

**UNCLASSIFIED**

**A 214253**

**Armed Services Technical Information Agency**

**ARLINGTON HALL STATION  
ARLINGTON 12 VIRGINIA**

FOR  
MICRO-CARD  
CONTROL ONLY

NOTICE: WHEN GOVERNMENT OR OTHER DRAWINGS, SPECIFICATIONS OR OTHER DATA ARE USED FOR ANY PURPOSE OTHER THAN IN CONNECTION WITH A DEFINITE GOVERNMENT PROCUREMENT OPERATION, THE U. S. GOVERNMENT THEREBY ASSUMES NO RESPONSIBILITY, NOR ANY OBLIGATION WHATSOEVER, AND THE FACT THAT THE GOVERNMENT MAY HAVE FORMULATED, FURNISHED, OR IN ANY WAY SUPPLIED THE SAID DRAWINGS, SPECIFICATIONS, OR OTHER DATA IS NOT TO BE REGARDED BY IMPLICATION OR OTHERWISE AS IN ANY MANNER LIMITING THE HOLDER OR ANY OTHER PERSON OR CORPORATION, OR CONVEYING ANY RIGHT OR PERMISSION TO MANUFACTURE, USE OR SELL ANY PATENTED INVENTION THAT MAY IN ANY WAY BE RELATED HERETO.

**UNCLASSIFIED**

**CONFIDENTIAL**

CLASSIFICATION CHANGED FROM

SEE AUTHORITY LISTED IN

UNCLASSIFIED

SUMMARY TECHNICAL REPORT  
OF THE  
NATIONAL DEFENSE RESEARCH COMMITTEE

Reproduced From  
Best Available Copy

This document contains information affecting the national defense of the United States within the meaning of the Espionage Laws, Title 18, U. S. C., 31 and 32, as amended. Its transmission or the revelation of its contents in any manner to an unauthorized person is prohibited by law.

This volume is classified CONFIDENTIAL in accordance with security regulations of the War and Navy Departments because certain chapters contain material which was CONFIDENTIAL at the date of printing. Other chapters may have had a lower classification or none. The reader is advised to consult the War and Navy Agencies listed on the reverse of this page for the current classification of any material.

Unclassified



**UNCLASSIFIED**

Manuscript and illustrations for this volume were prepared for publication by the Summary Reports Group of the Columbia University Division of War Research under contract OEMsr-1131 with the Office of Scientific Research and Development. This volume was printed and bound by the Columbia University Press.

Distribution of the Summary Technical Report of NDRC has been made by the War and Navy Departments. Inquiries concerning the availability and distribution of the Summary Technical Report volumes and microfilmed and other reference material should be addressed to the War Department Library, Room 1A-522, The Pentagon, Washington 25, D.C., or to the Office of Naval Research, Navy Department, Attention: Reports and Documents Section, Washington 25, D.C.

Copy No.

**9**

This volume, like the seventy others of the Summary Technical Report of NDRC, has been written, edited, and printed under great pressure. Inevitably there are errors which have slipped past Division readers and proofreaders. There may be errors of fact not known at time of printing. The author has not been able to follow through his writing to the final page proof.

Please report errors to:

JOINT RESEARCH AND DEVELOPMENT BOARD  
PROGRAMS DIVISION (STR ERRATA)  
WASHINGTON 25, D. C.

A master errata sheet will be compiled from these reports and sent to recipients of the volume. Your help will make this book more useful to other readers and will be of great value in preparing any revisions.

**UNCLASSIFIED**

UNCLASSIFIED

SUMMARY TECHNICAL REPORT OF DIVISION 6, NDRC

VOLUME 16

*Underwater Sound Equipment III*

# SCANNING SONAR SYSTEMS

OFFICE OF SCIENTIFIC RESEARCH AND DEVELOPMENT  
VANNEVAR BUSH, DIRECTOR

NATIONAL DEFENSE RESEARCH COMMITTEE  
JAMES B. CONANT, CHAIRMAN

DIVISION 6  
JOHN T. TATE, CHIEF

## CLASSIFICATION

(canceled) (changed to)

Unclassified

By authority of

*James H. Douglas*  
dated *8-2-60*

---

WASHINGTON, D. C., 1946

  
Unclassified

# NATIONAL DEFENSE RESEARCH COMMITTEE

James B. Conant, *Chairman*

Richard C. Tolman, *Vice Chairman*

Roger Adams

Army Representative<sup>1</sup>

Frank B. Jewett

Navy Representative<sup>2</sup>

Karl T. Compton

Commissioner of Patents<sup>3</sup>

Irvin Stewart, *Executive Secretary*

## <sup>1</sup>Army representatives in order of service:

Maj. Gen. G. V. Strong	Col. L. A. Denson
Maj. Gen. R. C. Moore	Col. P. R. Faymonville
Maj. Gen. C. C. Williams	Brig. Gen. E. A. Regnier
Brig. Gen. W. A. Wood, Jr.	Col. M. M. Irvine
Col. E. A. Routheau	

## <sup>2</sup>Navy representatives in order of service:

Rear Adm. H. G. Bowen	Rear Adm. J. A. Furer
Capt. Lybrand P. Smith	Rear Adm. A. H. Van Keuren
Commodore H. A. Schade	

## <sup>3</sup>Commissioners of Patents in order of service:

Conway P. Coe	Casper W. Ooms
---------------	----------------

## NOTES ON THE ORGANIZATION OF NDRC

The duties of the National Defense Research Committee were (1) to recommend to the Director of OSRD suitable projects and research programs on the instrumentalities of warfare, together with contract facilities for carrying out these projects and programs, and (2) to administer the technical and scientific work of the contracts. More specifically, NDRC functioned by initiating research projects on requests from the Army or the Navy, or on requests from an allied government transmitted through the Liaison Office of OSRD, or on its own considered initiative as a result of the experience of its members. Proposals prepared by the Division, Panel, or Committee for research contracts for performance of the work involved in such projects were first reviewed by NDRC, and if approved, recommended to the Director of OSRD. Upon approval of a proposal by the Director, a contract permitting maximum flexibility of scientific effort was arranged. The business aspects of the contract, including such matters as materials, clearances, vouchers, patents, priorities, legal matters, and administration of patent matters were handled by the Executive Secretary of OSRD.

Originally NDRC administered its work through five divisions, each headed by one of the NDRC members. These were:

- Division A — Armor and Ordnance
- Division B — Bombs, Fuels, Gases, & Chemical Problems
- Division C — Communication and Transportation
- Division D — Detection, Controls, and Instruments
- Division E — Patents and Inventions

In a reorganization in the fall of 1942, twenty-three administrative divisions, panels, or committees were created, each with a chief selected on the basis of his outstanding work in the particular field. The NDRC members then became a reviewing and advisory group to the Director of OSRD. The final organization was as follows:

- Division 1 — Ballistic Research
- Division 2 — Effects of Impact and Explosion
- Division 3 — Rocket Ordnance
- Division 4 — Ordnance Accessories
- Division 5 — New Missiles
- Division 6 — Sub-Surface Warfare
- Division 7 — Fire Control
- Division 8 — Explosives
- Division 9 — Chemistry
- Division 10 — Absorbents and Aerosols
- Division 11 — Chemical Engineering
- Division 12 — Transportation
- Division 13 — Electrical Communication
- Division 14 — Radar
- Division 15 — Radio Coordination
- Division 16 — Optics and Camouflage
- Division 17 — Physics
- Division 18 — War Metallurgy
- Division 19 — Miscellaneous
- Applied Mathematics Panel
- Applied Psychology Panel
- Committee on Propagation
- Tropical Deterioration Administrative Committee

## NDRC FOREWORD

AS EVENTS of the years preceding 1940 revealed more and more clearly the seriousness of the world situation, many scientists in this country came to realize the need of organizing scientific research for service in a national emergency. Recommendations which they made to the White House were given careful and sympathetic attention, and as a result the National Defense Research Committee [NDRC] was formed by Executive Order of the President in the summer of 1940. The members of NDRC, appointed by the President, were instructed to supplement the work of the Army and the Navy in the development of the instrumentalities of war. A year later, upon the establishment of the Office of Scientific Research and Development [OSRD], NDRC became one of its units.

The Summary Technical Report of NDRC is a conscientious effort on the part of NDRC to summarize and evaluate its work and to present it in a useful and permanent form. It comprises some seventy volumes broken into groups corresponding to the NDRC Divisions, Panels, and Committees.

The Summary Technical Report of each Division, Panel, or Committee is an integral survey of the work of that group. The first volume of each group's report contains a summary of the report, stating the problems presented and the philosophy of attacking them and summarizing the results of the research, development, and training activities undertaken. Some volumes may be "state of the art" treatises covering subjects to which various research groups have contributed information. Others may contain descriptions of devices developed in the laboratories. A master index of all these divisional, panel, and committee reports which together constitute the Summary Technical Report of NDRC is contained in a separate volume, which also includes the index of a microfilm record of pertinent technical laboratory reports and reference material.

Some of the NDRC-sponsored researches which had been declassified by the end of 1945 were of sufficient popular interest that it was found desirable to report them in the form of monographs, such as the series on radar by Division 14 and the monograph on sampling inspection by the Applied Mathematics Panel. Since the material treated in them is not dupli-

cated in the Summary Technical Report of NDRC, the monographs are an important part of the story of these aspects of NDRC research.

In contrast to the information on radar, which is of widespread interest and much of which is released to the public, the research on subsurface warfare is largely classified and is of general interest to a more restricted group. As a consequence, the report of Division 6 is found almost entirely in its Summary Technical Report, which runs to over twenty volumes. The extent of the work of a Division cannot therefore be judged solely by the number of volumes devoted to it in the Summary Technical Report of NDRC: account must be taken of the monographs and available reports published elsewhere.

Any great cooperative endeavor must stand or fall with the will and integrity of the men engaged in it. This fact held true for NDRC from its inception, and for Division 6 under the leadership of Dr. John T. Tate. To Dr. Tate and the men who worked with him—some as members of Division 6, some as representatives of the Division's contractors—belongs the sincere gratitude of the nation for a difficult and often dangerous job well done. Their efforts contributed significantly to the outcome of our naval operations during the war and richly deserved the warm response they received from the Navy. In addition, their contributions to the knowledge of the ocean and to the art of oceanographic research will assuredly speed peacetime investigations in this field and bring rich benefits to all mankind.

The Summary Technical Report of Division 6, prepared under the direction of the Division Chief and authorized by him for publication, not only presents the methods and results of widely varied research and development programs but is essentially a record of the unstinted loyal cooperation of able men linked in a common effort to contribute to the defense of their nation. To them all we extend our deep appreciation.

VANNEVAR BUSH, Director  
*Office of Scientific Research and Development*

J. B. CONANT, Chairman  
*National Defense Research Committee*

## FOREWORD

IN 1941, SECTION C-4, later Division 6, of the National Defense Research Committee, undertook a broad consideration of the steps which could be taken to increase the efficiency of echo-ranging sonar gear. This consideration led to undertaking a number of developments which, it was believed, might be promptly applicable to the conventional type of echo-ranging equipment employed at that time. In addition, it appeared that a quite radically different type of echo-ranging gear, designated as scanning sonar, probably offered decided advantages over methods previously developed. Consequently, a long-term program for the development of scanning sonar was authorized at two of the Section's laboratories, namely at the San Diego Laboratory of the University of California and at the Harvard University Laboratory at Cambridge.

The work at these two laboratories, although having the same general operating objectives, involved quite different physical methods. This particular summary report covers progress made in the development of scanning sonar based upon principles and methods adopted by or originating with the staff of the Harvard Underwater Sound Laboratory. It has been prepared by that organization and, because it is probable that scanning sonar will have a prominent place in the future art, the subject is presented in considerable detail.

Because of the course which the war seemed fortunately to be taking and because of other considerations, no attempt was made to rush into production apparatus based on the Harvard development. Consequently, the principal value of this work resides in its future applications. In this respect, one must assume that every effort will be made to develop sub-

marines which, both from aircraft and from surface ships, will be more difficult to locate and to attack successfully. If scanning sonar fulfills its promise, gear of this type should prove important in the detection and location of the submarine of the future. Its demonstrated performance has already indicated its potentialities for attaining other objectives in sub-surface warfare.

Other development groups are continuing this project and it is obviously desirable to provide these with reasonably complete information as to prior work. This has been the principal objective of this report and it is presented with the hope that it may serve this purpose.

The Division expresses its appreciation of the performance of the group of scientists and engineers engaged on this project under the able direction of Dr. F. V. Hunt, Director, and Dr. C. P. Boner, Associate Director of the Harvard Underwater Sound Laboratory. The Division also acknowledges the contribution of the Sangamo Electric Company which, under a Division contract, designed and produced a number of workmanlike models for test and demonstration.

During the four-year period over which this program has continued, the Division and the contractor have maintained close liaison with the Office of the Coordinator of Research and Development for the Navy and with the Bureau of Ships. By making facilities available and by giving advice and support, the progress of this development has been greatly facilitated.

JOHN T. TATE  
Chief, Division 6

## PREFACE

THIS VOLUME is devoted to an account of the development of scanning sonar, a method of underwater sound signaling which provides a continuous display of the position of all underwater objects within acoustical detection range. The development was begun in August 1941 at the Underwater Sound Laboratory, Harvard University [HUSL] (OSRD Contract OEMsr-287), and continued as an integral part of the sonar development program sponsored by Division 6 of the National Defense Research Committee. After shipboard trials of experimental equipment, pilot production was initiated in 1944 by the Sangamo Electric Company (Contracts OEMsr-1288 and NXsr-46933), and four Navy vessels had been equipped with prototype scanning sonar, designated XQHA, by the spring of 1945.

The outstanding feature of scanning sonar can be illustrated by comparing the different methods used in searching a large area by sound waves or by electromagnetic waves. The high velocity of propagation of electromagnetic waves makes it possible to search quickly to all useful ranges for any given azimuth bearing and to repeat this process at successive bearings rapidly enough to examine the entire horizon within an interval of a few seconds. A similar procedure has been used for many years, searching the sub-surface horizon by standard "searchlight" sonar, but the relatively low velocity of sound waves, even in sea water, makes such a process very slow. However, by inverting the searching processes it has been possible to overcome these time handicaps. This inversion consists in irradiating the whole horizon with a transmitted pulse of sound and in searching very rapidly at all azimuth bearings as the range increases slowly in accordance with the relatively low velocity of sound propagation. As a result of this interchange of slow and rapid search between range and bearing, it has been possible to devise sonar systems which scan the entire horizon to the range limits of expected detection within time intervals comparable with those required by search radar sets for coverage of the horizon to their maximum detection range.

This report presents the basic principles of omnidirectional scanning sonar systems, equipment design considerations, the construction of prototype equipment, an analysis of operating tests, and recommendations for future work in this field. It is arranged so

that the first three chapters constitute an account of the basic principles, design considerations, and performance expectations. Subsequent chapters recite in some detail the development work carried on during the period 1941-1945, and the report concludes with a chapter setting forth recommendations for future work.

The preparation of this report has been a group effort of members of the scanning sonar division and the editorial division of the Underwater Sound Laboratory, Harvard University. The first draft of the manuscript was assembled under the supervision of O. H. Schuck, with R. M. Scott, R. B. Bowersox, C. M. Wallis, R. B. Watson, and M. H. Hebb serving as chapter editors.

The development of scanning sonar has been carried out under the auspices of Division 6 as a part of Navy Project NS-142. The work described in this volume has at one time or another engaged the attention of almost the entire staff of the Harvard laboratory concerned with sonar equipment. The following tabulation lists those who have made principal contributions to this program:

Blumberg, R. K.	Lowance, F. E.
Boner, C. P.	McKittrick, M.
Bowersox, R. B.	Marlow, W. C., Jr.
Bundy, F. P.	Merritt, T. P.
Camp, L. W.	Morton, R. C.
Coleman, J. S.	Nash, H. E.
Cummerow, R. L.	Natwick, J. O.
Evers, J. L.	Nitchie, F. R., Jr.
Fromm, K.	Patterson, A., Jr.
Handel, N. E.	Payne, R. E.
Harrison, G. I.	Pellam, J.
Hathaway, J. L.	Rich, S. R.
Hebb, M. H.	Saunders, N. B.
Henderson, H. W.	Schuck, O. H.
Hesthal, C. E.	Scott, R. M.
Horton, C. W.	Smith, P. L.
Hunt, F. V.	Wallace, R. H.
Jones, F. B.	Wallis, C. M.
Knauss, H. P.	Watson, R. B.
	Whitmarsh, D. C.

Navy liaison was provided throughout the development by Capt. Rawson Bennett II, Bureau of Ships. During portions of this period, Navy liaison assistance was also provided by Comdr. C. L. Engleman and Comdr. J. C. Myers, Bureau of Ships; Comdr. M. R. Peterson, Comdr. R. D. Shepard, and Lt.

CONFIDENTIAL

Comdr. S. D. B. Merrill, Tenth Fleet; Lt. Comdr. R. G. Snider, ASDevLant; and Comdr. J. B. Knight, U. S. Navy Underwater Sound Laboratory. Grateful acknowledgment is also extended to the many Navy officers who gave assistance from time to time in connection with operating tests.

In addition to the foregoing members of the staff of the Harvard Underwater Sound Laboratory, C. H.

Lanphier, F. C. Holtz, J. S. Martin, W. W. Sherwood, and R. E. Rast of the engineering staff of the Sangamo Electric Company played important roles in the design of the XQHA prototype equipment manufactured by that company.

F. V. HUNT  
Director, HUSL

## CONTENTS

CHAPTER	PAGE
1 Introduction . . . . .	1
2 General Considerations in Scanning Sonar Design . . . . .	20
3 Performance Expectations with Scanning Sonar . . . . .	59
4 Mechanical Rotation Scanning Sonar . . . . .	77
5 Commutated Rotation Scanning Sonar . . . . .	116
6 Integrated Type B Scanning Sonar . . . . .	222
7 Electronic Rotation Scanning Sonar . . . . .	303
8 Test Methods and Techniques . . . . .	386
9 Theory of Beam Formation . . . . .	433
10 Summary Discussion of Scanning Sonar Problems and Proposals for Future Work . . . . .	475
Glossary . . . . .	513
Bibliography . . . . .	517
Contract Numbers . . . . .	531
Service Project Numbers . . . . .	532
Index . . . . .	533



## Chapter I

# INTRODUCTION

### 1.1 GENERAL DESCRIPTION OF SEARCHLIGHT SYSTEM

A BRIEF DESCRIPTION of the operation of sonar gear used prior to scanning equipment contributes to an understanding of the newer devices and techniques discussed later in this report. Most of the pre-scanning equipment either is, or is similar to, that commonly designated as QC and is of the searchlight type. A system of this kind first sends out a ping or pulse of sound in a particular direction under water, and then listens for echoes returning from that direction. If an echo is returned, the range of the reflecting target is determined from the time interval between emission of the ping and arrival of the echo, while its bearing is the direction from which the loudest echo is returned. The chemical range recorder and the *bearing deviation indicator* [BDI]<sup>1</sup> measure the respective quantities of range and bearing fairly accurately. The general shipboard arrangement of sonar gear of this type is shown in Figure 1.

The searchlight system has several operational limitations which are of interest in connection with the discussion of scanning sonar.

1. Since the projector is sharply directional, it detects a target at a given bearing only if it is trained in that direction when the ping is emitted and remains in that position long enough for an echo to be received from a target at the greatest possible range. This listening interval places an obvious limitation upon the speed in searching a given sector, and hence upon the efficiency of both screening and searching.

2. While a ship carrying searchlight sonar is attacking a target, it is impossible for the sonar operator to search for possible targets at other bearings or even to hear noise from other targets or torpedoes. Thus the ability of a searchlight-type sonar to protect the ship on which it is installed is limited.

3. Maintenance of sound contact is difficult when the target is conducting evasive tactics, or when the attacking ship is passing over the target. Furthermore, target wake, decoys, and wakes from other ships increase this difficulty. If contact with the target

is lost, searching a large sector again may be necessary.

4. The searchlight system projector is large and heavy and its operation requires it to be trainable in all directions, necessitating the use of extra mechanical gear.

5. The sonar operator must be well trained to operate the equipment skillfully and to interpret its indications correctly.

### 1.2 DESIRABILITY OF ALL-AROUND SEARCH AND PPI INDICATION

Early in World War II the need was seen for a search system giving simultaneous sensitivity through 360 degrees, and presentation on a *plan position indicator* [PPI] screen of continuous information on range and bearing of all targets within the maximum echo range. An omnidirectional search or scanning system of this sort would increase ship security by searching in all directions simultaneously, and by picking up echoes from multiple targets even during an attack on a specific target. Being continually alert in all directions, it therefore would detect approaching torpedoes.

Experience with the scanning sonars developed at Harvard Underwater Sound Laboratory [HUSL] has justified these expectations. If sea conditions permit reception of any echoes at all, contact with a target under attack is practically never lost, even though the target may be using evasive tactics. In addition, the systems tested have proved alert to noise sources, indicating their bearings by "noise radials" on the PPI screen. In test firings of torpedoes, detection on the screen has occurred in ample time to permit evasive maneuvers. Operator skill with the scanning-type sonar is less important than with the searchlight type. Instead of training the projector continually by a series of small steps, the operator sees the location of all targets within echo range at all times. The fact that the wake of a target and the target itself both appear on the screen aids the conning officer in conducting the attack.

In the scanning system searching at high speeds is automatic so that there is little danger that the opera-

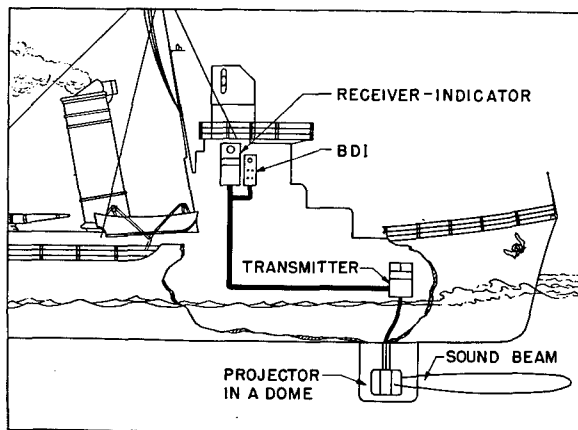


FIGURE 1. Destroyer installation of searchlight sonar.

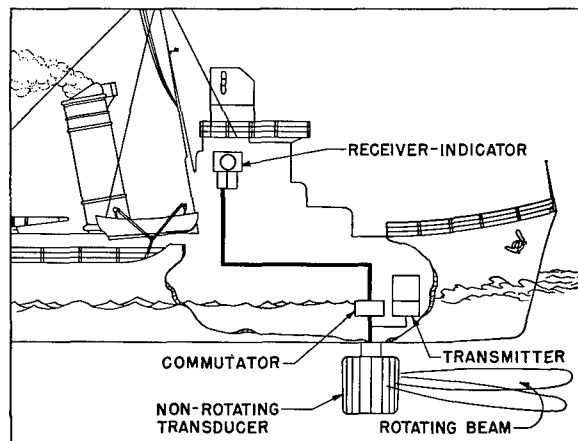


FIGURE 2. Destroyer installation of scanning sonar.

tor will miss any echoes. Even though he may not see the proper portion of the screen when an echo first appears, its repetition on successive pings and the persistence of the screen indication make it difficult to overlook the echo trace.

As mentioned above, the chief advantage of the PPI is in presenting all reflecting targets in their proper relationship to each other and to own ship. There is the problem of separating echo traces of undesired targets, such as rocks, from those of submarines. If the presentation is a relative position plot with own ship at the center, spots on the screen caused by rocks or other fixed targets move across the screen as a group, remaining fixed with respect to each other, as own ship moves. Echo traces from submarines or other moving targets, however, may be identified by their movements with respect to other spots.

It is also possible, with such a PPI screen, to present all targets and own-ship's motion in a true-bearing relationship. The entire display can be made to move across the screen at a rate to compensate for own-ship's motion, producing a geographical plot.

### 1.3 GENERAL DESCRIPTION OF HUSL SCANNING SYSTEM

The two outstanding characteristics of the scanning system developed at HUSL are, in brief:

1. Emission of a short omnidirectional ping.
2. Reception of the echo by a rapidly rotating beam of sensitivity.

The general arrangement of the gear is shown in the

block diagram of Figure 2. The sequence of events in operation is as follows:

The short ping is emitted in all directions simultaneously. Immediately following the ping, a sharp beam of receiving sensitivity scans the horizon very rapidly at rates varying from 30 rps to 500 rps. Any returning target echo is received by this rotating beam as it passes the target's bearing. It is amplified by a standard receiver and then brightens a moving spot on the PPI screen. The PPI scope is designed so that the spot, which is invisible in the absence of a signal, starts at the center of the screen with each ping and travels outward in a spiral. Since the rotations of the spot and the scanning beam are synchronized, an echo from a given bearing will brighten the moving spot at the corresponding bearing on the screen. The radius of the spiral increases at a uniform rate so that the distance from an echo brightened spot to the center of the screen indicates the target's range. In other words, the scanning sonar PPI presents a ship-centered map on which any given target is located correctly in range and bearing.

If the scanning beam is to pick up at least part of the echo from any target within echo range, regardless of bearing, the emitted pulse must be at least as long as the time required for one complete rotation of the scanning beam. For example, with a scanning rate of 30 rps the time required for one revolution of the scanning beam is about 33 milliseconds. If a target is 800 yards distant, one second, in which the scanning beam makes 30 revolutions, is required for the sound to go out and the echo to return. During this one second the dark spot on the PPI screen travels outward in a spiral which breaks

up the 800-yard range into steps of approximately 27 yards each. This range resolution can be increased by increasing the scanning speed to as much as 500 rps and correspondingly reducing the minimum length of the ping.

A source of noise in the immediate vicinity of own ship or of the target appears on the PPI scope as a bright radial streak, caused by the scanning beam receiving a signal each time it passes the noise source and thus brightening a corresponding spot on every spiral. This noise radial on the PPI scope gives the bearing of the noise source but not the range.

It should be noted that an echo from a small object is presented on the PPI screen as an arc of the spiral, the length of which corresponds to the width of the beam of receiving sensitivity which is being rotated. An extended target may give an echo whose length in time is greater than the time length of the ping, and the bright arc on the PPI screen is correspondingly wider in bearing and may also occur on successive spirals. The wake of a passing ship, for example, usually produces echoes which appear on the PPI screen as a long, bright streak covering a number of spirals. It has been found that the center of the arc gives a good approximation of the bearing of the target and can usually be measured to within a fraction of a degree by an operator with only limited experience.

Figure 3 is a photograph of the PPI screen showing a variety of targets. This picture was taken in Boston Harbor during a single ping and is typical of the appearance of the screen under shallow-water conditions when own ship is stationary. Usually the propellers of the attacking ship make sufficient noise in the water to produce a faint noise radial on the PPI screen in the aft direction.

The cylindrical transducer of the scanning system is composed of 36 or more vertical staves, which can be connected together for transmitting and whose individual signals are combined to form a sharp beam for receiving. During transmission all staves are connected in parallel to the transmitter to constitute a uniform cylindrical radiator. The sound distribution for an azimuthal scanning system is essentially the same in all horizontal directions, but is restricted usually to a fairly small vertical angle. During the reception, the staves are disconnected from the transmitter and connected separately to the scanning device. This may be a mechanically rotating capacitive or inductive commutator, or an

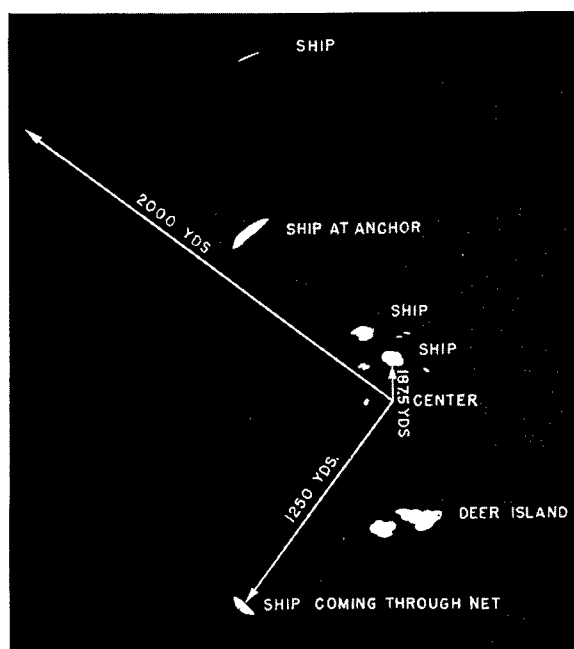


FIGURE 3. PPI screen showing several targets (CR/ER sonar).

electronic switching device, either of which contains the beam-forming network by means of which a single sharp beam of sensitivity is usually formed from about one-third of the total number of transducer elements. This beam is rotated at a rapid rate by means of the scanning commutator, so that the effect produced in reception is the same as if a highly directional hydrophone of the QC type were rapidly rotated under water at 30 to 500 rps. The receiver, transmitter, and other associated electronic equipment may be much the same as in the ordinary QC system, except that the omnidirectional cylindrical scanning transducer requires about 20 times as much electric power as the searchlight-type projector to produce the same emission intensity in a given direction. The type letters QH have been assigned by BuShips to this form of sonar.

#### 1.4 OTHER OMNIDIRECTIONAL SEARCH SYSTEMS

Several omnidirectional search systems other than the one described in this report have been under development by various groups. It is beyond the scope of this volume to describe these developments in detail, but their salient features will be described briefly.

An omnidirectional scanning system has been under development and experimental study by the British Navy. This version of scanning sonar has many features in common with QH sonar, including use of a multielement (72-element) cylindrical transducer. Multiple lag lines are connected to the transducer elements to provide 72 fixed sharp-beam patterns for each of which a separate amplifier and rectifier are provided. The charge on each rectifier capacitor, representing the amplitude of the signal coming from a particular direction, is scanned at high speed by a suitable electronic switch and presented on a PPI scope. This arrangement has been characterized as a storage system, since the entire length of the echo signal from a particular direction is stored in the output capacitor of a particular directional channel for subsequent scanning. In addition to providing for integration of the pulse over its entire length, the scanning frequency can be selected independently without reference to the length of the transmitted pulse. These are desirable features not present in the QH scanning system, but attained in the British system with a greatly increased complexity of the equipment.

Another system, characterized as *frequency modulation* [FM] sonar, received extensive development at the University of California Division of War Research [UCDWR], San Diego Laboratory. This sonar system, designated QL, is described in detail in another volume of the Summary Technical Report. In this apparatus, a continuous beam of sound is emitted by a directional transducer whose frequency varies linearly with time over approximately a 10-kc range—for example, 25 kc to 35 kc. The echoes, which are received by a second directional transducer pointed to the same bearing as the first, are amplified by a receiver and filter system that transmits only signals of a definite frequency. The oscillator that sends out transmitted signals serves also as the beat-frequency oscillator in the receiver, so that any echo signals returning to the second transducer give a signal in the receiver whose frequency differs by an amount which depends upon the range of the target. Thus, the range of the observed echo is determined and measured by the frequency of the echo as it passes through the heterodyne receiver. A bank of 20 different filters covering a suitable range of frequencies is customarily used. The output from these filters is scanned by electronic switching to give a continuous indication of all echoes at

any range for a particular bearing. This FM system gives an essentially continuous indication of all targets on a given bearing, whatever their ranges, but the various bearings must be scanned at a rather slow rate. The short-ping rapid-scan HUSL system, on the other hand, scans all bearings continuously, but must wait for echoes from different ranges, that is, until sound proceeds from the transmitter to the target and back to the receiver. Thus these two systems differ fundamentally in method of scanning.

A third scanning system, investigated to some extent by the Submarine Signal Company [SSC], is in effect an annular search device in which two directional projectors are used, one to transmit, the other to receive. These projectors are mounted with a fixed angle of training between them (180 degrees in the SSC test set) which remains constant while they are mechanically rotated about a vertical axis at speeds of from 9 to 80 rpm. One projector transmits a signal continuously into the water, and the other picks up echoes which may be returned from any point around the horizon. Both have fairly sharp directionality patterns. Thus, a target at a given range is illuminated by sound from the transmitting projector some time after that projector has passed the target's bearing and returns an echo which arrives at the receiving transducer, if the range and the speed of rotation are correct, at just the moment it is trained in the target's direction. This means that the range from which the echoes can be received at any given time depends on the rotating speed of the two transducers and the fixed angle between them. Because of the finite widths of the transmitting and receiving beam patterns, an annular area of finite width in range is being scanned for targets at any given speed of revolution of the projectors. The operator can vary the average range of this annular region at will by varying the rotational speed of the scanning transducers.

In tests the magnetostriction face and the crystal face of the QC-JK combination SSC projector have been used as the projector and receiver. With this outfit, a speed of 9.6 rpm was found to give a range band centered at about 2,500 yards, while a speed of 80 rpm gave a range band centered at about 300 yards. It was planned to record the echoes picked up by this system on a moving sheet of chemically treated paper at the correct range and bearing, with own ship at the center of the plot. By having the paper move at a rate proportional to own-ship's

CONFIDENTIAL

speed, a modified geographical plot was obtained in which own ship appeared to steer a straight course at all times. Such a plot may be said to be geographical, showing relative bearing rather than true bearing. This system is probably better suited for use as protective equipment than as an attack device since the high speed of projector rotation necessary for investigating close ranges during attack is mechanically difficult.

## 1.5 HISTORICAL SURVEY OF PRELIMINARY WORK ON SCANNING SONAR

One of the first problems undertaken by HUSL after its organization in the summer of 1941 was that of devising an omnidirectional search system to replace the QC, or searchlight-type, sound gear then in use. The first scheme discussed was a crossed-dipole system, analogous to existing radio direction finders, in which either two crossed-loop antennas or four vertical antennas (Adcock system) form a crossed-dipole receiving antenna system. Signals received from these antenna systems are applied through two separate amplifiers to the plates of a CRO, so that the point at which the electron beam strikes the scope face is deflected in a direction corresponding to the bearing of the signal source. A fifth antenna may be connected into the system to blank out the spot on one-half of its deflection cycle, and thus eliminate the 180-degree ambiguity of the bearing indication. A crossed-dipole scheme of this kind, in which rotation was accomplished by suitable modulation of the signals received from the separate dipoles, was one of the methods of producing a rotating beam under water which was tried and discarded very early in the history of HUSL.

Another system used in radio direction finding is the "Musa" system, in which a small number of antennas are connected to suitable networks to form a beam in the vertical direction that can be steered by varying the compensator network. This scheme of steering a beam of sensitivity by means of compensator networks, which can be changed by suitable commutators, is the basis of most of the scanning systems used under water.

Several German patents<sup>a, b, c</sup> dating from about 1930, propose this steerable beam of sensitivity in underwater direction finding. One such scheme, de-

scribed in a patent,<sup>a</sup> was apparently used on the German submarine captured by the British and re-named HMS GRAPH.

Another patent<sup>b</sup> is of interest here, because it included a proposal for a cylindrical transducer with elements which could be excited independently of one another. This transducer was in the form of a ring with teeth, somewhat like a motor armature stamping, made of laminated nickel sheets. Each tooth was to be wound independently to form a separate and independent element of the hydrophone. The vertical elements were then to be connected with electric compensating networks to give a unidirectional beam of sensitivity which could be steered to any direction by means of a commutator.

## 1.6 HISTORICAL DEVELOPMENT OF HUSL SCANNING SYSTEM

### 1.6.1 Earliest Studies

The method for underwater scanning first discussed at HUSL involved some principles of the FM system. In this scheme, a sawtooth frequency sweep of about 5-kc range in 10 seconds was to be broadcast under water in all directions. Any returning echo would be picked up by a directional transducer and heterodyned with the oscillator generating the outgoing signal. Thus, the difference in frequency between the outgoing signal and the echo would be a measure of the range, with a difference of 1,000 c corresponding to a range of 1 mile.

This frequency difference then would be amplified and applied to a frequency meter circuit, the output of which would be applied to a PPI scope to produce a radial deflection. Instead of using a spiral sweep on the CRO, the spot was to be rotated somewhere near the center by potentiometers geared to whatever mechanism was used to rotate the sharp pattern of the receiver sensitivity. When an echo arrived, it would deflect the spot radially from the center at the appropriate bearing of the target. The magnitude of this deflection from the center would be a measure

<sup>a</sup> W. Rudolph, U.S. Patent No. 1,977,974 (1934).

<sup>b</sup> Kallmeyer, DRP No. 620,872 (1934).

<sup>c</sup> Some other patents on the subject of electric compensating networks are:

H. Hecht and H. Stenzel, U.S. 1,893,741 (1933).

F. Lange, U.S. 1,971,688 (1934).

F. Fischer, U.S. 1,995,708 (1935).

of the frequency of the returning signal and, therefore, a measure of the range of the target. The rotating receiver pattern was to be scanned or rotated by some sort of mechanical commutator. No actual apparatus was built and the scheme was abandoned for a number of reasons. Construction of a projector capable of handling the wide range of frequencies without significant changes in amplitudes was difficult, as was providing a suitable sawtooth frequency sweep which would be truly linear. The additional difficulty of dead time associated with the flyback was encountered, for, as the sweep started over, it would be possible to receive echoes from objects just beyond the range being searched. Such echoes would have a frequency which, when heterodyned with the new frequency of the sweep, would appear on the scope at an incorrect range. Thus in practice it would be necessary to blank out a certain region of the scope and this was regarded as a major drawback.

The scanning method finally developed at HUSL was studied in some detail during the summer and fall of 1941 and the preliminary reports issued in December of that year.<sup>2</sup> At first, it appeared that a multiple array of small projectors might be connected to each other with networks, so that sharp beams could be formed in a number of directions. This idea was soon abandoned, however, in favor of a single transducer with multiple vertical elements which could be considered as individual transducers. The electromechanically rotated sharp-beam system was never constructed but is described below for its historical interest.

A 250-millisecond ping was to be sent out by a non-directional transducer which might be either the receiving or a separate transmitting transducer. The PPI was to be a cathode-ray tube with a spiral sweep of 4 rps synchronized with the rotation of the sharp receiving beam. Any echo picked up would be amplified and used to brighten the spot on the indicator at the appropriate bearing and range. The range could thus be read on the face of the PPI scope to within approximately  $\pm 100$  yards. A 36-element projector was to be used as a receiver with 36 separate electric compensating networks forming as many receiving beams. These beams would then be fed through a mechanical commutator which would rotate and switch from one beam to another. By use of a commutator, signals picked up by the various beams would be applied successively to the indicator to brighten the spot on the scope.

The indication on the PPI during reception of an echo would be a series of short arcs of differing intensity, the overall effects of which would be the equivalent of a single longer arc of variable intensity. There would be enough overlap in the beam in the different directions to make these 10-degree steps sufficiently sharp.

In order to transmit and receive with the same transducer, 36 send-receive relay contacts were to be used for connecting the transducer to the transmitter during the ping, and then to the compensator network and receiver for reception of echoes. Since considerations of wear would limit the commutator speed to comparatively low values with resulting poor range resolution, it was believed that this system would be chiefly applicable to protection of convoys, rather than to attacking vessels. Various designs were discussed but no apparatus of this type was built. However, these design studies are fundamental to later scanning sonar apparatus, and will be described here.

In searching at a range of 5,000 yards, 6.25 seconds must elapse between pings to allow time for the return of an echo from that distance; echoes from a particular target would accordingly appear only once in every interval of that length. This would make a PPI screen of comparatively long persistence necessary and, fortunately, such a screen, already developed for radar purposes, was available in limited quantities. It was planned to use 2-phase deflection coils on the PPI scope, and to provide a 2-phase a-c generator geared to the commutator shaft to give a 2-phase 4-cycle voltage synchronized with the rotation of the commutator. Thus the spot on the PPI could be made to sweep in a circular path synchronously with the rotation of the commutator. The radial motion of this circular sweep was to be produced by ring potentiometers in each phase of the deflection circuit. The movable contacts on these potentiometers were to be driven by a variable speed motor, so that the spiral on the PPI scope would be expanded at the proper rate to cover the entire face of the scope within the searching time. Thus, the expansion would take 1.25 seconds for searching a 1,000-yard range, and 12.5 seconds for a 10,000 yard range. It was planned to have the transmitter keyed by a cam on the commutator shaft, so that the pulse would always start when the spot on the PPI scope was at the 180-degree or stern position. Thus, any transient occasioned by the switching of the send-

CONFIDENTIAL

receive relay by the transmitter would occur in the after direction, where echo ranging is always very difficult because of the noise from own-ship's propellers. The receiver was to be a standard type with a 300-c band-pass which was considered sufficient for receiving dopplerized echoes. The gain on this receiver would be controllable as a function of the range. Thus, the receiver gain would be low just after the emission of the ping in order to discriminate against the reverberation, while at the same time echoes would be presented in the correct amplitude without overloading the receiver. Since it is generally true that the greater the target range, the weaker the echo, the gain of the receiver would be increased slowly with time. The cylindrical projector of laminated nickel, about 10 inches high and 15 inches in diameter, was to be built of 36 elements and mounted in a streamlined housing. A 36-element crystal projector suggested for the same purpose was expected to produce similar results. The transmitted pulse was to be broadcast rather than sent out in a sharp beam and about 20 times the total power would be required, but this was considered feasible.

Before undertaking the construction of a projector and a system of this kind, the transmitting patterns that might be anticipated from such a 36-element cylindrical transducer were computed. It was expected that these would be identical with the receiving patterns because of the reciprocal relationship between the two. If all 36 of the elements were used in transmitting at the same phase and amplitude, the pattern would be uniform in azimuth around the transducer and fairly sharp in the vertical plane, which would be desirable for broadcasting. During reception, however, it was necessary to have a pattern as sharply directional as possible. For this purpose, only a limited number of the elements should be connected and phased in such a way as to give a suitable beam pattern. Computations were made using, respectively, 25, 19, 13, and 9 elements at a time. These were made always with suitable compensating phase networks to lag the transmitted signals of the front elements with respect to those of the side elements. With such a phasing scheme, the wave generated by side elements would arrive at a plane through the front of the transducer at the moment when the front elements were generating an acoustic wave, so that these waves would be in phase with each other. In effect, all elements used in transmitting such a narrow beam pattern could be considered

ALL SPOKES ARE ACTIVE, HAVE  
EQUAL AMPLITUDES, AND ARE PHASED  
SO THAT ALL RADIATION IN DIRECTION  
"P" IS IN PHASE.  $kd=16$   $\alpha_0=5^\circ$

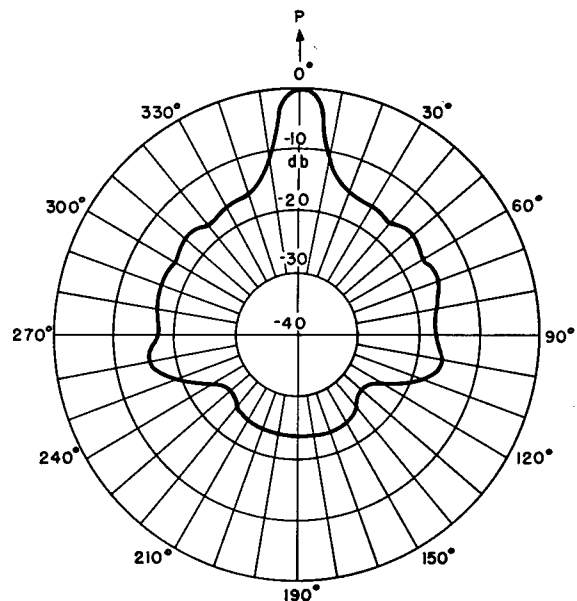


FIGURE 4. Directivity pattern of all spokes of 36-spoke cylindrical ring.

as located on a plane surface and therefore would be equivalent to a plane transducer. However, the elements at the front of the transducer would be facing in the direction of progression of transmitted wave, while the elements at the sides would be facing at angles away from that direction. Thus, the amplitude in the forward direction of the signal generated by the side elements would be somewhat less than that of the signal generated by the front elements. It was found possible to shade the signal from the side elements with respect to the signal from the front elements, and so obtain a beam pattern which, although somewhat wider than that obtained without such shading, had lower minor lobes at the sides of the main beam pattern. Examples of such calculated beam patterns for 36, 13, and 9 active sections are shown in Figures 4, 5, and 6.

In all proposals on scanning sonar, rotation of the sharp receiving beam pattern under water was to be accomplished by rotating a commutator, rather than the projector which would be difficult to rotate at high speeds. Two possible methods for obtaining the beam pattern were considered: one, before the commutation, by using a large number of separate

CONFIDENTIAL

Unclassified

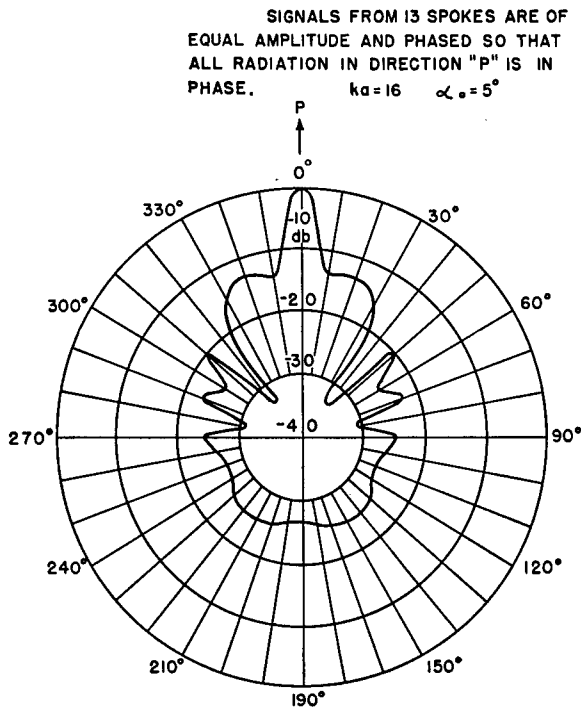


FIGURE 5. Directivity pattern of 13-spoke section of 36-spoke cylindrical ring.

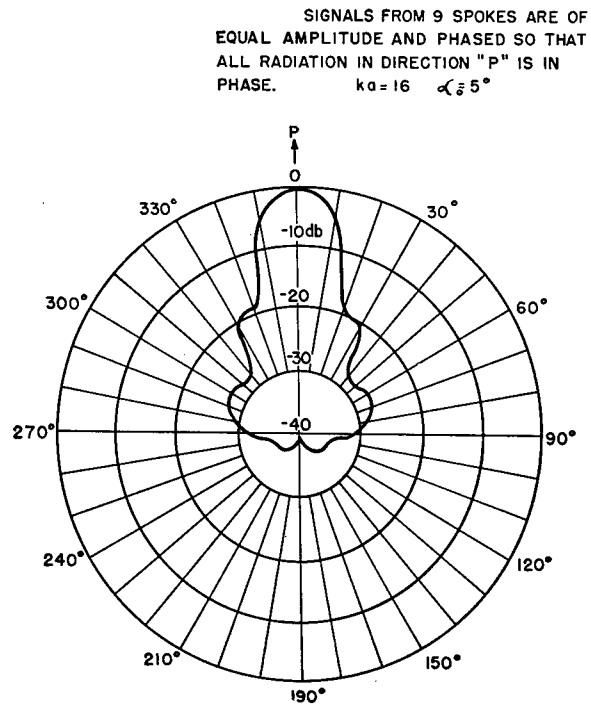


FIGURE 6. Directivity pattern of 9-spoke section of 36-spoke cylindrical ring.

compensator networks; and the other, by connecting the separate elements directly to the commutator and then, by means of the commutator, connecting a single beam-forming network to the various elements of the transducer in turn. This would produce a beam which could be steered step by step, from one bearing to the next, the size of a step being determined by the number of transducer elements. Apparently, 10-degree steps would be sufficient, and construction of a transducer and commutator system with more elements would be impractical. Later the scheme of using a commutator with capacitive or electromagnetic coupling instead of brush contact was conceived and developed. Capacitive commutators, which are discussed in detail later, have the advantage of eliminating the step-by-step feature of a mechanical commutator and allow fairly smooth commutation from one beam pattern to the next. This gives interpolation between the 10 sections of a 36-element transducer, and considerably more accurate bearing determination. Such a commutator can be rotated at higher speeds and accordingly gives a more exact determination of range, so that the system can be used for an attack on a target as well as for searching.

#### 1.6.2

#### MR Sonar System (Rotoscope)

In the summer of 1942, an echo-ranging system using a rotating directional hydrophone to receive echoes was proposed. The *rotoscope*, as far as is known, was the first system to embody this principle. It consisted of an omnidirectional transmitting projector, a directional receiving hydrophone rotating at 4 rps, and a receiving amplifier for brightening a spot on a cathode-ray tube. The dark cathode-ray spot, starting at the center at the instant the ping was emitted, traveled in a spiral so that its direction from the center of the scope face indicated target bearing, while its distance from the center indicated target range. Tests with a hydrophone rotating in water at 4 rps showed that noise generated by water turbulence was insignificant.

To test the principle of a rotating hydrophone in a scanning echo-ranging system, the rotoscope was set up on the barge *TIPPECANOE* during the summer of 1942. Echoes, reverberation, and noise were picked up in Boston Harbor and in the Charles River Basin, proving that this type of scanning system had possibilities for echo ranging.

Since the *TIPPECANOE* model was somewhat crude



mechanically, an improved model was built for installation on the 110-foot Diesel yacht AIDE DE CAMP. It had the same basic components as the first model except that the container, which rotated with the receiving hydrophone, was inside a stationary dome. Since the more accurate scanning echo-ranging systems were already being developed, this system was built primarily for experimental testing of ideas to be incorporated in other systems. Among the devices tested were *simultaneous lobe comparison* [SLC] brightening to reduce the number of spots appearing on the screen as a result of reverberation; receivers using *automatic volume control* [AVC] and *time-varied gain* [TVG] to reduce the effects of reverberation; amplitude modulation of the ping to determine the effect of greater peak power and modulation on reverberation and extended targets; and a system of measuring the length and phase of the ping with respect to the rotating microphone to get greater range accuracy. Many measurements of reverberation as a function of range and bearing were useful in the design of later systems. Because of the necessary long ping length, the rotoscope was greatly affected by reverberation and had a range accuracy of only  $\pm 100$  yards. Consequently, it was shelved as an echo-ranging device. It did prove useful for listening, however, so that the idea of employing a rotating microphone as a listening device to indicate the bearing of a noise source has been utilized for discovering torpedoes by their own noise in England and this country, especially in a modification of the WCA-2 echo-ranging equipment.<sup>3</sup> The last model of the rotoscope remained on TIPPECANOE during the summer and fall of 1942, and the improved system, on the AIDE DE CAMP from December 1942 to June 1943.

### 1.6.3 Early Electrically Rotated Systems

A method for rotating a beam of sensitivity by properly phasing several elements of a transducer composed of many independent elements around a circumference is described in *Progress Report on Sonic Locator Developments*.<sup>2</sup> Computations, making use of a time delay network or lag line for compensating the elements, showed the feasibility of producing a rotating pattern by this method. Two methods for rotating the beam of sensitivity continuously were considered. One involved tying the elements to a series of transformer primaries, one for each element, and then rotating the transformer sec-

ondaries and the beam-forming lag line inside the ring of primaries, the signal being taken off either on slip rings or through another rotating transformer. The second method was to connect the elements through transformers to capacitor segments on a stator plate, while the lag line, mounted on a rotor plate with similar segments, could be rotated over the fixed plate.

Experiments for smooth commutation were conducted and several transformers built into a linear array so that the secondaries could move past the primaries. It was found that a signal could be transferred by this method and that smooth, rather than step-by-step, commutation could be attained. A mechanical design was made and construction begun but abandoned when it was found that the capacitive commutator offered considerable promise and much less mechanical work.

The first experimental capacitive commutator consisted of two pieces of stiff cardboard with tinfoil segments glued on their surfaces. Experiments showed that when a signal was fed to the stationary segments and the corresponding segments on the other sheet rotated past the first group, a smooth commutation with a usable signal pickup resulted.

Following this basic experimentation, several laboratory models of the capacitive commutator were built and tested. From these early trials, considerable experience and information regarding the electric and mechanical design of the capacitive commutator were gained. A description of these early models and a historical account of the developmental work are given in Chapter 5. One of these units was used in conjunction with the first 36-element magnetostriction transducer, known as the "Medusa," to demonstrate the practicability of the scanning sonar principle.

Several pieces of electronic equipment were designed and built for testing the capacitive commutator. The first was a reverberation generator consisting of an oscillator whose amplitude and frequency were modulated by noise. The reverberation generator was connected through suitable isolation resistors to all the stator plates on the capacitive commutator. An "artificial water," consisting of a lag line equipped with taps, which could be connected to the stator plates of the capacitive commutator, was devised. This lag line gave phase lags to the output of a signal-frequency oscillator, so that signals produced at the commutator stator plates were similar to those gen-

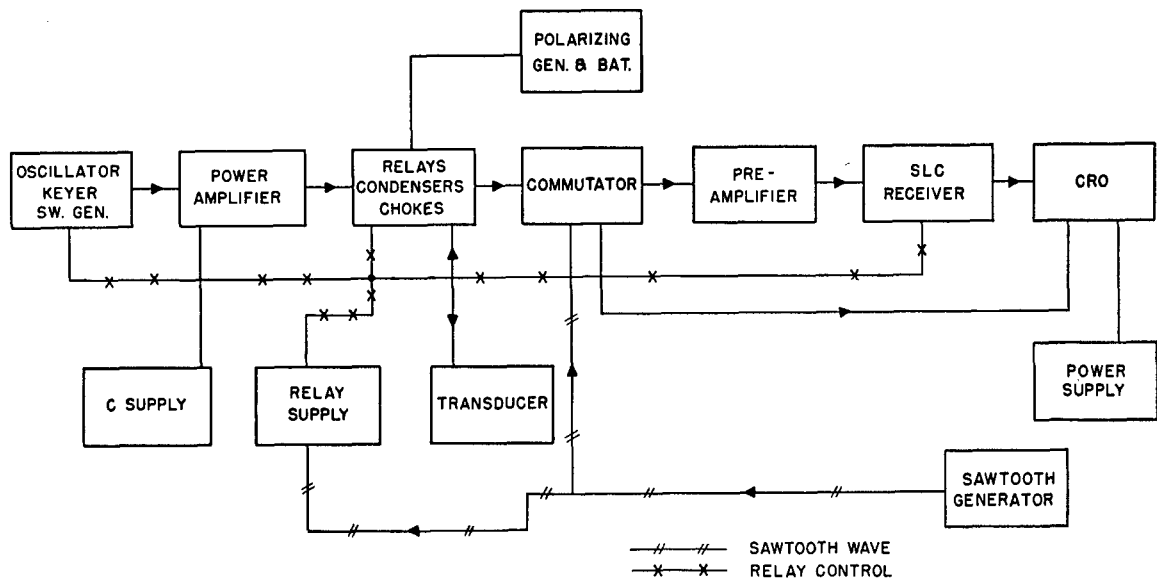


FIGURE 7. Early AIDE DE CAMP system (August 1943).

erated in the various elements of a multielement transducer receiving sound in the water from a distant point source. An "echo injector," which could introduce into the artificial water a short oscillator signal simulating an echo, was built for commutator and lag line compensator testing. The echo time was controlled by relay circuits associated with the reverberation generator, so that the echo could be introduced at any desired range and at a bearing determined by the connection of the artificial water to the commutator plates.

In order to facilitate the experimental study of beam-forming lag lines and their component tolerances, a laboratory commutator was built. It consisted of a 36-element flat-plate stator and rotor, surrounded by a safety shield, with relatively easy access to all components. It could be either motor-driven, at speeds up to 30 rps, or rotated by hand.

#### 1.6.4 First Workable Scanning Sonar System

The first workable scanning sonar system using a capacitive commutator was installed during June 1943 aboard the AIDE DE CAMP. The first transducer used with this system was Hebbphone I, made up of 36 magnetostrictive elements arranged in a circle. These elements were wedge-shaped stacks of nickel laminations 12 inches high and were mechanically and electrically independent. For transmission all

elements were electrically connected in phase, so that a nondirectional pattern was produced in the horizontal plane and a relatively sharp pattern in the vertical plane. During reception the system used a limited group of elements connected by a beam-forming phasing and shading network, while the remaining elements were connected to dummy loads.

At first polarizing current was supplied to Hebbphone I by a motor generator and later, to eliminate generator noise, by batteries. Suitable filter circuits were used to isolate the d-c and a-c signal channels.

A 36-pole double-throw relay was used so that the transducer could both transmit and receive. For reception each element was connected to an input transformer on the capacitive commutator, while for transmission all the elements were tied in a series-parallel combination and connected to the transmitter through an impedance-matching network. When the relay was in the transmitting position, one contact was used to start the transmitter, return the spiral sweep to the center of the PPI, blank the return trace, and start the TVG in the receiver.

A conventional class B 1.5-kw transmitter was used to drive the Hebbphone I. The signal, which had a frequency of approximately 22 kc, could be either amplitude- or frequency-modulated.

To rotate the beam of receiving sensitivity, a 30-rps 36-element commutator was used. In the rotor of this commutator there was a phasing and shading network connected to 12 of the rotating plates. Capacitive

tive slip rings were used to conduct a signal from the rotating phasing and shading network to the pre-amplifiers. With this commutator either amplitude or SLC brightening could be applied. A 3-phase 30-c sawtooth modulated voltage from a synchro attached to the rotor of the commutator was used to produce a spiral sweep on the PPI. Among the most important later modifications and additions were pulse transmitter circuits, true bearing presentation, and SLC brightening. The pulse transmitter circuits incorporated power supplies in which energy could be stored between pings and delivered to the transducer for only the duration of a ping. A signal fed to a synchro from the ship's gyrocompass was used to give true bearing presentation on the PPI—that is, bearing with respect to true north rather than to ship's course. With SLC brightening it was hoped to obtain greater bearing accuracy and to discriminate against reverberation.

This *commutated rotation* [CR] system was installed aboard the AIDE DE CAMP and field-tested at New London during November 1943. On November 8 the equipment was demonstrated to representatives of OSRD, BuShips, COMINCH, and the New London and San Diego laboratories. Approximately one week later a similar demonstration was held for several engineering concerns interested in manufacturing underwater detection equipment. Among these was the Sangamo Electric Company of Springfield, Illinois. Results of these field tests were most encouraging since they indicated that the sonar system under development at HUSL performed favorably as compared with other echo-ranging systems.

A block diagram of the early AIDE DE CAMP system is shown in Figure 7.

### 1.6.5 Development of CR Scanning Sonar

*Sangamo Participation.* Following the demonstrations mentioned above, NDRC and HUSL discussed with the Sangamo Electric Company the possibilities of engineering and manufacturing several pilot models of an echo-ranging system which would combine both scanning and searchlight features. BuShips later designated this system *QH sonar*. Early in February 1944 a prime contract (OEMsr-1288) between OSRD and the Sangamo Electric Company under which the company would make three QH scanning sonar systems for OSRD was drawn up.

The Sangamo system provided the searchlight and

scanning features by utilizing two commutators—one, a high-speed motor-driven commutator for rapidly scanning the sound horizon for echo-producing or noisemaking targets, and the other a hand-trained listening commutator for receiving along any chosen line of bearing. This made an audio response similar to that of other conventional echo-ranging equipment available for identifying targets and noise. Bearing deviation indication was omitted, but the rotor of the listening commutator contained a double lag line connected to the transducer so that right and left channel outputs could be obtained if BDI application were desired later.

Although, under the original negotiations, Sangamo was to commence active engineering work on March 1, 1944, work on the transducer and the capacitive commutator was delayed. At that time magnetostriction transducer design utilized d-c polarization of the active elements, permanent magnet polarization being still in the experimental stage. In view of the extensive simplification possible with permanent-magnet polarization, the Sangamo Electric Company delayed design work on the transducer until its practicability was determined at HUSL in April 1944. Subsequently Sangamo incorporated this principle in its transducer design.

Early in 1944, HUSL engaged in study and experimentation on various commutator designs and plate materials. As a result, a cylindrical glass plate arrangement was adopted for future experimental commutators. Certain alignment problems in the design appeared difficult in production, however, and after consultation with the mechanical design staff of HUSL, the Sangamo Electric Company offered an alternative construction, making use of a flat commutator plate with the beam-forming lag line mounted within the rotor, which was approved. Details of this construction are presented in Chapter 6.

Consultation between the engineers of the Sangamo Company and the HUSL research group continued throughout 1944 on design problems connected with the various components of this system. Some solutions were obtained from experimental equipment installed during this period on the USS SARDONYX and the USS CYTHERA.

#### USS SARDONYX INSTALLATION, MODEL 1

A formal demonstration of the QH type of sonar was given before Navy officials in February 1944. Tests were conducted on Experimental Model No.

1, made by HUSL and installed on the USS SARDONYX. Although the chief components of this system are described in greater detail later in this report, the salient features are outlined here.

A 36-element magnetostriction transducer (Model HP-1) was mounted on a standard QC hoist-train column and fixed in bearing with respect to the ship. The 36 channels were brought up to a choke box which served to carry d-c polarizing current to the transducer elements. From the choke box the 36 channels were carried to both the hand-trained listening commutator and the motor-driven scanning commutator. Connection was also made to the 22-kc transmitter. Relays in the choke box disconnected the commutators and receiver channels from the transducer during the transmitting or pinging period, and disconnected the transmitter during the receiving period between pings.

The pinging rate was controlled from a sweep generator which performed several functions: (1) supplying the field of a 3-phase generator mounted on the scanning commutator with a sawtooth current, starting from zero after each ping and increasing uniformly until its sharp drop to zero at the end of the next ping; (2) feeding a blanking pulse to the PPI tube during the flyback; (3) initiating transmitter keying at the same time and maintaining it for the desired ping length of about 0.035 second. The output of this 3-phase generator was applied to a 3-phase deflection coil arrangement around the neck of the PPI scope, thus producing a spiral sweep of the electron beam. This spiral sweep started at the center of the screen immediately after each ping, and spiraled outward with a uniformly increasing radius at a rate depending on the range setting or frequency of the sweep generator.

In each of the two commutators the 36 incoming channels were applied through step-up transformers to the 36 stator plates. For the scanning commutator, the output of the beam-forming lag line was fed to a brightening receiver and thence to the control grid of the PPI scope, the bias of which was adjusted so that the screen spot during the spiral sweep was just below the threshold of visibility when no echo was present. Consequently, the presence of a reflecting target was indicated by the brightened spot on the screen which, by its spiral sweep, represented both the range and bearing of the target with respect to the ship. For the listening commutator, the output of the lag line was applied to a listening receiver. Thus by

rotation of the hand-trained commutator, reception sensitivity was trained in the direction of the target and the entire echo received and made audible by a loudspeaker. The position of the listening commutator was controlled through a servo system by a handwheel on the PPI console.

The transmitter was of the master-oscillator power-amplifier type, capable of supplying about 2.5 kw during the transmitting period while pinging at 5-second intervals, with an average drain on the a-c power line of only 500 watts. This desirable feature was achieved by utilizing large storage capacitors in the rectifier unit which supplied plate power to the final amplifier. It represented a radical change in driver design from previous models and allowed far greater acoustic power to be put into the water. A detailed description of this transmitter is presented in Chapter 5.

The commutators used in the SARDONYX installation were of the radial type (Model M1-B) and are described in Chapter 5. The beam-forming lag line was placed inside the rotor and had two output leads connected through slip rings and brushes to a pre-amplifier mounted on the commutator unit.

The PPI, a magnetic-deflection type cathode-ray tube with a 7-inch long-persistence screen, was mounted on the sloping panel of a console approximately 45 inches high. On the console panel were located the overall gain and listening gain controls, and an off-on and range selector switch which could be set for noise-listening or for various ranges during echo ranging.

#### USS CYTHERA INSTALLATION MODEL 1

After several weeks of trials, Model 1 was transferred to the USS CYTHERA for more extensive tests. Much data pertinent to the general operation of a QH system, and Model 1 in particular were obtained during the spring and summer of 1944. With the Model 1 system, reasonably consistent echoes were received from submarine targets at ranges up to approximately 2,000 yards. Tests seemed to indicate that bearings were accurate to within 2 degrees. The listening channel was found to serve the valuable purpose of identifying multiple targets on the PPI by means of the doppler associated with each target.

#### USS CYTHERA INSTALLATION MODEL 2

The second QH sonar system made by HUSL, and designated Model 2, Serial 1, was installed on the

USS CYTHERA early in September 1944. Originally, it was to embody the specifications given to the Sangamo Company for its XQHA system, then under design. The transducer was to be a 48-element 26-kc magnetostriction type (HP-3), utilizing permanent-magnet polarization. Cylindrical glass plate commutators with 48 elements, Model 5, were to be employed, but because of the difficulties in the design and construction, plans were altered to permit the installation of a 36-element 22-kc transducer (HP-2B), and the 36-element radial disk commutators of the Model 1 QH system. Later, when this system was transferred to the USS BABBITT, the listening commutator lag line design was changed to give 2-channel output so that the bearing deviation indicator could be used experimentally.

In principle, operation of the Model 2 system was the same as for Model 1 but improved console design, provision for *maintenance of true bearing* [MTB], unicontrol of frequency, range recorder operation, and hand keying gave greater flexibility and control.

The PPI, cursor, and bearing scales occupied the central position on the console panel. The controls consisted of (1) a master gain control; (2) an off-on range switch which allowed operation as either a noise listening system or on any one of several ranges during echo ranging; (3) a keying selector switch which permitted either a chemical range recorder or the sweep generator to govern the ping rate; (4) a training handwheel on the side of the console to control the bearing cursor and also to position the listening commutator so that the listening beam would be trained automatically on the indicated bearing.

Attached to the cursor was a bug riding between an outer fixed scale which gave relative bearing and an inner scale which, driven by the ship's gyrocompass, gave true bearing. The gyro drive fed into the cursor through a mechanical differential to maintain true bearing.

The transmitter used in Model 2 was capable of supplying somewhat greater power output than that of Model 1. The unicontrol of frequency was accomplished in the following manner: A 60-kc fixed-frequency oscillator was located in the transmitter unit and a master tunable oscillator in the duplex receiver chassis supplied 82 kc to the transmitter and to the mixer stages of the two receiver channels. Thus a fixed intermediate frequency of 60 kc was assured in the receiver. In the transmitter, the difference beat

frequency between 82 kc and the 60-kc local oscillator was fed to the power amplifier.

The keying rate, depending upon the position of the switch, corresponded to ranges of 7,500, 3,750, and 1,500 yards and was controlled by contacts on a timing switch driven by a synchronous motor. For recorder operation the controls of the PPI sweep were arranged so that when the flyback of the recorder was adjusted to a decreased range, the sweep rate remained normal. A detailed description of these circuits is given in Chapter 5.

In December 1944 the Model 2 system was transferred from the USS CYTHERA to the USS BABBITT and a depth-scanning sonar system installed on the CYTHERA. In the BABBITT installation, a 100-inch streamlined dome was placed around the transducer and the lag line design in the listening commutator changed to permit the incorporation of BDI. The BABBITT installation also included a deep monitor so that pattern studies of the transducer-in-dome arrangement could be made. Tests of operation at high ship speeds carried on during the spring of 1945 showed that water noise increased with speed, and that maximum detection range decreased accordingly.

#### INTEGRATED TYPE B SONAR SYSTEM

Early in 1944 the Bureau of Ships requested NDRC to develop a vertical scanning system which would operate in conjunction with the QH horizontal scanning equipment. This project was assigned to HUSL and the combination designated as the *integrated Type B sonar system*. Although the system, its development, and its operation are described in detail in Chapter 6 of this report, the principal features are discussed briefly here. Two projectors are mounted on a single training shaft and enclosed in a dome. One, a standard QH type, is for horizontal scanning; the other, a similar unit, is for vertical scanning and is mounted on its side beneath the first. They are excited separately but synchronously by pulses from two transmitters operating at 26 kc and 38 kc.

To obtain accurate data and to keep the display on the screen steady, particularly in the vertical scanning system, the roll and pitch of the ship must be neutralized. This is accomplished by means of a gyroscopic stable element and a trunnion-tilt corrector of the kind used in fire-control systems but with modifications for this application. Two-axis stabiliza-

tion is used in the Type B system. Bearing-angle corrections, necessitated by the ship's roll and pitch, are introduced mechanically in the training system, while corrections of depth-depression angle are introduced mechanically by rotation of the depth-listening commutators and electrically by phase shifting in the indicator deflection circuits.

The horizontal and vertical scanning systems can be operated either separately or together. Present plans are for the horizontal system to be used alone during the target-search phase of the ship's maneuvers. When a target is detected and the range sufficiently reduced, the vertical system is put into operation and the attack initiated. The horizontal or azimuth system continues to operate as a search device throughout the attack in order to detect other possible targets.

The display equipment is on two consoles. The azimuth console contains the PPI scope for the azimuth scanning system and the BDI scope. On the panel are the gain controls for the two scopes, a projector relative bearing dial, a true bearing dial, a range switch, and the training control handwheel. On the depth console are the *elevation position indicator* [EPI] scope, its gain control and a range switch. The BDI and the listening channel can be used with either the azimuth or the depth-scanning system to indicate horizontal deviation.

To permit use of the BDI with the azimuth-scanning system, a stationary double lag line is fed from the right and left sides of the azimuth transducer. The two channels are combined into sum-and-difference outputs from which a listening channel and a bearing deviation indication are obtained. The rotatable training shaft, which is necessary if the two transducers are to be fastened together, thus serves the same purpose as the listening commutator in the QH system. The high-speed azimuth-scanning commutator is fed from the azimuth transducer in parallel with the stationary lag line and provides, through its scanning receiver, the echo pulses for the horizontal PPI. In order to use the BDI in the horizontal plane, when listening on the depth-scanning system, the depth-scanning transducer is split perpendicularly to its axis into right and left halves to give right and left output channels. These are combined into sum-and-difference channels; the sum channels are fed into the scanning commutator and into one of the listening commutators, and the difference channels are fed into the second listening commutator.

The echo signal from the scanning commutator is fed to a brightening receiver and thence to the control grid of the EPI scope. The outputs of the listening commutators are fed to the BDI listening receiver. Other features of the Type B system, such as unicontrol of frequency, ODN, and mechanical recorder control of keying, are described in Chapter 6.

#### TRIAL DEPTH-SCANNING SYSTEM

Scanning in the vertical plane had not been tried prior to the time at which plans for the integrated Type B system were formulated. It was highly desirable, therefore, that the practicability of this scanning method be tested at the earliest possible date. Information was needed concerning operation of horizontal BDI with vertical scan, effect of bottom echoes, surface reverberation, stabilization, and effect of the dome on receiving patterns. Consequently, early in July 1944, plans were made for a trial depth-scanning system. Procedures using available components were adopted and the system, developed through the summer and fall of 1944, was installed on the USS CYTHERA in December. After preliminary tests at New London, the ship was sent to Fort Lauderdale, Florida, where extensive tests were carried on during the winter and spring of 1945.

To save construction time, transducer laminations already on hand were used by scaling up the design of the integrated Type B 38-kc depth-scanning transducer to give the same beam patterns at 26 kc. The rest of the system was then designed for this frequency and the resulting transducer, while comparatively large, could be mounted on the standard QC training shaft. However, a special dome for protection from water forces was required.

The 26-kc depth-scanning transducer had 48 staves spaced around 270 degrees of its periphery, each stave being divided into a right and left section. As the transducer was mounted with its axis in the horizontal plane, a means of securing horizontal BDI was thereby realized. The echo-signal outputs from the right and left sections were combined to give sum-and-difference outputs. One sum channel was fed through the high-speed scanning commutator to the brightening receiver and EPI. A second sum channel and the difference channel were fed through two separate listening commutators to the BDI listening receiver.

In order to maintain contact with a target, as well as to determine accurately the depth depression angle

and bearing, stabilization of the system against roll and pitch of the ship was provided by two-axis stabilization, as planned for the depth-scanning portion of the integrated Type B sonar system, a Westinghouse Mark VIII Model 2 stable element and a Ford trunnion-tilt corrector being employed.

The transducer was energized by a storage-type transmitter delivering power in 35-millisecond pulses at a rate dependent upon the setting of the keying interval selector. The transducer was trained in azimuth by means of a training wheel on the BDI cabinet, while true and relative projector bearings were given by a bearing repeater unit. The direction of the listening channel in the vertical plane was determined by a control wheel on the EPI unit. This also rotated a mechanical cursor over the scope face, which with an angular scale made it possible to obtain directly the target depression angle. A chemical range recorder connected to the listening channel gave the slant range. A detailed description of this system and its performance is given in Chapter 6; however, it may be said here that its operation was satisfactory, that the possibility of operating a depth-scanning sonar was demonstrated, and that this installation allowed investigation of various problems for establishing design features of the depth-scanning portion of the integrated Type B sonar system.

#### 1.6.6 Development of ER System

The *electronic rotation* [ER] system in use in July 1945 was proposed in July 1943.<sup>4</sup>

Preliminary tests showed the fundamental principles of the new system to be sound, and work was begun on the preparation of a test rotor for an evaluation of the method. It was completed by August 12, 1943, and at that time the electronically rotated beam of sensitivity was demonstrated. An artificial transducer based on HP-1 (22-kc, 15-inch diameter) was used as the signal source. In this system the scanning speed was 60 rps, 36 triodes were employed as switching elements, and a mechanically rotated 3-phase generator was used to operate the rotor. The rotor output was viewed on a linear CRO screen whose sweep rate was synchronized with the switching rate so that the output of the rotor (the directivity pattern) was fixed on the face of the CRO screen. The resulting pattern was a beam of sensitivity having a major lobe 25 degrees wide at -6 db and minor lobes at least 14 db below the peak of the major lobe.

Results of tests on the first breadboard rotor proved the method to be practical. Tests completed by the end of August 1943 showed what component values would give the most satisfactory operation of the electronic rotor. Following this, construction was begun on an ER system to be installed on the AIDE DE CAMP. This gear included, instead of the large test rotor chassis, two smaller electronic rotor chassis containing approximately the same equipment as that used in the original model. Also incorporated in the shipboard rotor was a self-contained preamplifier system which was used to amplify the output of the rotor before transmission to the receiver equipment.

The electronic rotor was installed as a substitute for the capacitive commutator in the sonar system aboard the AIDE DE CAMP. Circuit connections were so arranged that the capacitive commutator could be switched out of the system and the electronic rotor substituted within a few minutes, thereby allowing comparison of the two systems.

The early trials of the electronic rotor system were successful to the extent that echoes were received and the proper representation achieved on the PPI. The beam patterns in the electronic rotor system were 2 to 3 degrees wider in the major lobes than the corresponding patterns in the capacitive commutator; the minor lobes were an average of 15 db down from the tip of the major lobes. There was, however, considerable variation in pattern uniformity around the entire azimuth circle, and the electronic rotor produced considerable electrical noise, caused chiefly by the method of switching and the electronic layout used. Comparative tests between the ER and the CR systems at this time were carried on at New London, where both systems were demonstrated to officials of the Navy Department, NDRC, and members of the HUSL staff. The electronic rotation system seemed able to pick up echoes and discover targets from the same ranges as the CR systems, but the PPI indications were more obscured by system noise than they were when the capacitive commutator was employed. Motion of the AIDE DE CAMP through the water produced a large arc of brightening in the stern direction caused by wake and propeller noises. Fogging of the PPI screen caused by noise peaks showing up at random for all bearing angles was also present. The results<sup>5</sup> achieved, however, demonstrated that the electronic rotation system was sound in principle and warranted further development to

eliminate the troubles found in this shipboard installation.

After the New London trials, fundamental investigations were undertaken to determine the best possible design of the beam-forming transmission or lead line. Other studies to improve the switching arrangement and to discover and develop other forms of switching were started. Lead line investigation revealed that for a particular transducer design and number of elements there is an optimum phase advance or lead per section in the line which will produce the best and most consistent rotor output patterns. Details of this investigation are discussed in Chapter 7.

The switching voltage generator finally adopted was a uniform-velocity lag line, or low-pass network,<sup>6</sup> which made possible the design proposed in July 1943 for electronic rotation, with a transmission line as a timing source for the switching voltage generator.<sup>4</sup> Because of the physical dimensions and availability of components, it was found possible to construct a switching lag line having a comparatively high fundamental frequency. That is, switching lag lines could be constructed so that a rotation of the receiving beam of sensitivity could be accomplished more easily at 200 or 500 rps than at the initial rotation speed of 60 rps employed in the first electronic rotor. This discovery opened a new field of application for the electronic rotation system. When the scanning speed is increased to 200 rps, it becomes possible to use a transmitted pulse length of only 5 milliseconds. The reduction of reverberation in a short pulse system of this sort permits it to locate small objects, a fact that had been previously reported by the British and others working in the field. Also it was hoped that the short-pulse system would give greater security to the echo-ranging vessel.

Investigation of other forms of vacuum-tube electronic switching at this time, in an attempt to improve upon the operation of the original rotor which employed triodes as switching elements, resulted in the development of an electronic switch which, in its operation, was less sensitive to the magnitude of the switching signal. This form of electronic switch required no opposing d-c bias to render it inoperative during periods of nonconduction.<sup>7</sup> Variations by as much as 6 db in the magnitude of the switching signal were possible. The self-regulating electronic switch, discussed and developed in January 1944, was set aside at this time in order to build a new

triode electronic rotor making use of the principles just described involving transmission lines for switching at high rotation speeds.

A second electronic rotor involving 18 double triodes was constructed for installation on the AIDE DE CAMP. It had a scanning speed of 200 rps, was housed in an X-3 BDI cabinet, and included a 36-element tube and circuit-testing mechanism whereby some of the difficulties involved in testing the earlier electronic rotor were surmounted. For this installation a new electronic spiral sweep, discussed in Chapter 7, was developed, a special transmitter able to supply the transducer (HP-1) with 18-kw average power during the 5-msec transmitted pulse was built, and a special tuned signal-frequency receiver developed.

The new 200-rps rotation speed ER sonar equipment had many of the characteristics predicted on the basis of short-pulse studies both at HUSL and elsewhere and was capable of detecting 3-foot spheres at distances as great as 450 yards.<sup>8</sup> Certain rules concerning the maximum discovery ranges for 3-foot targets under various conditions of bottom depth and thermal gradients in the surrounding water were formulated from these studies.

Qualitatively, one of the outstanding features of the 200-rps rotation speed system was the great improvement in range resolution and target definition on the PPI scope. The immediate bottom was depicted more accurately than in the slower rotation systems and permitted repeated observation of small objects, such as rocks and buoys, not previously discoverable. Also, because of the 5-millisecond ping length, the intensity of reverberation was considerably reduced. Range resolution permitted a 500-yard scale, as contrasted with the smallest range scale of 1,000 yards in the low-speed rotation systems. This 200-rps system is described in detail in Chapter 7.

After successful installation of the 200-rps ER system on the AIDE DE CAMP, construction of a system which would scan at still higher speeds seemed advisable. At about this time a 36-element 53-kc Y-cut Rochelle salt transducer built by the Brush Company for Naval Ordnance Laboratory was sent on loan to HUSL for possible incorporation into a high-frequency, high rotation speed system to be constructed especially for use with it. A 500-rps rotation speed system with a signal frequency of 53 kc was constructed. A new electronic rotor similar in layout and design to the 200-rps unit was built. A new transmitter capable of providing 2 kw of average power



during a 2-millisecond pulse, a new receiver, spiral sweep chassis, and a CRO viewing screen were constructed. This 53-kc equipment was incorporated into two cabinets housing all the electronic gear associated with the system. The 36-element transducer supplied the receiving signal to the electronic rotor, and a separate magnetostriction ring stack was used as the transmitting projector.

The operating characteristics of the system were as follows: The transducer pattern produced by the rotor was 38 degrees wide, 6 db down, with minor lobes averaging 15 db below the tip of the major lobe. The acoustic power radiated by the 53-kc transmitting ring stack was 175 watts as measured in the Charles River Basin when the system was installed for test aboard the HUSL calibration barge, *TIPPECANOE*. The receiving system had a sensitivity about 15 db lower than the 200-rotation speed system of the *AIDE DE CAMP*. Unfortunately, the combination of lower radiated power, poor receiving sensitivity, and poor beam formation of the rotor, made the 53-kc system comparatively inferior. In the Charles River Basin, however, a 3-foot test sphere, when towed by a rowboat, produced consistent echoes to ranges of 300 yards in water approximately 20 feet deep.

As a result of these comparatively successful tests, the equipment was shipped for analysis to the CUDWR-USRL testing station at Mountain Lakes, New Jersey, where its performance was not so satisfactory as in the Charles River. A possible reason for these poor results was the shallow water averaging 8 feet in depth, which greatly increased the reverberation level. After the tests at Mountain Lakes,<sup>9</sup> the equipment was dismantled and reinstalled aboard the *AIDE DE CAMP* at New London for sea tests.<sup>10</sup>

In summation, it can be said that the 53-kc system was incapable of detecting normal targets at ranges possible for other scanning systems. Because of the broad beam pattern, the detail of target presentation was poor, and the system seemed more susceptible to electric noise than any of the other scanning systems tried aboard the *AIDE DE CAMP*. Upon the return of the *AIDE DE CAMP* to the Boston area from New London, the 53-kc system was removed and has not been operated since then. The 200-rps outfit, originally installed aboard the *AIDE DE CAMP* was placed in operation again, and a series of tests was begun for detection of small objects.

Because of the successful operation of the 22-kc 200-rps ER system, the immediate construction of a

submarine system was proposed and new research directed toward replacing the triodes in the *AIDE DE CAMP* system with some other form of switch.

At about this time the use of copper oxide varistors, or rectifiers, as variable gain or loss elements in the signal frequency circuits was investigated.<sup>11</sup> It was soon discovered that the backward-to-forward impedance ratio for varistors, as measured under d-c conditions, could not be attained under ordinary circumstances with signal frequency conditions. This was caused by their comparatively high internal capacitance. Accordingly, a simple scheme to neutralize the capacitance of the electronic switch was devised and this resulted in much greater dynamic range between minimum and maximum loss. The insertion of a large capacitor in series with each varistor and charged by the varistor when it conducted on the peak of each switching cycle made it possible to cut off the electronic switch or varistor during most of the cycle as far as signal frequency was concerned. The varistor then behaved like a triode electronic switch and required little adjustment for switching purposes. At this time the building of transmission lines for switching purposes having characteristic impedances as low as 40 ohms and retaining the uniform characteristics of distortionless lines<sup>6</sup> was found possible.

An experimental varistor rotor, incorporating the above circuit modifications, gave a beam of sensitivity with the same characteristics as those produced by vacuum-tube electronic rotors. Its major lobe was 25 degrees wide 6 db down, while the minor lobes were 15 db to 16 db below the tip of the major lobe.

*ER Submarine System.* When the tests were substantially completed, HUSL was authorized to develop an ER sonar for submarines. As designed and built, the system incorporated two 48-element transducers, one mounted on the forward deck and the other beneath the hull. In the topside transducer, each element was tilted by an angle of 6 degrees with the vertical to overcome the unfavorable characteristics of negative thermal gradients frequently encountered in the sea. The system was designed to operate at a signal frequency of either 26 kc or 31 kc, and with a 330-rps scanning speed so that a 3-msec transmitted pulse could be used.

Factors peculiar to submarine installation made it necessary to locate the ER rotor inside the transducer so as to reduce the size of the cable brought through the pressure hull. Both crystal and magnetostriction

transducers, each type designed to accommodate an ER rotor, were built for experimental work. The rotor was a circular unit that could be quickly inserted or removed without disturbing the transducer elements or their connections. It contained 48 mutually interchangeable switching sections. Each section contained a varistor, a neutralizing capacitor, and a portion of the switching lag line.

The transmitter, sweep-range marking circuits, and receiver were built into three separate boxes and consolidated into one stack. A fourth box, containing the PPI, was a separate unit located at a convenient place in the submarine. A complete description and photographs of this system are presented in Chapter 7 of this volume.

The completed submarine sonar was tested at the HUSL Spy Pond Calibration Station during January 1945, and the receiving beam pattern produced by the rotor and transducer was satisfactory. The sensitivity was about 30 db above the reference level of thermal noise in 100 ohms. The system was capable of detecting echoes from 8-inch and 12-inch triplanes representing 3-foot and 5-foot diameter spheres respectively. The transmitter provided 3 kw of average power to the transducer during the 3-millisecond pulse interval.

The serious difficulty which evolved in operation of the submarine system was the inability of the varistors to withstand transmitting voltages. In transmission a certain amount of transmitter voltage leaked over into the varistor switch circuit by various paths and, as a result, individual varistors burned out after a short period of operation. A ring stack was then used as a separate transmitting projector so that no transmitter energy was fed to the transducer or the varistor rotor. The system with this modification was tested again at Spy Pond in February 1945 and was found to be satisfactory. The outfit was capable of picking up echoes from the 8-inch and 12-inch triplanes and delineated the character of the bottom at Spy Pond with comparative accuracy. Later, it was installed aboard a submarine.<sup>12</sup>

During the development of the submarine varistor electronic rotor, further investigation of the general properties of varistor electronic rotors seemed advisable. Consequently, a test setup was constructed and installed aboard the *TIPPECANOE*. A Brush crystal transducer, AX-89 No. 2, and a 36-element varistor rotor, with a variable-amplitude switching signal input to the lag line and the amplifier, to operate

with the rotor were used.<sup>13</sup> Results of this test indicated that the characteristics of the beam-forming lead line must be carefully adjusted to suit the transducer. During this experimental work a theoretical study on beam and pattern formation in electronic rotation was undertaken.<sup>14</sup> Many predictions were borne out in the fundamental tests conducted with AX-89 No. 2 and its rotor.<sup>15</sup> Experiments involving new forms of electronic switching to overcome the difficulties inherent in the use of varistors were performed. Varistors, although making satisfactory switches, are not uniform in their characteristics. Since the gain of each switch has a marked effect upon pattern shape and uniformity, it was found advisable to replace varistor rotors in the ER submarine sonar by rotors employing vacuum tubes. This change was effected just prior to the transfer of the scanning sonar research program from HUSL to the USNUSL at New London.

*Application of ER Scanning System.* The ER system was developed chiefly for use in submarines. Its short transmitted pulse provides greater security against detection, besides making the discovery of small objects possible. It is believed that, with the use of an ER system, a submarine should be able to detect mines and navigate mine fields. It is expected that the shorter transmission period possible with the ER system will increase the security of a submarine from detection by attacking enemy craft.

The ER system has no moving mechanical parts, so that its maintenance requires only normal radio-repair operations. Since the circuits are relatively complex, containing large numbers of component parts that have very close tolerances, maintenance techniques must be carefully worked out.

The short pulse gives the ER system a higher ratio of signal-to-reverberation noise than is possible in the CR system, and forms the basis of its superior ability to detect small objects. Design considerations are discussed in detail in Chapter 3.

The ER system gives better range resolution than the CR system because of its higher rotating speed. Bearing resolution is poorer, however, because of its inferior beam pattern, and this should be a subject for future development.

The high rotation speed of the ER system provides the possible advantage of creating a rotation doppler. That is, the rotor output signal, caused by a single frequency source in the water, acts approximately as if the transducer were physically rotated at the elec-

tronic rotation speed. Doppler components of the order of 10 kc are added to the signal frequency at certain bearings, and it may be possible to make use of this property to improve the system characteristics, as explained in Chapter 7.

The high rotation speed also has some inherently undesirable properties. Greater band widths in the receiving system are necessary to pass the shorter pulse generated by the rotor, and this tends to give poorer signal-to-noise ratios than are found in the slower systems. However, the most recent (April 1945) ER system has detected signals, under quiet conditions, as small in magnitude as those detected by any CR outfit.

### 1.7 PLANS FOR FUTURE WORK

Only the preliminary investigation of possibilities of scanning sonar had been completed when this was written (May 1945), and much work is incomplete. The construction of suitable transducers is both difficult and expensive, and it is suggested that some future work be directed toward simplifying manufacture. Obtaining sharper beams with smaller minor lobes is important because such an improvement would increase bearing accuracy, resolving power, and signal-to-noise and signal-to-reverberation ratios. Putting more acoustic power into the water for satisfactory echo ranging from high-speed ships and on noisy targets than is now used will be necessary. Also, permanent-magnet-polarized magnetostriction transducers or piezoelectric crystal transducers should be used to eliminate the necessity for polarizing current.

The beam-forming networks should be investi-

gated to increase ease of manufacture as well as to obtain sharper and cleaner beams. This is especially true in the case of ER systems where the beams are neither so sharp nor clean as theoretically they could be. Performing of beams and storage methods also merit attention. A listening channel should be developed for the ER system. The CR commutator can probably be reduced in size and rotated at higher speeds to permit shorter pulses and better range resolution. In any case, its design, both electrical and mechanical, should be refined.

Future work on the electronic components will undoubtedly be directed toward greater simplicity of circuits and ease of maintenance and operation. Items that should be investigated include receiver gain control, range-measuring circuits, underwater communication, test arrangements, a true sector-scanning system, expanded range sweep, reduction of interference from other pinging, doppler sensitization, own-doppler nullification, and storage line transmitters.

Any future overall design work on scanning or other sonars should start from the operator's point of view, the kind of information to be presented to the operator and what he must do with this information being considered first. The equipment should then be designed to obtain and present this data in the best and most convenient form.

As gunnery fire-control techniques are adopted to control attack, the operating function of sonar becomes that of fire-control director. It is therefore important to design the sonar as an integral portion of the complete attack system rather than as a separate unit, so that maximum efficiency of the entire system will be attained.

## Chapter 2

# GENERAL CONSIDERATIONS IN SCANNING SONAR DESIGN

### 2.1 BASIC DESIGN PARAMETERS— INTERRELATION

THE MAJOR DESIGN PARAMETERS of a scanning sonar system are determined primarily by the specific operational properties desired for the system. Normally, the specifications would state, among other things, the desired assured range for a given target under good water conditions; the range resolution, or minimum range difference between two targets on the same bearing which can just be distinguished; and the bearing resolution. A further specification would require that presentation of the echo position be easily interpreted and that the mode of indication should not tire the operator excessively. When used on submarines, there would be the additional requirement that the transmitted pulse of the scanning system should not be detectable by a surface ship.

These operational specifications place definite limitations upon the basic physical design parameters of the system. A quantitative study of the relations between the operational specifications and the design parameters is given in Chapter 3. Present discussion, however, is limited to an examination of the interrelationships of the various quantities.

The scanning sonar indicator is called a *plan position indicator* [PPI], and is usually augmented by a listening channel. On the PPI a unit radial distance on the oscilloscope face corresponds to a large distance in the water measured radially from the echo-ranging ship. Consequently, when the PPI range resolution is specified, the number of yards in the water which corresponds to a given distance on the PPI must be such that two spots, representing targets at the limit of resolution, can be distinguished on the oscilloscope face without causing the operator undue visual strain. On the other hand, ease of operation and interpretation demands that the outside rim of the oscilloscope face correspond to a range large enough so that an appreciable region around the ship is pictured and the range selector switch need not be changed too often during an attack. The scanning frequency must be chosen so that the time difference

required for echoes to reach the receiving hydrophone from two targets at the limit of range resolution cannot be less than the time required for one revolution of the spiral sweep. This determines a lower limit of the spiral sweep frequency. Moreover, the duration of the echo must be as great as the time required for one revolution of the spiral sweep. This condition is necessary in order to insure that the beam is pointed at the target within that interval in which the echo is passing the receiving hydrophone. Thus the lower limit of the scanning frequency also determines a lower limit of the pulse length. However, the pulse length must be made so short that echoes are not received from the same target on two successive turns of the spiral sweep, unless the target has such an extent in range. It is an experimental fact<sup>1</sup> that at normal echo-ranging frequencies the ratio of signal-to-reverberation level increases with decreasing pulse length. Since the range resolution essentially states the accuracy with which a target position can be determined, it is also a direct measure of range accuracy.

The pulse repetition rate is fixed by the maximum range, corresponding to the outside rim of the PPI oscilloscope face, since time must be allowed after a ping for the echo to go to and return from the greatest recordable range before another ping is initiated.

The maximum desired range fixes the upper limit for the echo-ranging frequency, since the attenuation of sound in the sea increases rapidly with frequency. For ideal sea conditions the optimum echo-ranging frequency is around 20 kc; however, under conditions of rough sea and strong temperature gradients the optimum frequency may be as high as 40 kc. For small object detection, long ranges are not required and high frequencies may be employed to reduce the transducer dimensions.

The specifications on the bearing resolution fix the sharpness of the major lobe of the receiving sensitivity pattern. If objects close together are to be shown, an extremely directional (narrow) beam is required. The beam width and the echo-ranging frequency determine the receiving hydrophone diameter. If the

rotating beam of receiving sensitivity is obtained from a stationary transducer by present methods,<sup>a</sup> certain conditions for smooth rotatability must be fulfilled (see Section 2.7 on transducers). The dimensions of the transducer, apart from conditions imposed by considerations of ship design, which are frequently the controlling factors in the specification of size, are fixed by the echo-ranging frequency. The specifications on bearing resolution may also put restrictions on the pulse shape of the transmitted ping, since modulation in the echo pulse may cause a substantial bearing error (see Figure 1). Unfortunately, the transmission of the echo through the water may also cause considerable modulation of the echo.

In the scanning system the transmitted ping is sent out in all directions simultaneously, while in a searchlight system the energy is concentrated in a narrow beam. For this reason the acoustic power which is emitted from the projector must be considerably higher for the scanning system if the same echo strength is desired from a given range. Moreover, it is found that in either system the power must be increased many times in order to increase the maximum obtainable range by a small fraction.

In normal long-ping echo ranging the advantages to be obtained with an aural indicator point to the desirability of retaining the listening channel in addition to the PPI. This rests upon the fact that the ear is a more sensitive echo detector than the PPI, especially when the echo has a doppler component due to target motion. The value of the listening channel decreases markedly, however, with decreasing pulse length, while the value of the PPI increases as the range is shortened. This is true because the aural quality of the echo is lost with the short pulse, while the screen persistence of the PPI reduces the fractional number of recordable echoes required to keep the picture of the target on the oscilloscope face as the pulse repetition rate increases. In long-pulse systems employing a listening channel, the band width of the receiver must remain broad enough to preserve the tonal quality of the echo and of the background noise. The band width must also be broad enough so that the doppler in the echo frequency does not shift the echo beyond the receiving band. In scanning systems there is a further shift in the echo frequency

<sup>a</sup> A cylindrical transducer which, considered by itself, is omnidirectional in the horizontal plane, with the cylinder broken up into staves so that shading and phasing circuits may be added.

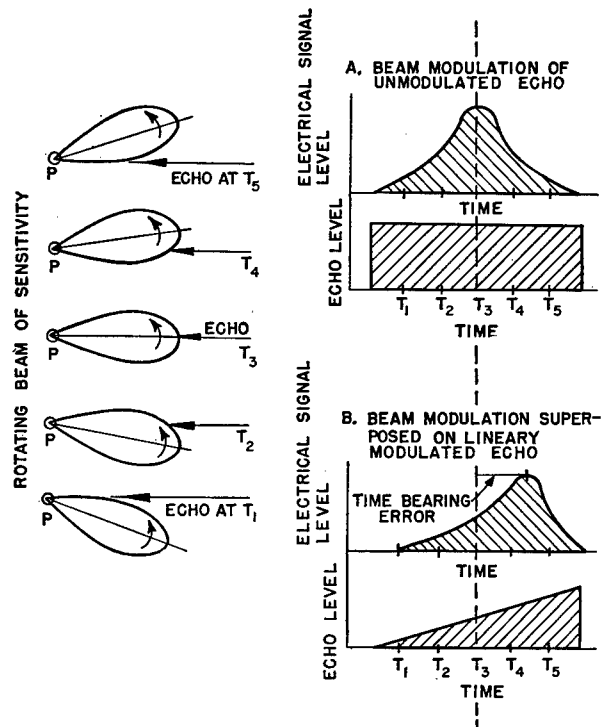


FIGURE 1. Diagram showing effect of echo modulation on bearing accuracy.

which is caused by the rotating beam of receiving sensitivity. This arises from the fact that there is associated with the rotating amplitude pattern a rotating phase pattern which causes a phase modulation of the echo just as the amplitude pattern causes an amplitude modulation. The phase modulation can in turn be thought of as a frequency modulation. Consequently, if it is decided that all echo levels less than, for example, 10 db down on the amplitude pattern must be passed through the receiver, the band width must be broad enough to pass the frequency after it has been shifted by own doppler, target doppler, and rotation doppler. The rotation doppler increases with scanning speed, resulting in an increase in band width and a corresponding decrease in the ratio of signal-to-noise level. This effectively sets an upper limit on the scanning speed and consequently a lower limit on the pulse length.

Scanning systems for submarines are further restricted by security considerations. It is at times desirable for the submarine to send out a single ping for a target range determination without risking detection by a surface vessel. Here the omnidirectionality of the transmitted pulse becomes a disadvantage, since all surface ships have an equal opportu-

nity to detect the submarine. In a searchlight system, only the ship ranged upon has a good opportunity. However, the total information obtained is correspondingly greater with the scanning system. With any system, security can be improved by echo ranging at an uncommon frequency, with a short pulse, and at the lowest power possible.

## 2.2 INDICATORS AND CONTROLS

The sources of information for a scanning sonar system are:

1. Noise—such as that coming from propellers of ships or submarines.
2. Signals—acoustical transmission.
3. Echoes—acoustical reflections.

Interference with the recognition and assimilation of this information is caused by:

1. Water noise.
2. Electrical noise.
3. Reverberation.

The primary information obtained includes one or more of the following factors for one or more sources such as targets, wakes, or bottom:

1. Slant range.
2. Azimuthal bearing (true or relative).
3. Depth angle.
4. Doppler.
5. Propeller or auxiliary noise—thus identifying target.
6. Target aspect (resolution permitting).
7. Signals (communication).
8. Miscellaneous information—covering less tangible factors, such as the difference in echoes from submarines and wakes as determined aurally.

By suitable operations the following additional information can be derived:

1. Horizontal range.
2. Depth.
3. Range rate.
4. Bearing rate.
5. Target speed, course, depth, and predicted future locations.
6. Condition of operation of the equipment.

In general this information is used in:

1. Search.
2. Attack.
3. Navigation.
4. Communication.
5. Testing and maintenance.

While the trend in scanning sonar design is to feed information obtained from the sonar equipment directly to attack directors and fire-control equipment and thus to make the operation of the system semi-automatic, the progress of sonar development has not yet reached beyond the necessity for consideration of the human element. The judgment of operator, conning officer, and other personnel must, therefore, be taken into account in designing for the sonar gear suitable indicators to present the information in the form which is most easily recognized, assimilated, and put to use.

Indicators may be classified in a general way by the method of their interpretation, such as hearing, sight, or touch. Any combination of these methods to indicate a single factor is an important consideration; for example, listening to an echo and seeing it on a screen at the same time may convey more information to an operator than the use of either sense alone.

Types of indicators that have been proposed or used are:

1. Cathode-ray tubes.
2. Mechanical devices such as rotating dials, drums, pointers, scales, cursors, bugs, etc.
3. Meters.
4. Recorders—chemical, spark, or direct inking.
5. Loudspeakers, headphones.

In designing the indicators for a system of scanning sonar, the following factors are important:

1. The number and location of persons needing the particular information, and the relative importance and accuracy of the information that each must have.
2. The degree of memory required.
3. The assignment of certain persons to specific functions, and the relative importance and frequency of use of the controls.
4. The background conditions such as noise level or lighting.
5. The possibility of using indicators jointly with other systems—such as radar.

Associated with each indicator may be one or more controls and miscellaneous electronic equipment, such as power supplies, the design of which is logically a part of the general indicator design problem. The designer must consider all pertinent Navy specifications to insure that the indicators are capable of satisfactory operation under the severe conditions encountered by naval sound gear, and that maintenance requires a minimum of effort and material. He must also consider the problem of training personnel to use the indicators.

### 2.2.1 PPI Scanning Display

With scanning sonar the most useful indicator for the operator in search and attack has been the PPI display, and for this purpose the persistent-screen cathode-ray tube is the most satisfactory indicator. The PPI display is a two-dimensional polar plot of the slant range and azimuthal bearing of all echo-producing objects within a given radius, usually up to about 4,000 yards. Noise sources are also shown, although with no indication of range.

This information may be displayed<sup>2,3</sup> as a ship-centered plot, geographic plot, mooring-board (target-centered) plot, or explosion-point-centered plot. The ship-centered plot seems most useful to the operator, the geographic plot to the plotter, and target and explosion-point-centered plots to sonar officers or conning officers.

*Maintenance of true bearing* [MTB] is generally applied to all but the ship-centered plot, in which case MTB is usually applied to the bearing cursor only, while the plot itself is in relative bearing.

#### SHIP-CENTERED PPI DISPLAY

The ship-centered PPI display has been considered most useful as an indicator for the operator in search and attack. Since the depth angle, except at close ranges, is small, such a plot represents a picture of a plane roughly parallel to the surface of the ocean. While the plot is usually portrayed in relative bearing with 000° relative up and away from the viewer, it is possible to apply MTB and have 000° true (north) always up and away from the operator. Since some sort of cursor or bearing line is customarily used, it is generally found more desirable for quick evaluation of the display to apply the MTB to the cursor and to keep the plot relative.

Scanning indication on the ship-centered PPI is ac-

complished by a spiral sweep whose angular position is synchronized with that of the scanning beam of sensitivity and whose radial velocity is constant, determined by the usable radius of the indicator and the time interval of the echo-ranging cycle. The maximum range is determined by the ability of the system to detect weak echoes. This is a function of frequency, sensitivity, power output, water noise, and the thermal gradients in the water. Echoes are indicated by brightening of the screen at a radius determined by the range of the reflecting object, while brightening occurs along whole "noise radials" in the case of noise sources.

#### GEOGRAPHIC PLOT PPI

This type of display is similar to that used in the *antisubmarine attack plotter* [ASAP]. Here the positions of both ship and target move; that is, the plot is stationary with respect to the surface of the ocean. While this type of display is more complicated and does not materially assist the operator, it does offer advantages in the plotting procedure, and possibly to the sonar officer and conning officer. For example, with the addition of scanning, the plotter is able to obtain information more rapidly, and in addition to plotting own-ship's movement and the motion of the primary target, he may plot additional targets or the positions and motions of friendly ships. Since precision of spot position is required, considerable attention should be given to the design so that the position is independent of such things as line voltage variation, humidity, temperature, or tube change. Early in 1945 an ASAP unit was modified<sup>4</sup> and adapted for a 30-rps PPI scanning and tested at HUSL with moderately satisfactory results.

#### BEARING INFORMATION FROM PPI

Bearing information may be obtained from a PPI screen by:

1. Estimation, where precision is not required.
2. Cursors, either mechanical or electronic.

If the gyro synchro order is available, MTB may be applied. This is of considerable assistance to the operator during change of ship's course and facilitates the reporting of true as well as relative bearing. The work of the plotter, sonar officer, and conning officer, both in attack and in search, is made easier when true-bearing information is available.

Both mechanical and electronic cursors have been

designed and tested. They may be compared on the basis of the following factors:

1. Screen visibility.
2. Cursor visibility.
3. Parallax.
4. Alignment of cursor to plot.
5. Accuracy.
6. Driving requirements.
7. Ease of setting.

Bearing cursors that have been tried are fundamentally either a radial line to center on echo spot, two radial lines at a fixed small angle to subtend the arc of the echo spot, or a combination of the two.<sup>5,6</sup> (The design considerations for various types of cursors are taken up in the section on range determination.)

It may be desirable in a system to repeat bearings at several locations and to use a bearing recorder. This consideration may affect the choice of cursor used. Where the cursor is coupled to a training system which requires appreciable time to change bearing, it may be made to move at greater speed than the training speed and thus show the intended order or eventual position of training before the actual training is accomplished, or it may be made to repeat the actual training accomplished.

When the PPI screen portrays a relative plot, MTB may be applied to the cursor by adding the training order to the gyro order and applying the result to the cursor drive system. This additional feature may be accomplished electrically with a DG synchro, or mechanically with differential gearing.

#### RANGE INFORMATION FROM PPI

Range information may be obtained from the PPI screen by:

1. Estimation.
2. Engraved scales.
  - a. Concentric rings.
  - b. Arcs on cursor.
3. Electronic schemes.
  - a. Range circles—fixed.
  - b. Adjustable length electronic cursor.
  - c. Adjustable range circle or caliper.

Estimation can be used satisfactorily when precision is not required. If this method is used, it is helpful to choose range sweep rates that produce swept ranges expressed in round numbers, with simple

multiplying factors as the range sweep rates are changed. Some systems key from a range recorder which produces swept ranges that may be odd figures, such as 3,750 yards. If, in this case, the sonar operator must estimate range also, it may be desirable to use a range sweep rate corresponding to 4,000 yards in order to make estimation easier, even though there is a slight loss of usable screen area.

Scales may be engraved as concentric circles on a transparent disk over the scope face. Where a mechanical cursor is used, arcs may be engraved on the cursor plate to produce a range scale. Engraved scales usually require illumination, such as edge lighting, to make them visible without affecting screen visibility.

In place of engraved scales for range, electronically brightened rings<sup>7</sup> may be introduced on the scope at intervals corresponding to those of the engraved range scales. These may appear continuously on the screen during echo ranging or may be made to appear when required by push button or switch control. The intensity of these marks should be adjustable.

An alternate scheme is to use an electronic bearing cursor<sup>5,6</sup> of adjustable length with the length control calibrated in range. The calibration could be a voltmeter scale which would lend itself readily to remote indication.

Another electronic range-measuring scheme is to use one brightened circle of adjustable radius, with the adjustment control calibrated in range.<sup>8</sup> To prevent interference with the echo, a nonbrightened arc or portion of the range circle may be included, the blank arc being made to center on the bearing cursor, thus, in effect, setting a caliper on the echo.

Whenever it is desired to read range accurately from the PPI screen with reference to mechanical markers, considerable care must be taken in design to make the indicator linear, stable (independent of slow or rapid line voltage changes), and free from parallax.

#### OTHER RANGE- AND BEARING-DETERMINING DEVICES

For purposes of remote repeating, plotting, or feeding attack directors, it may be desirable to have the sonar operator follow the target with a suitable pointer, and either mechanically or electrically feed information from the position and movement of this pointer, or spot, to the repeater, plotter, or attack director. In this case the operator may or may not have to determine range and/or bearing for himself. To prevent covering up parts of the screen it may be



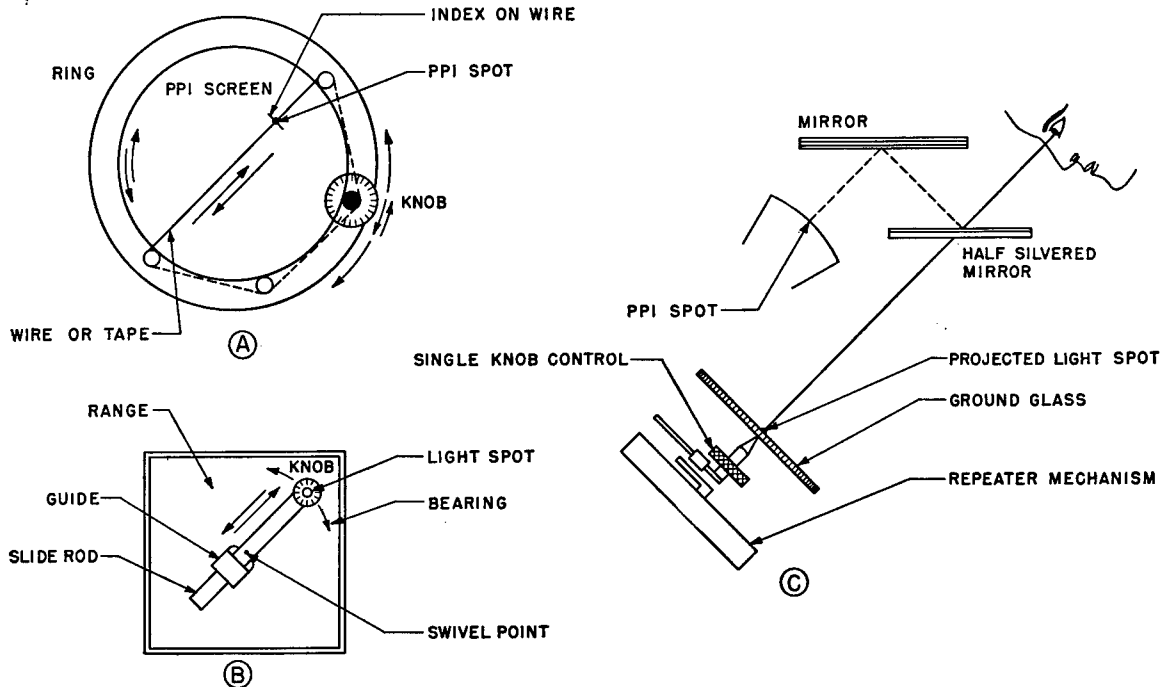


FIGURE 2. Proposed designs for range and bearing followers.

desirable to superimpose the follower spot on the screen by optical means.<sup>9</sup> (For example, see Figure 2.)

#### TUBE SIZE

The choice of the size of the cathode-ray tube is dictated by one or more of the following factors:

1. Number of persons having to view screen.
2. Centering of attention of chief operator; eye fatigue and accommodation.
3. Persistence, color, intensity.
4. Mechanical size, screen size, face curvature, edge wastage.
5. Type of deflection and neck size and shape.
6. Procurement problems and standardization, reliability, uniformity.
7. Power supply requirements.

The relative importance of the foregoing factors varies with the system, but the 5FP7 and the 7BP7 tubes are most useful.

Consideration must be given to magnetic shielding and the proper placement of any electromagnetic components whose fields may disturb the PPI indication. Amber and red filters have been commonly used to reduce eye fatigue from the initial flash of blue light while passing the yellow-green persistent after-

glow, and to reduce fogging of the screen by outside light.

#### 2.2.2

### Depth-Scanning Display

The depth-scanning display (see Chapter 6) differs from the azimuth-scanning or PPI display in two major respects:

1. Scanning does not take place through 360 degrees.
2. The area over which it is desired to scan is approximately a rectangle whose length is 1,500 yards or less and whose width (depth) is up to 400 yards.

Since depth scanning is to be used in conjunction with azimuth scanning, and because it seemed desirable to keep the types of components of both systems to a minimum and interchangeable, spiral-sweep scanning with beams of sensitivity rotating at constant angular speed have been used. An indicator adapted to this type of scanning, which shows target position in a vertical plane, has been designated *elevation position indicator* [EPI]. Its operation is similar to that of the PPI used for azimuth scanning, with own ship as the reference point for the plot.

The fundamental design problems peculiar to the

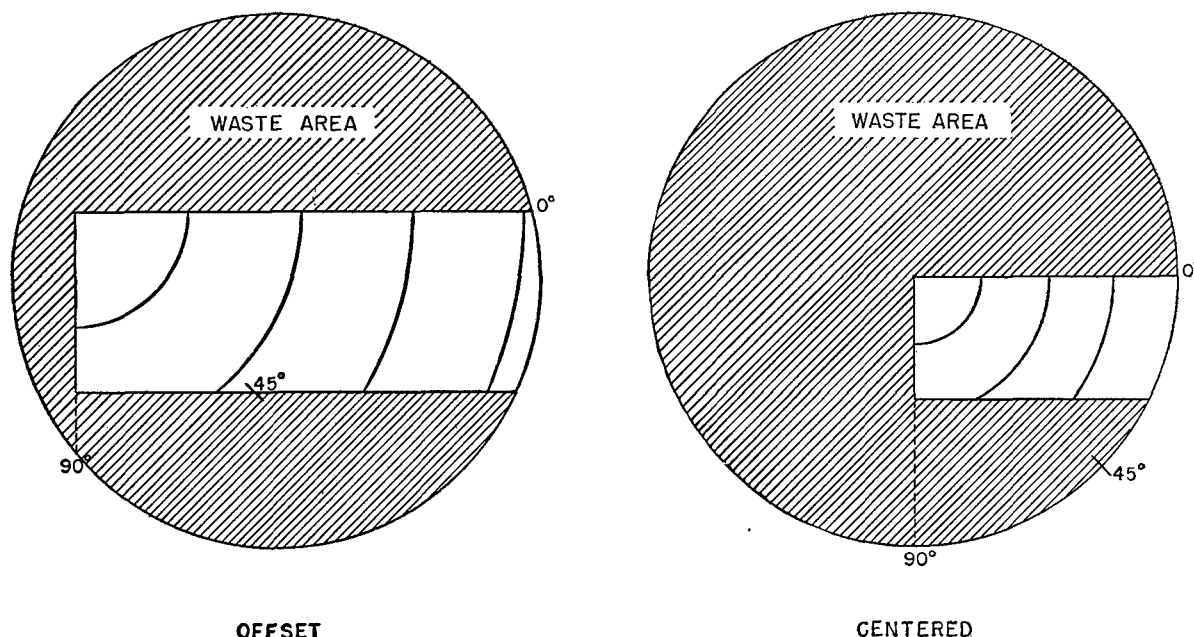


FIGURE 3. Depth-scanning indicator screen.

depth-scanning display are to reduce screen wastage, and to avoid depth angle distortion. A common problem is the provision of satisfactory cursor arrangements.<sup>10</sup> A fundamental cause of wastage of screen area when making use of circular sweeps is that the maximum vertical dimension at which submarine echoes would be expected is much smaller, perhaps 400 yards, than the horizontal range that may be obtained up to perhaps 1,500 yards. One way to reduce screen wastage is to offset the sweep center along a radius in a direction opposite to the center of the angle of desirable area of scan (see Figure 3). Details for accomplishing this offset, and difficulties existing because of efforts to combine a 64-element transducer and a 48-element commutator with this display are discussed in Chapter 6. Stabilization corrections of the scanning display are made by means of the mechanical rotation of the transducers as previously described, and correction in depth angle is made by means of a variable phase-shifting transformer inserted between the sweep generator and the deflection coils on the cathode-ray tube.

#### CURSORS FOR DEPTH-SCANNING DISPLAY

The information to be obtained from the *depth scanning sonar* [DSS] display is depth angle or depth, and horizontal or slant range. This information may be obtained by estimation, where accuracy is not re-

quired, or by using suitable scales, cursors, or spot followers.

Since, in the present DSS design, range is obtained from the listening channel, the depth-scanning display is required to furnish only depth (depression) angle. If there is no angular distortion, a simple cursor, geared 1:1 with a synchro order, may deliver the depth angle from the screen to remote points.

#### 2.2.3

#### Other Scanning Displays

While the PPI (ship-centered and geographic) displays and the ship-centered depth-scanning display have been used almost exclusively in scanning sonar work, there are other types of display, such as those used in radar work, which might merit the attention of designers of scanning sonar.

#### SCOPE DISPLAY

1. *A-scope display*. This is a plot of echo intensity versus range. It is particularly valuable in the accurate determination of range. The range interval shown may be restricted to a portion of the total range and this portion expanded to increase resolution and accuracy. Such a display would presumably be used in conjunction with a gating device on the scanning channel or as an alternative for the chemical range recorder on the listening channel.

2. *B-scope display*. This is a rectangular plot of range versus bearing, in which the echo intensity brightens the screen to form a spot. It is particularly valuable in determining bearings accurately at close ranges while retaining alertness at longer ranges. The locus of echoes from a straight-line target appears as a curved line. The bearings may be restricted and expanded when there is small angle of vision in the system, thus reducing scope area wastage and increasing resolution. Such an arrangement is used in the *NRL sector scan indicator* [SSI].<sup>11</sup>

3. *Elevation indicator* [EI]. Elevation angle versus range. This is like a B-scope on its side and may be used in depth scanning. It shows depression angle versus range. With amplification of a small range or depth angle it is called an *expanded elevation indicator* [E<sup>2</sup>I].

4. *Modified plan position indicator* [P<sup>2</sup>I]. The standard ship-centered PPI may be made open-centered by starting the sweep at a small definite radius. This improves bearing accuracy at close ranges. Angles are preserved but range distorted, so that a straight-line target is shown as a curved line.

5. *Precision plan position indicator* [P<sup>3</sup>I]. A gated portion of the PPI is greatly enlarged on a separate scope.

#### MECHANICAL DEVICES

Mechanical oscilloscopes and recorders for scanning purposes have been proposed. They offer the following advantages:

1. The screen may be made sufficiently large for plotting purposes.
2. It is possible to produce a permanent record.
3. They may be made visible in full daylight.

The systems that have been proposed<sup>12</sup> have a light source whose intensity is controlled by the echo or by other signal amplitude. This source may be made to move mechanically, or it may be stationary with the light beam moved by one or more mirrors or shutters; a combination of both may be used, thereby producing a spiraling spot of variable intensity.

#### 2.2.4 Listening Channel (Directed Beam)

A continuously rotating scanning system and its display fails to indicate three items of primary importance; namely, doppler, communication signals, and miscellaneous audible information. Further-

more, the bearing accuracy obtainable with a PPI display is apparently slightly inferior to that attainable with a *bearing deviation indicator* [BDI].<sup>13, 14</sup> It is, therefore, desirable to add a separately directed listening channel whose beam of sensitivity may be hand-trained at slow speed. Such a listening channel with its associated range recorder and BDI provides all the supplementary information needed.

#### AUDIO OUTPUT

Audio output is indicated by loudspeakers and headphones. The use of loudspeakers is preferable where background noise level permits their use, since they may be heard by more than one person. When this becomes objectionable, headphones may be used.

The following factors enter into the choice of auditory indicators:

1. Audio power required to drive the speaker or phone.
2. Level control, type and location.
3. Placement of speakers to direct sound to operator.
4. Protection from damage due to moisture, temperature, shock, or vibrations.
5. Fidelity.
6. Size.

The usefulness of an audio output depends greatly on the pulse length used. The directed-beam listening channel makes it possible to receive the full length of transmitted pulse. Short pulses, such as those of 1- to 5-millisecond length, produce only audible clicks. Some schemes have been proposed for enhancing the doppler effect by use of "shock-excited" high *Q* resonant circuits, but these were found to bring insufficient improvement.

Besides allowing the detection of doppler, an audible echo may convey "quality" information which is difficult to describe, but which enables a skilled operator to distinguish echoes of the target from those of wakes, whales, and so forth.

The combination of an echo spot on the screen and an audible echo is of greater value than either alone. The audible echo permits the operator to distinguish between screen traces coming from the target and those due to other noises and reverberation. The timing action of the screen enables the operator to pick out the true audible echo from other audible noises.

Fidelity must be sacrificed for the sake of signal-to-

noise ratio. The band pass of the audio channel has usually been designed to pass only the fundamental frequencies of the heterodyned signal, with provision for accommodating the expected target and own-ship doppler. The nominal beat frequency is usually 800 c, but an audio frequency of 500 c has sometimes been suggested in order to increase doppler detectability. The total amount of doppler shift possible must be considered.<sup>15</sup>

The use of *own-doppler nullification* [ODN] before the band-width-determining circuits reduces considerably the range of frequency encountered, and thereby permits a lower nominal frequency. Having determined the required bands of frequency which have to be reproduced, the designer should select a suitable speaker size and baffle to insure reasonably uniform and efficient reproduction of all frequencies within the band.

#### RANGE RECORDERS

Since the scanning channel delivers very short pulses compared to the transmitted pulse, marking on chemical recorders is difficult and the contrast of the mark is small. Also, since the scanning channel searches in all directions, it cannot select targets for the recorder unless some sort of high-speed gating is applied. The hand-trained listening channel thus becomes useful in providing a full-length echo pulse to mark the recorder, permitting selection of target for marking.

Thus far, only the chemical range recorder manufactured by the Sangamo Electric Company has been used. However, other types would presumably give normal performance. Test results using 30-millisecond pulses were quite satisfactory.

Since it is desirable to have a recorder gain control to get best marking and contrast, and since the signal to the recorder is also controlled by the sonar operator, there should be provided an excess of gain for the signal to the recorder, thus permitting sufficient signal control by the recorder operator.

The range recorder has sometimes been built into the main console or control unit of echo-ranging gear. This probably places more information and controls at the operator's disposal than he can reliably handle under the stress of attack. It is considered preferable to provide a separate location for the range recorder and to have a separate recorder-operator.

The range recorder must be synchronized with the echo-ranging cycle. To accomplish this, the recorder

is customarily used to key the scanning sonar, either through providing a keying contact or a suitable pulse to trigger keying circuits in the system. It is generally desirable to have the recorder contact, or pulse, determine the instant that keying functions commence but not to determine the length of transmitted pulse, blanking, and other sequences. The circuits should be so designed that double keying does not occur; that is, keying does not take place during the flyback of the recorder.

The foregoing paragraph deals with systems whose keying circuits are slaved to the recorder. With some types of keying circuits, however, this arrangement is either not possible or is extremely difficult to provide, and it has been necessary to slave the recorder to the system keying circuits. If more than one recorder is used, for remote repeater or other purposes, it is necessary to design the recorder so that it may be slaved to an external timing circuit.

Since the recorder generally is not used during search, but is in a stand-by condition, provision must be made in the recorder to change over from recorder keying to self or automatic keying, and vice versa. Suitable indication should be provided at any location concerned, to show whether the keying is being done by the recorder or the console circuits and at what range sweep rate it is taking place.

The recorder generally has functions other than recording range and providing keying. Some of these functions are:

1. Computing of time to fire.
2. Indicating range rate.
3. Averaging of intermittent data.
4. Determining aspect, identifying targets.

The recorder may furthermore be designed to provide additional functions such as:

1. Correcting for slant range.<sup>16</sup>
2. Determining depth.<sup>17</sup>
3. Transmitting range, range rate, and so forth to fire control or automatic training devices.<sup>18</sup>

#### BEARING DEVIATION INDICATOR

The use of the BDI with QC-type sonar makes it possible to obtain more accurate bearings and to obtain them with greater frequency. However, the accuracy and speed with which bearing information can be obtained from the PPI scope of a scanning sonar system are already considerably greater than those with which they can be obtained from a non-

BDI searchlight system. There is, accordingly, some question as to whether the addition of BDI to a scanning sonar system gives sufficient improvement to justify the additional complication. The answer to this question must be determined experimentally.

Assuming that the use of BDI or sector scan indicator is considered worthwhile, the following indicator design considerations are of interest: first, the BDI scope should be convenient for the operator who controls training; second, the type of BDI should be appropriate to the tactical use to be made of it, in both presentation and accuracy.

Types of BDI with considerable experimental background to date include the HUSL *lag line lobe comparison* Types X3 and X4, the Bell Telephone Laboratories *phase-actuated locator* [PAL], the CUDWR *right-left indicator* [RLI], and the HUSL *heterodyne BDI system*.<sup>19</sup> The last three use variations of the sum-and-difference principle. In addition, the SSI,<sup>11</sup> a proportionally indicating BDI, is under development at NRL.

### 2.2.5 Remote Indicators and Repeaters

Remote plan position indicators and bearing repeaters are needed for three fundamental reasons: (1) to convey the same information to several persons, each of whom is located in a different compartment or position in the ship; (2) to maintain a minimum equipment weight at higher positions in the ship; (3) to keep the volume of equipment small in such places as the bridge, where the space is at a premium.

While the design problems of such remote indicators and repeaters are in most respects similar to those of any other indicators, there are some considerations which are peculiar to their design. These are:

1. Size.
2. Shape for convenient location and mounting.
3. Controls necessary.
4. Completeness of information repeated.
5. Effect of repeater on other electronic parts of equipment.

Remote plan position indicators should be of minimum size and weight, and often have to be mounted in the bulkhead rather than on deck. The designer has to decide whether problems of cable insulation and so forth, or size and weight considerations, are the paramount factors when choosing the location of power supplies and other associated equipment. The

location may be in the repeater itself, or below in the main cabinets of the sonar gear.

### 2.2.6

### Arrangement of Controls

The arrangement of indicators and controls is an important design consideration. The designer must take into account operator convenience, design convenience, ease of maintenance, location on shipboard, and electronic limitations of the design. In locating the controls the designer must consider the following factors:

1. The number of operator functions must not be too great or confusion and loss of accuracy results.

2. Where, by proper design, a control can be eliminated without appreciable sacrifice in performance and maintenance, every effort should be made to do this. Controls divert attention.

3. When a control is needed for maintenance adjustment reasons only, it should be placed under cover to prevent confusion and incorrect adjustment.

4. Controls whose adjustment need only be made daily or at the time of changing watch should also be placed under cover, but in more accessible positions than maintenance controls.

5. Those controls and indicators which must be used often should be designed for ready identification and easy operation. They should be arranged on the front of the equipment in positions of relative importance.

6. Visual indicators should be placed to minimize parallax, distortion, reflections, and eyestrain, and to permit concentrated observation without physical strain.

7. Aural indicators should be placed to beam the sound towards the operator's head.

8. Since the majority of people are right-handed, training controls and hand keys should be on the right side.

9. Multiple control from one knob may have some advantages. Examples of this are seen in the two-speed training controls of the XQHA gear and the control of gain in dual-channel receivers (brightening and listening) by a single potentiometer. (See Chapter 5.)

The effect of repeater units upon the other parts of the electronic equipment must be considered. The loading effect of additional circuits, the need for simultaneous but independent operation of controls, the difference in background conditions, and the dif-

ference between components such as cathode-ray tubes are all factors which must be considered. It is probable that all the sonar circuits would be involved in these effects.

In locating the sonar components on shipboard, consideration should be given to the number and length of leads involved with different arrangements. Undesirable electrostatic and electromagnetic coupling between circuits occurs if cables are not properly positioned. Electrostatic and magnetic shielding may have to be used. Magnetic shielding is much more difficult in most cases, and cathode-ray tubes are very sensitive to stray magnetic fields from motors, relays, and synchros. Cables have appreciable capacitance and this may affect pulse shapes. Circuit components may be arranged to keep cables short and minimum in number, and circuits should be modified to have adequately low impedance.

#### PHYSICAL DESIGN CONSIDERATIONS

One of the problems that invariably arises in indicator design when cathode-ray tubes are used is that of locating the power supplies for the tube itself. From the standpoint of independence and easy maintenance, it is desirable to associate all power with the indicator. Space considerations, however, may make this location difficult to arrange, and the power supplies may have to be located remotely, perhaps with those for the receiving equipment. In the case of low-voltage supplies this is not difficult, but the high voltage required for the accelerating electrode of a magnetic-deflection tube presents a serious problem. It is much better to locate this power supply adjacent to the cathode-ray tube.

Since it is difficult to provide voltage stabilization for the accelerating electrode power supplies for cathode-ray tubes, it may be necessary to design the circuits associated with the cathode-ray tube in such a manner that the indication is made independent of line voltage variations, either of the rapid or slow type. Balanced deflection circuits are often possible, and may give adequate stabilization over the region of the screen that is of most interest. Safety devices such as interlocks, covers, and warning signs must be used. Since cathode-ray tubes may implode and cause serious injury to the person observing the scope, safety glass should be used in the colored light filter disk or the scope may be viewed through mirrors.

While it is desirable to reduce the number of controls, there are certain dangers in so doing. For ex-

ample, the on-off power switch has been ganged with the range-selector switch in some experimental models. As a result, in one instance the power was accidentally turned off during a practice run when an attempt was being made to change range. Since there was a minute and a half of time delay before the gear could be restored to operation, contact was lost and the run was a failure.

Adequate provision must be made to protect the components from the extreme shock and vibration encountered in naval applications. Since this often requires flexible mountings to permit mechanical filtering, provision must be made in cabling for flexing of the wires without damage.

#### 2.3

### RECEIVERS

#### 2.3.1

### General Considerations

The overall consideration in the design of receiving elements for sonar systems are: (1) reliability, (2) stability, (3) ease of servicing, (4) ease of manufacture, and (5) ease of operation. The importance of the various considerations is approximately in the order given above. These design factors apply to all types of receiving elements involved in the sonar system: scanning receivers, listening receivers, and BDI receivers. Moreover, each type of receiver involves certain factors that vary the design according to the task it is to perform.

#### 2.3.2

### Scanning Receivers

The essential function of the scanning receiver is to receive the signal from the transducer, as delivered via the commutator and lag line, and to amplify and convert it to a d-c signal. This signal may be applied to the brightening grid of a PPI scope so that a visual indication of any target within the sound field is indicated properly on the screen. In the design of such a receiver there are several factors to be considered and interrelated in order to achieve the best possible performance. These factors are discussed individually in order to simplify the analysis.

It is evident that the receiver has to tune over a limited frequency range. The choice of this range is dependent upon several factors of which the most important is the frequency response of the transducer. Transducers usually have a limited frequency response with the result that their efficiency is high

only in the neighborhood of the peak response. Often several ships are operating in the same area and it is difficult to avoid interference if all are operating on the same frequency. It has been the practice to use transducers with different resonant frequencies so that two searching ships could operate in the same area by the use of different operating frequencies. It is quite likely that this practice will continue in the future, supplemented by a limited degree of tuning.

Although the efficiency drops off rapidly with any deviation from the resonant frequency of the transducer, it is still possible to listen at other frequencies, but with a reduced signal-to-noise ratio. For instance, it is possible to observe high-energy signals, such as code transmission and pinging from nearby ships, even though the frequencies involved are quite far from the center of the transducer response characteristics. Thus, if the receiver is to be designed for use with a general type of sonar equipment, it may be desirable to have a tuning range large compared to the width of the transducer resonance. As an example, echo ranging is to be done only in the band from 18 to 24 kc; it may be desirable to construct a receiver that operates from 15 to 30 kc. The range of operation for the scanning-type equipment has extended from 14 to 55 kc in various experimental models. Current practice is to make the azimuth-scanning transducers for surface ships operate in the range of 20 to 26 kc. The trend toward higher frequencies is dictated by the physical size of the transducers, which are prohibitively large at low frequencies. The present design of depth-scanning transducers calls for a resonant frequency of the order of 38 to 40 kc.

Tuning should be accomplished by the use of a single dial, calibrated in frequency and operated by a vernier control for ease in selecting any particular frequency.

Another critical factor considered by the designer is that of band width. This is highly important, as the basic signal-to-noise ratio is a function of the band width of the receiving element. The noise energy present is directly proportional to the band width, and thus the narrowest width should be used that adequately passes the expected signal pulses and includes any frequency variations that are a function of the echo-ranging system. In order to arrive at an estimate of the necessary band width, the designer must consider the beam width of the transducer in the plane of rotation, the rotation frequency, the effect of own-ship doppler, and the effect of target

doppler. In existing models, ODN has not been applied to scanning systems, and hence the frequency of the received reverberation and echo varies from the transmitting frequency by this amount. In general for operation from surface ships, own-ship doppler is large compared to the target doppler. Present practice is to allow for as much as 30 knots of own-ship doppler, which at 20 kc amounts to 13.8 cycles per knot of ship speed. As the scanning beam looks both forward and aft, this amount of doppler must be provided for in both a positive and a negative sense. Thus the total frequency spread, due to this factor alone at 20 kc, must be  $\pm 30 \text{ knots} \times 13.8 \text{ cycles per knot}$ , or 828 c. At higher frequencies the band width that must be allowed because of this effect is proportionally greater.

Similarly, allowing for as much as 10 knots of target doppler, the frequency spread due to this factor at 20 kc is  $\pm 138 \text{ c}$ .

The calculation of the band width necessary to pass the pulse delivered by the rotating beam is slightly more complicated. In the case of azimuth scanning, where the effective beam width is approximately 20 degrees at 10 db down, it is necessary to proceed in the following manner:

The beam rotates at a rate of 30 rps in the present system, and only 20 degrees of azimuth is in view at any instant. Thus the band width necessary to pass the pulse delivered by the beam as it rotates past a source of sound is  $\frac{360^\circ}{20^\circ} \times 30$ , or 540 c. The total necessary band width is then the sum of all the above factors, or approximately 1,644 c (the band width is specified at 3 db down). This is given as a sample calculation for a particular frequency of operation of a specific transducer with a given beam width. Any variation in the elements considered must be accounted for in calculating the band width for a particular case. Good practice in the past has dictated the use of a band width slightly larger than that calculated by the above method to allow for errors in tuning and oscillator drift. Thus, in aligning the receiver, it would probably be adjusted for a band width of 1,800 c at 3 db down, rather than the 1,644 c calculated. This does not appreciably affect the signal-to-noise ratio and passes the signal pulse more faithfully than would be possible with the narrower band pass. An increase of band width of 2:1 increases the amount of noise present by 3 db.

It is well to consider the factors that determine the

noise present in the system. In general these arise from two sources; (1) noise developed in the electronic circuits, and (2) noise arising external to the electronic circuits. In the first case, assuming that the resistors are of good quality, the noise at the input grid can be calculated, knowing the resistance of the input circuit and the cutoff frequencies of the pass band.

The input resistance is determined by the lag line termination and the coupling circuit, as seen from the input tube grid. The sources of noise, external to the electronic equipment, arise from water noise due to turbulence about the transducer, electrical noise due to contacts such as the brush-to-slip-ring contact on the commutator, and electrical noise picked up from external fields. The latter can be minimized by the use of well-shielded low-impedance lines balanced to ground, and by minimizing the external fields of associated noise-generating equipment, such as motors. The water noise coming from the transducer is a basic limitation which can be minimized by proper dome construction, but cannot be eliminated. In addition to the water noise due to the motion of own ship through the water, there are other extraneous noises which may be received from the water because of sources of sound other than the target under observation. At best, in a quiet location, with transducers of the usual efficiencies, overall noise levels of the order of 1 microvolt are to be expected at the receiver input grid.

After deciding upon the tuning range and band width, the next question is how much gain is needed in the receiver. In this case there are two boundary conditions to satisfy: signal level available from the transducer and the signal level necessary to operate the indicating element. Echo-ranging experience has indicated that it is always necessary to provide a receiver that delivers maximum indication for signal levels from 1 microvolt to approximately 10,000 microvolts, or for a dynamic range of approximately 80 db.

Measurements upon the 7BP7 long-persistence cathode-ray tubes indicate that, for accelerating voltage of 6,000 volts or greater, the onset of brightening occurs at approximately +2 volts applied to the brightening grid (with respect to ground), and that the limit of brightening occurs at approximately 60 volts on the brightening grid. For lower accelerating voltages, the upper limit is considerably lower and is determined not by a cessation of brightening

with increasing grid voltage, but by defocusing of the beam. It is seen that the largest brightening dynamic range available with the present cathode-ray tubes is approximately 30 db. These figures apply for writing speeds encountered in 30-rps scanning sonars.

It is necessary, then, to provide sufficient gain so that a 1-microvolt signal on the grid of the first amplifier produces a d-c potential of approximately 60 volts on the brightening grid of the cathode-ray tube. Computing the gain, then, on the basis of voltage ratios alone, without regard to the impedances of the input grid and output circuits, a figure of approximately 156 db is calculated for the gain required. This is a fairly generous figure, and practice has indicated that the usual operating position of the gain control is such that only about 100 to 120 db of gain is in use.

As mentioned above, the necessity for providing operation over an 80-db dynamic range poses a rather severe problem for the designer. In listening systems this problem has been solved in the past by the use of limiters or *automatic volume control* [AVC], or such other schemes as *time-varied gain* [TVG]<sup>20</sup> and *reverberation controlled gain* [RCG].<sup>21</sup> In general, limiters are not considered desirable, as they tend to decrease the signal-to-noise ratio. Simple AVC likewise has the disadvantage of attenuating the echo signals following a strong burst of reverberation. The best methods devised thus far have been the use of TVG, and more recently, RCG. The latter is similar to a one-way AVC system in which the gain is allowed to increase with time after the ping, but never to decrease and has generally been found to be the most satisfactory method. It allows a maximum rate of recovery of gain after the ping, determined automatically by the amount of reverberation present.

The designer must select the proper time constant for the RCG circuit. It is evident that it must be longer than the 33 milliseconds required for one rotation of the beam, since otherwise the gain would increase too rapidly while the beam is passing through regions which are not returning large amounts of sound. This is particularly true for the depth-scanning system, for which the design differs to some extent from that for an azimuth-scanning system. The time constant, however, must not be too long, or the advantages of RCG as opposed to TVG are lost. It has been the practice to keep this time constant somewhat less than 50 milliseconds, and it would seem that its exact value is not critical. In listening systems



the time constant has been made as low as 10 milliseconds.

## 2.3.3

**Listening Receivers**

In designing a listening channel for a sonar system it is necessary to consider all the factors mentioned under scanning receivers discussed in the foregoing section. The requirements for the listening channel are somewhat different, however, so that it is necessary to consider its design separately.

In general, the same considerations with respect to tuning apply to the listening receiver as to the scanning receiver, and for a given system it is desirable to have both receivers cover the same tuning range. The pass band of the listening receiver, however, can in most instances be somewhat narrower than that of the scanning receiver. This improvement in selectivity can be made because the listening receiver listens in only one direction at a time and hence hears an echo pulse which approximates the whole length of the transmitted pulse. Thus, the actual echo pulse from a beam target as received by the 20-degree beam rotating at 30 rps is approximately  $\frac{20^\circ}{360^\circ} \times 33$  milliseconds = 1.9 milliseconds, whereas the listening beam trained in the direction of the target would hear the entire 33-millisecond pulse returning. Thus, in calculating the necessary band width for a listening receiver to be used with the scanning system having the characteristics described above, allowance would have to be made for target doppler, own doppler, and pulse length. This would give, as before,  $10 \text{ knots} \times 13.8 \text{ cycles per knot} = \pm 138 \text{ c}$  allowed for target doppler, plus  $1/0.033 = 30 \text{ c}$  allowed for pulse length plus 828 c for own doppler. The total band width required is thus 1,134 c. If an ODN is applied to the listening receiver, this band width may be reduced to 306 c. In general, since it cannot be assumed that the ODN functions perfectly, or that the oscillators involved do not drift, additional band width is usually allowed. The effect of this upon signal-to-noise ratio is not so unfavorable as might be expected, since the ear can discriminate between simultaneous sounds if they differ in character. Consequently over a wide dynamic range, the ear is able to detect an echo in the presence of considerable extraneous noise. This discrimination is completely lacking on the screen of the cathode-ray tube. Thus it is possible to allow greater band width in listening receivers than

would be indicated by the simple computation performed above. This selectivity is frequently accomplished by the use of an audio filter in addition to the usual r-f and i-f filters, so that it is not necessary to make the high-frequency pass band of the receiver as narrow as 500 cycles. However, intermodulation in portions of the receiver preceding the final bandwidth-determining filter must be avoided.

The amount of gain necessary in the listening receiver can be approximated from considerations similar to those given in the scanning receiver discussion. Assuming a plate load of approximately 5,000 ohms, it is necessary, then, to produce approximately 100 volts rms in the plate circuit of the output amplifier stage, to realize the desirable output power level of approximately 2 watts to the speaker unit. It is evident that the same considerations with respect to dynamic range apply to the listening receiver as to the scanning receiver. There is an optimum dynamic range in which it is desirable to work, but the received signals pass through the much larger dynamic range of approximately 80 db as the returning sound energy dies off after the ping. As a consequence, some system must be devised to lower the gain automatically at the time of the ping and to bring up the gain in some feasible manner as a function of time after the ping. In this respect, too, AVC has always been considered unsatisfactory. TVG is satisfactory but does not allow for the most effective use of gain control. That is, since the TVG is present without respect to the sound conditions existing at the moment, the gain returns in a definite manner determined by the time constants of the TVG circuit. Whenever the reverberation is small, echoes are at a disadvantage. The best solution has been the use of RCG, which makes it possible to use the maximum possible amount of gain at any given instant. Most recent practice has been to substitute for an actual gain control one which essentially sets the maximum amount of gain to which the RCG can return, so that the initial gain and the rate of recovery after the ping are independent of the control setting. RCG is designed to provide an audio signal which is within the comfortable dynamic range of the ear.

In a listening receiver it is necessary to provide a heterodyne oscillator in order to obtain an audio beat frequency. This oscillator must be stable and should have a dial accurately calibrated in cycles per second (audio beat frequency) to make operation as easy as possible. This permits a simple tuning proce-

dures enabling the operator to tune to zero beat with the heterodyne oscillator set at zero, and hence center the incoming signal in the pass band of the receiver. The calibration on the heterodyne oscillator dial also aids operators in centering the pitch of the audible beat in the middle of the audio filter.

Standard echo-ranging equipment has usually been provided with three types of audio filter selectivity; namely, peak, band, and flat. This additional complexity of control has not been entirely successful, and the present tendency is to provide only a rather broad band pass. The associated audio filter should have a band pass characteristic from 200 to 800 c for a center beat frequency of 500 c. It is still desirable to provide a switch whereby the filter can be eliminated and the system operated with a flat audio characteristic.

#### 2.3.4

### BDI Receiver

In addition to the scanning receiver and listening receiver included in a sonar system it may be desirable to have a BDI receiver. The main problems involved in designing a circuit to give bearing deviation indication are determining (1) where the phase information is changed to amplitude information; (2) where the two amplitude signals are compared to give a right-left deflection signal for presentation on the cathode-ray tube; and (3) how the circuits are arranged so that the two signals may be amplified while preserving the relationship between the signals. This last problem is exceedingly important and the different BDI circuits (noted earlier in the chapter) represent alternative attempts at a practical solution. In general, it is desirable to make the final comparison at high level in order to obtain a deflection signal for the BDI tube. This eliminates the need of high-gain d-c amplifiers. As a consequence, it is always necessary to build amplifiers that preserve relative amplitude between the signals and, in some cases, the relative phase between the two signals as well. The precise circuit arrangements of the various types of BDI are described in detail elsewhere.<sup>22</sup>

The X-3 type circuit gives excellent performance in practice but has been found difficult to manufacture because it is necessary to match accurately the band-pass characteristics of two filters with different center frequencies. It has proved difficult to maintain in service for the same reason. It has the advantage, however, of being a truly simultaneous comparison circuit.

Unlike Model X-3, the X-4 circuit does not perform simultaneous comparison but rather compares the signal arriving in the two steered channels at succeeding intervals of time. Although this system is not disadvantageous for echo ranging, it is less effective for accurate determination of the bearing of noise sources, whereas the X-3 is satisfactory for both noise and continuous signals. The erratic response of X-4 to noise is caused by the random nature of the noise itself. However, it has proved easy to manufacture and comparatively reliable in service and can be recommended for all uses where operation on noise signals is not important.

The sum-and-difference BDI principle has been applied to practical sonar by CUDWR in the RLI receiver. This system, by means of transformers, combines the signals from the two halves of the projector in such a way that two voltages result. One voltage is the vector sum of the voltages of the two halves of the projector, while the other is the vector difference. The difference voltage changes sign in accordance with the direction of deviation of the target bearing from the center line of the projector. The sum-and-difference voltages, as can be seen geometrically, are mutually perpendicular. It is necessary to bring them into phase so that they may be applied to a phase-sensitive detector to obtain d-c deflection signals for the cathode-ray tube and indicate the bearing deviation. In the usual sum-and-difference circuit, this phase shift is accomplished somewhere near the input. Thus far all sum-and-difference BDI'S have used two separate amplifiers, one for the sum signal and the other for the difference signal; these amplifiers must preserve both relative phase and relative amplitude. Phase must be preserved to within 1.5 degrees, and amplitude must not vary over 2 db if acceptable BDI operation is to be obtained.

This system gives excellent performance but is somewhat difficult to construct because of the limitations imposed by the necessity of preserving both phase and amplitude in the two amplifiers. This is particularly true since it is necessary to make the amplifiers track over a wide dynamic range in both phase and amplitude. The version built by the New London Laboratory for broad-band noise operation has worked satisfactorily. The Harvard version, although cumbersome in its use of a large number of transformers, also worked well. By using broad input filters or by eliminating them entirely, the sum-and-difference BDI can be made tunable like the X-4.

The PAL circuit developed by Bell Telephone Laboratories is slightly different from the sum-and-difference types mentioned above since the signals from the two halves of the projector are first separately amplified, then the sum-and-difference voltages are obtained and applied to a phase detector. This circuit was likewise developed for fairly broad-band noise listening and it has been successful for that purpose. The sector scan indicator now under development by NRL has not been used yet to any extent in the field. Its circuits are designed so that the amplitude of the indications is proportional only to the bearing deviation of the target, and is independent of signal level if the level is great enough to produce an indication. Proportional indication is produced over a limited sector within the projector pattern.

In choosing the type of BDI to be incorporated in a given sonar echo-ranging system, it is necessary first to decide just what types of operation the system is called upon to perform. This factor determines whether the relatively simple X-4 circuit can be used or whether it is necessary to use one of the other systems. Whenever operation upon noise signals is of minor importance, the X-4 is probably the best choice. However, when it is necessary for the system to operate satisfactorily with noise signals, one of the other circuits should be used. One advantage of the sum-and-difference type is that the sum channel can also serve as the main portion of the listening receiver.

Once the particular circuit has been chosen, however, the general design considerations are very similar to those previously discussed in the sections covering scanning and listening receivers. It is necessary that the BDI tune over the same range of frequencies as the listening receiver since in operation they are always used together. The same requirements of band width, dynamic range, and doppler allowance apply to the BDI receiver as were described under the section on listening receivers.

To improve the dynamic range it is necessary to include TVG or RCG as in the other receiving circuits. Again it has been found, in general, that RCG is the most satisfactory. TVG greatly improves the operation of the BDI but does not allow the receiver to adapt itself automatically to various acoustical conditions. As a consequence it must be manually adjusted to a compromise operating characteristic.

A d-c brightening voltage must be provided in order to brighten the spot on the cathode-ray tube screen as a function of received signal level. It is

usually desirable to limit the brightening voltage, as in the case of the scanning receiver. Again, in systems using high accelerating potentials on the cathode-ray tube (6,000 volts or higher), the use of a limiter is unnecessary.

## 2.4

## TRANSMITTERS

To obtain the best possible ratio of signal to noise, both electrical and acoustic, the transmitter should produce a maximum of power consistent with the power-handling capabilities of the transducer and its associated components, and at the same time fulfill the following requirements for a well-balanced design:

1. Low average consumption of power.
2. Steadiness of power consumption.
3. Light weight (consistent with design of other units of system).
4. Small size.
5. Reliability.
6. Ease of servicing.
7. Good performance.
8. Safety.
9. Reasonable cost.
10. Conservatively rated components.

Since these ideal characteristics are to some extent mutually incompatible, the final design requires a careful balance, emphasizing those factors of major importance and sacrificing those considered to be less important. Furthermore, the technical specifications set forth by the Navy have to be met.<sup>23</sup>

The types of scanning systems described in this report send out a discrete sound pulse whose length is dependent upon the scanning speed (see first section of this chapter for a discussion of pulse length requirements).

The shape of the transmitted pulse is usually rec-

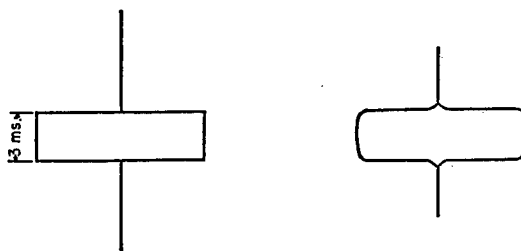


FIGURE 4. Square and rounded short pulses.

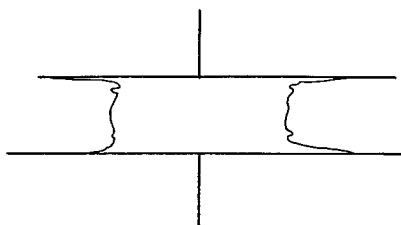


FIGURE 5. Poor pulse shape showing undesirable transients at beginning and end of pulse.

tangular. There is good indication that the detectability of short square pulses is appreciably greater than that of pulses with rounded corners (see Figure 4) and consequent lower harmonic development;<sup>24</sup> thus, on short pulse equipment, every effort should be made to assure a suitable envelope shape for the transmitted energy.

In equipment employing longer pulses (of the order of 30 milliseconds) when it is not the intention to prevent interception of the ping by enemy listening equipment, the actual shape of the pulse is of less importance. In any case, precautions must be taken to prevent transients (Figure 5) at the beginning and end of the pulse, since dielectric breakdown in the transducer, or in the cables and electric networks connected to it, may result from high-voltage peaks of short duration.

Some variation is permissible in the amplitude of the transmitted pulse; in fact, amplitude modulation has been employed in some experimental installations. It is generally considered unwise to permit a too abrupt variation in pulse amplitude, however, since it is possible to introduce bearing errors if the received echo envelope has an appreciable slope at the point cut by the receiving sensitivity beam (see first section of this chapter).

To avoid placing excessive current drain on the ship's power supply at periodic intervals and at the same time to effect a saving in component size and weight, it is desirable to use an energy-storage type of supply for the plate power of output tubes and other pulse equipment. The power may be stored up between pings at a comparatively low rate of power consumption, to be discharged periodically into the driver-amplifier stages during the ping. Since the rate of transmission of sound through water is so slow that an appreciable time interval must elapse between pings at the ranges usually employed, the efficiency of power supply utilization is obviously greatly increased. Weight and bulk, although items not so

significant as the improvement in electrical consumption, are greatly reduced. When it is considered that an ordinary continuous-duty power supply for a 10-kw transmitter would draw 100 amperes in pulses from a 110-volt line and would consist of very large transmitters and chokes, while a storage type of power supply would draw only 0.7 ampere continuously and require transmitters and chokes rated at less than 100 watts, the reduction in size and the increase in efficiency is apparent. These figures depend upon a duty cycle of 1 to 150 which would be the case for a transmitter producing 1/30-second pulses every 5 seconds. The increased amount of storage capacitor required, however, cancels in part the reduction effected in size of transformer and choke. The advantages of energy storage are less important in longer-pulse systems.

There are two principal types of energy-storage systems that may be used in scanning-sonar transmitter applications: (1) straight capacitor storage and (2) transmission lines, or pulse lines, of one form or another. Circuits showing possible designs appear in Figures 6, 7, and 8.

In any of these circuits the impedance into which the supply transformer delivers its power must be large in order to limit the primary current drain to some suitable figure. Such a high impedance may be obtained by inserting a resistor in the storage charging network (Figure 6) or by using a voltage-doubling

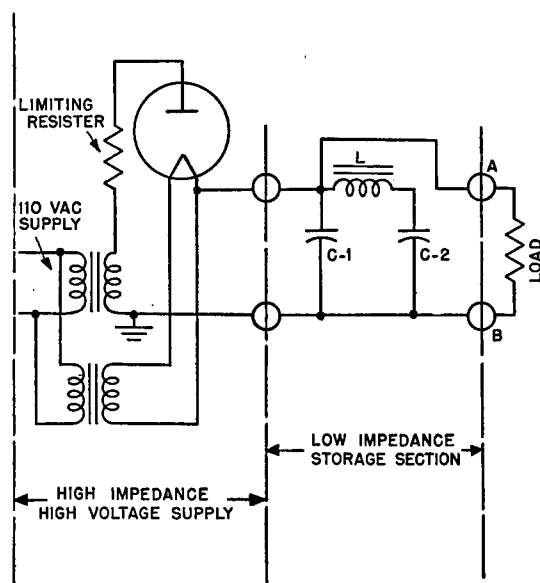


FIGURE 6. Half-wave rectifier with limiting resistor. Storage capacitors with choke.

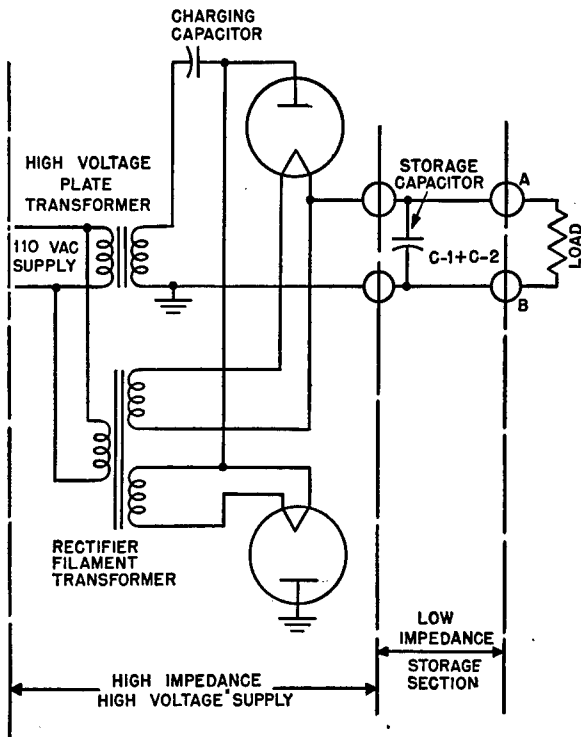


FIGURE 7. Voltage-doubling rectifier. Storage capacitor without choke.

circuit, such as that in Figure 7, in which a large impedance is offered by the charging capacitor. This second method is more efficient, since a minimum of power is dissipated in the capacitor.

Two proposed types of pulse line are seen in Figures 6 and 8. (The line in Figure 6 may be called a pulse line by courtesy only, as it consists of only one section of an unterminated line.) In operation, the vacuum tube load is placed across the points *A* and *B*. Keying the grid circuit of the tube (normally biased to cutoff) immediately places a low impedance across *AB*. If the reactor choke *L* were to be shorted out of

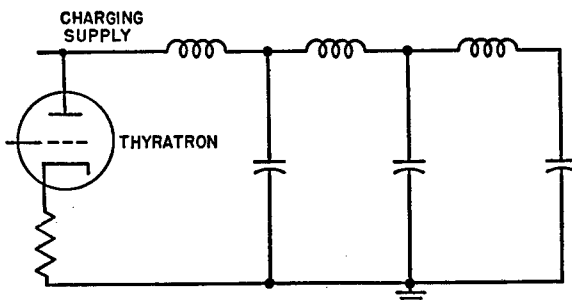


FIGURE 8. Pulse-forming transmission line.

the circuit thus reducing the storage section to a single condenser, as shown in Figure 7, the voltage would drop in a normal exponential curve determined by the values of the capacitors  $C_1$  and  $C_2$  and the load across *AB* (9A).

When the reactor choke is in the circuit, the voltage across *AB*, as condenser  $C_1$  discharges, falls somewhat faster than shown in Figure 9A; but this disturbance, reflected from the unterminated end of the filter, causes the voltage to rise again and decay as shown in Figure 9B. The values of  $L$  and  $C$  are chosen so that the point *F* on the curve of Figure 9B is reached coincidentally with the end of the pulse, resulting in the pulse envelope shown. Somewhat more energy is obtained in the pulse of Figure 9B than in that of Figure 9A, while the initial rate of drop in voltage is larger than in the first case. The results given by this circuit are crude compared to those that may be obtained from a pulse line with only one additional section (Figure 8); however, the

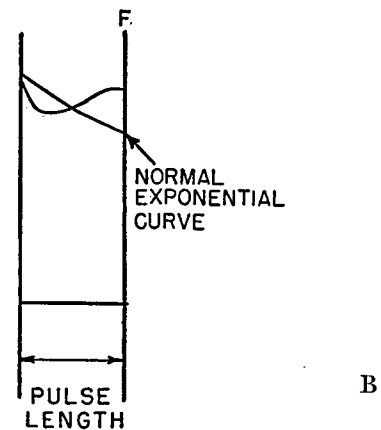
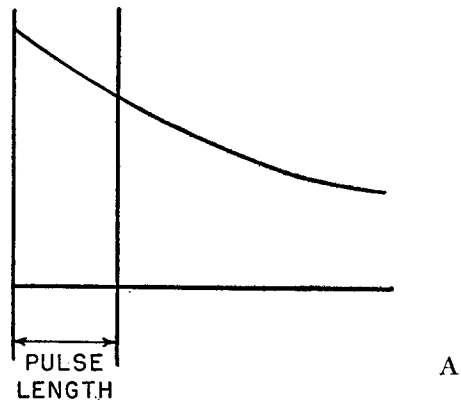


FIGURE 9. Pulse envelopes.

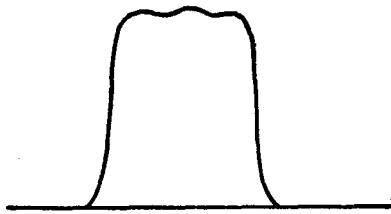


FIGURE 10. Voltage pulse obtained from line.

voltage of the pulse is the voltage to which the capacitors are charged.

The pulse line illustrated in Figure 8 is a relatively simple form of transmission line<sup>25</sup> which stores in its shunt capacitors the energy supplied to it until the line is terminated through a thyatron into the load. The type of pulse obtained, which may be shaped (within limits) to suit the requirements of the individual application, is shown in Figure 10. The fact that such a line must be initially charged to twice the voltage obtained from it on discharge may be a disadvantage in some cases. Power is drawn from the line by keying the plate voltage through the thyatron, thus removing strain on insulation except during pings, minimizing the danger of breakdown and increasing the life of the tube.

Most systems are improved by the inclusion of some means of controlling the output power of the transmitter. One of the simplest and most effective methods makes use of a variable auto-transformer in

the primary of the plate-supply transformer, allowing the plate voltage to be changed at will.

Other supplies—bias, low-power or low-voltage plate supplies, and the like—may be designed along conventional lines and in accordance with the particular requirements of the system. If a pulse line with pulse transformer is used, taps for bias and low plate voltages may be provided, with a consequent reduction in the number of necessary components.

In the so-called unicontrol system, a fixed frequency oscillator is incorporated in the transmitter unit. The output of this oscillator is then heterodyned with a signal supplied by another oscillator, usually located in the receiver unit of the system. The difference frequency (other frequencies being removed by a band-pass filter) is then used as the frequency of transmission. This unicontrol arrangement allows the transmitter-output frequency to be remotely controlled and also allows the entire scanning system to be tuned by one control. The diagram shown in Figure 11 illustrates a typical choice of frequencies and unit interconnections.

Systems have been built in which the transmitter-oscillator is required to sweep over a band of frequencies during the ping or to produce a noise-modulated signal. The frequency sweep may be produced by a reactance tube circuit if means are provided for varying the reactance-tube control-grid voltage in an appropriate manner during the ping. A gas tube noise-generator can be used to produce suitable noise frequencies for frequency or amplitude modulation of the transmitted signal.

In systems where one transducer is used for both transmission and reception, care must be exercised to prevent the transmitter from feeding over into the low-level receiving circuits. The most obvious solution is to operate the transmitter unit only during transmission, either by quenching it with a biasing voltage or by keying the plate voltage of either one or several of the transmitter stages. Both of these methods are practical. In unicontrol systems, one of the transmitter stages may be biased to cutoff during reception, which is usually sufficient to prevent feed-over through common ground circuits and other wiring.

Stability of output frequency should be achieved by voltage regulation, temperature compensation of capacitors,<sup>26</sup> stable mounting of coils, capacitors, and wiring, or other appropriate means. This is not a serious problem at the relatively low frequencies

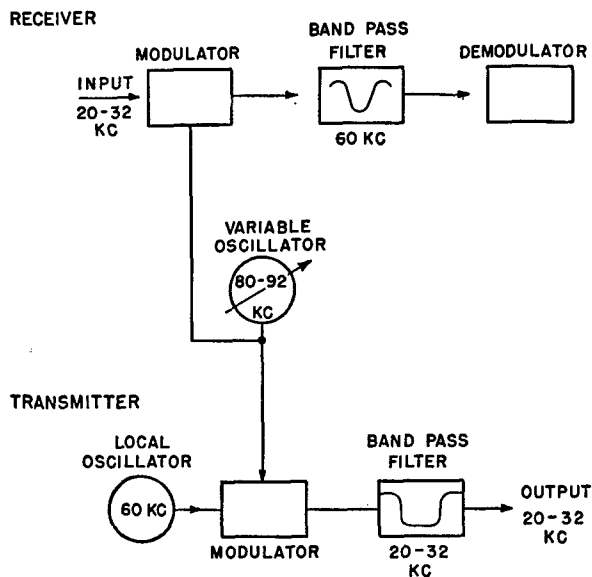


FIGURE 11. Example of unicontrol system.

CONFIDENTIAL

used in underwater sound transmission or with transducers and receivers having reasonably wide band-pass characteristics.

The initiation of transmitter operation is closely related to the timing of other circuit functions in the system. Without regard for the specific means of initiating the operation of the transmitter, the actual keying involves some form of timing circuit in the transmitter, by means of relay or electronic circuits. Relay contacts are difficult to adjust, are apt to bounce, and are not easily adapted for the control of pulse length while in operation. For these reasons electronic circuits of the "flip-flop" or modified multivibrator type are to be preferred. Keying should be performed in the relatively low-level circuits to avoid switching any large amount of power. If class C amplifiers are used in the final stages of the transmitter, a suitable pulse of energy applied to the normally overbiased grid operates the tube without changing the d-c grid-bias voltages. When pulse lines are used for plate power supply, the keying pulse is applied to the thyratron that terminates the line into the load impedance, and the pulse length is determined by the characteristics of the line.

The power amplifier portion of the transmitter commonly employs class C amplifier stages for maximum efficiency. If the transmitter is required to produce power over a fairly wide range of frequencies, low- $Q$  broadly tuned transformers (with consequently lower efficiencies) are required. If single-frequency transmission is employed, high- $Q$  tuned circuits allow the maximum class C efficiency to be achieved.

The requirement of high power for short periods has an important bearing upon the type of output power tubes chosen and on the method of rating them. Pulse modulator tubes originally designed for radar work are particularly useful, combining high cathode emission and small size (low plate dissipation). Since the plate dissipation can be averaged out, much in the same manner as the power consumed by the plate supply, the peak cathode emission and internal arc-over characteristics are often the limiting factors in the choice of tubes. Tubes that have been found useful are listed in Table 1.

Before provision for code transmission for underwater communication can be made, the energy storage characteristics of the power supply and the pulse-rate output tubes must be considered. Equipment designed to put out a 5-kw pulse 30 milliseconds

long, every second, would scarcely emit a single dash, or even a dot, before the power supply was discharged. This difficulty can be overcome if the code circuit is arranged to send short pulses of energy instead of relatively continuous pulses: a simple artifice is to modulate the transmitter-oscillator with

TABLE 1. Types of Tubes Suitable for Use in Power Output Stages.

Tube number	Type	Max plate voltage	Max cathode emission
838	triode	1250v *	—
2C26A	triode	3000v †	15a
304TH	triode	3500v *	10a
6C21	triode	2000v †	15a
829B	beam tetrode	30,000v *	250 ma *
3E29	beam tetrode	500v *	9a
715B	tetrode	5000v *	15a
5D21	tetrode	15,000v *	15a

\* Published values.

† Values used satisfactorily.

60- or 120-cycle energy during code transmission. A judicious choice of modulating voltage applied at a low-level stage enables the transmission of code at ordinary rates of speed at reduced power.

The two types of transducers commonly used (magnetostrictive and piezoelectric) present vastly different impedances to the transmitter, even after the reactive component of the load is tuned out, the impedance of the piezoelectric unit being appreciably higher than that of the magnetostrictive one. Matching the impedance of the transducer obviously is important if maximum power transfer is to be effected.

Although output transformer design may be varied to allow for the differences in the output tube characteristics and transducer impedance, the particular requirements of pulse transmission impose serious limitations on the transformer design. A brief consideration shows that tuned air-core transformers are essential if space and weight are to be kept within reason and appreciable power is used. The frequency band required must also be considered in the design of the output transformer, since this factor determines the  $Q$  of the tuned circuit.

The problem of transmitting power into the same transducer as used for reception, and at the same time providing protection for the receiving portions of the system, may be solved in several ways. Two of these are: (1) relays for disconnecting each of the necessary elements and connecting the transducer to the transmitter, and (2) electrical networks to accomplish virtually the same results.

Networks to isolate and protect the receiving elements of the system may be used in conjunction with one relay which for scanning systems appears to be a practical minimum. This relay switches or lifts one ground bus to prevent passage of the transmitting current through the receiving circuits while allowing it to pass through the transducer. Thyrite, a variable-resistance ceramic material, or neon lamps may be used across circuit elements requiring protection. If vacuum-tube rotors are used, a resistor in series with the grid circuit may be sufficient to protect the tube, but this may also become an important noise source. In some cases a balancing network may prevent harmful voltages from being developed across vital elements of the circuit, but this usually requires careful matching of a large number of components, as well as of the individual transducer elements.

## 2.5 SEQUENCE OF FUNCTIONS

In the scanning sonar, sufficient time must be allowed between the end of the display of one sweep and the beginning of the display of the next sweep for: (1) the protective circuits to operate; (2) the transmission of the ping to take place; (3) the spiral sweep to position itself to restart; and (4) the gain control to set the amplification of the signal to a value compatible with the intensity of reverberation.

The various time intervals and time-related events must be controlled by means of a timer. Each kind of timer has its own working time standard. An electronic system might use as a standard the time constant of a resistance-capacitance network. Most motor-driven timers use as a standard either the supply frequency or a governor.

There are two general types of electronic timing circuits: in one, the time interval is determined by the resistance-capacitance time constant of a relaxation oscillator; in the other type, either resistance-capacitance or inductance-capacitance determines the frequency of a sinusoidal oscillator. For sonar systems in which the maximum length of interval

is of the order of four or five seconds and which use the latter type of electronic timing circuit, it is best to operate the oscillator at a frequency of 80 or 800 c (10 yards or 1 yard per cycle), and use a frequency divider or counter to determine the length of the ping interval. The relaxation oscillator can also be used with a counting circuit. It is simple and has the further advantage of being able to supply a sawtooth voltage for the spiral sweep, and a sharp pulse for tripping the ping and blanking circuits at the proper time. It may be necessary, however, because of polarization of the dielectric, to include an inductor in the discharge path in order to discharge the sweep capacitor completely. It has the further disadvantage that it may be affected by changes in temperature and humidity.

A timer driven by a synchronous motor is as accurate and precise as its power supply frequency.<sup>27</sup> It is simple to design but is very apt to require maintenance because of the exposed contacts found in many designs. The contacts are also likely to chatter, causing erratic operation of the complete system. A motor whose speed is controlled by a governor is independent of the supply frequency, but the speed gradually changes as the brake on the governor wears. With any motor-driven timer, closing of the contact by the rotor keys the transmitter to produce the ping, trips the blanking circuit, and restarts the sawtooth sweep.

Since it is desirable to employ varying ping intervals in scanning, and hence different maximum ranges for the display, a range switch is necessary. When the equipment is being used to search for echo sources, the maximum range of detection is limited by the water conditions; thus one or two switch positions for search, corresponding to good and poor water conditions, are desirable. When the system is used for attack or navigation, shorter intervals between pings are desirable to give smaller maximum range, and hence greater range resolutions. Moreover, bearing determination is likely to be more accurate when the echo appears near the edge of the screen. In the case of mine detection, the range at which the mines can be reliably detected is expected to be small, 400 yards or less, so that one position of the switch is desired which displays such short ranges over a considerable portion of the face of the cathode-ray tube.

The spiral sweep for the PPI may be generated by either electromechanical or electronic means.<sup>28</sup> When



using the electromechanical method it is preferable to obtain the required rotating magnetic field in the PPI by connecting stationary polyphase deflecting coils to a polyphase generator. Either a 2-phase system or a 3-phase system may be used. The latter is easier to set up since accurately wound 3-phase units are available in the form of synchros. The sawtooth modulation of the polyphase voltages is achieved in this case by supplying the generator field with a sawtooth varying current.<sup>29</sup>

A second electromechanical method of spiral sweep generation is the rotating capacitor-generator. Either d-c or radio-frequency voltage upon one plate of the capacitor is modulated by a mechanical variation of the capacitance. The plates are shaped so that 2-phase sine-wave voltages are obtained. Range expansion is achieved by varying the amplitude of the voltage upon the fixed plate of the capacitor in accordance with the expanding sweep. If radio frequency voltage is used, the voltage to be applied to the deflection coils is obtained by using a detector or demodulator. The modulated, direct current may be applied directly to the deflection coils after amplification.

For high-speed rotation the necessary polyphase signal for the deflection coils can be generated electronically by using a multiphase oscillator or by using an ordinary sine-wave oscillator, followed by a phase-splitting network. The sawtooth modulation may be carried out either before or after the phase splitting. Because of the difficulty in making modulators track, it is most conveniently carried out before. Phase splitting is best done at low power levels because of the power losses associated with the splitting. Hence, it must be followed by a power amplifier for each phase. For simplicity, only 2-phase electronic systems have been used.

The sawtooth modulating sweep may be generated by either mechanical or electronic means. If a recorder or similar mechanical device is used to control the ping interval, a potentiometer can be attached to the moving element. A fixed voltage is placed across this potentiometer and the sawtooth sweep voltage taken from the slider. A sawtooth sweep can be generated most successfully, however, by means of the conventional capacitor charge and discharge type of circuit similar to that used in the cathode-ray oscilloscope. To secure stability of sweep rate and linearity of sweep voltage, the power supply must be regulated, and a means of producing a constant

charging current provided. Constant charging current is most easily secured by the use of a pentode tube in the charging circuit. These circuits are discussed more fully in Chapters 5 and 7.

A source whose current is exactly constant can be obtained also by using a voltage regulating system, with sufficient positive feedback to be metastable,<sup>30</sup> to keep the voltage across a resistor in the charging circuit constant. With any of the electronic systems of sweep generation it is usually desirable to have an isolating amplifier between the sweep generator and the point of application to avoid distortion.

The sawtooth sweep must be synchronized with the ping. This is most easily accomplished by letting the flyback, or return of the sawtooth sweep, initiate the ping. In the case of a mechanical timer the contactors that discharge the sweep capacitor can also be made to initiate the ping, after a time delay if necessary.

The polyphase sweep voltages must be synchronized with the rotation of the scanning beam. At present the method used in *commutated rotation* [CR] sonar is to couple the polyphase generator, usually a synchro, directly to the scanning commutator and drive them both by the same motor. For the *electronically rotated* [ER] sonar system, it is sufficient to use the same oscillator for the sweep as is used to rotate the beam of sensitivity. If a lag line is used to rotate the beam of sensitivity in ER sonar, the oscillator must be synchronized with the lag line, so that a pulse enters the lag line at the same instant that the previous pulse leaves it. This can be accomplished by connecting a discriminator to the beginning and end of the lag line and using the output of the discriminator to control the frequency of the oscillator through a reactance tube (see Chapter 7 for a more complete discussion).

Certain other factors must be considered in the design of the spiral sweep, since failure to allow for them introduces distortion. The hum level in the sweep circuit should be at least 80 db below the level of the sweep voltage. Harmonic distortion in the sweep amplifier must be kept to a minimum. The phase shift through the sweep voltage amplifier must be independent of amplitude, or else the bearing of the display changes with range. Regulation of the power supply may also cause this trouble. The deflection circuits can and should be compensated so that the size of the display is made nearly independent of line voltage. For the size of the display also to be in-

dependent of rapid transient changes in line voltage, time delays in the filters for the power supplies should be equal, and approximately equal to the lag in the change in heater temperature.

The ping length may be determined by a mechanical switch; for example, a pair of contacts. A knife-type switch is unsatisfactory, because the length of time that it must remain closed is so small. In general, it has been the experience at HUSL that mechanical contacts are not satisfactory because of their tendency to chatter and because of their maintenance requirements.

A multivibrator or self-blocking oscillator is well adapted for determining the ping length, since it operates well with an "on" interval of a few milliseconds and turns on and off in a few microseconds. An electronic network having associated mechanical parts has been used in the differentiated-pulse system of timing. Either the pulse used to actuate a relay, or the pulse formed by the discharge of the sweep capacitor, may be differentiated and the output used to key the transmitter.

Accurate and precise control of short ping length can be secured also by the use of a pulse line. Here, the ping length is determined by the time taken for a transient pulse to travel out and back along a transmission line made up of low-pass filter sections. As this time interval is dependent on the line constants, the ping length can be controlled by careful design and construction of the line. The pulse line has the additional advantage of storing energy between pings and giving up all its stored energy at the time of the ping so that the drain upon the power supply is small.

It is necessary to apply a blanking pulse to the PPI cathode-ray tube and to the BDI tube, when used, during return of the sweep to prevent any brightening by the transmitted pulse or by reverberation during return of the sweep. In a sonar system employing a listening receiver it is also necessary to blank the receiver during transmission of the ping to prevent an initial blast of sound in the speaker. In the ER sonar it may also be necessary to blank the switching voltage applied to an electronic rotor so as to prevent damage to rotor components during transmission of the ping. Blanking of the PPI tube should be long enough to allow any direct current transient due to return of the sweep to die out, and to allow the sweep to collapse to a sufficiently small value so that it restarts from approximately the center cathode-ray tube screen. In systems where an electronic cursor is

put upon the face of the cathode-ray tube during the dead time, it is necessary to blank the face of the cathode-ray tube before and after the cursor mark is placed upon it. This double blanking must be long enough to allow the switching transients to die out before the new portion of the display is started.

Receiver blanking may be accomplished by either reducing the gain of the system, or by shorting out the input signal. An additional contact upon a ping-ing or ping-interval relay can be used to do either. Electronically, the gain can be reduced either by driving the grid or suppressor negative, by reducing the plate or screen voltage, or by driving the cathode positive. A triode gate or switch may be used to short out the signal for the desired time.

Again it should be emphasized that all these time functions must be synchronized. It is necessary for the protective and blanking circuits to operate immediately after the sweep is blanked and to keep the dead time as brief as possible. The ping transmission must be delayed until all protective circuits are in operation, and yet must not be delayed longer than the time required for these circuits to become operative. In a system with two or more transmitters it is necessary to key the transmitters simultaneously in order to prevent the output of one transmitter from masking part of the echoes returning from the other. Where two transmitters are operating simultaneously at different ranges it is desirable to have the longer interval an integral multiple of the shorter.

With a dual indicating system, range-marking or range-determining circuits must be keyed at the same time to obtain identical range indications with both indicators. Bearings must likewise be synchronized.

## 2.6 MECHANICAL MOTIONS

### 2.6.1 Training of Listening Beam

To provide a listening beam in the CR sonar, an additional commutator with a synchro-controlled servo drive is used. Circuits are arranged so that the servo motor receives its signal from the cursor training handwheel directly, or through stabilization equipment.

Another method of positioning the receiving beam is to connect the beam-forming lag line directly to the transducer elements. This forms the receiving beam at a definite angle with respect to the transducer. If the transducer is then rotated mechanically

in a manner similar to the standard procedure of training QC projectors, the receiving beam can be positioned to the relative target bearing. Provision must be made in the scanning channel for cancellation of this motion if a relative bearing PPI is desired.

## 2.6.2

**Stabilization**

In order to obtain more data and to receive the data with greater accuracy, it becomes necessary to apply to the sonar equipment stabilization against the pitch and roll of the ship. There are at least two possible methods for introducing stabilization. The first is to position the projector mechanically according to the output functions of a stable element. These functions are *director train* [ $B'r$ ] *level* [ $L$ ], and *cross level* [ $Z'd$ ]. The BuOrd Bulletin, O.D. 3447, definitions are as follows:

*B'r Director train* (Stabilized Sight)—The angle between the fore and aft axis of own ship and the vertical plane through the line of sight (from the point upon which the range keeper or data computer bases its solution), measured in the deck plane clockwise from the bow.

*L Level angle*—Level angle measured about an axis in the horizontal plane; the angle between the horizontal plane and the deck plane, measured in the vertical plane through the line of sight. (Positive when the deck toward the target is below the horizontal plane.)

*Z'd Cross level angle*—Cross-level angle measured about an axis in the deck identified as the intersection of the plane of the deck with the plane through the line of sight perpendicular to the deck; the angle is measured between the vertical plane and a plane perpendicular to the deck through this axis. (Positive if, when one faces the target, the starboard side of the ship is up.)

The stable element gives these values as synchro orders which can be fed to the synchro-controlled servo systems directly attached to the three axes of the projector. Once the relative bearing and depression angle of the sound beam have been chosen, the stable element computes the necessary corrections to keep the beam trained always in the direction of the target during all changes in roll and pitch. A feature of this system is that the reference planes of both the bearing deviation indicator and the elevation deviation indicator are always in the horizontal

and vertical planes. From a maintenance point of view, this type of stabilization is not the most satisfactory. In one such system the level and cross-level control transformers, servo motors, and necessary mechanical components are located in a container which must be acoustically transparent, filled with an oil having the same impedance as sea water, and protruding from the bottom of the ship. This imposes the problem of building the motors and gears to operate in the oil without causing any noise at the projector face. The large number of moving parts in the oil, necessary to keep the projector stabilized, probably requires more maintenance than a fixed transducer. This system was developed by NRL as their integrated Type A sonar equipment.

The second type of stabilization is a two-axis system in which the outputs of the stable element are fed to a trunnion-tilt corrector. The trunnion-tilt corrector converts the three-axis corrections for roll and pitch to give train order in the deck plane and depression order in a plane normal to the deck. This system also keeps the center of the beam directed at the target during all conditions of roll and pitch. The reference plane of the BDI, however, does not remain vertical but is in the plane normal to the deck.

In the integrated Type B sonar the two signals from the trunnion-tilt corrector are used to position the receiving beam in space. The train order mechanically positions the transducer in azimuth with respect to the deck plane. Depression of the vertical beam is accomplished electrically by feeding the depression order to a servo attached to the listening commutators of the vertical scanning system.

In addition to positioning the listening beam, the scan indications on the cathode-ray tubes must be corrected to give azimuth in the horizontal plane and depression angle in a vertical plane. This can be accomplished by removing from the incoming scan information the components of train order and depression order which have been inserted by the stabilization equipment to stabilize the listening beam.

## 2.6.3

**Fire Control Information**

The purpose of sonar equipment is to supply information concerning any subsurface target. The present practice is to transmit the slant range, range rate, and bearing by word of mouth from the sonar operators to the conning officer. With these data and

the knowledge of own-ship's motion, the officer conns the attack.

The first means of improving this system would be to use conning aids such as templates or scales with which the conning officer would manually set up the problem from information supplied by the sonar operators. An improvement over this method would be to make an automatic geographical plot of the target and own ship. This has been accomplished in the General Electric attack plotter into which range, bearing, and ship motions are electrically inserted. More rigorous formulations of the complete attack problem have been solved by several different attack directors in which the bearing has been inserted by a synchro system, and the range has been received from the range recorder by a servo. Samples of this type are the Mark II, Mark III, and the Mark IV, Mod. O directors. All of these systems have shown some improvement in the utilization of the sonar data although the data are at times inaccurate and erratic.

The most successful method would appear to be one in which initial bearing and range are fed to rate-control mechanisms which commence generating ranges and bearings of the target. These generated values are then fed back to the primary sonar equipment to position both the bearing indicators and a cursor on the range recorder. The sonar operators now have only to introduce corrections to these generated values to produce accurate and consistent data. This system tends to eliminate some of the operational errors and to produce steady outputs from the sonar equipment. These more consistent data can now be inserted into the attack director which furnishes more accurate information for conning the attack.

#### 2.6.4 Synchro and Servo Requirements

Remote training of searchlight-type sonar systems was usually accomplished by observation of a repeat-back synchro indicator that was independent of the train-order system. While perhaps desirable for maximum assurance that no error is being introduced by the training not following the train order, such a system does not lend itself conveniently to the introduction of stabilization factors. If such a system is not used, more dependence must be placed on the reliability and accuracy of the servo systems that train the transducer or listening commutators. While

single-speed (1:1) synchro circuits are usually adequately accurate in comparison with the accuracy of sonar information under operating conditions, the dual-speed (1:1 and 36:1) systems are preferable for additional precision. The greater stiffness of servo systems with dual-speed synchro control may likewise be a determining factor towards use of the dual-speed arrangement.

Training speed of transducers has usually been limited by practical motor size limits to about 4 rpm. The very much smaller inertia of the listening commutator allows greatly increased training speeds without excessive motor size. A speed capability of 8 rpm is designed into the Sangamo XQHA sonar and even higher speeds should be readily obtainable, with the advantage that shifts from one target to another would require less lost time. High-speed servo operation usually leads to difficulties with either hunting or sluggishness, but these difficulties can be eliminated almost entirely by careful design. Specifications should be based on overshoot and lag error as functions of training speed.<sup>b</sup> Amplifier designs should be given particular attention to permit easy maintenance; to this end plug-in arrangements are attractive.

#### 2.7 DESIGN CONSIDERATIONS OF TRANSDUCERS

With multielement types of transducers such as are used in scanning sonar systems, the choice of frequency is a primary consideration, since this choice essentially determines the size of the transducer to be used. Experimental data have shown that for successful horizontal patterns to be obtained<sup>31</sup> with lag-line compensators, the value of  $ka/N$  must be less than, or equal to, 0.5. In this expression,  $a$  is the radius of the active face of the transducer;  $N$  is the number of elements in a full circle; and  $k$  equals  $2\pi f/c$ , where  $f$  is the frequency of the acoustic wave and  $c$  is the velocity of sound in the water. Therefore,  $ka/N$  is the center line to center line distance from element to element, expressed in wavelengths.

Both theory and experimental work have shown that the vertical pattern of a transducer becomes narrower as the vertical length of the individual element is increased. Figure 12 shows the total width of

<sup>b</sup> For high performance requirements, continuous-control servos are necessary; the most convenient arrangements use electronic amplifiers.

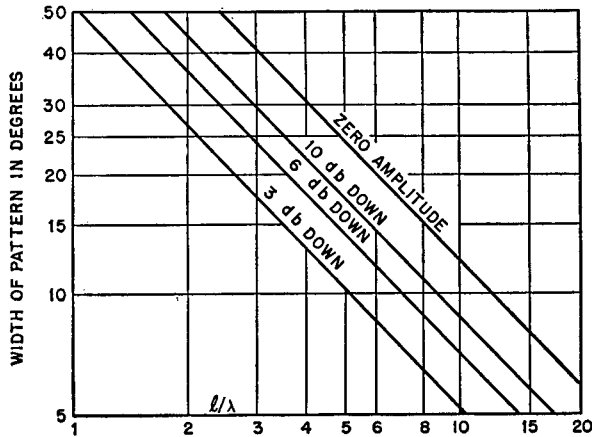


FIGURE 12. Total pattern width from square or line source at different levels below maximum.

pattern in degrees from a square or line source of dimension  $l$  at different levels below maximum. In this figure  $\lambda$  represents the wavelength of the sound wave in water. Narrower beams give better signal-to-noise ratio, as explained in Chapter 3, but are more subject to roll and pitch inconsistency. Maximum  $l/\lambda$  values of around 7 (that is, 18 inches at 26 kc), giving a pattern width of 12 degrees at  $-10$  db, have been used with reasonable success, but the best compromise from the overall operating viewpoint remains to be determined.

Careful consideration must be given to the phase angle existing between the sound energy falling perpendicularly upon the face of the element and the electric output of the element. It has been found from experience that while the actual value of this phase angle is unimportant, it must be uniform from element to element to within  $\pm 6$  degrees for satisfactory pattern formation.

This phase angle is made up of two parts, the first arising from the mechanical portion of the vibrating system, and the second arising from the electrical constants of the equivalent circuit. The mechanical part of the phase shift  $\beta$  for either magnetostriction or crystal transducers is given by

$$\tan \beta = \frac{2Q_m \Delta f}{f_r}$$

in which  $Q_m$  is the mechanical  $Q$  of the vibrating system,  $\Delta f$  is the difference between the resonant frequency of the individual element and the average frequency  $f_r$  of all the elements. In order that the variation of phase angle in the mechanical portion

of the system be within the desired limit,  $\Delta f$  or  $Q$ , or both, must be small. Since  $\Delta f$  can be kept small only by extreme precision of construction, transducers are usually designed with low  $Q$ . A  $Q$  of the order of 10 appears to be a good compromise between low efficiency and very low  $Q$ .

The electrical portion of the phase angle is given by

$$\tan \beta = \frac{2R\Delta X - X\Delta R}{4R^2 + X^2}$$

when the reactive component is tuned out, where  $\Delta$  indicates the difference of each individual element from the average element, and  $R$  and  $X$  indicate the average a-c resistance and the average reactance respectively, at the average resonant frequency. In order to satisfy the phase variation specification, therefore,

$$\frac{2Q_m \Delta f}{f_r} + \frac{2R\Delta X - X\Delta R}{4R^2 + X^2} < 0.1$$

should hold, since the two portions are independent.

The diameter of the transducer is determined in part by the size of the opening through which it must pass to be let out of the bottom of the ship. A standard size of this type of opening with dome is shown in Figure 13. If narrower beams are required, they can be obtained only by increasing the frequency or by increasing the size of the transducer.

The active materials to be used in the construction of this type of transducer are somewhat limited. Piezoelectric transducers may be constructed of either X- or Y-cut Rochelle salt crystals or Z-cut ammonium dihydrogen phosphate [ADP] crystals. Magnetostriction transducers normally are made from nickel or nickel alloy laminations. The choice of either the piezoelectric or magnetostrictive type of transducer depends upon the relative availability of materials, manufacturing convenience, and the electrical impedance desired.

In the mechanical construction of transducers, special consideration must be given to the water pressures to which these units are subjected. In addition, a transducer which is designed to be mounted topside on the deck of a submarine must be constructed to withstand the impact force of waves when the submarine is cruising on the surface.

This type of transducer generally varies from 500 to 1,000 pounds in weight. Consequently, special consideration should be given to means of handling a

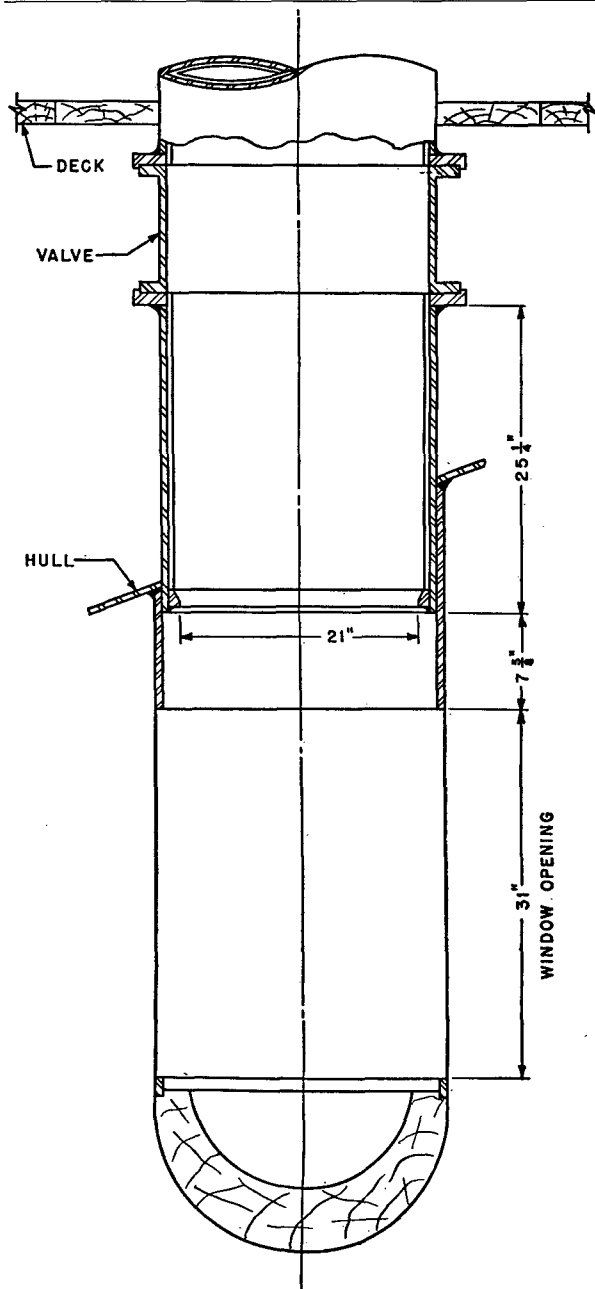


FIGURE 13. Standard QC-JK dome and hull opening.

piece of equipment of this kind, which is both delicate and heavy. Special care should be taken so that the active face of the transducer is not subjected to shock or undue pressure, such as contact with some sharp object. The material used in the structural part of the transducer should be either stainless steel or bronze casting to withstand the action of sea water. Transducers to be used bottomside on either ships or submarines normally are fastened to a standard QC flange.

In order to assure complete acoustic contact between the element faces and the rubber boot on a transducer, it has been the custom to vacuum-fill the space between them with castor oil. Recently constructed transducers, however, have been made with a slightly undersized boot which makes a pressure contact with the faces of the elements. A smearing of castor oil on the inside of the boot is used to assure good acoustic contact. It has been found that this type of construction gives greater efficiency and is much easier to handle during construction or replacing of elements than the oil-filled type. This method was used in the construction of several magnetostriction transducers, but up to the present time it has not been used on a crystal-type transducer. However, the presence of oil in crystal transducers gives a higher dielectric constant between electrodes than would be obtained with air, and thus may be more suitable for the high voltages necessary to obtain the desired power in this type of transducer.

Attention should be given to the kind of cable to be used. If it is possible to locate the rotor inside the transducer the cabling problem is considerably simplified, since the pair of wires from each element do not have to be brought out of the transducer itself.

It is desirable, upon transmitting, to get as much acoustic power as possible into the water. It has been found<sup>32</sup> that cavitation does not occur with a power less than 2 watts per sq cm with a 30-millisecond pulse or 20 to 30 watts per sq cm with a 3-millisecond pulse.

It is obviously desirable to use as small an amount of electrical power as possible and still put enough power in the water to be just under the cavitation point. In order to achieve this the efficiency of the transducer is of considerable importance. Experience has shown that it is difficult to obtain efficiencies over 30 or 40 per cent.<sup>33</sup>

Special consideration should be given to the desired impedance of the individual elements of the transducer. Various factors may enter into the determination of this impedance. Since it is desired to obtain the greatest possible power from the transducer, it is obvious that neither extremely high nor extremely low impedances would be satisfactory. In the case of a high impedance, large voltages and thick insulation would have to be used in order to obtain the desired power; while with low impedance values, large currents would be drawn necessitating heavy wire which, in some instances, would approach bus

bar proportions. Consideration must also be given to the components to be used in the transfer network, such as coupling transformers and capacitors.

It should be remembered that during transmission the elements are connected in parallel, whereas in reception the outputs of the individual elements are fed separately into a beam-forming device. Therefore, in order to match properly the impedances presented by coupling transformers when receiving, and to take account of the transmitting coupling capacitors, the impedances of the individual elements should be chosen with regard to the impedance values of transformers which are available, and also with attention to available sizes of transmitting coupling capacitors. It has been found from experience in design and construction that a reasonable value for the impedance of a magnetostriction transducer element is  $50 + j100$  ohms. This gives approximately  $1.04 + j2.08$  ohms for a 48-element transducer with the elements connected in parallel. These values can be obtained with magnetostrictive types of transducers, without using either extremely small or extremely large wire in the windings.

In general, crystal-type transducers have a much higher impedance than the magnetostrictive type. The 45-degree X-cut Rochelle salt crystals have been found to have considerable variation of impedance with temperature. A variation from  $140 - j1,200$  ohms at 0 C to  $60 - j700$  ohms at 18 C is not uncommon for this type of crystal transducer. Y-cut Rochelle salt crystals, which have much less impedance variation with temperature, have been found to have impedances averaging  $500 - j6,600$  ohms. The ADP crystals have been found to be more stable than either the X- or Y-cut Rochelle salt, and an average impedance for this type of crystal might be  $1,000 - j7,400$  ohms.

Table 2 lists all the multielement scanning sonar transducers used by HUSL, with the various systems developed. The table gives the names, dimensions, frequency, number of elements, material used for the elements, the systems in which they were used, the number constructed, and the manufacturer.

## 2.8 PRINCIPLES OF PATTERN FORMATION AND BEAM ROTATION

In the present section, the receiving pattern in a plane normal to the axis of the cylinder is referred to as the directivity pattern of a cylindrical trans-

ducer. (The pattern in the plane through the axis of the cylinder is approximately that of a line source having a length equal to that of the transducer.) It is obvious that the problem of pattern formation for scanning sonar is more complicated than for most other sonar systems. This is due principally to the fact that the active face of the transducer is cylindrical rather than flat in shape, as is usually the case for sharp-beamed searchlight system transducers. The necessity for rotating the pattern places relatively weak restrictions on it, so that the problem is reduced essentially to one of forming a stationary directional pattern.

The cylindrical transducer is divided into strips parallel to the axis of the cylinder. The receiving pattern is formed by combining the signals from these elements in a predetermined manner. This combining process involves weighting as well as delaying the various signals by different amounts to give a resulting pattern that is highly sensitive in one direction, while relatively insensitive in all other directions. A theory of pattern formation is given in Chapter 9 that tells how to attenuate and delay the various signals to yield a pattern of a given width. It appears that the time delays approximately compensate for the different time delays of signals in the water. That is, looking in at the electrical terminals, the transducer is made to appear flat. Once this is done, the usual shading techniques may be employed to suppress the minor lobes.

The above explanation is highly oversimplified. The size of the transducer in wavelengths and the number of elements in the transducer limit the narrowness of the pattern actually attainable. In Chapter 9 it is shown that the narrowest desirable pattern—that is, the pattern of minimum directivity ratio—is approximately that of a line source of length

$$l = (N + 1) \frac{\lambda}{2\pi},$$

where  $N$  is the number of elements and  $\lambda$  is the wavelength of the signal. The width of the major lobe 6 db down from the peak is then about  $435/(N + 1)$  degrees. It is also shown in Chapter 9 that if the minor lobes are to be low and the rotatability of the pattern is to be good, it is necessary that the width of the single elements should not be greater than half a wavelength. Practical considerations, such as handling and working with the laminations that are stacked to form the elements, make it desirable to

use as wide an element as possible. There is the temptation, therefore, to break this restriction and make the elements wider than half a wavelength. This has actually been done in certain cases to the extent of having elements as wide as  $5/9$  of a wavelength. There are indications that this is close to the limit.

When the elements are half a wavelength wide, the pattern of minimum directivity ratio is approximately that of a line source whose length is equal to the diameter of the transducer. This narrowest pattern has minor lobes which are only 13.5 db below the major lobe, so that it is necessary to sacrifice the

TABLE 2. Scanning Sonar Transducers.  
(Magnetostriction)

Name	Dimensions of active face (in inches)		No. of elements	Material used in elements	Frequency (in kc)	Systems for which designed	Manufacturer	No. of units constructed*	Remarks
	Diameter	Height							
Medusa	12	6	36	Nickel Ribs (residual magnetism polarized)	Flat	First CR System	HUSL	1	Discarded because of poor patterns and low efficiency.
Millerphone (Casketphone)	15	15	36	Nickel Tubes (Alnico magnet polarized)	22	CR System	HUSL	1	Discarded because of poor patterns.
Hebbphone—1	15	12	36	Nickel Laminations (current polarized)	21	CR & ER Systems	HUSL	1	First successful scanning sonar transducer.
Hebbphone—2	18	18	36	Nickel Laminations (current polarized)	22	CR System	HUSL	1	Leaked so that design was discarded and HP-2B built from same laminated stacks.
Hebbphone—2B	17½	18	36	Nickel Laminations (current polarized)	22	CR System	HUSL	1	Vacuum filled with castor oil.
Hebbphone—3	17½	4 stacks each 3¾ of active face—total 17½	48	Nickel Laminations Vinylite permanent—magnet polarized	27	Tests only	HUSL	1	Shaded vertically. Tight rubber boot, castor oil film contact.
Hebbphone—3S	17½ at top—21 at bottom	4 stacks each 3¾ of active face—total slant height 17½	48	Nickel Laminations p-m	27	Submarine ER System (Topside)	HUSL	2	6° taper.
Hebbphone—3DS	22.16	2 stacks each 3¾ of active face—total 8¾	48 on 270°	Nickel Laminations p-m	27	Preliminary depth scanning tests	HUSL	2	No. 1 used on CYTHERA.
Hebbphone—4	18	Design incomplete—like HP-3	36	Nickel Laminations p-m	27.2	....	....	....	Design discarded because of too high value of $ka/N$ .
Hebbphone—5	17½	4 stacks each 3½ of active face—total 16	48	Nickel Laminations p-m	25.5	XQHA (CR) System	Sangamo Electric Company	5 delivered	Like HP-3; not shaded.
Hebbphone—6	....	....	64	Nickel Laminations p-m	36	ER System	....	....	Design discarded; laminations too delicate.
Hebbphone—7	....	....	60	Nickel Laminations p-m	32	ER System	....	....	Design discarded in favor of 48 elements.
Hebbphone—8	14.7	2 stacks each 3 of active face—total 7¼	48 on 270°	Nickel Laminations p-m	38	Depth scanning in Integrated ASW Type B System	HUSL	4	Under construction.
Hebbphone—9	....	....	48	Nickel Laminations	31	ER System	....	....	Design incomplete.
Ring Ladderphone	12	10	48	Nickel Laminations p-m (complete ring)	36	Experimental Transducer	HUSL	1	Under construction.
SP	17.5	14	48	Nickel Laminations p-m	28	....	....	....	Design discarded for insufficient radiation loading.

\* As of May 1945.

CONFIDENTIAL



TABLE 2 (Continued)  
(Piezoelectric)

Name	Dimensions of active face (in inches)		No. of elements	Material used in elements	Frequency (in kc)	Systems for which designed	Manufacturer	No. of units constructed*	Remarks
	Diameter	Height							
CPI-1 # 770	13½	15¾	36	45° X-cut Rochelle salt	20	....	UCDWR	1	Patterns unsatisfactory.
AX-89	15¼	14¾	36	Y-cut Rochelle salt	22	CR System	Brush Development Company	2	One damaged; one used experimentally.
AX-104	7¼	4	36	Y-cut Rochelle salt	53	Experimental ER System	Brush Development Company	1	Loan from NOL.
AX-127	15½	12¾	48	ADP crystals	26	CR or ER System	Brush Development Company	Order outstanding	Interchangeable with HP-3 or HP-5. Shaded.
AX-132	14½ at top—16¾ at bottom	10 slant height	48	ADP crystals	32	Submarine ER System (Topside)	Brush Development Company	5	No. 1 in use; poor. No. 2 good.
AX-136	14½	10	48	ADP crystals	38†	Submarine ER System (Bottomside)	Brush Development Company	1 (5 more on order)	Good patterns.
AX-142	15	6	48 on 270°	ADP crystals	38	Depth scanning in Integrated ASW Type B System	Brush Development Company	Order outstanding for 4	One expected May 15, 1945.

\* As of May 1945.

† Designed for 32—actually 38.

width of the major lobe, which is the principal factor in determining directivity ratio, in order to reduce the minor lobes below some desired value.

The time delays and attenuations of each of the  $N$  elements are given in Chapter 9. It is found that the contribution of the elements at the sides and back of the transducer is small. From practical considerations concerning the compensating networks which introduce the attenuation and time delay, it is desirable to use as few elements as possible in forming the beam. It has been found in practice that it is possible to neglect elements which contribute 15 to 20 db less than the front elements, with the result that only the front 120 degrees or so of the transducer is used in the pattern formation. However, this neglect must not be pushed too far, since it may introduce rather high broad minor lobes around the side at 90 to 120 degrees with the principal direction.

There is one point that requires emphasis which has not been mentioned above. It was pointed out that time delay networks are used in forming the pattern. These time delays are relatively critical in controlling the width of the major lobe. It is, therefore, important not only that the time delay networks be constructed accurately, but also that variations be avoided in time delay introduced in the signals

before the pattern is formed. This accounts for the rather stringent requirements mentioned above for the uniformity of phasing of the individual elements of the transducer. It is easier to obtain uniformity in phase, which requires in turn uniformity of resonance frequency and sharpness of resonance, when the resonance is relatively broad. There are also strict requirements on the uniformity in sensitivity of the elements in order to get a good pattern.

Considerations such as the above, requiring precision in the construction of the elements of the transducer, do not apply so strongly to ER sonar as to CR sonar. This is because ER sonar, as designed at present, does not make optimum use of phase control in forming the pattern. Phase control is referred to here, rather than time delay control, because a lead line is used in ER sonar. This means that the best obtainable pattern for ER sonar is not so good as for CR sonar; in fact, in the present state of development the beam is 50 per cent wider. However, it still may be narrow enough for certain purposes.

The theory of pattern formation for ER sonar is quite different from that for CR sonar. All the elements are connected at equal intervals to a lead line which has a certain phase lead and attenuation per section. Thus each point on the lead line exhibits

CONFIDENTIAL

not only the signal of the element directly connected to the point, but also contributions from the signals from all the other elements after they have been phase-led and attenuated by the network. Finally, combining-circuits, actuated by a switching pulse, add the signals appearing at nearby junction points in certain proportions. The controllable parameters which determine the final patterns are, therefore, the shape of the switching pulse and the constants of the lead line.

## 2.9 COMMUTATOR DESIGN CONSIDERATIONS

### 2.9.1 General Considerations Concerning CR versus ER Commutators

The possibility of securing a beam pattern from a multielement cylindrical type of transducer and the manner in which this is accomplished has been discussed in the previous section. To rotate the direction of the beam of sensitivity, when the transducer is fixed in position, necessitates a switching device which in general has as many switching elements as there are elements around the periphery of the transducer. There are two general methods by which this rotation may be produced: (1) by use of a mechanically rotating device, or (2) by use of electronic circuits.

Where beam rotation is performed by mechanical means, as with the capacitive commutator, the minimum length of the pulse is determined in practice by the maximum allowable speed of the commutator rotor, which in turn is limited by mechanical stresses in the rotating parts. In the present state of development, the scanning speed is limited to 30 rps with a capacitive commutator but it seems likely that either an inductive or capacitive commutator could safely be rotated at considerably higher speed. With electronic rotation scanning, a much higher scanning speed can be obtained readily with a correspondingly shorter transmitted pulse. With short pulses, however, aural identification of echo signals by use of a listening channel is almost impossible, since little semblance of a tone is produced. The advantages derived from identification of targets by doppler effect are, therefore, lost.

Although CR scanning presents problems in mechanical design of the capacitive or inductive commutator, it is the more simple and direct means of

beam rotation. Once made, the commutator requires little maintenance and is very reliable in its operation. In the ER system no mechanical rotating parts are necessary, which is an advantage. A large number of circuit elements are required, however, including varistors or vacuum tubes. Varistors particularly are subject to failure and require close maintenance. The ER system has the advantage of higher signal-to-reverberation ratio because of its short transmitted pulse.

### 2.9.2 Capacitive or Inductive Commutators

With a cylindrical transducer having 48 elements evenly spaced around its periphery, it would be possible to form a receiving beam in any one of the 48 positions by use of a simple 48-position switch to connect the respective transducer elements to the proper points in the beam-forming network. However, as the beam could be formed only in these integral positions, the bearing of an echo source could be determined only to within 7.5 degrees. Since bearing accuracies of 1 degree or better are demanded, and it is impractical to build transducers with a very large number of staves, a means of rotating the beam and at the same time preserving the pattern between integral angular positions is necessary. This requirement necessitates the use of capacitive or inductive coupling methods. Both are practical, though the capacitive type has been used in all the developmental scanning sonars.

It is necessary that proper impedance matching be obtained between the transducer and the beam-forming network. Where, for example, the high impedance capacitive commutator is used, transformers with high impedance secondaries are needed.

The beam-forming network must introduce into the signals from the respective transducer elements time lags which compensate for those occurring in the water. Figure 14 shows that sound having a wave front parallel to *AA*, which is drawn at the time this wave front reaches the forward-looking transducer segments 1L-1R, arrives at 2L-2R, 3L-3R, and 4L-4R at increasingly later times. By introducing no lags in the outputs from 4L-4R and appropriately increasing lags in the outputs from 3L-3R, 2L-2R, and 1L-1R, the signals from all elements are brought together in phase to the receiver. As a result, the signal to the receiver is that which would have been obtained from a flat-face transducer whose elements are on the line

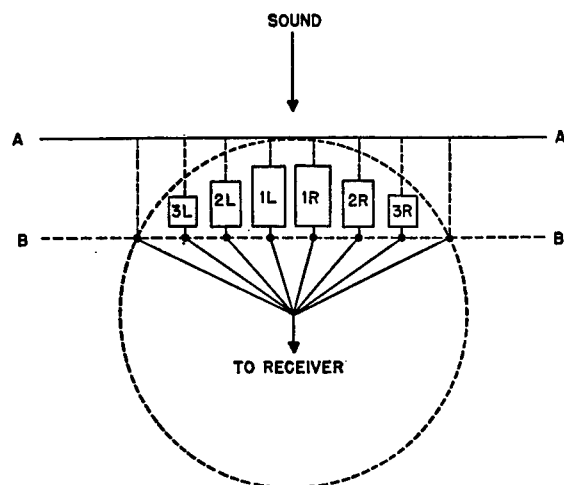


FIGURE 14. Basic principle of CR beam formation.

*BB.* The amplitude of this signal varies with change in the direction of the incident sound very much as it would from such a flat-face transducer. Also, as in the case of a flat-face transducer, reduction of minor lobes in the beam pattern is obtained by proper control of the amplitudes of the signals from the various transducer elements.

The output of the beam-forming network must be fed to the receiver through a coupling that allows rotation. When this has been done, the signal has all characteristics of that from a flat-face transducer which faces in a direction determined by the position of the commutator rotor.

Development to date has been devoted almost exclusively to the capacitive commutator, and the further discussion of design considerations are based on this type. Signals from the individual transducer elements are fed to an equal number of capacitive plates arranged in a circle, called the stator, which are faced by an identical set of plates mounted on a rotor. The beam-forming network or lag line is connected to a certain number of these rotor plates. As the plates form an arrangement of capacitors and do not touch, interpolation is obtained as the rotor is turned from one in-register position to the next; that is, the beam is rotated smoothly and continuously by movement of the rotor with only slight changes in pattern shape.

Limitations of mechanical design preclude the possibility of obtaining capacitances between pairs of rotor and stator elements much greater than about  $100 \mu\mu\text{f}$ . Consequently, with operating frequencies in the range from 20 to 40 kc, the commutator intro-

duces a reactance of 80,000 to 40,000 ohms into each signal channel. It is, therefore, essentially a high impedance device. Since a magnetostriction transducer has a low impedance per element (20 to 200 ohms), and the high impedance of a piezoelectric crystal transducer element must be transformed down to a similarly low impedance to avoid cable loss, input transformers are desirable for proper matching of circuit impedances.

The equivalent circuit for any one channel from magnetostrictive transducer element to beam-forming network is shown in Figure 15.  $R_c$  is the resistance of the network as seen from any rotor capacitor plate. At its resonant frequency the electrical  $Q$  of a magnetostrictive transducer element is generally in the neighborhood of 2. The transmitting capacitor, which during the receiving period is in parallel with the transducer, is usually of such value that the overall  $Q$  of the combination is near unity. If the transformer leakage inductance is small, the value of  $R_c$  should, therefore, be of the same magnitude as the capacitive reactance of the commutator. This follows from the fact that the beam-forming network is an energy sink, and to transfer maximum power from the transducer element to this network, the impedances  $Z_1$  and  $Z_2$  must be complex conjugates.

Figure 16 shows the method of feeding the echo signals into the beam-forming network, which is a shunt-fed lag line. The series resistances  $R'$  are required to attenuate the signals by certain amounts (see Chapter 6) to aid in the beam formation. The shunt resistances  $R''$  are adjusted to give uniform values of the input resistance  $R_c$  as seen from the rotor plates.

All the rotor elements are not connected to the

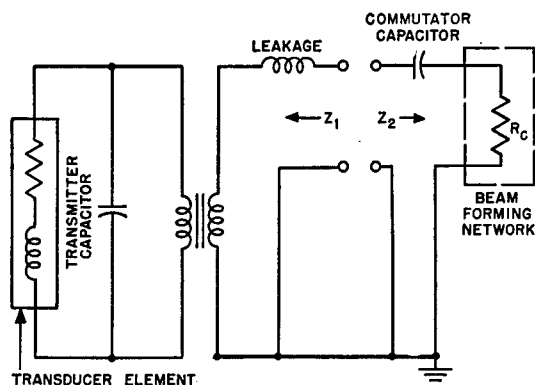


FIGURE 15. Equivalent circuit for one CR element channel.

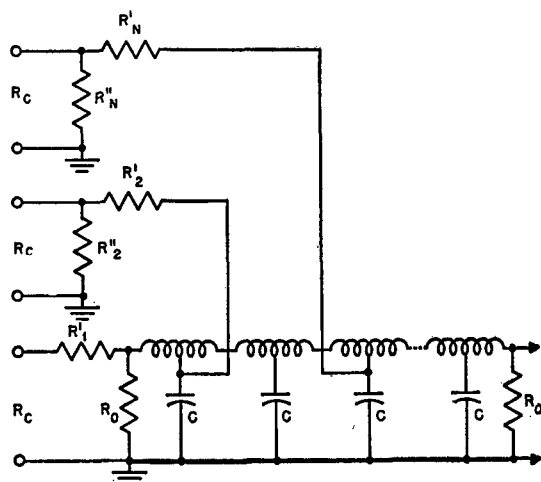


FIGURE 16. Method of feeding signals into lag line.

beam-forming network. Usually an even number of elements, called active elements, covering about 120 degrees of the transducer periphery are used to feed signals into the lag line. The number is determined largely by the following consideration: If it is desired to keep all minor lobes below  $-20$  db, enough rotor elements should be used so that the last one has a total attenuation of about 20 db. By total attenuation is meant that given by the pattern of the individual transducer stave together with the attenuation produced in the shading network (see Chapter 9). By using an even number of active rotor elements, the maximum sensitivity of the beam occurs in the direction of the center of the circular arc occupied by these elements and their corresponding transducer staves when the rotor and stator elements are in register. For those signal channels which are not connected to the lag line, the rotor plates should be terminated to ground by a resistance equal to  $R_0$ .

It is obvious that the various signal channels from the transducer cable junction box to the commutator—48 in number if a 48-element transducer is used—should have as uniform characteristics as possible. The input transformers should be tested individually to within close limits for uniformity of phase-shift and voltage-ratio characteristics. They should be located close to the commutator stator so that not more than one or two inches of lead is needed to connect the high potential end of any one secondary to its stator element. Transformers having electroshields between windings should be used, and the shields should be connected to the ground return of the secondaries. All leads should be kept as short as

possible; the high impedance leads should be well shielded electrostatically and the low impedance circuits well protected from magnetic pickup by the use of twisted leads. The ground connection on the lag line itself should not be made to the case or any metal part of the rotor shaft but should be made through a slip ring insulated from the shaft; it should make its first connection to the chassis or frame of the commutator at the input terminal of the preamplifier. A slip ring should be connected to the rotor shaft and grounded through a brush to the commutator frame with as short a lead as possible. This is to prevent noise arising in the rotor bearing from becoming mixed with the signal output of the lag line. The whole stator and rotor combination itself should be enclosed in an electrostatic shield. The commutator should be kept free from strong a-c magnetic fields when installed, since it is possible to generate an appreciable output because of the rotating lag line cutting this field.

In designing the beam-forming lag line, it is preferable to use a low-pass filter section whose phase shift is approximately a linear function of frequency, to match that which occurs in the water. The type of section is somewhat arbitrary; however, the bridged-T type, discussed in Chapter 6, has been used with considerable success. Toroidal coils using powdered molybdenum-permalloy cores are recommended for the inductive elements of the filter section. The line should be terminated at both ends in resistances which allow no energy reflection to take place at the center operating frequency of the system. If the filter sections have been properly designed, this termination should remain satisfactory over the sonar frequency range.

Considerable latitude in the choice of line impedance is possible. In general, it should have as high an image impedance as may be practical. However, an upper limit of approximately 15,000 ohms is imposed by stray capacitance effects, since in a high impedance line a few  $\mu\mu\text{f}$  of stray capacitance between a coil junction and ground may cause too great a change in the phase shift of a section. In selecting the line impedance, factors other than the stray capacitance must also be considered. If the line impedance is high, then the effective resistances shunted across the line at the signal-injection points become relatively low, and an excessive diminution of signal along the line results. On the other hand, if the line image impedance is made small compared to the

value of  $R_c$ , then only a small percentage of the echo signal appearing across  $R_c$  is impressed across the line at the injection point. The choice of line impedance is, therefore, a compromise between these two conflicting factors. Equations for calculating  $R'$  and  $R''$  for chosen values of image impedance  $R_c$  and amplitude shading are given in Chapter 6.

Signals from transducer staves equidistant from the head-on point may be applied to the lag line at the same injection point, or twin lag lines may be used. In the second case, the two lines are terminated on each other at their output ends, the output-signal lead being connected to their common junction point. This method results in half the bridging loss that occurs in the double-fed single lag line, but twice the number of inductors and capacitors are needed, as well as more space in the rotor. However, where right- and left-steered output channels are needed for BDI, the twin-line construction is necessary, and either separate terminations are required or an extra section must be inserted for the BDI comparison.

Once the phase lags necessary to form the beam pattern have been determined, the question of phase lag per line section and the number of sections must be considered. Fortunately, the phase delays required for the signals from the first four or five transducer staves away from the head-on point are almost exact multiples, so that uniform sections can be used. Those for successive elements do not follow this simple progression, however, and the designer is faced by the problem of finding the proper sized sections to fit the phasing requirements. One of the two following procedures may be used; either the line may be designed using uniform sections throughout with the phase shift per section selected to fit the overall phasing requirements as nearly as possible, or different sized sections may be used to meet the requirements in a more exact manner. The first method has several advantages from the manufacturing point of view, but in general does not yield quite so good a pattern in terms of minor lobe reduction as the second. Past experience seems to indicate that a  $\pm 5$  per cent tolerance in meeting the phase requirements at each injection point is permissible.<sup>34</sup>

If different sized sections are used, they should be designed to make the image impedance the same for each to avoid energy reflection at their junction points. This means that the cutoff frequency of each section should be several times greater than the operating frequency; preferably eight or nine times larger.

In selecting lag line elements, coils should be trimmed to within at least  $\pm 1$  per cent of the specified inductance at the expected operating frequency. The capacitors also should be selected to within the same tolerance. The terminating resistances at both ends of the line, after their values have been determined experimentally, should be selected to within  $\pm 1$  per cent of the proper values.

The quality of the beam pattern is more sensitive to deviations in phase shift at the injection points than to deviations in signal amplitude. For this reason it appears permissible to use 5 per cent RMA resistors in the shading network for the resistances  $R'$  and  $R''$  in Figure 16.

It was early suggested that the quality of the pattern in the interregister positions of the commutator could be improved by increasing the number of rotor segments and, therefore, the number of points at which signals are fed into the lag line. From the standpoint of lag-line design, this is not difficult; the main limitations lie in the mechanical design problems associated with increasing the number of rotor segments.

The output signal of the lag line must be brought out of the commutator rotor by means of some type of ring arrangement. If a contact type of slip ring is used, ring material and brush material should be such that together they have an extremely low contact resistance. With proper design and adjustment of brush pressure, the noise due to commutator rotation can be kept quite small, particularly if the slip ring is not required to carry appreciable current. There is always a tendency for slip rings to become noisy under service conditions. Nonconductive slip rings, either capacitive or inductive, are free from this trouble.

Since the circuit from the lag line to the preamplifier is a high impedance channel, the preamplifier must be mounted directly on the commutator or as close to it as possible. Design requirements for the preamplifier are:

1. Internal noise level less than thermal noise from the input impedance.
2. Low output impedance.
3. Gain reasonably independent of line voltage fluctuations and tube changes.
4. Amount of gain and frequency response in accordance with design of receiving portion of system. (This may or may not involve selectivity in the preamplifier.)

When dual preamplifiers are needed for BDI application, the requirements are more stringent. In addition to those already listed, these are:

5. Gain of the two channels must be the same, and remain the same with line voltage fluctuations, and tube changes.

6. Differential phase shift between the two channels must be very small, and remain small with line-voltage fluctuations and tube changes, over the operating frequency range.

The requirements in the first set are not difficult to meet with simple circuits, and those in the second set may be satisfied if negative feedback is used. Detailed descriptions of suitable designs used are given in Chapter 6.

#### MECHANICAL CONSIDERATIONS

The spacing between the rotor and stator capacitor segments is a function of their size and the required capacitance; experience indicates that the capacitive relation between the two sets of segments should be uniform to within  $\pm 12$  per cent of the total value. This corresponds to a  $\pm 12$  per cent variation in the air gap between the rotor and stator and includes both the overall variation in gap between the various rotor segments and their corresponding stator segments when the rotor is stationary, and the variation as a single rotor segment is moved from segment to segment of the stator. These capacitor segments may be of any material as long as they are conducting, corrosion-resistant, and mounted so that they can be rotated. One method of meeting the requirements involves cementing steel plates to an insulating disk and cutting the steel into segments. There are other methods, but to date the most successful is based on spraying and firing silver on the flat face of a circular insulator. The insulator itself can be any material which meets the requirements listed in Chapter 5, but, in general, a ceramic or glass seems to be the most satisfactory. Also in Chapter 5 is a discussion of the materials and metallizing methods tried at HUSL.

Two forms of commutators have been tried; the plate form, in which the segments are located on flat disks, and the cylindrical form, in which the segments are located on two concentric cylinders (see Chapter 5). These plates or cylinders must be nonconducting and strong enough to stand a high rotation speed. In addition, it must be possible to machine or grind them accurately and to mount them so that the air

gap between the stator and rotor is uniform, as described above.

High rotation speed is desirable from the electrical standpoint, but is limited mechanically. Large plates are needed to secure the required capacitances of about 100  $\mu\mu\text{f}$  between pairs of segments, but the smaller the plate, the faster it can safely be rotated. The maximum rotation speed that has been used is 1,800 rpm. It is possible that this can be increased when better plate materials and mounting methods are found, and possibly the cylindrical commutator could safely be rotated at a faster rate.

Fairly small plates can be made to meet both the electrical and the mechanical requirements if, instead of one rotor and one stator, two or more of each are connected in parallel. Tolerances on the uniformity of air gap may be relaxed if the rotating segments are connected in parallel and rotate *between* the stationary segments, which are likewise connected in parallel. In this case a decrease in capacitance on one side is accompanied by an approximately corresponding increase on the other. However, use of more than two plates has been found to complicate both manufacture and assembly to such an extent that quantity production does not appear practical for commutators of this type. Using a single rotor and single stator seems better, but as the active segment area is decreased, the air gap must also be decreased to maintain the 100  $\mu\mu\text{f}$  capacitance. The allowable variation in gap then decreases correspondingly, and a fairly definite practical limit is reached. As a compromise between these opposing electrical and mechanical requirements, an air gap of 0.0035 inch and two plates, 11 inches in outside diameter and  $4\frac{3}{8}$  inches inside segment diameter, are being used by the Sangamo Electric Company for the XQHA commutators. These have proved satisfactory. All plate form commutators made at HUSL have had double stators and rotors connected in parallel, as described above, with an air gap of 0.005 inch.

Both the rotor and stator may have electric connections to the individual capacitor segments. Two of the many possible methods of doing this have proved reasonably satisfactory in practice. Both of these are based on using fired silver coatings for the capacitive segments (see Chapter 5), the silver being carried through holes in the plates or cylinders. In one case, banana plugs are inserted into these holes, and in the other, bushings are soldered into the holes and leads soldered into the bushings. In general, it is

felt that the positive connection given by soldering is preferable to the banana plug method, but some difficulties have been encountered in making sure the bushings do not pull out.

Signals must be brought off the rotating section of the commutator, and two methods have been tried to date: (1) slip rings and brushes and (2) capacitive rings on rotor and stator. Experience at HUSL indicates that slip rings may be made of coin silver, or of some material with similar properties, but should be kept small so that the surface speed is low. Brushes should be of hard long-wearing low-dusting quality. Preforming of the contact area to the curvature of the slip rings seems of value in reducing noise. Low brush pressure and the use of several brushes in parallel on each ring also seems desirable. Brushes with contact areas of a silver-graphite compound have proved quite satisfactory for test commutators, but there is still considerable doubt as to how long they can stand up and remain quiet under continuous operation.

A better method from many standpoints involves no rubbing parts and requires only that a set of rings be rotated close to a similar stationary set, these being made the electrodes of a capacitor. The capacitive output introduces no electrical noise, and of course is excellent for continuous operation. This method, however, introduces the mechanical complications of mounting a second set of insulating plates and maintaining a second small air gap. In this case, though, constancy of air gap is not so critical as that on the input end, and the gap does not need to be so small, a gap of 0.008 inch having been used successfully. There are many possibilities for simplifying this capacitive output method, and it is also possible that the output could be taken off the lag line inductively.<sup>c</sup> For several reasons it is simpler to place the lag line within the rotating member. A stationary lag line might prove as satisfactory as the rotating one, but only one commutator has been built this way to date. This method simplifies commutator construction by reducing the number of parts which must be mounted, balanced, and rotated, but complicates it by requiring the number of output slip rings or capacitive or inductive couplings to be equal to the number of active rotor elements. This is a function of the total number of elements of the transducer; for some of the transducers as many as 22 rings are re-

quired. If, on the other hand, the lag line is rotated, only three output rings are needed with a double line and only two with a single line. This is a decided mechanical advantage. Commutators of this type are discussed in Chapter 5.

#### OTHER MISCELLANEOUS DESIGN CONSIDERATIONS

The initial assembly should be as simple and fool-proof as possible. Once the components are mounted and aligned, they should be pinned in place so that alignment can be regained if the commutator has to be taken apart. The possibility of servicing the commutator or replacing parts away from the factory, while desirable, has not been found practical in designs used thus far.

The fact that the commutator must be designed for continuous operation is important. It must be protected from salt spray, be as corrosion-resistant as possible, and be shock-mounted.

If the commutator output is to be through slip rings, rather than through capacitive or inductive coupling, it must be possible to remove and replace the brushes without disassembling the entire commutator.

For ease of manufacture, the scanning and listening commutators should be as much alike as possible. The most serious difficulty in manufacturing capacitive commutators is to maintain the required close tolerances in quantity production. Of course, good bearings and carefully fitted parts are required, but aside from special provisions for mounting and handling the fragile plates or cylinders, there is nothing in the commutators which cannot be made by normal precision methods.

### 2.9.3 Electronic Rotation Commutators

#### ELECTRONIC CONSIDERATIONS

In order to achieve scanning speeds of 200 rps and higher, it is necessary to use some electronic method of rotation. Electronic rotation is accomplished in two steps as follows:

1. A number of fixed beams of sensitivity are formed by compensating networks connected to a multielement transducer and are brought out to a number of terminals. For example, in the ER submarine sonar, each one of a set of 48 terminals is connected by sections of a lead line to the elements of the 48-element transducer, as indicated in Figure 17.

2. Electronic switches are connected to the ter-

<sup>c</sup> For a more complete discussion of the possible methods of accomplishing this, see Chapter 10.

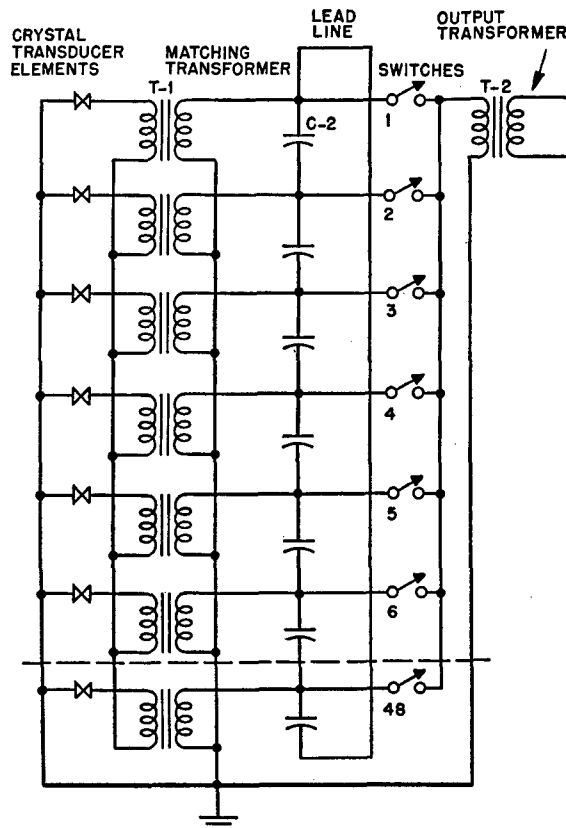


FIGURE 17. ER sonar rotor (simplified).

minals, as shown, and are operated in cyclic order so that the receiver is connected to each of the numbered terminals in succession, thus producing the effect of a rotating beam. Smooth rotation is produced by operating adjacent switches in various proportions; this also affects the shape of the rotating beam.

The simplest form which the compensating networks can take is a single lead-line ring in which the transducer segments form parts of the shunt elements. Such lines are described in a brief manner earlier in Chapter 2, and more fully in Chapters 7 and 9. Opera-

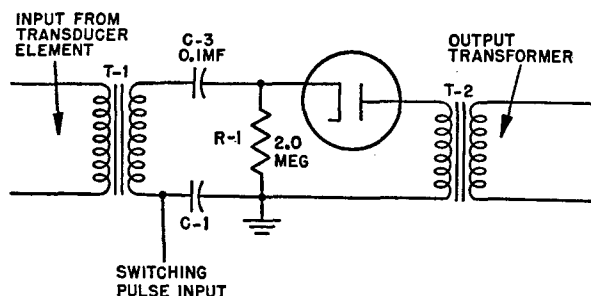


FIGURE 18. Sample diode switch.

tion of the electronic switches is controlled by application of appropriate voltage pulses. These switching pulses are applied cyclically to the respective electronic switches, their shapes determining the nature of the combination of signals from the various points on the lead line. In order to obtain such cyclic pulses it is convenient to use a lag line down which a pulse of the desired shape travels, and to obtain the switching voltages from equally spaced points on this line.

The switches indicated in Figure 17 are of the series type and may be rectifiers such as vacuum tube diodes or varistors, or they may be multielement vacuum tubes such as triodes or pentodes. Figure 18 shows a sample circuit to illustrate the action of a diode switch. Figure 19 shows a circuit of the lag line for use with diode switches. This line is not in the form of a ring and in order to insure that there is no gap or overlap in the motion of the receiving beam, it is necessary that the total delay of the line be equal to the period of rotation of the sweep. This represents a phase shift of 360 degrees or one wavelength of the fundamental component of the switching wave. If simple sine waves are used for switching, any desired type of delay line may be used, subject only to the restriction that the delay of the individual section is such as to make the total length of  $N$  identical sections equal to one rotation period, where  $N$  is the number of switching elements.

The use of sine waves for switching is desirable for many reasons; however, the actual switch conduction pulse must have a width considerably less than the 180 degrees provided by the sine wave. Pulse width has an important effect on the beam formation and is usually chosen between 30 and 50 degrees. If it is too narrow, the beam jumps from one position to the next; if it is too wide, the beam is unnecessarily widened. The sine wave is converted to a short conduction pulse by resistor-capacitor combinations. The resistor may be a separate component (see Figure 19,  $R_1$ ) or the back resistance of the switch (see Figure 17, switch). The capacitor ( $C_3$ , Figures 18, 19) is charged during the conduction pulse and discharges for the rest of the cycle. Since there always exists a considerable difference between the forward and the back resistance of any sine switch, the capacitor obtains and holds a bias which in effect permits the peak of each sine wave, in the form of short pulses, to be passed by the switch. The individual self-biasing of each element switch is self-compensating, so that the resulting pulse is nearly independent, in width and



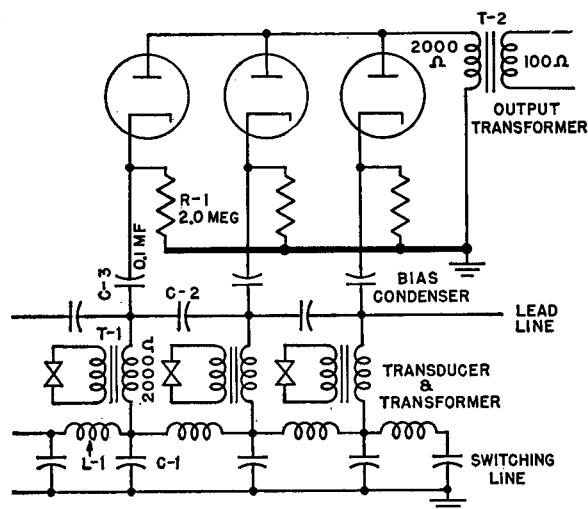


FIGURE 19. Switching lag line connections.

amplitude, of reasonably small changes in the amplitude of the sine wave.

An alternative method of switching requires pulses of exactly the proper shape and amplitude of the actual conduction pulse to be sent along the line. This means that the switching line must pass the desired pulse without appreciable distortion; in general, a more complex line is necessary to pass the requisite harmonics without change in time lag. In addition, this system imposes a more stringent requirement on the uniformity of the pulse along the line because of the absence of the self-compensation feature. While not recommended in the present state of scanning development, such methods may become desirable when, for improved beam formation, more precisely shaped switching pulses become necessary.

A large number of electrical specifications must be met in constructing a commutator of the ER type. The impedance of the switching line, at the switching frequency, must be low enough so that the diodes do not load the line and attenuate the switching pulse. For the same reason the  $Q$  of the coils used must also be high. In practice a total attenuation of  $11\frac{1}{2}$  db down the full length of the line has not been found excessive when the self-compensating feature mentioned above is used. The impedance of the transformer which matches the transducer element into the switching network must be made of the same order of magnitude as the impedance of the switching element in its conducting condition. Since the inductance of this transformer forms part of the lead line, this inductance must be taken into account when calculating the lead line capacitances. It must

be remembered that the act of switching generates a certain amount of noise and it is desirable to have the signal level as high as possible at the point where the switching occurs; at the present time these switching transients seem to be the greatest single source of noise in the system, but they have not prevented satisfactory operation.

The amount of phase shift in each section of the lag line determines the relative rate of rotation of the beam. If these phase shifts are not all equal, the beam rotates faster through some bearings than through others and the bearing indications are in error. All sections of the line must, therefore, be as nearly identical as possible. In practice, 3 per cent variations in the values of individual components may be tolerated without causing appreciable error in the bearing measurements. In addition, the frequency of the oscillator which generates the switching pulses must always be such that the total phase shift of the switching line is 360 degrees. If this were not true, there would either be a gap in the bearing indications on the PPI scope or an overlapping region, either of which would cause errors in the bearing determinations.

A frequency-discriminator circuit is at present connected to the switching lag line to give a positive or negative d-c voltage output whenever the phase shift differs from 360 degrees. This correcting voltage, through a reactance tube, controls the frequency of the oscillator to within  $\pm 0.5$  cycle. The synchronization between the switching frequency and the frequency of the sweep on the PPI scope is achieved by using the same oscillator as the source of both signals.

As the receiving beam pattern is rotated, its amplitude is a function of the switching elements. When varistors are used it is necessary to select them for uniformity of switching amplitude by means of a circuit similar to the one shown in Figure 18. The switching characteristics of diodes are usually sufficiently uniform so that no selection need be made.

#### MECHANICAL CONSIDERATIONS

The usual considerations of reliability apply to the ER commutator as to any other electronic apparatus. For one particular type of equipment designed for submarine use it was decided to install the commutator inside the transducer because of the difficulty of obtaining suitable pressure cable with a large number of conductors. For this purpose varistors were used as switching elements to eliminate the necessity

of furnishing heater current for diodes. These varistors were found liable to breakdown caused by transients during the transmitted pulse, but it was found that they could be protected by using 48 small neon tubes to couple the transducer elements to the transmitter.

The receiving transformer primaries were connected across the neon tubes; consequently, the voltage across the primaries never rose above the breakdown voltage of the neon tubes, or about 100 volts.

The physical size of the components used in the commutator was very much limited because of the

small available space in the transducer and the consequent crowding made the problem of assembly and wiring a difficult one. Every attempt should, therefore, be made to develop a suitable cable with enough conductors so that connections to each element may be brought out from the transducer and the commutator located inside the ship where it is available for maintenance and test. Diodes or other vacuum tube elements for switching are probably preferable to varistors because they have more uniform characteristics and are not so liable to breakdown under voltage overload.

CONFIDENTIAL

## Chapter 3

# PERFORMANCE EXPECTATIONS WITH SCANNING SONAR

### 3.1 DETECTABILITY OF ECHOES: NOISE

ANY ECHO-RANGING system employing sound is based on the principle that, following emission of a pulse of sound, reflecting objects return echoes that can be used to determine the location of the objects. In this discussion of sonar echo ranging, the reflecting objects are called "targets" and consist principally of enemy submarines, ships, and mines. Unfortunately, however, undesirable echoes are also returned. These come from a number of sources, the three most important being the ocean surface, the ocean bottom, and the ocean body itself. The resulting mixture of echoes from these sources is called reverberation. Other noises appearing in the sonar system but not originating in the emitted pulse include those caused by wave action, the motion of the ship and sonar gear through the water, propellers of own ship and other ships, and various forms of marine life. In addition, there are the purely electrical and mechanical noises in the receiving system and the ambient acoustical (or lighting) interferences at the indicators. The ability of an echo-ranging system to permit detection of the echo signal in the presence of interference from these other sources of sound determines its merit.

The characteristics by which the various echoes and noises can be distinguished will be discussed first. Following this, methods in which these distinguishing characteristics can be used in discriminating against undesired sounds while not interfering with indications of the desired ones will be considered.

The echo from a target is characterized by its return from a single direction. Ideally, it is a square wave pulse of a single frequency; usually, however, both its amplitude and phase are strongly modulated by interference. The effective intensity of the echo is independent of pulse length where the length is more than twice the target thickness; for shorter pulses it is proportional to the pulse length.<sup>1</sup> The frequency of a target echo differs from the frequencies of practically all other returning echoes, if the target has a component of motion relative to the water along the "line of sight." This difference is caused by the target doppler effect. A small amount of reverberation, picked

up on the minor lobes, may, however, have the same frequency as the echo.

The shifted frequency resulting from the total doppler effect may be written

$$\begin{aligned} f' &= f + \Delta f = f \left( 1 + \frac{2v_r}{c} \right) \left( 1 + \frac{2v_t}{c} \right) \\ &\cong f + \frac{2f}{c}v_r + \frac{2f}{c}v_t, \end{aligned} \quad (1)$$

where  $f$  is the initial frequency,  $f'$  is the shifted frequency,  $v_r$  is the velocity component relative to the water of the echo-ranging ship in the direction of the target,  $v_t$  is the velocity component relative to the water of the target in the direction of the echo-ranging ship, and  $c$  is the velocity of sound in the water. This formula shows that at 20 kc the shift caused by either ship's velocity is about 14 cycles per knot and is directly proportional to frequency. The frequency shift  $2f(v_r + v_t)/c$  is experienced by the target echo and is called the total doppler shift.

The characteristics of reverberation are similar to those of target echoes. Reverberation also exhibits the own-doppler shift  $2f v_r/c$  caused by motion of the echo-ranging ship, but since the reverberation echoes come from reflectors that are usually at rest with respect to the medium, the target doppler shift is zero. The coherence of the reflected signal depends on the general ocean conditions and the grazing angle. Minor doppler shifts may result from ocean currents and from the roll and pitch of the echo-ranging ship. Strong wave action may cause considerable frequency modulation of surface reverberation due to the motion of the reflecting surface. In consequence, the frequency of reverberation is not a definite quantity, but rather a spread of values, having the average value given by equation (1).

Reverberation is further characterized by the fact that its level fluctuates somewhat more violently than that of the echo. Its average intensity decreases less rapidly with range than echo intensity, and is directly proportional to the pulse length. Reverberation returns only from the region which has been "illuminated" by the beam of sound.

The general ambient noise of the sea is relatively

constant in amplitude over short periods of time and has a frequency spectrum that decreases at the rate of about 6 db per octave in the listening and echo-ranging bands.<sup>2</sup> On the other hand, the noise caused by snapping shrimp does not decrease at high frequencies in the echo-ranging frequency band.<sup>3,4</sup>

Ambient noises generally arrive from all directions. Shrimp noise may be directional if the shrimp bed is at a distance, but in such cases the noise level is too low to be troublesome.

The noise from ships, other than the echo-ranging vessel, has a relatively constant value over periods of time of the order of a pulse length. It has a frequency spectrum which decreases about 6 db per octave and its pressure level increases rapidly with increasing speed. It is further characterized by having directionality. The variation in pressure level with velocity is considerably greater in the case of a submarine, especially at periscope depth than for other types of ships. The noise from the echo-ranging ship itself includes the propeller noise from the stern as well as turbulence caused by the moving hull and the echo-ranging transducer.

In addition to the various sonic noises external to the receiving system, the system itself generates electric noise, such as thermal noise, microphonics, and transients caused by commutator and motor brushes, and relay contacts. Hum from the a-c power system and general crosstalk with other electric systems may also contribute appreciable noise. The input thermal noise of the receiver for the narrowest possible band width sets a lower limit beyond which the noise level cannot be reduced.

The transducer, in conjunction with any beam-forming circuits associated with it, is the first element of the receiving system, and consequently the first point at which discrimination against the various undesired noises is possible. By making the transducer directional, it is possible to discriminate against noises arriving from directions other than the target bearing. Thus ambient noise caused by marine life, reverberation, the echo-ranging ship, and sources in directions other than that of the target, can be discriminated against. This discrimination against directional sounds is given directly by the pattern  $q'(\theta, \phi)$  which expresses the efficiency of the transducer in reception in the direction  $(\theta, \phi)$  compared to the efficiency on the axis of the major lobe  $(0, 0)$ . If the projector pattern in transmission is called  $q(\theta, \phi)$  and that in reception  $q'(\theta, \phi)$ , where  $\phi$  is measured in the

azimuthal plane and  $\theta$  is measured in the vertical plane, the discrimination<sup>5</sup> in db against nondirectional noise is given by the receiving directivity index  $D'$ , which may be defined as:

$$D' = 10 \log_{10} d' \\ = 10 \log_{10} \frac{1}{4\pi} \int_0^{2\pi} \int_{-\pi/2}^{\pi/2} q'(\theta, \phi) \cos \theta d\theta d\phi \quad (2)$$

where  $d'$  is the receiving directivity ratio.

The discrimination in db against surface or bottom reverberation is given by the "surface" reverberation index,  $J_s$ :

$$J_s = 10 \log_{10} \frac{1}{2\pi} \int_0^{2\pi} q'(0, \phi) q(0, \phi) d\phi, \quad (3)$$

and the discrimination in db against volume reverberation is given by the volume reverberation index,  $J_v$ :

$$J_v = 10 \log_{10} \frac{1}{4\pi} \int_0^{2\pi} \int_{-\pi/2}^{\pi/2} q(\theta, \phi) q'(\theta, \phi) \cos \theta d\theta d\phi. \quad (4)$$

If the effective plane dimensions of the transducer are greater than  $2\lambda$ , where  $\lambda$  is the wave length of the signal in water, and there are no abnormally high side lobes, the values of these indices can be calculated from the angular half-width in degrees (6 db down) of the composite pattern  $q(\theta, \phi) q'(\theta, \phi)$  in the plane  $\theta = 0$ . If this half-width is called  $\Delta$ , then

$$J_s = 10 \log_{10} \Delta - 23.8 \text{ db}, \quad (5)$$

$$J_v = 20 \log_{10} \Delta - 42.6 \text{ db}, \quad (6)$$

$$D' = 20 \log_{10} \Delta - 40 \text{ db}. \quad (7)$$

The quantities  $J_s$  and  $J_v$  as determined from these formulas seem to be reliable to about  $\pm 1/2$  db for plane-faced transducers of the JK or QC types.  $D'$  is usually reliable to  $\pm 3$  db, but may be in error by as much as 10 db, since it is very critical with respect to the minor lobe structure.<sup>5</sup> Transducer patterns are more fully discussed in Chapter 9. The transducer

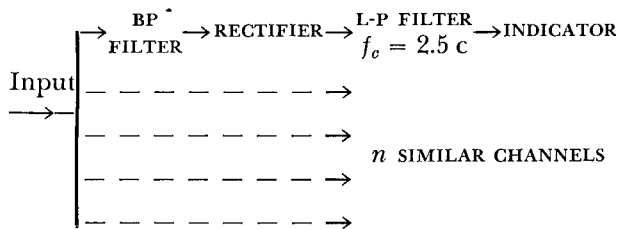
directivity pattern, of course, is not helpful in discriminating against the target's noise, which may still mask the echo, since both are from the same direction.

In addition to the directional discrimination of the transducer, noise discrimination of the system can be improved by the use of filters. In many cases, the frequency response of the transducer serves as a preliminary filter. Since most of the sounds to be discriminated against are noises with broad frequency spectra, the signal-to-noise discrimination of the receiver is very important. The noise energy in a narrow frequency band is directly proportional to the band width; consequently, if the minimum amount of noise is to be passed, the band width should be kept as narrow as possible. Furthermore, the band-width-limiting circuits should be located in the early stages of the receiver, where the level is low, so that cross-modulation products caused by nonlinearity will not be introduced into the acceptance band. The frequency spectrum of the echo pulse must also be considered, since the pulse consists essentially of a carrier frequency and two sets of modulation side bands. If the receiver band width is made too narrow, the side bands will be attenuated and considerable echo energy will be lost. For a given square pulse, the band width for the optimum signal-to-noise ratio is given by  $\Delta f = 1/2t_0$  cycles per side band, where  $t_0$  is the pulse duration in seconds and  $\Delta f$  is measured at 6 db down points.<sup>6</sup> Since it is seldom feasible to employ a single side band, this gives  $\Delta f = 1/t_0$ . If a narrower band is used, the pulse does not have time to build up to its maximum amplitude. In choosing a band width, the designer should remember that, because of doppler, the carrier frequency of the echo may vary over a considerable range.

In order to compare the signal-to-noise discrimination of various detectors, the following "ideal" detector will be used as a standard. The band width will always be made optimum for the pulse length used, and a sufficiently large number of individual bands will be employed side by side to secure a band wide enough to insure that doppler does not shift the signal frequency out of the total receiver band. The optimum band width will be taken as  $1/t_0$ ; however, this is too wide for present scanning systems, because the actual pulse is rounded and consequently has less extensive side bands than a square pulse. If the echo pulse is rectified, the pass band of the low-pass filter need be only half of  $1/t_0$ .

The human ear is inferior to the above "ideal" de-

detector from the standpoint of signal-to-noise discrimination. Since the ear of the operator is an important part of many types of underwater sound equipment, some of its properties will be discussed here. It is found that  $t_0$  must be at least 0.2 second if the ear is to attain its maximum response. For  $t_0 < 0.2$  second, the maximum signal intensity varies as  $t_0^2$ . Thus the ear is a much more sluggish detector than its effective signal-to-noise discrimination band requires. The following circuit has been proposed as representing the ear:



The cutoff frequency,  $f_c$ , of 2.5 c for the low-pass filter is determined by the response of the ear to pulses. Data on masking have shown that the band widths (6 db down) of the band-pass filters depend on frequency as follows:

Frequency (c)	Band Width (c)
125-500	30
1,000	36
2,000	60
4,000	120

These figures indicate that at the 0.2-second pulse length best adapted to it, the ear is 8 db less sensitive than the "ideal" detector and its sensitivity decreases as pulse length is shortened, being 11 db and 14 db lower for 0.1-second and 0.05-second pulse lengths respectively. These values refer to the signal-to-noise ratio and, since the band-pass filters have the critical band width, they indicate the ability of the ear to detect echoes against a noise background.

When using the visual detector it might be assumed that the doppler caused by the echo-ranging ship is nullified and the target speed is not greater than 10 knots, resulting in a doppler at 25 kc of  $\pm 175$  c, or a total spread of 350 c. The receiving band must be wide enough to pass a signal shifted by this amount plus the pulse side bands. Under these assumptions the following comparison can be made of the signal-

to-noise discrimination of different systems relative to the ideal detector.

TABLE 1. Signal-to-Noise Discrimination of Visual and Aural Systems.

Pulse Duration in sec	Ideal Detector Pass-band in c	Visual Detector Pass-band with 350 doppler shift in c	Ratio of Visual to Ideal in db	Ratio of Aural (125-500 cps) to Ideal in db
1.0	1	351	-25.5	-15
0.2	5	355	-18.5	-8
0.1	10	360	-15.5	-11
0.05	20	370	-12.5	-14
0.01	100	450	-6.5	-21
0.001	1,000	1,350	-1.3	-31

The band widths given refer to the supersonic channels. Only the pulse side bands need be considered in the audio channel if the supersonic signal is rectified.

These figures should not be applied to the scanning channel of a scanning sonar directly, since, if the beam is rotated through 360 degrees during the pulse length, the effective pulse length in this channel is the actual pulse length multiplied by  $2\Delta'/2\pi$ . Here  $\Delta'$  is the angular half width, measured in radians, at the half-power points of the scanning beam. The pulse shape, however, is approximately Gaussian rather than square after modulation of the echo by the scanning beam; consequently, the band width requirements may be slightly modified.

The factor that expresses the ability of a sonar system to distinguish an echo is called the *recognition differential*. It is defined as the number of decibels by which the echo must exceed the background in order to be recognized 50 per cent of the time. Since it depends on psychological and physiological factors associated with perception and identification, as well as on physical factors, the evaluation of this differential is difficult. Considerable empirical information has been collected on the probability of aural detection for relatively long pulse lengths,<sup>7-11</sup> but little is known about the detectability of short pulses.

The following is an empirical relation<sup>3</sup> for the probability  $Q$  that a nonfluctuating signal, masked by a fixed background, will be recognized when its actual intensity is  $I$  and the intensity for 50 per cent recognition probability is  $S_0$ :

$$Q = \frac{I^n}{I^n + S_0^n}$$

Here  $n$  depends on many factors, including the conditions of reception. For echo-ranging pulse lengths from a few milliseconds to 100 milliseconds,  $n$  is  $2.5 \pm 1$ . Under most conditions of echo-ranging, the signal intensity follows a Rayleigh distribution;<sup>1,3,4</sup> that is, the fractional number  $F$  of echoes whose levels exceed  $I$  is

$$F = e^{-\frac{I}{I_{av}}}$$

where  $I_{av}$  is the average echo level. Thus

$$dF = \frac{1}{I_{av}} e^{-\frac{I}{I_{av}}} dI,$$

and the echo recognition probability is

$$P = \int_0^\infty Q dF = \frac{1}{I_{av}} \int_0^\infty \frac{\left(\frac{I}{I_{av}}\right)^n}{\left(\frac{I}{I_{av}}\right)^n + \left(\frac{S_0}{I_{av}}\right)^n} e^{-\frac{I}{I_{av}}} dI. \quad (8)$$

This function varies quite slowly with respect to  $n$ . The important variable is  $S_0/I_{av}$ . A 50 per cent recognition probability results when  $I_{av} = S_0$ , or when  $10 \log (I_{av}/S_0) = 0.0$  db, and an 80 per cent recognition probability occurs when  $10 \log (I_{av}/S_0) = 7$  db. For present purposes the value of 80 per cent gives the more reasonable assurance of correct recognition or interpretation of the echo, and 7 db will be added

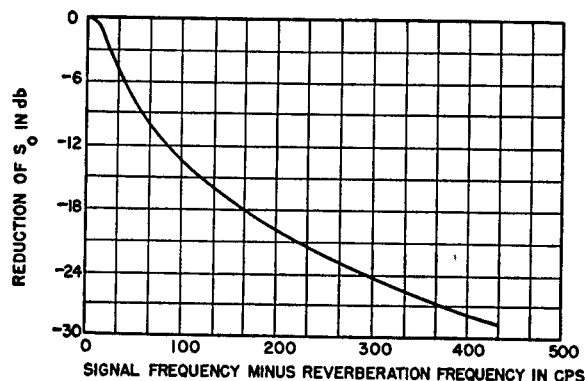


FIGURE 1. Reduction of masking effect due to target doppler 20 to 80 kc.

when this is desired. For a 100-millisecond pulse length and an 800-c listening frequency, the value of  $S_0$  is:<sup>3</sup> (1) 7 db below the noise in a 1-kc band centered at 800 c and (2) 3 db above the reverberation when this is the limiting factor and there is no doppler. The recognition level is considerably reduced when doppler is present, as shown in Figure 1. Table 2 illustrates the results of calculations based on the above assumptions.

TABLE 2. Calculated Recognition Levels.

Background	Average echo-to-background ratio for 80% recog. prob.
Noise in 1 kc band	0 db
Reverberation	
Relative target speed 5 knots	
20 kc	0 db
40 kc	-6 db
Relative target speed 15 knots	
20 kc	-10 db
40 kc	-17 db

The above values are very rough and may be radically modified by additional factors. For example, the echo quality, which depends on pulse length, is a very important factor in recognition. Echo periodicity is also important. When the background is largely reverberation, the recognition level can be lowered 4 to 5 db by employing a "chirp" instead of a constant frequency signal.<sup>3,12</sup> If the pulse length differs from 100 milliseconds, a correction can be made by referring to Table 1.

In the visual detector the echo quality, pulse repetition rate, and oscilloscope screen persistence have an important effect upon the recognition differential.

Available data on the visual detector indicate that the lowest value of signal-to-noise ratio that will result in an 80 per cent echo recognition probability is about 11 db. The condition required to realize this value is that  $\Delta f t_0 = 1$ , where  $\Delta f$  is the band width 3 db down and  $t_0$  is the pulse length. For the value  $\Delta f t_0 = 0.2$  or  $\Delta f t_0 = 12$  the signal-to-noise ratio must be 16 db for 80 per cent recognition. In a heterodyne system the audio-frequency band should not be narrower than that at the intermediate frequency required to pass a pulse without doppler. Investigators of the recognition differential for radar indicators have shown that type A and type B presen-

tations are approximately equivalent in the signal-to-broad-band noise ratio required for 80 per cent echo recognition; however, type A presentation is superior when the interfering signal is not of a random nature. These differences arise from the fact that type A presentation indicates by deflecting an electron beam, whereas type B system indicates by brightening a spot. The recognition differential of the visual channel of a QH system is about 10 db lower than that of the listening channel.<sup>13</sup> A small portion of this 10 db may be attributed to the difference in the band widths of the two channels, but the largest factors are probably commutator noise in the scanning (visual) channel and the psychological factors involved in aural versus visual perception.

### 3.2

## REVERBERATION— VOLUME, SURFACE, BOTTOM

As pointed out in the foregoing section, reverberation may be defined as the totality of undesired echoes returning to the echo-ranging transducer. These echoes are produced at any point in the medium at which there is a variation in the characteristic acoustic impedance. Volume reverberation represents the echoes resulting from oceanic variations such as the scattering of inorganic salt precipitates, or regions of abnormal density due to variations of temperature and salinity. Surface reverberation consists of the echoes from the surface or surface layer of the ocean which includes the region containing entrapped air bubbles. The air bubbles result mainly from wave action and may be present in a fairly thick layer after a storm. Bottom reverberation refers to the totality of echoes from the bottom of the ocean.

The simple theory of volume reverberation will be considered first.<sup>1</sup> In this discussion a spherical coordinate system will be employed in which  $\phi$  is measured in the azimuthal plane,  $\theta$  is measured in a vertical plane, and the origin is taken at the echo-ranging projector (Figure 2). The element of volume is given by

$$dV = r^2 \cos \theta dr d\theta d\phi.$$

If  $t$  is the time interval between the middle of the transmitted pulse and the middle of the returning echo,  $t_0$  the duration time of the pulse,  $t \gg t_0$ , and  $c$  the velocity of sound, then the range  $r$  of the volume element can be written as  $ct/2$ , and the thick-

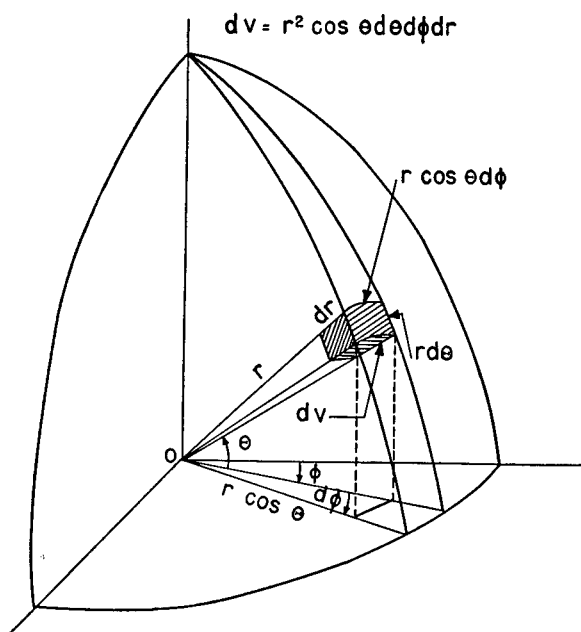


FIGURE 2. Coordinate system employed in computations of volume reverberation.

ness of the spherical shell from which echoes can be received simultaneously is  $ct_0/2$ . Then

$$dV = \frac{c^3 t_0^2}{8} \cos \theta d\theta d\phi. \quad (9)$$

Now if  $I_0$  is the power radiated by the projector per steradian in the direction  $\theta = \phi = 0$  ( $I_0$  is sometimes referred to as the intensity at unit distance from the projector), the intensity  $I_{dv}$  of sound that reaches the volume element  $dV$  is<sup>14</sup>

$$I_{dv} = \frac{I_0 q(\theta, \phi)}{\left(\frac{ct}{2}\right)^2} \cdot 10^{-\frac{A}{10}}, \quad (10)$$

where  $q(\theta, \phi)$  is the normalized transmitting intensity pattern of the projector.  $A$ , which is known as the transmission anomaly, is a dimensionless factor—depending on range and general ocean conditions—which accounts for other attenuation than that due to the inverse square divergence of the sound out to the range in question.

If  $m_v$  is the average coefficient of backward volume scattering ( $m_v$  has the dimension  $L^{-1}$ ), the average power scattered per steradian from the volume element is given by<sup>1</sup>

$$\begin{aligned} dW_v &= \frac{m_v}{4\pi} I_{dv} dV \\ &= \frac{m_v}{4\pi} \left[ \frac{I_0 q(\theta, \phi)}{\left(\frac{ct}{2}\right)^2} \cdot 10^{-\frac{A}{10}} \right] \left[ \frac{c^3 t_0^2}{8} \cos \theta d\theta d\phi \right] \\ &= \frac{m_v I_0 c t_0}{8\pi} q(\theta, \phi) \cdot 10^{-\frac{A}{10}} \cos \theta d\theta d\phi, \end{aligned} \quad (11)$$

and the intensity at the echo-ranging transducer of this sound scattered from  $dV$  is

$$\begin{aligned} dI_{dv'} &= \frac{dW_v}{\left(\frac{ct}{2}\right)^2} \cdot 10^{-\frac{A}{10}} \\ &= \frac{m_v I_0 t_0}{2\pi c t^2} \cdot q(\theta, \phi) \cdot 10^{-\frac{A}{5}} \cos \theta d\theta d\phi. \end{aligned} \quad (12)$$

If  $I'_0$  is the electric power produced by the transducer in reception in a sound field of unit intensity, and if  $q'(\theta, \phi)$  is the normalized transducer pattern in reception, the electric power produced at the receiver due to the element of volume  $dV$  is

$$dR_v(t) = dI_{dv'} \cdot I'_0 \cdot q'(\theta, \phi) \quad (13)$$

and the total electric power at the receiver is

$$\begin{aligned} R_v(t) &= \frac{m_v I_0 I'_0 t_0}{2\pi c t^2} \cdot 10^{-\frac{A}{5}} \int_{-\frac{\pi}{2}}^{\frac{\pi}{2}} \int_{-\frac{\pi}{2}}^{\frac{\pi}{2}} q(\theta, \phi) q'(\theta, \phi) \cos \theta d\theta d\phi. \end{aligned} \quad (14)$$

Integration is carried out over only half of the sphere, because it is assumed that  $q'(\theta, \phi)$  is zero on the back half. The integral then becomes the same as that in equation (4) and can be computed with reasonable accuracy from equation (6), if  $\Delta$  is computed from the geometric mean width of  $q$  and  $q'$ . This may be done when these patterns are similar, as they are in a searchlight type sonar. Here, however, an independent calculation will be made. Because the dimensions of the scanning sonar transducers are large compared to the wave length it is fairly true that in reception

$$q'(\theta, \phi) = \left[ \frac{\sin\left(\frac{\pi l}{\lambda} \sin \theta\right)}{\frac{\pi l}{\lambda} \sin \theta} \right]^2 \left[ \frac{\sin\left(\frac{\pi d}{\lambda} \sin \phi\right)}{\frac{\pi d}{\lambda} \sin \phi} \right]^2 \quad (15)$$



where  $d$  is the equivalent width and  $l$  is the equivalent length of a rectangular transducer giving the same lobe widths in the horizontal and vertical planes, at 3 db down, as those given by the actual transducer ( $l$  and  $d$  are both assumed to be large compared to  $\lambda$ ). During transmission,  $q(\theta, \phi)$  is non-directional in the  $\theta = 0$  plane and consequently is represented by the pattern of an equivalent vertical line source, where "equivalent" once again means that the length is so chosen that the actual pattern width and the line source pattern width agree at the 3-db down points:

$$q(\theta, \phi) = \left[ \frac{\sin\left(\frac{\pi l}{\lambda} \sin \theta\right)}{\frac{\pi l}{\lambda} \sin \theta} \right]^2. \quad (16)$$

Substitution of equations (15) and (16) in (14) gives

$$R_v(t) = \frac{4m_v I_0 I'_0 t_0}{2\pi c t^2} \cdot 10^{-\frac{A}{5}} \int_0^{\frac{\pi}{2}} \int_0^{\frac{\pi}{2}} \left[ \frac{\sin\left(\frac{\pi l}{\lambda} \sin \theta\right)}{\frac{\pi l}{\lambda} \sin \theta} \right]^4 \left[ \frac{\sin\left(\frac{\pi d}{\lambda} \sin \phi\right)}{\frac{\pi d}{\lambda} \sin \phi} \right]^2 \cos \theta d\theta d\phi,$$

where the factor 4 arises from the change in limits of integration, or

$$R_v(t) = \frac{2m_v I_0 I'_0 t_0}{\pi c t^2} \cdot 10^{-\frac{A}{5}} \cdot \frac{\lambda}{\pi l} \int_0^{\frac{\pi}{2}} \frac{\sin^4\left(\frac{\pi l}{\lambda} \sin \theta\right)}{\left(\frac{\pi l}{\lambda} \sin \theta\right)^4} \cdot d\left(\frac{\pi l}{\lambda} \sin \theta\right) \int_0^{\frac{\pi}{2}} \frac{\sin^2\left(\frac{\pi d}{\lambda} \sin \phi\right)}{\left(\frac{\pi d}{\lambda} \sin \phi\right)^2} d\phi.$$

If  $\pi l/\lambda \gg 1$ , the first integral is approximately  $\pi/3$ , the error being of the order  $\lambda/5l$ . The second integral can be shown<sup>15</sup> to be

$$\frac{\lambda}{2d} \left[ \int_0^{\frac{2\pi d}{\lambda}} J_0(u) du - J_1\left(\frac{2\pi d}{\lambda}\right) \right]$$

which, when  $2\pi d/\lambda \gg 1$ , reduces to  $\lambda/2d$ . Thus we may write

$$R_v(t) = \frac{m_v I_0 I'_0 \lambda^2 t_0}{3\pi c l d t^2} \cdot 10^{-\frac{A}{5}}. \quad (17)$$

The equivalent intensity  $I_v$  of volume reverberation at the receiver can now be defined by

$$I_v \equiv \frac{R(t)}{I'_0} = \frac{m_v c \lambda^2 t_0}{12\pi l d} \cdot \frac{I_0}{\left(\frac{c t}{2}\right)^2} \cdot 10^{-\frac{A}{10}}. \quad (18)$$

Further, since  $I_0$  is the power radiated per steradian, the square of the radiated sound pressure  $P_0(r)$  at any distance  $r$  is proportional to  $I_0/r^2$ . If we define  $P_0(1)$  as the sound pressure on the main beam of the projector at unit distance, then the volume reverberation pressure is given by

$$P_v = P_0(1) \sqrt{\frac{I_v}{I_0}} = \frac{P_0(1)}{\frac{c t}{2}} \sqrt{\frac{m_v c \lambda^2 t_0}{12\pi l d}} \cdot 10^{-\frac{A}{10}}.$$

Replacing  $ct/2$  by the range  $r$ ,

$$P_v = \frac{P_0(1)}{r} \cdot 10^{-\frac{A}{10}} \sqrt{\frac{m_v c \lambda^2 t_0}{12\pi l d}}. \quad (19)$$

The units to be used have not been specified; however, since sound pressure is almost universally measured in dynes per sq cm, C.G.S. units will be adopted here. In order to avoid introducing equipment constants, all pressures will be expressed in db relative to the pressure  $P_1$  on the main beam of the projector at a distance of one meter. It should be noted that, since pressure varies inversely with distance,

$$P_1 = \frac{1}{100} P_0(1).$$

Further, if  $r$  is measured in kilometers it must be multiplied by a factor  $10^5$ , since unit distance has been fixed as 1 cm.

Then twenty times the logarithm of both sides of equation (19) is taken, giving

$$20 \log_{10} \frac{P_v}{P_1} = 20 \log_{10} \frac{P_0(1)}{P_1} - 20 \log_{10} (10^5 \cdot r) - 2A + 10 \log_{10} \left( \frac{\lambda^2}{4\pi l d} \right) + 10 \log_{10} \left( \frac{m_v c t_0}{3} \right).$$

In the above expression  $10 \log_{10} \lambda^2 / 4\pi l d$  is by definition the directivity index  $D_e$  of an equivalent plane radiator of length  $l$  and width  $d$  which has the same horizontal and vertical beam widths, 3 db down on the intensity pattern, as the actual transducer. Also  $\lambda$  is the wave length of the signal. All quantities are measured in C.G.S. units except  $r$  which is in kilometers. By writing  $20 \log (P_v/P)$  as  $[P_v]$ ,

$$[P_v] = +40 - 100 - 20 \log_{10} r - 2A + D_e + 10 \log_{10} \left( \frac{m_v c t_0}{3} \right).$$

Then if it is assumed that  $A$  is proportional to  $r$ ; i.e. if  $A = \alpha r$ , where  $\alpha$  is the attenuation of sound in the sea in db per kilometer for the ocean state under consideration, the final expression for the volume reverberation pressure in db relative to  $P_1$  becomes

$$[P_v] = -60 + D_e - 2\alpha r - 20 \log_{10} r + 10 \log_{10} \left( \frac{m_v c t_0}{3} \right). \quad (20)$$

The expressions for surface and bottom reverberation pressures differ only in the values of the scattering coefficients involved, since in both cases the chief concern is with scattering from a horizontal surface; consequently, the development will be made in terms of the general coefficient  $m$ . The coefficient  $m$  will then be replaced by either  $m_s$  or  $m_b$  in the later computations, depending on whether surface or bottom reverberation is being considered. The development is quite similar to that given above for volume reverberation. If, however, the same coordinate system is used as in the case of volume reverberation, the surface elements must be taken parallel to a horizontal plane. Such a system is shown in Figure 3. The angle  $\psi$  represents the tilt angle of the transducer beam. Thus the element of area is

$$dA = r dr d\phi = \frac{c^2 t_0}{4} d\phi. \quad (21)$$

The intensity of the sound from the projector at the element of area is

$$I_{dA} = \frac{I_0 q(\theta - \psi, \phi)}{c^2 t^2} \cdot 10^{-\frac{A}{10}} \quad (22)$$

as in the case of volume reverberation, except that  $(\theta - \psi)$  now represents the vertical angle measured

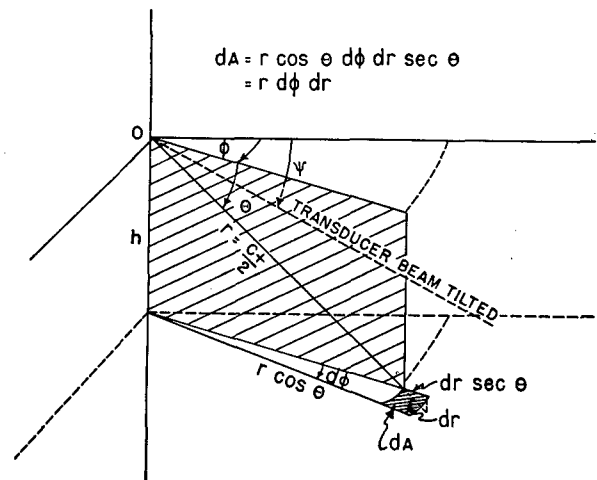


FIGURE 3. Coordinate system used in computation of surface and bottom reverberation.

from the tilted beam of the transducer. It has seemed desirable in some systems to tilt the transducer slightly upward to counteract the effect of strong negative thermal gradients. Further,  $\psi(t)$  is required for a treatment of depth scanning.

The coefficient of backward scattering  $m$  is defined<sup>1</sup> by the relation

$$i_0(\theta) = m \frac{I_{dA}}{4\pi} dA \quad (23)$$

where  $I_{dA}$  is the intensity of sound striking the element of area  $dA$  at the grazing angle  $\theta$  and  $i_0(\theta)$  is the power scattered backward per steradian in the direction  $\theta$ .

Term  $m$  is not necessarily constant; for a grazing angle  $(\theta)$  greater than 9 degrees it is a function of  $\theta$ . As indicated, it is to be replaced by either  $m_s$  or  $m_b$ . These coefficients further depend respectively on the state of sea and the type of bottom. For a grazing angle of 9 degrees,  $m_s$  varies from  $10^{-6}$  in a calm sea to  $10^{-2}$  in a very rough sea;  $m_b$  varies from  $10^{-3}$  to  $10^{-2}$  for rock bottom and from  $10^{-4}$  to  $10^{-3}$  for sand and mud bottoms.<sup>1</sup> Table 3<sup>16</sup> shows the distribution of  $m_b$  for a 9 degree grazing angle for various types of bottoms. The estimated quartile deviation is 5 db.

TABLE 3. Bottom Scattering Coefficients.

Bottom Material	$10 \log m_b$
Rock	-22 db
Mud, Mud-Sand	-30 db
Sand	-35 db

These values are constant<sup>17</sup> for any grazing angle less than 9 degrees; however, for  $9^\circ < \theta < 90^\circ$ ,

$$m_b = m_b(9^\circ) \cdot \frac{\sin^2 \theta}{\sin^2 9^\circ}.$$

From equation (23), the intensity of sound returned to the echo-ranging transducer is given by

$$dI_R = \frac{mI_{dA}}{\pi c^2 t^2} dA \cdot 10^{-\frac{A}{10}}.$$

As in the case of volume reverberation, the next quantity to be defined is the equivalent intensity of surface reverberation at the receiver which is  $I_s$ . Now

$$dI_s = q'(\theta - \psi, \phi) dI_R = \frac{mI_{dA} q'(\theta - \psi, \phi)}{\pi c^2 t^2} dA \cdot 10^{-\frac{A}{10}}.$$

This is the intensity of surface reverberation returned from  $dA$  effective in interfering with the desired echo in the receiver. Substituting from  $I_{dA}$  and  $dA$  from equations (22) and (21), gives

$$dI_s = \frac{mI_0 t_0}{\pi c^2 t^3} q(\theta - \psi, \phi) q'(\theta - \psi, \phi) d\phi \cdot 10^{-\frac{A}{5}}$$

or

$$I_s = \frac{mI_0 t_0}{\pi c^2 t^3} \cdot 10^{-\frac{A}{5}} \int_{-\frac{\pi}{2}}^{\frac{\pi}{2}} q(\theta - \psi, \phi) q'(\theta - \psi, \phi) d\phi$$

(24)

where again  $q'$  is assumed to be zero on the back half of the receiving pattern.

Again the patterns given by equations (15) and (16) will be employed, and it will be assumed that  $q(\theta - \psi, \phi)$  is nondirectional with respect to  $\phi$ . This is not true for the present depth-scanning transducer (see Chapter 6). Thus

$$I_s = \frac{2mI_0 t_0}{\pi c^2 t^3} \cdot 10^{-\frac{A}{5}} \left[ \frac{\sin\left(\frac{\pi l}{\lambda} \sin(\theta - \psi)\right)}{\frac{\pi l}{\lambda} \sin(\theta - \psi)} \right]^4$$

$$\int_0^{\frac{\pi}{2}} \left[ \frac{\sin\left(\frac{\pi d}{\lambda} \sin \phi\right)}{\frac{\pi d}{\lambda} \sin \phi} \right]^2 d\phi.$$

Again, if  $2\pi d/\lambda \gg 1$  the integral has the value  $\lambda/2d$ , and

$$I_s = \frac{m c I_0 t_0 \lambda}{8\pi d \left(\frac{c t}{2}\right)^3} \cdot 10^{-\frac{A}{5}} \left[ \frac{\sin\left(\frac{\pi l}{\lambda} \sin(\theta - \psi)\right)}{\frac{\pi l}{\lambda} \sin(\theta - \psi)} \right]^4. \quad (25)$$

If  $P_0(1)$  is the transmitted pressure at unit distance from the projector on the main beam, then the surface reverberation pressure at the receiver is given by

$$P_s = P_0(1) \sqrt{\frac{I_s}{I_0}} \\ = \frac{P_0(1)}{r^{3/2}} \cdot 10^{-\frac{A}{10}} \sqrt{\frac{m c t_0}{4\pi} \cdot \frac{\lambda}{2d}} \left[ \frac{\sin\left(\frac{\pi l}{\lambda} \sin(\theta - \psi)\right)}{\frac{\pi l}{\lambda} \sin(\theta - \psi)} \right]^2$$

Using C.G.S. units, referring pressures to  $P_1$  as in the case of volume reverberation, and expressing  $r$  in kilometers,

$$20 \log_{10} \left( \frac{P_s}{P_1} \right) \equiv [P_s] = 20 \log_{10} \frac{P_0(1)}{P_1} \\ - 30 \log_{10} (10^5 \cdot r) - 2A + 10 \log_{10} \frac{\lambda}{2d} \\ + 10 \log_{10} \frac{m c t_0}{4\pi} + 20 \log_{10} \left[ \frac{\sin\left(\frac{\pi l}{\lambda} \sin(\theta - \psi)\right)}{\frac{\pi l}{\lambda} \sin(\theta - \psi)} \right]^2$$

Now  $10 \log(\lambda/2d)$  is the directivity index of a line source of length  $d$  which has the same beam width, 3 db down on the intensity pattern, as the actual transmission pattern. If this index is called  $D_d$  and if  $A = \alpha r$ , then

$$[P_s] = -110 - 30 \log_{10} r - 2\alpha r + D_d + 10 \log_{10} \frac{m c t_0}{4\pi} \\ + 20 \log_{10} \left[ \frac{\sin\left(\frac{\pi l}{\lambda} \sin(\theta - \psi)\right)}{\frac{\pi l}{\lambda} \sin(\theta - \psi)} \right]^2. \quad (26)$$

If  $h$  represents the vertical distance from the transducer to the scattering surface,  $\theta = \sin^{-1} h/r$ . This expression holds for either surface or bottom reverberation.

The above theory does not take into account any ray paths other than the direct one. Actually there

may be many echo-ranging paths between the transducer and a point in the ocean. Frequently there is a smooth, flat ocean surface with nearly perfect reflectivity and for a "target" in the body of the ocean or on the bottom, there are four distinct "go-and-return" paths followed by the echo-ranging sound. If the sound intensity is the same along all paths, the average energy returned to the transducer is four times as great as that predicted by the above theory. In general, however, the four signals may be assumed to arrive in random phase, so that the total received signal fluctuates rapidly over small time intervals. Similar additional reflection may occur from the ocean bottom, especially from a shallow hard bottom, although in this case the coefficient of reflection is seldom unity. Actual sea conditions are usually such that there are many sound paths in which signals are attenuated by varying amounts. Since this factor is quite variable for different locations and sea conditions, no attempt will be made to incorporate it into the analysis. Failure to include it, however, will not alter the results by more than about 3 db, an amount which is considerably less than the uncertainties in the values of the scattering coefficients and recognition differentials.

### 3.3 NOISE—SEA, OWN, TARGET, ELECTRIC

As pointed out earlier, reverberation is not the only source of interference with the desired echo. Any one of the noises from the target, the echo-ranging ship, marine life, the turbulence of the sea, or the receiver itself may be the main factor in limiting the detectability of the echo. Experimental data concerning the magnitude of these factors have been accumulated during the last few years, but they are incomplete and in many cases inaccurate. In the present account only the facts as they are now known will be presented, with the admonition that the results are subject to continual revision as more information is gained.

Figure 4 represents the best available data on the ambient noise level of the sea.<sup>3</sup> The noise spectrum has been assumed to decrease at the rate of 6 db per octave in the ultrasonic range, because of the few measurements available at frequencies other than 24 kc. It should be noted that the pressure levels shown are not those that are effective in interfering with the echo. The directivity of the receiver must be

taken into account by adding algebraically the directivity index to the pressure level in db. A correction for band width may be made by assuming that the noise energy is proportional to the band width, e.g., for a 2-kc band width 3 db should be added to the values of Figure 4.

Figure 4 shows that the "self noise" in the 100-inch dome of the USS SEMMES (DD), at a speed of 10 knots, is equal to the ambient noise of the sea for sea state 6.<sup>2,3,4</sup> The spectrum of this noise decreases at the rate of about 6 db per octave. It has been found that the noise pressure varies approximately as the cube of the speed of the ship, which corresponds to an increase of 18 db in the noise level when the speed is doubled. The 100-inch dome contains a baffle which attenuates sound coming from the ship's propellers by at least 18 db.<sup>18</sup> Echo ranging at speeds greater than 10 to 15 knots is not feasible unless the transducer is enclosed in some kind of dome.

There are much more comprehensive data on target noise than on self noise. Target noise<sup>2</sup> is found also to decrease with frequency at the rate of 6 db per octave, and to increase with target speed at the rate of 18 db for doubled velocity. Table 4 shows the noise pressure at 200 yards (183 meters) caused by various targets moving at speeds of 20 knots. The values given are for a 1-kc band at 24 kc.

TABLE 4. Typical Target Noise Levels.

Type of Ship	Noise level at 200 yd in db vs. 1 dyne per cm <sup>2</sup> (at 20-knot speed)
Battleship	+13
Cruiser	+3
Destroyer or Destroyer Escort	-2
Merchant or Passenger	<div style="display: inline-block; vertical-align: middle;"> <div style="font-size: 2em; vertical-align: middle;">}</div> <div style="display: inline-block; vertical-align: middle;"> +6 (-7 at 12 knots) </div> </div>

This table gives average values, from which the value for any individual ship may differ appreciably. The value at any distance can be obtained by assuming a value for the transmission loss in accordance with the discussion in the next section. The noise<sup>2</sup> produced by an S-type submarine as a function of speed and depth is shown in Figure 5. Target noise is from a single direction and consequently is not discriminated against by the transducer directivity pattern, when the transducer is trained in the direction of the target.

If the speeds of the echo-ranging and target ships are not high, the electric noise of the receiving system

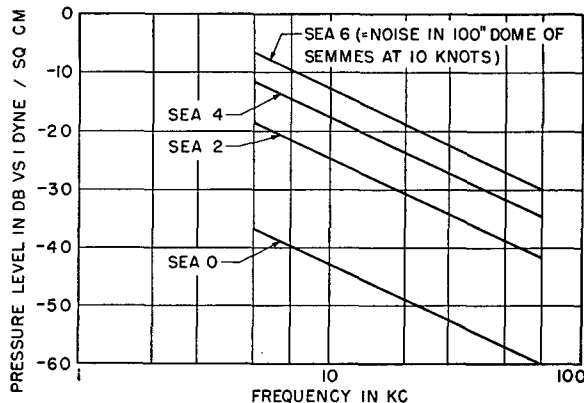


FIGURE 4. Ambient noise of sea in 1-kc band width.

may mask the returning echo. Normally, however, the electric noise is less than the self noise of the ship. Electric noise levels have been expressed here in terms of the equivalent noise pressure levels at the transducer so that they may be directly compared with the other noises. The directivity of the transducer is not involved in this case. Table 5 gives the

TABLE 5. Equivalent Electrical Noise Levels.

System	Equivalent Noise in Visual Channel	Equivalent Noise in Aural Channel
ER Submarine System	-15 db	...
CR QH Model II	-25 db	-35 db
CR XQHA	-29 db	-42.5 db

best available data<sup>19, 20, 21</sup> concerning the equivalent noise pressure (in db vs 1 dyne per sq cm) of the electric noise in several scanning systems.

The figures in Table 5 include the recognition differential of the system and actually represent the values of the smallest signals which can be detected consistently against the noise background.

### 3.4 TRANSMISSION LOSS, REFRACTION, TARGET STRENGTH

Transmission loss may be defined as the intensity loss of a signal in db in going from a point one meter from the projector to the range  $r$  expressed in kilometers. It is usually written as:

$$\overline{TL} = 20 \log_{10} r + 60 + A \quad (27)$$

where the first term accounts for the inverse square divergence and  $A$ , the transmission anomaly, accounts

for the remaining drop. The 60 db is introduced so that  $r$  may be entered directly in kilometers.

Classical theory attributes  $A$  to the attenuation of sound in the water but this does not correspond to the experimental facts. Actually the transmission anomaly is a function of general ocean conditions at a given time and place. Although all the factors that contribute to this anomaly are not known, the thermal gradient condition of the ocean is one of the most important. Actual attenuation plays a rather insignificant role at ordinary echo-ranging frequencies.<sup>14</sup>

While it has not been possible to find a general expression for the transmission anomaly, empirical equations have been derived for a special case.<sup>14</sup> Thus, if the total temperature variation in the upper 30 feet of the ocean is less than 0.3 F we can write:

$$A = \alpha r \quad (28)$$

where  $r$  is measured in kilometers and  $\alpha$  in db per km;  $\alpha$  is still called the *attenuation coefficient*, although this is not intended in the classical sense. Values of  $\alpha$  fitted over a band of thermal conditions are shown as a function of frequency in Figure 6. A rough correlation of  $\alpha$  with the depth  $D_t$  in meters to the top of the thermocline has been found; thus

$$\alpha = \alpha_0 + \frac{52}{h_t} \quad (29)$$

for the receiver above the thermocline, and

$$\alpha = \alpha_0 + \frac{76}{h_t} \quad (30)$$

for the receiver below the thermocline,

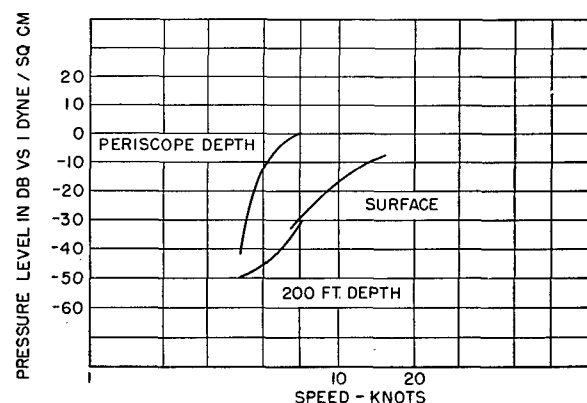


FIGURE 5. Curves of submarine noise versus speed measured at 200 yards (183 m); level in 1-kc band at 24 kc; S-type submarine.

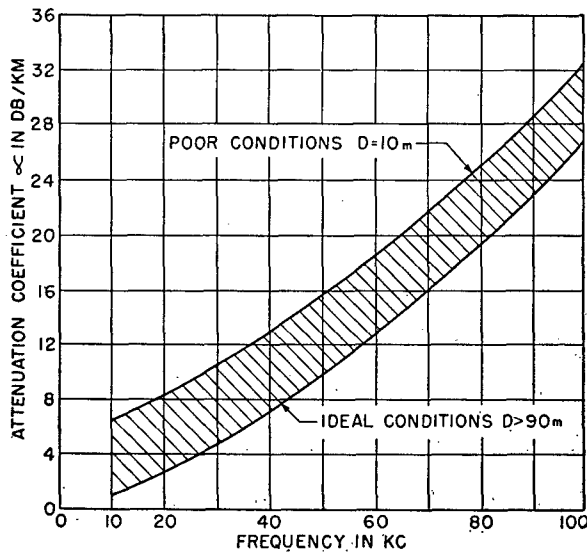


FIGURE 6. Curve of attenuation versus frequency over a range of thermal conditions.

where  $\alpha_0 = 0.15f + 0.00125f^2 - 0.8$  is the equation found by the least squares method that fits the data used for Figure 6. In this equation,  $f$  is the signal frequency in kc. The top of the thermocline is taken as the depth  $h_t$ , in meters, at which there is a sharp change in the thermal gradient. Under the thermal conditions stated, these values for  $\alpha$  are reasonably good for ranges greater than 1 km; however, the values may be too low for smaller ranges. For reasons not well understood, the transmission anomaly often tends to increase considerably at close ranges.<sup>14</sup>

The transmission anomaly is a function of the number of possible reflection paths and of the relative phases and amplitudes of reflected signals. Thus in shallow water where many reflection paths are possible, the transmission anomaly may decrease by 6 db or more.

A fairly good qualitative picture of the behavior of the transmission anomaly as a function of range can be found by plotting the actual ray diagrams of sound under the particular thermal conditions being studied. A case of considerable importance is that where there is a large negative temperature gradient. The sound beam is bent downward sharply, so that the path of the ray leaving the transducer and becoming tangent to the water surface limits the maximum range in echo ranging. Only sound reflected from the bottom or scattered from the ocean body penetrates the region beyond this limiting ray. This effect is observed as a sharp increase in transmission anomaly at

ranges greater than those indicated by the limiting ray. This type of refraction<sup>4</sup> is very common, especially in the South Pacific, where more than half of the time the ranges are limited to less than one kilometer.

Most other factors in range limitation are negligible in comparison with this strong refractive factor. Other types of refraction produce more complicated effects in the transmission anomaly. A comparatively rare condition is that referred to as a *sound channel* which results when there is a sharp change from a negative to a positive thermal gradient. The total sound energy is restricted to a narrow layer of water so that extremely long ranges are possible on targets within the layer. This is observed as a very small, or even as a negative, transmission anomaly.

In the study of echo-ranging problems it is necessary to introduce a quantity which can serve as a measure of the reflecting power of the target. This quantity is called the *target strength* and may be defined as the number of db which must be added to the transmitted intensity level measured at one meter from the projector, diminished by the transmission loss to the target and back, in order to obtain the echo intensity level at the hydrophone. Thus, if  $L_e$  is the echo level,  $L_1$  is the transmitted level at one meter, and  $T$  is the target strength,

$$L_e = L_1 - 2\overline{TL} + T. \quad (31)$$

The target strength of a perfectly reflecting sphere can be shown to be

$$T = 20 \log_{10} \left( \frac{R}{2} \right) \quad (32)$$

where  $R$  is the radius of the sphere in meters. It can be seen that  $T = 0$  for  $R = 2$  meters. Thus, the target strength can be considered as the ratio in db of the echo intensity level from the actual target to the echo intensity level from a sphere of 2-meter radius at the same range. Table 6 lists representative values of tar-

TABLE 6. Typical Target Strengths.

Type of Target	Target Strength	
	Beam Aspect	Stern or Bow Aspect
Sphere of radius 2 meters	0 db	0 db
Sphere of radius 20 meters	20 db	20 db
S-type submarine	$30 \pm 5$ db	$15 \pm 5$ db
Destroyer	17 db	6 db

get strength for various types of targets at frequencies in the neighborhood of about 24 kc.<sup>3,4</sup> Target strength should not depend strongly on frequency where the target dimensions are large and its surface irregularities small compared with the wavelength of the sound.

### 3.5 POWER AND TRANSMITTING DIRECTIVITY

In the discussion of reverberation earlier in this chapter the intensity of the sound at the distance  $r$  from the projector in the direction  $(\theta, \phi)$  was written

$$I_{dv} = \frac{I_0 q(\theta, \phi)}{r^2} \cdot 10^{-\frac{A}{10}} \quad (10)$$

where  $I_0$  is the power radiated by the projector per steradian in the direction  $(\theta = \phi = 0)$ , and  $q(\theta, \phi)$  is the normalized transmitting intensity pattern of the projector. In this expression  $I_0 q(\theta, \phi)$  expresses the power radiated per steradian in the direction  $(\theta, \phi)$ , so that the total power  $P_T$  transmitted is given by

$$P_T = I_0 \int_0^{2\pi} \int_{-\frac{\pi}{2}}^{\frac{\pi}{2}} q(\theta, \phi) \cos \theta d\theta d\phi. \quad (33)$$

Reference to equation (2) shows that this integral is  $4\pi$  times the directivity ratio in transmission. Thus, equations (10) and (33) show that if a given intensity is desired at range  $r$  on the transducer axis, the total acoustic power which must be radiated is directly proportional to the transmitting directivity ratio, which decreases as the beam width is reduced. In most echo ranging applications the greatest possible intensity at the greatest possible range is desirable, assuming, of course, that the refractive conditions are not limiting, which is seldom completely true for long ranges. The acoustic power which may be radiated into water is limited by the onset of cavitation. At atmospheric pressure this corresponds to a power of about 0.3 watt per sq cm of radiating surface, for pulses down to about 100 milliseconds. For much shorter pulses (of the order of only a few milliseconds) considerably higher power may be used. Practical considerations limit the area of the radiating surface. If the transducer is driven to cavitation, increases in the sound

intensity on the axis can be made only by decreasing the directivity factor—that is, by increasing the frequency and so narrowing the projector beam.

From a practical point of view, there is a beam-width limit below which it is not feasible to operate in echo ranging. This limit exists because of the rolling, pitching, and yawing of the echo-ranging ship. If, for instance, the angle of roll is considerably greater than the beam width, the target sometimes will be completely out of the beam. Under these conditions the target echo will be greatly attenuated by the beam pattern, especially when the target is abeam. This is true for both the transmitting and receiving patterns. The main beam of an ordinary pattern in a plane can be represented to a good approximation by means of a Gaussian function.<sup>22</sup>

Thus, the normalized intensity pattern of the transmitting beam in the vertical plane may be written:

$$[q(\theta, 0)]^2 = e^{-\left(\frac{\theta}{\delta_1}\right)^2}$$

where  $\delta_1$  is the value of  $\theta$  at which the intensity is  $1/e$  of the intensity  $I_0$  on the projector beam. The angle  $\theta$  is measured in the vertical plane relative to the direction of the beam. The beam may be assumed to be pointed first at the target and then swung through a vertical angle of  $\pm \theta_{\max}$  by the ship's motion. Since the forced roll and pitch of a ship in a resisting medium are generally aperiodic,<sup>23</sup> it may be assumed that all positions, within the extremes set by the angles of roll and pitch of the projected beam, are equally probable. This is somewhat optimistic, since on the average the angular velocity of the rolling ship will probably be greatest when the beam is pointed at the target. However, on the basis of the above assumption, the effective transmitted intensity  $\bar{I}_0$  in the direction of the target can be written as

$$\bar{I}_0 = I_0 \frac{\delta_1}{\theta_{\max}} \int_0^{\theta_{\max}} e^{-\left(\frac{\theta}{\delta_1}\right)^2} d\left(\frac{\theta}{\delta_1}\right).$$

This is the so-called error integral multiplied by  $\sqrt{\pi}/2$ . It is tabulated in Jahnke and Emde, *Tables of Functions*.

A similar factor must be introduced in order to calculate the effective intensity of the returning echo. If  $\delta_2$  refers to the receiving directivity pattern, then the

ratio  $\gamma$  by which the ship's motion has modified the average intensity of the echo is

$$\gamma = \frac{\bar{I}}{I} = \frac{\delta_1 \delta_2}{\theta_{\max}^2} \int_0^{\theta_{\max}} e^{-\left(\frac{\theta}{\delta_1}\right)^2} d\left(\frac{\theta}{\delta_1}\right) \int_0^{\theta_{\max}} e^{-\left(\frac{\theta}{\delta_2}\right)^2} d\left(\frac{\theta}{\delta_2}\right). \quad (34)$$

While there are many causes of fluctuation, this factor may be quite important in determining the value of  $I$  in equation (8). That is, if  $\bar{I}_1$  is the average echo level when the ship is not rolling (or pitching) then  $\bar{I} = \gamma \bar{I}_1$  will be the average echo level when the ship is rolling. A consideration of this factor will indicate what advantages are to be gained by stabilization in any individual case.

Table 7 gives the maximum values of  $\theta_{\max}$  for several types of ships when severe storm conditions do not prevail.<sup>24</sup>

TABLE 7. Roll and Pitch Amplitudes (in degrees).

Type	Navy Designation	Summary Roll	Pitch
Carriers	CV	$\pm 15$	$\pm 5$
Battleships	BB	$\pm 15$	$\pm 5$
(Converted Cruiser)	ACV	$\pm 20$	$\pm 7$
Carrier Escorts			
(Converted Merchant)	CVE	$\pm 20$	$\pm 7$
Carrier Escorts			
Heavy Cruisers	CA	$\pm 20$	$\pm 7$
Light Cruisers	CL	$\pm 30$	$\pm 10$
Destroyers	DD	$\pm 30$	$\pm 10$
Destroyer Escort	DE	$\pm 30$	$\pm 10$
Sub-Surfaced	SS	$\pm 20$	$\pm 10$
Sub-Submerged	SS	$\pm 5$	$\pm 2$
(Yacht Conversions)	PC	$\pm 30$	$\pm 10$
Sub Chasers			

For the following example, illustrative of the use of equation (34), the transducer involved is assumed to be HP-1.<sup>25</sup> A maximum roll angle ( $\theta_{\max}$ ) of  $\pm 15$  degrees is also assumed.

For the HP-1 transducer, the pressure pattern is very nearly Gaussian and has a width of about 18.5 degrees, 8.7 db (i.e.,  $1/e$ ) down. The width of the intensity pattern 8.7 db down is then  $18.5^\circ / \sqrt{2} = 13^\circ$ , so that the pattern half-widths of equation (34) are  $\delta_1 = \delta_2 = 6.5^\circ$ . Thus

$$\gamma = \left(\frac{6.5}{15}\right)^2 \left[ \int_0^{15} e^{-\left(\frac{\theta}{6.5}\right)^2} d\left(\frac{\theta}{6.5}\right) \right]^2$$

In *Tables of Functions*<sup>26</sup> it is stated that for an upper limit of  $\frac{15}{6.5} = 2.3$ , the error integral is 1.0 for all practical purposes. The above integral, then, has the value  $\frac{\sqrt{\pi}}{2} \cdot 1 = 0.886$ , and  $\gamma$  is given by

$$\gamma = \frac{\bar{I}}{I} = (0.433)^2 (0.866)^2 = 0.148$$

If this ratio is expressed in db, the effective average echo intensity  $\bar{I}$  is in this case 8 db below the value which would have existed if the ship had not been rolling.

If it is assumed that a given target can be detected at a maximum range of 1.5 km when the ship is not rolling and when the attenuation coefficient is 6 db per km, the maximum range when the ship is rolling may be calculated from the requirement that the one-way transmission loss must now be 4 db less.

The original transmission loss would be:

$$\overline{TL} = 20 \log_{10} 1.5 + 6(1.5) + 60 = 72.5 \text{ db,}$$

and when the ship is rolling through  $\pm 15$  degrees it would be:

$$\overline{TL'} = 72.5 - 4 = 68.5 = 20 \log_{10} r + 6r + 60.$$

This gives a range of slightly less than 1.2 km, so that the maximum range is reduced by 0.3 km.

### 3.6 COMBINATION OF FACTORS — CHARTS

The performance figure by which an echo-ranging system is ultimately judged is usually the maximum range at which the detection of a given target can be assured with average ocean conditions. It has been pointed out repeatedly that the numerical values of the factors which influence echo-ranging conditions, even for normal ocean states, are not well known at present; however, rough values do exist for the most important factors. It seems worthwhile to proceed with the calculation of maximum ranges in order to indicate thereby which design and performance factors impose the greatest limitations on maximum ranges. This calculation will give estimates of the ranges to be expected and may suggest improvements in design that will reduce the range-limiting factors.

First, curves of the effective pressures at the hydrophone for each type of noise will be calculated as a



function of range. For given conditions, one type of noise will predominate with respect to echoes arriving from a target at a given range, although at some ranges several types of noise may be equally effective. Next, the echo pressure levels, diminished by the proper recognition differentials for the predominant limiting noise or noises, will be plotted for several types of targets. The range at which the echo curve intersects the predominant noise curve will then correspond to the maximum detection range for the particular system, target, and ocean conditions chosen.

The calculation of the echo pressure level is made directly from equation (31) defining target strength, namely:

$$L_e = L_1 - 2\overline{TL} + T, \quad (31)$$

where

$$\overline{TL} = 20 \log_{10} r + 60 + \alpha r \quad (27)$$

and  $L_1$  is the transmitted pressure level on the transducer beam at a distance of 1 meter.

The curve of ambient noise pressure for a given sea state will be a horizontal line at the value indicated by Figure 4 for the operating frequency, adjusted for the receiving directivity index of the transducer. Thus,

$$L'_{an} = L_{an} + D'_e \quad (35)$$

where  $L'_{an}$  is the effective ambient noise level, and  $L_{an}$  is the ambient noise level for a nondirectional receiver. The receiving directivity index  $D'_e$  is inherently negative.

When the echo-ranging ship is sufficiently near a shrimp bed for shrimp noise to be a serious factor, it can be treated in the same manner as ambient noise.

The self noise of the echo-ranging ship is independent of range and, consequently will also be a horizontal line. The values which have been given for self noise are effective values so that no considerations of directivity are involved.

The electrical noise of the receiving system is also a horizontal line whose position depends upon the band width of the receiver.

The values for target noise are given for a range of 183 meters. It will be more convenient to reduce these values to the pressure at 1 meter by adding 45 db. A correction for the additional loss in transmission may

then be made for the desired range. Thus if  $L_{tn}$  represents the target noise at the distance 0.183 km from the echo-ranging ship and  $L'_{tn}$  represents the target noise at the echo-ranging ship, then,

$$L'_{tn} = L_{tn} + 45 - \overline{TL}. \quad (36)$$

The volume reverberation curve is given by equation (20). It will be remembered that  $[P_v]$  is measured relative to  $L_1$  (or  $P_1$ ), the pressure level at 1 meter from the projector, and is given by

$$[P_v] = -60 + D_e - 2\alpha r - 20 \log_{10} r + 10 \log_{10} \left( \frac{m_v c t_0}{3} \right). \quad (20)$$

Finally, the values of surface and bottom reverberation can be computed from:

$$[P_s] = -110 - 30 \log_{10} r - 2\alpha r + D_a + 10 \log_{10} \frac{m c t_0}{4\pi} + 20 \log_{10} \left[ \frac{\sin \left( \frac{\pi l}{\lambda} \sin(\theta - \psi) \right)}{\frac{\pi l}{\lambda} \sin(\theta - \psi)} \right]^2. \quad (26)$$

In all these equations the C.G.S. system of units is used, except that  $r$  is expressed in kilometers. For all practical purposes, meters and kilometers may be arbitrarily replaced by yards and kiloyards respectively, since the error introduced by so doing is negligible compared to the uncertainties existing in the analysis and in the evaluation of the experimental constants.

Illustrative calculations from the data on the electronic rotation [ER] scanning sonar tested on the AIDE DE CAMP are given in the next section and are followed by a comparison of experimental results with expectations arising from the calculations.

### 3.7 EXAMPLE OF CHART FOR ER SYSTEM ON THE AIDE DE CAMP

The following numerical data have been measured for the ER sonar on the AIDE DE CAMP mentioned in Chapter 1 and described in greater detail in Chapter 7.

1.  $L_1 = 110$  db above 1 dyne per sq cm.
2.  $D_e$  (transmitting) =  $-9$  db, pattern 15 degrees down 6 db,  $l = 30$  cm.

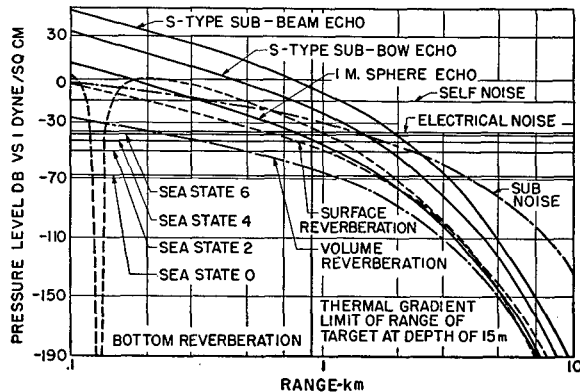


FIGURE 7. Chart for ER system on the AIDE DE CAMP;  $\alpha = 3$  db/km.

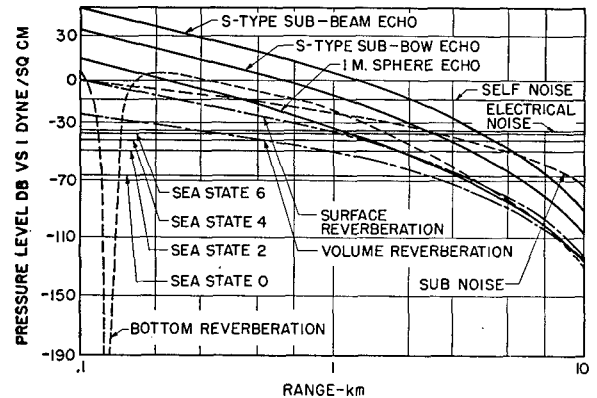


FIGURE 8. Chart for ER system on the AIDE DE CAMP; negative thermal gradient 0.1 F/3 m; 10-m thermocline;  $\alpha = 9$  db/km.

3.  $D'_e$  (receiving) = -23 db, patterns 15 and 25 degrees down 6 db.
4.  $f = 22$  kc,  $c = 1.5 \times 10^5$  cm per sec,  $\lambda = 6.8$  cm.
5.  $t_0 = 5$  milliseconds.
6. Scanning frequency = 200 c, so that effective  $t_0$  is  $5 \times \frac{25^\circ}{360^\circ} = 0.33$  millisecond.
7.  $\Delta f$  (receiver band width) = 4 kc.
8. Equivalent pressure of electrical noise level = -24 db vs 1 dyne per  $\text{cm}^2$ .
9. Indication is visual (PPI) and the recognition differential  $\delta$  is assumed to be +11 db.

The illustrative calculations will be made for a range of 2 km and the following assumptions made:

1. Three types of targets, namely, a sphere of 1-meter radius ( $T = -6$  db), an S-type submarine at bow aspect ( $T = +15$  db) and an S-type submarine at beam aspect ( $T = +30$  db).
2. Submarine is moving at 5 knots at periscope depth.
3. Ideal sound conditions exist for Figure 7.
4. A negative gradient of 0.1 F/3 m and a 10-meter thermocline exist for Figure 8. The last two assumptions give values of  $\alpha = 3$  db per km and  $\alpha = 9$  db per km respectively (see Figure 6).

The transmission loss at 2 km for  $\alpha = 3$  db per km is given by equation (27).

$$\overline{TL} = 20 \log_{10} 2 + 60 + 6 = 72 \text{ db}$$

The echo level from the submarine at beam aspect is given by equation (31).

$$L_e = 110 - 144 + 30 = -4 \text{ db}$$

This value is reduced by the recognition differential (11 db) before it is plotted; e.g.,  $L_e$  at 2 km is plotted as -15 db. The intersection of the echo curve and a particular interference curve will then give directly the maximum range under that interference condition alone.

From Figure 4, the ambient noise for sea state 4 at 22 kc is -25 db in a 1-kc band, or -19 db in a 4-kc band. Adding the receiving directivity index of -23 db gives an effective noise level of -42 db.

The "equivalent" pressure level of the receiver noise is 24 db below 1 bar. This quantity is measured by determining the minimum perceptible pressure in the water; thus it includes the -11 db recognition differential. The corrected equivalent pressure level is therefore -35 db.

It is assumed that the self noise at 10 knots and 22 kc is given by Figure 4 as -20 db in a 1-kc band, or -14 db in a 4-kc band.

The target noise is computed from equation (36), in which the value of  $L_{tn}$  at 183 meters is determined from Figure 5 as -12 db, so that the value at 1 meter is  $-12 + 45 = 33$  db. Again assuming a range of 2 km and taking  $\alpha = 3$  db per km, we obtain

$$L'_{tn} = 33 - 72 = -39 \text{ db.}$$

As before, 6 db must be added to account for the 4-kc band width; consequently, the plotted value is -33 db at 2 km.

The volume reverberation level is determined from equation (20). If  $m_v = 3 \times 10^{-10} \text{ cm}^{-1}$  is taken as an average value of the scattering coefficient,<sup>1,27</sup> then

$$[P_v] = -60 - 23 - 12 - 6 - 71 = -172 \text{ db.}$$

This pressure is relative to  $L_1$ ; the pressure relative to 1 dyne per sq cm is  $-172 + 110 = -62$  db.

The surface reverberation is calculated in a similar manner taking  $10^{-4}$  as the value of the scattering coefficient  $m_s$ . Since operation from a surface ship is being considered, the grazing angle at any appreciable range is less than 9 degrees, so that  $m_s$  is a constant. For the AIDE DE CAMP system  $\psi = 0$ ,  $\sin \theta = h/r = 0.003/r$ , where  $h = 0.003$  km is the transducer depth. It may be seen that the last term of equation (26) is negligible. Thus, if  $P_{ss}$  is sea-surface reverberation pressure,

$$[P_{ss}] = -110 - 9 - 12 - 9 - 22 + 0$$

$$= -162 \text{ db vs. } L_1, \text{ or}$$

$$-162 + 110 = -52 \text{ db vs 1 dyne per cm}^2.$$

For the calculation of bottom reverberation, a coefficient will be used between that for a mud-and-sand bottom and that for a rocky bottom, namely,

$$m_b = \frac{5 \times 10^{-2}}{\sin^2 9^\circ} \sin^2 \theta.$$

It may be assumed that

$$\sin \theta = \frac{h_b}{r} = \frac{0.03}{r},$$

where  $h_b = 0.03$  km is the vertical distance from the transducer to the bottom. The last term of equation (26) cannot be neglected for all values of  $r$  in this calculation. The equation may be rewritten, with  $P_{sb}$  denoting sea-bottom reverberation pressure, as

$$[P_{sb}] = 10 - 2\overline{TL} + 10 \log_{10} r + 10 \log_{10} \frac{0.12}{r^2} + 20 \log_{10} \left[ \frac{\sin \frac{0.13}{r} \pi}{\frac{0.13}{r} \pi} \right]^2$$

For  $r = 2$  km and  $\alpha = 3$  db per km,

$$[P_{sb}] = 10 - 144 + 3 - 15 + 0 = -146 \text{ db vs } L_1, \text{ or}$$

$$-146 + 110 = -36 \text{ db vs 1 dyne per sq cm.}$$

Figure 7 shows the complete curves of pressure level vs range for the ER sonar on the AIDE DE CAMP for  $\alpha = 3$  db per km.

Figure 8 is identical with Figure 7 except that  $\alpha = 9$  db per meter. A calculation<sup>28</sup> of the path of the limiting ray in the case of the 0.1 F/3 m negative temperature gradient shows that a target at a depth of 15 meters cannot be detected at ranges greater than about 0.9 km. This is a rather conservative value for the gradient.

A glance at Figure 7 shows that in ideal water conditions the maximum range on large targets is limited by the self noise of the echo-ranging ship. The maximum range can be increased by lowering the self noise; e.g., if the self noise were lowered about 20 db, the range of the submarine at bow aspect would be increased from about 1 km to 2 km. The limiting noise at 2 km would be the sum of the self noise, the electric noise, and the submarine target noise.

Figure 8 shows that the improvement indicated above is probably not worth while, because relatively small negative thermal gradients will limit the range to less than 1 km.

Both Figures 7 and 8 show that the ranges of small objects are severely limited by bottom reverberation in water of 30-meter depth. This conclusion was verified by the experimental work reported in the next section.

### 3.8

## EXPERIMENTAL RESULTS

A series of measurements of the maximum detection ranges of a sphere of  $1/2$ -meter radius was made with the ER sonar on the AIDE DE CAMP in water depths from about 15 meters to 100 meters in the vicinity of Boston. The target and transducer were both about 3 meters below the surface. The following empirical formula seems to fit the data fairly well:

$$r = 0.183 \log_{10} h_b - 0.133 \quad (37)$$

where  $h_b$  is the depth of the water in meters and  $r$  is the range in km at which 50 per cent of the echoes are detected.

Particular consideration will be given to the data obtained near Nahant in 30-meter water, with a sea bottom of mud, sand, and rock, since these were the conditions assumed in preparing Figures 7 and 8.

The range at which 50 per cent of the echoes were recognizable was about 0.135 km, which is in agreement with equation (37). The range at which 90 per cent of the echoes were recognizable was about 0.09 km. The difference in the two-way transmission losses

for the 0.09-km and 0.135-km ranges is 6 db, which indicates that, for this system and operator, the difference in average echo level for 50 and 90 per cent recognition probability is 6 db, which is considerably smaller than the value of 11 db given by equation (8) for 90 per cent recognition. The reasons for this discrepancy are not known; however, the indicator of this particular ER system undoubtedly has characteristics not present in other indicators. Also this value of 6 db is for only one set of conditions. The operator has reported that only those echoes causing appreciable persistence on the oscilloscope face were counted. The ship was rolling with a maximum angle of about  $\pm 15$  degrees when the measurements were made.

The value of the maximum calculated range of detection of a sphere of  $\frac{1}{2}$ -meter radius can be found from Figures 7 and 8. Since  $T = -6$  db for the 1-meter sphere and  $T = -12$  db for the  $\frac{1}{2}$ -meter sphere, the echo curve of the latter will be 6 db lower than that of the former. This gives a maximum range of about 0.16 km. It will be remembered that this value is for 80 per cent echo recognition probability, and that it is based on the assumption of no roll or pitch. The correction for 15 degrees maximum roll was calculated earlier as 8 db. On the average, the echo level should probably be 5 to 8 db (corresponding to 10 to 15 degrees roll) lower than the value used. If it is assumed that this difference must be made up in the transmission loss, the maximum range for 80 per cent recognition probability is about 0.11 to 0.13 km.

If it is assumed that the form of equation (8) is correct for the ER indicator and that 6 db is the value for the difference in average level for 50 and 90 per cent recognition, then we can interpolate for the 80 per cent value. This indicates that the level must be 3.5 db higher for 80 than for 50 per cent, and that it should be 2.5 db lower for 80 than for 90 per cent. When these corrections are applied to the 0.135-km and 0.90-km experimental values, a figure of about 0.110 km is obtained at the 80 per cent recognition value. This is to be compared with the calculated value of 0.11 to 0.13 km. The agreement seems to be well within the limits of error of the calculations, especially since peculiarities in minor lobe structure undoubtedly produce an appreciable modification

of the effective bottom reverberation at such close ranges.

Experimental work with ER sonar on large targets indicates that thermal gradients limit range in many cases. It was observed that 80 to 90 per cent echo recognition occurs up to a specific range and that no echoes were found beyond this range. This conclusion is in good agreement with Figure 8.

### 3.9

## FIGURE OF MERIT

From the experimental point of view, it is desirable to have a method of comparing different echo-ranging systems directly and under identical water conditions. The measurement of the maximum detection ranges for a given target does not necessarily afford a valid basis for the comparison of systems, since in many cases thermal conditions, rather than the characteristics of the system, limit the range. A consideration of maximum detection ranges is, however, of paramount importance in determining what "price" should be paid for any proposed "improvement" in the system. A definite measure of the improvement may be obtained by determining the *figure of merit*.

The figure of merit of a system is defined as the ratio, expressed in db, of the pressure level in the transmitted beam at 1 meter from the projector to the minimum detectable received echo level at the hydrophone. The figure of merit does not depend strongly on existing thermal conditions; however, thermal conditions may modify the reverberation level at the hydrophone, and this does influence the detectability of echoes. This is desirable because the discrimination against reverberation may be an important characteristic of the system. It must be emphasized that the figure of merit of a system as it has been defined has different values for different ranges, ocean conditions, and speeds of the echo-ranging ship.

The procedure employed in measuring the figure of merit is discussed in Chapter 8. Representative values for the QH Model II system, which is a commutated rotation sonar system, are 152 db for the listening channel and 142 db for the scanning channel. These values are for long ranges (low reverberation) with the echo-ranging ship at rest.

## Chapter 4

# MECHANICAL ROTATION SCANNING SONAR

### 4.1 GENERAL DESCRIPTION

WHEN THE WORK on scanning sonar was begun, it seemed clear that the easiest and most direct method of rotating a beam of receiving sensitivity would be simply to rotate a directional hydrophone in the water. This scanning method was known as *mechanical rotation* [MR] scanning sonar and the actual system which embodied it was given the name *rotoscope*. Two of these sonar systems were built; the first was installed on the HUSL calibration barge TIPPECANOE, and the second which was more complex, on the HUSL experimental yacht AIDE DE CAMP.

#### 4.1.1 Necessary Elements of MR Scanning Sonar

The essential functions of the rotoscope were (1) to send out a pulse of sound in all directions simultaneously, (2) to pick up returning echoes on the rotating hydrophone, and (3) to indicate the range and bearing of reflecting objects on a *plan position indicator* [PPI]. To accomplish these functions the following principal elements were required:

1. A cylindrical emitter capable of sending out a pulse of sound energy with equal amplitude in all directions.
2. A power amplifier to drive the emitter.
3. A method of controlling the emitted pulse in time and length.
4. A rotating directional hydrophone.
5. A receiving amplifier, either single-channel, or two-channel for use with *bearing deviation indicator* [BDI].
6. A plan position indicator.

Figure 1 is a block diagram of such a system. In this figure is shown a cylindrical projector which can emit sonic energy equally in all horizontal directions and which is energized by the transmitter. A receiving hydrophone with a horizontal directional sensitivity is shown being rotated by a motor drive. The signal from this rotating hydrophone is amplified by the receiving amplifier and used to brighten a spot on the cathode-ray tube plan position indicator. A timing device is necessary to initiate the ping at the

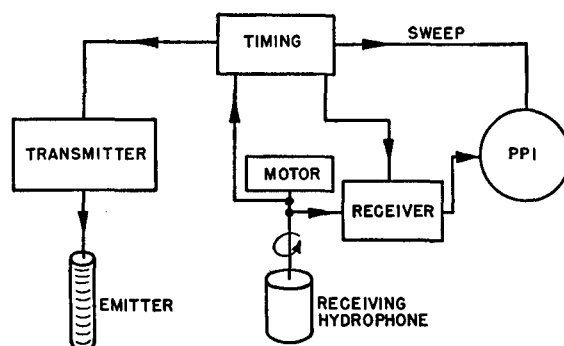


FIGURE 1. Block diagram of mechanical rotation scanning system.

proper instant and control its duration. This timing input also grounds the receiver input during the ping and produces flyback of the spiral sweep of the cathode-ray spot for the PPI. The timing must be controlled by the rotation of the hydrophone to insure proper sequence of operation and correct PPI indication.

The emitting projector used throughout the MR sonar development was a stack of commercially available ring-shaped magnetostrictive laminations resonating at 14 kc. This unit, as well as the receiving hydrophones, is described fully in the section on transducers.

The first receiving hydrophone was of Rochelle salt with a 6x6-inch active surface made unidirectional by a resonant steel backing plate. The receiving hydrophone used with the Model 2 rotoscope was a nickel tube magnetostrictive unit. This hydrophone was permanently polarized by magnets inside the tubes and each was electrically split for *simultaneous lobe comparison* [SLC] reception.

The receiver on the first model was known as the *automatic volume control* [AVC], or the 16-knob, receiver.<sup>1</sup> The Model 2 receiver was a TVG-AVC amplifier with approximately 120 db of gain. These receivers are discussed in detail later in the chapter. The Model 2 rotoscope also included a Model X-3 BDI receiver, retuned to 14 kc, which was used with the split hydrophone.

The original transmitter had a final power-amplifier stage capable of supplying 50 watts to the ring-



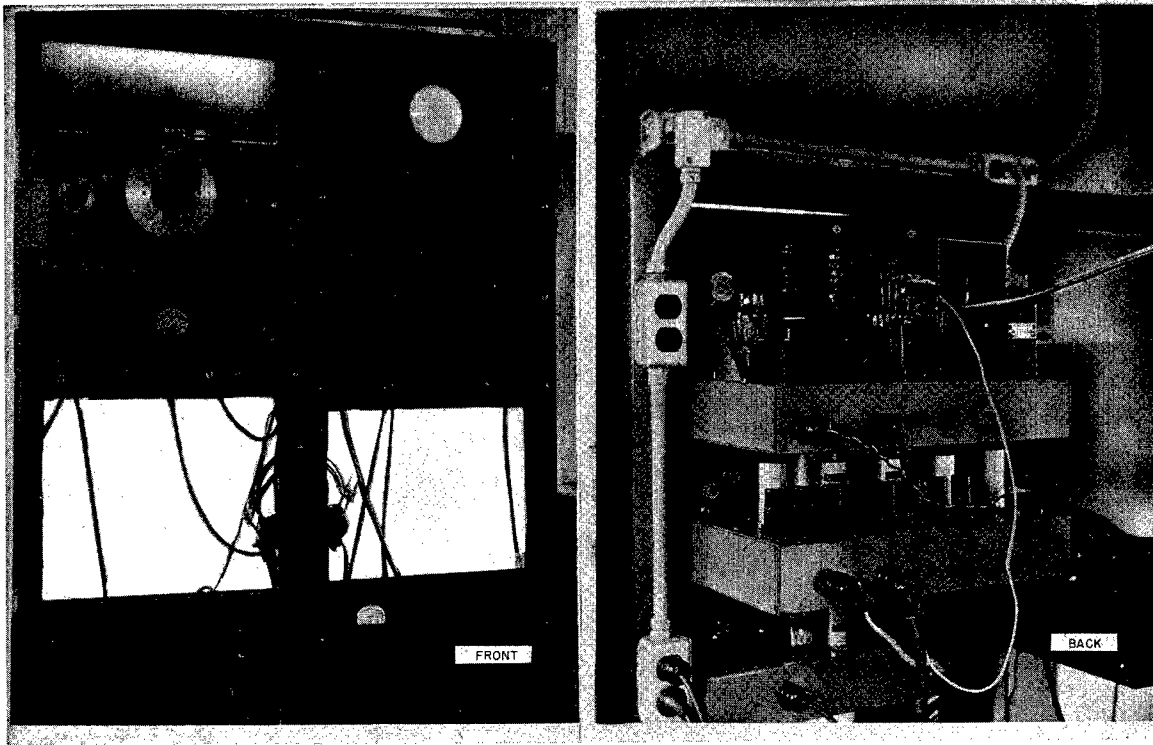


FIGURE 3. Model 1 rotoscope racks.

cathode follower to produce the sawtooth varying current in the deflection coils. The flexible shaft, for rotating the deflection coils of the PPI scope in synchronism with the hydrophone rotation, is shown in the figure, as is the keying chassis that controlled the ping by closing the polarizing circuit and the oscillator and power-amplifier circuit. The keying chassis also shorted the input to the receiver to prevent overload during the ping. Figure 3 shows front and back of the racks holding the electronic equipment of the Model 1 rotoscope.

## 4.1.3

**Model 2 Rotoscope**

Figure 4 is a block diagram of the Model 2 rotoscope as set up on the AIDE DE CAMP. Incoming sound was received on the hydrophone, which was rotated by the motor, and the resulting electric signal was passed through slip rings to the SLC amplifier or the amplitude receiving amplifier. From either of these, the signal could be put on the PPI by means of a selector switch. A low-pass filter was located in the receiving amplifier circuit. This unit, which was designed to pass rectified echo pulses but to reject

high-frequency noise pulses, could be switched in or out at the operator's discretion. The loud speaker was connected to the receiving amplifier at all times. The contact operated by a cam on the rotating shaft controlled the stepping relay, which in turn controlled emission of the ping, synchronization of the spiral-sweep generator, spiral-sweep flyback, the TVG initiation in both receivers, and the keying of the power amplifier. The keying of the polarizing current circuit for the ring-stack emitter is not shown in this diagram. Figure 5 is a photograph of the electronic chassis racks of this system on the AIDE DE CAMP.<sup>2</sup>

**4.2 EXPERIMENTAL WORK AND RESULTS**

Experimental work on MR scanning sonar began early in 1942 and continued into June 1943.<sup>2</sup> Although the description which follows deals primarily with the rotoscope development, it should be noted that much of the work was directed toward problems of scanning in general rather than mechanical rotation in particular. Considerable effort was devoted to the provision of experimental facilities

CONFIDENTIAL

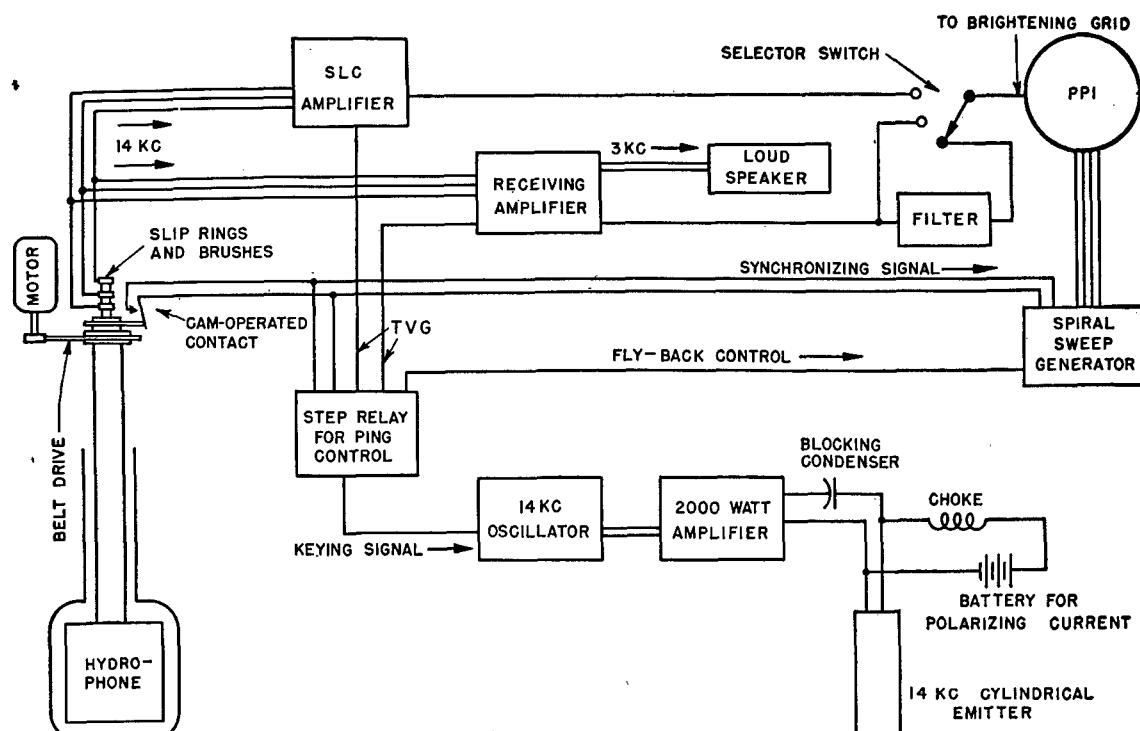


FIGURE 4. Block diagram of Model 2 rotoscope.

which were later used for *commutated rotation* [CR] and *electronic rotation* [ER] sonar and other projects.

#### 4.2.1 Preliminary Noise Tests in the Laboratory

Preliminary experimental work was carried on in the spring of 1942 by utilizing a subterranean crystal-growing vault located below the basement level of the Research Laboratory of Physics, Harvard University. This vault was watertight for protection against the high water table and provided a convenient testing tank.

One of the basic questions to be answered for the MR system was whether or not it would be possible to rotate a hydrophone without producing troublesome noise in the water. A preliminary test was made by rotating a 12-inch cylindrical dome in the water at 240 rpm. The rotating rig, designed for later use in the TIPPECANOE installation, was installed over the vault entrance for this purpose. The results obtained were encouraging in two ways; the rotating dome hanging from a universal joint proved to be reasonably stable without restraint below the joint, and the noise generated by rotation in the water was negli-

gible. A small crystal hydrophone placed inside the dome yielded no observable noise as a result of the rotation, although it was sufficiently sensitive to respond to noise produced by dangling a small metal object in and out of the water.<sup>3</sup>

#### 4.2.2 Pattern of Receiving Hydrophone When in Dome

The galvanized iron container for the hydrophone used in the above tests was designed to hold a 6x6-inch Rochelle salt transducer. The effect of this dome on the transducer pattern was investigated. Final results showed that the container sharpened the beam pattern somewhat in the vertical direction, and that the microphone in the dome made enough of an angle in the vertical plane so that the beam from one side of the crystal transducer was aimed at the source of sound, but the one from the other side was not.

Meanwhile, a new 6x6-inch hydrophone and container were under construction. In order to economize on size, the walls of the container were used as supports to hold the microphone. The patterns were found to be unsatisfactory and the container was rebuilt, with channels supported from the top to hold the hydrophone. The walls were thus supported

CONFIDENTIAL



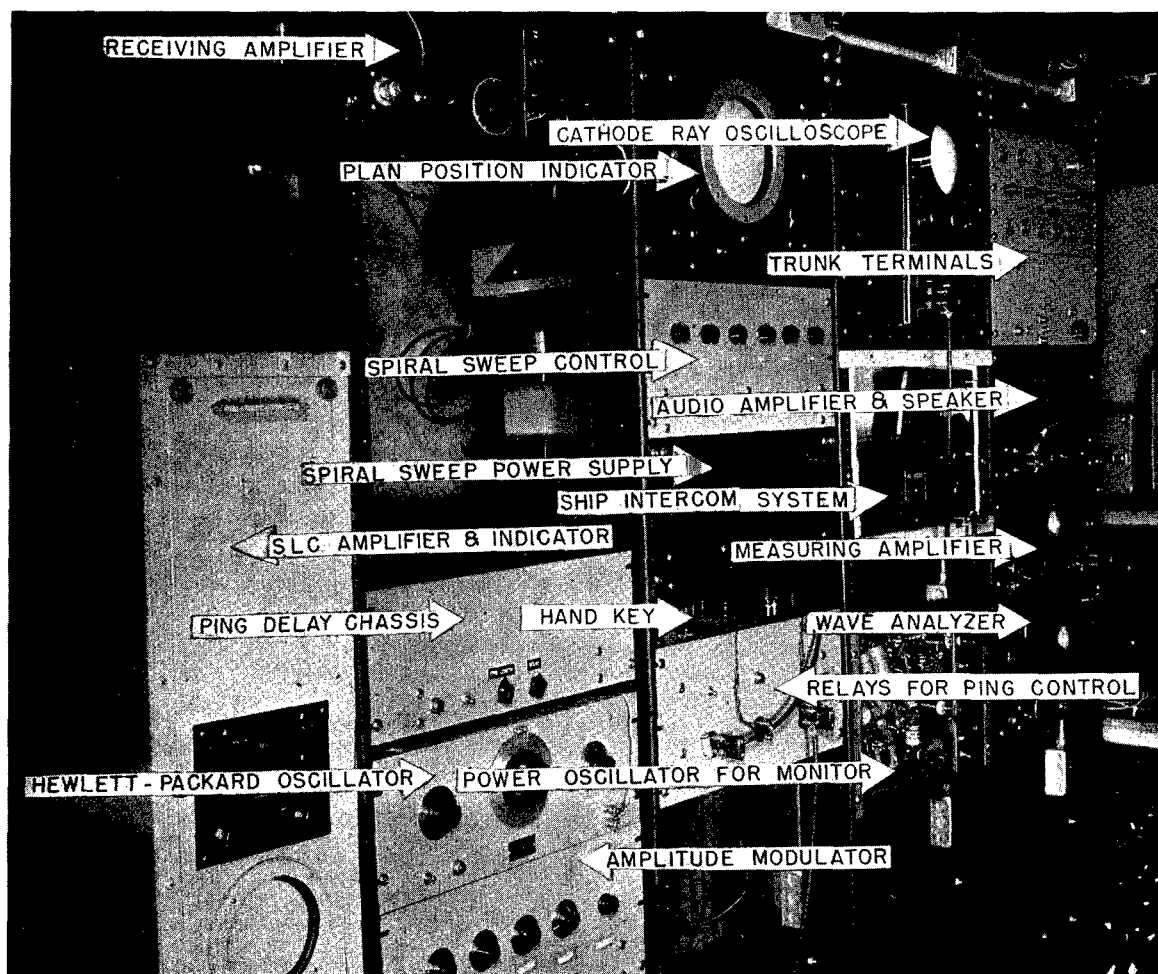


FIGURE 5. Model 2 rack and measuring equipment on the AIDE DE CAMP.

less rigidly than before and satisfactory patterns were obtained. This hydrophone was made unidirectional by using a resonant backing plate of steel backed with pressure-release rubber. A slab of plate glass was added on the front to give resonance at a frequency of 14.25 kc. The front-to-back discrimination was about 15 db.

#### 4.2.3 Installation of Model 1 Rotoscope

Preparations for a barge installation of MR sonar were begun in May 1942. By the end of July, the mechanical rotator described later in this chapter had been installed, and listening tests were made with encouraging results.<sup>4</sup> The original pipe support failed to run true, and steel tubing was substituted for the pipe below the universal joint. Power consumption was as follows:

1. Worm disengaged, motor running free—115 watts, 350 volt-amperes.

2. Dome rotating—200 watts, 400 volt-amperes.

Additional components of the system were installed as they became available. This equipment included the AVC receiver, the 14-kc ring-stack emitter, transmitter unit, the ping control and sweep mechanism, and the PPI unit.

On September 8, 1942, the equipment was inspected by a committee of Division 6, and brightening on a sector of a PPI screen was obtained, but pinging or reception of echoes had not yet been accomplished.<sup>5</sup>

#### NOISE REDUCTION

The usual installation difficulties were present and included the appearance of many varieties of noise. One principal source, pickup in the microphone

CONFIDENTIAL

cables, was reduced by improving the grounding of the cable shields, and by parallel-tuning the hydrophone and cable. A 40-millihenry coil and a capacitor of 0.0005  $\mu$ f were connected directly across the brushes. Radial lines, which appeared on the CR screen, were traced to noise arising in the brush and slip assembly. The slip rings were rebuilt using smaller rings,  $\frac{3}{8}$  inch in diameter, made of coin silver. The brushes were also redesigned using silver and being slit so as to form five fingers at the ends. Two brushes were used on each ring. After these changes were made, no further trouble from this source was experienced.

#### TESTS IN BOSTON HARBOR

To obtain a locality where water noise was relatively low, the barge with the installed equipment was towed to Pleasure Bay on September 15, 1942.<sup>6</sup> It was found possible to start the rotating rig by hand and to maintain its motion with power from a 1-kw gasoline-driven 60-cycle generator. A signal was put into the water by means of a 1x1-inch crystal projector, and appropriate brightening was obtained on a sector corresponding to the position of the source. It was found that 0.3  $\mu$ v across the 6x6-inch receiving transducer produced the minimum signal for good brightening. During this test, indications appeared on the PPI which proved to be caused by a small outboard motorboat about a  $\frac{1}{2}$  mile away.

No evidence of spurious brightening or brush noise was observed on this trip. Three days later, a second trip was made with the AIDE DE CAMP serving as tow vessel. It provided an extra source of 60-cycle power,<sup>7</sup> which freed the 1-kw generator aboard the barge to supply power for the output stage of the transmitter. The available power was still not adequate, however, to drive the amplifier to its rated 400-watt output. In these tests, the equipment again proved sensitive to target noise. Evidence of echoes consisted only in an extra bright spot superimposed upon the noise indication from the target. Water noises of undetermined origin caused appreciable trouble, so that it seemed necessary to find a quieter location.

#### TESTS IN CHARLES RIVER BASIN

On September 21, 1942, the barge was moved to the Charles River Basin where it was tied up alongside the measuring barge TYLER-TOO.

During tests, bright spots were observed on the

fourth or fifth turn of the spiral, indicating reception of echoes from an unidentified target located 1,000 yards upstream.<sup>8</sup> The gain was set so that reverberation appeared only on the first turn of the spiral. In this location, echoes up to 1,600 yards range were obtained, but there was no way of estimating the target strength of the reflector in comparison with that of a submarine.

Since the power that could be put into the water was limited by the 60-cycle sources, an attempt was made to increase the peak power for a given power consumption by employing amplitude modulation. A modulator was built that allowed a considerable choice of the amount and rate of modulation, and it was found possible to increase the peak intensity by this means. However, before any adequate evaluation of the equipment could be carried out, the rotating hydrophone was lost as a result of an accident. Though it was soon recovered, progress on the succeeding model was so well advanced that it was decided not to remount the Model 1 hydrophone, but to apply all possible effort to the completion of the Model 2 rotoscope.

The conclusions drawn from the Model 1 rotoscope experiments included the following:

1. The original slip rings caused trouble but the coin silver replacements with reduced dimensions were satisfactory.
2. The AVC receiving-amplifier characteristics were not satisfactory.
3. Rotation of the hydrophone in its container did not generate sufficient noise to cause trouble.
4. Difficulties with the mechanically rotated deflection coils led to the development of an electronic spiral sweep.
5. The work was handicapped by power limitations, both with respect to 60-cycle supply and to driving power obtainable from the 400-watt amplifier.
6. The lack of a calibrated target was a serious handicap.
7. The tests, as far as they went, revealed no fundamental difficulty in the way of scanning.<sup>9, 10</sup>

#### 4.2.4 Model 2 Rotoscope Experiments

The installation of the rotating microphone assembly on the AIDE DE CAMP was completed on October 23, 1942. This installation included the 12x12-inch tube-and-plate hydrophone, described later in

this chapter, mounted in the airtight rotation rig. The TVG receiver and a 7-inch cathode-ray tube PPI were installed. The 400-watt power amplifier was transferred from the TIPPECANOE to the AIDE DE CAMP together with the 14-kc ring-stack emitter. The ping-control relay unit was also installed in a crude form along with the electronic sweep circuit. Both of these are discussed in detail later.

The initial tests revealed various troubles, which were discussed in a 2-day conference, November 12-13, 1942.<sup>11</sup> Proposed improvements included:

1. Replacement of the 15-mil medium-temper nickel tubes by 10-mil soft nickel for greater sensitivity.
2. Shock-mounting of the 12x12-inch hydrophone to insulate it from mechanical vibration of the rotating support shaft.
3. Substitution of a cam-operated synchronizing switch for the gear-driven 4-cycle generator in order to eliminate gear noise.
4. Improvement of ground connections.
5. Reduction of electric noise from d-c motors.
6. Reduction of switching transients during the flyback of the spiral sweep.
7. Provision of means for training the rotating hydrophone by hand.

While these changes were being made, a 4.8-kva generator was installed on the AIDE DE CAMP, and the first trial of the complete Model 2 rotoscope was made December 19, 1942.<sup>12, 13, 14</sup> Tests and improvements on this model continued with minor interruptions until June 10, 1943, when it was removed to make room for CR scanning sonar equipment.

#### TESTS ON SYSTEM COMPONENTS

The 400-watt driver-amplifier caused considerable trouble until it was replaced in March 1943 by a 1.5-kw amplifier. An 8-db improvement in signal-to-noise ratio was obtained with the increased driving power. The new amplifier again made the 60-cycle power source inadequate, until an additional generator was installed.

The receiving amplifier was subject to numerous tests. Its TVG characteristics were measured and modified from time to time and interaction of the TVG setting with the main gain control was corrected.<sup>15</sup> The receiver had an output attenuator and it was found that at a commonly used setting of this attenuator the dynamic range was only 5 or 6 db. A rectifier and a filter, added in April 1943, were de-

signed to produce maximum brightening on a pulse shaped like that obtained by sweeping the receiving beam through a target echo. Under certain conditions the d-c method of brightening improved the appearance of the scope considerably.

Tests on SLC brightening were conducted with a Model X-3 BDI unit, modified for 14-kc operation.<sup>16</sup> Pattern measurements showed that the 12x12-inch hydrophone was not very satisfactory as a split projector;<sup>17</sup> nevertheless, it produced narrowing of echo images on the PPI scope. In general, the objection to SLC brightening was that spots due to electric noise and actual echoes all looked alike on the scope. The delineation of shore lines was less easy to interpret with SLC than with straight reception. It was noted that the recognition of echoes on the PPI screen was aided by the audible signals, even though the latter were quite short. Calculation showed that echoes of about 0.020-second duration were obtained which were sufficient for recognizing doppler.

Attempts to calibrate the 12x12-inch hydrophone after it was mounted were unsuccessful, partly because large fluctuations in the output occurred when steady sound was put into the water.

A ping-delaying device was installed in January 1943 and tested without appreciable success, largely because of the lack of constant echoes from the natural reflectors available. The purpose of this device was to improve range accuracy by bracketing the target between two successive turns of the spiral.<sup>18</sup>

Amplitude modulation of the ping was tried on various occasions, but no conclusion could be drawn concerning its effect on echo-to-reverberation ratio because of the lack of reliable echoes.

Reverberation studies received considerable attention. In the water accessible to the AIDE DE CAMP the strong bottom reflections could not be distinguished from surface and volume reverberation, and it was found that reverberation intensity fluctuated more or less in synchronism with the rotation of the hydrophone. Tests were conducted with the hydrophone stationary, pointed successively in different directions, and large variations in the reverberation pattern were obtained as a function of direction. Even in the deepest water reached by the AIDE DE CAMP—about 300 feet—effects of this kind were observed.<sup>19</sup> The reverberation studies were conducted partly with a high-speed level recorder and partly with a cathode-ray oscilloscope [CRO] provided with an auxiliary slow sweep. The sweep rate was

adjusted to agree with the pinging rate and photographs of the scope face were taken. Comparisons were made between the reverberation obtained with the 0.250-second ping required by the rotoscope's MR scanning system and the 0.035-second ping that was to be used in the CR scanning sonar.<sup>2</sup> The reverberation intensity was very much less in the latter case, but no statistical analysis of the data was made, since results of reverberation studies made at the San Diego Laboratory were available.

Tests of 39-kc operation were carried out. Since the hydrophone had a secondary response at 39 kc, a ring-stack emitter was made to match this frequency. The results of the tests were disappointing and it was found that the 39-kc pattern of the hydrophone was unsatisfactory, with minor lobes only 6 db down.

#### 4.2.5 Evaluation of Model 2 Rotoscope

Attempts to evaluate the rotoscope as an echo-ranging system were handicapped in many ways. The lack of a suitable target was a primary difficulty. The development of a reliable echo repeater was proceeding concurrently with these tests, but by the time the repeater was in satisfactory working condition, seasonal deterioration in water conditions in the vicinity of Boston had progressed markedly. On one occasion echoes from the repeater were received up to ranges of 200 yards. On another occasion they were obtained from the repeater at 1,600 yards, but not at shorter or longer ranges. Echoes on surface vessels were occasionally obtained up to the maximum of 3,800 yards, as estimated by comparison with the ping rate of the rotoscope, and at other times were completely unobtainable regardless of range.<sup>20, 21</sup>

One expedient which was tried in the test program was the modification of an echo repeater to send back signals with an artificial doppler. The ping reaching the echo-repeater hydrophone was made to key an oscillator set for a frequency differing slightly from that of the ping. In this way it was possible to recognize the signal from the echo repeater, even in the harbor in the presence of reflections from shore lines, bottom irregularities, and shipping.

Altogether, about 60 experimental trips were conducted, including two overnight trips to Gloucester to permit tests in 300-foot water off Cape Ann. On a few occasions the results were very promising but

there was no way of comparing the effectiveness of the reflectors with submarines. It was concluded that the reverberation level of a 0.250-second ping was too high for reliable echo ranging considering the beam pattern and sensitivity of the hydrophone being used. It may well be, however, that this conclusion was correct only for the shallow water in which tests were conducted and that peculiarities of the rotoscope receiver contributed to the unsatisfactory performance of the system.

The use of the mechanical rotation scanning sonar had not been contemplated for naval service, nor did it ever reach, in its echo-ranging form, a level of performance suitable for such service.

MR scanning sonar was developed to pave the way for the commutated rotation scanning systems. Application of the MR principle to listening systems for service use was, as mentioned in Chapter 1, carried out by other organizations.

#### 4.3

#### TRANSDUCERS

##### 4.3.1 15-inch Magnetostriction Ring-Stack Emitter

The emitter used throughout the HUSL experiments on the MR scanning sonar was a ring stack manufactured by the International Projector Company and was designed to be resonant at approximately 14 kc. Its general mechanical construction is shown in Figure 6. This photograph shows the top of the ring stack as it was suspended in the well of the AIDE DE CAMP. The laminations were made of 0.010-inch nickel annuli having an outside diameter of 5 inches; the overall height of the unit was 15 $\frac{3}{8}$  inches. The hydrophone was wound with 24 turns of Gencaseal insulated wire, which passed through holes near the periphery of the nickel annuli (see Figure 7).

The directionality of this unit is indicated in Figure 8 which shows the vertical pattern. The horizontal pattern was flat to within 1 db. Figure 9 shows the frequency response. No attempt was made to calibrate the field so that the exact nature of the curve was indeterminate; that is, when the curve was plotted, no corrections were made for the characteristics of the receiving hydrophone and amplifier.

Motional impedance curves,<sup>22</sup> taken both in water and in air while a 10-ampere polarizing current was used, showed that the impedance at resonance in air

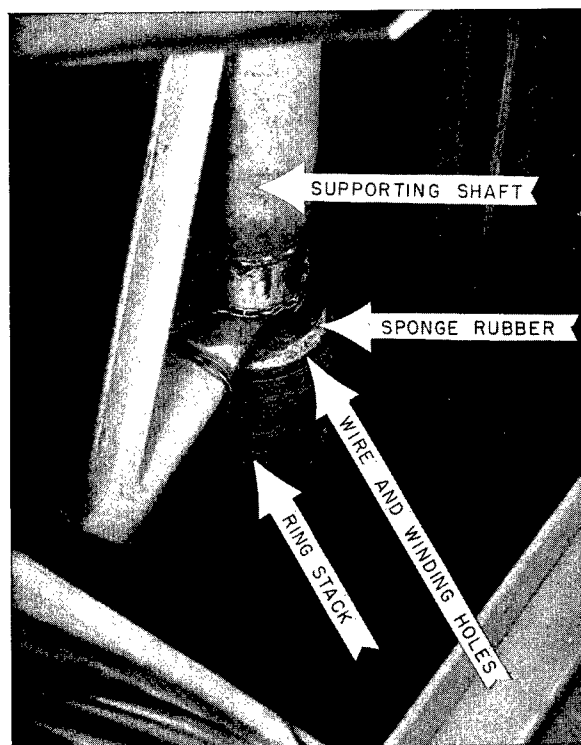


FIGURE 6. Ring-stack emitter (14-kc) mounted in AIDE DE CAMP well.

was  $11.6 + j32.32$  ohms, and the impedance at resonance in water was  $12.0 + j30.0$ . The mechanical  $Q$  in air was approximately 48, while the mechanical  $Q$  in water was 25. From these data the efficiency at resonance was computed to be 32 per cent.

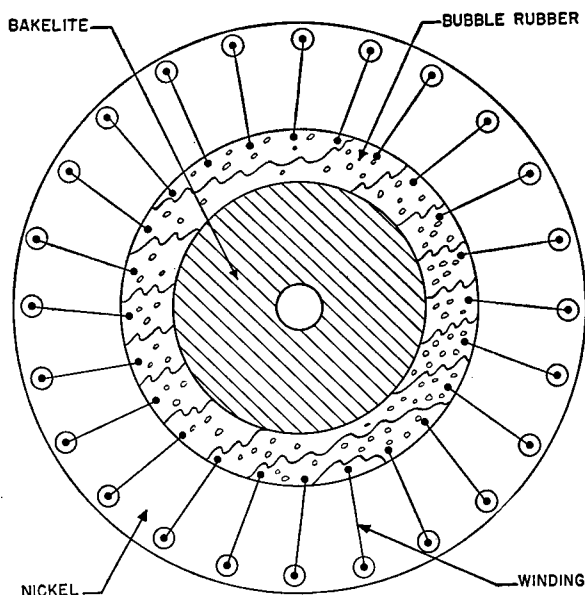


FIGURE 7. Horizontal section of 14-kc ring-stack emitter.

#### 4.3.2 6x6-inch Crystal Hydrophone

The first receiving hydrophone used with this system was a 6x6-inch crystal unit consisting of 4 sections, each section 3x3 inches with four parallel groups of six crystals in series. The crystals were 45-degree X-cut Rochelle salt,  $1\frac{1}{2}$  by  $\frac{7}{16}$  by  $\frac{1}{4}$  inches. Copper-foil electrodes were used, and clear Glyptal cement held the individual crystals together. The diaphragm was made of  $\frac{3}{8}$ -inch plate glass.

Since the crystal hydrophone was to revolve at a speed of 4 rps, it was necessary to surround it with a cylindrical container or dome. The general appearance of the first mounting will be seen from the drawing in Figure 10. The dome and hydrophone were both attached rigidly to the supporting shaft. Free-flooding holes in the cylinder allowed it to fill with sea water when in use. The patterns obtained with this hydrophone were poor, and in addition were double-sided since there was no backing plate on the hydrophone.

For this reason a second 6x6-inch crystal hydrophone was constructed and mounted inside a dome somewhat smaller than the first. As finally built, the hydrophone was supported at the top, thereby eliminating the mechanical connection at the sides between the container and the hydrophone. This arrangement produced patterns which were somewhat better than before, but still not so good as desired. The pattern of the hydrophone, with its backing plate, outside the cylindrical container is shown in Figure 11 while Figure 12 gives a pattern taken on the same hydrophone when mounted inside the container. Both patterns were taken at a frequency of 14 kc. No calibration was made in absolute terms, but a frequency response curve without correction for the characteristics of the measuring transducer is given in Figure 13.

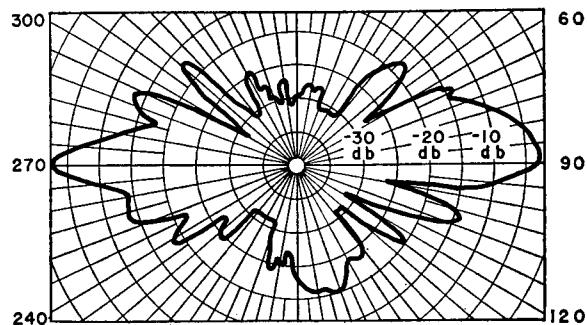


FIGURE 8. Vertical pattern of 14-kc ring-stack emitter.

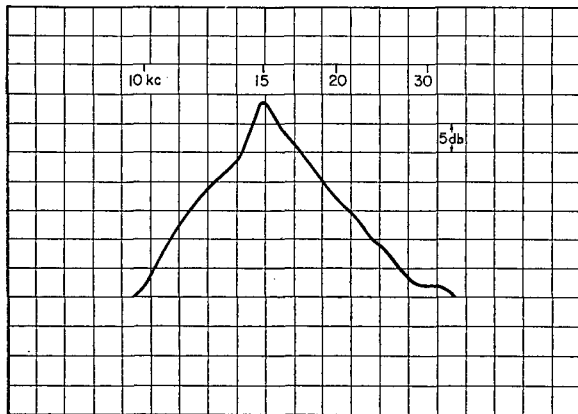


FIGURE 9. Frequency response of 14-kc ring-stack emitter.

The 6x6-inch crystal hydrophone was employed for the experiments on the barge *TIPPECANOE* as outlined earlier in this chapter.<sup>9</sup>

#### 4.3.3 12x12-inch Magnetostriction Hydrophone

The first definitive data obtained on a hydrophone for MR sonar were those taken on the 12x12-inch magnetostrictive tube hydrophone.<sup>23</sup> This hydrophone consisted of a steel diaphragm upon which were mounted 112 magnetostrictive nickel tubes, which in turn were surrounded by coils of magnet wire wrapped on wooden spools. The 112 coils were mounted between two pieces of 1/4-inch plywood to form a rigid mechanical unit, the coil assembly being held to the diaphragm by 16 stanchion bolts projecting up from its edges. The working assembly (i.e., the diaphragm, nickel tubes, and coil assembly) fitted into the hydrophone box, which was made of 1/16-inch steel. The thin edges of the diaphragm plate were clamped against a narrow rubber gasket to make the entire assembly watertight.

The diaphragm was made from a piece of steel 11 3/4 inches square and 3/8 inch thick; a 5/16-inch border around the edge of it was milled down to a thickness of 1/16 inch, and the remaining thick part of the plate was grooved diagonally by slots 1/16 inch wide and 5/16 inch deep. These served to cut the plate into 112 squares, approximately 1 inch on a side. The purpose of slotting the diaphragm was to reduce the mechanical coupling between the individual magnetostrictive units, thereby allowing each square with its individual tube assembly to act independently of the rest.

The nickel tubes were 0.015x0.375x3.7 inches and of medium temper. One such nickel tube was butt-soldered to each of the 112 full squares on the diaphragm, the coil assembly being used as a jig to hold the tubes in place while they were being soldered.

The coils were wound with 104 half-turns of No. 20 En SCC magnet wires on wooden spools which had overall dimensions of 15/16-inch diameter by 2-inch length and which had been boiled in paraffin before winding. The holes in the wooden spools were reamed out to 7/16 inch after the nickel tubes had been soldered in place. The 112 completed coils were glued with Glyptal cement between two pieces of 1/4-inch plywood in which had been drilled a pattern of 1/2-inch holes to match the holes in the wooden spools. The ends of the wires from the coils were drawn through small holes in the upper plywood plate. The entire coil assembly was then cooked in hot paraffin, allowed to cool, and then given a quick dip to put a coating of paraffin over all exposed surfaces. When the coil assembly was mounted, it was adjusted down

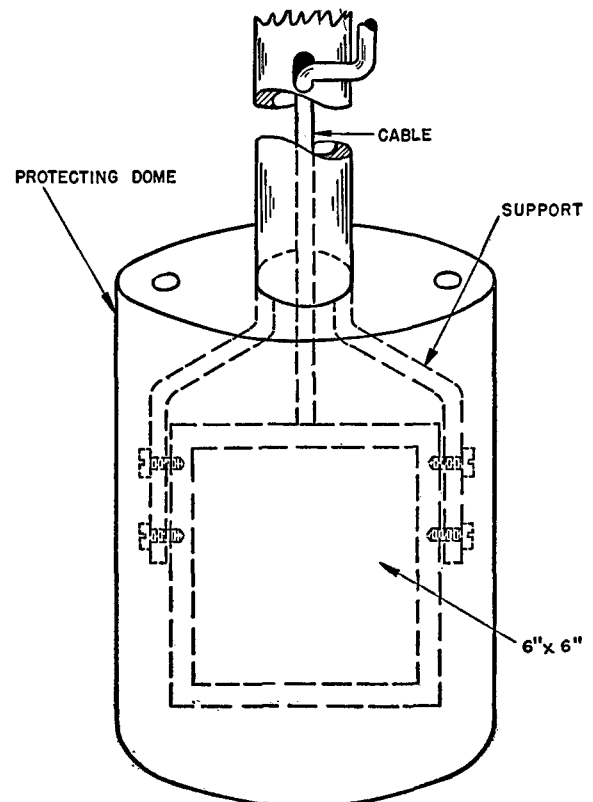


FIGURE 10. Sketch of 6x6-inch crystal hydrophone in dome.

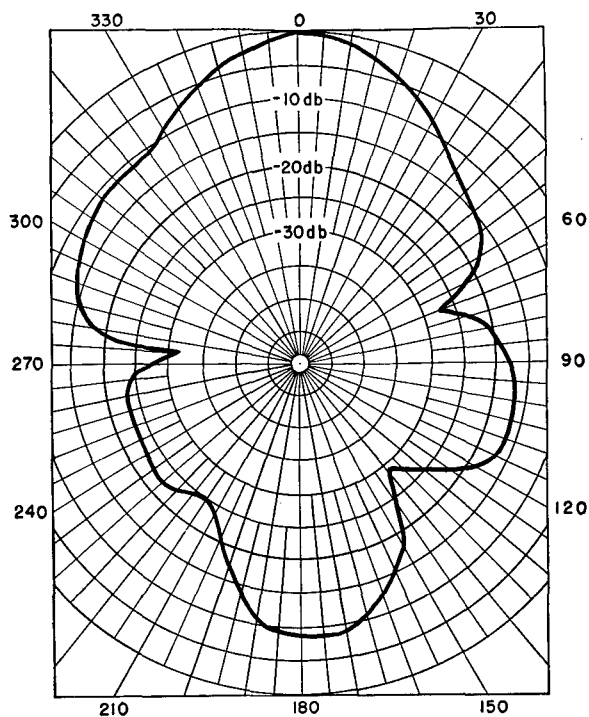


FIGURE 11. Receiving pattern of 6x6-inch crystal hydrophone (outside container).

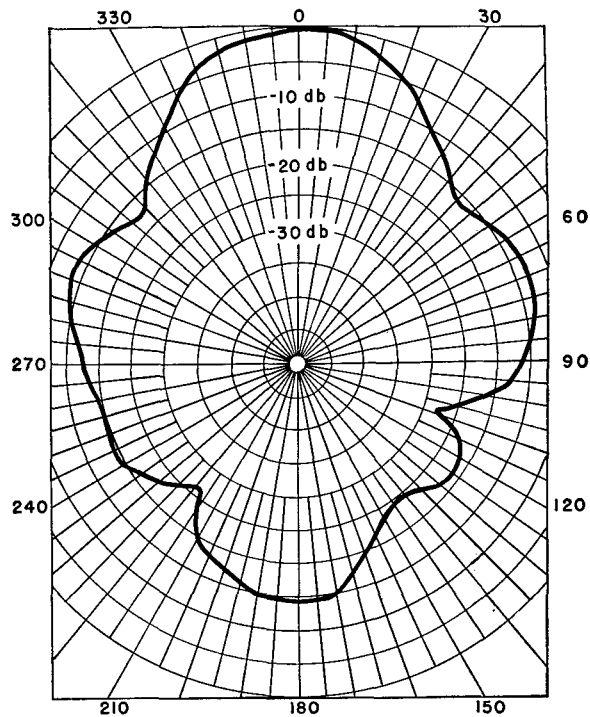


FIGURE 12. Receiving pattern of 6x6-inch crystal hydrophone (inside container).

close to the diaphragm plate so as to have the coils as near the bases of the nickel tubes as possible. This coil position had been shown to be approximately the best by certain simple preliminary experiments.

Magnetic polarization of the nickel tubes was provided by placing a 3/16-inch by 1 3/4-inch alnico magnet lengthwise inside each tube. The upper ends of the magnets were held in a symmetrical position by embedding each in the center of a piece of wooden dowel rod which was fitted loosely into the tube and

extended about 1/64 inch above its open end. To eliminate any possibility of the magnets and their wooden dowel keepers being thrown out of place by rapid rotation of the hydrophone, a plate of paraffin-boiled, 1/4-inch plywood was mounted on the same stanchion bolts that supported the coil assembly so that it just cleared the tops of the nickel tubes.

A sectional drawing showing the details described above is given in Figure 14.

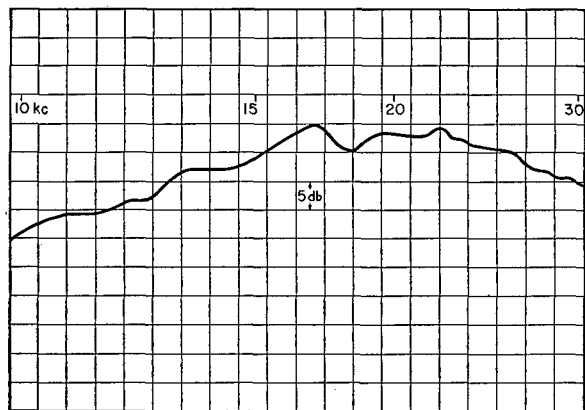


FIGURE 13. Frequency response of 6x6-inch crystal hydrophone.

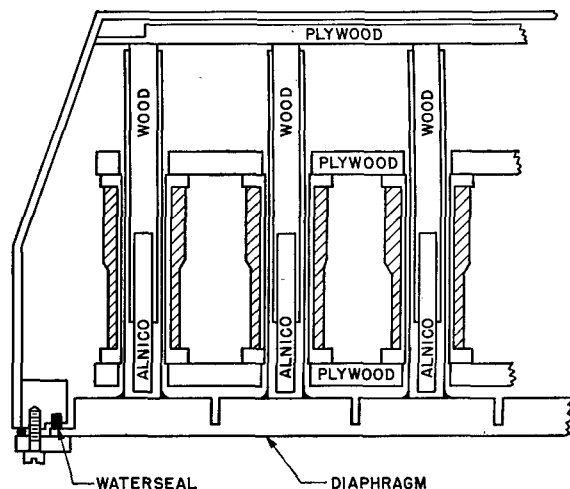


FIGURE 14. Cross section of 12x12-inch magnetostriction hydrophone.

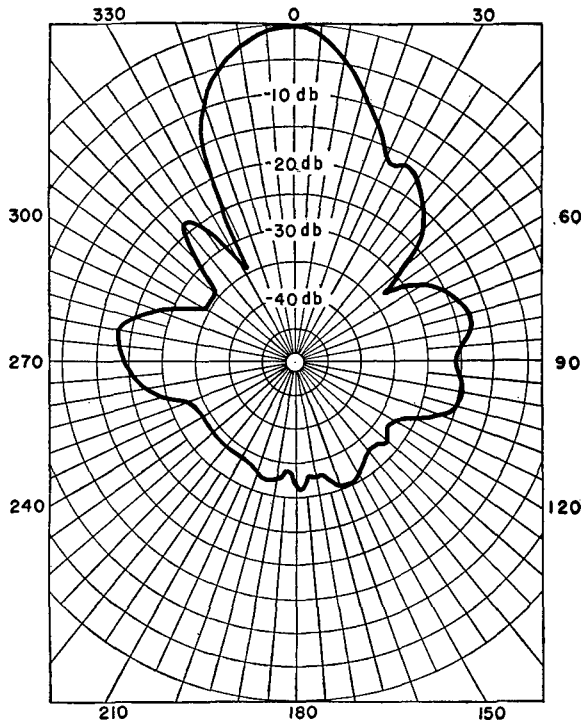


FIGURE 15. Receiving pattern of 12x12-inch magnetostriction hydrophone.

The hydrophone was divided electrically into right and left halves, with the coils in each half being connected in series. The original intention was that the a-c resistance of each half should be 200 ohms so that when the two halves were connected in parallel, the resistance would be 100 ohms. Unfortunately, however, the nickel tubing used in the construction of the hydrophone was of a different temper from the samples and the resistance in the finished unit was only about half the desired value.

The frequency response was found to remain about constant from 7 kc to 12 kc, then to increase about 20 db to a peak somewhere between 14.2 kc and 14.4 kc. Above this value, response decreased

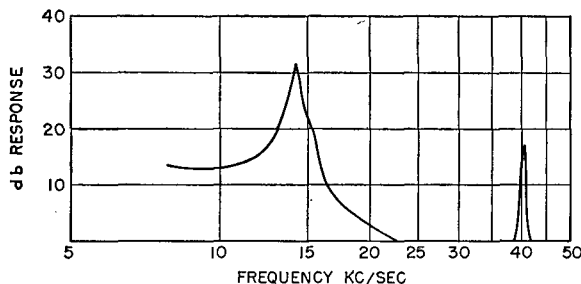


FIGURE 16. Frequency response for 12x12-inch magnetostriction hydrophone following rebuilding.

smoothly by about 30 db to a minimum at 23 kc and then remained very low until 40 kc was reached, where the response rose sharply to within 15 db of the former peak at 14 kc. The 40-kc peak was due to the vibration of the nickel tubes in the second longitudinal mode. The shape of the frequency-response peak at resonance indicated that the mechanical  $Q$  of the hydrophone was about 15.

The azimuth response-pattern is shown in Figure 15. The patterns taken with the hydrophone outside the dome are almost identical with those taken with it in the dome, except for a slight change in the shape of the minor lobes.

Reliable figures cannot be given for the absolute sensitivity of the 12x12-inch hydrophone because of difficulty with the standard comparison hydrophone on the day the measurements were made. By comparing with previous performance of the standard, it appeared that the following sensitivities (in decibels below 1 volt per bar) were obtained at the stated frequencies: at 10 kc, -98; at 15 kc, -68 (resonance); and at 20 kc, -99.

Tests with sample units indicated that proper annealing of the nickel tubes, and also a slotting of the tube, would increase the sensitivity of the hydrophone by approximately 35 db. Proceeding on this information, the hydrophone was rebuilt and the unannealed seamless nickel tubes were replaced with 0.010-inch slotted tubes, annealed in hydrogen at 1600 F.

The frequency response for the rebuilt hydrophone is shown in Figure 16. The mechanical  $Q$  of the hydrophone as obtained from the frequency-response curve was approximately 30, as contrasted with the value of 50 obtained from the impedance circle, and was essentially the same as before the unit was rebuilt.

The directivity pattern was not so good as before, the highest minor lobe being only 10 db down, but the degree of asymmetry was about the same. The impedance at the 13.5-kc resonance was found to be  $49 + j159$  ohms, the absolute sensitivity was 81.1 db below 1 volt per bar, and the directivity ratio was approximately 0.015 as compared with a theoretical value of 0.0101. The efficiency of the unit as a receiver was calculated to be approximately 9 per cent and as a projector approximately 13 per cent. The efficiency as determined from impedance loops in air and water was approximately 12 per cent.

Early in 1943, it was suggested that the 12x12-inch



magnetostrictive tube hydrophone be used at its higher resonance of 39 kc. A 2x6-inch cylindrical emitter was accordingly constructed so that tests could be made at that frequency. Although the sensitivity of the 12x12-inch hydrophone was lower by about 15 db at 39 kc than at 14 kc, the frequency for which it was constructed, it was expected that both reverberation and echo would be attenuated and that water noise would be less at the higher frequency. The chief reason for making such comparisons was to establish the relative importance of attenuation and sharpness of hydrophone pattern in scanning sonar systems. Tests made at 39 kc, however, indicated that the pattern of the 12x12-inch microphone at 39 kc was very poor, with minor lobes down only 6 db.

#### 4.4 ROTATING RIGS FOR MR SONAR

##### 4.4.1 For Model 1 Rotoscope

The Model 1 rotoscope, installed on the barge TIPPECANOE, used a 3-inch pipe to support the 6x6-inch crystal hydrophone. This pipe was actually in two pieces, but was joined together by a universal joint in an attempt to reduce vibration and to keep the hydrophone rotating smoothly in the water.

The driving motor was mounted on the top of the shaft-supporting structure and drove the shaft by means of a worm gear, while an extension of the motor shaft terminated in a gear box from which a variety of rotation speeds could be obtained for timing purposes. One shaft in the gear box rotated at 1/5 rps and was used to drive the PPI sweep-expander potentiometer. Another shaft rotating at 1/10 rps, supported a wheel on whose circumference were mounted two machine screws 180 degrees apart. During operation, these tripped a microswitch to produce the ping once every 5 seconds (4,000-yard range). A third shaft rotated at 36 rps was used to drive the flexible shaft which turned the PPI deflection coils through a 9:1 gear ratio on the neck of the cathode-ray tube of the PPI indicator.

The cable from the rotating hydrophone came through a water seal at the top of the hydrophone and ran up the inside of the shaft, by-passing the universal joint by coming out of the lower pipe and going back into the upper one. At the top of the pipe were five slip rings, of which three were used to take the signal from the hydrophone to the receiver. Two of these rings were for signal leads and the third was

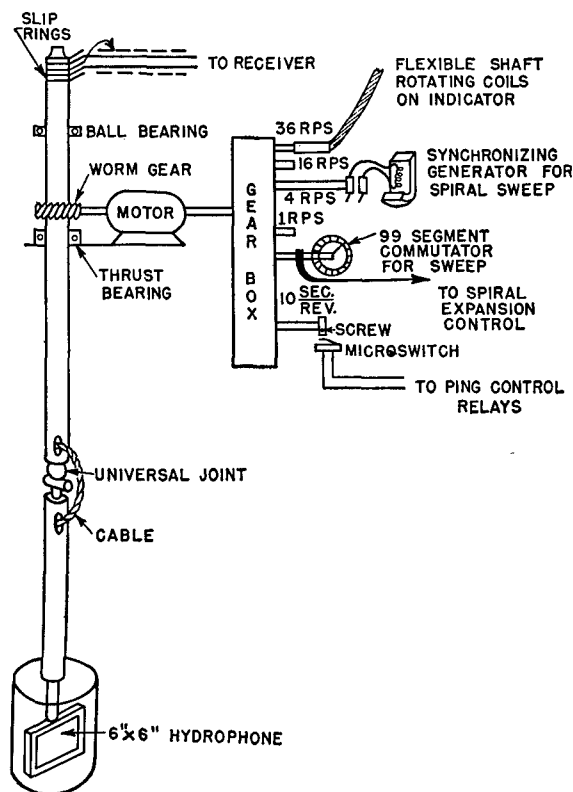


FIGURE 17. Diagram of rotation rig for Model 1 rotoscope.

for the cable shield. The two extra slip rings were supplied in case SLC should be used.

Figure 17 is a sketch of the rotating rig as used on the barge.

##### 4.4.2

##### For Model 2 Rotoscope

In the Model 2 rotoscope installed on the AIDE DE CAMP the hydrophone was supported on rubber mountings within a cylindrical container which rotated with it. Its supporting shaft ran up through a "cutless" rubber bearing and was supported by a thrust bearing at the top. It was belt-driven from a countershaft which in turn was belt-driven by an a-c motor (see Figure 18). The top of the rotating hydrophone shaft, as in Model 1, had five slip rings on which the cable from the hydrophone terminated, and had an attached cam operating a make-and-break contactor for ping control and synchronization.

The hydrophone container was surrounded by a thin stainless steel dome which remained stationary in the water. This outer dome was attached to a large

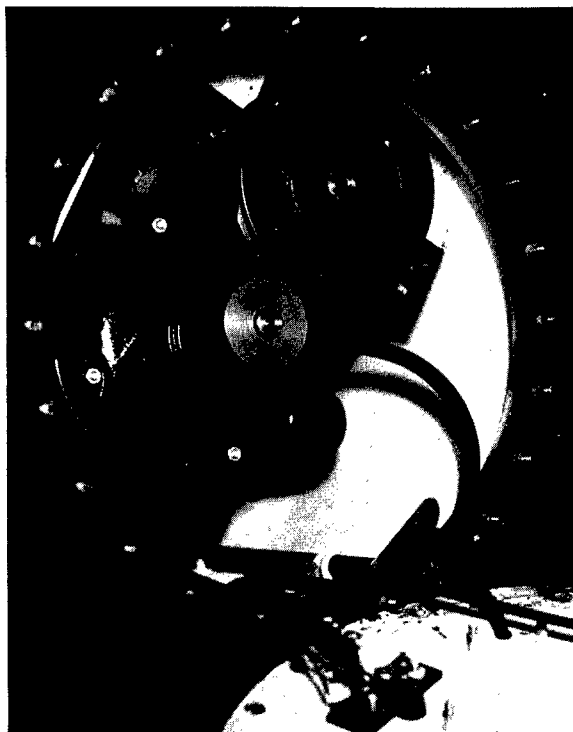


FIGURE 18. Top view of driving motor and countershaft, rotation rig for Model 2 rotoscope.

pipe surrounding the driving shaft and supported by the upper housing that contained the driving motor, slip rings, etc. The assembly is shown in Figure 19.

Both the hydrophone container and the stationary dome contained salt water which was later replaced by a solution of Prestone in water, to obtain some lubricating action on the cutless bearing. The whole assembly was watertight and nearly airtight. While in operation, air was pumped in to create a pressure of about 2 or 3 pounds per square inch to make certain that the water level in the assembly did not rise as high as the slip rings while the whole rotating system was in the lowered operating position, as the slip rings were then below the external water level. A 40-watt electric-light bulb was mounted in the upper housing near the motor and was kept burning while the motor was not in use in an attempt to keep moisture from injuring the slip rings and the driving motor. A crank fitting was installed on the top of the countershaft so that a crank inserted through a hole in the top cover could be used for manual training of the hydrophone. After initial adjustments had been made, this rotating rig performed in a satisfactory manner.

#### 4.5 INDICATORS FOR MR SCANNING SONAR

Both Model 1 and Model 2 rotoscope models were highly experimental in nature and so designed that each separate function was performed by a different chassis, usually with its own power supply. In both models, however, the actual echo indication was presented on a PPI type of display. In Model 1, a 5-inch special radar tube with a very small neck was used.

A high-voltage power supply of the conventional variety was mounted on the same chassis as the PPI scope. Figure 20 is a schematic diagram of the circuit used. The cathode-ray tube was of the magnetic focusing type which had a long persistence screen and used a second anode voltage of about 3,000 volts. The focusing was adjusted by means of a potentiometer which controlled the current through the focusing coil, while the intensity of the cathode-ray beam was controlled by adjusting the voltage on the first anode and on the grid. Signal from the receiver was applied

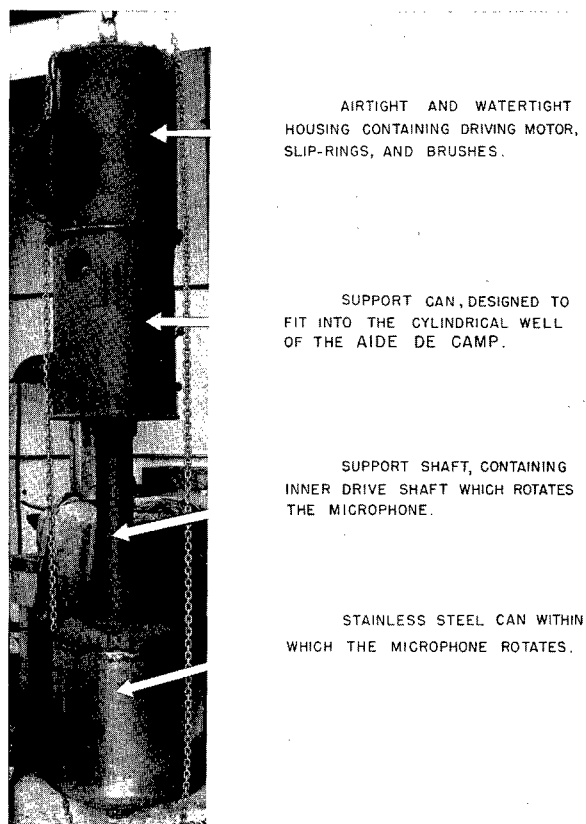
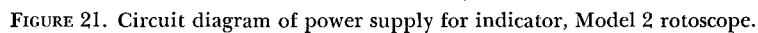
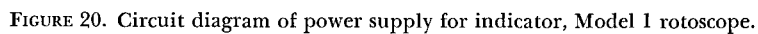


FIGURE 19. Assembly view of rotation rig for Model 2 rotoscope.

CONFIDENTIAL



CONFIDENTIAL

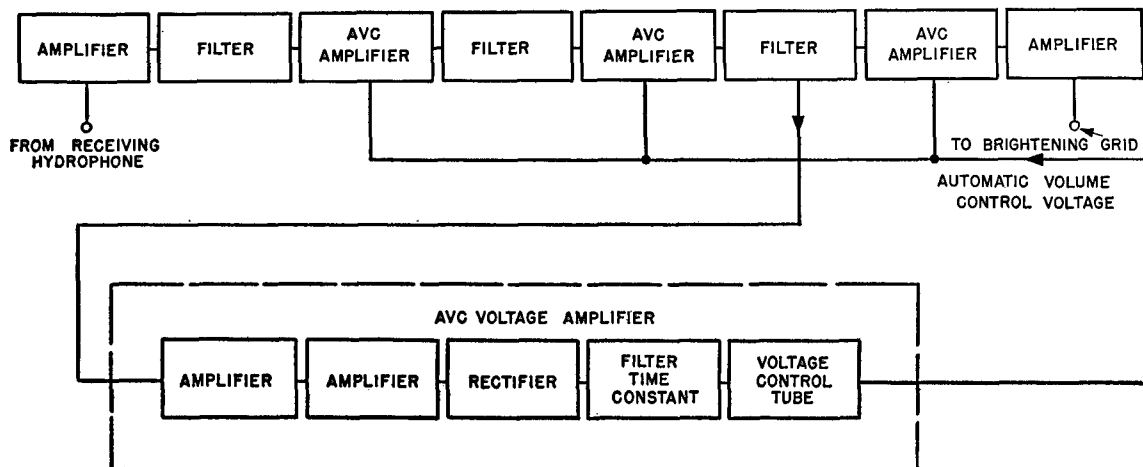


FIGURE 22. Block diagram of receiver, Model 1 rotoscope.

as a positive pulse to the grid of the cathode-ray tube in order to produce brightening of the spot at the appropriate range and bearing.

The spiral-sweep generating equipment is described in Section 4.8, "Spiral Sweep for MR Sonar."

The Model 2 rotoscope on the AIDE DE CAMP also used a cathode-ray tube as an indicator. This was a standard 7-inch, long-persistence screen type, similar to the Model 7BP7 which was later used in the Model XQHA scanning sonar. As in Model 1, the indicator chassis contained the power supply for the cathode-ray tube itself. Figure 21 gives a schematic diagram of this power supply, which again was of conventional type. The focus of the beam was controlled, as before, by a potentiometer in the focusing-coil circuit, while the intensity was controlled by varying the positive bias on the cathode of the tube. Two control potentiometers were included in the circuits of the deflection coils, so that the undeflected beam could be centered without the necessity of mechanically adjusting the focusing coil. The spiral in this case was produced by a 4-cycle electronic sweep synchronized with the rotation of the hydrophone by means of electric impulses, as discussed later in this chapter. Controls for adjusting the centering of the spot, the rate of expansion of the sweep, and the time of the rotation period were available on the front panel of the spiral-sweep chassis, which was mounted on the rack immediately below the indicator.

The receiver was mounted directly to the right of the indicator and had available only an input attenuator, an output volume control, and two TVG controls. As before, the operator controlled the fre-

quency of the ping by adjusting the Hewlett-Packard oscillator. This oscillator and an amplitude modulator were mounted on the rack below the receiver, with controls on the modulator to vary the frequency and percentage of modulation as well as the amplitude of the modulated signal. Among other controls available to the operator were a hand key for either automatic or hand pinging, and knobs for adjusting the length of the ping and the phase of the beginning of the ping with respect to the angular position of the receiving hydrophone.

In the Model 2 rotoscope installation on the AIDE DE CAMP, the received water signal was monitored at 3 kc by a loudspeaker operated with its own amplifier and fed from the output of the scanning receiver. There was a volume control on the speaker-amplifier chassis. Since the Model 2 unit, like the Model 1, was designed as experimental equipment for testing ideas to be used on later scanning systems, there were many adjustments to be made. Most of these, however, were pre-set, so that in actual operation the operator had only to adjust the receiver, and occasionally the background of intensity on the PPI indicator. Figure 5 shows a photograph of the indicator chassis in the rack of the AIDE DE CAMP.

#### 4.6 RECEIVERS FOR MR SCANNING SONAR

##### 4.6.1 Receiver for Model 1 Rotoscope

The receiver used on the Model 1 rotoscope was known as the AVC receiver-amplifier.<sup>1</sup> Figure 22 shows that it consisted of five stages of amplification.

As an understanding of its operation can be obtained by study of Figure 23, only a brief description will be given.

The first stage of the receiver was a fixed-gain amplifier while the second, third, and fourth were variable-gain stages. An RC filter was inserted after each of the first three stages to cut out frequencies below 2 kc so that flat response from 2 kc to 100 kc could be obtained, and any 60-cycle pickup eliminated. A 50,000-ohm resistor was put in series with each grid to suppress parasitics. The AVC voltage on the second, third, and fourth stages was obtained by feeding the signal from the output of the third stage into a two-stage amplifier ( $V_9$  and  $V_{10}$ ), rectifying and filtering it, and applying the resultant d-c voltage to the grid of the cathode follower ( $V_{12}$ ). The cathode of this triode was connected by a 0.5-megohm resistor to the  $-B$  supply, which was 50 volts below ground. The AVC voltage came off the cathode directly so that it was at  $-24$  volts, due to the voltage divider incorporated in the cathode circuit, when 6J5 ( $V_{12}$ ) was not conducting. When it started to conduct, however, the voltage on the cathode became increasingly positive and the AVC voltage varied from  $-24$  volts upward. This AVC voltage was applied to the grids of the 6J5 triodes ( $V_3$ ,  $V_5$ , and  $V_7$ ). Each tube acted as a variable arm in a voltage divider, for as its grid potential increased and it became increasingly conductive, the effective resistance across the tube decreased.

The output of the last receiver stage ( $V_8$ ) was applied through a coupling capacitor to the brightening grid of the cathode-ray indicator tube. The proposed peak-passer stage shown in Figure 23 was never incorporated into the circuit.

The controls 9 and 10 (variable resistors) controlled the amount of bias voltage supplied to the grids of the AVC tube ( $V_3$ ,  $V_5$ ,  $V_7$ ). The 6J5 AVC output tube ( $V_{12}$ ) was capable of supplying comparatively large amounts of power. This was necessary when the grids of the control tube ( $V_3$ ,  $V_5$ ,  $V_7$ ) became positive, as they did at high signal levels. Thus the time constant in the AVC circuit was made variable because it was desired that the level at the output of the amplifier follow down the reverberation decay curve as exactly as possible. At the same time, the time constant on the AVC had to be such as to pass an echo pulse without trying to follow it. Since little was known at the time about reverberation, the amplifier AVC time constants were made variable. Much

of this AVC circuit was designed to produce overcontrol in order to have the output-versus-input voltage as nearly flat as possible.

When this receiver was first designed, it had a flat frequency response from 2 kc to 100 kc, so that it could be used over a wide frequency range. The amplifier was designed to have a constant voltage output regardless of the input signal, with the exception that the recovery time involved for the AVC was set to allow a sudden burst of signal to rise above the controlled level. Later, to improve the signal-to-noise ratio, an LC filter for the plate load of the first stage was installed.

The dynamic properties of the receiver were adjustable. There were six controls for varying the time constant of the recovery rate of the AVC, input and output volume controls, a control for varying the signal supplied to the AVC control voltage amplifier, two controls for varying the output voltage with respect to the input voltage, and several bias controls. The AVC was capable of controlling input voltages within a range of 120 db from an input voltage of 5  $\mu$ v to 15 volts. The longest time possible for recovery of the AVC circuit when the signal level changed from 10  $\mu$ v to 100 mv was about 0.2 second. The AVC built-up recovery for the same change was about 0.7 second. Among the shortcomings of this receiving amplifier were the following:

1. To obtain optimum results, continual adjustment of the controls was necessary.
2. Above 0.1 volt of signal input, the AVC recovery rate was practically instantaneous.
3. The initial reverberation arrived when the amplifier was extremely sensitive, causing excessive brightening of the scope indicator at the beginning of the listening period. This disadvantage was later corrected by shorting the input to the amplifier during the pinging period.
4. Since there was no audio output from the receiver it was sometimes difficult to distinguish improper adjustment of the amplifier.
5. During the recovery period, for short recovery rates, the amplifier seemed to be regenerative for low frequencies.
6. The receiver was too broadly tuned.

#### 4.6.2 Receiver for Model 2 Rotoscope

The receiver-amplifier used with the Model 2 rotoscope was designed from experience with the first

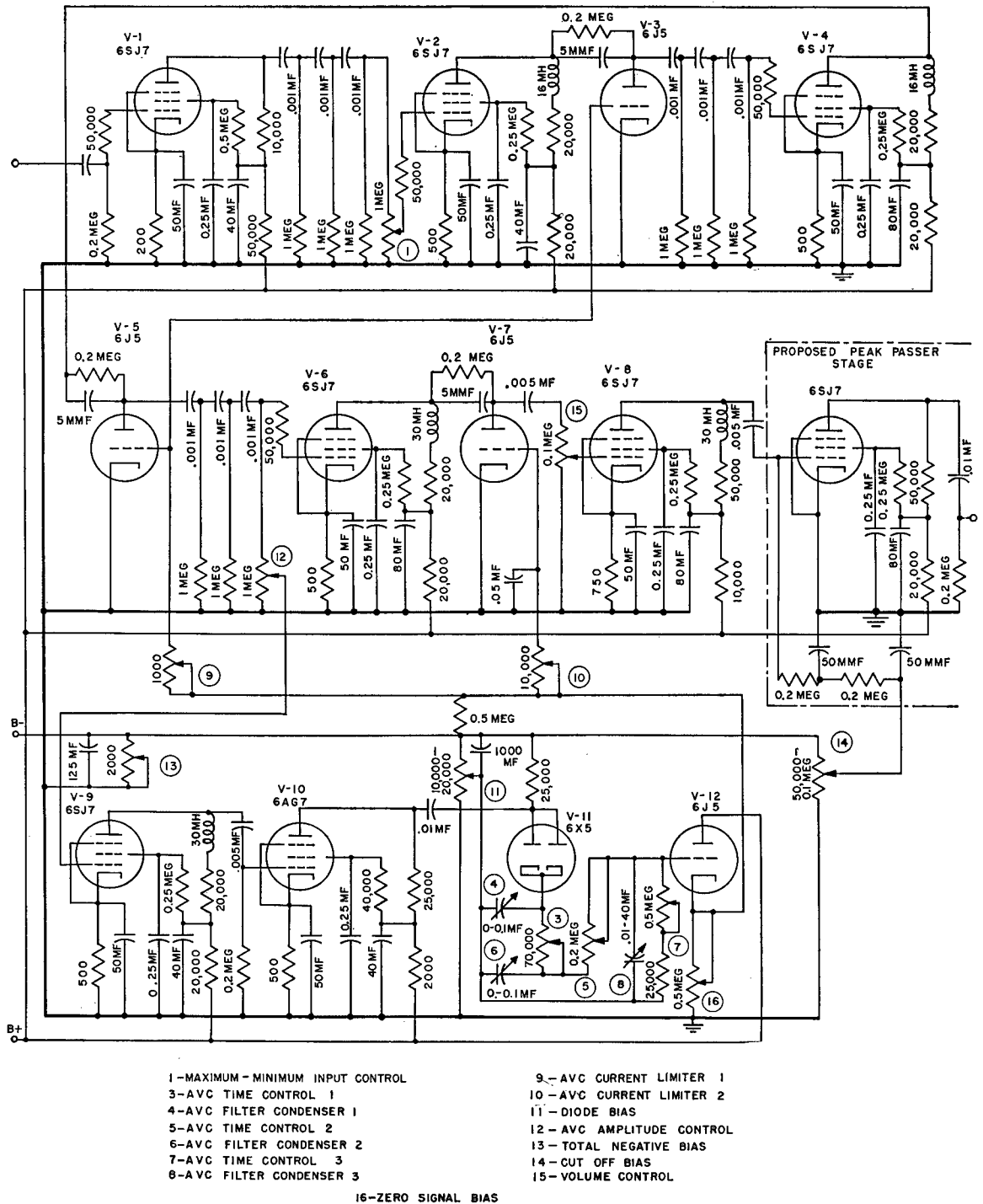


FIGURE 23. Circuit diagram of receiver and power supply, Model 1 rotoscope.

CONFIDENTIAL

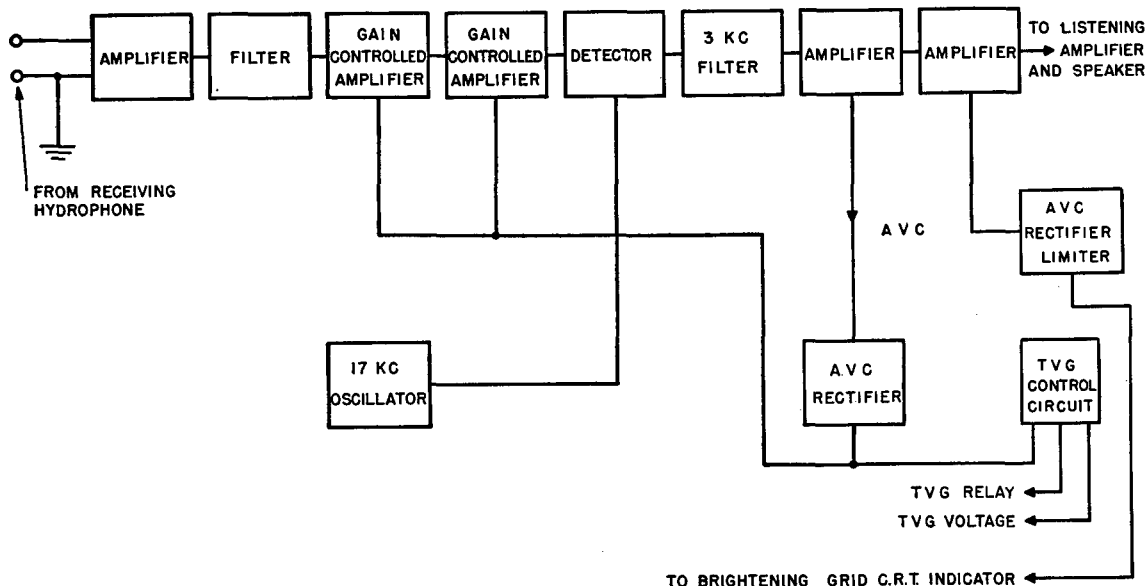


FIGURE 24. Block diagram of receiver, Model 2 rotoscope.

receiving amplifier. This unit included six stages of amplification, including a first detector as shown in the block diagram given in Figure 24. There was 140-db voltage gain from input to output, which later was reduced to 120 db. The circuit diagram is shown in Figure 25 as it was originally designed. The first three stages were ordinary pentode amplifiers using high-gain tubes. The grids of the second and third amplifiers were controlled by automatic volume control and time-varied gain voltages. In the fourth stage, which employed a 6SA7, the incoming 14-kc signal was heterodyned against a 17-kc signal supplied by the 6J5 local oscillator. The band-pass filter had a band width of 600 cycles, centered at 3 kc. The output of the filter was further amplified in each half of the 6S7 and then fed to a separate listening amplifier and speaker unit. The schematic diagram of this amplifier is shown in Figure 26. It consisted of a single 6SN7 amplifier and phase inverter, and the two halves of a second 6SN7 in push-pull driving a loudspeaker. In the receiver-amplifier the output from the second half of the first 6SN7 was also fed to a 6H6, where the signal was rectified, limited to 12 volts output, and used to brighten the PPI scope.

To obtain an AVC voltage, the output of the first triode in the 6SN7 was also rectified through a 6H6, and applied to a 0.02- $\mu$ f capacitor with a 100,000-ohm potentiometer across it. The resulting d-c voltage supplied the AVC bias to the grid of the second and

third amplifier stages. In series with the AVC bias was a capacitor discharging through a resistor which gave time-varied gain control. This TVG control was keyed during the ping transmission, rendering the amplifier insensitive immediately after the ping and allowing the sensitivity to increase gradually with time. To do this, 135 volts negative bias was applied during the ping to a 1- $\mu$ f capacitor connected between ground and the negative end of a 135-volt battery. The TVG voltage was fed to the control grids through the AVC potentiometer. The 1-meg-ohm potentiometer across the TVG capacitor determined the time constant and the swinger selected the initial TVG voltage to be applied.

The AVC, which had a comparatively rapid recovery rate, was removed from the circuit soon after experimentation was begun, because experience indicated it was seldom used. Another potentiometer was put across the TVG capacitors, permitting an adjustment of the time constant of the TVG circuit in order to match the reverberation decay rate in the water. The two TVG controls then permitted: (1) adjustment of the amount of blocking voltage applied to the control grid, and (2) adjustment of the time required for the grid to recover.

This receiver was put into use in November 1942, and continued in use until June 1943, when the Model 2 rotoscope was removed from the AIDE DE CAMP. During this period several changes were made

CONFIDENTIAL





in the circuit. A line-to-grid transformer was installed in the input. This provided better matching for the feeder line from the hydrophone to the grid, and also cut down the rather large amount of extraneous pick-up in the first stage. Some adjustments were made in the output 6H6 to produce the proper limiting for brightening of the scope. Twelve volts was finally decided on as the limit for brightening voltage. Figure 27 is a diagram of the final form of the receiver.

As the PPI indication was adversely affected by high-frequency propeller noise, which spotted the screen, a cathode follower and d-c filter circuit were incorporated into the brightening channel. This circuit is shown in Figure 28. The filter cut off at a frequency of 200 cycles, thereby attenuating high-frequency noise by an appreciable amount.

The operation of the MR system with its 0.25-second ping was greatly impaired by reverberation. Consequently, during the latter part of its experimental life, an attempt was made to obtain better discrimination between echoes and reverberation by using BDI brightening.<sup>24, 25, 26</sup>

A bearing deviation indicator was used as a monitor. Its use was possible since the 12x12-inch microphone was split for operation with BDI. The sweep was keyed with the ping, and the long-range sweep was used, giving 4,000 yards indication. Because the transducer was sweeping through an echo, the BDI gave deflections first in one direction and then in the other. This indication was used only in conjunction with the PPI scope, since obviously no bearing could be read from the BDI scope due to the transducer rotation. It did, however, give an indication of echo range.

For use with MR sonar a standard Model X-3 BDI unit, whose block circuit diagram is shown in Figure 29, was stripped of the cathode-ray tube circuits and all other circuits after the final amplifiers in the end channel (see dashed line in Figure 29). The lag line and oscillators were tuned for a 14-kc signal frequency.

As shown in this figure, the signals from the two halves of the projector were fed through two separate input amplifiers, employing tuned transformers in their input circuits, to the converter tubes. A 60-degree lag line joined the two channels at points between each amplifier and converter tube, thus connecting directly the 10-kc converter to the left half of the projector and to the right half through the lag

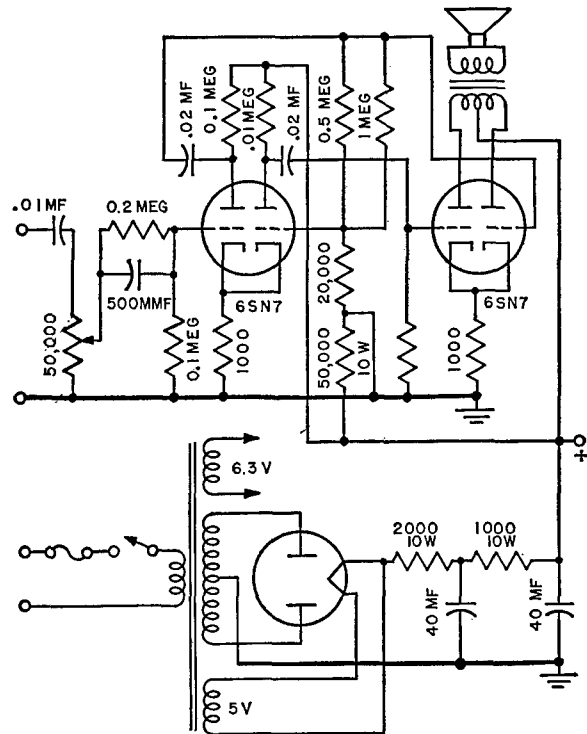


FIGURE 26. Circuit diagram of speaker amplifier, Model 2 rotoscope.

line. Similarly, the 7-kc converter was connected directly to the right half of the projector and to the left half through the same lag line. The lag line introduced a time delay of a few microseconds so that the 10-kc converter received a maximum signal when the echo approached from a point slightly to the right of the projector bearing, and the 7-kc converter received a maximum signal when the echo came from a point slightly to the left of the projector bearing.

For MR brightening<sup>27</sup> the channel signals were rectified separately in the same polarity and applied to the control grids on a 6SN7 as a push-pull amplifier which had common cathode degeneration (see Figure 30). This amplifier had normal gain for the difference between the two grid signals and was highly degenerative for the common component of the signals on these grids. The plates of the amplifier were connected to a transformer in such a way that the voltage developed across the secondary was proportional to the time rate of change of the plate current. As the microphone rotated past the bearing of the echo, a pulse was received first on one channel and then on the other. Since the difference-amplifier amplified only the difference, a positive then a negative pulse

This pulse was narrower than the pattern of sensi-

tivity on the hydrophone and so produced a short echo trace. Figure 30 shows the modified brightening circuit which was substituted for that portion of the standard BDI circuit to the right of the dashed line in Figure 29. In the final model there was a low-pass filter of 36-cycle cutoff frequency between the rectifiers and the grids of the difference-amplifier to increase discrimination against noise.

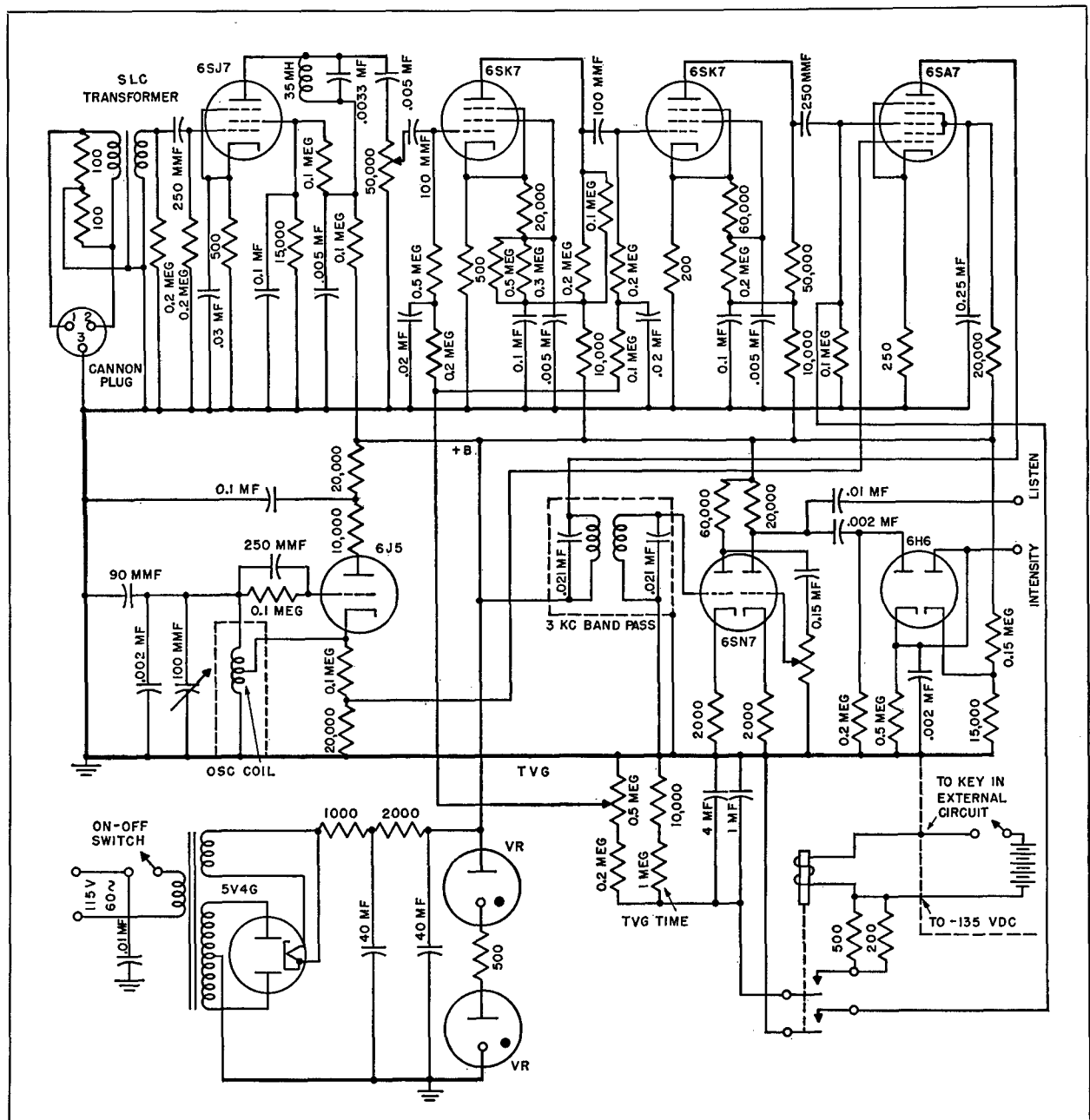


FIGURE 27. Circuit diagram of revised receiver, Model 2 rotoscope.

CONFIDENTIAL

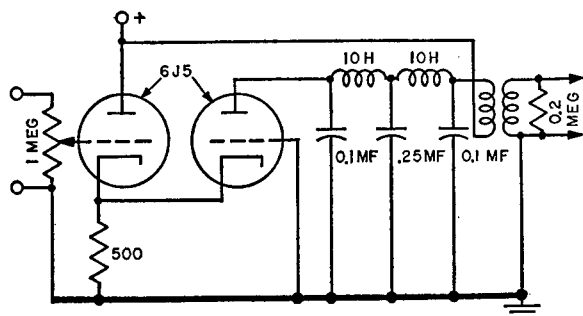


FIGURE 28. Circuit diagram of output filter for Model 2 rotoscope.

Since reverberation is likely to be fairly nondirectional and applies approximately the same signal to both halves of the projector, no voltage change should occur on comparison of the two channels, and no brightening should appear for reverberation. An echo, on the other hand, being directional, should cause the greatest voltage change on comparison and produce good brightening. Since target noise is directional, brightening would also be produced by such noise sources.

The system worked reasonably well and produced rather strong enhancement of echoes as well as suppression of part of the reverberation. After operating tests were made, however, it was finally decided that the simpler amplitude brightening, which gave more "quality" in the display, was the more satisfactory of the two.

#### 4.7 TRANSMITTERS FOR MR SCANNING SONAR

##### 4.7.1

##### 400-watt Transmitter

The first transmitter used in the Model 1 rotoscope on the TIPPECANOE was a small oscillator amplifier, tunable from 12 to 20 kc. It had a 6L6 push-pull parallel output capable of supplying approximately 50 watts to the 14-kc ring-stack emitter. In August 1942, this transmitter was replaced by one capable of putting out a nominal power of 400 watts. This unit was used for the experimental work on Model 1 and for several months on the Model 2 rotoscope on the AIDE DE CAMP. The tube and circuit arrangement is shown by the schematic diagram of Fig-

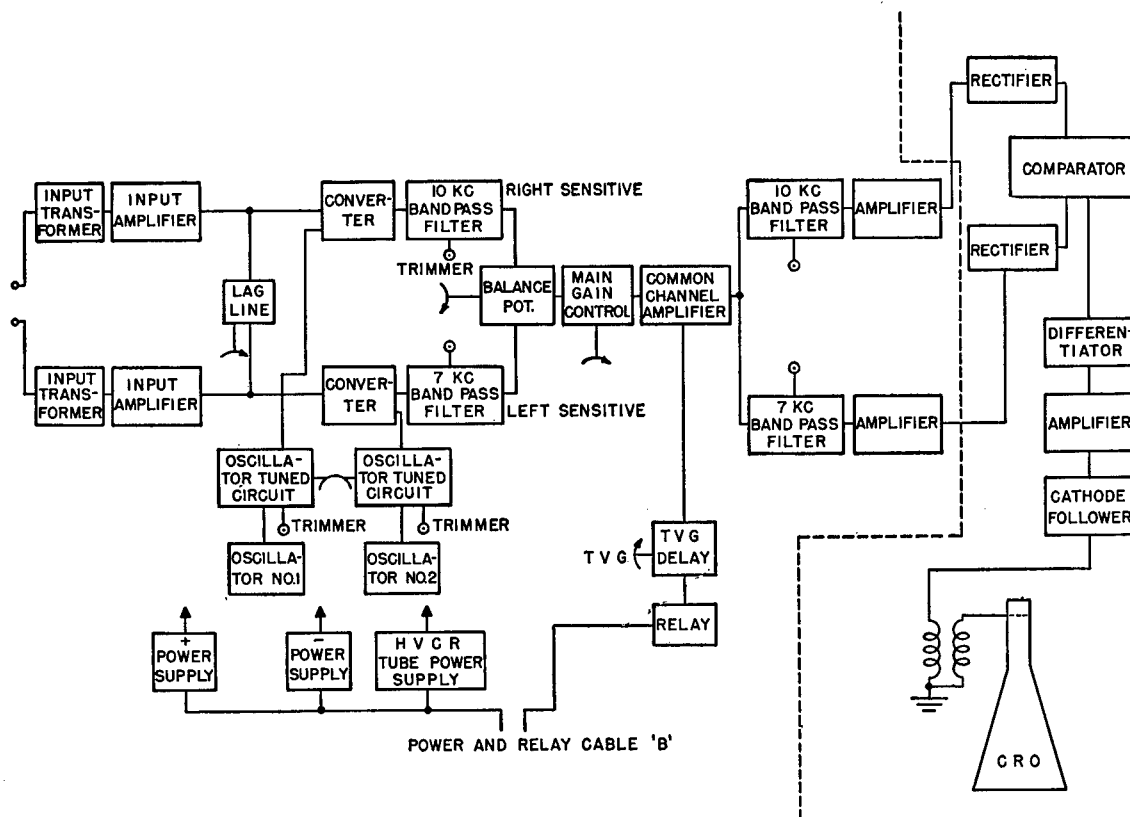
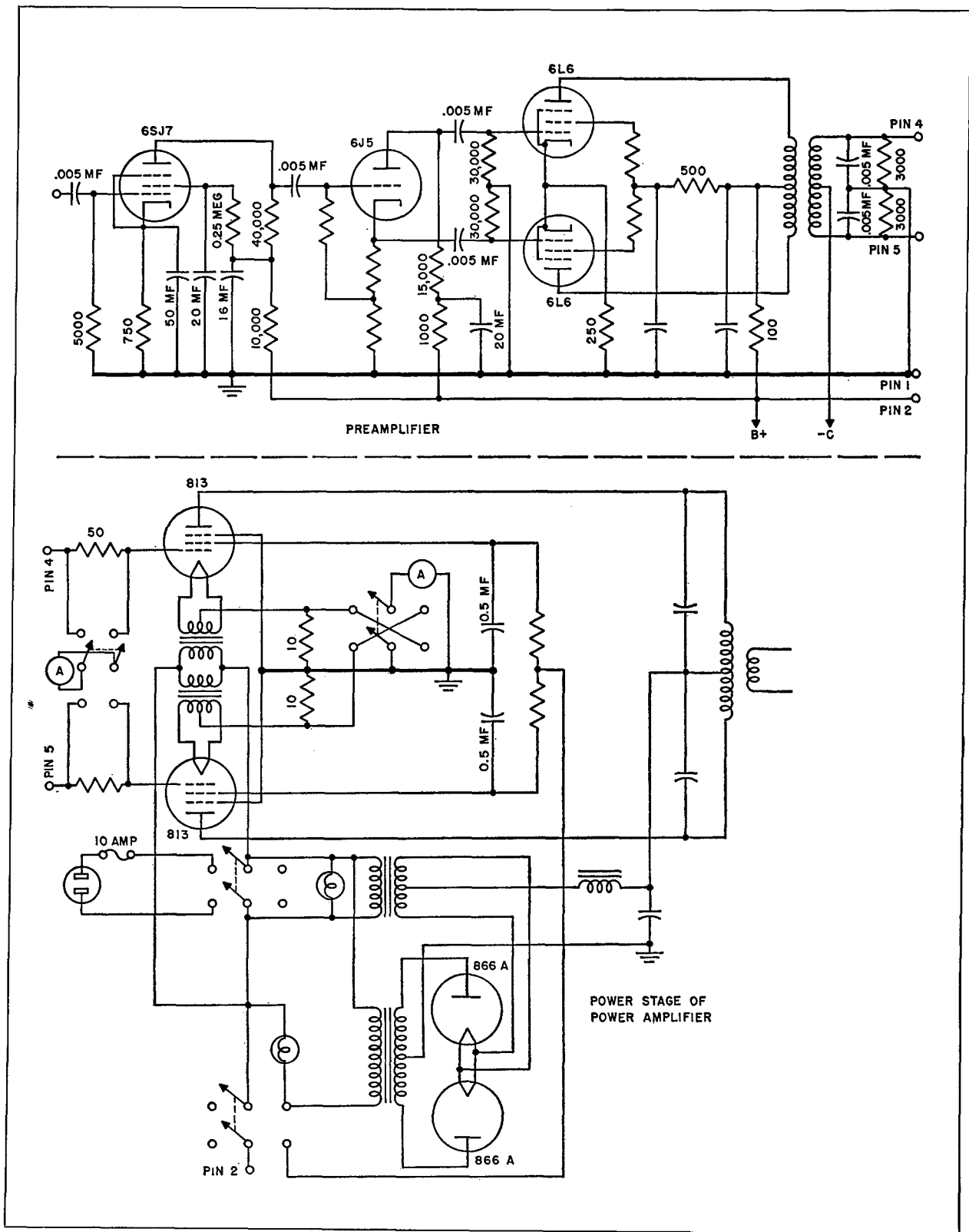


FIGURE 29. Block diagram of BDI Model X-3.

CONFIDENTIAL





CONFIDENTIAL



of covering a range from 12 kc to 20 kc was used to feed two 6J5's in a phase-inverter stage, which fed push-pull 6L6's driving push-pull 813's. These in turn drove the output stage consisting of a pair of 833A's in class C. Although the oscillator incorporated in the power amplifier covered only 12 to 20 kc, a jack was provided on the oscillator panel so that an external oscillator might be plugged in to allow the full frequency range of the power amplifier to be utilized. The whole power amplifier, except for the power supply for the final stage, was mounted in an

enclosed rack with safety switches provided on the door interlocked with the power-control circuit. The power supply for the output stage was mounted in a separate cage placed at one side of the rack. At the top of the rack was a control panel which had all the power switches, overload protection devices, thermal time-delay switches, etc. Relays operating from the 110-volt a-c line were provided to switch the filaments and each of the two high-voltage supplies separately for tuning-up purposes.

The oscillator chassis contained the oscillator,

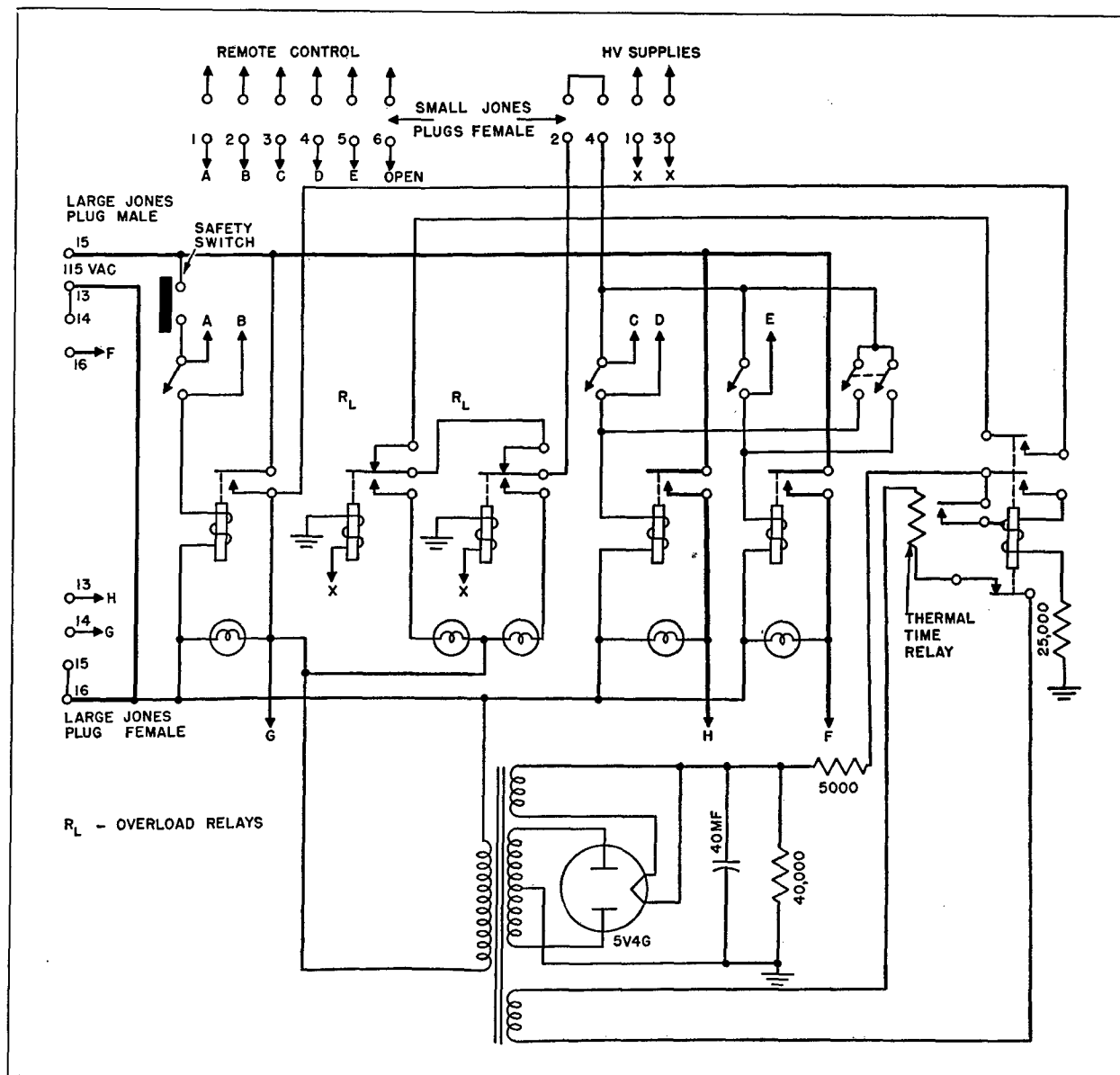


FIGURE 34. Circuit diagram of control panel, 1.5-kw transmitter.

CONFIDENTIAL

phase-inverter, and push-pull 6L6 stages. In addition to its own power supply, it also contained a power supply to provide operating current for the pinging relay and bias for the driver and final stages. On the panel there was a jack to connect an external oscillator, a gain control to control the excitation to the succeeding stages, a vernier dial to control the frequency

of the oscillator, and a switch to choose between the internal oscillator and external excitation.

The driver chassis, containing a push-pull 813 driver stage and 200-volt power supply, produced 125 watts of r-f power.<sup>11</sup> The only front panel components on the driver were a meter and a selector switch, which allowed the operator to read the plate current

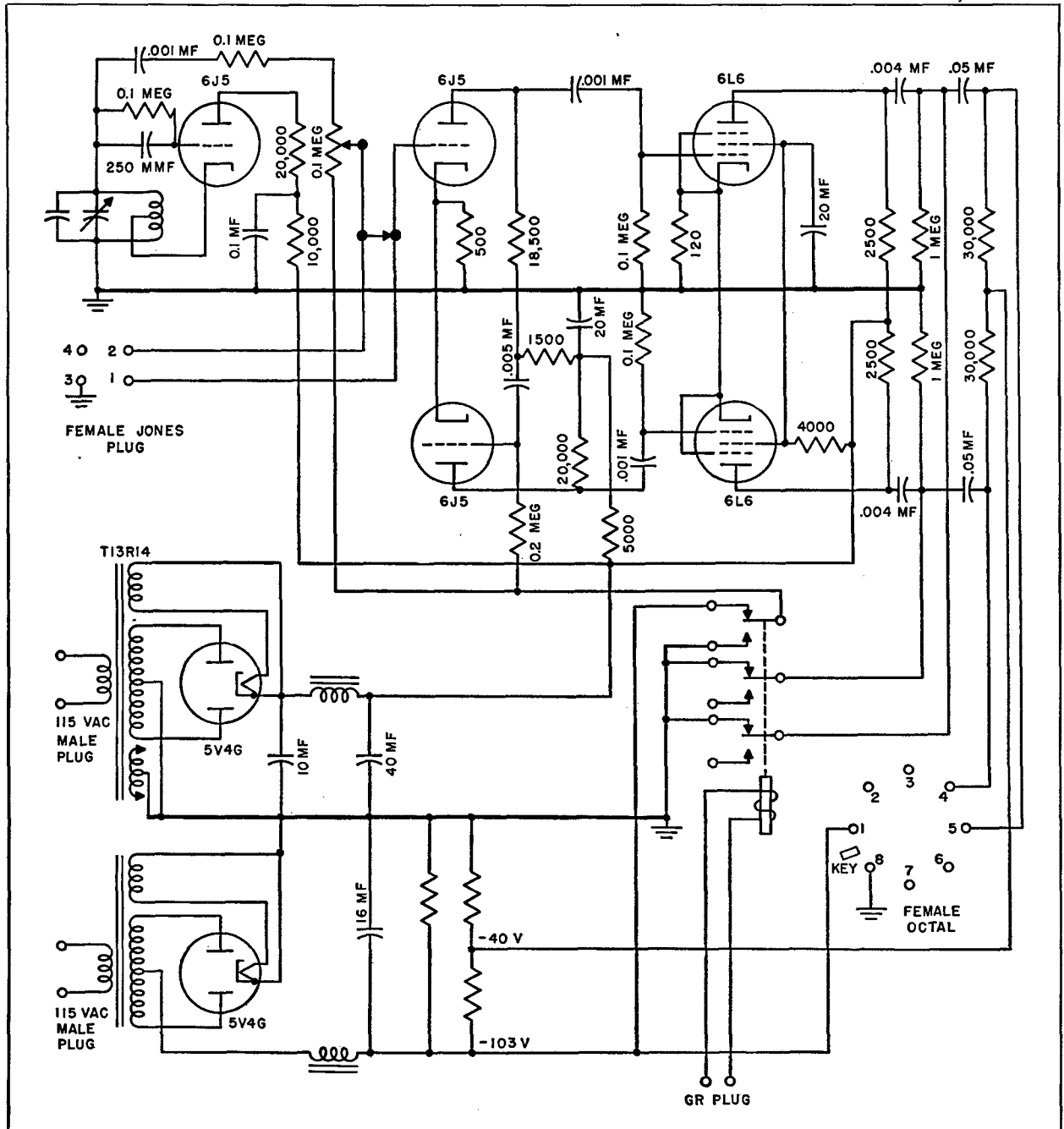


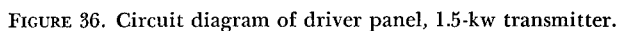
FIGURE 35. Circuit diagram of oscillator chassis, 1.5-kw transmitter.

CONFIDENTIAL



the grid current to each of the final tubes separately, and the total plate current plus total grid current.

The power amplifier was used as set up for the first few weeks. Later, the jack in the front panel of the oscillator chassis was used, permitting employment of the modulator. The Hewlett-Packard oscillator and the modulator were mounted remotely from the power amplifier, and the signal from the modulator was fed through the jack in the power amplifier. This gave convenient control of the excitation amplitude and modulation from the operating position. This



**CONFIDENTIAL**

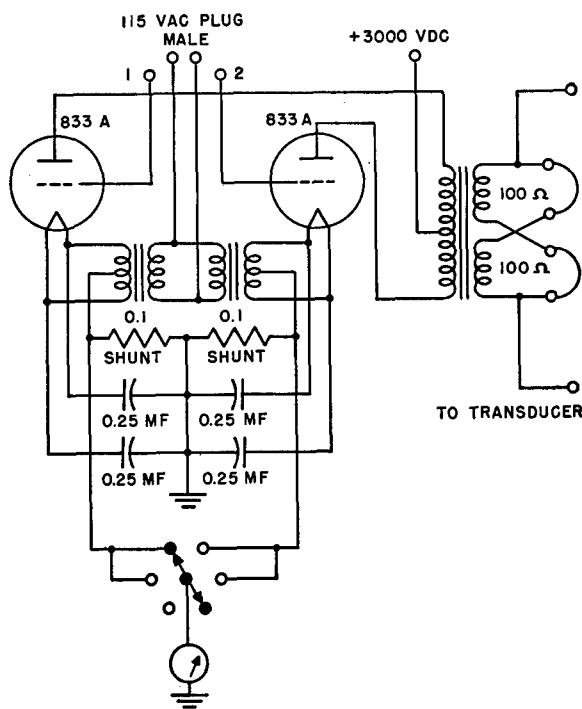


FIGURE 37. Circuit diagram of final stage, 1.5-kw transmitter.

power amplifier was used on MR scanning sonar until the Model 2 rotoscope was removed from the AIDE DE CAMP.

#### 4.7.3 Ping Control for Model 1 Rotoscope

The Model 1 rotoscope on the TIPPECANOE had a rather simple ping control<sup>27</sup> as indicated in Figure 39. Since it was required that the length of each transmitting period be at least 0.25 second, which was the time for one complete rotation of the hydrophone, it was necessary that the transmitter energize the emitting transducer for 0.25 second. A wheel rotating once in every 10 seconds in the gear system of the rotating hydrophone drive was used to control the ping interval and the ping length. Two screws, 180 degrees apart on the circumference of this wheel, were used to engage the spring on a microswitch as the wheel rotated. The length of the ping could be adjusted with a fair degree of accuracy by moving the microswitch slightly with respect to this wheel. The microswitch actuated four relays, d-c power being supplied by a 117Z6 tube used as a half-wave rectifier on the 110-volt 60-cycle line. These relays performed the following functions:

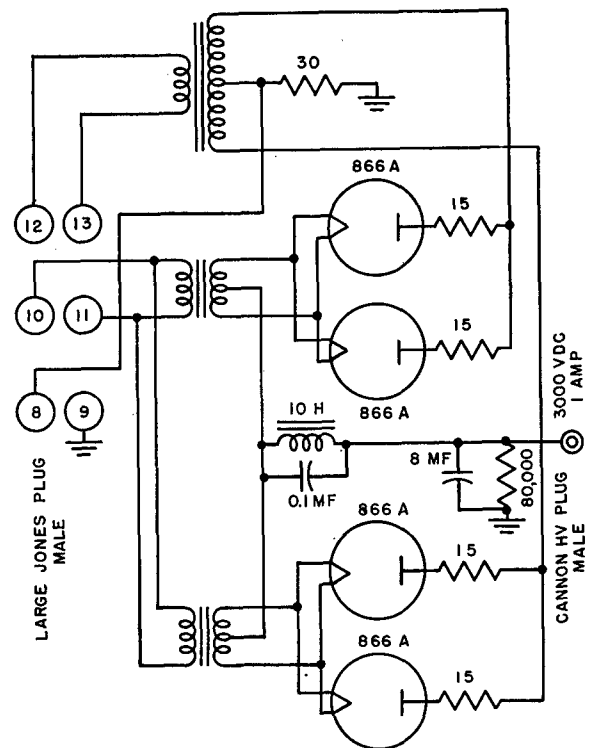


FIGURE 38. Circuit diagram of power supply for final stage, 1.5-kw transmitter.

1. Connected the Hewlett-Packard oscillator to the power amplifier, thereby producing the ping. In the "off" position, the input to the power amplifier was grounded.

2. Connected the battery for polarizing the ring stack into the transducer circuit.

3. When an electronic spiral sweep was used, the third relay brought the spiral sweep back to the center to permit it to expand on the next listening period.

4. The fourth relay was a spare and later was used to short-circuit the receiver input during the ping period.

Later, two additional screws were mounted 90 degrees from the two already on the ping-control wheel so that it was possible to work at half the range but with two pings on one spiral.

#### 4.7.4 Ping Control for Model 2 Rotoscope

In the Model 2 rotoscope, the pinging operations were somewhat more complicated. The ping-control mechanism performed the following operations at the time of the ping:

1. Synchronized the spiral sweep.

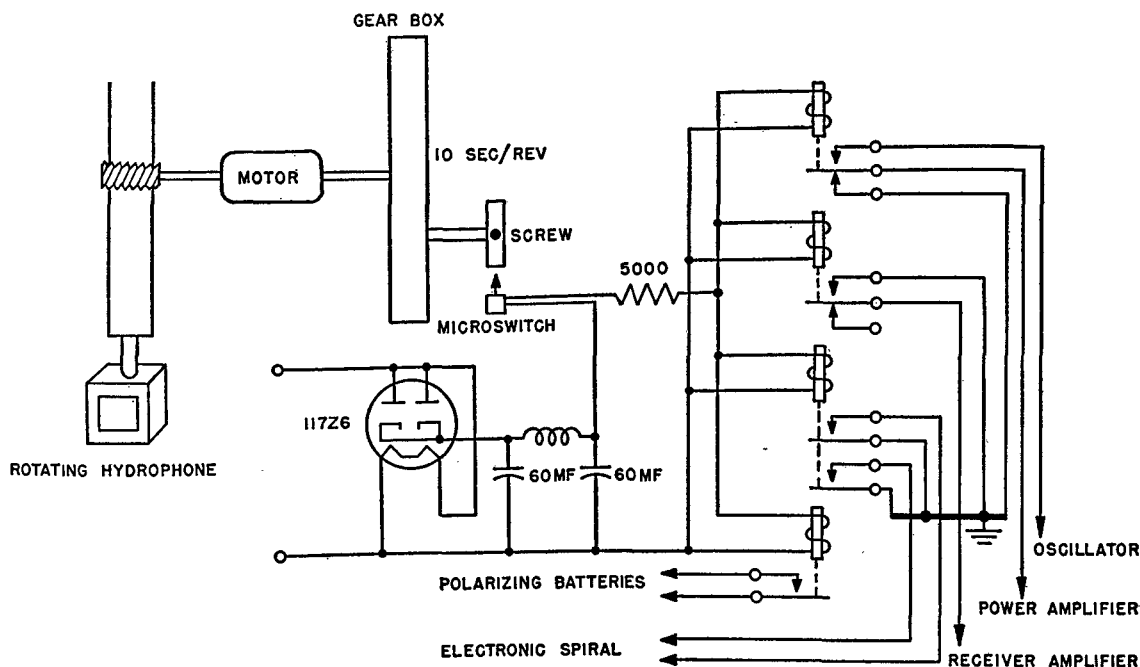


FIGURE 39. Diagram of ping-controlled circuit, Model 1 rotoscope.

2. Sent the polarizing current through the emitter hydrophone.
3. Keyed the transmitter.
4. Reset the spiral sweep.
5. Applied the TVG voltage to the receiver.
6. Reset the BDI sweep.
7. Closed the circuits on the ping-delay circuit (only in later experimentation).

The controlling item of the ping-control circuit was a multicontact step relay (see Figure 40) of the type used for machine switching in telephone work.

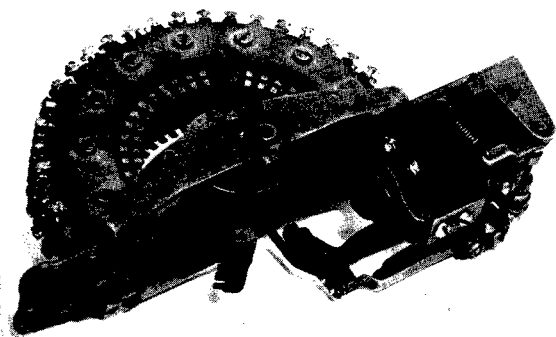


FIGURE 40. Photograph of step relay for ping control, Model 2 rotoscope.

As will be seen in the photograph it had a series of 21 groups of 6 contacts arranged in a semicircle. Six insulated contact arms rotating together on a common shaft one step at a time wiped each set of contacts consecutively through 21 steps. A ratchet gear drove the contact arms one step at a time by means of an electromagnetic coil, permitting six operations to be initiated simultaneously or in any order. Since the wiper arm moved very rapidly in passing from one contact to the next, it touched each set of contacts for practically 0.25 second when the actuating impulses were supplied at the rate of 4 per second. A diagram of this ping-control system in its final form is given in Figure 41.

On the shaft of the rotating hydrophone, a cam-operated contactor was mounted which made contact for 180 degrees of each rotation. This device gave a d-c voltage in the form of a square wave with  $\frac{1}{8}$  second on and  $\frac{1}{8}$  second off to control the stepping relay. These contacts are illustrated in the grid cathode circuit of the 6L6 ( $V_1$ ) in the diagram of Figure 41. The power supply through the 6X5 ( $V_2$ ) supplied negative voltage to the grid of the 6L6 ( $V_1$ ) to keep it cut off until the contactor on the rotating shaft was closed, at which time the grid and cathode were shorted together, permitting the 6L6 to conduct for  $\frac{1}{2}$  rotation or  $\frac{1}{8}$  second. In the plate circuit of this

CONFIDENTIAL

tube was a 110-volt 6-ma d-c relay, which closed when the 6L6 conducted. This relay was then closed for an interval of  $\frac{1}{8}$  second out of every revolution. A pair of contacts actuated the telephone step relay; the wiper arms then moved one step for each revolution of the hydrophone. In the dotted box labeled "Telephone Relay," the contacts are shown at one of the 21 positions of the relay and the wiper arm.

When the arms reached the No. 4 position on the step relay, each pair of contacts shown inside the dotted box were made, thus producing the ping.

The second pair of contacts on the 6-ma 110-volt relay which controlled the step relay were used to synchronize the spiral sweep, by supplying a 45-volt square wave d-c signal through a variable resistor to the grid of the oscillator tube in the spiral sweep.

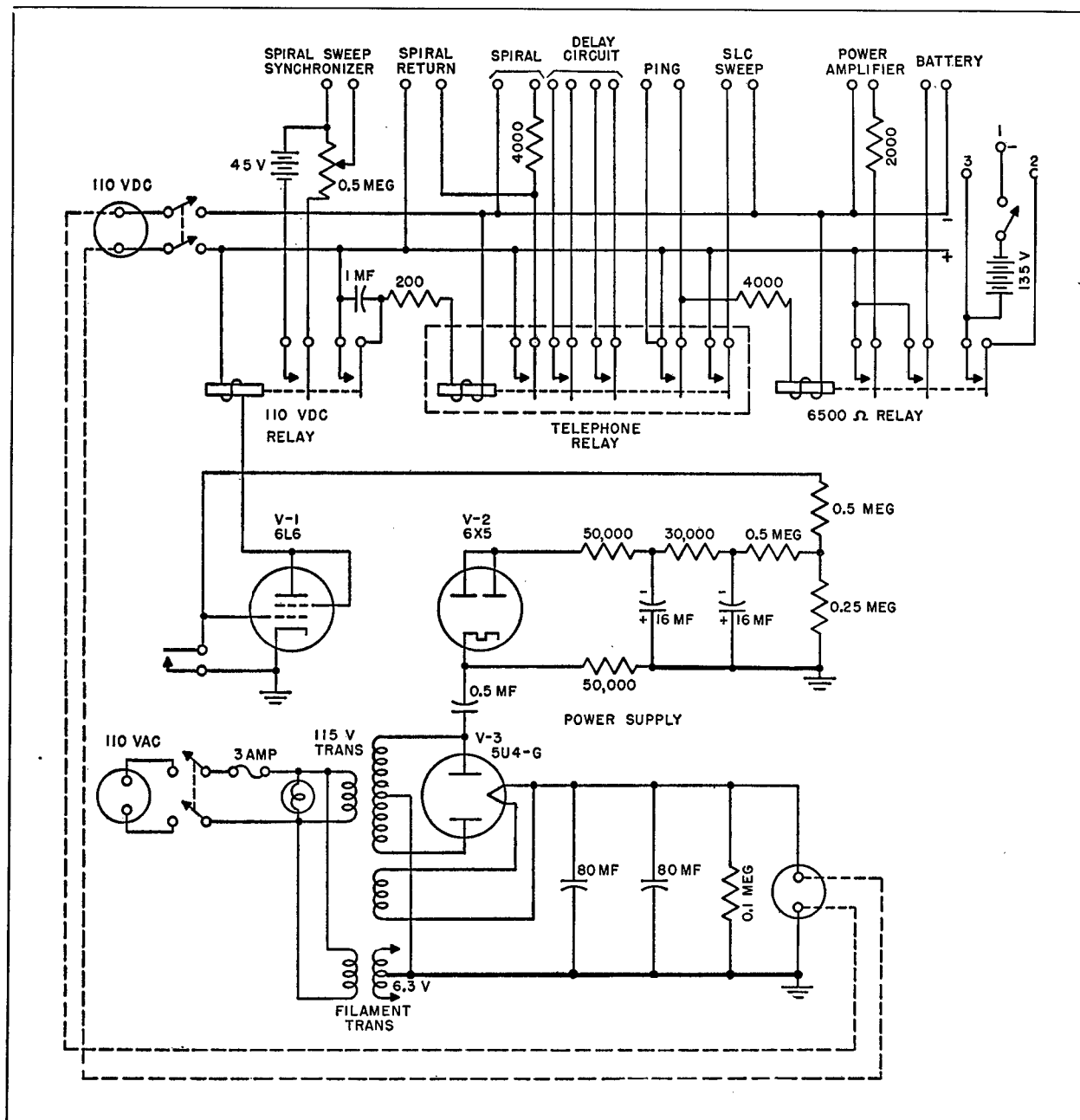


FIGURE 41. Diagram of ping-control circuit, Model 2 rotoscope.

CONFIDENTIAL

Since the length of this square wave was  $\frac{1}{2}$  cycle of the oscillator, the latter was synchronized with the rotation of the hydrophone.

Since the step relay had 21 sets of contacts, one set of which was the wiper-arm connection, and since the wiper arm paused for 0.25 second on each set of contacts, a very convenient 5-second sweep cycle was available for listening.

One of the six circuits in the stepping relay was used to actuate the spiral-sweep return relay, which was located in the spiral-sweep chassis. Two other sets were used to close the circuits necessary in the ping-delay chassis, which will be described later. A fourth set actuated the sweep reset relay in the BDI receiver. A fifth set of contacts actuated the ping relay, which was thus closed for 0.25 second to produce a 0.25-second ping. The ping relay was a 6,500-ohm d-c relay that closed three sets of contacts. The first of these connected the oscillator to the power amplifier. The second pair actuated the relay which put polarizing current through the 14-kc ring-stack emitter. The third pair of contacts put a negative 135 volts on the TVG circuit in the receiver. There was a switch in the TVG circuit (available on the front panel of the ping-control chassis) so that the negative voltage could be cut off from the TVG chassis in case the operator desired to ping without using the TVG. It was later found to be necessary to parallel the polarizing contact on the ping relay with a set of contacts on the step relay, so that the polarizing current could be turned on one step before the ping. This was done when it was found that a measurable amount of time was required for the current to build up in the 14-kc ring-stack emitter and that polarizing current had to be established already when the ping started in order to produce a square pulse of sound in the water.

In operation, then, the contactor on the hydrophone shaft closed for  $\frac{1}{2}$  of each revolution. This in turn actuated the 6L6 ( $V_1$ ) which closed the 110-volt 6-ma relay once for each revolution. This relay, in turn, moved the telephone step relay one step for each revolution and, at the same time, supplied a synchronizing signal for the spiral-sweep oscillator. When the wiper arms on the step relay moved to the position of the No. 2 contacts, the spiral was returned to the center. At step No. 3 the spiral was held at the center and the polarizing current was turned on. At step No. 4 the spiral was held at the center; the two delay circuits were closed, the ping relay was closed to

the transmitter, and the polarizing current remained on; TVG voltage was applied to the receiver; the SLC sweep was returned; and the two ping-delay contacts were closed. At step No. 5 all the circuits were released except the two ping-delay circuits which were held for steps No. 5 and 6. From step No. 6 on through step No. 1, the circuits were all opened. The spiral sweep was returned two steps before the ping to allow the transients generated by the return to subside.

A multileaved key on the top of the ping-control chassis had one pair of contacts connected in parallel with the ping-control relay contacts on the step relay, thus permitting hand-keying. The second set of contacts on this key were paralleled across the spiral-return contacts on the step relay. If this key were pushed halfway down, a ping would be produced without resetting the spiral, and, if the key were pushed to the bottom, a ping would be produced and the spiral reset. The ping-control relay could also be actuated by the ping-delay chassis.

The circuit relays themselves were external to the ping-control chassis; i.e., the spiral-return relay was in the spiral-sweep chassis, the polarizing relay was near the polarizing batteries, and the power-amplifier relay was incorporated in the power-amplifier circuit. The voltages for synchronism and for TVG, however, were supplied from batteries located in the ping-control chassis.

#### 4.7.5 Ping-Delay Circuit for Model 2 Rotoscope

It was decided to try to secure better range information by controlling the phase of the ping with respect to the hydrophone position and increasing the length of the ping slightly from 0.25 second.<sup>19</sup> The circuit for this purpose required several batteries, a 2050 thyratron, and a 6J5 triode, as shown in Figure 42. The stepping relay closed the two circuits indicated in this diagram and these circuits were held closed for three steps on the relay, or 0.75 second, starting when the ping would ordinarily begin, that is, at step No. 4. When the grid circuit of the 2050 thyratron was completed, the grid voltage began to rise as the capacitor C was charged from the battery through the variable resistor  $R_c$ . When the 2050 thyratron fired, the relay in its plate circuit closed through the circuit completed by the stepping relay. When the plate circuit closed, the ping was emitted

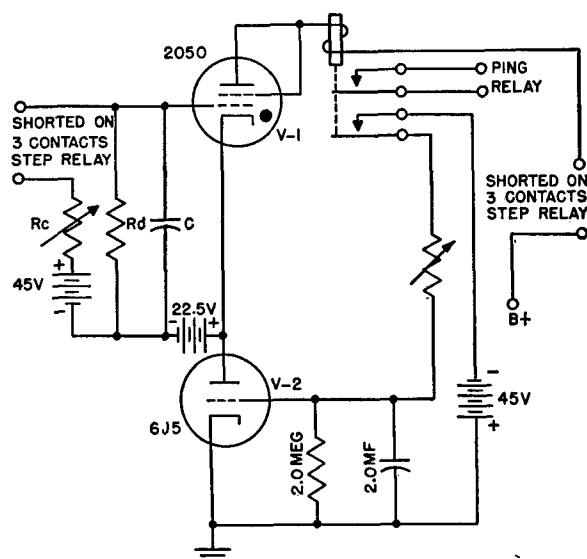


FIGURE 42. Circuit diagram of ping-delay circuit, Model 2 rotoscope.

since one pair of contacts on this relay controlled the ping relay in the ping-control chassis. The second set of contacts on this relay, when closed, permitted current to flow from the 45-volt battery through the variable resistor to charge the capacitor in the grid circuit of the 6J5. When the grid of the 6J5 became sufficiently negative, this tube stopped conducting, and since it was in the cathode circuit of the 2050 thyatron, this tube also stopped conducting. This

opened the plate-circuit relay and stopped the ping. The bias was then reset on the 2050 thyatron by the 22½-volt battery, since by this time the telephone relay had opened the grid circuit and the negative voltage had leaked off the grid capacitor of the 6J5 tube. The delay circuit thus was reset and ready to fire on the next ping cycle. By varying the value of the variable resistor in the grid circuit of the 2050 thyatron the amount of delay in the initiation of the ping could be controlled from 0 to 0.4 second; changing the resistor in the grid circuit of the 6J5 tube permitted control of the ping duration from 0.04 to 0.275 second. Calibrations indicated that the ping-delay and ping-length settings were reproducible with fair accuracy. This ping-delay circuit was used in the latter part of the experimentation with the Model 2 rotoscope.

#### 4.8 SPIRAL SWEEP FOR MR SCANNING SONAR

##### 4.8.1 Mechanical Sweep Used on Model 1 Rotoscope

The mechanically controlled spiral sweep, shown in Figure 43, was used on the Model 1 rotoscope. The deflection coils rotated mechanically around the neck of the cathode-ray tube which was used for the PPI display. The coils were mounted in a bakelite ring which was rotated by means of a flexible shaft and suitable gearing from the receiving hydrophone shaft. Because the coil assembly rotated once for each rotation of the transducer shaft, direct synchronization between the bearing of the hydrophone and the indicator spot was secured. The sweep signal was fed to the deflection coils through slip rings. Rigidly mounted near the top of the rotating shaft was a 99-segment commutator-type potentiometer and brush, which rotated around the outside of the potentiometer and was geared to the hydrophone shaft so that it made one revolution in 5 seconds. The brush, as it rotated around the commutator, picked off an increasing d-c voltage which was fed to the grid of a cathode follower and varied the current in the deflection coils to produce an almost linearly expanding spiral sweep. When the brush passed from the end to the beginning of the potentiometer the cathode-ray spot was returned to the center of the tube screen. There were a few imperfections in the spiral caused by the step-wise character of the potentiometer, and

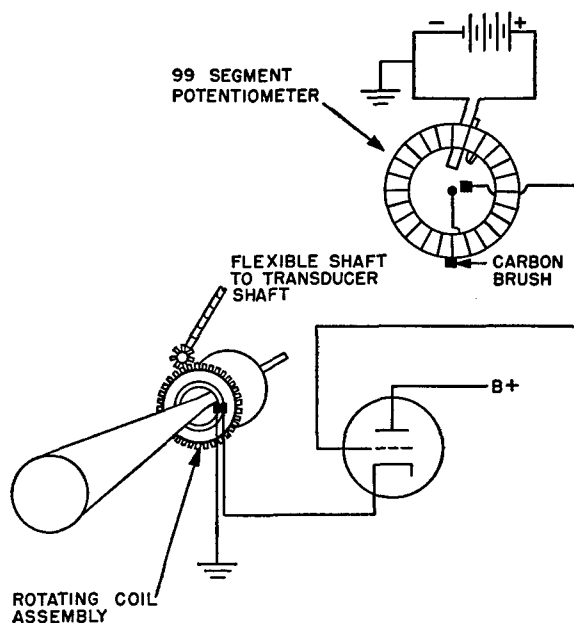


FIGURE 43. Diagram of spiral sweep, Model 1 rotoscope.

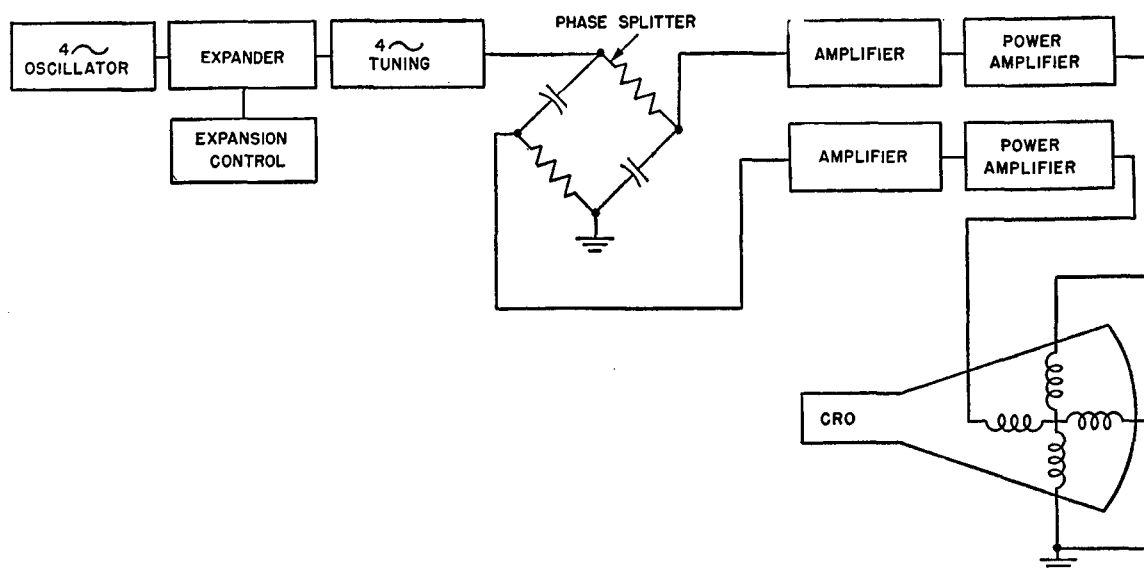


FIGURE 44. Block diagram of electronic spiral sweep, Model 2 rotoscope.

by the brush shorting from one segment to the next. There was also a small 120-cycle variation caused by incomplete filtering of the current supplied to the cathode follower.<sup>30</sup> Although a very usable spiral was produced by this system,<sup>9</sup> there were certain disadvantages from a mechanical point of view: it required accurate alignment of the gearing and careful adjustment of the coil support, which had to rotate at 240 rpm around the neck of the CRO tube. This mechanical spiral sweep was used, however, until the Model 1 rotoscope was replaced by Model 2.

#### 4.8.2 Electronic Sweep Used on Model 2 Rotoscope

In order to overcome the difficulties experienced with the mechanical spiral sweep used on the Model 1 rotoscope, and also to allow the indicator to be mounted at a distance from the rotating hydrophone, an electronic spiral-sweep was built for the Model 2 rotoscope and was used throughout its experimental program.<sup>31</sup>

A block diagram of the circuit arrangement is given in Figure 44, and the final circuit which was used is given in Figure 45. A 6SJ7 tube and a 6F6 tube operated as an oscillator of the RC type. Synchronization was effected at first through a 4-cycle signal supplied by a generator coupled to the rotating hydrophone shaft. This method of synchronizing was found to introduce considerable wave-form distortion and was later replaced with one using a 4-cycle

square wave, generated by a contactor on the shaft of the rotating hydrophone, as shown in Figure 46. The contactor closed a relay 4 times per second, and sent d-c pulses to the 6F6 grid in the 4-cycle oscillator in the sweep circuit. Although the oscillator was built to operate at three frequencies — 4 c, 10 c, and 30 c — the 4-c frequency was the only one used with the Model 2 rotoscope. The output of the oscillator was fed through a potentiometer to the No. 3 grid of a 6SA7 used as an expander tube, while the No. 1 grid of this tube was fed with a sawtooth bias voltage having a period of 5 seconds and an adjustable lower voltage limit. This sawtooth voltage was obtained from the potential difference across a capacitor which was charged to -300 volts at the time of the ping and then allowed to discharge to ground during the sweep period. The expanding 4-cycle signal was fed through a 4-cycle filter, in which the secondary of a power transformer served as the inductive element, to an RC phase-splitting bridge-type network. Two signals 90 degrees out of phase were thus secured; each was fed through a separate power amplifier and cathode-follower circuit to one of the deflection coils. Centering was provided by an adjustment of 6V6 bias obtained from the negative 300-volt supply through a voltage divider and potentiometer. An adjustable potentiometer between the amplifier and cathode-follower stages in each channel permitted signal equalization and control of the amplitude of sweep expansion.

Various shortcomings were discovered and cor-

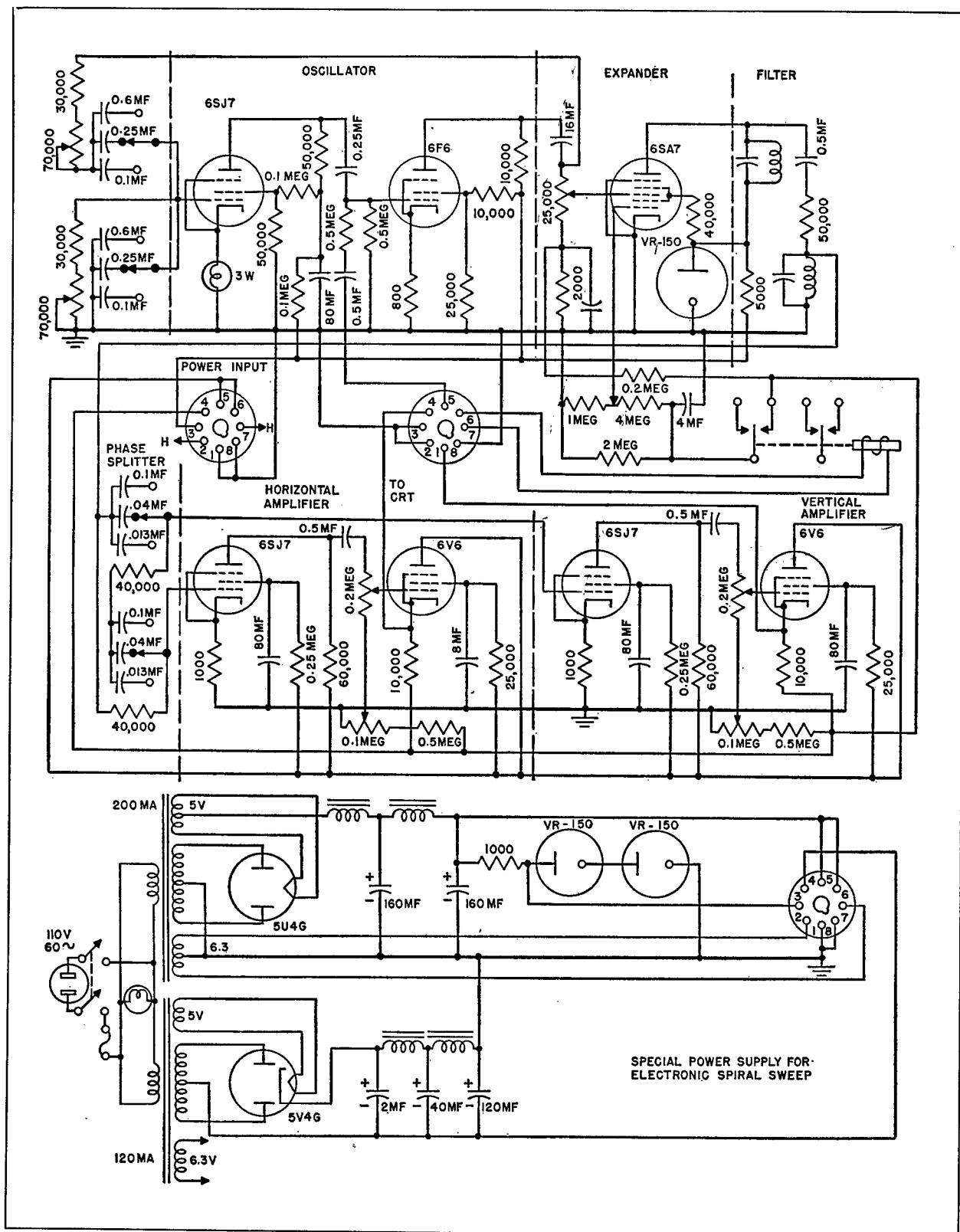


FIGURE 45. Circuit diagram of electronic spiral sweep, Model 2 rotoscope.

CONFIDENTIAL



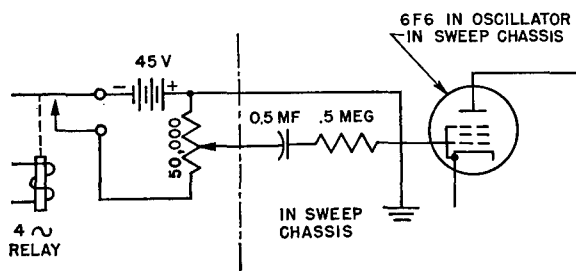


FIGURE 46. Circuit diagram of synchronizing circuit for spiral sweep.

rected during the development of these circuits. Little difficulty was encountered in getting the oscillator to work properly, although phase shifts with respect to the synchronizing signal occurred with change in frequency. While the oscillator would lock with the synchronizing signal at any frequency from 3.75 to 4.25 c, there was considerable variation in the phase at which the oscillator synchronized with the square-wave synchronizing pulse.

Considerable trouble was encountered in the expander circuit. The first system tried (see Figure 47A) used a 6J5 triode in the plate circuit in parallel with the plate-load resistance of the first amplifier tube after the oscillator, the 6J5 triode plate resistance

acting as part of a voltage divider. The relay reset the spiral to zero during the ping, and, when the relay was released, an 80- $\mu$ f capacitor began to charge from the negative 45-volt battery through suitable resistors. A potentiometer selected the amount of the bias to be put on the grid of the 6J5 triode, and as the capacitor charge became more and more negative, the grid potential decreased towards cutoff. The plate resistance of the 6J5 tube then increased, and more and more signal was fed to the phase-shift network. The one drawback to this was that the coupling capacitor between the 6J5 and the following stage became charged. Since its discharge time constant was long, it was necessary to remove the charge with an extra pair of contacts on the relay, as shown in Figure 47A. This system worked fairly well, except that several turns of the spiral were needed to establish equilibrium conditions.

Several schemes were tried in which the expansion was carried out after the phase-splitting operation. However, these were judged to be unsatisfactory and single channel expansion before phase splitting was again adopted, as shown in Figure 47B. In this case the 6SK7 tube with 6J5 triode was used as the plate-circuit potentiometer. Although extra contacts on the ping relay were used to ground the grids of both

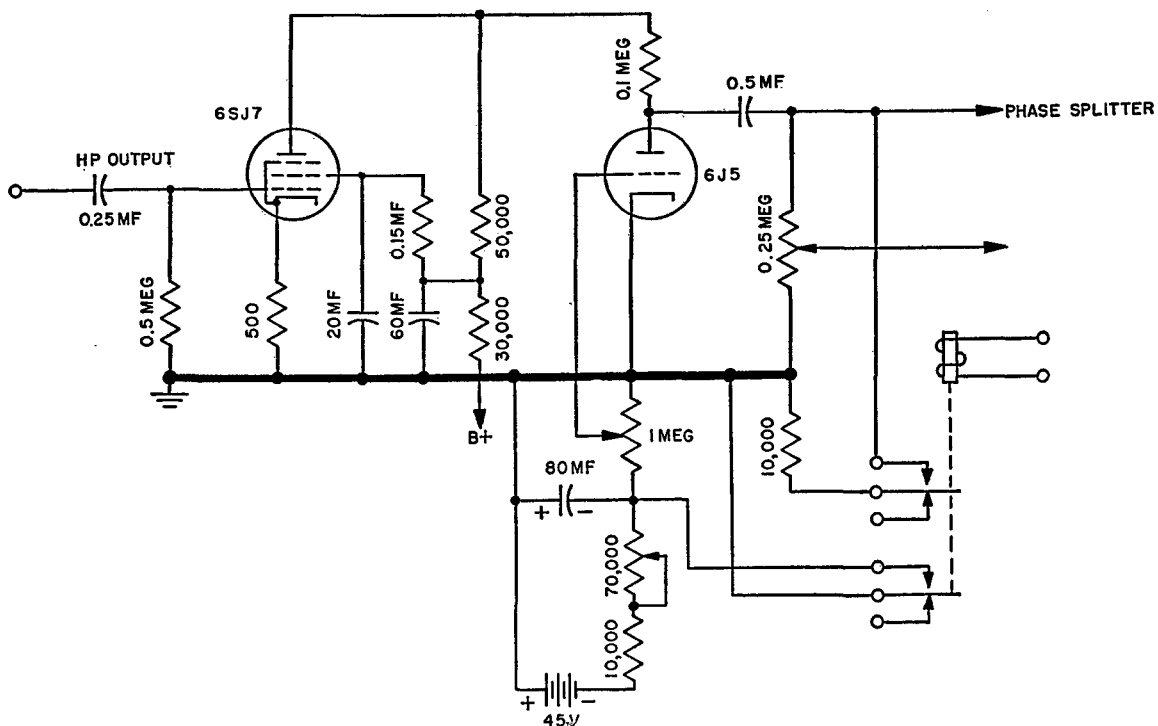


FIGURE 47A. Circuit diagram of early experimental spiral-sweep expanders.

CONFIDENTIAL

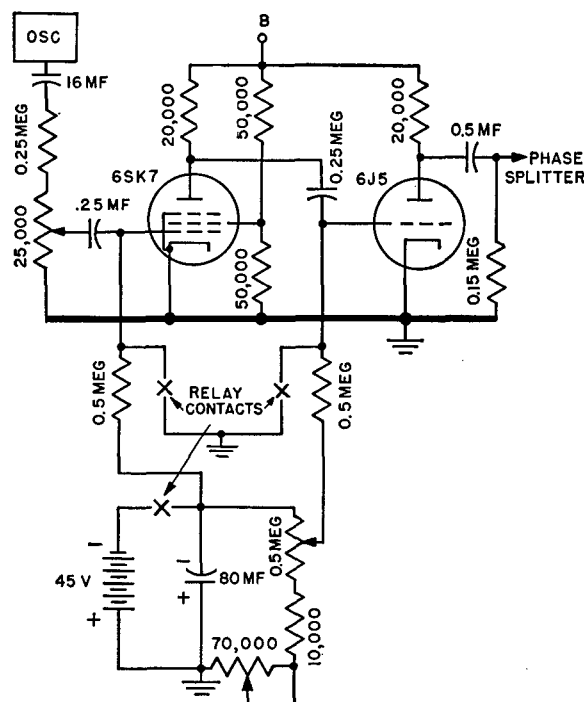


FIGURE 47B. Circuit diagram of modified experimental spiral-sweep expander.

tubes during the ping interval, some charge remained on the blocking capacitors (probably due to dielectric hysteresis), resulting in nonlinearity of the sweep expansion at short ranges. The arrangement finally adopted has already been described in connection with Figure 46. Since residual transients could not be entirely eliminated, the resetting of the spiral to the center was started two steps ahead of the stepping relay (0.5 second) before the actual start of the ping.

There were, of course, other difficulties. It was necessary to use an LC rather than an RC filter in the output of the expander stage to keep time constants low. Since the deflection coils obtained a bucking current from the negative power supply, and since the time constants of negative and positive power supplies were not identical, there was some spot drift with change in line voltage. The drain on the positive power supply varied as the 4-cycle signal from the expander changed. Since at this low frequency the power supply had appreciable regulation, some feedback to the oscillator occurred, the amount varying with the progress of the expansion cycle.<sup>13</sup> This resulted in a slight phase shift relative to the synchronizing signal from the beginning to the end of the cycle, and caused a slight change in indicated bearing with range.

Despite its lack of perfection the sweep circuit shown in Figure 46 permitted reasonably satisfactory operation of the Model 2 rotoscope, and was used throughout the experimental work with this system. For the CR scanning sonar work it was abandoned in favor of a rotating polyphase generator, but was again used in an improved form in the high-speed sweeps required for the electronic rotation scanning systems described in Chapter 7.

#### 4.9 SUGGESTIONS FOR FUTURE WORK

Since the primary purpose of the experimental work on mechanical rotation scanning sonar was to accumulate experience and develop techniques that would be useful in the commutated rotation and electronic rotation types, the work was not pursued to the point of realizing a completely satisfactory system. Some of the techniques developed have already been applied by other organizations to listening systems, and should a demand ever arise in the future for a particularly simple version of scanning sonar, the MR type might well be considered a possibility. While two transducers would probably still be required, each could be of far simpler construction than the multielement transducer required in the CR or ER units. Furthermore, no complex commutators or electronic rotors would be needed.

The outstanding disadvantage of the MR sonar is the slow rotation speed imposed by the necessity of rotating physically the receiving hydrophone in the water, with a consequent limitation of range resolution and signal-to-noise ratio. There is no assurance, however, that the 4-rps systems built at HUSL were operating at the maximum practicable speed. The question of what the maximum practicable speed should be is therefore one which deserves investigation. It is likely that the limiting factor would be water noise, rather than power for rotation. The direct approach to answering this question would be to mount a hydrophone in a suitable dome and measure the noise as a function of speed. Peripheral speed would probably be the determining factor. In the Model 2 rotoscope the peripheral speed was 14 feet per second. In order to match the reasonably satisfactory performance of the QH Model 2 scanning sonar (CR type), which used a rather wide beam and a rotation speed of 30 rps, the peripheral speed would have to be increased to about 65 feet per second. The power, which for the Model 2 rotoscope

was about 0.1 hp, would be increased to about 2.3 hp. This is reasonable, particularly since direct coupling could be used. In fact, one arrangement has been suggested in which the motor would be built into a watertight dome with the directly coupled hydrophone.<sup>32</sup> Liquid filling in the lower half of the container would be necessary to provide acoustic transmission.

Among the reasons for a lack of satisfactory results with the rotoscope systems were the limitations of the available transducers, which were characterized by broad patterns, excessive side and back sensitivity, and extremely low efficiencies. The developments of the last few years in the art of transducer design would undoubtedly allow considerably improved performance.

## COMMUTATED ROTATION SCANNING SONAR

## 5.1 GENERAL DESCRIPTION

THE MODEL XQHA scanning sonar, built by the Sangamo Electric Company as a preproduction model<sup>1</sup> during the latter part of 1944, was selected to explain the functional requirements and operation of *commutated rotation* [CR] sonar because it embodied most of the durable features found desirable by HUSL for such an underwater-sound detection system.

A block diagram showing its functional operation is shown in Figure 1. Photographs, schematic diagrams, and more detailed explanations of the operation of the various circuits are given in later sections of this chapter.

The *receiver unit* of the Sangamo model contains the send-receive transfer network and relay, the listening and scanning commutators, and a dual channel amplifier. The transfer relay is closed during transmission by a relay-actuating tube operated from the keying unit and range selector in the *indicator control unit*. The relay, when actuated, removes the short across the output of the transmitter, disconnects the ground side of the receiving channel at the input transformers, and removes the negative bias from the modulator in the transmitter, which thus is allowed to operate and transmit a pulse of power to the transducer. During reception the transfer relay remains in the normal position, in which the transmitter output is grounded to prevent any possible noise or signal feed-over into the receiver. The low side of each of the 48 receiving- and 48 listening-commutator input transformers is also grounded, and the contacts which short out the negative bias to key the oscillator are open.

The output of the transmitter is fed through a bank of 48 capacitors, each of which is in series with a transducer element. During transmission, these are all paralleled and tuned by a common coil. During reception, signals generated in the transducer elements are fed to the 48 commutator segments through 48 step-up transformers. The rotor of the commutator, operating at approximately 1,800 rpm, scans the segments of the stator 30 times per second while the beam-forming lag line, which revolves as an integral

part of the rotor, forms a narrow beam pattern of receiving sensitivity at a specific bearing by correcting the phases and amplitudes of the voltages of several segments on each side of that central bearing segment. The output of the rotor is conducted through a set of slip rings to a preamplifier consisting of a pentode amplifier stage, a band-pass filter, and a cathode follower. The output of the cathode follower is fed through a shielded cable to the receiver.

The scanning receiver consists of a tuned amplifier (a ganged capacitor controls the tuning of the heterodyne oscillator and the first tuned stage of the scanning and listening amplifiers) followed by a band-pass filter, second and third stages of amplification each followed by a band-pass filter, a rectifier, and a cathode follower which feeds the brightening grid of the cathode-ray indicator tube, the *plan position indicator* [PPI]. The first two stages of the receiving amplifier are controlled by a master gain control in the indicator control unit as well as a *reverberation-controlled gain* [RCG] circuit. The RCG bias is rectified from the output of the listening amplifier and is established in coincidence with the keying of the transmitter by a tube actuated from the keying unit and range selector in the indicator control unit.

The input circuits of the listening commutator are paralleled with those of the scanning commutator; there is one transfer network for both commutators. A preamplifier identical to that on the scanning commutator feeds the commutator output signal to the listening receiver, the first two stages of which are identical with those of the scanning amplifier-receiver, being tuned by the same ganged capacitor and controlled by the same master gain control and RCG circuits. There is an auxiliary gain control between the second stage and the modulator following it. The modulator feeds a band-pass filter and a second modulator which produces the difference frequency of 800 c used for listening. The output of the second modulator is amplified, passed into a cathode follower feeding an 800-cycle band-pass filter and into a power output stage which operates the loudspeaker and the chemical range recorder.

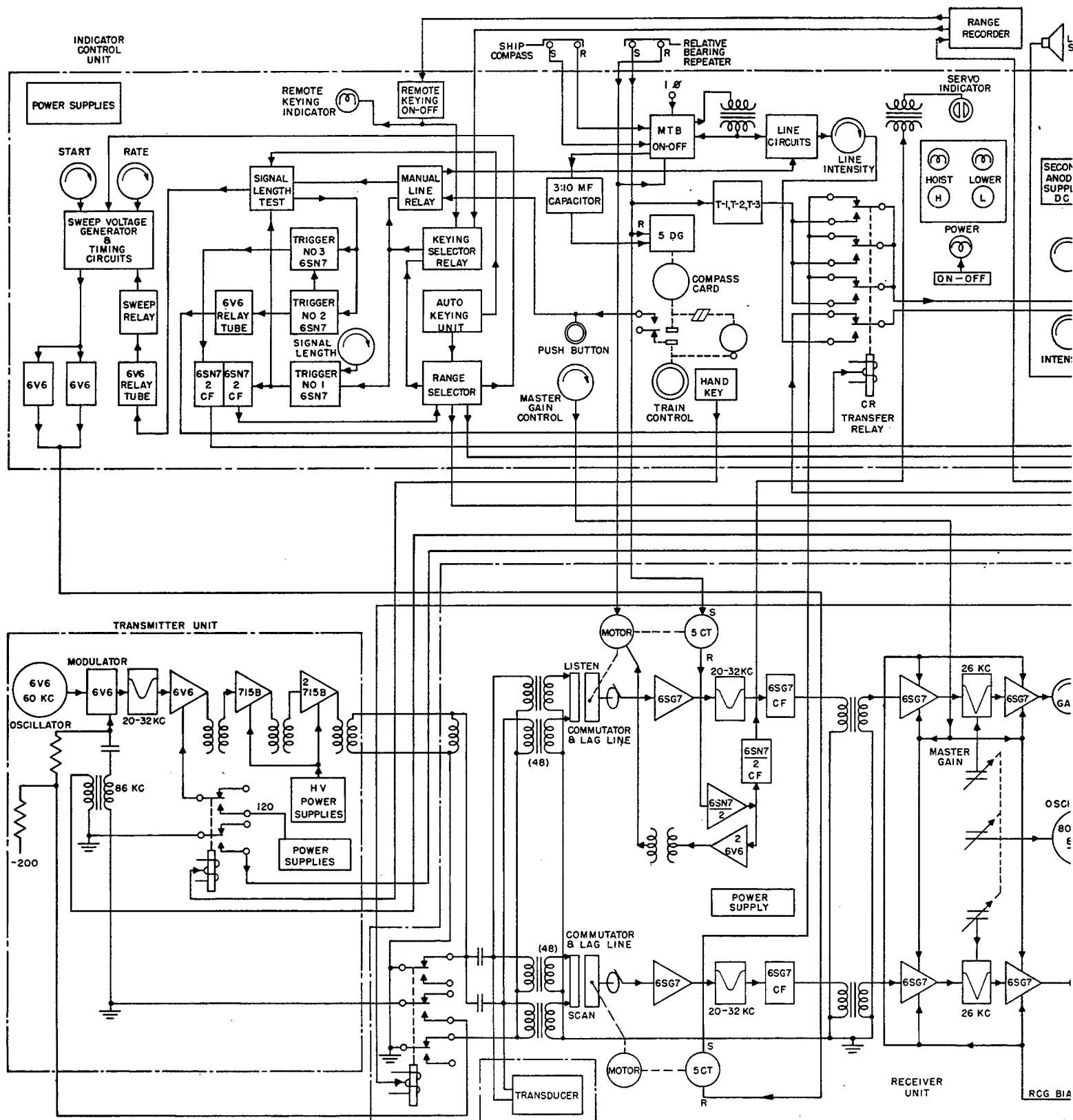
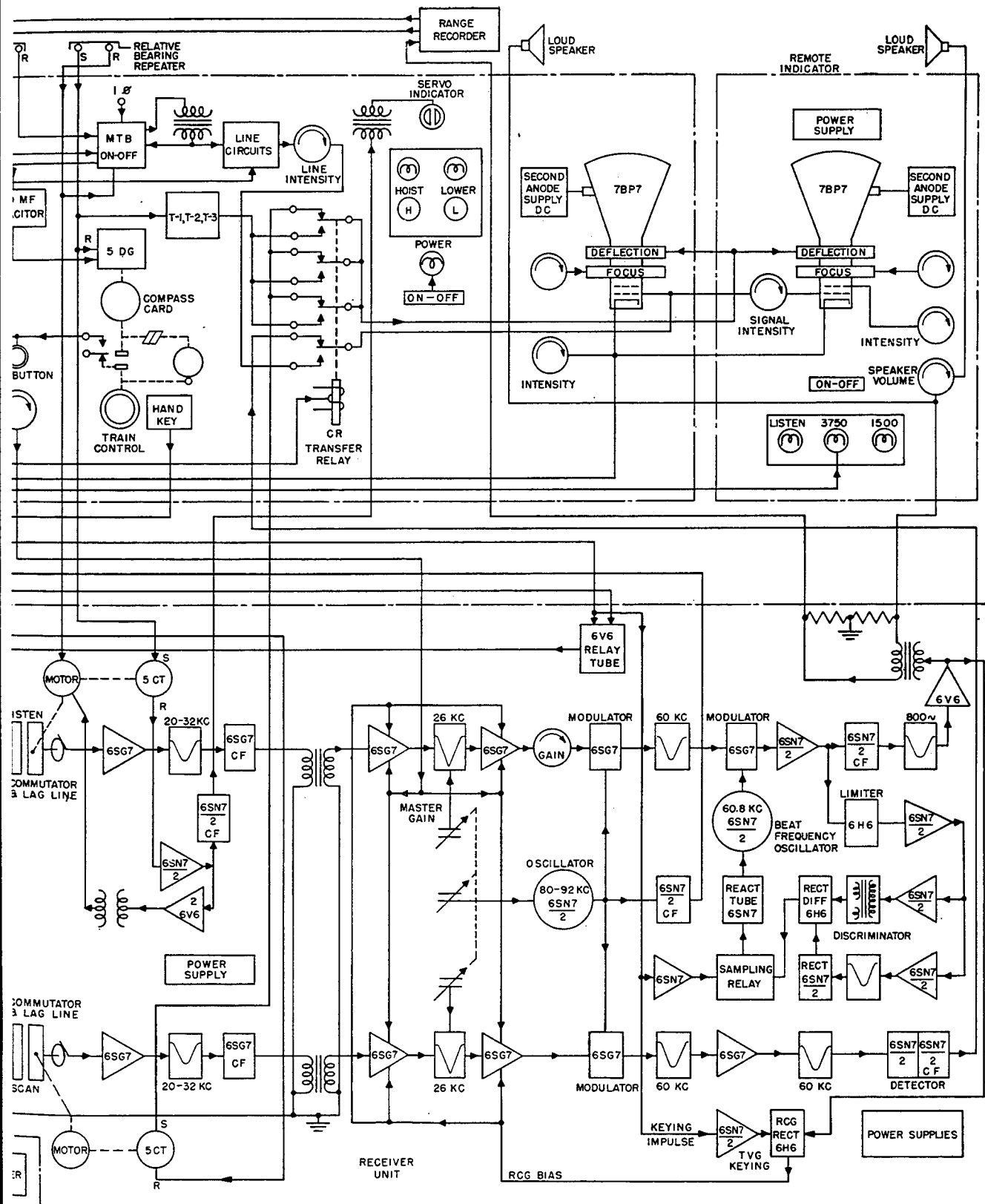


FIGURE 1. Block diagram of Sangamo Model XQHA scanning sonar.



Block diagram of Sangamo Model XQHA scanning sonar.

CONFIDENTIAL

To compensate for change in frequency caused by own-ship's speed, a group of circuits for *own-doppler nullification* [ODN] is included which acts on the beat-frequency oscillator. The ODN feature operates as follows: the amplified output of the second modulator is limited, amplified, and further amplified by two separate channels, one of which feeds a discriminator coil, the other a band-pass filter. The discriminator feeds a rectifier to provide the correction bias to a reactance tube for adjusting the frequency of the beat-frequency oscillator; the output of the second channels, when rectified, provides a second corrective bias to prevent the discriminator bias from shifting in the negative direction as a result of spurious cross-overs occurring in the discriminator response. A sampling relay operated from the keying and range selector unit samples a portion of the reverberation during each ping period and corrects the beat-frequency oscillator to produce an 800-cycle output from the modulator. Requisite power supplies are included in the receiver unit.

The *transmitter unit* contains a local oscillator, the output of which is combined with the unicontrol oscillator signal from the receiver unit in a modulator tube. During the receiving period the modulator tube is overbiased to prevent signal output; during transmission this bias is removed by the transfer relay in the receiver unit. The ping length is determined by the length of time this relay holds down, but can be varied by controls in a trigger-tube circuit which is in the indicator control and determines the length of the current pulse in the relay coil.

The output of the modulator is filtered and applied to the grid of the power-amplifier driver tube, which is transformer-coupled to the grids of two power output tubes which drive the transducer through a suitable matching transformer. The transfer relay and impedance-matching network are contained in the receiver unit and have already been described. Control of the transmitter output power is obtained by varying the plate voltage of the output tubes by a variable-ratio auto-transformer in the primary of the plate supply transformer.

The transmitter is an impulse type which employs large storage capacitors for the plate supply of the power output tubes. The transmitted pulse at the slowest pinging rate develops a total power input of 7.8 kw to the transducer. Since the transducer acoustical efficiency is from 30 to 40 per cent, the result is 3 kw of sound power transmitted into the water. This

type of transmitter is extremely economical, its average power input being only about 550 watts.

Provision for underwater code communication at reduced output is made by incorporating in the transmitter a relay which applies a 120-cycle modulating voltage to the tube that feeds the power-amplifier drivers. This relay also actuates the transfer relay in the receiver unit, which in turn allows the modulator in the transmitter to operate in the manner described above. The transmitter output then consists of short pulses of energy produced at a 120-cycle rate. The hand key that energizes the communication relay is located on the indicator control unit. Suitable high- and low-voltage power supplies are provided.

The indicator control unit contains the cathode-ray tube on which range and bearing information developed by the system is presented as a PPI display, the circuits associated with the tube, the necessary operator controls, and the timing circuits which operate the various portions of the system in correct sequence. A bulkhead-mounted loudspeaker and the chemical range recorder were located near the indicator unit.

The PPI cathode-ray tube is provided with a focusing coil and a deflection coil assembly. The latter is actually a 3-phase 5 CT synchro stator coil wound to match the output of the synchro generator mounted on the scanning commutator. A 3-phase alternating current whose frequency is equal to the scanning speed and whose amplitude is sawtooth modulated at the ping rate is supplied by the 5 HCT synchro generator to the deflection coil, causing the cathode ray to spiral out from the center to the circumference of the tube. As the synchro generator is geared directly to the scanning commutator rotor the spiral-sweep rotation is synchronized with the scanning commutator rotation; its rate of increase of radius is proportional to the range setting. The rectified signal output from the scanning amplifier-receiver is applied to the control grid of the cathode-ray tube, resulting, when an echo is received, in a bright arc on the fluorescent tube face which, in angular position, indicates the target bearing and, in radius, the target range. Externally generated sounds, such as propeller noises, produce a brightened sector whose angular position indicates the bearing of the sound source. The brilliance of the indication can be varied by an intensity control.

The output of the listening amplifier-receiver is supplied to a loudspeaker and the chemical range

recorder. The listening commutator rotor is trained, through a synchro-controlled servo system, by a hand-wheel which positions the bearing cursor line on the PPI, a dial being provided to indicate bearing order. *Maintenance of true bearing* [MTB] is provided through synchro connection to the ship's gyrocompass, but the training control can be converted to relative bearing by throwing a switch MTB on-off in the indicator control unit.

A cursor line on the face of the PPI scope is produced automatically during the transmission interval, but can also be applied at will during any part of the receiving interval by pressing a button that energizes the cursor circuit. During the transmitting period, a separate relay disconnects the PPI deflection coil from the synchro generator on the scanning commutator, connects it to a set of transformers fed from the hand-trained synchro, and simultaneously applies a 60-cycle signal, synchronized in proper phase relation to the synchro order, to the grid of the PPI tube, to produce a line on one-half the scope. The intensity of this cursor line is varied by a separate control.

The length of time between pings is determined either by a mechanical timer in the indicator unit or by the chemical range recorder. The recorder, when turned on, automatically takes control of keying unless the remote keying on-off switch was turned off. The keying pulse from either of these sources sets off three trigger circuits: the first gives a pulse which actuates the transfer relay in the receiver unit and operates the sweep discharge relay. The second generates a pulse that controls the length of time the PPI deflection coil and grid transfer relay operate. The third generates two blanking pulses which are applied to the PPI tube to blank out display of transients caused by collapse of the magnetic field in the deflection coil and by the switching operation. The first of the two blanking pulses is over in time for producing the bearing cursor line; the second, which is initiated by the cessation of the pulse from the second trigger circuit, blanks the scope while the deflection coils are being reconnected to the spiral-sweep supply.

A test circuit to check the length of the transmitted pulse is embodied in the indicator unit. When this circuit is placed in operation, trigger circuits No. 2 and 3 are inoperative, so that blanking and deflection coil switching does not occur. Further, the circuit is so arranged that the spiral-sweep keying is dissociated from the transmitter keying to allow observation of the transmitted pulse signal as a bright spiral trace on

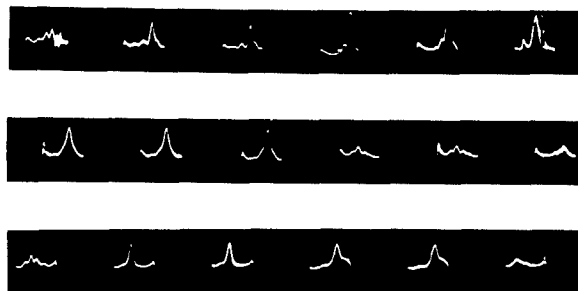


FIGURE 2. Receiving directivity patterns obtained with Medusa transducer and whirling dervish commutator.

the PPI tube. A spiral with a slight overlap indicates a pulse length slightly longer than one scanning rotation period, and adjustment of the transmitted pulse length can be made by varying the pulse length from trigger circuit No. 1. The sweep voltage generator produces a sawtooth wave initiated by the keying unit through the sweep relay. This linear sawtooth wave is fed into the rotor of the synchro generator which produces the spiral sweep.

## 5.2 EXPERIMENTAL WORK ON CR SCANNING SONAR SYSTEM

### 5.2.1 Medusa and Rotating Tubes

The first CR system used a 36-element vertical nickel tube transducer known as Medusa (see Section 5.3 on transducers for CR sonar), so named because of the large number of wires emerging from the top of the perimeter of the transducer. (See Figure 10.) The capacitive commutator used with Medusa was known as the whirling dervish and is described later in this chapter. It was an early model commutator unit built with the lag line and 10 amplifier tubes mounted on the rotor and rotated at 10 rps.

The transducer and commutator were tested at the HUSL barge, where patterns were photographed as they appeared on the cathode-ray oscilloscope. These patterns,<sup>2</sup> recorded for each 20 degrees around the transducer, are given in Figure 2. A 14-kc ring stack, used as a projector and driven by a power amplifier, provided sound in the water for echo ranging in the Charles River Basin. Echoes were received from the opposite bank of the river on this first experimental system. No indicator was used other than a CRO and a high-frequency analyzer for listening.<sup>3</sup>

About October 16, 1942, the system was taken aboard the AIDE DE CAMP for a short series of tests.



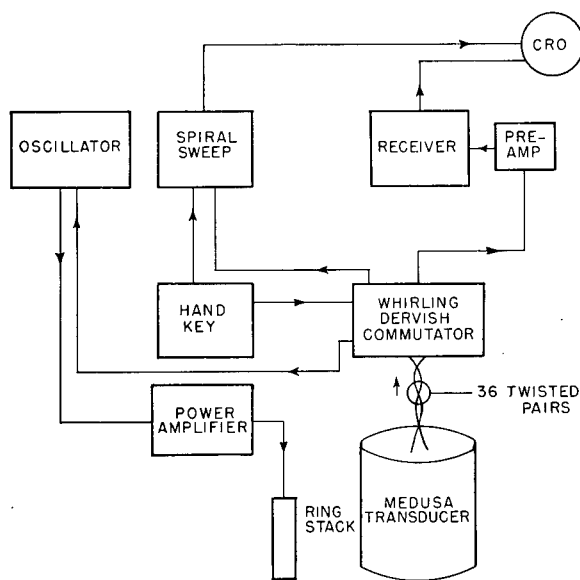


FIGURE 3. Block diagram of Medusa, whirling dervish scanning sonar of AIDE DE CAMP.

The transducer was located in the forward well of the AIDE DE CAMP, with the capacitive commutator placed on the floor next to the well. A 400-watt transmitter feeding the 14-kc ring stack was used as a source of sound in the water. The signal output from the commutator was fed through a preamplifier to a receiver built for use in *mechanically rotated* [MR] sonar and known as the *time-varied gain* [TVG] receiver (see Chapter 4). The output of the receiver was then fed to the brightening grid of a 7-inch cathode-ray tube built for MR use. The electronic spiral sweep of this tube rotated at 10 rps, and was synchronized with the commutator rotation by an electric contact on the rotor. A hand key was used to reset the spiral and key the transmitter. The keying interval was controlled through relays by a contactor on the commutator rotor shaft so that the ping length equalled the time of one revolution of the rotor; however, the ping sequence had to be manually initiated.<sup>4</sup> Figure 3 gives a block diagram of the system used.

Experimental tests made in Boston Harbor indicated that with a constant 14-kc signal fed into the ring stack, located in the aft well of the AIDE DE CAMP, radial brightening was produced on the indicator, showing that a pattern was being produced and rotated. However, tests also showed that the bearing indication changed when the transducer was turned in the water. This undesirable effect occurred because

the individual hydrophone elements of the transducer differed in their directional pattern and sensitivity. Moreover, the commutator was noisy, from both electrical pickup and microphonics. When listening, with the commutator stationary, a rotor position was found at which a very good echo could be identified by ear. With the rotor running, the noise level was higher, and because of the shorter duration of the echo, aural identification was difficult. No echoes were identified on the cathode-ray indicator screen, but noise from passing ships and other noise sources was indicated.<sup>5</sup> The general result was encouraging, but it was apparent that a more efficient and uniform transducer was necessary. Consequently, it was decided to build a laminated-stack multiple-element transducer for the scanning system.

### 5.2.2 Auditorium Demonstration System

While a new transducer was being designed and built for further work on the scanning problem, the electronic components of a new system, to operate at 22 kc, were designed and built. During development, the system was set up in the laboratory and tested by artificial means. A block diagram of this system, as finally evolved for demonstration purposes, is shown in Figure 4. It uses a cathode-ray tube PPI on which the spiral sweep is produced by a synchro stator coil assembly around the neck of the tube. The sweep voltage is obtained from a 3-phase synchro generator mounted on the capacitive commutator shaft, the generator field being excited by a sawtooth varying current. A DG synchro is inserted in the sweep circuit between the generator and the cathode-ray tube so

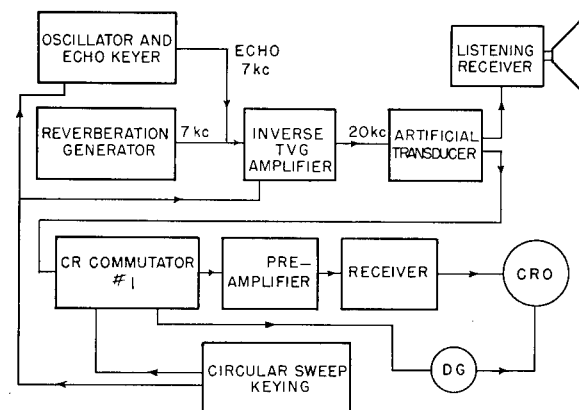


FIGURE 4. Block diagram of laboratory demonstration system.

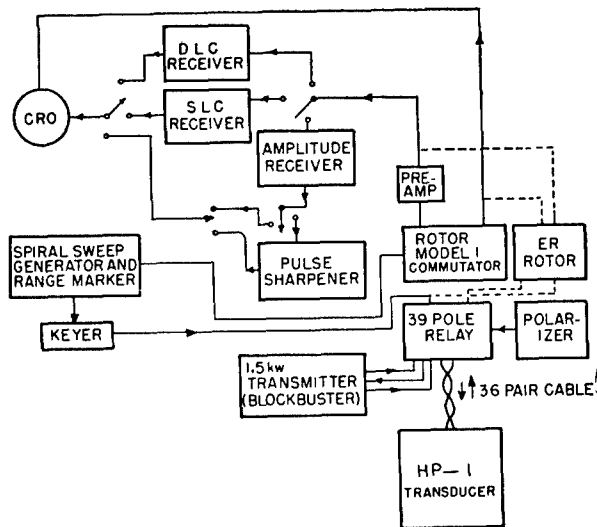


FIGURE 5. Block diagram of AIDE DE CAMP CR/ER scanning system.

that the position of the indication can be varied in bearing. The sawtooth generator controls the keying of the system. To simulate the echo signal, a reverberation generator was developed and built for this particular application, the echo being formed by it and an oscillator signal keyed through a time-delay relay mechanism in such a manner that the echo would appear at any desired range on the PPI. The signal from the reverberation generator and oscillator is fed through an amplifier with inverse TVG to produce reverberation levels and level changes with time similar to those actually occurring in water. This signal is then fed through an artificial transducer which produces the appropriate time lags between the signal voltages reaching the various commutator elements. From the commutator the signal is fed through a preamplifier and a receiver to the brightening grid of the cathode-ray tube indicator. A listening receiver and loudspeaker are connected to the artificial transducer so that it is possible to hear the signal that is being fed through the CR system. The ideas incorporated into this system were later used in developing the *operator training equipment* [OTE].<sup>6</sup> This system was used as a laboratory test for the development of new components and for demonstrations to interested parties of the Navy, Merchant Marine, and OSRD.

Concurrently with this work, experiments were carried on to develop a better sweep circuit. Although a capacitor-type sweep was tried,<sup>7</sup> the synchro type was

found to be more satisfactory and was eventually adopted for use on all CR systems. Considerable research on receivers, methods of pulse sharpening, *simultaneous lobe comparison* [SLC], and amplitude brightening was carried forward during this period; these developments are discussed in the sections of this chapter having to do with receivers and sweep and timing circuits. Tests were made on some doppler brightening arrangements but they were not successful. During this period much time was also spent in the search for a proper plate material to be used in the capacitive commutator. Since a scanning speed of 30 rps was deemed necessary for using the short-ping technique, a commutator capable of rotating at 1,800 rpm had to be designed. A detailed discussion of the developmental work on commutators is given in Section 5.4 of this chapter. The commutator finally decided upon for the demonstration system, and later used in the system on the AIDE DE CAMP, was the one designated as Model 1.

### 5.2.3

## Aide de Camp System

The first laminated-stack 36-element transducer, known as *Hebbphone 1* [HP-1], was installed in the forward well of the AIDE DE CAMP. This formed the basis for the AIDE DE CAMP system which was actually first installed in June 1943, and was given extensive field tests during October and November at New London with a submarine target.

Although minor changes in the system components were made from week to week, the block diagram given in Figure 5 shows the overall arrangement of circuits used throughout the whole history of this system. HP-1 was used both as a transmitting and receiving projector at 21 kc. It is a type which requires d-c polarization at all times. The received signals from the transducer elements were introduced into the Model 1 commutator and its associated beam-forming lag line. The lag line's output signal was amplified in a preamplifier, and then applied to the receiver equipment. A receiver amplified the signal and produced a brightened spot on the cathode-ray tube PPI. There was also a spiral sweep controlling the keying circuits which keyed the 1.5-kw transmitter for transmission.

Part of the time, and for the New London tests, a 60-rps scanning ER rotor was installed, which could be substituted for the CR Model 1 commutator by

changing four connection plugs. This is described in Chapter 7.

The electronic receiver equipment consisted of three receivers: a *delayed lobe comparison* [DLC] receiver used almost exclusively with ER; an SLC receiver; and a linear amplitude receiver—used almost exclusively with the CR system. There was also a pulse-sharpening circuit for the output of the amplitude receiver, which the operator could use or not as he wished. The receiver connections were arranged so that any one of them could be connected by suitable switches to the preamplifier output signal channel and to the PPI. The spiral-sweep generator fed a sawtooth excitation current to the synchro generator rotors to produce a spiral sweep on the indicator. The ranges used were 1,000, 2,000, and 4,000 yards. The range-marker circuit put a brightened ring, equal to one turn of the spiral, on the PPI four times during a sweep cycle, thus separating the range into four equal parts in an attempt to make the estimation of range fairly accurate by interpolation between these range marks. The PPI used was the 7-inch cathode-ray tube employed in the laboratory system. However, this was later replaced by a 12-inch tube with a mechanical cursor for reading bearing.

Operation of the keying system was initiated by the spiral flyback voltage which was differentiated and used to start the keying chassis in its keying sequence. During reception, the elements of the transducer were connected independently to the commutator unit; during transmission, all elements were connected in parallel to the transmitter. This was accomplished by means of a 36-pole relay.

The keying sequence was as follows: When the transducer relays closed, the receiver circuit was broken and a pulse fed to the transmitter keying relay which allowed the transmission of a high-frequency signal into the transducer. At the end of the ping, the transmitter relay, and then the transducer relays, opened, thereby connecting the transducer to the receiving circuits. This somewhat complicated interwiring of relays was necessary to prevent the transmitter from feeding power into the commutator or any part of the receiving system.

This system worked very well, producing good echoes from surface ships, bottom, and underwater objects. The Model 1 commutator produced a good pattern with the HP-1 transducer, and rotated the beam smoothly. Insulation breakdown inside HP-1 occurred near the end of July, which necessitated its

removal for repair. In the meantime, the AIDE DE CAMP was used for other work so that the CR system was not back on board until September 1943.

Numerous tests were made in July, September, and October. One of these was the test of the various receivers. (See Section 5.6 of this chapter.) By using a floating echo repeater of the buoy variety<sup>8</sup> as a target, it was finally decided that the linear amplitude receiver produced the best indications. The SLC and DLC receivers produced an on-off type of indication, and the amplitude receiver with sharpening produced a pulse too sharp and without sufficient discrimination between echoes and noise. The linear amplitude receiver produced a half-tone effect that delineated channels, ledges, rocks, and other bottom singularities, making identification of echoes in the presence of such interference much easier.<sup>9</sup>

The possibility of a true-bearing PPI was also investigated. A DG synchro was installed in the sweep channel between the synchro generator on the commutator and the deflection coils on the PPI tube. The rotor in the DG synchro was positioned by a servo motor which was driven by the output from a photoelectric-cell compass follower. This arrangement gave magnetic rather than true bearing. The system worked successfully, but was confusing to operators whose instruction had been limited to experience on the relative bearing plot.

During the change from 7-inch to 12-inch indicators, it was noted that while the 12-inch size gave a larger plot, the actual information received was not improved and the spiral appeared much coarser.<sup>10</sup>

Shortly before the New London trip, a transmitter utilizing the duty-cycle pulse-type circuit was installed. With this circuit the same pulse power could be obtained from a much more compact transmitter than the one designed for 1.5-kw continuous service. This unit is described in Section 5.7 of this chapter. It worked well for an experimental model and its general design was later adopted for all scanning sonar systems.

During November of 1943 the AIDE DE CAMP was stationed at New London where field tests on the CR system continued, using a submarine as target. Sometimes it was possible to follow the submarine at periscope depth, or a little deeper, out to 4,000 yards. At other times it was impossible to detect the target at ranges over 1,500 yards. Under reasonable water conditions the system followed the evasive maneuvers of the submarine readily.

CONFIDENTIAL

During this test period, sharpening of the beam and reduction of minor lobes in the system were improved.<sup>11</sup> Records were made of echo amplitude and the sensitivity of the system was determined.<sup>12</sup> A study of range errors, error distribution, and echo amplitudes was made.<sup>13</sup>

Experience with range determination on this CR scanning sonar may be summarized as follows: Range observation of the PPI was quite simple, but observed ranges appeared to have errors of  $\pm 64$  yards, which is much greater than the intrinsic sonar error of  $\pm 15$  yards, showing that the indicating method left much to be desired.

The results of these tests also indicated that the average bearing error was approximately 6 degrees. This error was not introduced by the method of rotation, since an experiment to check this point indicated that the direction of the maximum beam sensitivity was always within 2 degrees of the direction indicated by the capacitive commutator.

During the whole experimental period, behavior of the spots on the CRO indicator corresponding to echoes received from the target indicated that there was an uncertainty of approximately  $\pm 10$  degrees as to the precise bearing of the target. This erratic motion was possibly caused by the ship's yaw and bearing errors which derived from amplitude modulation of the echo.

In regard to echo strengths, it was found that at 000 degrees relative bearing, with the submarine at 1,000 yards at beam aspect, good echoes were returned from only about 25 per cent of the pings, as observed on the PPI screen. Observable echoes were returned from perhaps 30 per cent, and the remaining 70 per cent of the pings produced no spot on the screen. To obtain quantitative data on the performance of the system, careful measurements of transmitted power and receiving sensitivity were made, and the figure of merit of the system was determined to be 122 db,<sup>12</sup> which is definitely low for a sonar system. Further study of the echo intensity data indicated that they were consistent with the behavior to be expected, under the thermal conditions then prevailing, from a sonar system with this figure of merit and a submarine with a target strength of something under 10 db.

While the AIDE DE CAMP was at New London, the CR system was demonstrated to representatives of the Navy and of interested manufacturing concerns. On the return trip from New London a stop was

made at Newport, and the CR system, as a listening device, was tested for its ability to detect torpedoes.<sup>11</sup> The AIDE DE CAMP lay off the edge of the firing range at about 2,000 yards from the control tower. A torpedo could be followed by its noise from the time it was launched until the end of its run, the noise producing a brightened radial sector on the PPI that indicated its bearing.

After the return from Newport, a second pulse-type transmitter was substituted for the one that had been on board. Because of its higher power output, a better signal-to-noise ratio was obtained. Other changes also were made. In the initial installation the transducer polarizing current was supplied by three heavy-duty storage batteries connected in parallel, producing about 60 amperes of polarizing current. These batteries were so connected that they could be charged by a motor-driven generator while not in use. As this system was too noisy, a General Electric oxide rectifier unit and filter, capable of producing about 50 amperes at 5 volts, was installed in the place of the batteries and generator, making a much cleaner installation.

A change was also made in the transfer network. A method of connection, using blocking capacitors and inductors that required but one relay in the ground returns of the rotor input transformers, was tested and proved satisfactory. The HP-1 transducer was removed, repaired, and reinstalled in late December. At that time the first CR console, known as the CR/ER Model 1, No. 1, was installed for tests before it was to be placed on the USS SARDONYX at New London.

A series-tuned, thyrite, send-receive, transfer network was used with moderately good results for a few weeks in December and January 1944, on the Model 1 rotor on the AIDE DE CAMP. The circuit diagram is shown in Figure 20. No tuning adjustments were necessary after they were made initially at HUSL. The minimum detectable signal was approximately the same as with the transformers, and the pattern was equally good. The chief drawback was the necessity for fixed tuning at only one frequency.

5.2.4

### Model 1 CR/ER Sonar

In February 1944, the CR/ER console, Model 1, No. 1, the Model 1 commutator rotor, the HP-1 transducer, and its choke box were removed from the AIDE DE CAMP. These units and the components

CONFIDENTIAL

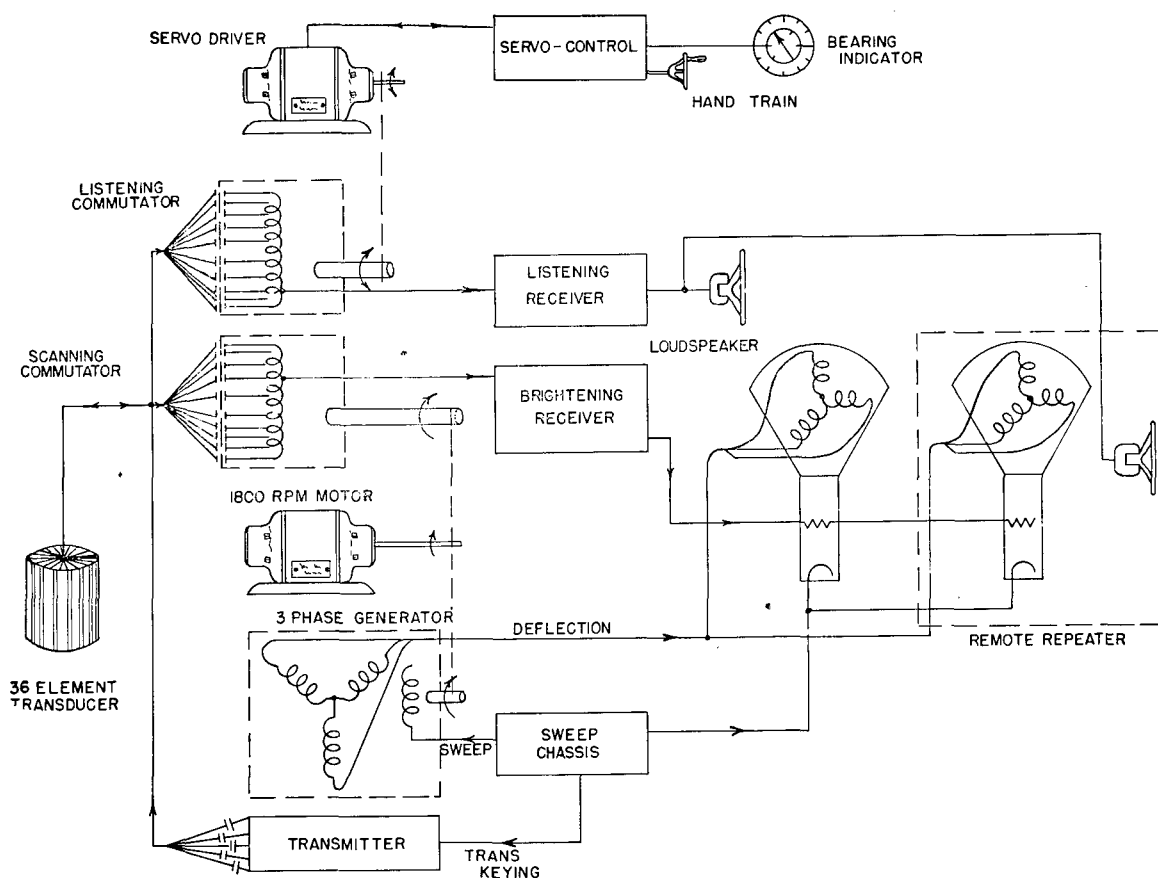


FIGURE 6. Block diagram of Model 1, Serial 1, CR scanning sonar system.

necessary to make a complete CR system were installed on the USS SARDONYX about February 21, 1944. The block diagram of the system as installed is shown in Figure 6. The components did not differ much from those in the experimental system on the AIDE DE CAMP except that the electronic chassis were placed in two cabinets.

The main improvement in this system was a second commutator paralleled with the first and used for listening. It was hand-trained, thereby giving the equivalent of a regular searchlight-type sonar in addition to the scanning sonar. The regular scanning commutator rotated at the usual 1,800-rpm speed and performed the scanning operation, while the listening commutator was positioned by a servo motor which acted as a follow-up for a hand-operated synchro system controlled by a knob at the top of the console. A bearing bug next to this knob repeated the position of the rotor. The output of the listening commutator was applied to a listening receiver. In this manner, the listening beam could be trained,

and the echo received and made audible by a loudspeaker.

A second improvement was the use of a remote repeater station which included a PPI scope and a loudspeaker. These were both in parallel with the main indicator and speaker so that the conning officer on the bridge could also see and hear what the operator was seeing and hearing. The PPI had the brightened ring range-marking circuit as used on the AIDE DE CAMP, but a switch was installed so that the range marks were applied only when desired.<sup>14</sup>

The HP-1 transducer was installed first, but on February 28, the HP-2 transducer became available and was installed. Some difficulty was encountered with three or four leaking elements of HP-2; these elements were removed from the circuit and it worked satisfactorily without them. As installed at first, the choke box used the 36-pole relay system for the send-receive change-over, but this was later replaced by a send-receive network requiring only one relay (see Figure 21). The transmitter was of the

CONFIDENTIAL

pulse type (see Section 5.7 of this chapter), and a GE oxide rectifier battery charger was used for polarizing the transducer. The ER rotor was not used although the console had been designed as a CR/ER console.

From February 21 to March 3 operation of the CR equipment was demonstrated.<sup>15</sup> On one test run during this period, it was found that with a submarine target 500 yards away, 14 pings out of 20 gave good echo indications on the screen, while at a range of 1,500 yards on the same target, 8 pings out of 20 gave good indications. During other tests the operator was able to hold contact with the submarine at times up to 3,000 yards, while audible echoes could be heard at greater ranges. The discovery range of the target was consistently of the order of 2,000 yards. The power in the water at this time was measured at various values between 11 and 25 acoustic watts.<sup>16</sup>

On March 1 the HP-2 transducer was removed and the HP-1 reinstalled. On some trial tests made at this time with HP-1, the maximum range for echo identification on the PPI was found to be about 2,200 yards with the maximum audible range of 3,800 yards.

The CR Model 1 QH system was aboard the USS SARDONYX for about one month and then was removed because of the urgent need of ship facilities for other programs. Near the end of May this equipment was installed on the USS CYTHERA. As the sea chest on the USS CYTHERA was too small to permit the installation of the HP-2, the HP-1 was used. In July the HP-1 transducer unit was removed and the AX-89, a Brush crystal transducer, was installed and used for a few days until speed tests were tried. At this time, the rubber boot water-seals broke down and water reached and damaged the crystals. The transducer was removed while repairs were made, and HP-1 was used for approximately two weeks.

During June 1944 an attempt was made to determine the accuracy of bearing indication of this system. Several runs were made past a triplane target, anchored 1,000 yards east of Sea Flower Reef in Fisher's Island Sound. The data taken included ship's bearing, range reading on the chemical recorder attached to the listening channel, and bearing indication as given on the PPI. These results showed a mean deviation of 1.1 degrees. No corrections were made for irregularities in bearing produced by ship's yaw.<sup>17</sup>

On July 18, 1944, tests using a submarine as the target were run in an effort to determine maximum dis-

covery range. The transducer used was the repaired AX-89 crystal unit. This range was found to be approximately 1,800 yards with the minimum contact range being about 200 yards. A visual figure of merit on this system at the dock was found to be 127 db.<sup>18</sup> In trial runs made while testing for torpedoes fired by the submarine, maximum echo ranges of 1,500 yards to 2,100 yards were obtained on the submarine target.

During July and August 1944 the QH Model 1 gear on the USS CYTHERA was used to listen for torpedoes fired by a submarine in an attempt to determine the discovery range of the fired torpedo and the range at which the torpedo was lost. Where water conditions permitted detection of echoes, observations were made of the range and bearing of the submarine at 10- or 20-second intervals. In making these tests, the QH operator kept the listening channel trained on the noise source as the torpedo approached the ship. He called out bearings as rapidly as possible. These data and time intervals were recorded. Particular note was made of the time at which the lowering pitch of the propeller whine indicated the end of the run. Records were kept during the torpedo run by making photographs of the remote PPI scope, which had been set up in the ship's laboratory room for this purpose. Torpedo ranges in all cases were calculated from the known speed of the torpedo and from the time it was under observation both before and after it crossed the target-ship's track. In all, 27 firings were observed during July and August.

The following are some of the conclusions drawn from the tests:

1. All the torpedoes were detected on approach except one which was fired from almost directly astern. This was not noted until it had passed the ship.
2. In some cases the firing time recorded from the bridge observation post was earlier than that obtained from the sonar gear, but the reverse was more frequently true.
3. Initial detection occurred at ranges up to approximately 3,400 yards.
4. The tests indicate that QH sonar on a target ship may be useful for scoring of torpedo firing tests whether day or night.
5. The chance of evading a torpedo after it is detected by QH sonar can be estimated from the time required for the ship to answer its helm, in relation to the time lapse between initial detection on the

CONFIDENTIAL

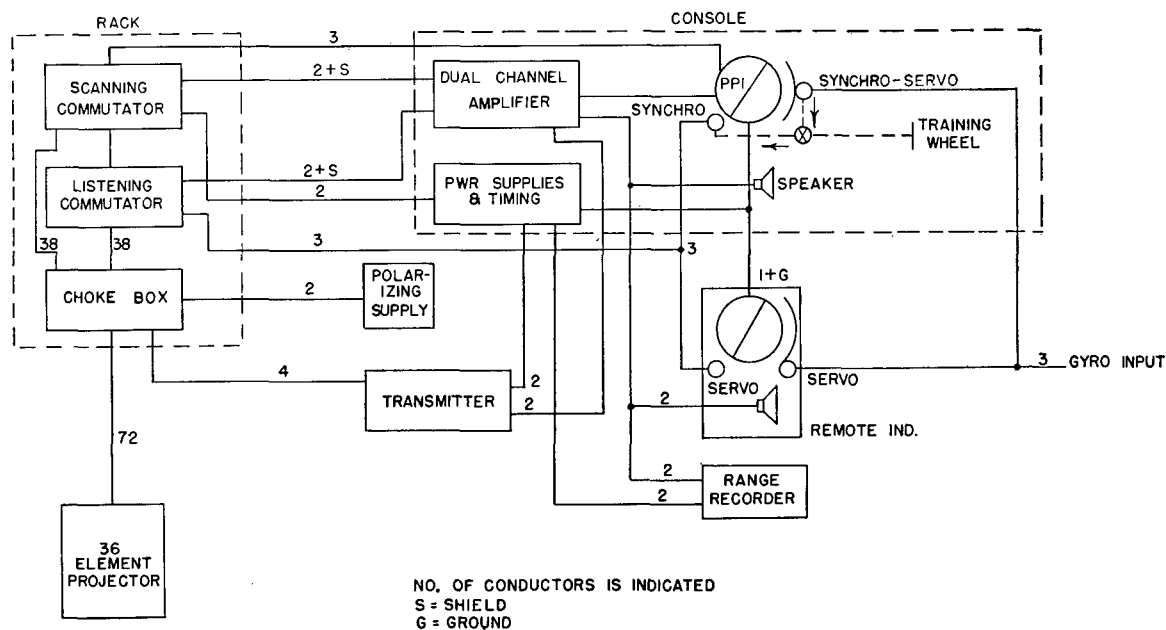


FIGURE 7. Block diagram of Model 2 CR scanning sonar system.

PPI screen and the arrival of the torpedo at ship's track.

6. The information from these tests suggested the possible application of QH gear to counter-mining or disabling approaching torpedoes before they reach the target.<sup>19</sup>

### 5.2.5 Model 2 CR Scanning Sonar

In September 1944, the QH Model 1 was removed from the USS CYTHERA and Model 2 was placed aboard. This was essentially the same type of system but was to be the prototype for the Sangamo Electric Company's XQHA scanning sonar. A block diagram is given in Figure 7. The main difference between Model 1 and Model 2 was in the use of a 48-element transducer and two 48-element commutators. At the beginning, the 48-element transducer was unavailable, and the HP-2B, the rebuilt HP-2, was installed in its place. The principal differences between Model 2 and Model 1 were for convenience and the incorporation of circuits found desirable in Model 1.

The sweep circuit, instead of being electronically controlled, was controlled by a mechanical timer device using a synchronous motor. The range was read from a chemical recorder connected into the listening receiver. A circuit for recorder keying of the timing circuits was incorporated, but provision was also made for automatic keying when the recorder

was disconnected. The console had an MTB indication for training the listening rotor through synchro connection to the ship's gyrocompass on the true bearing of a target. There was also a true-bearing dial mounted around the outside of the PPI. The listening rotor position was controlled by the position of the bearing cursor on the PPI rather than by a separate control. Unicontrol of frequency through the whole system was secured by control of the heterodyning frequency: a single control adjusted the heterodyne frequency of the listening receiver, scanning receiver, and transmitter. The remote PPI had a true-bearing dial and a speaker which was connected to the listening channel. Hand keying for communication and a new choke box and transfer network employing only one transmit-receive relay were installed.

In October some tests were made on QH Model 2 to determine the maximum discovery range using a triplane target. Taking an average of three runs, this appeared to be about 2,500 yards. Echoes were obtained from passing ships up to ranges of 2,200 yards. Propeller noise from many of these ships was observed at an estimated range of 4,500 yards. The average figure of merit, with the ship docked, varied from 137 to 142 db on the scanning channel, and from 147 to 152 db on the listening channel. With a submarine target, good echoes were obtained at ranges varying from 2,500 to 3,200 yards.

CONFIDENTIAL

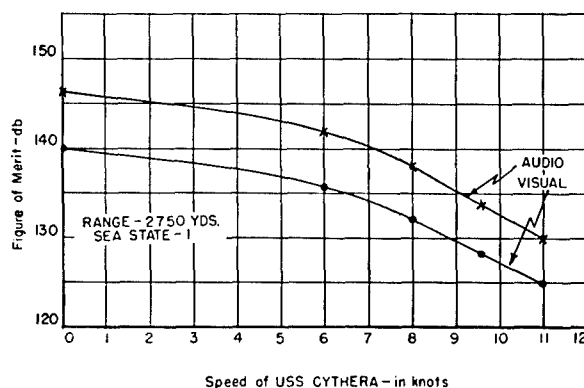


FIGURE 8. Variation of figure of merit with speed, QH Model 2 scanning sonar.

During one series of tests, the figure of merit was measured at 0, 6, 8, 9½, and 11 knots. The dynamic monitor injected a signal into the installed monitor hydrophone B19H No. 9 so that the echo appeared on the PPI screen at a relative bearing of 341 degrees and a range of 2,750 yards. These data<sup>21</sup> were taken in sea state 1 with transducer HP-2B without a dome, and are plotted in Figure 8.

During January and part of February 1945 the QH Model 2 was transferred from the USS CYTHERA to the USS BABBITT and a standard 100-inch dome placed around the transducer. A change was made in the receiver gain control system so that TVG, AVC, and RCG could be varied by the operator. A *bearing deviation indicator* [BDI] was installed on the listening channel after a double lag line was incorporated in the listening rotor but, because of imperfections of the Model 2, it was unsuccessful. Later BDI was successfully used with the Sangamo Model XQHA.

In March 1945 the USS BABBITT with the HUSL Model 2 QH sonar installation was taken to New London where several tests of its operation with a submarine target were made. The results indicated that at speeds up to 23 knots a submarine at periscope depth was detectable at about 2,000 yards, while at 25 knots the range was about 1,000 yards, and at 28 knots, about 500 yards.<sup>22</sup> At 15 to 20 knots, where ranges of 2,000 yards were observed, propeller noise of the submarine was detectable at 7,800 yards, but there was no indication on the PPI.<sup>23</sup>

During April an attempt was made to determine the interference resulting from the operation of scanning sonar at various frequencies by two ships in close proximity. The second ship, the USS GALAXY, was equipped with the Sangamo Model XQHA

sonar, Serial No. 1. Various runs were made with the USS BABBITT following a zigzag course which varied her range to the USS GALAXY from 4,000 yards to 300 or 400 yards, while the latter ship maintained a straight course at constant speed. The two ships used signal frequencies between 24 kc and 28 kc. Interference was considered to exist when the BABBITT's signal became strong enough to produce brightening on the minor lobes of the GALAXY's XQHA gear. The results are given in Figure 9.<sup>24</sup>

Several demonstrations were made for interested personnel while QH Model 2 was aboard. In the latter part of April this system was removed from the USS BABBITT and Sangamo Model XQHA scanning sonar Serial No. 3 was installed.

#### 5.2.6

### XQHA System

A description of the Sangamo XQHA scanning sonar has been given at the beginning of this chapter and a much more complete description is available in the instruction book.<sup>1</sup> The transducer design followed closely that of the HUSL HP-3 design, although there were some minor mechanical changes. The mechanical design of the commutator disks was carefully worked out to permit maintenance of close tolerances. Provision was made in the beam-forming lag line design to allow application of BDI to the listening channel. A compact mounting arrangement of the commutators permitted their placement in one

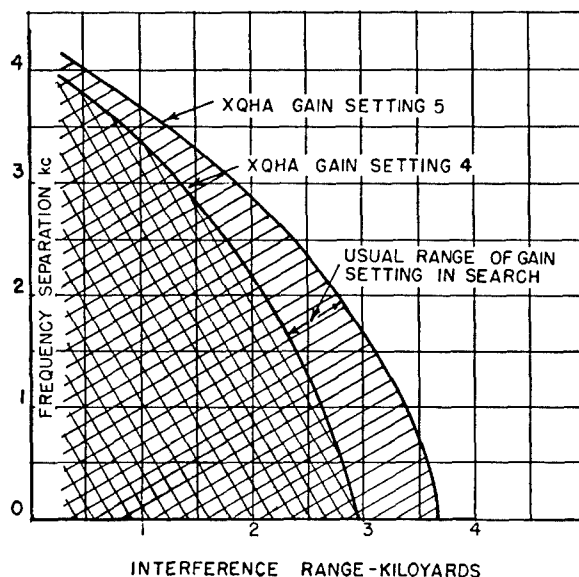


FIGURE 9. Interference ranges with two CR scanning sonar systems.



cabinet with the junction box components, the pre-amplifiers, servo amplifier, and the two-channel uni-control receiver. All components were designed with Navy standards and Service requirements in mind.

Four Model XQHA scanning sonars were built by the Sangamo Electric Company, three under contract with OSRD (OEMsr-1288) and one under contract with the Bureau of Ships (NXsr-46933). The first transducer, known as Type HP-5 Serial 1, was sent to HUSL (see Section 5.3, "Transducers"). When the first commutator was completed, it too was sent to HUSL and the combination of transducer and commutator tested. Results were gratifying: the patterns were better, both in shape and uniformity, than any obtained in the previous development work.<sup>25, a</sup>

After being tested by HUSL,<sup>26</sup> the Serial No. 3 transducer was sent to the USRL measurement station at Orlando, Florida, where it was assembled with the remainder of the Serial No. 2 system which was shipped directly from the Sangamo Electric Company. An intensive test program had been planned by USRL in consultation with HUSL engineers and was carried out with results confirming those obtained on the first transducer and commutator at HUSL.<sup>27</sup> Particular attention was paid in both these sets of tests to variations in the shape of the receiving pattern as the commutator plates moved from one "in-register" position to the next. Systematic changes were found, but considered too insignificant to have an appreciable effect on the accuracy of bearing determination. Nevertheless, study of methods for improvement was stimulated.

Following tests at Orlando, the Serial No. 2 system was shipped to San Diego for operating tests in locating small objects by the University of California Division of War Research [UCDWR]. Subsequently it was returned to the Sangamo Electric Company for incorporating improvements developed after its original construction, and it was then sent to the USRL measurement station at Mountain Lakes, New Jersey, for further qualitative tests. To aid in making these tests, signal simulator equipment, originally built at HUSL for laboratory testing of scanning sonar components, was also sent to Mountain Lakes. This equipment as originally developed had been applied to the Sangamo attack teacher QFA-5 to permit simulation of scanning sonar attack procedures, but was superseded by a simulator unit, Type 2, part of the complete setup known as OTE-5.<sup>28</sup>

The third and fourth Sangamo HP-5 transducers were sent to HUSL for tests, with representatives of the Sangamo Electric Company assisting. Having proved satisfactory,<sup>26</sup> Serial No. 4,<sup>29</sup> was installed on the USS SEMMES, under supervision of Sangamo Electric Company representatives, as part of the Serial No. 4 system contracted for by the Bureau of Ships. The Serial No. 2 HP-5 transducer was installed on the USS BABBITT, as part of the Serial No. 3 system, the work being supervised by HUSL engineers. In each of these installations the transducer was protected by a 100-inch streamlined dome originally designed for the QGA searchlight-type sonar.

Model XQHA scanning sonar Serial No. 1, whose transducer had been the first tested at HUSL, was installed on the USS GALAXY, to provide facilities for further development and improvement, as well as for quantitative tests. There were two nonstandard features that required preliminary checking. The first was the absence of a dome to protect the transducer. It was believed that for the 12-knot maximum speed of the USS GALAXY a series of nine nickel bands about the boot were adequate to avoid its being pulled away from the elements. The second nonstandard feature was the unusually long cable of 110 feet instead of 45 feet to the transducer, which was required for convenient installation of the remainder of the system. Neither the banding nor the extra-long cable produced deleterious effects on pattern formation or sensitivity.<sup>25</sup> After installation, intensive tests were carried out to determine the detailed performance characteristics of the system.<sup>30-32</sup>

Later, the USS GALAXY went to New London for operating tests with a submarine target under conditions of interference from the QH Model 2 scanning sonar then still on the USS BABBITT. These tests were made under the supervision of a representative of the Bureau of Ships, and with the cooperation of HUSL personnel. Quantitative data were also obtained on the average target strength of the submarine target as a function of range and were found to agree well with the value expected from previous measurements (see Chapter 3).<sup>33</sup>

The first modification of the Serial No. 1 system on the USS GALAXY was for BDI operation. A dual-channel preamplifier had been built and tested.<sup>34, 35</sup> This was installed and a series of measurements made to define the BDI performance.<sup>36, 37</sup> It had been expected that the pattern distortions in the commutator interregister positions might introduce serious

BDI errors, but these actually proved very small. In fact, only by the most refined techniques could the resulting BDI errors be measured accurately, as they were generally less than a half-degree.

The use of a 100-inch dome with the XQHA Serial No. 3 scanning sonar on the USS *BABBITT* was for making operating tests at high ship speeds. Following a series of quantitative tests to insure performance equivalent to that of XQHA Serial No. 1 on the USS *GALAXY*,<sup>38</sup> a series of noise measurements was made at different speeds. These were made under the direction of a representative of the Bureau of Ships. While showing a steady deterioration of the figure of merit with increased speed, they indicated that satisfactory operation with this dome was possible to something over 20 knots.<sup>22, 23, 39</sup> These results were of particular interest in connection with plans for the integrated sonar systems described in Chapter 6.

XQHA Serial No. 4, which was installed on the USS *SEMMES*, was tested by representatives of the Bureau of Ships and, after some minor difficulties, it performed as well as the other systems.

Two other HP-5 transducers were built by the Sangamo Electric Company during the spring of 1945. The main structure of HP-5 Serial No. 5 was strengthened and modified to be part of the integrated Type B sonar, as described in Chapter 6. After satisfactory tests of performance,<sup>40</sup> it was set aside awaiting its intended use. HP-5 Serial No. 6 was an experimental unit constructed for answering several questions on manufacturing tolerances. After testing, this unit<sup>41</sup> was returned to the Sangamo Electric Company.

### 5.3 TRANSDUCERS FOR CR SONAR

#### 5.3.1 Medusa

The primary aim in construction of the first transducer (Medusa) was to prove that a directive receiving beam of sensitivity could actually be rotated in the water. It accordingly designed for simplicity of construction, broadness of resonance, and economical use of nickel (which was then considered a factor of importance). A sketch of this transducer is shown in Figure 10. Its active elements were arched shells of thin nickel soldered to a 1/2-inch thick bronze cylinder, and wound in pairs as shown in Figure 11, such an arrangement having proved reasonably satisfac-

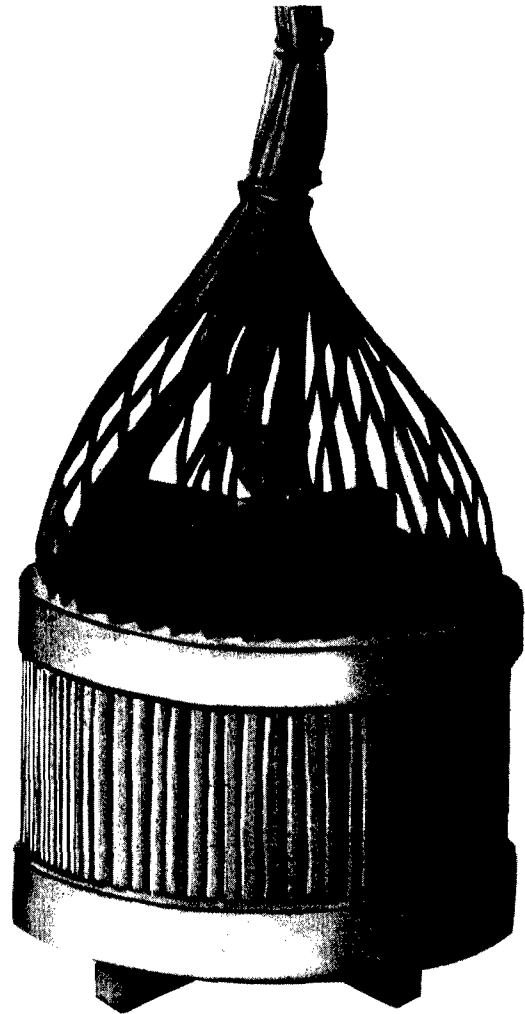


FIGURE 10. Assembly view of Medusa transducer.

tory in an early *sound gear monitor* [SGM] transducer known as the Type S-3.<sup>42</sup> Polarization was by remanent magnetism induced by passing a heavy current through the windings. There were 36 elements arranged on a 12-inch circle. From each of these a shielded pair was brought out separately, and the 36 lead pairs were then bunched into a cable for connection to the commutator.

Measurements on Medusa were made in October 1942. They showed that the performance of the individual elements varied considerably from one to another. It was therefore not surprising that the patterns formed in conjunction with the commutator were not very good. Table 1 summarizes the results of pattern measurements made by turning the commutator while holding the transducer stationary.<sup>2, 43</sup>

TABLE 1. Compensated Pattern Characteristics Measured with Medusa.

Frequency (kc)	No. of mike element toward sound source	Approx. width in degrees of main lobe (6 db down)	Minor lobe below major lobe (db)	Relative sensitivity of major lobe (db)
14	0	72	12	0
	9	36	10	-6
	18	78	10	-7
	27	62	3	-6
20	0	44	8	0
	9	42	10	-2
	18	45	10	+1
	27	57	6	-3
25	0	27	1	0
	9	27	6	-5
	18	39	11	+3
	27	44	5	+2

## 5.3.2

## HP-1

In view of the inherent difficulties and limitations associated with the arrangement used in Medusa, a design adapting the principle of the asymmetrical laminated magnetostriction stack<sup>42</sup> to cylindrical form was developed. The 36 elements were individually made up of stacks 12 inches high, their laminations having the form shown in Figure 12, and arranged on a 15-inch diameter face circle. The laminations, which were of 0.005-inch oxide-annealed nickel, were consolidated with a synthetic resin adhesive, and the resulting solid stacks were wound through slots with a single winding that carried both the d-c polarizing current and the a-c signal current. Since current polarization was used, transmission at high power was possible. It was expected that such stacks could be individually tested before assembly into the transducer in order to insure uniformity, and that the resulting transducer would be adequately strong and durable.

In the original design it was expected that the stacks would be directly exposed to the water. The elements operated as free resonators, with greater motion at the light outer end than at the heavy inner end, the motion of the lighter outer end producing useful radiation into the water. To allow direct immersion, the windings were made of wire with heavy impervious (Gencaseal) insulation. Figure 13 shows four stacks so wound. Cast end caps were provided to

form a smooth surface over which to bend the wire, and to aid in mounting the stacks. Preliminary tests on stacks wound in this manner showed satisfactory insulation resistance, as well as gratifying efficiency and uniformity. However, when a complete transducer was assembled from such stacks, gradual deterioration of insulation resistance was observed. It was almost impossible to wind the wire with sufficient care to avoid damage to the insulation.

Because of the troubles with winding insulation, it was decided to immerse the stacks in castor oil contained in a rubber boot. A design to permit this was worked out, and is shown in Figure 14. The 72 leads from the 36 elements came out of the oiltight compartment through individual water seals to a terminal board, and to this terminal board were fastened the wires of two 36-conductor cables. An early stage of the assembly is shown in Figure 15. After assembly with the boot, the stack compartment was vacuum-filled with castor oil. To prevent bulging, wire bindings were applied to the boot, as may be seen in the assembled view in Figure 16.

Measurements on the completed transducer show good uniformity of elements, in both sensitivity and

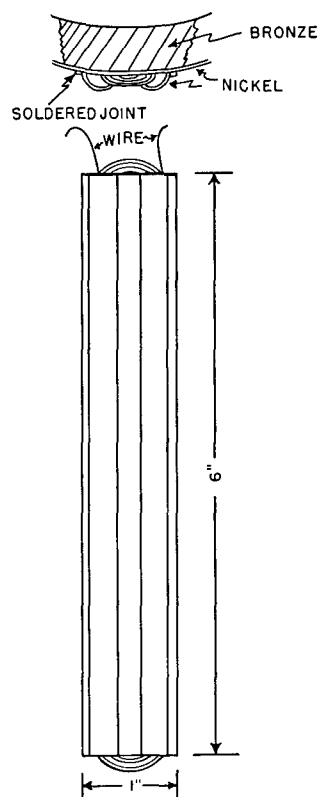


FIGURE 11. Single Element of Medusa.

CONFIDENTIAL

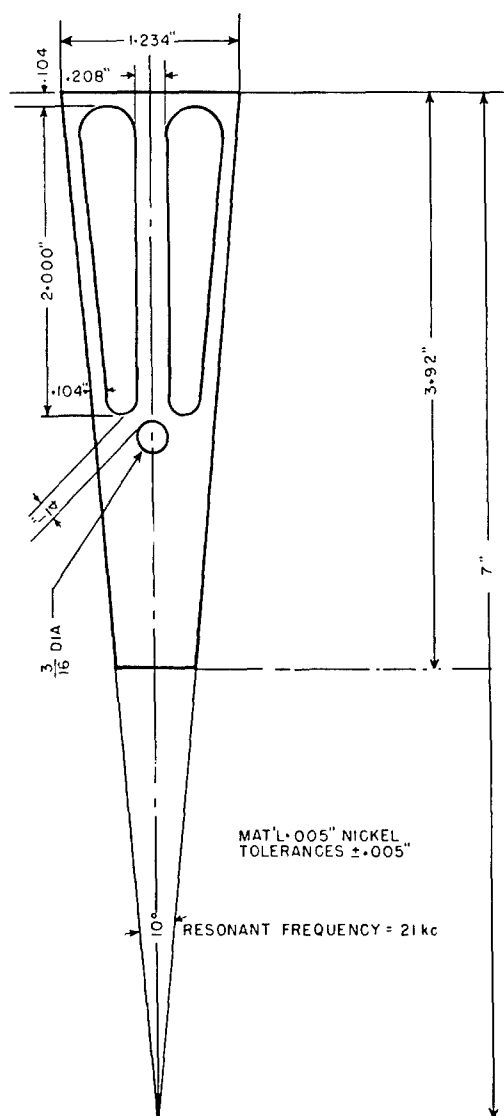


FIGURE 12. HP-1 lamination.

pattern.<sup>44</sup> With all elements in parallel, the frequency response in transmission was as shown in Figure 17. The double-peaked response was due to coupled modes of vibration which were unavoidable with the three-leg design of the lamination. From a vertical transmission pattern, as given in Figure 18, a directivity ratio of 0.13 was calculated. Calculations indicated an efficiency of 11.4 per cent at the 21-kc resonance—a value lower than expected from preliminary tests on the individual stacks, but adequate for echo-ranging purposes. In fact, in view of its broad response, it compared favorably with current designs of searchlight-type sonar transducers. Imped-

ance measurements showed the average individual stack impedance to be  $21 + j67$  ohms.

With a beam-forming lag line designed to compensate 10 elements, this transducer gave patterns of the form shown in Figure 19, which is an average pattern; some were better, some poorer. Such patterns were considered reasonably satisfactory for scanning sonar service, and this transducer gave satisfactory performance.

In order to provide polarizing current during both the transmitting and receiving periods, with the elements acting individually in reception, a separate feeding choke and blocking capacitor were provided for each element. In this, as in all later systems, where a single transducer is used for transmission and reception, a transfer or change-over network is necessary. The change-over mechanism was initially a set of multiple contact relays which were closed by a keying pulse originating in the sweep circuit.<sup>45</sup> To insure that the transmitter did not ping while any relay bank was in the wrong position, a set of contacts on each bank was wired in series with the keying control circuit. These relays were rather large

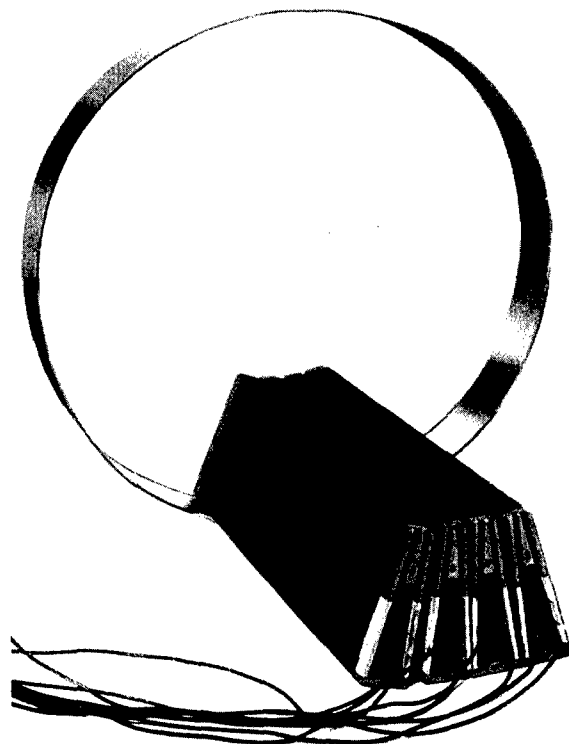


FIGURE 13. HP-1 transducer elements.

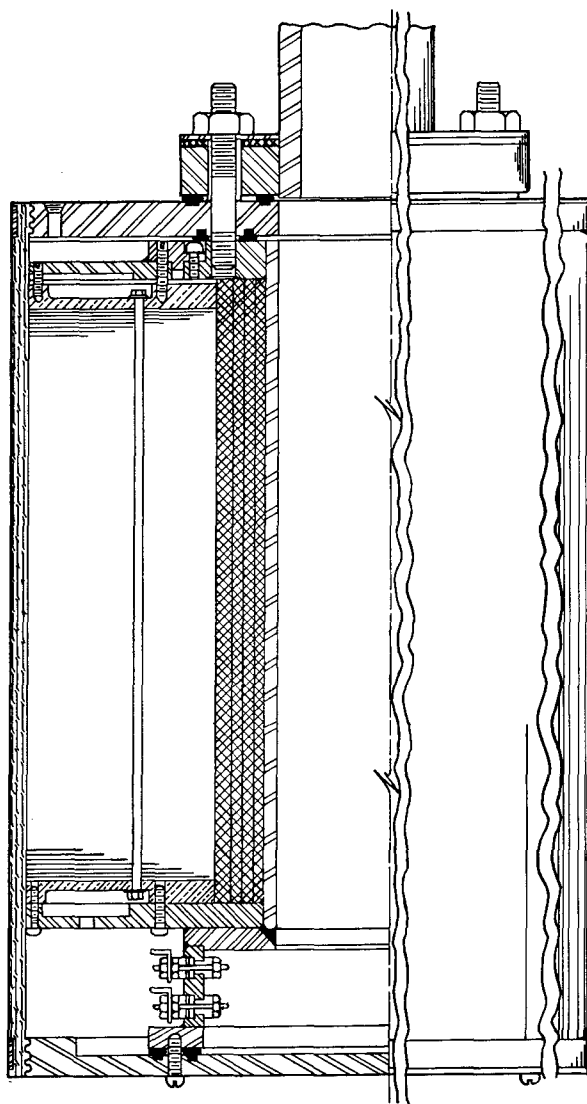


FIGURE 14. Assembly drawing of HP-1 transducer.

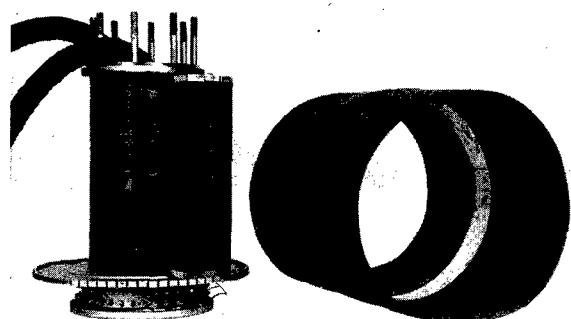


FIGURE 15. Partial assembly view of HP-1 transducer.

and were later replaced by a smaller telephone type of relay.

The use of relays in sound gear, if it were possible to use other schemes, was undesirable because they often required maintenance, especially those with many contacts. Circuits for eliminating the relays or reducing their complexity were suggested. One idea tested involved the use of disks made of thyrite, a material whose resistance decreases rapidly with increased voltage. Because the receiver input voltages were very low (of the order of microvolts) and the transmitter output is high (of the order of 100 volts or more), the introduction of thyrite permitted the transfer operation without relays. Such a circuit is shown in Figure 20. T1 to T36 are the magnetostriction-type transducer elements. To provide a d-c polarizing current which was not excessive, pairs of transducer elements were fed in series. A series-resonant circuit was formed by each 26-mh coil and a thyrite unit, the latter having a capacitance of 1,500  $\mu\mu\text{f}$ . Trimmer capacitors compensated for variations in thyrite capacitances and choke inductance. During reception, when potential across the thyrite disks

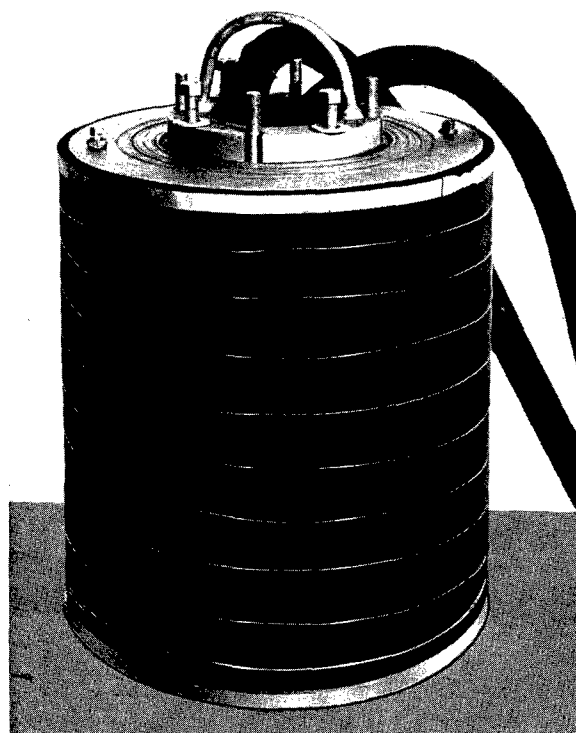


FIGURE 16. Assembled view of HP-1 transducer.

CONFIDENTIAL

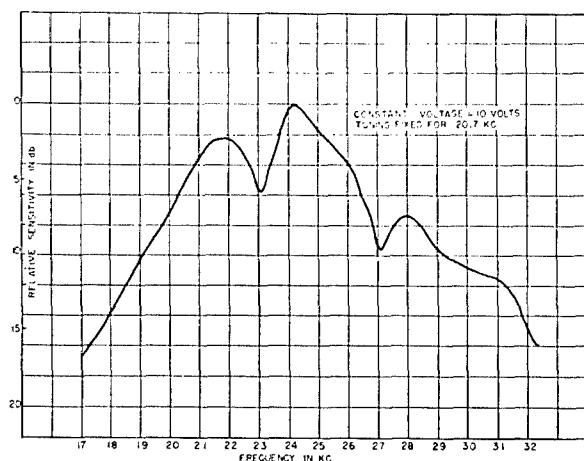


FIGURE 17. Frequency response in transmission, HP-1 transducer.

was a few microvolts, resistance was high and each series-resonant circuit coupled its transducer element to a commutator stator plate, as well as effecting an impedance transfer. During transmission resistance dropped to a very low value, effectively grounding the thyrite end of the 26-mh chokes. Because the impedance of the 26-mh chokes was high, little transmitting power was lost in the disks. Moreover, very little voltage appeared across the thyrite disks, so that the receiver circuits were protected.

The circuit performed as expected, but because the capacitance and resistance of the thyrite ele-

ments varied, the process of selecting suitable units—those whose capacitances and resistances were nearly alike—caused the rejection of a large percentage of units. Another disadvantage was that change in the frequency of operation was not practical because of the high  $Q$  of the series circuit. These disadvantages made this circuit unsatisfactory for production devices.

A later transfer-circuit development, shown in Figure 21, used a single relay for the change-over from transmission to reception. In reception, one contact grounded the high side of the transmitter output, thus putting the blocking capacitors in parallel with the transducer elements, and another contact grounded the common low side of all the commutator input transformer primaries. During transmission both grounds were removed, and the transmitter fed all the transducer elements in parallel through the individual blocking capacitors in series connection. Since the ground return of the commutator input transformer primaries was broken, they floated at transducer-element potential. This circuit proved very satisfactory and was used with all subsequent transducers. In later transducers not requiring a polarizing current the d-c feeding chokes were omitted, but the blocking capacitors retained because of their transfer network function.

After being in use for over a year the HP-1 transducer was completely reconditioned by incorporating design improvements. New windings were put on the stacks, with pressure-release material between the windings and the laminations. After this, transmis-

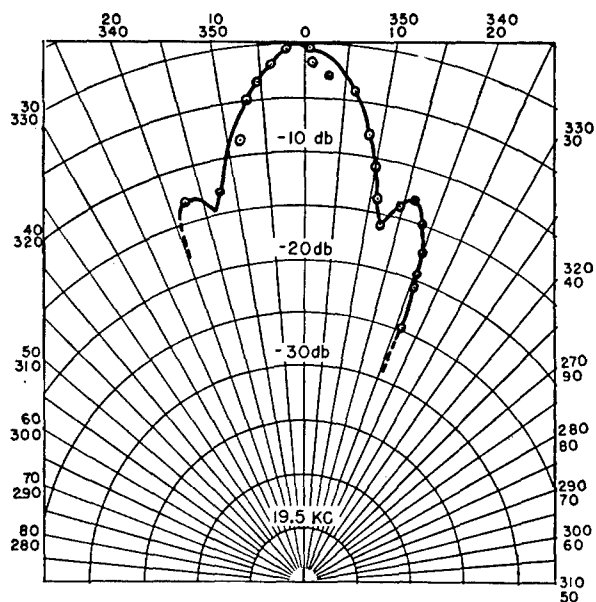


FIGURE 18. Vertical transmitting pattern, HP-1 transducer.

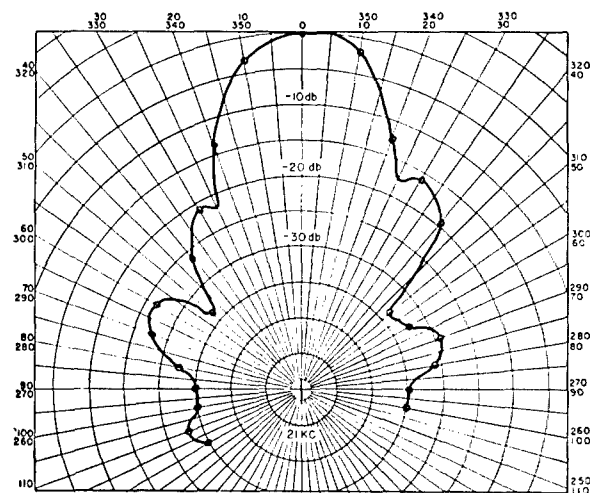


FIGURE 19. Average receiving directivity pattern with 10 elements compensated, HP-1 transducer.

CONFIDENTIAL

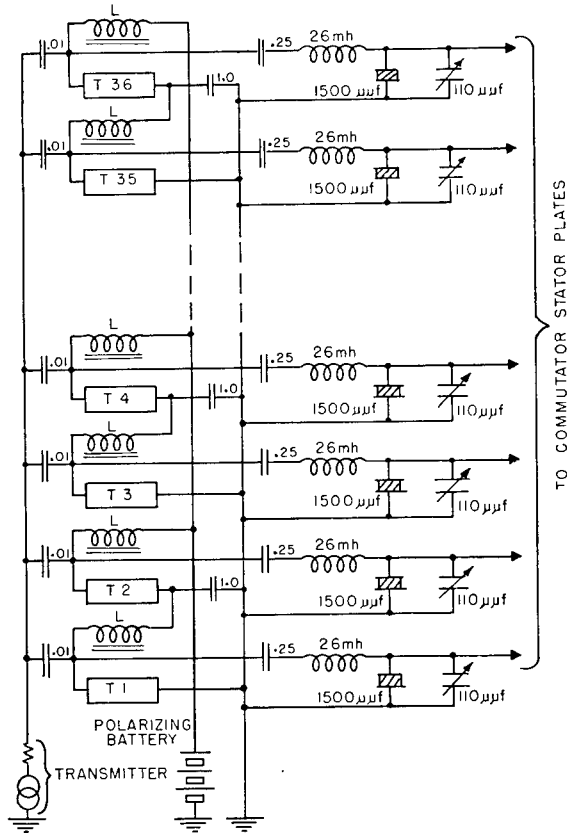


FIGURE 20. Send-receive network using thyrite.

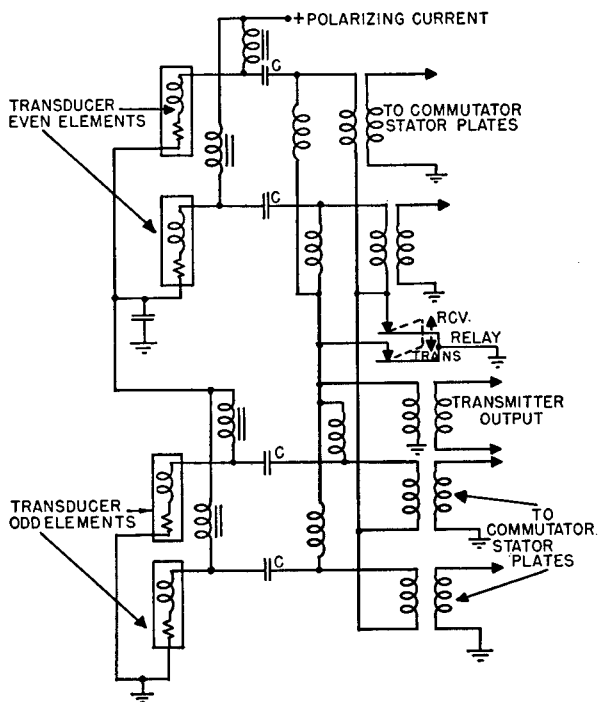


FIGURE 21. Transfer network used with HP-1.

sion measurements indicated an efficiency of 32 per cent at 20.7 kc.<sup>46</sup>

### 5.3.3

### HP-2 and HP-2B

Plans for the QH Model 2 scanning sonar included a new transducer which would be an improvement over HP-1. Improved directivity in both transmission and reception was accomplished by increasing both the diameter and length to 18 inches. In addition, replacement of individual elements was provided by sealing each into a separately removable container. To increase the efficiency, the liquid filling was abandoned, and only the active face was loaded. The asym-

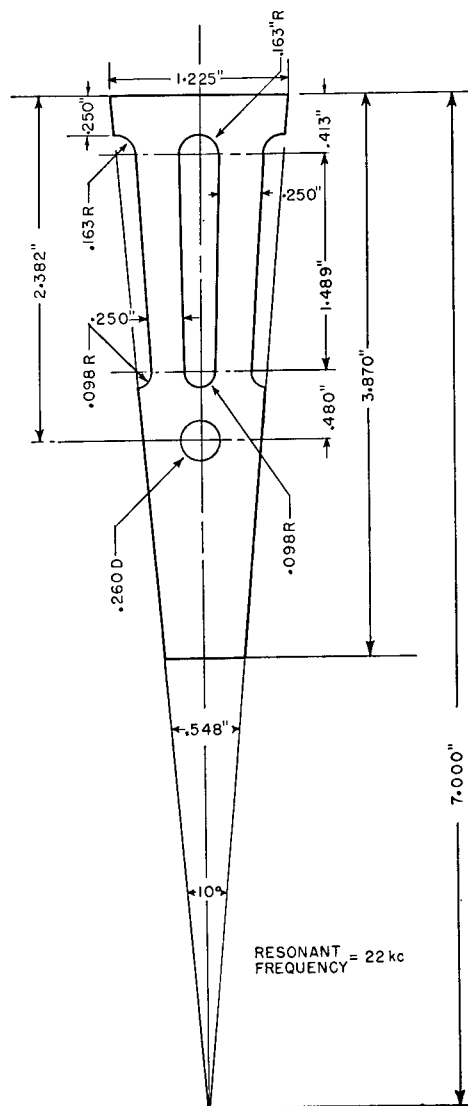


FIGURE 22. HP-2 lamination.

metrical laminated stack design used in HP-1 was retained, but, in order to simplify winding and avoid multiple resonances, the two-leg lamination shown

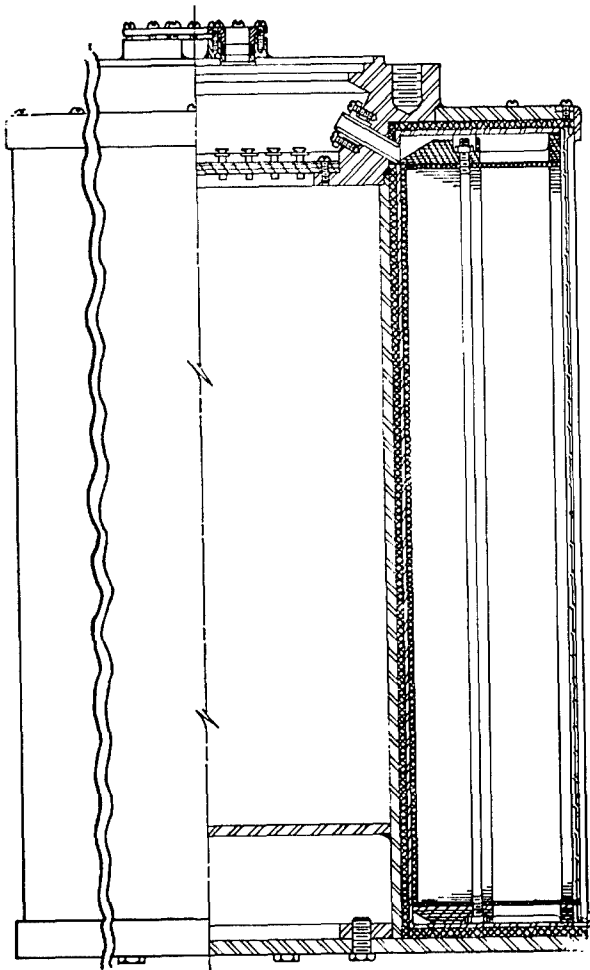


FIGURE 23. Assembly drawing of HP-2 transducer.

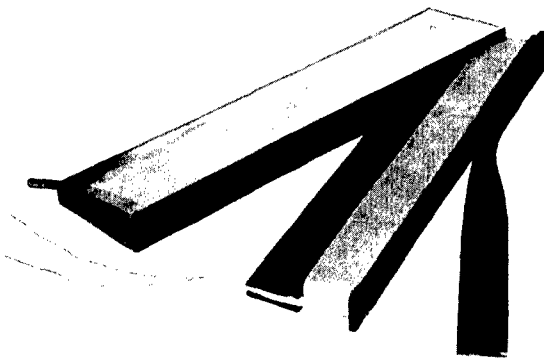


FIGURE 24. Construction of canned element for HP-2 transducer.

in Figure 22 was adopted. Polarization was still by a d-c component through the windings. An assembly drawing of this transducer is shown in Figure 23.

The laminations were of 0.010-inch oxide-annealed nickel, and consolidated with a synthetic resin adhesive into stacks 18 inches high, then wound with 50 turns of solid enameled wire over pressure-release material, and inserted into stainless steel containers lined with pressure-release material. As indicated in Figure 24, a rubber face was cemented to the active edges of the laminations, and then to the inside lip of the container. Leads from the element were brought out through a plastic seal in the tube. This passed through a water seal into the interior of the transducer frame, and there the leads were attached to a terminal board that permitted easy connection of the cables. The assembled transducer is shown in Figure 25.

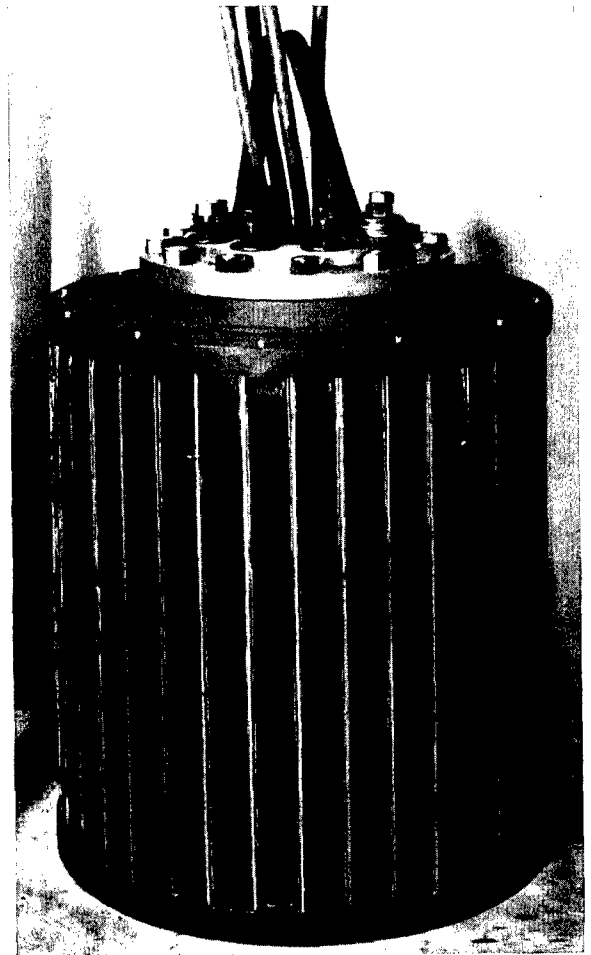


FIGURE 25. Assembly view of HP-2 transducer.



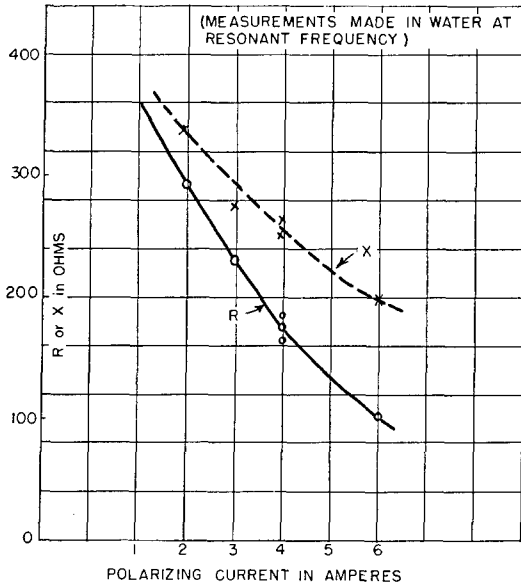


FIGURE 26. Average measured impedance of HP-2 elements.

Impedance measurements on individual HP-2 elements mounted in containers showed potential efficiencies of the order of 50 per cent. Values of the resistive and reactive components of the impedance are given in Figure 26 as a function of polarizing current. Variations in impedance and sensitivity of the individual elements were satisfactory, but variations in resonant frequency were larger than expected.<sup>47</sup> The distribution curve shown in Figure 27 indicated that there were two definite groups. This was ascribed to probable differences in the consolidating procedure that the two contractors making the stacks used.

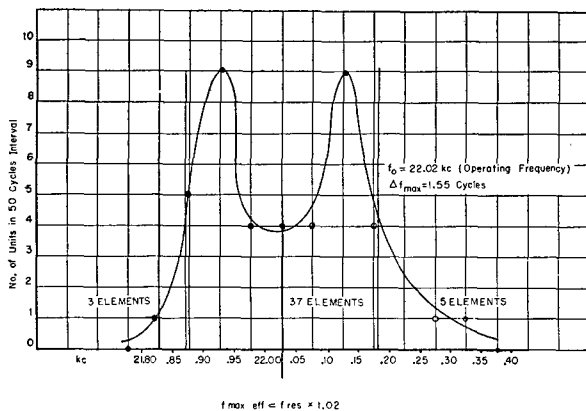


FIGURE 27. Distribution of resonant frequencies for 45 elements of HP-2 transducer.

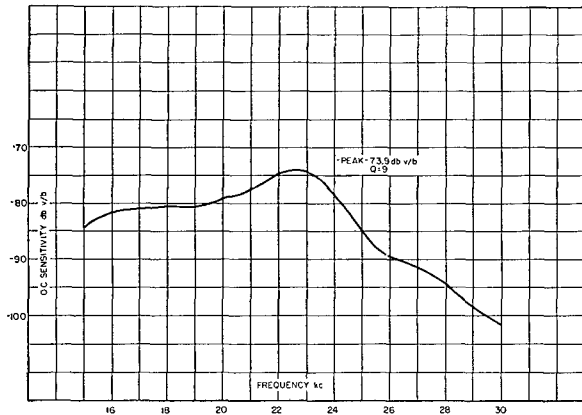


FIGURE 28. Receiving frequency response of HP-2 transducer.

Measurements on the assembled transducer<sup>48</sup> showed that with all elements connected in parallel the overall sensitivity variation in the azimuthal plane was about 4 db. The frequency response is given in Figure 28, and the vertical transmitting pattern in Figure 29. From this pattern the directivity was figured to be 0.075, and from this the efficiency was calculated to be about 26 per cent.

With 10 elements compensated by an appropriately designed lag line, receiving patterns of the form shown in Figure 30 were obtained.<sup>49</sup>

With these results, HP-2 was a decided improvement over HP-1 from the electroacoustical point of view. From the mechanical or service viewpoint, however, it was definitely unsatisfactory. It was impossible to maintain a permanently watertight bond between the rubber faces and the containers, and this transducer was redesigned, using the castor-oil-filled rubber-boot construction that had proved satisfactory in the reconstruction of HP-1. An assembly drawing of the reconstructed HP-2 transducer, which was known as HP-2B, is shown in Figure 31. Trans-

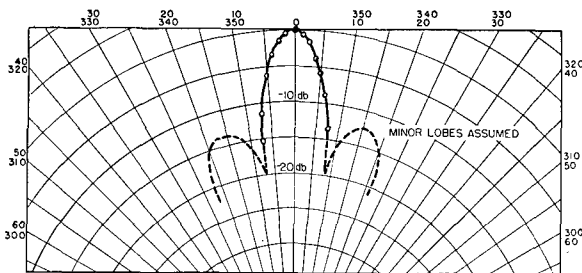


FIGURE 29. Vertical transmitting pattern of HP-2 transducer (22 kc).

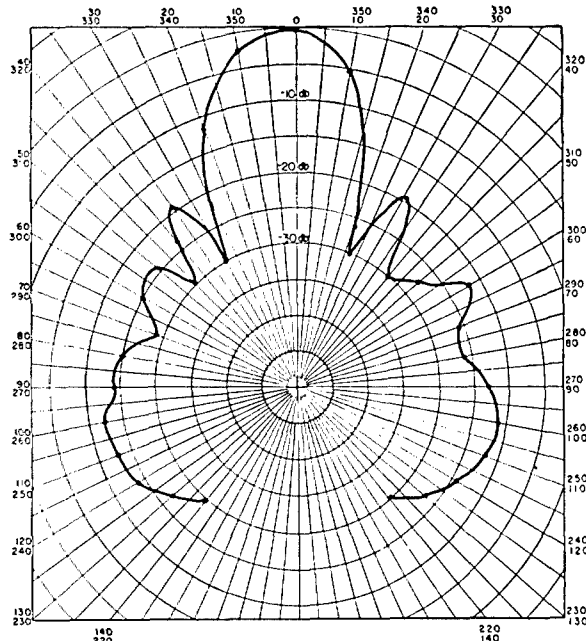


FIGURE 30. Average receiving directivity pattern with 10 elements compensated, HP-2 transducer (22 kc).

mission measurements<sup>46</sup> showed that the efficiency was now about 33 per cent.

The HP-2B transducer was installed as part of the QH Model 2 scanning sonar on USS CYTHERA at New London, and further measurements were made on board, using the *installed sound gear monitor* [ISGM] transducer.<sup>50</sup> An azimuthal transmitting pattern is given in Figure 32 showing a variation of about  $\pm 1.3$  db. A typical receiving pattern taken with 10 elements compensated is shown in Figure 33, the rotor being turned. A similar pattern with the rotor stationary while the transducer was turned is shown in Figure 34.

The HP-2B transducer was used in the QH Model 2 scanning sonar with a transfer network essentially the same as that shown in Figure 21. While there was some variation among the elements of the transducer, even greater variations were introduced by the d-c chokes and isolating capacitors in the transfer network, which also absorbed about half of the power supplied by the transmitter. This led to the development of permanent-magnet-polarized transducers.

#### 5.3.4

### HP-3

HP-1 and HP-2 required a d-c component in the windings for adequate polarization, but the undesirability of this was recognized early and research

toward achieving permanent-magnet-polarization of the HP type of asymmetrical magnetostriction lamination had begun. When, as a result of satisfactory demonstrations of the QH Model 2 scanning sonar on the USS CYTHERA, the development of a prototype transducer became necessary, the HP-3 design was developed. After small-scale tests at HUSL on sample elements using sintered oxide magnets, the Sangamo Electric Company adopted the design for its HP-5 transducer. While the HP-3 transducer was originally intended for a prototype model, the Sangamo HP-5 was actually completed first, and the HP-3 lamina-

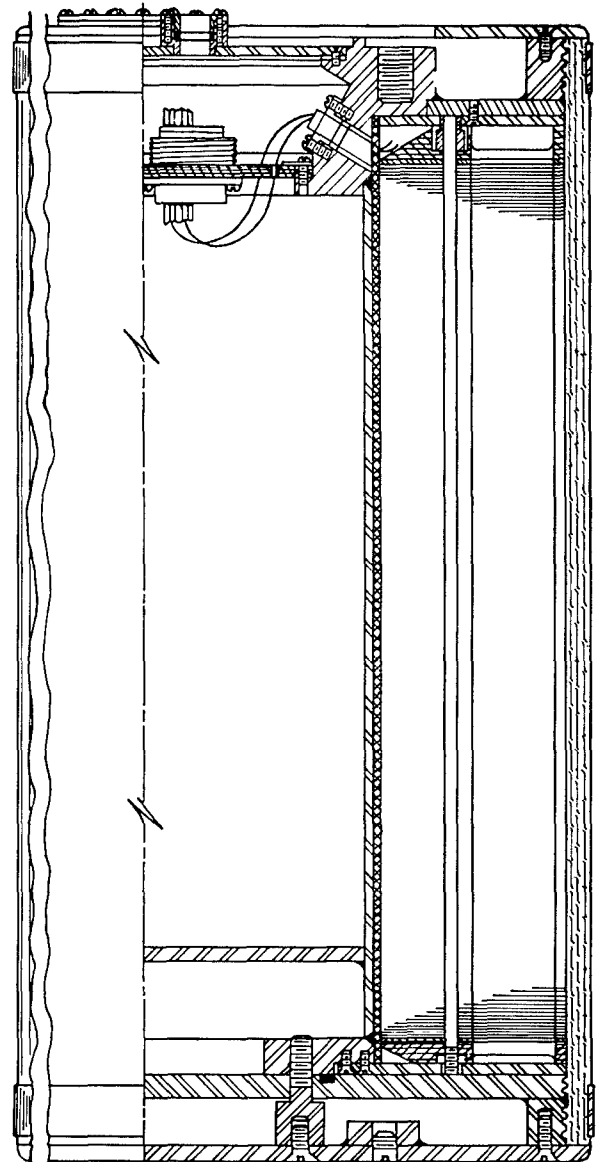


FIGURE 31. Assembly drawing of HP-2B transducer.

tion was used for experimental purposes in the HP-3S transducer (see Chapter 7), and in the HP-3DS transducer (see Chapter 6).

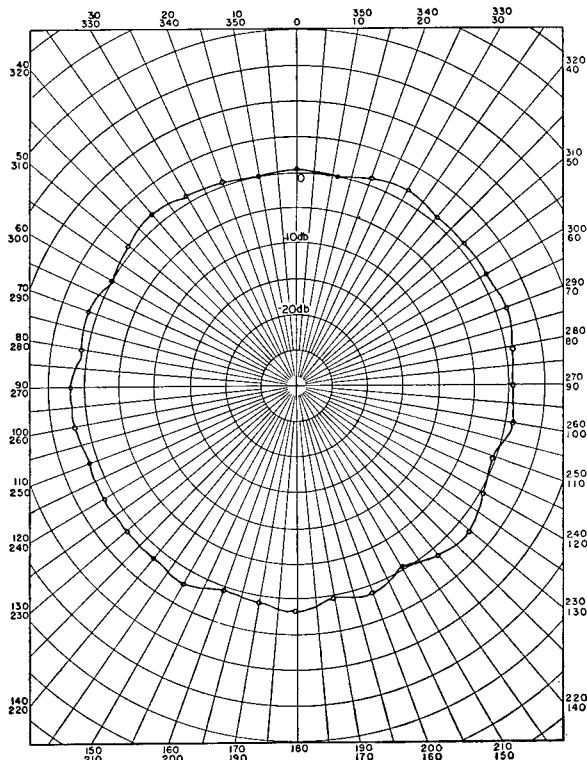


FIGURE 32. Horizontal transmitting pattern, HP-2B transducer (22 kc).

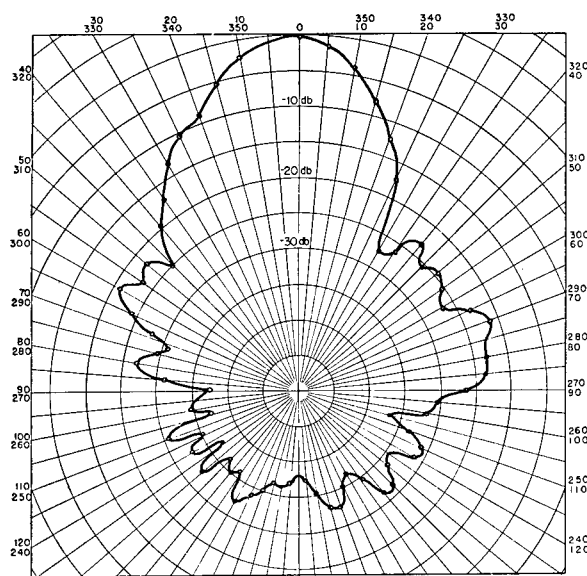


FIGURE 33. Typical receiving directivity pattern with 10 elements compensated, commutator rotated, HP-2B (22 kc).

An outline of the HP-3 lamination is shown in Figure 35. While this lamination followed the general two-leg design of the HP-2 lamination, a slot was provided in the heavy end to accommodate a loosely fitting, transversely magnetized, sintered oxide magnet. These laminations were consolidated with synthetic resin adhesive into stacks approximately  $3\frac{3}{4}$  inches high, and were wound with enameled wire over pressure-release material. (The presence of the slot greatly facilitated this operation.) The magnets were then inserted and magnetized in place.

The HP-1 and HP-2 transducers had 36 elements. In order to reduce the spurious sensitivity in the neighborhood of 110 and 250 degrees (see Figure 30), theory indicated that the face width should be no greater than a half wavelength. The only way to keep the beam narrow was to use more than 36 elements, and the HP-3 lamination was accordingly designed with 48 elements in the complete circle.

No vertical shading had been used in HP-1 and HP-2, and their vertical directivity patterns were essentially those of line sources, with first minor lobes only 13 db down. For investigating the practicability of simple shading in reducing these minor lobes, the HP-3 transducer was designed with each vertical stave (or element) composed of four of the unit's  $3\frac{3}{4}$ -inch stacks. Experiments with sample

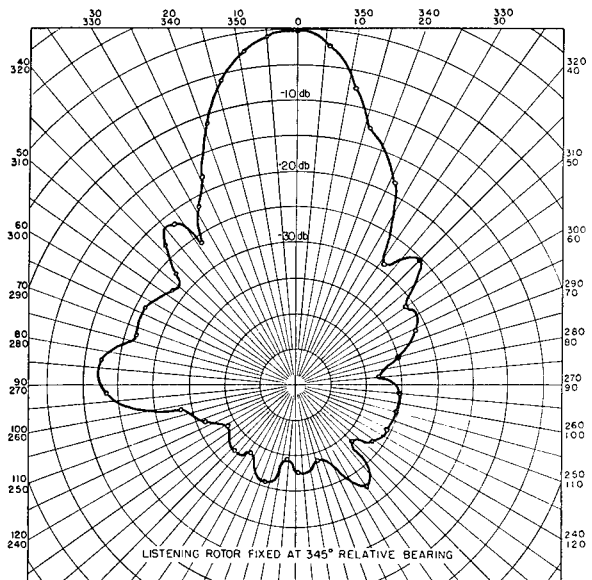


FIGURE 34. Typical receiving directivity pattern with 10 elements compensated, transducer rotated, HP-2B transducer (22 kc).

CONFIDENTIAL

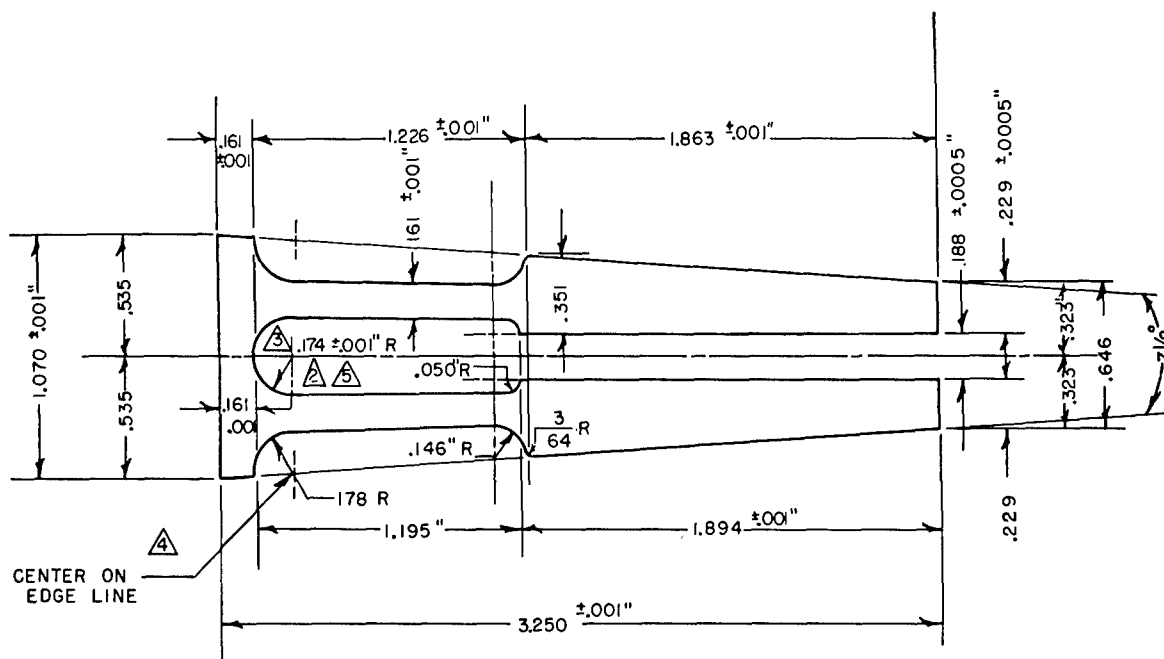


FIGURE 35. HP-3 lamination.

staves showed that a useful reduction in the minor lobe amplitudes could be obtained by exciting in the ratio 1:2:2:1.<sup>51, 52</sup>

The development of the HP-3 lamination and the design of the HP-3 transducer are covered in considerable detail elsewhere,<sup>42</sup> and only a brief description of the transducer will be given here. Figure 36 shows the assembly, and Figure 37 a photograph of the transducer before the boot was applied. A rubber strip, fitting the curvature of the inside of the boot, was cemented to the active edges of the laminations of the four stacks forming each stave. When the slightly undersized boot was applied, its tension held it to these strips, and good acoustic contact was assured by a film of castor oil. A photograph of the assembled transducer with boot in place is shown in Figure 38.

Extensive measurements were made to determine the uniformity of the laminated stacks comprising the HP-3 transducer,<sup>53</sup> and it was found that by proper control of the consolidating process and of the magnetization of the permanent magnets, entirely satisfactory uniformity could be achieved. Tests of the completed HP-3 transducer showed that its performance was very close to expectations.<sup>52</sup> However, since it has not been used in an actual scanning sonar system, and since its performance is similar to that of

the Sangamo HP-5 transducer, these tests will not be discussed.

### 5.3.5

### HP-5

When the practicability of constructing PM-polarized transducer elements had been demonstrated at HUSL, the Sangamo Electric Company began design of the HP-5 transducer. It followed closely that of the HP-3 transducer, the differences being mechanical rather than electrical or acoustical, and being directed particularly toward ease of construction for quantity production. The lamination design was almost exactly that of the HP-3 lamination, but improved methods of punching, annealing, and consolidating were developed to reduce the amount of handling. With the cooperation of HUSL engineers, production methods of testing the consolidated and wound stacks were developed, and it was found possible to produce a highly uniform product.

Figure 39 shows the mechanical design of the HP-5 transducer. The four stacks of a stave, which in the HP-3 had been assembled into a unit stave, were here mounted separately, each in its own layer. Because their bakelite end caps were keyed into holes in metal spacing rings, a very rigid assembly resulted. Recesses in the end caps permitted connections to the windings after assembly, and a terminal board at the bot-

tom allowed easy connection of the cable. A diaphragm in the spool casting carried a cable seal, so that the transducer would be watertight independently of mounting. In the model built for the XQHA system a special cable with pot-head seal was used. The modified unit built for the integrated Type B sonar had standard Navy packing gland (terminal tube) seals to accommodate an internally blocked cable from the HP-5 and also two ducts for cables from the depth-scanning transducer attached below (see Chapter 6). At the upper end of the spool casting

were threaded studs and a sealing ring to fit a 12-inch QC-type mounting flange.

Figure 40 shows the assembled HP-5 transducer for the XQHA scanning sonar. The rubber boot is of particular interest since it was maintained in acoustic contact with the elements by its own tension. The outer faces of the rubber strips cemented to the laminations were curved to fit, and castor oil was introduced at assembly as a further insurance of good acoustic contact.

The individual elements of the first HP-5 transducer had an average resonant frequency of 25.5 kc; their  $Q$ 's averaged a little over 12. From the variations in resonant frequency, the phase variations in the generated voltages appeared to be within the range of  $\pm 5$  degrees. Sensitivities of the individual elements were within  $\pm 1$  db of the average.<sup>25,54</sup>

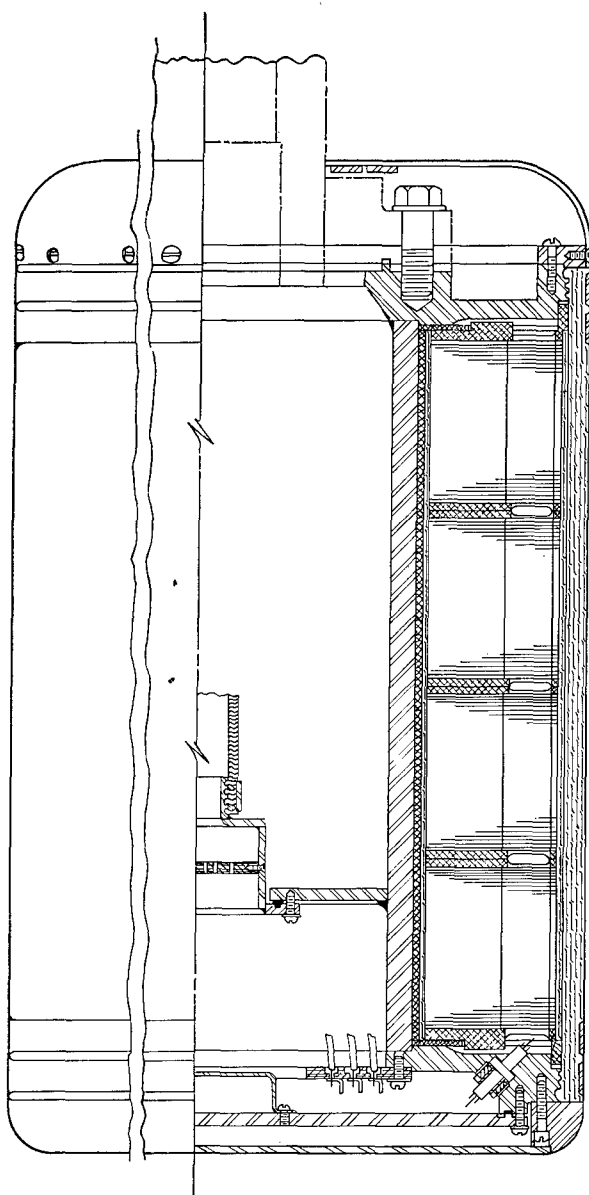


FIGURE 36. Assembly drawing of HP-3 transducer.

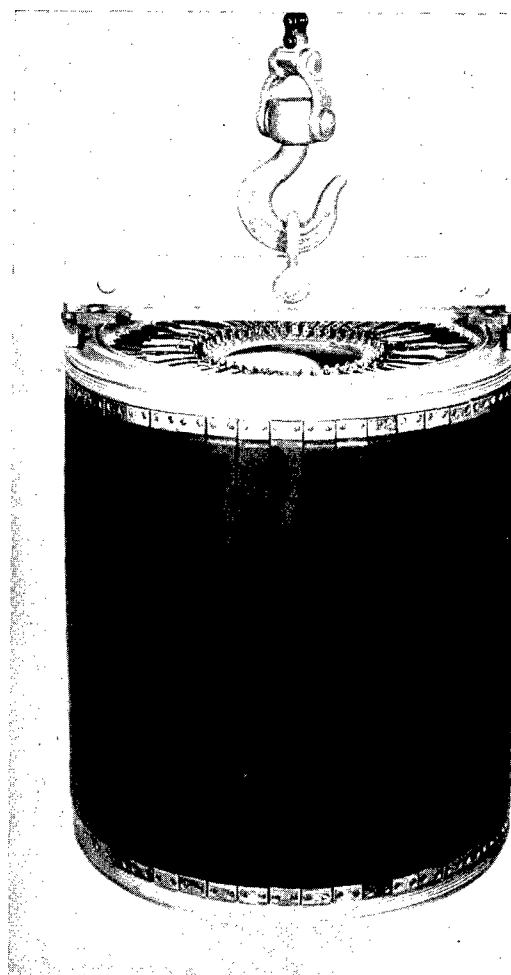


FIGURE 37. Assembly view of HP-3 transducer without boot (inverted).

CONFIDENTIAL

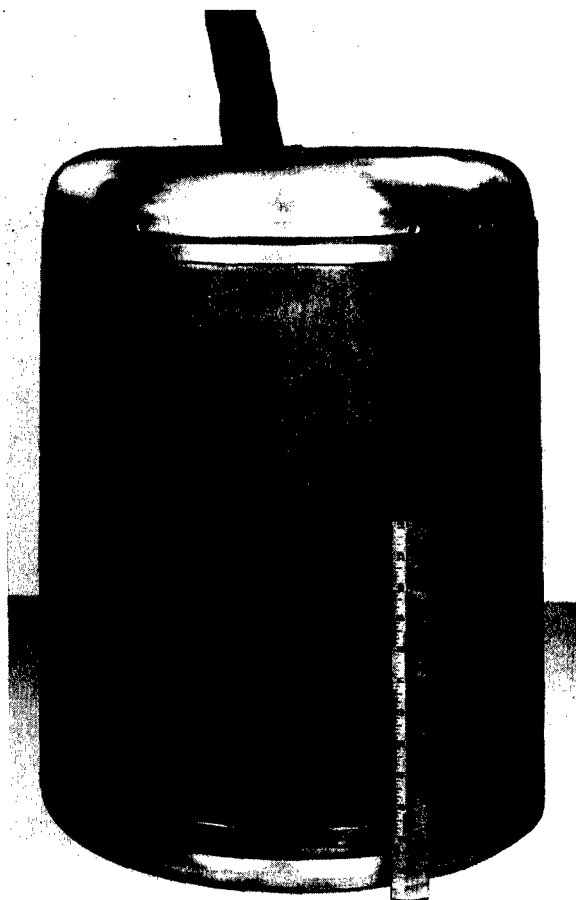


FIGURE 38. Assembly view of HP-3 transducer with boot.

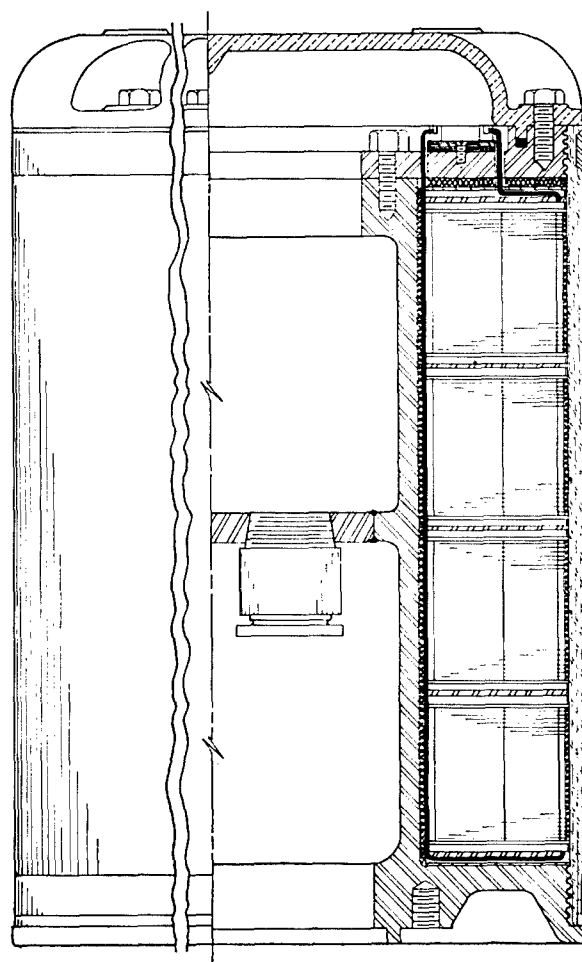


FIGURE 39. Assembly drawing of HP-5 transducer.

Their admittances averaged  $2.3 + j6.1$  millimhos. A typical horizontal pattern of a single element is shown in Figure 41. With all elements connected in parallel, the horizontal directivity pattern was uniform to  $\pm 1$  db. The vertical pattern is shown in Figure 42 and is representative of vertical patterns obtained on individual elements.

The directivity ratio was 0.085, and this, with the sensitivity of  $-103.2$  db vs 1 volt per bar and the impedance values, gave a receiving efficiency of 36 per cent. However, measurements of transmission efficiency gave considerably lower values. By the spring of 1945, six HP-5 transducers had been constructed and tested.<sup>25, 26, 29, 40, 41, 54</sup> All proved at least as good as Serial No. 1, indicating that quantity production of transducers for scanning sonar service is entirely practical.

One unit, Serial No. 1, which was installed on USS GALAXY without a protecting dome, was modified in

appearance from that shown in Figure 38. To insure acoustic contact despite water forces, nine thin nickel bands were stretched around the boot. Tests before installation proved that they had no measurable effect on the acoustic performance of the transducer.

The transfer network used with the HP-5 transducer was similar to that used with the HP-1 and HP-2, except that provision for polarizing current was unnecessary. The chokes supplying the polarizing current to the transducer elements and the separate transmitter tuning inductors were omitted. The simplified network is shown in Figure 43.

### 5.3.6 Other Magnetostriction Types

Early in the development work on scanning sonar, work was done toward developing magnetostriction transducers that would use less nickel, which was then a critical material. In the HP type of design, only that



FIGURE 40. Assembly view of HP-5 transducer.

small part of the nickel in the leg of the lamination is working magnetostrictively, the remainder being simply part of the mechanical resonator. Attempts were accordingly made to produce compound resonators in which the use of nickel was limited to the mag-

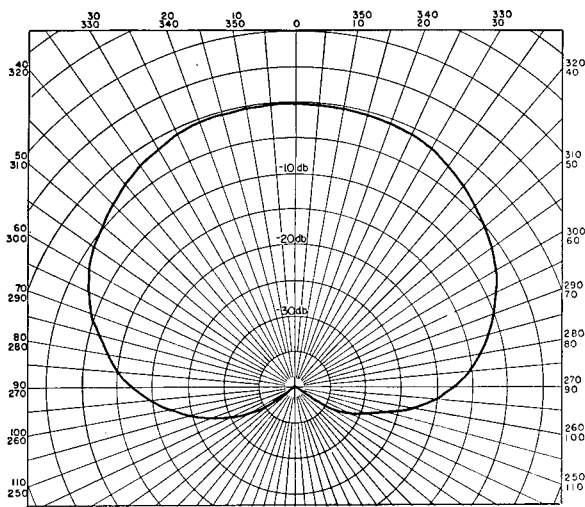


FIGURE 41. Single element receiving pattern, HP-5 transducer.

netostrictive energy transformation function. The remainder of the resonator was made of a less critical material, such as steel or bronze. Laminations punched from a composite welded strip were tried with little success. An adaptation of the tube and plate design, which was widely used in depth-sounding and searchlight-type echo-ranging sonars, was actually built and tested;<sup>55, 56, 57</sup> however, it proved to have variations between elements that were too great to permit satisfactory scanning sonar operation. Another design using laminated nickel sheets in place of the tubes was subject to the same faults. These transducers are discussed in detail elsewhere.<sup>42</sup>

### 5.3.7 Piezoelectric Types—CPI-1 and AX-89

While most of the scanning sonar was developed with magnetostriction transducers, the virtues of piezoelectric transducers were always kept in mind, and procurement of such units from organizations equipped to make them was early initiated. The first one obtained was made by the University of California Division of War Research and was known as

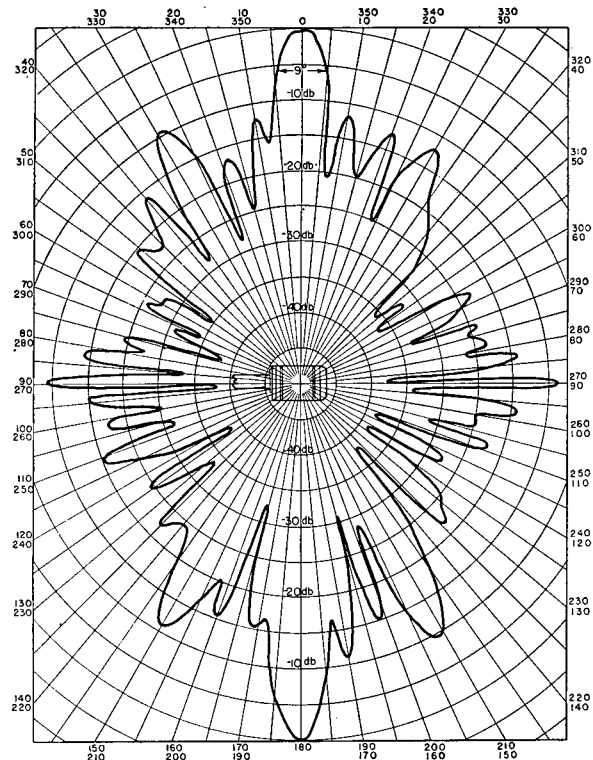


FIGURE 42. Vertical directivity pattern, HP-5 transducer.

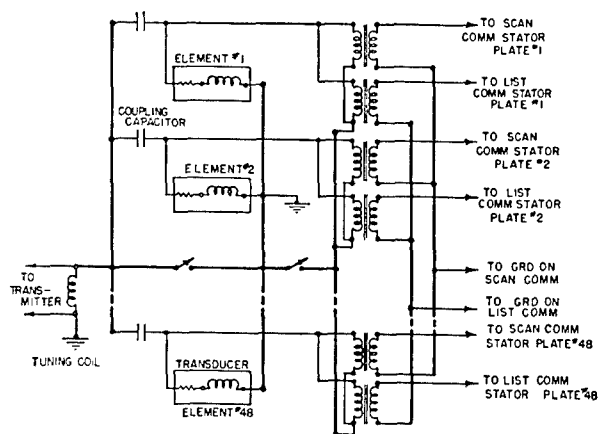


FIGURE 43. Transfer network for HP-5 transducer.

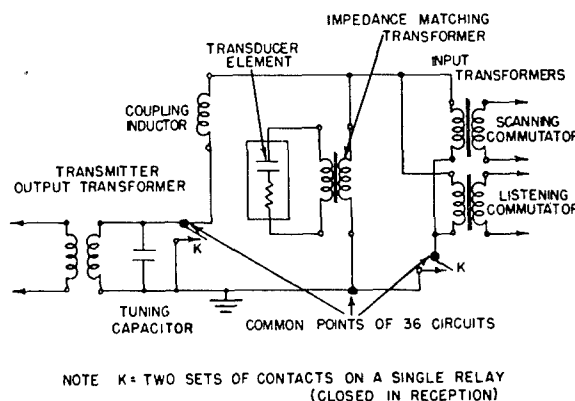


FIGURE 44. Transfer network for piezoelectric transducer.

CPI-1 No. 770. It has 36 elements made of X-cut Rochelle salt crystals. Impedance tests on the individual elements showed fairly large variations from one to another and large changes in the average as a function of temperature.<sup>58</sup> Although the open circuit sensitivities were fairly uniform, it was found impossible, because of these variations in impedance, to transform the high crystal generator impedances down to values convenient for running in cables and feeding constant loads without introducing intolerable large phase variations. The resultant patterns were accordingly quite unsatisfactory,<sup>59, 60, 61</sup> and the unit was never used in any complete scanning system.

The second piezoelectric transducer was the AX-89, made by the Brush Development Company. It too was a 36-element unit, but used Y-cut Rochelle salt crystals. Unfortunately, it was damaged by leakage before tests were made on it. After partial repairs, the unit was used for a short time as a part of the QH Model 2 sonar on the USS CYTHERA with fair success. Measured pattern widths averaged 30 degrees at -6 db.<sup>62</sup> Since 22 degrees had been obtained from the commutator with artificial water, the uniformity of the transducer was considered rather unsatisfactory. A second similar unit constructed by the Brush Development Company was used only in the ER scanning sonar development and its construction and performance are described in Chapter 7.

The transfer networks used with these piezoelectric transducers were similar to those used with PM-polarized magnetostriction transducers, as may be seen in Figure 44. Because the impedance of the piezoelectric transducer element is high, a transformer was inserted in the circuit to lower the impedance to

permit cabling the leads. The installation of such transformers in the AX-89 transducer is shown in Figure 45. With the capacitive transducer, coupling and tuning reactances had to be opposite in sign to those used with the inductive magnetostrictive elements.



FIGURE 45. Impedance matching transformers in AX-89 transducer.



## 5.4

## COMMUTATORS

The design considerations and functional requirements of the commutator unit used with the CR scanning sonar have been discussed in Chapter 2. It should be remembered that these requirements and design criteria were not at first evident but evolved through experience. The developmental work was centered almost exclusively on the capacitive type of commutator in order to exploit promptly the first available method which would perform the required functions for efficient, simple, and reliable operation.

## 5.4.1

## Inductive Commutator

A second type of electromechanical commutator, the inductive type, was considered for early scanning sonar development. The original design called for 36 transformers, each having a stationary primary and movable secondary. The secondaries were to be mounted on a rotor inside the primaries, with a small air gap between their magnetic cores. Each primary was to be connected to a transducer element, with some of the secondary coils connected into the lag line. The cores were to be built up of thinly lami-

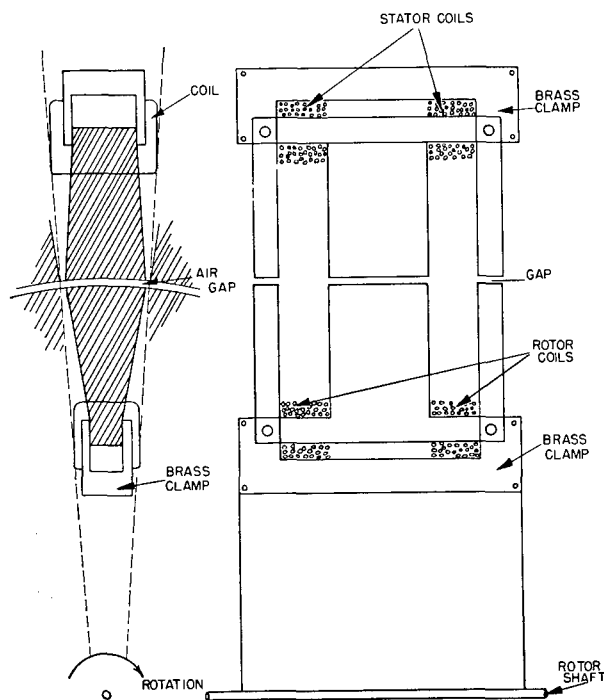


FIGURE 46. Sketch showing early inductive commutator design.

nated high mu material and clamped together in a brass supporting structure. The general design is shown in Figure 46.

Construction on an experimental model was started early in July 1942, but because of difficulties in meeting the transformer design requirements and the rapid and successful development of the capacitive commutator, construction was stopped. The possibilities and advantages of this type of commutator are discussed in Chapter 10.

#### 5.4.2 Design of Capacitive Commutator Historical Account

*First Cardboard Commutator.* The first capacitive commutator was a crude device built in August 1942. Its chief purpose was to verify the principle of smooth commutation for this type of instrument, with particular emphasis on the behavior of its output signal in reference to its input signal during the process of transfer from one position of commutator segment matching to another. The commutator consisted of two circular cardboard disks approximately 8 inches in diameter, each having eight segments of tin foil cemented to one face as indicated in Figure 47A. The two disks or plates had a common center and faced each other, with a sheet of ordinary typewriter paper between them to serve as a dielectric and insulating medium.

In operation, a signal voltage was applied to each of the eight segments on one plate, called the stator, from a phasing network which gave approximately 90 degrees phase displacement between the voltages impressed on successive segments. One segment of the second plate or rotor was connected to one pair of terminals of a cathode-ray oscilloscope, and a reference voltage from the stator was applied to the second pair of terminals. As the rotor was slowly turned, ellipses were observed on the CRO, and from these the phase and amplitude of the voltage appearing on

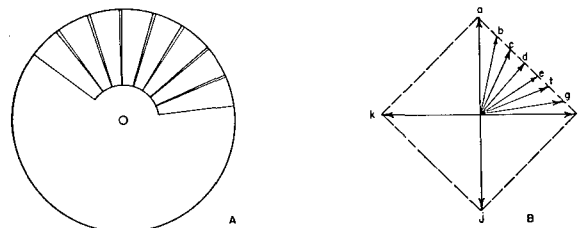


FIGURE 47. Sketch of first sectored disk and vector diagram of its rotation.

CONFIDENTIAL

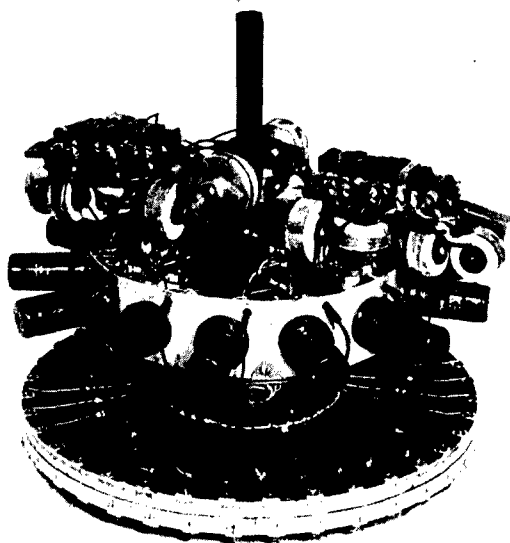


FIGURE 48. Assembly view of whirling dervish commutator.

the rotor segment could be deduced. A vector plot of this voltage is shown in Figure 47B. The vector equivalent of the voltage moved smoothly through the positions (*a, b, c, . . . h*) as the segment moved in position from directly above one stator segment to the position directly above its neighbor. Further rotation caused the vector to move smoothly to the positions *j, k*, etc. From this rather simple experiment it was concluded that smooth rotation of a beam pattern was possible with the capacitive type of commutator, a discovery which led directly to the development of the capacitive commutator at HUSL.

*The "Whirling Dervish."* The second capacitive commutator was more elaborately built and eventually was used for actual rotation of a beam pattern. Originally, it had two flat plates 12 inches in diameter, which were made of 1/2-inch-thick glass-base bakelite. On each plate, 36 sector-shaped segments of aluminum foil were cemented with equal spacing around 360 degrees. The rotor plate was mounted to rotate around a vertical shaft centered in the stator plate. The air gap distance between the plates was about 0.038 inch, giving a capacitance of about 16  $\mu\text{pf}$  between the pairs of capacitor segments.

All the rotor segments were connected through 1-megohm resistors to ground, except that an additional connection was made from one segment to the

input circuit of a CRO. Again, tests showed that the rate of change of phase of the voltage appearing on this segment was nearly constant with uniform rotation. It was concluded, therefore, that if the phase difference between voltages on successive stator segments were reasonably small, a smooth change in the phase of the voltage appearing on any rotor plate could be secured by rotation without appreciable change in its amplitude.

It was next proposed to equip the rotor with slip rings for continuous rotation. To test the efficacy of the above principle for beam rotation, a beam-forming lag line was added; then an array of ten tubes (Type 6SJ7) was arranged around the periphery of a cylindrical plate—all being mounted on the rotor member. The tubes were added to provide isolation between transducer and lag line and also to introduce amplitude shading. Several slip rings conducted the lag line output signal from the rotor and the supply voltages to the tubes. At this stage of development the commutator became known as the "whirling dervish." A photograph of the unit is shown in Figure 48, and the electrical circuit diagram of the rotor connections in Figure 49. Because of the tendency of the bakelite plates to warp, they had to be refaced and the aluminum foil segments replaced several times during experiments.

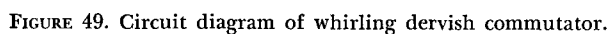
The whirling dervish was used with the first artificial transducer to demonstrate in the laboratory the possibility of forming satisfactory directivity patterns. It was later used on the AIDE DE CAMP with the Medusa transducer to obtain the first rotatable beam pattern from a projector in water.

*The Die-Block Model.* If a capacitive commutator were to be used for rapidly rotating a receiving beam, a material less subject to warping and changes in shape was needed for the plates. Therefore, a third commutator was designed and built to meet a 600-rpm speed requirement. Initially, the rotor plates were made of Die-Block, a commercial plastic-impregnated plywood which was supposed to retain its shape to a high degree. Aluminum foil was used for the 36 capacitive segments on each plate and the unit was placed with its shaft vertical.

The lag line was enclosed in the rotor, and its output brought out through capacitive rings. Signals were fed into the line through L-type resistor networks in the same manner as used in all later commutator models. The line itself consisted of a number of constant-K low-pass filter sections having uniform

ments were cemented to the glass. Figure 50 shows the unit, with the artificial transducer phasing line located on the bench below the commutator unit.

With these alterations, the commutator was, on one occasion, operated successfully at a speed of 1,800 rpm, although the next test was unsuccessful. The cause of its failure is unknown. The rotor glass plate



**CONFIDENTIAL**

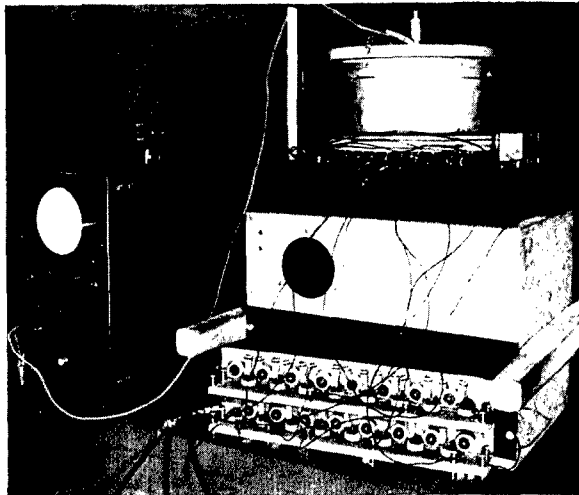


FIGURE 50. Assembly view of Die-Block commutator.

disintegrated and associated parts of lag line, glass, and wire were distributed around the laboratory with some near misses to personnel.

#### CAPACITIVE COMMUTATOR, MODEL 1

The Model 1 commutator was the first practical capacitive commutator designed for a rotation speed of 30 rps. A photograph of the unit as later modified is shown in Figure 51. The commutator proper was separately mounted and isolated from the chassis frame by the use of Lord rubber mountings symmetrically placed about its center of gravity.

Starting with the end furthest from the driving motor the commutator chassis contained:

1. A bank of 36 *input transformers* attached to a single plate. These were Audio Development transformers No. 3479 with 100-ohm primaries and 50,000-ohm secondaries. One element of the 36-element transducer was connected to the primary of each transformer. The secondaries were connected through holes in the end plate to the stator segments, these leads being kept as short as possible to minimize pick-up of extraneous noise.

2. *Commutating stator plates.* The two stator plates were 8 inches square, and they and all other plates were made of 1/2-inch-thick Mycalex. Since Mycalex is an insulator, to make one surface of each plate a conductor, 16-gauge steel was cemented to that surface. The steel was ground until the faces were flat and parallel and then cut into 36 separate sector-shaped segments, the active area of each being approximately 1.19 square inches. Later, two screws

were added to each segment to hold it in place. After mounting, the segments on the two stators were electrically connected together. The stators were separated by ground spacers so that the air gaps between them and the rotor, which rotated between them, were .005 inch on each side. They were mounted on four 1/2-inch rods and three screw adjustments were provided to simplify alignment at assembly.

3. *Commutating Rotor Plate.* The rotor plate was between the two stators and was 8 inches in diameter, 1/2-inch thick, and had 36 metallic segments on each side, the segments on the two sides being connected in parallel. The capacitance between any one pair of commutator segments was approximately 100  $\mu\text{mf}$ ; the use of a doubly faced rotor between two stator plates provided compensation for subsequent minor variations in air gap.

Each capacitor segment of the rotor was connected to the lag line, which, in this model, was rotated. The sections of the beam-forming lag line were attached to bakelite pieces mounted inside a cylinder of 16-gauge steel. This cylinder was constructed in two parts so that the lag line could be wired and added to the commutator after the plates had been mounted and aligned.

Experimental work on lag line design to improve its beam-forming characteristic was carried on with this model. Toroidal coils using powdered molybdenum Permalloy cores were first used as inductive components. The earliest lag line designs employed the constant-K type filter section. Later, however, the bridged-T type filter section (see Chapter 6) was substituted with considerable improvement in beam pattern.

4. *Output Rotor and Stator Plates.* The output of the lag line was taken off capacitively rather than by

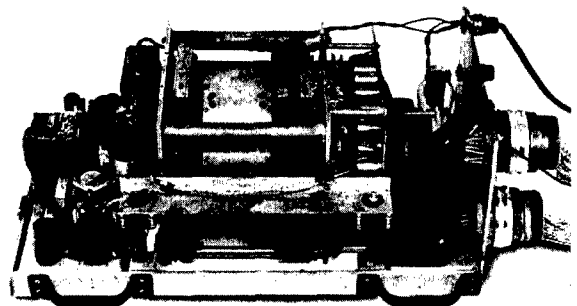


FIGURE 51. Assembly view of Model 1 commutator.

slip rings as in subsequent models. This was done by another pair of plates, comprising a single rotor plate and a single stator plate on the other side of the lag line cylinder. Their size and construction was the same as the commutating plates and the spacing between them was about .008 inch. Instead of being segmented, their metallic surfaces were cut into three concentric rings of equal area. Three output rings were needed because the lag line was double to make SLC reception possible. There was, however, one slip ring which was used to give a positive ground connection. The ring itself was coin silver and the brush contact area was a silver graphite compound.

5. *Motor and Sweep Generator.* The commutator driving motor was a 1/2-hp, 1,725-rpm motor with a shaft extending from each end. One end was connected through a flexible coupling directly to the commutator rotor shaft. The sweep generator was a GE industrial type synchro generator whose stator was rewound to have a high impedance suitable for excitation from vacuum tubes.

This commutator assembly, approximately 36 inches long, 14 inches wide, and 10 1/2 inches high, was completely enclosed. Input connections to the transformers were made through four 18-terminal Jones plugs mounted close to the transformers; all other connections were made through Amphenol connectors.

*Modification.* After about a year of operation the Model 1 commutator was remodeled, the primary changes being directed toward decreased size and accomplished by using a small 1/40-hp motor, changing the input transformers to the smaller size Audio Development transformer No. A3770, and replacing the GE industrial type synchro generator (selsyn) with a standard size 5 CT synchro. Because of its high-impedance rotor this synchro was satisfactory as a sweep generator, but not so satisfactory as the original rewind generator. This loss was accepted because of the advantages of a standard synchro and the convenience of smaller size. At the same time a preamplifier and power supply were added. After this modification the dimensions were 24x12 3/8x10 1/2 inches.

#### CAPACITIVE COMMUTATOR, MODEL 2 (EXPERIMENTAL UNIT)

A second design was undertaken, the primary requirement being relative ease in disassembling, changing, and reassembling for laboratory experimentation.

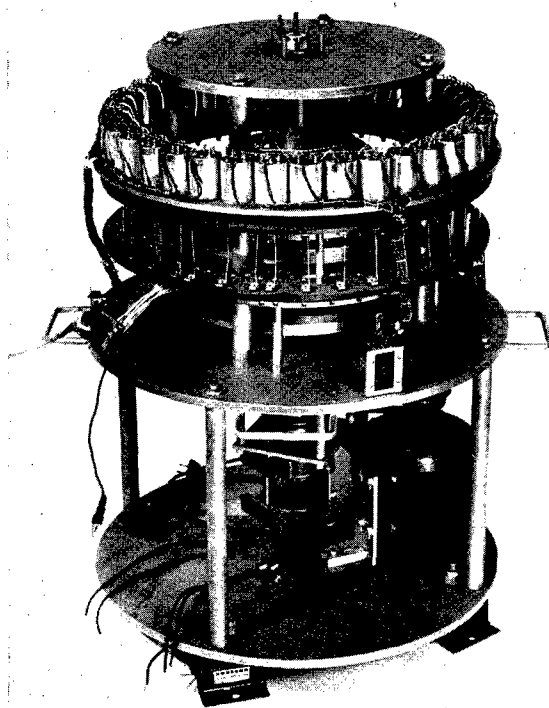


FIGURE 52. Assembly view of Model 2 commutator.

In this model the shaft was made vertical rather than horizontal. Space for the lag line was provided in a cylinder on top of the rotor assembly. The plate assembly was below this and the sweep generator and motor at the bottom of the commutator. (See Figure 52.)

The lag line was rotated as in Model 1, but because of its location, it could be reached and changed without disassembling the entire commutator. Its elements were mounted on bakelite plates and the entire unit was shielded by a 16-gauge steel container between two bronze castings.

Directly below the lag line was the commutating rotor which was made of 1/2-inch Mycalex, 12 inches in diameter. The larger diameter was necessary to secure the required capacitance without a second stator. One surface was made conducting by cementing a 16-gauge steel plate to the Mycalex, and then cutting into 36 segments of approximately 2.78 sq in. area each. Because this commutator was planned to rotate at speeds up to 3,600 rpm, the rotor plate was rigidly secured in a heavy bronze casting for protection.

The commutating stator was so mounted that the

spacing between it and the rotor could be varied. It was positioned axially by four rods which also supported the top rotor bearing plate. The 36 segments of the stator surface were connected to 36 banana plugs mounted on a bakelite ring around it.

The input transformers were mounted around the capacitor plates on a single plate which could be plugged as a unit into the banana plugs attached to the stator segments. An additional plate was provided so that small capacitors could be added in series with the stator segments to simulate reduction in gap capacitance, if desired.

Directly below the commutating plates were two output plates of the same size and material. The output stator plate was about 1½ inches from the commutating stator plate and was mounted and positioned in the same way. One surface of each output plate was made metallic by a silvering process described later. (See Section 5.4.3 on commutator plate materials.) These surfaces were cut into 12 concentric rings of equal area, 12 being provided to allow the installation of a stationary lag line, if desired, in the experimental program. In this case leads from any 12 active segments on the rotor commutating plate could be connected directly to the 12 rings on the output rotor plate.

Coupled to the end of the rotor shaft was a GE industrial type synchro generator used as a spiral-sweep generator. As in the Model 1 commutator, the rotor was rewound for a higher impedance. The unit was belt-driven by a 1/12-hp synchronous Bodine motor and a knob and dial were provided at the top for hand-training. All connections were made through Jones plugs and Amphenol plugs. The commutator was approximately 22 inches in diameter, about 34 inches high, and the whole assembly mounted on U. S. Rubber Company isolators.

The Model 2 capacitive commutator was used at HUSL to investigate the problem of air gap tolerances. Variations in the rotor-to-stator plate spacing due to the stator plate unevenness were simulated electrically by changes in the overall series capacitance of the commutator produced by the insertion of capacitors between any one of the 36 stator segments and its input transformer. Likewise, variations in the rotor-to-stator spacing due to rotor plate unevenness were simulated electrically by changes in the series capacitance produced by the insertion of capacitors between the active rotor plates and the feed-in points to the lag line. Test results indicated that a tolerance

of approximately  $\pm 12$  per cent in air gap variation was allowable without serious deterioration of beam pattern.<sup>62</sup>

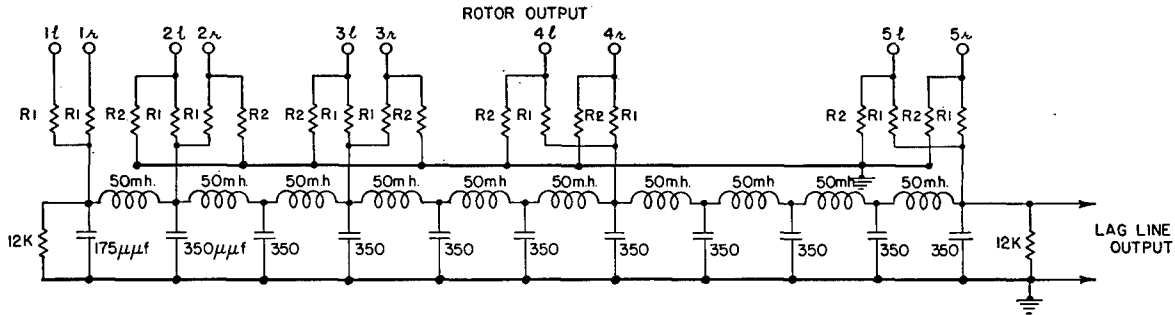
#### CAPACITIVE COMMUTATOR, MODEL 3

A third design was begun in anticipation of the need for two commutators to be installed with the QH scanning sonar on USS SARDONYX. Originally the Model 2 commutator was to be completed and tested before starting the third design, but, because of the press of time, several assumptions were made so that the Model 3 design and construction could proceed. Three Model 3's were built, redesigned, and two of them rebuilt and installed before the Model 2 was completed. The design was begun in the latter part of July 1943, and was completed late in August 1943.

The basic difference between Model 3 and other commutators was the stationary instead of rotating lag line. To accomplish this and to give a double lag line for SLC reception five plates were used, three being stators and two rotors. The center stator plate corresponded to the commutating stator plate in previous commutators, and both sides were surfaced with metal cut into 36 segments of approximately 2.19 sq in. active area each. On each side was a rotor plate with 36 segments cut into the metallic surfaces facing the commutating stator plates, and 10 concentric rings of equal area cut into the metallic surfaces on the back. These corresponded to the output rings on other commutators. The ten active segments on one side were electrically connected through holes in the plate to the rings on the other side. Opposite each rotor plate was a stator plate whose metallic surface was also cut into 10 concentric rings. These were the output stators and their rings were connected directly to the sections of the lag line.

The stator plates were clamped together and mounted on four rods, the distance between them being determined by accurately ground spacers. They were adjustable as a unit but not individually. The rotors were mounted to the shaft in such a way that they could also be adjusted as a unit, the distance between being determined by a spacer. The air gaps used for both input and output were .005 inch. To make SLC reception possible, the centers of the active segments on the two rotors were offset by 10 degrees when they were mounted to the shaft.

All plates were made of ½-inch-thick Mycalex, the rotors being 10 inches in diameter, and all plates were



R1 AND R2 ARE SELECTED SO AS TO PRESENT 25K TO THE ROTOR OUTPUTS AND TO GIVE THE ATTENUATIONS SHOWN ON THE SHADING CURVE

$\frac{C}{\lambda} = ka = 20$   $f \approx 20.4$  KC  
LINES GIVES  $30^\circ$  PER SECTION

FIGURE 53. Circuit diagram of beam-forming lag line, Model 3 commutator.

coated with silver by a method described in the next section. The stators were silvered 5/8 inch beyond the outside diameter of the rotor and connections from the input transformers were made to soldering lugs bolted to the stator in this space. Input transformers were mounted around the plates.

The lag line was double to allow SLC reception, and half of it was attached to each end of the rotor section. Figure 53 gives design data on the lag line for this commutator.

The entire rotor section was mounted on Lord mounts for isolation from motor and other vibrations. The motor was a 1/12-hp, 1,725-rpm Robbins and Myers motor mounted on Lord isolators and connected to one end of the rotor shaft by a flexible coupling. The final design used a 1 CT synchro coupled directly to the other end of the rotor shaft.

The preamplifier and power supply were built into this model. Figure 54 shows the preamplifier and Figure 58, the power supply, which was the same as for Model 1B. The preamplifier was double, half of it being mounted at each end of the rotor section. All

connections to the commutator were made through Amphenol plugs.

Construction was started on three Model 3 commutators but, after completion and testing of one, the stationary lag line proved unsatisfactory. Following the completion of two Model 1B commutators, the original Model 3 commutator was converted to this type and used as a listening rotor. It was first installed with the Model 1 as part of the QH Model 1 sonar on the AIDE DE CAMP.

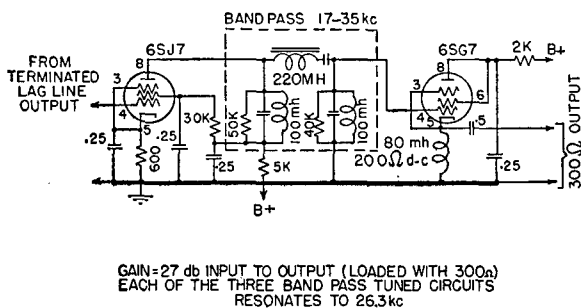
#### CAPACITIVE COMMUTATOR, MODEL 1B

This unit consisted of one rotor between two stators, a rotating lag line with conductive slip ring rather than capacitive output, the usual spiral-sweep generator and motor, and a preamplifier and power supply. The commutating plates were 10 inches in active diameter, made of 3/8-inch Mykroy and coated with silver by the Metaplast process. (See Section 5.4.3 on commutator plate materials.) The two stators were mounted as before and separated by ground spacers allowing a .005-inch air gap on each side of the rotor.

The rotor was attached to a collar on the shaft, to which were also attached the lag line and a slip ring collar (see below).

The stators were metallized on one side only, 5/8 inch beyond the outside of the rotor, and this metal surface was cut into 36 segments. Connections to the stator segments were made as in Model 3. After mounting, the segments of the two stators were connected in parallel.

Both surfaces of the rotor were metallized and cut into 36 segments of approximately 1.92 sq in. area each. The two sides were connected in parallel by silvering the insides of 36 holes through the plate.



GAIN = 27 db INPUT TO OUTPUT (LOADED WITH 300Ω)  
EACH OF THE THREE BAND PASS TUNED CIRCUITS  
RESONATES TO 26.3 kc

FIGURE 54. Circuit diagram of preamplifier, Model 3 commutator.

CONFIDENTIAL

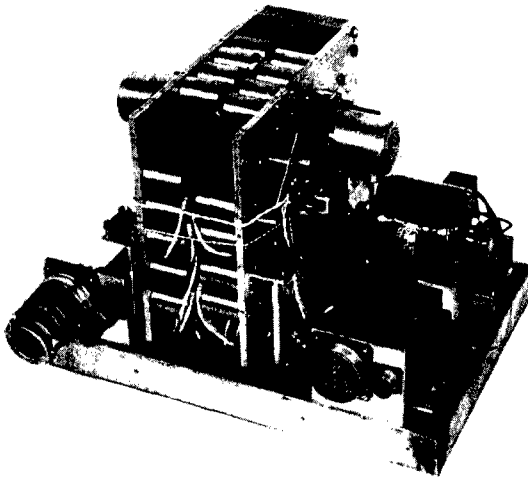


FIGURE 55. Assembly view of Model 1B commutator.

These holes also provided a simple means of making connections to the lag line. Figure 55 is a photograph of this unit.

The lag line components were mounted on bakelite pieces inside a heavy ring fastened to a plate on the shaft collar. This could be assembled and wired as a unit and then completely inclosed by putting on a spun metal cover. Leads to the lag line sections were attached to a ring of 36 banana plugs extending through the lag line plate and could be plugged into the silvered holes in the rotor plate as a unit. This lag line design is shown in Figure 56.

The three output leads for the lag line were connected to silver-plated brass slip rings attached to a bakelite collar. The brushes, with a contact area of silver graphite compound, were made by the Radiation Laboratory at MIT. Two brushes were used in parallel on each ring to reduce electrical noise.

Since the size 1 CT synchro used in Model 3 as a spiral-sweep generator did not have the output expected, a GE size 5 CT synchro was used for Model 1B. This was coupled directly to the rotor shaft with a flexible coupling. It was found experimentally that of the 5 CT synchros made by different manufacturers, only those made by GE had the high rotor impedance required to permit satisfactory excitation by the vacuum tubes used.

In order to shorten the commutator still further, the motor was mounted on the end with the synchro, rather than on the opposite end as before. A 1/40-hp, 1,725-rpm capacitor start-and-run Bodine motor was coupled to the rotor shaft by a Link-Belt silent chain. This proved satisfactory in operation but was noisy. A small discrepancy between the size of the sprocket on the motor and the one on the rotor shaft was used to bring the rotation speed up to about 1,800 rpm. The overall size of the commutator unit was 17x15x15 inches.

Both the preamplifier and the power supply chassis were complete in themselves and could be assembled and wired separately. The circuit diagrams of these two units are shown in Figures 57 and 58.

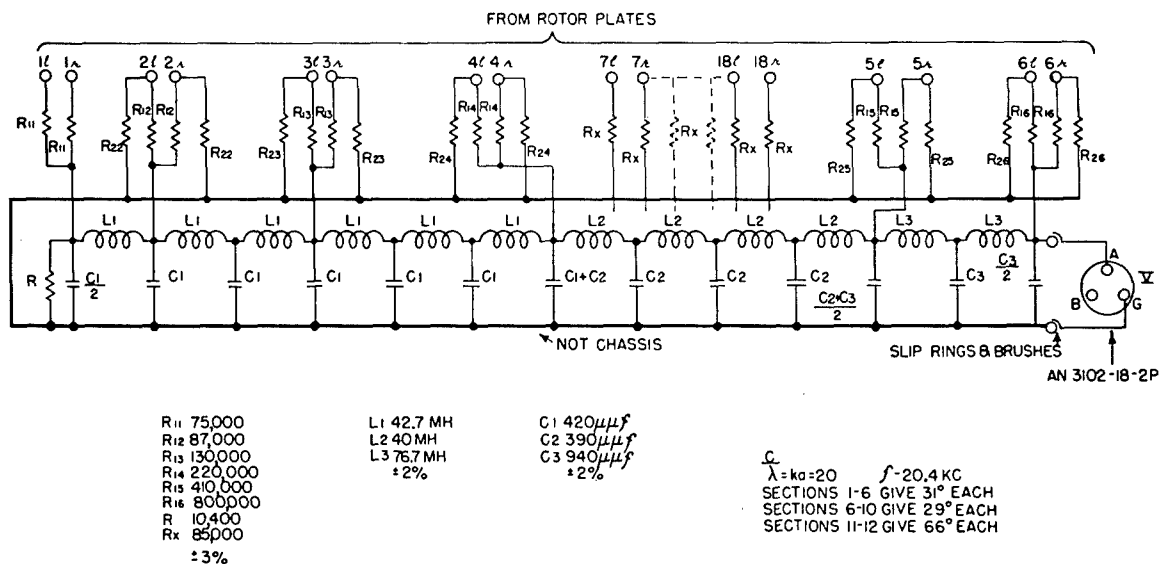


FIGURE 56. Circuit diagram of beam-forming lag line, Model 1B commutator.

CONFIDENTIAL



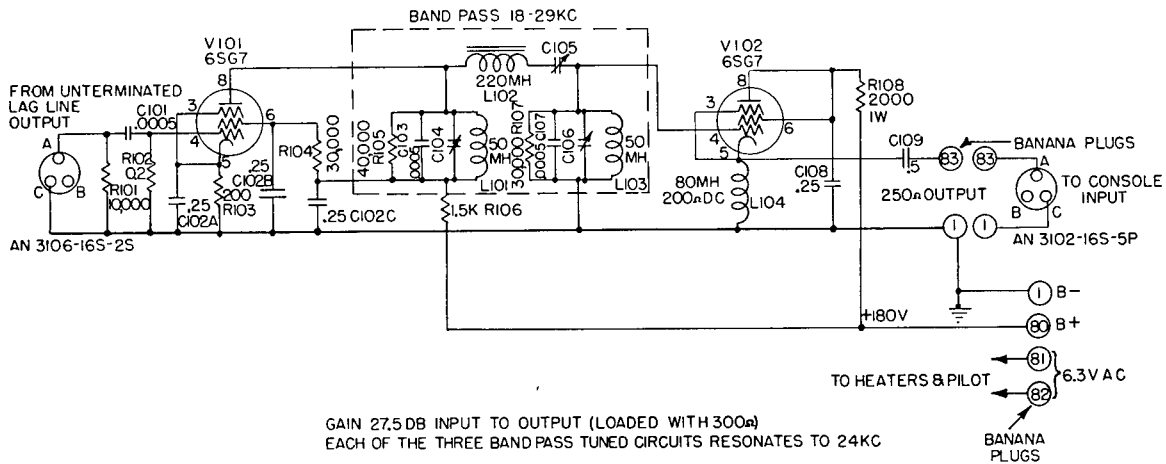


FIGURE 57. Circuit diagram of preamplifier, Model 1B commutator.

## MODEL 1B LISTENING ROTOR

The Model 1B was converted to a listening rotor by replacing the Bodine motor drive with a servo system composed of:

1. The 5 CT synchro already coupled to the rotor shaft.
2. A 27-rpm Brown Instrument Company servo motor, No. 76750-3, geared to the rotor shaft to give a 9-rpm rotation speed.
3. A 2-watt servo amplifier Model 3, shown in Figure 59.

One scanning and one listening Model 1B commutator were used with the QH Model 1 sonar which was installed on USS SARDONYX and later transferred to USS CYTHERA. These models also served as the prototype of the commutators manufactured by the Sangamo Electric Company as part of the XQHA systems.

## CAPACITIVE COMMUTATOR, MODEL 4

Because of the large number of parts involved and the difficulty of assembling a multiple-plate commutator, a fourth design was undertaken which was a radical departure from previous designs in that two concentric cylinders were substituted for the flat plates. (See Figures 60 and 61.)

In this model the rotor was a cylinder about  $6\frac{3}{4}$  inches OD, mounted for rotation inside a stationary cylinder with .005-inch clearance all around. The inside of the stator and the outside of the rotor were coated with a fired silver, as described in the following section. Both cylinders were made of Pyrex by the Corning Glass Company and delivered to HUSL ready for installation. The segments were cut longitudinally and the connections to them were made by plugging banana plugs into silvered holes. The active area of each segment was approximately 3.35 sq in.

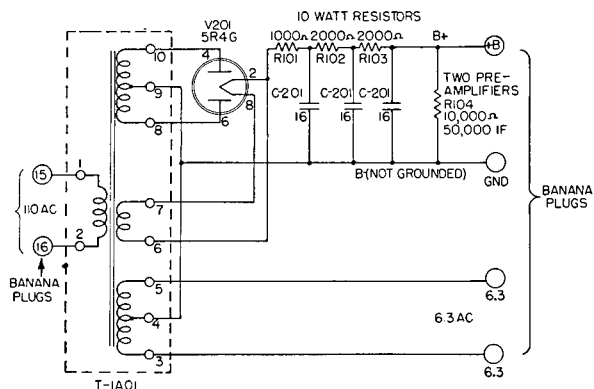


FIGURE 58. Circuit diagram of power supply for pre-amplifier, Model 1B commutator.

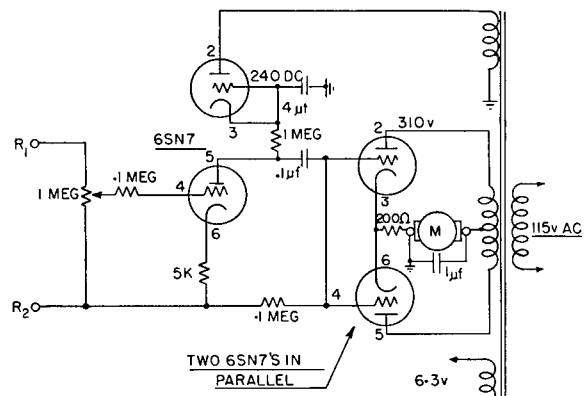


FIGURE 59. Circuit diagram of Model 3 servo amplifier.

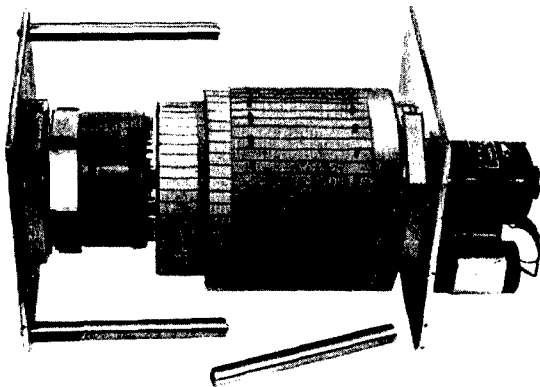


FIGURE 60. Disassembly view of Model 4 commutator.

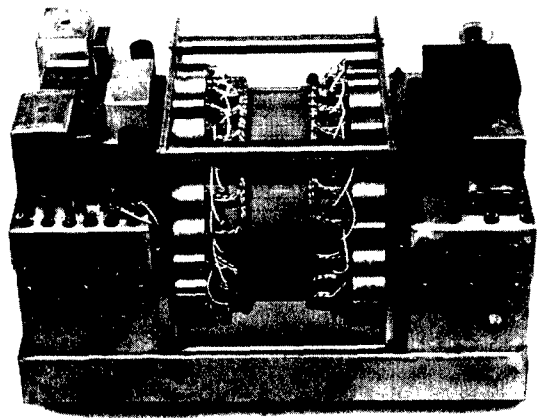


FIGURE 61. Assembly view of Model 4 commutator.

These cylinders were mounted on castings which were carefully fitted into their inside surfaces. To reduce stress caused by differential expansion between the glass and the casting material, only six points of the castings were in contact with the glass. Since it was necessary that these castings have essentially the same coefficient of thermal expansion as the Pyrex, two low-expansion alloys, developed by the Westinghouse Research Laboratories, were used. One was a modification of Invar, designated Research Heat No. 5121; the other, developed in an effort to make the castings corrosion-resistant, was an iron-chromium-cobalt alloy designated Research Heat No. 5132. The

cylinders were positioned radially only by these castings; axially, they were held in place by steel rings attached to the castings and clamped against their ends. For protection, thin corprene washers were used between these rings and the glass. The castings that positioned the stator also formed housings for the rotor bearings; consequently, their inside and outside surfaces had to be concentric to a high degree of accuracy. Likewise, surfaces for the casting for the rotor had to be concentric.

The lag line was considerably compressed for mounting inside the rotor. Space was allowed for a double lag line for SLC reception, although the com-

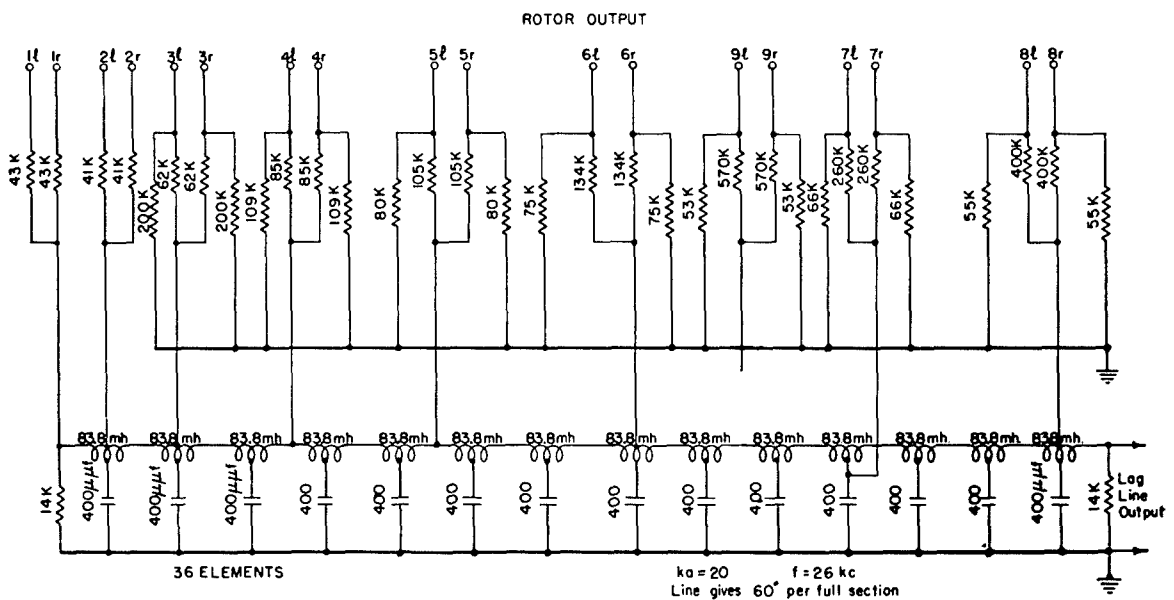


FIGURE 62. Circuit diagram of beam-forming lag line, Model 4 commutator.

CONFIDENTIAL

mutators built had only single lag lines. The electric design of this lag line is shown in Figure 62. Three output leads from the double lag line were brought through the casting at the rotor end to three slip rings. The brushes used were the same as those used on other models and could be removed without disassembling the entire commutator. To reduce electrical noise, six brushes were used on each slip ring.

The commutator was to be used for either scanning or listening, and two motors were therefore built into it. The scanning motor, a 1/40-hp, 1,725-rpm capacitor start-and-run Bodine, was mounted on one end of the rotor and permanently coupled to its shaft by a flexible coupling. The servo motor for listening was made by the Brown Instrument Company and geared to the other end of the rotor through an idler which could be engaged by moving a lever. This lever also tripped a microswitch which shifted the a-c power from the scanning to the servo motor. The sweep generator, a size 5 CT synchro made by the General Electric Company, was coupled directly to the rotor shaft on the servo motor end. Both motors and the synchro were attached to the end plates of the rotor and the whole commutator unit was mounted on Lord mounts.

The power supply and preamplifier were parts of this unit and could be connected by detachable plugs as in Model 1B. All electric inputs to the commutator were through Amphenol AN plugs. The input transformers were Audio Development Type A3770 mounted around the stator. The dimensions of the complete commutator were  $18\frac{3}{4} \times 11\frac{1}{4} \times 10\frac{1}{2}$  inches, and it could be mounted in a standard relay rack.

Because of the small air gap and the rigid requirements for uniformity, the problem of mounting the cylinders was difficult. Consequently, there was some question as to whether the unit could be readily made on a mass production basis. During the design period of the Model 4, the design of the XQHA commutator units was discussed with the representatives of the Sangamo Electric Company. As a result, a design using two identical flat glass plates with fired silver segments was adopted.<sup>1</sup> This design has proved readily manufacturable, and has given satisfactory performance.<sup>27, 31</sup> Commutators of this design are used in the integrated Type B sonar (see Chapter 6).

#### CAPACITIVE COMMUTATOR, MODEL 5

The only difference between this and Model 4 was that Model 5 had 48 input transformers, and the sil-

ver surfaces on the cylinders were cut into 48 rather than 36 strips. This gave an active area of approximately 2.5 sq in. for each segment.

#### 5.4.3

### Commutator Plate Materials

The considerable amount of experimental work to develop a satisfactory arrangement for forming and mounting the capacitive commutator segments is described here. The ideal material for commutator plates would have the following properties:

1. Nonconduction
2. Low dielectric constant
3. Ease of machining
4. Mechanical strength to stand high rotation speeds and resistance to shock
5. Very high dimensional stability—no cold flow or warping over a period of time
6. Nonhygroscopic
7. A surface to which conducting material can be attached easily and firmly
8. Ability to hold its shape and dimensions at the high temperatures required to fire silver on its surface, if this method of metallizing is to be used
9. Ready availability

A large number of materials were considered but, since no one material possessed all these properties, only two or three were actually used. The hardest requirement to meet was the one of dimensional stability. The few materials actually used will be discussed in detail, but for reference all materials considered are listed below. The number in parenthesis after each material indicates the primary requirement it failed to satisfy.

1. A steel plate as base with porcelain standoffs holding separate steel segments [(3 & 4), mechanical complexity]
2. Die-Block (5)
3. "Hy-Den" (bakelite impregnated wood) (5)
4. Injection molded hard bakelite (5)
5. Canvas-base bakelite (Formica, Micarta, F. B. E.) (5 & 6)
6. Glass-base bakelite (8 & 9)
7. Polystyrene (5 & 7)
8. Lucite (5)
9. Vinylite (5)
10. Mycalex } (8)—see below
11. Mykroy }
12. Plate glass (4)
13. Pyrex—see below

- |                            |   |            |
|----------------------------|---|------------|
| 14. Porcelain (3)          | } | —see below |
| 15. Prestite (3)           |   |            |
| 16. Isolantite (3)         | } | —see below |
| 17. Alsimag (3)            |   |            |
| 18. Ebony—Asbestos (5 & 6) |   |            |

#### MYCALEX AND MYKROY

With the exception of the cylindrical commutator all formally designed commutators constructed at HUSL had either Mycalex or Mykroy plates. These two are essentially the same, except for minor differences in composition.

Mycalex is a mixture of 60 per cent mica, 30 per cent low fusing glass, and 10 per cent water. It is pressed dry and cold, completely dried, then heated to the fusing point of the glass and pressed again while hot. The result is a material which meets most of the requirements described above, but which is not strong enough mechanically for mass production. It can be machined under water with comparative ease, but in general should be handled like glass. The point on which it is definitely not satisfactory is point 7, since there is much difficulty in finding a method of metallizing the surface which would be practical for mass production.

Mykroy, being essentially the same as Mycalex, is subject to the same troubles, but is better on point 8, since it can stand a slightly higher temperature. (See below.)

#### PYREX

Thus far Pyrex met all requirements satisfactorily, and production models were made with Pyrex plates, although mechanical strength and resistance to shock could be better.

#### ALSIMAG

Alsimag is a steatite and is representative of the handling of ceramics in general. It has about four times the mechanical strength of glass, can easily be produced in quantity by molding, and provides an excellent bond for a metal surface. Its one drawback is that, like all ceramics, after being fired it is too hard for further changes, except by grinding. Unfortunately, a 10-per cent shrinkage which occurs during firing makes it impossible to locate small holes, etc., accurately, since they must be put in before firing. However, it can be ground easily, and it seems that a commutator could be designed which would overcome this difficulty. Once fired, Alsimag plates can be

reheated as high as 1000 C, with no change; so metallizing is a simple process. From an admittedly incomplete study it seems probable that, with further development, Alsimag would be the most satisfactory of the materials considered.

This approach is subject to the basic limitation that the insulating material is also the structural supporting member. Any future study should include composite structures, in which the separate functions of insulation and structural support are performed by the most suitable materials in each case.

#### METALLIZING METHODS

A satisfactory method of securing conducting surfaces on the insulating plates has been very difficult to find. All that is required is that the surface be conducting and that it be possible to cut it up into segments or rings without its coming off. For the first attempts, 16-gauge steel plates were cemented to Mycalex plates, using Vinylseal as the adhesive. This was done for the Model 1 commutator, but before being used the plates loosened and screws had to be added to hold them in place. Because of its brittle quality, tapping into Mycalex is not practical.

Attempts were made to attach 16-gauge steel plates to Mycalex by using Cycle-Weld as the adhesive, first by cementing steel directly to the Mycalex and later by cementing it to a bakelite filler and then cementing the filler to the Mycalex. Both methods were unsatisfactory because the surface of the Mycalex was weaker than the bond, and the plates could be pulled off along with a very thin layer of this surface. With the bakelite "sandwich" other difficulties were also encountered.

Since cementing proved unsatisfactory, several other methods, listed below, were tried. Only the first two were successful, but it is possible that some tried only on Mycalex could be used on glass or on Alsimag.

1. Spraying and firing silver
2. "Metaplatinizing"
3. Spraying hot metal
4. Vacuum plating
5. Sputtering
6. Mirror silvering

A liquid silver manufactured by the Hanovia Chemical Company of Newark, New Jersey, looked very promising after preliminary tests. It was a colloidal suspension of very finely divided silver in an organic compound. It was sprayed on with a regular

paint spray gun and then the plates brought up to a temperature determined by the type of silver and the plate material. This volatilized the organic compound and left a coating of metallic silver. However, many troubles were encountered in applying it to Mycalex, the chief being that the firing temperature required for silvering (450 C) was very close to the softening point of the Mycalex. This required very careful control in heating the plates, and even then the quality of the bond between the silver and the Mycalex was unpredictable. Under no conditions were plates successfully heated to this temperature without some change of dimensions or flatness. Although Mykroy could stand a little higher temperature, it was unsatisfactory because of warping. Actually two Mykroy plates were successfully coated by this method for the Model 2 commutator, as well as all the plates for the Model 3 commutator. However, to compensate for the warping, several thick layers of silver were put on and then burnished flat.

The fired silver method of coating was essentially the same as that used by the Corning Glass Works in coating their Pyrex disks for the XQHA commutator manufactured by the Sangamo Electric Company. No trouble was encountered there, first, because the plates were very carefully annealed before reheating for the silvering, and, second, because the firing temperature for silvering was not near the softening temperature of the glass.

Considerable work with this method of silvering on Alsimag brought excellent results. Alsimag is resistant to heat shock and, consequently, temperature control is not nearly so critical as with Mycalex or glass. In addition, it can stand temperature up to 1000 C without warping, this being considerably above that required for firing silver (800 C). The resulting bond is excellent, and the silver can not be scraped off.

Another successful method of plating was achieved by the Metaplast Corporation of New York and required no heat. In this process, a very thin bonding coat was put on, and then additional thickness built up by regular silver plating methods. The two Model 1B commutators used in the USS SARDONYX installation were plated by this method. Because of the press of time, only a bonding coat was put on these commutators, but after about six months of operation they had to be recoated and the silver built up to about .0005 inch. Care had to be exercised in doing this, however, for once the coat became thick enough

to be continuous, in the sense that a metal plate is continuous, it could be peeled off.

This method had many advantages over cementing steel to the plates. The chief advantage of the fired silvers or Metaplating was that the coating could be put on in any shape without machining. After being plated and fired, the surface could be cut into segments simply by scratching along a straight edge rather than by milling. The coating was noncorrosive and, provided it was thin enough, could not be peeled off. It would stand a great deal of wear and tear in normal handling and assembling and it vastly simplified the problem of making connections to the segments, because the metallic coat could be carried on through holes and to any point desired. This made it possible either to plug into these holes or to solder lugs into them as was done in the Sangamo XQHA commutator.

5.5

## INDICATORS

This section contains descriptions of the indicators used in the various CR scanning sonars. In the early part of Chapter 2 design considerations were discussed and may be referred to in evaluating the units described here. Many recognized operating conveniences were omitted in early experimental designs so that time and effort could be saved until the value of the fundamental scanning sonar principles had been established.

5.5.1

### Use of MR Indicator for Medusa Tests

For general preliminary testing in the laboratory, commercial cathode-ray oscilloscopes were used as indicators. For example, to observe patterns, the horizontal deflection amplifier was driven by the linear sweep, synchronized with the rotation of the beam of sensitivity, thus making the abscissa represent bearing; the vertical deflection amplifier was fed from the output of the receiver, so that the ordinates represented signal intensity. A linear plot of the beam pattern in rectilinear coordinates was then obtained (see Figure 2).

From the beginning of the work on scanning systems, a cathode-ray tube was used as the indicator to give a plan position indicator [PPI] display. Such an indicator, using a magnetic deflection cathode-ray tube with 2-phase spiral sweep, was built for the roto-

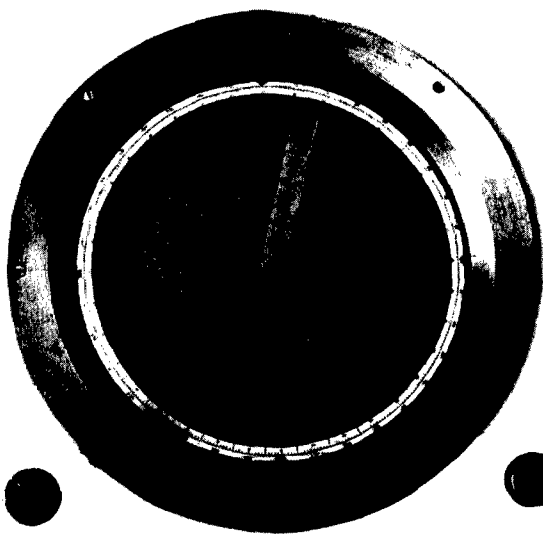


FIGURE 63. Operator's view of 12-in. PPI.

scope MR scanning sonar. Details of construction and use are found in Chapter 4. It was used as the indicator unit in the scanning sonar system using the Medusa transducer in tests conducted on the AIDE DE CAMP in October 1942. The PPI performed satisfactorily and the test results gave sufficient evidence that a CR scanning system could be made to function.<sup>4, 5, 63</sup> No further work was done using this PPI on CR systems. It was transferred to the rotoscope program and continued to perform satisfactorily in that work for some time.

#### 5.5.2 Use of 7-Inch CR Tube in the Auditorium Demonstration System

After the first tests of a scanning sonar system were made in the Charles River Basin, a CR system was set up in the laboratory in order to develop the electronic portions of the system and to permit demonstrations to be given. The indicators used in this system consisted of a 7-inch cathode-ray tube PPI and a loudspeaker. The speaker was not then intended as a part of a scanning sonar system but was used in demonstrations for comparing patterns on the PPI with the corresponding aural indications of echo and reverberation in the usual searchlight-type sonars.

The construction of the PPI was very simple. The

7-inch, long-persistence-screen (P7 phosphor) cathode-ray tube was mounted in a standard 14-inch relay rack panel behind a color filter, and the focusing and deflection coils were supported on wooden blocks. Only the control for intensity was provided on the panel. Signal was applied to the brightening grid through a step-up transformer, about 27 volts being required for full brightening. The deflection coil assembly was the 3-phase stator winding of a Diehl 5F synchro. The scanning speed used was 30 rps. This indicator was used in the laboratory for demonstrations and for testing<sup>64</sup> of spiral sweeps. SLC brightening was also used later in tests on quenching<sup>65</sup> of the screen persistence (see Chapter 2).

#### 5.5.3 12-Inch PPI on Aide de Camp

The third CR scanning sonar was installed on the AIDE DE CAMP in June 1943 (see Section 5.2.3 of this chapter on experimental work). The first indicator used was the PPI with a 7-inch cathode-ray tube that had been used in the laboratory CR system. This was later replaced, however, by an improved design incorporating the following innovations:

1. A 12-inch cathode-ray tube.
2. A mechanical cursor to assist in reading the range and bearing of target echoes.
3. True- or relative-bearing display by use of a DG synchro in the spiral-sweep circuit.
4. Electronically brightened range circles on the PPI screen.

The 12-inch tube was of the long-persistence (P7) type using magnetic deflection and focusing. The deflection coil was a 3-phase stator of a type 5F synchro (Diehl). The scope was mounted inside a steel housing which was supported by the front panel, and which in turn supported the focus and deflection coils and permitted their adjustment by allowing movement with respect to the cathode-ray tube. Also supported by the front panel were the bezel ring (which held the protective transparent disk), the light filter disk, and the mechanical cursor with its gears and control knob. A bearing scale was engraved on the outer portion of the protective disk and the bearing was read against a pointer carried by a large ring supporting the outer end of the cursor. This ring was supported by wheels and was connected by gearing to the control knob so that it could be positioned by the operator.

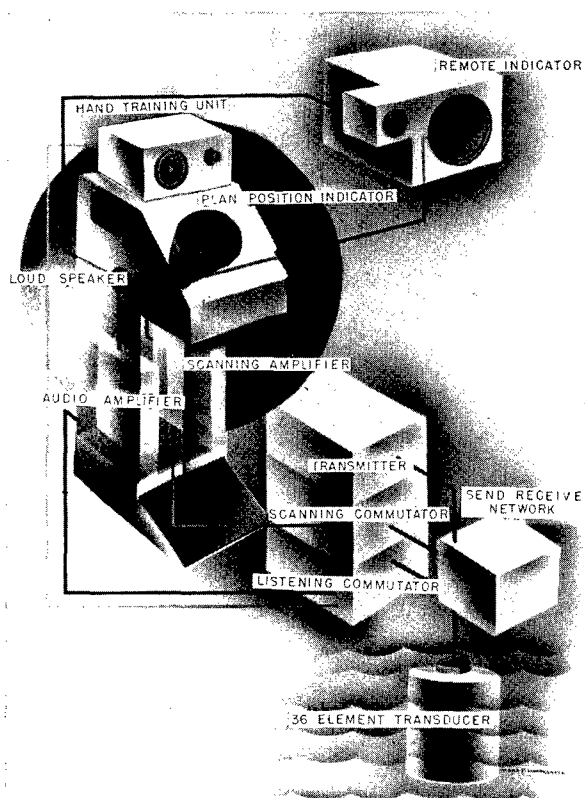


FIGURE 64. Arrangement of units in QH scanning sonar, Model 1.

Figure 63 is a photograph of the PPI front assembly. No other controls were provided on the PPI panel, and no lighting was provided to make the scales visible.

The power supplies for the CRO were on a separate chassis. The true-bearing display was accomplished by inserting a 5 DG synchro between the sweep generator and the deflection coils, its rotor being positioned by a servo motor controlled by a magnetic-compass follower.<sup>66</sup>

During the tests on the AIDE DE CAMP considerable attention was given to console design factors, in particular, the size and relative position of the PPI with respect to the operator. The following general conclusions were drawn:

1. A 7-inch scope was more desirable than a 12-inch.
2. The mechanical cursor was very useful.
3. The true-bearing display could be obtained readily with the DG synchro in the sweep circuit, but the display was confusing to the operator.

4. The electronically brightened range marks<sup>67</sup> were unsatisfactory because of the bright flash of light which distracted the operator.

Following the AIDE DE CAMP tests, the 12-inch scope PPI was removed from the ship and mounted in a mockup console, and used for tests and demonstrations of PPI tube size versus bearing accuracy.<sup>68, 69</sup>

#### 5.5.4 QH Sonar, Model 1 Indicator Console

The Model 1 QH Sonar was installed and tested on the USS SARDONYX and later on the USS CYTHERA (see Section 5.2.3 of this chapter). In this system (Figure 64) the indicator control unit for the sonar operator was built in the form of a console (Figure 65). A

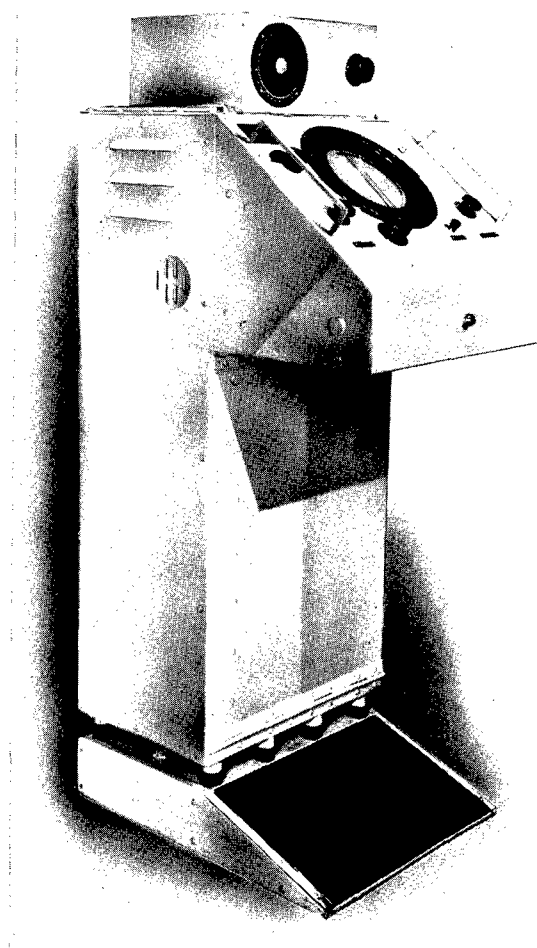


FIGURE 65. Console, QH scanning sonar, Model 1.

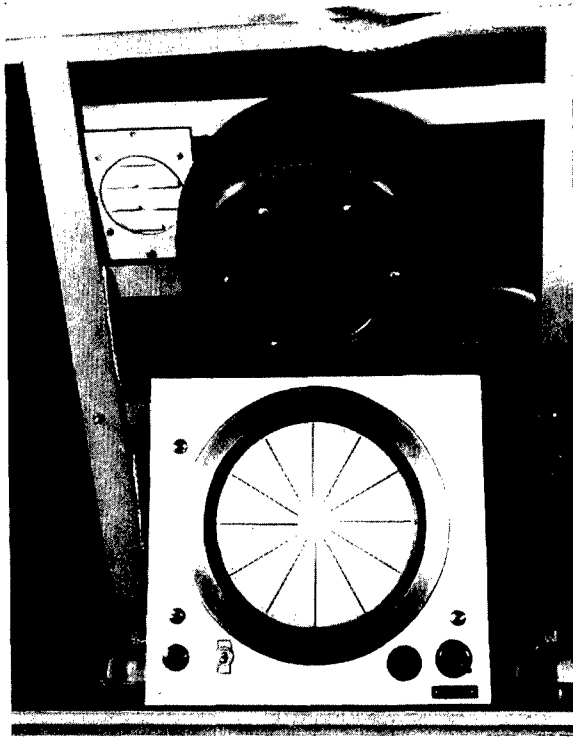


FIGURE 66. Repeater PPI and speaker, QH scanning sonar, Model 1.

remote PPI and loudspeaker were also provided (see Figure 66). This was the first attempt to design a complete operational CR sonar system.

The console was 45 inches high, 18 inches wide, and 24 inches deep overall. The sloping panel containing the scope and controls made an angle of  $37\frac{1}{2}$  degrees with the horizontal. It was designed so that when the operator was seated before the console, the PPI scope would be in such a position with respect to the operator's head that he could readily view the screen. The operating controls are indicated in Figure 65. The following recessed controls were located behind a hinged lid on the sloping panel:

1. Bearing-scale light switch, bright or dim.
2. Scope intensity control.
3. Range-circles brightness control.

In addition to the PPI the operator also had other indicators in the listening rotor repeat-back bearing dial and the loudspeakers. These are also shown in Figure 65. The CRO focus control was located inside the console and was reached through the top lid. Other controls in the console were not considered as operational controls and are treated in other sec-

tions of this chapter. The remote indicator had an on-off switch, a pilot light, and an intensity control (see Figure 66). In order to make all parts readily accessible for maintenance, all chassis were hinged to swing outward (see Figure 67).

The PPI tubes in both the console and repeater were type 7BP7, equipped with 3-phase deflection-coil assemblies which were stators of size 5 synchros.

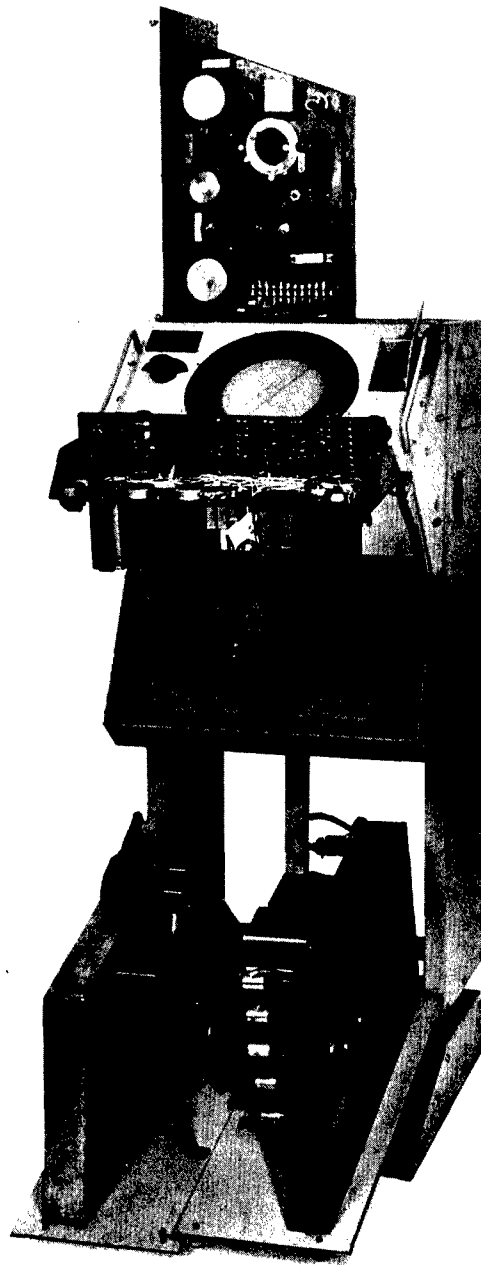


FIGURE 67. Open console, QH scanning sonar, Model 1.



The power supplies for the console scope were mounted on a chassis in the lower part of the console, as shown in Figure 67.

The hand-training unit for the listening commutator (see Figure 64) contained a 5 CT synchro geared to the manual knob and a 5F synchro to drive the repeat-back dial. The console scope-bearing cursor and scale were edge-lighted to permit the operator to see the cursor and the bearing marker at the end of the cursor.

Since the center of gravity of the console was practically over the front rubber mountings, a base was provided to prevent it from tipping forward when not fastened down. This also served as a footrest (see Figure 65).

There were several defects in the console design. At the time the design of the console was started, the importance of the listening channel was not realized, and hence none was at first provided. Consequently, there was neither sufficient space within the console to mount the listening receiver and associated parts, nor room on the front panel to place the training control, speakers, or bearing indicator. The training control and bearing dial were, therefore, not easily accessible. The loudspeakers were placed one on each side of the console. This made it very difficult to hear the audio output signals since they were beamed away from the operator.

The range marks proved to be unsatisfactory, because they were confusing rather than helpful in estimating range. The design of the keying circuits was such that the system could not readily be keyed by a chemical recorder. While it was not realized at the time, the ganging of the on-off switch with the range selector was undesirable because the equipment could be turned off inadvertently during an attack run and the time delay would disable the equipment for an appreciable length of time. Absence of maintenance of true bearing on both the scope-bearing console and the hand-training unit for listening was evident.

#### 5.5.5 Model 2 Console and Repeater

Figure 68 shows the functional position of the Model 2 console, remote indicator, and range recorder in the complete system.<sup>70</sup> Figures 69, 70, and 71 show the console and remote indicator. Figure 72 shows the front panel of the control unit in greater detail. With this model all defects mentioned for

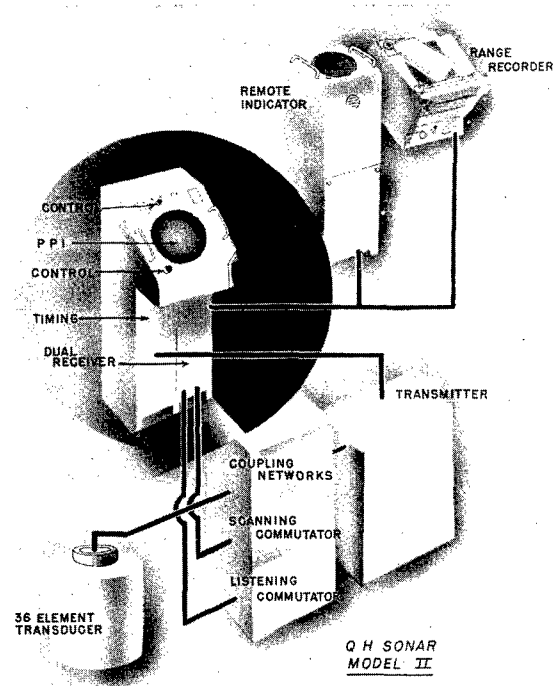


FIGURE 68. Arrangement of units in QH scanning sonar, Model 2.

Model 1 were corrected with the exception of the ganging of the on-off switch with the range selector. In addition, other improvements were made, such as reduction of the number of operational controls, addition of the bearing and range cursor on the remote indicator, and greater reliability in the electronic circuits and components.

The console was of the same general shape and construction as the Model 1 console. It differed in the following respects, however:

The hand-training wheel was located on the lower right corner of the front panel. This positioned the bearing cursor through a 36-to-1 gear reduction and differential gearing, thus permitting changes in ship's course to be added by a servo system controlled by the ship's gyrocompass. By this means, MTB was applied to the cursor. The cursor was a transparent strip having engraved radial lines about 20 degrees apart and a range scale consisting of engraved arcs at intervals corresponding to 100, 250, and 500 yards respectively for range selection settings of 1,500, 3,700, and 7,500 yards.

Both the scanning and listening channels were controlled by a common gain control. The hand key was moved to the front panel and located behind a hinged door (see Figures 69 and 70). A switch to trans-

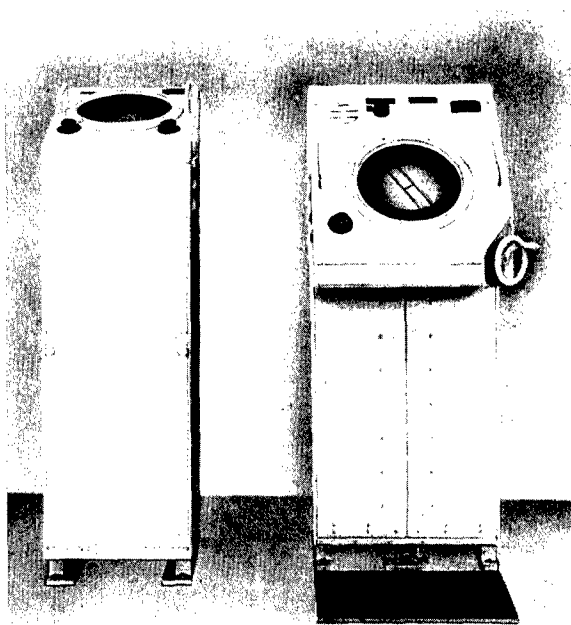


FIGURE 69. Repeater and console closed, QH scanning sonar, Model 2.

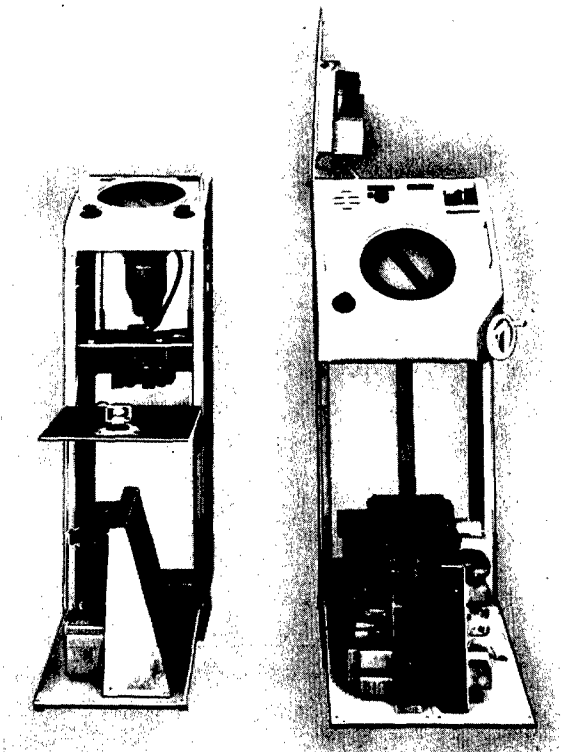


FIGURE 70. Repeater and console open, QH scanning sonar, Model 2.

fer keying control from the console to the chemical recorder was added. The on-off and range selector switch was provided with lights indicating the position of the switch. The above five controls were the only ones required for operation. Scope adjustments, namely, range start, range limit, focus, and intensity, were accessible by lowering the power-supply-sweep chassis (lower left side of console). These may be seen in Figure 70. The loudspeaker was placed on the front panel.

The cursor and true-bearing scales tended to stick and consequently not follow accurately. Because the drive was mechanically complicated, careful alignment and accuracy of construction were required to prevent this difficulty. Figure 73 is a schematic diagram of the training system with its associated deflection circuits. All synchros were standard with the exception of the sweep generator, which was a 5 CT with its rotor rewound for higher impedance and equipped with special brushes for high-speed rotation. The deflection coils were 5 CT stators especially wound for higher impedance.



FIGURE 71. Rear view of repeater and console, QH scanning sonar, Model 2.

CONFIDENTIAL

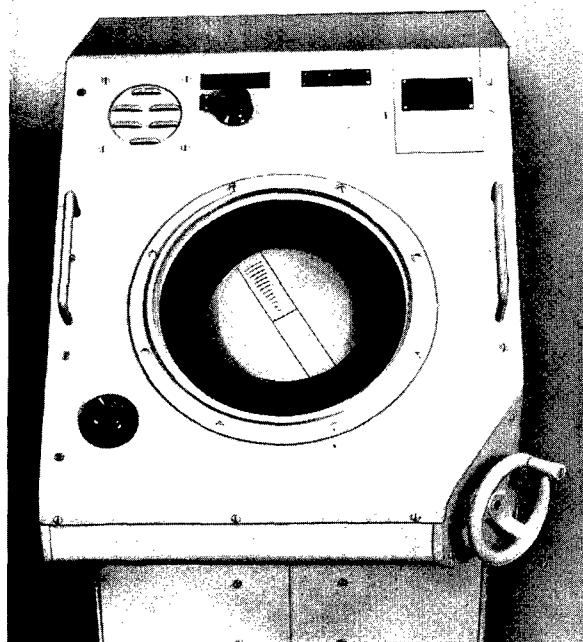


FIGURE 72. Operator's view of console panel, QH scanning sonar, Model 2.

The remote indicator had a PPI scope with cursor and bearing-dial assembly similar to that in the operator's console. Two controls were provided, audio gain (including on-off switch) and scanning gain control. A speaker was provided in the front panel. The remote indicator was rather large, because of the presence of synchros and other iron-cored components which had to be kept away from the cathode-ray tube to prevent their fields from causing spurious deflections.

The second anode power supply for the console scope was located on the lower left chassis of the console (see Figure 70). The schematic diagram of this power supply is shown in Figure 107. Figure 74 shows the schematic diagram for the remote indicator power supply.<sup>70</sup>

Four servo amplifiers were used in the system. These were all identical and readily replaceable or interchangeable. Figure 75 is a schematic diagram of these amplifiers.

The range marks on the mechanical cursor were difficult to interpret because of the choice of selected range; which gave multiplying factors of 2.5 and 5

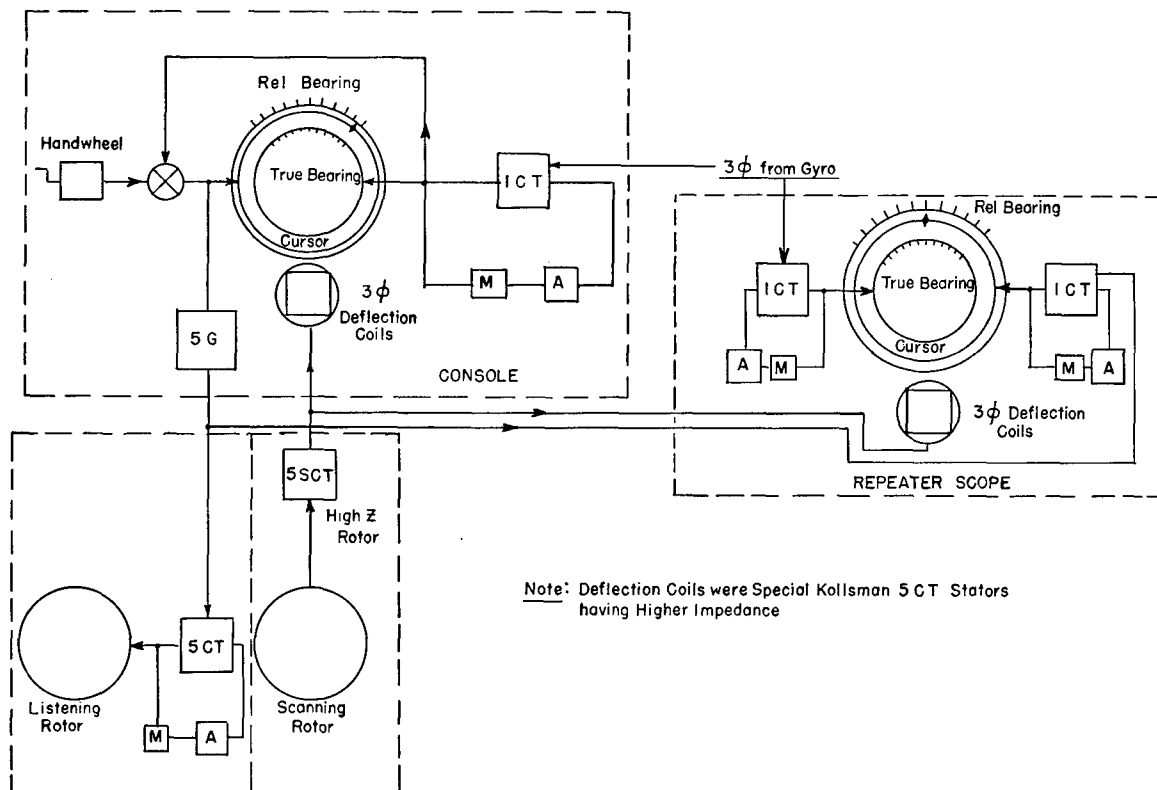


FIGURE 73. Schematic diagram of training and deflection system, QH scanning sonar, Model 2.

CONFIDENTIAL

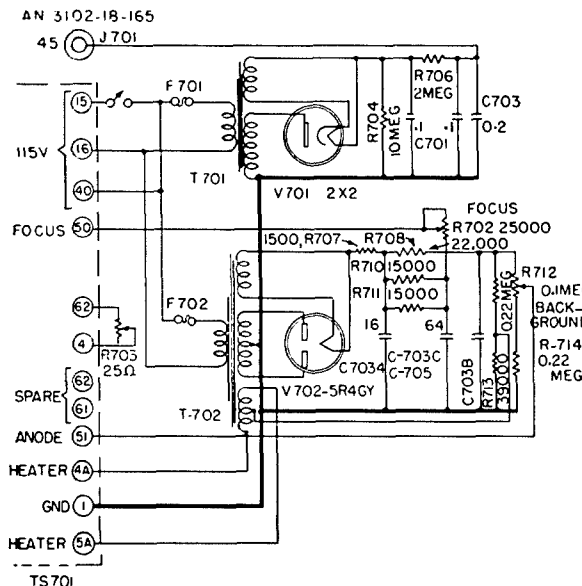


FIGURE 74. Circuit diagram of repeater power supply, QH scanning sonar, Model 2.

for the longer ranges. The particular choice of range limits was based on those used in the standard chemical range recorder, which could key the system during attack runs. The cursor was supported by a ring rotating about the center of the scope face, which also carried a diamond-shaped bug to indicate cursor bearing. Outside the ring there was a fixed relative-bearing scale and inside was a true-bearing scale positioned by the same servo system which drove the differential gearing for the handwheel and cursor.

Some of the defects of this system were as follows:

1. There was considerable backlash in the hand-training wheel.
2. The true-bearing scale and the cursor would sometimes stick, making them inaccurate.
3. Some difficulties were experienced with the lighting of the cursor and bearing scales.
4. The ganging of the on-off switch with the range selector was undesirable.
5. No lighting was provided for the keying selector switch (local or remote). If thrown to remote (recorder) when the recorder was not keying, the beam would go off the screen and the current in the sweep tubes would become excessive. A limiter should have been provided.
6. No hoist control was provided.
7. The speaker on the remote indicator was inadequate.

In general, however, the indicators on this system

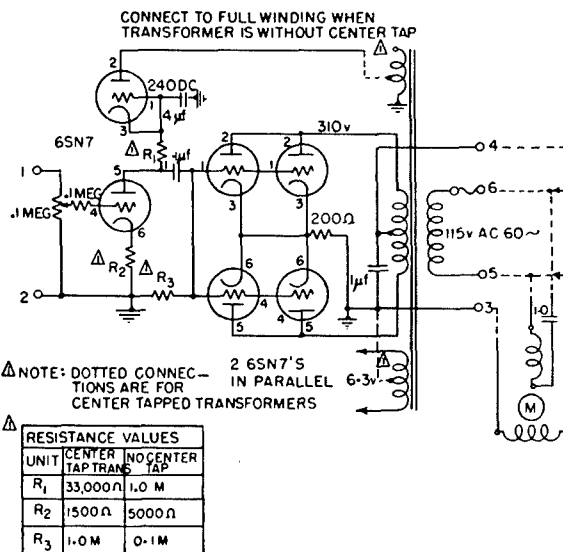


FIGURE 75. Circuit diagram of servo amplifier, Model 3.

performed very well. The console design was good, and accessibility for maintenance was excellent. The equipment was reasonably independent of line voltage variation effects.

#### 5.5.6 Indicators for 26-kc Depth-Scanning Sonar

The 26-kc depth-scanning sonar<sup>71</sup> was set up to test the performance of a complete depth-scanning system so that information would be available for designing the integrated Type B sonar (see Chapter 6), in which depth scanning would be combined with azimuth scanning. There were no particular changes in the indicators, descriptions of which are given in Chapter 6.

#### 5.5.7 XQHA Indicators

The Model XQHA scanning sonar indicators included the following units:

1. The indicator control unit (console)
2. The remote indicator
3. The chemical range recorder
4. The loudspeakers
5. The remote-bearing indicator

The reader may refer to the block diagram in Figure 76 for the functional relations of the indicators to the

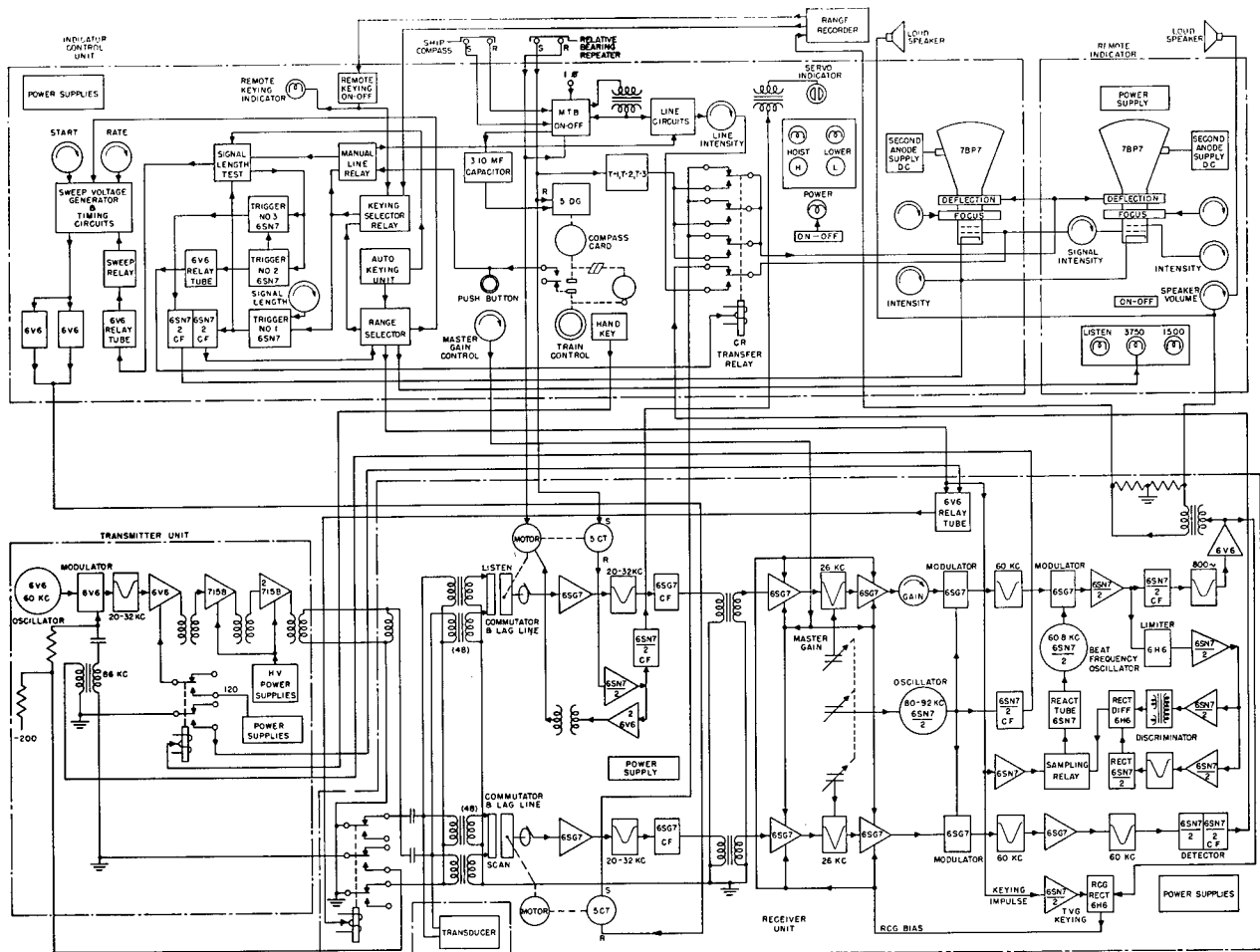


FIGURE 76. Block diagram of Model XQHA scanning sonar.

system. As this system is described in detail in reference 1 and briefly at the beginning of this chapter, only the chief essentials of the indicators are described here.

The following innovations were introduced into the XQHA equipment:

1. An electronic cursor replaced the mechanical cursor of Model 2. This eliminated three of the four servo systems of Model 2 and reduced mechanical gearing problems at the expense of requiring additional tubes and relays.
2. The true-bearing indicator was a dial below the scope and was designed so that only that portion of the dial was visible which was near the true bearing to be read.
3. Instead of having the cursor repeat the position of the commutator, a neon lamp indicated whether or not the servo system was satisfied. The operator

was able to position the cursor quickly to determine new target bearings.

4. A battle-damage switch was provided to shift from true bearings to relative bearings in the event of failure of the ship's gyrocompass system.

5. Controls and indicator lamps were provided for the hoisting and lowering of the transducer.

6. An indicator was provided to show whether keying was done by the control unit or the recorder. Control of change-over was placed at the recorder.

7. A separate on-off switch was used to reduce the likelihood of inadvertent shutdown of equipment during an attack run.

8. Provision was made to determine on the PPI screen the transmitted pulse length in terms of rotation period.

The indicator control unit, shown in Figures 77 and 78, was the operating station of the complete

CONFIDENTIAL

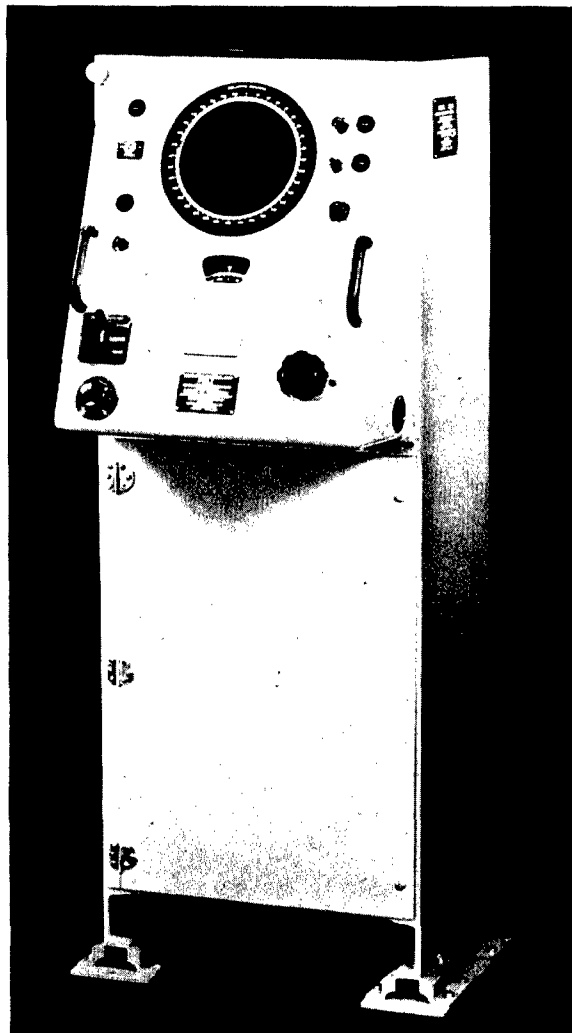


FIGURE 77. Indicator control unit, Model XQHA scanning sonar.

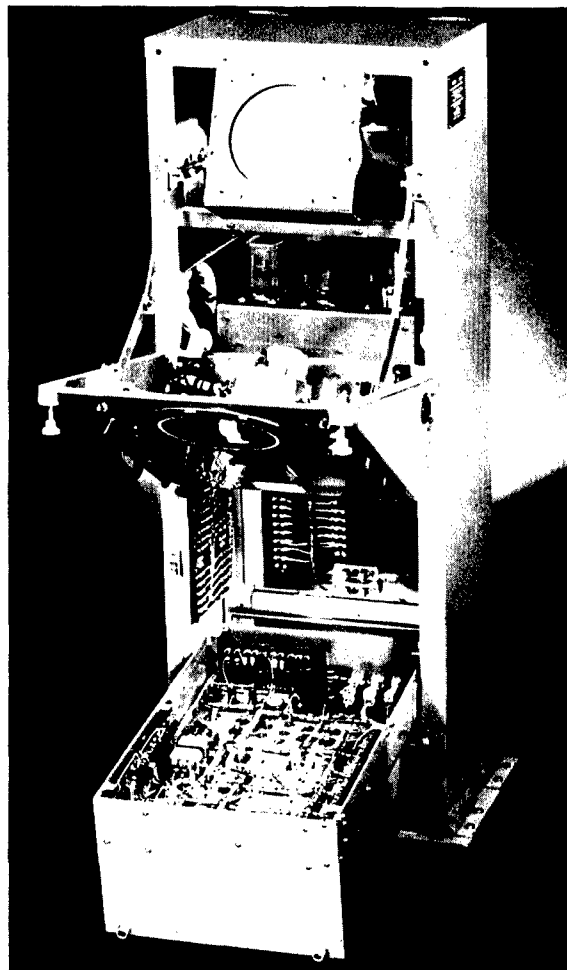


FIGURE 78. Indicator control unit open, Model XQHA scanning sonar.

system. It contained the PPI controls and was designed to conserve space. The elements of the unit were:

1. The cabinet assembly
2. Control panel assembly
3. Power supply and keying chassis
4. PPI tube assembly
5. The deflection chassis
6. The second anode power supply

The cabinet construction may be deduced from Figures 77 and 78. The PPI tube assembly is shown in Figure 79. The following controls and indicators were located on the main control panel:

1. PPI screen surrounded by relative-bearing scale.
2. Bearing indicator dial (normally would show true bearing of listening channel when MTB switch is changed to on).
3. Transducer hoist and lower control buttons and indicator lamps.
4. Indicator light to indicate condition of listening commutator servo system (whether listening channel is trained to position indicated by cursor).
5. Power switch and pilot light.
6. Local-remote keying indicator light and switch.
7. Push button switch for electronic cursor.

CONFIDENTIAL

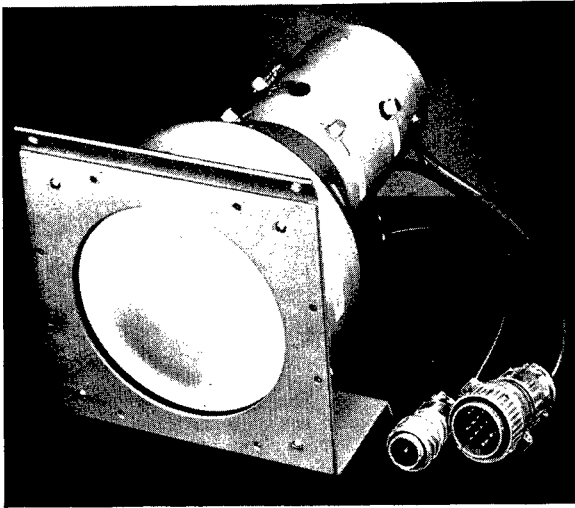


FIGURE 79. CRO tube assembly, Model XQHA scanning sonar.

8. Range selector toggle switch.
9. Gain control for scanning and listening channels.
10. Hand-training knob for training listening beam and positioning cursor.
11. Hand key for communication purposes.

The true bearing dial was mounted on the spindle of a 5 DG synchro whose position determined the cursor position, and whose electric order controlled the training of the listening commutator. The stator of the 5 DG was connected to the ship's gyro while its rotor was driven mechanically by the training knob. A clutch-and-gear assembly permitted two rotation speeds of the synchro rotor by the knob, 18:1 and 1:1. The higher speed was chosen by pushing the knob in before rotating it.

When properly aligned, the output of the synchro rotor was an electric order representing the relative bearing of the electronic cursor and the relative bearing of the listening beam of sensitivity (if the neon lamp were not lighted). The bearing shown on the bearing card was the true bearing of the cursor and commutator. Because changes of the ship's course were introduced by the gyro order, the true bearing of the cursor and listening commutator remained constant if the hand-trained knob was not turned (MTB).

The PPI indicator plot was in relative bearing, since the sweep generator was geared directly to the

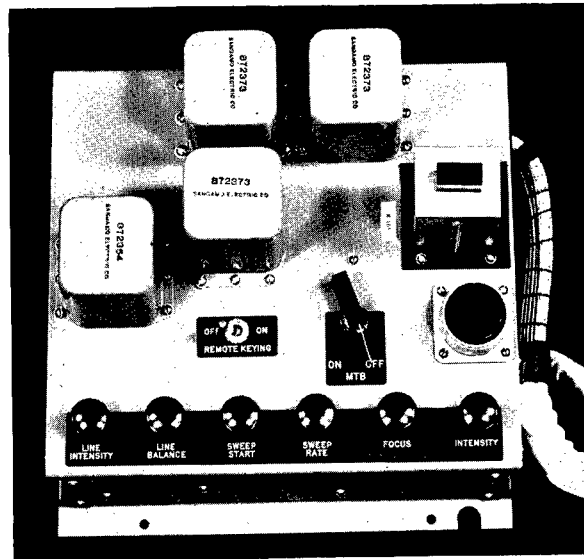


FIGURE 80. View of deflection chassis, Model XQHA scanning sonar.

shaft of the scanning commutator. The generator was so adjusted that the 000-degree relative bearing was at the top of the screen.

Figures 80 and 81 are photographs of the deflection chassis and the second anode power supply for the PPI tube. The deflection chassis contained the following controls: potentiometer controls for PPI intensity and focus, sweep start and limit control, and the electronic-cursor-line balance control and intensity control. Figure 82 shows a schematic diagram of the circuits involved in keying, the PPI tube display, and the electronic cursor, as well as the PPI tube power supplies. Figure 83 is a schematic diagram of the circuits concerned with the directional control of the scanning and listening beams of receiving sensitivity.

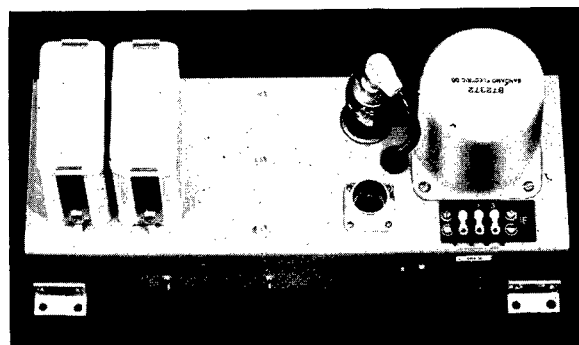


FIGURE 81. View of second anode supply, Model XQHA scanning sonar.

Photographs of the remote indicator unit are shown in Figures 84 and 85 and a photograph of the remote indicator control chassis in Figure 86. Controls for intensity, focus brightening level, and speaker volume were provided.

A standard CAN-55139 chemical range recorder was used. When the main control switch of the recorder was turned to on, contacts operated a relay in the indicator control unit, switching the control of keying to the recorder which supplied a positive pulse to initiate the keying cycle. The listening receiver supplied the echo signals to mark the recorder. Provision was made to energize a standard bulkhead-mounted bearing repeater if desired.

Operation with the indicators of the Model XQHA scanning sonar was satisfactory. The electronic cursor proved convenient, and its simplicity and lack of parallax were appreciated by operators. In preliminary tests in the spring of 1945 accuracies of  $\pm 1$  degree, with respect to pelorus bearings, were indicated and extensive tests to obtain further data were planned. BDI was added and performed as well as with searchlight-type sonar; tests were planned to determine whether or not its inclusion was justified in terms of increased accuracy or ease of operation.

#### 5.5.8

### Geographic Plot

To investigate the possibilities of geographic plotting with scanning sonar, changes were made in a General Electric *attack plotter* [ASAP],<sup>72</sup> Mark I, Mod. 2, Serial 556, to adapt it for use with QH gear.<sup>73</sup> Laboratory tests using OTE 5,<sup>28</sup> Serial 1, were made and also shipboard tests on USS CYTHERA in conjunction with QH sonar Model 1, Serial 1.<sup>74</sup> Further tests were conducted in the spring of 1945 in conjunction with the Model QFA-5 attack teacher.<sup>28</sup>

Changes were made on the echo-amplifier chassis and the sweep chassis of the ASAP. Those in the echo amplifier will be described first. Because the amplitude of the signal from the receiver of the QH sonar was sufficient for brightening the cathode-ray tube in the ASAP, it would have been possible to apply this signal directly to the ASAP grid without an intervening amplifier. However, since the time required to put on own-ship's spot and the predictor line was somewhat greater than the blanking time on the QH sonar, it was necessary to incorporate a special circuit in the ASAP for blanking out indication on the ASAP for the time taken for own-ship's spot and the elec-

tronic predictor line. The modification required to perform this operation is shown in Figure 87. Tube V303 is a cathode follower which feeds the signal to the cathode-ray tube grid. The other half of V303 is connected as a diode limiter to keep excessive signal level from being applied to the CRO grid. Blanking is accomplished by connecting the grid of the cathode-follower tube to a bleeder, one end of which is connected to the negative bias supply voltage, and the other end to the plate of V304. This thyratron tube fired when the relays were thrown in the ASAP, and its plate potential thus fell to a very low value. When this operation occurred, the grid bias of the cathode follower was dropped to cutoff value. This kept any signal from the QH receiver from arriving at the grid of the cathode-ray tube during the time when the relays in the ASAP were being operated.

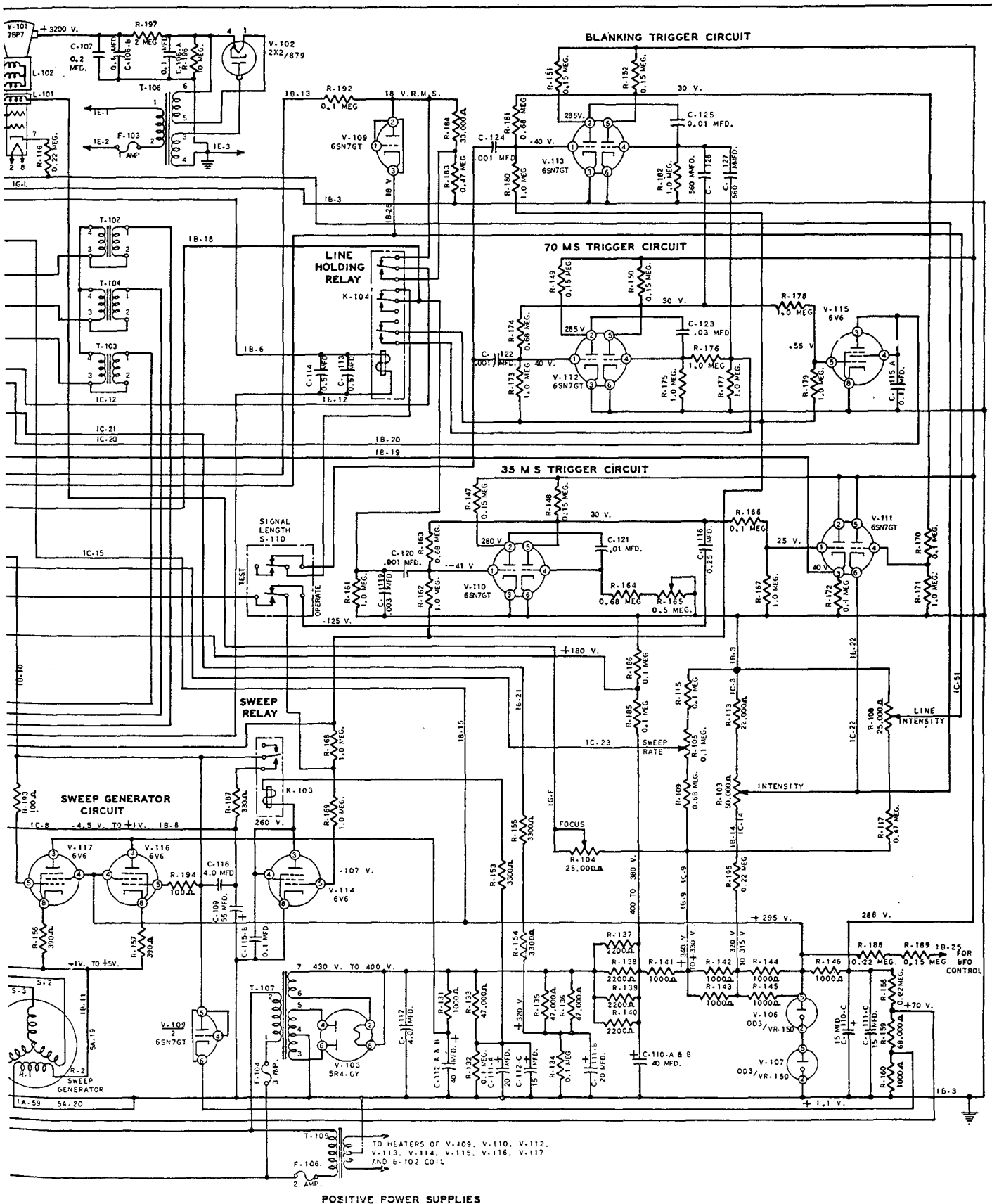
In order to retain the short-echo feature of the ASAP, the signal from terminal No. 329 furnished the input for a three-stage amplifier in which double differentiation of the echo pulse occurred. The output of this amplifier was applied to terminal No. 324 of the full-echo switch. Short echo, which gave a narrower peak to the echo pulse generated by the QH receiver, was thus provided. It was found that this narrow peak was about half the width of the ordinary pulse and was centered on the peak of the original pulse as closely as could be ascertained. However, even the shorter pulse obtained with this double differentiating arrangement was not short enough to duplicate the normal appearance of the ASAP indication, and unless a method of obtaining an even shorter pulse can be developed, the attempt to shorten the normal scanning pulse is probably not worth while.

The other changes were made on the sweep chassis in such a way as to allow the spiral sweep to be applied to the sweep coils of the cathode-ray tube in place of the original linear sweep. Those changes are quite simple in form and may be seen in Figure 88. The sweep signal from the QH spiral-sweep generator was fed through the 5 SCT synchro, to the Scott-connected transformers built into the ASAP. The sweep signal was fed directly through R504 to terminal 8 on relay A.

In order to return own-ship's spot to the center of the circle each time a pulse was transmitted, the inductor L502 was replaced by the secondary of a transformer, Audio Development Type A3920. Additional circuits were so arranged that a capacitor was dis-







ying and CRO control. Model XQHA scanning sonar.

2

CONFIDENTIAL

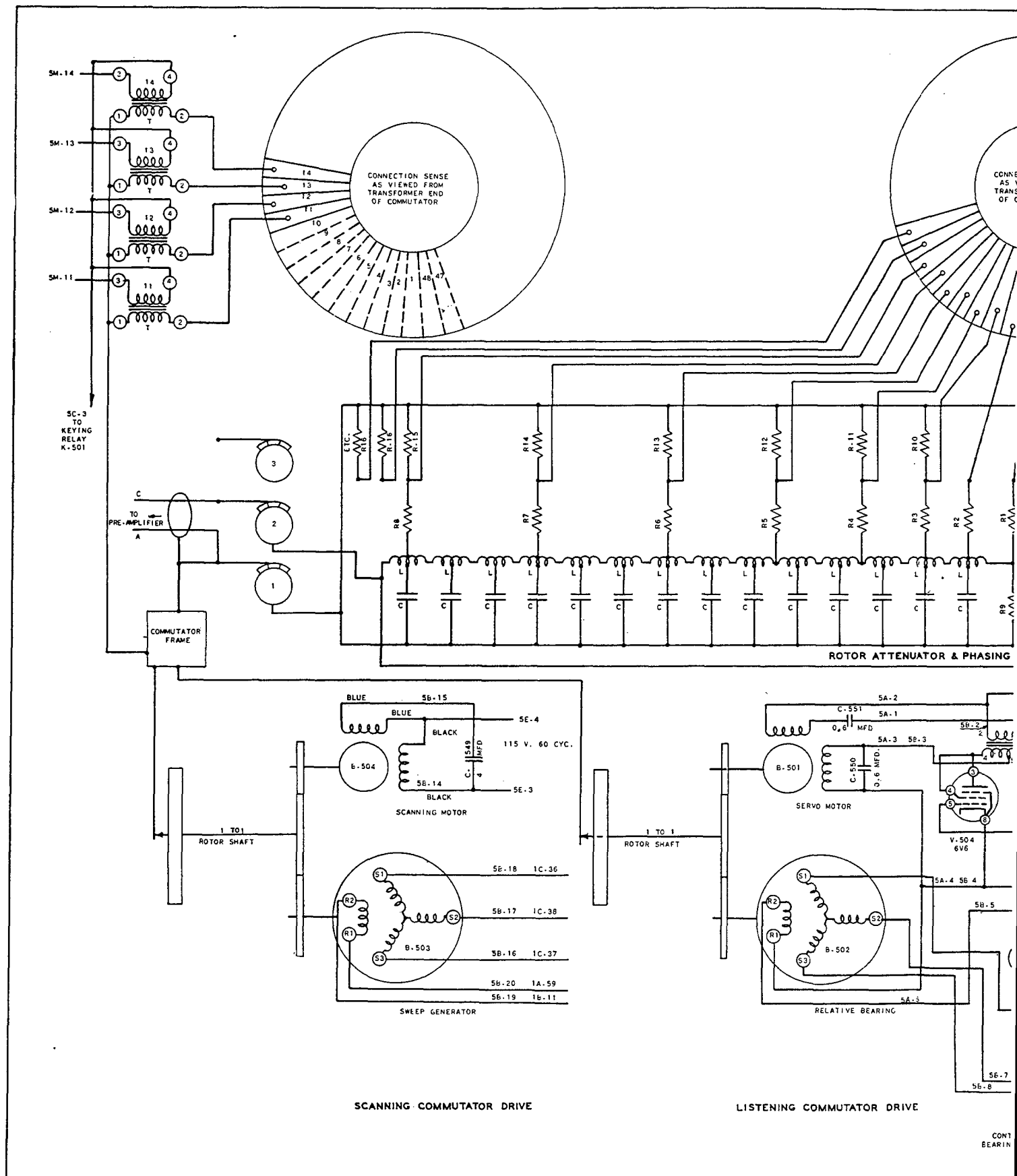
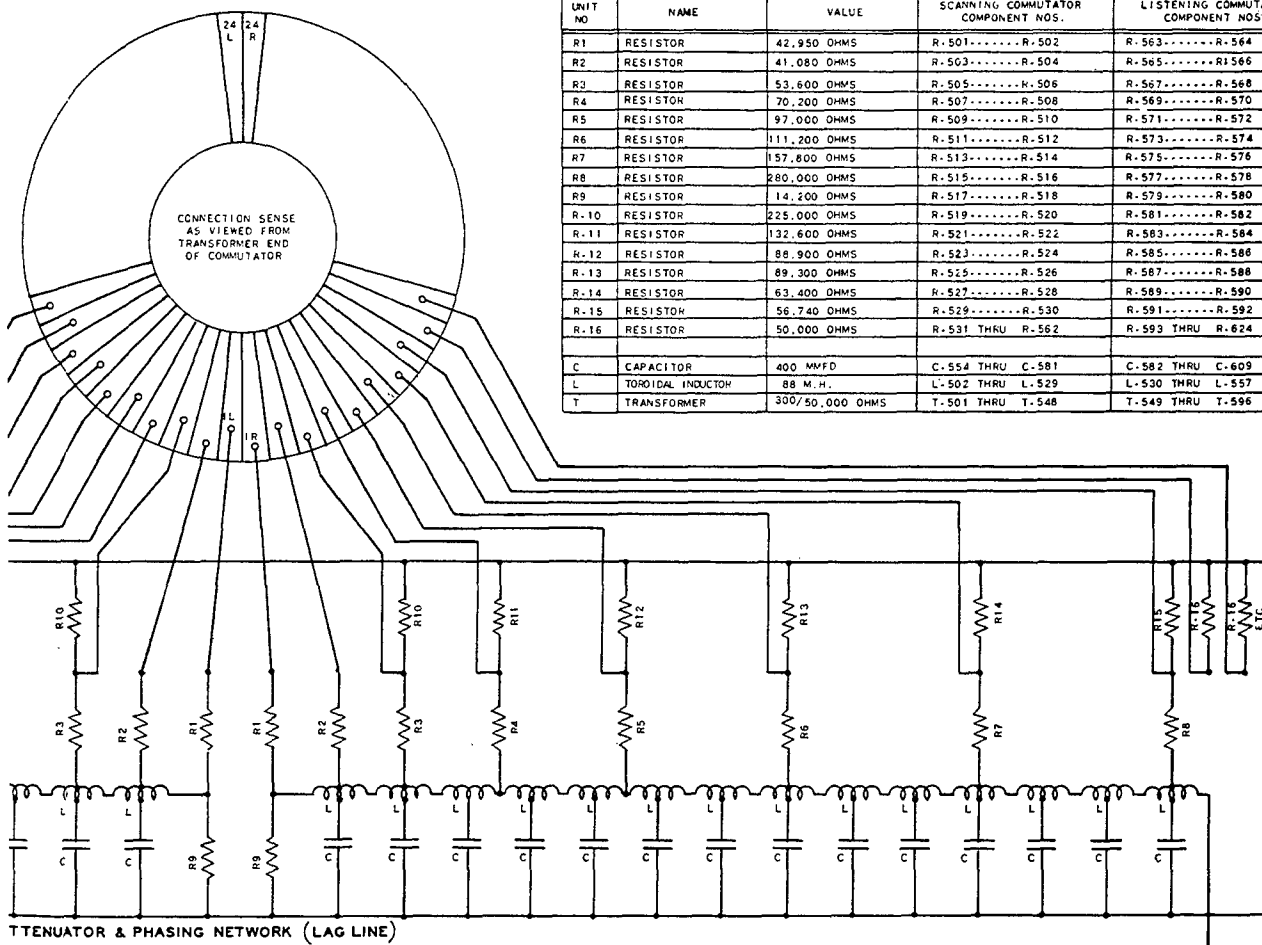
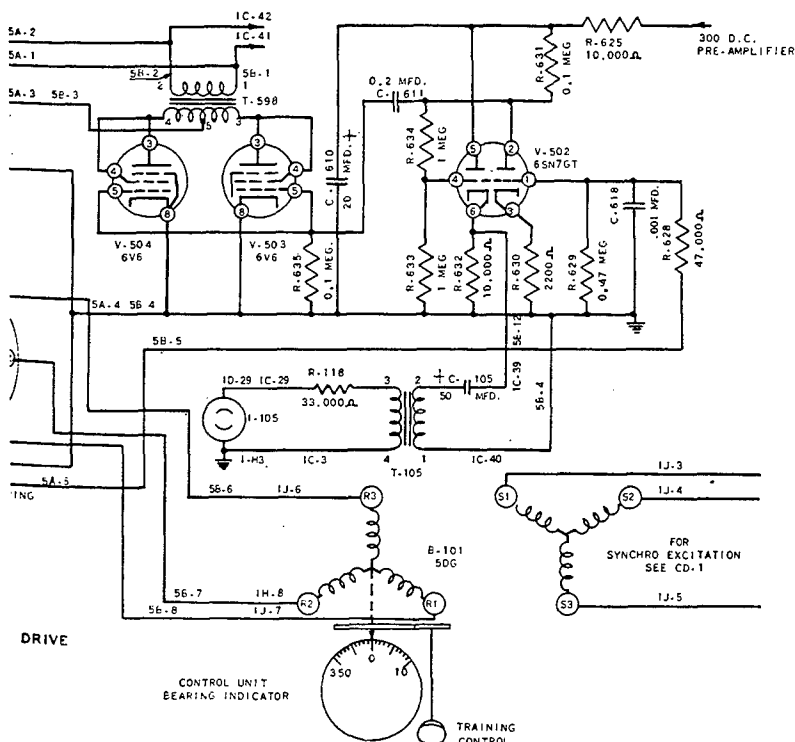


FIGURE 83. Circuit diagram of directional sensitivity control, ?

1



UNIT NO	NAME	VALUE	SCANNING COMMUTATOR COMPONENT NOS.	LISTENING COMMUTATOR COMPONENT NOS.
R1	RESISTOR	42,950 OHMS	R-501.....R-502	R-563.....R-564
R2	RESISTOR	41,080 OHMS	R-503.....R-504	R-565.....R-566
R3	RESISTOR	53,600 OHMS	R-505.....R-506	R-567.....R-568
R4	RESISTOR	70,200 OHMS	R-507.....R-508	R-569.....R-570
R5	RESISTOR	97,000 OHMS	R-509.....R-510	R-571.....R-572
R6	RESISTOR	111,200 OHMS	R-511.....R-512	R-573.....R-574
R7	RESISTOR	157,600 OHMS	R-513.....R-514	R-575.....R-576
R8	RESISTOR	280,000 OHMS	R-515.....R-516	R-577.....R-578
R9	RESISTOR	14,200 OHMS	R-517.....R-518	R-579.....R-580
R-10	RESISTOR	225,000 OHMS	R-519.....R-520	R-581.....R-582
R-11	RESISTOR	132,600 OHMS	R-521.....R-522	R-583.....R-584
R-12	RESISTOR	88,900 OHMS	R-523.....R-524	R-585.....R-586
R-13	RESISTOR	89,300 OHMS	R-525.....R-526	R-587.....R-588
R-14	RESISTOR	63,400 OHMS	R-527.....R-528	R-589.....R-590
R-15	RESISTOR	56,740 OHMS	R-529.....R-530	R-591.....R-592
R-16	RESISTOR	50,000 OHMS	R-531 THRU R-562	R-593 THRU R-624
C	CAPACITOR	400 MMFD	C-554 THRU C-581	C-582 THRU C-609
L	TOROIDAL INDUCTOR	88 M.H.	L-502 THRU L-529	L-530 THRU L-557
T	TRANSFORMER	300/50,000 OHMS	T-501 THRU T-548	T-549 THRU T-596



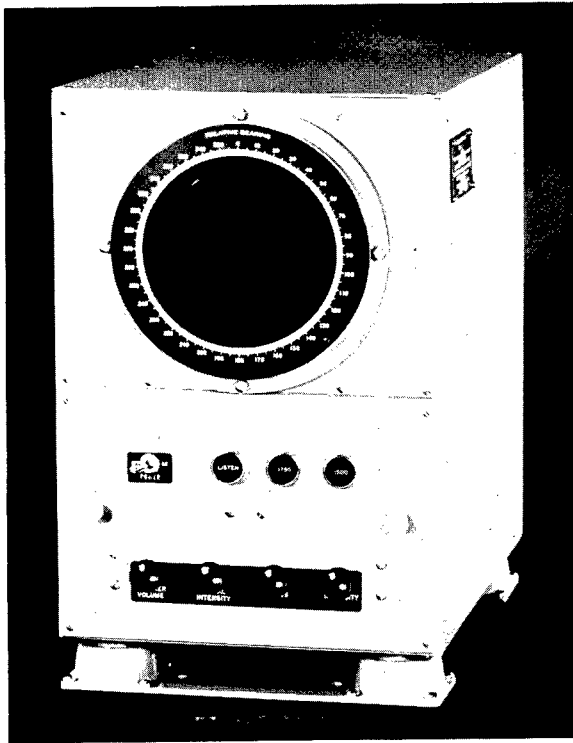


FIGURE 84. Remote indicator unit, Model XQHA scanning sonar.



FIGURE 85. Interior view of remote indicator unit, Model XQHA scanning sonar.

charged through the primary of this transformer at the time of the ping, and this oscillatory discharge demagnetized the deflection coils on the scope, and thus allowed own-ship's spot to return to the correct position each time. Figure 88 shows at B the manner in which two of these transformers were connected in series so that a single 0.1- $\mu$ f capacitor could be discharged through their primaries. The additional relay charged a capacitor during the listening period and discharged it at each pulse transmission. Since the horizontal and vertical deflection sweep circuits in the ASAP were exactly alike, only one of these has been diagrammed in Figure 88. No change was made in the electronic predictor line. These changes permitted the retention of all normal ASAP functions. It was also possible to replace quickly the two modified chassis by standard units.

The equipment was installed on USS CYTHERA. Two methods of connection were tried. First, the standard ASAP chassis were inserted and the ASAP connected to the listening channel of the QH gear. The 5 SCT synchro normally used to change the relative bearing of the projector to true bearing was used

to change the relative bearing of the cursor to true bearing. This was done by applying the signal from the cursor generator synchro to the 5 SCT stator and driving the 5 SCT rotor shaft by means of a 5 F synchro energized by the gyro system, the true-bearing signal coming from the 5 SCT winding. The plotter was synchronized without any difficulty with a signal from the keying circuit of the QH gear. With this arrangement the appearance of the ASAP screen was essentially the same as that obtained when using ordinary QC gear. The attack plotter when operated in this manner appeared to be entirely satisfactory.

Following this, the modified echo and sweep chassis were installed in the ASAP. The 5 SCT was reconnected to place its windings between the QH plan position indicator deflection circuit and the ASAP input, still using the 5 F to drive the rotor shaft with gyro order. Some difficulty was encountered here because, when the 5 SCT was connected so as not to cause serious loading of the sweep generator circuit, the spiral amplitude on the plotter was insufficient. When the connections to the 5 SCT were reversed, sufficient amplitude was obtained to give a suitable

CONFIDENTIAL



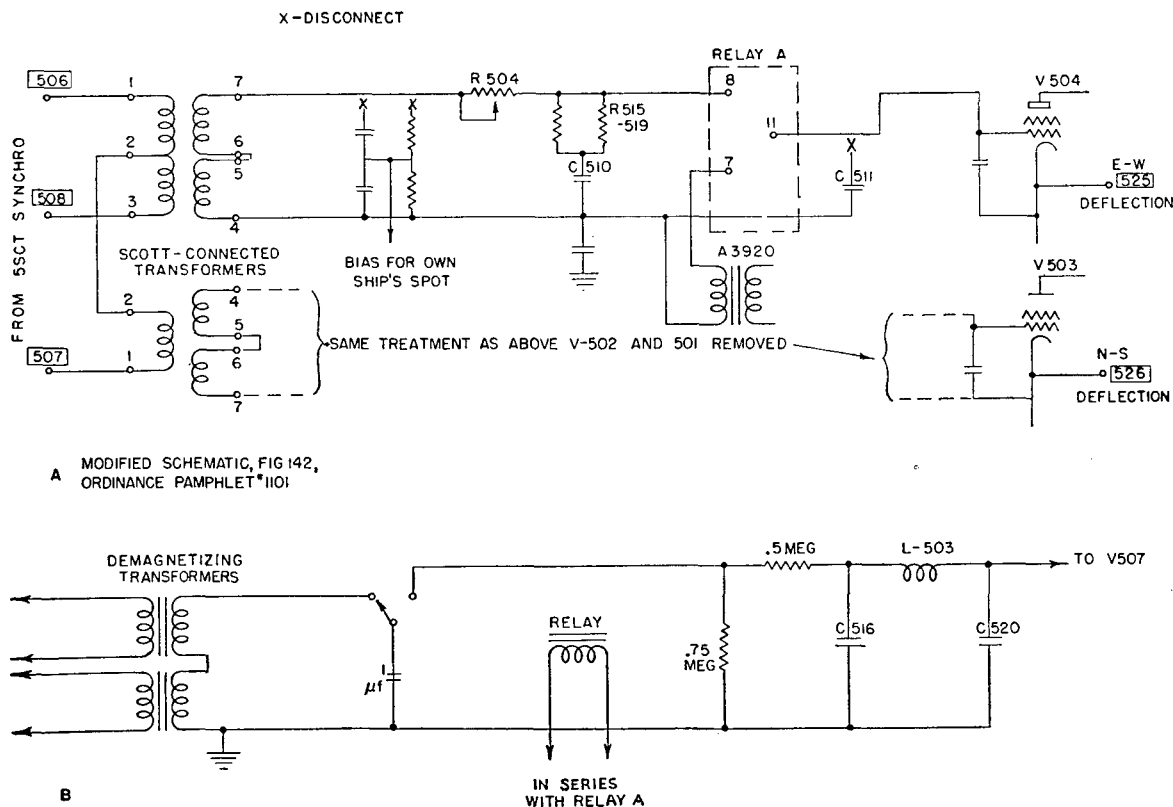


FIGURE 88. Circuit diagram of modifications in ASAP sweep chassis.

One innovation in this receiver was a scheme for varying its gain in accordance with the sawtooth excitation on the spiral-sweep generator. Because the angular velocity of the spiral sweep was constant, the tangential speed of the spot on the indicator screen increased with the radius. This resulted in lowered intensity and reduced persistence as the radius increased. To overcome this, the sawtooth voltage, which had a negative slope, was fed through a potentiometer control to the grid of a 6J5 triode. The cathode of this tube was grounded and its plate tied to the screen of the second 6SG7 amplifier tube; a series resistor connected the screen to the B+ supply. Through variation of the plate resistance of the 6J5 tube, the screen potential was varied so as to increase the receiver gain in direct proportion in the sweep radius. A second pair of contacts on the TVG relay grounded the screen of the 6SG7 to blank the receiver during transmission.

The r-f tuning was adjusted to center the pass band at about 23 kc. The coil coupling was adjusted to flatten the top of the selectivity curve (slightly

greater than critical coupling). The band width at -6 db was 1,900 cycles, and at -20 db, 2,500 cycles.

The preamplifier for this system used two tubes. The first was a 6SG7 pentode amplifier. A doubly tuned transformer coupled the plate of the 6SG7 to the grid of a 6SJ7 tube connected as a cathode follower to give a low output impedance. A 10,000-ohm to 25,000-ohm transformer connected the preamplifier to the commutator output terminals.

### 5.6.3

## SLC Brightening Receiver (Aide de Camp MR System)

It had been proposed that SLC brightening schemes might accomplish a sharpening of the PPI trace, improve the signal-to-reverberation noise ratio, and improve the gain-control operation in a scanning system.<sup>76</sup> To test the possibilities of such a scheme, a Model X-3 BDI was modified for use as an SLC brightening receiver for the MR scanning sonar. This receiver and its operation are described in Chapter 4 in connection with the MR sonar.

CONFIDENTIAL



FIGURE 89. Rear view of chassis B and C of receiver, AIDE DE CAMP ER/CR scanning sonar.

#### 5.6.4 Scanning Receivers Used with Aide de Camp ER/CR Scanning Sonar

During the summer and fall of 1943, the components of an ER/CR system were built and installed on the AIDE DE CAMP. (A block diagram of this system is shown in Figure 5.) Although it was called the AIDE DE CAMP ER/CR system, several different types of receivers were built and tested with it. Descriptions of two of these are given on the following pages.

##### CHASSIS A, B, AND C RECEIVER

This particular receiver was so named because it consisted of three chassis labelled A, B, and C. Chassis A was the preamplifier; chassis B held the r-f and i-f portions of an X-3 type of SLC circuit; chassis C contained the detectors, difference amplifier, differen-

tiator, and pulse amplifiers. Photographs of chassis B and C are presented in Figures 89, 90, and 91. Schematic wiring diagrams of the chassis units are shown in Figures 92, 93, and 94, respectively.

As initially designed, the preamplifier contained two signal channels, each using a 10,000-ohm to 25,000-ohm input transformer with a 6J5 cathode follower. However, as tests indicated a need for improved selectivity to reduce noise, the preamplifier was redesigned to incorporate a band-pass filter and to increase the gain (see Figure 95). With this changed design the preamplifier had a gain of 35 db at 23 kc. The dynamic range was 64 db, and the maximum undistorted signal output was 3.8 volts when loaded with the chassis B input circuits.

In the first design of chassis B (see Figure 92), the two channels each had an input transformer with a tuned secondary, from which the 23-kc signals were applied to the grids of two 6SG7 mixer tubes. Oscillators at 30 kc and 33 kc fed the screens of these mixers, and in their plate circuits were located band-pass filters centered at 7 kc and 10 kc. The outputs from these filters were fed to a common balance-control potentiometer and a common manual-gain-control potentiometer. The combined 7-kc and 10-kc signals were amplified in two stages of resistance-coupled amplification using 6SG7 pentodes, and then fed to chassis C. Automatic gain control was accomplished by varying the bias on the signal grids of the two 6SG7 tubes. Some of the signal appearing at the chassis B output terminals was fed back to the grid of a 6N7

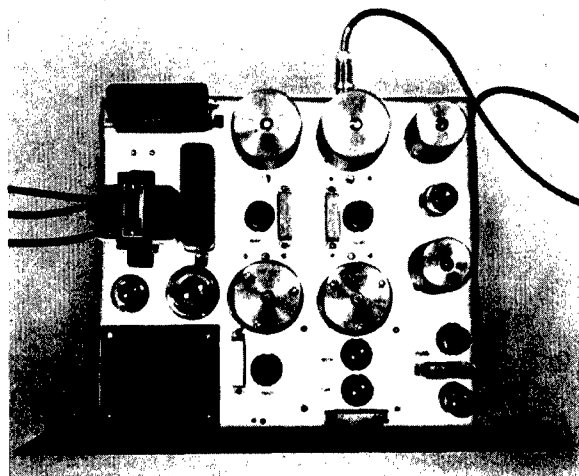


FIGURE 90. Top view of chassis B of receiver, AIDE DE CAMP ER/CR scanning sonar.

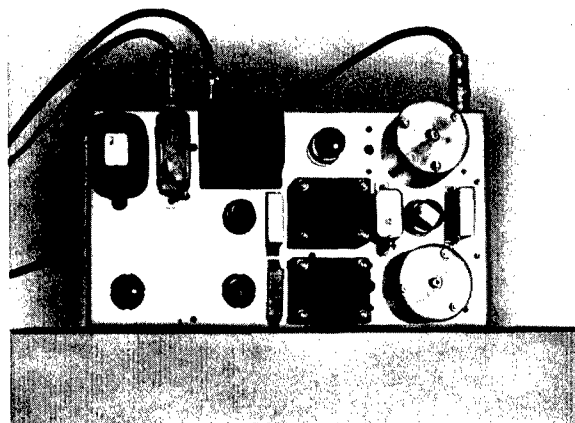


FIGURE 91. Top view of chassis C of receiver, AIDE DE CAMP ER/CR scanning sonar.

CONFIDENTIAL



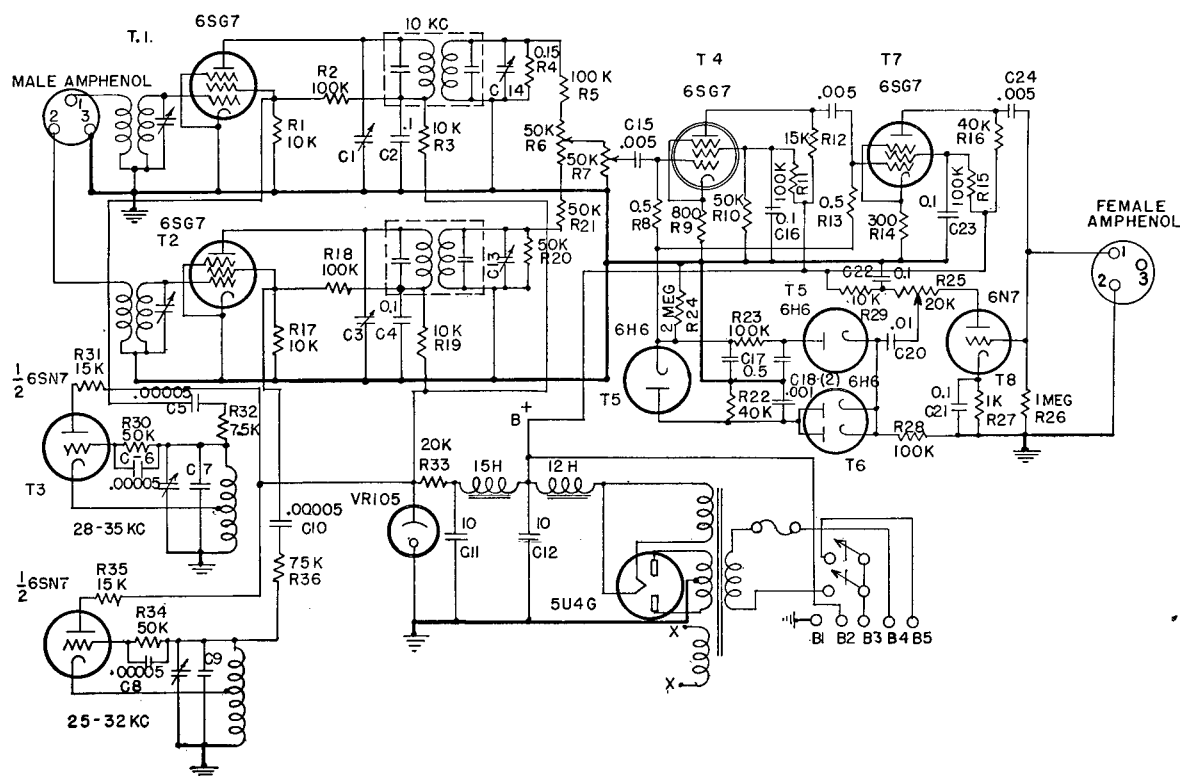


FIGURE 92. Circuit diagram of SLC receiver (chassis B), AIDE DE CAMP ER/CR scanning sonar.

amplifier having a control potentiometer in its plate circuit. Its adjustable output was fed to two rectifiers; one charged a  $0.5\text{-}\mu\text{f}$  capacitor with the energy picked up in the receiver circuits from the transmitter signal, and the resulting negative voltage was fed to the grids of the 6SG7 tubes, thereby reducing the receiver gain. A 2-megohm resistor discharged this bias voltage at a slow rate. The other rectifier also produced a negative voltage, but because of the much shorter time constant of its associated RC circuit, the rectified voltage followed the energy level variation of the reverberation or noise. A diode, T5, was connected between the two negative rectifier outputs in such a manner that the  $0.5\text{-}\mu\text{f}$  capacitor discharged through 40,000 ohms in parallel with the 2.0 megohms, provided that the voltage output of the second rectifier was lower than that of the first. This circuit arrangement comprised one type of RCG. If the reverberation died out rapidly, the gain was restored rapidly; otherwise restoration was slow. The relative rates were determined by the two RC time constants, which were approximately 0.02 second and 1.0 second respectively. Later the circuits of the chassis B unit were modified as shown in Figure 93. Chassis C (see

Figure 94) contained the remainder of the receiver. The output signal from chassis B was fed to the primaries of two filter transformers (band-pass) where the 7-kc and 10-kc components were separated and each signal component fed to a separate triode (6SN7), operating as a detector. The two rectified outputs were impressed directly onto the grids of a second pair of 6SN7 triodes which comprised the difference amplifier. The plates of the difference-amplifier tubes were connected to the push-pull primary of a transformer.

The two pulses present in the two transformer primaries were similar to those shown in Figure 96A. The resulting difference is shown in Figure 96B. The derived pulse appearing in the secondary of the transformer is illustrated in Figure 96C. The latter was amplified by the 6SG7 amplifier and then fed through a gain-control potentiometer to a 6J5 cathode-follower output stage. To blank the receiver during transmission, a pulse was fed to the grid of a 6V6 connected as a triode. Because the plate resistance of this tube formed the lower leg of the screen divider for the 6SG7 amplifier, when the positive blanking pulse was applied to the 6V6 grid, its plate resistance dropped,

CONFIDENTIAL

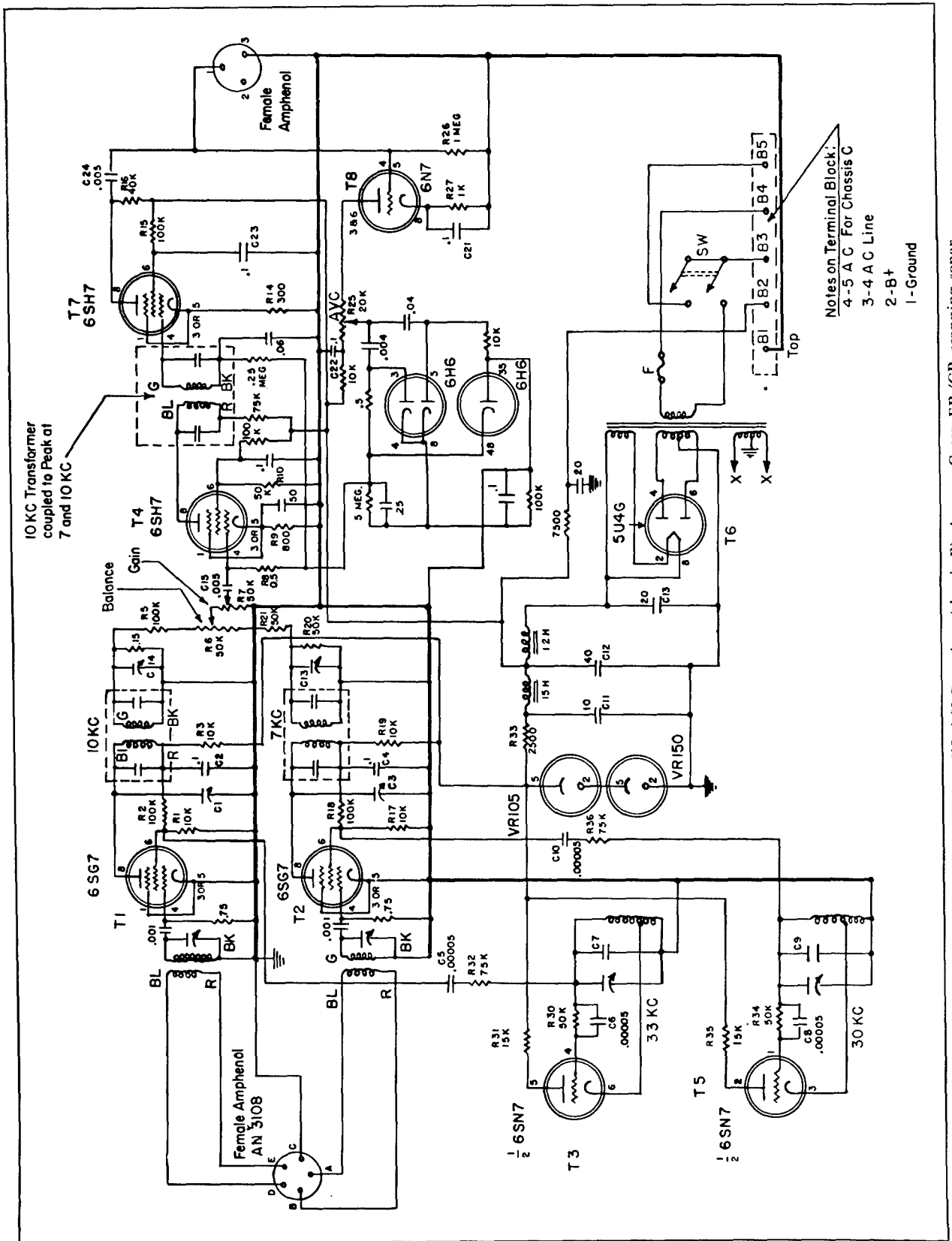


FIGURE 93. Circuit diagram of modified SLC receiver (chassis B), Amd de Camp ER/CR scanning sonar.

CONFIDENTIAL

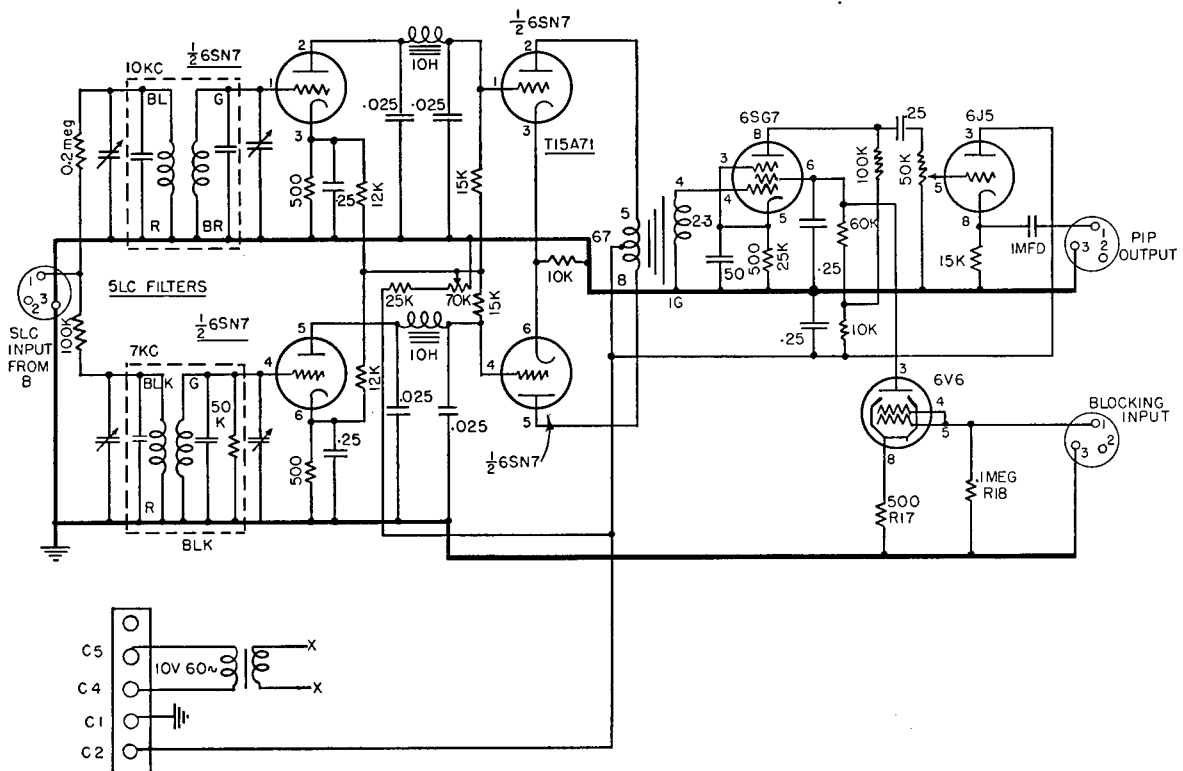


FIGURE 94. Circuit diagram of receiver output (chassis C) AIDE DE CAMP ER/CR scanning sonar.

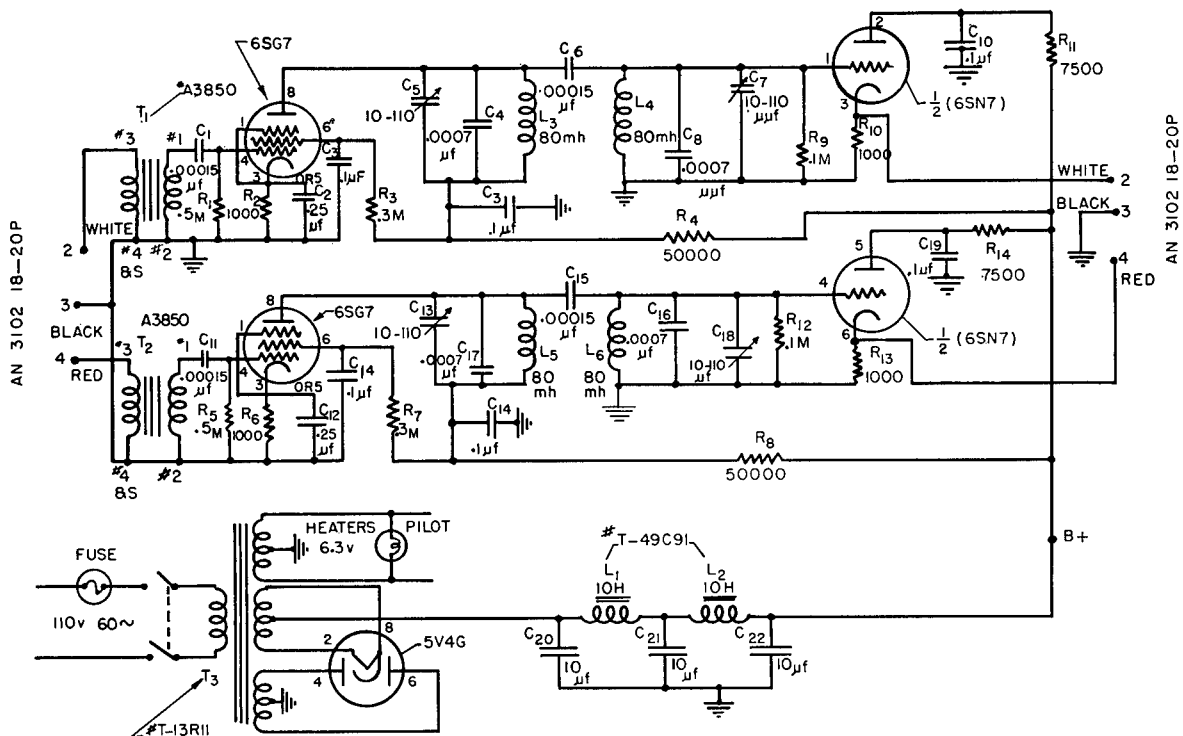


FIGURE 95. Circuit diagram of redesigned preamplifier (chassis A) AIDE DE CAMP ER/CR scanning sonar.

CONFIDENTIAL

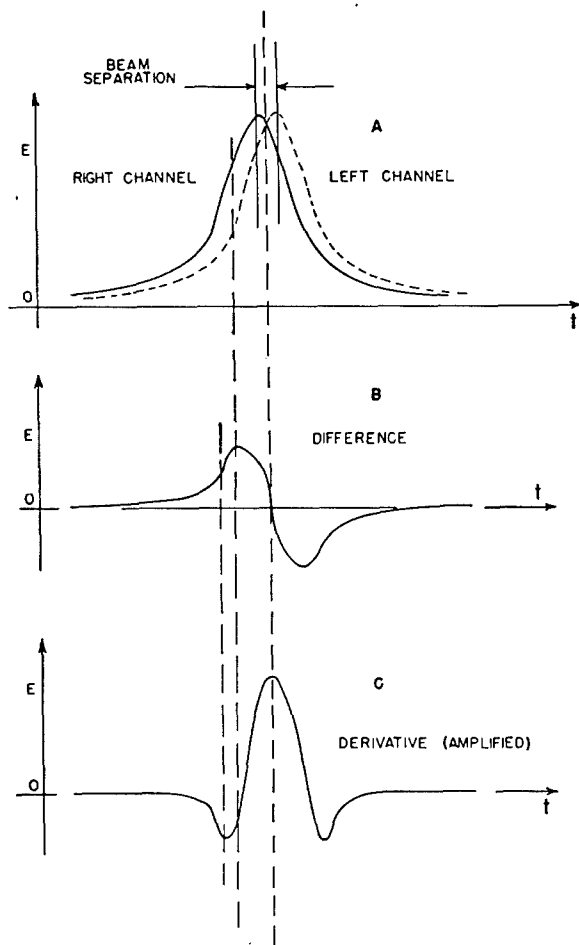


FIGURE 96. Pulse forms for SLC brightening.

reducing the screen voltage of the 6SG7, and consequently reducing the receiver gain. A potentiometer was used to adjust the positive potential on the detector plate and cathode, and on the difference-amplifier grid circuits.

This receiver system was tested aboard the AIDE DE CAMP in comparison with three other types of sonar brightening receivers.<sup>9</sup> Considerable trouble was experienced with poor connections, feedback difficulties, and noise. Although the receiving system worked well enough for comparative tests to be made, it was felt that the receiver-amplifier was not sufficiently free from constructional difficulties.

#### THE AMPLITUDE-BRIGHTENING RECEIVER

A circuit diagram of the amplitude-brightening receiver, used with the AIDE DE CAMP system is shown in Figure 97. This unit had three amplification stages preceding the diode detector which was the second

half of the 6SN7. This was followed by a cathode-follower stage. The signal output of the amplifiers was also fed through relay contacts to a 6H6 rectifier for gain control. The resulting TVG voltage was applied to the grids of the first two amplifier tubes through a potentiometer which adjusted the amount of TVG. Additional gain control was obtained by returning the cathode of the first amplifier to an adjustable positive reference point. The chassis contained a 5Y3 full-wave rectifier and filter for plate supply.

The receiver was originally designed for RCG, but was converted to TVG shortly after installation on the AIDE DE CAMP. Its gain was approximately 115 db, and maximum undistorted output was obtained with a signal input of 0.1 volt. The equivalent input noise voltage at maximum gain was  $1.1 \times 10^{-7}$  volt. The pass band was 2 kc wide, 3 db down, and was centered at 22.0 kc.<sup>77</sup>

#### 5.6.5 Receivers for QH Scanning Sonar Model 1

During early tests of the Model 1 system aboard the AIDE DE CAMP a small laboratory audio receiver was connected to the scanning channel preamplifier output to test the possibility of listening with scanning systems. Figure 98 is a schematic of this simple heterodyne unit with self-contained speaker and power supply. Tests indicated that the use of a listening channel offered several advantages in the identification of targets. However, own-ship's propeller noise, which appeared once for each revolution of the beam of sensitivity, was very annoying.

#### LISTENING RECEIVER

As a result of the testing program carried out during 1943 it was decided that a listening channel consisting of a separate commutator, paralleling that used for scanning, a separate preamplifier, and a separate listening receiver be provided. A new receiver was designed to accomplish the listening function. Figure 99 is a schematic diagram of this superheterodyne-type receiver, which was mounted in the console as shown in Figure 67 and is the chassis hinged to the top of the console. Two units were built, the second for the Serial 2 system. In the second unit the following minor changes were made (refer to Figure 99): a 0.006- $\mu$ f by-pass capacitor was added to the cathode of V101; R108 was changed to 0.1 megohm;

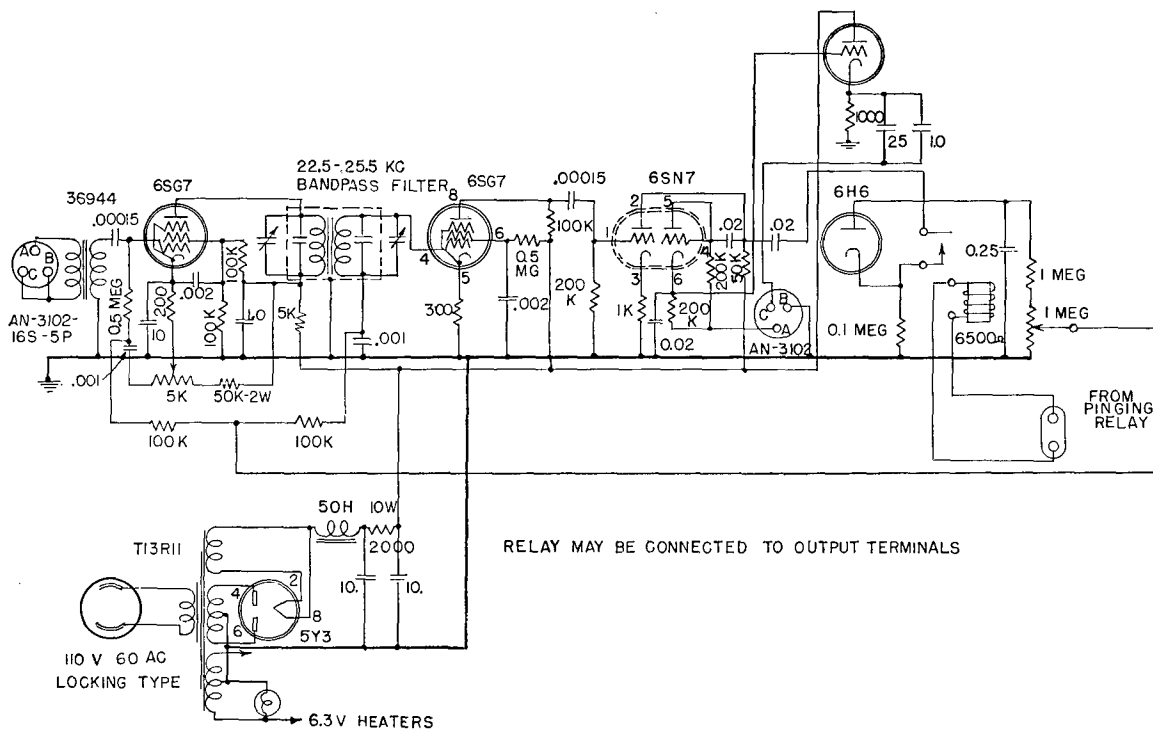


FIGURE 97. Circuit diagram of amplitude-brightening receiver, AIDE DE CAMP ER/CR scanning sonar.

NOTE: L1 -170 MH IN AIR  
L2 -200 MH IN AIR

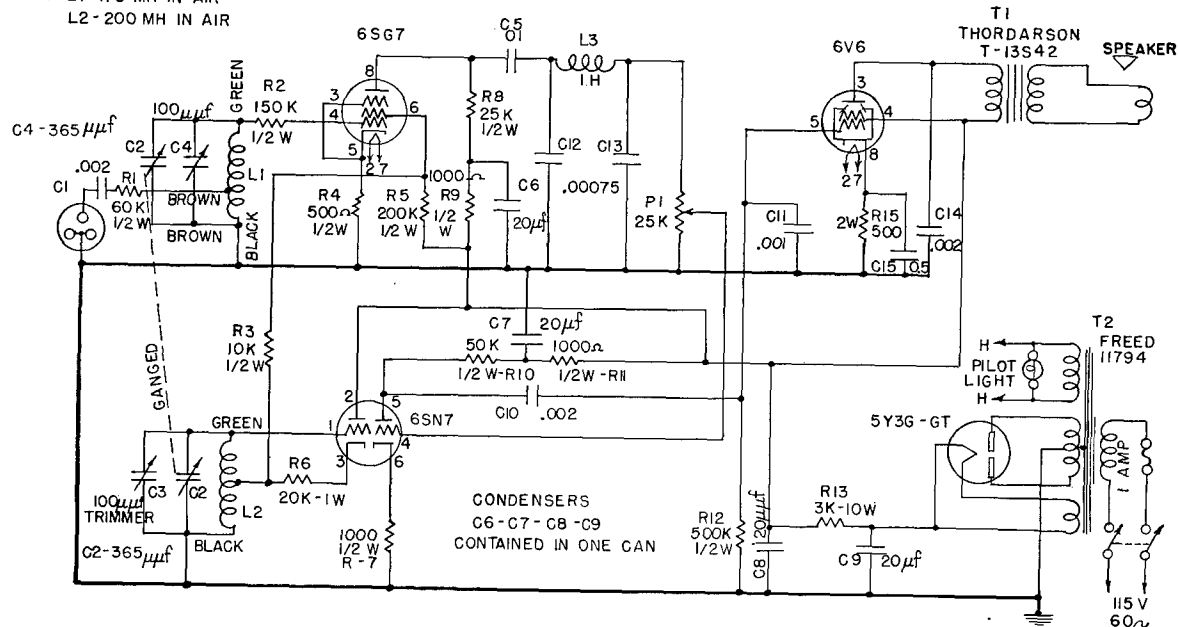


FIGURE 98. Circuit diagram of heterodyne listening receiver QH scanning sonar, Model 1, Serial 1.

CONFIDENTIAL

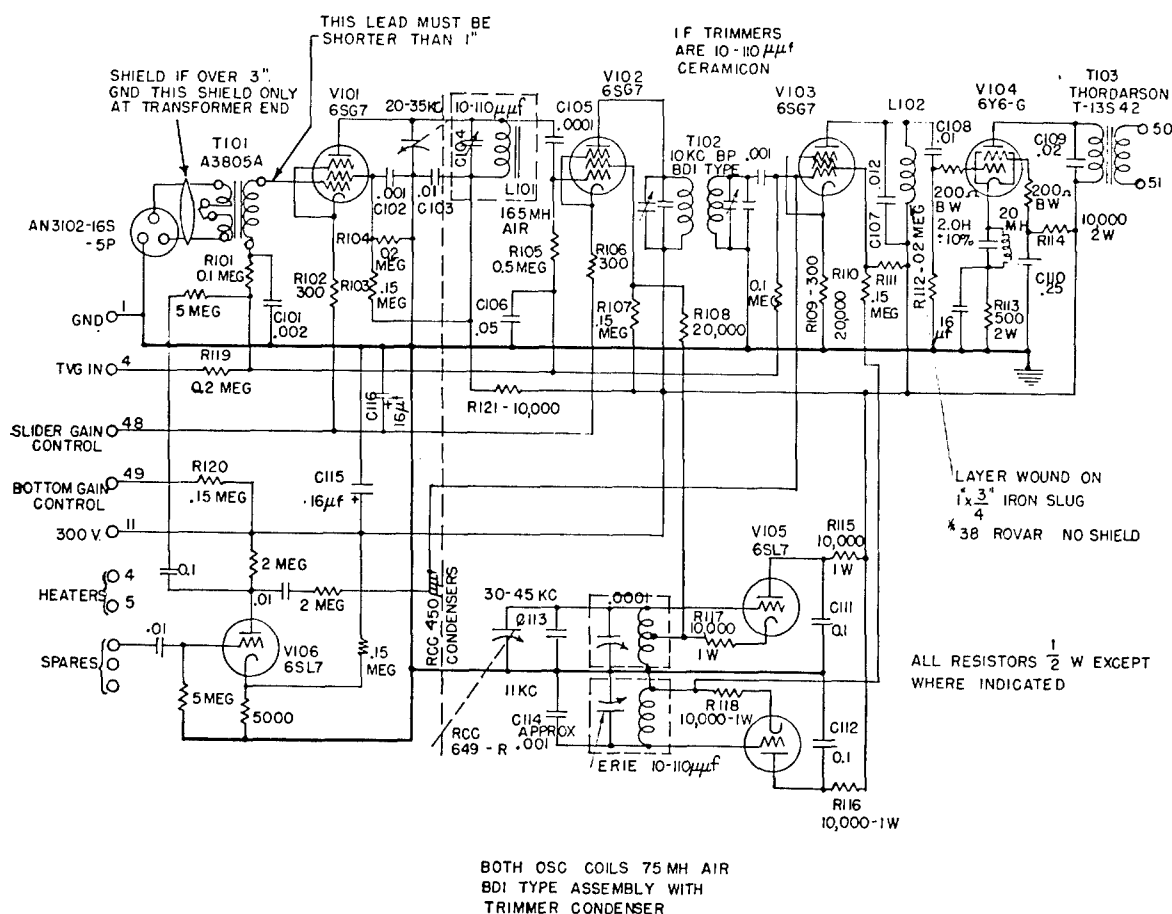


FIGURE 99. Circuit diagram of listening receiver, Serial 2, QH scanning sonar, Model 1, Serial 1.

the 2-megohm resistors associated with the plate circuit of V106 were changed to 0.75 megohm; and terminal 51 on the output was grounded.

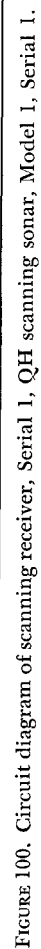
The electric characteristics<sup>78</sup> of these receivers were as follows: the sensitivity for 1-watt output was 7.0  $\mu$ v at 23 kc and 4.8  $\mu$ v at 35 kc. The maximum power output was 5 watts into a 10-ohm load, and required 50- $\mu$ v input at 23 kc and 24- $\mu$ v at 30 kc. Tracking of the voltages through the r-f and oscillator-tuned circuits was within  $\frac{1}{4}$  db from 23 to 45 kc. The high-frequency oscillator voltage delivered to the screen of the first mixer (V102) was 7 volts at 30 kc and 2.5 volts at 45 kc. The intermediate frequency was 10 kc and the second (heterodyne) oscillator was tuned to 11 kc, the 1-kc image response being 15 db down. The overall response gave a peak at 1-kc audio output and was down 6 db at 750 and at 1,300 c. The volume control gave an attenuation range of 57 db.

The receiver controls included frequency, gain, and TVG. The frequency-control dial was mounted directly on the variable capacitor shaft on the chassis.

The gain control, which was a potentiometer mounted on the console panel, controlled the cathode bias on the first two stages of the receiver. The TVG voltage was common to and obtained from the scanning receiver, its control being located on the scanning receiver chassis (to be described later in this section). The two receivers used a common power supply.

#### SCANNING RECEIVER

The first scanning receiver (Serial No. 1) for the Model 1 QH scanning sonar was built according to the schematic diagram shown in Figure 100. It was of the superheterodyne type using an intermediate frequency of 10 kc, and controls included frequency, gain, and TVG. The gain control shown on the receiver schematic was actually mounted for remote control on the front panel of the console. Provision was made to blank the output during transmission. Two 6SG7 r-f amplifiers were employed as the initial stages, with a tuned circuit in the plate of the first 6SG7 to provide r-f selectivity. A 6SG7 mixer or first



CONFIDENTIAL





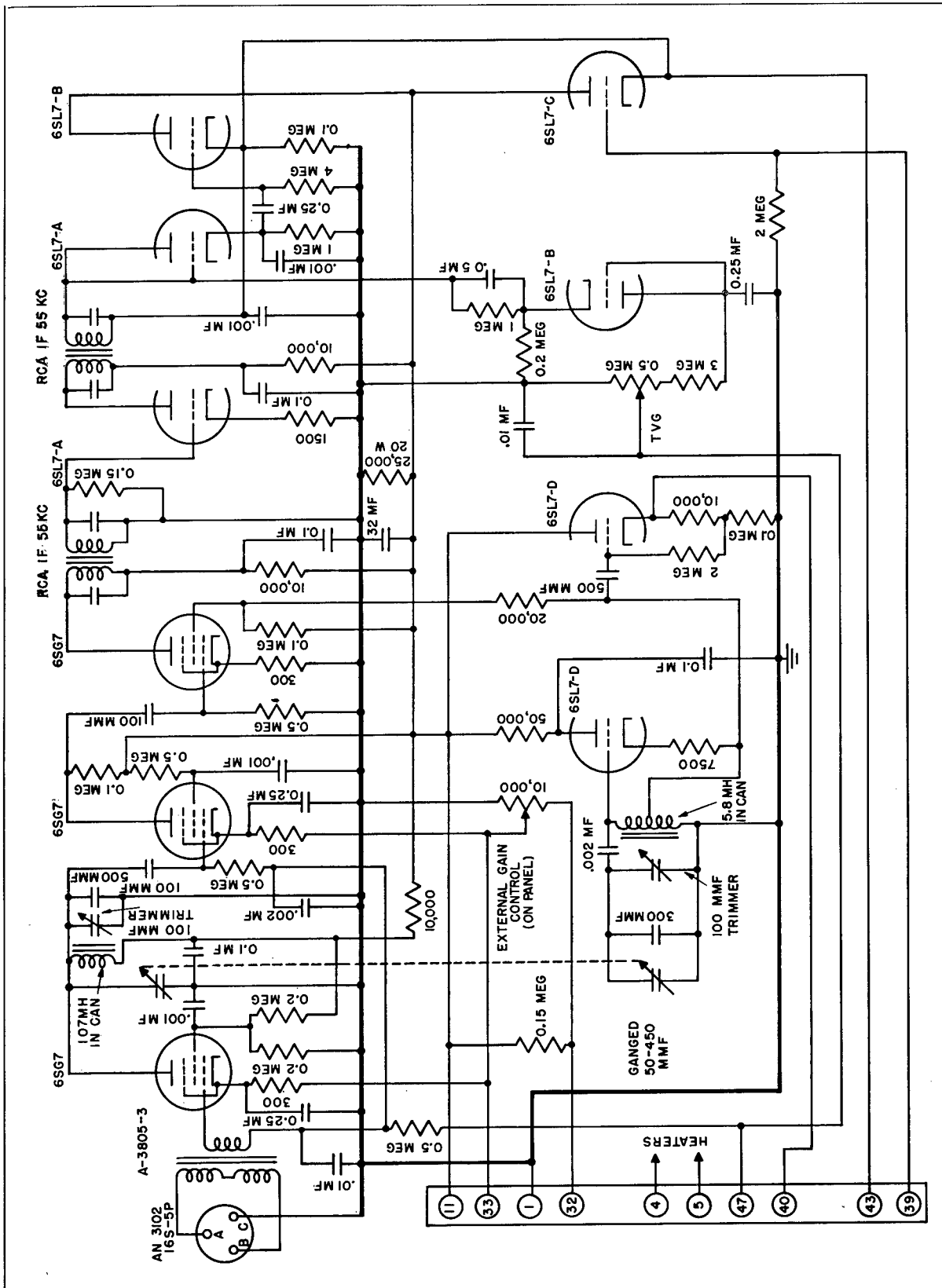


FIGURE 102. Circuit diagram of unicontrol scanning receiver, QH scanning sonar, Model 1, Serial 2.

CONFIDENTIAL

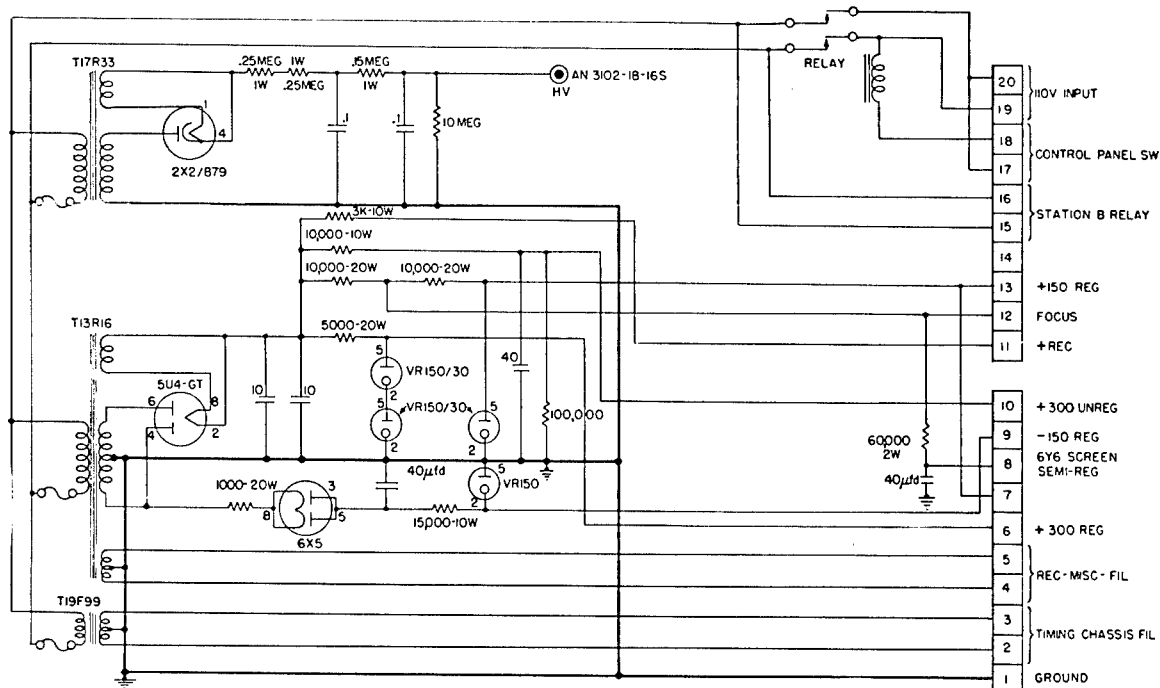


FIGURE 103. Circuit diagram of power supply, QH scanning sonar, Model 1, Serial 2.

detector was used having the oscillator voltage injected on its screen; an i-f transformer coupled its output to a 6SN7 i-f amplifier which used a single-tuned circuit in its plate circuit to increase further the selectivity. The other triode portion of the 6SN7 served as the oscillator. One half of a 6H6 was used as the second detector and the other half as the TVG rectifier. The TVG 1.0- $\mu$ f capacitor was charged by rectifying the output of the i-f amplifier from the signal picked up in the receiver during the transmitting period. A 6SN7 tube served as a cathode-follower output stage and a cathode-follower blanking amplifier.

Gain control action was obtained by a 10,000-ohm tapered potentiometer which adjusted the cathode bias on the two 6SG7 amplifiers. The i-f output was also brought directly out of the chassis for use as an alternate brightening output. Figure 101 is the schematic diagram of the Serial No. 2 receiver chassis, which was similar to Serial No. 1.

These receivers were tunable from 20 to 35 kc. The gain control had a range of 75 db; the overall voltage gain was 150 db at 25 kc; the noise level was  $3 \times 10^{-8}$  volt of input for 1 volt of output. One  $\mu$ v of input at 25 kc produced 32 volts of output.

The Serial No. 2 receiver was used in the QH Model 1, Serial 1, scanning sonar. A third receiver

was constructed for the Serial 2 system. Figure 102 is the schematic diagram for this chassis. Unicontrol of frequency was incorporated in the receiver to allow simultaneous frequency adjustment of the receiver beat-frequency oscillator and transmitter-output frequency.

In this receiver two 6SG7 r-f stages were used, followed by a 6SG7 mixer stage with the oscillator voltage injected at its screen. By a single control, the r-f stages could be tuned from 20 to 33 kc, and at the same time the oscillator frequency tuned from 75 to 88 kc, the intermediate frequency being fixed at 55 kc. One half of a 6SL7 was used as the oscillator; the other half served as a cathode follower to feed the oscillator voltage to the transmitter. In the transmitter unit this signal was mixed with that from a 55-kc fixed oscillator to produce a 20- to 30-kc output signal for the transmitter. A twin-triode (6SL7-A in Figure 102) served as the i-f amplifier tube and second detector tube. The output of the i-f stage caused by the pickup in the receiver during the transmitting period was rectified by half of a 6SL7-B, diode-connected, to initiate TVG control. The other half of 6SL7-B was used as a cathode-follower output stage. A third twin-triode (6SL7-C) was used as a blanking cathode follower. Gain control was obtained by using a potentiometer controlling the cathode bias in the two r-f

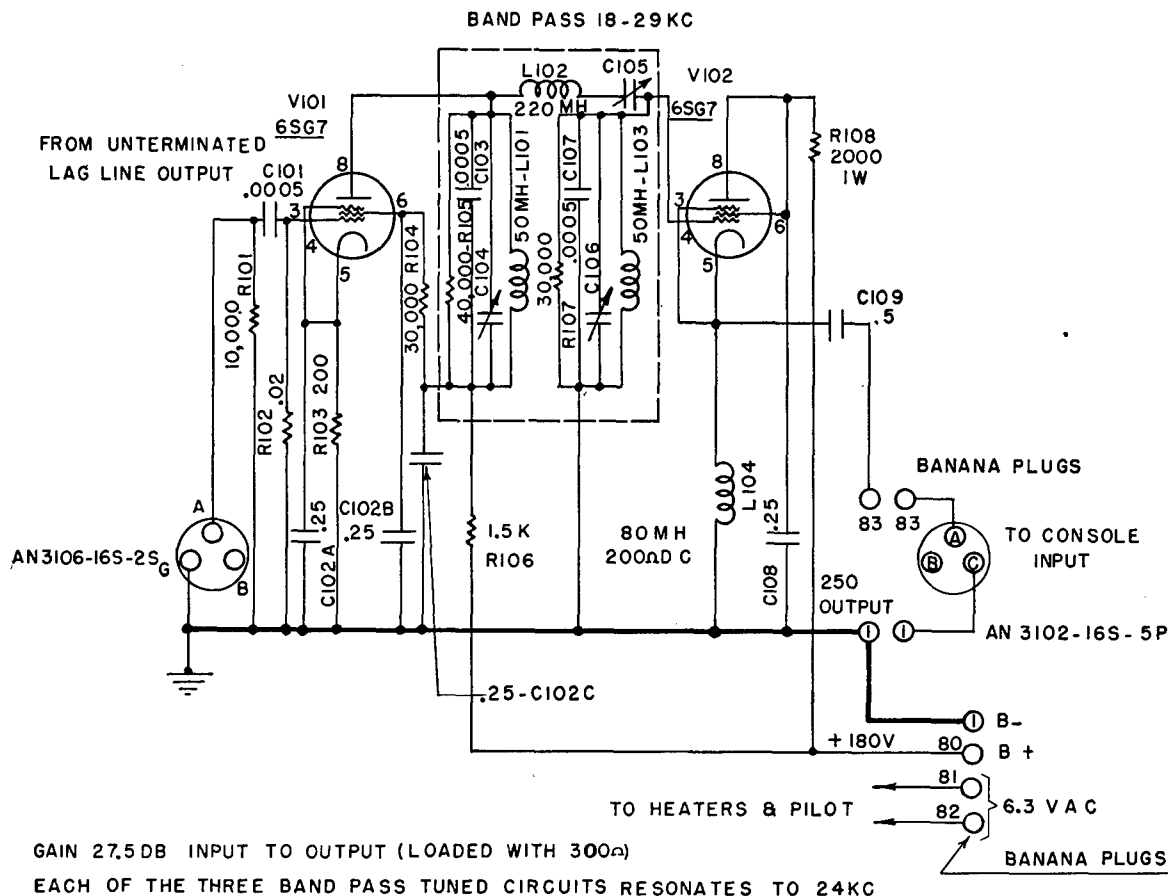


FIGURE 104. Circuit diagram of preamplifier, QH scanning sonar, Model 1.

stages. TVG was also applied to the grids of these stages; a potentiometer controlled the amount of TVG voltage applied. The frequency control was a two-section variable air capacitor.

Figure 103 gives a circuit diagram of the power supply used in the console. This unit furnished power for the scanning and listening receivers, the sweep chassis, and the CRO. Figure 104 gives a circuit diagram of the preamplifier, identical units being used in both the listening and brightening channels.

### 5.6.6 Receivers for QH Scanning Sonar Model 2

In the QH scanning sonar Model 2 both the listening and scanning receivers were combined in one chassis.<sup>70</sup> Their tuning range was from 20 to 32 kc. A single oscillator on the receiver chassis provided the heterodyning signal for both receivers and the transmitter, thus giving unicontrol of frequency.

TVG and gain control circuits were also common to both receiver channels. The use of this design simplified the circuits, reduced the number of controls, and conserved space. Figures 70 and 71 show the position of the dual-channel receiver in the console. Figure 105 is a schematic circuit diagram of the receiver.

Two receivers were constructed with almost identical circuits. However, the mechanical layout chosen in the first receiver complicated wiring, placed controls in inconvenient positions, and was considered unsatisfactory. For this reason the first receiver was not used, but a second proved satisfactory. The major difficulties in the design and testing were parasitic oscillations and cross talk between channels. These were solved by the use of parasitic suppressors in the form of 100-ohm wire-wound resistors in several grid circuits. Cross talk occurred between the initial two amplifier stages in one channel and those in the other.

The r-f amplifier stages of both channels were

CONFIDENTIAL



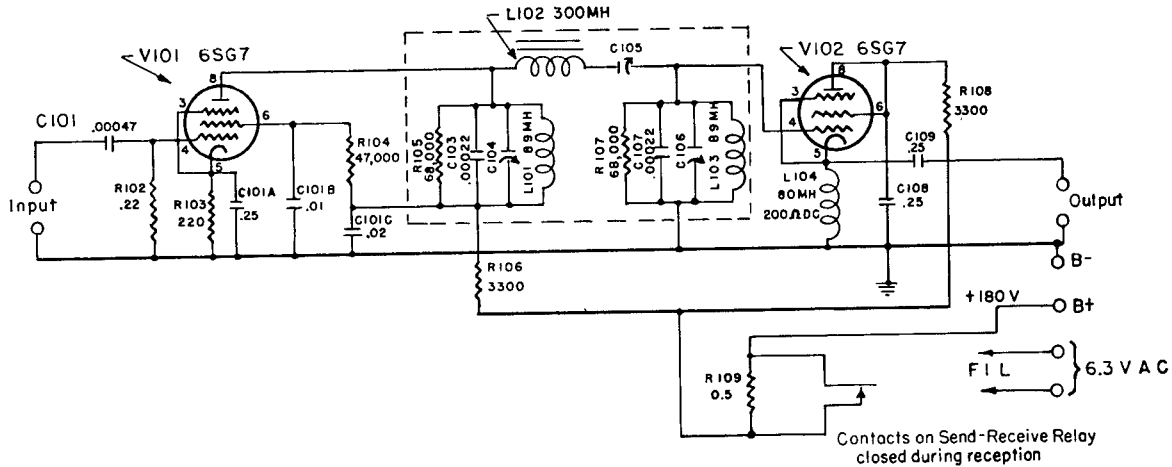


FIGURE 106. Circuit diagram of 26-kc preamplifier.

Cross-talk measurements between channels gave the following results, with the common gain control at its maximum setting:

Condition of test	Frequency (kc)	Output from listening channel (volts)	Output from scanning channel (volts)
10- $\mu$ v input to listening channel with its gain control on position 2 (see audio gain control in Figure 105)	20	1.9	7
	30	2.1	8
10- $\mu$ v input to scanning channel with listening gain control at maximum	20	0.22	150
	30	0.60	150

The preamplifier used in the Model 2 system was the same as that for Model 1 (see Figure 104). Because the resonant frequency of the transducer used in the Model 2 system was 22.5 kc, while that of the first production model (by Sangamo Electric Company) was to be 26 to 28 kc, another preamplifier filter was designed and bench-tested in breadboard form to center the band-pass near the 26- to 28-kc region. Figure 106 shows the schematic wiring and circuit constants of this preamplifier.

Figure 107 is a schematic of the power supply and sweep chassis used with the Model 2 system. The design and operation of the latter are discussed in a later section of this chapter. The power supply furnished power for all the console circuits except the servo amplifiers. Care was taken in its design to eliminate effects of line voltage variations on the critical circuits, particularly in the PPI display. The circuits were first compensated for slow variations by proper

choice of the percentage regulation for each element. Then, to insure that compensation would hold for rapid variations, identical time constants were chosen for critical circuits. In this way satisfactory compensation of line voltage fluctuations was obtained.

### 5.6.7 Preamplifier Filter Design for QH Sonar

Following tests of the QH Model 2 sonar, investigation of filter designs was carried on to improve their characteristics, in order to meet the more stringent requirements of BDI application and good manufacturing practice. It was decided that these filters should meet the following requirements:

1. The band-pass should center on 26 kc and should be 7 kc wide.
2. To function in the plate circuits of high gain tubes, such as 6SG7, the filter impedance should be high (at least 50,000 ohms).
3. To meet the requirements of BDI application, two or more such filters, properly constructed for quantity production, should have phase shifts over the entire pass band which would not differ by more than  $\pm 2.5$  degrees.
4. Pi sections should be used for convenience in feeding d-c potentials to the associated vacuum tubes.

After several types were designed and tested,<sup>79, 80</sup> it was found that the one shown in Figure 108 had the best overall operating characteristics and would be manufacturable in quantity. Its band-pass characteristic is shown in Figure 109.

Two preamplifiers incorporating this filter design

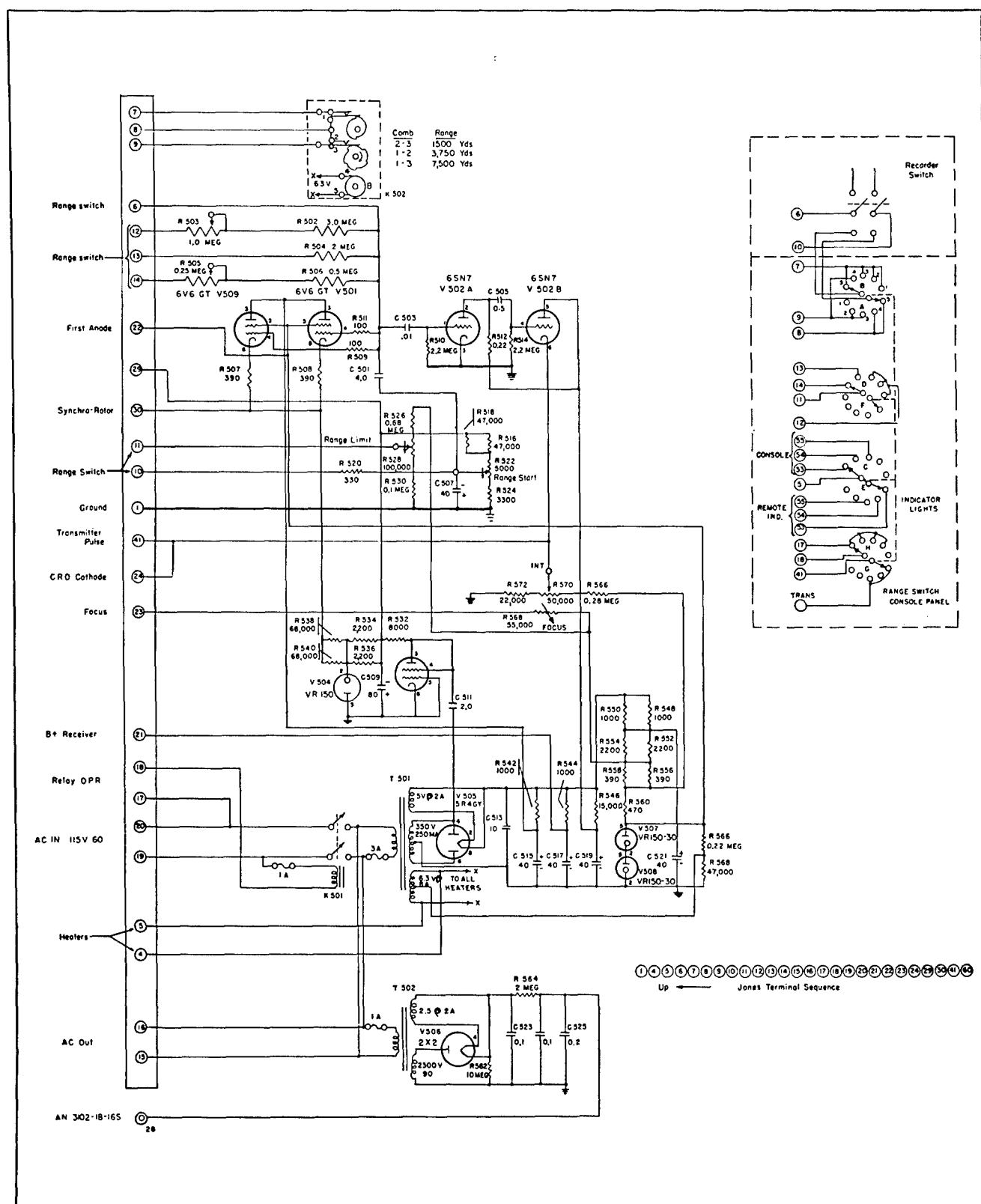


FIGURE 107. Circuit diagram of power supply and sweep chassis, QH scanning sonar, Model 2.

CONFIDENTIAL

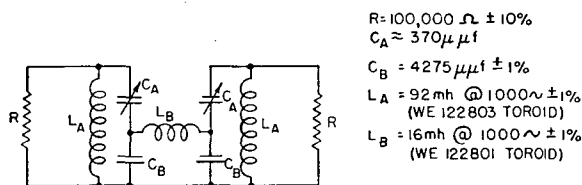


FIGURE 108. Circuit diagram of band-pass filter for pre-amplifier.

were compared for phase shift, a point of great importance in BDI application. The result is shown in Figure 110.

The filter alignment procedure was to open the series link ( $L_B$ , Figure 108) and tune the shunt circuits at center frequency (26 kc),  $C_A$  being variable. The coils used in the filter were:

$L_A = 92 \text{ mh at } 1,000 \text{ cycles } \pm 1 \text{ per cent}$   
(W. E. 122803 toroid)

$L_B = 16 \text{ mh at } 1,000 \text{ cycles } \pm 1 \text{ per cent}$   
(W. E. 122801 toroid)

The calculation of the constants of the filter was made by first designing the ordinary constant-K band-pass filter of the type shown in Figure 111, assuming impedances, band-pass, and center frequency. A transformation showed that the circuits of Figures 108 and 111 produced the same effects, assuming the following relations between circuit component values:

$$L_A = 2L_2$$

$$L_B = \frac{L_1}{2C_1} \left[ \frac{1}{\left(1 + \frac{C}{2C_1}\right)^2} \right]$$

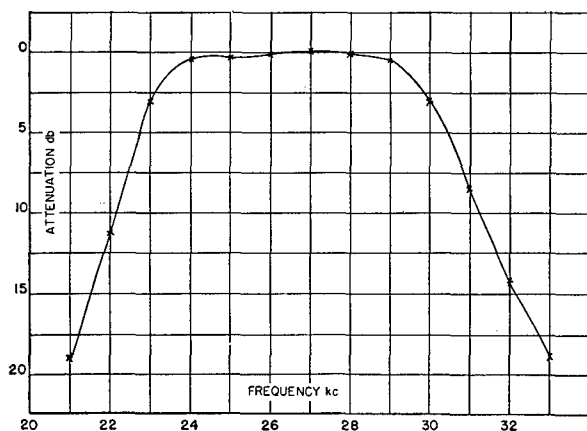


FIGURE 109. Frequency response of band-pass filter for preamplifier.

$$C_A = 2C_1 + C$$

$$C_B = C \left( 1 + \frac{C}{2C_1} \right)$$

$$C = \frac{C_2}{2} - C_d$$

where  $C_d$  is the distributed capacity associated with  $L_A$ .

### 5.6.8 Receivers for 26-kc Depth-Scanning Sonar

The depth-scanning sonar had two receivers, a scanning receiver for brightening the *elevation position indicator* [EPI] scope, and a second for listening and BDI operation. Three identical preamplifiers were used, one in the scanning channel, and two in the sum-and-difference channels to the BDI listening receiver. Each preamplifier was mounted on its commutator and had its own power supply; the design was the same as for the QH Model 2, with the filter pass band centered at 26 kc. Both the scanning and listening receivers for the 26-kc DSS system are described in detail in Chapter 6.

### 5.6.9 Receivers in the Model XQHA Scanning Sonar

The receivers in the Model XQHA scanning sonar, designed and constructed by the Sangamo Electric Company, were based fundamentally on those in the QH Model 2 sonar. However, the mechanical layout was different and RCG and ODN (own-doppler nullification) were incorporated at the request of the Bureau of Ships. The receiver chassis and its power supply chassis were mounted in the two upper

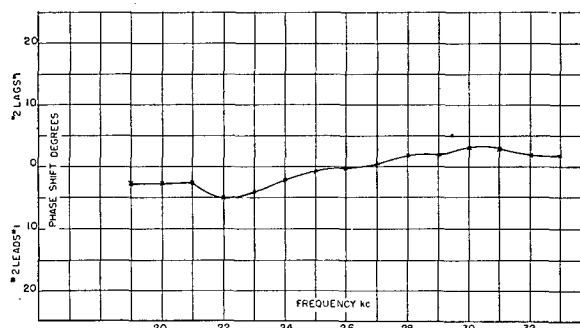


FIGURE 110. Difference in phase shift in two preamplifiers.

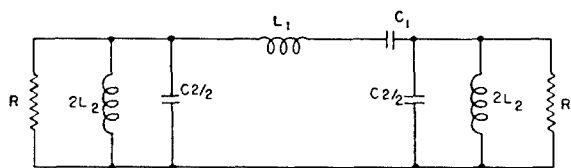


FIGURE 111. Equivalent circuit of band-pass filter for preamplifier.

sections of the receiver unit (Figures 112 and 113), the lower portion of which contained the commutators, transfer network, and the preamplifier and servo chassis (located adjacent to the commutators: see Figure 113, right side). The receiver chassis is shown in Figure 114 and the power supply chassis in Figure 115; a circuit diagram for the preamplifiers, receiver, and power supply is shown in Figure 116.

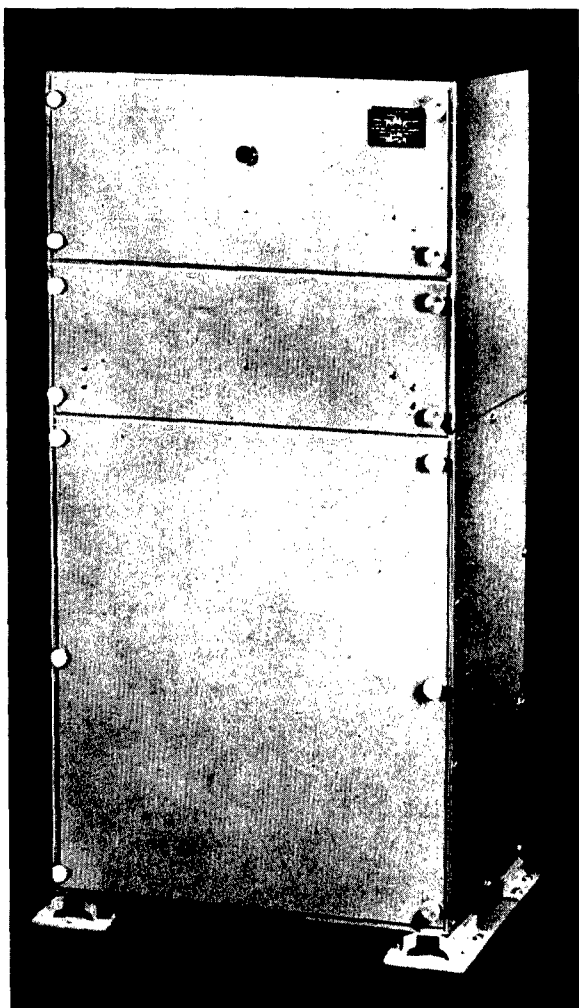


FIGURE 112. Front view of receiver unit, Model XQHA scanning sonar.

Transfer of the receiver position from its location in the console of QH Model 2 to the receiver-commutator unit of the XQHA system permitted reduction of size and weight in the indicator control unit (console). This was desirable to keep the system weight low in the ship and to conserve space in the already crowded portions of the ship where the operator's station was normally located. This also made it unnecessary to transmit signals at low levels from the

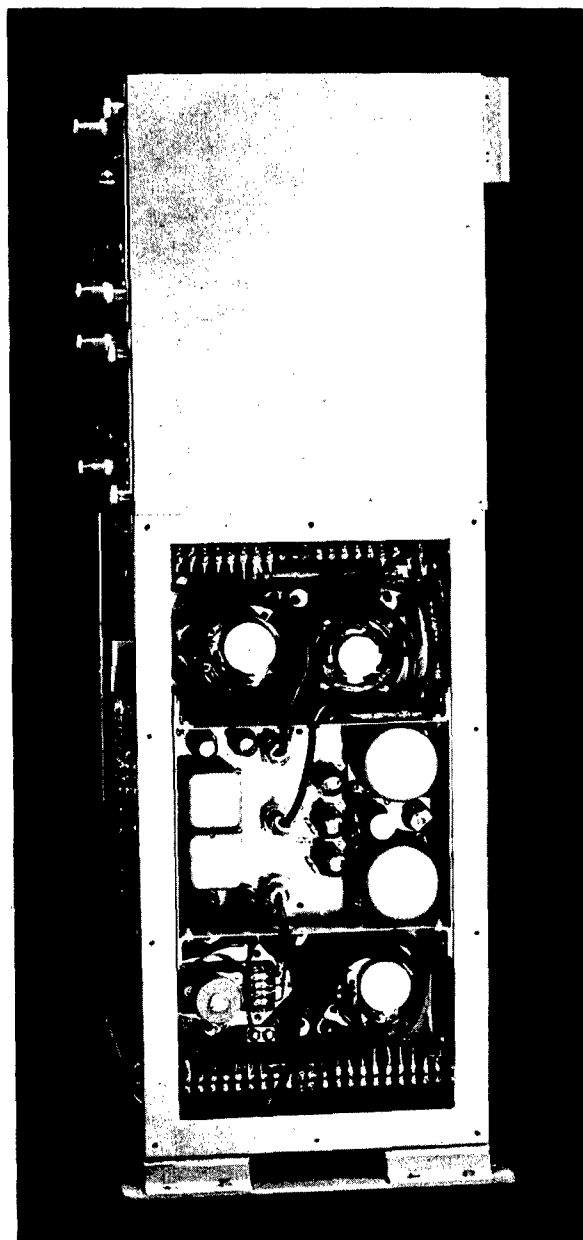


FIGURE 113. Right side view of receiver unit, Model XQHA scanning sonar.

CONFIDENTIAL



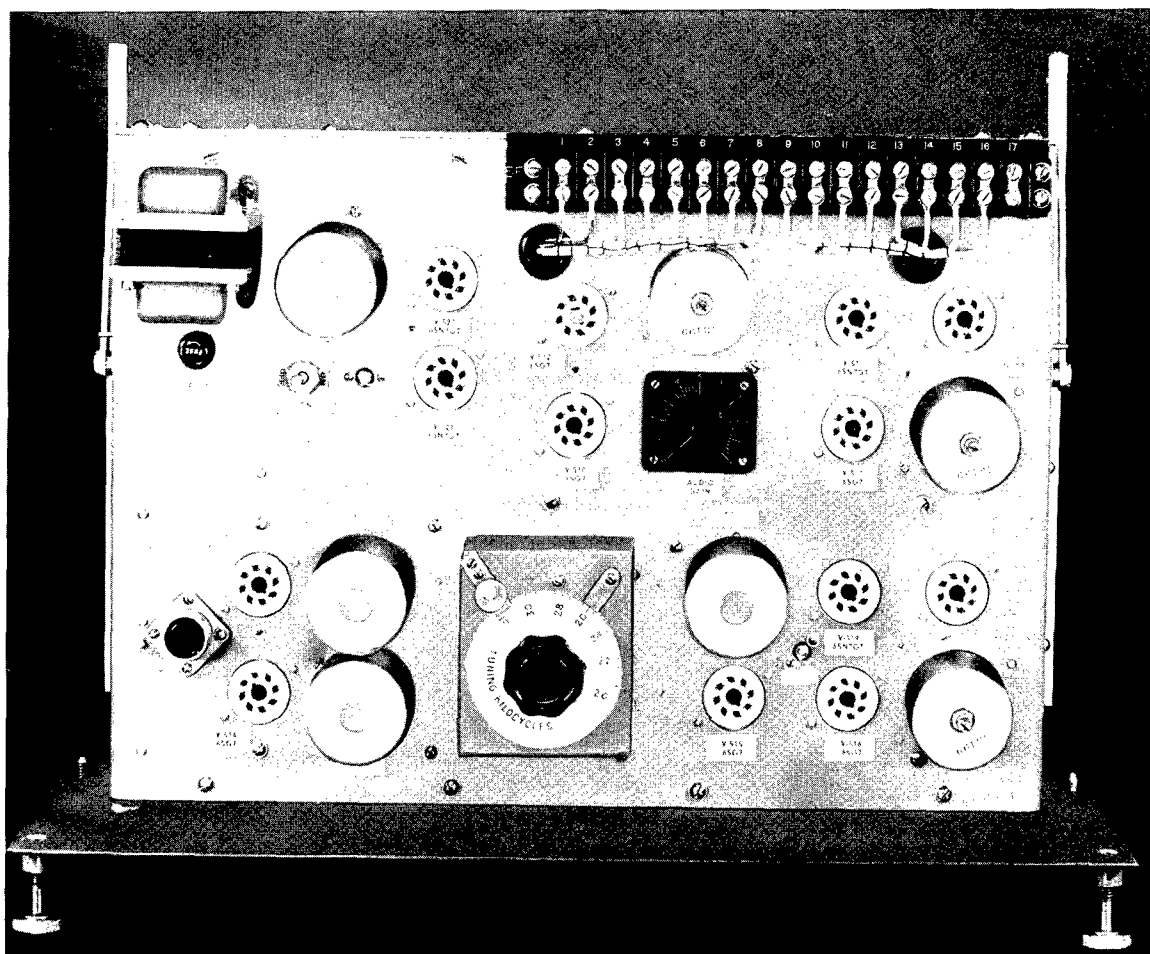


FIGURE 114. Top view of receiver chassis, Model XQHA scanning sonar.

lower sound room to the operating position, and thus reduced the likelihood of electric noise pickup.

Only those portions of the receiver circuits which differ greatly from those of the Model 2 system will be discussed here. (A complete description is given in reference 1.) The only change in the preamplifiers was in the band-pass filter. This had a higher impedance which increased the amplifier overall gain by about 5 db. The scanning channel was like that of the QH Model 2 receiver, except for a different input transformer (identical with the commutator input transformers). The listening channel also used this input transformer and followed essentially the same design in its r-f and i-f stages as used in the QH Model 2 scanning sonar. The heterodyne oscillator circuit was modified to permit variational control of frequency either by a reactance tube (for ODN) or by a manual beat-oscillator control. The audio ampli-

fier had an added 6SN7 (V-513) which served as a stage of resistance-coupled amplification and a cathode follower. An audio band-pass filter was inserted between the latter stage and the output tube (V-522), its pass band extending from 550 to 1,100 cycles.

The ODN was of the reverberation-controlled type, which sampled the audio signals caused by reverberation and, from their frequencies, corrected the beat oscillator to compensate for doppler shift caused by the component of own-ship's motion along the listening beam of sensitivity.<sup>81</sup> This represented the first use of ODN in CR scanning systems. One difficulty appeared when the target-ship's propeller noise was picked up; then ODN action was erratic, and no distinction could be made between reverberation and any other audio signals present during the sampling period.

The ODN circuit operated as follows (refer to Fig-

CONFIDENTIAL

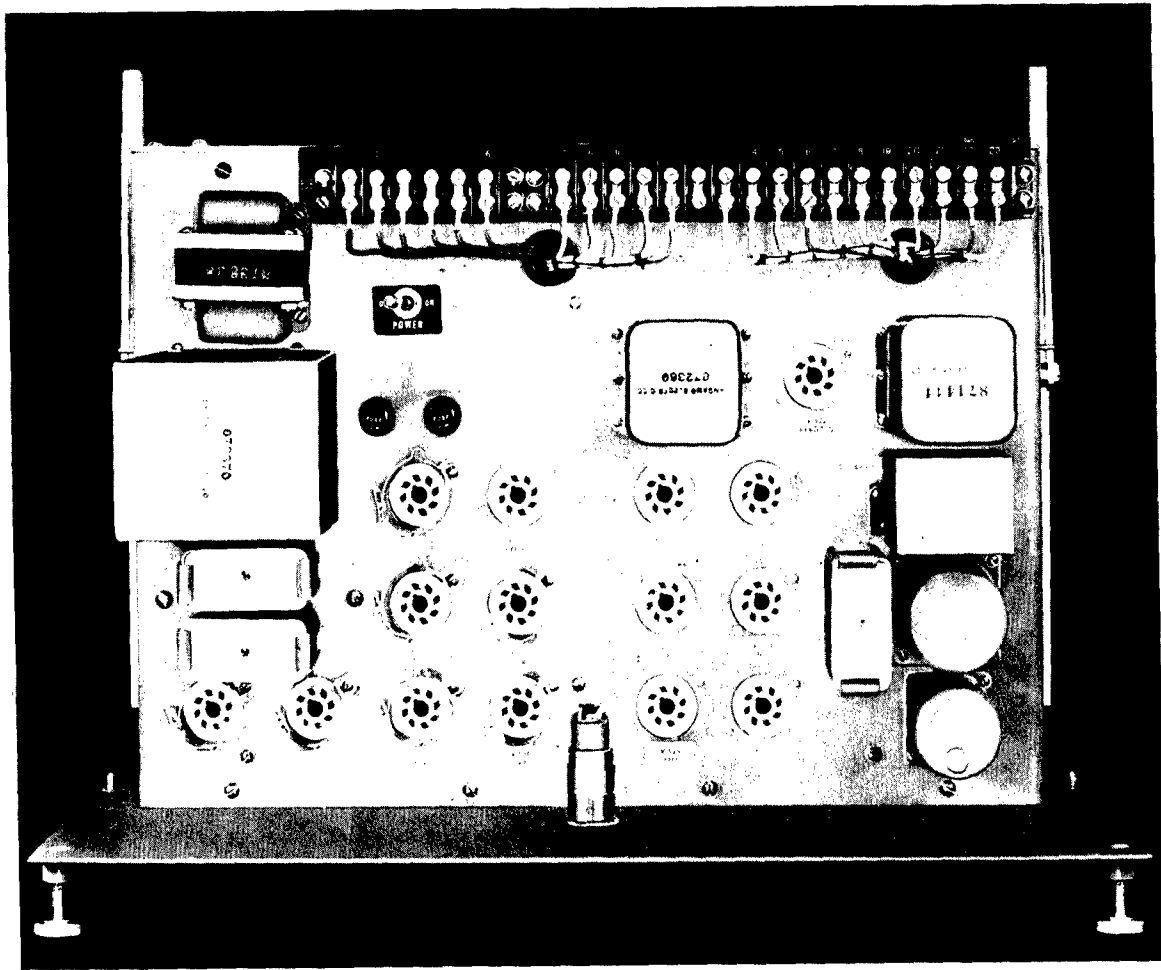


FIGURE 115. Top view of power supply chassis, Model XQHA scanning sonar.

ure 116): The audio signal, obtained from V-513, was passed through a clipper stage (V-523), which limited its amplitude to a peak value of 4.5 volts. Sufficient audio signal was necessary to insure limiter operation. The signal was then amplified by V-524 (two stages) and applied to the discriminator transformer T-606. The primary voltage was introduced in series with the secondary center tap, so that the secondary voltages in each half were vectorially added to the primary voltage. Each vector sum was rectified (tube V-525), and the resulting d-c outputs were compared to give a measure of the frequency deviation. The transformer was so tuned that at resonance (800 cycles) the secondary voltages were 90 degrees out of phase with the primary voltage, and 180 degrees out of phase with each other. The rectified sum voltages were thus equal, and their difference zero. If the signal frequency were shifted from 800 cycles, the phase

relations between the primary and secondary voltages changed, and the sums were no longer equal. The rectified voltages, being unequal, produced a difference voltage (d-c) whose polarity depended upon whether the signal frequency was less or greater than 800 cycles. This voltage was used to charge a capacitor C-663 during the sampling period (when relay K-503 was closed. The shunt leakage resistance across the capacitor being high, its voltage would then remain constant during the remainder of the echo-ranging cycle. This voltage was used to control the grid of a reactance tube V-521,<sup>81</sup> which in turn controlled the frequency of the heterodyne oscillator V-520. If the rectifiers V-525 were properly polarized, the reactance tube effect was to restore the audio output frequency to approximately 800 cycles during the sampling period.

Because the audio signals applied to the discrimi-

CONFIDENTIAL

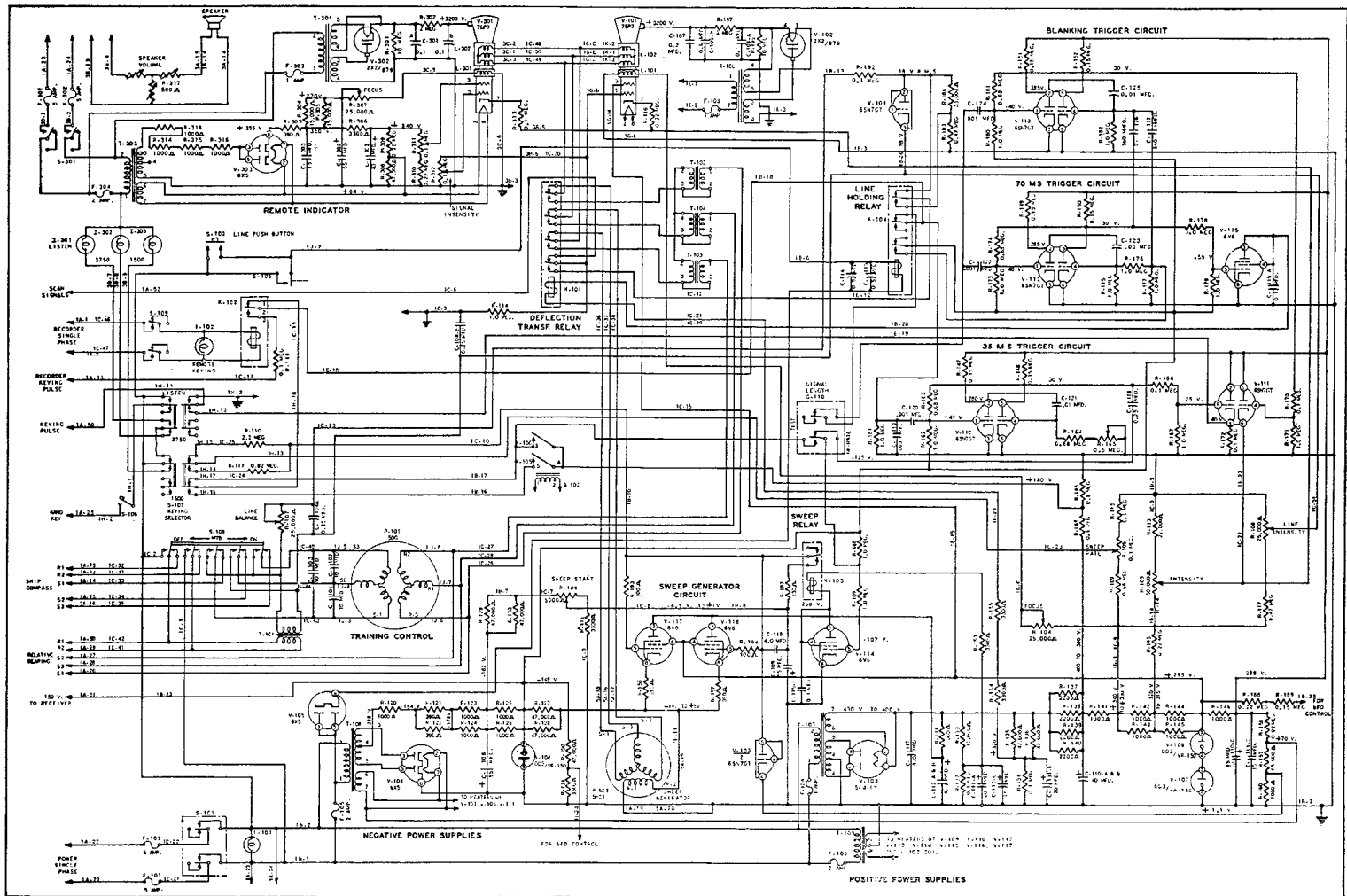


FIGURE 82. Circuit diagram of keying and CRO control, Model NQHA scanning sonar.

CONFIDENTIAL

nator usually had a high harmonic content, a false balance indication could occur if the signal frequency was just half the center frequency of the discriminator. To prevent this, signal was taken from the plate of the first section of V-524 and amplified by the first section of V-526 in the plate circuit of which was a parallel-tuned circuit resonant at about 350 cycles. The second section of V-526 rectified the voltage across this tuned circuit, and the resulting direct current was introduced in the proper polarity into the comparison circuit. Thus, the voltage produced to charge C-663 could not become reversed in the neighborhood of 400 cycles. Because the instantaneous frequencies of reverberation signals fluctuate, it was necessary to provide an averaging effect over an appreciable period of time. The circuit used to operate the ODN relay K-503 was so designed that the contacts closed immediately after transmission and remained closed approximately 0.37 second. As the charging circuit for C-663 had appreciable resistance (approximately .22 megohm) and an additional resistor R-758 (.22 megohm) was placed in series, the time constant for charging and discharging C-663 (when K-503 was closed) was sufficiently long to permit averaging out rapid variations in discriminator output.

Provision was made for manual beat-oscillator control. The grid circuit of the reactance tube V-521 included the switch, S-501, which permitted the connection of the grid to either the ODN capacitor C-663 or to the manual beat-oscillator control. Additional details of this circuit are given in reference 1, including a discussion of the ODN relay timing circuits.

Reverberation control of gain was accomplished in the following manner: The grid circuits of the r-f stages in both channels (V-509, V-510, V-514, and V-515) were returned to pin 8 of V-527, as shown in Figure 116. This point was connected to ground through resistors R-735 and R-734 with a capacitor C-668 across the latter. This common point was also connected to the plate of a triode V-528 and to the cathode of a diode V-527. The cathode of the triode was returned to a divider between the -150-volt supply and ground, composed of R-726 and R-727, the latter being by-passed with an electrolytic capacitor C-660. This placed the cathode potential at -60 volts direct current. The grid of this circuit was returned to a divider which consisted of R-728 and R-729. One side of this divider was connected to the -150-volt d-c supply, and the other to the keying pulse circuit

which was normally at +40 to +50 volts direct current. The grid was thus normally at approximately -87 volts direct current with respect to ground and -27 volts direct current with respect to the cathode, biasing the triode to cutoff. When the keying pulse appeared, the pulse circuit potential changed from +40 to +200 volts direct current, the grid of the triode was driven positive, and the tube conducted. Since its cathode was negative with respect to ground, current flowed through R-735 and R-734 to charge C-668 negatively. The plate of the triode N-528 was thus about 50 to 55 volts negative with respect to ground, and the grids of the two receiver channels, being at this same potential, approached cutoff and the gain was reduced to a level which did not overload the amplifier but permitted the transmitter signal to mark the recorder. During the time the keying pulse was present, C-668 was charged up to approximately the potential of the triode plate. At the end of the keying pulse the triode was again cut off and the bias voltage for the r-f stages immediately became the potential across C-668. The resistor R-734 discharged C-668 at a slow rate.

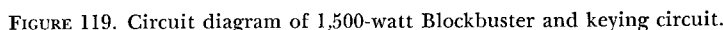
The common point referred to above was also connected to the cathode of a diode V-527, whose plate was connected to ground through the resistors R-733 and R-732. This gave another discharge path for C-668. The time constant of this circuit was such as to restore the gain very rapidly—that is, to within 5 db of maximum within 0.1 second. This latter discharge occurred as long as no reverberation or other audio signal was present. If reverberation was present the audio signal at the plate of the output tube V-522 appeared across R-767 and was rectified by the other diode of V-527 to produce a negative voltage across C-667. This raised the negative potential of the plate of the first diode in V-527 and prevented discharge of C-668 through the diode when the potential of C-668 was less negative than the first plate of V-527 (pin 5). Thus there was a potential across C-668 for control of gain which started at a high negative value and decreased at a rate depending on the amount of reverberation.

## 5.7 TRANSMITTERS FOR CR SCANNING SONARS

The development of the transmitters used in the CR scanning sonars required finding adequate solutions to four fundamental problems:

CONFIDENTIAL





This multitube amplifier was not constructed, because calculations indicated that its output power would be too low. Nevertheless, the design brought out the idea of using only a single relay in the transfer

In the initial designs the blocking-type oscillator had circuit constants selected to produce output pulses of practically square wave form with a carrier frequency of the order of 20 kc, a duration of 30 msec, and a pulse rate which was variable from one pulse every 6 seconds down to one every second. Various tubes were tried, including types 810, 811, 813, 828, 838, and 8005. The 813, as a pentode, gave very good square wave pulses, had excellent frequency stability, and an output of 1 kw. The outputs of the 811, 828, and 838 were limited to lower values because of in-

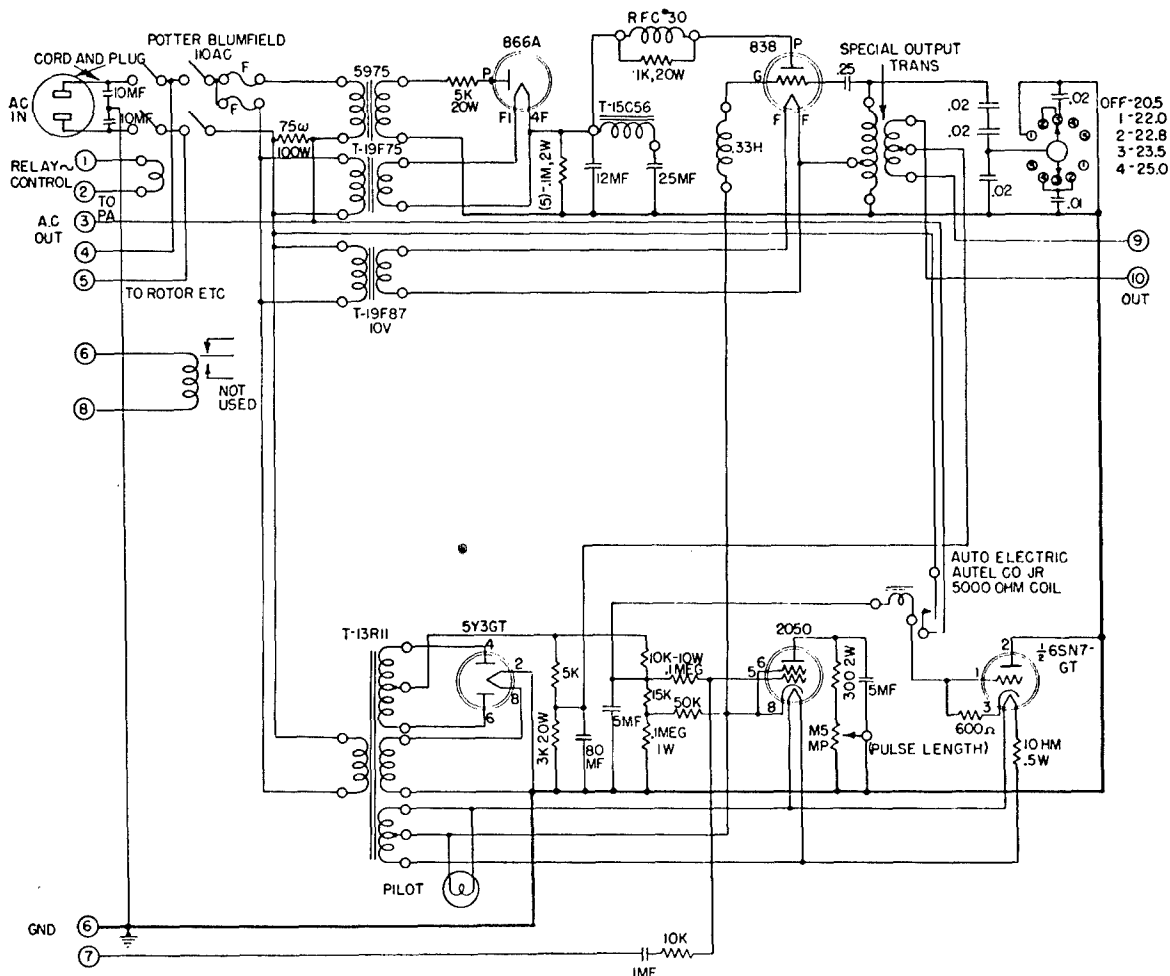


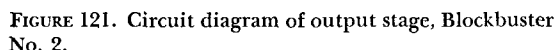
FIGURE 120. Circuit diagram of 400-watt driver, Blockbuster No. 2.

ternal arcing or saturation of cathode emission. The 8005 was discarded because of the large number of defective units. The 810 gave the most output, 3.3 kw, but the frequency stability was not good. Following these tests, a blocking-oscillator chassis and power supply were constructed using the 810 tube. This unit gave 4.3 kw on short pulses and 2.0 kw with 35-msec pulses. In the attempt to synchronize the pulse interval, keying was tried, the 810 circuit being converted to a straight Hartley oscillator keyed by a grid-blocking bias which was removed for the duration of the pulse by means of a 6L6 keying tube. This gave good results, although capacitor failures forced a reduction of the power to 1.4 kw, delivered to a load of 18 to 45 ohms.

The transmitter was installed aboard the AIDE DE CAMP. When tested, it drew 250 watts average from

the 115-volt supply line. At this time it was revised to work into a 75-ohm load without reduced output power and the 6L6 keying tube was replaced by a type 2050 thyratron. A delay interval introduced by a 6SN7 was added in the keying circuit to permit operation of the send-receive relays before transmission. Figure 119 is the schematic of this No. 1 Blockbuster in its final form.

During the testing of the No. 1 Blockbuster, a second transmitter was started. This used the 400-watt (sometimes called the 500- or 600-watt) driver, with an 838 tube as an oscillator, and with associated power supply and keying circuits (see Figure 120). This driver was similar to the No. 1 Blockbuster, and was connected to an 810 tube used as an amplifier to give a power output of 2.5 kw. These experiments led to the construction of a master-oscillator-power-ampli-



fier [MOPA], comprising the No. 2 Blockbuster. The 400-watt driver was used to excite push-pull 838 tubes (see Figure 121), which gave a power output of 2 kw into a 100-ohm load for a 30-msec pulse. An unsuccessful attempt was made to hand-key the circuit for communication purposes.

### 5.7.4 Transmitter for QH Scanning Sonar Model I

The principles used in the Blockbuster transmitters were applied to the design used with the QH scanning sonar Model 1 on USS SARDONYX and USS CYTHERA. This transmitter was constructed on two chassis, one containing the power supply and keying circuits, the other containing the oscillator and amplifier circuits. Figure 122 is a schematic wiring diagram of the latter unit. The output power obtained was 3 kw into a 100-ohm load using a 30-msec pulse and 5,000-yard keying rate. While testing this unit in the laboratory, neutralization of the final power amplifier was tried but did not seem to improve its performance. At first considerable trouble was encountered with the amplifier output transformer. It was rebuilt using Litz wire and having better insulation, with the result that both its characteristics and breakdown strength were improved. The final design included secondary taps which would properly feed into either a 20-ohm or a 225-ohm output load. Fig-

ure 123 shows a sectional view of the transformer. With the improved transformer, approximately 4 kw of power output could be obtained with a 2,200-volt plate supply for the final amplifier. Hand-keying of the transmitter was successfully accomplished by adding resistance in the power supply of the transmitter circuit. Since no provision was made to operate the send-receive relays, the Model 1 system could not be used for communication purposes.

Figures 124 and 125 are schematic wiring diagrams for the power supply keying circuit, the send-receive relay keying circuit, and the power supply circuit. Each keying circuit received its triggering pulse from the sweep control circuits at terminal No. 42. Several tubes were tried in the power supply keying circuit—types 2050, 6V6, 6L6, and 6Y6—the 6Y6 being chosen. This tube keyed the 838 oscillator by decreasing its negative grid bias during transmission. A potentiometer in the 6Y6 circuit was provided to control and adjust the transmitting pulse length. In the send-receive relay keying circuit, a 2050 tube furnished the relay keying pulse. The power supply circuit is also shown in this figure. The circuit diagram shown in Figure 126 is that of the circuit in the choke box, which contained the send-receive relays and the

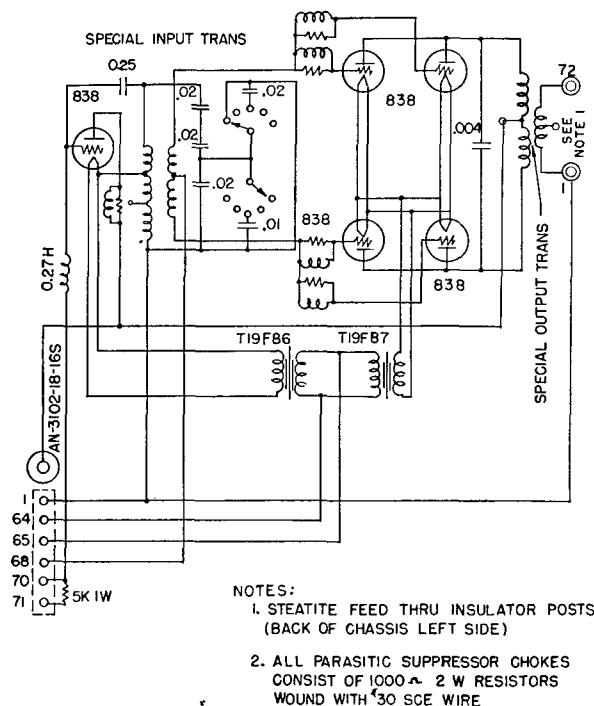


FIGURE 122. Circuit diagram of MOPA for transmitter, QH scanning sonar, Model 1.





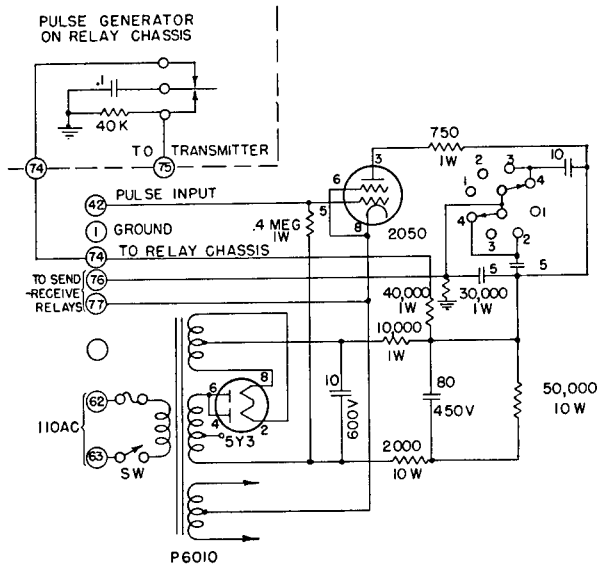


FIGURE 125. Circuit diagram of relay keying circuit and power supply, QH scanning sonar, Model 1.

filters, a spark gap (fixed or rotary) in series with the power supply output, and a tuned circuit, the latter being coupled to the transducer as indicated in Figure 127A. It was also proposed that a gap having sufficient spacing to prevent arcing at the normal power supply voltage be used and that an additional voltage in series with the gap and sufficient to initiate the arc be introduced. This voltage was to be either a high-frequency a-c pulse—say 2 mc—or a continuous a-c excitation keyed by a vacuum-tube relay (Figure 127B). Although some work was done on this system (the 2-mc oscillator and a rotary gap were constructed), because of the pressure of other work, the program was not continued. Later some experimental work was done using thyratrons and pulse lines in connection with ER sonar development which of-

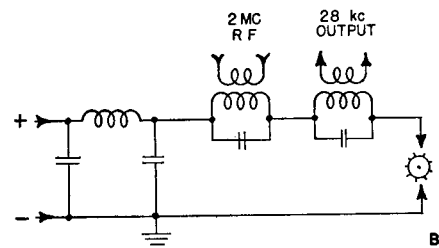
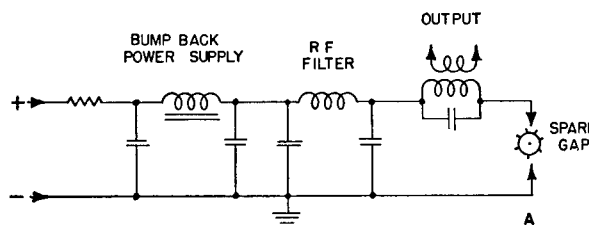


FIGURE 127. Basic spark transmitter circuits.

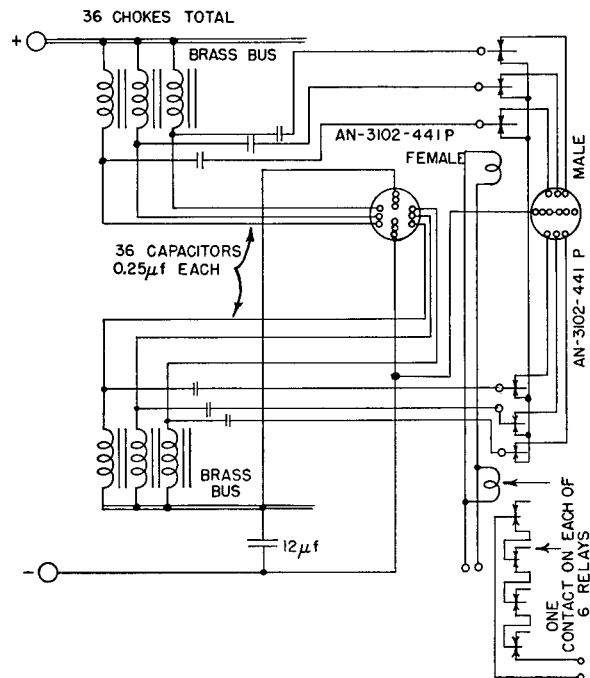


FIGURE 126. Circuit diagram of choke box, QH scanning sonar, Model 1.

ferred similar possibilities of simple transmitter construction. This is described in Chapter 7.

In developing the transmitter for the Model 2 scanning system, several tube types were tested. Type 829 proved unsuitable, but types 715B and 304TH, when used in the final amplifier stage, gave outputs of 8 kw and 10 kw, respectively. Types 8005 and 807 were used as driver tubes for the 304TH tubes, using cathode coupling. The 807 gave insufficient output, and even with type 8005, difficulty was encountered in driving the 304TH tubes. The 715B was chosen as the most suitable, additional reasons for this choice being its lower filament power requirement, and the removal of type 304TH from the Navy-approved list. The use of interstage transformer coupling (in the driver plate) proved better than cathode coupling.

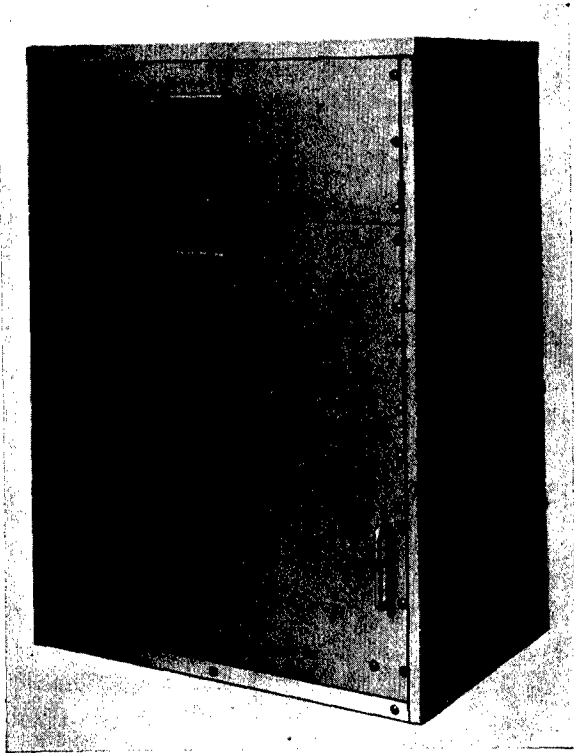


FIGURE 128. Front view of transmitter, QH scanning sonar, Model 2.

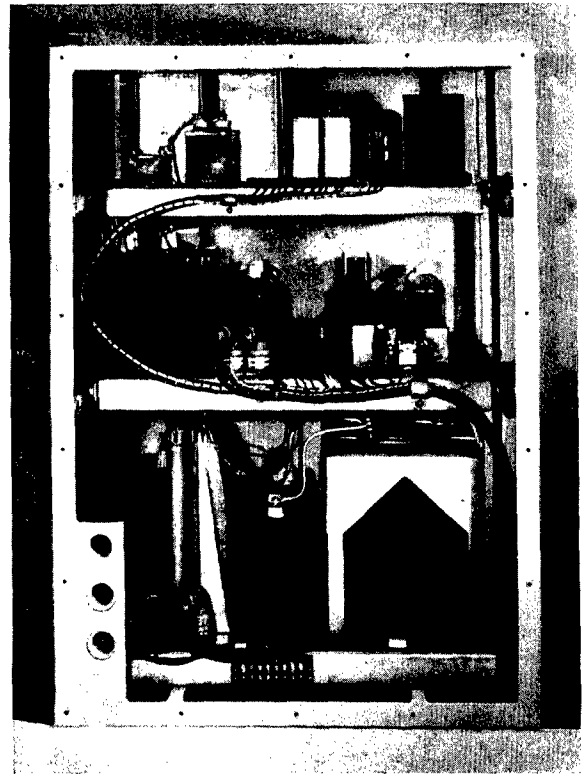


FIGURE 129. Rear view of transmitter, QH scanning sonar, Model 2.

The Model 2 transmitter was then constructed, using two 715B tubes in parallel as a final amplifier. These tubes were driven by a single 715B, and this in turn by a 6V6GT buffer amplifier. Difficulty was encountered with undesired feedback. For hand-keying with limited power output, a feedback circuit was tried using a 6V6 to rectify some of the output, the resulting voltage being filtered and used as a bias for the 6V6GT amplifier. Radio-frequency feedback troubles prevented this circuit arrangement from working out satisfactorily. Another scheme for underwater communication was tried in which 120 cycles was used in hand-keying to modulate the signal frequency and thereby to reduce the average drain on the power supply. This was satisfactory because the arrangement did not involve a feedback path.

Although unicontrol tuning (see Figure 11) had been proposed for the QH Model 1 system and a receiver incorporating the necessary circuits had been constructed, no provision had been made for this feature in the transmitter. However, the Model 2 transmitter was designed for unicontrol, and functioned satisfactorily. The common heterodyning oscillator

was in the receiver, with its output coupled through a cathode follower to the transmitter. Because of the length of the coupling line and its capacitance, the high-frequency signal (80 kc to 91 kc) was considerably attenuated, and it was necessary to use a step-up transformer at the transmitter end of the line. Figures 128 and 129 are photographs of the transmitter finally designed and built. It was constructed with three chassis. The bottom chassis contained the high-voltage power supply; the middle chassis, the driver and output amplifier; the top chassis, the low-voltage power supply, converter, and keying unit. The chassis were mounted on roller slides for easy access in maintenance. The only adjustment provided was a potentiometer which controlled the pulse length.

Figure 130 is the circuit diagram for the high-voltage power supply chassis. The on-off switch on the console-supplied power to operate relay K301, which connected the transmitter to the ship's power line. A time-delay relay S-301 prevented excessive line current during the warm-up time of the rectifier and amplifier tubes (715B tubes require  $\frac{1}{2}$  to 3 minutes for heating). C-301, L-301, and C-302 formed the bump-

CONFIDENTIAL





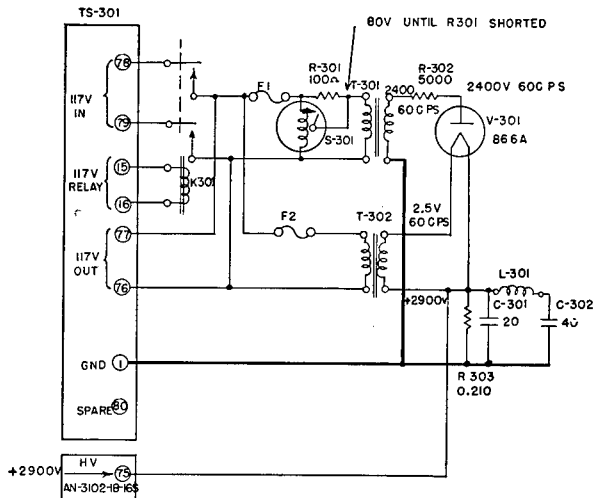


FIGURE 130. Circuit diagram of transmitter power supply (chassis A), QH scanning sonar, Model 2.

back filter (see below) and R-303 served as a bleeder resistor for this supply.

Figure 131 is a circuit diagram of the driver and

output amplifier, which had three stages of amplification with transformer coupling.

Figure 132 is a schematic diagram for the converter chassis. A full-wave power supply supplied 720 volts for the 715B screens; 310 volts for the V-304 keying tube, V-303 oscillator, and V-305 converter; and -280 volts for grid bias on the 715B grids and in the converter and keying tube chassis. The 120-cycle voltage used in the hand-keying circuit was obtained from the rectifier through a 1- $\mu$ f capacitor.

Keying was accomplished by the relay K-302, located in the plate circuit of V-304, which removed the negative bias from the converter screen, and the short circuit from the transmitter output. At the same instant, the ground return for the commutator input transformer primaries was opened. The positive keying pulse obtained from the sweep circuits in the console drove the grid of V-304 positive. Since the grid was normally biased to cutoff, the positive pulse caused plate current to flow, closing the relay. Also as a result of grid current in V-304, the capacitor C-310 was charged by the positive pulse. This charge

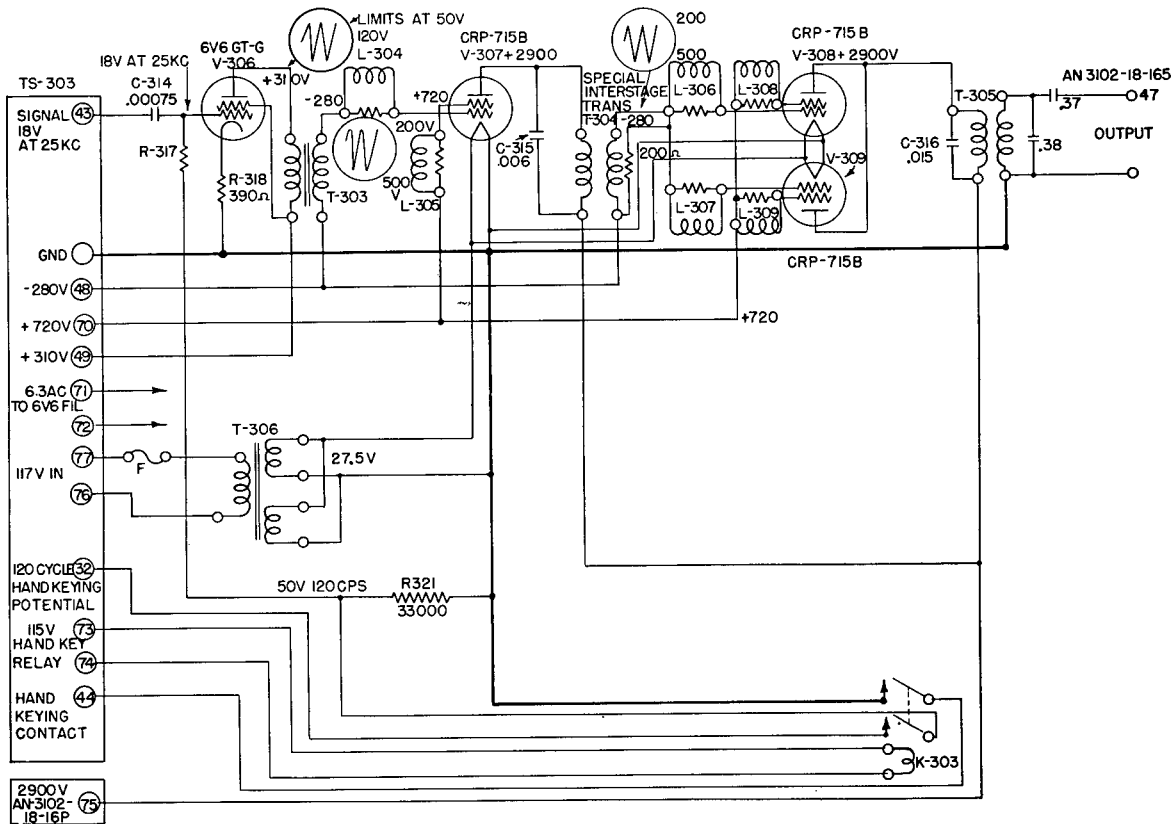


FIGURE 131. Circuit diagram of transmitter driver and output stages (chassis C), QH scanning sonar, Model 2.

CONFIDENTIAL

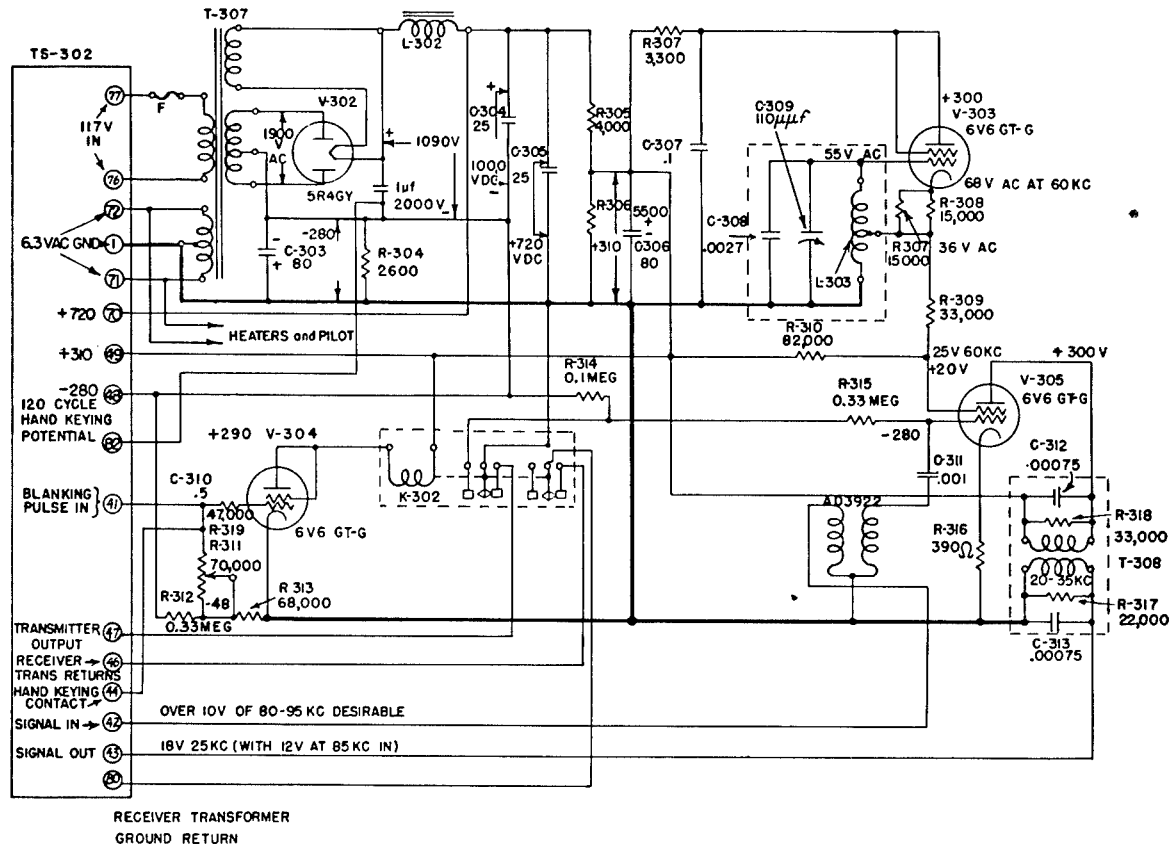


FIGURE 132. Circuit diagram of transmitter keying unit power supply (chassis B), QH scanning sonar, Model 2.

leaked off through resistors R-311 and R-313 until the tube was again cut off. Since the time constant was made adjustable by making R-311 variable, the length of time that the relay was closed could be controlled to fix the proper pulse length.

Frequency conversion was accomplished by mixing the unicontrol oscillator output (80 kc to 92 kc) with a 60-kc output from the local oscillator, V-303, to produce 20-kc to 32-kc signal. This conversion took place in V-305, the high frequency being fed to the control grid and the 60 kc to the screen, and a filter T-308 separated the 20 kc to 32 kc from the higher frequencies in the mixer output. The 20-kc to 32-kc output was used to excite the 6V6 amplifier on the third chassis. For code communication, operation of the hand-key closed relay K-303 (Figure 132) which operated K-302 (Figure 132) by removing the bias on V-304 and connected the 120-cycle voltage across R-321, causing modulation of the r-f signal. Later, a 200-ohm resistor was added across the secondary of T-304 and, for tuning the output load, a .38- $\mu$ f capacitor was shunted across the secondary of T-305 and

a .37- $\mu$ f capacitor placed in series with the output lead.

Figures 133 and 134 show the choke box, which contained the circuits necessary to introduce a polarizing current to the transducer, and to complete the send-receive network. It also served as a junction box for interconnection of the transducer cable, the two commutator input cables, and the transmitter output cable. The 7-mh chokes and .05- $\mu$ f coupling capacitors were provided to tune the transducer circuits to the proper impedance. These, with the .38- $\mu$ f and .37- $\mu$ f capacitors mentioned in the preceding paragraph, reflected a 50-ohm load across the secondary of the output transformer T-305.

The general construction of the final amplifier output transformer (also the one used between the driver and final amplifier stage) is shown in Figure 135 and Figure 136. This transformer was designed to work into a 50-ohm resistive load and reflected approximately 750 ohms when tuned to 28 kc with .015  $\mu$ f. Unloaded (interstage use), the tuning capacitor required for 28 kc was .006  $\mu$ f. The primary self-induc-

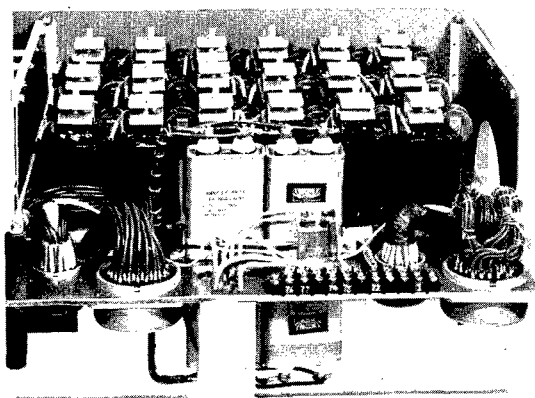


FIGURE 133. Rear view of choke box, QH scanning sonar, Model 2.

tance was 5.6 to 6.0 mh, the coil having 295 turns of No. 15-36 Litz wire in a universal winding with  $\frac{1}{4}$ -inch throw. The secondary had four spiral-wound pies of 45 turns each, using No. 15-36 Litz wire. Its self-inductance was 1.75 mh.

A few difficulties were found on installation.<sup>83</sup> The long ground leads involved in the send-receive networks between transmitter and choke box caused

trouble due to noise pickup and pickup of signal frequency in the unicontrol circuit. Shortening these leads solved this difficulty.

Initially, the installation on USS CYTHERA used the choke box<sup>83</sup> from the Model 1 system. Later this was removed and the choke box described above was installed.<sup>84</sup> Considerable power loss occurred in the choke box. The measured transmitter output was 6,450 watts. The power output of the choke box into the transducer was 3,800–2,950 watts. Thus, the choke box efficiency was about 44 per cent, and the power lost about 3,600 watts.

Some investigation<sup>85</sup> was made of temperature compensation of the oscillators in the QH Model 2 sonar. Since the time rate of change of temperature was extremely rapid in the tests, it is doubtful that the tests were at all representative owing to the different thermal inertias of various materials involved.

#### 5.7.6

### Bump-Back Filters

In designing transmitters for CR scanning sonars, the fundamental problem was to obtain a supersonic acoustic signal in the water in the form of a pulse as powerful as possible without producing cavitation. With standard construction this would have required

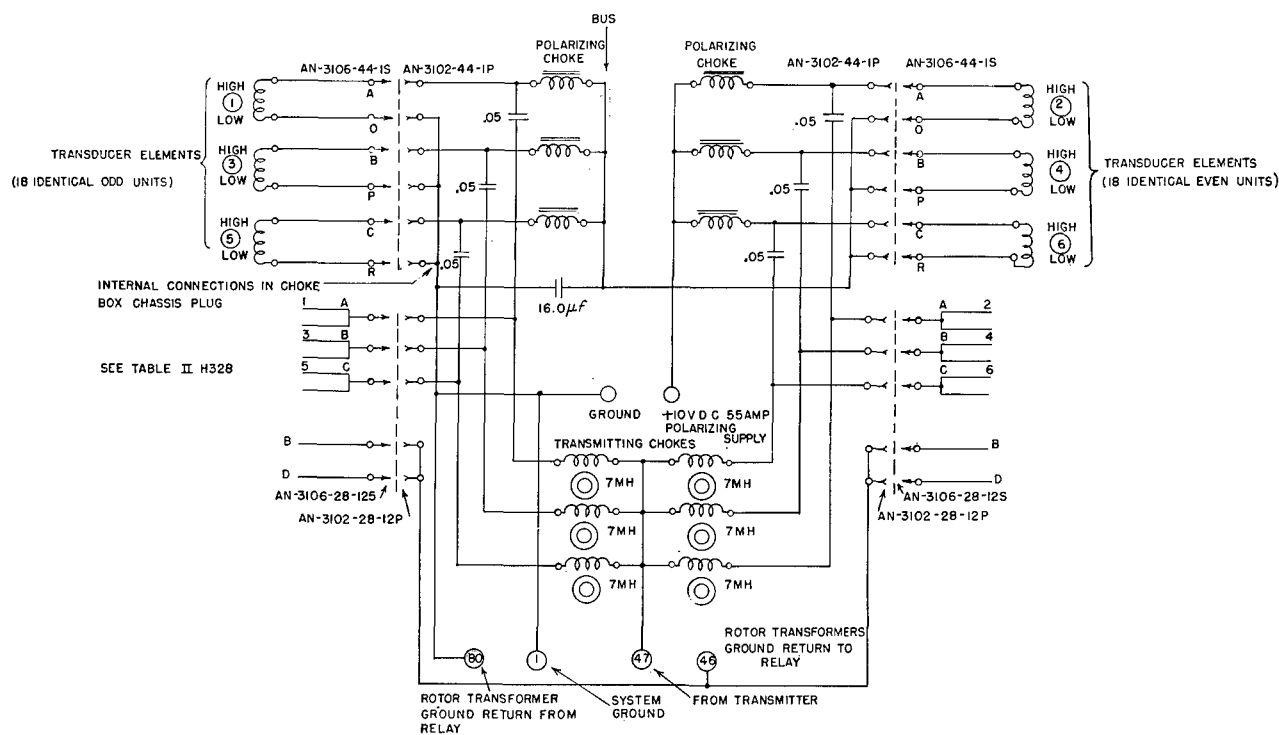


FIGURE 134. Circuit diagram of choke box, QH scanning sonar, Model 2.

CONFIDENTIAL



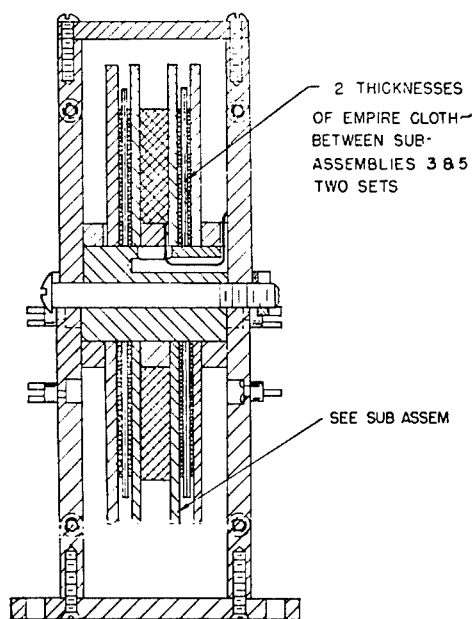


FIGURE 135. Assembly cross section, transmitter output transformers, QH scanning sonar, Model 2.

a large power supply to produce several kilowatts of electric power. Since signal power was actually needed for about 3 per cent of the time (30-msec pulses at 1-second intervals), this meant inefficient utilization of space and transmitter components, unless some means were found to store energy during the unused portion of the duty cycle.

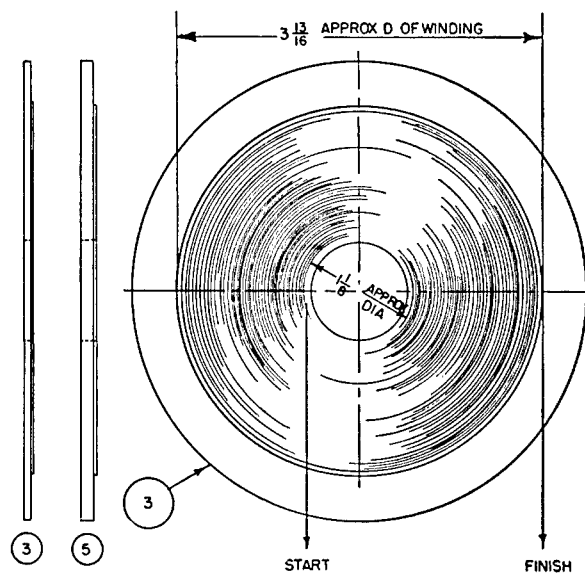
Radar systems were faced with a similar problem and developed the energy-storage or duty-cycle type of power supply, which stored energy in a filter by charging at a slow rate between pulses and discharging at a fast rate during the pulses.

A transmitter utilizing the charge and discharge of a large capacitor for its plate supply was first used at HUSL in the transmitter for the "Anchor" project,<sup>86</sup> but was unsuccessful. A similar arrangement was to have been used in the 36-tube amplifier which was not constructed. It was then suggested<sup>87</sup> that the simple aperiodic condenser discharge circuit used previously might be replaced by a filter using both inductance and capacitance, thus allowing more than one parameter for adjustment, and perhaps enabling the discharge curve to be made to approximate a flat-top pulse.

Further tests<sup>88</sup> established the fact that low-pass filter networks could be designed to produce approximations of square wave pulses. Conferences were

held with Radiation Laboratory personnel, the general methods for radar work were disclosed, and a comparison was made of the factors involved in radar applications and in sonar work.<sup>89, 90, 91</sup> These are pulse length, repetition rate, and peak power.

In the development of the Blockbuster transmitters, a simple pulse-forming filter was used. The rectifier charged capacitors in a low-pass pi-section filter (see Figures 121 and 129). The characteristics of this bump-back filter can be shown by analyzing and comparing the circuits of Figures 137A and 138A.<sup>92</sup> The first circuit represents the use of a straight capacitor storage system, and the second, the simple bump-back filter used in the CR sonar transmitter power supplies.  $R$  in each case represents the load on the power supply during transmission of the pulse. While the actual load was probably neither purely resistive nor constant, the assumption of a constant resistance load served to predict the experimental results with reasonable accuracy. The switch  $SW$  represents the effect of pulsing a class C amplifier by considering it to close only for the transmitting period. The capacitors are considered to be charged to a voltage  $E_0$  by the rectifiers.



NOTE:

FIX COIL TO PARTS (3) & (5) USING ACETATE TAPE. APPLY 2 EMPIRE CLOTH RINGS, FIX ANOTHER SPIRAL COIL TO SECOND EMPIRE CLOTH RING USING ACETATE TAPE. CONNECT INNERLEADS OF COILS. WINDINGS MUST BE AIDING.

FIGURE 136. Details of coils, transmitter output transformers, QH scanning sonar, Model 2.

The load current for the two cases may be found from the approximate expressions

$$i = \frac{E_0}{R} e^{\frac{-t}{R(C_1 + C_2)}} \quad (\text{circuit, Figure 137A})$$

and

$$i = \frac{E_0}{R} e^{\frac{-t}{R(C_1 + C_2)}} [1 - A \cos(\omega t - \pi/2)] \quad (\text{circuit, Figure 138A})$$

when

$$A = \frac{2\omega L C_1 C_2}{R(C_1 + C_2)} \quad \text{and} \quad \omega = \frac{1}{\sqrt{L \frac{(C_1 C_2)}{C_1 + C_2}}}$$

Since the output voltage will be proportional to this current, the pulse shapes will be as shown in Figures 137B and 138C. In the first case the voltage falls off with a slope determined by the time constant  $R(C_1 + C_2)$ . In the second case the average slope is the same, but the initial slope is determined by the time constant  $RC_2$ , and the average slope is modulated by the current through the inductor  $L$  and capacitor  $C_1$  (see Figure 138B). This is a damped oscill-

ating current having a frequency determined closely by

$$f = \frac{1}{2\pi \sqrt{L \frac{C_1 C_2}{(C_1 + C_2)}}}$$

The current through the choke is approximately expressed by (see Figure 138B)

$$i_1 = \frac{E_0 C_1}{R(C_1 + C_2)} e^{\frac{-t}{R(C_1 + C_2)}} (1 - \cos \omega t)$$

Besides reducing power supply size and increasing efficiency, the bump-back filter thus controls pulse shape. The latter factor was of interest for three reasons: It was desirable to have the echo strength independent of bearing but, if there were considerable slope in the pulse envelope, this would not be true; extreme slope would produce serious bearing errors; and, it was thought that proper shaping of the pulse

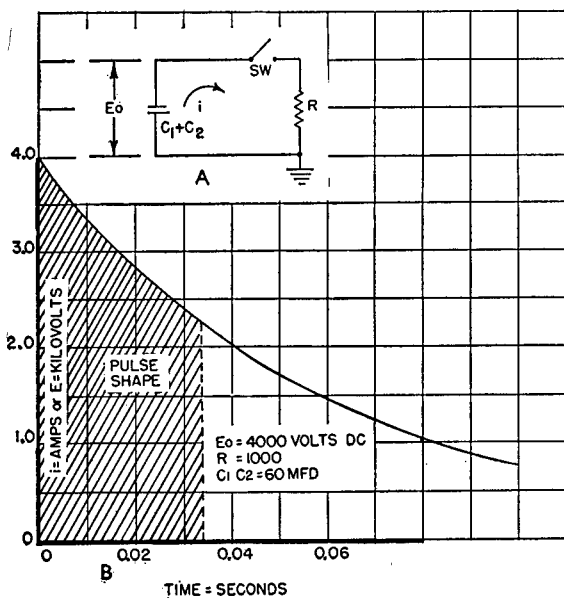


FIGURE 137. Current variation with straight capacitive filter.

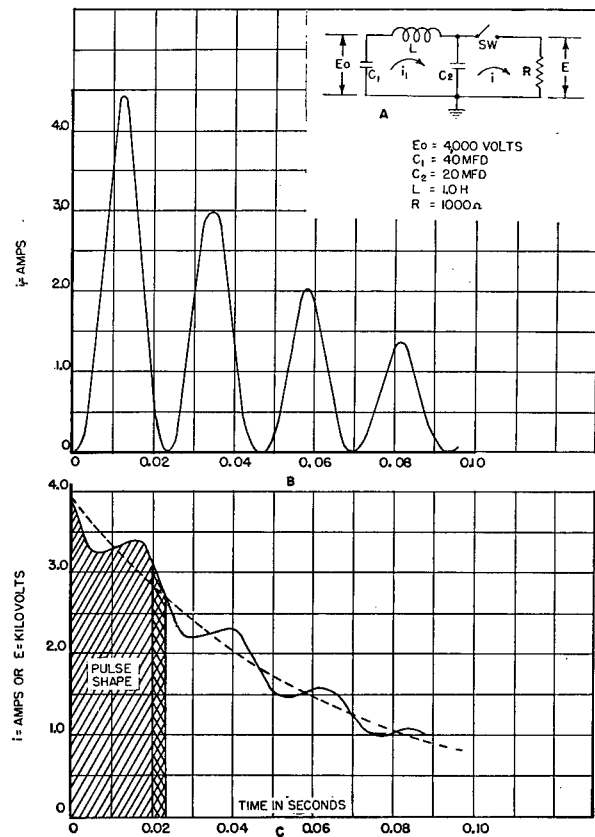
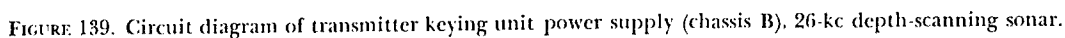


FIGURE 138. Current variation with bump-back filter.

CONFIDENTIAL



In the 26-kc depth-scanning sonar transmitter, designed and built at HUSL, a choke (T17COOB in

Figure 139) was added to the screen supply for the three 715B tubes. The action of this choke was as follows: at the beginning of the pinging period, a considerable drop in the screen voltage occurred because of the impedance of the screen choke and the very rapid rise in the screen current. Hence, the screen potential was low at first, and this tended to limit the initial high surge of plate current through the tube. With proper choke inductance, the net effect was to round off the initial sharp peak in the signal pulse which was otherwise obtained without the screen choke. Figure 140 is a sketch showing the approximate effect of the choke with and without the use of the bump-back filter in the plate supply. Photographs of the transmitting pulse envelope as appearing on a CRO are shown in Figures 141, 142, and 143. These show the results of varying the operating conditions in the transmitter.

#### SANGAMO METHOD

Sangamo Electric Company engineers found that in testing the amplifier circuits of the QH Model 2 system transmitter, the high initial screen and grid currents of the 715B tube dropped the screen supply voltage and raised the grid bias voltage very rapidly during the initial portion of the signal pulse. However, if the screen voltage were reduced to approximately 150 volts, the screen would draw no current; and below 150 volts, the screen current reversed because of the high screen secondary emission, and charged the power supply filter. At these low voltages,

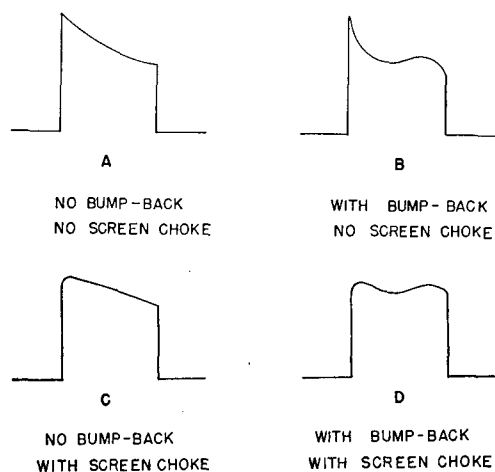


FIGURE 140. Output pulse shapes with and without screen choke.

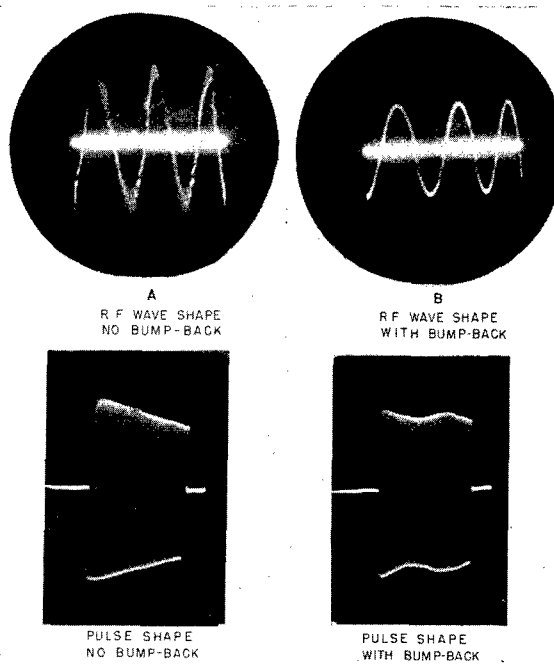


FIGURE 141. Output wave forms and pulse shapes, with and without bump-back filter, 26-kc depth-scanning sonar.

the output pulse was quite rectangular but the power was low. In the final design of their transmitter, it was decided to hold the screen supply voltage to about 350 volts, and to add sufficient capacitance in the supply filter to hold its voltage reasonably constant during the pulse period. The grid bias supply filter was split into two sections, additional capacitance and bleeder action being added to the section for the final amplifier grids to hold the bias voltage constant. The grid current for the intermediate stage was not excessive.

While the bump-back filter held up the end of the pulse, it made the initial portion steeper, while the average power remained practically the same. The Sangamo Electric Company decided that a simple capacitor storage system would perform satisfactorily and the elimination of the rather large choke was welcomed. For rapid pinging (short ranges) the capacitors did not charge to full voltage, so that the power output was suitably reduced.

It was also found at the Sangamo Electric Company that by proper variation of the driving signal level the pulse shape could be controlled and its slope reduced. Figures 144A, B, and C show this effect.

Figure 145 shows a keying circuit which was devel-

CONFIDENTIAL

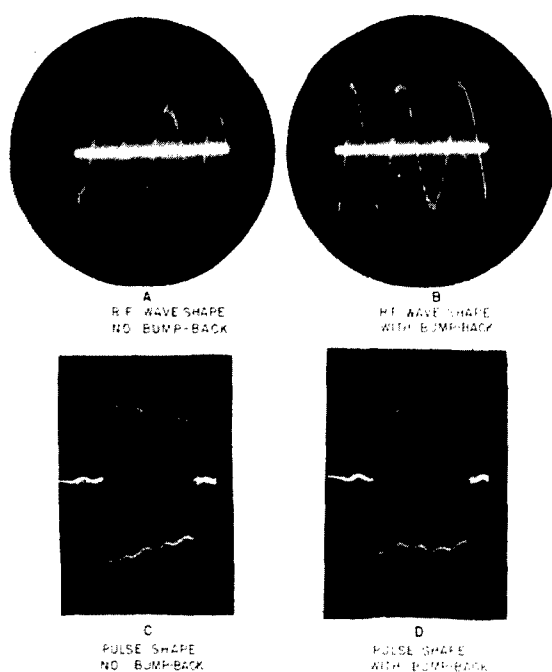


FIGURE 142. Wave forms and pulse shapes at grid of final amplifier, with and without bump-back filter, 26-kc depth-scanning sonar.

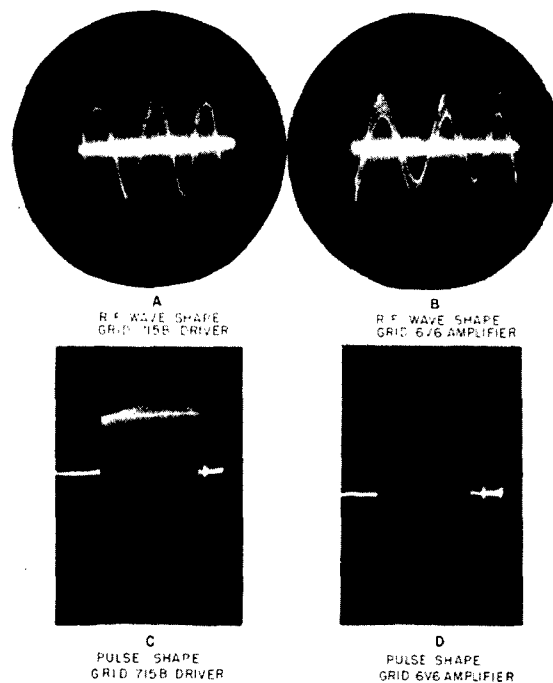


FIGURE 143. Wave forms and shapes, grid of 6V6 amplifier and grid of 715B driver, 26-kc depth-scanning sonar.

oped by the Sangamo Electric Company in order to control the pulse shape of the driver output. The normal keying circuit for the mixer tube merely removed the grid bias during transmission by grounding the grid end of the resistor  $R_2$  through relay contacts marked *SW*. This gave a rectangular driving pulse. By inserting a choke,  $L$ , shunted by the resistor  $R_1$  in series with switch *SW*, the driving pulse could be shaped as shown in Figure 144. This method of shaping had one disadvantage. The driving signal level to the primary of the input transformer (Figure 145) had to be held quite constant. This made for a critical circuit—especially critical to any reduction in the signal.

#### 5.7.7 Transmitter for Model XQHA Scanning Sonar

The transmitters as designed and constructed by the Sangamo Electric Company for Model XQHA scanning sonar<sup>1</sup> were based on those used with the HUSL QH Model 2 scanning sonar. Four identical units were constructed and tested (see previous sec-

tions). There were six basic differences between the XQHA and the QH Model 2 transmitters:

1. A higher plate supply voltage was used in the XQHA transmitter-amplifier tubes (4,200 versus 2,900 volts direct current), which, with the use of permanent magnet polarization and other improvements in the transducer, increased the efficiency, and raised the acoustical power output.
2. The bump-back feature in the power amplifier supply filter was dropped, and a straight capacitive filter used.
3. A buffer amplifier was added between the 60-kc oscillator and the converter stage.
4. The screen and bias power supplies were changed to permit energy storage operation.
5. The circuits controlling pulse length were changed and provision made to measure the pulse length on the PPI scope.
6. The mechanical layout and construction were changed to adapt them to Sangamo production practice and interpretations of Navy requirements.

Figures 146 through 150 show photographs and a circuit diagram of the XQHA transmitter.

CONFIDENTIAL

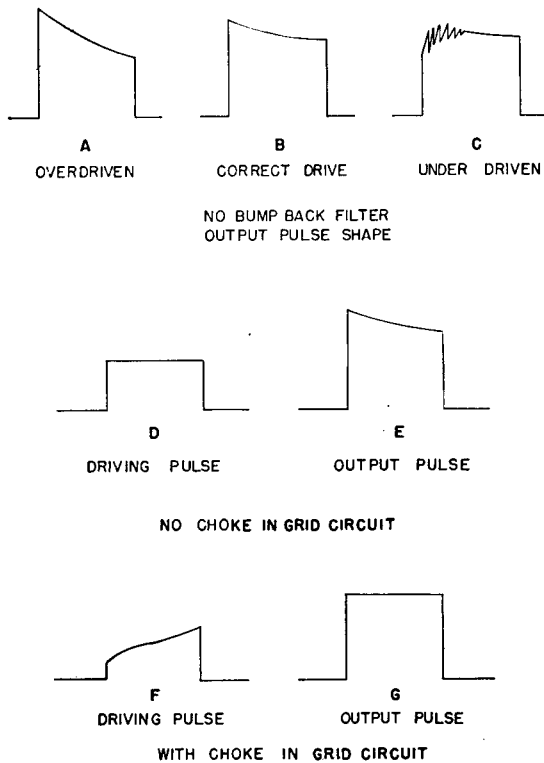


FIGURE 144. Pulse shapes with excitation control.

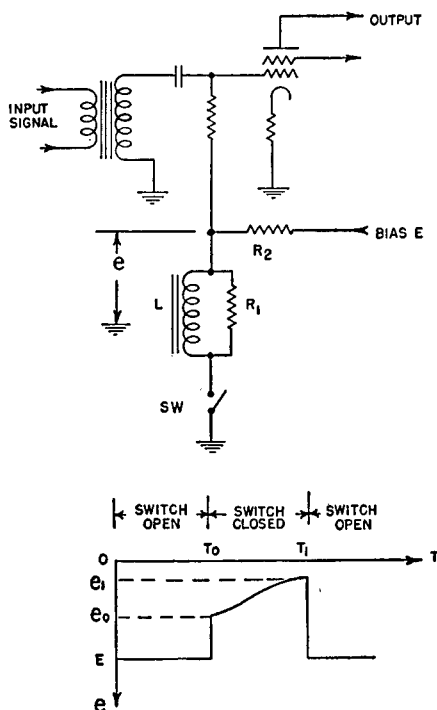


FIGURE 145. Diagram of shaping circuit for excitation control.

## 5.8 SWEEP AND TIMING CIRCUITS

### 5.8.1 Functions for a CR Scanning System

In a CR scanning sonar there are several functions which must be closely coordinated and therefore require close control of time intervals. These functions are:

1. Generation of the spiral sweep for the plan position indicator display.
2. Range determination.
3. Timing of the ping interval.
4. Blanking of the PPI screen during the flyback period or return of the sweep.
5. Control of the ping period.

#### GENERATION OF SPIRAL SWEEP FOR PPI DISPLAY

In general, all scanning sonars have used a PPI display with a spiral sweep that started from the screen center, representing the position of own ship, and expanded to the edge of the screen. With a magnetic deflection system, it was therefore necessary to produce a rotating magnetic field within the cathode-ray tube and at the same time to increase its strength linearly with time. To do this, it was necessary to use a coil assembly having proper space-phase relationships between coils and fed by polyphase voltages, the amplitudes of which followed a sawtooth variation. Various schemes of producing sawtooth-modulated polyphase voltages have been used. In all of these the chief problem was to obtain sufficient power to produce the desired spiral expansion on the PPI screen without distortion.

In one early design using a two-phase sweep system, the sweep was generated entirely by electronic circuits, synchronization being obtained by a contactor attached to the scanning commutator shaft. A signal of sweep frequency was modulated in sawtooth fashion before it was split into the two phases necessary for the PPI deflection circuit. In all other designs, a rotating generator device coupled to the scanning commutator shaft was used. One of these was a sinusoidal capacitor mechanism described later in this section; however, the most practical and successful means of obtaining the polyphase sweep voltages has been the use of a polyphase a-c generator coupled to the scanning commutator shaft. Two-phase generators were first used, but were later discontinued in favor of three-phase units.

Sawtooth current excitation was supplied to the

CONFIDENTIAL

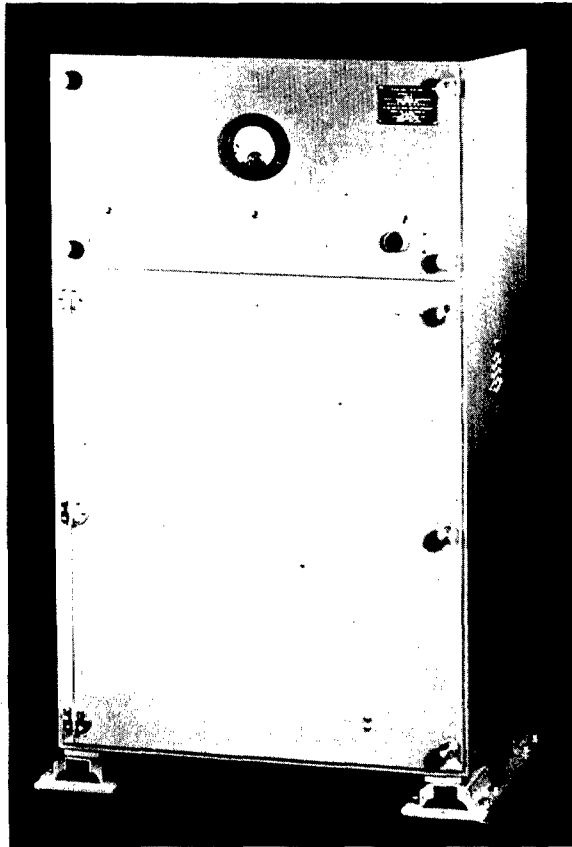


FIGURE 146. Front view of transmitter unit, Model XQHA scanning sonar.

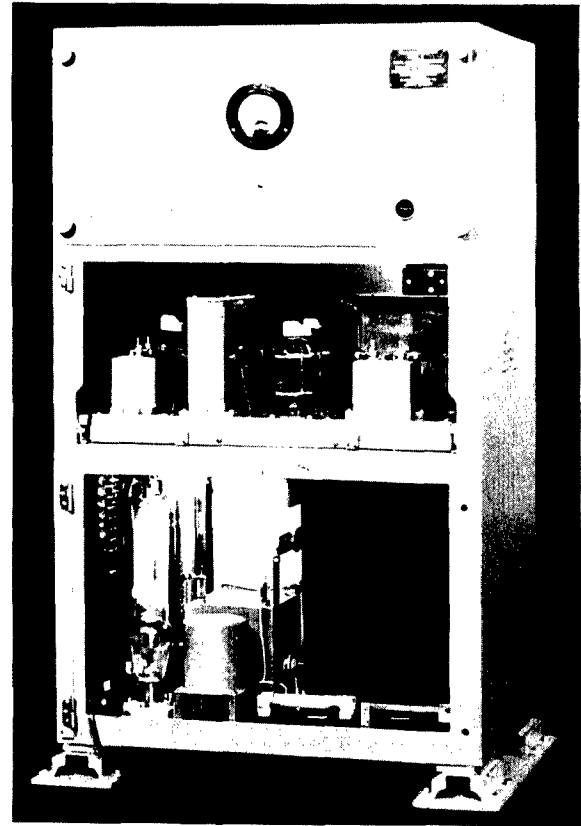


FIGURE 147. Front interior view of transmitter unit, Model XQHA scanning sonar.

rotor field of the a-c generator, which produced the requisite sinusoidal polyphase emf's. For synchronization, the unit was directly coupled to the scanning commutator shaft. Since two-phase deflection coils were the first standard equipment, they were used with the two-phase sweep generator and in some cases with a three-phase sweep generator and Scott-connected transformers. In the more recent CR scanning sonars, three-phase spiral-sweep generators and three-phase deflection coils have been used throughout.

#### RANGE DETERMINATION

The function of range measurement is associated with time because the velocity of sound in sea water is substantially constant, and the range is therefore determined by the time lapse between the emission and return of the sound pulse. The early CR systems had no means of range determination other than a visual estimate based on the known approximate maximum range of the PPI display. In the later CR

systems (HUSL QH Model 2 and the Sangamo Model XQHA), a chemical range recorder was used as an auxiliary means of more accurate range determination. When used, the recorder was connected to the output of the hand-trained listening channel.

#### TIMING OF PING INTERVAL

The time interval between pings was another function whose accurate control was necessary to the successful performance of the CR scanning sonar. In the first experimental systems, the operator initiated the ping by means of a hand key, the length of the ping period being determined by a simple type of relaxation oscillator. In later systems, both electronic circuits and mechanical timers were used to control the time interval between pings. These are discussed later in this section.

#### BLANKING OF PPI SCREEN

Blanking pulses applied to the PPI tubes are neces-

CONFIDENTIAL

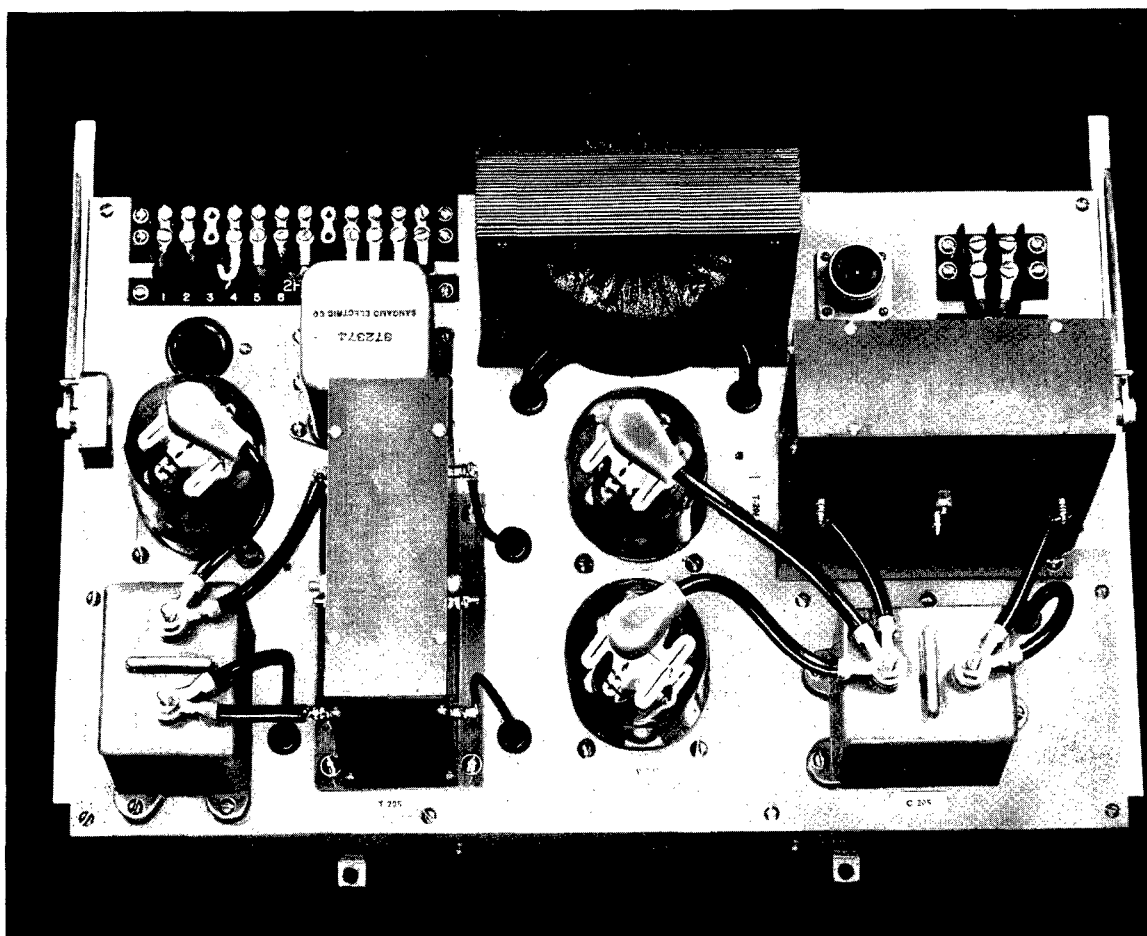


FIGURE 148. Top view of power amplifier chassis, transmitter unit, Model XQHA scanning sonar.

sary to blank the tube during the periods when the spiral sweep is being collapsed to the center of the tube screen. The present method is to make the cathode of the PPI sufficiently positive so that the brightening cannot occur. The blanking was made originally for only the duration of the transmission interval. In later designs, it was made longer because many of the switching transients did not die out until an appreciable time had elapsed. In the XQHA system the blanking was complicated because of the necessity of "painting" an electronic cursor line on the screen during the return of the sweep.

#### CONTROL OF PING PERIOD

The pulse length was originally determined by the length of time required for the scanning commutator rotor to make one revolution. This was done by means of a contactor and relays. Subsequently, the length of time that a relay was held closed by the

action of an energizing pulse was used to determine the ping length. This system was replaced by one utilizing a differentiating circuit whose time constant, with certain critical voltages, determined the ping length. Other methods were used; all are described in detail later in this section.

#### 5.8.2

### Early Sweep Development

#### ALL-ELECTRONIC SWEEP

The first experimental CR scanning system used the electronic spiral sweep from the MR system. No range-determining system was used, and the timing of the transmitted ping was done by hand. There was no blanking of the returned trace. The length of the transmitted ping was determined by a pair of interlocking relays.

The spiral sweep is shown in block diagram in Figure 151, and in detail in Figure 152. A simple con-

CONFIDENTIAL



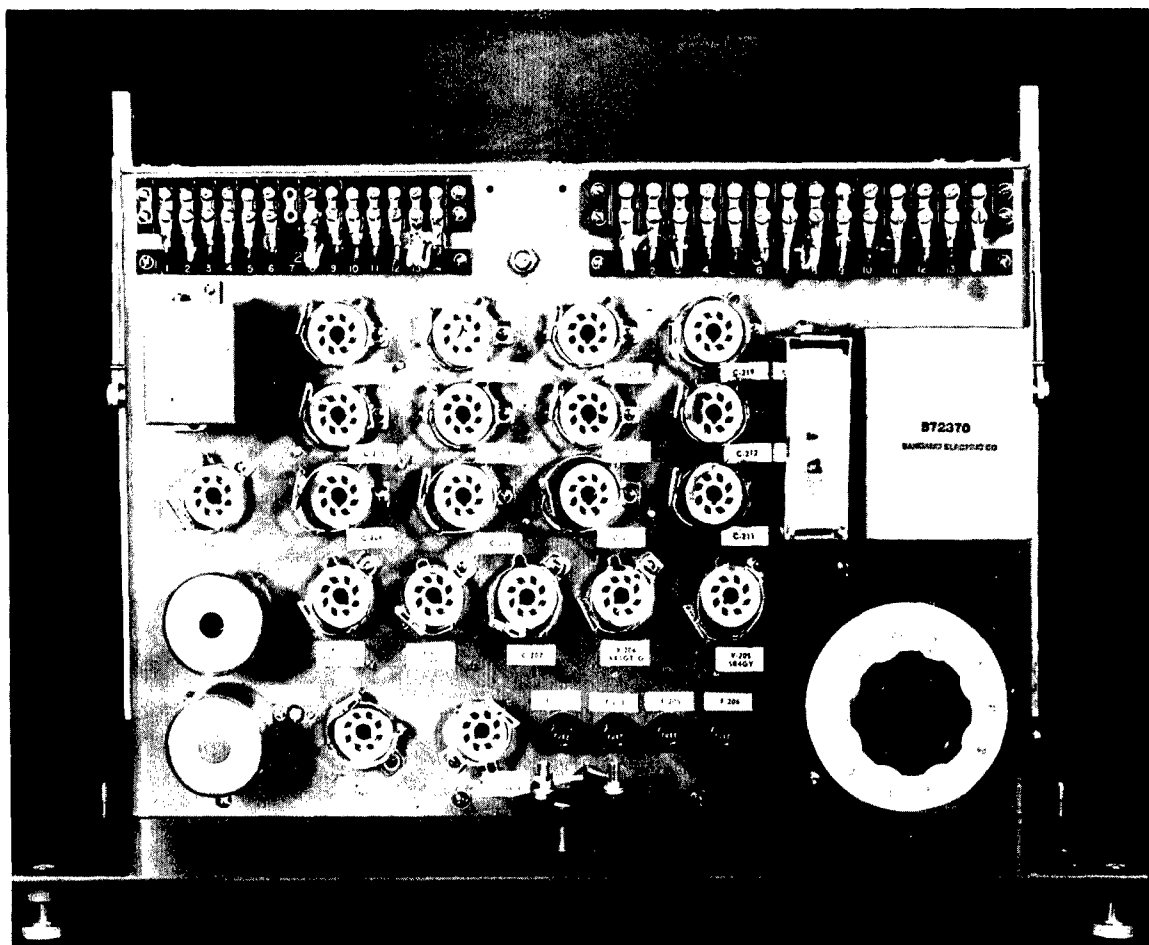


FIGURE 149. View of converter chassis, transmitter unit, Model XQHA scanning sonar.

tactor on the rotating shaft of the commutator was used to synchronize the signal from an RC sine wave oscillator. The oscillator supplied voltage to a modulator which in turn produced a sawtooth-varying modulation of the voltage. The output of the modulator was applied through a bridge-type phase splitter into a pair of power amplifiers and thence to the 2-phase deflection coil assembly around the neck of the cathode-ray tube. All these units were designed to operate at 10 c for this trial system.

The saw tooth sweep was generated by the discharge of the 80- $\mu$ f capacitor (C101) through the bleeder connected across it. During the time of transmission of the ping, the four switches S1, S2, S3, S4, shown in the network (Figure 152) were closed simultaneously, connecting the capacitor to the battery and the grid returns of the 6SK7 and 6J5 directly to the negatively charged side of the capacitor, and shorting the sweep output. Hence, immediately after trans-

mission of the ping, the two tubes were biased nearly to cutoff, and as the capacitor discharged, the bias decreased, allowing the gain of the tubes to increase. Because the output of the oscillator was applied to the grid of the 6SK7 with which the 6J5 was cascaded, the output of the 6J5 was a sine wave voltage starting at almost zero amplitude and increasing linearly with time to some maximum value. The switches also effected prompt return of the spiral sweep to the starting point.

The bridge type of phase splitter was adopted shortly before the first trial of the CR scanning method, and was used with it. This phase splitter consisted of a bridge circuit formed by two capacitors and two resistors, all having the same reactance or resistance at the operating frequency. With this circuit arrangement, a phase-lead and a phase-lag section were connected across the source. When the capacitors were of equal value and the resistors were of equal value,

CONFIDENTIAL

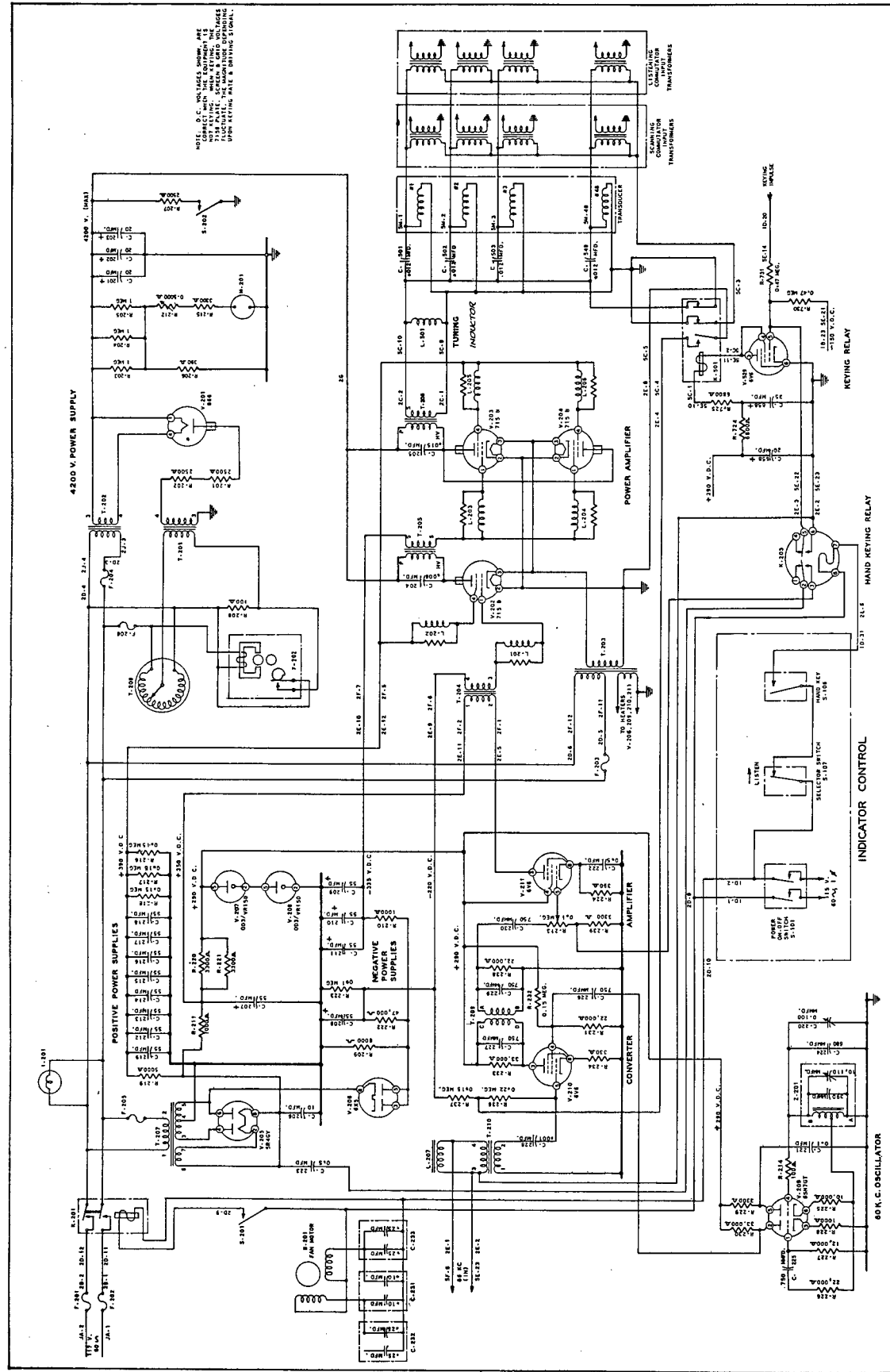


FIGURE 150. Circuit diagram of transmitter, Model XQHA scanning sonar.

CONFIDENTIAL



the phase difference between the two output points of the bridge were exactly 90 degrees for all frequencies of interest. For the operating frequency, at which the reactances and resistances were numerically equal, the two output voltages were equal in magnitude. The two outputs of the phase splitter were amplified to provide sufficient current through the two-phase PPI deflection coils to give the desired beam deflection.

It was noted on the first field trip<sup>63</sup> that the spiral sweep was far from perfect. Transients were troublesome at the beginning of the spiral; voltages for synchronizing influenced brightening; and 60-cycle hum interference was noticeable. Fluctuations in the supply voltage, produced by the normal operation of the apparatus, had very pronounced effects on the cathode-ray tube. On the second field trip, the spiral sweep of the CR trace was obtained with a manually controlled sweep because of the severe transients that remained in the modulator. A further difficulty was that the phase of the oscillator shifted with a change in synchronizing signal. It was thought that it would be possible to use transformer coupling at the 10-cycle frequency to eliminate d-c transients. Work along this line was discussed in Chapter 4.

As previously stated, initiation of pulse transmission was manually controlled by use of a hand key. A contactor actuated by the scanning commutator provided a voltage pip at each revolution of its rotor. When the hand key was closed, the first succeeding pip produced by the shaft contactor operated a switching system composed of two relays which were so interlocked that the relay operating the transmitter closed at this time and stayed closed until a second pip, generated by the next closing of the contactor, released it.<sup>95, 96, 97</sup>

Following the tests of the CR trial system on the AIDE DE CAMP, extensive developmental work on spiral sweeps was carried on, leading to an all-electronic type and mechanical types using rotating capacitors and polyphase a-c generators.<sup>7</sup> The necessity for a better spiral-sweep generator than that used in the MR system grew out of the more stringent requirements of the CR system, including accurate synchronization of the sweep rotation with that of the capacitive commutator.

At a conference at HUSL during November 1942, other methods of securing range and bearing indication were discussed.<sup>98, 99</sup> After careful consideration of all the suggested methods for the production of a

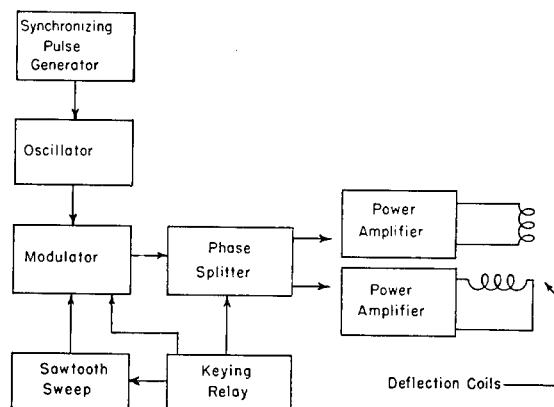


FIGURE 151. Block diagram of sweep circuit for first CR trials with Medusa transducer.

spiral sweep, that of a capacitive modulator was chosen as most promising for immediate development.<sup>100</sup> Other methods proposed the use of two- or three-phase synchro generators. A two-phase generator was rewound for this use, but was discarded because of poor output wave form. A small Elinco synchro was also tried but found unsatisfactory. Further development of the synchro generator method is described below.

#### ROTATING CAPACITIVE SWEEP GENERATOR

A rotating capacitor with two sets of rotors spaced 90 degrees apart was received for testing. It was incorporated in the circuit shown in Figure 153 which was designed and built early in December 1942. V104 was used to linearize the sawtooth-varying voltage across the 2- $\mu$ f capacitor (C101). This voltage was applied to two rotating sinusoidal capacitors, *a* and *b*, mounted on the commutator, the outputs of which were therefore sawtooth modulated voltages with a frequency equal to the rotation frequency of the commutator, and with 90 degrees phase difference. This sweep was then applied to the deflection coils through two amplifiers, each with low output impedance. Initiation of the sweep was accomplished by use of a switch S1.

The spiral-sweep generating capacitor was a KS-8534 capacitor built by the Allen D. Cardwell Manufacturing Company for radar applications, and consisted of four sets of stator plates and two sets of rotor plates mounted on a shaft. Rotation of this condenser produced two outputs, both approximately sinusoidal and 90 degrees out of phase. This condenser was modified mechanically to obtain better operation and



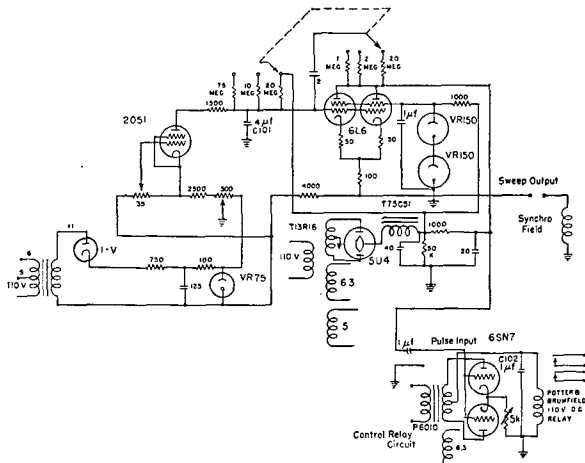


FIGURE 154. Circuit diagram of sawtooth generator for spiral sweep, auditorium system.

rapid restart of the sweep. The 4- $\mu$ f (C101) sweep capacitor was charged from the positive supply through one of three resistors which determined the maximum range of the sweep. A second charging circuit, coupling the plate and grid, was used to linearize the sweep, and was also switched. The sweep was restarted when the plate voltage of the 2051 thyatron, which was the voltage across the sweep capacitor, became sufficiently positive with respect to the cathode to fire the thyatron. The 35-ohm potentiometer was used to control this firing point. The 300-ohm potentiometer controlled the initial radius of the spiral sweep.

The positive pulse appearing in the plate circuit upon discharge of the sweep capacitor was used for operating a control relay to close the transmitter relay, to blank the scanning receiver, and to produce the initial gain reduction for the receiver TVG circuit. The pulse triggered a grid-controlled rectifier whose output closed the control relay, and charged a 1- $\mu$ f capacitor (C102) across the relay coil. The relay remained closed until the capacitor had partly discharged, thus determining the length of the transmitted ping.

In this auditorium demonstration system, the sweep generator was a GE 110-55 volt three-phase synchro transmitter which had a maximum of 3 volts of direct current applied across its field winding. A GE three-phase 55-55 volt differential synchro was inserted between the generator and the stator coil of a Diehl 115-volt synchro repeater around the neck of the cathode-ray tube, so that the bearing of the display could be changed in synchronism with the

position of the rotor of the DG. The shaft of the DG was positioned according to the compass heading of the imaginary ship so that the resultant display was a plot in true bearing rather than relative bearing.

#### 5.8.4 Further Sweep Development

Because synchros were difficult to obtain at the time of these experiments, a search was made for some other type of polyphase spiral-sweep generator.<sup>7</sup> A Kollsman two-phase synchro, type 738 (similar to Size 1 synchro), which required an amplifier in each output phase to supply the requisite power to the deflection coils, was tried. The wave form was excellent, and a circle which appeared perfect to the eye was obtained.

To get more voltage from this generator, its rotor field was rewound to obtain 180 ohms resistance. More than enough voltage was then generated to expand the spiral from the screen center to well beyond the outside of the PPI tube with a 6F6 cathode follower in the sawtooth sweep circuit. The linearity was considerably improved and the wave form was still good.

Further tests showed that a Size 1 synchro generator did not generate sufficient voltage without amplifiers to give full-scale PPI deflection. The next choice was a GE 5 CT synchro as the three-phase spiral-sweep generator. For a short period a standard two-phase deflection coil assembly was used with the unit, conversion from three- to two-phase being effected by use of a Scott-connected transformer network. Later the three-phase generator with three-phase deflection coil spiral sweep was adopted in all further scanning sonars.<sup>101</sup>

#### 5.8.5 Sweep and Timing Circuits for the Aide de Camp ER/CR Scanning Sonar

The ER/CR scanning sonar, installed on the AIDE DE CAMP, used the same type sawtooth sweep-generator circuit that had been developed for the auditorium demonstration system except that the parallel 6L6 cathode followers were replaced by a single 6F6. The circuit, shown in Figure 155, has just been discussed.

Up to this time range determination had been largely a visual estimation of the radial distance of the echo spot from the center of the PPI face. This procedure was dependent upon the linearity of the



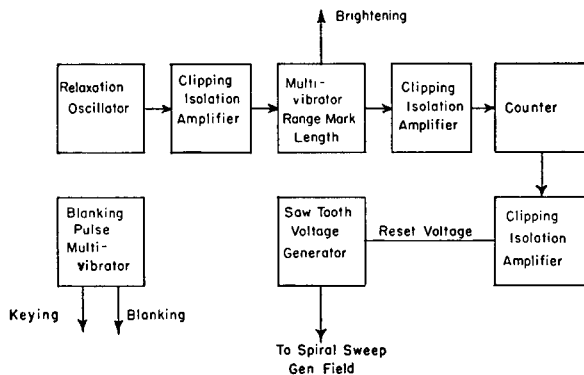


FIGURE 157. Block diagram of sweep generator and range marker, AIDE DE CAMP ER/CR scanning sonar.

The isolation amplifiers were conventional resistance-coupled triodes, operated as clippers to pass only negative input pulses. The multivibrators were standard units. The counter was a device in which a capacitor was charged stepwise, one step by each brightening pulse. After a sufficient number of pulses, the capacitor was charged to such a potential that the  $\frac{1}{2}$ 6SN7 (V106) triode conducted. The grid of this triode was connected to the capacitor through the secondary of a transformer, and its cathode was biased at 105 volts positive by means of the VR tube bleeder. The plate of the triode was connected to a more positive potential through the primary of the transformer. The windings were so phased that as the plate current started to flow, the grid was driven further positive, increasing the plate current and thus setting up a violent oscillation one-half cycle long which discharged the counting capacitor and allowed the cycle to restart. This discharge pulse, being negative,

was passed through the clipper isolation amplifier.<sup>105</sup>

The first 6Y6 (V108) in the sawtooth sweep circuit was a reset tube and was used to discharge the two 10- $\mu$ f capacitors connected to the grid of the second 6Y6 (V109), on receipt of the positive pulse from the clipping isolation amplifier. By using two 10- $\mu$ f capacitors and a charging resistor with each, a sawtooth varying current with a nearly constant rate of growth was obtained. It will be noted that the sawtooth sweep and the range marker required two well-stabilized power supplies, as well as eight tubes. The sawtooth voltage was used with the spiral-sweep generating synchro to produce the spiral sweep on the cathode-ray tube. The blanking pulse was used to short the output of the receiver as in the auditorium system.

The pinging relays and controls were changed between installation on the AIDE DE CAMP and the installation of the counting-marking chassis. The original ping-length control shown in Figure 158 consisted of a time-delay multivibrator, a ping-length multivibrator, and an electronic switch. The electronic switch consisted of a pair of diodes with transformer-coupled input and transformer-coupled output so that the bias could be changed to make them conducting or nonconducting, and hence pass or not pass the signal from the oscillator to the driver. The time-delay multivibrator was a standard unit operated by the short differentiated positive pulse from the sweep circuit upon its first grid. When it returned to its normal state, the positive pulse on its first plate tripped the second multivibrator, thus opening the electronic switch. After the .05- $\mu$ f capacitor in the circuit of the second grid of the ping-length multi-

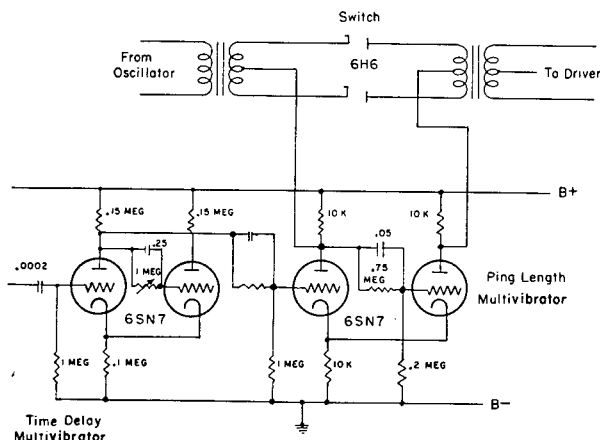


FIGURE 158. Circuit diagram of original ping length control, AIDE DE CAMP ER/CR scanning sonar.

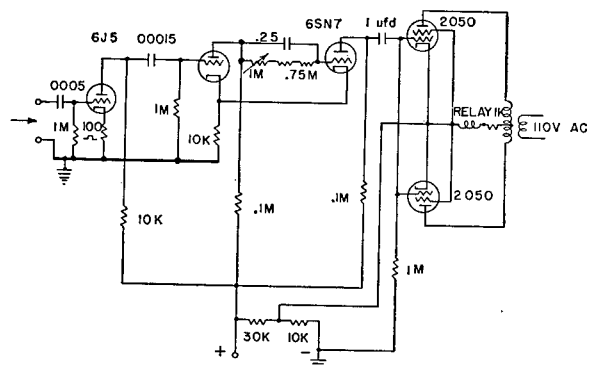


FIGURE 159. Circuit diagram of final ping control, AIDE DE CAMP ER/CR scanning sonar.



brator had discharged sufficiently, the circuit returned to its normal condition and the switch was closed.

The final ping-control circuit for this system is shown in Figure 159. The sweep discharge pulse was differentiated, and then amplified. The amplified pulse tripped a type of multivibrator whose output was a square positive pulse which was fed to two grid-controlled rectifiers. The current through the full-wave rectifier actuated the transmitter relay.

Range determination by means of the chemical range recorder was tried at about this time. The signal in the scanning channel was gated by a tube which was made conducting for a few degrees at a preset bearing, allowing the echo signal pulse to pass through to the chemical recorder. This was not very successful, partly because the information from the given bearing was presented to the chemical recorder only during the time that the scanning beam of sensitivity was pointed along that particular bearing. Later, the incorporation of the listening channel allowed direct and much better application of the chemical range recorder.<sup>106</sup>

Although complicated, the counter sawtooth sweep circuit operated satisfactorily. After about three months of operation, it was decided to increase the count from three to four; however, its operation was never quite so good as with the original adjustment.<sup>107</sup> Though similar range-marking systems have been used successfully elsewhere,<sup>108</sup> some doubt as to the ability of this circuit to perform properly had been expressed earlier. These doubts led to the development of the *dynamic monitor*.<sup>109</sup> An extended discussion of linear sweeps will be found in the section on ER system sweeps.<sup>110, 111</sup>

As in the auditorium demonstration system a DG was introduced into the spiral-sweep circuit between the spiral-sweep generator and the three-phase deflection coil to obtain a true-bearing plot. This reduced the spiral from a full 6 inches to 4 inches, but it was still usable for the experimental work.

#### 5.8.6 Sweep and Timing Circuits for QH Scanning Sonar, Model 1, Serial 1

In the Model 1 system the spiral sweep was generated by a synchro used as a three-phase generator, attached to the commutator shaft; and was applied to the PPI tube by means of the stator of a synchro

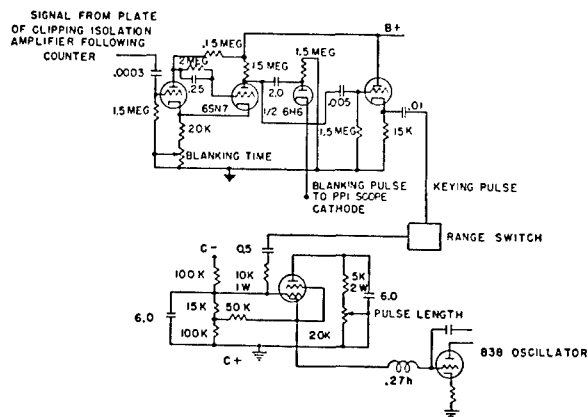


FIGURE 160. Circuit diagram of sweep and timing, QH scanning sonar, Model 1, Serial 1.

around the neck of the tube. The sawtooth excitation for the rotating field winding of the sweep generator synchro was generated and controlled by a separate all-electronic sweep circuit. This circuit also generated the pulse which made the range-mark circles, the blanking pulse, and the keying pulse. The maximum ranges were 1, 2, and 4 kiloyards. The range marks were spaced at fractions of  $\frac{1}{4}$ ,  $\frac{2}{4}$ ,  $\frac{3}{4}$ , and  $\frac{4}{4}$  of the maximum range. The range-marking pulses were applied to the scanning receiver to produce the range circles.

The timing circuits were essentially the same as those used on the AIDE DE CAMP in the ER/CR system, namely: the relaxation oscillator, the three clipping isolation amplifiers, the range-marking length circuit, the counting circuit, and the sawtooth sweep circuit (see Figure 157). The blanking pulse generator and keying pulse generator, with the ping-length control circuit, were changed and are shown in Figure 160. The blanking pulse generator was a multivibrator of the type described in the previous section. The output of the third clipping isolation amplifier (see Figure 157) was differentiated, and the resultant pulse tripped the multivibrator. Its square wave output was applied to the cathodes of the PPI tubes through a diode  $\frac{1}{2}$  6H6, which prevented any brightening during the blanking time. In addition, the blanking pulse was differentiated and applied to the transmitter-power-supply chassis to key the transmitter. A description of the operation of the transmitter keying circuits is given in Section 5.7 on transmitters in this chapter. There was no muting of the audio channel in the Serial 1 system.

The range determination was still largely a prob-

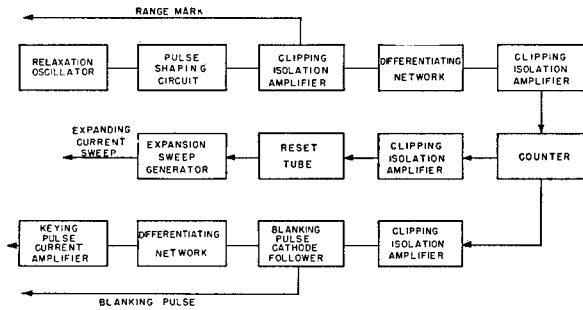


FIGURE 161. Block diagram of timing circuits, QH scanning sonar, Model 1, Serial 2.

### 5.8.7 Sweep and Timing Circuits for QH Scanning Sonar, Model 1, Serial 2

The timing circuits for Serial 2 were again all-electronic, furnishing range-marking pulses to the PPI. The principal change was the substitution of a 6SL7 lead-lag relaxation oscillator for the VR tube relaxation oscillator and the number of circuit components was reduced by a partial redesign. However, the circuit was still somewhat complicated and required many compensation resistors which had to be switched when the range was changed.

A block diagram of the timing circuits is shown in Figure 161 and a circuit diagram in Figure 162. The range marks were applied in the same manner as in the QH Model 1, Serial 1 system. The sawtooth current sweep was fed into the field of a synchro generator as in Serial 1. The balance of the spiral sweep was the same. The keying and blanking pulses were also applied in the same manner as in Serial 1.

The relaxation oscillator was a twin triode (V101A and V101B) connected as a cathode-coupled multivibrator. Its square pulse output was doubly differentiated in the pulse-shaping circuit. A variable resistor controlled the first time constant in the differentiation and hence determined the length of the range

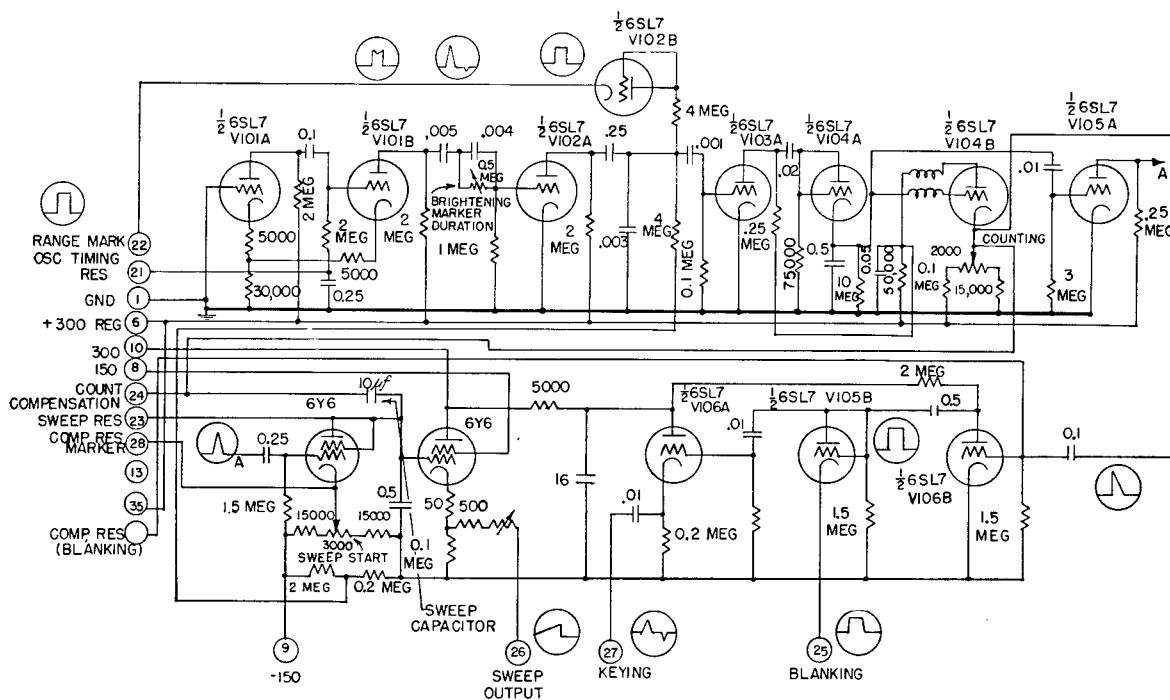


FIGURE 162. Circuit diagram of timing circuits, QH scanning sonar, Model 1, Serial 2.

CONFIDENTIAL

mark. The clipping isolation amplifiers were substantially the same as those used in Model 1, Serial 1 system. A diode, V102B, was used as a switch to prevent differentiation of the brightening pulse from producing a darkened zone following the range mark. The positive pulse output of V102A was differentiated by a simple RC network and applied through the next clipping isolation amplifier, V103A, to the counting circuit. The counting circuit was similar to that described in the AIDE DE CAMP ER/CR sonar sweep and timing circuit.

The negative step created by the discharging of the counting capacitor was passed through a clipping isolation amplifier V105A, similar to the preceding clipping isolation amplifiers, and the resultant positive pulse was applied to the grid of the reset tube. This reset tube discharged the sweep capacitor and hence reinitiated the sweep.

The sawtooth sweep started with substantially zero current flowing through the 6Y6 sweep generator tube; this occurred when the grid was biased to about -75 volts. The current increased as the grid became more positive because of the charging of the sweep capacitor through the sweep resistors.

The pulse formed on the cathode of the counting circuit discharge tube passed through the clipping isolation amplifier, V106B, and appeared as a positive pulse upon the grid of the cathode follower, V105B, whose cathode was connected to the cathode of the PPI tube. Thus, the PPI was blanked for the duration of this pulse. A simple RC network differentiated this pulse and applied it to the grid of another cathode follower, V106A, which delivered the differentiated pulse at low impedance to the keying chassis.

#### 5.8.8 Timing and Sweep Circuits for QH Model 2 Scanning Sonar

The timing circuits in the QH Model 2 scanning sonar differed considerably from those used in Model 1, and are shown in Figure 163. The basic design<sup>113</sup> was laid down by March 1944 and the assembled circuits were used for a short time in the laboratory with OTE-5 before installation on USS CYTHERA.<sup>70</sup> The fundamental timing element in Model 2 was a mechanical timer which was driven by a synchronous motor and had two pairs of contacts, one of which closed at time intervals corresponding to 1,500 yards and the other at intervals corresponding to 3,750

yards; interconnection gave a time interval corresponding to 7,500 yards. This timer replaced the relaxation oscillator, pulsing circuits, isolation circuits, and counter of Model 1.

The spiral-sweep circuit was substantially unchanged. A GE 5 CT synchro was directly coupled to the scanning commutator to serve as a three-phase spiral-sweep generator, its field being furnished by a sawtooth excitation current. The constants of the sweep circuit were adjusted so that the spiral expanded to the full radius of the tube on each sweep, for ping rates of 1,500, 3,750, and 7,500 yards respectively.

The mechanical timer shorted a 4.0- $\mu$ f capacitor across which the sawtooth sweep voltage appeared, thus restarting the sweep. The synchronous motor which drove the cams on the timer unit was originally a 115-volt 60-cycle motor.<sup>114</sup> It was expected that difficulty would be encountered because of the small size of the wire and the motor was therefore rewound for 6.3 volts 60 cycles, gaining the added advantage of retaining synchronism over a much wider voltage range.

Previously, an attempt had been made in the HUSL shops to build a mechanical timer<sup>115</sup> consisting of a motor-driven lucite cam with brass inserts, and using brushes to contact the inserts and thus discharge the sweep capacitor. Brass particles carried by the brushes onto the lucite made continuous contact so that the capacitor was continuously discharged. Thereafter, the Sangamo Electric Company *automatic keying unit* [AKU] was adopted. It had two arms, which were operated by cams in rapid succession, so that contact was made for only 1 msec. Burning of the contacts was prevented by discharging the 4- $\mu$ f (C501) sweep capacitor through a 330-ohm resistor. (See Figure 163.)

The negative side of the sweep capacitor was connected to a voltage divider which controlled the starting point of the sawtooth sweep. The sweep capacitor was charged through one of three resistors determined by the setting of the range switch upon the console. These resistors were of such value that the voltage across the sweep capacitor at the end of the sweep period was the same for each maximum range, the rate at which the sweep capacitor charged, and hence the range scale, being determined by the potential of the charging source. This potential was controlled by the setting of the range limit potentiometer connected between the positive supply and ground.

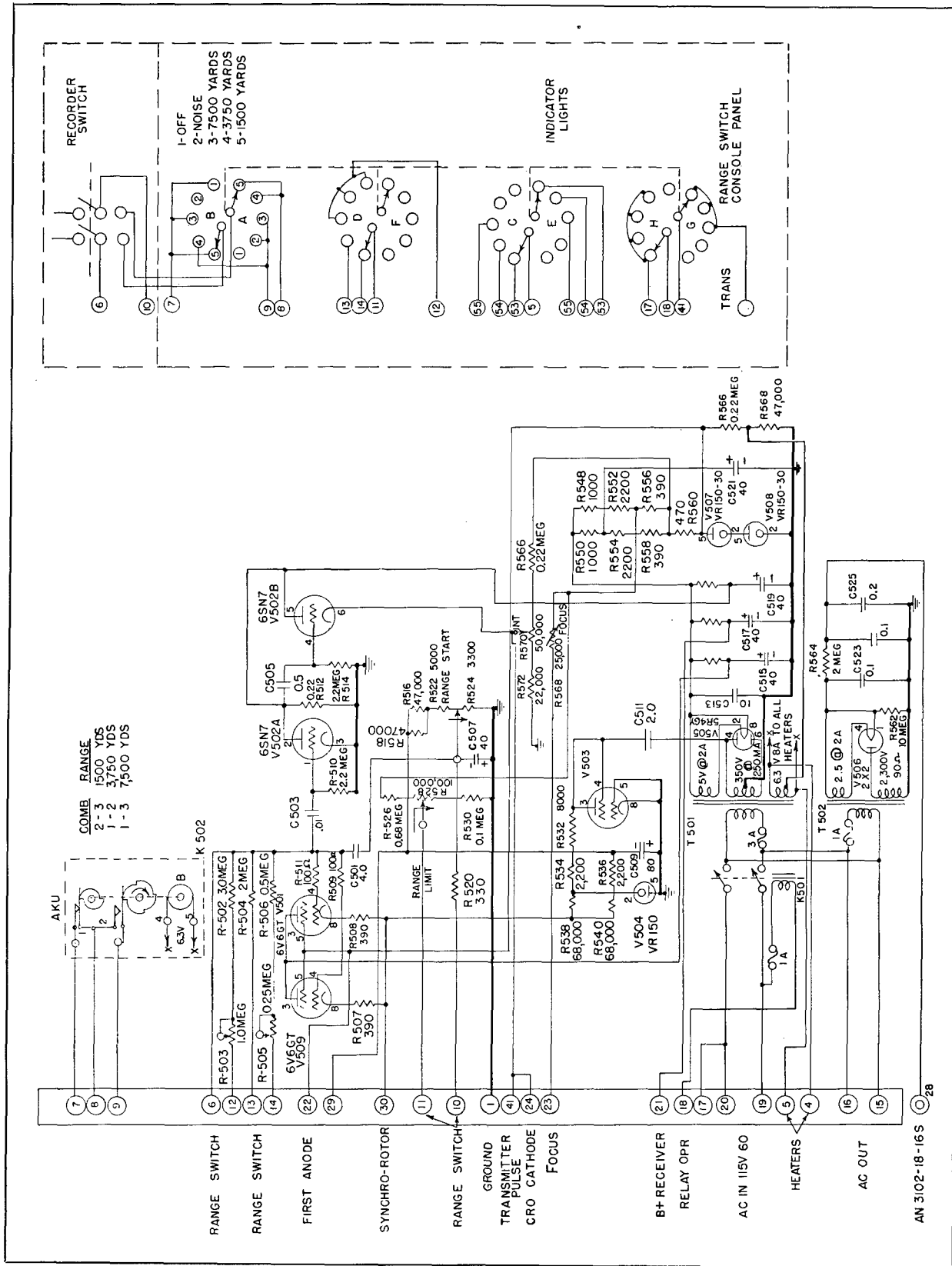
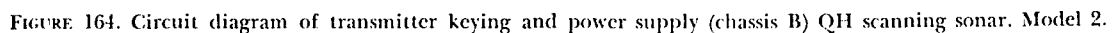


FIGURE 163. Circuit diagram of timing circuits and power supply, QH scanning sonar, Model 2.

CONFIDENTIAL



The keying was done normally by the mechanical contactor. When the chemical range recorder was in use, the keying impulse was received from the recorder instead of from the timing switch by operating a switch on the console to recorder keying. The ef-

The QH scanning sonar, Model 2, was so constructed that it could be used with the standard attack plotter. This presented a geographic plot of own ship

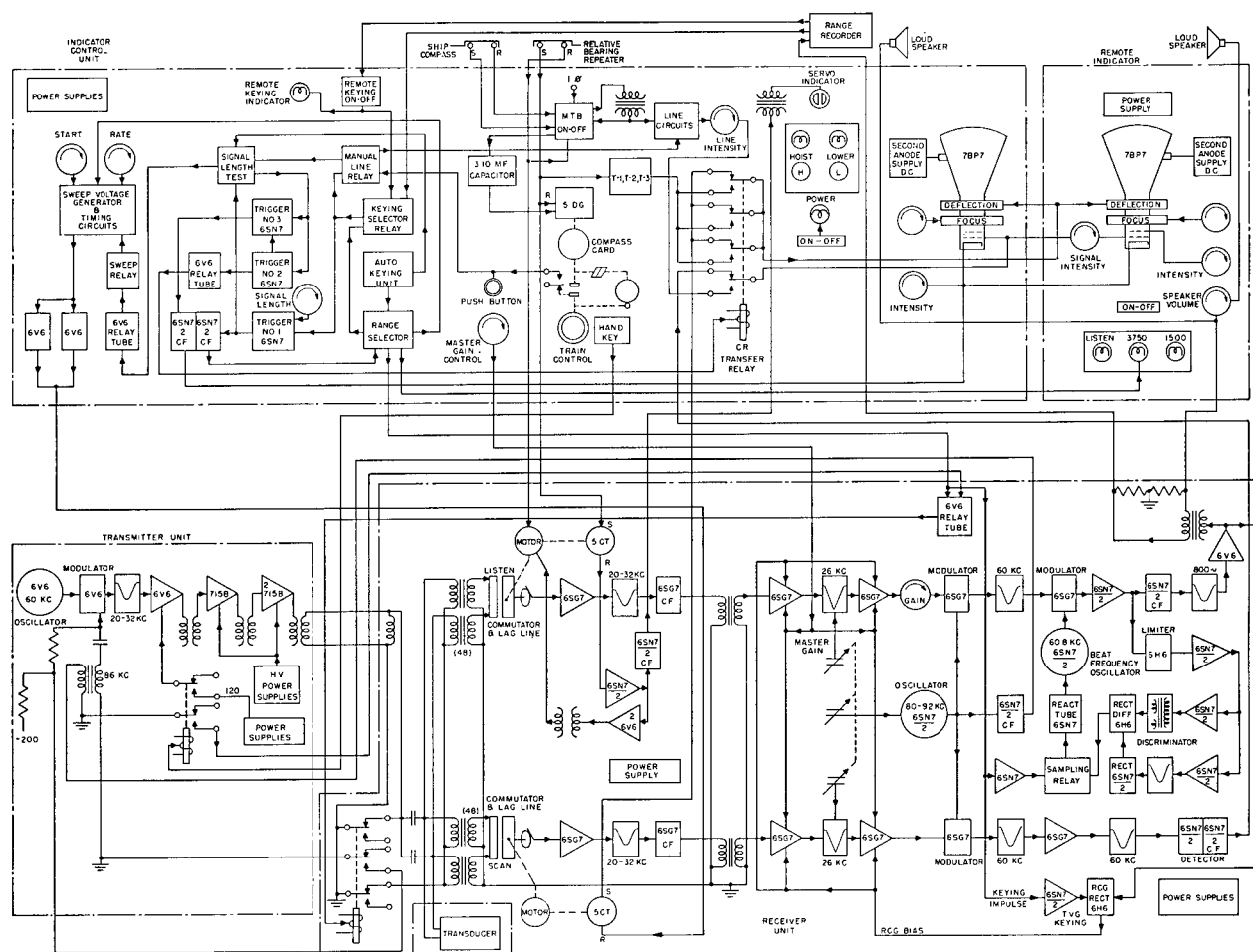


FIGURE 165. Block diagram of Model XQHA scanning sonar.

and all targets. Timing and sweep considerations for this application are given earlier in the present chapter.

### 5.8.9 Sweep and Timing Circuits of the Model XQHA Scanning Sonar

The sweep and timing circuits of the XQHA scanning sonar<sup>1</sup> were similar to those of QH Model 2. The significant features and actions of these circuits are:

1. Determination of range was made from visual estimate of the PPI screen, after consideration of range-marking circles and variable-length electronic cursor.<sup>117, 118</sup>
2. The time interval between pings was determined by an AKU timer described in the preceding

section. The transmitted pulse length, blanking pulses, and electronic cursor action were obtained by means of trigger circuits initiated by the AKU timer, resulting in operation of suitable relays.

3. An electronic cursor was used for measurement of bearing on the cathode-ray tube face, applied at the beginning of each ping or by hand keying.

4. Automatic or hand keying of the system was provided to allow for communication; connection was also provided for recorder keying.

5. The spiral-sweep generating circuit was similar to that used in QH Model 2, with minor modifications.

6. Means were provided for calibrating the length of the transmitted pulse. A circuit diagram of the sweep and timing circuits is shown in Figure 82, and a block diagram in Figure 165.

CONFIDENTIAL

## 5.9 APPRAISAL OF CR SCANNING SONAR

### 5.9.1 Appraisal of XQHA Scanning Sonar

Based on the experience which HUSL has had with the Model XQHA scanning sonar and with the other experimental models leading to it, the following preliminary appraisal is presented as a list of its strong and weak points.

#### STRONG POINTS

1. Continual alertness in all directions, one of the original aims, has been achieved, except (in common with all echo-ranging systems) for the bearings directly aft, where own-ship's screw noise considerably reduces the effectiveness of both listening and echo ranging.

2. Ease of operation in comparison to that of the searchlight-type sonar has been improved by reducing the number of controls and by giving the operator a more comprehensive picture of what he is doing. While receiving, through the listening channel, all information normally available by a searchlight-type sonar, the PPI display gives additional information without additional effort for the operator. Through coordination of aural and visual impressions, targets may be more quickly identified, contact may be maintained or regained more surely when lost, and a more consistent and rapid flow of sonar information delivered. Range-recorder operation is facilitated, and a maximum accuracy in determining firing time is assured. Moreover, it is possible that less training will be needed for adequate operation.

3. Potential reliability has been increased by having essentially two systems, either of which may be used alone. Although such units as the transducer, junction box, and transmitter are common to both systems, it is possible for the listening commutator, listening receiver, speaker, or recorder to fail and still allow satisfactory detection with the scanning channel and the PPI. On the other hand, failure in the scanning commutator, receiver, or indicator still allows operation of the listening channel in accordance with usual searchlight sonar techniques.

4. The adaptability of the system to the future incorporation of improved equipment is good. The fact that the listening channel beyond the commutator is essentially a searchlight-type sonar allows incorporation of all electronic modifications developed for such echo-ranging systems for improving the recognition of echoes, such as doppler sensitization or automatic

target training. Interchangeable design of XQHA scanning and listening commutators and receiver components simplifies the repair problem.

5. The scanning sonar transducer in the azimuth system can be fixed with respect to the ship, and therefore requires no training shaft. This is a distinct advantage over the QC gear, both in installation and maintenance.

#### WEAK POINTS

1. Figure of merit for the scanning channel is less than that for the listening channel, causing a slight reduction in theoretical maximum detection range. Whether or not this reduction is apparent under operating conditions, and whether or not it is offset in practice by continual alertness on all bearings, must be determined by operating trials.

2. Multielement transducers and commutators are expensive and difficult to build, test, and install, and are presumably more liable to breakdown than the simpler transducers used in searchlight-type sonars. Provision for transducer replacement from within the ships would therefore be desirable.

3. With present design, no provisions have been incorporated as part of the XQHA sonar to permit monitoring while in service.

### 5.9.2

### Operational Evaluation

Comprehensive measurements have already been made (as described earlier in this chapter) to determine the performance of the Model XQHA scanning sonar in terms of its physical characteristics, such as power, sensitivity, noise level, beam patterns, inherent bearing accuracy, and figure of merit. These measurements indicate that the operating capabilities of the system should be at least equal to those of any searchlight-type sonar. However, since they permit only an inference as to operating capabilities, they should be considered merely as the first step in the evaluation program, signifying mainly that the system is a fit candidate for further investigation. A comprehensive program of evaluation under operating conditions is necessary to obtain a clear picture of the tactical value of this new type of sonar.

In laying out the test program, the strong and weak points of the system indicated above might well be considered subject to proof. Ease of operation will be extremely important, and tests with operators having different amounts of training should be made. The

consistency and rapidity of the flow of information under various conditions of roll and pitch should be investigated to determine the limitations of narrow vertical beam pattern in XQHA sonar. Both electronic and mechanical PPI cursors should be tested in order to obtain operating criteria to guide future design specifications. The effect on operating efficiency of interference from other sonar equipment, particularly that of the same type, should be given attention.

Accuracy of bearing information is of extreme importance. It is well known, as a result of tests with the bearing deviation indicator, that the inherent accuracy of a system, determined under ideal conditions, is never realized in actual operation with a moving submarine target. The effective accuracy under such practical conditions must be found, both for comparison with that obtained with standard searchlight-type sonars and also for use in the design of future fire-control equipment. Another question for future sonar design is whether or not BDI equipment, either of the normal types or of the proportional *sector scan indicator* [SSI] type, will give any appreciable improvement in accuracy under operating conditions.

### 5.9.3 Proposals for Future Development

Various modifications and improvements on the present CR scanning sonar systems should be carried

out, as well as other more general problems. Problems of interest are:

1. The bearing deviation indicator, both of the normal type and the proportional SSI type, appears to be applicable to the listening channel, and this application should be investigated. Studies of BDI accuracy in this arrangement had been started in the spring of 1945.

2. Short pulse and multiple-spaced pulse transmissions seem to be applicable, and investigations of their usefulness in enhancing the detectability of small targets had already been started in the spring of 1945.

3. *Maintenance of close contact* [MCC] provision through control of the transducer pattern has been proposed and some work carried out on this problem in the summer of 1945 by USNUSL, New London.

4. Geographical plan position indicator display has been applied at HUSL to the attack teacher. Further work should be carried out on this problem to obtain better accuracy.

5. Monitoring arrangements have been of great value during the experimental work, and should be further developed for inclusion in service installations.

6. More general problems involving studies of CR scanning sonar for future work are discussed in Chapter 10.



## Chapter 6

# INTEGRATED TYPE B SCANNING SONAR

### 6.1 GENERAL DESCRIPTION, ARRANGEMENT OF INTEGRATED TYPE B EQUIPMENT AND OPERATIONS

#### 6.1.1 Introduction

IN JUNE 1944, the Harvard Underwater Sound Laboratory [HUSL] was asked to consider the adaptation of scanning sonar principles to depth determination, and to propose a design for a complete sonar system that would include azimuth scanning for search and depth scanning for attack, and that would give required stabilized information to fire-control equipment. A proposal for such a system was presented to the Bureau of Ships on July 14, 1944. This system, using a 2-axis stabilized<sup>1,2</sup> depth-scanning system to obtain the fire-control information, was designated by the Bureau of Ships as *ultimate Type B*; and a system proposed by the Naval Research Laboratory [NRL] to meet the same requirements, using a 3-axis mechanically stabilized searchlight sonar for obtaining the fire-control information, was designated by the Bureau of Ships as *ultimate Type A*. Both systems proposed the use of the QH azimuth-scanning system. The Bureau of Ships requested that an experimental model of the Type B system be available by October 1, 1944, and a production prototype by January 1, 1945.

The Harvard Underwater Sound Laboratory was requested by the National Defense Research Committee [NDRC] (Section 6.1) to proceed with the study of Type B, and a program was set up which called for: (1) theoretical and experimental investigations of the possibility of depth scanning itself; and (2) future detailed design and development of the complete system. While earlier discussions and reports referred to this system as *ultimate Type B scanning sonar* it was later designated by HUSL as *integrated Type B sonar*, and is so designated in this report.

An extensive program of experimental testing was carried out on depth-scanning sonar, following the designing, development, and construction of suitable equipment. Installation of the equipment for these tests was made on the USS CYTHERA. Concurrently

with certain portions of this work, an overall design was formulated for the integrated Type B sonar. Complete and detailed designs were made for the consoles, and development work was carried forward on other parts of the equipment in the light of experience gained in the USS CYTHERA tests and by tests on QH Model 2 horizontal-scanning system and on the Sangamo XQHA system (see Chapter 5). Construction and preliminary testing were carried out on an HP-8D transducer for the depth-scanning portion of the integrated Type B sonar. Interconnections between the various portions of the sonar equipment and between the sonar equipment and the attack director were worked out in detail with particular reference to ship installation. Design and development continued at HUSL until April 1945, when the HUSL sonar program was transferred to NRL at New London. In the spring of 1945, however, when it became apparent that the remaining development and construction could not be completed prior to July, construction work on the integrated Type B prototype was transferred to the shops at U. S. Navy Underwater Sound Laboratory [USNUSL].

This chapter describes in detail the HUSL investigation of depth scanning, including the design and construction of the depth-scanning transducer HP-8D. It also describes the proposed design for the integrated Type B sonar, and the projected installation and operation of this device on a suitable ship such as the USS BABBITT.

Integrated Type B sonar was designed to give information about the location of a subsurface target in terms of bearing, range, and angle of depression. The principal requirements are: (1) maintenance of a continuous search through 360 degrees in the horizontal plane; and (2) presentation of accurate data on range, depth, and bearing for a given target after it is discovered.<sup>3,4</sup>

#### 6.1.2 Functional Requirements

The first basic requirement of integrated sonar is the maintenance of underwater search through 360 degrees of azimuth to the maximum range possible. This can be obtained by methods employed in the

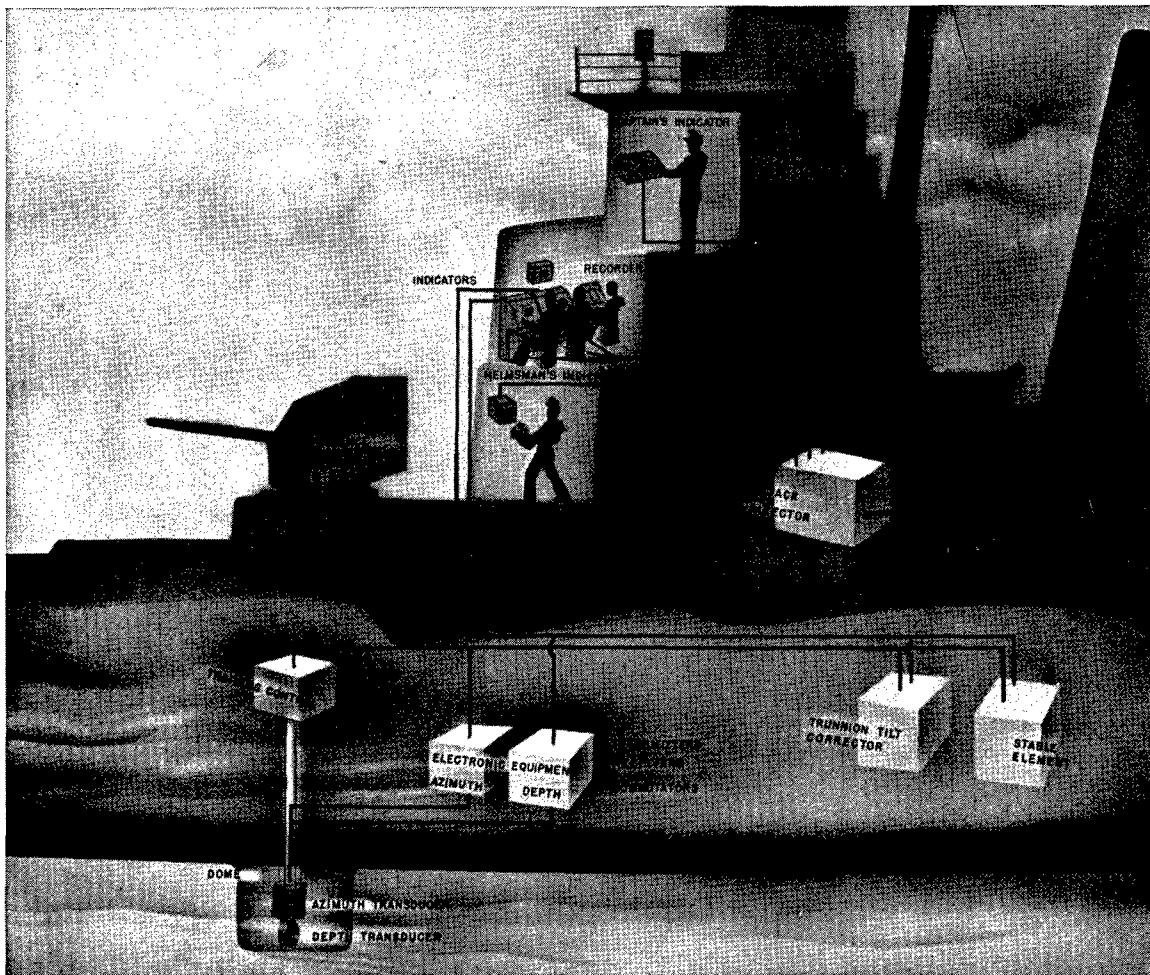


FIGURE 1. Ship arrangement of components for integrated Type B sonar.

conventional QH horizontal-scanning system. Here a cylindrical transducer mounted beneath the hull of a ship provides a relatively narrow vertical beam while scanning or listening in the horizontal plane. Deep targets in the immediate vicinity of the ship, therefore, cannot be detected or followed.

The depth-scanning portion of integrated sonar, which normally would be used for targets at ranges less than 1,000 yards, is required to provide information on azimuth, slant range, and depth angle. In this system a cylindrical transducer mounted beneath the hull of the ship, with its axis parallel to the deck plane, provides a relatively narrow horizontal beam while scanning or listening in the vertical plane. This system, therefore, cannot scan the horizon for targets but can follow deep targets in the immediate vicinity of the ship.

The desired requirements<sup>5</sup> are as follows: (1) range accuracy  $\pm 5$  yards for ranges under 1,000 yards; (2) bearing accuracy  $\pm 1/4$  degree; and (3) depth-angle accuracy  $\pm 1/2$  degree, for depth between 50 and 800 feet at 500-yard range. It was expected, however, that the range accuracy would approximate  $\pm 10$  yards for ranges under 1,000 yards, and that the bearing accuracy would approximate  $\pm 1/2$  degree. Original specifications called for a frequency of 50 kc or less. To give the desired bearing accuracy, it was thought desirable to use the *bearing deviation indicator* [BDI] for the azimuth direction of the signal.

In order to maintain contact with a target, and to obtain the desired accuracy in determination of its depth angle and bearing, it is necessary to incorporate stabilization in the depth portion of this system. Two-axis stabilization, requiring a trunnion-tilt corrector

CONFIDENTIAL

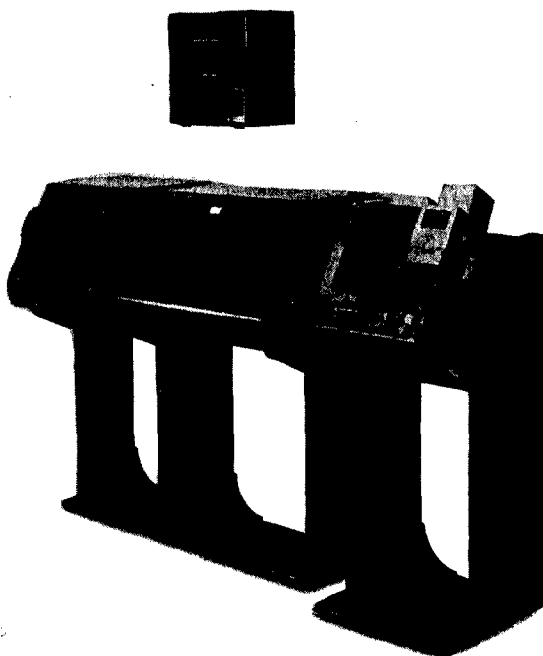


FIGURE 2. Consoles for integrated Type B sonar.

in addition to the gyroscopic stable element, was by far the most convenient to apply in this case. Output of the trunnion-tilt corrector can be used mechanically to correct in azimuth the training of the transducer and the depression angle of the depth-listening beam, and used electrically to correct the *elevation position indicator* [EPI] and *plan position indicator* [PPI] scanning displays.

Obtaining proper range data requires the use of a chemical recorder to give time range. Temperature gradient correction applied to time range and measured depth angle (in the attack director) provides slant or horizontal range and true depth angle or depth.

The final functional requirement of the system is to combine all the information in an attack director that produces data for conning an attack on the target.

### 6.1.3 Operation and Location of Components

Location in a ship of the various components of integrated Type B sonar is shown in Figure 1. As indicated in the figure, there are three positions to which intelligence should be carried from the various

elements in the system. The captain's indicator, which is located on the navigation bridge, consists of the indicators necessary to show the outputs of the attack director. The helmsman's indicator is located at the helmsman's position and shows only the course to be steered during attack. The depth console, azimuth console, range recorder, loudspeaker, and control panel should be located in the sound room (see Figure 2).

Operation of the system during attack should be carried out by three operators in the sound room. During search, the presence of the azimuth operator alone is required. His duties consist of watching the azimuth console, noting a target, and notifying the other two operators, one of whom operates the depth console and the other the range recorder. The azimuth operator trains the transducer to keep on the target. During attack the depth operator depresses the depth-listening beam for the same purpose. During search only the azimuth console is energized. The depth operator turns on the depth console when he comes on duty and the range-recorder operator turns on the range recorder. When the range has closed to approximately 1,000 yards, the azimuth operator throws an attack-search switch so that data for the attack originates in the depth system.

On making a contact, the azimuth operator sets the bearing cursor to the echo, using the handwheel on the azimuth console. He then tracks the target in bearing either by observation of the echo spot on the PPI or by the BDI screen next to the PPI. During attack the azimuth operator continues to track the target using the BDI. Either he or a standby operator watches the PPI for any further targets so that the system remains alert in all azimuth directions, even during attack.

During attack, the depth operator, using the handwheel on the depth console, tracks the target by keeping the cursor on the EPI centered on the echo spot. The range-recorder operator, using a handwheel, keeps the cursor on the range trace at all times. Gain controls are provided for the three operators; range switches are provided for the azimuth and depth operators. While it is intended that each operator concentrate on adjustment of the controls on his particular equipment, the three are placed close together, enabling each operator to obtain from the other's equipment the information pertinent to his own needs. Information obtained from these three operations is given to the attack director, which provides

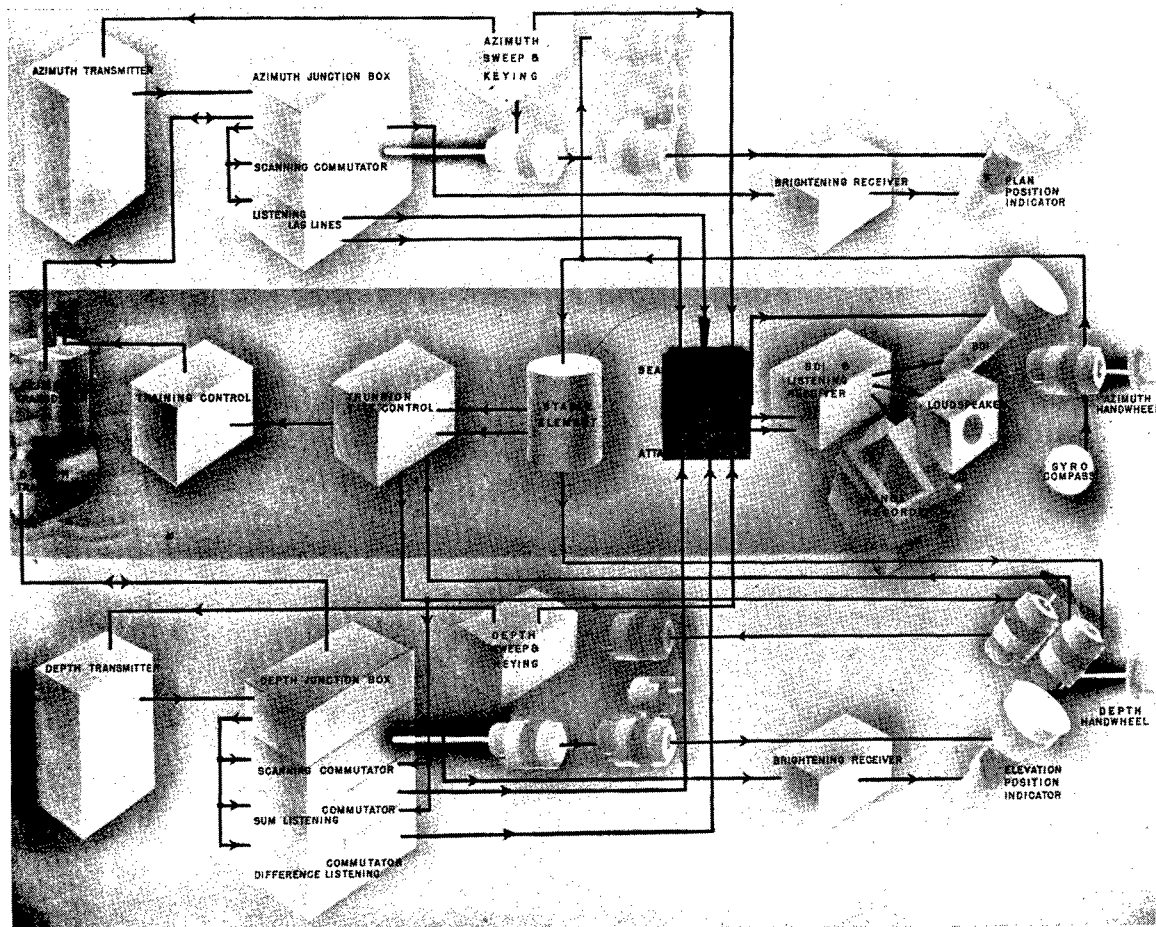


FIGURE 3. Block diagram of integrated Type B sonar.

necessary data to the conning officer and to the helmsman. Other controls, including on-off, hoist-lower, stabilization switch, and computer on-off are also in the sound room on a control panel. This panel is removed from the consoles to avoid confusion during operation. There is a separate gain control on the loudspeaker to control the initial level of sound; there is also a band-filter switch. The circuit design should be arranged so that adjustment of these other controls is not necessary during operation.

All other electronic and mechanical elements of the system should be located below decks. In general the stable element is positioned close to the center of roll of the ship. The trunnion-tilt corrector is placed near the stable element. Electronic equipment is located in the lower sound room to provide accessibility, and to be near the transducers, which are beneath the hull of the ship. The attack director should be

located in the computing room with other fire-control equipment.

Two transducers are included in this design, one for azimuth scanning and listening, and one for depth scanning and listening. Both are mounted on the same training shaft. These transducers are mounted in an enclosing dome which is streamlined to allow proper operation for high ship speeds and is acoustically transparent to allow both azimuth and depth scanning.

A more detailed block diagram of the integrated Type B sonar is shown in Figure 3. There are three distinct sets of electronic gear. The first set is used for transmission and reception during search, using the azimuth part of the system. It consists of the azimuth transmitter, junction box, transducer, scanning commutator and fixed lag line, phase-shifter for phase correction of scan, brightening receiver, and PPI (in

CONFIDENTIAL

the azimuth console). The second set performs the same functions as the first during attack for the depth-scanning portion of the equipment. It consists of the depth transmitter, junction box, transducer, commutators, phase-shifter for phase correction of scan, brightening receiver, and EPI (in depth console). The third set is used for BDI and listening. It consists of a sum-and-difference BDI receiver, a BDI indicator (in the azimuth console), and a loudspeaker. The audio output to the loudspeaker should also be available as input for the range recorder. Also, the third set of components is switchable so that the input to it is obtained from either the azimuth or depth system.

The stabilization equipment consists of a stable element, trunnion-tilt corrector or computer, and the two phase-correction synchros in the azimuth and depth systems. It stabilizes rotation of the transducers which are mounted on a common shaft, rotation of the commutators which form the depth-listening beam, and the indications on the PPI and EPI.

#### 6.1.4

### Fire Control

The final design of integrated Type B sonar provides for the use of an attack director to control the ordnance used in a submarine attack and to provide information to aid the conning officer in making the attack.

## 6.2 EXPERIMENTAL WORK AND RESULTS

#### 6.2.1

### Schedule of Work

A fundamental problem was raised in the design of integrated Type B sonar: the general consideration of depth scanning.

Depth scanning had not been tried previously, and a number of specific problems were immediately apparent. The surface of the water, the bottom of the ocean, and the hull of the ship form three reflecting surfaces that complicate the vertical scanning problem by producing various apparent images or echoes not associated directly with the target. Refraction of the sound ray, because of pressure and temperature gradients in the water, produces improper values of depression angle and may limit range and depth of detection of a target. The azimuth portion of integrated Type B sonar, in order to preserve adequate signal-to-noise ratio for search, must have a relatively narrow vertical beam, and is, therefore, unable to

maintain accurate bearing determination at large depression angles. Consideration had to be given the use of horizontal BDI on the depth-scanning system, as well as the usual listening and scanning beams. The type of indication used for the depth-scanning system had to be distinctive and yet comparable to the type used for the azimuth-scanning system. In order to obtain the requisite accuracy in depth angle and range, stabilization of the sonar system was required to counteract effect of the ship's roll and pitch. Application of stabilization to a full-size sonar system for standard echo-ranging frequencies had not been previously made, and required investigation. Ability to maintain contact with the target by using depth scanning combined with horizontal BDI in the depth-scanning system was a point to be determined. In addition, the dome that houses the transducer had to be investigated for its effect on the transmitted and received sound.

A number of theories were held concerning these questions on the depth-scanning principle, but there was little or no experimental evidence available. In an effort to find answers to these questions as quickly as possible, the 26-kc *depth-scanning sonar* [DSS] was developed and installed on the USS CYPHERA.

#### 6.2.2

### Development of the 26-kc Depth-Scanning Sonar

The two major problems to be solved with the 26-kc depth-scanning sonar installed on the USS CYPHERA were the development of a suitable transducer and a suitable BDI-listening receiver.

The HP-3DS transducer was designed so that depth angles from 0 to 90 degrees could be scanned at all times, independent of roll and pitch of the ship up to angles of 30 degrees. It was of the cylindrical magnetostrictive type, with the axis of the cylinder horizontal, and with 48 magnetostrictive staves disposed around 270 degrees of the transducer, from the top of the cylinder downward to the bottom and up to the horizontal on the rear side. It was necessary to use about 120 degrees of elements to form the listening and scanning beams. Referring to Figure 4, it is seen that in order to form such a beam 30 degrees behind the vertical downward, elements had to be included up to the horizontal on the rear side of the transducer. Figure 5 is a photograph of the transducer HP-3DS mounted in place. The outside diameter of the transducer was about 24 inches, and the length of the cyl-

inder about 13 inches. The diagonal dimension across the center of the cylinder was about 27 inches. This dimension determined the turning circle of the transducer, and therefore the necessary size of any dome enclosing the transducer. The overall height was about 30 inches from the bottom to the top of the mounting flange. Each stave of the transducer was divided into right and left halves to allow BDI operation of the system.

The BDI listening receiver used the sum-and-difference principle. Its development was primarily concerned with stability, unicontrol of frequency, and remote gain control problems. The general principle of this BDI circuit was to (1) add the voltages from the two halves of the transducer and amplify the sum in one channel, (2) subtract the two voltages and amplify the difference in another channel, (3) shift the phase of each of these resultant voltages by 45 degrees in such a way as to produce a 90-degree difference in phase, and (4) combine outputs of both channels in a phase-sensitive rectifier to give a d-c voltage for operation of the BDI right-left indicator. The sum channel was also used to provide voltage for brightening the spot on the right-left indicator and to provide signal power for operating the standard range recorder and the loudspeaker. Thus, this receiver performed both the functions of a BDI receiver and a listening receiver at the same time. Only one pair of commutators was necessary to provide the BDI and listening functions, the outputs from these commutators being attached to the two inputs

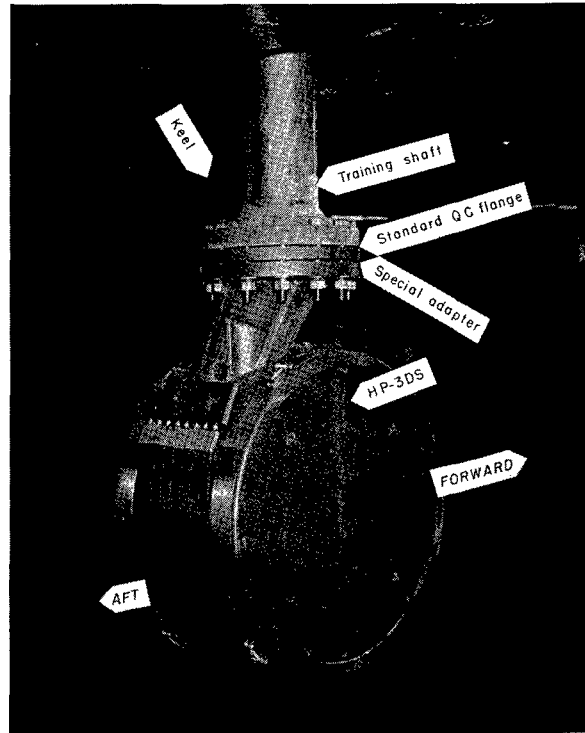


FIGURE 5. Installation of HP-3DS on USS CYTHERA.

of the BDI listening receiver. Stability of the receiver was obtained by use of negative feedback in all amplifier circuits, and by careful choice of circuit components. The receiver was designed to include unicontrol of frequency. Simplicity of gain control was obtained by using varistors as gain-control elements in such a way that the gain of both channels of the amplifier could be modified simultaneously and identically. This was an important consideration since both the gains and phases of the two channels had to be matched at all times. The control voltage for modifying the gain was direct current, making remote gain control possible.

The principal components of the system as installed on the USS CYTHERA are shown in Figures 6 and 7. Figure 6 shows the signal circuits. A send-receive relay was used to connect the transducer to the transmitter for transmission and to the commutators for receiving. Output of the scanning commutator, which rotated at a speed of about 1,800 rpm, was connected through a preamplifier to the scan-brightening receiver and then to the brightening electrode of the cathode-ray tube in the EPI. Signal outputs from the two listening commutators were connected through preamplifiers to the BDI listening receiver,

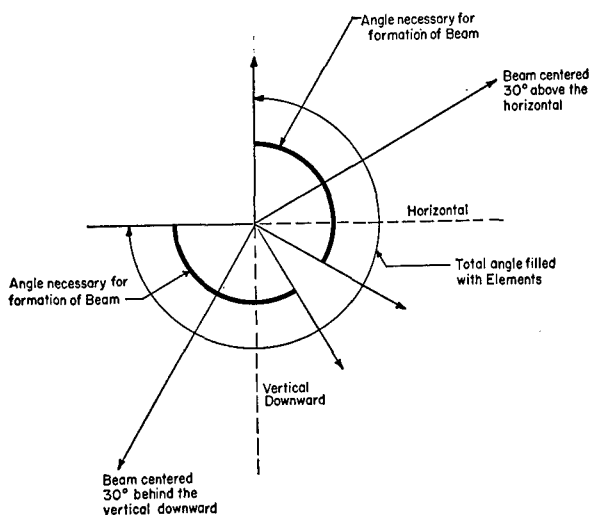


FIGURE 4. Transducer elements needed for beam formation in depth-scanning sonar system.

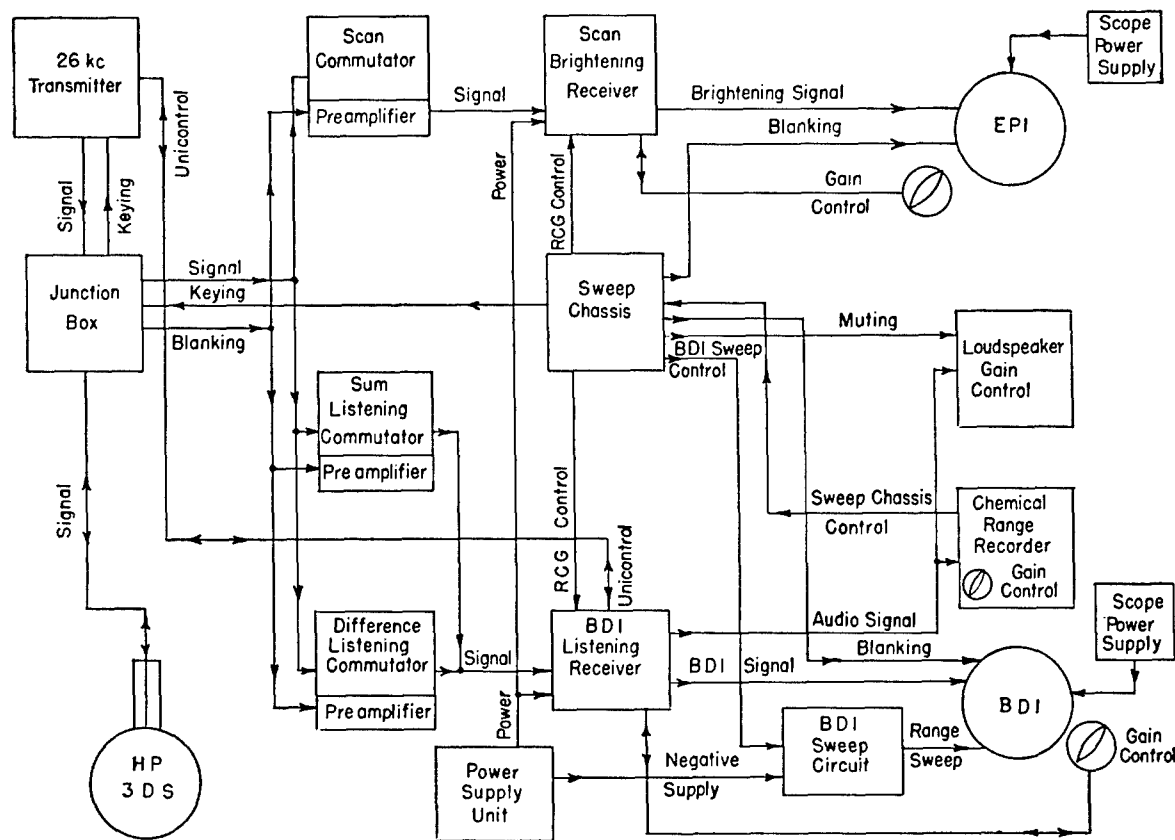


FIGURE 6. Depth-scanning sonar electronic units, USS CYTHERA.

and then to the BDI cathode-ray tube, the loudspeaker, and the range recorder. Synchronizing and timing of the transmitted pulse, and generation of the various sweeps and blanking wave forms were accomplished by circuits in a sweep chassis. A separate sweep chassis was included for the BDI range sweep, which was, however, coordinated with the first sweep chassis. The unicontrol circuit involved connections between the BDI listening receiver and the transmitter. Suitable power supply units were provided for the two receivers and the BDI sweep circuit, and the other units had self-contained power supplies.

Figure 7 shows the synchro control and display circuits. The spiral sweep for the cathode-ray tube in the EPI was generated by a synchro used as a 3-phase a-c generator, attached mechanically to the commutator. The output of this generator was modified in phase by a differential synchro used as a rotatable phase-shifting transformer, and was then applied to the deflection coils of the cathode-ray tube in the EPI. Motion of the depth-angle handwheel at the elevation position indicator (1) turned a cursor placed across

the face of the EPI cathode-ray tube; (2) turned a synchro which electrically transmitted the depth angle combined with level from the stable element to the trunnion-tilt corrector; and (3) turned a synchro which provided electrical signal to correct the EPI display. Motion of the handwheel at the BDI scope turned a synchro which electrically transmitted bearing to the stable element. A switch was arranged to make rotation of the handwheel either true or relative bearing. To obtain true bearing, own-ship's course was obtained from the ship's gyrocompass through a gyrocompass converter unit. The electrical output of the stable element, plus the sum of level and depth angle obtained from the synchro turned by the depth handwheel, were transmitted to the trunnion-tilt corrector. Outputs from the trunnion-tilt corrector were sonar train order and sonar depression order. The sonar train order was used to train the transducer through an amplidyne servo system, and the sonar depression order was used to position the listening commutators through a servo system. In addition, the sonar depression order was combined

CONFIDENTIAL

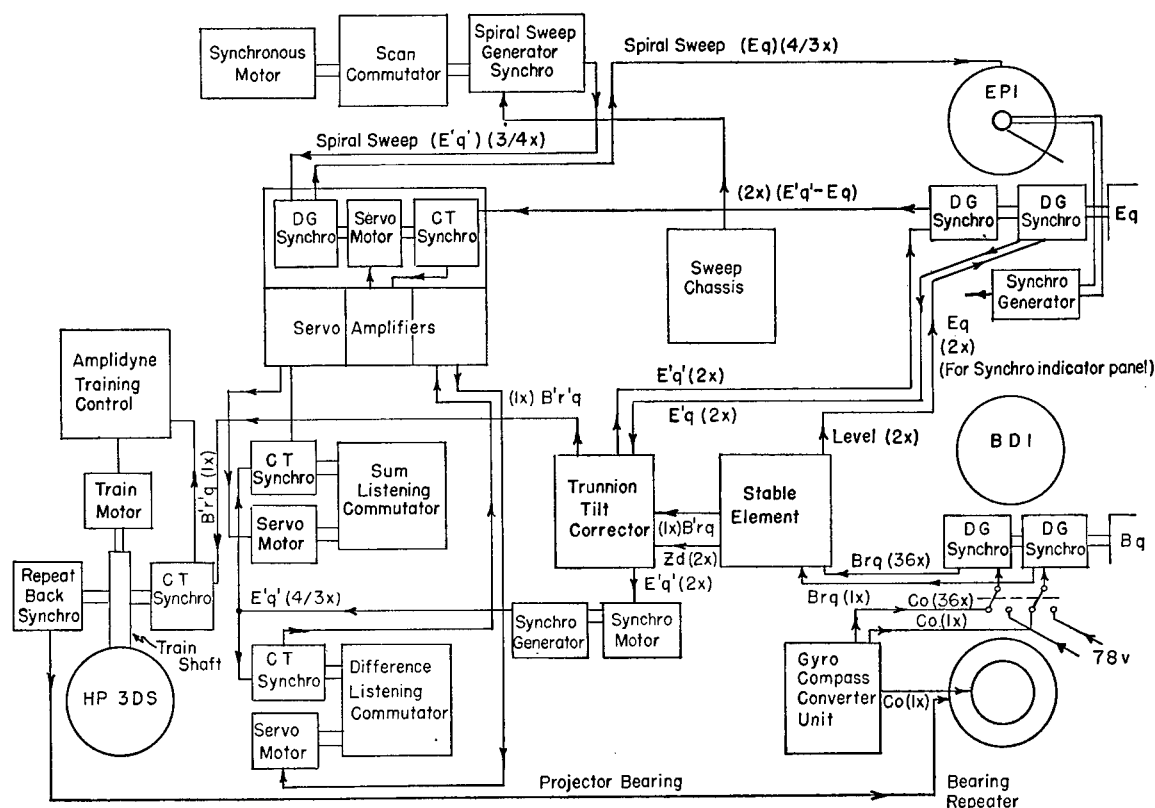


FIGURE 7. Depth-scanning sonar synchro controls, USS CYTHERA.

with depth angle in the differential synchro turned by the depth handwheel to give an electrical signal. This signal corrected the EPI display by means of the phase-shifting transformer.

A detailed description of the installation on the USS CYTHERA is given in the installation book.<sup>6</sup> Figure 8 shows installation of the electronic equipment. Figure 9 shows the trunnion-tilt corrector in the sound laboratory in the forward part of the ship. The stable element was mounted near the center of roll of the ship in the forward part of the engine room. Figure 10 shows the EPI, BDI, and range recorder. These units were mounted in the sound laboratory on a table of proper height for operation by two operators seated in front of the EPI and BDI and by a third operator standing in front of the range recorder. The brightening and BDI listening receivers were rack-mounted next to the table (see Figure 8) for convenience in tuning the system and adjusting the beat-frequency oscillator in the audio output. The sweep chassis and test equipment were mounted in a rack next to the receivers. A third rack contained the junction box, servo amplifiers, and the three commuta-

tors. The transmitter was placed next to the three racks. The trunnion-tilt corrector and a synchro indicator panel were placed on a work bench along the port side of the laboratory.

The transducer HP-3DS was mounted on the existing QC hoist-train shaft on the ship (see Figure 5). A dome was used to protect the transducer from unnecessary strains during roll and pitch and from the forward motion of the ship, and to provide a certain amount of streamlining. Since no standard dome was available which would allow full 360-degree rotation of HP-3DS and which was suitably transparent for depth scanning, a special dome was procured from the Budd Manufacturing Company. This dome was made of 0.030-inch stainless steel with a minimum of bracing to avoid acoustic interference and reflections. A photograph of the dome as installed on the USS CYTHERA is shown in Figure 11.

In order to make experimental checks on the behavior of the depth-scanning transducer, a deep monitor was constructed and installed on the USS CYTHERA. This monitor consisted of a 1-inch-high magnetostriction ring stack, whose resonant frequency



was about 26 kc,<sup>7</sup> and which was mounted on the end of a long heavy-walled steel tube. Figure 12 shows sketches of the transducer after being enclosed in a resinox casting. The mounting tube was placed inside a standpipe in the ship and could be raised or lowered so that various depth angles could be set from 20 degrees above the horizontal through 0 to 60 degrees below. Figure 13 shows the upper end of this mounting tube, the hoisting mechanism, and the square angle-iron piece used to keep the inner tube from rotating. As shown in Figure 14, the deep monitor was situated forward and slightly to port of the depth-scanning transducer HP-3DS. Because of strength and accuracy considerations, the deep monitor was not usable to its full extent unless the weather was calm and the ship was not under way. However, there was also installed an early model of the *installed sound gear monitor* [ISGM]<sup>8, 9</sup> whose streamlining was sufficient to permit operation at the USS CYTHERA's maximum speed of 14 knots. Measurements and operation checks for 0-degree depth angle were therefore possible with the ship under way. The position of the ISGM is shown in Figure 15.

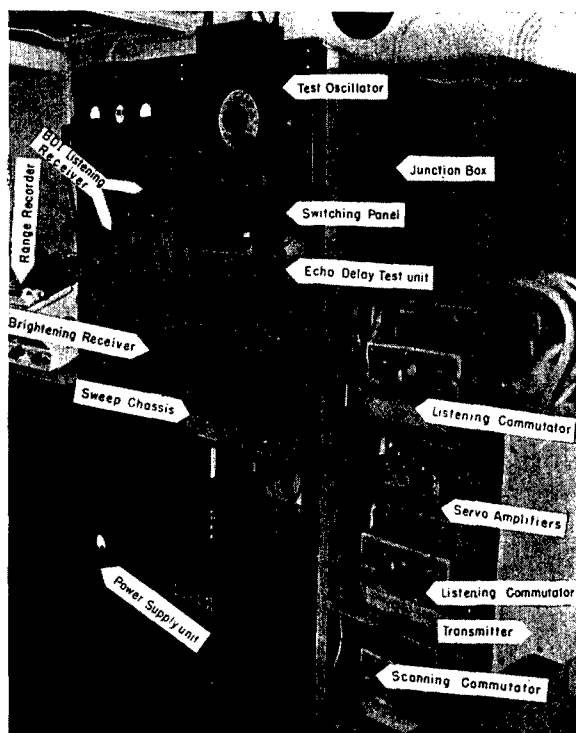


FIGURE 8. Installation of electronic equipment for 26-kc DSS on USS CYTHERA.

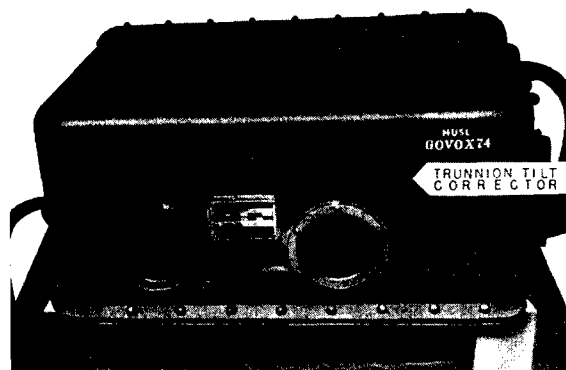


FIGURE 9. Installation of trunnion-tilt corrector for 26-kc DSS on USS CYTHERA.

### 6.2.3 Results of Tests on 26-kc Depth-Scanning Sonar Installed on the USS Cythera

The depth-scanning sonar installed on the USS CYTHERA was tested quite comprehensively in order to determine the degree of usefulness of depth scanning and to test this particular installation. The work was carried on mostly at Port Everglades, Florida, a site chosen because of the reasonably deep water and generally good weather conditions. The installation was made at the Boston Navy Yard and completed at New London. The trip to Port Everglades gave opportunity to check the electrical circuits. The first two days after arrival were spent in preparing for a demonstration to Navy personnel.<sup>10</sup> This was a qualitative demonstration but pointed the way to a number of quantitative tests which were made later. The primary items indicated for investigation were (1) the importance of the bottom echo and (2) the apparent width of the target spot on the EPI.

To test operation of the transducer, commutators, and preamplifiers, a large number of patterns were taken, both vertical and horizontal, in reception as well as in transmission.<sup>11</sup>

The vertical patterns were taken by placing the deep monitor at a specific depth angle and then rotating one of the depression commutators to obtain the pattern. The stabilization system was by-passed since both HP-3DS and the deep monitor were attached to the ship. The *portable polar chart recorder* [PPCR]<sup>12</sup> was used to record the patterns; its synchro-control circuit was connected to the synchro control on the commutator. There were two commu-

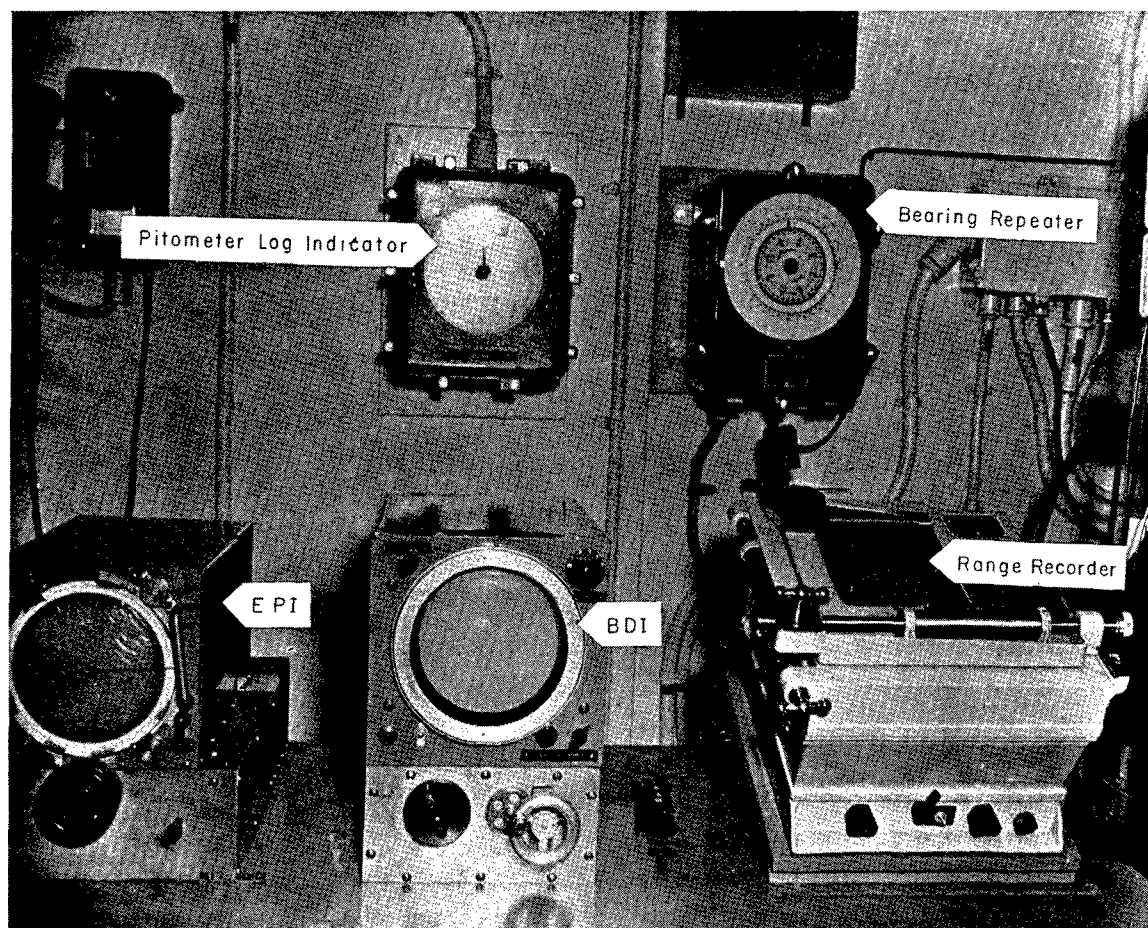


FIGURE 10. Installation of indicators for 26-kc DSS on USS CYTHERA.

tators on which vertical patterns were taken, the sum-listening commutator and the scanning commutator. The scanning commutator was converted for servo-controlled rotation to obtain patterns.

These patterns showed that the sound beam was somewhat wider in the vertical plane than expected from measurements on the commutators made in the laboratory with an artificial transducer and at the Spy Pond testing station with the HP-3DS transducer and the sum-listening commutator.<sup>13</sup> The beam width 10 db down from the maximum varied from 15 to 20 degrees, depending on the depth angle, compared to values of 14 to 15 degrees measured in the laboratory. Figure 16 shows the values of beam width plotted as a function of depth angle. The first minor lobes on the vertical patterns were somewhat higher than expected but did not produce false target echoes. Figure 17 shows a typical vertical pattern. The center of the pattern varied somewhat from the depth angle

with a maximum difference of 3 degrees. Measurements with the deep monitor showed no irregularities in attenuation of the sound caused by transmission through the dome.

Because of the importance of the bottom echo, values of response on the pattern for 90-degree depression were of interest. Down to a 50-degree depth angle, the response remained at least 14 db below the peak of the major lobe. Some very high minor lobes observed at angles above the horizontal were attributed to the image of the deep monitor in the hull of the ship and were considered of no importance for actual targets.

Horizontal patterns were taken by setting the deep monitor at a given depression angle and then rotating the HP-3DS transducer through a complete revolution. The PPCR was connected so that the rotation of its table corresponded to rotation of the transducer. In the horizontal plane, two types of pattern were

CONFIDENTIAL



FIGURE 11. Installation of cylindrical dome on USS CYTHERA.

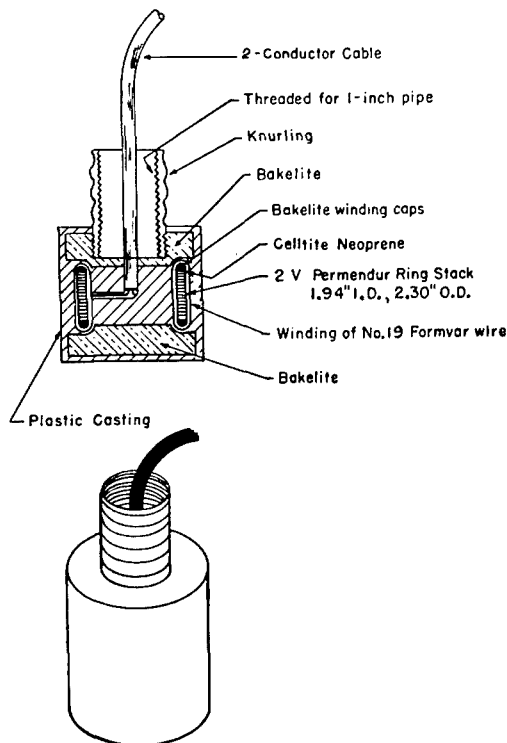


FIGURE 12. Deep monitor transducer.

taken, sum patterns from the sum commutator, and difference patterns from the difference commutator. It was considered important to obtain both of these in order to estimate the possible behavior of the BDI circuit. In general, the horizontal patterns were very good, and it was assumed that BDI operation should be equally good. The width of the horizontal pattern at 10 db down from the maximum was 22 degrees, which agreed well with the computed value. As the deep monitor was lowered for larger depth angles, the sound beam traced out a cone as HP-3DS was rotated, so that the apparent pattern became wider. The measured widths followed the calculated values very well. This again indicated little or no effect of the dome on the sound beam. Figure 18 shows the values of beam width plotted against depth angle for the sum commutator. Figures 19 and 20 show the beam widths and separation plotted against depth angle for the difference commutator. The heights of the minor lobes relative to the major lobe were found to be fairly close to the computed values, except for depression angles above the horizontal where reflection from the bottom of the ship could occur. Figures 21 and 22 show typical sum and difference patterns, respectively.

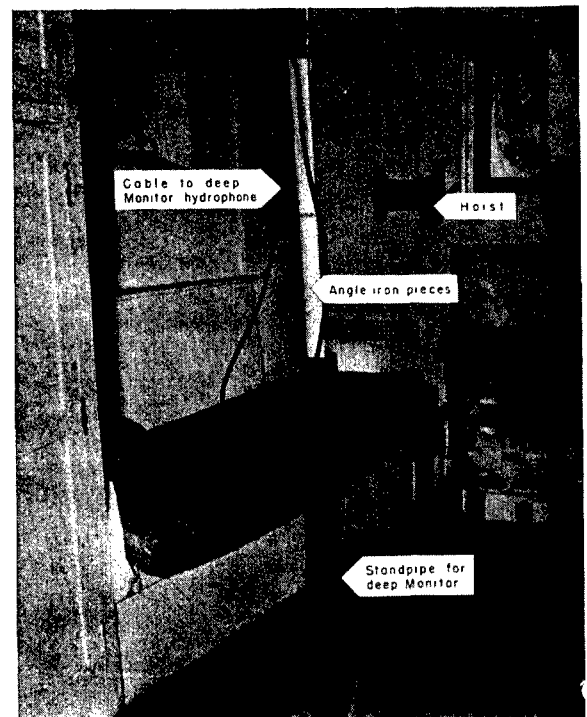


FIGURE 13. Top of installation of deep monitor on USS CYTHERA.

CONFIDENTIAL

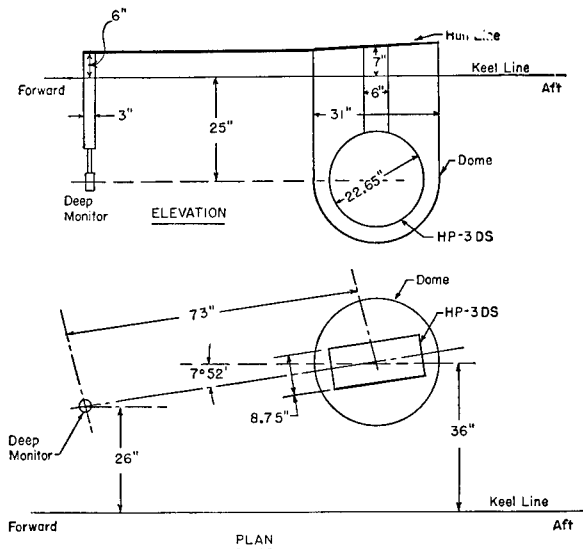


FIGURE 14. Physical arrangement of HP-3DS and deep monitor on USS CYTHERA.

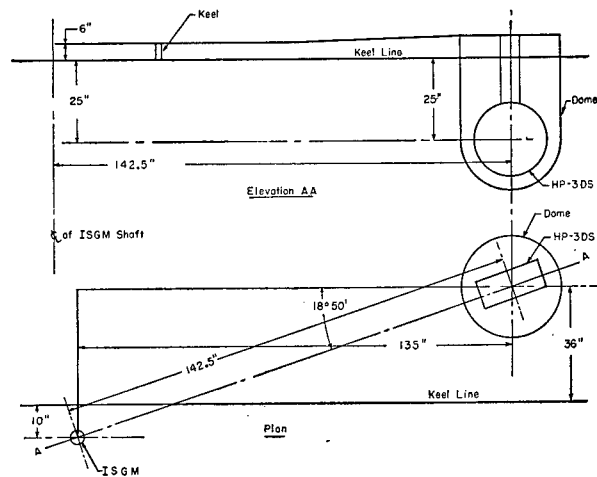


FIGURE 15. Physical arrangement of HP-3DS and ISGM on USS CYTHERA.

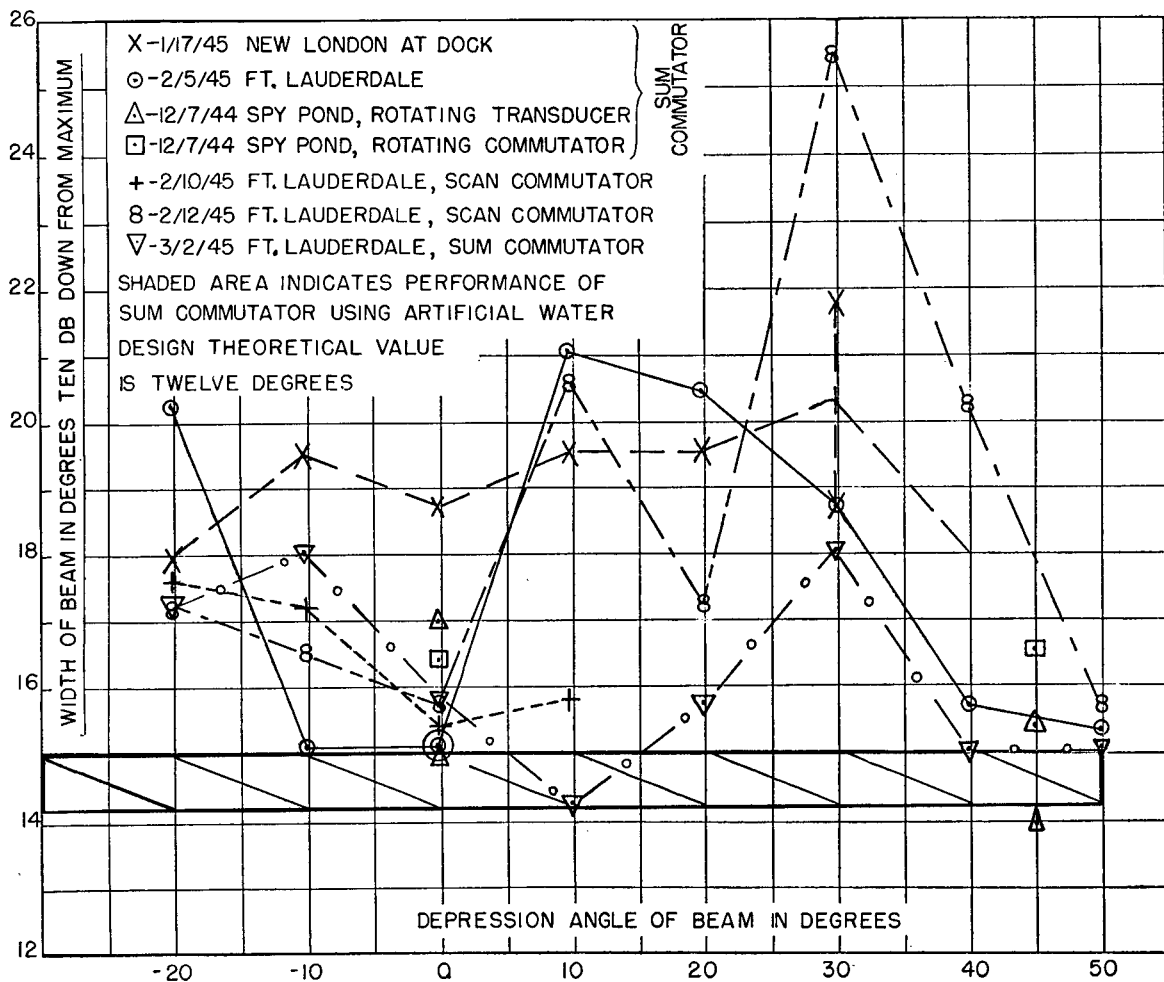


FIGURE 16. Vertical beam widths, depth-scanning sonar.

CONFIDENTIAL

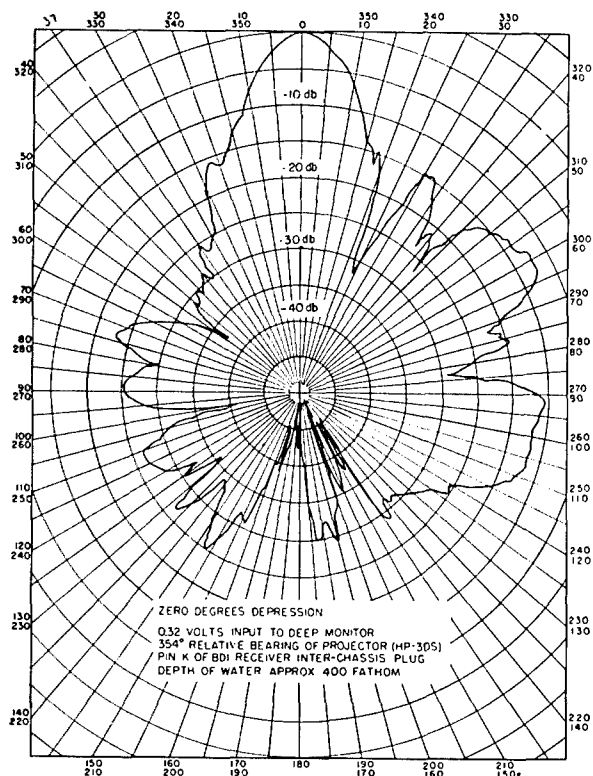


FIGURE 17. Typical vertical sum pattern.

Transmitting pattern<sup>14,15</sup> were taken by setting the deep monitor at a given depression angle and observing the amplitude of the transmitted ping at the deep monitor with a cathode-ray oscilloscope. The experimental values as a function of depth angle showed much more irregularity than was to be ex-

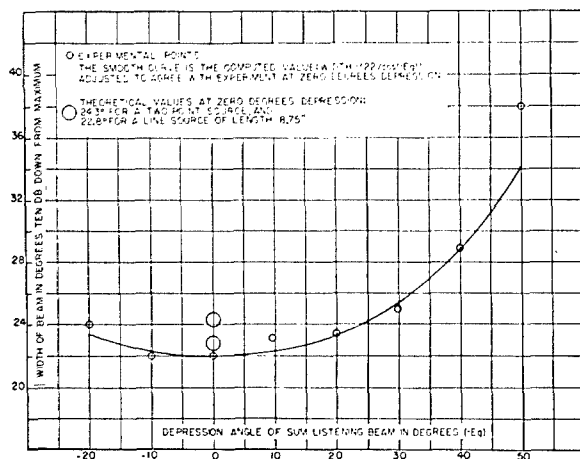


FIGURE 18. Horizontal width of sum-listening beam for 26-kc DSS.

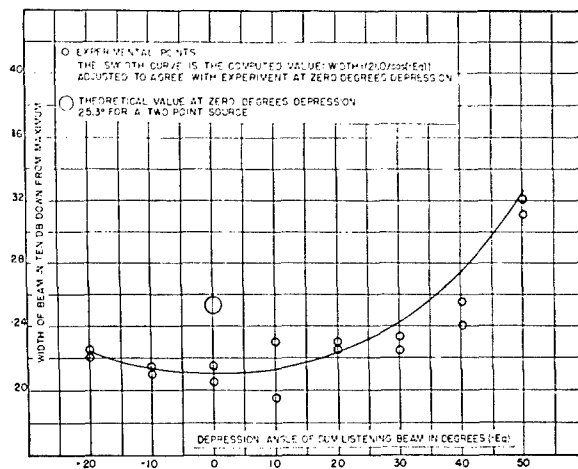


FIGURE 19. Horizontal width of difference-listening beams for 26-kc DSS.

pected from the data taken at HUSL on the transducer. Figure 23 shows typical values.

An approximate calculation shows that the effect of the image of HP-3DS in the hull of the ship could produce an interference pattern whose magnitude from maximum to minimum would be about the same as the observed irregularity. Observations made with the deep monitor over a small range of depth angle did not show the details of this computed interference pattern, since the deep monitor transducer was large enough to average out such details. A similar calculation shows that an interference pattern might be obtained at long range due to this image effect, causing the transmitted pattern to be far from

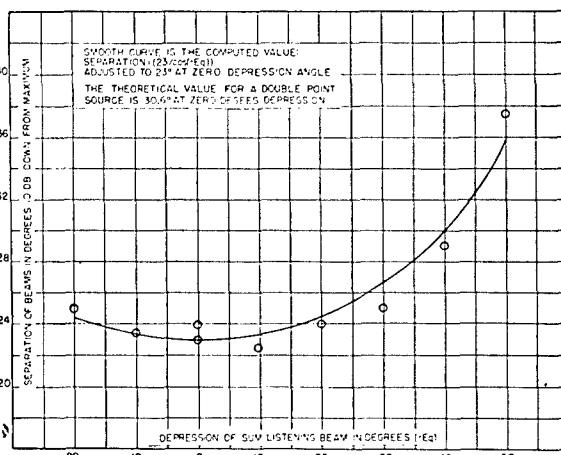


FIGURE 20. Horizontal separation of difference-listening beams for 26-kc DSS.

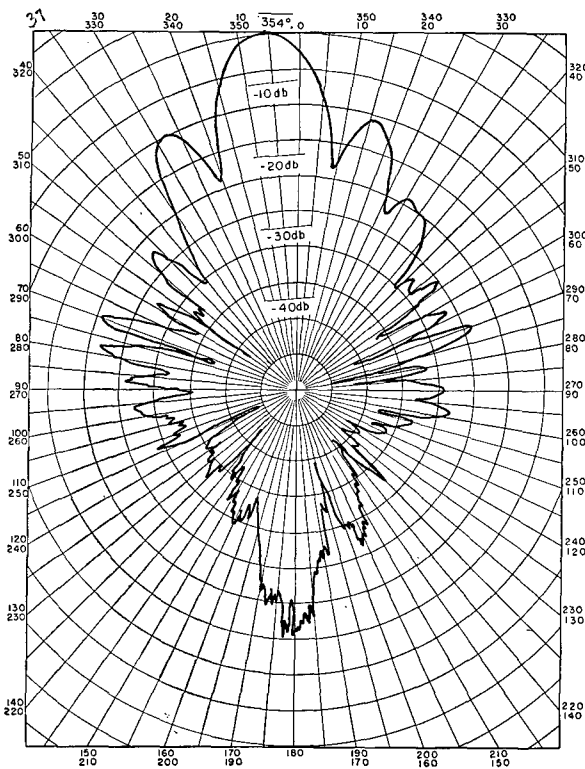


FIGURE 21. Typical horizontal sum pattern for 26-kc DSS installed on USS CYTHERA.

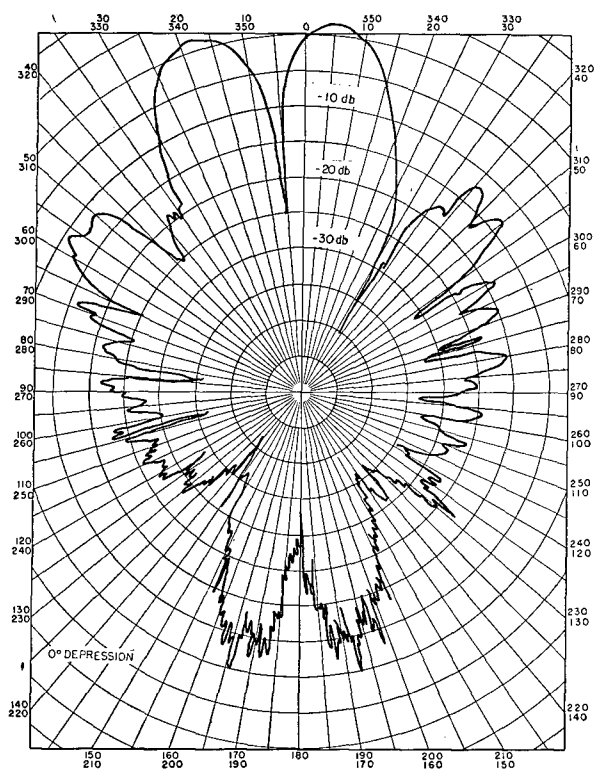


FIGURE 22. Typical horizontal difference pattern for 26-kc DSS installed on USS CYTHERA.

uniform. In general, this image effect and the resultant interference patterns form a fundamental limitation on depth scanning unless the image is effectively eliminated. For long ranges, this limitation may amount only to variation of strength of the received echo. More importantly, for an extended target it may result in incorrect determination of depth angle because of variation of the strength of the received echo from various parts of the target.

The initial operations of the depth-scanning system showed that the bottom echo was extremely strong and appeared both in the scanning and listening indications of the system.<sup>10</sup> The appearance of the bottom echo on the EPI is shown in Figure 24.<sup>16</sup> Zero elevation is horizontal in this photograph. The strength of the bottom echo was so great that response was obtained on all the minor lobes of the receiving pattern, which appeared as a half circle to a full circle. A full circle resulted from a reflection of the echo from the ship's hull. For larger ranges, as seen in the photograph, the bottom echo appears as approximately a straight line, though bent upward at the rear, for depth angles greater than 90 degrees. The shape of the bottom echo resulted from the fact that

the indication was not true, but that 90 degrees of depth angle was spread out to occupy 120 degrees on the face of the cathode-ray tube. At still greater

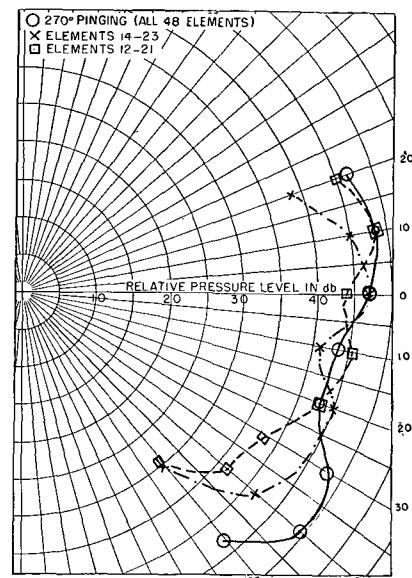


FIGURE 23. Transmitting pattern for HP-3DS installed on USS CYTHERA.

CONFIDENTIAL

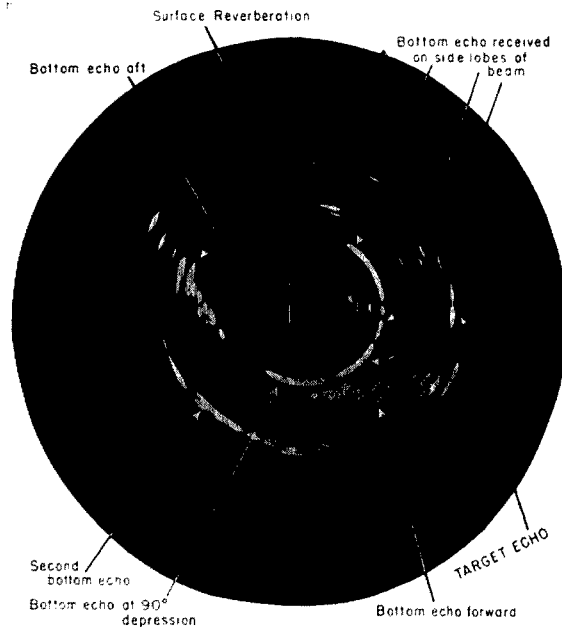


FIGURE 24. Bottom echo effect on EPI display for DSS. Range, 600 yd; target depth, 100 ft; depression angle, 3 degrees; water depth, 300 yd.

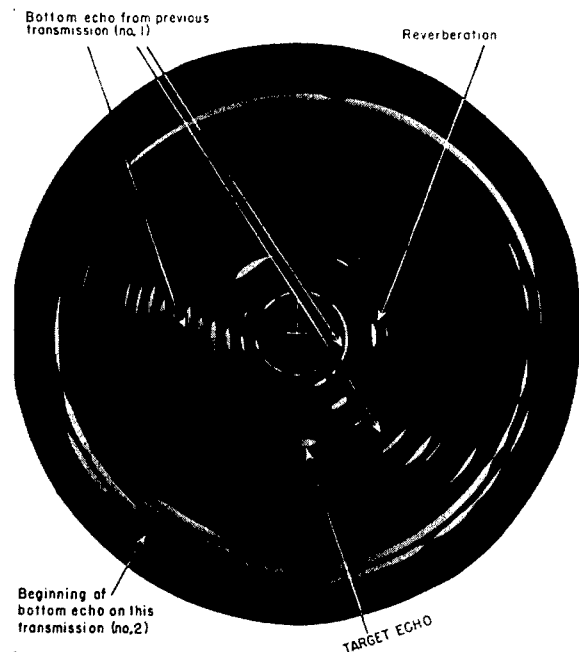


FIGURE 25. Bottom echo effect on second transmission, EPI display for DSS. Range, 300 yd; target depth, 800 ft; depression angle, 60 degrees; water depth, 700 yd.

ranges, a second bottom echo is observed, due to multiple reflections between the bottom and the surface of the water. It is obvious that a target occurring at the range of the bottom could be obscured by the bottom echo or that an echo might be missed on the EPI because of the large number of dots on the screen due to the bottom echo. In shallow water it was found that the pinging rate might be such that the bottom echo returned during the period of time represented by a succeeding ping. An example of this is shown in Figure 25. It is obvious that the bottom echo from the preceding ping obscures the screen during the second ping interval and, therefore, the target might again be lost. As the water became deeper the bottom echo became of less importance, and in very deep water it disappeared entirely because of the absorbing nature of the sediment on the bottom. An example of this is shown in Figure 26. In order to evaluate this effect quantitatively, a large number of measurements were made of the apparent target strength of the bottom (defined, as in the case of a submarine target, as the size of the equivalent perfectly reflective sphere). The apparent target strength increased with depth of sea and satisfactorily followed the computed value. Figure 27 summarizes the values obtained.<sup>17</sup> The computed value was adjusted to fit the points by

assigning a proper reflection coefficient for the bottom: a value which turned out to be surprisingly low (about 0.04). Despite this, the target strength of the bottom was found to be at least equal to or greater

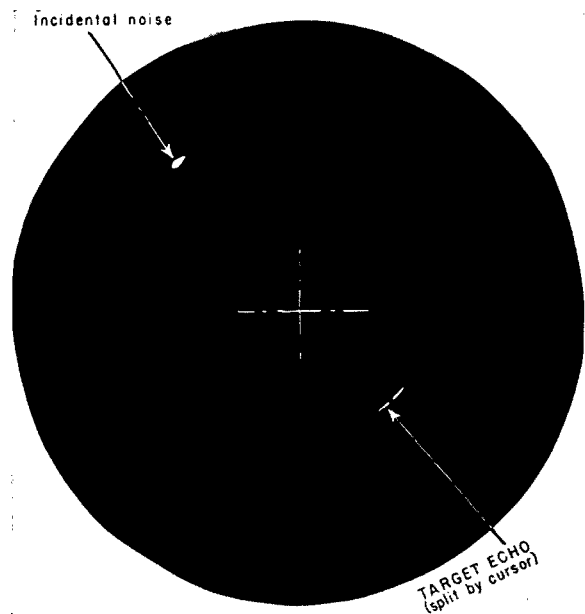


FIGURE 26. Target echo on EPI display for DSS. Range, 180 yd; submarine 360 feet deep; depression angle, 40 degrees; 1,500 fathoms.

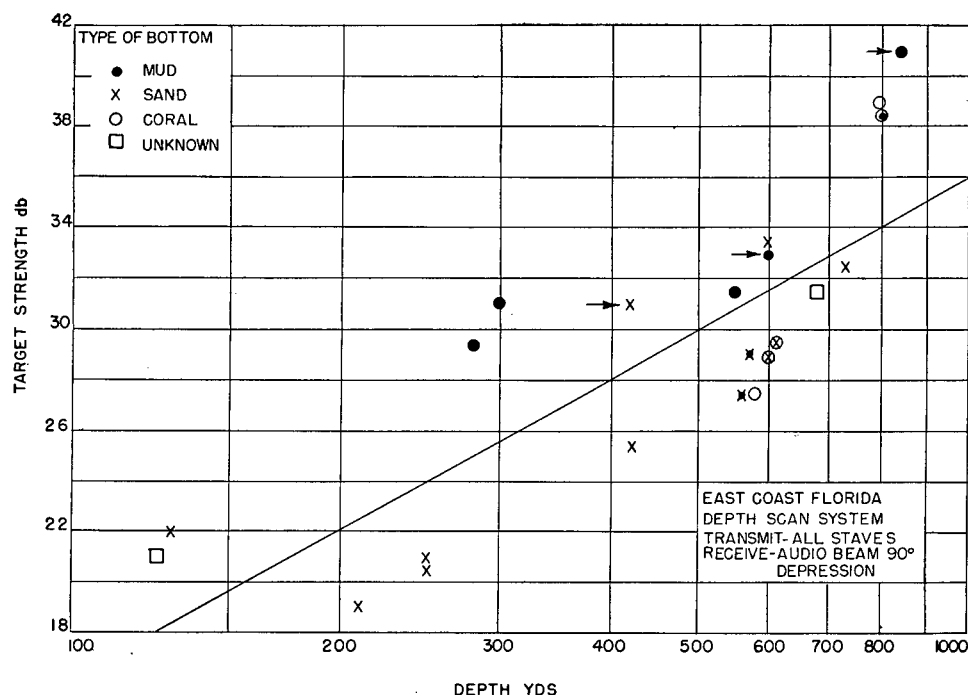


FIGURE 27. Ocean bottom target strength versus depth.

than the target strength of a typical submarine for all depths greater than 300 yards.

Reduction of the strength of the bottom echo can be accomplished in two ways. The first is by improving minor lobes of the scanning pattern so that the circle observed at the range equal to the depth of the sea is eliminated. The second is by pinging with a directed beam whose intensity would be reduced toward the bottom, instead of pinging with the nondirectional beam obtained by exciting all elements of the transducer equally. Such a directed beam was obtained by exciting only ten of the transducer elements. Measurements of the transmitted beam are shown in Figure 23 for an arrangement using ten elements centered on the horizontal and for an arrangement using ten elements centered 10 degrees below the horizontal. A second experiment was carried out to determine the effect of a differently directed beam.<sup>18,19</sup> The projector for the QBF gear installed on the USS CYTHERA was used for transmission, and the depth-scanning transducer HP-3DS was used for reception. The QBF projector had a pattern such that the output was down 20 to 25 db at a depression angle of 90 degrees. The QBF gear was trained, in accordance with the information obtained on depth-scanning sonar, for ranges shorter than

those for which contact could be maintained on the QBF system. It was found possible to make successful runs directly over a submarine at depths of 200 and 400 feet in water that was 1,800 feet deep. Subsequent use of this composite system in shallower waters indicated equally successful operation. The bottom echo did not appear on the EPI screen in sufficient strength to be confusing so far as the target was concerned, and there was no difficulty in following target echo through the range equal to the depth of the water. A set of measurements was taken to show relative strength of the bottom echo as a function of the listening beam depression angle and as a function of the type of transmitting beam used. These are summarized in Figure 28. This curve has an arbitrary 0-db value, which may be made absolute from the values given in Figure 27.

In relatively shallow water, confusion resulting from appearance of the bottom echo on the second ping may be avoided by using alternate pinging with the screen of the EPI blanked during the interval for the second (omitted) ping.<sup>16</sup>

Measurements of the target strength of a submarine were made, and the values obtained agreed quite well with those published in other reports. This was an encouraging sign, because it indicated that the

CONFIDENTIAL



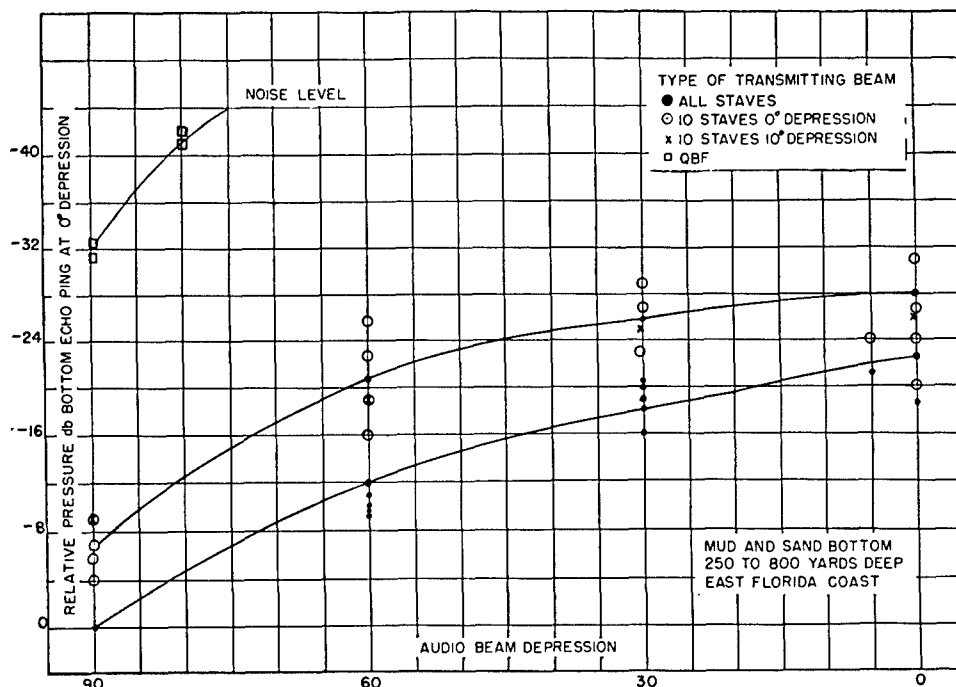


FIGURE 28. Relative bottom strength versus type of transmitting beam versus depression audio receiving beam.

overall operation of the system was in accordance with theory.<sup>20</sup>

The visual figure of merit of the system<sup>21</sup> was measured and the values obtained compared well with the QH Model 2,<sup>22</sup> when it was installed on the USS CYTHERA. (See Table 1.) The audio figure of merit for 12-knot speed was 130 db. The value for QH Model 2 was 130 db at 11 knots.

The listening channel operated quite satisfactorily. The only difficulty encountered was, again, the bot-

TABLE 1. Figure of Merit for DSS on the USS CYTHERA.

Speed	Visual Figure of Merit	
	DDS	QH Model 2
0	133	140
12	125	125

tom echo. The direct bottom echo had no doppler shift in frequency, but the echo of the bottom at various ranges, that is, for depression angles other than 90 degrees, had a definite doppler which changed as the depression angle increased. This effect was most noticeable when the listening beam was pointed forward or aft because of reception of the bottom echo on the back and side lobes as well as the major lobe of the beam. At the same time, the target

itself might have a still different doppler. If the beat-frequency oscillator was adjusted for best reception of the target, it was often difficult to judge the doppler effect of the target because of this confusing effect of bottom-echo doppler. It might be possible to differentiate the target from the bottom by this difference in doppler, but the actual doppler shift of the target would be difficult to determine.

Typical pictures of the EPI scope are shown in Figures 24 and 26. Appearance of the bottom echo has already been discussed. There seemed to be a small amount of surface reverberation, and occasionally wake echoes were observed on the surface. However, the region between the surface reverberation and the bottom echo was quite free from signal. When the transducer was trained aft, propeller noise as well as wake echo obscured the screen for values of depth angle down to 30 degrees. Some electric noise also appeared, but in general neither electric noise nor water noise appeared to any great extent on the screen.

When the stabilization system was tested after installation, it was found that the system operated in the right direction and that the corrections had about the proper magnitude. The training control was not very satisfactory because a sudden turn of the azimuth handwheel caused a considerable amount of over-

CONFIDENTIAL

shoot and oscillation at the projector. The defect was eventually improved,<sup>23</sup> but all the servos in this system could have benefited by an increase in stiffness.

The synchro indicator panel contained a number of synchros which indicated the various values transmitted by synchro orders. It was intended, by means of a movie camera synchronized with a high-speed light source, to photograph the dials on these various synchros in order to obtain data on stabilization and check on the operation of various servos. Unfortunately the synchros were not suitable for this application, and the panel was never used in its original form; lack of time prevented rebuilding.

The BDI listening receiver, being a first development unit, was subjected to numerous tests and was modified in a number of particulars before it operated properly. The measurements of the sum and difference patterns on the transducer indicated definitely that the BDI receiver should work properly, and good BDI deflection patterns were obtained after some effort.<sup>24</sup> A typical measured BDI deflection curve is shown in Figure 29.

In the original design of the BDI receiver, a *reverberation-controlled gain* [RCG] circuit was included. The gain reduction was initiated by the original reverberation level and the circuit then allowed the gain to increase according to the reverberation level. The strength of the bottom echo was great enough to reinitiate the gain reduction, hence, to modify the proper action. For this reason, the gain reduction initiation was later obtained from the blanking pulse in the sweep chassis. Transformers feeding the phase-sensitive detector also caused trouble by introducing improper phase shifts and wave-form distortions, but after the transformers were replaced the phase-sensitive detector operated properly.

Despite the lack of suitable BDI indications during the early part of tests on the system, it was found fairly easy to locate and follow a target, provided the general area for search was known. This was particularly true in deep water where there was no bottom echo. In this situation, a submarine target could be followed from about a 1,300- to 120-yard range; that is, directly over the submarine, or for depression angles from 0 to 90 degrees. Contact was readily maintained while passing over the target until about 40 degrees depression when the receiver was trained aft, at which time propeller noise obscured the echo. While the maximum observed range on a submarine target was 1,300 yards, good echoes were sometimes

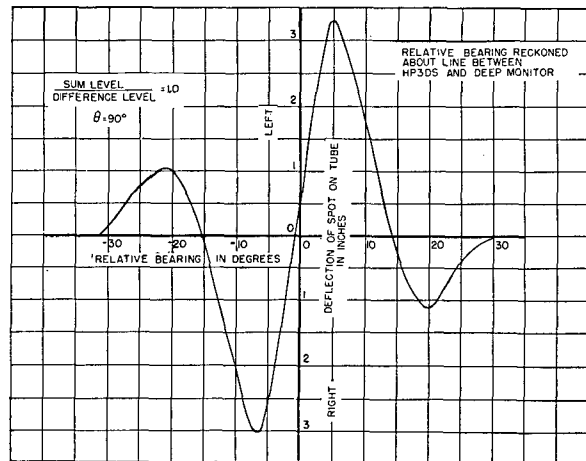


FIGURE 29. Typical BDI deflection curve, depth-scanning sonar.

obtained from surface targets out to 3,750 yards. In the absence of BDI indications, contact was maintained by listening to the echo, watching the EPI, and using cut-on procedures. Difference between the target and its wake was readily observed by noting the doppler shift. Temperature gradients in the waters, near Port Everglades, in which most of the tests were made, were very slight and did not appreciably limit operation of the system.

As an overall test of the complete installation, the USS CYTHERA followed several runs of a submarine from the greatest detectable range to depth angles of very nearly 90 degrees. A typical plot of slant range and depth versus time is shown in Figure 30. Also plotted is the actual depth of the target obtained from the log of the submarine. Experimental depth values were computed from range and depth angle. The depth was 2,350 yards and the water was at a constant temperature of 61 F down to a depth of 400 feet. Depression angles were measured by recording the cursor settings of the EPI. From curves of the three runs (shown in Figure 30), the apparent depth seems to be a function of range (as plotted in Figure 31). If it is assumed that there was a systematic error of 3 degrees in the depth angle and a correction of this amount was made, then the observed depth is closer to the reported depth from the target. The original setting of the zero of the elevation angle was made in dry dock at a time when the keel of the ship was horizontal. When the ship was in water the keel may not have remained horizontal, so that calibrations carried out using the deep monitor may have been in error. In

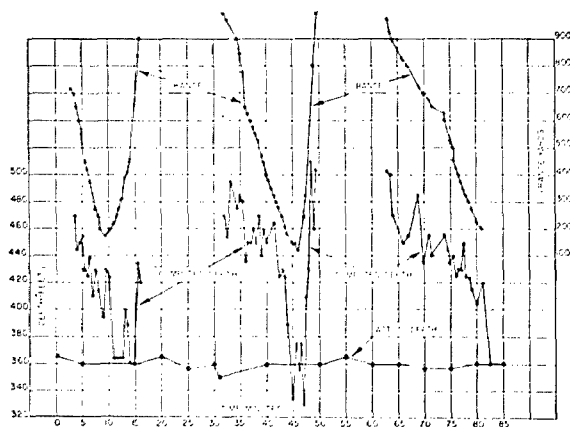


FIGURE 30. Range and depth of target versus time.

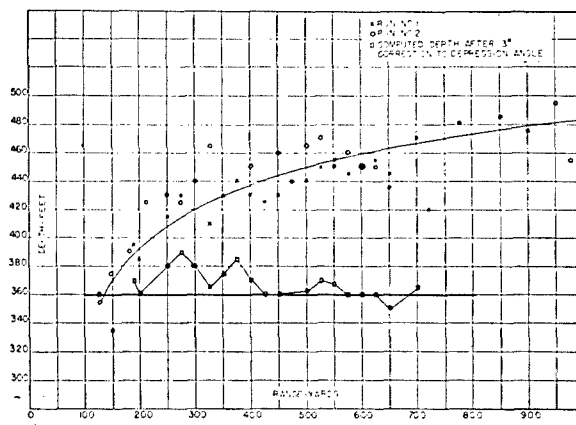


FIGURE 31. Apparent depth versus range of target.

addition, there may have been some error in the servo mechanisms which stabilize the indication on the EPI.<sup>25</sup>

#### 6.2.4

### Conclusions

Tests carried out on the depth-scanning system installed on the USS CYTHERA proved that depth scanning was a feasible system and that it followed in general the prediction made for it. Several specific items arose which had to be considered in the application of depth scanning to the integrated Type B sonar. One of these was reduction in strength of the bottom echo. Various schemes were proposed for the use of a directional transmitting pattern,<sup>26,27,28,29,30</sup> and one or two of these were carried out on the experimental installation. The use of a lag line, or lines, in forming a transmitting beam should be considered theoretically. A pattern of the type shown in Figure 32 might be found useful, if practical means could be devised to form such a beam. It has the obvious advantages of reducing both the strength of the bottom echo and the strength of any target image in the surface of the water.

The particular sum-and-difference BDI receiver used caused trouble in the experimental work—to the extent that it was not recommended for use in the integrated Type B sonar unless further development work was carried out on it. In particular, the bridge-type varistor vario-losser circuits used did not have sufficient dynamic range and power-handling capacity. As expected, it was found that center indication of the target was always correct, though right and left deviations were at times incorrect when the varistors

introduced spurious phase reversals. Some difficulty in obtaining proper BDI operation was due to inability to line up properly the two listening commutators. A means of alignment should be provided.

The transmitter, junction box, commutators (except as mentioned above), and transducer were found satisfactory for use in integrated Type B sonar. Patterns taken on the transducer show that it was quite satisfactory for depth scanning and for application to a BDI-type circuit. Tests on the transmitter showed that it operated properly, though some detailed recommendations were made in regard to the keying-control circuits in order to keep the pulse length constant and to retain the pulse shape. The stabilization feature of the system was found to work properly, although it was not possible to make detailed tests in the experimental work. It was recommended that the

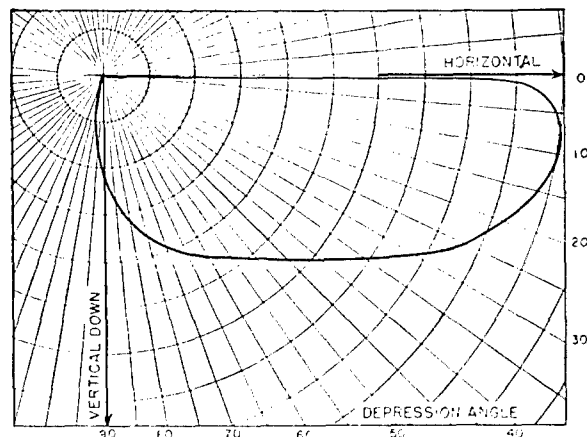


FIGURE 32. Proposed pattern for transmission for depth-scanning sonar.

various servo systems in the synchro-control circuits be kept quite stiff in order to obtain proper operation of the servos and to retain a suitable instrumental accuracy in the system.

The depth-scanning system proved to have the distinct advantage of allowing the operator to keep on the target by reference to the scanning indicator (EPI), so that momentary loss of the target by the incorrect choice of depression angle could be corrected without searching for the target.

### 6.3 TRANSDUCER, TRANSFER NETWORKS

#### 6.3.1 HP-3DS Depth-Scanning Transducer<sup>13</sup>

The depth-scanning transducer<sup>31</sup> HP-3DS was designed and constructed in order to carry out investigations on the principle of depth scanning and to prepare for detailed design and construction of a depth-scanning transducer for the integrated Type B sonar. Since it was hoped to construct such a model fairly rapidly, the time factor was important in the first tests on depth scanning. Owing to the immediate availability of HP-3 magnetostrictive laminations, the detailed design of HP-3DS included these laminations taking into account, however, the various general design considerations.

Both depth-scanning transducers HP-3DS and HP-8D were designed on the basis of the same general requirements,<sup>4</sup> except for the maximum allowable size. The general requirements were as follows:

1. The vertical beam width should allow possible measurement of depth angle to  $\frac{1}{2}$  degree at 1,000-yard range. It was decided that the vertical beam width should be about 9 degrees wide and 6 db down from the maximum in order to meet this requirement.

2. The horizontal beam width should be such that the entire target would be contained in the beam at all times for all target aspects and useful ranges. It was decided that the horizontal beam width should be about 20 degrees wide 10 db down from the maximum in order to meet this requirement. (Thus, for example, a beam-on target 300 feet long at a range of 150 yards would be entirely included in this beam.)

3. The depth-scanning transducer should have such dimensions that it would fit into a standard 19-inch sonar sea chest, so that it could be used on a standard sonar hoist train. (This dimensional re-

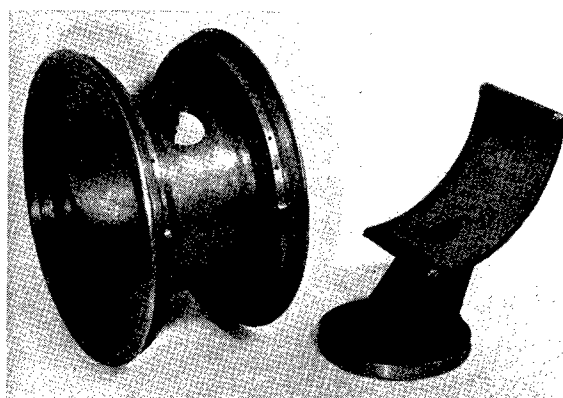


FIGURE 33. Spool, gooseneck, and end flanges for HP-3DS transducer.

quirement was not met by HP-3DS, but was met by HP-8D.)

4. The depth-scanning transducer should be constructed to allow examination of depression angles from 0 to 90 degrees independent of roll and pitch of the ship. In meeting this requirement, it was assumed that the combined effect of roll and pitch would not exceed 30 degrees under normal conditions of operation.

5. It was envisaged that when the depth-scanning sonar was being used in attack, it should be independent of any other sonar system which might lose contact with the target for large depression angles. For this reason, it was required that the depth-scanning transducer be constructed so that target bearing deviations could be determined. This requirement was met by making each element on the transducer in two halves, thus providing effective right and left halves in the transducer for BDI operation.

The depth-scanning transducer HP-3DS met all except the dimensional requirement. In order to obtain the necessary vertical beam width it was decided that a 64-element cylindrical transducer, 10 wavelengths in diameter, would be satisfactory. The diameter of the active face of the cylinder was accordingly made about 23 inches, since the frequency of HP-3 laminations used was 26 kc.<sup>32</sup> To obtain the required horizontal beam width, an active length of element of about eight inches was necessary. Actually, HP-3DS laminations were being consolidated for other purposes in stacks  $3\frac{3}{4}$  inches long. Two of these stacks with end caps on each gave a length of  $8\frac{3}{4}$  inches, producing a pattern of 22.5 degrees width 10 db down from the maximum (see Chapter 9). The use of two such stacks in each element automatically satisfied

requirement No.5 above since such element then consisted of right and left halves.

A total of 48 elements arranged around 270 degrees of the transducer were used as explained in the pre-

TABLE 2. Characteristics of the Staves and Stacks Used in Scanning Sonar Transducer HP-3DS. Frequencies Are Referred to a Temperature of 23.5 C.

Stave No. on spool	Prod. No. of stave	Right half			Left half		
		Prod. No. of stack	$f_G$ (kc)	$G_{max}$ (mmhos)	Prod. No. of stack	$f_G$ (kc)	$G_{max}$ (mmhos)
1	XLI	337	27.100	128	351	27.100	93
2	LXVII	619	26.095	112	639	.105	102
3	XLIV	99	27.100	120	77	.105	119
4	LXVIII	627	.115	101	629	.100	96
5	XL	173	.110	102	225	.110	131
6	XXX	417	.115	103	259	.110	116
7	XXXVIII	183	.115	95	185	.115	103
8	XLVII	321	.120	115	239	.120	114
9	LXIV	647	.110	103	617	.130	98
10	XLV	419	.125	107	421	.125	102
11	XVII	233	.125	112	199	.125	114
12	XXIX	67	.135	115	369	.130	93
13	XXXV	171	.135	120	107	.135	124
14	XXXII	247	.135	122	31	.140	114
15	XXXVI	55	.140	105	163	.140	110
16	LXIX	475	.150	109	491	.130	111
17	LXIII	645	.150	98	641	.140	110
18	LXIII	463	.140	103	455	.165	113
19	XLVI	109	.150	113	113	.150	98
20	LXV	501	.140	115	607	.160	107
21	XXXIII	409	.150	84	179	.155	120
22	XX	181	.155	110	327	.155	114
23	XXIV	119	.160	114	315	.155	109
24	XXIII	243	.160	113	251	.160	93
25	XIX	143	.160	108	215	.160	114
26	LIX	481	.160	115	503	.160	114
27	LVI	469	.165	109	467	.170	112
28	LII	453	.170	101	451	.170	118
29	XIV	365	.170	107	381	.170	115
30	XI	203	.170	115	245	.170	123
31	X	397	.170	107	387	.170	93
32	III	349	.175	105	399	.175	101
33	VI	347	.175	110	155	.175	119
34	VIII	389	.175	86	323	.180	115
35	LI	609	.185	105	479	.170	85
36	XII	411	.185	102	59	.185	124
37	IX	415	.185	130	149	.180	119
38	V	61	.185	124	383	.185	87
39	LX	483	.200	117	499	.185	105
40	XV	603	.210	119	637	.180	122
41	IV	393	.195	102	343	.195	114
42	LIV	613	.195	114	601	.195	108
43	I	413	.195	96	309	.200	110
44	L	477	.195	111	457	.210	102
45	LXV	493	.210	87	495	.205	100
46	XVI	605	.200	112	611	.220	125
47	VII	57	.215	129	103	.210	124
48	LXII	485	.220	94	509	.215	119

vious section. Figures 33 through 39 are photographs of the HP-3DS transducer in various stages of construction. Table 2 shows the electrical characteristics of the various stacks used in the transducer.

Selection of a suitable cable for HP-3DS was complicated by the 192 wires necessary. The first cable used for test work is shown in Figure 39 and was later replaced by two sections of a Navy Type Cable TTHFA-50 with suitable cable seals.

The transducer was electrically coupled to three commutators during reception, and to the transmitter on transmission, by means of a transfer network including a junction box and various transformers. The junction box included coupling capacitors, a send-receive relay, and a tuning coil. The transformers were mounted directly on the commutators but formed an integral part of the transfer network. The wiring diagram for the transfer network is shown in Figure 40. Figure 41 shows the rack containing the junction box and three commutators.

The transfer from transmission to reception was accomplished by means of a double-pole single-throw switch, (switches  $S_1$  and  $S_2$  Figure 40), which during reception grounded the common points on the various sum transformers and also grounded the common

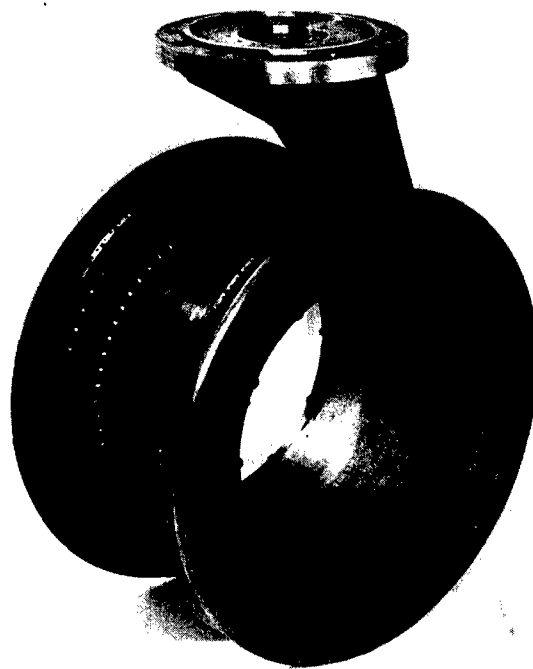


FIGURE 34. Assembly of spool, end flanges, and gooseneck for HP-3DS transducer.

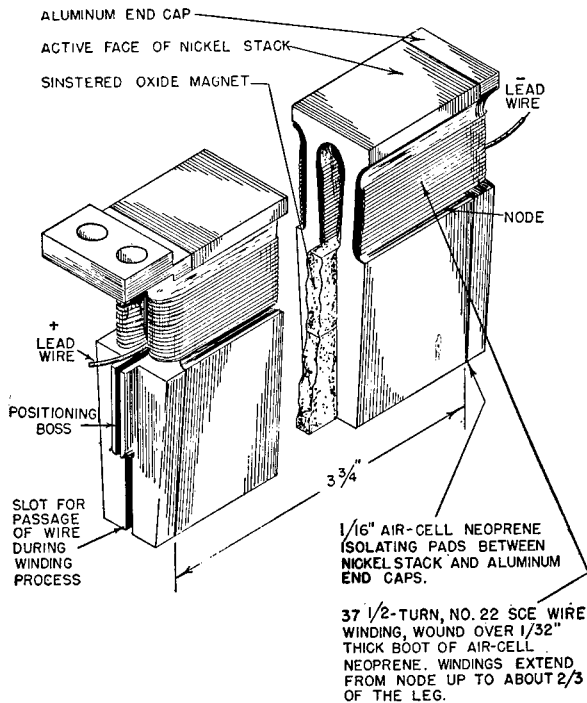


FIGURE 35. HP-3 stack as used in HP-3DS transducer.

points of the various coupling capacitors. During the transmission interval, this switch was open, and the receiving transformers were ungrounded and inactive, so that the transmitter fed the 96 transducer

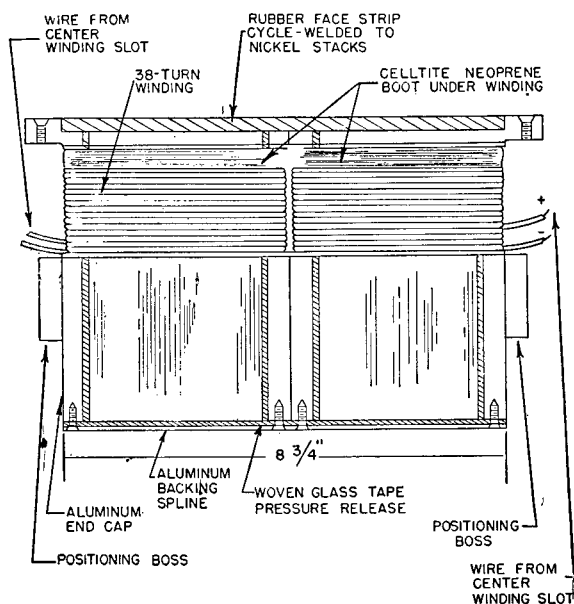


FIGURE 36. Side view of stave-like element used in HP-3DS transducer.

stacks in parallel, each through a series capacitor ( $C = 0.051 \mu\text{f}$ ). The total impedance of the 96 stacks and capacitors in parallel was about  $0.27 - j0.96$  ohms. To tune out this amount of capacitance, a tuning coil was placed in shunt across the transmitter to ground. This coil had an inductance of  $6 \mu\text{h}$  and was built of heavy Litz wire in such a manner that it would carry the very large circulating currents obtained during transmission. During reception (see Figure 40), the switches  $S_1$  and  $S_2$  were closed. Each pair of elements, right and left (shown as 1L, 1R, etc., in Figure 40), was, therefore, connected to a transformer so that the output of the transformer was the difference between the voltages generated by the two halves. This transformer was center-tapped and led to the mid-point of the two halves of the transducer element through the primaries of two other transformers, whose outputs were then proportional to the sum of the two voltages developed by the two halves of the transducer element. These sum-and-difference voltages were led to the commutators (see next section of this chapter).

The transducer was carefully tested at Spy Pond before being released for installation. In all these tests, the junction box was used with the sum listen-

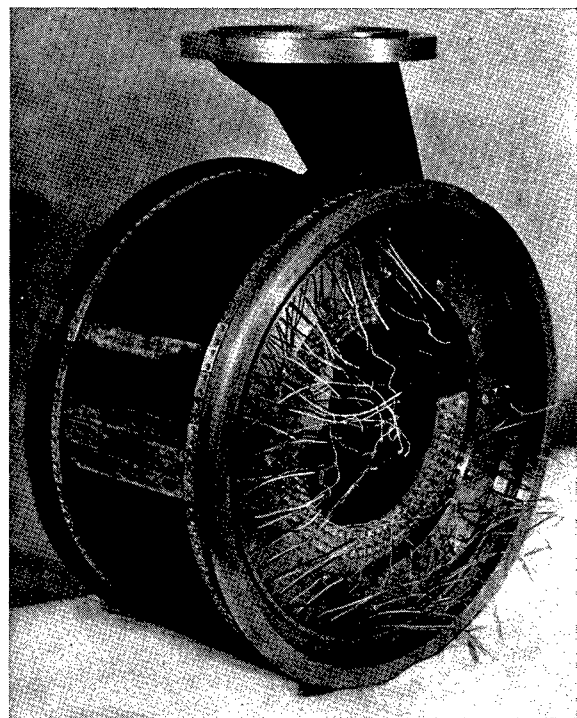


FIGURE 37. Assembly of elements on HP-3DS transducer.

ing and scanning commutators. The difference commutator was not available so the connections to it were short-circuited. The 6- $\mu$ h tuning coil was not available but was not necessary in these tests. Figure 42 shows the basic circuit used. All measurements were made with the axis of symmetry of the transducer spool in the vertical direction; that is, with the transducer on its side, the right side up and the left side down.

The following measurements were made:<sup>13</sup>

1. Receiving patterns were taken through the sum-listening commutator by rotating the commutator with the transducer in fixed positions, and vice versa. All patterns were taken at 26 kc with

the sound source at a distance of 24 feet, unless otherwise specified.

2. Receiving patterns of all elements in parallel were taken.
3. Patterns were taken for various single stacks.
4. Frequency responses of various single stacks were taken.
5. Impedance measurements were made on some single stacks.
6. Transmitting patterns with all elements in parallel were taken.
7. Patterns were taken in the BDI plane by noting the response of a B19B transducer mounted in a horizontal position and raised and lowered at known distances in front of the HP-3DS transducer.
8. Phase measurements were made between pairs of stacks and between pairs of elements at a frequency of 26 kc as a function of stack position.

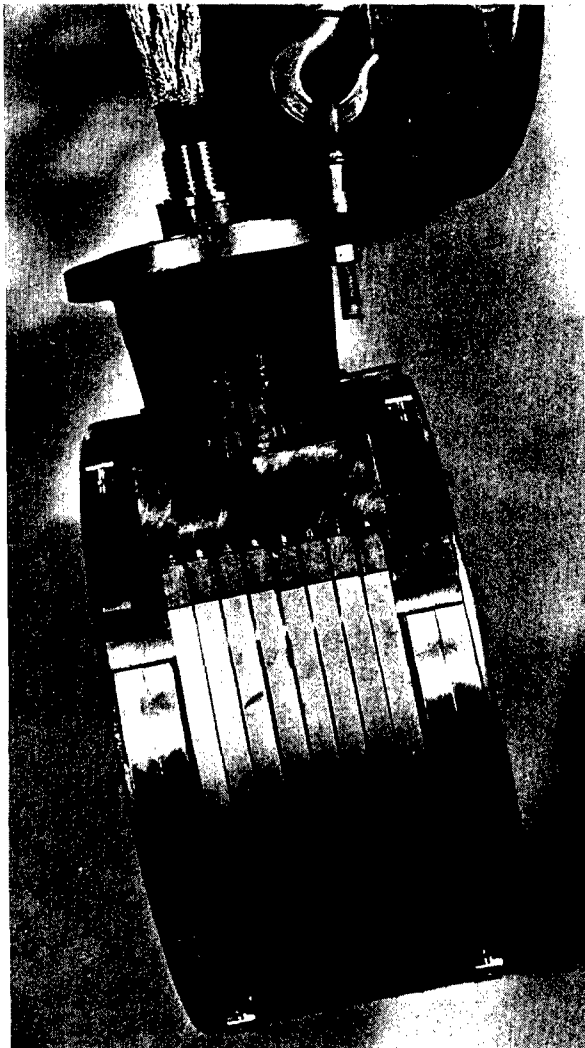


FIGURE 38. Assembly of HP-3DS transducer showing nickel bands over surface of rubber boot.

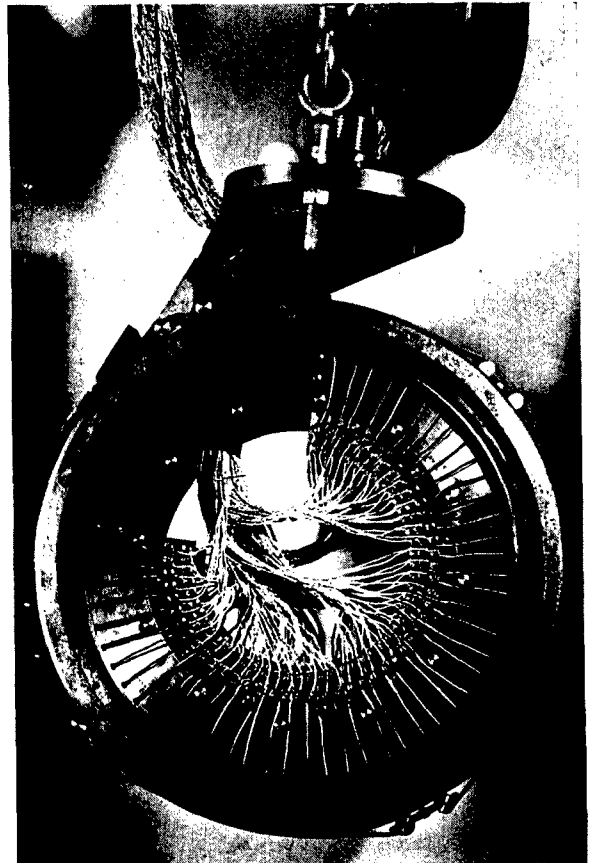


FIGURE 39. Cable connection to HP-3DS transducer.

CONFIDENTIAL

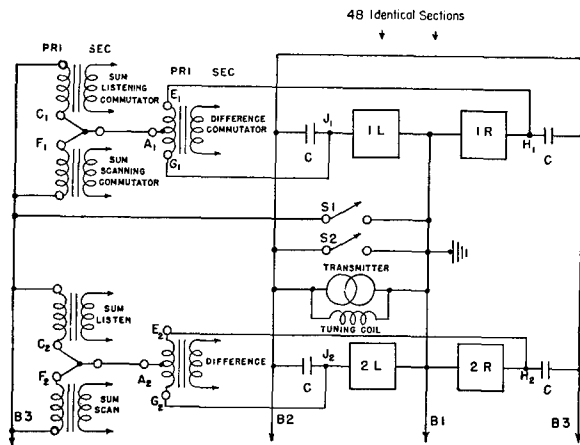


FIGURE 40. Wiring diagram of transfer network for 26-kc DSS.

9. Phase measurements were made between pairs of stacks and pairs of elements as a function of frequency.

Standard test methods were used in making these measurements. The results of these measurements showed that HP-3DS was suitable for use as a depth-scanning transducer. The patterns obtained with the commutator were slightly wider than computed (15 degrees at 10 db down from the maximum) but were considered satisfactory. The receiving pattern with all elements in parallel showed that a nearly nondirectional pulse should be obtained on transmission for the 270 degrees of arc covered with elements. The frequency response measurements showed that the main resonance occurred at 27 kc. Patterns in the BDI plane were not good and more satisfactory measurements for evaluation of the BDI operation were taken after installation (see preceding section). Phase measurements showed the phase difference between voltages generated in the various stacks and the stack on the acoustic axis to be somewhat greater than computed. This factor is important in the behavior of the combination of transducer and commutator in producing a suitable directional beam of sensitivity.

When phase measurements were made, responses of the elements were also taken. This was done to obtain information on the proper amounts of attenuation to use in the lag line to give the degree of amplitude shading that would make the side lobes of the acoustic receiving pattern sufficiently low. The pressure amplitude pattern was found to be midway between the theoretical patterns for stiff and soft baffles.

Efficiency of the transducer was computed to be about 30 per cent.

### 6.3.2 HP-8D Depth-Scanning Transducer

The depth-scanning transducer for the integrated Type B sonar was designed in accordance with the general requirements listed in Section 6.3.1. These requirements specified the vertical and horizontal beam widths, the angles that must be scanned, and the split construction necessary for BDI service. In addition, it was specified that the transducer should have such dimensions that it would be accommodated in a standard 19-inch sea chest.

In considering the design of integrated Type B sonar, it was proposed that the azimuth scanning for search be combined with depth scanning for attack (see first part of this chapter). Two transducers were

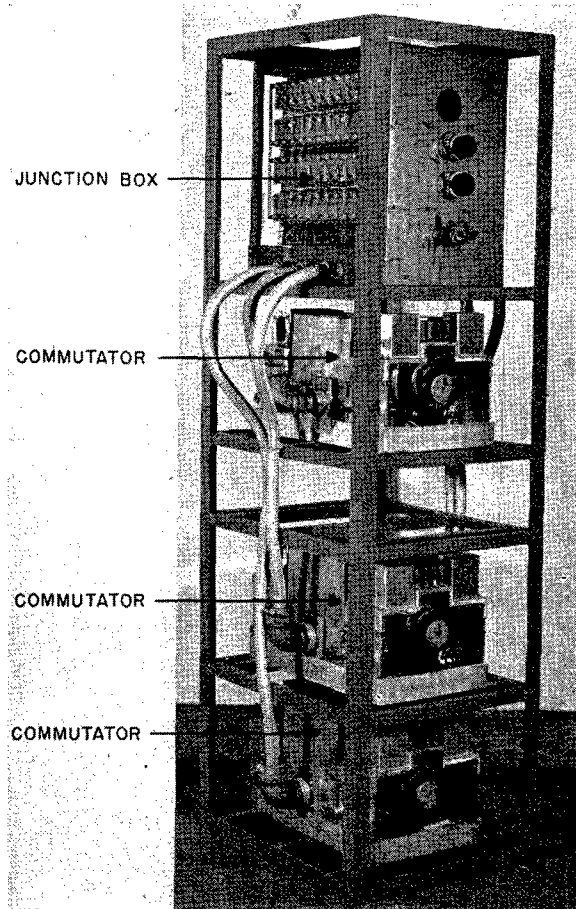


FIGURE 41. Junction box and commutator assembly for 26-kc DSS.



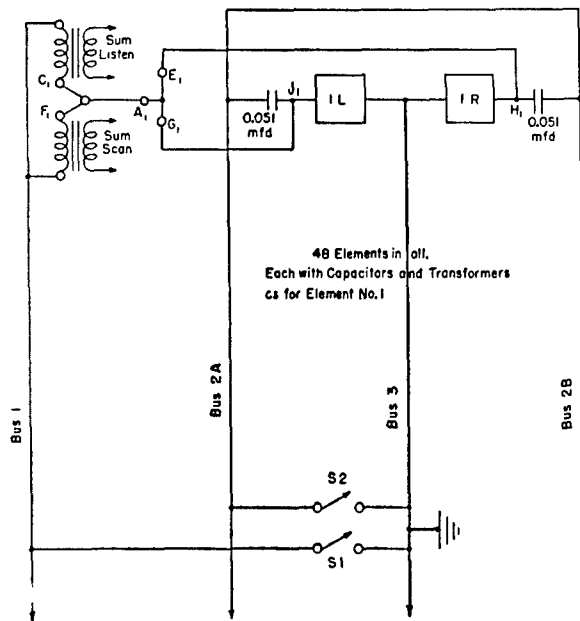


FIGURE 42. Transfer network for Spy Pond tests of HP-3DS transducer.

needed, and it was proposed that they be mounted on the same hoist-train shaft so that only a single opening in the hull of the ship would be necessary. It was pointed out,<sup>5</sup> however, that a maximum depth of only 50½ inches below the keel of the ship could be allowed without interference in dry-docking. This made the mounting of two transducers on the same shaft somewhat difficult. Consideration was given to various possible schemes of mounting the transducers separately<sup>33</sup> and of placing the transducers at different points of the hull. All these proposals led to some acoustic shadowing of one transducer by the other, or

to unduly complicated design of the dome. They also required two hoist-train mechanisms, if the transducer was to be retractable within the ship when not in use. Therefore, it was decided that for integrated Type B sonar, an effort would be made in the design to keep the transducers within the limit of 50½ inches below the keel of the ship, but mounted on a single shaft.

The mounting of HP-8D on the same shaft as the azimuth-scanning transducer raised a question of training. Since the depth-scanning transducer was to scan in only one plane, it had to be trained to point towards the target. The azimuth-scanning transducer, however, did not require training, as commutators could be used to point the beam of sensitivity at the target. Therefore, a scheme was considered for rotating only the depth-scanning transducer. This led to considerable mechanical difficulties. To avoid these it was decided to rotate both transducers simultaneously.

For the reasons discussed above, it was desirable to make the depth-scanning transducer HP-8D small. To retain the desired beam widths, a considerably higher frequency than that used for HP-3DS was required. To avoid interference between the azimuth-scanning and depth-scanning systems, different frequencies were used for the two transducers. Since 26 kc had been chosen for the azimuth-scanning transducer, 40 kc was chosen for HP-8D.

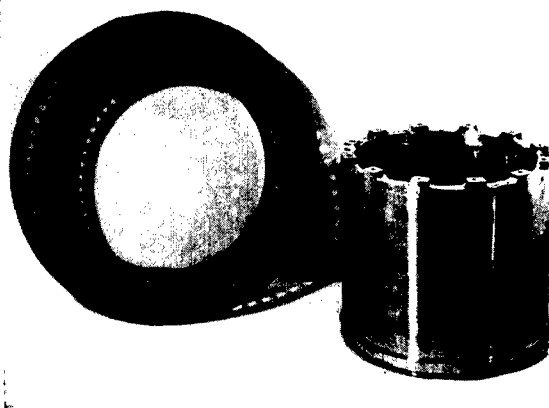


FIGURE 43. Spool and spacer for elements for HP-8D transducer.



FIGURE 44. Spool and spacer for elements, assembled, for HP-8D transducer.

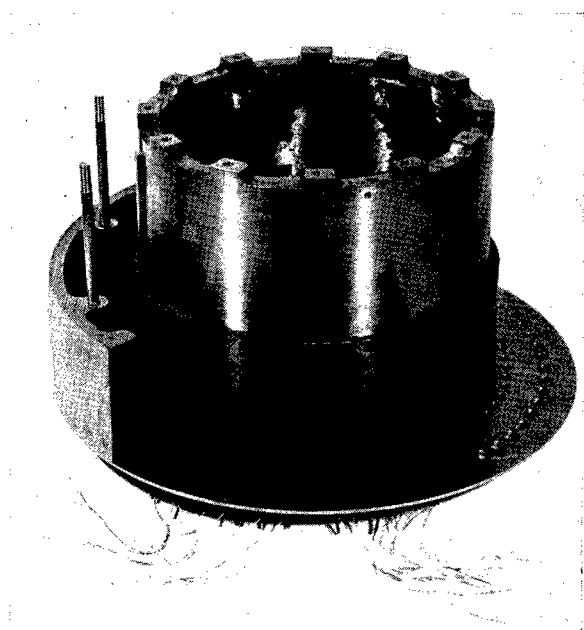


FIGURE 45. Assembly of first set of stacks and spool of HP-8D transducer.

The depth-scanning transducer HP-8D then met all the requirements listed in Section 6.3.1 and was designed to be mounted underneath the azimuth-scanning transducer HP-5 and to be turned on the same shaft with HP-5. In order to meet the vertical beam width requirement of 9 degrees at 6 db down from the maximum it was decided that a 64-element cylindrical transducer would be satisfactory, and that an active-face diameter of about 15 inches would be needed at 40 kc.<sup>32</sup> Design of laminations to be used

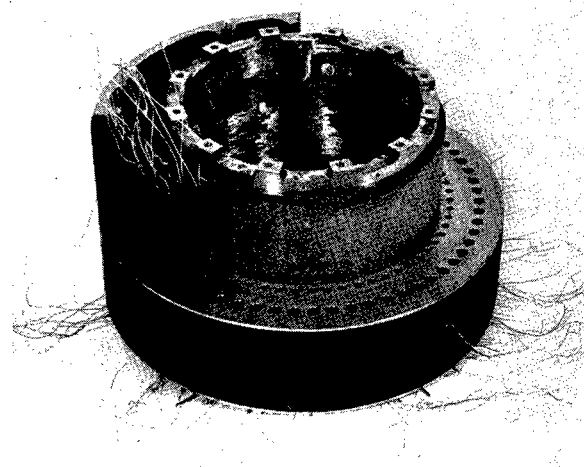


FIGURE 46. Assembly of second set of stacks on HP-8D transducer.

for HP-8D was, therefore, made on this basis.<sup>34</sup> To meet the horizontal beam width requirement of 20 degrees at 10 db down from the maximum, the HP-8D laminations were consolidated in stacks 3 inches long, and two such stacks were placed together to form an element 6 inches long, with an additional  $\frac{1}{2}$  inch for separation between the stacks. The pattern for an unshaded  $6\frac{1}{2}$ -inch element was computed to be 19.3 degrees at 10 db down from the maximum. This was considered satisfactory to meet the requirement. The use of two such stacks in each element automatically satisfied the requirement for BDI operation of the depth-scanning system by providing right and left halves for each element. As explained for the HP-3DS transducer, a total of 48 elements arranged around 270 degrees of the transducer satisfied the requirements for scanning the depth angles from 0 to 90 degrees, allowing 30 degrees leeway on each end of the range for pitch and roll (see Figure 4).

The requirement that the HP-8D transducer was to be mounted underneath the HP-5 transducer led to some changes in mechanical design of the depth-scanning unit. These were primarily changes in form of the upper flange structure attaching HP-8D to HP-5, and in arrangement of cable ducts to carry the cables from HP-8D through HP-5 without making

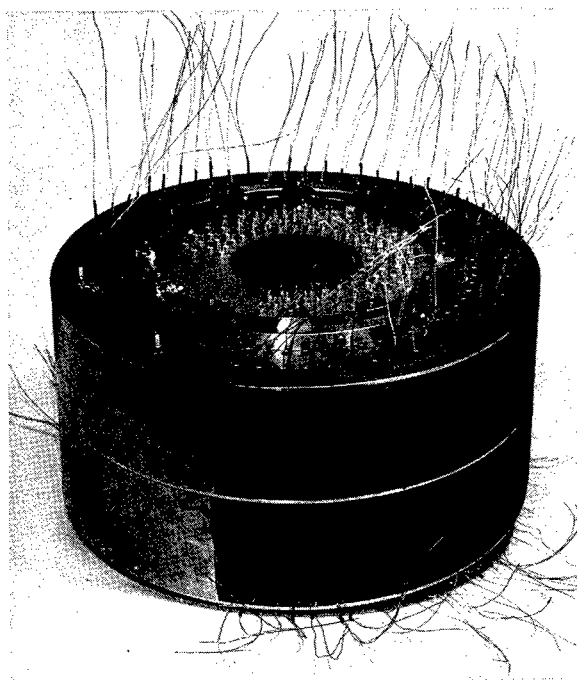


FIGURE 47. Assembly of stacks on spool, terminal board in place, HP-8D transducer.

CONFIDENTIAL

either transducer vulnerable to leaks in the other. Experience in the construction of HP-3DS led to other detailed changes in the construction of HP-8D, particularly in regard to the supporting structure for the transducer.

Figures 43 through 52 are photographs illustrating the construction and assembly of HP-8D.<sup>35</sup> Table 3

TABLE 3. Electrical Measurements of Elements for HP-8D No. 2.

Element No.	Right Half			Left Half		
	Stack No.	$f_G$ (kc)	$G_{max}$ (mmhos)	Stack No.	$f_G$ (kc)	$G_{max}$ (mmhos)
1	72	.39.115	90	19	.39.500	101
2	102	.470	87	21	.480	112
3	229	.395	90	48	.400	92
4	22	.425	80	51	.440	101
5	27	.360	97	192	.360	98
6	211	.380	91	30	.365	112
7	201	.350	93	13	.350	99
8	142	.315	86	37	.315	102
9	224	.330	97	61	.335	99
10	42	.330	82	207	.325	112
11	122	.330	78	215	.320	104
12	123	.310	95	38	.300	102
13	206	.310	92	189	.300	103
14	199	.305	96	178	.300	108
15	140	.300	88	182	.305	117
16	196	.295	90	125	.290	109
17	144	.290	78	214	.285	120
18	155	.280	102	150	.285	108
19	152	.280	98	217	.285	115
20	174	.285	85	203	.285	128
21	80	.270	102	170	.270	110
22	117	.265	116	212	.255	117
23	115	.265	110	127	.255	118
24	116	.265	105	181	.265	122
25	146	.265	82	172	.265	122
26	157	.265	107	198	.255	118
27	153	.270	87	205	.265	117
28	230	.275	102	171	.275	121
29	14	.280	87	83	.275	110
30	162	.270	107	209	.280	122
31	121	.285	107	101	.280	108
32	186	.290	87	237	.280	107
33	179	.290	95	213	.295	115
34	139	.300	90	191	.290	101
35	238	.315	82	193	.305	107
36	149	.310	93	33	.315	113
37	184	.315	102	219	.305	111
38	63	.310	99	49	.300	102
39	56	.335	79	195	.320	105
40	41	.330	86	202	.320	118
41	84	.345	83	151	.335	103
42	68	.350	92	12	.350	107
43	25	.345	96	24	.330	95
44	111	.380	91	110	.375	98
45	228	.395	87	210	.375	98
46	91	.415	86	17	.435	96
47	95	.445	85	31	.475	107
48	124	.475	94	59	.445	97

gives the electrical characteristics of the various staves used in the HP-8D, Model 2 (stainless steel castings).

Prior to release of HP-8D No. 2 for installation this equipment was given a series of tests at the barge test station as follows:

1. Vertical patterns were taken (a) on a number of elements at the resonance frequency, (b) on one group  $\pm 2$  kc from resonance, and (c) on one group at the second harmonic frequency.
2. Vertical patterns were taken on various groups of elements in parallel, at the resonance frequency and at  $\pm 5$  kc from resonance.
3. Vertical patterns were taken on the transducer in conjunction with the commutator.
4. Frequency responses were taken on a number of elements.
5. Horizontal patterns were taken for one element only.
6. Phase measurements were made, and amplitude responses were taken simultaneously on four groups of elements.
7. Admittance measurements were taken for the right and left halves of the transducer with all elements in parallel in each case; and impedance measurements were taken on each individual stack.
8. A frequency response was taken with all elements in parallel, and under the same condi-

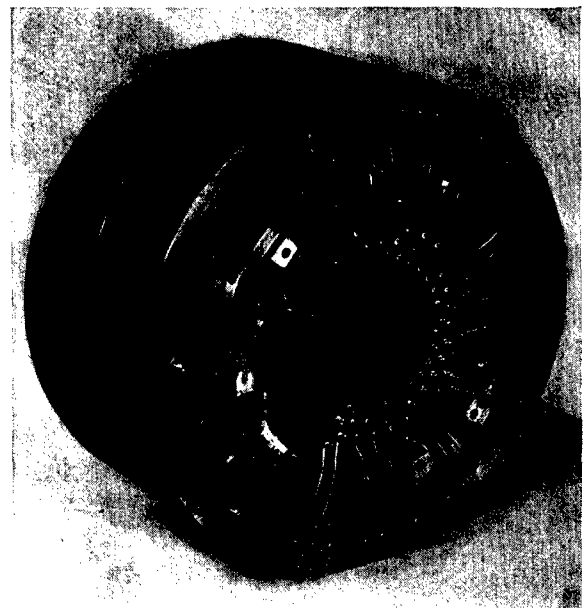


FIGURE 48. Wiring of stacks to terminal board, HP-8D transducer.

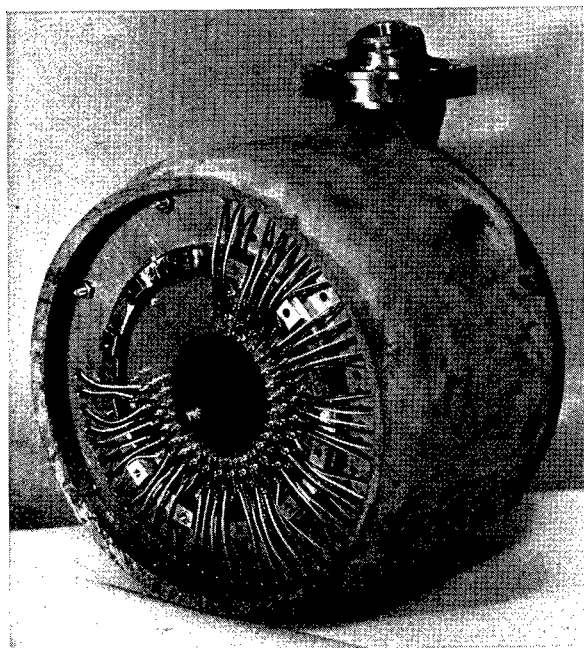


FIGURE 49. Assembly of rubber boot over elements, with one end flange in place, HP-8D transducer.

tions a measurement was made of the field obtained by using HP-8D No. 2 as a transmitter, and the impedance of the transducer was determined. These data were used to compute the efficiency of HP-8D No. 2.

Standard test procedures were used in making these measurements. Dummy mountings were made available for these tests, as shown in Figure 53. The dummy HP-5 transducer was removed when taking vertical patterns. Analysis of the data led to the following conclusions and results:

1. The HP-8D No. 2 transducer proved satisfactory as a depth-scanning transducer, operated at 38 kc.
2. The HP-8D No. 2 transducer operated best into a lag line designed for about the computed  $ka = 32$  at 40 kc. (This result was derived from the phase measurements.)
3. Vertical patterns taken with the commutator connected to the transducer gave a beam width of 12 degrees, 10 db down from the maximum; side lobes were at least 15 db down, and back radiation at least 22 db down from the maximum.
4. The one horizontal pattern gave a beam width of 13.5 degrees, 10 db down from the maximum,



FIGURE 50. Assembly with both end flanges in place, side view, HP-8D transducer.

with the first minor lobes being 10 db down from the maximum.

5. The efficiency of the transducer was computed to be about 30 per cent.
6. Amplitude measurements, taken at the same

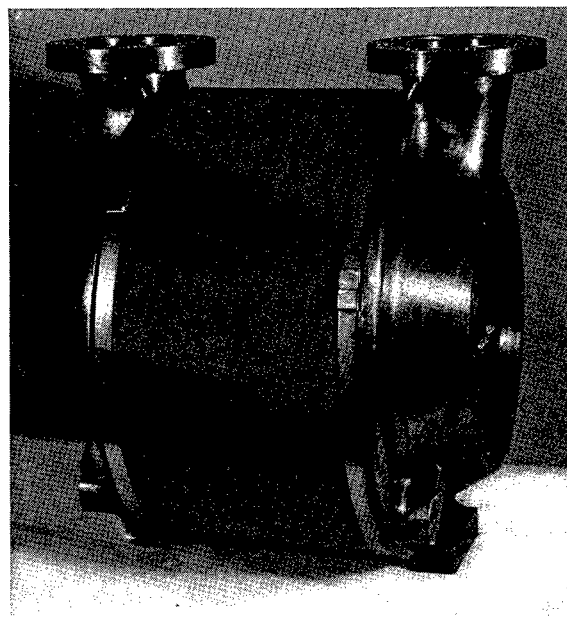


FIGURE 51. Assembly with both end flanges in place, front view, HP-8D transducer.

time as the phase measurements, provided data for computation of the attenuation to be used in the lag line to achieve proper amplitude shading for reduction of side lobes in the vertical pattern.

7. Receiving patterns taken with various numbers of elements in parallel showed the various possibilities for transmission patterns using these combinations. The pattern for all elements in parallel showed that omnidirectional transmission could be obtained for nearly the entire 270 degrees of arc covered with elements.

The transfer network connecting the transducer to the three commutators for the depth-scanning portion of integrated Type B sonar was the same as that used with HP-3DS, except that values of the various circuit elements were different. The wiring diagram is shown in Figure 40. Value of the coupling capacitor  $C$  was made  $0.033 \mu\text{f}$  on the basis of a stack impedance of  $16 - j27$  ohms.<sup>36</sup> For the parallel combination of 96 stacks, each with its capacitor in series, the resultant impedance was  $0.167 - j1.044$  ohms, and the necessary tuning coil had an inductance of  $4.5 \mu\text{h}$ .

The cable for HP-8D No. 2 was procured from the Collyer Wire and Cable Company according to the HUSL specifications.<sup>37-40</sup> The primary problem involved in construction was the need to combine flexibility (bending and torsion) and complete internal

blocking in a cable composed of 53 pairs. Two cables were used for HP-8D No. 2 totaling 106 pairs, 96 being required and 10 being spares.

Considerable experience which had been gained in developing cables for HP-3DS was used in evolving cable specifications for HP-8D No. 2. The first experimental cable (see Figure 39) was too large and stiff, being covered with a fire hose, and was not blocked. The second experimental cable used the Navy Type TTHFA-50 (two sections) with suitable blocking at the ends,<sup>41,42</sup> but was too stiff.

The first lot of cable delivered by the Collyer Wire and Cable Company<sup>38,39</sup> was satisfactory except for incomplete blocking.<sup>43</sup> This difficulty was remedied in the cable of later deliveries.<sup>39</sup>

### 6.3.3 HP-5 Transducer, Modified

The transducer for the azimuth-scanning portion of integrated Type B sonar was a modified HP-5 transducer. The changes were entirely mechanical; the same acoustic properties were maintained as those



FIGURE 52. Assembly with cables in place, HP-8D transducer.



FIGURE 53. Mounting means for tests of HP-8D No. 2 transducer.

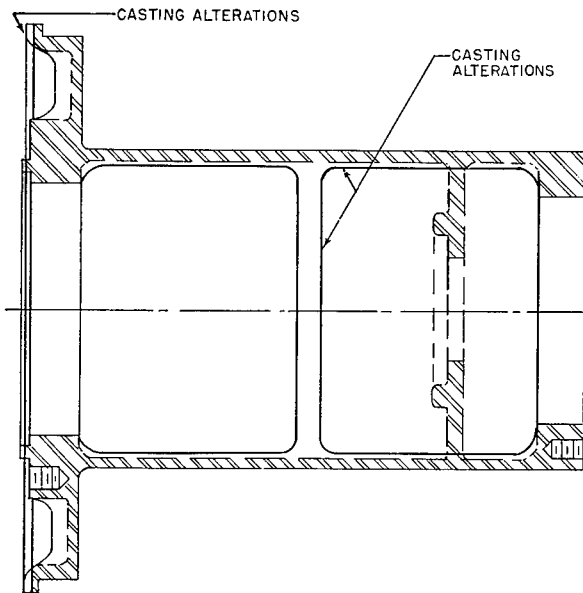


FIGURE 54. Modifications in spool of HP-5 transducer.

of the standard HP-5 transducer which is discussed in Chapter 5 and in the transducer report.<sup>31</sup> There were two primary mechanical modifications, (1) a change in the spool that supported the transducer elements, and (2) a change in the bottom end cap.

The spool had to be made stronger by increasing the wall thickness 50 per cent to take the strain of the HP-8D transducer suspended from it. The partition across the spool holding the cable seals was moved from near the bottom of the spool to near the top. This was done to accommodate the cable ducts from the HP-8D transducer, which were, of necessity, brought through the spool of the HP-5 transducer. Because of dimensional limitations in this partition, which in the modified form held seals for three cables (two from HP-8D and one from HP-5), the original HP-5 cable pothead was changed to a standard cable gland. Access to the duct and cable glands was facilitated by the new location of the partition. Figure 54 is a drawing showing the various changes made in the spool.

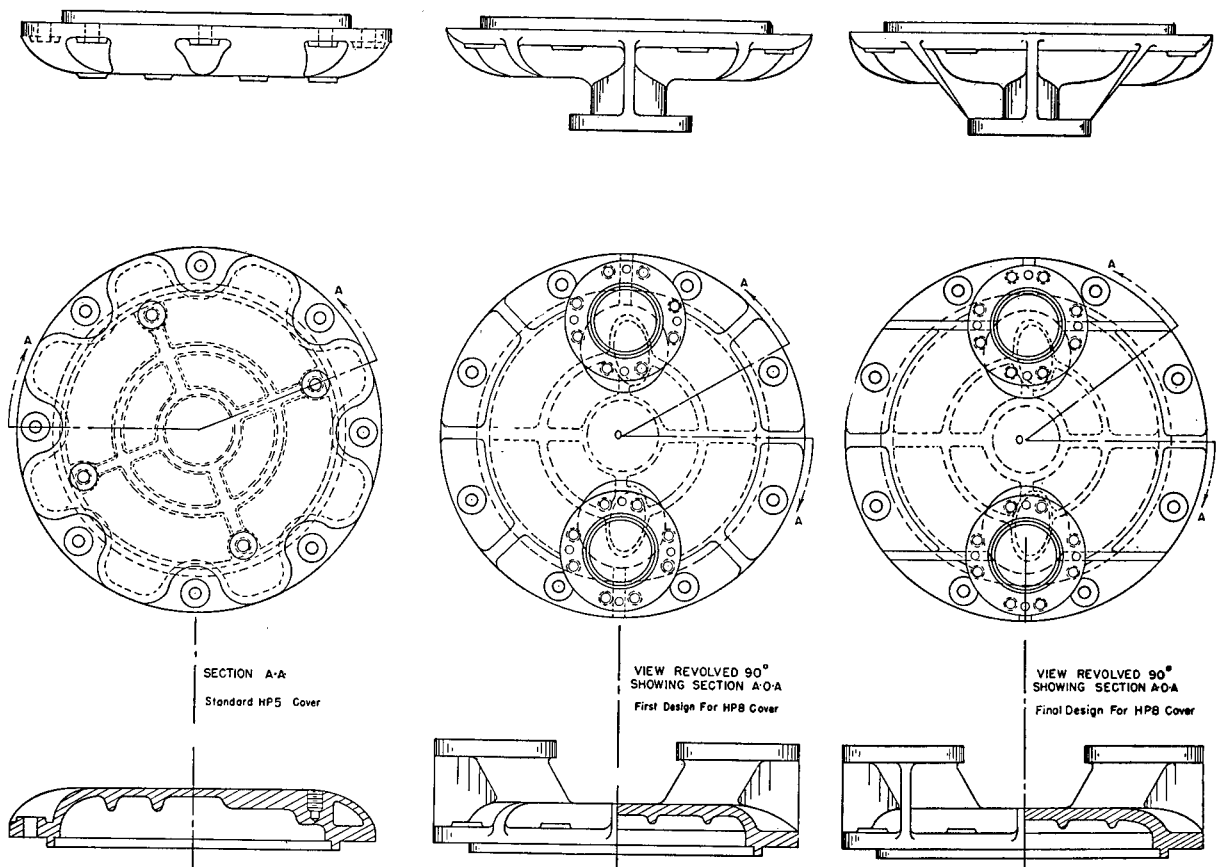


FIGURE 55. Cover casting, HP-8D transducer.

CONFIDENTIAL

In the standard model of the HP-5, the bottom end cap was a solid piece, with a removable waterseal around the outside for servicing the cable connections. In the modified model the cap was changed to have a double-yoke construction extending downward and ending in flanges which met the mounting flanges for the HP-8D. The end cap was strengthened by the addition of ribs to carry the strain of the HP-8D transducer suspended from it. Figure 55 shows the various changes made in the end cap.

The problem of providing sufficient strength to support the combination of HP-8D and HP-5 transducers was considered in some detail. On the ship on which the units were mounted, results were computed for the worst possible case, assuming that 90 per cent of the strain occurred because of a roll of 45 degrees from center with a total period of eight seconds, and that the other 10 per cent was caused by pitch. On this basis, the present designs for the HP-8D and the modification of HP-5 were suitable. The resulting design was forwarded to the Bureau of Ships and approval obtained for mounting such a combined unit on a QCJ-8 hoist-train shaft on the USS *BABBITT*.

When the first model of HP-5 properly modified for use in the integrated Type B sonar was tested,<sup>44</sup> it was found to be similar in performance to previous models of HP-5 with the normal end cap. Maximum variations in directional patterns were found to be within a 3-db band at 25.5 kc. The maximum variation in resonance frequency for the various elements in the transducer was found to be  $\pm 0.12$  kc, about an average of 25.735 kc. Extreme values of  $Q$  were 10.5 and 12.9, representing a variation of  $\pm 1.2$ . Extreme values of sensitivity of  $-83.6$  and  $-81.5$  db ( $v/b$ ) represented  $a \pm 1$  db ( $v/b$ ) variation. This performance was considered to be entirely adequate in the light of experience with the previous HP-5 transducers and their operation in the XQHA scanning sonar.

#### 6.4

### COMMUTATORS

#### 6.4.1

### Commutator for 26-kc Depth-Scanning Sonar

The three commutators used in the 26-kc depth-scanning sonar were the Model 5 48-element cylindrical glass plate units. The mechanical design is described in Chapter 5. A photograph of the one com-

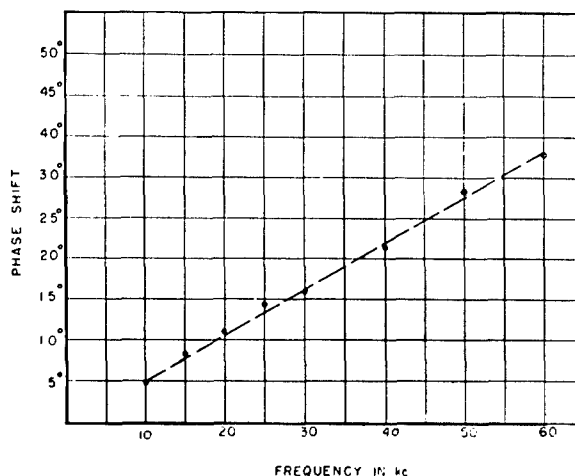


FIGURE 56. Phase shift curve. Audio Development Company transformer No. A 3770.

mutator unit (Figure 61 in Chapter 5) shows the manner in which the transformers and cabling were arranged.

The 48 transformers used on each commutator were selected for as nearly identical phase shift and voltage ratio characteristics as possible. In selecting a set for any one commutator, the phase shift was held to within  $\pm 1$  degree of a mean value, which was about 14 degrees at 26 kc. The transformers used on the difference-listening commutator were Audio Development Type A 4876, which has an impedance ratio of 50 to 50,000 ohms. The phase-shift frequency characteristic of Type A 3770, which is identical to Type A 4876 except for absence of the center tap, is

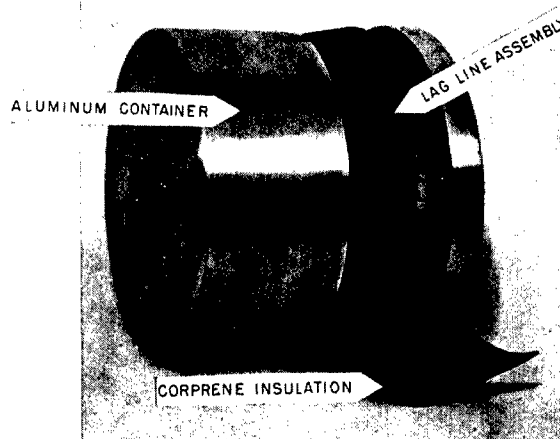


FIGURE 57. Lag line and container, partially assembled, commutator for 26-kc DSS.

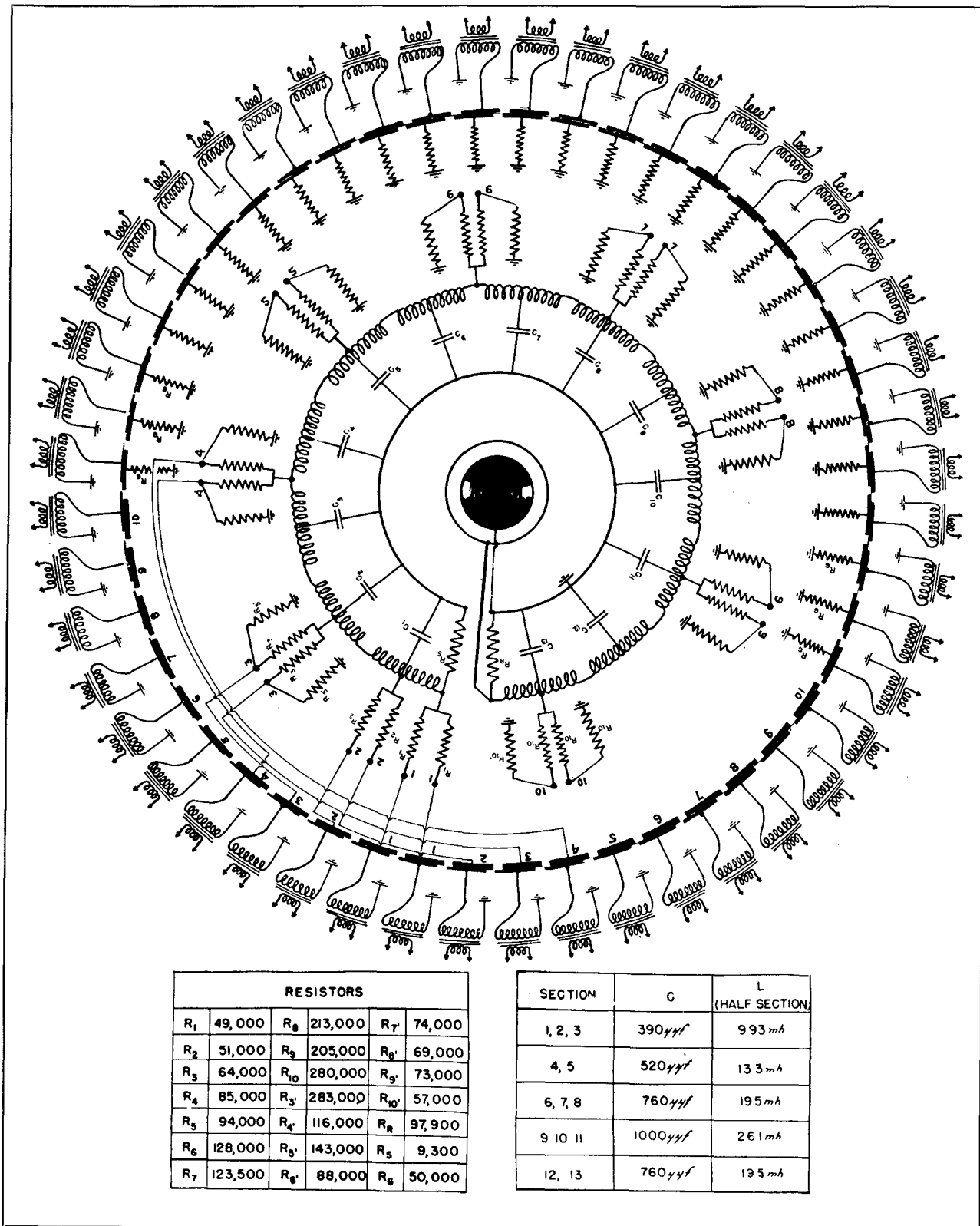


FIGURE 58. Capacitive commutator, 26-kc DSS.

CONFIDENTIAL



shown in Figure 56. Audio Development Type A 4567, having an impedance ratio of 25 to 50,000 ohms, was used on the scanning and sum-listening commutators.

Connections from 20 of the 48 rotor plates were made to the feed-in points on the beam-forming lag line through resistor networks, while the remaining 28 rotor plates were connected to signal ground through 50,000-ohm resistors. All lag line components were enclosed in an aluminum container placed within the rotor. Photographs of the assembly are shown in Figure 57 and in Chapter 5, Figure 60. The lag line output was brought out of the rotor through a pair of slip rings and brushes to the preamplifier. A third slip-ring assembly furnished a means of directly grounding the lag line container to the commutator frame to reduce bearing noise as there was no electrical connection inside the rotor between the signal ground and the container shield. Figure 58 shows the electrical circuit arrangement between the rotor plates and the lag line. For the sake of clarity, connections between rotor plates 5,5 and the feed-in points 5,5 and those of higher numbered points, are not drawn. Values of the circuit components are indicated in this figure.

The beam-forming lag line consisted of a number of low-pass T sections of the type shown in Figure 59. The series arm of the T consisted of the two halves of a toroidally wound coil-connected series aiding. The shunt arm of the T was the capacitance  $C$ . The phase shift of such a section is practically a linear function of frequency over a wide frequency range. This linearity is achieved to a considerable degree by the effect of the distributed capacitance between the halves of the coil, although it is not critically dependent upon the value of this distributed capacitance.

Each coil half was trimmed to within 1 per cent of the specified inductance at the operating frequency of the system; the capacitors were selected to within 1 per cent of their specified values. The line was terminated at both ends by resistors whose values gave smooth-line operation when the attenuating resistor networks and the equivalent transducer-element impedances were bridged across the line. Figure 60 shows the curve of signal amplitude along the line when fed from the "head end" (at  $R_s$  in Figure 58).

#### LAG LINE DESIGN PROCEDURE

The filter section (Figure 59) is a bridged-T type (see Chapter 9). If, in designing the line, the param-

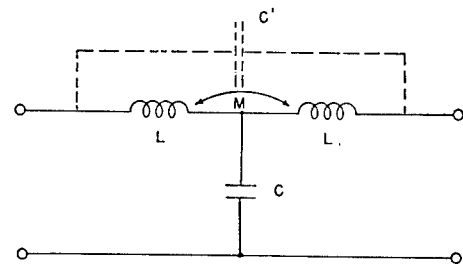


FIGURE 59. Low-pass T section for lag line, 26-kc DSS.

eters are selected so that  $C$  is large compared to the distributed capacitance  $C'$ , then calculations for a mid-series  $m$ -derived section with

$$m = \sqrt{\frac{1+k}{1-k}}$$

can be used with negligible error.

The equations for the  $m$ -derived section (Figure 61) in terms of the parameters of its constant- $k$  prototype are:

$$L_1 = m L_{1p}; L_2 = \left( \frac{1-m^2}{4m} \right) L_{1p};$$

$$C_2 = m C_{2p}; \text{ where } m = \sqrt{1 - (f_c/f)^2};$$

$f_c$  being the cutoff frequency equal to  $\frac{1}{\pi} (L_{1p} C_{1p})^{-1/2}$ . Assuming zero attenuation, the phase shift in the pass band is

$$\beta = \sin^{-1} \frac{m \frac{f}{f_c}}{1 - \left( \frac{f_x}{f_c} \right)^2}$$

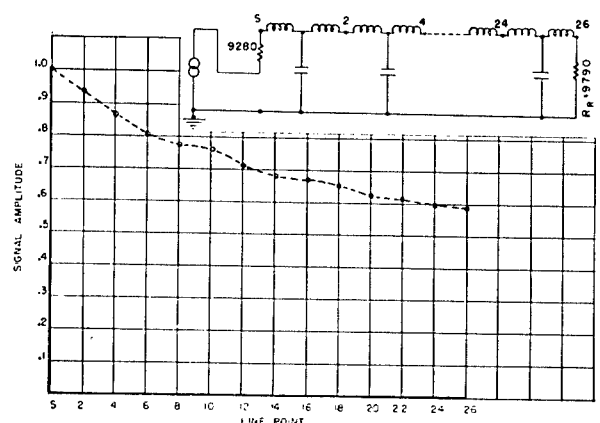


FIGURE 60. Amplitude curve of lag line, 26-kc DSS; attenuation network and loading resistors connected to line feed-in points.

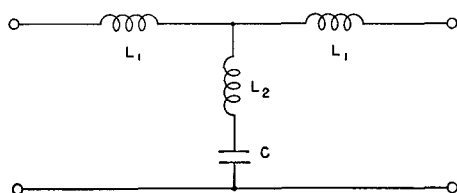
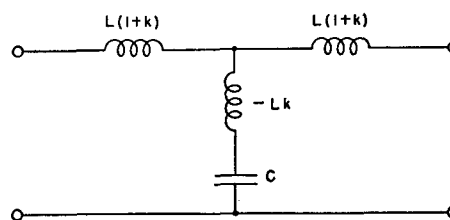
FIGURE 61.  $m$ -derived lag line section, 26-kc DSS.

FIGURE 62. Equivalent circuit of lag line section, 26-kc DSS.

where  $f_{\infty}$  = frequency at which the attenuation is extremely high,

and  $f$  = operating frequency.

Suppose each half of a coil used as the series arm in a T filter section has a self-inductance  $L$ , and the coupling coefficient between the halves is  $k$ . If the coil halves are connected series aiding, then the equivalent circuit is that shown in Figure 62. Comparing this circuit with that in Figure 61, it may be seen that the former is a series  $m$ -derived type, having

$$L(1+k) = mL_{1p}; \quad -Lk = \left(\frac{1-m^2}{4m}\right)L_{1p};$$

$$C = mC_{2p}; \quad \text{giving} \quad m = \sqrt{\frac{1+k}{1-k}}.$$

The cutoff frequency in terms of the phase shift angle  $\beta$ ,  $m$ , and the operating frequency  $f$  is

$$f_c = f \sqrt{\frac{m^2}{\sin^2 \beta/2} + (1-m^2)}.$$

If the image impedance of the line is  $R_0$ , then

$$L = \frac{(m^2 + 1)R_0}{4m\pi f_c}; \quad C = \frac{m}{\pi f_c R_0};$$

$$R = R_0 \sqrt{1 - \left(\frac{f}{f_c}\right)^2}.$$

The last four equations are used in designing a filter section to give the required phase shift. In using these equations a value of  $k$  is assumed, and a preliminary measurement of several toroidal coils is made to check its probable value. The coupling coefficient of the Western Electric Company toroids, used in the commutator lag lines, varies between 0.83 and 0.93. Fortunately, any value of  $k$  between these limits affects only slightly the values of  $L$  and  $C$  necessary to give a desired phase shift. Further discussion of this type of filter section is given in Chapter 9.

With the depth transducer having a  $ka$  of 32 at the operating frequency of 26 kc, the phase lags necessary to give a narrow beam pattern, measured from the head end of the line to each successive injection point, are given in the first row of Table 4. These are calculated from the equations given in Chapter 9 under ER lead line design.

TABLE 4. Phase Lag Values of 26-kc Depth Transducer.

Injection Point	1,1	2,2	3,3	4,4	5,5	6,6	7,7	8,8	9,9	10,10
Phase Lags ( $\beta$ )	0°	17.6°	52.8°	104°	174°	258°	358°	471°	594°	725°
Scanning Commutator Lag Line ( $\beta$ )	0°	17.1°	51.2°	107°	179°	264°	361°	474°	593°	731°
Sum-Listening Commutator Lag Line ( $\beta$ )	0°	17.3°	50.0°	103°	174°	262°	358°	474°	592°	730°
Difference-Listening Commutator Lag Line ( $\beta$ )	0°	16.5°	51.3°	106°	175°	261°	359°	474°	591°	728°

The values given in the second, third, and fourth rows were obtained by use of a 13-section lag line using four different sized filter sections. They were measured with the attenuating resistor networks bridged across the line. Table 5 gives the pertinent design data on the lines used in the three commutator units.

TABLE 5. Design Data of Lag Lines in Commutators (Scanning, Sum and Difference).

Section No.	Phase Shift Per Section (in degrees)	$L$ (in mh)	$C$ (in $\mu\mu\text{f}$ )	WE Coil Used
1,2,3	35.2	9.9	390	D-122802
4,5	46.0	13.3	520	D-122802
6,7,8	64	19.5	760	D-122803
9,10,11	80	26.1	1020	D-122803
12,13	64	19.5	760	D-122802

Signals from the various transducer elements were attenuated by the series resistors between the rotor plates and injection points on the lag line. The required amplitude at each point, stated as a fraction of the first amplitude, is given in the first row of Table 6.

TABLE 6. Signal Amplitude Values on Lag Line of 26-kc Transducer.

Injection Point	1	2	3	4	5	6	7	8	9	10
Signal Value with respect to that at point 1 (theoretical) . . . . .	1.0	.975	.915	.844	.75	.65	.54	.45	.35	.27
Values obtained in Scanning Commutator . . .	1.0	.95	.91	.83	.75	.66	.52	.48	.31	.260
Values obtained in Sum-Listening Commutator . . .	1.0	.97	.91	.84	.74	.66	.56	.45	.35	.274
Values obtained in Difference-Listening Commutator . . .	1.0	.97	.89	.88	.74	.65	.58	.45	.36	.28

The remaining rows give the values obtained in the three lag line assemblies. The approximate values of the series resistors can be calculated in the same manner that resistors in a voltage divider would be determined if the signal loss along the lag line were taken into account.

#### DETERMINATION OF SHADING RESISTORS

Referring to the circuit in Figure 63, let it be assumed that the resistive load on the lag line side of the rotor plate is to be  $R_c$ . This must be the same for all rotor plates, whether they are connected to the line or terminated in series resistors to ground. If they are grounded, shunt resistors are needed in addition to the series units.

Let  $\alpha_n$  = the required signal amplitude at  $n$ th injection point as a fraction of that at the first, assuming there is no lag line loss. (Values given in Table 6.)

Let  $l_n$  = the signal amplitude at  $n$ th injection point as a fraction of the head end amplitude when a signal is fed into this end of the line (ordinate of curve in Figure 60.) Then for the  $n$ th feed-in channel the series resistance is

$$R_n' = \frac{R_c}{\alpha_n l_n} - \frac{R_0}{2}.$$

The shunt resistance is

$$R_n'' = \frac{R_c}{1 - \alpha_n l_n}.$$

As the calculations are dependent on  $l_n$ , one or two trials may be necessary to evaluate correctly the value of  $l_n$ . To check its value, the bridging resistance should be calculated for the various injection points. These values should be connected across the line, and the values of  $l_n$  should be determined experimentally. As used, the bridging resistance is that resistance which the attenuating network and the transducer impedance effectively shunt across the line at the feed-in point. The approximate value of this resistance at the  $n$ th injection point is

$$R_n = \frac{2R_c}{2\alpha_n l_n - \alpha_n^2 l_n^2} \quad \text{if} \quad \frac{R_0}{2} \gg R_c.$$

If the line is doubly fed; that is, if the signals from a pair of rotor plates are fed into the same injection point,  $R_n$  is half the value given by the above equation.

The output signal was fed through the slip ring and brush assembly directly into the preamplifier. The bus to which one end of each transformer secondary was connected, the shield ground, and the lag

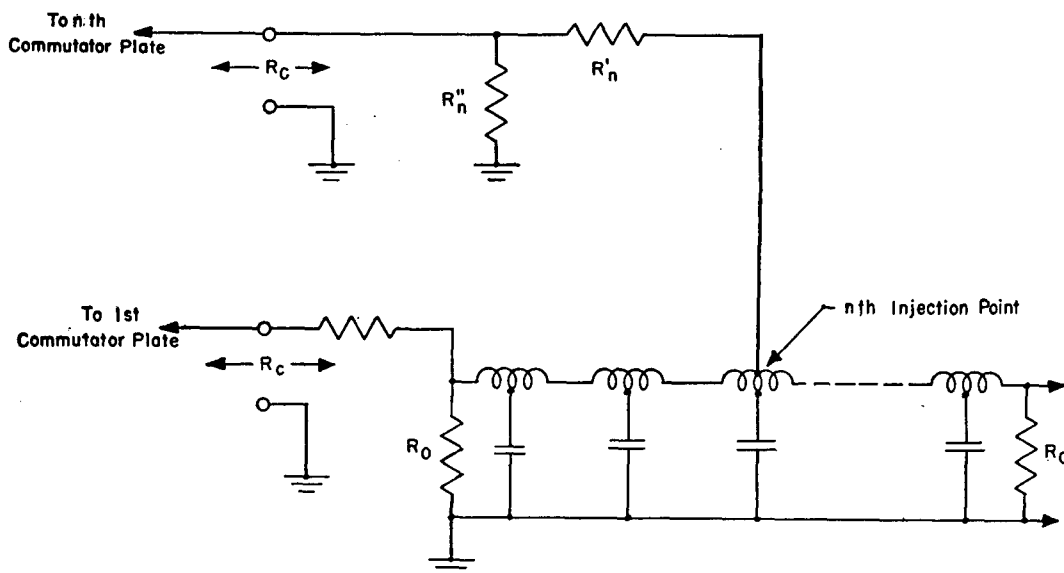


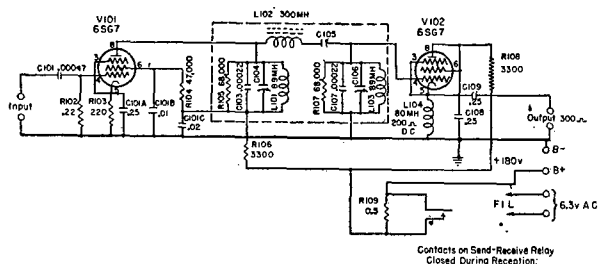
FIGURE 63. Connections from commutator to lag line, 26-kc DSS.

line signal ground were all tied together at the input ground terminal on the preamplifier. A schematic wiring diagram of the latter unit and its power supply are shown in Figures 64 and 65. The characteristics of its band-pass filter are discussed in Section 6.6 on receivers. A wiring diagram of the service connections on the commutator frame is given in Figure 66. All electric connections to each commutator unit were made detachable by use of A-N cable connectors. It should be pointed out that as far as the synchro generator, servo motor, driving motor, preamplifier, etc., are concerned, all three commutator units were identically wired.

The three commutator units and the junction box were mounted tierwise in a rack (shown in Figure 41). The junction box was placed at the top of the rack with the difference-listening, sum-listening, and scanning commutators underneath, in the order listed.

A chassis (not shown in the picture), mounting the two servo amplifiers for the servo motors on the listening commutators, was located between the two listening commutators. This chassis also contained a phase-correction servo unit which introduced stabilization into the scanning spiral-sweep circuit.

Although design characteristics of the transducer used on this system were those of one having 64 elements, only 48 elements encompassing 270 degrees were mounted. As previously pointed out, signals from these elements were fed to the 48 stator plates of the scanning commutator. When the commutator and its directly connected sweep generator rotated at uniform speed, the deflection coils of the EPI were supplied with sweep currents which moved the spot around through 360 degrees for 360 degrees rotation of the commutator rotor, whereas, in the same time, the scanning beam actually moved only 270 degrees



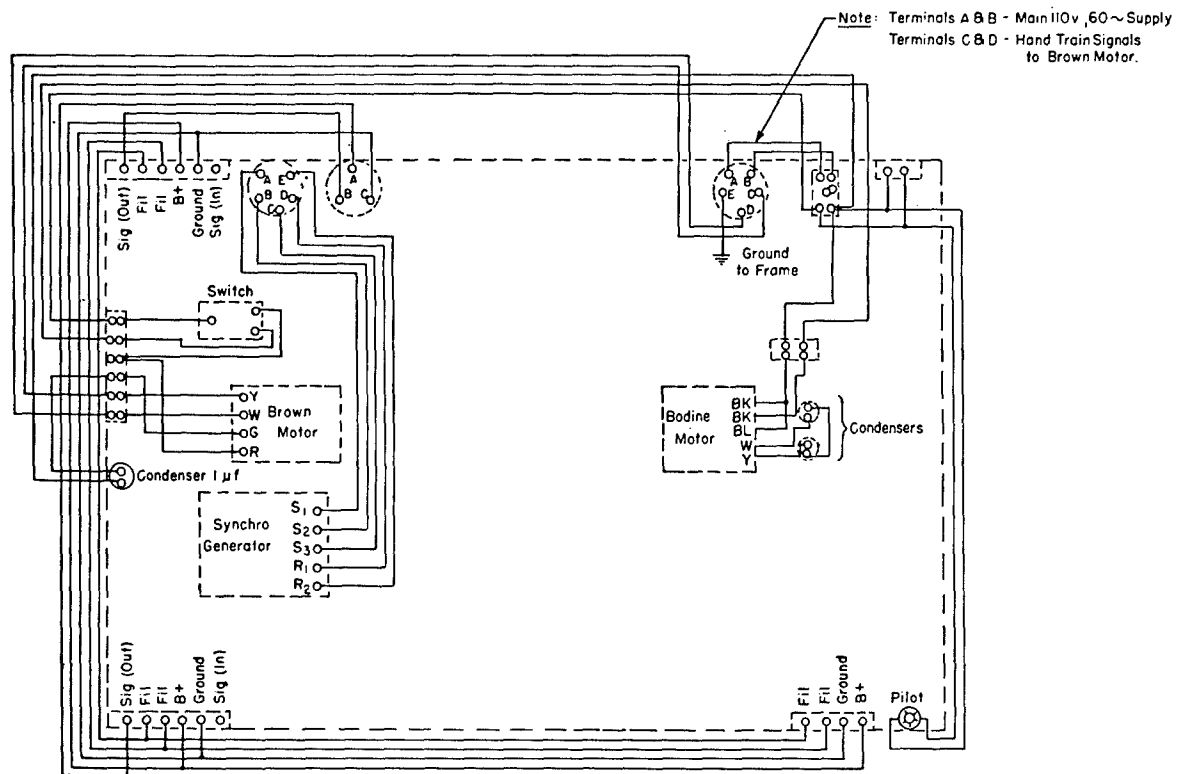


FIGURE 66. Service wiring, commutator frame, 26-kc DSS.

around the transducer. Consequently, 90 degrees of true depression angle was pictured on the EPI as an angle of 120 degrees (see Section 6.4.2 of this chapter).

Several schemes for correcting or orthogonalizing the screen display were considered and tried.<sup>45,46</sup>

However, in using the 48-element scanning commutator, no simple means of correction was found, so that it was decided to use a 64-element commutator for the

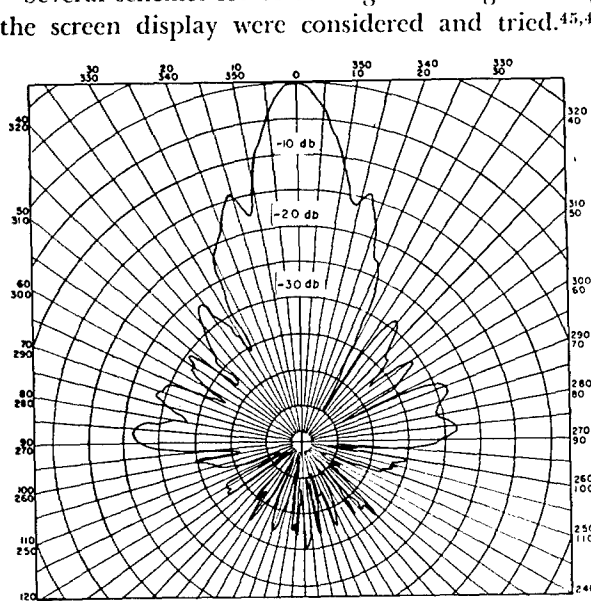


FIGURE 67. Pattern taken with artificial transducer on DSS scanning commutator, frequency of 26 kc, position 1,1.

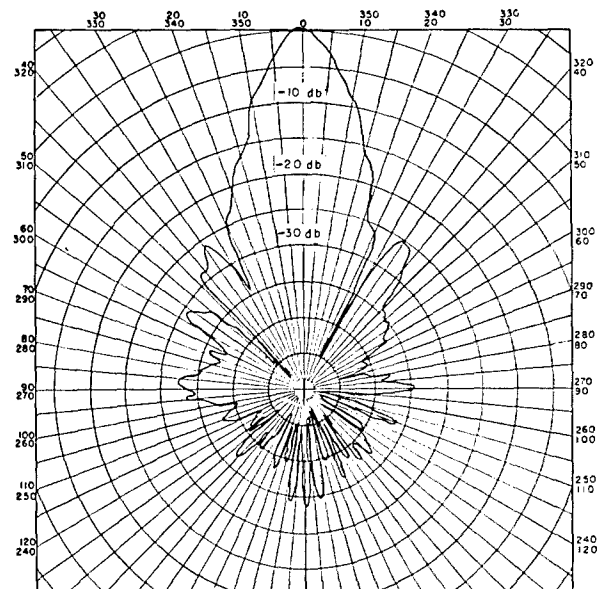


FIGURE 68. Pattern taken with artificial transducer on DSS sum listening commutator, frequency of 26 kc, position 1,1.

CONFIDENTIAL

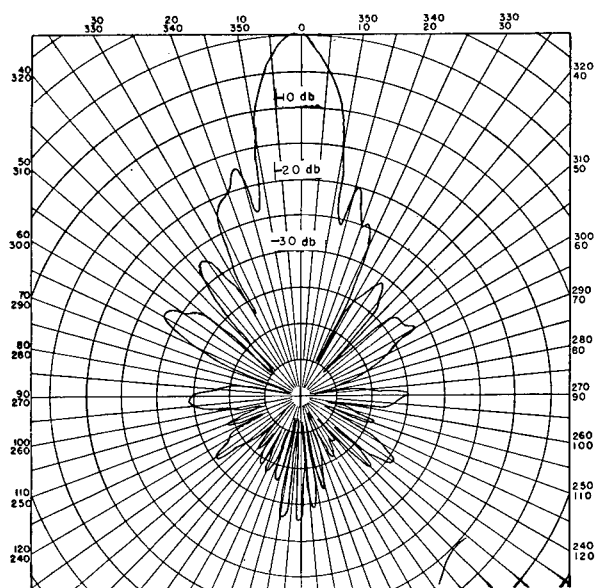


FIGURE 69. Pattern taken with artificial transducer on DSS difference listening commutator, frequency of 26 kc, position 1,1.

depth-scanning unit in the final design for integrated Type B sonar.

Figures 67, 68, 69 show representative patterns obtained with the three commutators using an artificial transducer (see Chapter 8). Each commutator was given an extensive series of pattern tests. This involved the taking of a series of beam patterns with the effective head-on element of the artificial transducer connected in turn to each one of the 48 stator plates of the commutator. This was accomplished by use of a 96-pole 48-position rotatable switch connected into the system between the commutator input terminals and the artificial transducer. Although construction details of all three were essentially the same, the patterns obtained on the scanning commutator in general did not show the uniformity which characterized those of the two listening units.<sup>47</sup>

The width of the major lobe in the pattern of the scanning unit varied from 12 to 20 degrees at the 10-db down point as the transducer was rotated. The major lobes of the listening commutators remained generally at a constant width of 13 degrees.

#### 6.4.2 Commutators for 38-kc Depth-Scanning Portion of Integrated Type B Sonar

The 38-kc vertical-scanning commutators to be used in integrated Type B sonar were made by the Sangamo Electric Company and were similar to those

used in the Model XQHA scanning sonar.<sup>61</sup> A photograph of the scanning unit is shown in Figure 70.

The beam-forming lag line was located in a cast aluminum cylindrical dish bolted to the flange which mounted the rotor plate. The rotor conducting segments were connected to the lag line by short pin connectors in a manner identical with that used to connect the stator plate and the input transformers. Signals from 22 rotor segments were fed into the lag line, and the other 26 segments were grounded through 53,000-ohm resistors.

The output of the lag line was connected to silver slip rings mounted on the shaft by means of suitable insulators. Carbon-silver brush members inserted through the rear wall of the front end bell engaged the slip rings. A shielded cable connected the brushes to a preamplifier which was mounted on the cradle frame.

The commutator shaft was gear-driven at a 2-to-1 reduction by a 3,500-rpm 1/20-hp induction motor. The drive was made through helical gears to insure smoothness of rotation and reduction of noise. A 5 HCT synchro-control transformer was driven by the large gear on the commutator shaft at rotor shaft speed to serve as the sweep generator providing a 3-phase voltage of a frequency identical with the angular speed of the commutator rotor. The output of this generator was to furnish the spiral sweep for the EPI scope. Both motor and control transformers were mounted in a cast plate which was doweled and bolted to the front end bell.

The construction of the listening commutator was identical to that of the scanning unit, except for the method of rotor drive. The front end plate of this unit was replaced by one on which were mounted two synchro-control transformers and a 2-phase 1,800-rpm servo motor. This servo motor was fastened to a gear casing which was mounted to the end plate. The total reduction from the motor to the helical pinion, which drove the rotor gear, was 204:1. The two synchro-control transformers were 2-speed and 36-speed units. The gear ratios between these and the commutator rotor shaft were such that one complete revolution of the rotor resulted in 1½ revolutions of the 2-speed CT and 27 revolutions of the 36-speed CT. The reason for this unusual gearing was that 48-element commutators were used in conjunction with what was in effect a 64-element transducer.

When describing the 26-kc DSS commutators it was mentioned that successful orthogonalization of the

EPI scope (true representation of depth depression angle) could not be obtained satisfactorily by artificial means. As the first 38-kc commutators were ordered from the Sangamo Electric Company prior to

installation of the trial depth-scanning system, and at that time orthogonalization seemed possible, a 48-element commutator for the scanning unit was requested. But, in view of subsequent investigation,<sup>46</sup> a

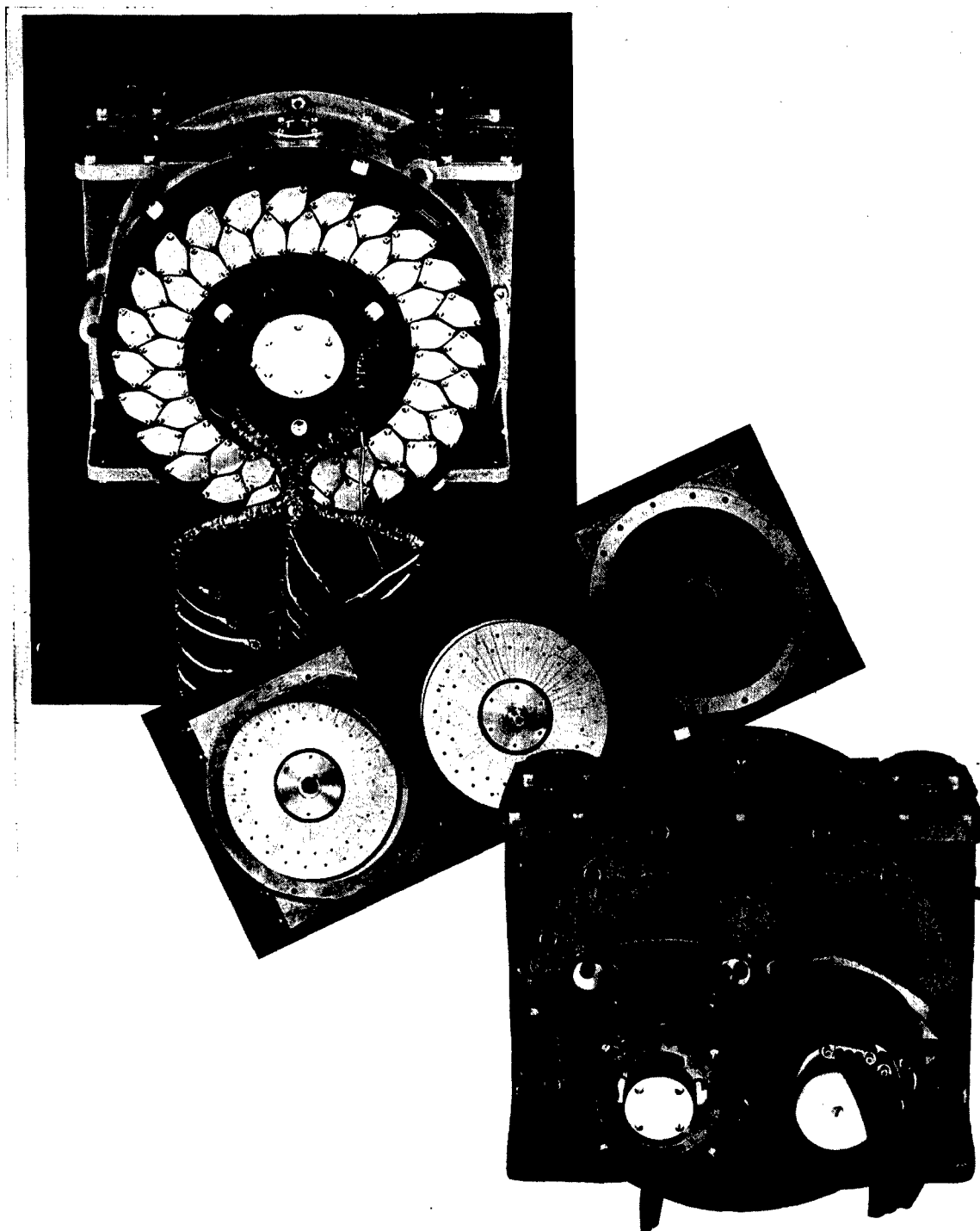
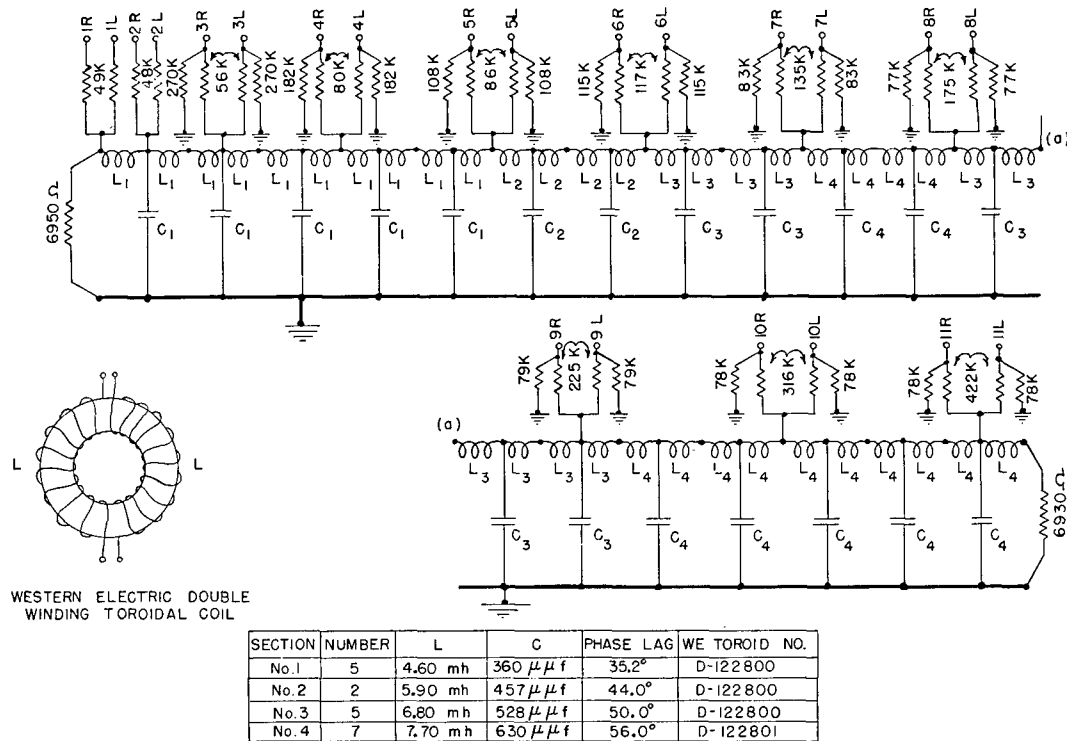


FIGURE 70. Sangamo Electric Company commutator for integrated Type B sonar.

CONFIDENTIAL

FIGURE 71. Schematic diagram of 40-kc lag line,  $ka = 32$ , integrated Type B sonar.

64-element commutator was ordered, by which a true depression angle on the EPI screen was automatically obtained. The listening commutators continued to be 48-element units, since correction of their angular position could be made by proper gear ratios between their synchro-control transformers and the rotors. Proper initial alignment is to be facilitated by provision of an index mark on the rotor gear which is to be visible from the front end.

The input transformers used on the commutators were also made by Sangamo Electric Company. Type D-871360, having an impedance ratio of 33:50,000 ohms, was used on the scanning and sum-listening commutators. A Type C-871351, using a center-tapped primary and having an impedance ratio of

66:50,000 ohms, was used on the difference-listening unit. In selecting a set of 48 transformers for any one commutator, the phase shift was held to within  $\pm 1$  degree of a mean value, approximately 10 degrees at 38 kc.

The beam-forming lag line used in each of the commutators was of the same type as that used in the 26-kc system (see beginning of this section). The electrical connections between rotor segments and the lag line were similar to those shown in Figure 58, except that signals from 22 rotor segments were fed into the lag line instead of 20. This number was increased in an attempt to reduce the minor lobes in the beam pattern.

The lag line used in the first 48-element scanning

TABLE 7. Phase Lag Values of 40-kc Transducer ( $ka = 32$ ).

Injection Point	1,1	2,2	3,3	4,4	5,5	6,6	7,7	8,8	9,9	10,10	11,11
Phase Lag ( $\beta$ ) Desired (in degrees)	0	17.6	52.8	104	174	258	358	471	594	725	870
Value of ( $\beta$ ) Measured (in degrees)	0	17.3	51.4	103	174	263	364	477	604	748	892



TABLE 8. Signal Amplitude Values of 40-kc Transducer ( $ka = 32$ ).

Injection Point	1,1	2,2	3,3	4,4	5,5	6,6	7,7	8,8	9,9	10,10	11,11
Signal Value											
Desired	1.0	.975	.915	.841	.75	.65	.54	.45	.35	.273	.20
Value											
Measured	1.0	.975	.89	.82	.70	.63	.535	.45	.35	.265	.205

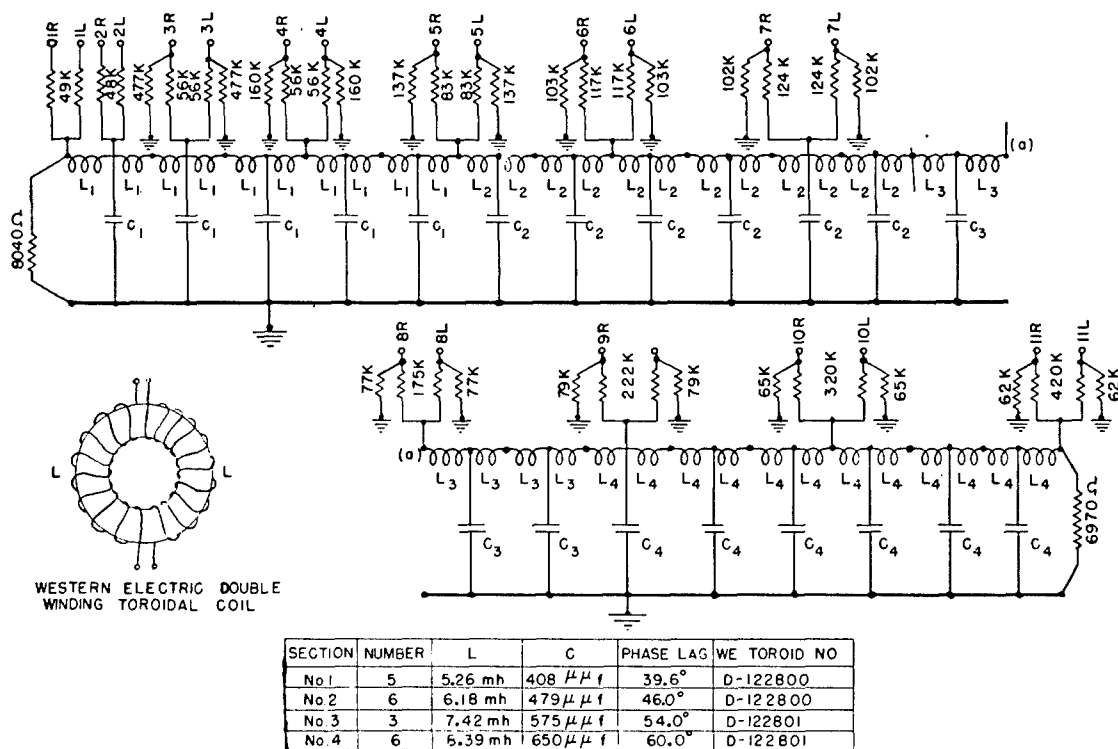
commutator was designed to meet the phasing requirements of a 40-kc transducer having a  $ka = 32$ . It was a 19-section line using four sizes of filter section and having an image impedance of 7,000 ohms. Other data relative to its design are given in the wiring diagram shown in Figure 71.

The phase lags necessary to give a narrow beam pattern for  $ka = 32$  at 40 kc, measured from the head end of the line to each successive injection point, are given in the first row of Table 7. Values quoted in the second row are those measured with the lag line assembled and with attenuating resistor networks attached.

The required signal amplitude at each injection

point, stated as a fraction of that at the first injection point, is given in the first row of Table 8. The second row gives the values obtained on the assembled line.

Tests made on magnetostriction cylindrical transducers, particularly the 26-kc depth-scanning unit HP-3DS, showed that the effective diameter of such a transducer was larger than its actual diameter. In the case of the HP-3DS this was approximately an 11-per cent increase in its apparent acoustic diameter. Consequently it seemed advisable to anticipate this phenomenon by designing the lag lines for the two depth-listening commutators to meet the phasing requirements of a transducer having an apparent  $ka = 36$  at 40 kc. Figure 72 gives the design data for the

FIGURE 72. Schematic diagram of 40-kc lag line,  $ka = 36$ , integrated type B sonar.

CONFIDENTIAL

TABLE 9. Phase Lag Values of 40-kc Transducer ( $ka = 36$ ).

Injection Point	1,1	2,2	3,3	4,4	5,5	6,6	7,7	8,8	9,9	10,10	11,11
Phase Lag ( $\beta$ ) Required	0	19.8°	59.4°	118°	195°	291°	404°	531°	668°	819°	982°
Value of ( $\beta$ ) Obtained, Sum-Listening	0	21.5°	62.0°	116°	198°	291°	408°	535°	675°	825°	1008°
Value of ( $\beta$ ) Obtained, Diff-Listening	0	20.5°	61.5°	118°	200°	289°	406°	528°	661°	815°	1012°

second and third lag lines. These lines were designed to have the same image impedance as that of the first design; that is, 7,000 ohms. The phase lags necessary to give narrow beam patterns, as calculated from theory, are given in Table 9 in the first row. The second and third rows also give the values obtained with each line assembled in its shield container and with the attenuating networks connected.

The preamplifier used on each commutator was a 3-stage unit employing Type 6SG7 and 6SL7 tubes. A schematic wiring diagram of the circuit is given in Figure 73. Voltage gain from input to output of the cathode follower stage was approximately 33 db, with about 18 db of negative feedback between the triode and the pentode stages. Both the amplifier and its power supply were located on one chassis, which was mounted in an inverted manner on vibration insula-

tors to the front end of the commutator cradle frame. It was found that the phase shift through such an amplifier was constant, and that supply voltage variations had negligible effect on the overall gain.<sup>48</sup>

The three commutator units used for the vertical-scanning portion of the integrated Type B sonar were located in one rack with the associated junction box. Each unit, including the junction box, was designed so that it could be removed from the rack with minimum effort.

Representative patterns obtained on the three depth-scanning commutators are shown in Figures 74, 75, and 76. These patterns were taken with two artificial transducers for use at 40 kc, one having an effective  $ka$  of 32 and the other having an effective  $ka$  of 36. In each case the actual beam width was 4/3 of that indicated.

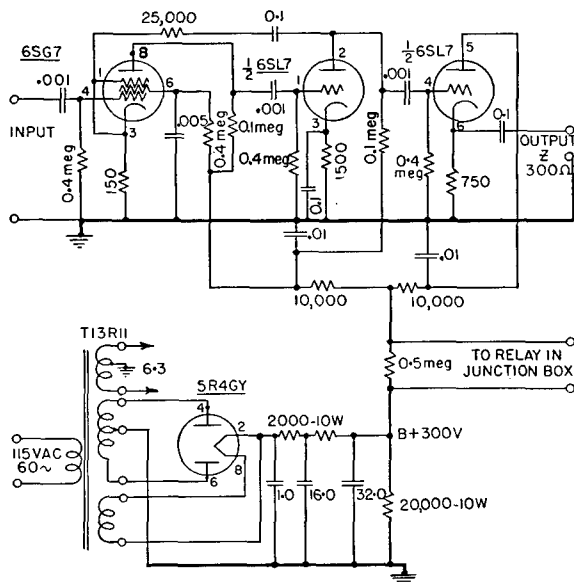


FIGURE 73. Preamplifier and power supply for integrated Type B sonar.

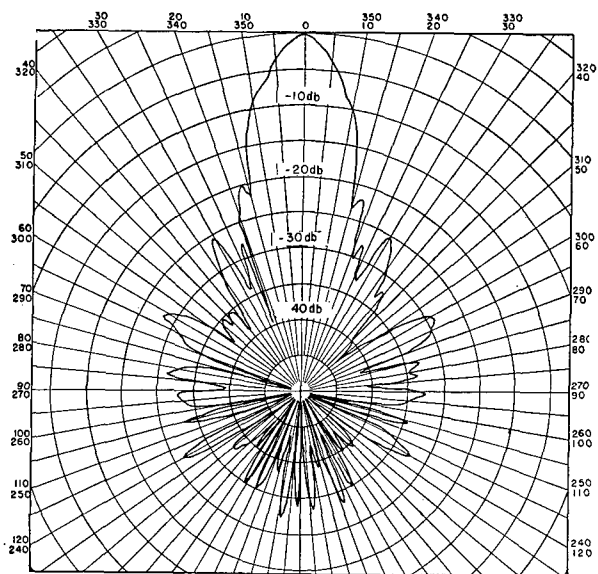


FIGURE 74. Pattern taken with artificial transducer ( $ka = 32$ ) on scanning commutator, Sangamo No. 9, position 1,1, integrated Type B sonar.

CONFIDENTIAL

### 6.4.3 Commutators for 26-kc Azimuth-Scanning Portion of Integrated Type B Sonar

The 26-kc azimuth-scanning portion of the integrated Type B sonar utilizes one high-speed scanning commutator and two stationary beam-forming lag lines. Since the transducer is mounted on a hoist-train shaft that is trained in azimuth, rotatable listening commutators are not needed to direct the listening beam in the horizontal plane. Figure 77 shows the circuit connections of the azimuth section from transducer to commutators.

The scanning commutator was made by the Sangamo Electric Company and is identical with that used in the Model XQHA scanning sonar. Its mechanical design and method of drive are the same as those of the vertical-scanning unit shown in Figure 70. The lag line is the same as that used in the Model XQHA scanning sonar gear. It is a double lag line; one line is fed with signals from transducer elements on the right side, the other with signals from the left side of the head-on bearing point. The output ends of the two lag lines are terminated on each other with output signal leads connected to their common junction points. A wiring diagram of this line is shown in Figure 78. Sixteen active rotor segments are used to introduce the echo signals into the lag line, while the

other 32 segments are terminated through 50,000-ohm resistors to ground. The commutator is mounted on vibration insulators in a cradle frame similar to that used to hold the vertical-scanning units. The pre-amplifier is identical with the one described in Section 6.4.2, and is fastened to the frame in the same manner. The 48 twisted pair connections from the input transformer primaries are brought around to terminal boards located on each side of the commutator assembly.

The stationary listening lag line unit utilizes the transformer ring assembly and lag line assembly of the Sangamo XQHA commutator. The two lines have the same input circuit connections as the high-speed scanning unit, where signals from one side of the transducer head-on point are fed into one line, while signals from the other side are fed into the other line. However, to secure right and left output channels, the two lag lines are terminated separately by resistances to give smooth-line operation. Each channel is fed into a separate preamplifier. After coming out of the two preamplifiers, the right and left channels are combined (Figure 77) to give the sum-and-difference output signals that are introduced into the bearing deviation indicator listening receiver. This is done in order that the same type of input circuit can be available when the single bearing deviation indicator listening receiver is switched

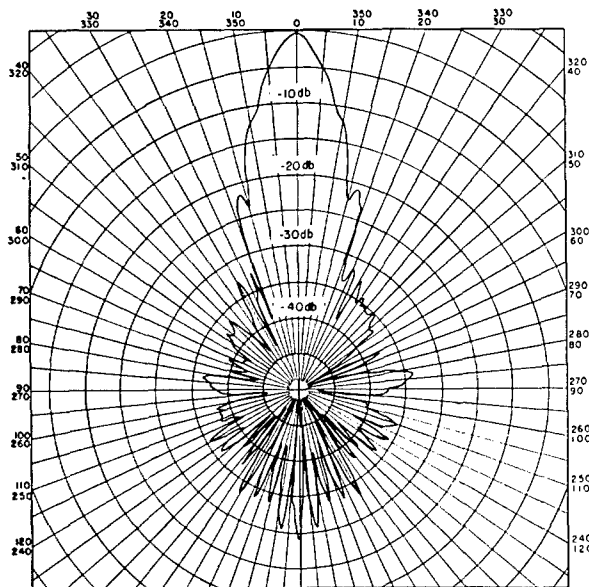


FIGURE 75. Pattern taken with artificial transducer ( $ka = 36$ ) on sum listening commutator, Sangamo No. 10, position 1,1, integrated Type B sonar.

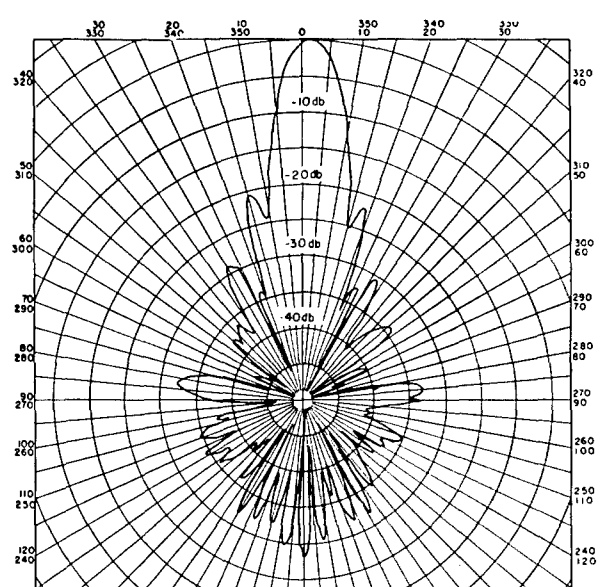


FIGURE 76. Pattern taken with artificial transducer ( $ka = 36$ ) on difference listening commutator, Sangamo No. 11, position 1,1, integrated Type B sonar.

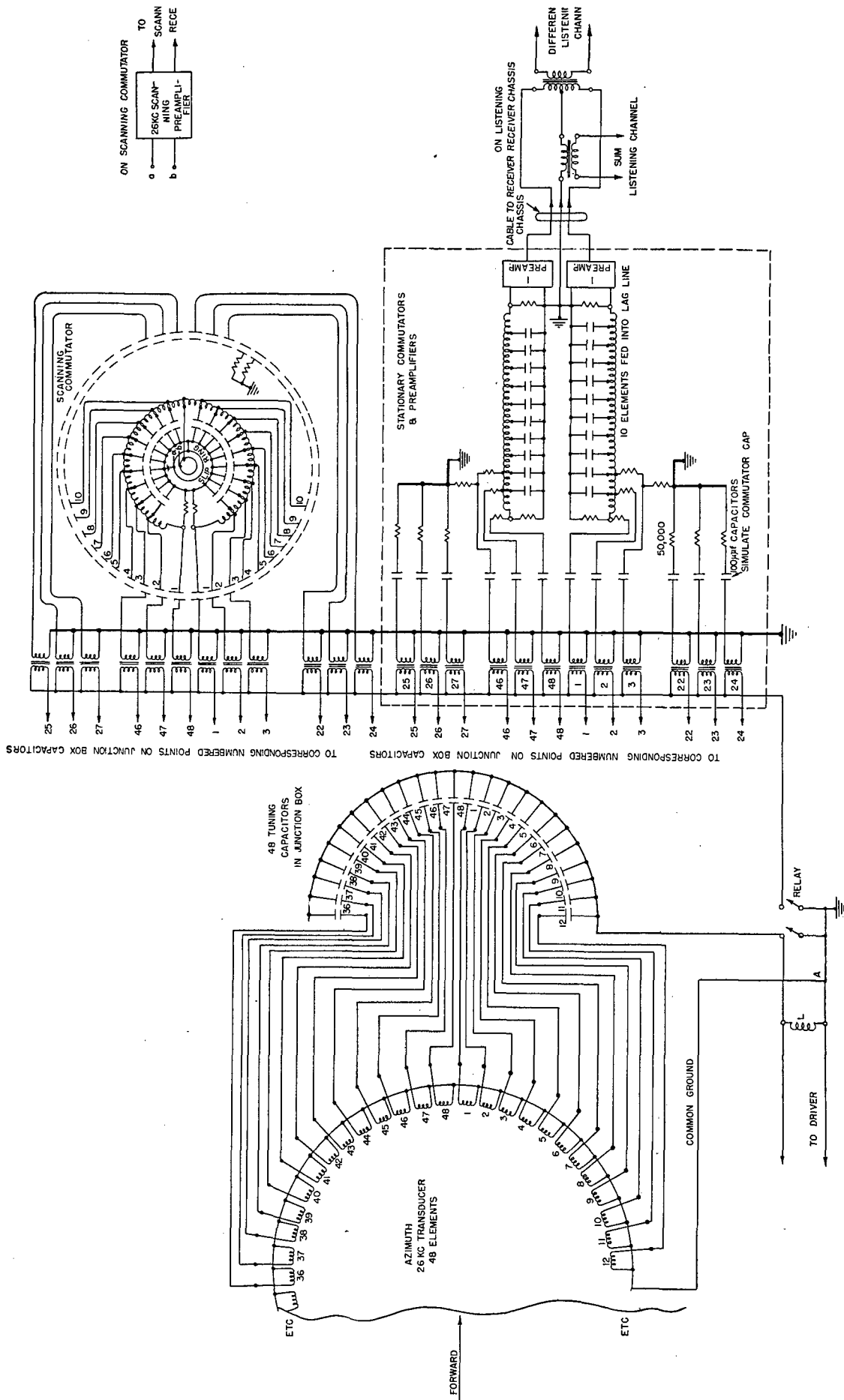


FIGURE 77. Transducer-junction box-commutator connections of azimuth-search section of integrated Type B sonar.

CONFIDENTIAL

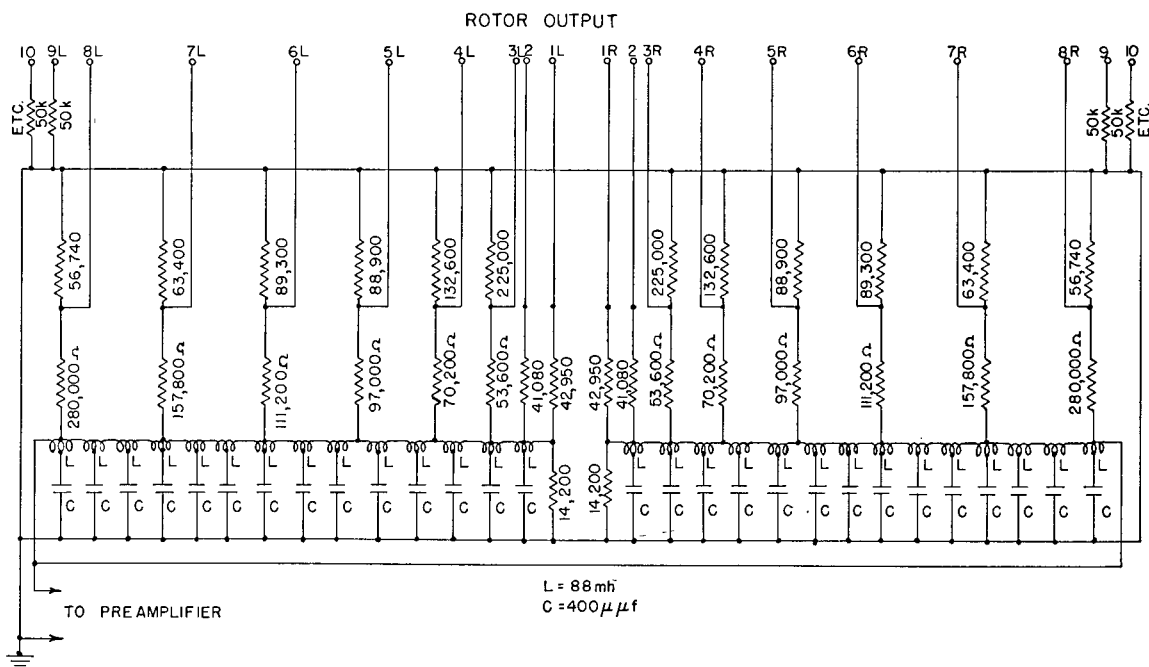


FIGURE 78. Wiring diagram of Sangamo Model XQHA lag line.

from the 38-kc depth-scanning system to the 26-kc azimuth-scanning system.

The transformer ring with its 48 transformers and the lag line assembly is bolted onto a spindle stud fixture which is welded to the cradle frame, while 48-

100- $\mu$ mf capacitors of the postage stamp variety serve as the connection links between transformer secondaries and the lag line input pins. These capacitances simulate those between the rotor and stator segments in the regular commutator, insuring proper imped-

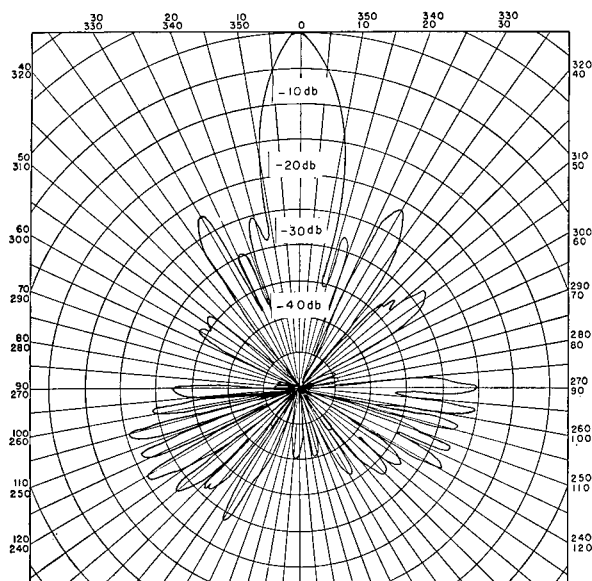


FIGURE 79. Receiving directivity pattern of 26-kc Model XQHA scanning sonar, transducer fixed, commutator rotated.

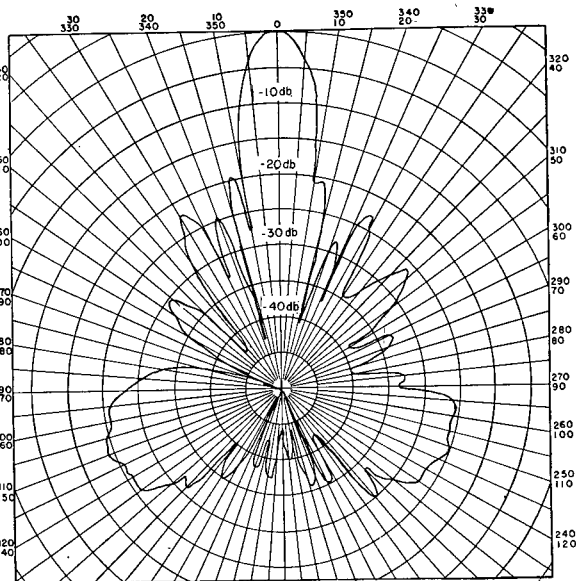


FIGURE 80. Receiving directivity pattern of 26-kc Model XQHA scanning sonar, commutator fixed in register position, transducer rotated.

CONFIDENTIAL

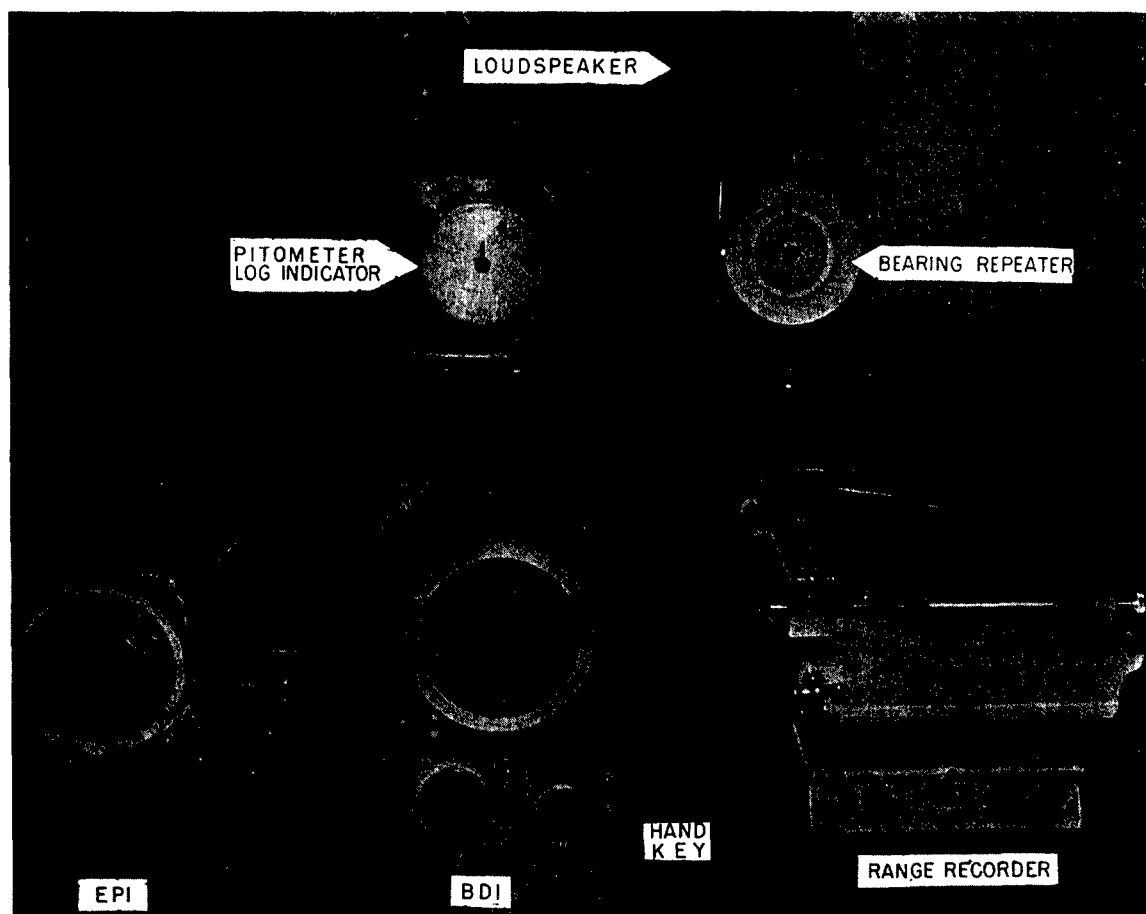


FIGURE 81. Indicators for 26-kc depth-scanning sonar.

ance matching in the input circuits. As in the other units, the 48 twisted pairs from the transformer primaries are brought around to terminal boards on the cradle frame. The input circuits of the scanning commutator and of the stationary lag lines are paralleled in the transfer network.

The horizontal-scanning commutator and the stationary listening lag lines unit are located in the azimuth commutator rack with the transfer network (junction box) and the servo amplifiers for the vertical-listening commutators. All cabling to the rack is brought into the bottom of the rack in the same manner as that used in the depth rack. Design of the rack assembly is such that each unit may be pulled out part way for test, or removed entirely for repair or replacement. The rack is 19 inches square and about 5 feet high. The back and top panels are welded to the frame; the two side panels and the front panel are detachable. Two typical patterns obtained using

similar commutators in a standard XQHA system are shown in Figures 79 and 80.

## 6.5 INDICATORS, STABILIZATION, FIRE CONTROL

### 6.5.1 Indicators for 26-kc DSS

Indicators for the 26-kc depth-scanning system installed on the USS CYTHERA were experimental units.<sup>6</sup> Cathode-ray tube assemblies built for other purposes were functionally modified for this system, but no attempt was made to satisfy all operational requirements. The EPI (see Figure 81) used a 7-inch cathode-ray tube with its power supply and focus and intensity controls built into the cabinet (see Figure 82). A master gain control for the brightening receiver was mounted on the face of the cabinet. A circular piece of lucite, cut as a gear with a wire set from the

CONFIDENTIAL

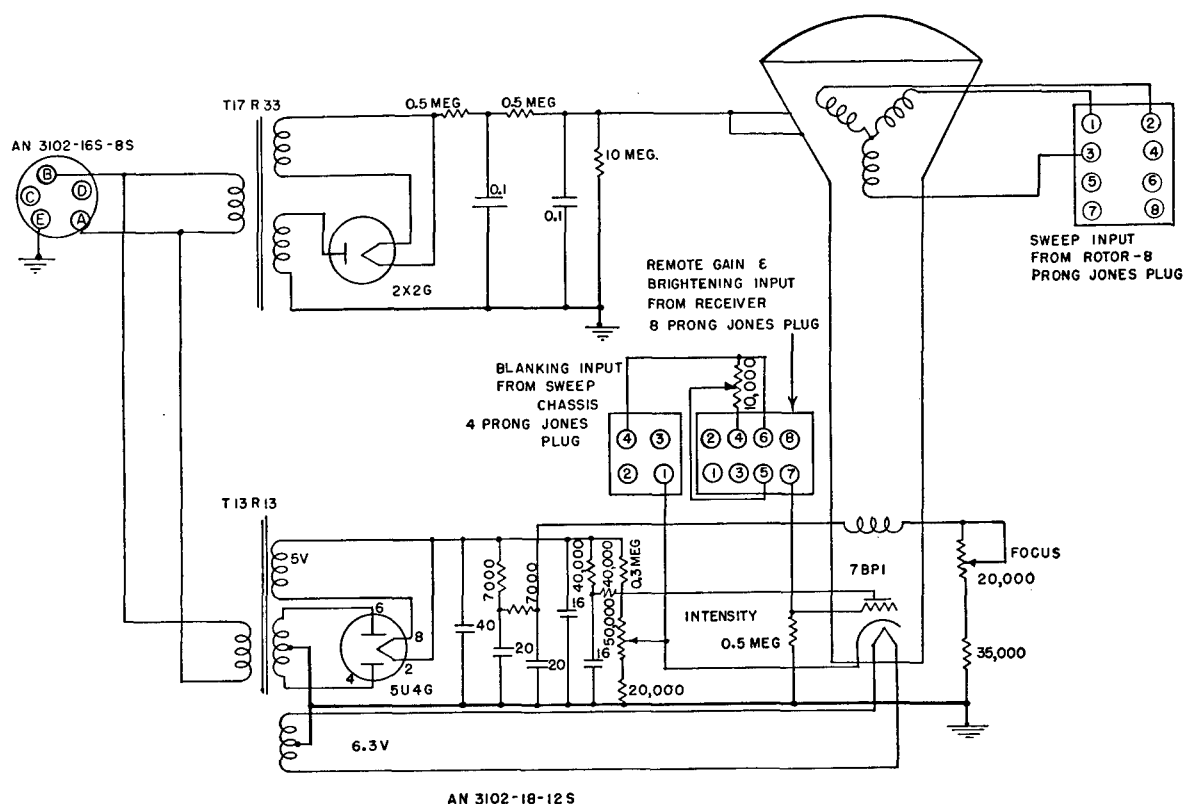


FIGURE 82. Schematic diagram of EPI 26-kc depth-scanning sonar.

center to the rim along a radius, was mounted over the face of the tube to serve as a cursor. Mounted below the cathode-ray tube cabinet was an additional section containing two DG synchros and one synchro generator mechanically geared to the handwheel. The first DG was used to add the elevation angle to the level signal from the stable element. The sum was then used as the director elevation order to the trunnion-tilt corrector. The second DG was used to obtain the difference between the depression order and the actual depression angle. This difference was used to correct the scan indication by positioning a phase-shifting transformer. The synchro generator was used as a direct repeater to the synchro indicator panel for depression angle.

A second indicator was built for the BDI in which a 7-inch cathode-ray tube was used to show the BDI deflection (see Figure 81). A standard high-voltage power supply and the standard BDI sweep circuits (Figure 83) were mounted in the rear of this cabinet. An additional 350-volt negative supply for the BDI sweep was fed in from an external source (Figure 84). On the face of the cabinet there were four controls—

focus, intensity, master gain control (for the BDI listening receiver), and sweep (range switch). An additional section which contained two DG synchros, a 78-volt transformer, and a two-position rotary switch was mounted below the main cabinet. The two DG synchros were geared to a handwheel which inserted the bearing. These synchros were geared in the ratio of 1 and 36 respectively, and the first of these was geared 36:1 to the handwheel. Their electric outputs were fed directly to the stable element. The rotary switch was used to control the *maintenance of true bearing* [MTB] system: when the switch was in the true position, the gyro information was fed into the stator of the two DG's; when in the relative position, 78 volts was applied across the stator windings.

A standard range recorder was used in this first installation, the signal input being fed from the audio channel of the BDI listening receiver.

It was desirable to put in a direct repeat-back indicator between the projector shaft and the operating position because of the complications of feeding the relative bearing through the stable element, trunnion-tilt corrector, and the projector. This unit was

CONFIDENTIAL

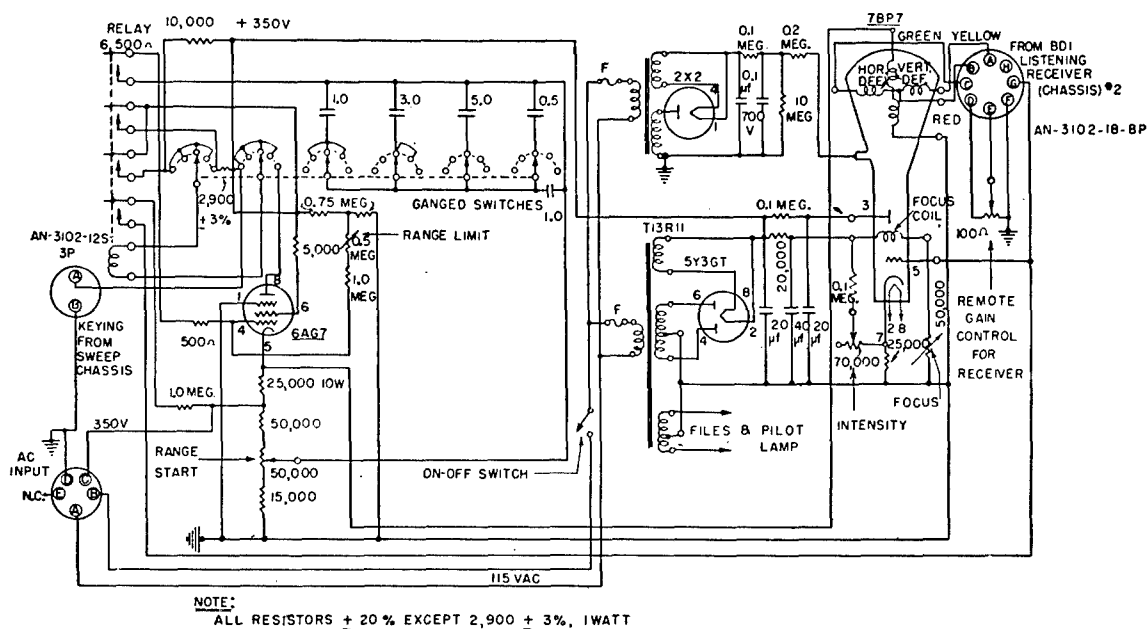


FIGURE 83. Schematic diagram of BDI 26-kc depth-scanning sonar.

a standard Submarine Signal Company bearing-repeater unit with gyrocompass indication on the center dial.

The Navy had specified a change from the old 800-cycle center listening frequency to a new 500-cycle

center listening frequency which they considered would make doppler changes easier to recognize. This lower frequency made it imperative to have a speaker which would reproduce low frequencies down to 200 cycles. To reproduce these low frequencies efficiently, HUSL found that an 8-inch speaker would be required. One of these speakers was mounted in a wooden case and attached to the bulkhead in front of the BDI operator<sup>49</sup> (see Figure 81).

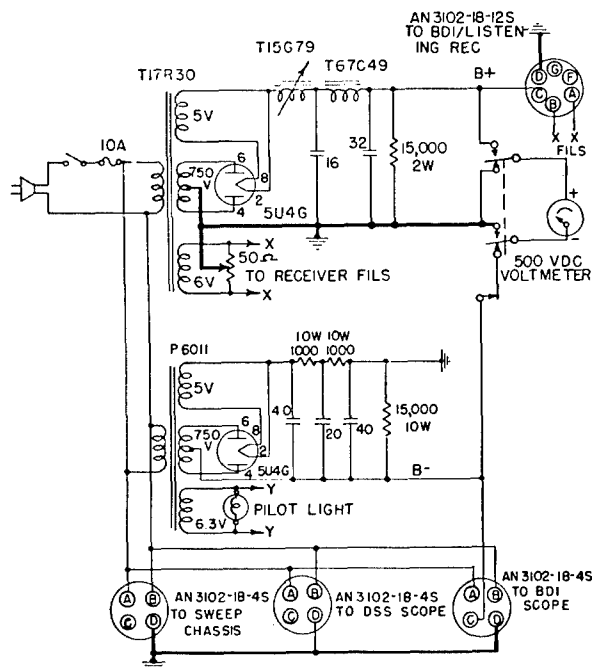


FIGURE 84. Power supply for receivers and indicators, 26-kc depth-scanning sonar.

#### 6.5.2

#### Stabilization for 26-kc DSS

The synchro-control and display circuits for the 26-kc DSS system are shown in Figure 85. The stable element used with the 26-kc DSS system was a Westinghouse Manufacturing Company Mark 8, Model 2. This unit measured and transmitted level and cross level at 2- and 36-speed and included an attachment for correcting the relative bearing for deck tilt. A complete description of the design and operation of this unit is found in the instruction book prepared by Westinghouse Electric and Manufacturing Company.<sup>60</sup>

The outputs of a stable element are generally used for 3-axis stabilization. However, it has been pointed out in Chapter 2 that for the depth-scanning sonar equipment 2-axis stabilization was required.<sup>3,50</sup> To accomplish this a sonar trunnion-tilt corrector was



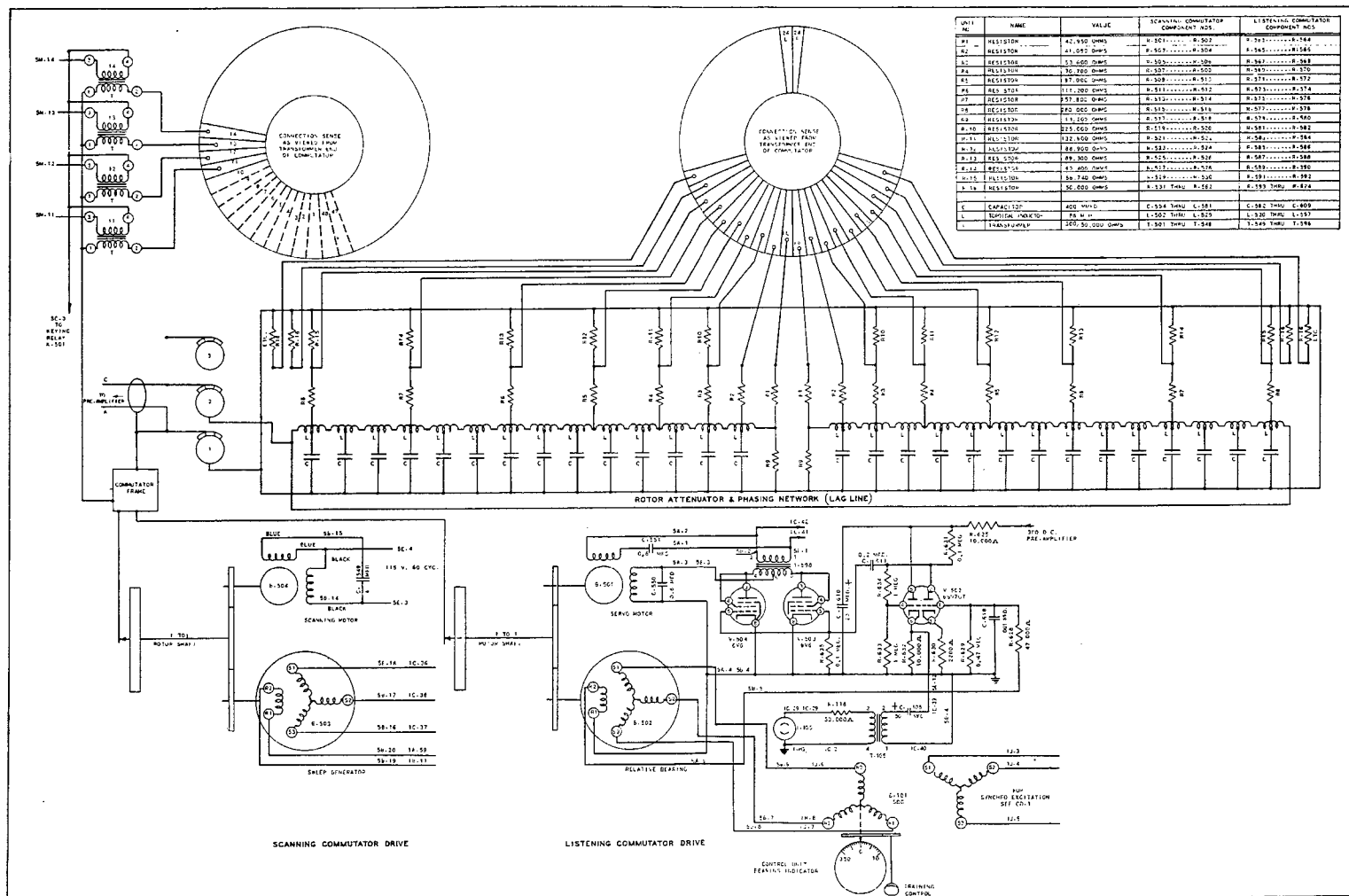


FIGURE 83. Circuit diagram of directional sensitivity control, Model NQUA scanning sonar.

CONFIDENTIAL

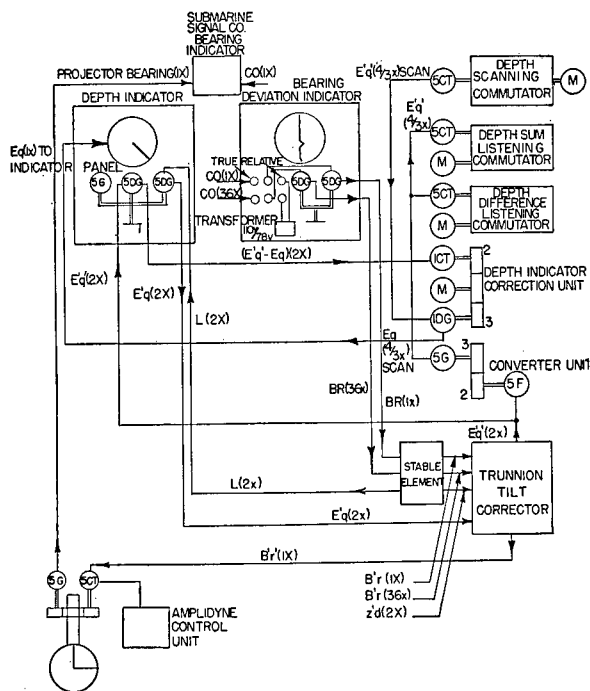


FIGURE 85. Synchro schematic diagram for 26-kc depth-scanning sonar.

added. This unit took information from the stable element and computed the sonar train order,  $B'r'q$ .

$B'r'q$  — **TRAIN ORDER** — The angle between the fore and aft axis of own ship and the plane through the line of sight (from the point upon which the range keeper or data computer bases its solution) perpendicular to the deck, measured in the deck plane clockwise from the bow.

The trunnion-tilt corrector also computed the sonar depression angle,  $E'q'$ .

$E'q'$  — **ELEVATION ORDER** — The elevation of the line of sight above the deck, measured in a plane, perpendicular to the deck, through the line of sight.

A converted searchlight trunnion-tilt corrector built by the Ford Instrument Company was used in the experimental installation aboard the USS CYTHERA. The major change was the conversion of the bearing input servo from a 1-speed system to a 1- and 36-speed system. Limits, name plates, and dials were also changed.

The depth-scanning commutator caused the scanning beam to rotate in a plane normal to the deck. Thus, when a target echo was received, its depth angle as measured by the commutator was an angle

which was  $4/3$  the sonar depression order, or  $4/3 E'q'$  (see Section 6.4.2). The angle which should appear on the depth-scanning indicator should not change with the roll and pitch of the ship, and should be  $4/3$  the true elevation angle of the target, or  $4/3 E_q$ .

$E_q$  — **ELEVATION ANGLE** — The elevation above the horizon of the line of sight (from the point upon which the range keeper or data computer bases its solution), measured in the vertical plane through the line of sight.

In order to accomplish this change from  $E'q'$  to  $E_q$ , it was necessary to subtract from the electrical signal of the sweep generator on the commutator an amount equal to the difference between these two quantities,  $4/3(E'q' - E_q)$ :

$$\frac{4}{3}E'q' - \frac{4}{3}(E'q' - E_q) = \frac{4}{3}E_q.$$

In order to produce the quantity  $4/3(E'q' - E_q)$ , a differential generator was attached to the depression handwheel and the quantity  $E'q'$  at 2-speed was fed from the trunnion-tilt corrector to the stator winding of this differential generator. The rotor was then turned by means of the handwheel which subtracted the quantity  $2E_q$ . The resulting signal  $2(E'q' - E_q)$  was then fed to a servo which was geared to the rotor of a phase-shifting transformer at a ratio of 2:3. This phase-shifting transformer was placed between the sweep generator and the deflection coils on the cathode-ray tube (see Figure 86).

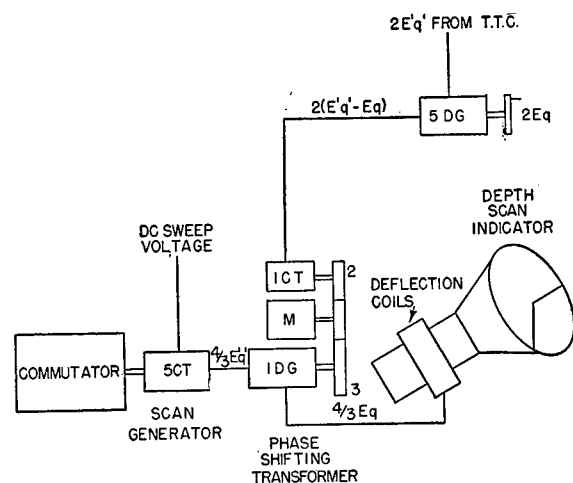


FIGURE 86. Depth indicator correction arrangement for 26-kc DSS.

CONFIDENTIAL

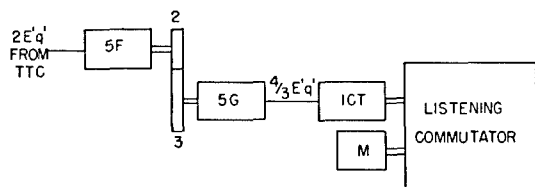


FIGURE 87. Converter unit for 26-kc DSS.

Since the installation aboard the USS CYTHERA was unorthogonalized (see previous section), a converter unit had to be inserted between the output of the trunnion-tilt corrector and the listening commutators. This converter unit consisted of a 5 F synchro follower which received the signal from the trunnion-tilt corrector ( $2E'q'$ ) and was geared at a ratio of 2:3 to a 5 G synchro generator which then fed the  $4/3 E'q'$  signal to the servos attached to the listening commutator (see Figure 87).

The manufacturing specifications of the Westinghouse stable element required that the maximum training speed be not more than 6 rpm and the accelerations in training should not exceed 36 degrees per second per second. This latter specification did not meet the requirements of the system as installed aboard the USS CYTHERA. Under normal circumstances the sonar operator, when training from one bearing to another, turned the handwheel at a speed which did not exceed 6 rpm. However, the accelerations and decelerations were much greater than the specified 36 degrees per second per second. In operation aboard the USS CYTHERA, when the operator trained to a new bearing and stopped the handwheel, the stable element generally overshot the bearing by approximately 6 degrees. This overshoot was amplified in the trunnion-tilt corrector and caused the servo system of the training shaft to oscillate as much as 15 degrees before coming to the required bearing (see Section 6.2). The total errors of the trunnion-tilt corrector were very small (approximately 25 minutes) in comparison with errors in the stable element and training shaft.

### 6.5.3 Indicators for Integrated Type B Sonar

Indicators for the integrated Type B sonar were designed according to specifications laid down by the Bureau of Ships and the Bureau of Ordnance.<sup>51,52</sup> The equipment was required to be as light as possible

because of its position topside; therefore, only the minimum equipment needed for operation was located in the consoles. The number of controls requiring operation during attack was also kept at a minimum. This requirement led to a study of operating needs and relegation in the design of all nonessential controls to the lower sound room.

In the design of these consoles<sup>53,54</sup> much thought was given to the reliability and serviceability of each unit. Drawer construction is used to provide accessibility. The consoles can be attached to pedestals designed specifically for that purpose or to any designated table or bulkhead-mounted framework, and are protected from shock and vibration by isolation mounts. A removable stuffing tube plate at the rear of each console facilitates attachment of cables. Spurious deflections of the cathode-ray tubes were minimized by keeping the synchros and servo motors at the greatest possible distance from the tubes and by using magnetic shielding.

On the front of the depth console (see Figure 88) are the depth-scan indicator, a gain control, a range selector switch, and a depth-angle control handwheel. The focus, intensity, and centering controls for the cathode-ray tube are located on the inside of a drawer

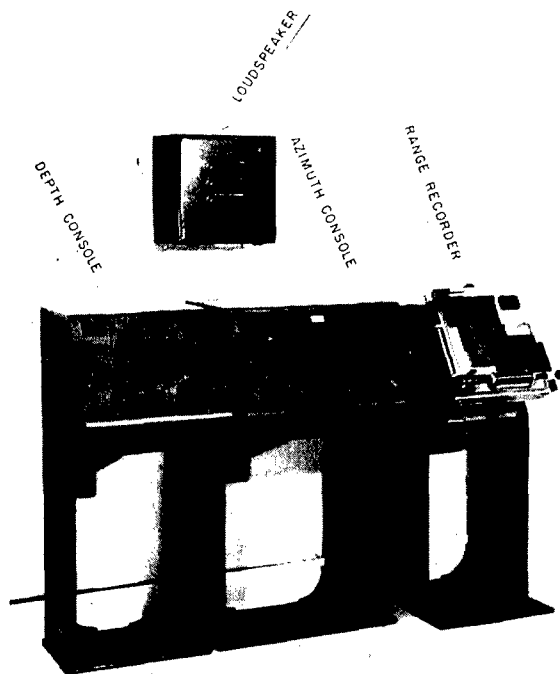


FIGURE 88. Indicators for integrated Type B sonar.

which can be released by pushing a button on the front of the console. A phone jack is supplied in the front left corner to provide a connection for headphones if desired. The handwheel is geared to two size 5 synchro generators which are arranged to transmit depth angle at 2- and 36-speed. This information is supplied to the stabilization equipment which in turn positions the two listening rotors. The signal from these two generators, in addition, is applied to a servo arrangement which positions a mechanical cursor over the face of the depth-scan indicator. Centering controls permit alignment of the cathode-ray tube sweep center with the mechanical center of rotation of the cursor.

On the front of the azimuth console (see Figure 88) are the following components: the azimuth-scan indicator, the BDI indicator, the master gain control for each of these indicators, the range selector switch, the true-bearing drum dial, the relative projector bearing dial, the cursor push button, the attack-search switch, and the training handwheel. The true-bearing drum dial is positioned by a synchro which receives a true-bearing signal from the computing circuits in the control rack. The projector bearing dial is a direct repeat-back system from the training shaft of the projector. This dial is used because the different functions introduced by stabilization equipment make it desirable to have a direct indication of the area being searched.

The handwheel is geared to two size 5 differential generators to produce bearing synchro signals at 1- and 36-speed. The output of the two differential generators when a director-aided-tracking mechanism is used is ship's course plus a bearing correction. This signal is then combined with the computed true bearing from the director to produce the actual relative bearing, which is then transmitted through the stabilization equipment to train the projector. When the director-aided-tracking mechanism is not used, information from the differential generators becomes a relative bearing by turning the handwheel an amount equal to true bearing. This relative bearing is transmitted through the stabilization equipment to train the projector. Further explanation of the computing and stabilization circuits is described in Sections 6.5.2 and 6.5.5 of this chapter.

Focus and intensity controls for both cathode-ray tubes are located on the inside of a drawer which is released by pushing a button on the front of the console. A phone jack is supplied on the console at the

front corner to provide a connection for headphones if desired.

The range recorder for the integrated Type B sonar is supplied in this design by the Bureau of Ordnance and is arranged to take its signal from the audio channel of the BDI receiver, which may be switched to either the azimuth- or the depth-scanning portions of the system. The recorder has a cursor servoed from the range-rate control mechanism in the attack director. In addition to the servo, a handwheel is arranged on the side to introduce spot corrections to the range. Then the actual position of the cursor is repeated back to the attack director by means of a synchro repeater system.

The speaker for the integrated Type B sonar is an 8-inch speaker in a separate case shock-mounted to the bulkhead (see Figure 88). This size speaker was chosen in the design to provide adequate low-frequency response, as described in the first part of this chapter. On this cabinet face there is an on-off control, a volume control, and a band selector switch. The band selector switch determines the frequency response by use of a filter.

#### 6.5.4

### Control Rack

In order to increase the flexibility of the proposed experimental installation of integrated Type B sonar on a suitable ship, a control rack was designed to contain supplementary controls for the system (see Figure 89). A number of these controls are unnecessary for a production type of installation; the remainder will be designed into the different units of the integrated equipment.

The top panel contains power switches and cable terminals. Below these power switches, on the same panel, are three switches labeled relative-true, stabilization, and attack-director. The relative-true switch introduces the feature of MTB when placed in the true position. The stabilization switch disconnects all stabilization from the sonar equipment. When disconnected, the stable element and the trunion-tilt corrector do not have their main power supply shut off; only the energizing power to the synchros involved in the stabilization is disconnected. The attack director switch is used to disconnect the aided-tracking mechanisms of the attack director from the sonar equipment and, like the stabilization switch, disconnects only the synchros. It is arranged to allow continued self-operation of the aided-track-

CONFIDENTIAL

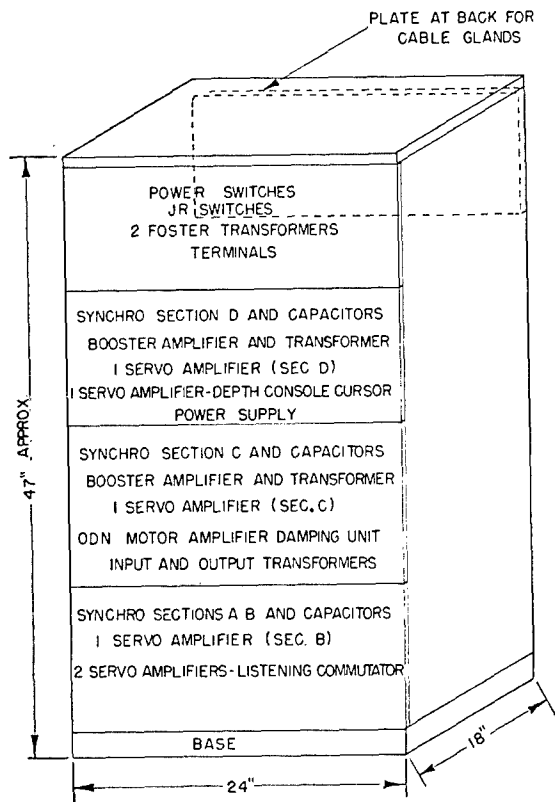


FIGURE 89. Sketch of control rack, for integrated Type B sonar.

ing mechanisms. The circuits for the two switches are arranged so that each operates independently. This makes it possible to operate either stabilized or unstabilized circuits, with or without aided-tracking mechanisms.

The second panel contains (1) the synchro section D (see Figure 89), (2) one servo amplifier for this synchro section, (3) a booster amplifier and transformer for the input to the resolver, (4) a power supply to supply the booster amplifiers in this and one other panel, together with a motor amplifier in another panel, and (5) one servo amplifier used to control the cursor on the EPI in the depth console.

The third panel contains (1) the synchro section C, (2) one servo amplifier for this synchro section, (3) a booster amplifier and transformer to supply the resolver, and (4) a damping unit, motor amplifier, and transformers to amplify the output from the resolver for the ODN computer in the BDI listening receiver.

The bottom panel includes (1) the synchro sections A and B, (2) a servo amplifier for synchro section B, and (3) two servo amplifiers which are used to drive

the listening commutators in the depth-scanning system.

Easy accessibility to the three lower panels is provided by drawer-type construction and electrical-plug connection to the rack.

#### 6.5.5 Stabilization for Type B Integrated Sonar

At the present time the schedule for installing integrated Type B sonar aboard the USS *BABBITT* calls for the installation of a Westinghouse stable element Mark 8 similar to the one installed aboard the USS *CYTHERA*. The Bureau of Ordnance has under development another stable element designated as Mark 7, to be built by the General Electric Company. This unit will not be available for sonar work before the end of October 1945. One of the first units to be manufactured by General Electric has been allotted to the integrated Type B sonar and when it becomes available will be installed in place of the Westinghouse Mark 8. During the time the Mark 8 stable element is aboard, a Ford Instrument Company searchlight trunnion-tilt corrector converted for sonar use will be employed, modified for 2- and 36-speed depression, and 1- and 36-speed bearing operation.

Under the arrangement where a Mark 8 stable element and a trunnion-tilt corrector are used, it is possible to stabilize only the sonar equipment. When the Mark 7 stable element is installed, it will be used to stabilize the antisubmarine weapon in addition to the sonar equipment. This weapon may be 1-axis, 2-axis, or 3-axis stabilized. Under any one of these conditions, the relative bearing of the weapon will be transmitted to the stable element where the level, cross level, and director train will be computed for this given bearing. These same values of level, cross level, and director train which are computed for the weapon bearing will also be transmitted to a Mark 23 sonar computer, manufactured by the Arma Corporation. This computer will then solve the necessary sonar train order and sonar depression order for 2-axis stabilization of the line of sight to the target (see Figure 90).

The integrated Type B sonar will include a search portion which is to be essentially a QH azimuth-scanning sonar. In the design of the search portion, the listening beam was formed by connecting the lag lines directly to the transducer elements, and was rotated

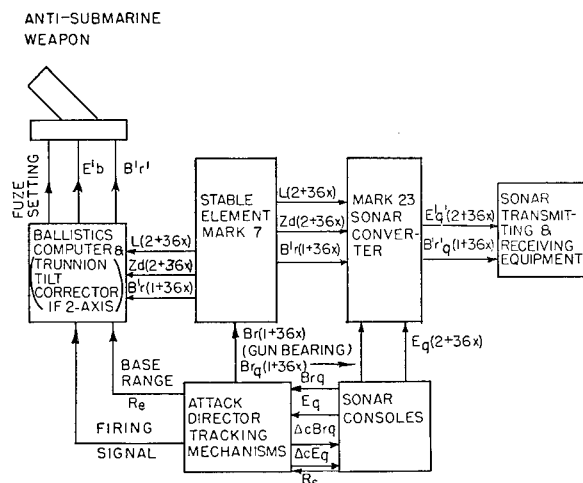


FIGURE 90. Proposed stabilization plan for test program aboard USS BABBITT, integrated Type B sonar.

by training the projector. This type of operation was explained in Chapter 2. The azimuth-scanning commutator will cause the scanning beam to be rotated in a plane parallel to the deck plane. Thus, when the target echo is first received, its bearing as measured at the commutator will be equal to the sonar train order for that target less the amount of projector train at that instant. The angle which should appear on the azimuth-scanning indicator is one that does not change with the roll and pitch of the ship and should be the actual relative bearing of the target. To present this relative bearing properly on the azimuth-scanning indicator, the projector must be trained until the BDI deflection is zero. The bearing then measured at the commutator will be 0 degrees. If the electrical signal of the sweep generator on the commutator is changed in phase by an amount equal to the *relative bearing*  $[Br]$ , then indication on the azimuth-scan indicator will appear directly as  $Br$ . This will be accomplished (see Figure 91) by inserting a differential generator, used as a phase-shifting transformer, between the sweep generator on the commutator and the deflection coils of the cathode-ray tube. The rotor of this differential generator will be moved by an angle equal to  $Br$  by a servo in the computer section of the system (described later).

In order to obtain the quantity  $Br$  when the attack director is used, the relative-true switch on the control rack will be turned to the relative position and the director switch will be turned to the on position (see Figure 91). The *computed relative bearing*  $[cBr]$  from the computing mechanisms in the attack direc-

tor will then be applied to the two 5 F synchro followers in the computing section of the control rack, which will position the rotors of two size 5 differential generators. The stators of these synchros are to be supplied with a correction signal so that the output of the rotors will be *correct relative bearing*  $[jBr]$ . This correction signal is to be obtained from two size 5 DG's in the console whose rotors are positioned by the handwheel so that the BDI is kept centered. The correct relative-bearing signal is then applied to a servo arrangement which will position the phase-shifting transformer for correcting the azimuth-scan indicator and a resolver for obtaining the cosine of  $Br$  for the ODN circuit. The correct relative-bearing signal also will be applied directly to the stable element to stabilize the projector at the proper bearing.

When the attack director is not used, 78 volts will be placed across the stators of the two 5 F synchros in the computer section, which then will position the rotors of the two 5 DG's at zero relative bearing. If the relative-true switch is then positioned in the true position, the ship's course will be applied to the stators of the two size 5 DG's in the console. If the handwheel is turned an amount equal to the true bearing, the two size 5 DG's will then apply relative bearing to the stators of the two size 5 DG's in the computer circuit, and these two DG's in turn will apply relative bearing to the servo and the stable element as described above.

In the design for the integrated Type B sonar, the depth-scanning commutator had 64 segments in place of the 48 used in the experimental 26-kc system. Forty-eight of the segments are connected to the 48 elements of the transducer. The remaining 16 segments are grounded. By using this 64-element commutator the angularly distorted display which was accepted in the USS CYTHERA installation can be avoided. Thus, when a target echo is received, its depth angle as measured at the commutator is the sonar depression order,  $E'q'$ . Details of the method of correcting this angle to present the actual depression angle on the scan indicator are slightly different from those used on the experimental installation for USS CYTHERA. The following description can be understood more easily by referring to Figure 91. Located in the depth console are two 5 G synchros which are positioned by the handwheel to an angle equal to the actual depression angle. These synchros transmit this angle  $E'q'$  (at 2- and 36-speed) to the computer section of the control rack, where, through a servo, it posi-



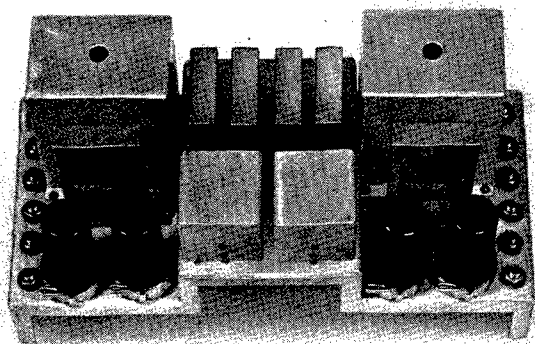


FIGURE 92. Top view of preamplifier.

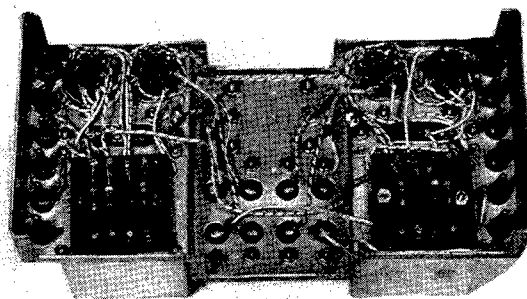


FIGURE 93. Bottom view of preamplifier.

tions the rotors of four DG's and a resolver. The first pair of DG's are used to add the level signal from the stable element to the depression angle to obtain director depression angle  $E'q$  which then is applied to the trunnion-tilt corrector. The second pair of DG's are used to obtain the difference between  $E'q'$  and  $Eq$ . The output of this second pair of differentials is applied to another servo which positions the rotor of a differential generator, which is used as a phase-shifting transformer between the sweep generator on the depth-scan commutator and the deflection coils on the depth-scan indicator. The resolver is used to obtain the cosine of  $Eq$  which is used in the ODN circuit.

The listening commutators on the depth-scanning portion of the integrated system are standard 48-segment commutators. However, the servo system is geared to the rotor at a ratio of 2:3 in order to compensate for the angular distortion as previously explained.

It is desirable to provide for removing the stabilization, both for damage control and for testing. The installed sound gear monitor (attached to the ship) may be used as a reference. By throwing the stabilization on-off switch to the off position, the effects of stabilization on the listening and scanning beams can be removed. This is accomplished by applying the signal from the two 5 G's in the depth console directly to the servos attached to the depth-listening commutators, thus positioning the beam at  $Eq$ . Then also, the training control receives its signal directly from the 5 DG's in the bearing computing circuit and, thus, eliminates the effect of the stable element and the trunnion-tilt corrector.

The training control for the integrated Type B sonar is a standard QCJ-8 unit with amplidyne control or a similar unit. The control amplifier will be modified by the RCA Manufacturing Company to operate from 1- and 36-speed synchro signals in place of the normal 36-speed signal.

It should be noted that throughout this system all signals are transmitted at double speed in order to obtain an accuracy of  $\frac{1}{4}$  degree or better. All bearing angles are transmitted at 1- and 36-speeds while elevation, level, and cross level are transmitted at 2- and 36-speeds. This has been arranged to conform with Bureau of Ordnance practices.

#### 6.5.6 Fire Control for Use with Integrated Type B Scanning Sonar

The integrated Type B sonar has been designed to make use of the latest developments in sonar fire-control equipment.<sup>55</sup> The first portion of this equipment is the aided-tracking mechanisms. On the first installation aboard USS BABBITT a Mark 4, Model 0 attack director will be used when it becomes available. This attack director incorporates aided-tracking mechanisms to generate the relative bearing and the slant range. After preliminary tests an additional box will be added which will contain an aided-tracking mechanism for the depression angle. All this equipment will be supplied by the Bureau of Ordnance and is being developed by Librascope, Inc., under the supervision of Section Re4b of BuOrd.

Under the design of the preliminary system, the bearing aided-tracking mechanism provides a computed relative bearing to the sonar equipment. The

CONFIDENTIAL



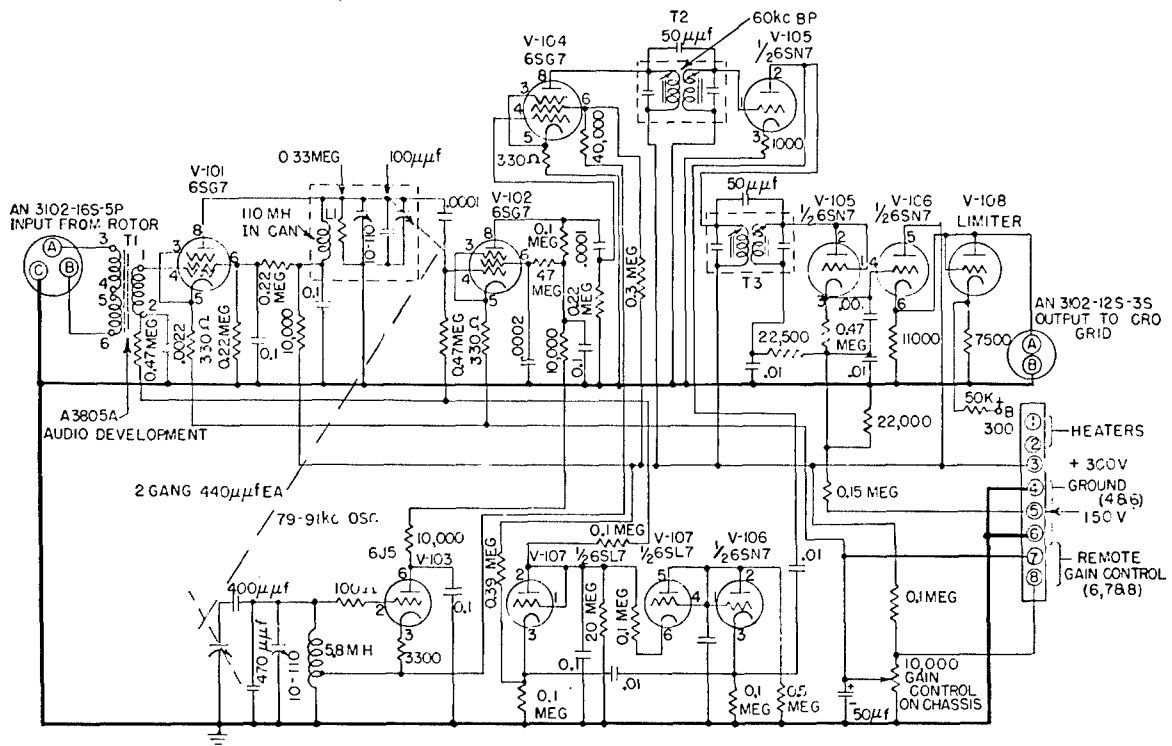


FIGURE 94. Wiring diagram for scanning receiver.

sonar operator can then insert corrections to bring this computed bearing to the actual bearing as indicated by the BDI. When using scanning sonar, it is often desirable to investigate a second target which may appear on the scanning indicator. This is possible if the operator disconnects the aided-tracking mechanisms from the sonar equipment and then proceeds to train in the direction of the new target. When returning to the original target and reconnecting the attack director, the computed bearing causes the projector to train to a new position which may be more than 5 degrees away from the actual bearing of the target. To insert a 5-degree correction into the aided-tracking mechanism immediately would cause an error in the bearing rate set up within the director. To correct this error would take a considerable number of corrections inserted at the sonar handwheel. Under the latest proposed system<sup>22</sup> (not included in this first design) the aided-tracking mechanism does not furnish a computed bearing, but furnishes increments to the initial bearing set up by the sonar operator. Therefore, after searching a second target and repositioning the cursor to the original echo, there is no large bearing error. If at this point the cursor continuously leads or lags the echo, the hand-

wheel can be used to insert small corrections which change the bearing rate. During this time of correction, bearing errors are very small and the rates are corrected in the proper manner.

When calculating the depth and horizontal range of a deep target, it becomes necessary to make corrections for the temperature gradients in water. This is done with an automatic temperature-gradient corrector. The preliminary model of this unit requires the slant range and depression angle to be inserted by hand operation. The bathythermograph information can be interpreted in terms of several thermal layers in the water and the depth of each layer can be inserted into the machine by means of hand-operated knobs. The actual depth of the submarine then appears on a dial as depth in feet. It is contemplated that additional models can be built after a period of field testing has shown what modifications are required.

In addition to the aided-tracking mechanisms as described in a previous paragraph, the Mark 4, Model 0 director is essentially a computing device for computing the course-to-steer and time-to-fire to make a successful attack. The Model 0 has been designed for use with present-type depth charges and ahead-

thrown ordnance. This computing portion of the director has been given exhaustive tests under the direction of ASDevLant.<sup>56</sup> When new ordnance is developed, a new attack director will be designed that will include some of the computing sections required for correcting the scanning indicators, as well as changes necessary to direct the new type of ordnance.

The extensive use of depth charges during this war has shown some of the defects in this type of attack. One of these faults is the long "blind" time required when the submarine is deep, which permits the submarine to make evasive maneuvers between the time of loss of contact and the explosion of the depth charge. The use of present ahead-thrown weapons is not entirely satisfactory because of their limited range and the necessity of getting the ship close to a collision course at the time of firing. Both of these conditions could be overcome if a large charge could be fired from a stabilized gun-type of thrower. The specifications for this type of unit would include a means of varying the range to which the charge could be thrown; also it would be arranged to train approximately a total of 270 degrees. Such a gun-type thrower has been proposed by Section Re4b of the Bureau of Ordnance and is at the present time under consideration.

6.6

## RECEIVERS

### 6.6.1 Preamplifiers for 26-kc Depth-Scanning Sonar

There were three identical preamplifiers used in the receiving channels in the depth-scanning sonar installed on the USS CYTHERA. One of these amplified the signal from the scanning commutator and the other two amplified the signals from the two listening commutators. The output from the first was connected to the scanning receiver and the outputs from the other two were connected to the BDI listening receiver. A photograph showing the preamplifier and its power supply mounted on the commutator is shown in Figure 61 in Chapter 5. Figures 92 and 93 show top and bottom views of the preamplifier alone. The preamplifier as installed on the commutator was made in dual form; that is, two complete preamplifiers were provided, although only one of the two was used. This came about because the original design called for two preamplifiers to handle dual outputs from each lag line, whereas in this application only one was required. (For QH scanning sonar, see Chapter 5.)

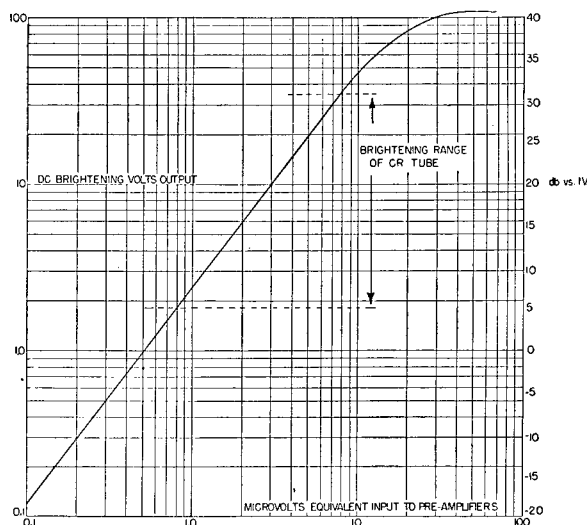


FIGURE 95. Scanning receiver performance: output versus input.

A wiring diagram for these preamplifiers is shown in Figure 106 in Chapter 5, under "Receivers for QH Scanning Sonar, Model 2." Each preamplifier contained two stages of amplification, separated by a band-pass filter.<sup>57</sup> The first stage (6SG7) was coupled to the band-pass filter, which was 7 kc wide 3 db down from the maximum, and was centered at 26 kc. The second stage 6SG7 was used as a cathode follower so that the output was at low impedance, and it was not necessary to have a short connection from the preamplifier to succeeding parts of the receiver. The overall voltage gain of the preamplifier was approximately 33 db.

During the time of transmission, the gain of the preamplifier was reduced to a very low value by the insertion of a resistor between the positive plate supply and the preamplifier. This was accomplished by contacts on the send-receive relay. Thus during transmission, any leakage voltage appearing at the output of the commutator did not appear as a large amplified voltage at the output of the preamplifier.

### 6.6.2 Scanning Receiver for 26-kc Depth-Scanning Sonar

The scanning receiver for the depth-scanning sonar installed on the USS CYTHERA amplified the signal from the preamplifier on the scanning commutator, and delivered a d-c signal to the brightening grid of the cathode-ray tube in the elevation position indicator, so that a spot appeared on the screen of the tube for every signal received. This receiver was es-

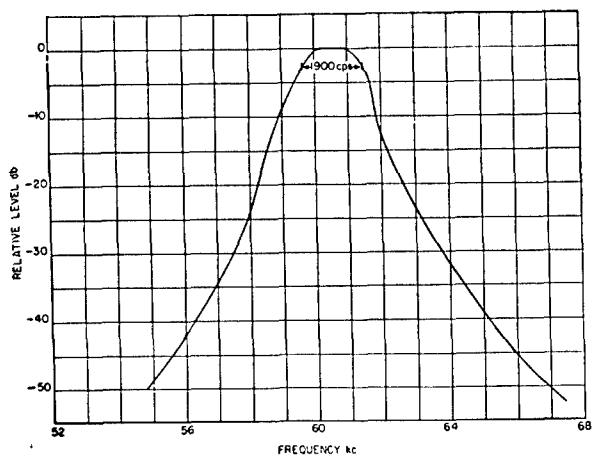


FIGURE 96. Scanning receiver, i-f filter response.

essentially the same as the CR Model 2 receiver described in Chapter 5, except for rearrangement of the chassis layout. The wiring diagram is shown in Figure 94. A remote manual gain control was used, mounted on the EPI, in parallel with a local manual gain control. A *reverberation-controlled gain* [RCG] circuit was also used, which operated from the level of reverberation received. During the time of transmission, high signal voltages were developed as a result of leakage in the input of the receiver. Signal taken from the plate of the last intermediate-frequency amplifier tube was fed to a triode ( $\frac{1}{2}$  6SL7), used as a biased rectifier. The fixed cathode bias allowed it to rectify only those signals which were above a certain level. A capacitor connected in the grid-returns of the r-f stage (6SG7) and the mixer (6SG7) was, thereby, charged negatively with respect to ground. As a consequence, these tubes were nearly cut off and the overall voltage gain of the receiver was reduced by at least 100 db. During the time of reception, the negatively charged capacitor discharged to ground through a second biased rectifier ( $\frac{1}{2}$  6SL7). The time constant of this discharge circuit was approximately 10 milliseconds, neglecting the action of its biasing circuit. A third rectifier ( $\frac{1}{2}$  6SN7) provided the bias for the rectifier in this discharge circuit, the bias being a d-c potential proportional to the amount of reverberation present at any instant. The discharge of the negatively charged capacitor was thus controlled by the magnitude of the reverberation at any instant, and the rate of recovery of gain of the receiver was also a function of the reverberation since the gain depended on the voltage on this capacitor.

The maximum available voltage gain in the receiver was 150 db, measured from the input grid (rms a-c volts) to the d-c amplifier output (d-c volts); maximum voltage output possible without distortion was about 90 volts (d-c). Figure 95 shows the output-versus-input characteristic. The receiver had a band width of about 2 kc at 3 db down from the maximum, as indicated by the i-f filter response shown in Figure 96. The mixer oscillator (86-kc) was tunable over a band from about 80 to 91 kc, so that the receiver itself was tunable from 20 to 31 kc. The receiver introduced no measurable electrical noise by comparison with normal water noise.

The cathode-ray tube in the EPI first showed a perceptible brightened spot for a voltage of 1.8 volts with respect to ground, applied to the brightening electrode. For an accelerating voltage of 3,600 volts, a brightening voltage of 38 volts made the spot on the tube face begin to defocus. For this reason, the voltage output from the receiver was limited so that it would not be greater than 38 volts. This was accomplished in the installation on the USS CYTHERA by adding a rectifier ( $\frac{1}{2}$  6SL7) as a limiter at the output, biased so that it began to limit at 38 volts.<sup>6</sup>

Under normal darkened sound room conditions, with the intensity control on the EPI adjusted so that the spot was just not visible in the absence of any signal, brightening was observed for voltages of slightly over 1 volt applied to the brightening electrode. Therefore, it was necessary to keep voltage outputs arising from electrical and water noise down to about 1 volt. It was found that with an overall gain of about 130 db (including preamplifier), water noise just began to brighten the spot on the cathode-ray tube. Since the preamplifier had a gain of 33 db, the gain of the receiver for this measurement was about 100 db, representing its greatest useful gain.

The intensity control on the cathode-ray tube could be used to suppress unwanted noise so that brightening would not be noted until the brightening voltage reached a value considerably greater than 1 volt. Under such circumstances, it would be possible to overlook weak signals which were only of the order of magnitude of the noise signal. However, very strong signals could be received under these conditions without defocusing. This was a desirable situation for strong signals since the defocusing effect led to poor estimation by the operator of the angular position of the spot.

The ideal situation would be to increase the range

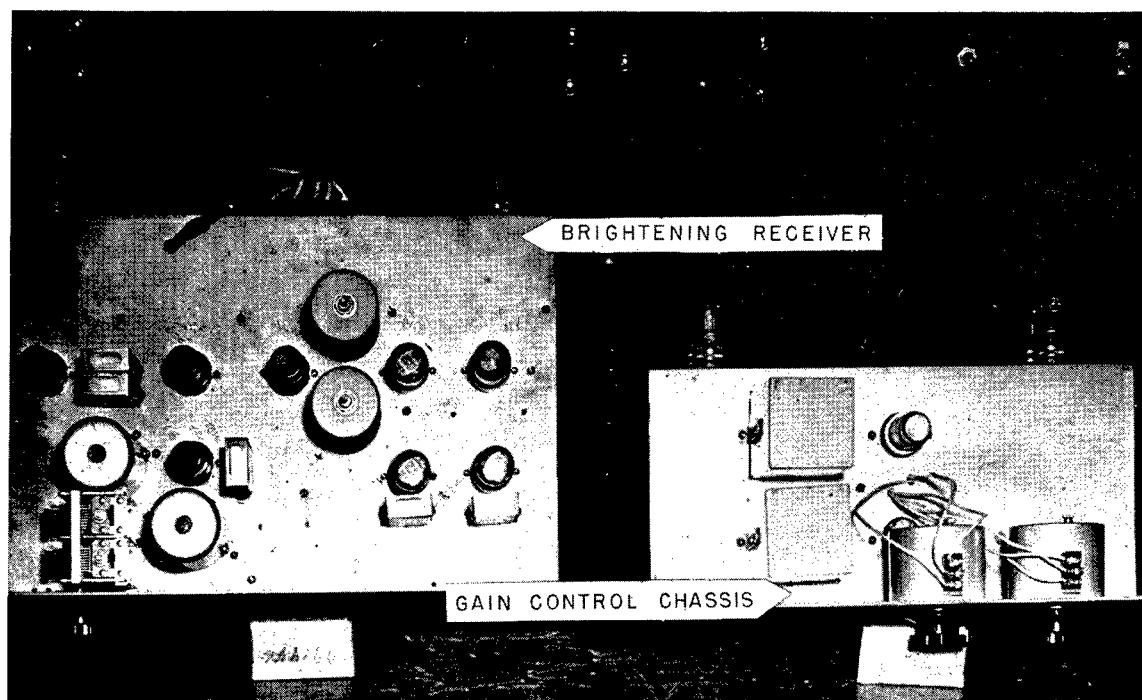


FIGURE 97. Top view of scanning receiver chassis and gain control chassis.

of brightening of the cathode-ray tube without defocusing, in order that both weak and strong signals could be obtained at the same time without changing the intensity control. One means of doing this would be to increase the accelerating voltage on the cathode-ray tube. Another method would be to increase the effect of the limiter at the output of the brightening receiver, so that strong signals would all be limited to the same voltage output value.

Figures 97 and 98 are photographs of the brightening receiver, and show the construction and layout of the various components. Considerable care was taken to keep signal lead wiring down to a minimum because of the high gain originally thought necessary. The receiver proved perfectly stable at full gain. Power for operating the receiver was taken from the power supply on the sweep chassis. Figure 99 shows the position of the brightening receiver in the receiver rack.

#### 6.6.3 BDI Listening Receiver for 26-kc Depth-Scanning Sonar

The BDI listening receiver used in the depth-scanning sonar installed on USS CYTHERA was designed to incorporate in one unit the function of a listen-

ing receiver, giving outputs to loudspeaker and range recorder, and that of a BDI receiver, giving an output to the bearing deviation indicator scope. Any BDI receiver requires two channels. It was advantageous to use a sum-and-difference type,<sup>58</sup> since one of the two channels (the sum channel) could also be used as the listening channel. This type of circuit also had the advantage of inherently maintaining a high order of accuracy in zero deviation bearing, while having only relatively modest requirements on equality of gain and phase shift in the two channels. In addition it was possible, by utilizing the new principle of 2-phase heterodyning, to achieve tunability over a wide frequency range.

Figure 100 shows a block diagram of the BDI listening receiver. The general principle of the sum-and-difference type of BDI circuit used was as follows: (1) take the signals from the two halves of a transducer; (2) add them vectorially and amplify the resultant signal in one (sum) channel; (3) subtract them vectorially and amplify the resultant signal in another (difference) channel; (4) shift the relative phase of these resultant signals by 90 degrees so that they are brought into phase (plus or minus); and (5) combine the outputs of the two channels in a phase-sensitive rectifier to give a d-c voltage for operation of

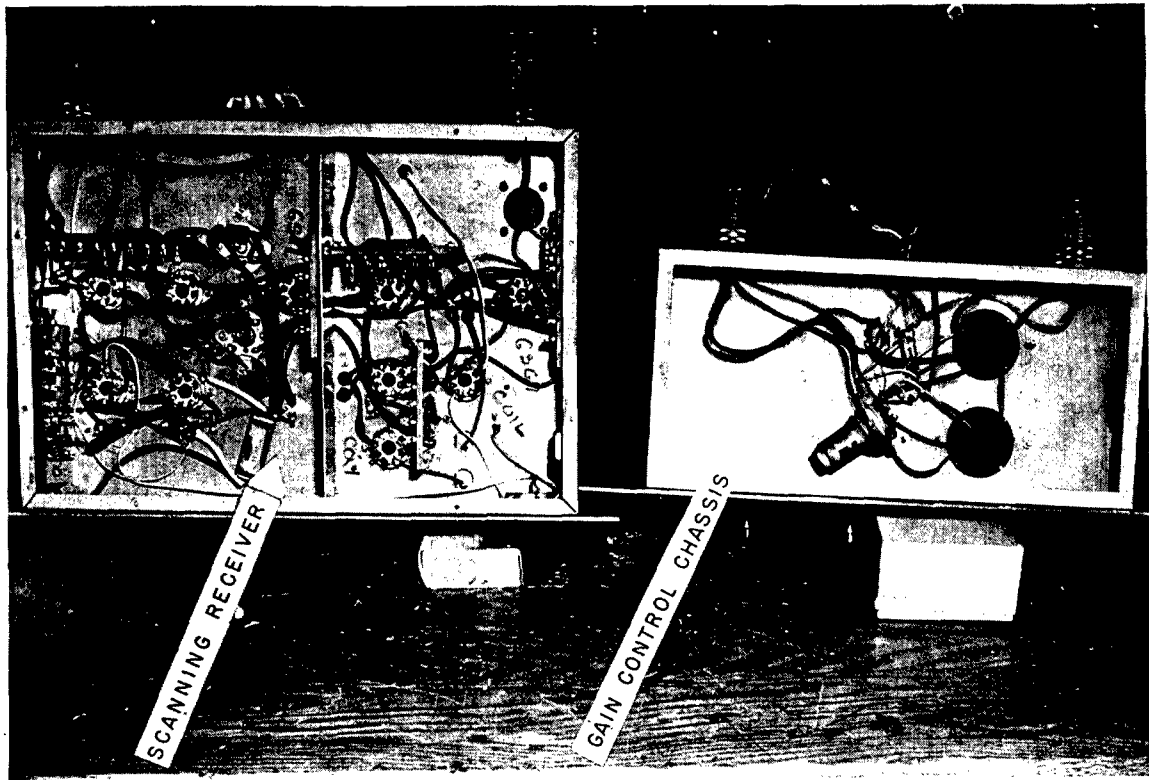


FIGURE 98. Bottom view of scanning receiver chassis and gain control chassis.

the BDI right-left indicator. The vector relations involved for equal gains in the two amplifier channels are illustrated in Figure 101.

This BDI listening receiver required the construction of two amplifier channels which preserved relative phase and amplitude up to the point of the phase-sensitive detector, except that a 90-degree relative phase shift between the channels was required at some point in the circuit prior to the phase-sensitive detector. In this receiver, the 90-degree relative phase shift was introduced between the local oscillator and the injection signal points at the modulators (mixers) in the two channels. This procedure took advantage of the easy tuning of a superheterodyne circuit, while maintaining the required 90-degree phase differential over a wide frequency range by combining a lead line and a lag line. Relative phase shift in the two amplifier channels was held to within  $\pm 15$  degrees. This small shift was assured by careful construction of the circuits providing the selectivity, which were band-pass filters following the modulators, and by using identical feedback-stabilized amplifiers in the two channels. Relative gain was kept within  $\pm 1$  db throughout the range of manual and reverberation-

controlled gain. This gain was assured by using varistor vario-losser circuits controlled from a common source for each channel. Such a varistor circuit used a d-c control voltage which varied the attenuation of signal voltage through the circuit. Because a d-c signal voltage was used, control was possible from a remote position. It was desirable to have suitable filtering of the control voltage at the point of application to eliminate the effects of pickup along the remote connecting wires. Because of the uniformity among a stock group of varistors, the variation of loss through them for a given control voltage was nearly the same; and an application of the same control voltage to two circuits in two different channels introduced the same loss. Prior to the phase-sensitive rectifier, amplification by vacuum tubes was introduced only in the form of feedback-stabilized dual-stage units, thereby separating the functions of gain and gain control. Only two tube types were utilized in design and construction of this amplifier, 6SL7 and 6V6.

The wiring diagrams for this receiver are shown in Figures 102, 103, 104, and 105. The outputs from the two preamplifiers connected to the two listening com-

CONFIDENTIAL

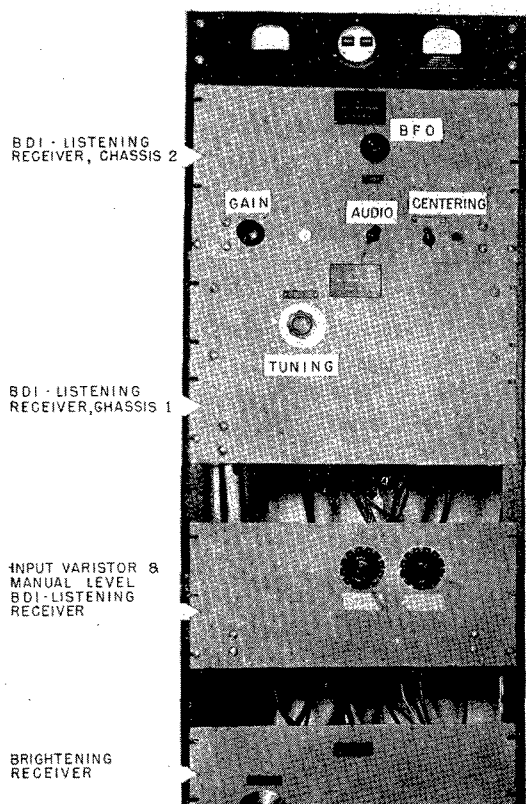


FIGURE 99. Rack mounting for receivers.

mutators (sum-and-difference listening commutators and respective preamplifiers) were connected to the sum-and-difference channel inputs in the first chassis of the receiver. Transformers at the inputs to the two channels coupled the signals to two varistors used as vario-losser circuits for RCG, whose outputs were transformer-coupled to bridge-type balanced modulators using varistors. A local oscillator circuit, using one-half of a 6SL7 tube whose frequency was centered at 33 kc, was coupled through one half of a cathode-follower tube (6SL7) to two phase-shifting circuits. This local oscillator was tunable over a range from 31 to 35 kc; since the intermediate frequency was 7 kc, the receiver was tunable from 24 to 28 kc. One of the two phase-shifting circuits was a 45-degree lead line which fed an amplifier tube ( $\frac{1}{2}$  6SL7), the output of which was coupled to the varistor modulator of the difference channel. The other phase-shifting circuit was a 45-degree lag line which was connected to an amplifier tube ( $\frac{1}{2}$  6SL7) whose output was coupled to the varistor modulator of the sum channel. The

output from the varistor modulator in each channel was coupled to a band-pass filter which selected the difference frequency. This filter was a constant- $k$  section with a design impedance of 600 ohms. It had a band width of 2.6 kc, 3 db down from the maximum, centered at 7 kc. Its rejection requirements were eased by the fact that the modulator was a balanced carrier-suppression type. To pass a total doppler shift of  $\pm 40$  knots, including both own doppler and target doppler, a band width of 1.4 kc was required. The actual band width used was greater than this to avoid possible phase differences between the two filters in the two channels near the cutoff frequencies. The response characteristic of one of these filters is shown in Figure 106. It was found that the two filters agreed in response over the pass band to

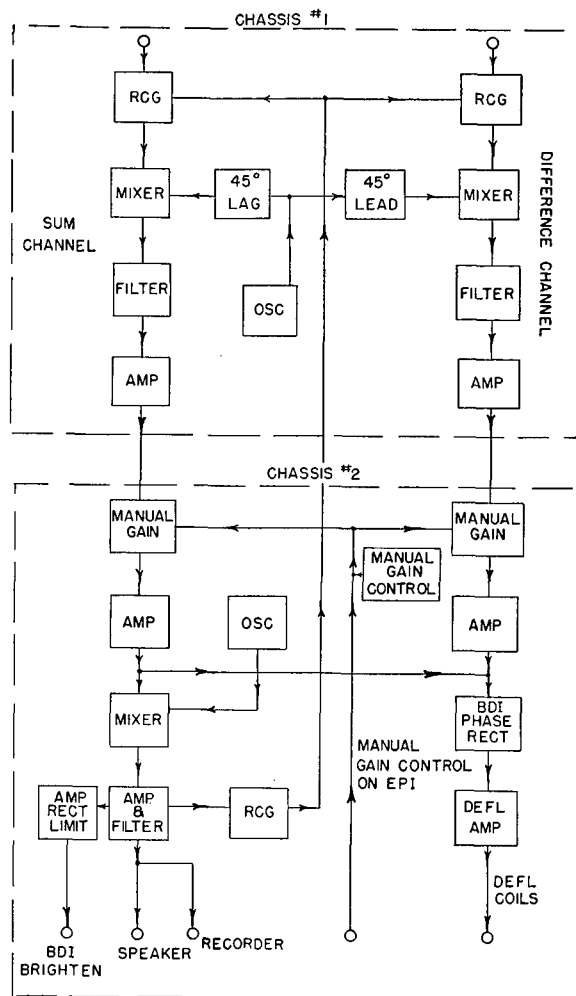


FIGURE 100. Block diagram of BDI listening receiver, 26-kc DSS.

CONFIDENTIAL

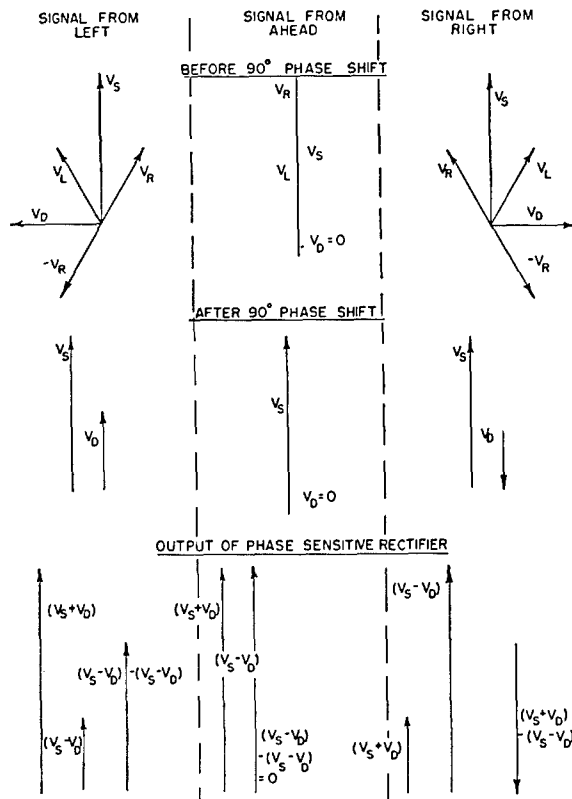


FIGURE 101. Vector relations for sum-and-difference BDI.

within  $\pm 1/4$  db. As shown in Figure 107, maximum phase differences between the two filters were within  $\pm 2$  degrees over the range to the  $-30$  db down points in the frequency response.

Since a 90-degree phase difference had been introduced between the voltages applied from the local oscillator to the two varistor modulators, there was a 90-degree difference between the side-band signals selected by these two band-pass filters. The output of each of the filters was transformer-coupled to a two-stage amplifier (6SL7), which was stabilized by about 18 db of negative feedback and which had a gain of about 40 db. The output of this amplifier was transformer-coupled at a 600-ohm level (in each channel) to the second chassis, the signals in the two channels were applied to two varistor vario-losser circuits for manual gain control. Approximately 40 db of gain control was available, this control being achieved by applying d-c voltage from a voltage divider to both of the varistor circuits simultaneously. The signals from these varistors were amplified by two-stage amplifiers (6SL7) identical to those described above, whose outputs were applied to a phase-sensitive rectifier circuit using a 6SL7 tube. The filtered output from this

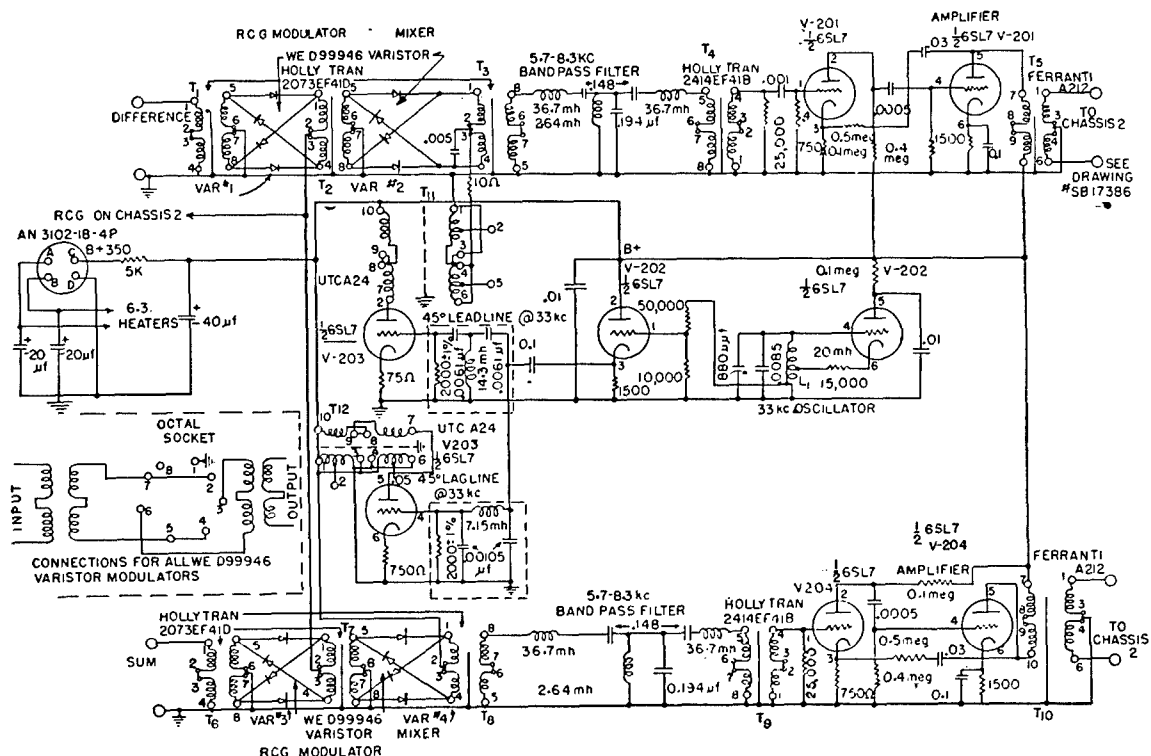
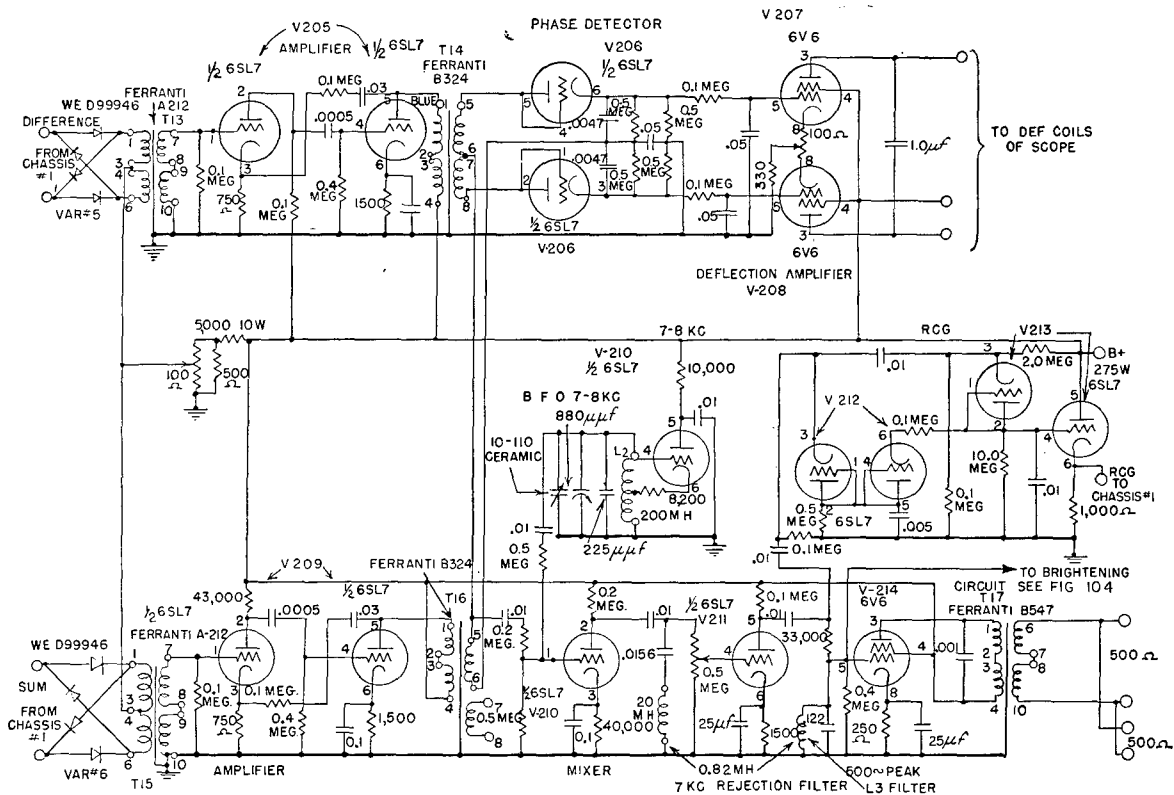
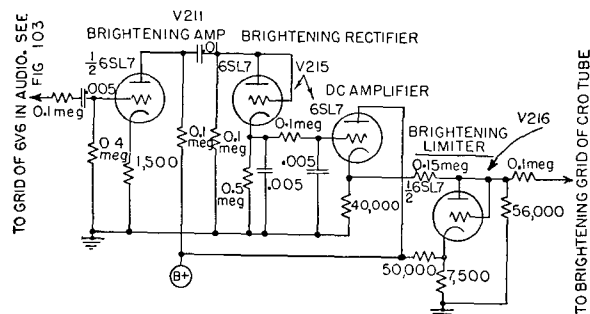


FIGURE 102. BDI listening receiver chassis, No. 1.

CONFIDENTIAL



rectifier was a push-pull d-c signal which fed the grids of a push-pull d-c amplifier (6V6 tubes). The plates of the amplifier were connected to the deflection coils of the BDI right-left indicator in order to give the right-left indication. A small potentiometer in the cathode circuits of the 6V6 tubes allowed for a centering adjustment when tubes were changed. When the amplifier was in use, no centering adjustment was necessary.





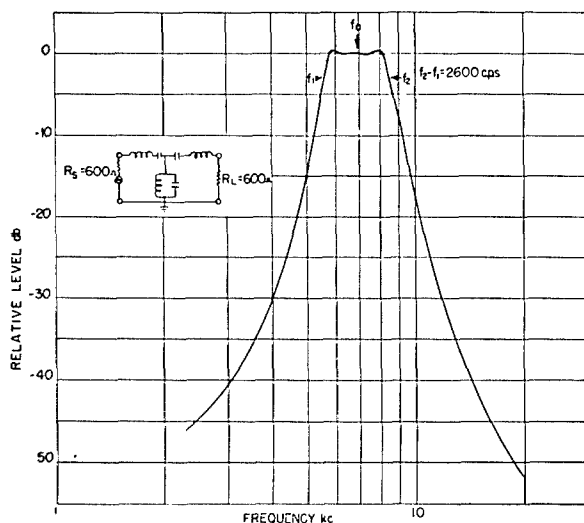


FIGURE 106. BDI listening receiver, i-f filter response.

signal of 7.5 kc from a beat-frequency oscillator was also applied to the modulator, whose output was filtered to remove the high frequencies and to choose the difference frequency. This difference frequency (500 c) was amplified by the second  $\frac{1}{2}$  6SL7 and the output was coupled to an audio filter, peaked at 500 c to reduce further the amount of intermediate-frequency (7-kc) signal present. The audio output signal from the amplifier ( $\frac{1}{2}$  6SL7) was applied to a power amplifier (6V6) whose output was passed through a transformer to drive the loudspeaker and the range recorder at 500-ohm impedance level with a maximum undistorted output capability of about 2 watts.

Further, the audio signal from the  $\frac{1}{2}$  6SL7 amplifier was applied to the brightening circuit for the BDI scope. In this circuit, the signal was amplified in a

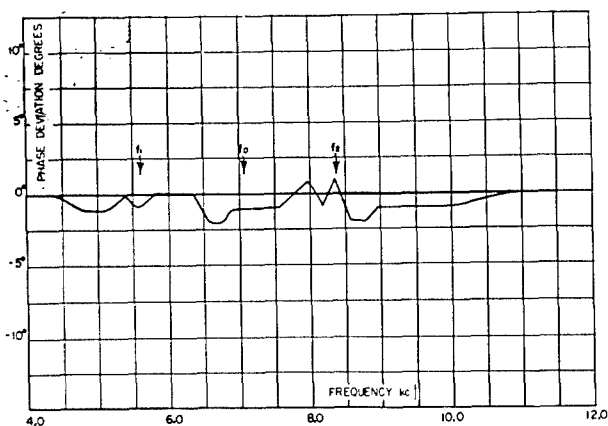


FIGURE 107. BDI listening receiver, phase differences between channels versus frequency.

$\frac{1}{2}$  6SL7 triode and then rectified in a  $\frac{1}{2}$  6SL7 used as a diode. The d-c output of this tube was filtered and fed to a d-c amplifier ( $\frac{1}{2}$  6SL7) used as a cathode follower, whose output was limited by a biased rectifier ( $\frac{1}{2}$  6SL7 used as a diode). The limited signal was applied to the brightening grid of the BDI cathode-ray tube.

Audio signal from the  $\frac{1}{2}$  6SL7 amplifier was also applied to an RCG circuit. This circuit was identical to that in the brightening receiver (see Section 6.6.2 on scanning receivers), except that the negative voltage developed on the RCG capacitor was applied to the grid of a  $\frac{1}{2}$  6SL7. The d-c voltage developed across the cathode resistor for this tube was connected to the RCG varistor at the input of each receiver channel. The total range of RCG thus available was 40 db in each channel.

A power supply chassis provided filament and positive voltage for the BDI listening receiver, also a negative voltage (350 volts) for the sweep on the BDI indicator.

The maximum gain of the amplifier, measured from the input grids of the preamplifiers associated with the receiver to the grids of the deflection amplifiers, was 140 db for each channel. Variation in gain was accomplished by varistors as described above. Since the control voltage, either in the manual gain control or the RCG control, was applied to a pair of

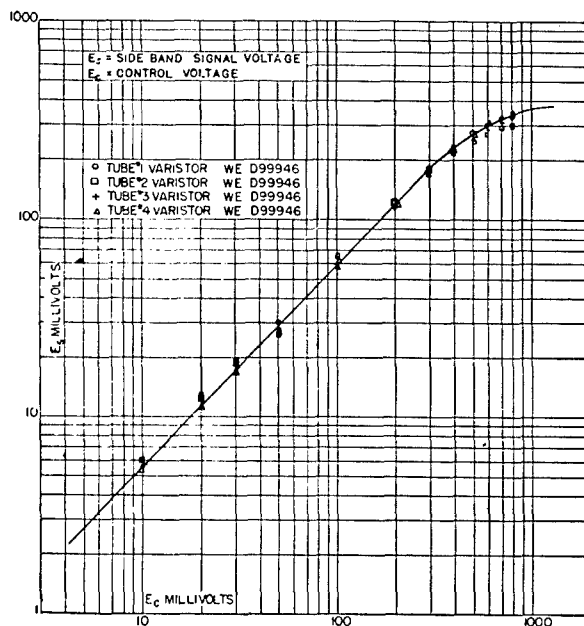


FIGURE 108. Varistor balanced modulator, output versus input, various varistor units.

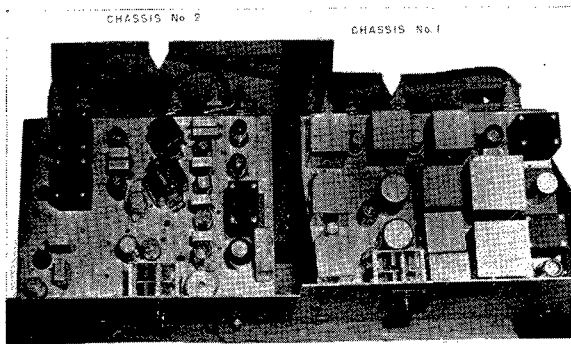


FIGURE 109. Top view of BDI listening receiver.

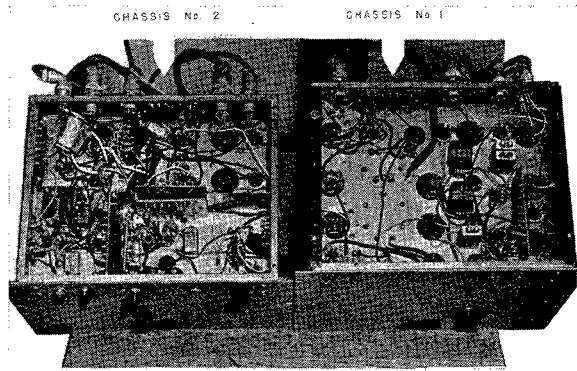


FIGURE 110. Bottom view of BDI listening receiver.

varistors simultaneously (one in each channel), the gain in the channels tracked to within one-half decibel throughout the control range of 80 db, (40 db of manual control and 40 db of RCG). Figure 108 shows the control range for four varistors.

Under normal darkened sound room conditions, the cathode-ray tube used in the BDI first showed a brightened spot for a voltage of about 1 volt, with respect to ground, applied to the brightening electrode. Since the maximum voltage allowable without defocusing was about 38 volts, the brightening limiter tube at the output of the brightening circuit was set to begin to limit at this voltage. To avoid any brightening from electrical noise and water noise, voltages due to such noises had to be kept down to about 1 volt at the output of the brightening circuit. It was found, as for the scanning receiver, that water noise at the input to the preamplifiers overshadowed any electrical noise, and amounted, under average conditions, to about 1  $\mu$ v on the first grids of the preamplifiers.

In order to obtain proper operation of this receiver, considerable care had to be taken in actual layout and construction. The channels were made as symmetrical as possible to avoid such incidental phase shifts and variations in gain as were caused solely by placement of components. Figure 109 shows the top of receiver chassis No. 1 and No. 2, and Figure 110 shows the bottom view of the same two chassis. Figure 99 shows the rack mounting of the receiver.

Following bench tests, a preliminary test of the BDI listening receiver was made aboard the USS GALAXY, demonstrating BDI operation of the system on a QC projector and proving the tunability of the receiver. Preliminary values of gain and RCG were set up at this time. Later this BDI listening receiver

was used on the installation of depth-scanning sonar on the USS CYTHERA. Since it was a first development unit, it was subjected to a number of tests and modified in a number of particulars before it operated properly.

The gain-control circuits were subjected to considerable attention. The range of RCG available was only 40 db, obtained by means of the varistor circuit at the input to the first chassis of the receiver. This was found to be insufficient, partly because of the very strong bottom echo. For this reason, the set of varistors used for gain control purposes at the input of chassis No. 2 were connected for RCG operation, giving a total of 80 db of RCG range. The maximum gain of the receiver was set manually. Any reduction of gain from the maximum possible from the receiver then limited the amount of RCG available. Thus, if the maximum gain was manually lowered by 40 db, only 40 db of useful RCG was available. Later tests on the operation of the receiver indicated that the varistor gain-control circuits caused some phase distortion between the signals in the two channels as a function of the control signal. This was important because the individual varistors behaved differently, destroying the uniformity of phase between the two channels of the amplifier. Further, for certain values of high-frequency signal and control signal, the varistors produced considerable distortion. This did not cause trouble in the first chassis, since the varistors' gain-control circuit was followed in the receiver by a filter section selecting the desired frequency and rejecting any distortion products. However, in the second chassis no such filter was present, and the distortion products were applied directly to the phase-sensitive rectifier. Again, different varistor units did not distort in the same manner, so that the uniform-

CONFIDENTIAL

ity of operation between the channels was destroyed. The effect of distortion was more important in chassis No. 2 because the signal was at a higher level than it was at the input of chassis No. 1. To overcome this difficulty of distortion, it was essential that the control voltage on the varistors be kept above a few tenths of a volt, and this left only a small range of operation of the circuits. To increase the range again to a useful value, a similar varistor circuit was placed just prior to the input to chassis No. 1 and a pair of attenuators were added at this same point to provide manual gain control. All manual gain control was centered in these attenuators, and the varistor circuits were set for a constant control voltage and, therefore, for reasonably good operation in the RCG circuits. Figure 97 shows a top view of this extra gain-control chassis, and Figure 98 shows a bottom view of the same chassis.

The RCG circuit, as originally designed and built, provided variation in gain which was initiated by the beginning reverberation level and then varied afterward according to the continuing reverberation level. The strength of the bottom echo was great enough to reinitiate the gain variation and, hence, to modify the proper RCG action by reducing the gain to a considerable extent for ranges at and just beyond the value equal to the depth of the bottom. For this reason, initiation of the gain variation by the RCG circuit was taken from the blanking pulse of the sweep chassis, so that reinitiation prior to the next transmission was impossible.

Because they introduced unequal phase shifts, the transformers coupling the two-stage amplifiers in the two channels of the second chassis to the phase-sensitive rectifier were replaced by two other transformers with better characteristics. The phase inequalities were thereby reduced and the phase-sensitive rectifier operated properly.

Considerable difficulty was experienced due to the 7.5-kc heterodyne oscillator which produced the 500-c audio signal. It was observed that this signal was leaking into the intermediate-frequency stages of the receiver which operated at 7 kc. It was very difficult to remove this leakage completely because rearrangement of parts, more effective shielding, and a more suitable selection of frequencies would have been necessary.

BDI deflection curves were taken for the receiver by using a signal from the deep monitor as a test signal. Figure 111 shows the curves taken with the bear-

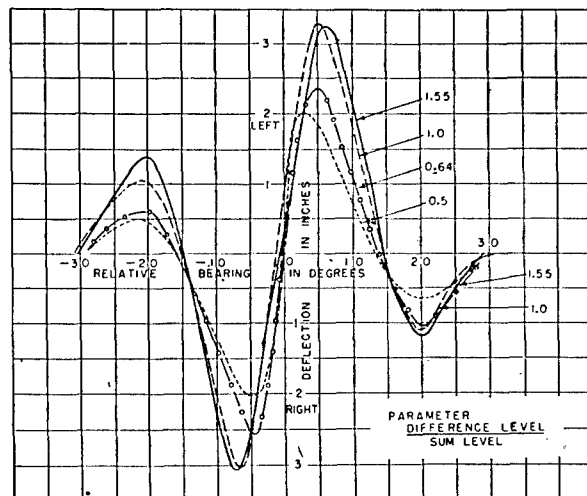


FIGURE 111. Measured BDI deflection curves.

ing of the deep monitor arbitrarily set at 0 degrees. The fact that the curves do not all intersect the horizontal axis at 0 degrees is primarily because it was not possible to set the transducer accurately to a desired bearing. While taking data, the gain of the difference channel was held constant, and relative gains of the two channels were varied by changing the gain of the sum channel. The curve for the ratio equal to unity ( $\theta = 90^\circ$ ) was taken as the best curve for normal operation.

The tests on the USS CYTHERA and first construction difficulties led to several suggestions for improved design and construction of receivers for this system. The necessity for uniformity of amplitude and phase for the two channels of the amplifier limits the use of varistors for gain control purposes to the regions of varistor operation which do not produce phase or amplitude distortion. Such distortions can be accepted only if they are identical for each varistor circuit. Under these conditions, it is desirable to follow them with suitable filters to reject all harmonics generated. The use of varistors as modulators is satisfactory, provided a filter is used to select the proper side band. Since there is a restriction of the operation range of varistor vario-lossers when they are used for gain control purposes, it was proposed that auxiliary manual gain controls be provided for the two channels. These would be in the form of standard matched attenuators mounted on a common shaft and operated remotely by a servo mechanism. It was also suggested that other forms of circuits using varistors be investigated, such as that in which the varistor forms one part of a potentiometer.

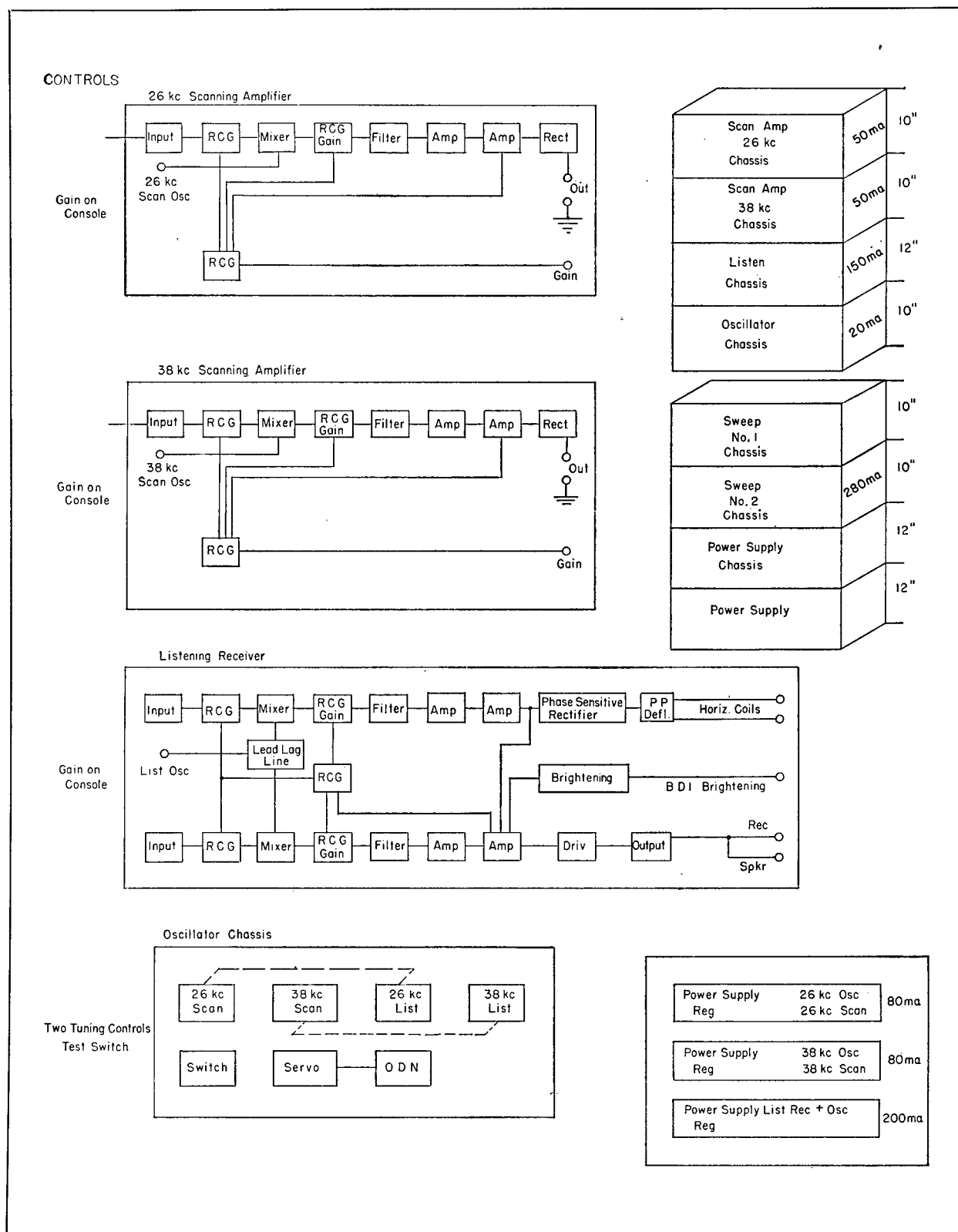


FIGURE 112. Block diagram of integrated Type B sonar scanning receivers.

CONFIDENTIAL

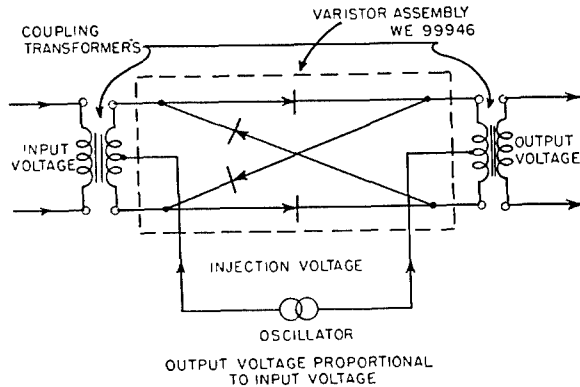


FIGURE 113. Varistor-bridge balanced-modulator circuit.

A better selection of frequencies for the receiver oscillators might make it possible to avoid cross talk between the intermediate-frequency channel and both local oscillators, and still allow maximum simplicity in constructing filters used in the intermediate-frequency portion of the receiver.

#### 6.6.4 Receivers for Integrated Type B Sonar General Considerations

The receivers for integrated Type B sonar were designed so that they would include the best features of and suggestions for improvements arising from tests on the 26-kc DSS receivers. In general, therefore, the designs were similar to those described in the two previous sections. Three receivers were designed: these were an azimuth-scanning receiver, a depth-scanning receiver, and a BDI listening receiver. Original plans called for these units to be built as nearly identical as possible so that parts and circuits could be standardized for manufacturing and maintenance. Thus, in this design, all preamplifiers would be made the same. The receivers are to be provided with suitable oscillators so that a common intermediate frequency, and, therefore, identical intermediate-frequency channels, can be used for all three receivers. Amplifier sections in the receivers are built as packaged units incorporating feedback-stabilized sections to give suitable gain and phase-shift stability.

Control of these receivers was designed to allow independent tuning of depth or azimuth systems. At the same time, a switching arrangement is to be provided to use the BDI listening receiver on either the depth or azimuth system. Gain control is carried out by a varistor vario-losser circuit. Other methods were suggested because difficulties were experienced with

the bridge-type vario-losser circuits (including cathode-bias, grid-bias, and attenuator controls). The final design will await further experimental work. The listening receivers are to be supplied with computed corrections for own-doppler frequency shifts but no doppler correction was planned for the scanning receivers. The possibility of applying *own-doppler nullifier* [ODN] to the scanning channel and coordinating the scanning and listening ODN functions is discussed in Chapter 10. A test switch is to be provided for suitable routine test operations.

#### 6.6.5 Preamplifiers for Integrated Type B Sonar

Figure 73 shows the wiring diagram for the preamplifier. This design does not include tuning so that the preamplifier may be used in either the depth or azimuth system. The design is conventional, using a two-tube resistance-coupled amplifier with negative feedback applied from the plate of the second stage to the cathode of the first stage. The output from this two-tube amplifier is coupled to a tube used as a cathode follower, to provide a low impedance output for coupling to succeeding stages of the receivers. Preliminary attempts to improve stability still further, by including the third tube in the feedback loop, showed that such a design was undesirably critical in choice of components.

The power supply is conventional. A high resistance is located between the power supply and the high-voltage input to the amplifier. This resistor is short-circuited by means of the send-receive relay during the receiving interval to allow normal operation of the preamplifier. During the transmitting interval the resistor is not short-circuited and the gain of the amplifier is very low to minimize leakage voltage from the transmitted signal.

This preamplifier was designed for mounting on the cradle supporting a commutator, and the chassis layout was planned with this in mind. The chassis is shock-mounted to avoid vibration from the commutators or other sources.

#### 6.6.6 Scanning Receivers for Integrated Type B Sonar

The preliminary block diagram showing the design of the two scanning receivers is shown in Figure 112. In this design, an input circuit is coupled to an

RCG circuit, followed by a mixer to produce the intermediate frequency. The mixer output is coupled to another RCG circuit, which also incorporates the manual gain circuit. Next is the intermediate-frequency filter, which selects the proper side band from the mixer. The output from the filter is amplified and passed to a rectifier which includes a limiter. This rectified output is then applied to the brightening grid of the cathode-ray tube in the appropriate indicator.

These two receivers, for the depth and azimuth systems, were designed to be identical except for the input circuits. Each input circuit includes a band-pass filter which selects the proper signal from the associated preamplifier. Thus, for the azimuth system the signal from the preamplifier is 26 kc, and the filter is set for a center frequency of 26 kc. Likewise, for the depth system the signal from the preamplifier is 38 kc, and the filter is set for a center frequency of 38 kc. The RCG and manual gain-control circuits use varistor units. Coupling to the varistor circuits utilizes transformers because of the low impedance of the varistor bridge circuits. The filter in the input circuit is of low impedance, since it couples from a cathode follower in the preamplifier into a low-impedance varistor circuit. Where filters are followed or preceded by low-impedance varistor circuits, the filters are of balanced form in order to avoid the use of coupling transformers. The filters at the inputs of the receivers are carefully constructed to be as nearly identical as possible. The filters in the intermediate-frequency section of the receivers are also carefully constructed so that they can be interchangeable and can have definite values of loss and phase-shift characteristics. The two scanning receivers are, therefore, practically interchangeable in this design except for the input filters.

The oscillators for these receivers were designed as parts of a special oscillator chassis, to allow tuning of the complete depth and azimuth systems by means of only two tuning controls. The oscillators for the scanning receivers are of conventional design, and the tuning capacitors are mounted on the two shafts used for tuning control of the two systems.

#### 6.6.7 BDI Listening Receiver for Integrated Type B Sonar

As shown in Figure 112, the BDI listening receiver for integrated Type B sonar is to the sum-and-differ-

ence type.<sup>58</sup> The general operation of the receiver is the same as before. The input circuits were designed to include the filters necessary to choose the proper frequency from the outputs of the two preamplifiers. Switching is provided to connect the proper local oscillator, depending on the use of the receiver in the depth or azimuth system. The same switch connects suitable lead-lag lines to produce the 90-degree phase shift of the injection signals to the two mixers. The outputs from the receiver are to be applied to the BDI scope, the recorder, and loudspeaker, and are to be utilized in the RCG circuit which operates on the general principles discussed in the two foregoing sections.

The two channels of this receiver were designed to be as nearly identical as possible. The filters in the input circuits are identical with the ones used in the scanning receivers and are built with sufficient care so that the phase and amplitude characteristics of the two filters are close enough to meet the requirements of uniformity necessary between the two channels. The RCG and manual gain-control circuits and mixers use varistor units. Coupling to the varistor circuits is accomplished the same way as in the scanning receiver. The filters in intermediate frequency portions of the channels are identical in center frequency with those used in the scanning receivers, and constructed with sufficient care to meet the requirements of phase and amplitude necessary for the BDI listening receiver. A narrower pass band is desirable in order to take full advantage of the longer pulse length. The amplifiers in the receiver are composed of two-stage feedback-stabilized units as described earlier in the present section. The only exceptions are the driver stage for the audio signal to the loudspeaker and the range recorder, and the d-c deflection amplifier at the output of the BDI phase-sensitive rectifier, which are similar to those used in the 26-kc DSS. The rectifier and limiter in the brightening circuit include a better limiting circuit than that used in the 26-kc DSS.

The choice of the intermediate frequency for the receivers was determined by two factors: (1) ease in construction of the necessary filters; and (2) selection of a frequency that would be sufficiently removed from the various oscillator frequencies to facilitate the elimination of cross talk. The particular value of 18.5 kc was found to satisfy these two requirements fairly well for both azimuth and depth systems of the integrated Type B sonar.

The oscillators for this receiver are of conventional design and were designed as parts of the special oscillator chassis described previously. The oscillators are also provided with variable capacitors controlled by a servo system for ODN.

#### 6.6.8 Control Circuits for Receivers for Integrated Type B Sonar

All three receiver designs described in the previous section use varistor-bridge circuits for both gain control and mixer functions. The varistor-bridge balanced-modulator circuit operated very satisfactorily for the mixer function in the 26-kc DSS, since the injection voltage from the oscillator was always greater than the signal voltage. The output voltage at intermediate frequency, therefore, was always a linear function of the input voltage at received high frequency. The side-band output bore a definite phase relationship to the input signal and injection signal, independent of the level of the input signal. This type of circuit is illustrated in Figure 113. It had the further advantage of balancing out both applied voltages, thus easing requirements on the subsequent filter.

The varistor-bridge vario-losser circuit did not fulfill the gain-control function as well as the mixer function. In use as a gain-control circuit the injection voltage was a variable d-c control voltage, so that the output varied in some manner according to this d-c voltage when the input voltage was constant. This type of circuit is illustrated in Figure 114. The operation of this circuit was reasonably satisfactory when the control voltage was kept always larger than the input signal voltage. The output then was a linear function of the control voltage, and the phase shift between the input and output voltages remained es-

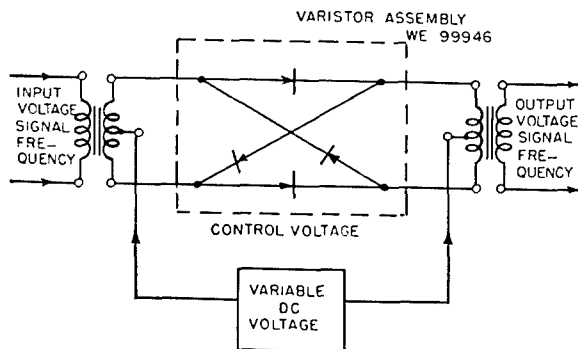


FIGURE 114. Bridge-type varistor vario-losser circuit for gain control.

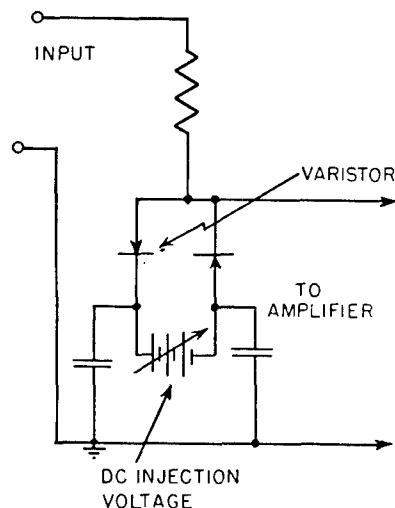


FIGURE 115. Varistor potentiometer gain-control circuit.

entially constant. However, when the control voltage was of the order of magnitude of the input voltage or lower, the vario-losser circuit produced distortion in the output voltage and the phase shift through the circuit no longer remained constant. For these reasons, it was necessary to restrict the range of operation of the varistor vario-losser circuits in the 26-kc DSS. This limited the amount of gain control available for a given vario-losser circuit, so that additional vario-

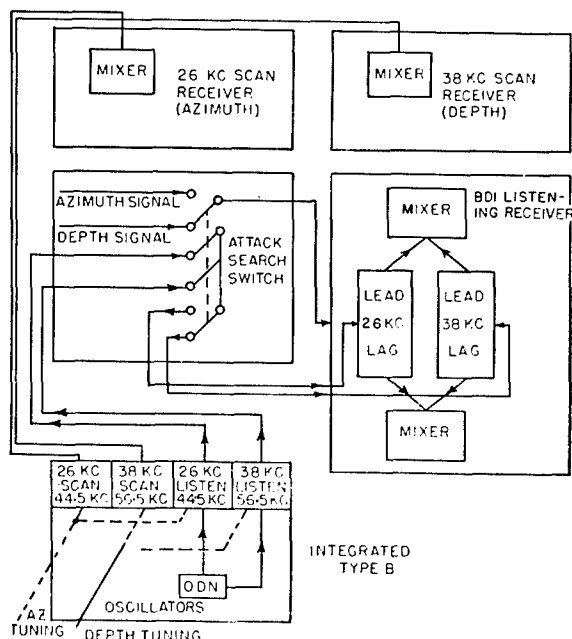


FIGURE 116. Attack-search switch and receiver portion of unicontrol system.

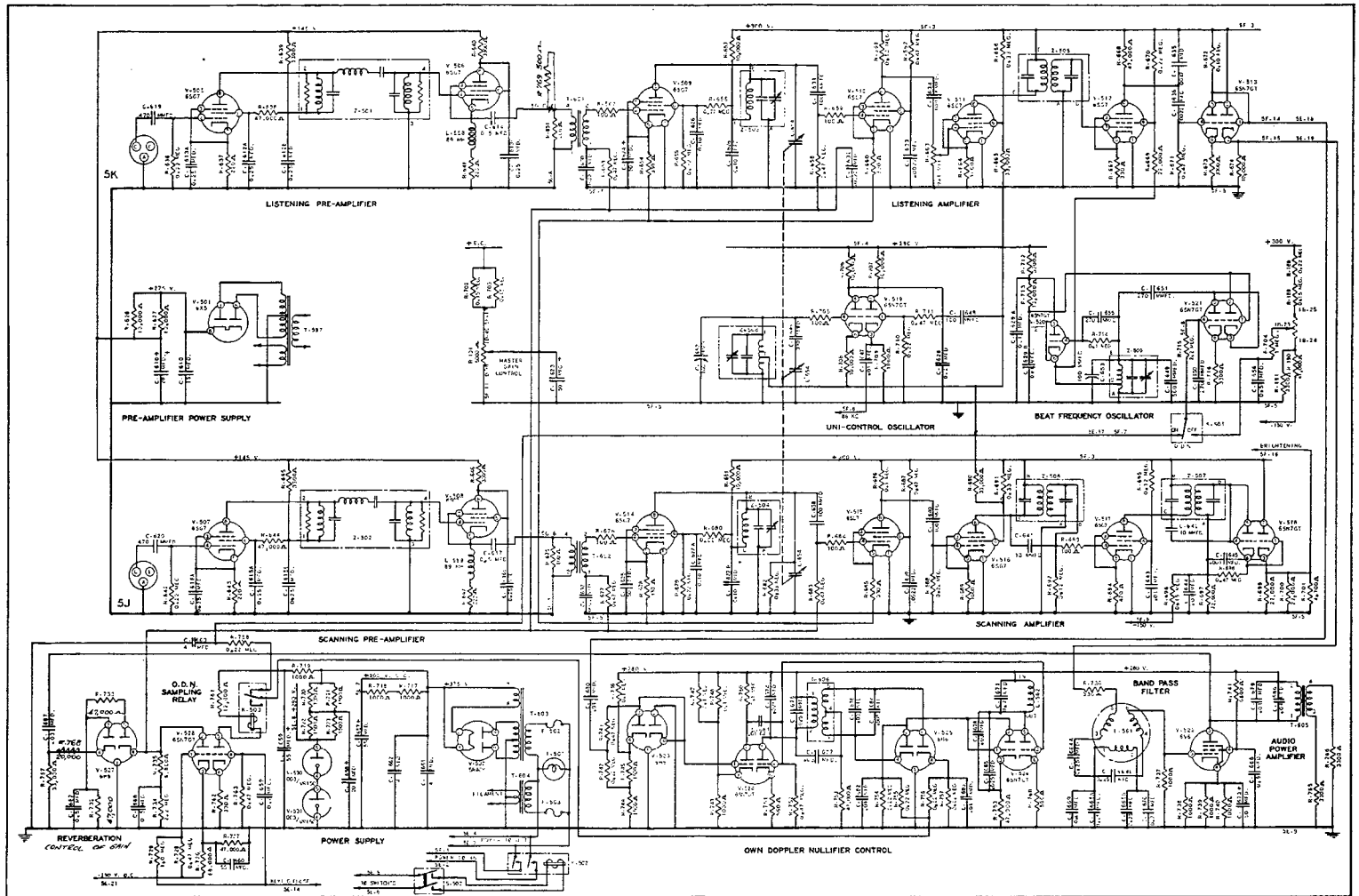
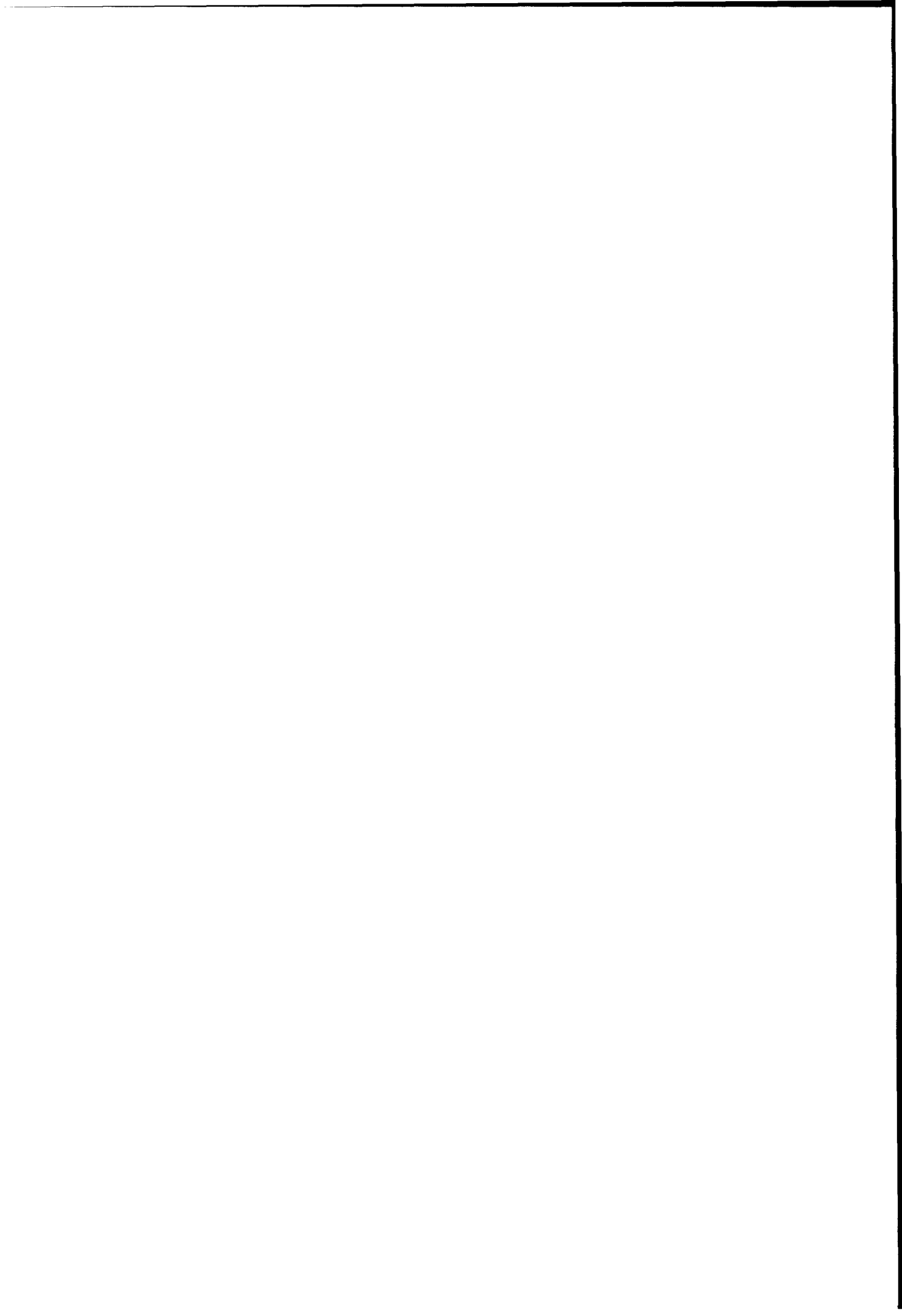


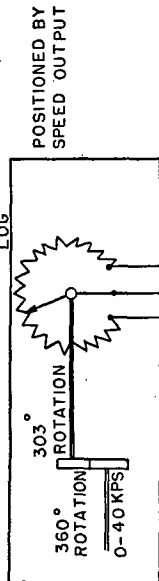
FIGURE 116. Circuit diagram for preamplifiers, receiver, and power supply, Model NQHA scanning sonar.

CONFIDENTIAL





G.R. 214-A 2000 ~  
LOCATED IN PITOMETER



SET BOTH  
POTENTIOMETERS  
TO 16V

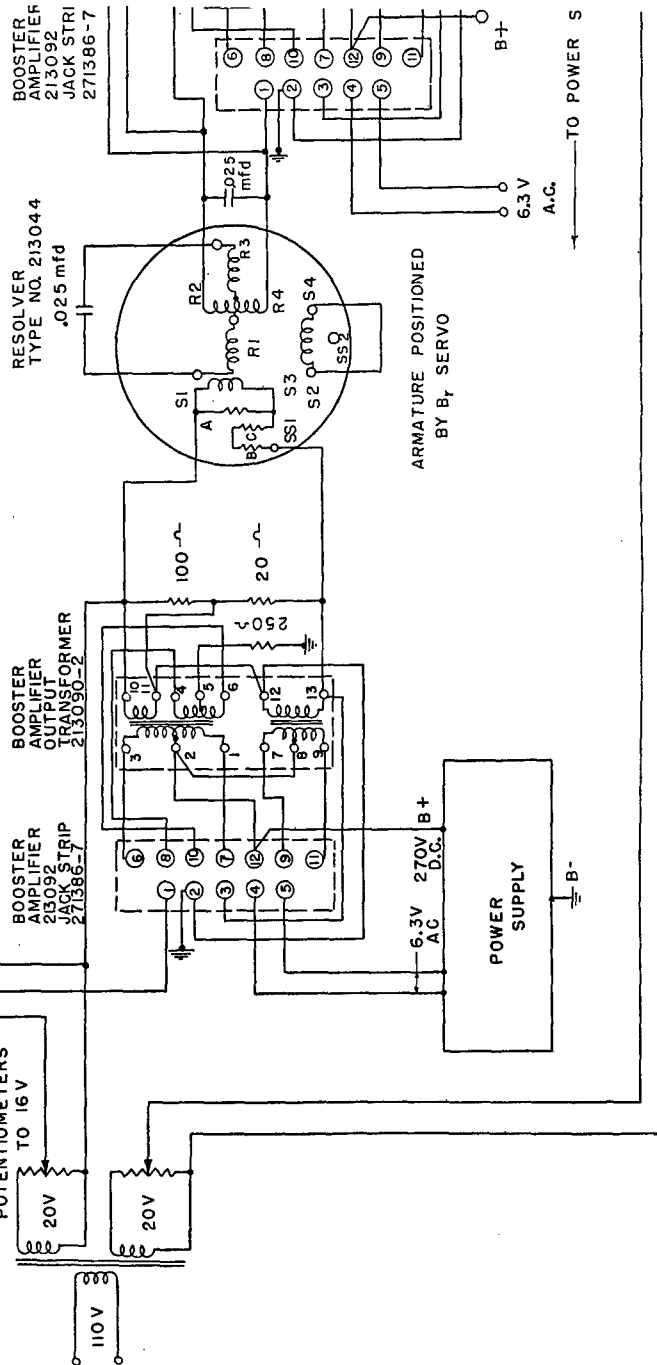
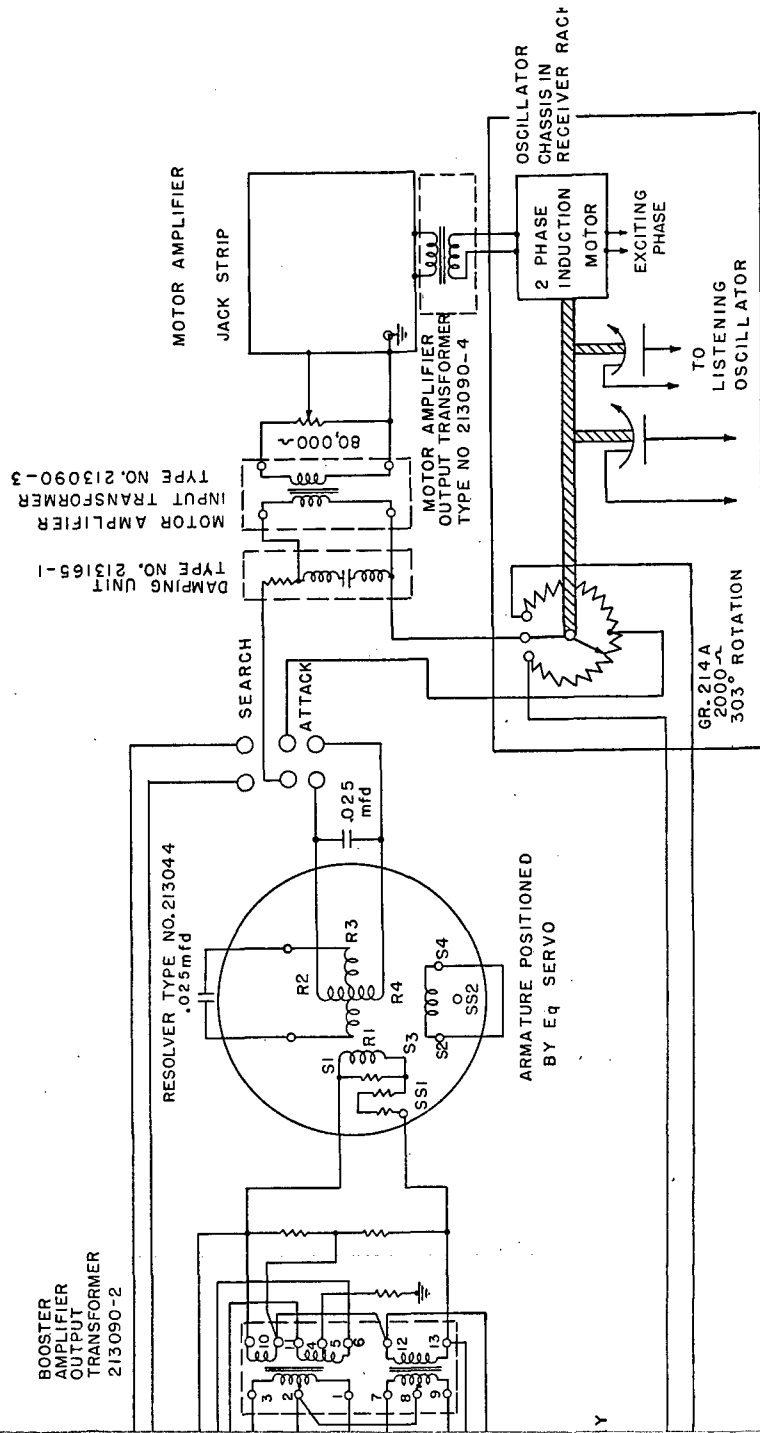


FIGURE 117. ODN





for integrated Type B sonar.

CONFIDENTIAL

2 of 2



losser circuits were incorporated to give the necessary amount of control.

The definite advantage of the varistor vario-losser circuit was that the control was the same for any varistor assembly selected at random, provided that the above restrictions were observed. Also, the control voltage was a d-c voltage, so that remote control was easily available. With these circuits it was readily possible to obtain instantaneous, identical, remotely controlled gain for two channels. This was the most important consideration in recommending their use for gain control in the BDI listening receiver for the integrated Type B sonar. The instantaneous change of gain was extremely useful in obtaining rapid RCG, and the remote feature made remote manual gain control simple.

The remote manual gain-control feature in this design was intended at first merely to vary the maximum d-c voltage applied to the varistor circuits and thus to limit the maximum gain. This method, however, further restricted the amount of RCG available. A separate varistor could be added for this manual gain control. It was suggested to use a pair of attenuators on a common shaft, as a method of applying manual gain control for the two channels of the BDI listening receiver. This method does not lend itself to remote control except by means of a servo system to rotate the attenuator shaft, and it cannot be made instantaneous as is required for RCG. For a single-channel receiver such as the scanning receivers, where tracking between two channels is not required, instantaneous and remote control may be obtained by using a variable d-c cathode bias or grid bias. Such a system was used on the scanning receiver for 26-kc DSS, using cathode-bias control, but could not be used in two channels where identical control is necessary, because the control function changes considerably from one tube to another when chosen from stock.

A potentiometer-type vario-losser circuit as shown in Figure 115 was suggested. This circuit utilizes the variation in impedance of the varistor units as a function of the d-c control voltage, to control the gain of an amplifier stage. It was expected that this method might prove useful if the phase shift, produced by the varistor units as a function of d-c control voltage, was not too great and did not vary appreciably from unit to unit.

It was concluded in the design that gain control should be obtained with varistor circuits if the diffi-

culties with these circuits could be resolved in further investigation. It was also concluded that filters should be added after all varistor circuits in order to remove any harmonics generated.

Tuning control of the receivers is obtained by mounting all the various oscillators on the same chassis. Both tuning capacitors for the azimuth system are mounted on one shaft, and both tuning capacitors for the depth system are mounted on another shaft. Thus only one control will be needed for tuning each system, and the tuning controls will be independent of each other. Unicontrol of frequency (described previously) will be used for each system.

In order to allow operation of the BDI listening receiver in either the depth or the azimuth system, a search-attack switch is used. The functional arrangement of this switch is shown in Figure 116, insofar as it involves the receivers; the unicontrol features are not shown. The attack-search switch connects the proper mixer oscillator to the mixer through the proper lead-lag line. Simultaneously when transferring from search to attack, it transfers the input signal from the azimuth system to the depth system and selects the proper filters at the input to the receiver.

In this design ODN is obtained by means of an electrical-mechanical computer. A diagram of this computer is shown in Figure 117. Principles of ODN correction are discussed in Chapter 10. In order to compute the own-doppler frequency shift, it is necessary to form the product  $S_o \cos B_{rq}$  for the azimuth system, where  $S_o$  is own-ship's speed and  $B_{rq}$  is the relative bearing of the target. This is done by means of a resolver (Arma Type No. 213044). The electrical input is made proportional to own-ship's speed by means of a voltage obtained from the pitometer log. The rotation of the armature of the resolver is made proportional to  $B_{rq}$  by attachment to the servo for  $B_{rq}$ . By virtue of the operation of the resolver, the electrical output is then  $S_o \cos B_{rq}$ . By means of the attack-search switch, this quantity is transmitted (on the search position) to a servo mechanism which positions the rotor of a variable capacitor by the necessary amount to change the frequency of the azimuth mixer oscillator, supplying the BDI listening receiver, so that it compensates for the doppler shift in the frequency of the received sound. Thus, it keeps the intermediate frequency of the receiver constant at all times, except for target doppler shift.

For the depth system, it is necessary to compute the

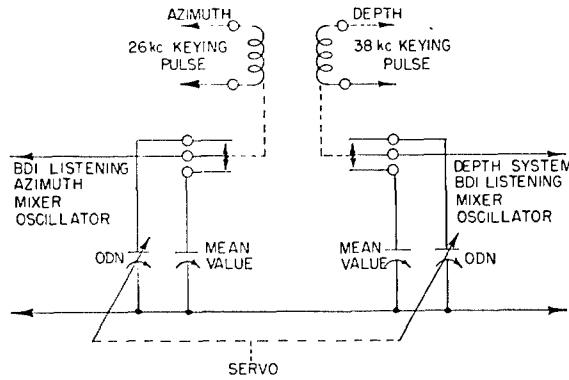


FIGURE 118. ODN and tuning capacitors.

product  $S_a \cos B_{rq} \cos E_q$  as the doppler shift in frequency, where  $E_q$  is the depression angle of the target. To do this, the electrical input to a second resolver is made proportional to  $S_a \cos B_{rq}$ , as described above. The armature of this second resolver is rotated by means of the  $E_q$  servo, described in the previous section on indicators. By the operation of this resolver, the electrical output is  $S_a \cos B_{rq} \cos E_q$ . By means of the search-attack switch, this quantity is applied (on attack) to the same servo mechanism and positions a second variable capacitor on the same shaft as the first. This second capacitor adjusts the frequency of the depth mixer oscillator supplying the BDI listening receiver by the amount necessary to compensate for the doppler shift in the frequency of the received sound and to keep the intermediate frequency of the receiver constant at all times, except for target doppler shift. The ODN capacitance change is, in each case, independent of receiver tuning and, therefore,

subject to slight errors. (See Chapter 10.) However, with the intermediate frequency used, and with proper choice of  $L/C$  ratios, these errors are kept to only a few cycles per second, even at the extremes of the useful tuning range. Only one capacitor is used, since only one of the two ODN-controlled oscillators is working at any given time, but use of two separate units is relatively simple and reduces the possibility of circuit interaction through switch capacitance. Because the i-f pass band of the BDI listening receiver will be narrower than that in the scanning receivers, it is desirable to use the BDI listening-mixer oscillators in the unicontrol systems to set the transmitted frequencies. The ODN corrections must be removed during the transmission periods. To do this the ODN capacitors are replaced with mean value capacitors by using contacts on relays operated by the keying pulses, as indicated in Figure 118. Such switching would be unnecessary if the scanning-receiver mixer oscillators were used for unicontrol, but such a procedure would require greatly increased precision in tracking the scanning and BDI listening-mixer oscillators for each system. From the viewpoint of stability during service the arrangement described above seemed more desirable.

## 6.7

## TRANSMITTERS

## 6.7.1 Transmitter for 26-kc Depth-Scanning Sonar

The transmitter used for the 26-kc depth-scanning sonar installed on the USS CYTHERA was similar to

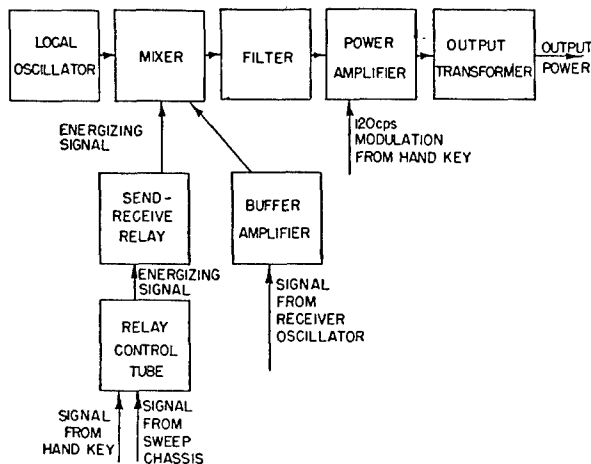


FIGURE 119. Block diagram of transmitter for 26-kc depth-scanning sonar.

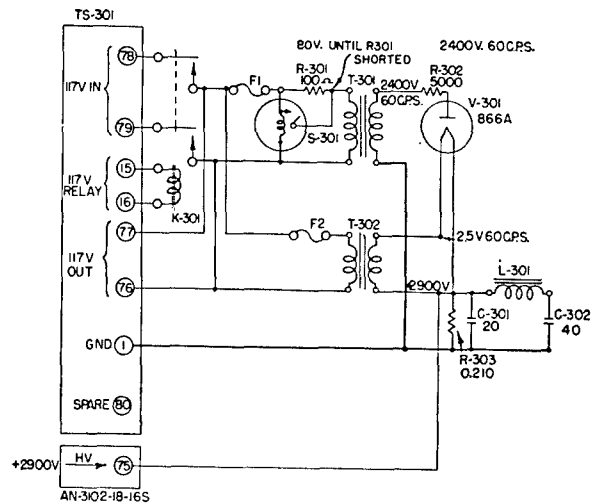


FIGURE 120. Wiring diagram of transmitter power supply, Chassis A, 26-kc depth-scanning sonar.

that built for the QH Model 2 sonar described in Chapter 5, but several modifications were made to satisfy requirements of the depth-scanning sonar. A block diagram of the transmitter is shown in Figure

119 and detailed wiring diagrams are shown in Figures 120, 121, and 122.

The major modification was in the unicontrol circuit. The frequency of the local oscillator in the trans-

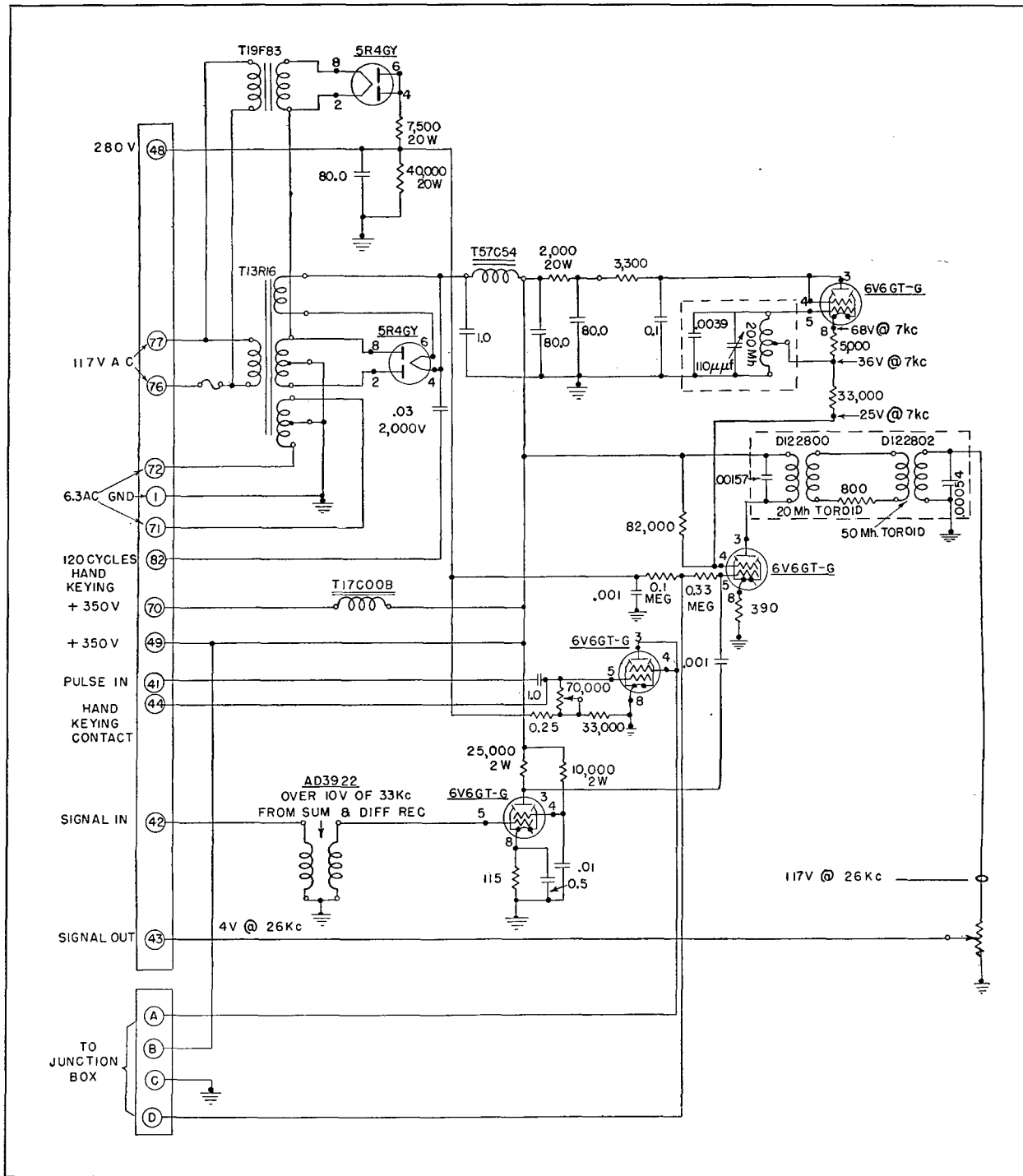


FIGURE 121. Wiring diagram of transmitter keying power supply, Chassis B, 26-kc depth-scanning sonar.

CONFIDENTIAL



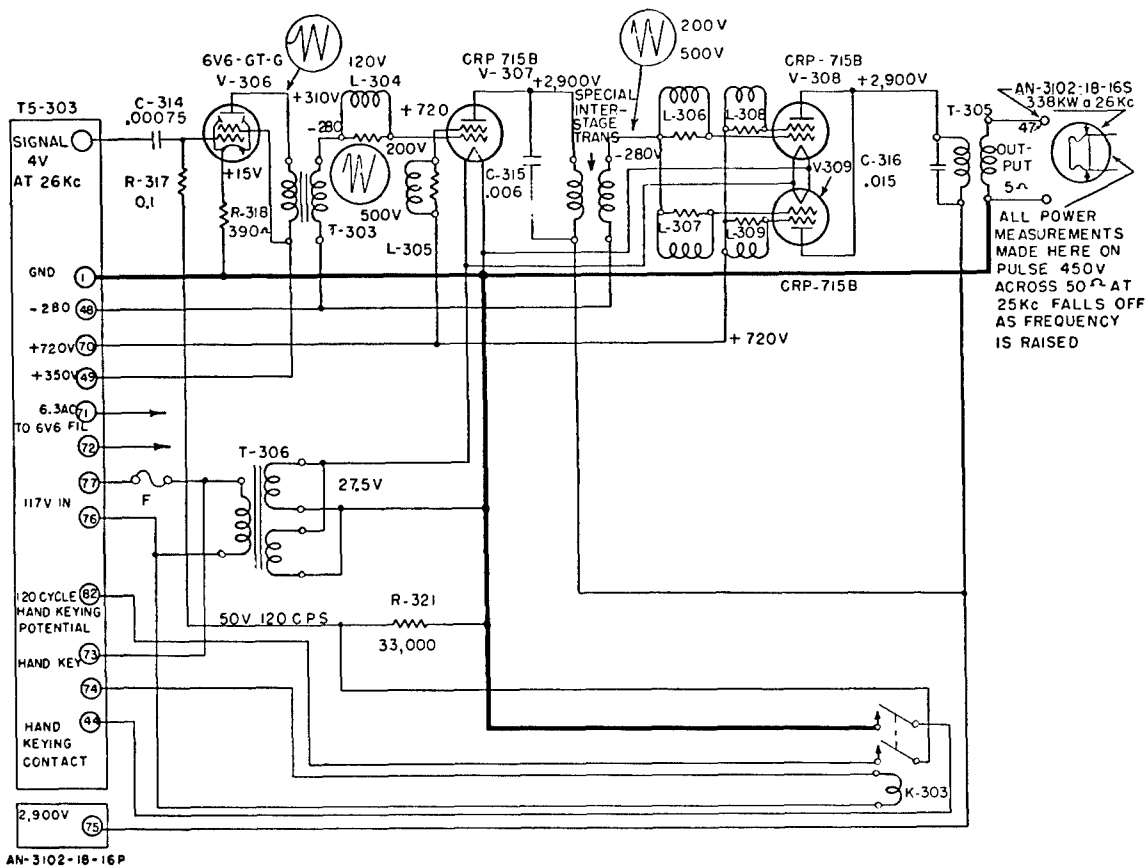


FIGURE 122. Wiring diagram of transmitter driver, Chassis C, 26-kc DSS. (Output voltage indicated is for original output transformer and does not hold when 50-w output is changed to 5 w. Voltage should then be about 130 v across 5 w.)

mitter being only 7 kc (the intermediate frequency of the BDI listening receiver), the requirements on the filter for selecting the 26-kc side band were more stringent. Its band width was only 2 kc at  $-3$  db. The keying circuit was modified so that the send-receive relay keyed the mixer stage. The interstage couplings, which had been originally designed to operate at 21 kc, were found satisfactory for 26-kc operation.

The output transformer was replaced with one wound for a 5-ohm output impedance in order to match the impedance of the depth-scanning transducer and its associated transfer network.

The power output from the transmitter was 3.4-kw peak, measured into a 5-ohm resistive load. The relative power output (in per cent of the peak value), as a function of load resistance, is shown in Figure 123. It is seen that maximum power output was obtained for a load of 6.8 ohms, slightly greater than the nominal output impedance. Control of the output pulse shape is discussed in the section of Chapter 5 on transmitters.

#### 6.7.2 Controls for Transmitter for 26-kc Depth-Scanning Sonar

Keying of the transmitter was effected through a send-receive relay which was actuated indirectly by a pulse from the sweep chassis. The various functions of this relay are illustrated in Figure 124. Three contacts were used to mute the three preamplifiers by placing resistors between the high-voltage supply points of the preamplifiers and their respective power supplies (see Section 6.7.1). One contact was used to lift from ground the common bus bar for the sum transformers in the junction box. A second contact was used to lift from ground the common bus bar on the coupling capacitors from the transducer elements to the transmitter. A third contact was used to energize the mixer tube in the transmitter. The relay coil was energized from the relay control tube in the transmitter.

Figure 121 shows details of the keying circuit of the transmitter. The pulse from the sweep chassis was

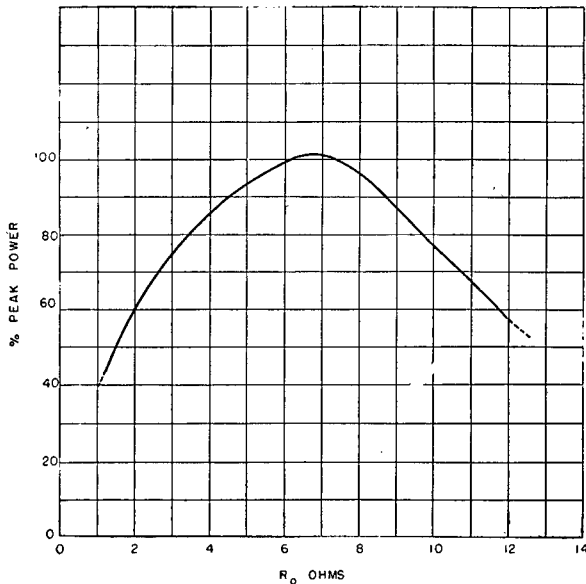


FIGURE 123. Power output versus load resistance characteristics of transmitter, 26-kc DSS.

applied to the grid of a 6V6 GT tube which conducted for the 35-millisecond duration of the pulse, thereby actuating the send-receive relay.

### 6.7.3 Integrated Type B Sonar Transmitters

It was planned that the two transmitters for the integrated Type B sonar should be similar to those constructed by the Sangamo Electric Company for

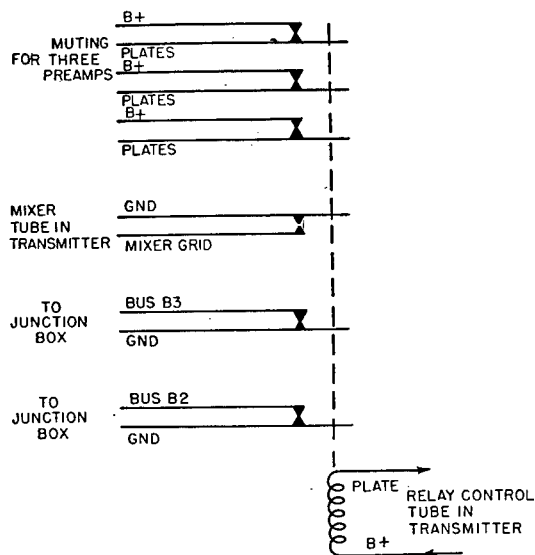


FIGURE 124. Send-receive relay connections, 26-kc DSS.

the XQHA scanning sonar (see Chapter 5). In this design, the transmitter for the azimuth portion of the system remains essentially the same, while that for the depth portion is modified for operation at 38 kc instead of 26 kc. This necessitates modifications in the local oscillator and mixer associated with the unicontrol tuning arrangement, in the interstage coupling transformers, and in the output transformer which was designed to accommodate the low impedance presented by the HP-8D depth-scanning transducer. The modifications for unicontrol, which are described in detail later, include the addition of mixer stages, suitable buffer amplifiers to introduce signals from the receiver oscillators, and an adjustment of the frequency of the local oscillators to suitable values for each transmitter.

### 6.7.4 Control Circuit for Transmitters for Integrated Type B Sonar

In the design, the keying circuits for the integrated Type B transmitters operate indirectly by pulses from the sweep chassis (see following section). These pulses energize send-receive relays through relay-control tubes, which mute the preamplifiers in the receivers during the transmitting interval, disconnect the transfer networks for the transducers, and energize the mixer tubes in the transmitters. Thus, the relays will

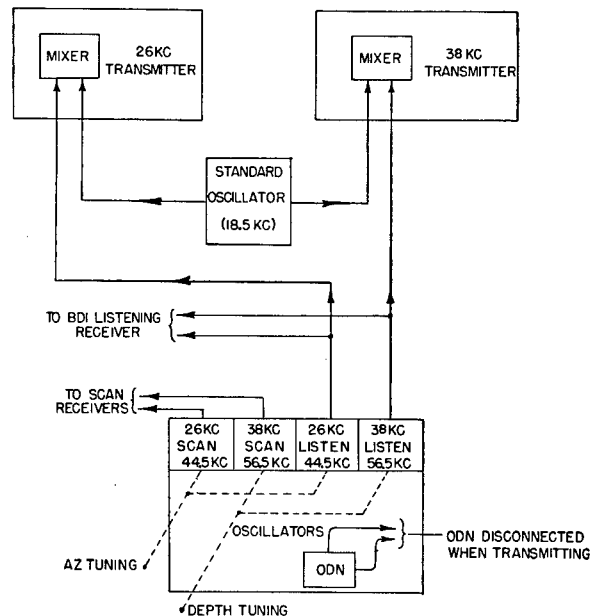


FIGURE 125. Unicontrol system for transmitter, integrated Type B sonar.

have approximately the same number of functions and the same operation as shown in Figure 124.

Frequency control of the transmitters is obtained through unicontrol circuits of the type that has been described previously for a single transmitter. The same general arrangement is used, but in the case of integrated Type B sonar it is applied to two transmitters. Details of the unicontrol system as it affects the transmitters are shown in Figure 125. When transmitting, ODN compensation is removed from the oscillator circuits in the receivers, and the oscillator outputs are mixed with the outputs from local oscillators in the transmitters. Although, as shown, a common local oscillator could be used for both transmitters, it actually was preferable to use two separate oscillators, one associated with each transmitter, in order to make better provision for damage control.

## 6.8 SWEEP AND COORDINATION OF PING TIMING

### 6.8.1 Requirements and Functions

The general functions of sweep and timing circuits have been discussed in Chapter 5. The one additional requirement for the integrated Type B sonar is the necessity for coordinating operations of the azimuth- and depth-scanning sonars. Independent operation is also necessary in case of battle damage to one of the systems. The specific functions of the sweep and timing circuits for the integrated Type B sonar are: (1) for azimuth-scanning sonar, spiral sweep and blanking pulse for PPI, and transmission pulse control; (2) for depth-scanning sonar, spiral sweep and blanking pulse for EPI and transmission pulse control; (3) for controls common to both sonars, sweep and blanking pulse for BDI, muting pulse for loudspeaker, coordination of transmission pulses, recorder or automatic recycling of either system or the combined systems, and hand-keying controls for communication.

### 6.8.2 Sweep Circuits in 26-kc Depth-Scanning Sonar

The 26-kc depth-scanning sonar utilized sweep circuits very similar to those used for the QH Model 2 sonar, described in detail in Chapter 5. Figure 126 shows the detailed wiring diagram. The circuit operations were initiated by a Sangamo AKU timer, with available range values of 750, 1,500, and 3,650 yards.

The spiral-sweep generator and blanking pulse amplifier were the same as for QH sonar Model 2 except for the range values mentioned. A separate relay tube and relay were added to operate the speaker muting during transmission, and to initiate the BDI sweep circuit, which was a standard X-3 BDI circuit<sup>58</sup> contained in the BDI indicator. The BDI sweep circuit is shown in Figure 127. The pulse used to operate the transmitter was obtained from the blanking pulse amplifier.

Provision was made for range-recorder operation of the timing function by paralleling the contacts on the range recorder with those on the Sangamo timer. When the synchronous motor on the Sangamo timer was stopped, it delivered no pulses and the system was recycled every time the recorder stylus began a sweep.

Hand keying for underwater communication was provided, and since the transmitter used a storage type of high-voltage power supply, the 120-cycle modulation arrangement described in Chapter 5 was used.

### DEFECTS IN TIMING AND KEYING CIRCUITS

The timing and the keying circuits of the 26-kc depth-scanning system were not entirely satisfactory. In this system, the determination of the ping length depended upon the length of contact of the mechanical contactors. These were not wholly reliable and, because of the number of capacitively coupled circuits which tend to affect the pulse length, the transmitted pulse length was not constant as range was varied. As a result, it was necessary from time to time to change the bias on the transmitter relay tube in order to obtain the proper length of transmitted pulse. As has been pointed out previously, a more satisfactory method of ping-length determination is to use electronic circuits of the flip-flop type which can be made independent of other variables.

### 6.8.3 Timing and Coordination Circuits for Integrated Type B Sonar

The timing, sweep, and ping-coordination circuits needed for the integrated Type B sonar were by far the most complex circuits which have been required for scanning sonar equipment.<sup>59</sup> In addition to the various sweeps and blanking pulses, it is necessary to provide keying pulses for two transmitters (azimuth and depth systems). It is also necessary to provide a



FIGURE 126. Schematic diagram of sweep chassis, 26-kc DSS.

synchronization method whereby the keying interval of the azimuth transmitter is a simple multiple of the keying interval of the depth transmitter and synchronous with the keying of the depth transmitter when both are in use. Provision should be made for obtaining signal inputs for the BDI listening re-

ceiver from either the azimuth or the depth system, and for synchronizing the BDI sweep with that of the system with which it is being used. Since the PPI was designed to have an electronic cursor, it is necessary to provide a relay which operates during the period of transmission and connects the deflection coils of

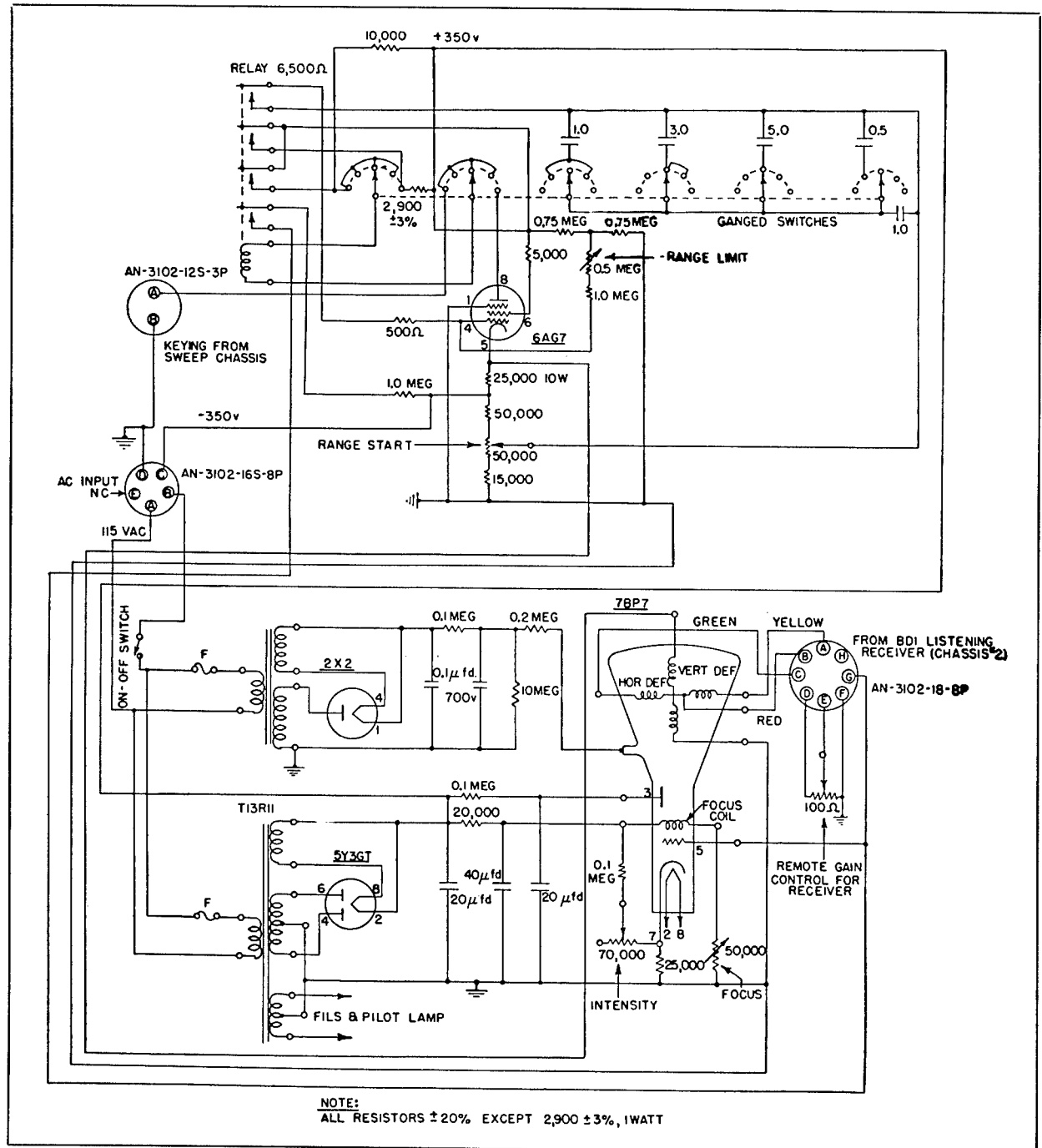


FIGURE 127. Schematic diagram for bearing deviation indicator, 26-kc DSS.

CONFIDENTIAL

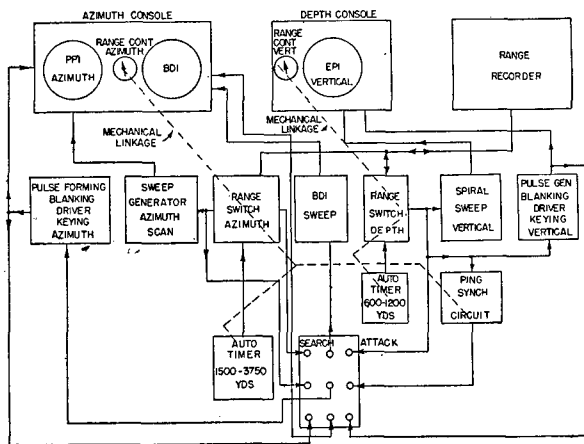


FIGURE 128. Functional diagram of timing and ping control circuits, integrated Type B sonar.

the PPI to a synchro signal input. Provision should be made for automatic internal timing of the pings of the two systems, as well as for the use of the range recorder as the timing element in either of the two systems separately or for timing both during the period of an attack. It is necessary to provide circuits which determine the ping length of the two systems accurately and independently of other variables.

The accompanying block diagram (Figure 128) illustrates the interrelationship of all these necessary functions for the integrated Type B sonar. At the top of the diagram are the blocks representing the azimuth and the depth consoles. Two range switches are provided, one on each console. The range switch on the azimuth console always controls the range sweep of the PPI and also controls the range sweep of the BDI when the search-attack switch is in the search position. The range switch on the depth console always controls the range sweep of the EPI and also controls that of the BDI when the search-attack switch is in the attack position. The dotted lines on the block diagram indicate mechanical linkages between these switches and other parts of the circuit associated with them. The search-attack switch shown at the bottom of the diagram is used to change primary control of the sonar gear from the azimuth to the depth system.

There are three necessary switching functions on the search-attack switch: (1) The BDI sweep is changed over so that it is initiated by the timing circuits of the depth system; (2) the blanking pulse for the BDI is switched over so that it also will originate from the depth system; and (3) whenever the depth system is operating, the basic timing of the azimuth

ping is controlled by the timing circuits of the depth system through a ping synchronization circuit, which insures that the interval between pings of the azimuth system is a simple multiple of the ping interval of the depth system (see Figure 128). Two automatic timing circuits are provided, one for the azimuth system with possible intervals of 1,500 and 3,750 yards, and one for the depth system with possible intervals of 600 and 1,200 yards. In addition, a range recorder is provided which allows the possibility of obtaining any range interval from about 100 to 3,750 yards. It is supplied with marking signal from the BDI listening receiver, and is arranged to supply keying pulses to that system (depth or azimuth) to which the BDI listening receiver is connected.

Although these arrangements are quite complicated, they allow complete freedom of operation of the components of the Type B sonar, effectively providing four echo-ranging systems. This insures against breakdown of any fraction of the equipment, as it is possible to obtain echo-ranging information from other combinations of the equipment not affected by the breakdown. The four possible echo-ranging systems are: (1) listening, range recorder, and BDI using azimuth transducer; (2) listening, range recorder, and BDI using depth transducer; (3) scanning in azimuth; and (4) scanning in depth. Each of these systems allows the operator to find targets and determine range and bearing.

Figure 129 shows the actual schematic circuit diagram of one electronic system designed to perform all these functions. By the spring of 1945 this system had not been used in an integrated Type B sonar, but its various portions had performed satisfactorily in breadboard form. It was planned that development work should continue since other possible arrangements had been suggested<sup>59</sup> and seemed to merit investigation.

A consideration of the tuning and control circuits described above indicates that there are some drawbacks from an operating standpoint. Three main switches are used to set up the operating conditions at any time; the azimuth-range switch, the depth-range switch, and the attack-search switch. Thus, it is necessary for the operator or sonar officer to observe the positions of three switches in order to determine the mode of operation of the system at any given moment. It is possible that during the excitement of an attack, errors can be made in setting these three switches.

#### 6.8.4 Proposed Timing and Coordination Circuit for Integrated Type B Sonar

A new system shown in Figure 130 was proposed to overcome the difficulties mentioned above. This uses one switch to perform all major control functions of the integrated system with four available switch positions. Positions 1 and 2 allow for search procedure with azimuth ranges of 3,750 and 1,500 yards respectively. The depth system can be used in these positions but only one automatic range (1,200 yards) is available. Positions 3 and 4 on the switch are attack positions. In the attack position only one range (3,750 yards) is available for the azimuth system. The depth system, however, recycles automatically at 1,200-yard range in position 3 and at 600-yard range in position 4. All sweep circuits are switched to correspond to these ranges. This single switch also controls the BDI listening channel inputs, by automatically switching from azimuth to depth reception as the switch changes from search to attack position.

Since one main switch performs the major control functions during an attack, the position of this switch immediately indicates to the operator or sonar officer all of the essential conditions of system operation at any given moment. Furthermore, the switch is arranged so that the extreme left (No. 1) position is the usual search position. After contact with a target, the switch is arranged so that advancing it to the right one step at a time arranges the circuits properly in the appropriate sequence for attack procedure. This feature relieves the operators of the responsibility of setting three switches for each new operating condition desired as the attack proceeds.

It is difficult to perform all switching functions with a single switch and yet maintain a high degree of flexibility in the system. In this design, auxiliary switches are provided to perform minor functions and to permit maximum flexibility of operation of the integrated system components. On-off switches are provided in the keying circuits of both the azimuth and depth systems. These switches permit the operator to stop or start the pinging of these two systems independently. On the off position the switch permits noise listening with the particular system involved. The on-off switch on the depth system provides an additional function. It is arranged so that whenever it is in the on position, the automatic (or recorder) keying of the azimuth system is disconnected and a synchronizing circuit is inserted. This

allows the azimuth driver to ping only at integral multiples of the ping interval of the depth system. This is true whether the timing of the ping is performed by the automatic timer or by the recorder. Thus, if the recorder is being used to key the azimuth system while the depth system is inoperative, and the depth system is suddenly turned on, the recorder keying is switched to the depth system and the azimuth system is synchronized with it. However, the signals for the recorder trace continue to come from the azimuth system as long as the main control switch remains in the search position.

Switch points on the recorder allow the recorder to take over complete control of the timing of the system whenever the recorder is turned on. This operation disconnects the automatic keying for both depth and azimuth and provides instead a keying pulse from the recorder. Whether the recorder or the azimuth system times the depth is determined by the position of the depth system on-off switch, as explained before.

It is true that this proposed system of timing and control circuits causes a slight loss in the operating flexibility of the integrated Type B sonar. However, the gain in operating ease due to the simplicity of the controls involved was expected to more than offset the loss. This control system allows only one depth-scanning range (1,200 yards) while the control switch is on search. Only one azimuth range (3,750 yards) is available in the attack position. These ranges represent those which would normally be needed in each case. Experience with sonar systems has always indicated that operator controls should be few and extremely simple. The second of the two control systems described above seems to meet these criteria better than the first.

#### 6.9 APPRAISAL OF INTEGRATED TYPE B SONAR

The work that was carried out on integrated Type B sonar at HUSL followed two general lines: (1) theoretical and experimental investigations of depth scanning; and (2) detailed design of the integrated Type B sonar. The first part of this program called for considerable research and development work. The depth-scanning system, including stabilization, was set up and tested on an experimental basis. The investigation and experience with azimuth-scanning

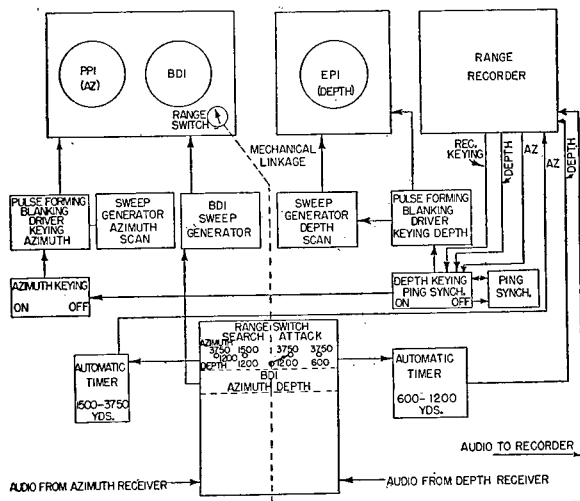


FIGURE 130. Functional diagram of suggested timing and ping control circuits, integrated Type B sonar.

systems led to the general design of the integrated Type B sonar, which was partially constructed but not completed or tested by HUSL.

The experiments on depth scanning were successful to the extent that the system operated as expected. It was found possible to hold contact with a target from ranges of about 1,300 yards and at a depth angle of 0 degrees, to a depth angle of 90 degrees, with the target immediately below the experimental ship. Reverberation did not appear to be a disturbing factor, but the echo from the bottom of the ocean was extremely disturbing for both the scanning and listening portions of the depth system. It was found that disturbance because of the bottom echo could be minimized by transmitting on a directional-type beam rather than on the nondirectional beam as originally used. On the basis of these data it is recommended that, in future experiments, the transmitting beam provide approximately constant echo strength from a target at constant depth as the range from ship to target changes. Some difficulties were observed in obtaining proper depth angles for a target at known depth angle. An effort should be made in future work to evaluate the effects on operation of the system caused by the target-image in the surface and by inhomogeneities in the water path between the target and the experimental ship.

The experiments on depth scanning also included the taking of data to measure quantitatively the strength of bottom echo compared to the strength of target echo, for various bottom conditions and for

various aspects of the target. No careful measurements were made of the operation of the stabilization feature for the depth-scanning system, but, qualitatively, the stabilization acted in the manner expected.

The design of the integrated Type B sonar included both a stabilized depth-scanning system and an azimuth-scanning system. It was assumed that the azimuth-scanning system was to be used in search to discover targets at as long ranges as possible, the use depending in some instances upon water conditions and in others upon ship speed. It was assumed that the depth-scanning system was to be used in attack to follow the target at the shorter ranges and to furnish accurate positional data for attack computation. Under these assumptions, the azimuth-scanning portion of the system determined only the bearing and range of the target, while the depth-scanning portion determined bearing, range, and depth angle of the target. Originally it was anticipated that the integrated Type B sonar might give information about an underwater target within the following accuracies:  $\pm 10$  yards in range for ranges less than 1,000 yards;  $\pm 1/2$  degree in depth angle for depths between 50 and 800 feet at a 500-yard range; and  $\pm 1/2$  degree in bearing for all ranges to the maximum obtainable range with the system. However, the experimental data presented in this chapter indicates that these accuracies can be attained only under ideal test conditions.

The integrated Type B sonar has a number of distinct advantages over other sonar gear. Original detection of a target by the azimuth-scanning portion of the system is obtained by watching a single indicator without moving any controls. Following detection, placing the cursor of the PPI on the target and keeping it there allows further detection of the target on the EPI without moving any other controls. Use of the BDI technique allows continued bearing determination even when the target is no longer detectable on the azimuth-scanning portion of the system. Continuous maintenance of contact with a minimum of effort is thereby accomplished from the original detection throughout the time that the target remains within detectable range, including very short ranges and depth angles to 90 degrees. Because of the ability of this system to retain contact with the target to very short ranges and large depth angles, the conning officer should be able to make a better judgment of the evasive behavior of the target and be able to avoid the uncertainty now existing when contact is lost.



With the addition of a suitable attack director (now under development) to include depth angle in its computations, the problem of attacks on the target should be simplified and, on the average, attacks should be more successful. Upon availability of trainable gun-type ordnance, the effect of the first rounds on the target can probably be taken into account by spotting in the outputs from the system, so that the attacks should become even more successful.

For navigational purposes, the system could be adapted with ease for detection by the PPI of surface ships, buoys, reefs, or other obstacles near the surface. The EPI could be used to examine the bottom in the direction of, or at any angle to, the direction of motion of the ship, and could also be used to detect submerged objects on the bottom or between the surface and the bottom for any particular direction.

## ELECTRONIC ROTATION SCANNING SONAR

## 7.1 ELECTRONIC ROTATION SCANNING SONAR

## 7.1.1 General Description

THE *commutated rotation* [CR] scanning system had certain well recognized limitations. Chief among these was the fact that the rotation speed was limited by the mechanical strength of the commutator, thus putting a lower limit on the pulse length that could be used. It was early recognized that higher rotation speeds could most conveniently be obtained by means of *electronic rotation* [ER] methods. In addition, it was thought that the mechanically rotating commutator (as in the CR system) would prove difficult to build and maintain because of the very close tolerances involved, while the ER rotor could be assembled and repaired by anyone equipped to do electronic repair work. Consequently, development work on the ER system was accelerated after the summer of 1943, and finally culminated in the submarine system which was tested on the USS DOLPHIN at New London in March 1945. This ER system is described in some detail later in this section.

The higher scanning speed of the ER system was of importance in three ways: first, with the higher rotation speed the spirals on the *plan position indicator* [PPI] were spaced closer together and there was a consequent increase in the accuracy with which the range of the target could be measured; second, with a short ping, higher signal-to-noise ratio was obtained; third, with the short pulse output it was also possible to obtain considerably higher peak power in the acoustical pulse without materially increasing the size of the transmitter and necessary power supply.

Figure 1 shows a block diagram for a typical ER sonar system. A short, high-frequency pulse from the transmitter was fed to the cylindrical transducer through the transfer network, and was emitted as a nondirectional ping. The echo was received by the transducer, was conducted through the transfer network to the beam-forming network and to an electronic rotor, was amplified by the receiver and then supplied in the form of a short d-c pulse to a PPI. Sweep and timing circuits were similar to those used in the CR system, except that the sweep was initially

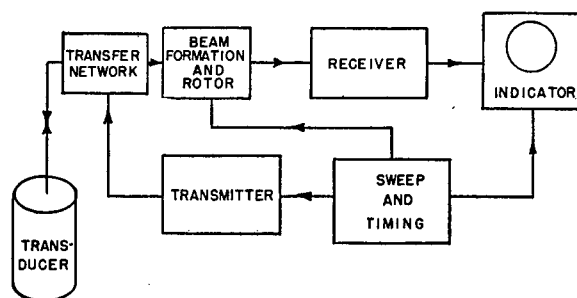


FIGURE 1. Block diagram for ER sonar.

generated by a low-frequency oscillator instead of a mechanically rotated polyphase generator. Rotation of the beam of sensitivity was accomplished by means of a switching signal fed to the electronic rotor, at a rate that varied from 200 to 500 rps for different models. The length of the ping was, as in the CR system, equal to the time taken for one rotation of the scanning beam.

In order to produce electronic rotation, it was necessary to connect each element of the transducer to a corresponding switch which could be operated by means of a d-c pulse. Typical elements used for this purpose were vacuum tubes, such as triodes or diodes, or dry rectifiers, such as the copper oxide or selenium varistor type. A sequence of switching signals was obtained by sending the switching pulse down a network of the low-pass filter type with the number of sections equal to the number of transducer elements, and with a total time lag equal to the required time of rotation of the beam pattern. Since it was found possible to use the tip of a sine wave as a switching pulse, this switching line, or lag line as it was generally called, had a total phase shift equal to 360 degrees at the frequency of the sine wave used. The sine wave was obtained from the same oscillator which generated the spiral sweep on the PPI, so that there was always synchronization between the position of the switching pulse on the rotor and the position of the electron beam on the PPI.

Since this method was equivalent to a single-pole 48-position switch, rather than a multipole 48-position switch as represented by the CR commutator, it was not convenient to use a set of 16 or more lag lines in order to form the beam pattern. Instead, it was

necessary to have a set of 48 preformed beam patterns which could then be connected into the receiver by means of the above set of switches. In order to obtain a beam pattern, signals from the various elements of the transducer were advanced in phase by a lead line so that the outputs of elements at the sides of the transducer were in phase with that from the element at the most forward point on the transducer. This lead line was essentially a high-pass filter network whose series elements were capacitors connected from one element of the transducer to the neighboring element and whose shunt inductive reactances were usually the transducer elements themselves. Smooth rotation of the beam pattern was accomplished by having the switching pulse broad enough to operate two or more switches simultaneously and in proper proportion.

#### 7.1.2 Submarine Scanning Sonar Model XQKA

A typical example of a complete ER scanning sonar is the equipment built for use on a submarine and installed on the USS DOLPHIN from March to May 1945.<sup>1</sup> Figure 2 is a photograph of the electronic part of the equipment as installed in the forward torpedo room of the USS DOLPHIN. The top unit in the photograph is the indicator. The chassis immediately under the indicator unit contains the receiver and power supply. The next contains the sweep, range marker, and oscillator chassis, while the bottom unit is the transmitter. It can be observed that the indicator unit had all the controls necessary for use by the operator; it could be located in any convenient position in the ship remote from the rest of the gear. In the photograph, the three cabinets are shown stacked on top of each other, but they were three separate units and could be placed in any convenient locations with interconnecting cables. A motor generator set of about 1½-kva capacity and the two transducers constituted the remainder of the equipment. One of these transducers was mounted on the hoist-train shaft which had been used for the bottomside QC transducer. The other transducer was mounted on the top deck of the submarine at a point just forward of the capstan.

Figure 3 shows a block diagram of the submarine ER sonar equipment. At the extreme left side of the diagram is the transducer assembly containing the



FIGURE 2. Submarine ER sonar installation.

transducer itself, the transfer network, the beam-forming lead line, the electronic rotor, a relay, and the discriminator circuit. All of this electronic equipment was installed in the central cavity of the crystal transducer. The transducer was a 48-element ADP (ammonium dihydrogen phosphate) crystal type made by the Brush Development Company.

The receiver, described in detail in a later section of this chapter, was essentially a flat r-f amplifier with two band-pass filters, plus a detector and output circuit. The indicator for the submarine ER system and the sweep, timing, and range-marking circuits are also described later in this chapter.

### 7.2 EXPERIMENTAL WORK AND RESULTS

#### 7.2.1 60-cycle ER System for Aide de Camp

In the summer of 1943, work was begun on the problem of finding a means of forming a beam from the signals generated by the elements of a multiele-

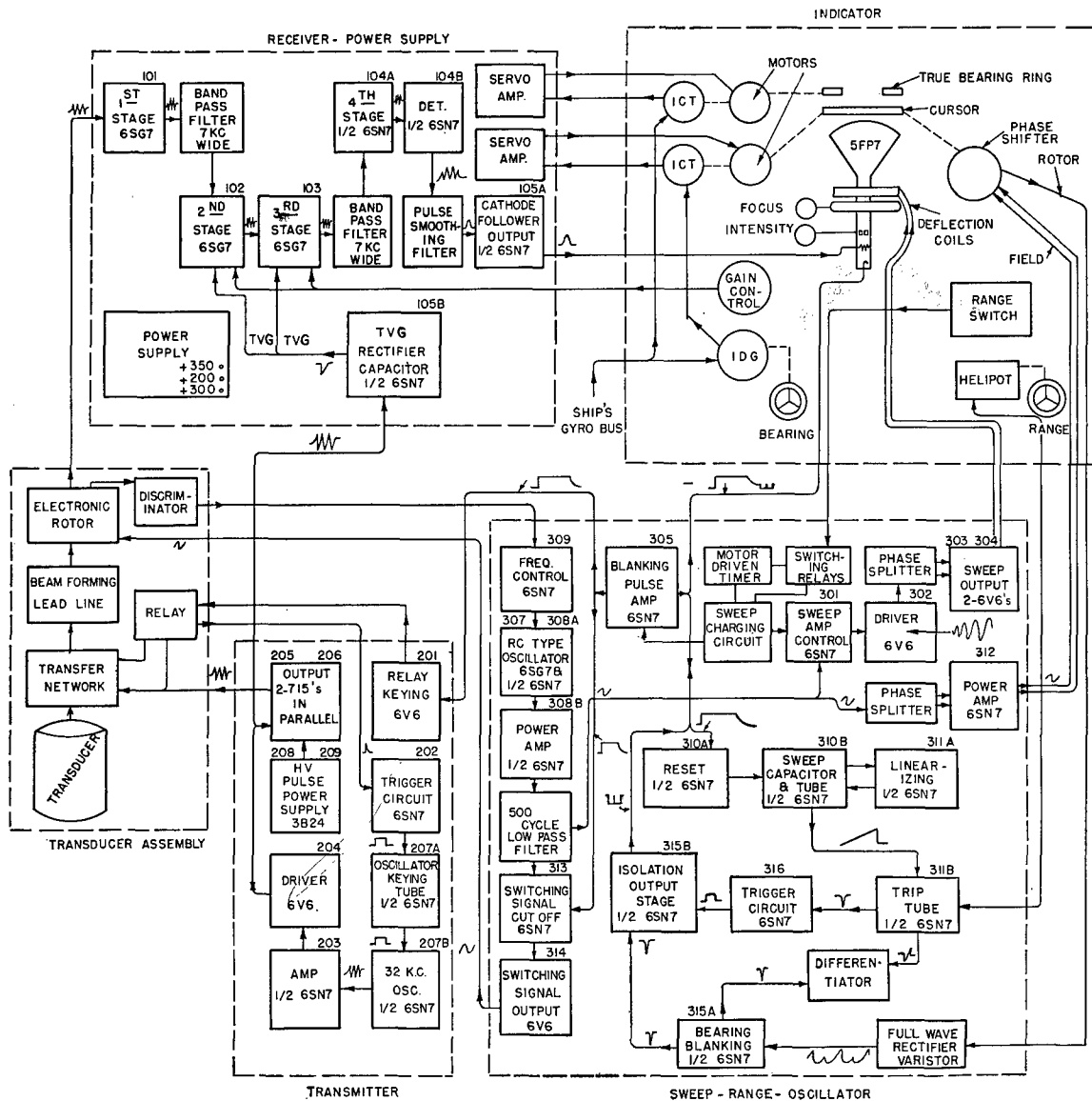


FIGURE 3. Block diagram, submarine ER sonar.

ment cylindrical transducer and a method of rotating this beam by electronic means. A great deal of work was done in the laboratory between July 1943 and September 1943 in order to produce a workable electronic rotor that could be used to take the place of the CR commutator (see section on ER rotors for the details of their development). As a result of the laboratory tests, a shipboard model electronic rotor scanning sonar system was developed for installation and test abroad the AIDE DE CAMP. This system included an electronic rotor with 18 twin triodes as electronic switches, controlled by switching pulses

from a 3-phase synchro used as a 3-phase generator and a resistor phase-splitting network which split the 3-phases into 36 phases for switching purposes. The beam-forming lead line consisted of a set of capacitors connected from element to element of the magnetostriction transducer so that a complete circular array was formed. Figure 4 is a photograph showing the rotor, phase splitter, and the motor generator set used for switching purposes in this system on the AIDE DE CAMP. Figure 5 is a block diagram of the same system. Since the rotation speed was 60 rps, this was designed as the 60-cycle ER system. Other units

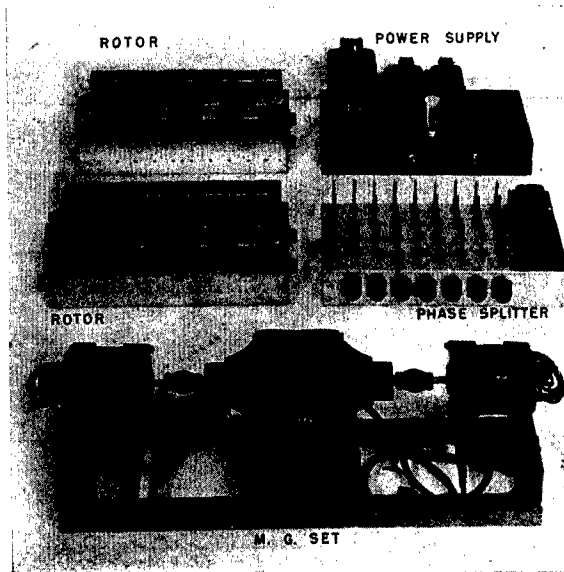


FIGURE 4. Rotation components 60-cycle ER sonar.

in the system not shown in the photograph were mainly the same ones which were then being used on the AIDE DE CAMP for the CR sonar experiments.

As may be seen from the photograph, the rotor itself was built on two standard-size chassis with 9 tubes containing 18 elements on each chassis. Audio Development Type 3805-A transformers were used to couple from the magnetostriction hydrophone to grid impedance and can be seen on top of the chassis. On a separate standard chassis was constructed a power supply to operate the electronic rotor. The fourth chassis shown is the phase-splitting unit de-

scribed in the following section on ER rotors. The motor generator set in the lower part of the photograph contained in the 3,600-rpm motor in the center, driving two standard General Electric synchros as a 3-phase switching generator and a 3-phase spiral sweep generator respectively.

By referring to the block diagram in Figure 5, the operation of this system may be followed. The transducer used was the 36-element magnetostrictive type, known as HP-1 and described in Chapter 5. It was connected by means of a 36-pair cable to the polarizer unit, and also by means of an additional 36-pair cable to a 36-pole double-throw relay. This relay acted as a send-receive relay, connecting all of the elements of the transducer to the electronic rotor during reception and connecting the transducer elements in parallel to the transmitter during transmission. The electronic rotor output was fed to the receiving amplifier, then into the delayed lobe comparator and brightener, and then in the form of a pulse to the grid of the PPI CRO. At the same time, the 3-phase generator used as a switching generator fed the resistive phase-splitting network, while the spiral sweep generator received a sawtooth waveform current from the timing and keying chassis for excitation of its rotor. The output of the sweep generator was fed to the deflection coils of the PPI CRO in the form of a 60-cycle 3-phase sine wave whose amplitude was continuously increasing during the time of the sweep. The transmitter and receiver were the same ones that were used in the second CR sonar system which was installed concurrently with the ER system aboard the AIDE DE CAMP. A description of the receiver, transmitter, polarizer, timing chassis, and send-receive relay may be found in Chapter 5.

The *delayed lobe comparator* [DLC] indicated in the block diagram was an addition to the usual CR system intended to narrow the brightened arc. It is described in the section on ER receivers later in this chapter.

During the fall of 1943, this 60-cycle ER system was tested on the AIDE DE CAMP at the same time that tests were being made on the CR system. Comparisons were made between the two systems, and in addition, the ER receiver was used both with and without the delayed lobe comparison circuits. (See Section 7.6.1 on receiver design.) This DLC system of brightening performed as expected in narrowing the brightening arc due to any given target. As a consequence, the PPI display seemed sharper than the display with

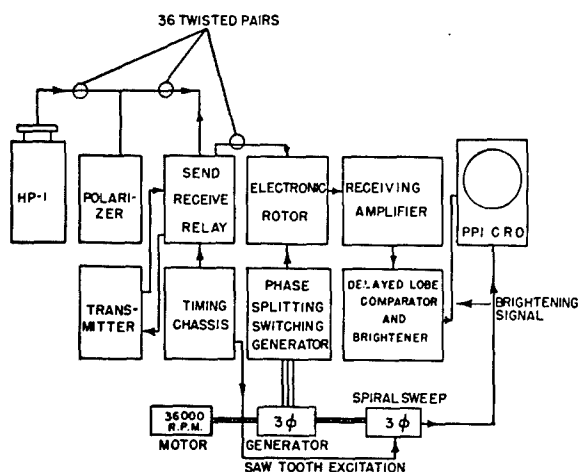


FIGURE 5. Block diagram of AIDE DE CAMP 60-cycle ER sonar.

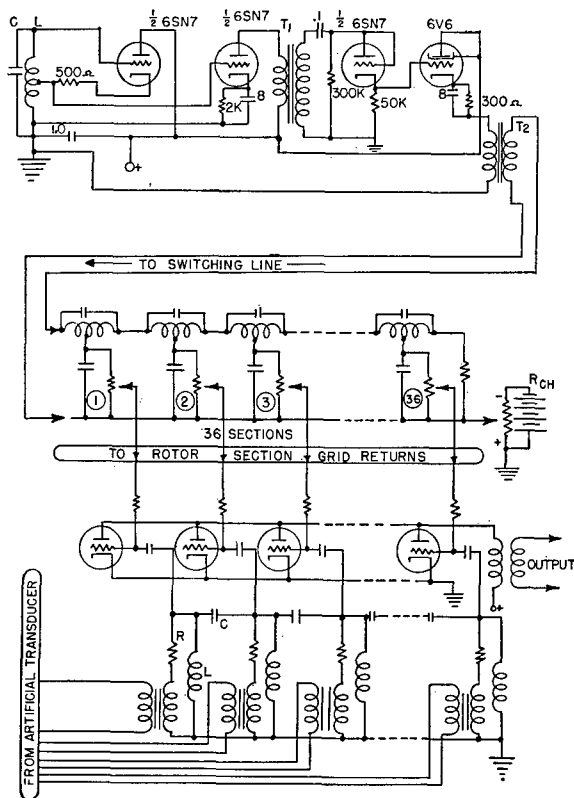


FIGURE 6. Circuit diagram of 200-cycle laboratory rotor.

amplitude brightening only. The disadvantage of using delayed lobe comparison was in its enhancement of electric noise. Short noise impulses present in this system were represented as high intensity spots on the screen. The high intensity was caused by the fact that the differentiator circuits which were employed intensified all signals whose amplitude rate of change was great with respect to time. Noise impulses were thus intensified out of proportion. This property caused the abandonment of delayed lobe comparison.

During the trip of the AIDE DE CAMP to New London in November 1943, a series of experiments was made on echo consistency, target discovery distance, and sensitivities of the ER and CR systems.<sup>2, 3</sup> From the results of the tests during the fall of 1943, it was concluded that although the electronic rotation method was successful and could produce a useful echo, the system had certain disadvantages as compared with the capacitive rotation system. The CRO was noisier in the sense that noise impulses interfered with the proper identification of actual echoes on the CRO screen of the PPI. This was subsequently

found to be caused by the method of construction of the electronic rotor which was microphonic. It was also caused by the fact that the rotated transducer pattern produced by the ER commutator was inferior to that produced by the CR commutator from the same transducer. The minor lobe structure was more prominent and the width of the major lobe was greater, as was the variation in major lobe maximum amplitude.

### 7.2.2 200-cycle ER System for Aide de Camp

As a result of the tests of the 60-cycle rotation ER scanning sonar system, plans were made for an improved system to operate at 200-c rotation. A laboratory prototype electronic rotor was built in accordance with the schematic wiring diagram shown in Figure 6. A bridged-T type of transmission line was used as a switching generator and is shown at the center of the diagram. At each junction a potentiometer

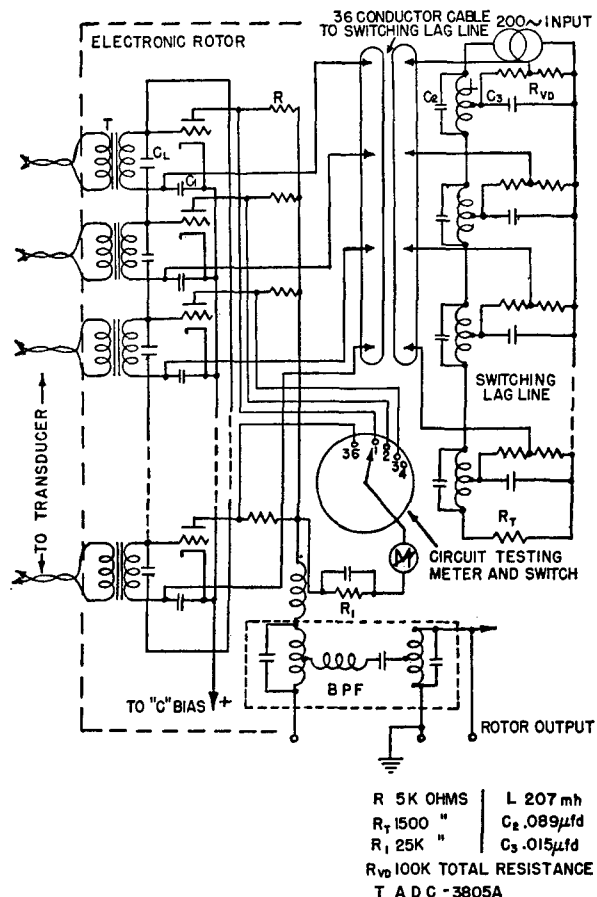


FIGURE 7. Circuit diagram of electronic rotor, 200-cycle ER sonar.

CONFIDENTIAL

meter, shown next to the encircled numbers running from 1 to 36, was included to make possible the equalization of switching signal amplitude along the various sections of the lag line. At the top of diagram is shown the pulse-generating circuit used to supply switching pulses to the switching line. One half of a 6SN7 acted as a Hartley oscillator operating at 200 cycles, and drove the other half of the 6SN7 as an amplifier. Another half of a 6SN7 was used as a peak rectifier charging a  $0.1\text{-}\mu\text{f}$  capacitor so that conduction through the capacitor and tube was limited to approximately 90 degrees out of 360 degrees. This rectifier then acted to clip or limit the original sine wave to provide the pulse needed on the switching line. The pulse was amplified by a 6V6 connected as a cathode follower through a transformer  $T_2$  to supply energy to the switching line at an impedance of 1,500 ohms. Values of lead line components L and C were then varied to produce the best pattern at the output of the rotor as judged by means of the standard laboratory test arrangement, which consisted of an artificial water amplifier, and a synchronized linear sweep CRO.

As a result of the laboratory investigations described above, the 200-cycle ER system was built for installation aboard the AIDE DE CAMP. The schematic wiring diagram of its electronic rotor is shown in Figure 7, which illustrates some significant differences between the 200-cycle rotor on the AIDE DE CAMP and the 200-cycle rotor built in the laboratory. In the first place, in the AIDE DE CAMP rotor the shunt elements in the beam-forming lead line were formed entirely from the transducer impedance as seen through matching transformers. It was found that by using the impedance of the HP-1 elements as shunt impedances in the lag line and by the proper choice of capacitors, the desired beam pattern could be obtained.

Another circuit change involved in the AIDE DE CAMP electronic rotor was the inclusion of a circuit-testing meter and switch, shown at the right center of the diagram in Figure 7. This circuit-testing meter and switch was simply a single-pole 36-point selector switch whose stationary contacts were all connected to the respective plates of the switching tubes. The rotating arm was connected through the microammeter and a suitable series resistance to the plate voltage supply of the electronic rotor. By switching from point to point, therefore, it was possible to measure the plate current in any of the triode switching

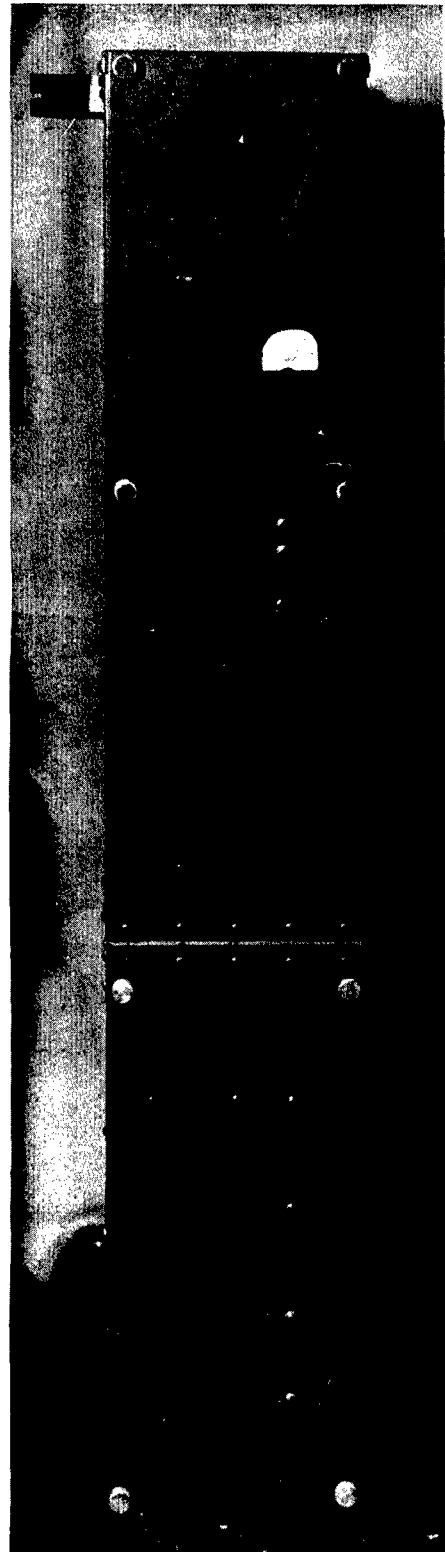


FIGURE 8. Front view of rotor, 200-cycle ER sonar.

CONFIDENTIAL

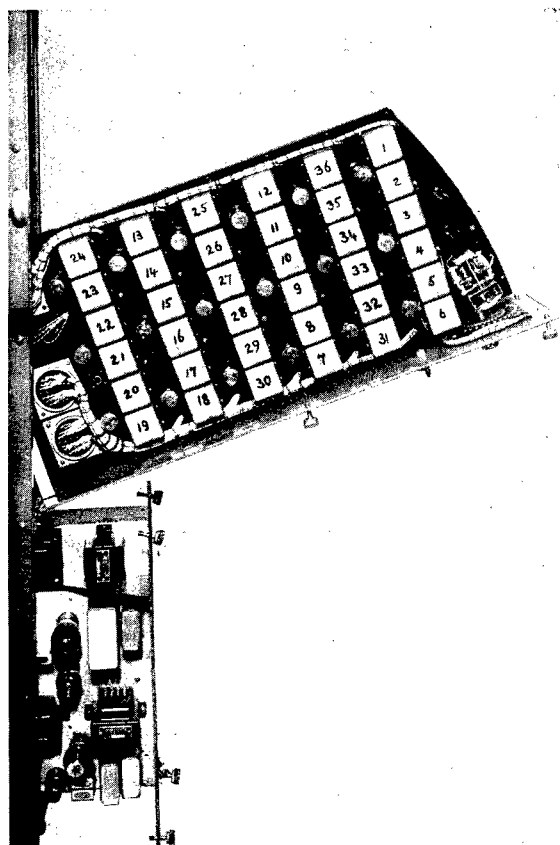


FIGURE 9. Interior view of rotor, 200-cycle ER sonar.

elements. In this way, any irregular operation was evident immediately upon turning the selector switch to the appropriate circuit. The tube could then be tested, and if found to be in proper operation, the trouble could be located among one of several components or connections in this particular circuit.

The switching lag line employed was the same as for the 200-cycle laboratory rotor. However, after setting the potentiometers so that the switching signal amplitude was of correct value in all the 36 circuits, the resistance ratios were measured and the potentiometers were replaced with fixed resistors. The cut-off bias for the triode switching tube was also changed from the grid circuit to the cathode circuit of all the switching tubes. For this purpose, all the cathodes were connected together and brought to a positive voltage control potentiometer on the front panel of the electronic rotor.

Figure 8 shows a photograph of the front panel of the 200-cycle rotor used on the AIDE DE CAMP. Figure 9 shows a photograph of the rotor chassis swung out of its cabinet.

Among other new equipment constructed for this 200-cycle AIDE DE CAMP ER system were a high-power pulse-type transmitter, a new transfer network, a 200-cycle spiral sweep for the PPI scope, and a switching pulse generator. Figure 10 shows a schematic diagram of this latter circuit. It may be seen that it is nearly identical in operation with the pulse generator shown at the top of Figure 6. At the bottom of Figure 10 is shown the regulated power supply that was built on this same chassis. The spiral sweep used in this system is described in some detail in Section 7.8 on sweep generation and range marking. The 200-c signal, developed by the first oscillator of the switching generator described above, was applied to the input of a pair of triodes acting in cascade, while the bias of this triode pair was varied according to a sawtooth voltage. The output of the 2-tube amplifier was then a 200-cycle sine wave signal whose amplitude increased linearly with time over the receiving period. This output was then split into two quadrature components which were impressed through suitable amplifiers upon the two-phase deflection coils of the PPI.

The transmitter used with the 200-cycle AIDE DE CAMP ER system was an 18-kw transmitter, developing this average power in a transmitted pulse length of 5 milliseconds. It is described later in this chapter.

The transmit-receive network used in the AIDE DE CAMP 200-cycle ER system is shown in Figure 11. At the left side of the drawing is shown the input of a keying pulse which was derived from the spiral sweep chassis described in Section 7.8 on sweep generation. At the time of transmission the relay shown in its normally open position was closed. The transmitter chokes  $L_2$  had a common return which was ungrounded by the relay and, thereby, made ready to receive a transmitted pulse. The common return was permanently connected to the transmitter through tuning capacitor C, as indicated in the diagram. The transmitter pulse was initiated by the upper contact on the relay, marked "key to transmitter." At the time of the transmitted pulse, the common return of the primary of the rotor input transformer, shown at the bottom of the diagram, was ungrounded by the same relay. This created a potentially balanced system in the electronic rotor, so that under perfect balance conditions no potential difference existed upon any rotor primary. In this way the electronic switches in the rotor were protected from voltage overload during periods of transmitter operation. At the upper



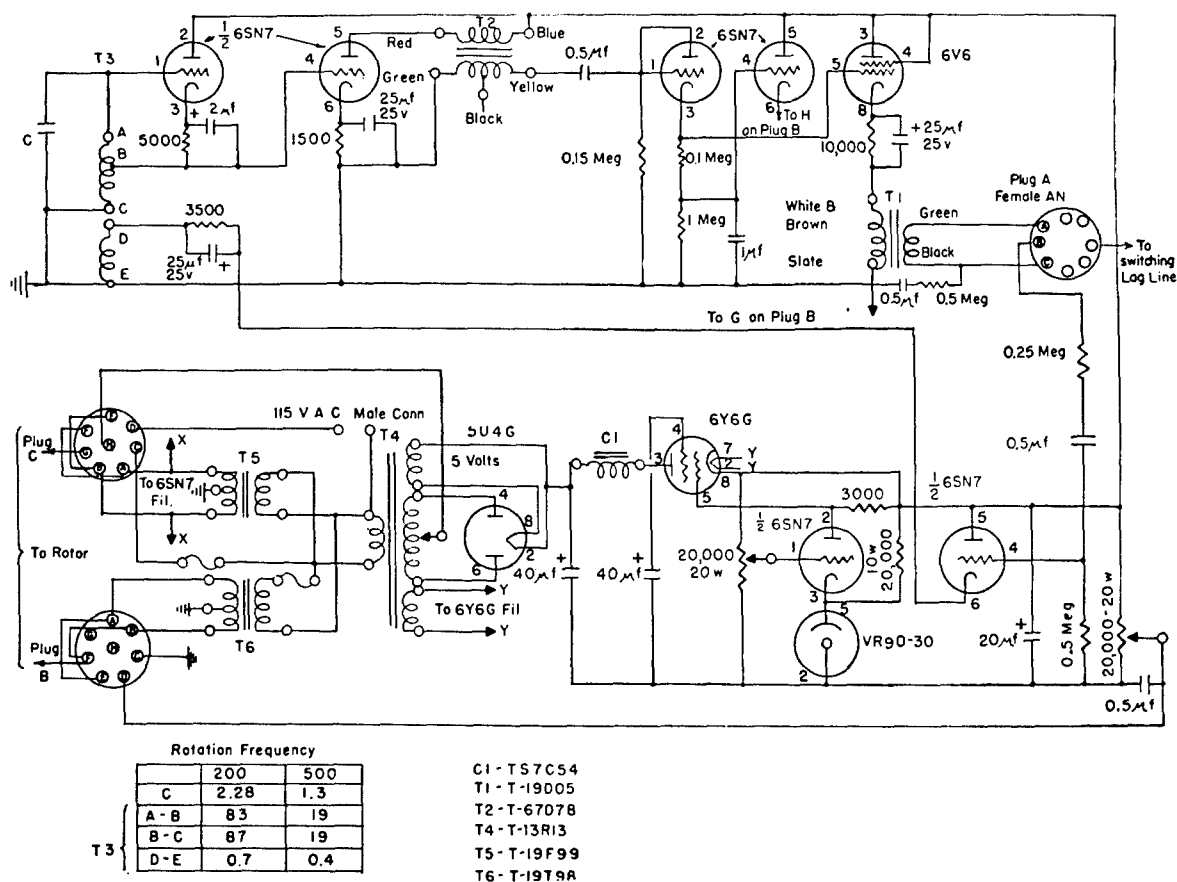


FIGURE 10. Circuit diagram of switching pulse generator.

portion of the drawing are shown the polarizing chokes and d-c polarizing source arrangement. Each polarizing choke  $L_1$  was connected in series with the corresponding element marked by X on the top of the diagram. During reception all transmitter chokes  $L_2$  were returned to ground through a large blocking capacitor shown at the left of the relay. This eliminated any possibility of energy transfer from one transducer element to another element in the network via the continuous star-connected network of transmitter chokes. At the same time all rotor transformer primaries were connected to ground by means of the same relay lead. By means of this connection the transformers were able to receive any signal present in the appropriately connected transducer element.

The first tests made with the AIDE DE CAMP 200-cycle system were on the pattern produced by the 200-cycle electronic rotor when connected to the HP-1 transducer. Measurements showed a major lobe with

an average width of 25 degrees and minor lobe structure averaging 16 db below the tip of the major lobe. The maximum deviation in width of patterns was  $\pm 6$  degrees. The minor lobe structure varied in height below the major lobe between the limits of 13 and 24 db.

Other tests made on this system showed that it was capable of indicating echoes from large targets, such as surface ships or island shoals, at ranges as great as those obtainable using the CR system. Under Boston Harbor conditions echoes were obtained out to 3,500 yards. The display on the PPI, according to observers, compared favorably with that of the CR system.

A series of observations was made to determine the relative usefulness of fixed-frequency transmitter output versus a frequency sweep (21 to 23 kc in 5 milliseconds). Observations on the AIDE DE CAMP system at 200-cycle rotation speed tended to indicate that there was no improvement in echo consistency, diminution of reverberation, or decrease in fluctuation of

CONFIDENTIAL

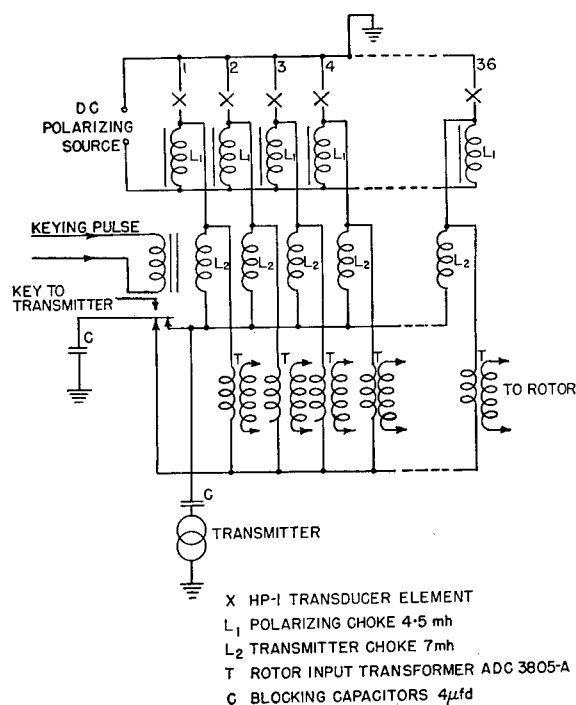


FIGURE 11. Circuit diagram of receive-transmit network ER sonar.

background noise due to frequency sweep as compared with single-frequency transmission. Furthermore, the use of a single frequency permitted the operation of the transmitter at the frequency corresponding to the greatest response in the HP-1 transducer, so that the average acoustic power was greater. In these same transmitter tests performed with the 200-cycle AIDE DE CAMP system "white" noise was tried as a transmitter source in place of a single frequency. A white noise generator was connected through an appropriate band-pass filter to the power amplifier used in the transmitter, and was tested against both the frequency sweep and the single-frequency type of operation. This white noise type of pulse produced by far the poorest results of the three tested, presumably because of power limitations as compared with single-frequency or glide-frequency operation.

Tests were begun on the AIDE DE CAMP to discover the usefulness of the 200-cycle rotation speed system as a small object locator. This system, making use of a 5-millisecond transmitted pulse, was found to have a considerable merit as a small-object locator when compared with a longer pulse system. The reference memorandum<sup>4</sup> describes the results of the tests made

in the detection of a 3-foot sphere against range and against depth of water in which the AIDE DE CAMP was being operated. The results of these tests indicated that a 3-foot sphere could be detected by a transducer hung 7 feet below the surface of the water at a range in yards approximately equal to the depth of the water in feet; that is, in 400 feet of water consistent echoes were returned from a 3-foot sphere at ranges of 400 yards. Partly as a result of these successful tests, a system was planned for use on submarines utilizing a short pulse and the high rotation speed which is possible with an ER scanning sonar system.

### 7.2.3

### 53-kc 500-cycle ER System

During the AIDE DE CAMP tests of the 200-c system, there became available to HUSL a Brush crystal transducer, AX-104, originally designed for the Naval Ordnance Laboratory [NOL], consisting of 36 vertical elements of Y-cut Rochelle salt crystals, resonant in the vicinity of 53 kc. It was decided, because of the possibility of using higher rotation speeds at the higher signal frequency, to construct a 500-c ER system using this transducer. This system became known as the 53-kc system, and its rotor is shown schematically in Figure 12. By comparison with Figure 7 it may

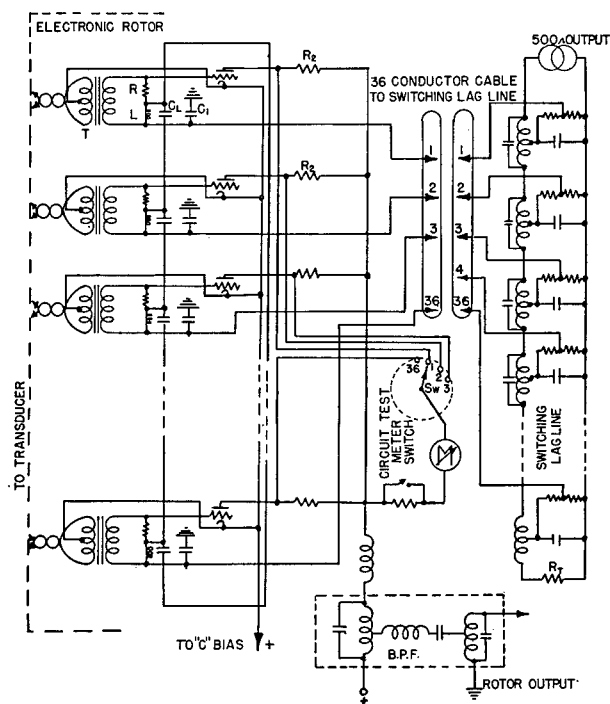


FIGURE 12. Circuit diagram of rotor, 53-kc ER sonar.

be seen that this 500-cycle rotor is very nearly the same as the 200-cycle rotor used in the previous systems. A transmission line was used for switching, and 18 6SN7 double triodes were used as electronic switches. Additional resistors and inductors were used in this lead line in place of the reactance of the transducer elements. A preamplifier was also built into a portion of the rotor chassis.

In order to couple the crystal transducer to the electronic rotor, transformers were mounted inside of AX-104, transforming the high capacitive reactance of the transducer to a low impedance with inductive reactance. The impedance at the secondary terminals of the transducer transformers was designed to be approximately  $50 + j100$  ohms at 53 kc. Twisted-pair cables were connected to the output of the transducer transformer to connect the transducer to the rotor which was external to the transducer. The rotor input transformers in the case of the 53-kc systems were Audio Development Company Type 3922.

A spiral sweep was especially constructed for the 53-kc system and is described in detail in Section 7.8.1 on spiral sweep requirements. It was an electronic spiral sweep, modeled after the sweep used successfully in the AIDE DE CAMP 200-cycle system, and incorporated a Sangamo mechanical timer to initiate the transmitted ping and thus to determine the fundamental timing operation for the entire system.

The transmitter is described in detail in Section 7.7 of this chapter covering that unit. It operated directly into a ring stack with a resonant frequency of 53 kc. Because of the transmission into a separate transducer, it was not necessary to incorporate any transmit-receive network in the 53-kc system. Keying was accomplished simply by the initiation of the transmitter pulse at the appropriate time as determined by the mechanical timer in the spiral sweep chassis. At the same time the spiral sweep chassis generated a blanking signal which blanked the return sweep of the PPI CRO.

This 53-kc system was installed upon the barge TIPPECANOE on the Charles River during the summer of 1944. A 3-foot sphere was brought into the river and towed as a target for the tests made at that time. This sphere produced easily visible echoes at distances as great as 300 yards in water of 20-foot depth. This performance was thought to be caused principally by the short transmitter pulse length, namely 2 milliseconds, and its inherently higher echo-to-reverberation ratio, since tests proved the receiver pat-

terns to be highly unsatisfactory. Major lobe widths averaged 35 degrees at a point 6 db below the tip of the major lobe, and showed considerable variation from element to element around the transducer. Widths were found as narrow as 28 degrees and as wide as 45 degrees. These poor transducer patterns, as compared with those obtained on the AIDE DE CAMP 200-cycle system, were caused by the transducer which had not been designed for this purpose. There were probably considerable phase differences between the outputs of the various elements, as the frequency response was found to differ greatly from element to element in the transducer.

During the tests in the Charles River, the AIDE DE CAMP was brought into the Basin for a detectability test in which the standard 24-kc WEA-1 echo-ranging sonar installed aboard the AIDE DE CAMP was used to listen for the transmitted pulse of the 500-cycle 53-kc system.<sup>5</sup> It was found that the transmitted pulses, although at a frequency of 53 kc, were easily detected by the WEA-1 operating at a frequency of 25 kc. These pulses were heard in the WEA-1 system as short loud clicks, and were seen as sharp deflections on the standard X-3a *bearing deviation indicator* [BDI] connected to the WEA-1. The source of the short click in WEA-1 and BDI equipment at 25 kc was the frequency spread of the short duration sharp-cornered pulse at 53 kc. It was suggested that pulse be tailored in order to reduce the frequency spread transmitted into the water,<sup>6</sup> and thereby reduce detectability. Subsequent theoretical work has suggested a Gaussian form of a pulse to give the minimum bandwidth for a pulse of a given time duration.

The 53-kc system was then transported to the Mountain Lakes Testing Station of the Underwater Sound Reference Laboratory [USRL] for tests and evaluation. Echo ranging was conducted in Crystal Lake against 2- and 3-foot spheres and against a hollow iron cylinder 8 inches in diameter. This system, because of its poor receiving patterns, as discussed in an earlier paragraph, and because of the relatively high system noise level, produced unsatisfactory results in these tests.<sup>7</sup>

The 53-kc system was then shipped from Mountain Lakes to New London where it was installed aboard the AIDE DE CAMP. The system there was compared with the WEA-1 installation on board for the detectability of small objects as well as for the determination of maximum discovery range of standard targets. High internal electric noise and generator noise

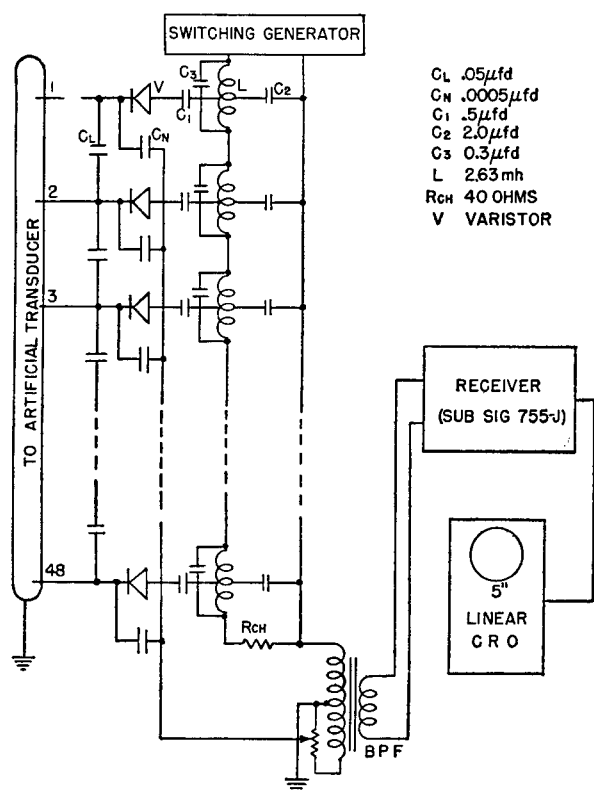


FIGURE 13. Circuit diagram of laboratory varistor rotor.

aboard the AIDE DE CAMP caused considerable difficulty. However, again because of the poor receiver-transducer patterns, the system proved decidedly inferior to the WEA-1. It proved inferior also to the standard 22-kc 200-cycle ER system previously installed.

## 7.2.4

**Submarine ER Sonar**

This system, which was also known as the 300-cycle varistor system, was based on the use of the varistor as an electronic switch. The investigation of copper oxide rectifiers for possible incorporation into electronic rotors is described in detail in Section 7.4 on ER rotors. Figure 13 is a schematic diagram of the rotor used in breadboard form for these tests in the laboratory. In test, it was connected to a suitable artificial transducer having output terminal impedances equivalent to those of a magnetostriction transducer. It was used to produce a rotating pattern of sensitivity, which upon passage through a Submarine Signal Company [SSC] Receiver Type 755-J was viewed by means of a linear-sweep cathode-ray oscilloscope. The switching transmission line, whose characteristic

impedance was 40 ohms, was incorporated into the large breadboard rotor and was supplied with either pulses or sine waves having a repetition frequency of 300 cycles. This transmission lag line was constructed so that a signal appearing at the beginning of the line would be absorbed in its terminating resistance  $1/300$  second later. To accommodate the 48 varistor switches of this rotor the line was divided into 48 elements so that it could be used with future 48-section transducers. The lead line in this case consisted of a set of capacitors (marked  $C_L$  in Figure 13) connected so that one was between each adjacent pair of transducer elements. Since the copper oxide rectifiers have a rather high capacitance it was necessary to connect a set of neutralizing capacitors  $C_N$  to one side of the primary of the output transformer as indicated in the diagram. The capacitors  $C_1$  were coupling capacitors which served also to maintain sufficient d-c bias on the varistors to keep them in the cutoff state except at the moment when the switching pulse was being applied. The switching lag line was of the bridged-T type originally used in the 200-cycle system. Noise and pattern tests made upon this breadboard rotor in the laboratory indicated that Western Electric Company varistors would be entirely satisfactory for switching purposes and it was decided to incorporate them in the rotor to be built for the submarine system.

The submarine system has already been described early in this chapter, while the details of the transducer, indicator, receiver, transmitter, and sweep chassis can be found under their proper headings. Figure 14 shows a schematic diagram of the varistor rotor incorporated in the submarine system. It was designed to be inserted into the transducers available for this purpose, which included AX-132 and AX-136 built by the Brush Development Company, and HP-3S built at HUSL. The varistor rotor wiring diagram shows the usual bridged-T switching lag line at the top of the diagram. The  $0.04\text{-}\mu\text{f}$  capacitors shown near the center of the diagram are for the lead line. Just below these lead line capacitors are the 48 separate matching transformers. At the bottom of the diagram are the 48 crystal elements of the transducer, each with its associated neon lamp which is used as part of the transfer network. The use of these  $1/4$ -watt neon tubes in the transfer network was necessary because the varistors were unable to withstand the same voltages upon transmission as the corresponding triode tubes in the previous rotor. At the right-hand

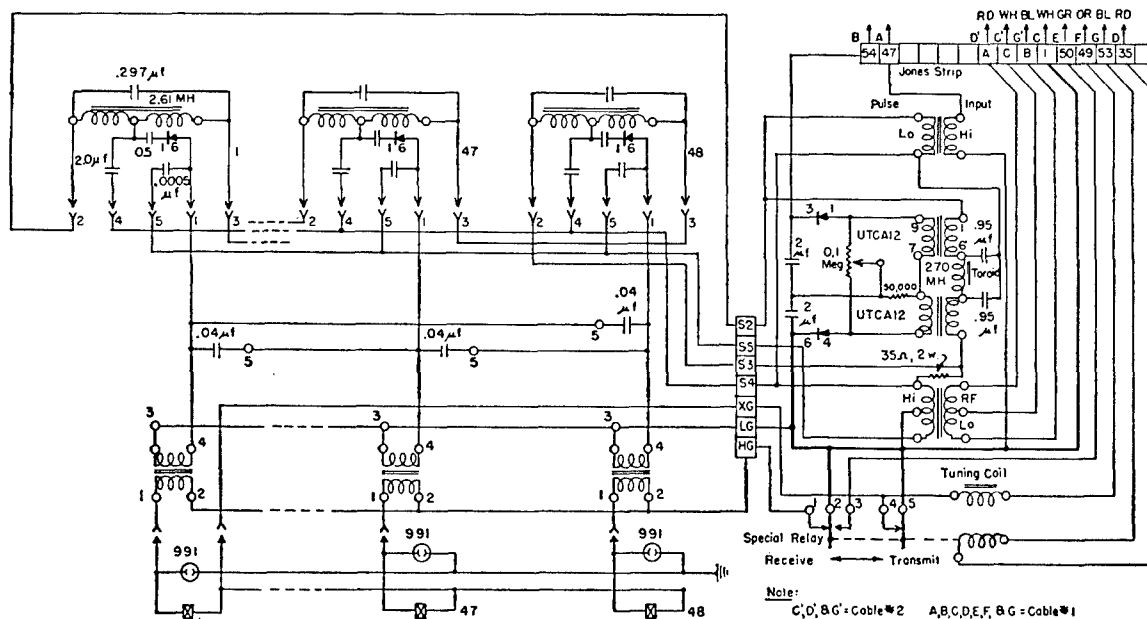


FIGURE 14. Circuit diagram of varistor rotor Model 1A, submarine ER sonar.

side of this diagram is indicated the discriminator network for maintaining the switching oscillator frequency at the correct value. This effects a total phase shift of 360 degrees in the switching lag line.

The first transducer to become available for the submarine system was AX-132, No. 1. For initial tests this transducer with its varistor rotor was installed with the remainder of the system at the HUSL Calibration Station at Spy Pond. Pattern measurements were made and found to correspond closely with those obtained in the laboratory on the breadboard rotor and discussed under ER rotors. Noise measurements were made and it was found that signals of the order of 0.3 mv were visible, as against the 0.7-mv minimum obtained with the laboratory varistor system. The better shielding afforded by the location of the varistor rotor inside the transducer was thought to cause this.

The chief difficulty experienced with the first installation of the submarine system at Spy Pond was the inability of the varistors installed inside the transducer to withstand the application of transmitter voltage to the system when a transfer network, similar to the one used with the 200-cycle rotor, was tried. As a result, a magnetostriction projector ring stack was incorporated into the first submarine system. Eight- and 12-inch triplanes were lowered into the water at Spy Pond and were readily detected by the sub-

marine system at ranges of about 150 to 200 yards. As a result of these tests, the submarine system was installed aboard the submarine USS DOLPHIN at New London at the end of February 1945. A series of tests was undertaken to determine the maximum range of discovery of certain small objects. In one of the tests a triplane 12 inches across was discovered at ranges of 1,400 yards and less. Subsequent tests on another day showed the system capable of producing consistent echoes from 3-foot mine cases at ranges of 900 yards.<sup>8</sup>

Meanwhile, experiments were begun at the laboratory to circumvent the varistor destruction which was involved in the first test of transmission direct into the AX-132 crystal transducer. An arrangement was developed to protect the varistors.<sup>9, 10</sup> In this circuit, as indicated at the bottom of Figure 14, transmitting power was applied to the crystal transducer through a series of 48 neon lamps. The drop across the neon lamps was of the order of 100 volts instead of the 2,000 or more volts developed across the input transformer primaries as originally designed. Rough measurements indicated that about 1 kw of power was lost in the neon lamps at each pulse when about 5 kw of power was applied to the transducer assembly by means of the transmitter. (See Section 7.4 on ER rotors for further description of this transfer network.) This system was then incorporated in an electronic rotor built into AX-136 and mounted aboard

the USS DOLPHIN on the bottomside QC training shaft available for that purpose, and it was also installed in a second AX-132 topside transducer. Throughout all of the tests on the USS DOLPHIN, none of the neon lamps failed in operation nor were any of the varistors burned out until the end of the tests, when one of the transmitter output tubes became defective and placed very large transients on the transducer assembly. Two transducers were used aboard the USS DOLPHIN, the AX-132 No. 2, mounted topside, and the AX-136 No. 1, mounted on the bottomside training shaft. Both of them were equipped with the neon lamp transmit-receive network.

The results of tests made on the USS DOLPHIN with the above gear were satisfactory, depending on echoing conditions. On days when a bathythermograph record showed an isothermal condition all the way to the bottom, the results were excellent. Consistent echoes were obtained from small objects, such as dummy mine cases, at ranges out to 600 yards and with discovery ranges of 1,500 yards.<sup>11</sup>

#### TRIPLANE DETECTION

Triplanes were used principally in the preliminary phases in March to check the operation of the equipment before the practice mine field was laid out completely. On the first field trip, twelve-inch triplanes were used as targets laid in the form of a square 1,000 yards on the side. The topside AX-132 transducer was used while a separate transmitting ring stack was used at the same time. The targets were placed at 25-to-45-foot depths in 120 feet of water while the USS DOLPHIN maneuvered at periscope depth, corresponding to approximately 55 feet from the keel to the surface. The AX-132 was thus at a depth of 28 feet. No differences were observed as a result of the varying depths of the target while the maximum discovery range was found to be 1,400 yards. Many echoes were followed in to ranges of about 200 yards with consistent echoes all the way in. Triplanes were again used about a week after the initial tests, at which time the bottomside AX-136 transducer was tested. On this occasion five triplanes were planted in a straight line to simplify the maneuvering problem. Very poor results were produced by the topside transducer. With the bottomside transducer, however, a maximum range of 800 yards was obtained. A 12-inch triplane at a 25-foot depth gave the best results throughout the day. It returned echoes on an average of 80 per cent of the pings sent

out, while the remaining 12-inch triplanes returned only 10 or 20 per cent of the pings. The 8-inch triplane, which was planted on one end of the line, was never seen at any range. During the day echoes were observed at ranges of from 900 to 1,200 yards, on an unknown target, which later turned out to be a friendly submarine operating in the same area.

#### MINE DETECTION

A practice mine field was laid out about 3 miles east of Block Island in water about 120 feet deep. This field was laid in two parallel rows with 13 mines in each row at varying depths from the surface to the bottom; the distance between the rows was 500 yards, while the distance between individual mine cases in each was 100 yards. The standard 3-foot spherical mine cases used were filled with plaster of Paris and air in the same proportion as a standard live mine would be filled with TNT and air. Among the problems studied in the work on the mine field, besides the gaining of a general impression of the operation of the system and obtaining operating experience were:

1. Consistency of echo return,
2. Effect of depth of target on echo return,
3. Bearing accuracy,
4. Bearing resolution,
5. Ability to con a course through the mine field from PPI indications, and
6. Ability to follow mines to within 100 yards' range.

In general, ranges obtained on the 3-foot mine cases were greater than had been anticipated, and the maximum was found to be 1,500 to 1,600 yards. At extended ranges the chance of obtaining echoes became very small, however, while targets at fairly short ranges of 600 to 1,000 yards came in with much more consistency. The following table giving the percentage of pings returning echoes at various ranges is of interest:

Range (yards)	Percentage pings giving echoes
0 - 150	75%
150 - 600	90%
600 - 1000	40%
1000 and over	15%

In general, it was found that those targets at a depth more nearly comparable to that of the transducer, be-

tween 40 and 70 feet, gave the most consistent echo return. In addition to this numerical check, on at least one occasion 11 mines were observed at once in a row on the 1,500-yard scale. This further indicated the ability of the system to receive echoes at reasonable ranges without much regard for the depth of the target.

Bearing accuracy checks made with this gear were few. The observations that were made were usually consistent to  $\pm 1$  degree, and no difference in consistency was observed as between mines and other targets. Probably as a result of the fairly broad receiving sensitivity pattern, it was found difficult to resolve mines only 100 yards apart at ranges of over 300 yards because of the broad PPI indications of the echoes.

Some work was done with a surface target in order to check the ability of the equipment to echo-range on such a target. The destroyer used as a target lay dead in the water, while the USS DOLPHIN spiraled outward from a very short range to rather long ranges. To check the bearing accuracy, coincident readings were taken of center bearings of the targets on the PPI scope and of masthead bearings by the periscope. After a 5-degree correction was made for what was assumed to be an error in the setting of the PPI deflection coils, it was found that the readings from the PPI and the bearing readings from the periscope agreed with each other to within  $\pm 1$  degree. During this check a count was kept on echoes returned for pings sent out. Between the ranges of 150 and 1,000 yards, no echoes were missed for over one hour. When the destroyer was under way, it was much more difficult to obtain echoes from her as a target because many echoes were lost in the noise from the destroyer propellers. When the destroyer was making 12 knots, the screws were followed by the noise indications out to 1,400 yards range, but when the destroyer was making 25 knots, contact was made at 3,500 yards and lost at 1,900 yards as the result of passing through the wake of the destroyer. The contacts could undoubtedly have been made again and at a range greater than 3,500 yards if the tests had continued to a greater range.

#### TORPEDO DETECTION

For this purpose torpedoes were fired both from the USS DOLPHIN and from another submarine. In 11 cases, except that of one run, the torpedo was detected at the moment of firing. In this one run, the torpedo

was not picked up until it was within 4,000 yards of the USS DOLPHIN. Some of these runs were erratic, but at no time was there any difficulty in determining the bearing of the torpedo by means of the noise indications on the PPI. In the case of the four torpedoes fired from the USS DOLPHIN, it was found possible to follow them to the end of their runs at distances of about 5,000 yards. In every case the torpedo would have been detected at a range sufficiently great to allow for evasive action on the part of the USS DOLPHIN.

#### DEPTH CHARGE DETECTION

One depth charge was set off at a distance of 700 yards, while the USS DOLPHIN was on the surface, and later three standard 300-pound depth charges were dropped while the USS DOLPHIN was submerged. This string was set to explode about 300 yards apart at a range of 750 yards from the USS DOLPHIN. The result of the concussion on the PPI was a complete, but not intense, brightening over the whole scope face. As the range switch was set on the 1,500-yard range at the time, it is evident that approximately two seconds must have elapsed during the general commotion following the explosion. Approximately five or ten seconds after the explosion was heard, it was possible to obtain sharp echoes from the turbulence by echo ranging with the sonar gear. An echo could be obtained from this turbulence for 20 minutes and more after the explosion had occurred. When the three depth charges were set off at ranges of 100 yards apart 750 yards away, echoes were obtained after each explosion, but no separate echo was ever seen. Apparently the turbulence from the charges overlapped sufficiently to make it impossible to resolve the individual explosions.

During these tests the output power was measured by means of a B-19J hydrophone. The AX-136 bottomside transducer was found to produce about 900 watts of acoustic power at 33.6 kc. At the same frequency and pinging rate of the 300-yard rate, the AX-132 topside transducer gave 1,500 watts acoustic output in the water. The tests on the topside transducer were made by means of a monitor hydrophone, permanently installed on the deck of the submarine.

Before this series of field tests was carried out, it had been hoped that the 3-millisecond pulse used in transmission would confer a great measure of secrecy on the system while echo ranging. However, a surface ship working with us reported that their standard QC

CONFIDENTIAL

gear gave a sound like someone hitting the loud-speaker case with a hammer. The standard 755 receiver, tuning from 18 to 30 kc, picked up the ping at any point on the dial with the projector trained on the sound source.

Throughout most of the tests, the wide-range monitor was connected to the installed topside monitor hydrophone and was left in the beat position, with the frequency dial set at approximately the frequency of the transmitted pulse. The amount of information about what was going on outside was considerable, and it was found at least on one occasion that distinct echoes could be heard even with the nondirectional monitor hydrophone. In addition, reverberation would draw the pulse out long enough in time so that a definite frequency could be recognized and measured by means of a beat-frequency method.

## 7.3

**ER TRANSDUCERS**

## 7.3.1

**HP-1 Transducer**

The rebuilt version of this transducer was used with the 60-cycle ER sonar and again with the 200-cycle ER sonar on the AIDE DE CAMP. It was a 36-element magnetostriction transducer with a resonant frequency of about 22 kc.

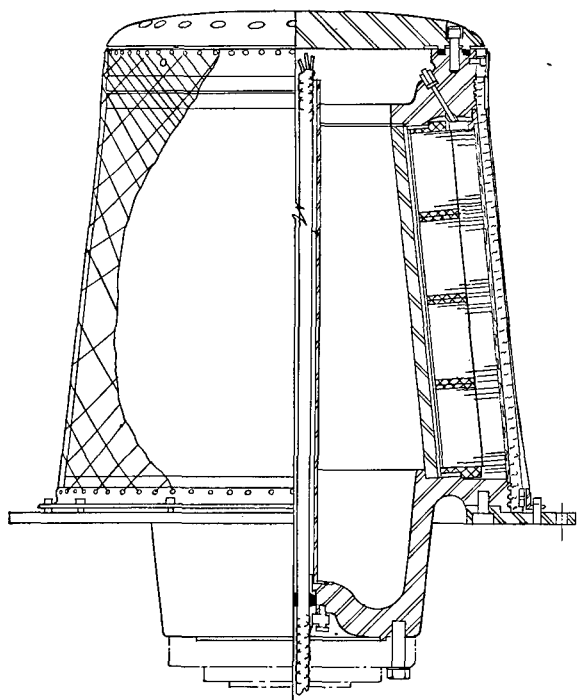


FIGURE 15. Assembly cross section of HP-3S transducer.

## 7.3.2

**HP-3S Transducer**

This transducer was designed to be mounted on the deck of a submarine for use with the submarine ER sonar. Each element consisted of four shorter elements of the type used in the construction of HP-3 and discussed in Chapter 5. The 48 elements of the transducer were polarized by permanent magnets and were arranged in the form of a cone inclined upward at an angle of approximately 6 degrees to the vertical through the center of the transducer. Figure 15 is an assembly drawing showing the general construction of the unit. A partial assembly of the transducer is shown photographically in Figure 16. The transducer was designed with special strength considerations so that it would withstand both wave action, when the submarine was on the surface, and high pressures, when the submarine was submerged. Its central portion was designed to contain the electronic rotor.

The impedance characteristics of the individual

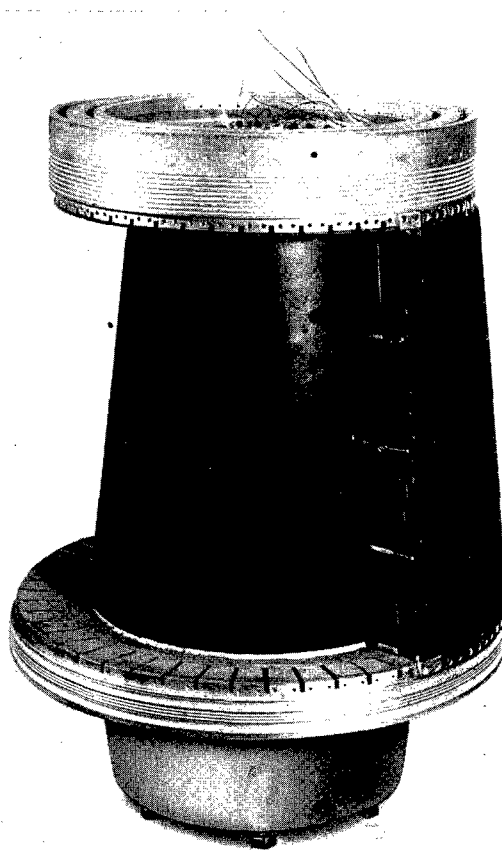


FIGURE 16. Partial assembly view of HP-3S transducer.

CONFIDENTIAL



staves were similar to those of HP-3, the average impedance being  $15.7 - j25$  ohms at resonance in water.

## 7.3.3

**AX-89 No. 2**

This 36-element Y-cut Rochelle salt crystal transducer, with a resonant frequency of about 24 kc, was originally constructed for use with a CR system. It was used on the barge for tests on lead lines and beam pattern formation. A more complete discussion is found in Chapter 5.

## 7.3.4

**AX-104**

This transducer was obtained on loan from the Naval Ordnance Laboratory following its construction at the Brush Development Company. It was composed of 36 crystal stacks arranged circularly with an active face diameter of  $7\frac{1}{4}$  inches, each element having an active face height of 4 inches. The crystals were Y-cut Rochelle salt and were resonant at approximately 53 kc. The mechanical construction of the transducer is shown in Figure 17, and a photograph is given in Figure 18.

Because of the high impedance of this crystal trans-

ducer it was necessary to insert cathode followers in the output of each element before entering the cable, thus making the output impedance of the amplifier approximately 700 ohms. Since it was impossible to drive the transducer through the cathode followers, no transmitting data were obtained on this unit. However, sufficient receiving data and impedance measurement data were collected so that a clear picture was obtained of its performance. Later on, transformers were installed in place of the cathode followers, but the transducer was still not used for transmitting.

Impedance versus temperature measurements were made on this unit at 53 kc, and it was found that the average equivalent shunt impedance of individual elements changed from  $250 - j185$  ohms at 0 C to  $225 - j190$  ohms at 18 C. It is to be noted that the variation here was considerably less than with the X-cut crystal transducer CP-1 No. 770, described in Chapter 5.

Figure 19 shows a horizontal receiving pattern for this transducer obtained with all 36 elements receiving in parallel. The greatest deviation from this average in this pattern is  $\pm 3$  db, this being compara-

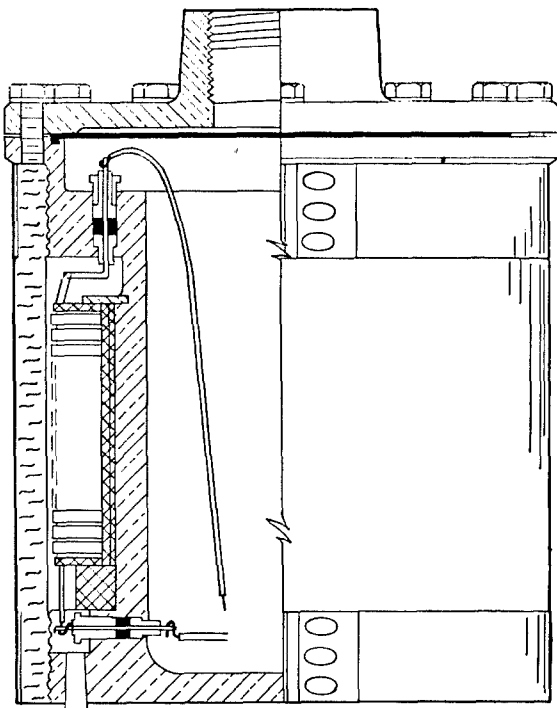


FIGURE 17. Assembly cross section of AX-104 transducer.

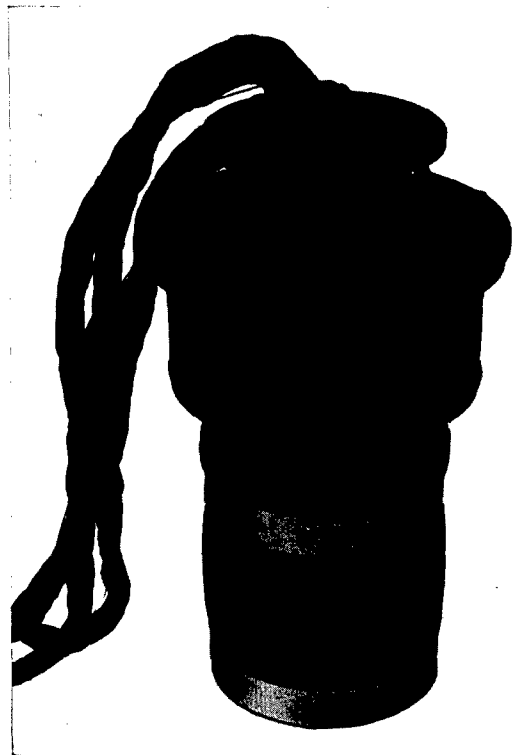


FIGURE 18. Assembly view of AX-104 transducer.

CONFIDENTIAL

ble to that of similar patterns for other scanning sonar-type transducers.<sup>12</sup>

Figure 20 shows the response of AX-104. The  $Q$  as calculated from this curve is approximately 3.1. Measurements from admittance and impedance circles indicate the efficiency at resonance and the maximum efficiency of this unit to be approximately 21 per cent, and the potential efficiency to be 30 per cent.

Figure 21 shows a vertical receiving pattern for the AX-104 transducer with all elements in parallel. The directivity ratio as calculated from the pattern for the parallel array is 0.14. This may be compared with a value of 0.13 for HP-1 and 0.075 for HP-2.

Figure 22 shows a receiving pattern obtained with a 10-element lag line designed for this transducer. The highest minor lobes for all 10-element groups were approximately 20 db down, and the average major lobe width at 6 db down was 20 degrees.

This transducer was used in connection with the 53-kc ER system demonstrated at the Mountain Lakes Reference Laboratory as described in an earlier section of this chapter.

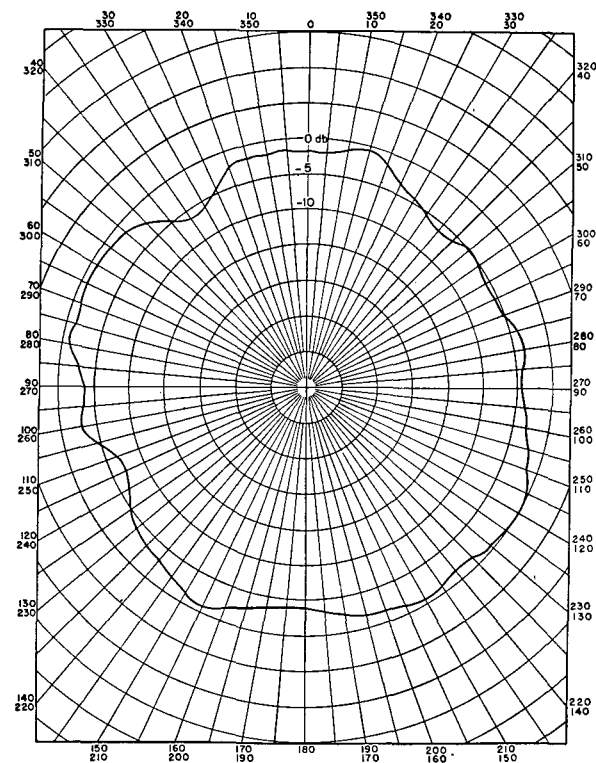


FIGURE 19. Horizontal receiving pattern with 36 elements in parallel, AX-104 transducer.

### AX-132 No. 1

The AX-132 transducer was constructed by the Brush Development Company. This was a 48-element crystal unit, constructed of ADP crystals. These crystals were made into staves arranged conically and inclined upward at an angle of approximately 6 degrees to the vertical through the center of the transducer. The design of this transducer is shown in Figure 23, and it is shown photographically in Figure 24. The active face was 10 inches in height,  $14\frac{1}{2}$  inches in diameter at the top, and  $16\frac{3}{4}$  inches in diameter at the bottom. The unit was designed to be mounted on the deck of a submarine.

Admittance measurements made on each of the 48 elements of the transducer indicate that the elements tend to be grouped into two admittance groups. The average impedance for the elements in one group, as calculated from the admittance data, was  $894 - j7320$  ohms, and for the elements in the second group, it was  $1190 - j7430$  ohms. The impedance for all of the elements connected in parallel was approximately  $23.8 - j160$  ohms. All of the impedance values given

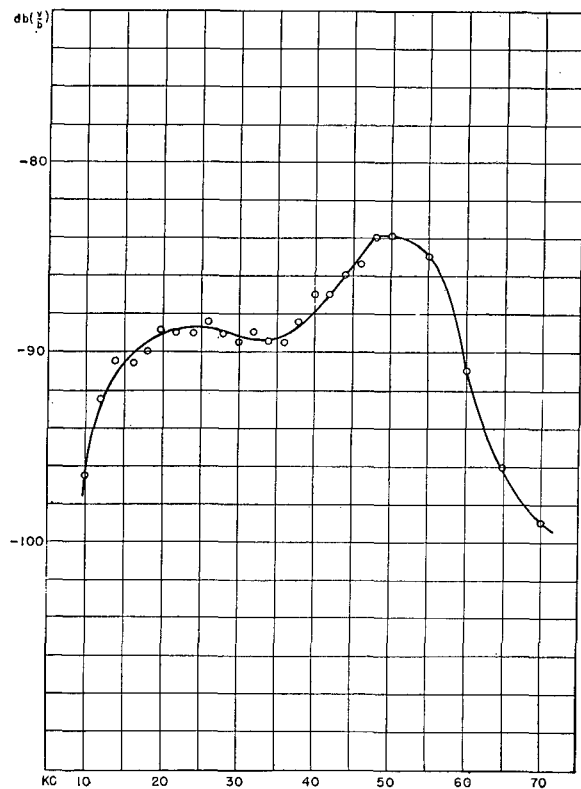


FIGURE 20. Frequency response, AX-104 transducer.

CONFIDENTIAL

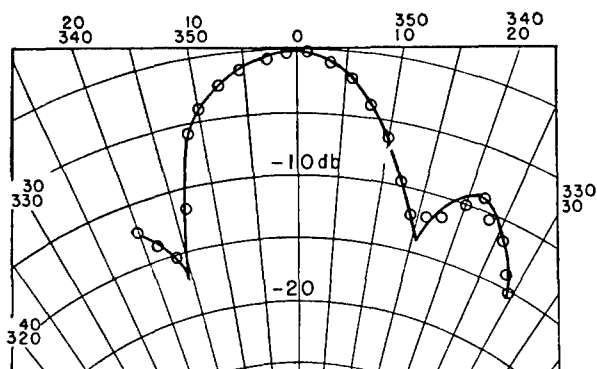


FIGURE 21. Vertical receiving pattern with all elements in parallel, AX-104 transducer.

here were derived from admittance data taken at a frequency of 32 kc.<sup>13</sup>

The curve in Figure 25 represents the transmitting response with all of the elements connected in parallel. The mechanical  $Q$  as calculated for 31 kc is 3.1. It is to be noted that the response at the second harmonic frequency of 60 kc was only 1 db below that at the resonant frequency.

Figure 26 shows the horizontal receiving pattern for this transducer with all elements in parallel.

An average of the horizontal patterns made on each of the 48 elements is shown by the solid curve in

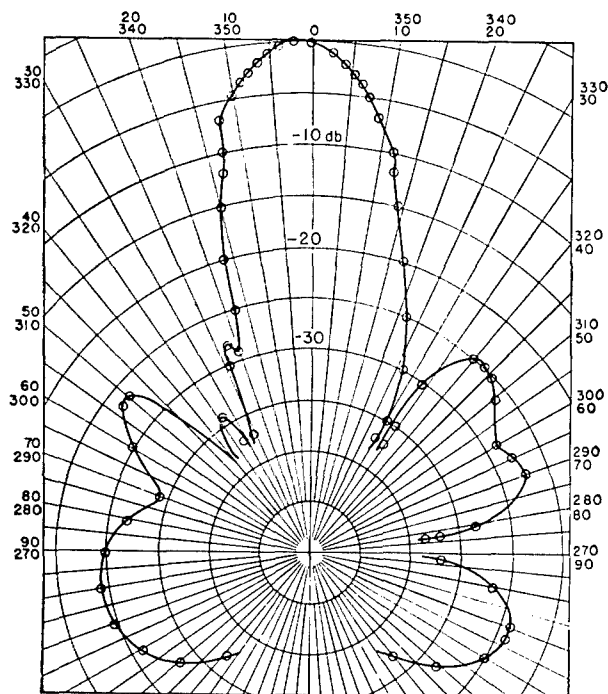


FIGURE 22. Horizontal receiving pattern with 10 elements compensated, AX-104 transducer.

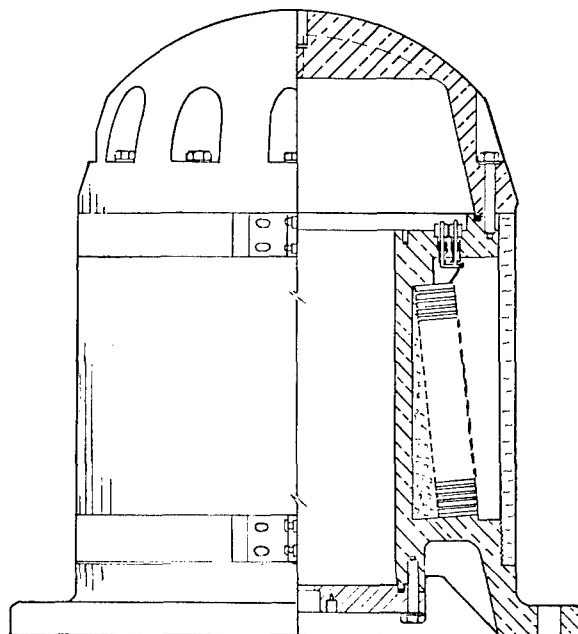


FIGURE 23. Assembly cross section of AX-132 transducer.

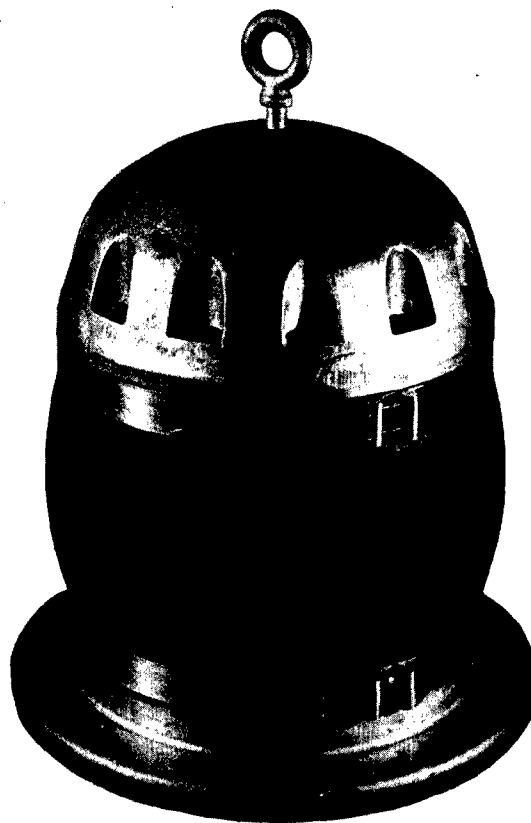


FIGURE 24. Assembly view of AX-132 transducer.

CONFIDENTIAL

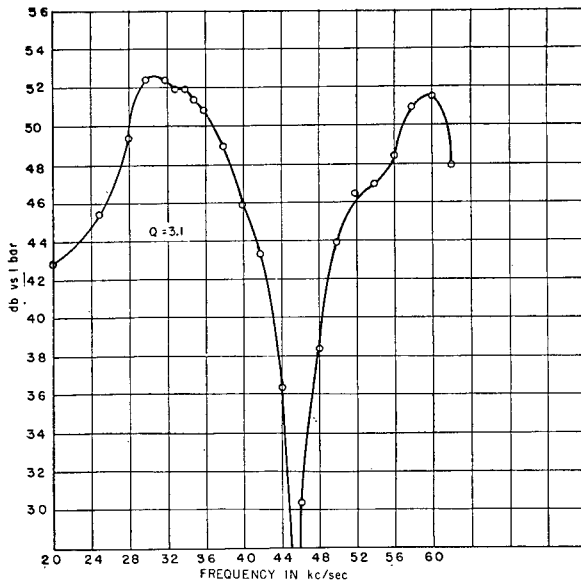


FIGURE 25. Transmitting frequency response for AX-132 transducer No. 1.

Figure 27. In this figure are also shown the theoretical patterns for a single element of the type used in the transducer with pressure release baffle and stiff baffle.

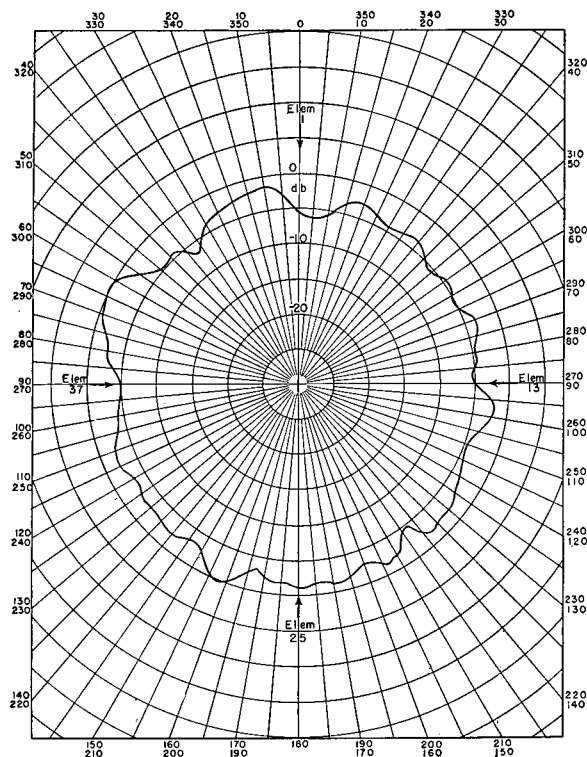


FIGURE 26. Horizontal receiving pattern for AX-132 transducer No. 1.

It is seen that the observed pattern coincides within a few db with the theoretical pattern for a pressure release baffle. The vertical receiving pattern, made with all elements of the AX-132 in parallel, is shown in Figure 28. This pattern is not complete because the curve shown is taken only within the limits between which the measuring hydrophone could be moved. It was assumed, however, that the minor lobes on the left side of the central beam were similar to those on the right side, and the directivity index was calculated on this basis to be 0.08.

A total of six Type AX-132 crystal transducers were delivered to HUSL by the Brush Development Company and tested at the Spy Pond Calibration Station. All the measurements on these transducers gave results that were very nearly the same as those obtained with AX-132 No. 1, except that in general the individual elements in any one transducer were more closely like each other than were the elements in AX-132 No. 1.<sup>14-18</sup>

For example, the admittance measurements made on individual elements for the last five transducers show that the elements tended to be grouped close together instead of in two groups, with the exception of certain single elements in transducers No. 4 and No. 6. Circles drawn on the admittance diagram so that all the points were included had radii that were less than 2 per cent of the magnitude of the vector admittance.

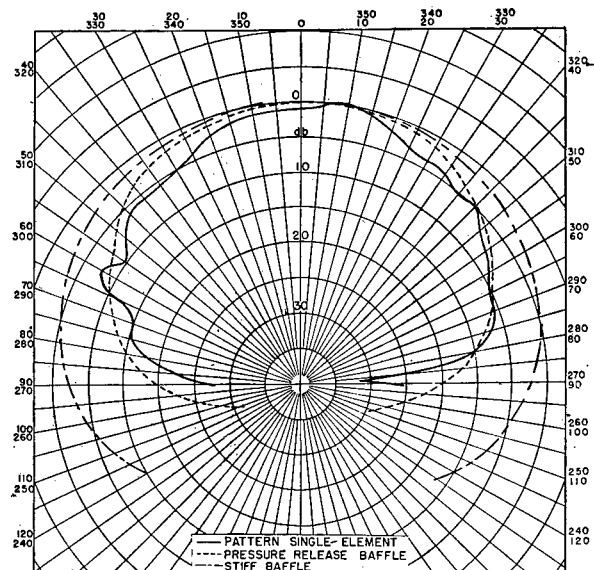


FIGURE 27. Horizontal single-element pattern of AX-132 transducer No. 1.

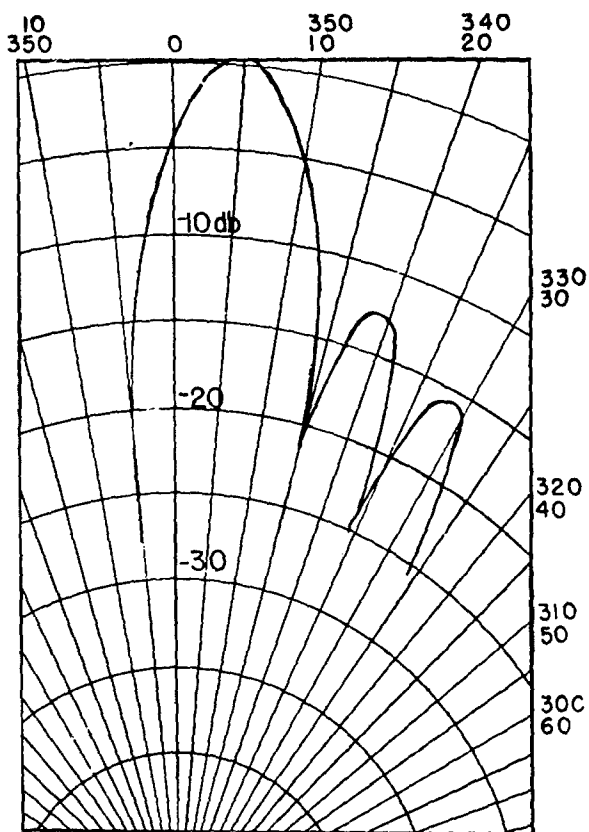


FIGURE 28. Vertical receiving pattern of AX-132 transducer No. 1.

The resonant frequencies of all of these transducers was very close to 32 kc as measured on about one fourth of the individual elements in each case. Horizontal transmitting patterns were taken with all elements connected in parallel and in all cases were found to be flat within  $\pm 1$  db as the transducer was

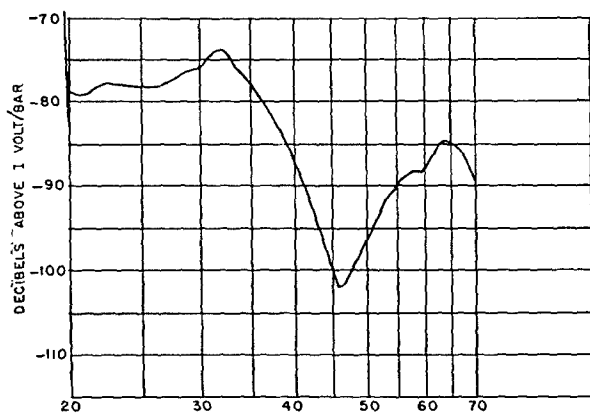


FIGURE 29. Receiving frequency response for single element of AX-132 transducer No. 6.

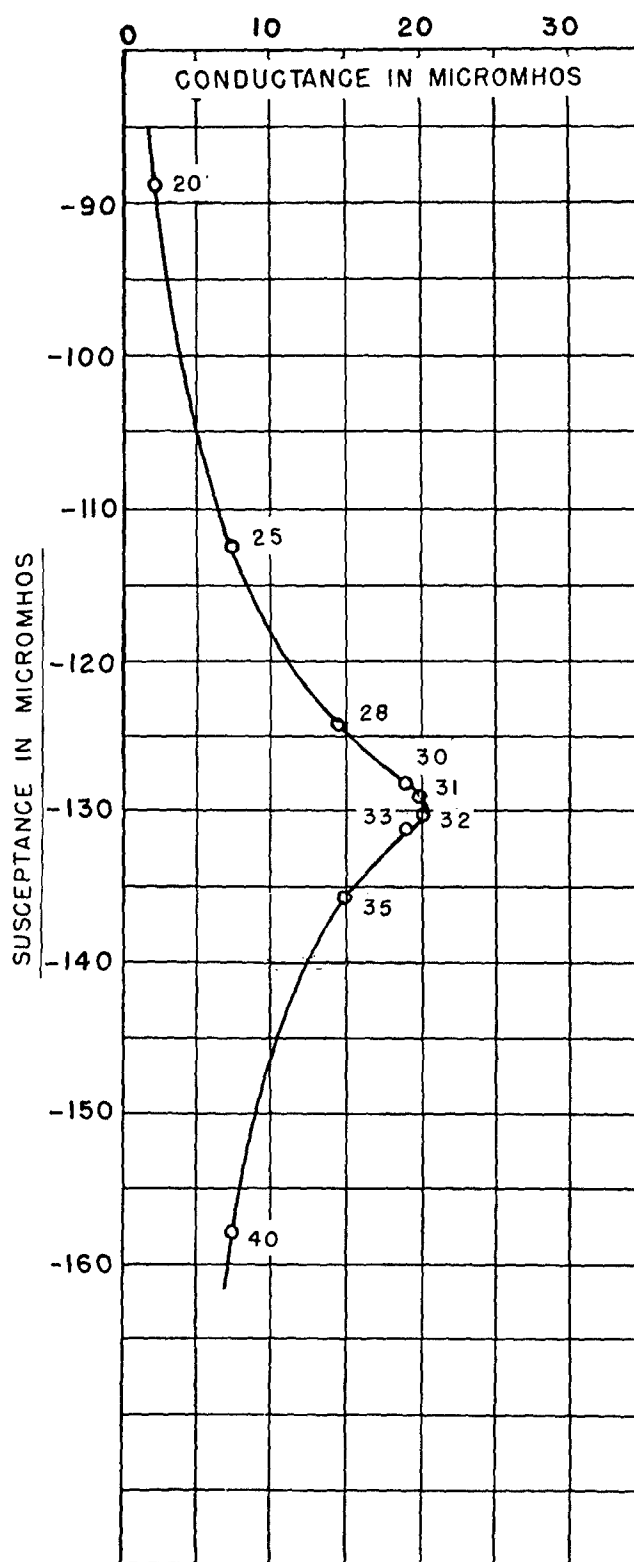


FIGURE 30. Admittance locus of single element of AX-132 transducer No. 6.

CONFIDENTIAL

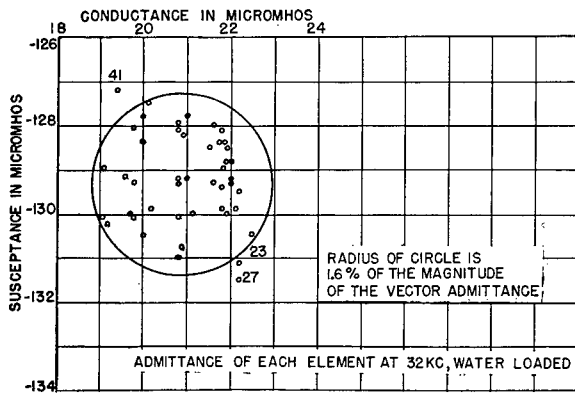


FIGURE 31. Plot of element admittances, AX-132 transducer No. 6.

rotated 360 degrees. Figure 29 shows the receiving response of a single element; Figure 30 the admittance of a single element at different frequencies; Figure 31 an admittance plot for all elements at 32 kc; and Figure 32 the transmitting pattern of all elements in parallel at 32 kc.

### 7.3.6 AX-136 Crystal Transducer No. 1

This transducer was an ADP crystal unit manufactured by the Brush Development Company and de-

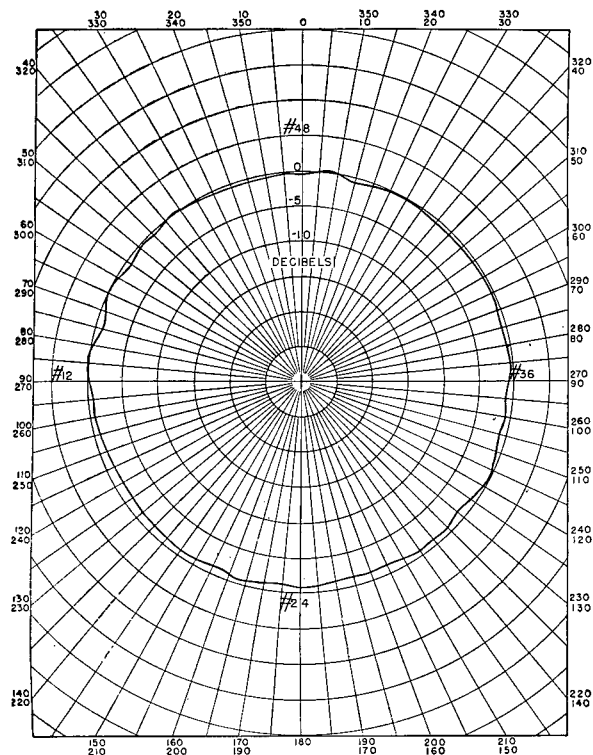


FIGURE 32. Horizontal transmitting pattern with all elements in parallel, AX-132 transducer No. 6.

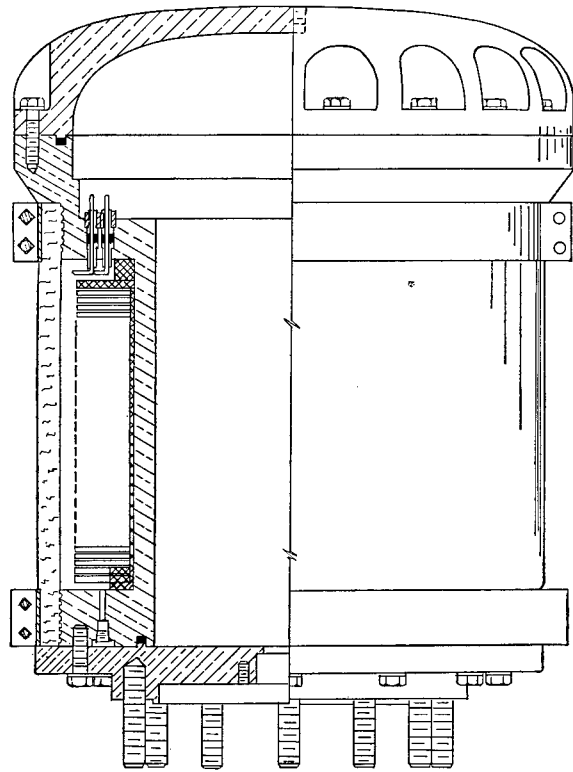


FIGURE 33. Assembly cross section of AX-136 transducer.

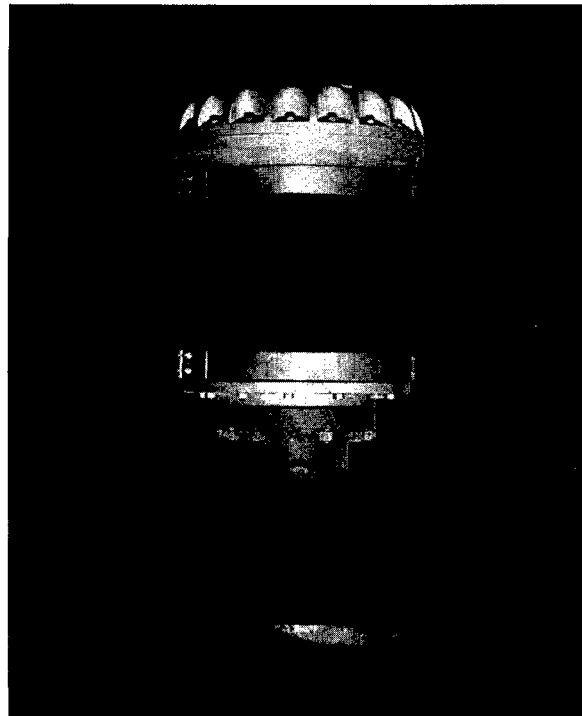


FIGURE 34. Installed view of AX-136 transducer.

CONFIDENTIAL

signed for bottomside mounting on a submarine. The elements were arranged vertically around the surface of a cylinder, the active faces of the crystals forming a surface having a diameter of  $14\frac{1}{2}$  inches. The general construction of the unit is shown in Figure 33, and the unit itself is shown photographically in Figure 34.

The average admittance of a single element of this

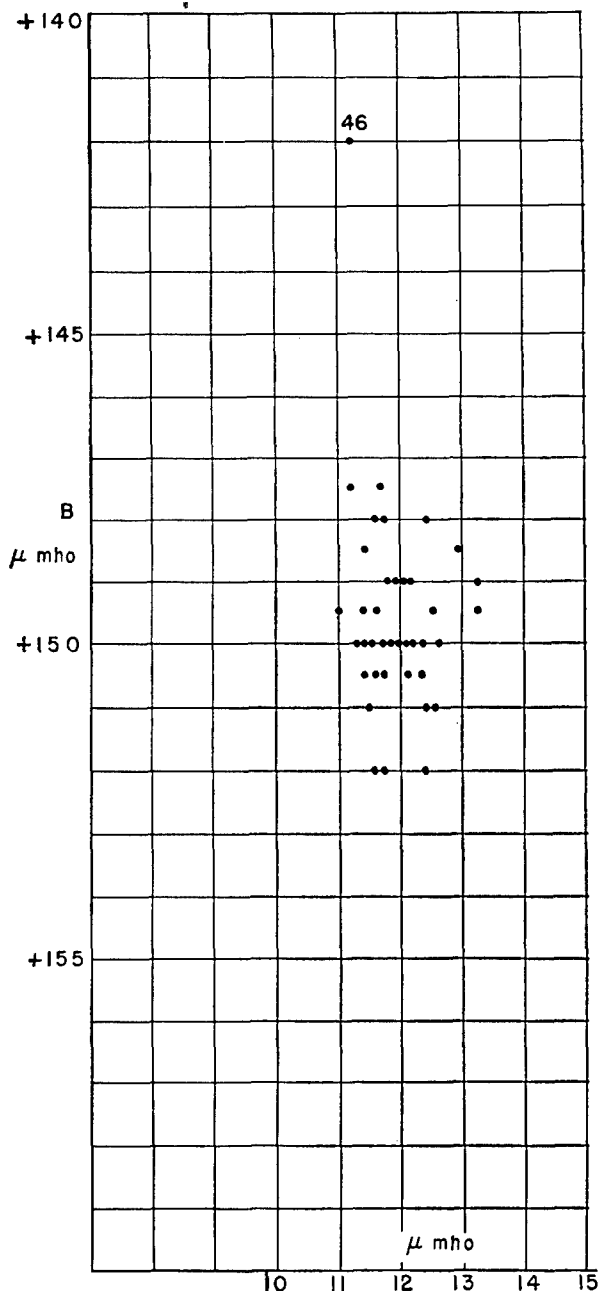


FIGURE 35. Plot of element admittances, AX-136 transducer No. 1.

transducer was  $11.95 + j149.6$  micromhos. The average impedance of all the elements in parallel was  $11.05 - j138.5$  ohms, and the average impedance of a single element was  $532 - j6650$  ohms. Figure 35 shows the admittances of all the separate elements plotted on the same graph at 32 kc. Several of the points marked on this graph represent two or more different elements.<sup>19</sup>

Figure 36 gives the response of all 48 elements in parallel while transmitting with a constant power input to the transducer of  $5.6 \times 10^{-5}$  watt. As can be seen from this graph, the transducer had a resonant frequency near 40 kc, and when used as a transmitter had about 4 db more output at 40 kc than it did at 32 kc which was the intended operating frequency.

A horizontal receiving pattern of an individual element is shown in Figure 37. This was taken at 32 kc and, within experimental error, this is equivalent to the receiving pattern of any of the other single elements. Figure 38 shows the horizontal receiving pattern taken with all elements receiving in parallel at 32 kc. This is seen to be flat to within  $\pm 1$  db.

The efficiency of the transducer was calculated from the acoustic field measurements and the measured impedances of the transducer itself, on the assumption of a directivity ratio of 0.1 for the transducer as a whole and about 0.02 for a single element. As a transmitter the efficiency was calculated to be 13 per cent at 32 kc and 34.4 per cent at 40 kc. As a receiver the efficiency of the transducer was calculated to be 20 per cent at 32 kc.

In all, six AX-136 transducers were built and delivered by Brush Development Company. Measurements at Spy Pond indicated a transmitting efficiency of 40 per cent at 32 kc for AX-136 No. 4, a typical unit.<sup>20</sup>

Admittance measurements made on individual elements showed them all to be grouped close together. As described in the previous section, circles may be drawn around all of the points on the admittance diagram for each transducer with a radius about 2 per cent of the magnitude of the vector admittance. As on

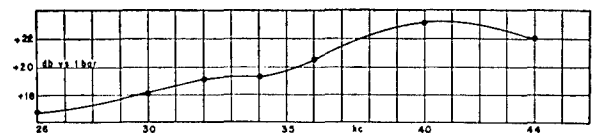


FIGURE 36. Transmitting frequency response with all elements in parallel, AX-136 transducer No. 1.

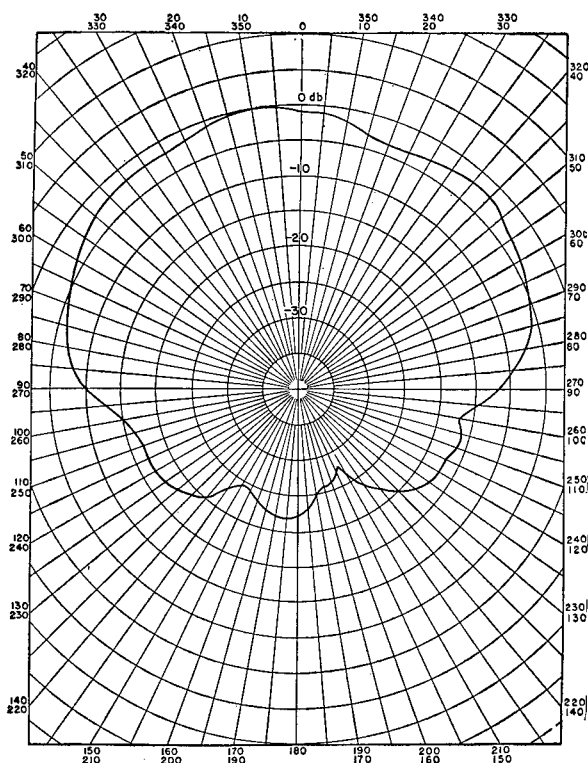


FIGURE 37. Horizontal receiving pattern of single element, AX-136 transducer No. 1.

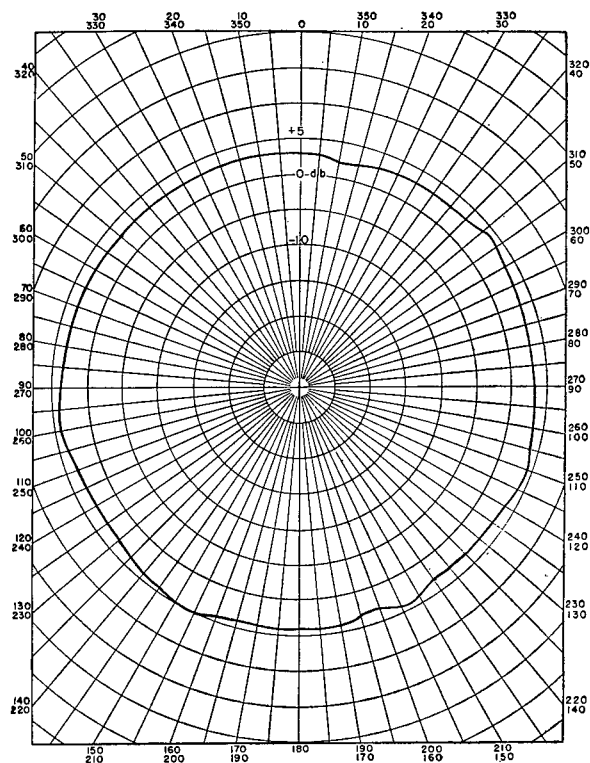


FIGURE 38. Horizontal receiving pattern with all elements in parallel, AX-136 transducer No. 1.

AX-132 transducers, the transmitting patterns of all elements in parallel showed deviations no greater than  $\pm 1$  db in a horizontal plane. Details of the measurements are given elsewhere.<sup>21-25</sup>

### 7.3.7 54-kc Ring-Stack Transducer (54 ARS No. 1)

Since cathode followers were placed in the output of each element of the AX-104 transducer to reduce the impedance, it was impossible to transmit with this transducer. Consequently, a ring stack was constructed to be used for transmitting. This transducer was constructed of rings of approximately 1-inch inside diameter by 1.2-inch outside diameter. Its general construction is shown in Figure 39. It was made in two sections in order to allow a choice of directivity. The length of each section was  $3\frac{1}{2}$  inches.

The horizontal transmitting pattern of individual sections of this transducer, or of both sections in series, was flat to within  $\pm 1$  db. The vertical transmitting pattern of a single section and of both sections in series<sup>26</sup> is shown in Figure 40 and Figure 41.

The transducer was used only with the two sections in series, and for that case the impedance in water was  $20 + j400$  ohms and in air  $100 + j25$  ohms. These values were taken at approximately 54 kc (the resonant frequency of the transducer) with a polarizing current of 2 amperes.

### 7.3.8 28-kc Ring-Stack (28 ARS No. 5)

This transducer was designed to be used with the ER submarine system for transmitting. The rings in this transducer were approximately 2-inch inside diameter by 2.3-inch outside diameter. Its general construction is shown in Figure 42, while Figure 43 shows a photograph of the unit as it was mounted near the JK hydrophone on the deck of the USS DOLPHIN.

The transducer was resonant at approximately 31 kc and had a horizontal pattern flat to  $\pm 1$  db.<sup>26</sup> The impedance at resonance in water was approximately  $400 + j240$  ohms, and in air was approximately  $870 - j87$  ohms, when a polarizing current of 5 amperes was used. No vertical patterns were taken on this unit; consequently, there is no indication of its



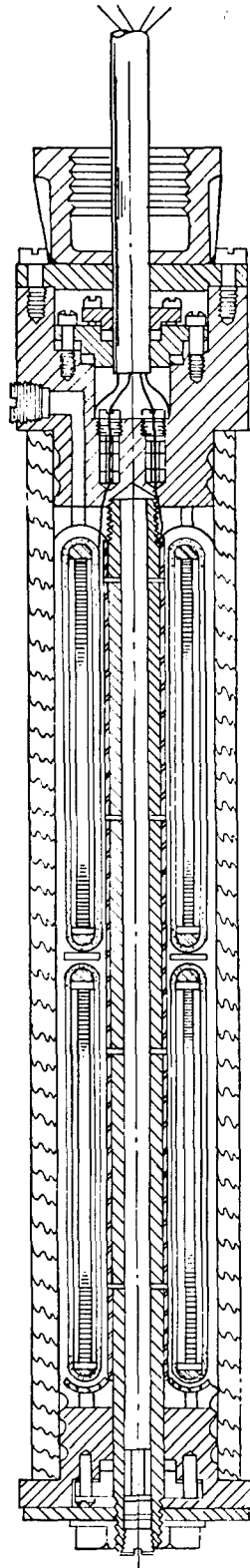


FIGURE 39. Assembly cross section of 54-kc ring-stack transducer.

directivity. The potential efficiency of this unit, as determined from impedance circles, was 71 per cent.

#### 7.4

#### ER ROTORS

##### 7.4.1 Functional Parts of Electronic Rotor

The electronic rotor is that combination of circuit and transmission line components that produces a rotating beam of sensitivity when connected to a multielement cylindrical transducer. It can be described as consisting of three main sections: the first is the compensating lead line network to which the transducer elements are connected; the second is an array of electronic switches equal in number to the number of elements in the transducer; the third is the switching generator which operates the electronic switches.

##### 7.4.2

#### Operation of Lead Line in Pattern Formation

Figure 44 shows a multielement cylindrical transducer array connected to a lead line. Each element numbered from 1 through 48 is connected to a point on the lead line. These points are numbered 1' through 48'. The action of the combination of transducer and lead line is hereinafter referred to as the first stage of pattern formation. Just below the lead line is shown a number of electronic switches, diagrammatically represented as circles, numbered 1 through 48. The action of the electronic switches on the lead line and transducer combination is hereinafter referred to as the second stage of pattern formation.

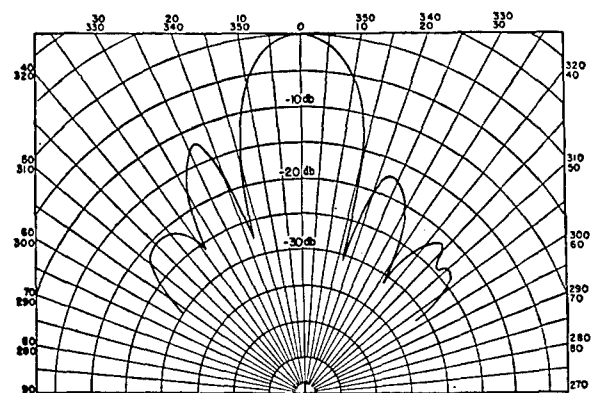


FIGURE 40. Vertical transmitting pattern of one section, 54-kc ring-stack transducer.

CONFIDENTIAL

When the transducer is receiving sound from a point source at an infinite distance, a pattern is produced along the lead line which has both amplitude and phase components. Figure 45 is the amplitude pattern of the first stage of ER sonar. Figure 46 is the associated phase pattern. (See Chapter 9 for the method of computing these patterns.) It is seen from the amplitude pattern that the width of the pattern, 6 db down, is 22 degrees, and the height of the principal minor lobe is 11 db with respect to the tip of the major lobe. Other minor lobes exist as shown alongside the first principal minor lobe in descending amplitude order.

It is seen that the slope of the phase pattern, with respect to bearing, is greatest in the amplitude pattern minima and flattens out for each amplitude pattern maximum. It is also seen that the flattening of the phase curve occurs most prominently in the major lobe and in the first minor lobe, with only minor inflections occurring for each succeeding minor lobe.

This first stage pattern of ER sonar is scanned by means of an appropriate group of electronic switches. Referring again to Figure 44, it is seen that all of the electronic switches have a common output. Below the array of switches is seen the curve of conductivity versus bearing position. A given switch conducts signals from its input to the common output only when the conductivity of the switch is greater than zero. The conductivity wave is shown as the tip of a sine wave having a base width of 40 degrees (bearing angle sector), so that only those switches lying directly above the conductivity (in the drawing) wave may contribute signal from their input to the common output. This conductivity wave is made to progress to the right by means which are referred to hereafter as

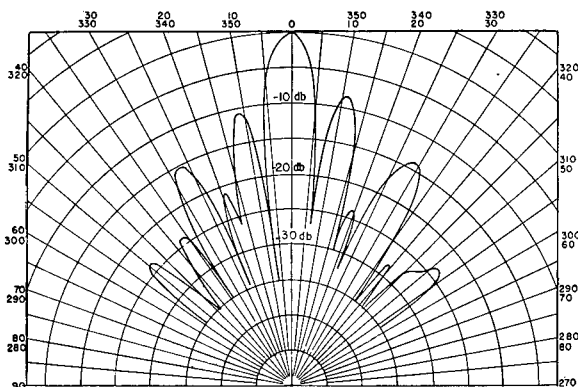


FIGURE 41. Vertical transmitting pattern of two sections, 54-kc ring-stack transducer.

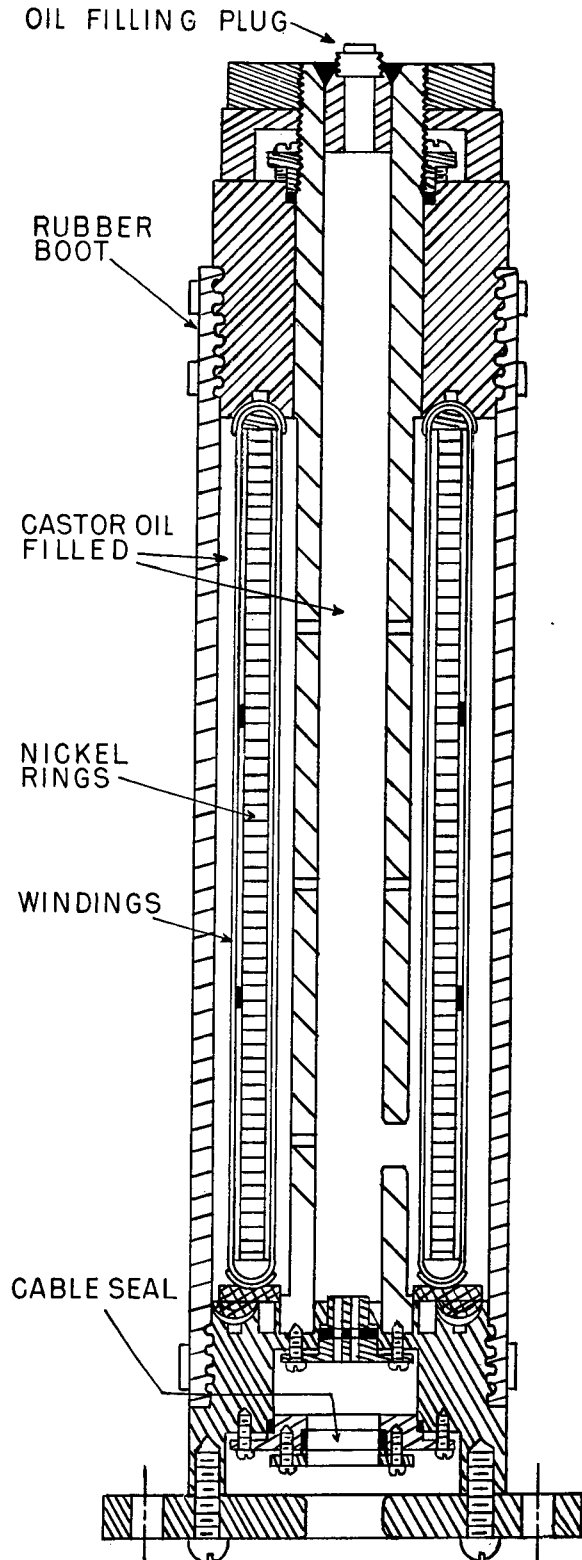


FIGURE 42. Assembly cross section of 28-kc ring-stack transducer.

CONFIDENTIAL

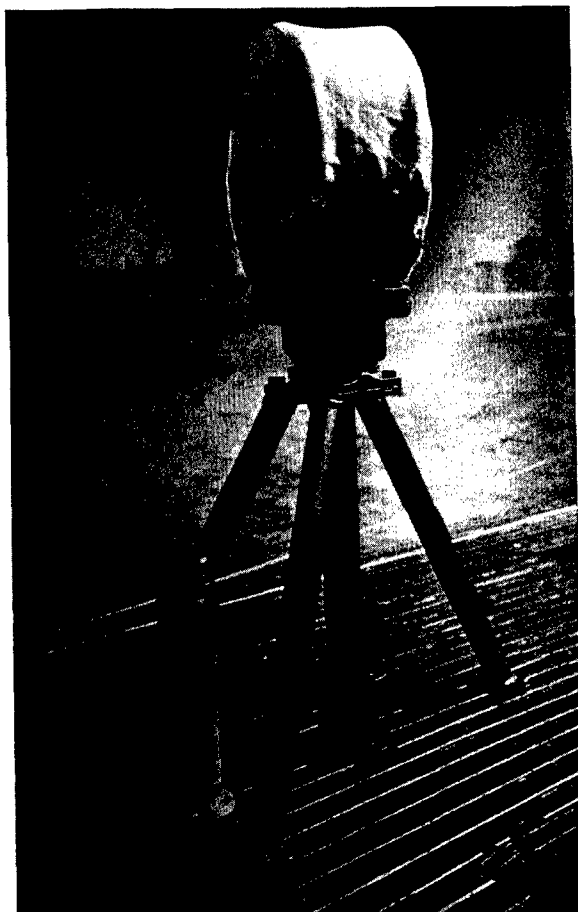


FIGURE 43. Installed view of 28-kc ring-stack transducer.

the switching generator. The motion of the conductivity wave is repeated smoothly by starting a new wave at the beginning, as the old one is absorbed at the end. This gives the effect of a rotating conductivity wave which moves from 1 on through to 48 and around again without discontinuity.

The pattern shown in Figure 45 is considerably modified by the second stage of pattern formation, which appears in Figure 47. In the pattern shown in Figure 47, a particular shape of conductivity wave is assumed; namely, three electronic switches are assumed to be conducting in the ratio  $1 : x : 1$ , where  $x$  varies between 1 and 4. In practice this may be accomplished by using a broad wave which progresses as indicated in Figure 44. It is seen by comparing Figures 45 and 47 that the width of the major lobe is not changed appreciably by the second pattern-forming process, whereas the height of minor lobes is considerably altered. The first minor lobe decreases in

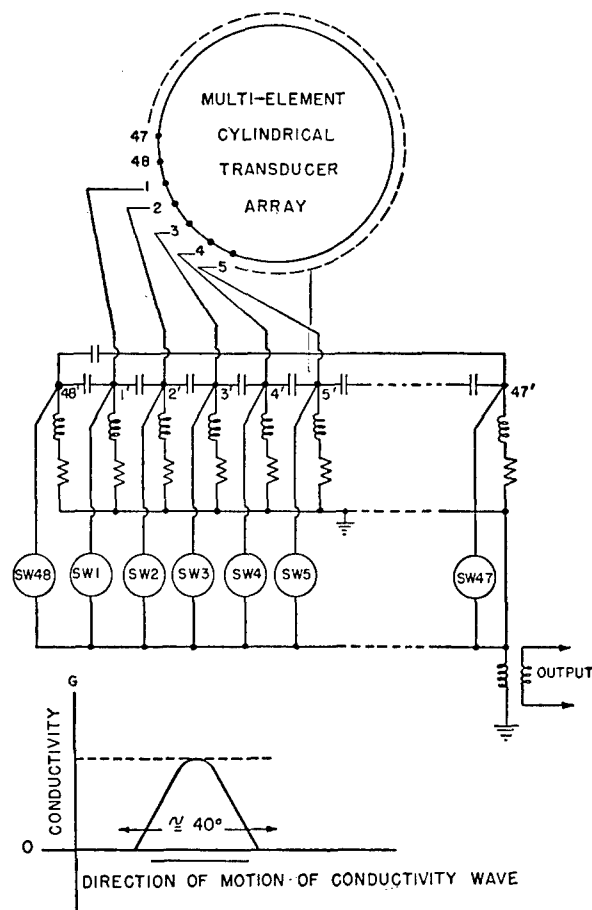


FIGURE 44. Schematic diagram to illustrate ER pattern formation.

height from  $-11$  db, in the case of the first stage pattern, to values between  $-13.5$  and  $-16$  db, according to the value taken for  $x$  in the ratio  $1 : x : 1$ . The second pattern formation then serves mainly to decrease the amplitude of the minor lobes in the rotating pattern.

By choosing the tip of a sine wave for a conductivity wave form in operating the electronic switches, an additional desirable property is obtained; namely, signals from the individual elements in the transducer and its associated lead line are commutated smoothly into the output circuit of the rotor. By this means, it is possible to interpolate between elements in the transducer and lead line array to determine accurately the bearing of a particular source, even though it lies between the elements in the array.

Another property of electronic rotation can be seen by referring to Figure 46. The output of the electronic rotor produces a pattern having a certain

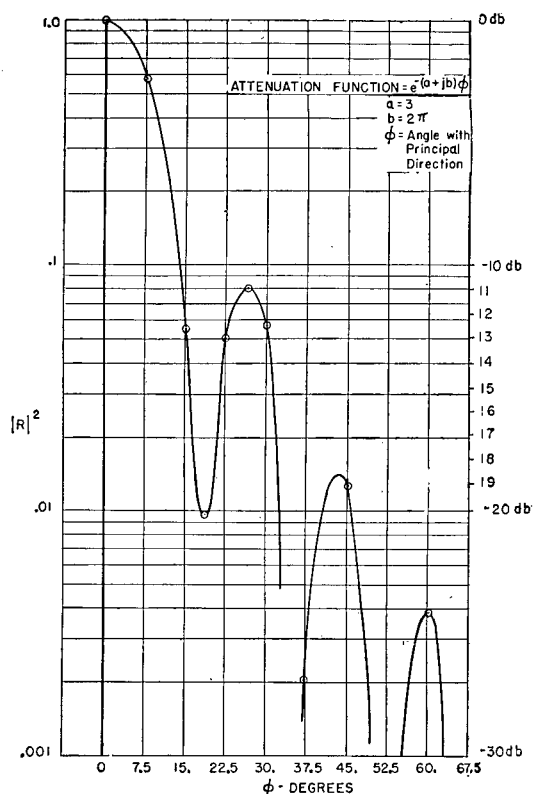


FIGURE 45. Amplitude pattern in first stage of ER pattern formation.

phase relationship, compared with the phase of the voltage developed, when the center of the major lobe is pointing in the direction of the source. For example, at 15 degrees bearing from the center of the source, the phase of the voltage in the electronic rotor

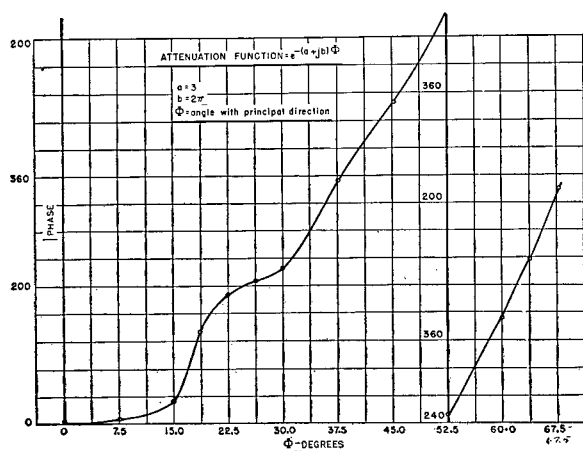


FIGURE 46. Phase pattern in first stage of ER pattern formation.

output lags zero-bearing phase by 32 degrees. From 15 to 22½ degrees, it is seen that the slope of the phase-versus-bearing curve is much greater. A leveling off is seen between 22½ and 30 degrees, from which point the phase-versus-bearing-angle curve is seen to rise sharply. The slope of the phase-angle curve, when multiplied by the frequency of rotation, equals the doppler produced instantaneously by the electronic rotor. That is, since the pattern rotates at a known speed and since the phase of the voltage in the output of the rotor has a known rate of change with bearing and, therefore, with time, a frequency deviation results which is added instantaneously to the received signal frequency. In the case of the electronic rotor used in the submarine ER sonar, this doppler (which is referred to as rotation doppler to distinguish it from the ordinary ship doppler), was as great as 9,000 c on either side of the central signal frequency. Clearly, by utilizing band-pass filters in the output of the electronic rotor, it is possible to reject entirely those components of the rotor pattern

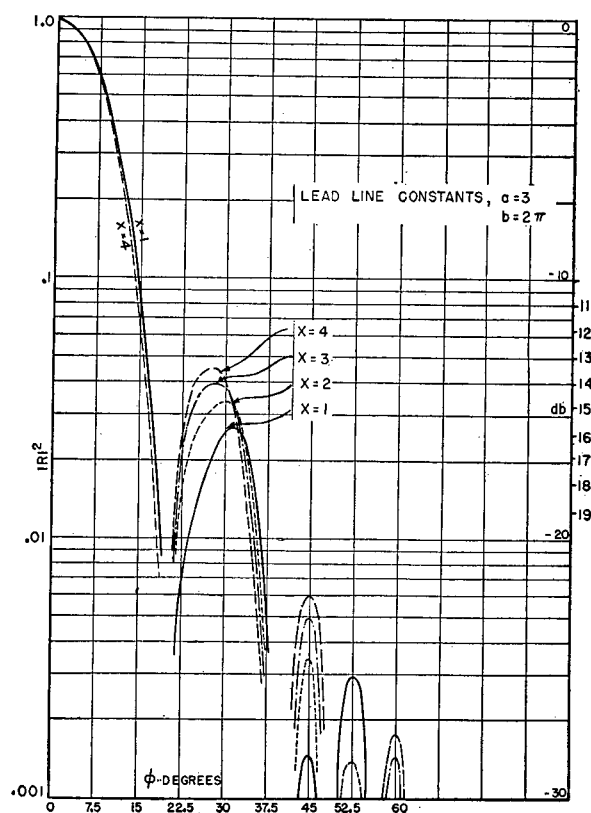


FIGURE 47. Amplitude patterns in second stage of ER pattern formation (three elements conducting in the ratio 1:x:1).

CONFIDENTIAL

having sufficient doppler imposed upon them to take the signal outside the limit of the band-pass filter. This principle was utilized in the submarine system electronic rotor and had the effect of wiping out any signal beyond a bearing angle of 50 degrees. This was true because, in general, those lobes farther than 50 degrees either side of the major lobe had the greatest doppler imposed upon them by the electronic rotor.

There are certain limitations on rotation speed due to the relationship between signal frequency and rotation frequency. In the average electronic rotation system, the major lobe traverses a given target in approximately 1/10 of a revolution. During this 1/10 of a revolution signal frequency is transferred from the transducer to the rotor output in accordance with the shape of the major lobe. It is desirable to have the shape of the major lobe accurately represented in the rotor output, and a given number of cycles at signal frequency are required to delineate properly the shape of the pulse. By experimentation it was found that fewer than 7 cycles at signal frequency made it impossible to do this; consequently, a practical rule was established which dictates that the rotation frequency be no greater than 1/100 of the signal frequency. In this manner it is guaranteed that at least 10 cycles of signal be passed by the electronic rotor to delineate the major lobe of the transducer pattern.

At various times in the past, consideration has been given to the idea of allowing the electronic switches to influence the action of the lead line in the first stage of pattern formation during the conduction of the given electronic switch. These thoughts have taken two major forms. Figure 48 illustrates the use of the Miller effect, and Figure 49 illustrates the use of the varistor, or similar control device, as a reactance element.

Referring to Figure 48, it was thought that profitable use might be made of the fact that the input capacitance of a triode is a function of the gain of the tube. A lead line and generator were connected as shown and the phase difference between points *B* and *A* was recorded versus the grid voltage of one half of a 6SL7 duo-triode. It was found that considerable effect was produced as the bias of the 6SL7 was varied between cutoff and some maximum value. This is shown in the table at the right side of the figure. It was felt that the conducting triode at the center of the pattern could be made to reduce the phase shift in those sections of the lead line in which the conduction wave was operating. In this way it was supposed

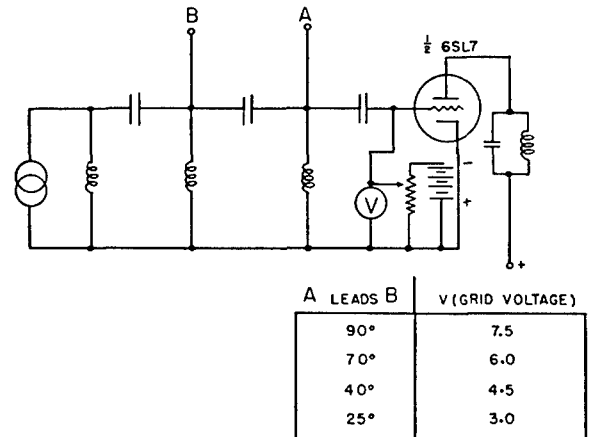


FIGURE 48. Arrangement for testing influence of Miller effect on lead line.

that the pattern produced by the electronic rotor could be made more nearly the theoretical pattern achieved in CR sonar.

The circuit shown in Figure 49 was proposed in a memorandum in November 1944.<sup>27</sup> This memorandum proposed the use of the electronic switch in an elaborated arrangement of the Miller-effect circuit. In this circuit the impedance could be made into any form desired; including inductive, capacitive, resistive, or negative resistive impedance, or any combination of these. No significant work has been accomplished in this field, however, because of the additional number of independent variables added to the general problem. Because of the uncertainty of the effects produced upon the lead line by the switching mechanism, (whether by Miller effect, by intentional reactance circuits, or by straight resistance loading, as in the case of the varistor and the diode), all electronic rotors produced thus far are designed to have a minimum of these effects.

The characteristics of the lead line have been found to exert considerable influence over the shape

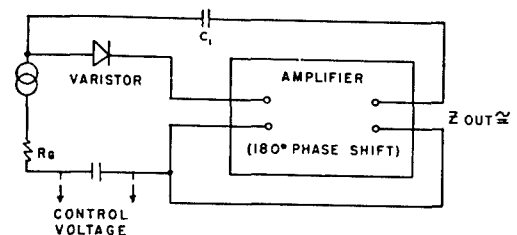


FIGURE 49. Arrangement for using varistor as a reactance element.

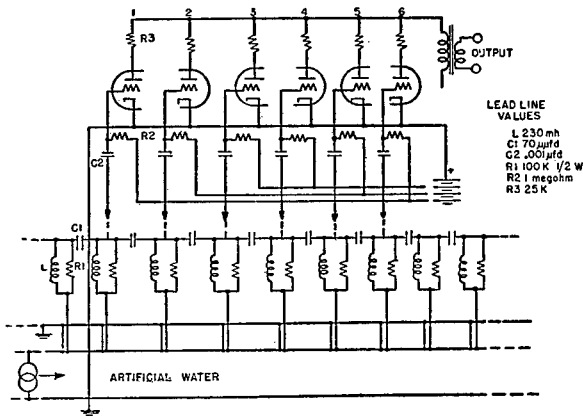


FIGURE 50. Circuit diagram of preliminary experimental electronic rotor.

of the pattern produced by the electronic rotor. Some of these effects have been discussed earlier in the present chapter. In more general terms, the lead line can be considered as possessing two independent variables, each of which has an effect upon the shape of pattern. These variables are (1) the phase shift per section of the transmission line and (2) the attenuation per section. It has been found that for each transducer and frequency, there is an optimum phase shift and attenuation which can be found experimentally, and which with the impedance desired in the lead line completely defines the circuit components necessary.

#### 7.4.3 Experimental Work in Lead Lines

Beam pattern formation by means of a lead line was first attempted in July 1943. Figure 50 shows the schematic wiring diagram of the experimental setup. An artificial transducer (see Chapter 8) connected in series with an inductance  $L$  and a resistance  $R_1$  formed the shunt element of the beam-forming lead line network. Capacitor  $C_1$ , shown along the top of the beam-forming lead line in the diagram, completed the connection from section to section and created a constant- $K$  high-pass type of lead line compensator. The lead line (of which only a part is shown in Figure 50) was 36 sections long, connected at both ends to form a continuous ring. A group of triode elements, shown as elements 1, 2, 3, 4, 5, and 6 in the diagram, was connected so that signals impressed upon their grids were amplified and brought to a common plate output circuit. The individual grids were attached to sections of the lead line adjacent to

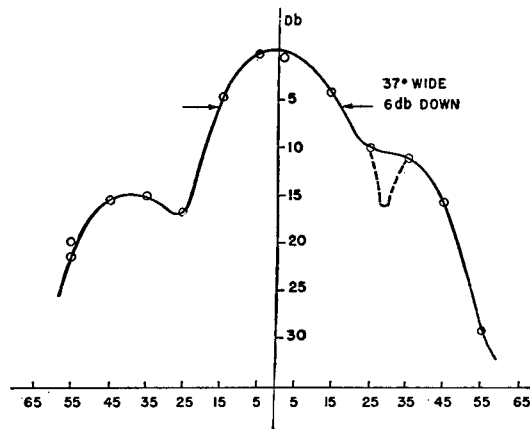


FIGURE 51. Beam pattern produced by preliminary experimental electronic rotor.

one another, and the signal frequency current in the common plate output circuit was measured. By moving the six grid contacts from position to position along the lead line and by plotting the common output, a pattern was produced (Figure 51) which was, therefore, the beam pattern of this first electronic test rotor. Amplitude shading was produced in the electronic switching elements. Thus, triodes 3 and 4 contributed the greatest amount of signal to the common output circuit. Triodes 2 and 5 were biased to contribute one half as much as 3 and 4. This was done, as shown at the right side of Figure 50, by connecting greater negative grid bias to triodes 2 and 5 than to 3 and 4 and still greater bias to triodes 1 and 6. It was hoped by this means to simulate conditions easily attained in actual electronic rotation in which a sine-wave switching pulse is applied to the individual grids.

In August 1943, further experiments on lead line constants were performed with a complete 60-cycle rotation system shown in Figure 52. A 3-phase 60-cycle generator and phase-splitting network, as described later, were used to feed the triode grids with a succession of switching pulses. The lead line is shown at the bottom of Figure 52 with a typical section labeled  $C_3$ ,  $L_2$ , and  $R_3$ . Thirty-six lead line sections were fed by an artificial transducer and in turn fed signals on to the vacuum tube switches shown at the center of the figure. The output of the rotor was connected through an amplifier to the vertical deflection plates of a CRO with linear horizontal sweep. Figure 53 is a block diagram of the test setup used in the laboratory for observing the effect on pattern formation as lead line component values and switch-



process repeated for attenuation values between  $-1$  and  $-7$  db per section. By the process of varying the frequency input to the artificial transducer an adequate range of lead per section was tested, and by the process of varying the conduction pulse width these two parameters were related.

The first, and one of the most important, results obtained during these tests was the realization that for attenuation values much less than 3 db per section, enough signal energy was transmitted around the rear half of the lead line to cause excessively high back sensitivity and high minor lobes in the region from 90 degrees through 180 to 270 degrees. However, it was found that attenuations of much greater than 3 db per section produced a perceptible widening of the major lobe; for example, a 6-db per section attenuation value produced a major lobe of 40 degrees in width compared with major lobe widths of 24 degrees using 3 db per section. In this manner it was ascertained that 3 db per section is the best compromise value of attenuation in order to obtain narrow major lobes without too great back sensitivity. It was also found that phase advance of about 60 degrees per section at the signal frequency and conduction pulse widths of about 20 degrees 6 db down produced the best patterns. These values were confirmed as being optimum by later experiments on the AIDE DE CAMP 200-cycle ER sonar using the HP-1 transducer and on the submarine ER sonar using the AX-132 transducer. In both of these cases, the phase advance of 60 degrees per section yielded patterns of 24 degrees in width 6 db down, with minor lobe heights 15 to 20 db below the major lobe height.

Figure 55 shows the various forms of high-pass or phase-advancing lines investigated as a substitute for the straight constant- $K$  type of lead line used in the AIDE DE CAMP tests. The line shown as A is the lead line that was decided upon for all future work using magnetostriction transducers. In this line the transducer itself is represented as  $R$  with  $+jX$  in series, and capacitors  $C$  form the series elements of the lead line. With  $R$  approximately  $0.04 X$  in magnitude, capacitance values  $C$ , which would give 60 degrees per section of phase shift, also produced optimum attenuation per section to produce the best pattern using a 36-element 15-inch transducer at 22 kc. This pattern, in the case of a 36-element transducer of 15-inch diameter operating at 22 kc, was found to be 25 degrees wide with minor lobes 17 db down.

At B is shown a lead line having the same charac-

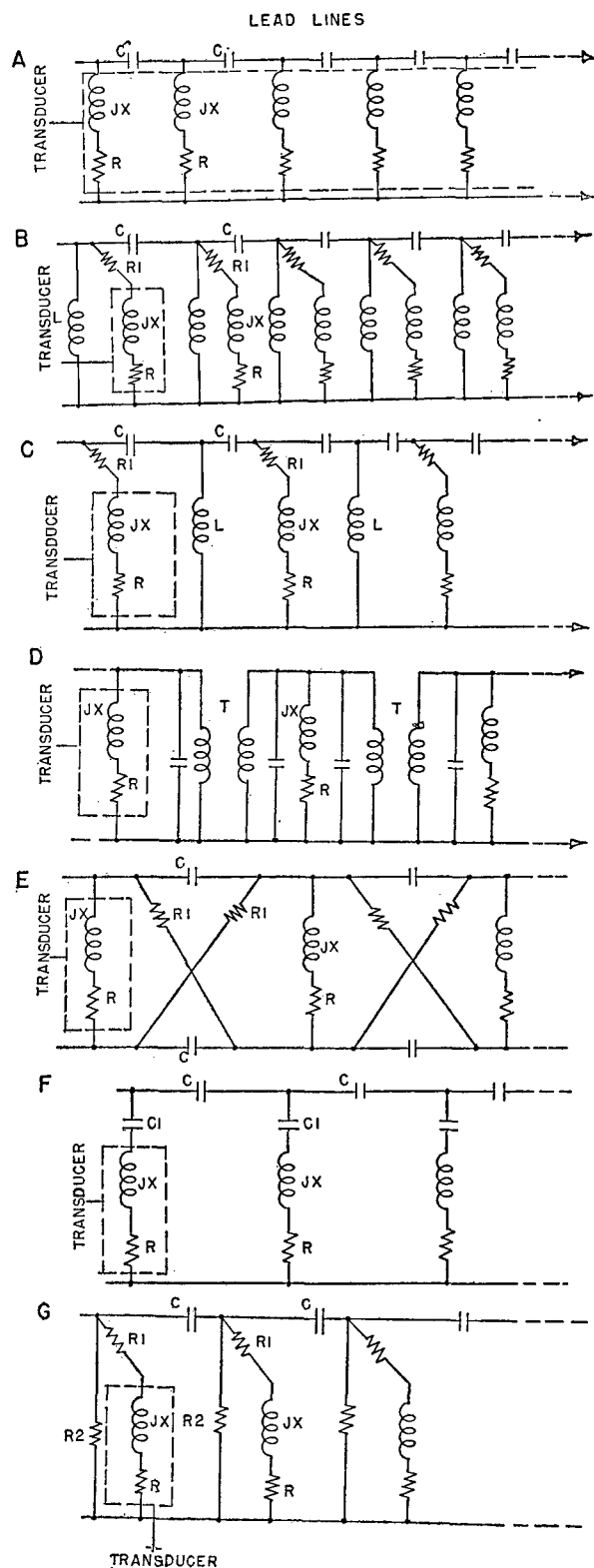


FIGURE 55. Types of lead lines investigated.



teristics as that in A, but in which the shunt element impedance is influenced more by inductance  $L$  and resistance  $R_1$  than by the transducer element impedance  $R$  and  $jX$ . The advantage of using a lead line such as this lies in the fact that transducer impedance need not be specified, but that by means of a bridging resistor  $R_1$  the impedance of the transducer can be effectively isolated electrically from the lead line. If it were found impossible to design magnetostriction or crystal transducers so that the relationship between  $R$  and  $jX$  is that necessary for lead line A, then lead line B could be resorted to. Its chief disadvantage lies in the fact that a certain amount of electrical power loss is incurred in resistor  $R_1$ , the bridging resistor, and it is, therefore, less desirable than the lead line A, which has effectively no bridging loss.

Line C embodies the isolation features of line A, but brings the signal from a particular transducer to a point midway between lead line shunt sections, shown as  $L$  in the figure. It was thought possible to get more uniform pattern formation by increasing the number of sections in the lead line. This proved to be without foundation.

Lead line D is an attempt to produce phase advance by the mistuning (that is, tuning to a lower frequency) of a series of transformers for coupling, shown in the diagram as  $T$ . This line proved to have greater dependence of pattern on frequency than desired.

Lead line E, a lattice type, was tried in an effort to reduce the amount of change of phase shift or lead with respect to frequency. It was found to have too great a loss per section for optimum pattern production. Patterns produced with lead line E had major lobes approximately 1.5 times the width of those produced by lead line A. The introduction of  $L$ , or some inductance in series with  $R_1$ , in each case was thought to be too complicated to warrant competition with lead line A.

Lead line F is an  $m$ -derived lead line. Again this was an effort to reduce the variation of phase shift with frequency, but this lead line proved to have no advantage over lead line A, while it had the disadvantage of being more complicated.

Lead line G was an RC lead line constructed for experimentation with a noninductive lead line. It proved to be a failure because the attenuation developed in one radian of phase shift was about 6 db per section or 3 db higher than lead line A.

When lead line A is used, the transducer imped-

ance becomes a part of the lead line. In this case, the ratio of resistance to inductance in the impedance of the lead line determines the transducer characteristics desired. In general, transducer impedances equal to  $R + jR$  satisfy the requirement that the lead line possess 3 db attenuation per section. A proper choice of the series capacitor yields the required phase shift of approximately 60 degrees.

If it is found impossible to produce this relationship of resistance to reactance, it becomes necessary to use a bridged form of lead line, such as lead line B. In this case, the transducer impedance is made approximately equal to the lead line impedance. These impedance values yield the least loss in the transfer of energy from the transducer to the lead line.

Transformers are used when the electronic switches operate at impedances different from those of the transducer. For example, the triode vacuum-tube rotors of the AIDE DE CAMP 60-cycle and 200-cycle ER sonars and the 53-kc ER sonar required, for the sake of power economy, the highest possible impedance at the grids of the vacuum-tube switches. In these cases the transducer impedance was transformed upward by means of suitable impedance-matching transformers before introduction into the switching grids. It has been found most satisfactory to operate triode grids at an impedance of 50,000 ohms. In such circumstances, the transducer is matched directly to the grid of the tube by means of a suitable transformer, such as Audio Development 3805-A, for matching 100-ohm transducers to 50,000-ohm grid circuits. It has been found possible to connect the lead line capacitors at high impedance between adjacent grids, thus reducing the size of capacitors needed.

Transmitter coupling networks, also known as transfer networks, introduce into the system an additional complicating impedance. Such networks should not interfere appreciably with the desired phase shift and attenuation in the lead lines. This has been found possible by a method that is described later in this section.

In January 1945, the Brush transducer AX-89 No. 2, a 36-element Y-cut Rochelle salt crystal transducer, was used for a series of tests aboard TIPPECANOE, the test barge in the Charles River. These tests were concerned with the fundamental behavior of lead lines in pattern formation and with varistors as switching elements. Figure 56 shows the schematic wiring diagram of the arrangement used. In the upper right corner the switching lag line is shown. In this case, it

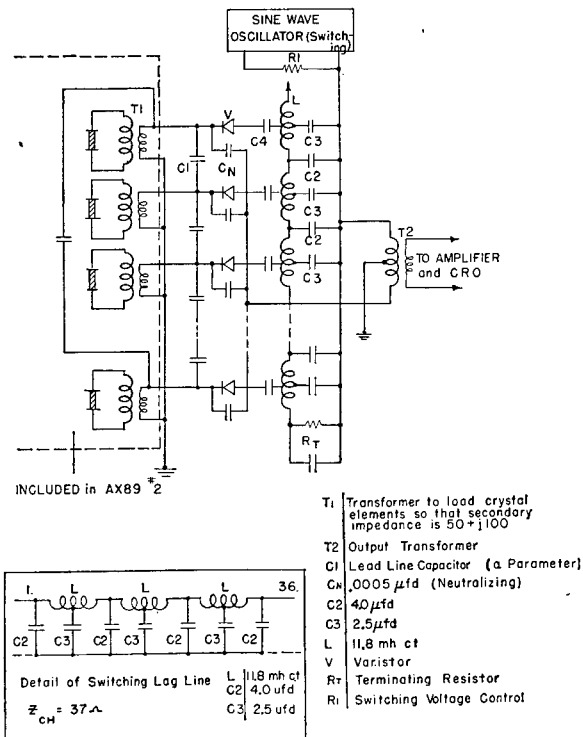


FIGURE 56. Arrangement for electronic rotor tests on barge TIPPECANOE.

is a shunt arrangement having a characteristic impedance of 37 ohms. Thirty-six varistors served as switching elements, and the transducer transformers were mounted inside AX-89 No. 2. Signals were brought out by means of a cable consisting of 36 twisted pairs. The varistor rotor shown was connected by means of the twisted-pair cable to AX-89 No. 2 and was then connected to a small wide-band amplifier whose output was led to the vertical plates of a linear-sweep CRO. The sweep frequency was externally synchronized with the switching voltage input to the switching lag line of the test rotor. Aboard the barge TYLER Too was placed a transmitting projector which received signal from a Western Electric oscillator. The tests included the behavior of pattern production versus magnitude of switching signal input, lead line parameters, and the type of varistors used.

The following conclusions<sup>28</sup> were arrived at as a result of the tests on TIPPECANOE with the AX-89 No. 2 transducer and varistor rotor:

1. The pattern width is widest when the number of varistors conducting is a maximum; decreases as the number of conducting varistors is decreased; and reaches an optimum value which is a function of the

pattern forming lead line. As the number of varistors conducting is decreased still further, the major lobe width does not change significantly. It would appear, therefore, that there is an optimum conduction pulse width consistent with a given pattern. This width is  $\frac{3}{4}$  of the optimum pattern width.

2. Minor lobe height decreases as the number of conducting varistors is increased. In general the optimum conduction pulse given in conclusion No. 1 results in minor lobe heights averaging -16 db with relation to the tip of a major lobe. (This can be said for at least AX-89 No. 2, but has been observed generally in the behavior of other electronic lead line rotors.)

3. The choice of lead line parameters has a profound effect upon pattern formation. These may be juggled for each particular transducer to obtain best results. In the tests performed, a lead line formed by inserting 0.04- $\mu$ f capacitors gave patterns averaging 25 degrees in width with minor lobes averaging 16 db down. A lead line formed with 0.06- $\mu$ f capacitors gave average patterns approximately 3 degrees wider with minor lobes an average of 4 db stronger. Patterns formed using no lead line whatsoever averaged 40 degrees in width with minor lobes as strong as in the first case.

4. It has been shown that the characteristics of varistors have a profound effect upon the uniformity of pattern production. It would appear that these must be held within tolerance of  $\pm 10$  per cent.

#### 7.4.4

### Switches

Electronic switches used in electronic rotors must be capable of control of the transfer function so that the switch may follow a prescribed conduction pulse form, which has been found to be the tip of a sine wave. The gain of the switch in the nonconducting condition is required to be at least 50 db less than the maximum gain, if back sensitivity is down by 40 db. Also, the switch must not introduce excessive noise into the system. In general, a level of switching noise at signal frequency no greater than 0.25 microvolts at 100 ohms has been achieved.

The band pass required to accommodate the signals generated by the electronic rotor is a function of the rotation speed and the width of major lobe attained in the pattern. In general,<sup>29</sup> the band pass required is equal to the rotation frequency times  $\frac{3}{2}$ , the reciprocal of that fraction of a rotation cycle

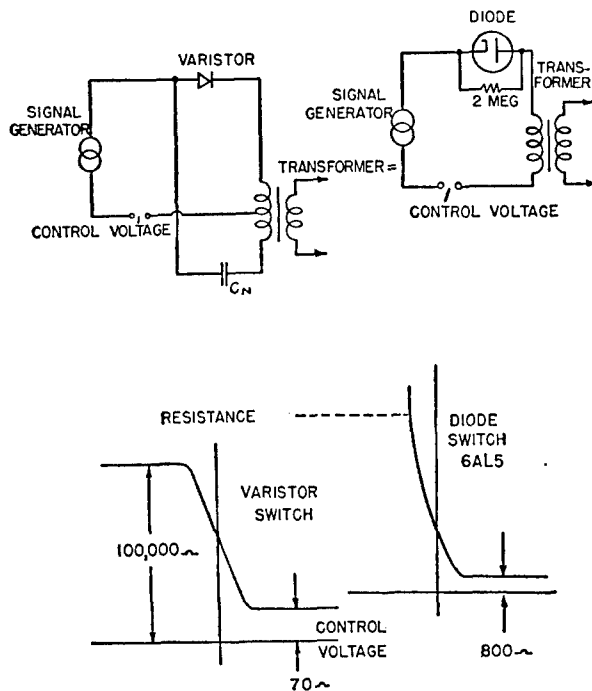


FIGURE 57. Principles of operation of varistor and diode switches.

occupied by the major lobe at the 8.7 db down points. In the practical case, the submarine system which has a rotation speed of 300 c and a major lobe 30 degrees wide would require a bandwidth of 5.4 kc. The submarine system, then, would operate best with a 5-kc band-pass filter in the output of its electronic rotor.

The electronic switches used in ER rotors may be divided into four basic types. The first, illustrated in Figure 57, is a varistor switch. As can be seen in this figure, the resistance of a varistor to the passage of small signal frequency current is a function of the control voltage. At control voltages more negative than  $-1$  volt, the varistor has a resistance (commonly referred to as its back resistance) of 100,000 ohms or more. In the forward direction, at control bias values greater than  $+\frac{3}{4}$  volt, the varistor has a resistance of 70 ohms. The varistor has in addition an internal capacitance that must be neutralized by capacitor  $C_N$  (shown in the upper left drawing) used in the normal "plate" type of neutralization circuit.

The varistor is equivalent to a diode in its operation. In the diode shown at the right side of the diagram in Figure 57, the neutralizing capacitor  $C_N$  may be omitted because of the low internal capacitance of diodes. It is seen that the diode reaches a minimum resistance of 800 ohms to the passage of signal cur-

rent, compared with 70 ohms in the case of the varistor. Also, an external resistance is shown equivalent to the varistor back resistance.

The varistor is commonly applied in a self-biasing switch circuit shown in Figure 58. In such a circuit the applied switching voltage is rectified by the varistor and the rectified current charges the capacitor  $C$ . The back resistance of the varistor is approximately 10,000 times its front resistance, so that the discharge time of the capacitor is accordingly longer than its charging period. The capacitor rapidly accumulates a charge which acts to bias off the varistor, except during the short conduction period, during which signal in the varistor input circuit is transferred to its output circuit. A pulse of signal then is passed to the output circuit having the envelope shape of the tip of a sine wave.

The varistor has the valuable property of possessing an impedance approximately equivalent to the impedance found in magnetostriction transducers. In the case of crystal transducers, transformers are needed to transform the high crystal impedance down to varistor impedance. Varistors have the disadvantage of requiring neutralization of the comparatively high capacitance existing across their plates.

Varistors have the definite advantage of being passive elements. This makes possible their inclusion in such comparatively inaccessible places as the interior of transducers.

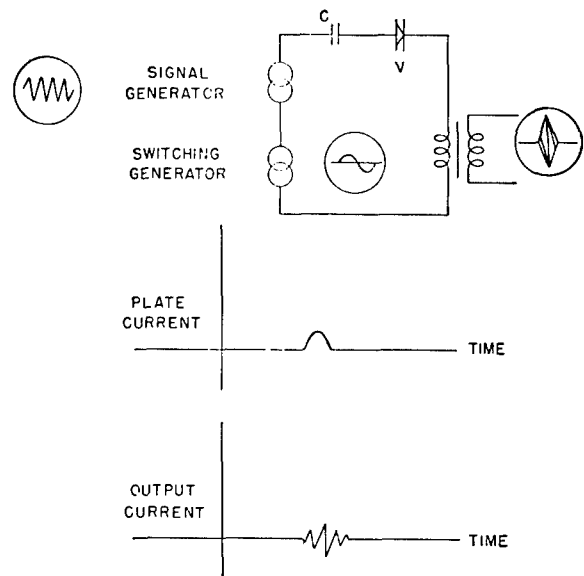


FIGURE 58. Principle of operation of self-biasing switch circuit.

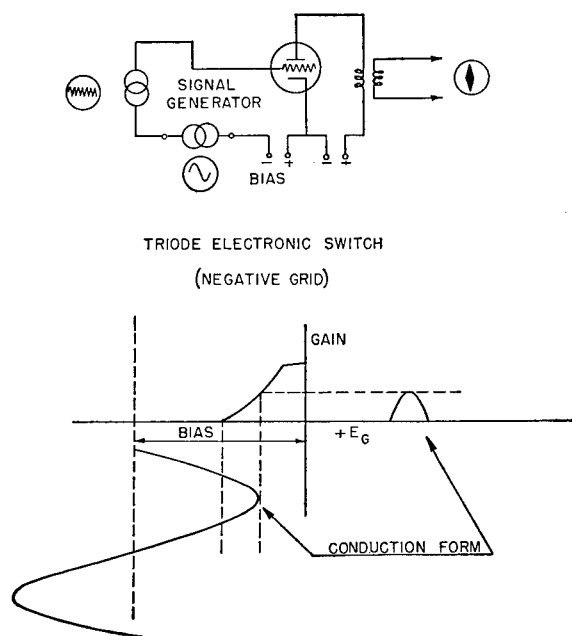


FIGURE 59. Principle of operation of triode switch circuit.

Varistors have the disadvantage of being far more nonuniform in characteristics than the average vacuum tube. Also, they have been found to be easily damaged by the application of high transmitter voltage.

Among vacuum-tube switches investigated at HUSL, only the triode type of switch was incorporated into electronic rotors. For this purpose a Type 6SN7 duo-triode was used. In both the AIDE DE CAMP 60-cycle system and the 200-cycle system, as well as in the 53-kc system, 36 triode elements in 18 tubes were employed. All of the cathodes were tied together and a high positive bias was applied between this point and ground, thus cutting off all of the elements. A given triode would conduct only if enough positive switching voltage were present so that the tube would be brought into a conducting state. Figure 59 shows such a switch. In this type of switch the voltage appearing at the 36 grids must be carefully balanced so that equality is obtained over a range of not more than  $\pm 1/4$  volt in the 36 circuits. In general this necessitated the employment of 36 carefully chosen voltage dividers or a 36-potentiometer system. Also in such a switch it is required to regulate carefully the amplitudes of both bias and switching voltage to insure that the switches operate at the proper point. This adjustment was found to be quite critical and consequently became the motivat-

ing factor in the development of a self-biasing switch such as the varistor switch previously described.

Plate switching, in which grids and cathodes are maintained at fixed-bias potentials and in which each plate receives operating voltage from a switching lag line, was proposed in a memorandum<sup>30</sup> and was tried in October 1944. It was found to require plate power pulses of such great amplitude and of such short duration that a transmission line for switching could not be successfully built to handle such a pulse without considerable distortion. For this and other reasons, the signal-to-noise ratio in a plate triode switch was found to be considerably poorer than in a triode switch in which switching is accomplished in the grid circuit.<sup>31</sup>

A pentagrid, or multielement electronic switch, is diagrammed in Figure 60. In such a switch it is possible to use the advantages of self-regulation and self-bias, discussed above under varistors, and to benefit from the separation of signal from switching circuits, which is impossible when the varistor is used. The waveforms developed in various parts of the circuit are shown in the small circles. Alternative forms of multielement operation have been proposed, including a method of screen grid switches in which signal is applied to the screens while switching voltage is applied in the usual peak rectifier manner to the first grid. Another method was to use suppressor switches in which switching voltage is applied to the suppressor of a vacuum tube while signal voltage is applied at grid No. 1. None of these schemes has been operated in an electronic rotor.<sup>32,33</sup>

#### 7.4.5

### Switching Generators

All electronic rotors require a polyphase switching generator for proper operation. This generator, by supplying either sine waves, or pulses having the

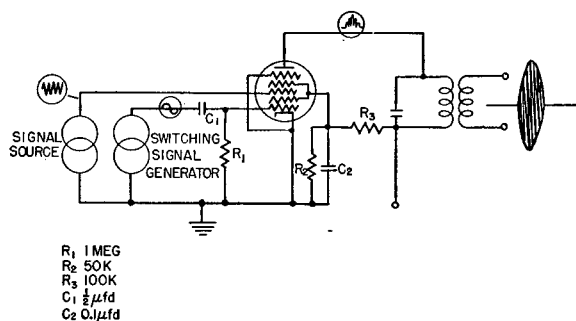


FIGURE 60. Circuit diagram of pentagrid switch.

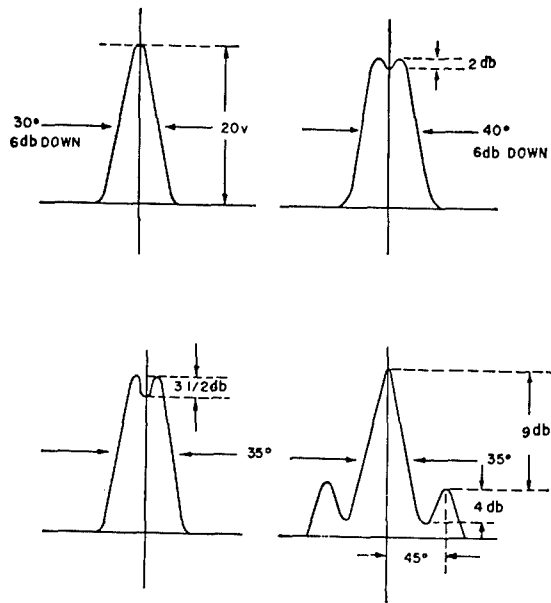


FIGURE 61. Types of conduction pulse forms.

shape of tips of sine waves, serves to operate the individual switching elements. The fundamental repetition frequency of the generator determines the rotation speed of the transducer pattern of sensitivity. The polyphase operation of the switching generator requires a number of phases separated by the same interval. For example, a 36-element electronic switch requires that the positive peak of switching voltage be delivered to the switches at 10-degree intervals in successive rotation during each revolution. It is the cyclic appearance of the positive peaks that causes the electronic switching elements to operate in a rotary sequence.

It has been found by experimentation with the pulse shapes, shown in Figure 61 encompassing four shapes of pulses, that the pulse form producing best operation is the tip of a sine wave 35 degrees wide at its base. This sine wave tip is generally clipped from a broader sine wave tip or, in some cases, from a complete sine wave by the electronic switch itself.

Figure 62 shows the method which was adopted for the first polyphase generator. A three-phase generator, which in this case was a standard GE synchrotype 5 DG, was driven by a single-phase 3,600-rpm motor to produce a 3-phase 60-cycle voltage of good waveform and of 100-volt amplitude. The 3-phase voltages at the output of the switching generator were then connected to three transformers, whose secondaries were center-tapped and connected at the

center tap to form the neutral of a 6-phase star-connected system. Each of the phases, shown as roman numerals I through VI inclusive, were then connected to a ring of resistances, shown in the diagram as  $R_1, R_2, R_3$ , and  $R_3, R_2, R_1$ , chosen so that a phase shift of 10 degrees per resistor junction would be achieved. From each resistor junction to the neutral was connected a potentiometer shown as P in the table of values at the right of the diagram and lettered as A through T on the diagram. These were adjusted so that the amplitudes of switching voltage at the arm of each potentiometer were made equal. This is necessary in the case of a resistive phase-splitting method, because the amplitude of the voltage developed at a given resistor junction decreases, as does a radius vector drawn from the center of a circle to a chord. Referring now to Figure 62, each of the triode grid returns was connected to the points shown as A, etc., and, in this manner, triodes 1 through 36 were made to conduct in succession.

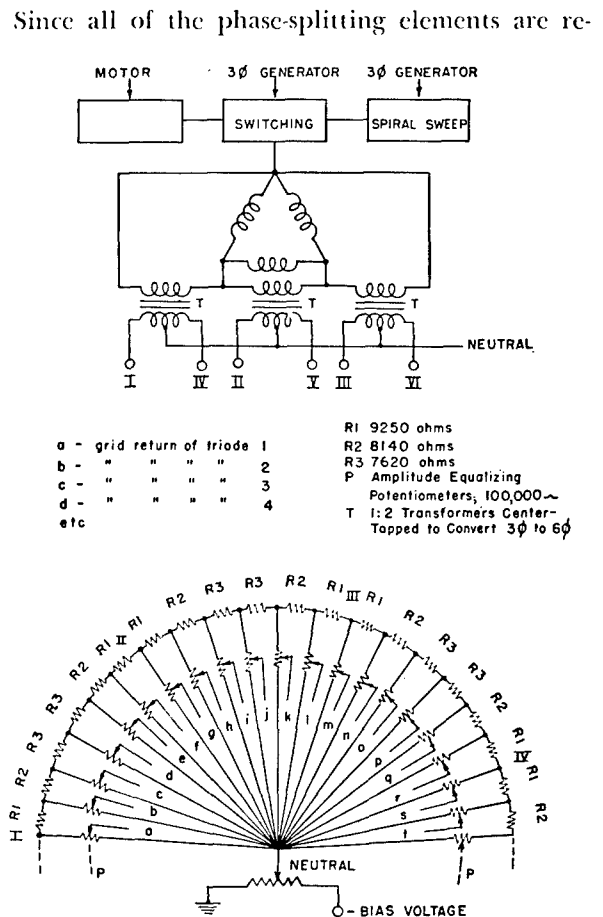


FIGURE 62. Circuit diagram of phase-splitting switching generator.

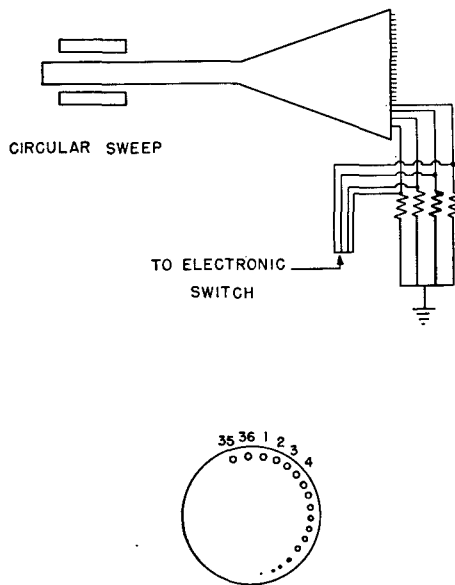


FIGURE 63. Arrangement for using cathode-ray tube as switching generator.

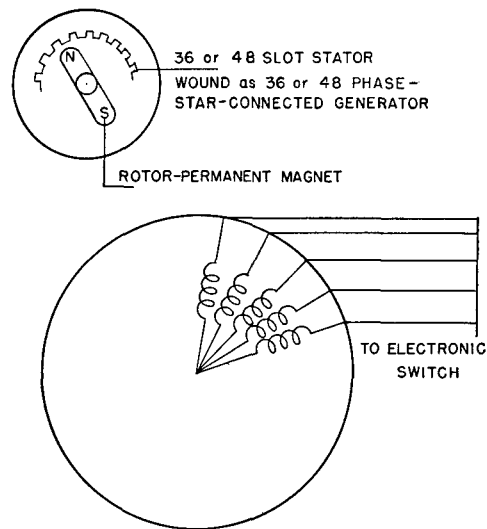


FIGURE 64. Arrangement for using rotating polyphase generator as switching generator.

sistive, an advantage of the rotating machine and phase splitter is that proper phase-splitting action is accomplished regardless of generator frequency. The chief disadvantage is the fact that by requiring a rotating machine for operation the rotation speed is limited to 60 cycles when standard parts are used. One of the objects of the development of electronic rotation is the creation of a system capable of much higher rotation speeds.

A cathode-ray switching generator was proposed as shown in Figure 63. Procurement was investigated, but it was found that none of the commercial firms manufacturing cathode-ray tubes would undertake the development of a special tube of this type.

A standard electric motor stator frame having 36 slots was found, and this machine was wound as a 36-phase star-connected generator. A pair of Alnico magnets were machined and mounted as a rotating field. The machine was driven by a 3,600-rpm motor for the purpose of producing a switching signal in each of the windings of the 36-phase generator (see Figure 64). A suitable pulse was developed by this machine and was close enough to the shape desired to warrant the commercial production of several models of this machine for further laboratory testing. A contract was let with the Westinghouse Company to produce six machines having 36-phase stators and three having 48-phase stators to meet the requirements of

transducers then under construction at HUSL. Unfortunately, in the time allotted, the Westinghouse Company could not produce a generator sufficiently free from distortion of the developed pulse to satisfy the requirements of the ER system.

Also investigated was the method of binary counter-switching shown in Figure 65, which consists of seven pairs of triodes connected in multivibrator circuits with feedback return. In the resistor matrix (shown below the diagram) there is one combination of resistors connected to either the left or right line shown in each pair of lines, that produces the most positive pulse at a given point in the rotating cycle. It is seen by examination of the positions of the resistors in this matrix that point No. 1 is most positive first, then point No. 2 follows, and so on, so that a positive pulse is developed in rotation in a 36- or 48-phase system. A model of this binary counter switching generator was built but it was found that the component tolerances and number of parts proved prohibitive, so that the development was dropped.

Transmission lines were first conceived as switching mechanisms for electronic rotors in July 1943.<sup>34</sup> It was proposed at that time to use a delay network 36 sections long having a phase lag of 10 degrees per section at 60 cycles for the operation of an array of 36 triode elements. Sixty-cycle sine waves were to be introduced at the beginning of the line and absorbed

CONFIDENTIAL

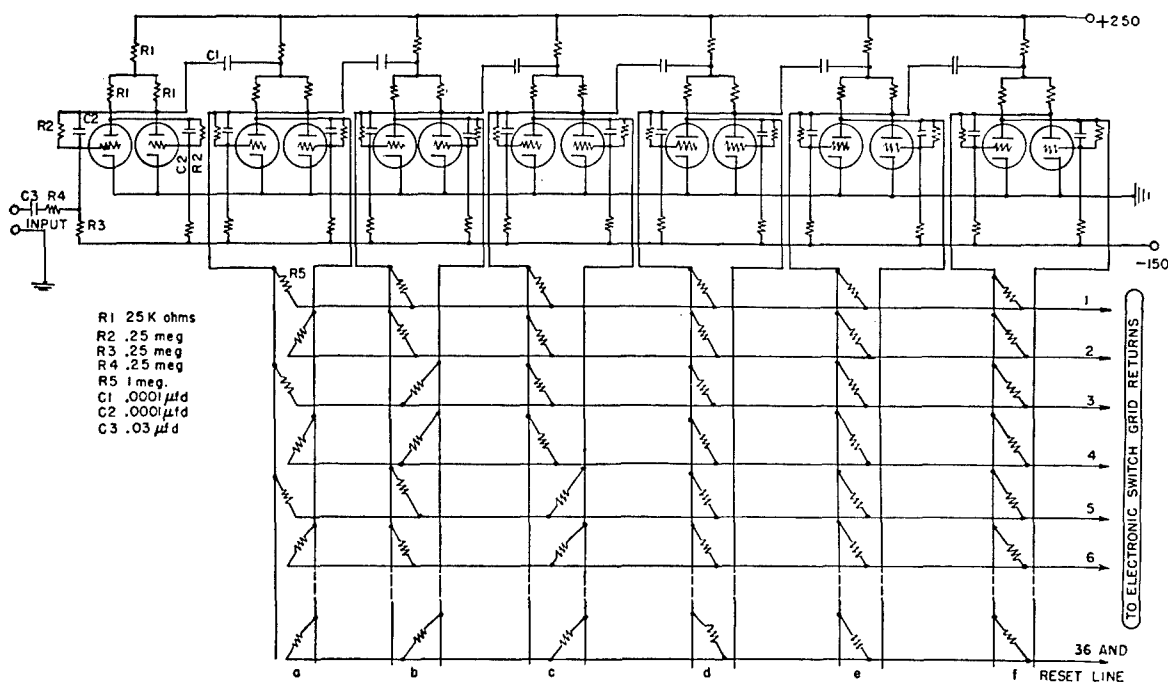


FIGURE 65. Circuit diagram of binary counter-switching generator.

in its terminating resistance at a point 360 degrees later. As the positive peak traveled down the lag line, it caused the triode connected to that given lag line section to conduct. A negative bias was used to cut off all triode elements when not in the presence of the positive peak. This principle was found successful and was adopted for all rotors except the first two experimental models.

The first experimental electronic rotor operated at a 60-c rotation rate. A switching lag line built to operate this particular rotor was unsuccessful because of saturation in the iron core inductances. (This line is shown at the top of Figure 66.) It had to be abandoned in favor of the resistive phase-splitter switching generator supplied by a rotating 3-phase generator.

The development of suitable transmission lines for use in electronic rotation was begun in November 1943. These transmission lines are of three general types. The first type employed was an  $m$ -derived line, in which  $m$  equals 1.3. It was designed to have linear phase shift versus frequency characteristics up to the 10th harmonic of the fundamental switching frequency. This line employing 72 coils and 36 capacitors for 36 elements, was considered over-complicated although it performed satisfactorily. It was designed to be distortionless over the wide frequency range

previously mentioned. Thus switching pulses could be applied to the line and suffer no distortion by the line itself in their travel from the beginning to the termination. This line is the second diagram of Figure 66.

A new type of bridged-T line was developed at this time<sup>35,36</sup> and was constructed with 36 inductances and 72 capacitors. It was found to be more economical in space and construction time than the  $m$ -derived line. It has been employed in the 200-cycle and 500-cycle vacuum-tube rotors as well as in Models I and 1A of the submarine ER sonar. This line is shown second from the bottom of Figure 66.

A derivative of the bridged-T switching lag lines has been developed<sup>37</sup> which has the virtue of requiring half the number of inductances for a given line. Such a line requires only 25 inductances and 48 capacitors for a 48-element line. This is the type of lag line used in the Model 2 submarine ER sonar rotor and in the TIPPECANOE test rotor setup. This is shown as the lowest portion of Figure 66. This latter line uses fewer coils than the bridged-T type above, but more capacitance, and it occupies approximately the same total volume.

One of the problems involved in the operation of a lag line as a switching generator is the accurate synchronization of switching frequency to the constants

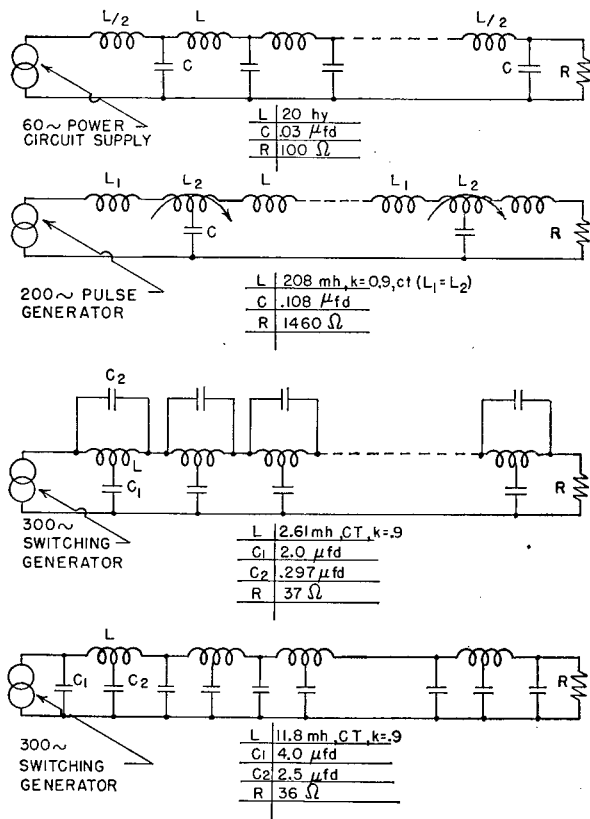


FIGURE 66. Types of transmission lines used as switching generators.

of the lag line. If, for example, switching frequency was lower than the fundamental line frequency as defined above, a gap would appear in the rotation of the system since the positive peak would have been absorbed in the terminating resistance a short time before the application of a new pulse. If the applied frequency were too high, then it would be possible for two groups of switches to be operated at the same time. Accordingly, bearing errors and beam distortion would result.

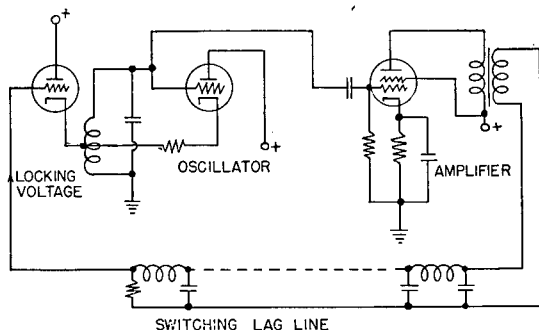


FIGURE 67. Circuit diagram of switching generator with phase-locked oscillator.

Several methods have been proposed for the control of the switching oscillator to synchronize it with the lag line. The first of these involves the use of a blocking oscillator in which the arrival of the positive peak at the end of the line is used to trigger off the next cycle. This was found to be less desirable than other forms of synchronization, because of the unstable character of the blocking oscillator.

A second form of synchronization is that in which signal from the end of the lag line is coupled directly back into the oscillator circuit, thus forming a feedback path 360 degrees long at some given frequency. This is similar in operation to a Hewlett-Packard type of oscillator, in which a given phase shift is required for proper oscillation and which, occurring at only one frequency, tends to lock the oscillator into stable operation. Figure 67 shows a circuit that was used in the 200-cycle AIDE DE CAMP system. In this case, signal was taken from the end of the lag line and coupled to the oscillator by means of a 6J5 triode.

Both of the systems described above proved inferior in operation to the frequency discriminator circuit (shown in Figure 68) that was employed in the submarine ER sonar. In this system the phase difference between signals at the beginning and end of the switching lag line is compared by a BDI-type phase-

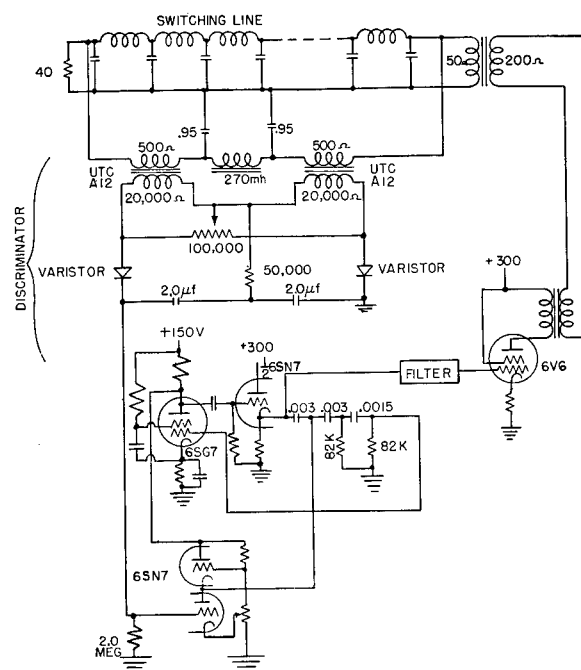


FIGURE 68. Circuit diagram of switching generator with discriminator-controlled oscillator.



sensitive discriminator circuit to correct the frequency of the switching oscillator. The oscillator is an RC phase-shift type in which the signal from the plate of a pentode amplifier is fed into an RC network, whose phase shift is 180 degrees, and then fed back to the grid of the pentode amplifier. The first resistance of the feedback network was replaced by a triode combination whose effective resistance was controlled by the d-c voltage from the discriminator. This circuit had great sensitivity. It held the switching oscillator within  $\pm 0.1$  cycle of the correct operating frequency under any of the conditions encountered thus far.

Pulse generators, used for the application of switching voltage to transmission lag lines in electronic rotors, are required to supply a pulse whose positive peak has the shape of the tip of a sine wave. The amplitude required for the proper operation of the switching line is a function of the type of electronic switch employed and of the impedance of the lag line. The repetition frequency of the pulse generator is determined by the constants of the lag line, which are in turn determined by the rotation speed desired in the electronic rotor.

The pulse repetition rate is that frequency at which the delay in the entire lag line is equal to one wavelength. For example, a transmission line having 36 sections, in which each section introduces a phase lag of 10 degrees at 200 cycles so that a total delay of 360 degrees occurs at the 200-cycle point, must be supplied with pulses having a 200-cycle repetition rate.

Vacuum-tube rotors, employing triodes in which no current is drawn from the switching mechanism, permit the use of switching lag lines of higher impedance than do rotors using current drawing devices such as varistors. In the lag lines built in this laboratory, a 1,500-ohm characteristic impedance has been used to operate vacuum-tube electronic switches, while lag lines of between 35 and 50 ohms have been considered suitable for varistor switches.

In the case of the vacuum-tube switch in which a common bias is used to cut off all switches, except those under the direct influence of the positive switching pulse peak, it has been found economical to clip the sine wave generated by the fundamental switching oscillator so that the total switching voltage applied to the switching lag line is minimized. In the case of the 200- and 500-cycle vacuum-tube rotors, the tip of a sine wave having a base width of 90 degrees

was applied to the switching lag line. This pulse tip was 20 volts high and was opposed by bias voltages of  $-23$  volts. Had sine wave been employed instead, a total sine wave amplitude of 72 volts (peak to peak) would have necessitated a negative bias of  $-39$  volts. Thus, a saving was effected by clipping the switching sine wave so that a pulse of smaller amplitude would be applied to the lag line.

In the case of varistors, where no opposing bias voltage is used (each varistor generates its own cutoff bias in a peak rectification circuit) and in which only three volts rms of sine wave switching voltage is required for proper operation, nothing is gained by clipping the voltage applied.

In the case of nonrectifying switches necessitating the use of a common opposing bias, it is found necessary to equalize the applied switching amplitudes appearing at the 36 or 48 lag line junctions. This requires a system of a corresponding number of resistive voltage dividers, which must be carefully adjusted so that the amplitude of switching voltage available for each electronic switch is held within  $\pm 1/4$  volt. It is this stringency which motivated the search for a type of electronic switch that does not require such careful voltage equalization.

With the varistor switch, or the pentagrid converter switch (in fact, any self-regulating switch) it is found possible to omit the voltage-divider networks.

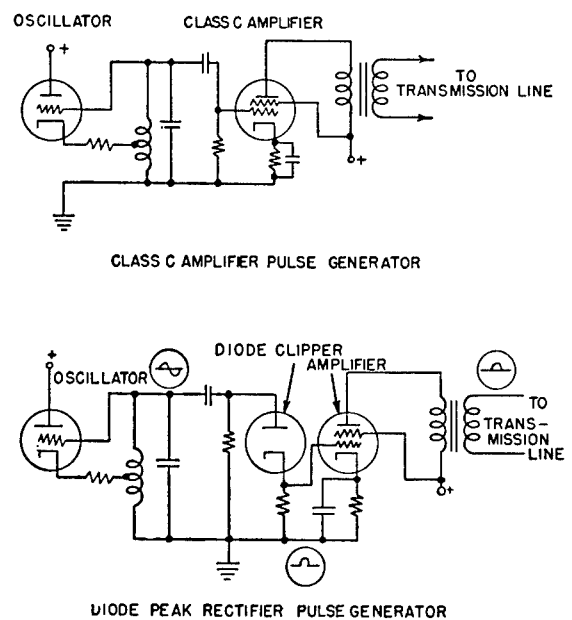


FIGURE 69. Circuit diagrams of clipping types of switching pulse generator.

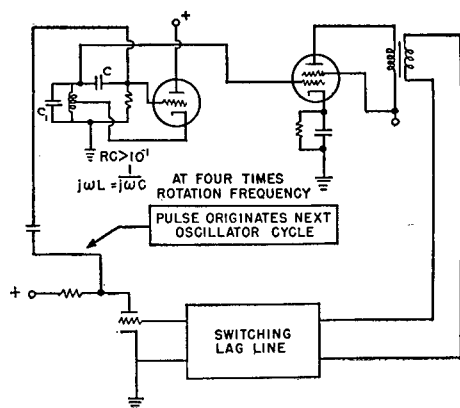


FIGURE 70. Circuit diagram of blocking oscillator type of switching pulse generator.

Such switches have been found to operate successfully over a range of  $\pm 2$  db in applied switching voltage, with negligible effect upon their switching characteristics. The self-biasing feature of the switch takes care of the differences in applied amplitudes.

Voltage sources for transmission lag lines have taken three general forms. A sine wave source consisting of a discriminator-stabilized RC phase shift oscillator has been used in all of the submarine systems. A second form was a sine wave oscillator followed by a clipping circuit as used in the 200-cycle and 500-cycle systems. The third form tried was the blocking oscillator, not used in any system.

Figure 69 shows the application of the oscillator to two forms of clipper circuit for conversion into properly shaped pulses. At the upper half of the diagram is shown a class C amplifier which is self-biasing so that it passes only the positive tip of the oscillator voltage to the lag line. The lower diagram shows a peak rectifier diode used for the same purpose. The current flowing through the diode generates a voltage across a small resistance placed in series with the diode cathode, which is then amplified in a class A amplifier and passed on to the lag line, shown at the right of the drawing.

Figure 70 shows a blocking oscillator type of pulse generator in which only a portion of a sine wave is actually generated, in which case the oscillator blocks itself off in the manner commonly used in radar circuits. This last type was found to be unstable and was not included in any system.

The power requirements of the vacuum-tube high-impedance type of lag line and of the low-impedance low-amplitude lag line used in varistor switches are

approximately the same. From  $\frac{1}{4}$  to 1 watt of power is required as a steady-state input to the lag lines. In no case has it been found necessary to use any larger switching generator output tube than a Type 6V6. This is applied through a suitable impedance-matching transformer to the lag line.

#### 7.4.6 Summary of Electronic Rotor Designs

The preceding sections have discussed design criteria of the various components of electronic rotors. Table 1 gives the essential data on those rotors which were used in experimental ER sonars.

The rotating generator and resistor phase-splitter switching generator were applied to both the laboratory 60-cycle rotor and the AIDE DE CAMP rotor. The laboratory rotor was constructed on a large breadboard for purposes of easy adjustment of component parts. The AIDE DE CAMP 60-cycle rotor, which is shown in Figure 4, used the same system features but was reduced to the form shown for installation aboard ship. This system employed 18 duo-triodes, and used impedance-matching transformers to match the low-impedance transducer to the grid circuits.

The AIDE DE CAMP 200-cycle rotor was likewise a compact version of the laboratory rotor. Eighteen duo-triodes were used in connection with a switching generator of the transmission line type. This rotor was built into a BDI type of cabinet, its chief difference from the laboratory rotor being the inclusion of a tube-testing switch and meter for checking the operation of the tubes while the system was in use. The switching oscillator was phase-locked to the lag line.

The 53-kc 500-cycle rotor differed from the AIDE DE CAMP 200-cycle rotor in only two respects: (1) the switching lag line was constructed for 500-cycle rotation and (2) the lead line impedance was 10,000 ohms rather than 50,000. The lower impedance was necessary because of the stray capacitive coupling at the higher signal frequency. This rotor was constructed in a BDI cabinet and employed a tube-testing circuit. Its lag line was phase-locked to the switching oscillator.

The laboratory varistor rotor was a breadboard version of the submarine rotor Model 1. The switching lag line operated at 300 cycles and no transformers were needed to couple the low impedance from the artificial (magnetostriction) transducer to the rotor.

The submarine system embodiment of the 48-sec-

TABLE 1. Details of Rotors Used in Complete ER Sonars.

ER Rotor	Type of switch	Switching generator	Rotation frequency	Signal frequency	Transducer	Number of elements	Spiral sweep	Mechanical arrangement
60-cycle rotor AIDE DE CAMP system	$\frac{1}{2}$ 6SN7 triodes, externally biased	36 $\phi$ resistive phase splitter, 36 potentiometers to equalize amplifiers	60 ~	22 kc	HP-1 Magnetostrictive	36	3 $\phi$ generator excited by sawtooth rotor current	Constructed on five chassis, interconnected by cables
200-cycle rotor AIDE DE CAMP system	$\frac{1}{2}$ 6SN7 triodes, externally biased	200-cycle lag line, pulse input. Synchronized by oscillator feedback	200 ~	22 kc	HP-1 Magnetostrictive	36	Electronic sawtooth modulation of signal from switching oscillator	Constructed inside BDI cabinet
500-cycle rotor, high frequency system	$\frac{1}{2}$ 6SN7 triodes, externally biased	500-cycle lag line, pulse input. Synchronized by oscillator feedback	500 ~	53 kc	AX-104 Y-cut Rochelle salt crystal	36	Electronic sawtooth modulator of signal from switching oscillator	Constructed inside BDI cabinet
Submarine system rotor	Varistors, self-biased	300-cycle lag line, sine wave input. Synchronized by frequency discriminator	300 ~	32 kc	AX-132 AX-136 ADP crystals	48	Electronic sawtooth modulation of signal from switching oscillator	Constructed inside transducer

tion laboratory varistor rotor used the same switching lag line to operate the varistor switches but employed a network of matching transformers to transform the high capacitive impedance of the crystal transducers AX-132 and AX-136 down to the required impedance  $60 + j80$  ohms. A frequency-discriminator circuit was used to synchronize the switching oscillator to the lag line. The submarine system contained no preamplifier built into the rotor because the rotor was installed inside the transducers. This represented a fundamental departure from the procedure followed in the vacuum-tube rotors.

The 36-element self-biasing varistor rotor used in the TIPPECANOE setup made use of a double  $\pi$  section switching lag line shown at the bottom of Figure 66 instead of the bridged-T type of line used in all previous systems. This rotor involved only 36 elements because of its operation in connection with AX-89, a 36-element, 18-inch diameter, Rochelle salt Y-cut crystal transducer of 25-kc resonant frequency. Since the rotor was used only for tests, it employed no synchronization circuits to adjust the switching oscil-

lator to the lag line, a function which was performed manually.

#### 7.4.7 Transmit-Receive Networks

A transmit-receive network is required in the ER system so that transmission into all of the elements of the transducer may be accomplished with these elements connected electrically in parallel, while in the receiving condition each element may be connected to the rotor as an individual circuit element. Another requirement is that the transmit-receive network absorb a minimum of power and permit the transducer to be utilized at full efficiency during transmission. Still another requirement is that the transmit-receive network introduce no spurious paths which transfer energy from one element to any other element in the receiving condition.

The first ER system, namely the 60-cycle AIDE DE CAMP system, made use of a 36-pole double-throw relay bank. In an effort to eliminate the large number of relay contacts, the capacitive transmit-receive net-

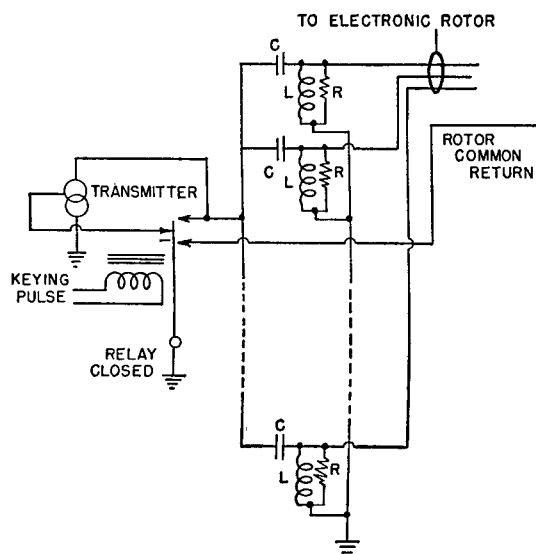


FIGURE 71. Circuit diagram of capacitive transmit-receive network.

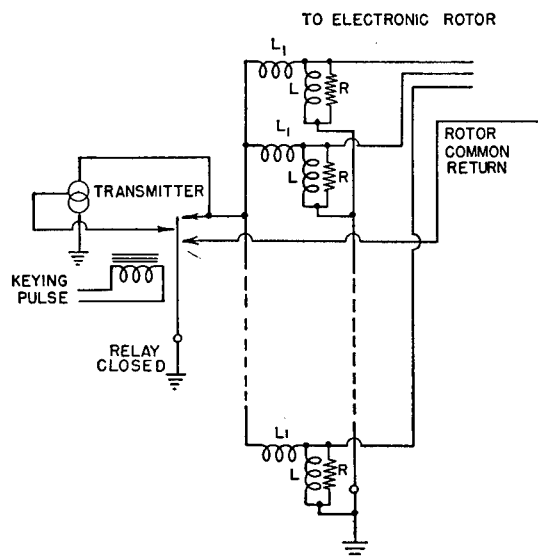


FIGURE 72. Circuit diagram of inductive transmit-receive network.

work was evolved as shown in Figure 71. The signal relay shown at the left of the drawing is normally open. In this condition the common return, coming from the rotor network at the right side of the diagram, is grounded through the relay leaf. The transmitting capacitors  $C$  are likewise grounded. Under these circumstances, the capacitors are simply paralleled with the transducer elements, represented as the inductance  $L$  and resistance  $R$  in the diagram. The capacitors  $C$  may have reactance which is large compared to the transducer element impedance, in which case they represent only a light reactive load on the transducer elements. Under other circumstances, they may tune the inductance in the transducer elements to resonance at the operating frequency, serving to increase the voltages developed by the transducer in reception. The fact that their common point is grounded in reception prevents energy originating in any transducer element from reaching any other transducer element across the capacitive network.

In transmission (as shown in Figure 71), the rotor common return is disconnected from the transducer common return so that no potential difference exists among the transducer elements in transmission. All points in the rotor network are raised to the same potential; hence, no potential differences are obtained across rotor elements. This condition is true only when all transducer impedances and all capacitive reactances are identical. With 5-per cent toler-

ance components, a reduction in potential may be obtained across each rotor element of 30 to 40 db, compared with the case in which the common rotor return is not disconnected.

One difficulty encountered in the case of the capacitive transmit-receive network is the transfer of energy from transducer element to transducer element caused by transformer effect. Adjacent windings, having a coefficient of magnetic coupling of the order of 0.1, transfer considerable amounts of energy between them because of the fact that at some frequency the transmitting capacitors tune the element inductances to the same frequencies. This is very much like the action which takes place in a double-tuned i-f transformer. In the case of HP-1 in the 200-cycle AIDE DE CAMP system, energy transfers of as high as -4 db occurred, element to element, at a frequency only 3 kc removed from the operating frequency. It was finally decided to eliminate this form of coupling by the use of the inductive transmit-receive network diagrammed in Figure 72. The principles of this network are the same as those of the capacitive network described above. However, by the use of inductive elements, tuning and energy transfer problems were eliminated. The only design criterion employed was to make the coupling inductance at least five times the transducer inductance so that it did not interfere with the proper operation of the lead line in which the transducer impedance was a shunt element.

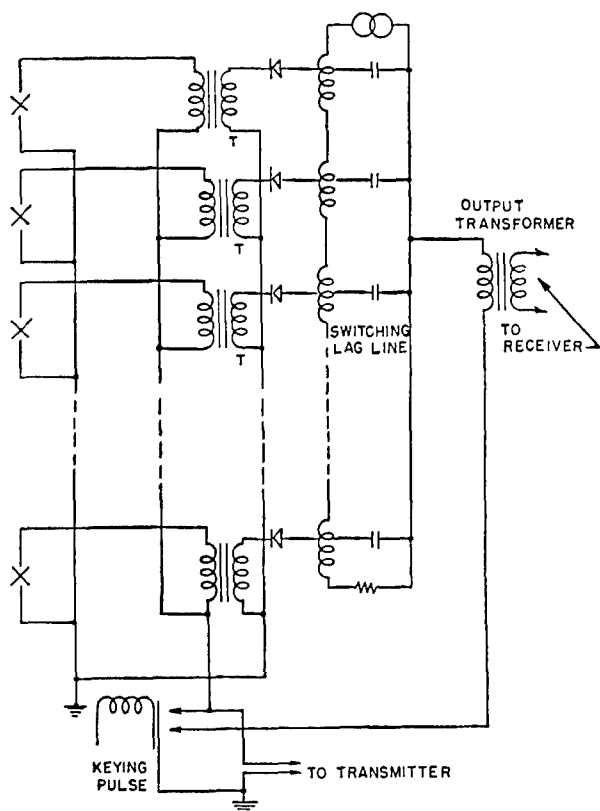


FIGURE 73. Circuit diagram of preliminary transmit-receive network, submarine ER sonar.

Figure 73 shows the transmit-receive network tried in the first Model 1 submarine rotor. This system was found inadequate because the varistors proved incapable of supporting more than 10 volts rms of signal voltage without breakdown. The capacitance to ground of the switching lag line network nullified in part the disconnecting effect of the relay leaf used for that purpose, so that the balance desired in this

form of transmission network was not obtained. In practice, the 2,000 volts appearing across each transducer element was reduced by only 26 db to 100 volts across some varistors, thus causing breakdown. Another factor influencing the poor balance obtained was the nonuniformity in element impedance of the early AX-132 and AX-136 transducers. As a result of these considerations, the coupling network shown in Figure 74 was finally developed.<sup>9</sup> In this coupling network the transducer elements are connected to the transmitter in series with neon lamps of Type 991, eliminating almost entirely any voltage appearing across the transducer transformer windings. This is the system that was used aboard USS DOLPHIN (Figure 75).

#### 7.4.8

### Mechanical Construction of Electronic Rotors

The electronic rotor of the AIDE DE CAMP is shown in Figure 4. This form of mechanical construction of a vacuum-tube rotor was abandoned in favor of the single-cabinet type of construction shown in Figure 8. Visible on the front panel is the tube-testing meter and selector switch as well as the on-off switch and pilot lights and the bias control. The base of the BDI cabinet contains the power supply and pulse generator. The switching lag line is mounted on the back of the rotor cabinet. Figure 9 is a view of the inside construction of the rotor itself. The preamplifier can be seen at the top of the chassis behind the tube-testing switch. The array of 36 transformers and 18 tubes occupies the remainder of the chassis space. Interconnections among the elements of the rotor are

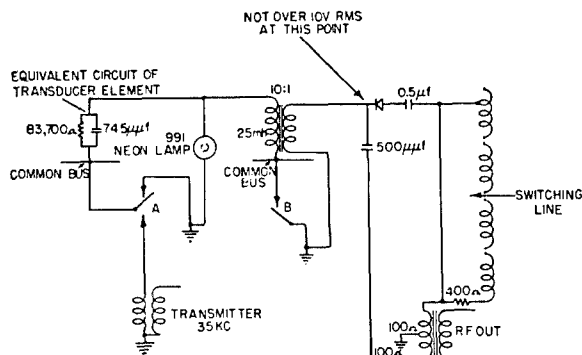


FIGURE 74. Circuit diagram of transmit-receive network with protective neon lamps, submarine ER sonar.

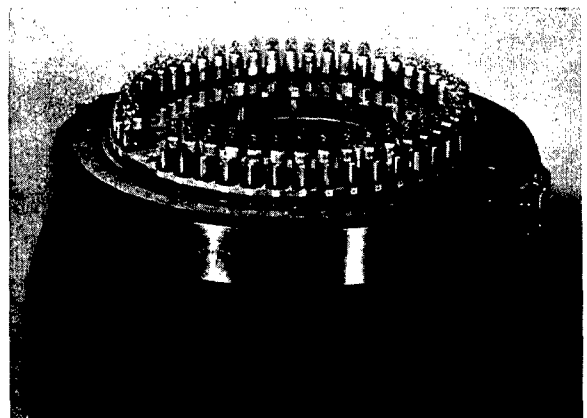


FIGURE 75. Installed view of protective neon lamps on AX-132 transducer, submarine ER sonar.

CONFIDENTIAL

made by means of AN plugs, some of which are visible at the bottom of this chassis.

The electronic rotor of the 500-cycle 53-kc ER sonar was, with respect to mechanical construction, exactly the same in every detail as the 200-cycle rotor. However, a departure was made in the rotor for the submarine ER sonar, which was designed for inclusion inside the transducer. It was, therefore, constructed in part as a right circular cylinder 9 inches in diameter, to be inserted in the hole provided in the submarine transducers. The component parts of the submarine rotor were designed, as discussed below, to be readily removable for tests and replacement. These parts were constructed on identical removable sub-chassis which were interchangeable for purposes of replacement.

Figure 76 is a photograph of the assembled electronic rotor which was designed for installation inside the AX-132 or AX-136 transducers. Incorporated in the rotor were the signal frequency lead line, the switching lag line, all of the varistor switching elements, all of the neutralizing capacitors, the input

transformer that fed the switching lag line, the electronic rotor output transformer, the transmit-receive relay, and the pulse repetition rate control circuits. Figure 77 shows two views of an individual rotor sector.

Figures 78 and 79 show the upper or fixed section of the electronic rotor. The projector-matching and transmitting transformers were arranged with the lead line capacitors near the top of the unit. A circle of 49 banana plugs connected the projector elements to the rotor (48 elements and ground). Also installed in this upper section were the input and output transformers, the synchronizing circuits, and the relay.

Submarine ER sonar rotor Model 1A was designed for insertion into the AX-132 and AX-136 transducers. Model 1 was designed earlier (but completed later) for insertion into the HP-3S transducer, and differed slightly in arrangement of parts at the top of frame, as may be seen in Figure 80.

Experience with the first submarine ER sonar electronic rotor Model 1 indicated that only the varistor elements were particularly vulnerable to damage and would require replacement under normal circumstances. For this reason a Model 2 rotor was designed in which a double  $\pi$  section type of lag line was employed to reduce the number of parts, and in which all the varistors were mounted at the top of the rotor. They were, therefore, readily accessible for test or replacement without removing the entire rotor from the transducer. A photograph of this rotor is shown in Figure 81. Connections to the transducer elements and to the external circuits were made with screws

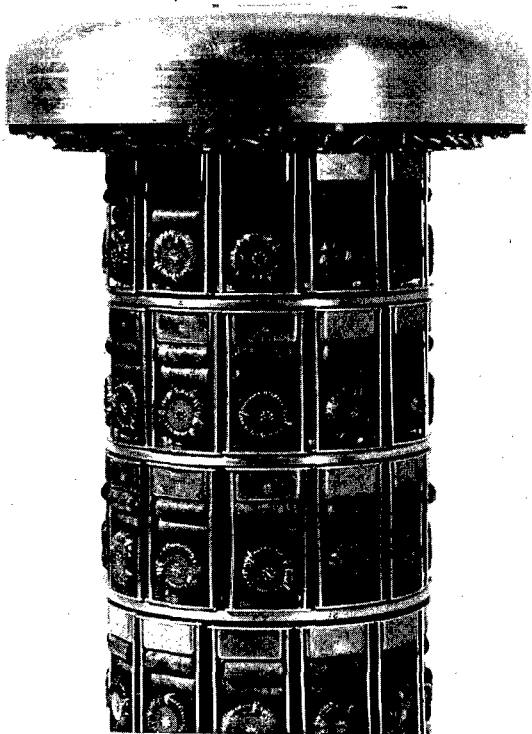


FIGURE 76. Assembled view of electronic rotor Model 1A, submarine ER sonar.

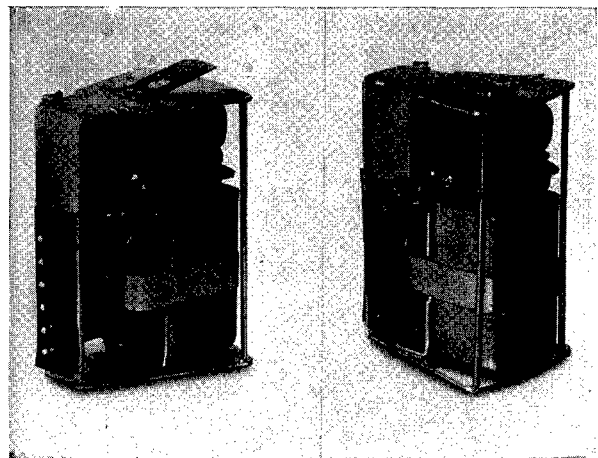


FIGURE 77. Front and back views of sector, electronic rotor Model 1A, submarine ER sonar.

CONFIDENTIAL

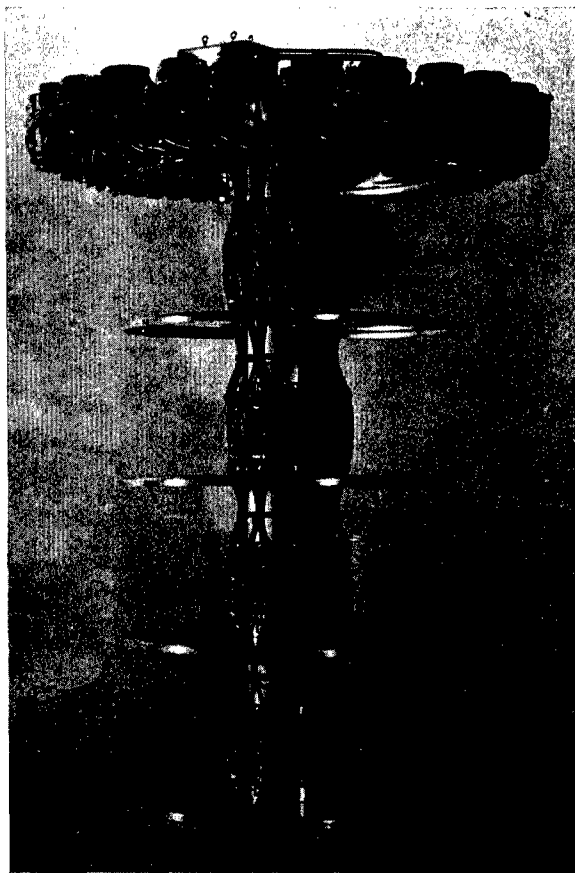


FIGURE 78. Side view of electronic rotor Model 1A with sectors removed, submarine ER sonar.

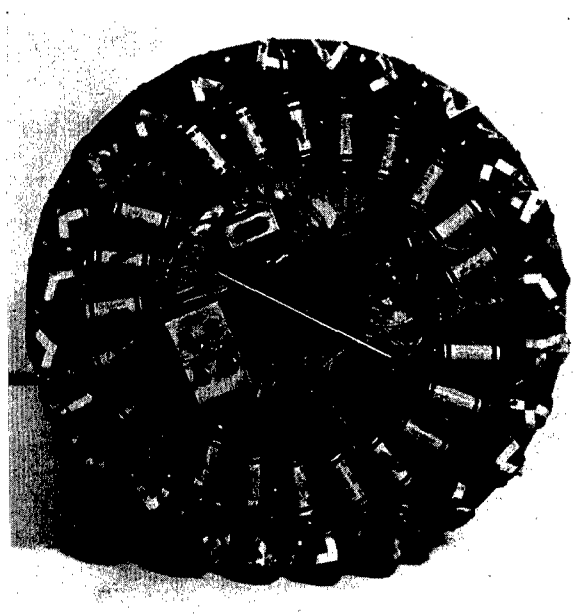


FIGURE 79. Top view of electronic rotor Model 1A, submarine ER sonar.

and Shakeproof soldering lugs. This rotor was designed for accommodation in the AX-132 and AX-136 transducers.

#### 7.5 INDICATORS AND CONTROLS

Early laboratory tests on ER systems were conducted using a commercial type of cathode-ray oscilloscope with linear sweep or with a PPI display of makeshift design. In the discussion to follow on the development of ER scanning sonar indicators, the types and capabilities vary from a simple PPI cath-

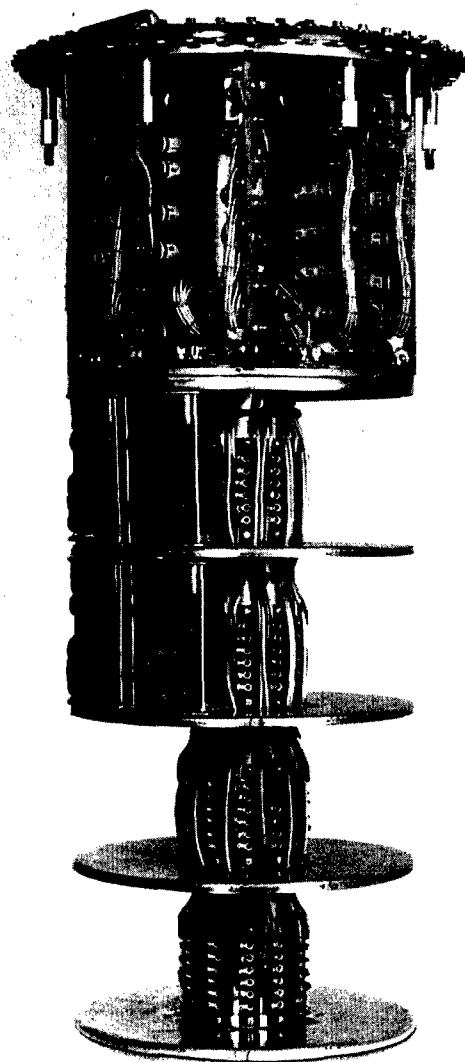


FIGURE 80. Partially assembled view of electronic rotor Model 1, submarine ER sonar.

CONFIDENTIAL

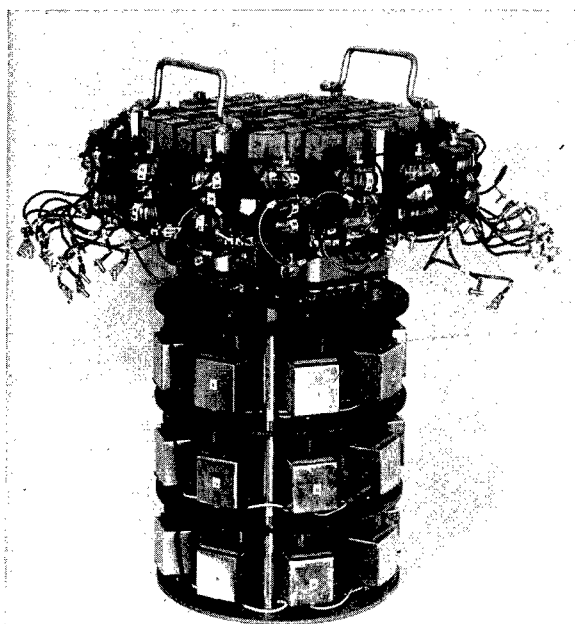


FIGURE 81. Assembled view of electronic rotor Model 2, submarine ER sonar.

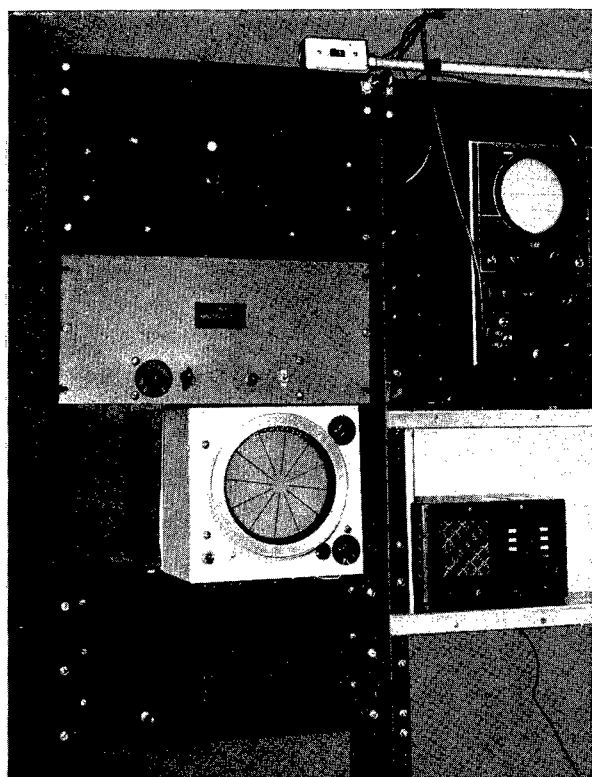


FIGURE 82. Front view of 200-cycle ER sonar indicator.

ode-ray tube, with only relative bearing engraved on the filter over the face and with controls on individual chassis of the system, to the submarine ER sonar indicator cabinet, which contained all the necessary controls grouped at the operator position.

#### 7.5.1 Indicators for 60-cycle ER Sonar

On the AIDE DE CAMP 60-cycle ER sonar a panel-mounted cathode-ray tube indicator was used. Operator controls were on their respective chassis. A mechanical cursor was used over a relative bearing scale engraved on a yellow filter placed over the tube.

#### 7.5.2 Indicators for 200-cycle ER Sonar

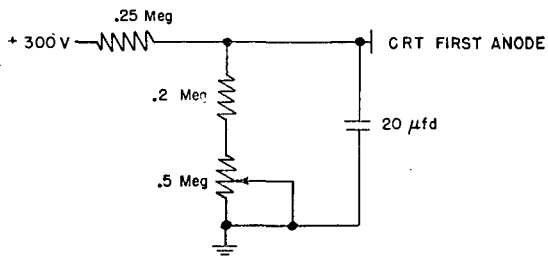
A CR repeater scope, or remote indicator, was used in this experimental system (see Figure 82). Designed primarily as a compact remote indicator, the indicator was  $17\frac{1}{2}$  inches long,  $10\frac{5}{8}$  inches wide, and  $10\frac{1}{8}$  inches high. In the center of the panel was located a 7BP7 cathode-ray tube, around which the controls were symmetrically grouped. A relative bearing scale was provided by engraving the filter placed over the tube.

Inside the scope housing, two chassis mounted at right angles contain the high- and low-voltage power supplies and their associated voltage-divider networks. (See Figure 83 for a schematic diagram of this sonar repeater scope.) Adjustments necessary to regulate the display were on the individual chassis in the rack of ER scanning equipment. Four ranges of 500, 1,000, 2,000, and 4,000 yards could be selected by means of the range switch on the switch chassis.

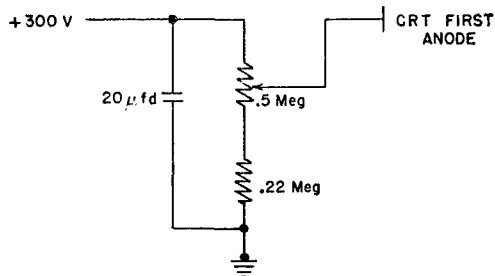
Standard 2-phase deflection coils were utilized, which produced a spiral that was not so uniform as desired. Toward the end of the sweep there was a tendency for the deflection to become square or to develop other irregularities. Further experimentation, to improve the circularity of the spiral, indicated that the entire source of nonuniformity was not in the deflection coils, but was partially developed in the output of the sweep chassis. To correct the deflection coil distortion, the stator coil assembly of a 2-phase 2-pole Kollsman generator was used. (The order for this assembly specified "Stator coil assembly, SK455-901, 2-phase 2-pole generator stators, I.D. of winding 1700 on both ends.") By experimenting in reversing the leads of the coil it was possible







A USED IN 53 kc ER SONAR



B USED IN SUBMARINE ER SONAR

FIGURE 85. Circuit diagrams of PPI intensity controls.

the repeater scope bolted to the top as shown in Figure 86.

Three scanning ranges of 600, 1,500, and 3,000 yards could be selected by the 5-position range switch. The two other positions were power on-off and a stand-by which open-circuited the blanking pulse used to key the transmitter on the No. 2 or listening position. At this setting, which was used in a warm-up period, or when the ER sonar was being used for listening only, the transmitter was not keyed. To aid in the operation of the gear the receiver gain control was moved from the receiver proper to the indicator panel. The measurement of range of an echo depended upon operator judgment, as range-marking was not employed. Use was again made of the engraved filter for reading relative bearing. An interior view of the PPI chassis is shown in Figure 87.

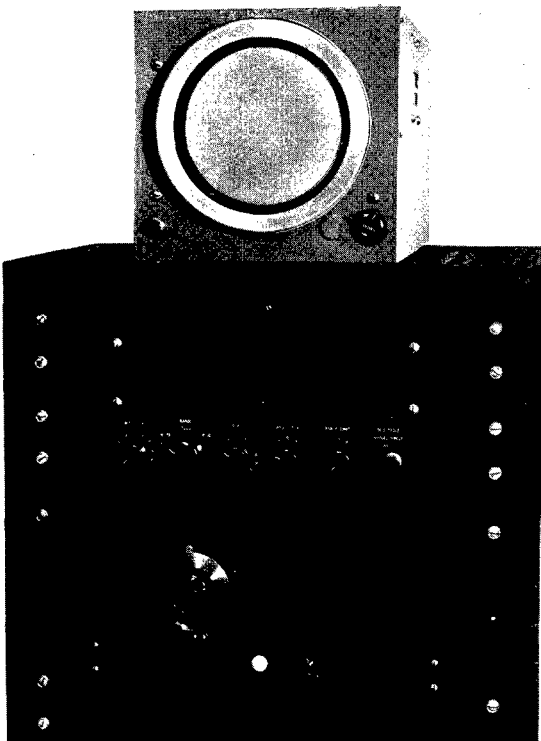


FIGURE 86. Front view of 53-kc ER sonar indicator.

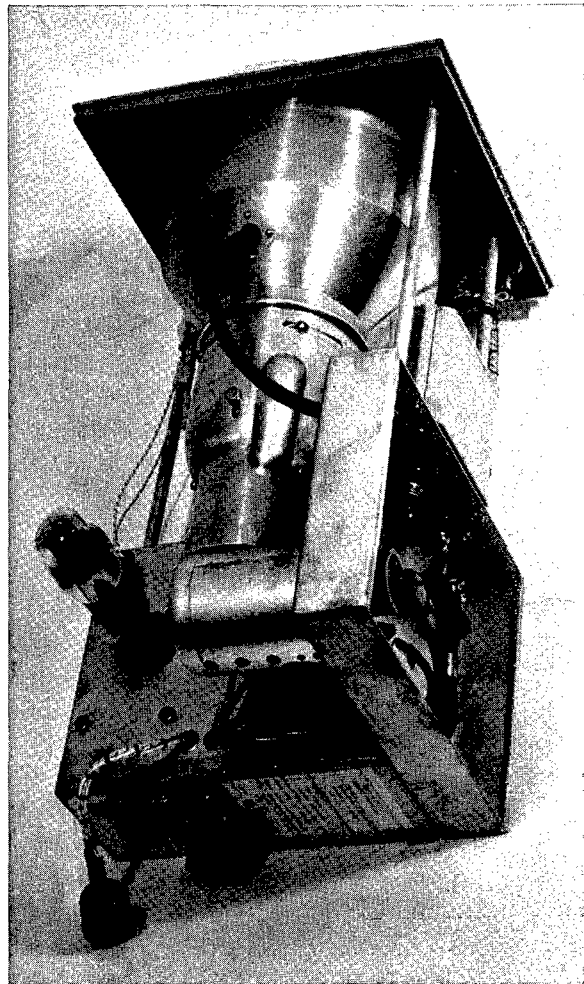


FIGURE 87. Interior view of 53-kc ER sonar indicator.

CONFIDENTIAL

#### 7.5.4 Indicators for Submarine ER Sonar

In the design of an indicator for the submarine ER sonar, particular thought was given to physical size and location of controls. As indicator development had already been undertaken by outside companies, as well as by HUSL, it was profitable to borrow from this experience. A Western Electric mounting designed for a PPI-BDI indicator was available as a sample, complete with blueprints. Around this sample was designed the submarine ER sonar indicator cabinet. Controls for the system were divided into two classifications: (1) those to be manipulated by the operator during normal operation of the equipment were to be on the indicator, while (2) those requiring only occasional adjustment were to be located on their respective chassis. By making the indicator a compact unit, the problem of mounting it in the restricted spaces available on shipboard was considerably simplified.

With the exception of the back plate, the outside case, measuring  $16\frac{1}{4}$  inches wide,  $11\frac{7}{16}$  inches high, and  $14\frac{1}{4}$  inches deep, was constructed of a  $\frac{3}{8}$ -inch aluminum casting. As the front panel was attached directly to various components of the indicator, it was bolted to the main casting of the chassis. Two rails, or tracks, inside the case on each side engaged runners on the chassis to bear its weight. A 40-prong Cannon plug (DPR 40-33 and DPR 40-34 assembly, Cannon 1412-1 receptacle, Cannon 1412-2 plug) was used as a practical means of connecting the cable to the chassis while also allowing removal of the chassis without unscrewing numerous terminal strips. The receptacle was secured to the back of the case, with the bail of the receptacle connected mechanically to a handle on the outside of the case. The plug was mounted on the chassis, in such a way that as the chassis was pushed into the case it slid into the 40-terminal receptacle gear rack channel. Raising the handle on the case closed the plug. On the front top left side there was a cutout in the case. When the chassis was in place, the focus control, intensity control, and battlephone plug were directly behind this window and accessible to the operator. Six retaining screws on the front panel held the chassis in position.

Both true and relative bearing information was presented. On the inner plastic transparent window over the face of the cathode-ray tube was scribed a pair of lines constituting the cursor. (See Figure 88.) This window was mechanically attached to the rotat-

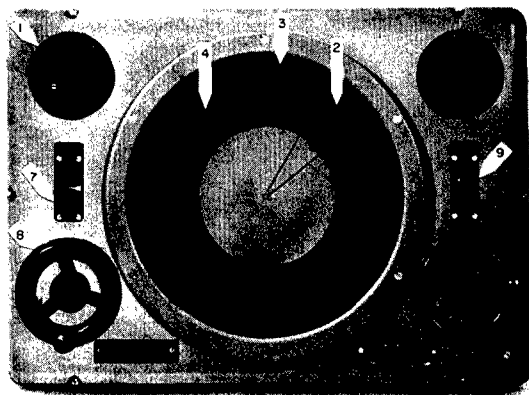


FIGURE 88. Front view of submarine ER sonar indicator.

ing middle ring (2) which had engraved on it a diamond-shaped pointer, or bug. Rotation of the bearing hand wheel (8) set in action a servo system, driving a motor that was gear- and shaft-connected to the middle or relative bearing ring. Therefore, if the bearing hand wheel was turned until the two lines straddled the echo being observed on the face of the cathode-ray tube, the bug indicated bearing relative to the ship on the outside ring (3), which was fixed in position, and the true or compass bearing upon the inner ring (4).

*Maintenance of true bearing [MTB]* was also a feature of the bearing system. To accomplish this the leads coming into the indicator box from the gyro were wired to a 1 CT synchro (5) whose shaft was geared to the gyro ring as shown in Figure 89 and Figure 90. The gyro voltage was also applied to the 1 DG synchro (6) geared to the bearing hand wheel, and through the 1 DG synchro to another 1 CT synchro (10) whose shaft was geared to the cursor ring. For differences between zero position as indicated by the gyro circuit and zero position on the 1 CT synchro rotor attached to the gyro ring, the synchro rotor developed 60-cycle voltages proportional in magnitude and in sign to the angular difference existing between these two positions. This voltage was used via a servo amplifier to drive the 2-phase motor which positioned the gyro ring.

The output of the DG synchro was a set of voltages corresponding to the sum of the mechanical position angle of the shaft and the voltages corresponding to the gyro order. The voltage output of the 1 CT synchro attached to the bug ring was proportional in magnitude and phase to the difference between the

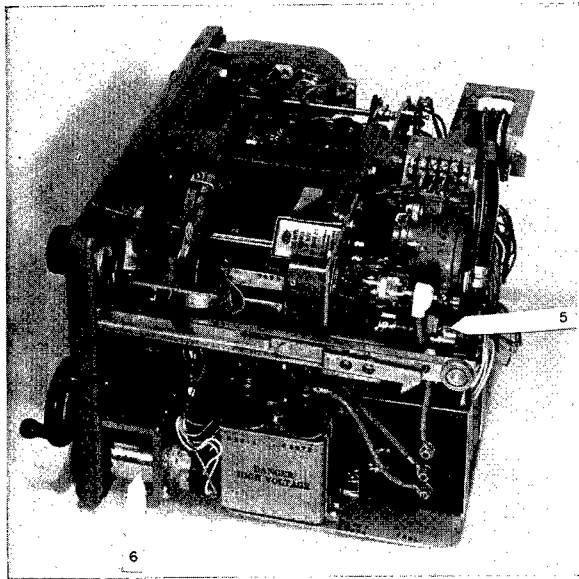


FIGURE 89. Interior view, right side, of submarine ER sonar indicator.

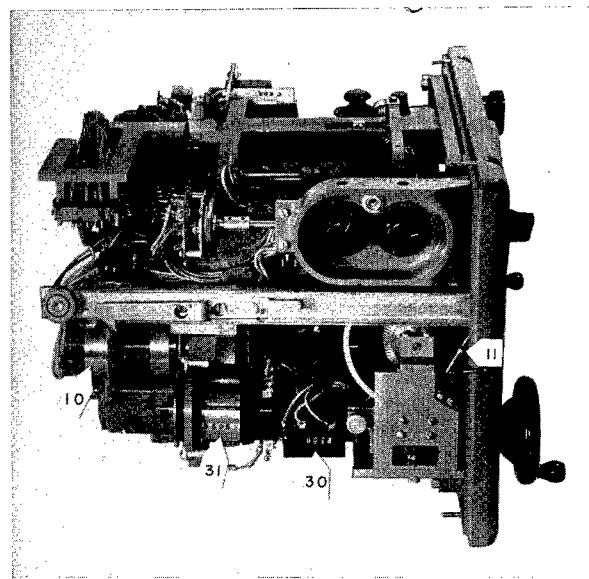


FIGURE 90. Interior view, left side, of submarine ER sonar indicator.

bug ring position and the sum of the gyro order and the angle through which the bearing wheel had been rotated. Output of this 1 CT was amplified by another servo amplifier in the receiver chassis and used to drive the 2-phase motor geared to the cursor ring (see Figure 91 for the circuit diagram). By reversing the phase of the signal to the motor the direction of rotation reversed, so that the mechanical and electrical differences were reduced to zero for changes in either direction.

To illuminate the bearing dials a miniature bulb (19/32 inches long, 7/32 inches in diameter, GE 2-amp special midget screw base) was placed behind the diamond bug on the inner rotating ring. Electrical contact was made by two slip rings on the outside of the ring, so that the light could follow the rotation. Illumination of both the bearing light and the range dial light could be varied by the dial illumination intensity control R505 (circuit diagram, Figure 91). Geared to the cursor ring was a phase-shifting transformer in the range-caliper circuit (see Section 7.8 on sweep generators) that insured that the blank sector of the range circle was centered on the bearing indicated by the bug.

Three indicators were constructed for the submarine ER sonar. These were alike except in the arrangement of various parts which comprised the high-voltage supply for the cathode-ray tube. The high-voltage transformer and rectifier tube were not

sufficiently protected in the first indicator and were relocated and shielded in Serial Nos. 2 and 3 to provide greater safety for the operator. At the same time the rectifier tube was changed from a 2X2 to a 3B24 for greater reliability. The same circuit diagram was used for all three.

7.6

## ER RECEIVER

7.6.1

### Design Considerations for ER Receivers

#### BANDWIDTH

The choice of the bandwidth to be passed by an ER sonar receiver depends primarily upon the required functional performance of the system. It is necessary to know whether or not *own-doppler nullification* [ODN] is to be applied, and whether it is desired to echo-range on surface ships as well as on small objects. The rotation speed and the width of the beam pattern also must be known.

To take a particular case, that of the submarine ER sonar, the object may be to observe noise radials from target sources or to echo-range on surface craft traveling up to 30 knots. It may be assumed that ODN is not applied to the receiver and that own-ship's speed is 10 knots. Furthermore, a rotation speed of 330 c may be assumed and beam widths 30 degrees at points 6 db down.

CONFIDENTIAL

First attention may be directed to that portion of the bandwidth which must be provided to take care of doppler introduced by own-ship and target motion. This motion has been assumed to take place at a

maximum of 40 knots. Since, at 30 kc the doppler shift is 21 cycles per knot, it requires  $\pm 840$  cycles or a total bandwidth of 1,680 cycles.

Next, consideration may be given to the increase

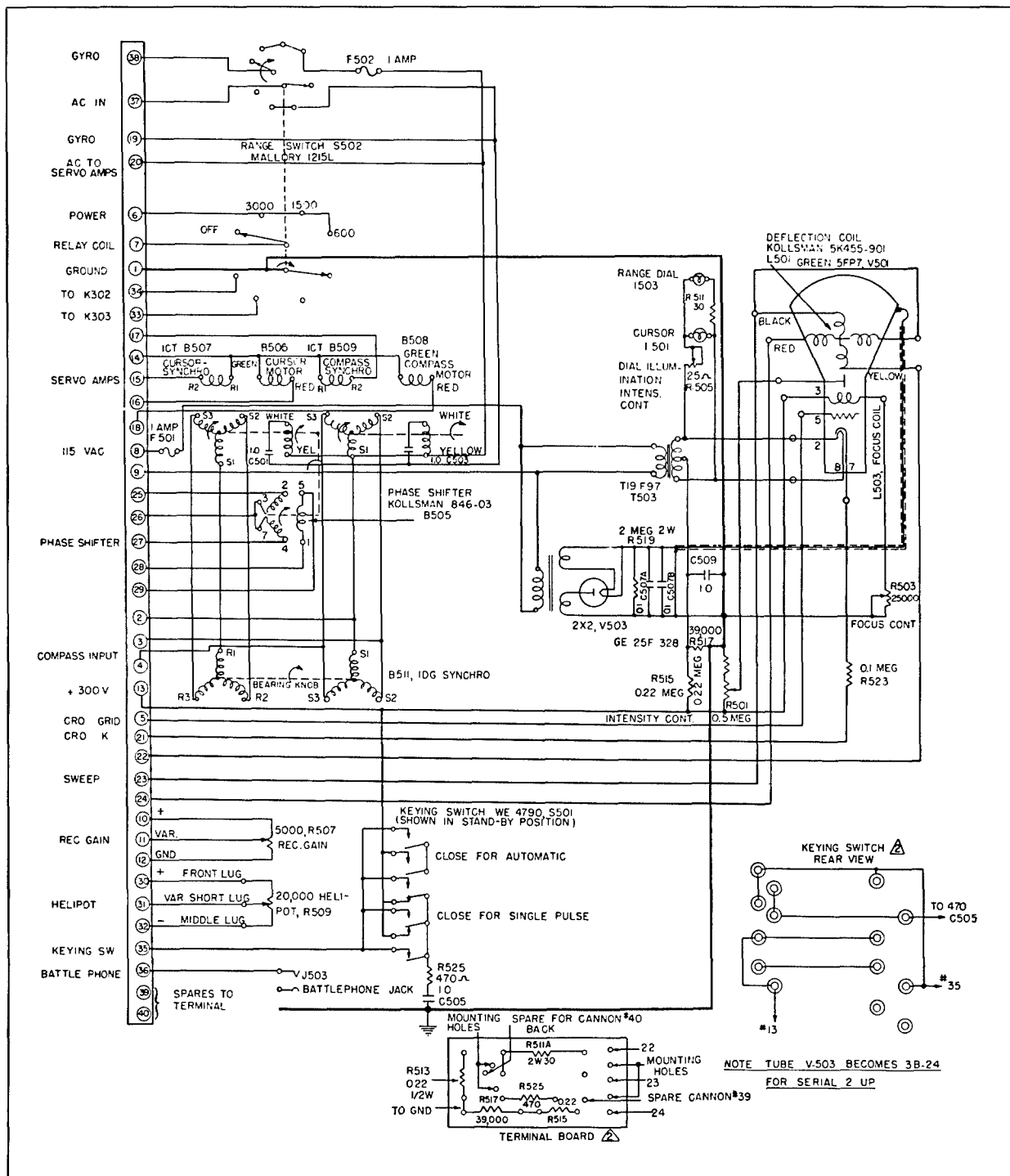


FIGURE 91. Circuit diagram of submarine ER sonar indicator, Model 1, Serial 1.

CONFIDENTIAL

in bandwidth which must be provided to accommodate the short pulses that come through the rotor and appear as echoes to the receiver. Since the rotation speed is 330 c, a transmitted pulse of 3 milliseconds in length is necessary to avoid dead areas. (See Section 7.8 on sweep generators in the present chapter.) With a beamwidth of 30 degrees, a returning echo from a target is intercepted for a period equal to  $30/360$  of the time for one rotation, or 0.25 milliseconds. In this case, therefore, a bandwidth of 4,000 cycles would be necessary.

The combined bandwidth necessary to accommodate the doppler shift as well as the echo without undue distortion is approximately 5.6 kc. In addition to this,  $\pm 200$  cycles should be allowed to compensate for slight mistunings of the transmitter. This means that a total bandwidth of 6 kc is necessary. It is well to note here that noise radials are not affected by doppler considerations, since these radials are caused by more or less white noise sources and doppler shifts are unimportant.

From the above discussion it is seen that if it were possible to obtain 10-degree beams, it would become necessary to have a bandwidth of approximately 12 kc in order to accommodate the short echo pulse. Although the narrower beam would provide additional discrimination against water noise, the broader band would increase the receiver noise. Moreover, it should be noted that doppler considerations contribute a relatively minor portion of the total bandwidth required in systems having a high rotation speed sharp beam.

One of the advantages of keeping the bandwidth narrow is to reduce some of the minor lobes of the pattern produced by the lead line. This reduction occurs because the high rotation speed of the switching action introduces a rotational doppler which shifts the frequency of the signal in the minor lobes away from that in the major lobe. There may, however, be an increase in the width of the major lobe if the band-pass is made too narrow.

In case preamplifiers for each transducer element are utilized ahead of the switching elements, the band-pass of these preamplifiers need only be wide enough to pass the doppler shift due to own-ship and target motion, and to include the width necessary for the full transmitted pulse. In the present ER system this pulse is 3 milliseconds. There is a great deal to be gained from the standpoint of signal-to-noise ratio by introduction of preamplifiers.

#### RECEIVER GAIN

The overall gain of the system must be sufficiently large that the limiting noise, whether water noise at sea state zero or thermal noise in the transducer, brightens the indicator. The amount of gain necessary depends upon the bandwidth of the receiver, and upon whether or not narrow bandwidth preamplifiers can be included for each element in the transducer. In the case of a crystal transducer, which is a relatively high impedance source, experience would indicate that the limiting noise is thermal noise arising in the transducer.<sup>38</sup> In the case of ER sonars so far constructed, 150 db of voltage amplification was included. The input impedance of these receivers was approximately 100 ohms. The receiver output stage was a cathode follower with considerably more power capabilities than were needed to drive the grid of the cathode-ray tube. It was required to deliver 100 volts (peak) to the grid of the indicator tube.

#### OUTPUT FILTERS

In order to apply a unidirectional pulse to the brightening grid of the cathode-ray tube, it is necessary to rectify and filter the output of the amplifier. The characteristics of this filter must be such that no appreciable distortion of the pulse corresponding to the echo is introduced. For a 0.25-millisecond pulse, the bandwidth should be 4 kc. However, there is considerable doubt as to the necessity of passing very low frequencies. There might be some advantage in elimination of d-c components due to power supply variations by the use of transformer coupling to the grid of the PPI scope. By locating this transformer close to the CRO grid, it would be possible to reduce the gain of the rest of the receiver through approximate matching of the output stage to its load.

The output filter may be of any type that satisfies the requirements regarding cutoff frequency to accommodate the pulse length. For the case cited above, in order to obtain a distortionless output pulse, the phase shift must be nearly linear with frequency to 4 kc. Moreover, since the transient response of the filter is the important factor, its impedance should be nearly independent of frequency. The carrier component should be down at least 30 db.

#### AUTOMATIC GAIN CONTROL

The type of automatic gain control (*time-varied gain* [TVG], *automatic volume control* [AVC], or *reverberation-controlled gain* [RCG]), to be used

in the receiver requires very careful consideration. Its purpose is to control the gain of the receiver with time in such a way that reverberation neither overloads the receiver circuits nor obscures the display on the PPI by excessive brightening, while the receiving sensitivity is maintained at the highest usable level. The initial charge and the rate of decay of the TVG circuit depends upon several factors. The shortest range at which it is desired to receive echoes must be known in most cases. The minimum possible range is determined primarily by the transfer network, and secondarily by the blanking pulse to the oscilloscope. Since the transfer networks normally require about 10 milliseconds to operate and must be maintained in an operated condition until after the transmitted pulse, the normal ER blanking pulse is about 30 milliseconds, 10 of which precede the transmitted pulse and need not be considered. The operator is then "blind" for an interval of 20 milliseconds, which corresponds to a range of approximately 16 yards from the transducer. Assuming that the purpose is to see an object 20 yards distant, then the receiver has to be able to receive strong echoes 25 milliseconds after the transmitted ping. Hence, the TVG bias must not be so great that the receiver is completely blocked after 25 milliseconds. A bias sufficient to cause a reduction in gain of 40 db at this time should be sufficient. If provision is made to restore the gain gradually to its full value as the indicated range increases from 100 to 600 yards, most conditions should be accommodated.

RCG has not yet been used on ER systems. If it should be desired to employ it, similar considerations would apply as for TVG, with the additional factor that the time constant of the grid bias circuit of the discharge tube must be extremely rapid compared to the rotation rate of the ER beam. This is so that a noise source is not allowed to maintain the bias on the discharge tube throughout the rotation period of the beam. As an alternative, RCG could be cut out for noise listening.

#### DELAYED LOBE COMPARISON

The delayed lobe comparison scheme<sup>39</sup> is a device for sharpening the echoes received in ER sonar. Figure 92 shows the delayed lobe comparison circuit, as well as a diagram from which its action may be more readily understood. The output of the receiving amplifier delivers a signal to a delay network, or lag line.

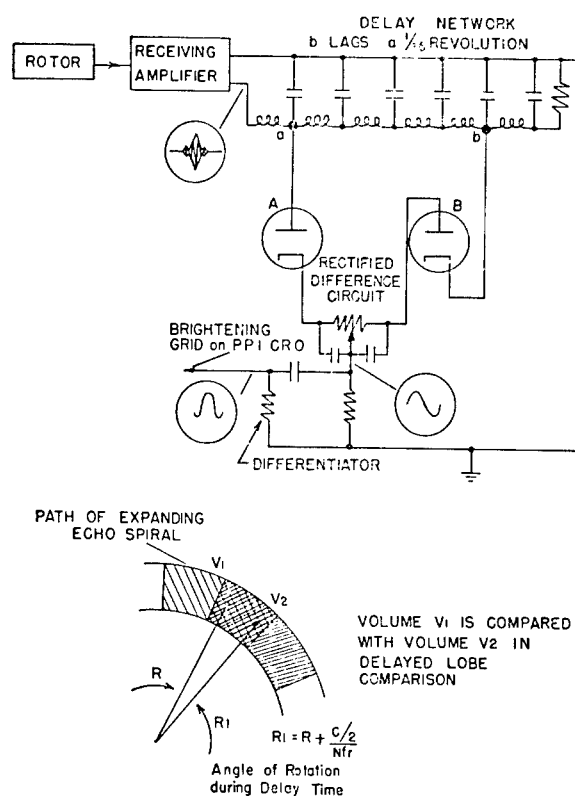
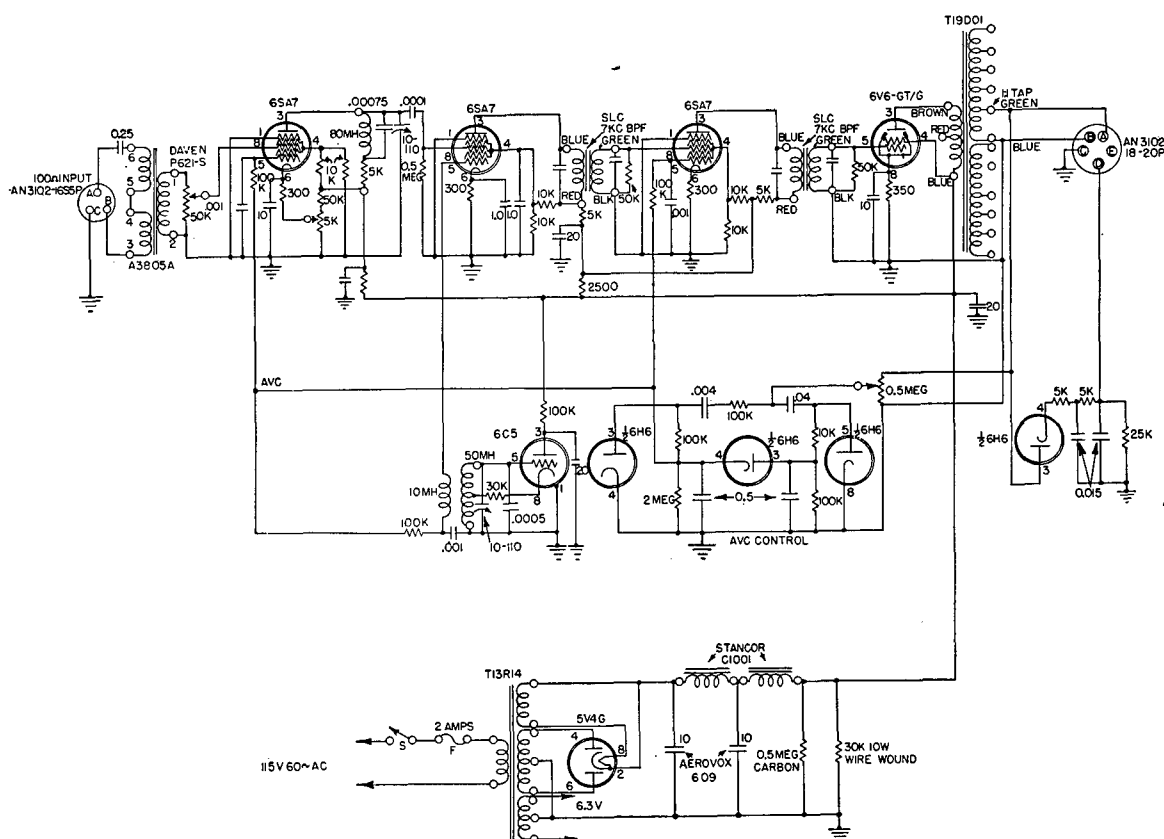


FIGURE 92. Circuit diagram of delayed lobe comparison system.

A and B equal to the length of time taken by the tip of the major lobe in traversing the angle subtended by one transducer element. In the case of the 36-element transducer this time was 1/36th of a rotation, or 10 degrees out of the 360 degrees in a rotation cycle. Signal amplitude at point A is compared with signal amplitude at point B. In the circuit shown, the difference is taken and differentiated to cause sharper brightening representation than would be possible in using the pulse amplitude alone. The output of the receiving amplifier has a shape or pattern as shown in the small circle at the beginning of the delay network. The pattern travels down the delay network and is rectified so that the envelope of the pattern is presented by rectifier A in a positive sense to the difference circuits. The output of the pattern, delayed as it appears at rectifier B, is presented to the difference circuits in a negative sense. The combination of the envelopes of the pattern as rectified and subtracted, rectifier B from rectifier A, is shown in the small circle near the center of the difference circuits. After passage through the RC differentiator, a signal is pro-



duced having a shape as shown in the small circle, at the output of the differentiator circuit. This output pulse is applied to the brightening grid on the PPI CRO, and has a negative lobe where the difference signal has a negative slope, a positive lobe where the difference signal has a positive slope, and another negative lobe at the end of the difference signal. The new brightening pulse is a narrower pulse than the original one, with the peak lying midway in time between the time when the signal arrived at point A and the time when the signal arrives at point B in the delay network. The representation on the PPI scope is, thus, a very short arc lying at the correct range and bearing.

### TUNING RANGE; CHOICE OF INTERMEDIATE FREQUENCY

In some cases ER receivers have been designed around fixed frequency systems, and fixed-tuned r-f receivers have been used. However, in some instances it is desirable to have the sonar receiver tunable over a range of at least a few kilocycles in order to avoid interference between equipments installed in ships

that may be operated in fairly close proximity. In the case of the Model XQHA scanning sonar receivers, this tuning range has normally been of the order of 10 kc (see Chapter 5). In view of interference measurements made with two ships carrying QH scanning equipment, it seems reasonable to assume that 5-kc tuning range would be sufficient for a QH receiver.<sup>40</sup>

Since the bandwidth of an ER receiver must be considerably greater than that of a QH receiver (approximately 6 kc compared to 2 kc), an intermediate frequency high enough (50 to 100 kc) to obtain this bandwidth is advisable. In order to eliminate interference from other ER equipments, a tuning range of 15 kc may be necessary. Experience has shown considerable interference from another vessel putting signals into the water at 23 kc, when the ER gear on the searching ship was tuned to 33 kc. If dual-channel receivers are utilized in ER systems as they now are in QH systems, some difficulties can be avoided if the intermediate frequency is not an exact multiple of any signal frequency.

In certain applications where it is important that



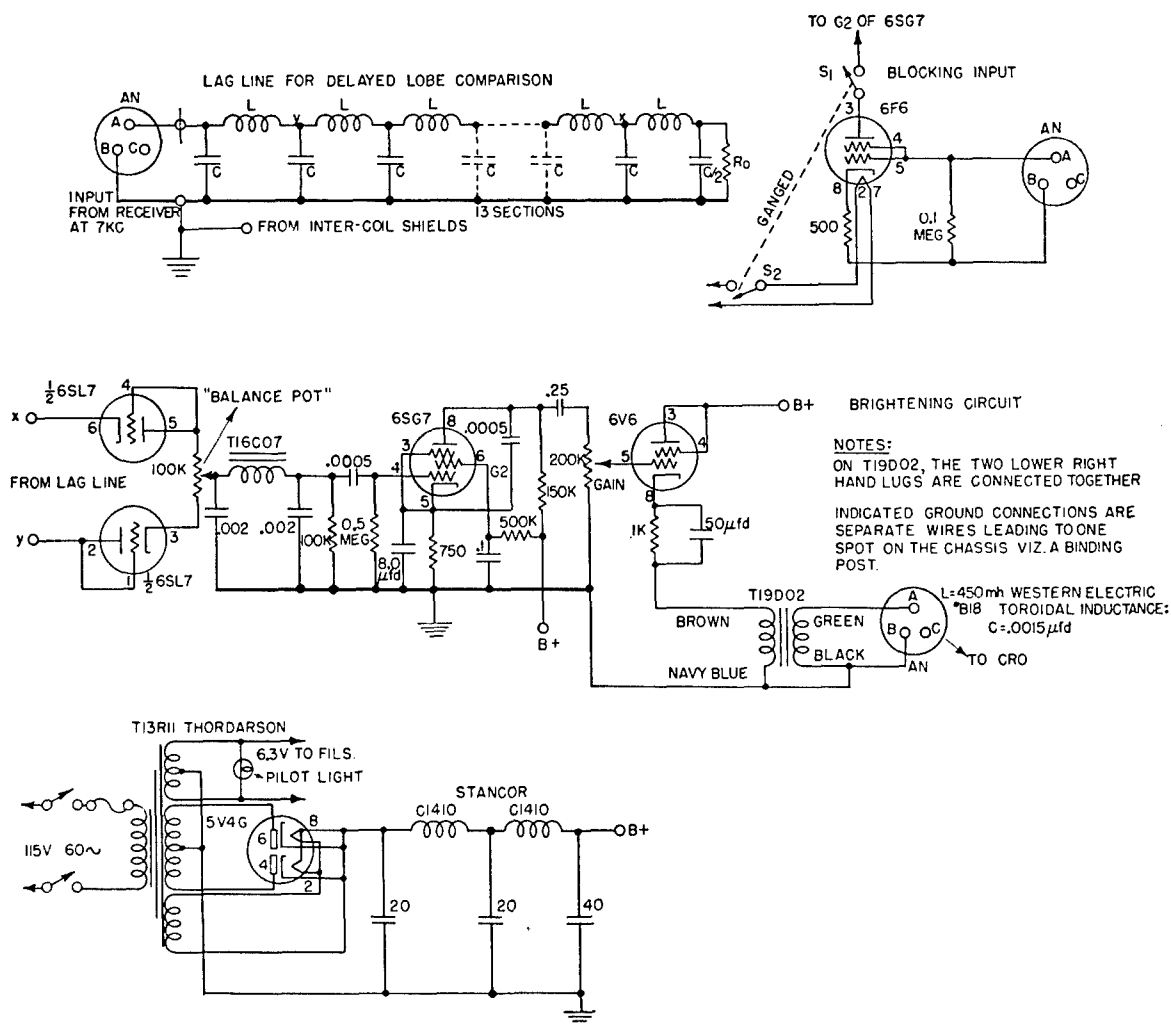


FIGURE 94. Circuit of delayed lobe comparator and brightening chassis for 60-cycle ER sonar.

phase shift be constant through two channels, an intermediate frequency should be adopted that is as low as is consistent with the required band pass. Care should be taken to keep the local oscillator frequency as far removed from the intermediate frequency as possible.

#### DYNAMIC RANGE OF AN ER RECEIVER

The dynamic range of an ER receiver, or any scanning receiver, should be at least 30 db. An outstanding factor in the overload characteristics should be that, for very large signals, limiting occurs without blocking. The only precaution necessary to insure that blocking does not occur is to keep the RC time constants in the grid circuit shorter than the period of one cycle of the incoming wave. It should be noted here that blocking occurs on steady-state signals when

it would not do so under transient conditions. For this reason, ER receivers should be tested both under steady-state conditions and under transient conditions. Although the signals being discussed here are transient in character, reverberation may appear to the receiver much more like a steady-state signal.

#### 7.6.2 Receivers for 60-cycle ER Sonar

The 60-cycle ER sonar on board the AIDE DE CAMP used a delayed lobe comparison receiver. This receiver (Figure 93) was interchangeable by means of switches with a *simultaneous lobe comparison* [SLC] receiver and also an amplitude receiver with a pulse-sharpening output. These other receivers were built for the use of the CR system and are described in Chapter 5. A circuit diagram of the delayed lobe

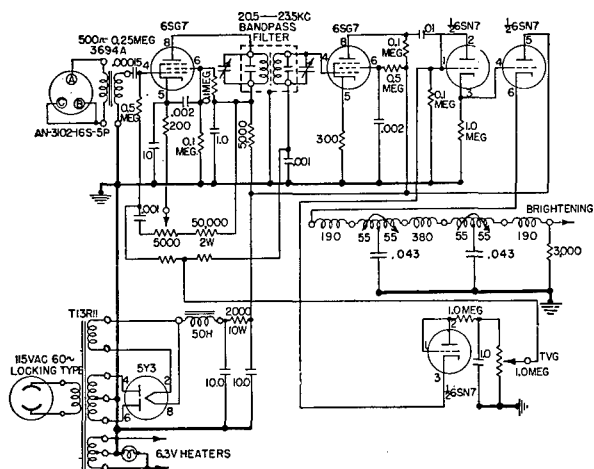


FIGURE 95. Circuit diagram of receiver for 200-cycle ER sonar.

comparator and brightening chassis is shown in Figure 94.

#### 7.6.3 Receiver for 200-cycle ER Sonar

The 200-cycle 22-kc ER sonar as installed on the AIDE DE CAMP used a revised CR amplitude receiver from the AIDE DE CAMP. Figure 95 gives the circuit diagram in the revised form. The receiver had a total

bandwidth of approximately 3.5 kc, centered at 22 kc, and the voltage amplification was approximately 95 db, with the preamplifier located in the rotor producing another 35 db.

#### 7.6.4 Receiver for 53-kc ER Sonar

The 500-cycle 53-kc rotation ER sonar used a superheterodyne receiver. Figure 96 is a schematic of this circuit.

#### 7.6.5 Receiver Used with Laboratory Varistor Rotor

For tests on the varistor rotor as used in the laboratory, a Type 755-J Submarine Signal Company receiver was used. This receiver had a 100-ohm balanced input which was directly connected to the output transformer on the varistor rotor. In general the receiver was of the superheterodyne type with tuned r-f stages and a tunable local oscillator. The total tuning range available was from 18 to 37 kc.

As used in the tests the receiver was tuned to 24 kc, the frequency of operation of the artificial transducer connected to the rotor. The second oscillator (c-w switch) was turned off and the i-f filters were set at the

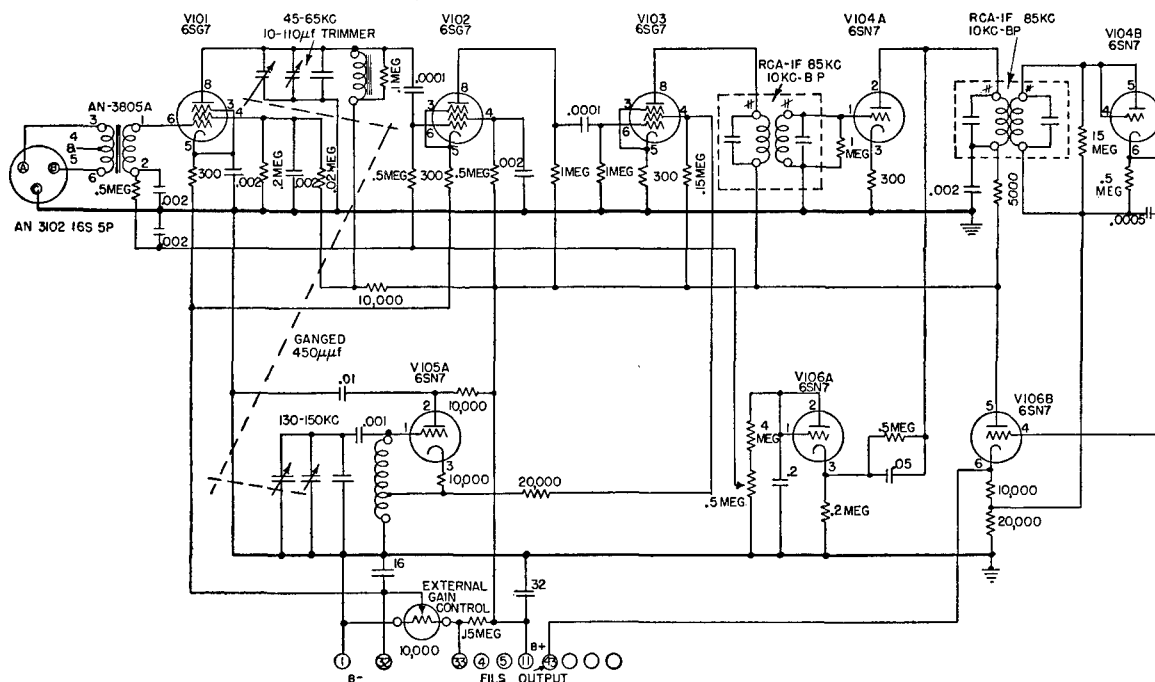


FIGURE 96. Circuit diagram of receiver for 53-kc ER sonar.

CONFIDENTIAL

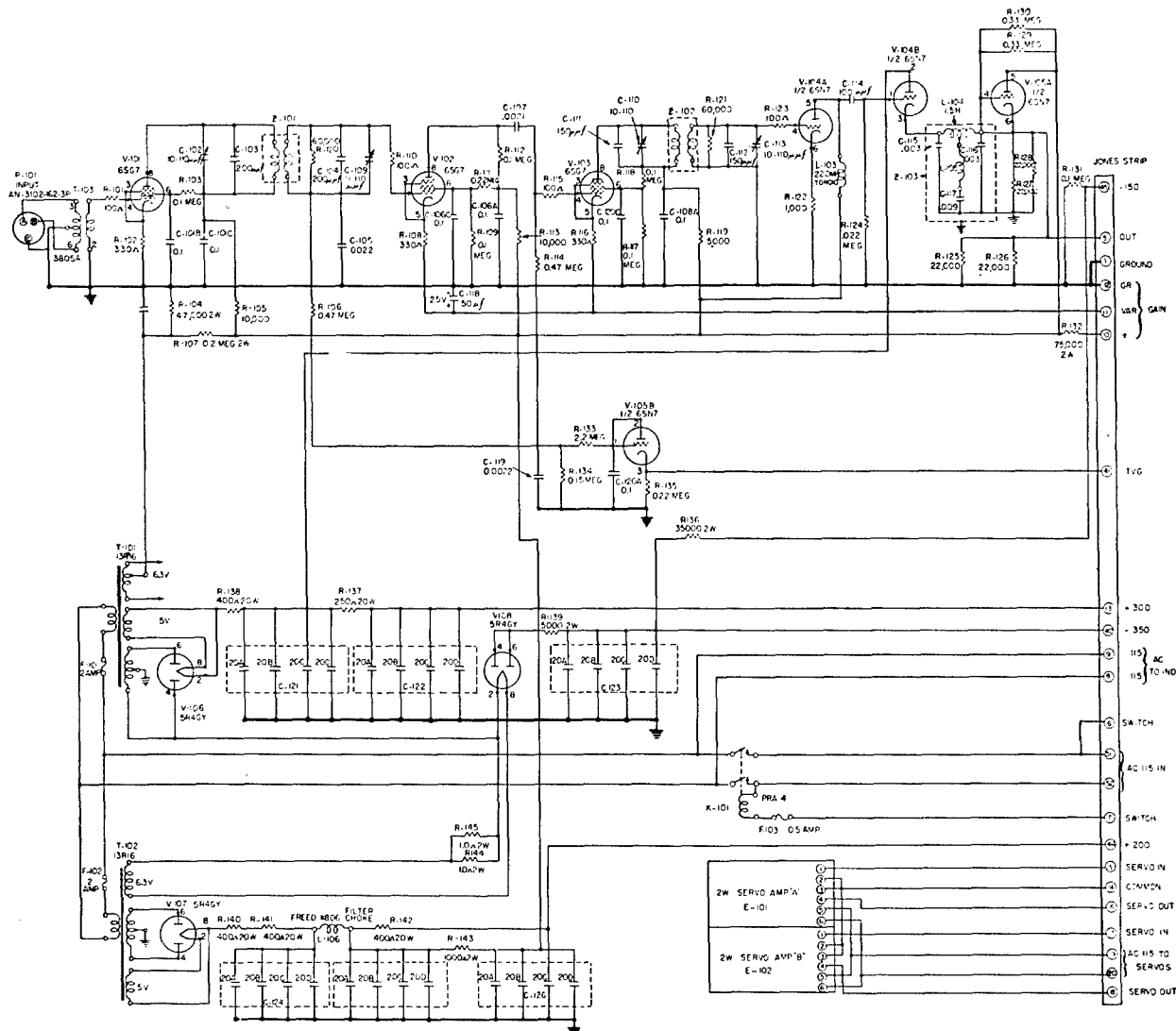


FIGURE 97. Circuit diagram of submarine ER sonar receiver, Model 1, Serial 3.

broad position, while the audio filters were set at the flat position. Under these conditions the bandwidth of the receiver was about 3 kc at points 3 db down. It was found that this receiver had adequate gain and suitable filter characteristics for use with the ER system when connected in the manner indicated above. It was interesting to note that as the receiver bandwidth was narrowed, the output pattern became wider until finally, on the narrowest possible bandwidth positions, no pulse came through at all.

#### 7.6.6 Receivers for Submarine ER Sonar

The receivers used in the submarine system were of *fixed-tuned signal frequency type*.<sup>41</sup> To date there

have been three such receivers constructed to operate at a frequency of 32 kc and differing only slightly in construction. Figure 97 is a circuit diagram of Serial No. 3.

The receiver could be tuned over  $\pm 1$  kc by means of the trimmer capacitors on the filters. The center frequency was adjusted to 32 kc and could be shifted over a considerable range by removing or adding fixed filter capacitors. Tentative specifications for these receivers were set forth in a memorandum.<sup>42</sup> These specifications were as follows: "The receivers will be tuned to a fixed frequency of about 31 kc with a band-pass 7.5 kc wide, 2 db down; 9 kc wide, 3 db down; 15 kc wide, down as far as possible. The voltage amplification is to be 150 db with an input im-

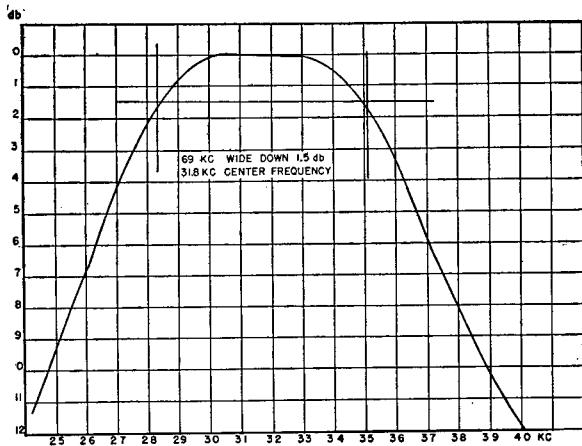


FIGURE 98. Band-pass transformer characteristics for submarine ER sonar receiver.

pedance of approximately 200 ohms and a maximum output pulse of 140 volts. The receiver must be capable of utilizing a maximum input voltage of 0.02 volt. Remote gain control should have a control of at least 70 db smoothly distributed over the rotation of the potentiometer. The receiver should have a true TVG action with gain at intervals after transmitting approximately as follows:

- 0.1 second—20 db below full gain
- 0.5 second—6 db below full gain
- 1.0 second—full gain

This TVG performance should be independent of the setting of the gain control to less than 4 db. Input pulses at the tuned frequency as short as 0.2 millisecond should be reproduced in the output pulse without appreciable transient distortion."

Receiver Model 1, Serial No. 3 differed from the other receivers in that the band-pass filters were hermetically sealed. A typical response curve for one of these units is shown in Figure 98. It is noted that coupling was such as to give a flat top on the band-pass characteristic, even though a dip in the center of not more than 0.5 db would have been tolerable. The existing circuit incorporated the use of variable ceramic capacitors across the primary and secondary of the filter units, which made it possible to change the center frequency over a small range. If a greater change was necessary, larger or smaller fixed capacitors had to be used. The inductance for these filters was a 100-mh universal wound coil of No. 38 wire on a  $\frac{3}{8}$ -inch by  $\frac{1}{2}$ -inch powdered iron slug. A rectifier

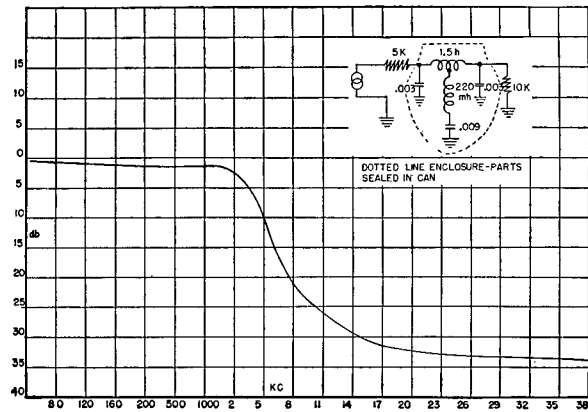


FIGURE 99. Output filter characteristics for submarine ER sonar receiver.

and low-pass filter (Z103 in Figure 97) to give a d-c pulse out of the r-f envelope was incorporated in the receiver. This filter did not present a constant impedance with a changing frequency, but had a cutoff frequency of 5 kc with an impedance of about 10,000 ohms. For characteristics of the filter see Figure 99.<sup>43</sup> By actual test the output filter was able to pass a pulse of 0.1-millisecond duration without causing transients greater than 26 db below the level of the peak of the pulse.

The TVG circuit in the receiver used one half a 6SN7 triode (V105B, Figure 97) as a rectifier of part of the transmitted pulse and to charge capacitor C120A to a negative potential. This negative potential was applied to the control grids of the second and third stages in the receiver and was allowed to decay through a 2.2-megohm resistor. It was found advisable in the field to connect a multipoint switch and a set of resistors in place of R134 so that there was a choice of the maximum TVG potential to be applied to these grids. Under some conditions, it was found that the reverberation was so small that it was desirable to have as little TVG as possible. The manual gain control was in the form of a variable cathode bias supplied to the cathodes of these same two stages.

The dynamic range of this receiver was measured by means of a standard signal generator, using a signal at 32 kc modulated 100 per cent by 1,000 cycles in one case and by 400 cycles in a second case. Figure 100 shows the dynamic ranges of the receiver for these two cases. The 0-db reference level was defined to be a 5-mv input from the signal generator with 1-volt output.

CONFIDENTIAL



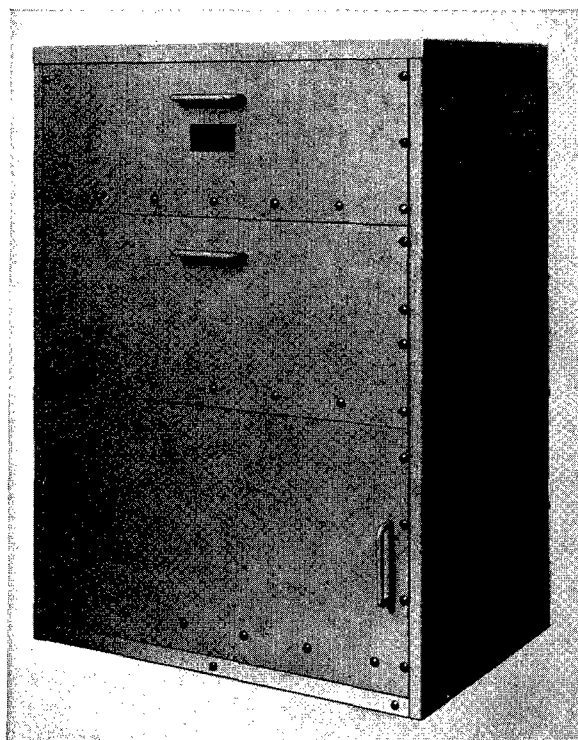


FIGURE 102. Front view of 200-cycle ER sonar transmitter cabinet.

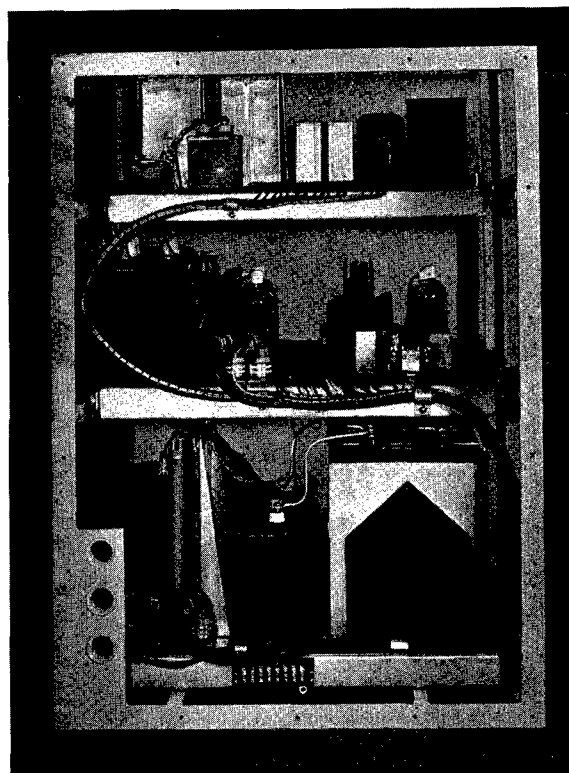


FIGURE 103. Rear interior view of 200-cycle ER sonar transmitter.

The high-voltage power supply consisted of three 2- $\mu$ f 7,500-volt capacitors, with a choke of 0.4 henry connected as a "bump-back" filter (see Chapter 5). A 4,200-volt a-c plate supply transformer operated through a Variac from the ship's supply with the necessary rectifier and rectifier filament transformer. A protective time-delay relay was placed in the primary of the transformer. Screen, bias, and low plate voltages were developed by a separate power supply giving both positive and negative voltages.

A separate keying chassis contained a trigger tube circuit, with pulse length controllable from 1 to 15 milliseconds and from 13 to 40 milliseconds operating into the grid of a normally over-biased triode. Radio-frequency signal was also fed to the same grid from an external oscillator. The output of the triode was developed across a 450-mh toroid coil connected as a transformer. Since it was the intention to use the keying chassis as a piece of laboratory equipment, a second amplifier, consisting of a 6V6 also operating into a 450-mh toroid transformer, was incorporated. A 2-volt signal from an oscillator fed into the device would produce a pulse output of over 100 volts in

the 20- to 60-kc range. This chassis had its own power supply (see Figure 101).

The power amplifier consisted of a 6V6 low-power driver operating into a 3922 Audio Development unit connected as a step-up transformer to drive the grid of an over-biased 715B, which in turn drove, through a step-down transformer, two 715B's in parallel. This output stage fed the transducer and its tuning network through a step-down transformer matching a 50-ohm output impedance. The interstage and output transformers were identical; their construction is described in Chapter 5. The power output of the transmitter unit into a noninductive load with approximately 5,500 volts on the plates of the power tubes was 15 kw for a 5-millisecond pulse at 22 kc.

This breadboard transmitter<sup>45</sup> was replaced by a permanent unit incorporating certain refinements, the desirability of which was indicated by experience gained during its use on the AIDE DE CAMP. A local oscillator was built in with reactance tube control of its frequency. The reactance tube and oscillator were operated from a voltage-regulated supply, affording sufficient stability to allow the transmitter frequency

CONFIDENTIAL

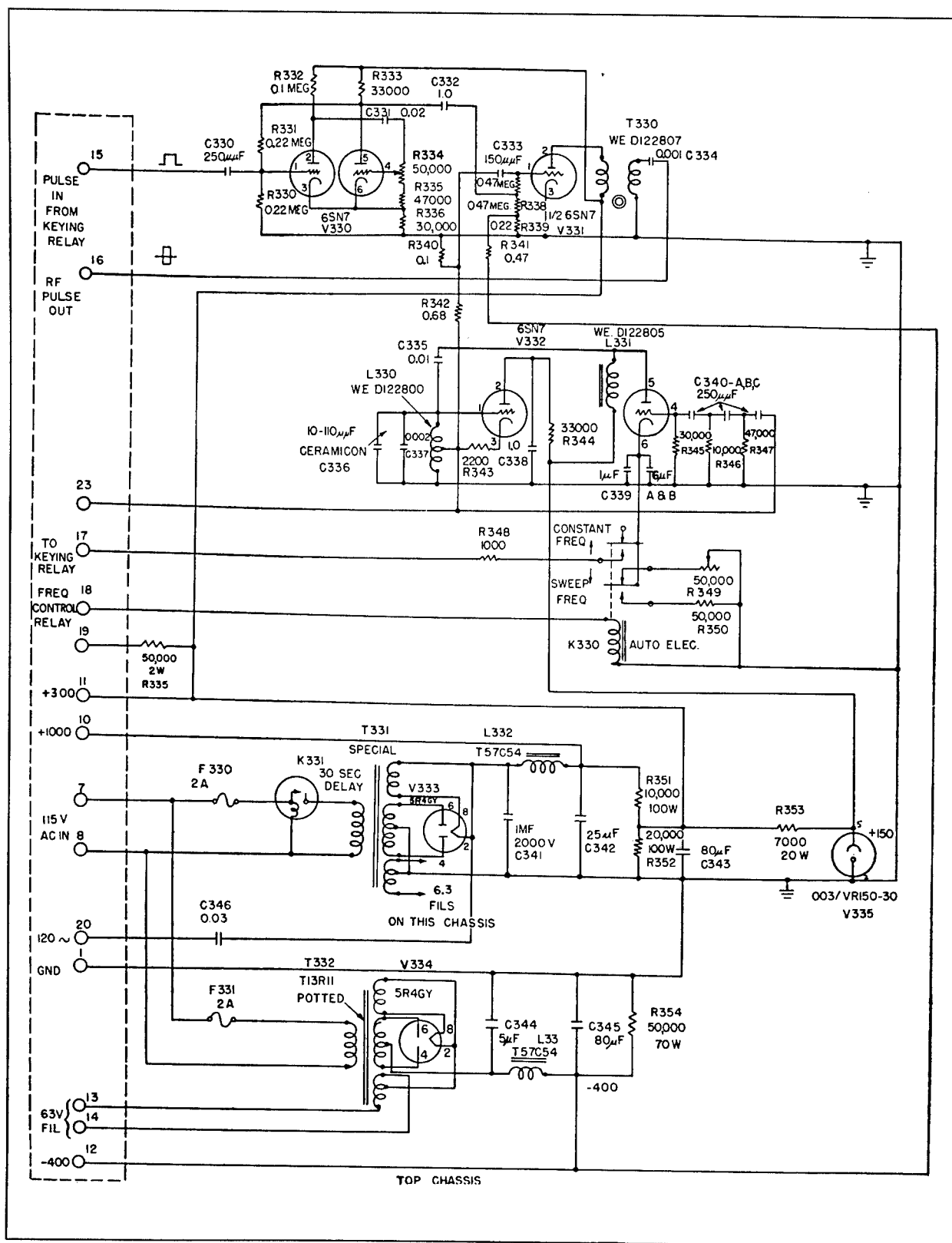


FIGURE 104. Circuit diagram of keying, oscillator power supply chassis for 200-cycle ER sonar transmitter.

CONFIDENTIAL

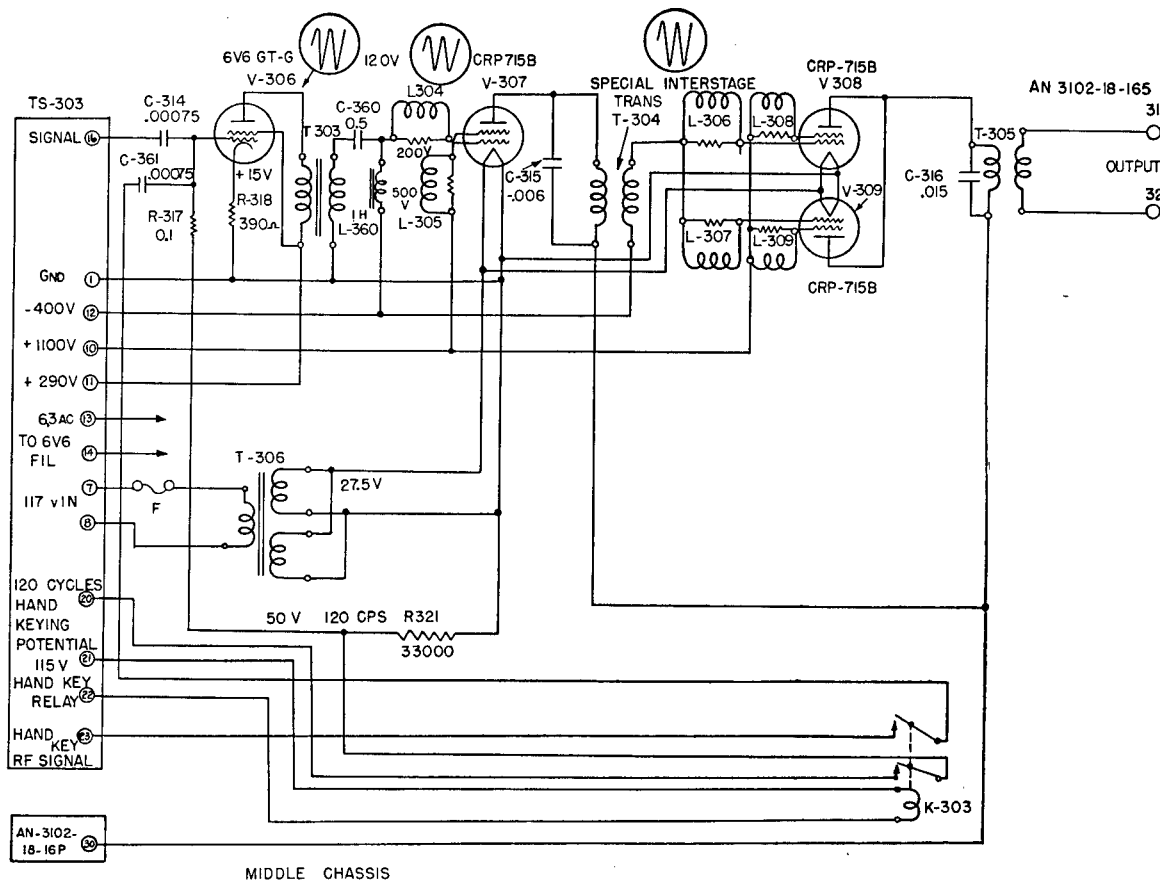


FIGURE 105. Circuit diagram of power amplifier for 200-cycle ER sonar transmitter.

to be determined by a potentiometer in the reactance tube circuit. A relay was arranged so that the transmitter could be remotely switched to either frequency sweep or c-w output. The frequency sweep was 2 kc, centered on 21.7 kc. Separate positive and negative low-voltage power supplies were used to avoid the complications of a bleeder circuit.

Figures 102 and 103 show the mechanical construction used. This transmitter produced 11.5 kw at 21.7 kc into a noninductive load when supplied with 105 volts a-c, 60 cycles. With 115 volts a-c line voltage, the power output was 16.2 kw average, with an average power consumption of 4.5 amperes from the a-c supply when transmitting one 5-millisecond ping per second.

Figures 104, 105, and 106 show the circuits used in this transmitter. The circuits for keying, oscillator, and power supply were contained in a separate chassis, the circuit diagram of which is given in Figure 104.

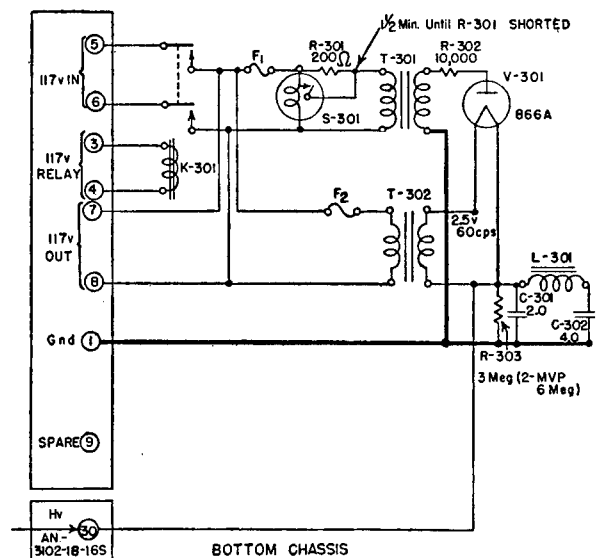


FIGURE 106. Circuit diagram of high-voltage power supply for 200-cycle sonar transmitter.

CONFIDENTIAL



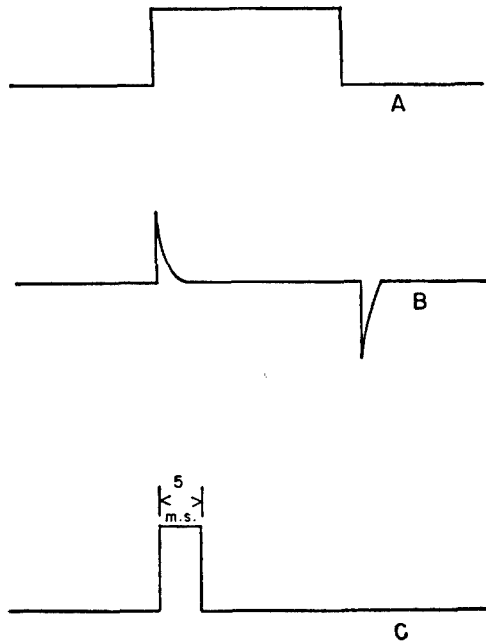


FIGURE 107. Pulse forms appearing in keying circuits of 200-cycle ER sonar transmitter.

Terminal 15 on this chassis was supplied with a positive pulse, formed by a pair of contacts on the transfer relay situated in the transducer matching and tuning circuits. This square pulse was differentiated by the capacitor C330 and the resistor R330 and applied to the first grid of the trigger-tube circuit V330. The output of this trigger-tube circuit was a square pulse of the required time length. (For pulse shapes, see Figures 107 (A), (B), and (C).) This square pulse from the trigger-tube circuit was then applied to the grid of V331 in such a way as to render this triode conductive. The grid of V331 is normally biased to the cutoff point by means of a bleeder from the negative power supply. The length of the square pulse, which was used to control the length of the ping, could be adjusted by means of the potentiometer R334 in the grid circuit of the second half of the trigger tube. The signal frequency voltage was developed by a Hartley oscillator circuit consisting of one half of V332. This signal frequency was applied to the grid of V331, which then acted as a gate to control the length of the transmitter pulse. The frequency of the oscillator could be controlled by the trimmer capacitor C336 and was in addition controlled by a reactance tube circuit consisting of the second half of V332. Thus, by varying the grid potential on the reactance tube, the frequency of the oscil-

lator could be changed at will. This was utilized in a frequency sweep during the transmitted pulse. The bias on the grid of the reactance tube V332B could be controlled by a choice of cathode resistors. Relay K330 could be thrown either to include the resistor R349 or the resistor R350 in the cathode circuit. R349 was a potentiometer which could be set by hand so that any desired frequency could be produced from the oscillator. When R350 was used, the initial frequency of the oscillator was raised about 1 kc above the average value. At the time the keying pulse was sent out, the cathode was grounded by the keying relay through a 1,000-ohm resistor, and the 7- $\mu$ f capacitors on the cathode circuit were allowed to discharge, thus producing a frequency sweep. This drop in cathode voltage was timed to coincide with the pulse length being produced by the operation of the trigger circuit, so that the frequency of the oscillator was swept approximately 2 kc during the pulse. This, in effect, caused the pulse frequency to sweep through 2 kc, centered at 21.7 kc.

Figure 105 is a schematic circuit diagram of the power amplifier for the 200-cycle ER sonar transmitter. The signal pulse, which was formed by V331 in the keying and oscillator chassis, appeared on terminal 16 and was amplified by the 6V6 power tube V306. This amplified pulse was applied to the grid of the 715B driver tube V307, via the coupling transformer and an isolation capacitor C360. This isolation capacitor was necessary to prevent voltage breakdown between the primary and the secondary of the coupling transformer. Parasitic suppressor chokes, consisting of chokes in parallel with resistors, were formed by winding the choke with No. 30 wire, utilizing the resistor as a winding form. These suppressors were connected to each of the grids of V307. The pulse was applied through a special interstage transformer to two 715B power output tubes, V308 and V309, connected in parallel. The grids of these power output tubes were likewise protected by parasitic suppressors of the type used on the driver stage. Driver and output tubes usually had sufficient negative over-bias to prevent plate current flow, even if the line voltage supply fell to 100 volts. A special transformer T305 was used in the plate of the power output tubes in order to match the plate impedance of these tubes to the input impedance of the transducer. The primary of this output transformer was tuned by C316. The interstage transformer T304, between the driver and the output stages, and the out-

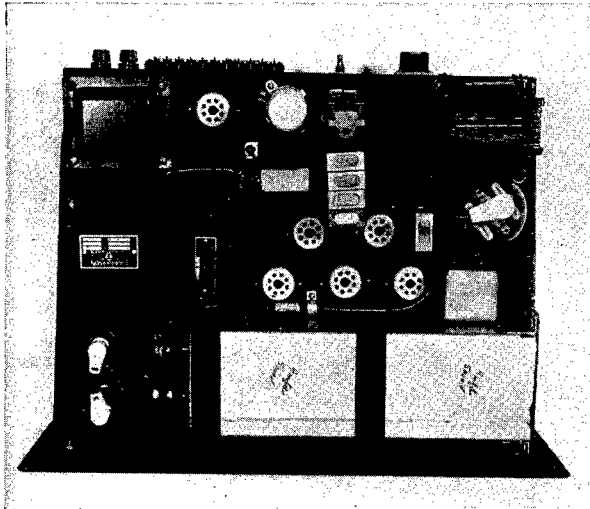


FIGURE 108. Top view of 53-kc ER sonar transmitter.

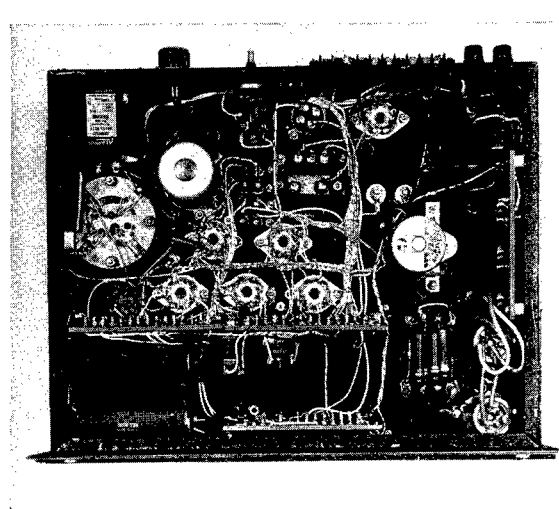


FIGURE 109. Bottom view of 53-kc ER sonar transmitter.

put transformer T305 were identical in construction and are described in Chapter 5. The size of capacitor necessary to tune these transformers to the same frequency was a function of the load impedance placed on the secondary, so that C315 and C316 were different in capacitance although tuned to the same frequency. A separate filament transformer T306 was used to supply the heater current to all of the driver and output tubes with their heaters connected in parallel.

### 7.7.3 Transmitter for 53-kc ER Sonar

For the 53-kc 500-cycle system the transmitter was modified considerably and was made smaller. Figures 108 and 109 show the mechanical construction of the transmitter and Figure 110 is the circuit diagram.

A detailed description of the operation of the circuits used is as follows:

V301 was a beam tetrode used to throw a relay K301 connected in the plate circuit. The tube was normally biased to cutoff, so that the positive blanking pulse from the CRO indicator applied to the grid would cause the relay to close momentarily. The length of time the relay remained closed was determined, to some extent, by the size of the input capacitor C301, and the bleeder network R301, R302, and R303, and by the pulse that initiated the relay operation.

When relay K301 closed, a positive pulse was applied to the grid of the trigger tube V302 which de-

termined the pulse length of the transmitter output. This positive square pulse from the trigger circuit was coupled to the grid of V303A which was normally biased to the cutoff point. The oscillator signal was fed to the same grid from the cathode of the oscillator tube V306A. Thus V303A was used to key the output of the oscillator, which was on continuously. The output of V303A was transformer-coupled to a 6V6 driver stage V304 and a step-up transformer T302 was placed in the plate circuit of V304. This applied the grid-drive potential to the single 715B output tube.

Frequency sweep of the transmitting pulse in the 53-kc system was obtained from reactance-tube control of the oscillator V306B. Between pings, the oscillator operated at a frequency higher than that of the center frequency of the system, and on the closing of K301, a positive potential was applied through R336 to the cathode circuit. The time constant of the combination of R336 and C311 determined the rate of frequency sweep. This time constant was adjusted so that the frequency sweep was approximately 4 kc, centered on 53 kc during the 2-millisecond pulse interval.

### 7.7.4 Transmitters for Submarine ER Sonar

The transmitters for the submarine ER sonar were developed directly from the 53-kc transmitter just described, with modifications made necessary by the

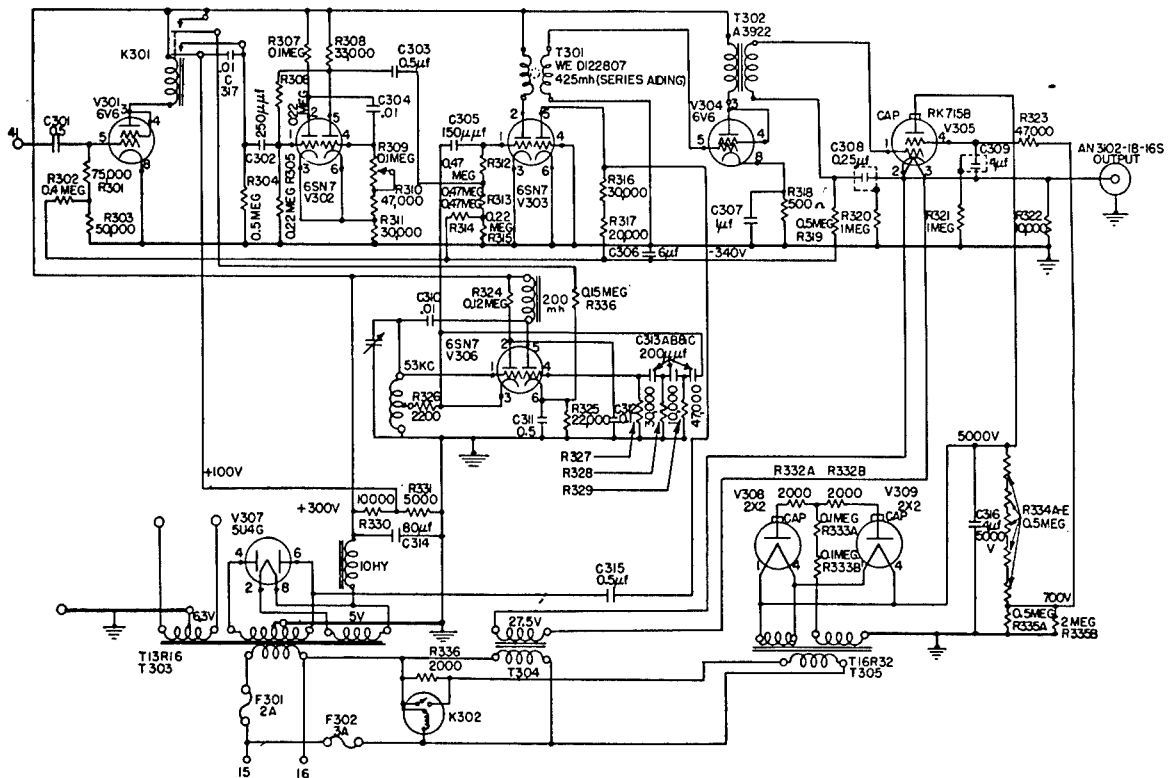


FIGURE 110. Circuit diagram of transmitter for 53-kc ER sonar.

mechanical and electrical requirements of the new system and those shown to be necessary as a result of experience with the 53-kc equipment in operation.

The Model 1 submarine transmitter unit was built on a standard Submarine Signal Company Type 755 receiver chassis and was designed to fit into the cabinet commonly used with this receiver. Two 715B tubes were used in parallel to feed the transducer load through an output transformer. The power supply storage capacitance was raised to 8  $\mu$ f at 5,000 volts to give increased power. Substantially the same trigger, keying, reactance tube, and amplifier circuits, heretofore described, were used. Figure 111 is a photograph of the Serial 1 unit.

Since continued failure of the plate supply transformers rendered this model transmitter unusable, a second model was developed and Model 1 was not used. A voltage doubling plate and filament transformer combination, originally used in radar applications, was readily available. The size of these units necessitated a complete rearrangement of parts and a removal of the low-voltage supplies. The circuits of Model 2 transmitter is described in detail with ref-

erence to its circuit diagram which is given in Figure 112.

V201, a beam tetrode, was supplied the CRO blanking pulse through terminal 21. The tube was nor-

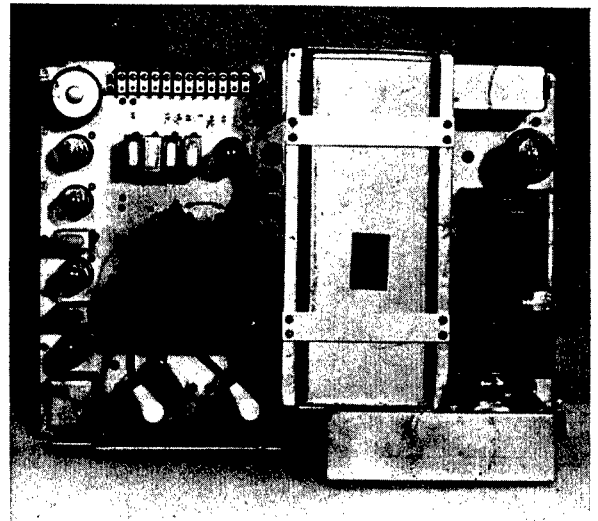
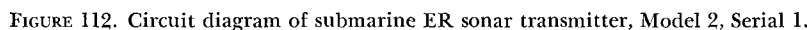


FIGURE 111. Top view of submarine ER sonar transmitter, Model 1, Serial 1.

CONFIDENTIAL



The output of the oscillator was amplified by V203

Figures 113 and 114 are photographs of the Model 2 transmitter. T205 was a 2,500-volt a-c 300-wa transformer, which together with C213, V208, and V209 constituted the voltage doubling circuit. T206, a dual filament transformer, was necessary because of the requirement for separate filament supplies insulated to the full supply voltage above ground in a voltage doubling system. C213 was made sufficiently small to introduce a high impedance into the power supply circuit, limiting the maximum current drain to a

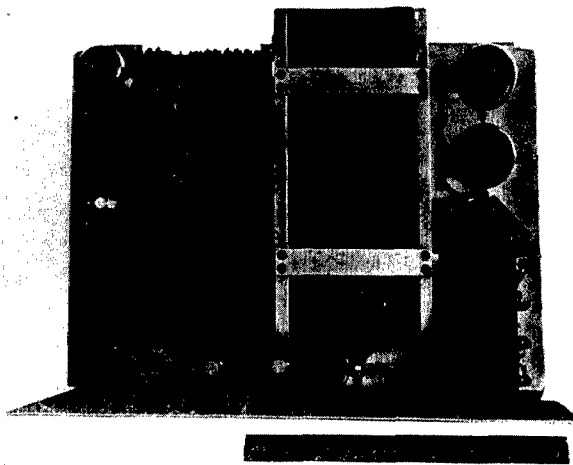


FIGURE 113. Top view of submarine ER sonar transmitter, Model 2.



FIGURE 114. Bottom view of submarine ER sonar transmitter, Model 2.

value compatible with the power output required and the time between pings. Type 3B24 rectifier tubes were used. These were capable of carrying a great deal more current continuously than were the 2X2's previously used in Model 1, so that no protective resistance in series with the tubes was necessary.

No reactance-tube control of frequency was employed in the Model 2 transmitter, since it had been decided that the improvement gained from the frequency sweep did not warrant the additional circuits involved. This design proved completely satisfactory as no difficulty was experienced with the transformers. The power output on the 3,000-yard range was 7 kw average into a noninductive load.

#### 7.7.5

### Pulse Lines

In the fall of 1944, research was begun on a pulse line, similar to those used in radar transmitters, which might be used as an energy-storage system to form a high-voltage d-c pulse to drive a power-oscillator tube.<sup>46</sup> It was hoped that line could be designed to give a better shaped pulse than could be obtained with the present storage capacitor in the transmitter and that the line would occupy less space than the storage capacitor. Theory on such lines is given in Chapter 9. Up to the present time a number of different pulse lines have been designed and tried out, both with and without pulse transformers, but the results so far have been unsatisfactory. It has been possible to produce pulses with a peak power output of 20 kw, but the pulse shape was only slightly better

than that produced by the single storage capacitor system, and the space and weight have been at least as great as that used by the single capacitor.

The pulse lines are in general low-pass type filter networks in which the capacitors may be charged relatively slowly by a high-voltage rectifier source.<sup>47</sup> The line is then discharged through a load by means of a spark gap or a thyratron tube. The pulse amplitude is equal to one half the voltage to which the line is charged, and the pulse width is determined by the electrical length of the line.

Figure 115 shows the type of line tried at first, with the resultant pulse shape. The ripple across the top of the pulse formed by this line was an objectionable feature, as was the steepness of the sides of the pulse at the base line. The ripple from this type of line was greatly reduced by making the cutoff frequency of

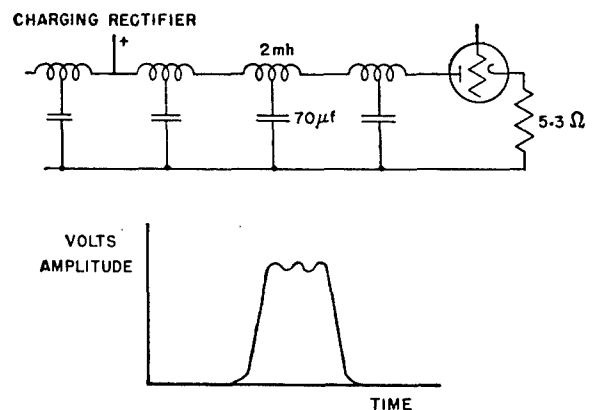


FIGURE 115. Circuit diagram of T-section pulse line.

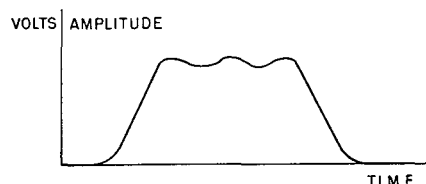
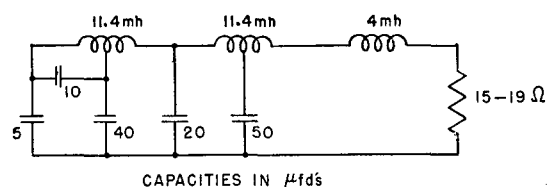


FIGURE 116. Circuit diagram of modified T-section pulse line.

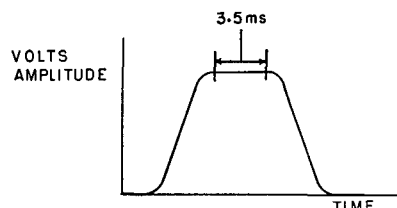
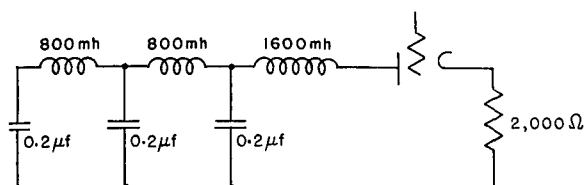


FIGURE 117. Circuit diagram of constant-K pulse line.

the line less than  $n/\tau$ , where  $n$  is the number of sections in the line, and  $\tau$  is the time duration of the pulse. The shape of the pulse at the base line was not greatly improved by any of the methods tried.

Early in 1945, two different types of pulse line were set up with promising results; one of these was a modification of the T-section network and the other was a constant-K network. Figure 116 shows the modified T-section type with its resultant pulse shape. The extra capacitor was added experimentally to help flatten the top of the pulse. The pulse obtained with this line represented a peak power output of 40 kw at an impedance of about 20 ohms. It would be difficult to wind the inductances to give a higher impedance than 20 ohms without resorting to iron cores, with the consequent danger of saturation effects.

A constant-K network was designed with hypersil iron-core inductances and was found to give good pulse shapes.<sup>48,49</sup> Figure 117 shows the line used with the pulse shape obtained.<sup>50</sup>

## 7.8 SWEEP GENERATOR AND RANGE MARKING

### 7.8.1 Spiral Sweep Requirements

The electronic rotation scanning sonar required for its PPI display, a spiral sweep that is synchronized in its start with the emitted ping and with the range-determining device and is, in addition, synchronized in bearing with the rotating beam pattern.

The spiral sweep was usually formed by amplitude-

modulating a circular sweep with an expanding or radial sweep. The circular sweep may be generated by either mechanical or electronic means. The mechanical generator could be a 2- or 3-phase rotating machine. However, since the ER commutation is done electrically, the sweep generation is best done electrically. The customary electronic sweep generator consisted of a single-phase oscillator operating at the rotation frequency, followed by a modulator and a phase-splitting network. Two quadrature signals from the phase-splitting network were amplified by power amplifiers and used to drive 2-phase deflection coils on the magnetic deflection cathode-ray tube. The expanding sweep usually fed to the modulator was the voltage across a capacitor, which was being charged through a resistor from a source whose voltage might or might not be compensated to make the expanding sweep linear.<sup>51,52</sup> If a simple non-linear charging circuit is used, the linearization may be carried out in the modulator. If the sweep is linear, then a linear modulating circuit must be used. The expanding sweep is reset by means of a shorting element that discharges the capacitor.

### 7.8.2

### Sequence Control

In any system a certain sequence of operations must be performed. The face of the cathode-ray tube must be blanked at the end of the PPI display and must remain blanked until all of the pinging functions are completed. At the same time as, or immediately after, the face of the cathode-ray tube is

blanked, the expanding sweep must be reset and the rotation pulse to the rotor must be blanked, if the rotor is such that it requires this protection. If the system has an audio or BDI channel, this should be blanked at the same time. When these steps have been completed, the transmitter must be keyed while a timing circuit makes the length of this ping equal to the time for one revolution of the scanning sensitivity beam. After the end of the ping, the various blanking and protecting circuits must be returned to their receive condition, and the cathode-ray tube must again be made sensitive to brightening by any returning sound. The dead time, during which the face of the cathode-ray tube is blanked, should be held to a minimum because the time lost between the blanking of the face of the cathode-ray tube and the emission of the ping reduces the rapidity with which information is obtained. The time interval between ping and the rebrightening of the face of the cathode-ray tube determines the minimum range from which echoes may be seen.

## 7.8.3

**Range Determination**

The ER scanning system is adaptable to range determination by several methods such as (1) marks engraved upon the protective cover of the cathode-ray tube, (2) brightening marks placed electronically at fixed ranges, or (3) a brightened mark adjustable to any desired range that may be indicated on a separate indicator. The first two systems give an approximate range only and depend for accuracy on the linearity of the sweep. The third method is the most accurate and may be varied by using a separate scope for range measurement.

The ways in which these various timing functions have been carried out is described in connection with the various ER scanning systems. The operation of each circuit modification is described with the system in which the modification was introduced. The operation of the submarine system is described in greatest detail as representative of the best methods at present.

## 7.8.4

**Sweep and Timing Circuits for 60-cycle ER Sonar**

The 60-cycle switching frequency ER sonar, installed in the AIDE DE CAMP in October 1943, used the QH Model 1 indicator (12-inch cathode-ray

tube), keying chassis, and 15-kw transmitter. The sweep for the cathode-ray tube was generated by a synchro connected directly to one end of a bench grinder motor. Another synchro connected to the other end of the motor supplied the switching voltages to the rotor. The sweep, timing, and send-receive circuits are discussed in Chapter 5.

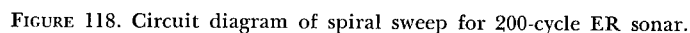
## 7.8.5

**Sweep and Timing Circuits for 200-cycle ER Sonar**

The sweep circuits for this system differed from those used in the CR system, since the 200-cycle switching and rotation frequency was too high to be obtained by means of a mechanical generator such as used with the 60-cycle system. In this, and succeeding systems, a vacuum-tube oscillator was used to generate both the switching and the sweep voltages. The sweep signal was split into two phases 90 degrees apart, amplified by a pair of power tubes, then applied to 2-phase deflection coils in order to produce a circular sweep whose radius was controlled by an amplitude-modulating circuit.

The circuits used in this first installation are shown in Figure 118. The 6V6 driver had a tuned plate circuit which by-passed the low frequency and d-c components of the signal and passed on only the 200-cycle component to the phase-splitting network through the coupling transformer. The coupling transformer was subsequently replaced by a coupling capacitor. The output of one phase of the phase-splitting network was the unshifted signal, attenuated to the same level as the signal for the quadrature phase. The quadrature phase was formed from the unshifted phase by shifting it approximately 90 degrees by means of an RC circuit. The outputs of the phase-splitter went to the grids of the pair of 6V6 cathode followers. The deflection coils were directly connected to the cathodes of the 6V6 followers. Subsequently, transformer coupling was used, as shown in the circuit diagram in Figure 119.

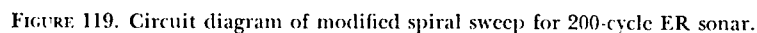
Originally, the timer was merely a multipoint switch with the stop removed so that it could be rotated continuously. The rotating contact of the timer was attached to one side of the sweep capacitor and the fixed contacts were attached through the range selection switch to the other side. Thus, when the timer closed a contact connected through the range switch to the sweep capacitor, the sweep capacitor



There was no method of range determination incorporated into this 200-cycle system.

After the 200-cycle system had been in use for a few months, a 53-kc system with a 500-cycle switching frequency was built (see circuit diagram in Figure 120). The range start and range limit circuits were the same as those which had been used previously. The timer was a 6.3-volt mechanical contactor driven by a synchronous motor which was built especially for HUSL by the Sangamo Electric Company. The contacts closed every 1,500, 3,750, or 7,500 yards (assuming the sound velocity in the water to be 4,800 yards per second) and remained closed for 1 milli-





The changes in the 53-kc system from the 200-cycle system were in the modulator which generated the expanding 2-phase 500-cycle sweep, in the blanking circuit, and in the sweep power output circuit which drove the deflection coils. The only item added was a phase-shifting network in the 500-cycle input to the sweep expander, so that adjustment of the relative

The modulator made use of the twin triodes in a

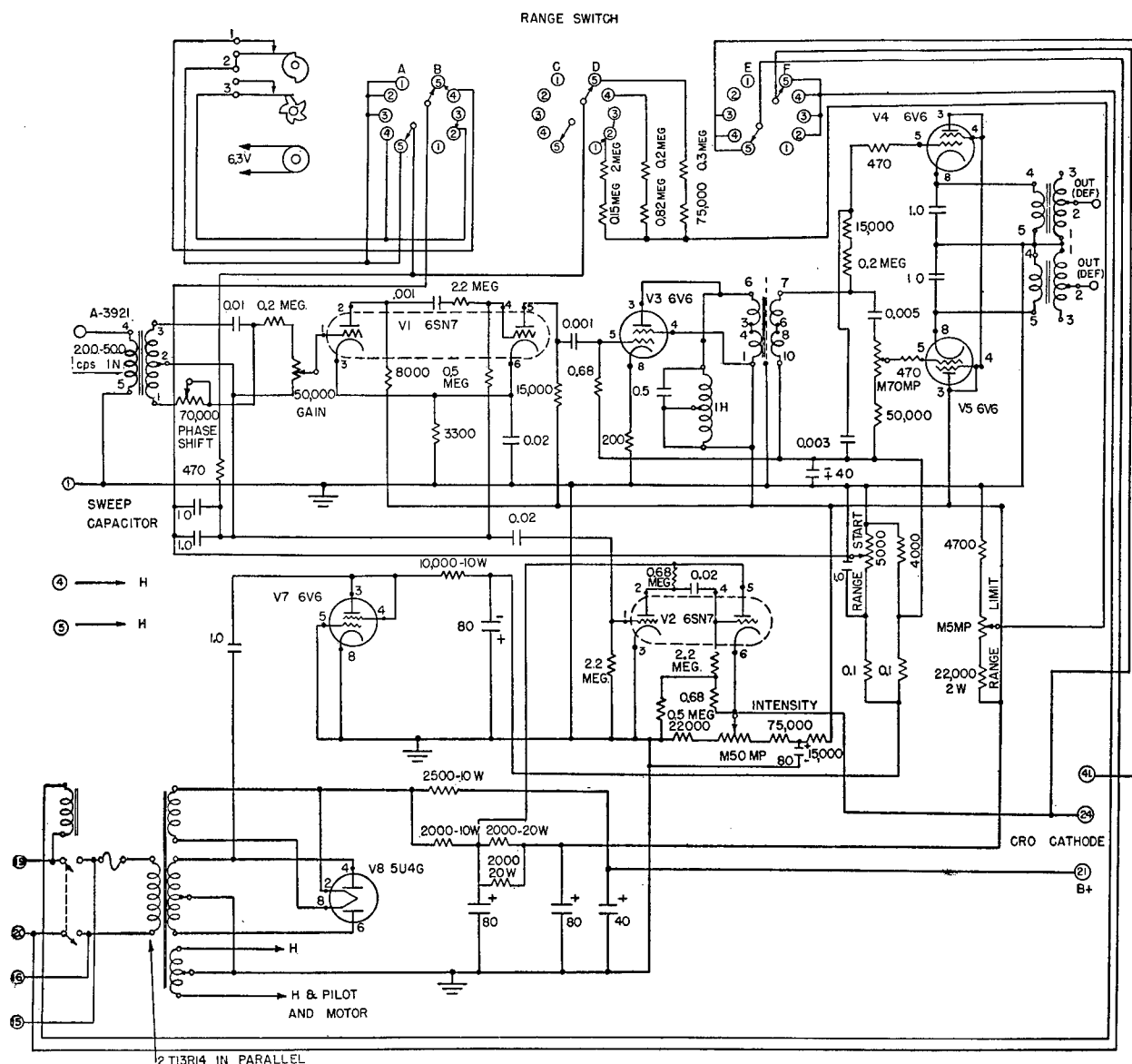


FIGURE 120. Circuit diagram of spiral sweep for 53-kc ER sonar.

6SN7.<sup>58,54,55</sup> When the bias on these triodes was increased beyond the normal value, the gain fell off considerably. A linear expansion range of 15 to 1 is possible in each triode. The grid returns for both triodes were made to the expanding d-c voltage. The 500-cycle a-c signal, which was to have its amplitude changed, was applied directly to the grid of the first triode. A fixed attenuator was incorporated in the coupling network between the first and second triodes, so that the level of the signal at the grid of the second triode would be reduced to approximately the

same value as the level of the signal at the grid of the first triode. This prevented excessive harmonic distortion without introducing excessive hum. By very careful choice of all the components, particularly the plate load resistors, the degree of expansion was made directly proportional to the bias.

The phase-splitting network in this model consisted of two RC sections, one phase lead, and the other phase lag. There was a phase shift in each of these channels of approximately 45 degrees at the switching frequency of 500 cycles.

CONFIDENTIAL

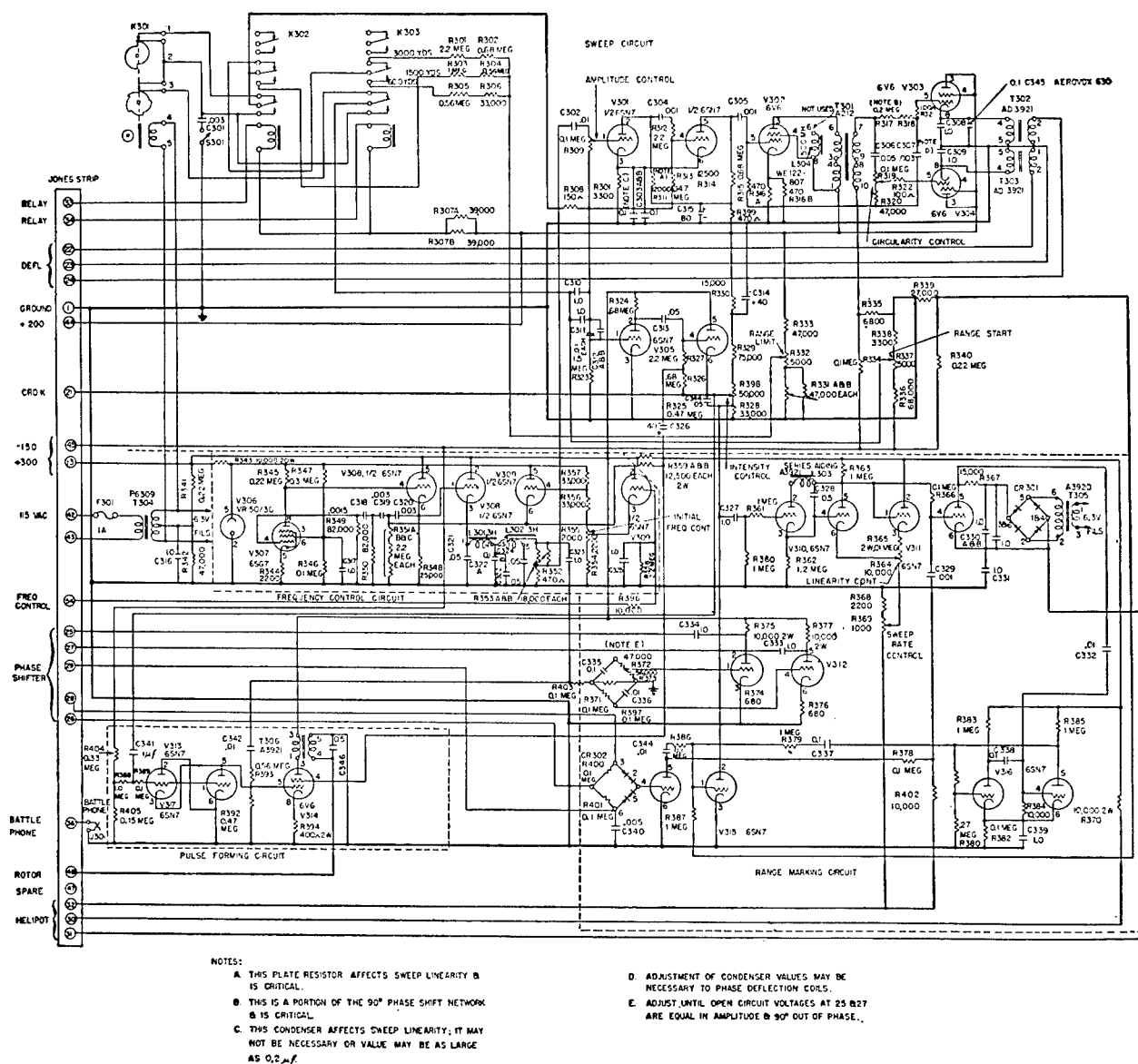


FIGURE 121. Circuit diagram of sweep, range, and oscillator chassis, submarine ER sonar, Model 1.

The blanking pulse was sharpened without resorting to a multivibrator by increasing the voltage across the sweep capacitor. This voltage could be increased without increasing the change of gain excessively, because, at the same time, resistance was added to the cathode return of the expander tubes. The larger pulse then formed upon discharge of the sweep capacitor cut off the first of the blanking triodes, and thus produced a flat-topped blanking pulse. The second triode of the blanking circuit was biased beyond cutoff, so that the tail of the capacitor discharge was also clipped off. The bleeder from the

cathode biasing arrangement increased the apparent input impedance, as well as the height of the blanking pulse. The timing of the ping, by means of the blanking pulse, and the control of the ping length is fully discussed in the foregoing section on transmitters.

### 7.8.7 Sweep, Timing, and Range-Marking Circuits for Submarine ER Sonar

The submarine system<sup>1-42</sup> was built in four separate boxes. One was the indicator box containing

CONFIDENTIAL

the PPI display and all of the controls, a front view of which is shown in Figure 88. The other three boxes contained (1) the transmitter chassis, (2) receiver chassis, and (3) the chassis upon which were mounted the sweep circuit, range-marking circuit, oscillator circuit, timer, and pulse-generating circuit for switching the varistor rotor. The last named was known as the SRO chassis and its circuit diagram is shown in Figure 121. Photographs of the top and bottom of the chassis are shown in Figures 122 and 123 respectively. Two models were built, and are described separately.

In the first, the sweep circuit and the blanking and pulse-generating circuits used were almost identical with those used in the 53-kc system. The oscillator was built from a description in the literature<sup>56</sup> and was found to be satisfactory. The timing portion of the range-marking circuits was developed especially for this system.<sup>52, 57, 58</sup> (The phantastron<sup>52</sup> circuit was originally tried, but was not satisfactory with an unregulated power supply.)

The sweep circuit supplied the two-phase 300-cycle switching voltage of increasing amplitude to the deflection coils of the indicator box. This voltage started at a negligible amplitude at the time that sound was put into the water. It increased to a sufficient value to give deflection to the edge of the tube by the end of the time required for the sound to travel to and return from the range to which the selector switch upon the indicator box was set.

The range selector switch (1) shown in Figure 88 had three positions allowing ranges out to three different maxima (that is, 3,000, 1,500, and 600 yards) to be indicated on the face of the cathode-ray tube before the new sweep was started. To effect a change in range, this switch controlled a pair of relays in the SRO chassis.

In order that the range could be determined accurately, a range-marking circuit was incorporated into the system. This circuit put a bright ring on the face of the cathode-ray tube at the same place that an echo would appear, returning from the range indicated on the drum dial at the left (7) in Figure 88. This bright ring was blanked under the cursor so that it would not interfere with any echo which might be returning from the direction indicated by the cursor. The hand wheel in the lower left corner of the panel (8) (Figure 88) turned this dial and the potentiometer (30) (Figure 90) attached thereto, delivering a voltage to the range marking circuit in the SRO chassis that was proportional to the range indicated on the

dial. The range-marking circuit then decreased the voltage at the cathode of the cathode-ray tube at the proper time to put the range mark on the face of the tube, and restored the normal voltage while the sweep was passing under the cursor.

This restoration of voltage, which produced the blanking of the range mark in bearing, was timed in accordance with the phase of the output from the rotor of the phase shifter (31) (Figure 90) in the indicator box. The rotor of this phase shifter was geared to and turned with the bug ring, so that the phase of the output corresponded to the position of the bug ring. The stator of the phase shifter was excited by a 2-phase voltage of constant amplitude at the rotation frequency coming from the SRO chassis.

The oscillator supplied voltage with a frequency of approximately 300 cycles for the sweep and range circuits, as well as for switching the varistors in the rotor. The exact frequency of this oscillator was determined by a discriminator in the rotor so that continuous scanning would be given by the rotor.

The pulse generator in Model 1, Serial 1, was merely a power amplifier for the sine wave used in switching.

The cathode potential of the cathode-ray tube was raised, during the return of the spot to the center of the tube, by means of the blanking circuit in the SRO chassis, thus blanking the return trace; that is, preventing the face from brightening.

The following pages describe the SRO circuit operation in detail. The sweep consisted of a voltage amplifier followed by a phase-splitting network and a power amplifier. The gain-controlled portion consisted of two half 6SN7 triodes V301 which were biased nearly to cutoff, with greatest bias at the start of the sweep, and least bias at the end of the sweep. With the resistors and voltages used in this circuit, the amplification of these triodes was proportional to the decrease in bias. The amplification-bias characteristic had a slight curvature which compensated for the curvature of the capacitor's voltage-time characteristic. The bias was obtained from the negative supply through the range start potentiometer, R337, which determined the bias at the start of the sweep, and was decreased by current from the 200-volt positive supply through the range limit potentiometer R332 and the charging resistors R301 through R306. The capacitors C310 and C311 were discharged to return the sweep to the center of the face of the cathode-ray tube by the mechanical timer.

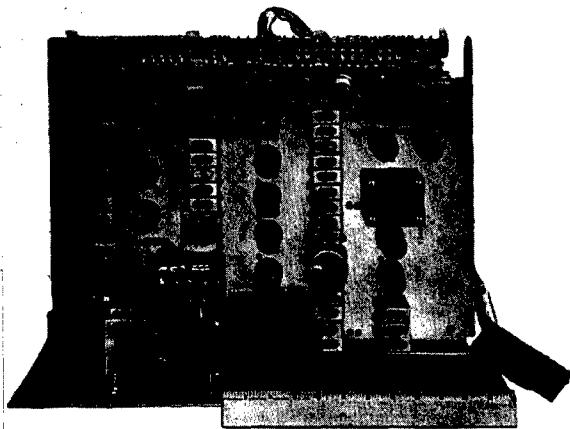


FIGURE 122. Top view of sweep, range, and oscillator chassis for submarine ER sonar, Model 1.

This timer was composed of two contactors actuated by cams driven by a synchronous motor. The capacitors were then charged through that pair of

the charging resistors which were connected by the relays for the maximum range in use. The relay coils were energized from the positive supply through the range selection switch on the indicator box. When the range switch was in the 3,000-yard position, neither relay was energized. The current flow through the large resistors R301 and R302 hence was small and the capacitor charged slowly. For the 1,500-yard range one relay was energized, and for the 600-yard range the other relay was energized, thus inserting either R303 and R304 or R305 and R306 into the circuit and permitting the capacitor to charge to the same voltage in shorter lengths of time. The contacts on the motorized contactor K301 were also switched by the relays, so that on the 600-yard range the contactor shorted and hence discharged C310 every 750 milliseconds; on the 1,500-yard range, every 1.87 seconds; and on the 3,000-yard range, every 3.75 seconds. The contacts stayed closed for only a few milliseconds, and the sweep recommenced from the center as soon as they opened.

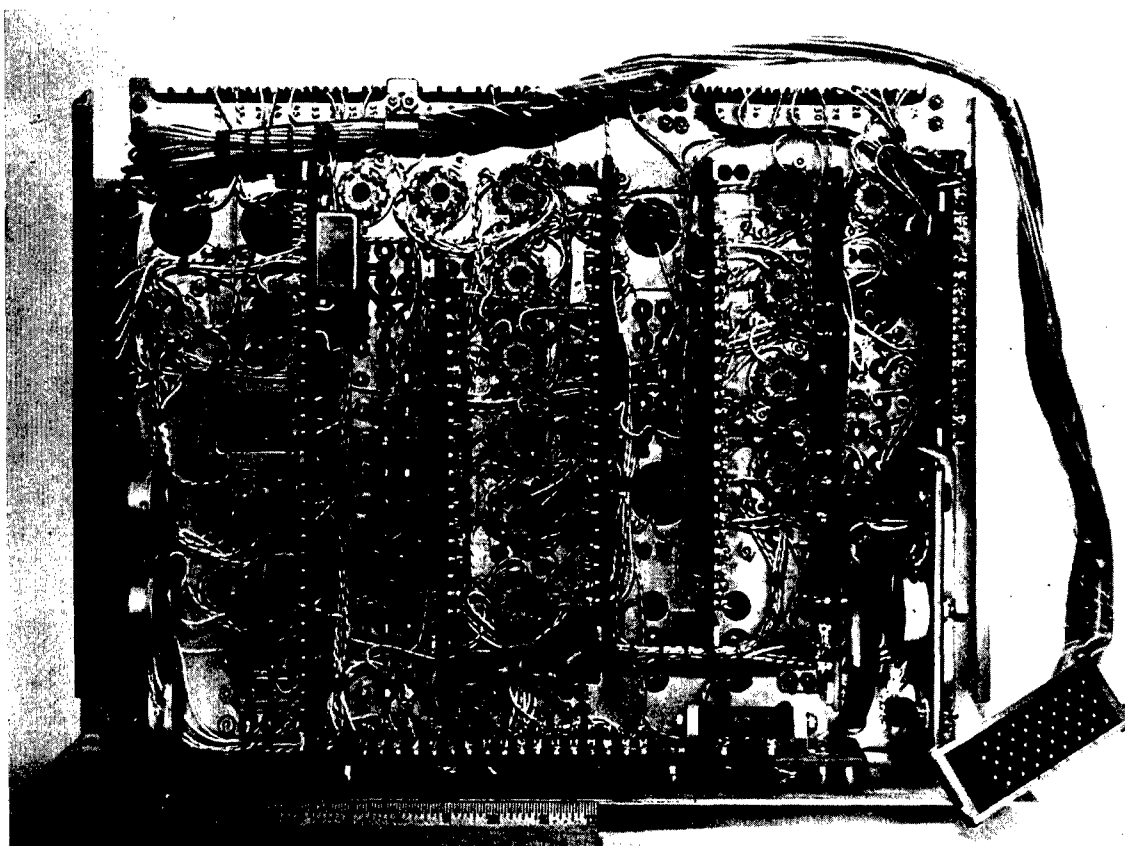


FIGURE 123. Bottom view of sweep, range, and oscillator chassis for submarine ER sonar.

CONFIDENTIAL

The alternating voltage, which was amplified by this variable gain amplifier, came from the bleeder R353 and R352 at the output of the oscillator section. Its amplitude was controlled by the potentiometer R309 in the grid circuit of V301A. Since only the variation in gain of these triode sections was needed, and not the gain itself, the excessive signal amplitude at the plate of the first triode was attenuated through the bleeder R312 and R313. The output of this gain control section was resistance-coupled to the first 6V6 in the power amplifier stage by C305 and R315 which had a small time constant so that the d-c control voltage was kept out of the power amplifier. This 6V6 was transformer-coupled by T301 to the bridge-type phase-splitting network. The portion of the bridge formed by R317, R318, and C307 delayed the switching frequency by a small amount so that it was given a slight phase lag. The portion of the divider formed by C306, R319, and R320 shifted the phase of the switching frequency in the opposite direction to introduce enough phase lead so that the difference in phase between the grids of the two 6V6's, V303 and V304, was 90 degrees. This phase-shifting network gave 90 degrees phase shift over an extended range of frequencies. However, the amplitude of the phase lag section decreased as the switching frequency increased, and the amplitude of the phase lead section increased as the frequency increased, so that the potentiometer R319 was incorporated to make the amplitudes of the quadrature voltages at the grids of the 6V6's equal. This control was called a circularity control, since the spiral on the face of the cathode-ray tube would be egg-shaped if the control were in the wrong position. V303 and V304 were cathode followers transformer-coupled by T302 and T303 to the deflection coils in the indicator box.

At the time capacitor C310 was discharged by the contactor and the sweep returned to the center, there were electrical disturbances and acoustical disturbances if the system was transmitting. This placed extraneous and erratic marks upon the face of the cathode-ray tube. To prevent this, the pulse generated by the contactor discharging C310 was differentiated by the circuit C312 and R323, amplified by V305A, and applied to the cathode of the cathode-ray tube in the indicator box by means of the cathode follower V305B. V305B was normally biased beyond cutoff and had no effect upon the rest of the circuit, except during the blanking time. The normal potential at

the cathode of the cathode-ray tube was determined by the potentiometer R398 in the bleeder from the positive supply. This potentiometer, by controlling this potential, controlled the background intensity of the cathode-ray tube.

When the keying switch (9), shown in Figure 88, was in the automatic position, plate voltage was applied to a keying tube in the transmitter, and a pulse of sound was put into the water by the projector each time the sweep returned to the center. With the keying switch in the single position, a pulse of sound was put into the water the first time that the sweep returned to the center of the scope. No further sound was emitted no matter how long the key was held down, because the plate circuit of the keying tube was supplied by the charge upon capacitor C405 for the first pulse and the capacitor was thereafter discharged so that no plate voltage was applied. The capacitor was recharged when the switch was allowed to return to its normal position.

To echo-range, the key was put into either the automatic or single position. In the automatic position a short pulse of sound was put into the water at the start of each sweep. Any echoes appeared on the face of the cathode-ray tube as bright arcs with bearings corresponding to the bearings of the echo sources and at distances from the center roughly corresponding to the ranges of the echo sources. To determine the range accurately, the range hand wheel was turned until the range-marking circle and the brightening from the echo source coincided and formed a complete ring. The range of the echo source could then be read on the range dial. The mark was independent of the range switch setting, so that if the range dial were set to a greater range than the maximum being displayed, the circuit produced no bright ring. It was unnecessary to read the dial more closely than 10 yards because ranges determined by echoes were always in doubt by that amount, and that was the precision required.<sup>59, 60</sup>

The range mark could be removed from the visible portion of the sweep by turning the range hand wheel (8) to the left until the range scale (7) (see Figure 88) read 0, or by turning the hand wheel to the right until the scale read 3,000 yards.

The range-marking circuit consisted of six triodes and two twin triodes performing separate functions. The first triode was a reset tube, the second a sweep tube, the third a linearizing tube, the fourth a trigger tube, the fifth and sixth generated the range mark

CONFIDENTIAL

pulse, the seventh and eighth served as a power amplifier to supply the phase shifter in the indicator box, the ninth formed the bearing blanking pulse, and the tenth injected the range mark into the rest of the circuit.

V310 was the reset tube. The blanking pulse made its grid positive through C327 and R361, thereby causing it to conduct, whereas it had normally been biased beyond cutoff. When this reset tube conducted, it discharged the sweep capacitor C328 through the inductor L303. The inductor and the capacitor had more influence upon the current during the discharge of the capacitor than did the internal resistance of the reset tube, so that the capacitor was completely discharged within the 50-millisecond interval that the cathode-ray tube was blanked.

The sweep capacitor C328 was then recharged slowly through R363 and R362. The charging current flowing through R362 raised the potential of the grid (pin No. 4, V310B) to about 24 volts above ground. If the grid became more positive, the sweep tube V310B would pass more current, thus increasing the voltage drop across R363, and decreasing the potential on the grid of the sweep tube by virtue of the fact that the voltage across C328 cannot change instantaneously. If the grid of the sweep tube became less positive than 24 volts, the reversed effect would take place. Hence, the grid potential must remain 24 volts. Since the voltage across R362 was constant, the current through it was constant. Consequently, the charge on the capacitor and the voltage across the capacitor increased linearly with time.<sup>58</sup>

The linearizing tube V311A was a cathode follower whose cathode potential follows the potential of the plate of the sweep tube. This tube with the bleeder R365 and R364 increased the potential of the cathode of the sweep tube as the potential of the plate of the sweep tube increased, thus compensating for the limited gain of the sweep tube. When the potentiometer R364 (linearity) was adjusted so that the voltage division across this bleeder was equal to the voltage amplification of the sweep tube, these two tubes formed a circuit having very high gain. This maintained the voltage at the grid of the sweep tube constant, regardless of what the potential at the plate of the sweep tube might be. The potentiometer R369 (range rate) was in a bleeder from the positive supply and the position of its slider determined the potential to which the sweep and linearizing tubes held the

grid of the sweep tube. Thus, by varying this potentiometer, the rate at which the capacitor C328 was charged was varied, and hence the sweep rate was changed. A system of calibration using the timer as a time divider was worked out for use in setting the sweep rate potentiometer, the linearity potentiometer, and the range zero, and is described briefly at the end of this chapter.

The bleeder containing R369 also included the helipot in the indicator box. The cathode of the trip tube V311B was connected to the slider of the helipot. The plate voltage of this tube was supplied by the transformer T305, the varistor rectifier CR301, and the filter capacitor C330. At the start of the sweep the potential of the more positive side of the sweep capacitor C328, and hence of the grid of the trip tube, was low, so that the trip tube did not conduct. When the voltage across the sweep capacitor rose to about one volt less than the voltage at the slider of the helipot, which was also the voltage of the cathode of the trip tube, the trip tube conducted. The pulses, which were always on the grid of the trip tube, were amplified and appeared at the plate. These pulses came from the bearing blanking pulse generator V315A and were differentiated through the network formed by C329 and R366 so that a sharp pulse was provided for triggering the range-marking pulse generator. The plate of the trip tube was capacitively coupled to the grid of V316B.

V316 was a conventional pulse-generating circuit, except that, once it had been tripped, a long time was required for the circuit to recover and become sensitive to a new tripping pulse. This prevented successive spurious range marks on the face of the cathode-ray tube. The plate of V316B was normally at a small positive potential with respect to the cathode, because the tube normally had no bias. When a negative pulse was received from the trip tube, the plate of V316B became positive, so that V316A, which was formerly biased beyond cutoff, now conducted, driving the grid of V316B negative beyond cutoff and holding it there for about 3 milliseconds. The positive pulse formed at the plate of V316B was capacitively coupled to the grid of V315B, which was normally biased beyond cutoff. V315 now conducted, short-circuiting the cathode of the cathode-ray tube to ground, and thereby putting a bright mark on the face of the cathode-ray tube.

The bearing blanking of the range mark was positioned by means of a pulse derived from the output

of the phase shifter in the indicator box, which was powered by the two-phase power amplifier V312. The output of the oscillator was attenuated by R403 and split into two phases by the bridge network C335, R372, R373, R371, and C336, in the same fashion in which the phases were split in the sweep power amplifier. Each phase was amplified by one half of V312, so that sufficient power was given to energize the stator windings in the phase shifter in the indicator box. The rotor of the phase shifter in the indicator box was connected to the rectifier bridge formed by R400 and R401 and the varistor rectifier CR302. This full-wave rectifier was unbalanced by the capacitor C340, so that the output, which was always negative, instantaneously rose to zero volts only once during a cycle of the switching pulse. As the phase shifter was rotated, the phase of the voltage out of the rotor was lagged smoothly. Thus the instant of time at which the output from this unbalanced rectifier reached zero was delayed from the start of the switching pulse cycle by the fraction of a cycle equal to the rotation from its zero position of the bug dial on the indicator box. Thus, this time of zero bias always occurred when the spot that was sweeping over the face of the cathode-ray tube to form the sweep spiral was directly under the cursor. The grid of V315A was beyond cutoff by virtue of the negative output of this full-wave rectifier, except during the short interval of about 1/12 of a switching frequency cycle. During this cycle the output rose to zero, at which time the tube conducted and the plate became negative. This square pulse was capacitively coupled to the grid of V315B, where it cut off V315B at the proper time to blank the range mark under the cursor. It was also attenuated and differentiated to put a continuously repeating sharp pulse on the grid of the trip tube.

The oscillator consisted of a voltage amplifier tube V307, a regulator tube V306, a pair of cathode follower current amplifiers V308, and a resistance tube V309, with a phase-lead phase-shifting circuit and a low-pass output filter. The phase-shifting network formed by C320 and the resistance tube, C319 and R350, and C318 and R349, shifted the phase of the switching frequency through 180 degrees, and thereby attenuated it. V307 amplified the shifted signal to its former level and inverted the phase so that the signal was in phase with the input to the phase-shifting line. The frequency at which the phase shift was exactly 180 degrees was determined by the a-c resistance between the junction of C320 and C319 and

ground. This resistance was the internal or plate resistance of V309A which changed with the cathode potential of this tube. Thus, a very small change in the potential of the grid of V309B made a large change in the potential of the cathode of V309A, a large change in the a-c resistance between capacitors C320 and C319 and ground, and a large change in the frequency of the oscillator. The discriminator circuit in the rotor produced a positive or a negative voltage depending upon whether the switching pulse left the switching line before or after the next switching pulse started down the line. This discriminator circuit thus controlled the switching frequency by controlling the bias of V309B. The potentiometer R355 controlled the potential of the cathode of V309B, and was used to center the discriminator output to  $\pm 0.1$  volt at the proper frequency when the system was initially set up, or when it was necessary to change tube V309. The filter formed by L301, L302, and the three capacitors prevented the distorted portion of the oscillator wave from reaching the rest of the circuits.

The output of the oscillator was coupled to the grid of V314. This 6V6 was an ordinary power amplifier and was transformer-coupled to the terminal No. 48 from which the switching pulse was led to the rotor.<sup>61, 62</sup> To protect the varistors in the rotor during transmission this pulse was blanked; that is, it was not sent to the rotor during the time that the cathode-ray tube was blanked. This was accomplished by means of V313 which was biased beyond cutoff, except during the blanking pulse, at which time the two triodes acted as a short circuit from the grid of V314 to ground.

The transmitted pulse or ping length was determined in the transmitter chassis. (See Figure 112.) The blanking pulse from the SRO chassis was introduced to the transmitter chassis at terminal 21, causing the 6V6 tube V201 to conduct and operate the d-p d-t relay shown in the lower right corner of the rotor schematic in Figure 124. This relay grounded terminal 50, causing the tube V202, which was connected as a "flip-flop," or multivibrator, to send a square pulse to the grid of the first half of V207, which keyed the oscillator. The square pulse out of V202 had a length of approximately 3 milliseconds, the time for 1 cycle of the sweep. The length of this pulse was determined by the adjustment of the 1/10-megohm potentiometer between the grid and cathode of the second half of V202. The send-receive



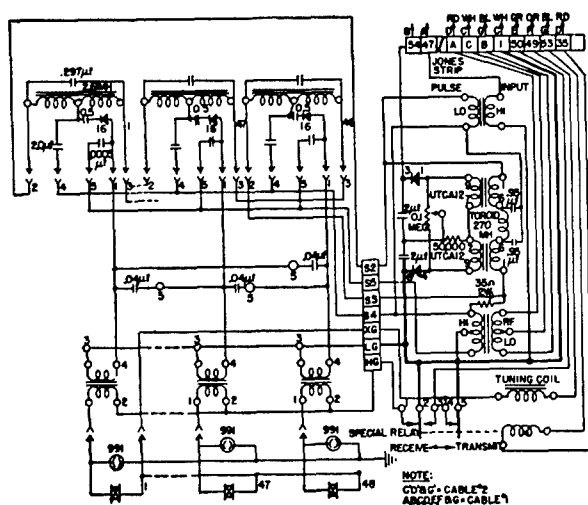


FIGURE 124. Circuit diagram of varistor rotor for submarine E.R. sonar, Model 1A.

relay, at the same time that it actuated the transmitter multivibrator, switched the projector from receiving to transmitting.

The second submarine system which was built differed sufficiently from the first to be called Model 2. Its sweep and timing circuits are shown in circuit diagram, Figure 125. The send-receive networks are described earlier in this chapter. No change was made in the ping timing circuits. The sweep timing and range determination circuits were substantially the same, except that the mechanical timer used in Model 1 was replaced by an electronic timer in Model 2.<sup>63</sup> A circuit diagram of the electronic timer, which developed as a logical outgrowth of the range marking circuit, is given in Figure 126.<sup>57</sup>

The linearly expanding voltage of the range-marking circuits was used to modulate the circular sweep, to get the spiral sweep, and to determine the sweep interval. This was done by attaching a potential divider to the expanding voltage output in the range-marking circuit. The potential at the tap of this divider, the control point, then rose to a given value which was equal to, was  $2/5$  of, or was  $1/5$  of, the potential to which the expanding sweep in the range-marking circuit had risen. The potential to which the control point rose was determined by a multivibrator circuit which generated the blanking pulse. The sweep of the control point was used directly to drive the grids in the sweep amplifier.

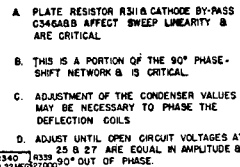
By December 30, 1944, this circuit had been incorporated into the Model 2 SRO chassis. The prin-

cipal modifications were that the average potential of the sweep output was lowered by means of a voltage divider between B+ and C-, and two blanking pulses had been incorporated. One of the blanking pulses was used to reset the sweeping circuit and was about 20 milliseconds long. The other blanking pulse, about 40 milliseconds long, was applied to the cathode for blanking of the PPI display, so that the switching transients were allowed to die out completely before the display restarted. The two pulses started at the same time.

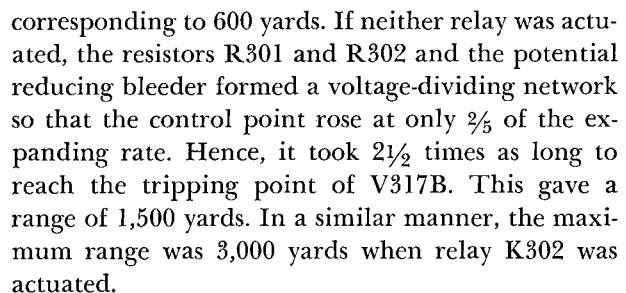
The operation of this interval timer can be understood most readily by following it through a complete cycle. As the end of the sweep was reached, grid No. 1 of V317B became sufficiently positive so that this tube began to conduct. This drove the grid of tube V317A negative, cutting off this tube and putting a sharp positive pulse on the grid of V305A. V317B continued to conduct until capacitor C301 had discharged through resistor R325 sufficiently so that V317A again began to conduct. As V317A started to conduct its cathode became positive, thus cutting off V317B and restoring the current to V317A. This operation took about 40 milliseconds and produced a square-top blanking pulse which V305A applied to the cathode of the cathode-ray tube. When the plate of V317B went negative, the pulse was differentiated by the capacitor C310 and resistor R361, cutting the tube V305B off for about 20 milliseconds. This caused the grid of V310B to be made positive for 20 milliseconds. During the time that V310B conducted, the inductor L303 and the plate resistance of tube V310B determined the discharge characteristic of capacitor C328, which was the sweep capacitor. Thus, the sweep capacitor was completely discharged and the circuit returned to equilibrium by the end of the 20-millisecond period. Meanwhile, the grids of the sweep amplifier tube V301 had been returned to their starting potential because they were connected to the sweep capacitor through the potentiometer R331 and the relays K302 and K303.

The voltage across R362, and hence the current through it, was held constant by the tubes V310A and V311B. The linearity control R364 was adjusted so that the positive feedback from tube V311B to V310A was sufficient to make the pair of tubes metastable. This adjustment insured constant current into capacitor C328 and, hence, a linear sweep.

If the relay K303 was actuated, the control point on the potential reducing bleeder was connected



directly to the sweep capacitor. Hence, the control point was swept at the full expanding rate and reached the tripping voltage of V317B after a time



There are two fundamental methods of obtaining a linear spiral sweep. One method is to use a linearly

**CONFIDENTIAL**

expanding sweep to operate a linear modulator. The other method is to use a nonlinear expanding sweep with a nonlinear modulator whose characteristics compensate for the nonlinearity of the expansion voltage generator. A linear sweep with linear expander was used in the submarine ER sonar, Model 2. (An analysis of the method used to achieve the linearly expanding voltage is given in reference 57.) A linear sweep may be approximated by using a small fraction of an exponential sweep. There are several ways of doing this. One method is to charge the sweep capacitor to only a very small fraction of the source voltage. The other methods rely upon creating an apparent source whose voltage is much higher than the actual source voltage, as, for example, by the use of a pentode "constant current" tube. The characteristic of most electronic expanders contains some region such that, when operated by a reasonably small portion of an exponential expanding voltage, they give a reasonably linear characteristic. The early ER sweeps all used this type of compensation.

A linear sweep could be obtained by using a counter to actuate some sort of stepping device to move the circular sweep out just one step for each cycle of the counter.

The greatest obstacle to sweep linearization has been the transient which accompanies the return of the sweep to the center. The time for recovery of normal sweep display was about 60 milliseconds with the synchro generator used in the 60-cycle system. The potentiometric coupling used in the expander of subsequent systems was incorporated to reduce this recovery time, as was also the tuning or low-frequency by-passing of the driver tube following the expander.

Sweeps must be stabilized so that they are independent of slow and rapid changes in supply voltage, frequency, and waveform of the power supply; of slow and fast changes in temperature and humidity; of aging of components; and of other factors, such as the polarization of the dielectric in the sweep capacitors. Timing can be stabilized with respect to all these factors, except power supply frequency, by using a synchronous motor. The sweep and timing functions may be stabilized against changes in power supply voltage and/or waveform by using voltage regulation for all of the components. The sweep and timing may be made independent of age and change of components by making the timing dependent solely upon elements which are stable.

Independence of the supply voltage is achieved by making the time interval measurement and time rate measurement both from the same power supply. In this case, the time constants in the filter supply must be of the same order as the longest intervals in any variational time sequence, so that transients are removed by integration. When it is necessary to depend upon two or more supplies then time constants must be identical, so that sharp transients in the power supply have identical effects upon the supplies. A variation of this scheme is used to compensate the extent of the sweep display for changes in power supply voltage.

Oscillator amplitude, expanding voltage amplitude, or modulator output is increased as the power supply voltage increases, so that the increased stiffness of the beam of the cathode-ray tube keeps the limit of the sweep display constant, as the voltage upon the anodes of the cathode-ray tube is increased.

For the bearing of the display to be independent of range, it is usually necessary to have well regulated supplies.<sup>52,64,65,66,67,</sup>

#### 7.8.9

### Sweep Calibration

The method of sweep calibration for the submarine ER sonar Model 2 is given in Chapter 8. Model 1 required a less extensive calibration method because the 6.3-volt timer used to generate the sweep ran accurately at 16 rpm from any supply voltage of 8/10 volt to 8 volts provided that the supply frequency was exactly 60 c. This calibration procedure is given in the instruction manual<sup>1,58</sup> and may be described briefly here.

A range-calibrating switch on the SRO chassis allowed the operator to connect the contacts of the mechanical timer to the sweep circuit so that the sweep was displaced at 0.75-second intervals equivalent to 600-yard intervals in range. These displaced points could be readily located by the range marker with the sweep on the 3,000-yard range scale, and their position read on the range dial. Thus a measure of the linearity of the range marker scale could be obtained, while a calibration of the scale could be made from the fact that the first displaced point should occur at 590 yards, the second at 1,190 yards, and so on at 600-yard intervals. The 10-yard (12.5-millisecond) discrepancy in the range of the first mark represents the time lag between the action of

the timer and the occurrence of the ping itself. Controls were provided on the SRO chassis for adjusting the linearity and rate of the range marker circuit, while a zero setting screw was provided on the range dial in the indicator unit.

In the development of the range determination system for the submarine sonar systems, a chemical recorder was used for calibration purposes.

The considerations for oscillator stability are fundamentally the same as those for sweep stability.<sup>68</sup>

The oscillator to be stabilized is that which generates the circular part of the spiral sweep. It must be stabilized not only in frequency, but also in phase. Locking of the phase of the display to the bearing of the scanning beam is achieved by using a single oscillator for both. It has been found advisable to use a closed cycle system to lock the frequency of the oscillator to the rotating member. The discriminator circuit described above was developed to perform this function.

## Chapter 8

# TEST METHODS AND TECHNIQUES

### 8.1 TRANSDUCER TEST METHODS AND TECHNIQUES

DETAILED TEST METHODS and techniques are described in various sections of the report on transducers.<sup>1</sup> These sections also include a description of the application of these methods to scanning sonar transducers.

#### 8.1.1 Transducers to be Tested

The various types of scanning sonar transducers have been described in earlier sections of this report and elsewhere.<sup>1</sup> They fall into three classifications:

1. The plane type of transducer used in reception in the *mechanically rotated* [MR] scanning system.
2. The cylindrical type of transducer, sometimes called ring stack or ring emitter, used for transmission in MR sonar and in one model of *electronically rotated* [ER] sonar.
3. The multielement cylindrical type of transducer used for both transmission and reception in *commutated rotation* [CR] and ER sonar, both of which make use of auxiliary devices to obtain rotation of the receiving beam of sensitivity while the transducer remains stationary.

#### 8.1.2 Basic Transducer Tests

All types of scanning sonar transducers should undergo some preliminary tests to determine their characteristics and their efficiency for scanning application. Basic measurements that should be made for MR sonar receiving transducers are:

1. Reception patterns taken both in the vertical and horizontal planes.
2. Sensitivity measurements of the transducer.
3. Impedance measurements of the transducer.

Measurements which should be made on the transmitting transducer for MR sonar application are:

1. Transmission patterns taken in both the vertical and horizontal planes.
2. Sensitivity measurements of the transducer as a hydrophone.
3. Impedance measurements of the transducer.

4. Output-acoustic-power versus input-power measurements at the operating frequency of the transducer.

Basic measurements that should be made on multielement cylindrical transducers for use in systems in which the transducer is stationary and has a rotatable sensitivity pattern are:

1. Reception patterns on single elements, taken both in the vertical and horizontal planes.
2. Reception patterns of the transducer with all or a portion of the elements connected in parallel, taken both in the vertical and horizontal planes.
3. Phase-difference measurements among the various elements with the cylindrical axis of the transducer vertical—that is, in the same position as that used for taking patterns in the plane to be scanned.
4. Sensitivity measurements of each element over sonar frequency range.
5. Sensitivity measurements of the transducer as a whole, with transducer elements—either all or a portion of them—connected in parallel.
6. Impedance measurements of each element.
7. Transmission pattern of the transducer as a whole in the horizontal and vertical planes, with all or a portion of the elements connected in parallel.
8. Output-power versus input-power measurements at the operating frequency of the transducer.

#### 8.1.3 Results of Transducer Tests

The data obtained from the basic tests on a scanning sonar transducer are used in several specific ways to evaluate the transducer for scanning.

1. Patterns are used to test uniformity among the various elements of a multielement transducer, to determine the effective baffling of the elements for computation of beam-forming lag lines (see Chapter 9), and to determine the characteristics of the transmitted beam of sound. For MR sonar, patterns are used to determine the receiving beam of sensitivity.
2. Sensitivity data are used to test uniformity among the various elements of a multielement transducer, to determine the optimum frequency of operation, to compute the mechanical  $Q$  and to compute the efficiency of the transducer.

3. Phase measurements are used to test phase uniformity among the various elements of a multielement transducer, and to compute the phasing requirements in the lag line used for forming a suitable beam of sensitivity.

4. Impedance (or admittance) measurements are used to compute the efficiency of the transducer, to determine the resonant frequency, to compute the mechanical  $Q$  (with and without inclusion of the transducer-core losses), and to determine uniformity among the various elements.

5. Measurements of acoustic-power output and electric-power input are used in the computation of the efficiency of the transducer.

6. Measurements, in water at a suitable test station, of impedance (or admittance) for each stave at the resonant frequency, and also at a frequency where the motional impedance is negligible, are used to check uniformity among the elements and to check the effect of assembly, as well as to determine the sensitivity of each stave at the operating frequency. The reception pattern of all elements in parallel at the operating frequency is used to check the transmitting measurements under this condition.

For multielement transducers, the electrical impedance, sensitivity, and reception patterns of the various staves must fall within a suitable tolerance established from previous basic measurements. For MR units, the leakage tests must be satisfactory, the transmission pattern must be uniform within a tolerance set by basic measurements, and the receiving transducer must have a suitable pattern defined by basic measurements.

Specific means for carrying out these tests are, of course, dependent on the design of the transducer, its mechanical shape and size, and the purpose for which it is intended. Various devices may be used to speed up accumulation of data, such as automatic pattern plotters, sensitivity meters, etc. Such instruments should be selected according to the particular transducer to be tested, and specific routines worked out for their use.

#### 8.1.4 Production Testing of Sonar Transducers

Production testing of a transducer involves a set of tests to evaluate the transducer in a minimum of time and with a minimum of effort. The entire set of basic tests previously described cannot be used as a series of

production tests. Furthermore, additional tests should be made during the process of assembly. A specific routine must be worked out for any particular unit, but certain general tests are suggested to assure proper operation of the transducer.

Tests prior to complete assembly should include:

1. Strength tests on all load-carrying parts.
2. Spot checks on dimensions.
3. Leakage tests on completed castings.
4. Careful inspection of magnetostrictive laminations and of the consolidation process of these laminations, and some simple tests on uniformity of the resultant staves and on uniformity of electrical characteristics.

Tests following the assembly should include:

1. Spot checks on placement of staves during assembly and after assembly.
2. Leakage test on completed unit.

### 8.2 COMMUTATOR TESTS

Since the commutator is such a vital part of a scanning sonar system, it is very important that it be adequately tested. The individual components entering into its construction should be tested before assembly, as should each subassembly, and the complete commutator tested for satisfactory operation. These statements apply equally to both CR and ER types. Because of the considerable differences between these two systems, the subassembly and overall tests are discussed separately.

#### 8.2.1 Component Tests

Much trouble in later stages of construction can be avoided by testing each component before assembly. Undesired phase shift, for example, in just one input transformer may lead to poor beam-pattern formation over a considerable sector.

##### INPUT-TRANSFORMER MEASUREMENTS

Quantities of interest are turns ratio (or impedance ratio), input impedance, phase-shift characteristics, and in some cases, an insulation breakdown test and tests of the accuracy of the center tap location.

The turns ratio is considered as the ratio of open-circuit voltage across the primary to that across the secondary measured at the mean of the frequencies over which the transformer is to operate. The measurement should be made by means of a vacuum-tube

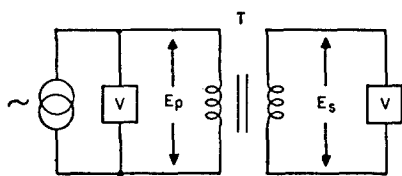


FIGURE 1. Arrangement for measuring turns ratio.

voltmeter with high-input impedance (see Figure 1).

The impedance ratio of the transformer may be considered as equal to the square of the turns ratio, or may be determined more directly by measuring the primary input impedance when the secondary is terminated in its rated load impedance.

One method of measuring the input impedance is illustrated in Figure 2A. This method gives the magnitude of the impedance without regard to the phase angle, as does the substitution method illustrated in Figure 2B. The phase angle may be determined with the arrangement shown in Figure 2C, in which the standard lag line<sup>2</sup> is adjusted to have phase shift to match the phase angle of the input impedance. The slope of the trace is proportional to the magnitude of the input impedance. An impedance bridge<sup>1</sup> may also be used.

Figure 3 illustrates two methods for measuring phase shift through a transformer. In Figure 3A the phase shift is determined from the width of the Lis-

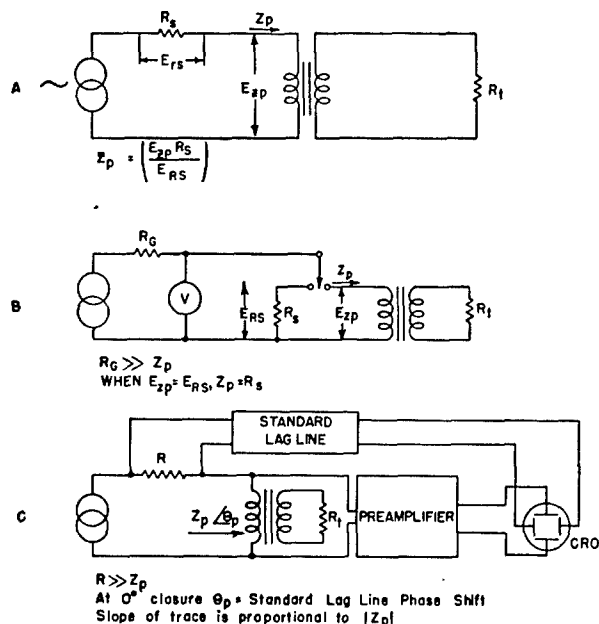


FIGURE 2. Arrangements for measuring transformer input impedance.

sajous ellipse. In Figure 3B the width of the ellipse is reduced to zero by compensating the phase shift through the transformer with an equal phase shift introduced by the standard lag line.<sup>2</sup> This arrangement is useful for checking a large number of transformers that are supposed to be identical, and may be modified to use a standard transformer instead of the standard lag line, as shown in Figure 3C. Amplitude differences between the standard transformer chosen as a reference and the one under test are indicated by change in the slope of the line on the oscilloscope. Phase differences are indicated by an elliptical figure rather than a straight line, and limits may be set for the tolerable width of the ellipse. The oscillator frequency may be swept through any desired range while the observations are being made.

In some cases where balanced circuits are used, it is necessary to maintain certain tolerances with regard to the accuracy of the transformer center tap. The

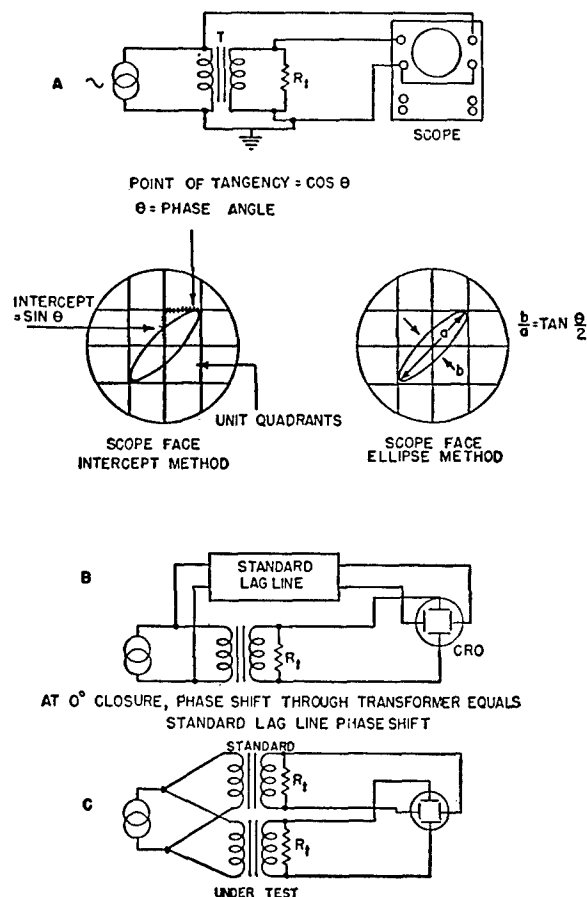


FIGURE 3. Arrangements for measuring phase shift through a transformer.

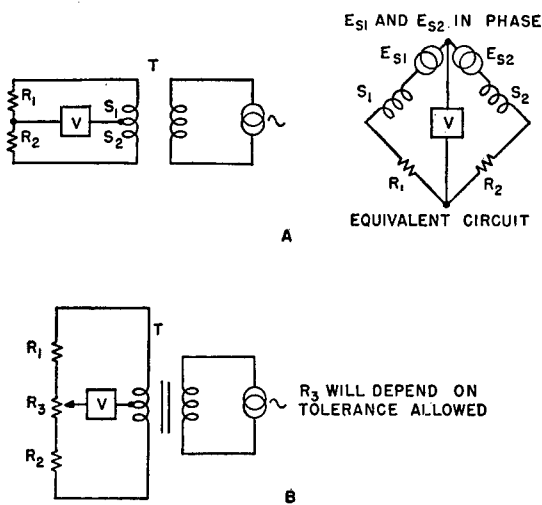


FIGURE 4. Arrangement for checking center tap accuracy.

bridge techniques illustrated in Figure 4 may be used to check the accuracy of the center tap. When the bridge is balanced (Figure 4A), the voltmeter reads zero, and  $R_1/R_2 = S_1/S_2$ . For production testing the circuit shown in Figure 4B is convenient since it permits the setting of tolerances.

In certain sonar applications, particularly in ER sonar, the insulation between the primary and the secondary of the input transformers may be subjected to potential differences of 100 or 200 volts during transmission. It is desirable to test the insulation of such transformers at a voltage considerably in excess of any peak voltages which might occur in use, for example, at twice the rated voltage of the transformer plus 1,000 volts, and to apply this voltage for a short interval of time. The use of a high-impedance d-c source with a current-indicating device such as that shown in Figure 5 has been found satisfactory.

#### LAG-LINE OR LEAD-LINE COMPONENTS

Toroidal coils wound on high-permeability dust cores have been used in lag lines and lead lines. The

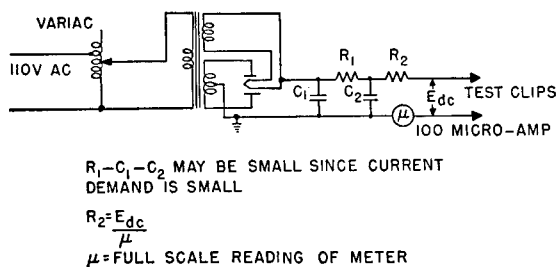


FIGURE 5. Arrangement for checking insulation leakage.

inductance of the individual coils should be measured at the operating frequency to insure that the desired tolerance is maintained. The arrangements shown in Figure 6 may be used in making the inductance measurements. That given in Figure 6A is the ordinary Q-meter circuit and depends upon the adjustment of the standard capacitor to give an amplitude maximum in the voltmeter reading. It is not so precise as that of Figure 6B, which depends on phase indication. The d-c resistance of coils may be determined by means of an ordinary Wheatstone bridge.

The capacitors for lag lines and lead lines may be checked by means of a capacitance bridge.

Resistors may be checked with a Wheatstone bridge. In experimental work the termination and shading resistors are often chosen after the lag line has been assembled, as described in the following section.

#### 8.2.2 Subassembly Tests for Commutator

After the inductors and capacitors for a lag line have been checked, the line may be assembled in breadboard fashion. Line termination resistors and the resistors for the shading networks must then be chosen.

Methods that have been used in determining the proper termination resistors are shown in Figure 7. In Figure 7A the voltage across successive points along the line is measured and plotted, and the process repeated with different values of terminating resistor  $R_t$  until no reflection at the termination is indicated. A quicker method is shown by Figure 7B

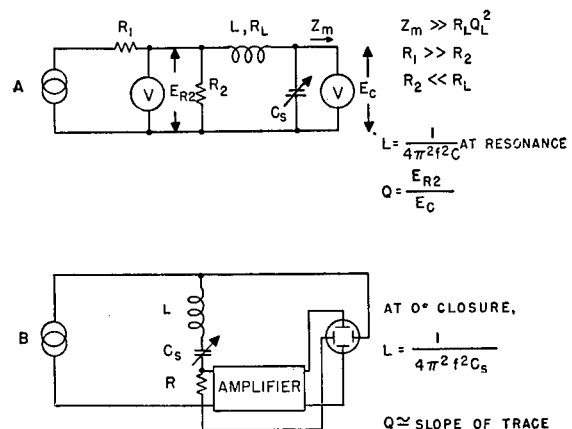
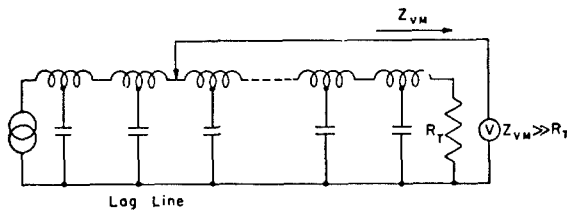


FIGURE 6. Arrangements for determining coil inductance.





A

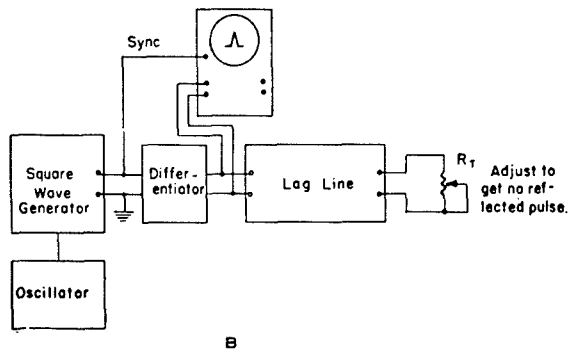


FIGURE 7. Arrangements for determining proper terminating resistances.

in which reflections from the termination are observed directly. A sharp pulse is fed into the input end of the line. If the terminating resistor does not have the correct value, one or more reflected pulses will be seen on the *cathode-ray oscillograph* [CRO] following the initial pulse. The terminating resistance should be adjusted until the reflected pulse has zero or minimum amplitude. Several reflected pulses of small amplitude are usually observed because of variations in impedance along the line. If the correct tolerance of components has been observed, these pulses are of negligible amplitude. The same procedure may be used to terminate the line at the other end. It is not sufficient to assume that the two resistors should be of the same value.

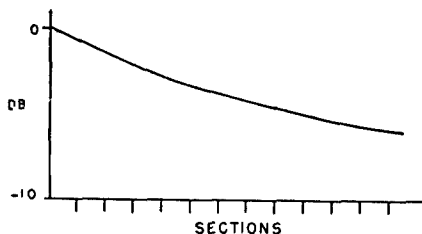


FIGURE 8. Example of curve of voltage along lag line.

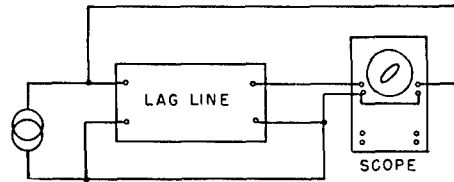


FIGURE 9. Arrangement for measuring total phase shift of lag line.

The arrangement shown in Figure 7A gives a check on standing waves along the line. Figure 8 shows a typical curve of voltage versus sections of line. Irregularities in this curve are evidence of standing waves. The total attenuation is also found from this measurement.

The total phase shift of the terminated line may be measured as shown in Figure 9. The frequencies at which the trace on the scope is a straight line are the frequencies for which the phase shift is a multiple of 180 degrees. These frequencies are plotted as shown in Figure 10, and the total phase shift at the design frequency is read from the curve. The plot should be a straight line through the origin. Accurate means should be provided for checking the frequency calibration of the oscillator.

The cumulative phase shift through the lag line may be measured section by section, with the arrangement shown in Figure 11A. Measurements are carried beyond 360 degrees by simply adding 360 degrees (or the proper multiple thereof) to the phase angle as read from the standard lag line. A phase-meter may also be used, as shown in Figure 11B, if less accuracy can be tolerated.

The resistors for the shading network must be chosen carefully. The correct value of each resistance may be calculated as described in the section on commutators in Chapter 6. The resistors  $R_1$  of Figure 12 are used during this test to simulate the impedance looking back into the commutator. When the com-

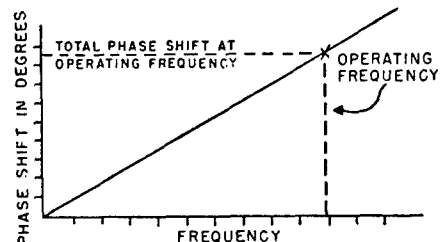


FIGURE 10. Sample curve of total phase shift versus frequency.

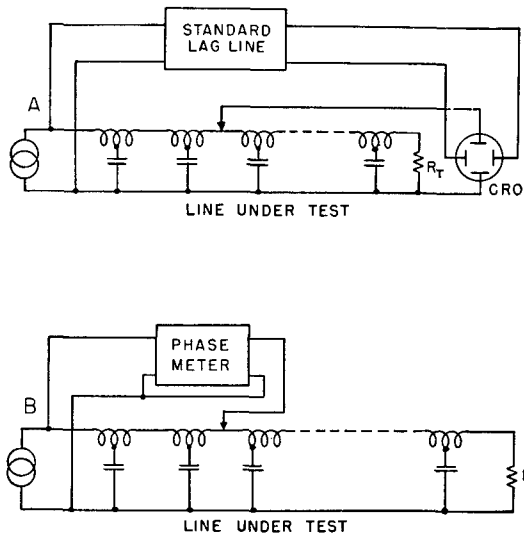


FIGURE 11. Arrangements for measuring cumulative phase shift.

mutator is finally assembled, the resistors  $R_1'$ ,  $R_1''$ ,  $R_2'$ ,  $R_2''$ ,  $\dots$ ,  $R_n'$  and  $R_n''$  are connected to the rotor plates of the commutator at points  $a$ ,  $b$ ,  $c$ , etc.

After these shading resistances have been computed, resistors having these values are connected to the line as shown. The generator is placed in series with the  $R_1$  resistor at point  $a$ , and the frequency is set at the desired value. The generator output is adjusted until  $VM_2$  reads a convenient multiple of unity. The reading of  $VM_1$  is noted. The generator

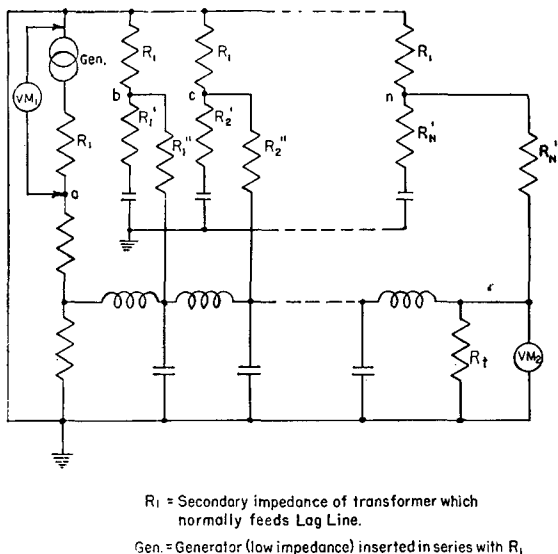
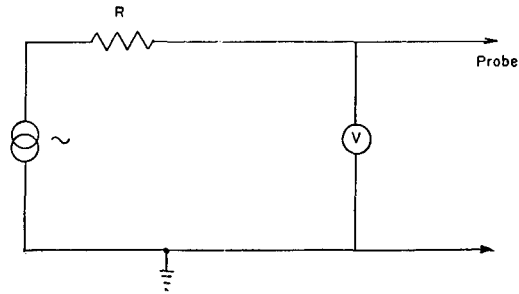


FIGURE 12. Arrangement for experimental determination of shading resistor values.



$R$  = Same value as impedance of circuit to be measured.  
 $R_0 \ll R$

FIGURE 13. Arrangement for rapid check of input impedance uniformity.

is then transferred to be in series with the  $R_1$  resistor at point  $b$ , and the voltmeter  $VM_1$  is connected between point  $b$  and ground.  $R_1''$  is adjusted until the reading of  $VM_1$  is the same as the previous reading.  $R_1$  is then adjusted until  $VM_2$  reads the value computed for correct shading. If the reading of  $VM_1$  has been disturbed,  $R_1''$  must be readjusted, and then  $R_1'$ . In this manner the final correct value of each resistor is determined.

The impedance of the assembled lag line with shading network at any point may be measured with any of the arrangements shown in Figure 2.

### 8.2.3 Assembly Tests on CR Commutators

After the commutator has been assembled, measurements of the spacing between plates should be made in order to determine whether it is the correct

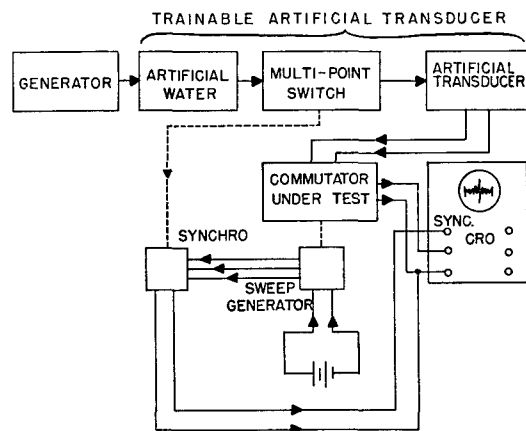


FIGURE 14. Arrangement for oscilloscopic observation of commutator beam patterns.

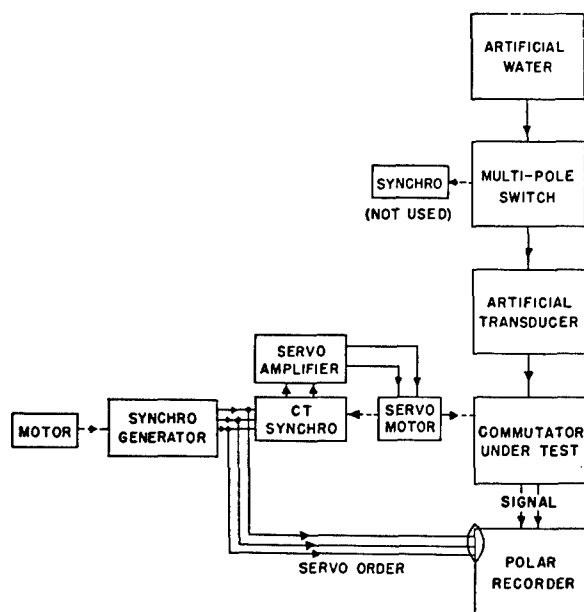


FIGURE 15. Arrangement for automatic plotting of commutator beam patterns.

value and is uniform with rotation. Thickness gauges may be used, but measurement of capacitance is more accurate. Excessive vibration should not occur when the commutator is brought up to speed.

After the input transformers have been wired, tests may be made to check the uniformity of the input impedances of the different channels with any of the arrangements shown in Figure 2. An arrangement that allows a rough check to be made very quickly is shown in Figure 13. If the impedance has the desired value, the meter reading will decrease by exactly 6 db when the probes are applied to the input terminals.

Beam pattern measurements are perhaps the most important of all measurements to be made on the finished commutator unit. Figure 14 shows a suitable arrangement for checking scanning beam patterns with an oscilloscope and a trainable artificial transducer. The latter device is described in a succeeding section, and instructions for use are given in an instruction manual.<sup>3</sup> It comprises an "artificial water" (which is a lag line tapped to give phase differences corresponding to those in the signals from the respective elements of a scanning sonar transducer when receiving sound in the water), a multipoint switch to change the apparent direction of the incident sound, and networks to simulate the impedances of the actual transducer elements. The commutator is driven at its normal scanning speed and its output signal is

applied to the vertical deflection plates of the CRO. A linear sweep is used, synchronized by the signal from the sweep generator on the commutator. As the multipoint switch is rotated, one step at a time, the beam pattern for each corresponding direction appears in linear form on the CRO screen. Estimates of beam width and the bearings of minor lobes are facilitated by adjusting the sweep length to 36 divisions of a ruled mask. The synchro on the multipoint switch acts as a phase shifter for the synchronizing pulse, and keeps the pattern stationary on the CRO screen. Tolerance limits may be drawn on the face of the CRO for major lobe amplitude and width, and minor lobe amplitude. Variations in the patterns over the frequency range of interest may be checked quickly by changing the frequency of the signal generator.

This arrangement has been useful in experimental work and seems very well adapted for production testing as the beam patterns in each of 48 directions may be checked in less than a minute. The presence of defective components or improper connections is seen immediately from changes in the beam pattern, and the fault is quickly located. It is adaptable only to a commutator that is scanning, but its speed makes it desirable for the testing of listening commutators as well. This may be done if the drive motor assemblies for scanning and listening commutators are made interchangeable, as has been done in the Model XQHA scanning sonar.

When a permanent record is desired, the CRO may be replaced by a voltmeter to measure the signal output of the commutator. In this case the commutator is not scanning, but is rotated by hand to selected bearings, and the readings of the voltmeter are plotted point by point. If the position of the rotor is not easily adjusted directly, it may be controlled from a synchro generator through the listening rotor

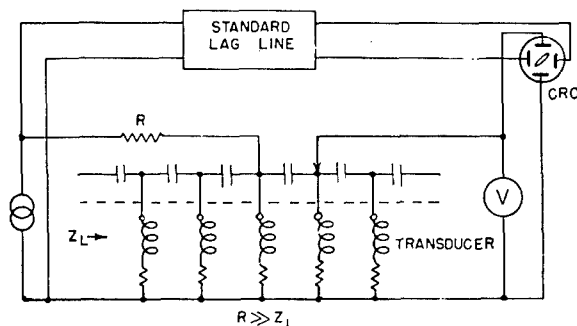


FIGURE 16. Arrangement for phase and voltage measurements on lead line.

servo drive. Interchangeability of drive assemblies thus allows the beam patterns of a scanning commutator to be plotted, as well as those of a listening commutator.

Point-by-point plotting is tedious and tends to obscure detail in the patterns. The patterns may be plotted automatically, preferably with a polar recorder,<sup>4</sup> by using the arrangement shown in Figure 15. Here the turntable servo and the commutator servo are both controlled from the synchro generator, which may be rotated slowly by hand or by a motor. The smoother rotation possible with the motor results in smoother and therefore more accurate patterns.

#### 8.2.4 Electronic Rotor Tests

Checking of individual components for proper value and uniformity may be accomplished by use of the methods previously described. Only tests on sub-assemblies and on the completed rotor are discussed here.

##### LEAD-LINE MEASUREMENTS

Since the transducer elements form the shunt legs of the lead line, a transducer, either actual or artificial, must be connected to the lead line. Signal of the operating frequency is introduced at one point through a high resistance. Phase measurements at successive points may be made with a standard lag line and CRO as shown in Figure 16, and the phase shifts for each section may be determined by taking differences. Alternatively, a phasemeter may be used to measure the phase shift of each section directly. Amplitude measurements may be made at the same time to determine the attenuation of each section.

##### SWITCHING LAG-LINE MEASUREMENTS

Terminations and total and cumulative phase shifts of the assembled switching lag line may be measured by means of arrangements such as those already described for beam-forming lag lines. However, because of the low frequencies involved (about 300 c), the standard lag line may not be convenient for measuring the cumulative phase shift, and a goniometer technique may be preferable. Such an arrangement is illustrated in Figure 17. The goniometer, which may be a 2-phase synchro, is adjusted to give 0 degrees Lissajous closure on the CRO, and the phase shift is read directly from its dial. Modifications

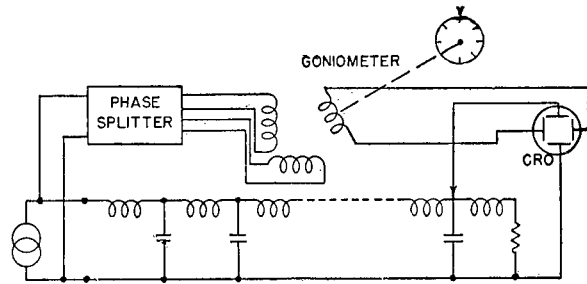


FIGURE 17. Goniometer arrangement for phase measurement.

using variable resistors have been proposed.<sup>5</sup> Another method uses a CRO plus a decade capacitor and a decade resistor. The scope is used to indicate only 0 degrees or 180 degrees phase shift. The decade boxes are used to produce a known phase shift in the same way as a standard lag line. The frequency is measured by comparison with a standard oscillator.

The proper operating frequency for the switching lag line is that at which it has a total phase shift of exactly 360 degrees. This may readily be determined with the arrangement shown in Figure 9. As an alternative method the frequency control discriminator may be connected, and its rectified output, measured on a d-c voltmeter, may be used to indicate 360 degrees total phase shift (assuming that the discriminator has already been checked for balance).

##### DISCRIMINATOR ADJUSTMENT

The following procedure may be used in adjusting the discriminator: the frequency supplied to the switching lag line is set to give 360 degrees shift as indicated by CRO closure, and the discriminator balanced by means of its balance potentiometer at zero output. The action of the discriminator may then be checked by varying the switching frequency and observing the discriminator output voltage. Best discriminator action, as measured by volts output per cycles per second frequency change, is obtained if the rectifiers in the discriminator have a high backward resistance. If varistors are used, they should be selected on the basis of this property. An ordinary ohmmeter may be used for the resistance measurements. There are, however, two varistor elements in each mounting enclosure, and since the two may not be identical (hence the need for the balance potentiometer), it is preferable to pick those which show high sensitivity when tested in an actual discriminator circuit. While an actual switching lag line may be

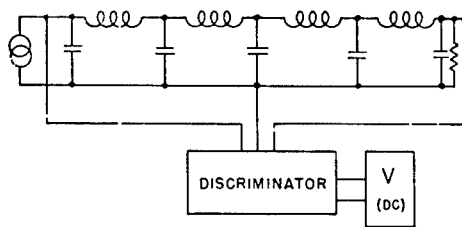


FIGURE 18. Arrangement for adjusting discriminator.

used in adjusting the discriminator, it is often more convenient to have a simpler line for this purpose. Such a test line may have far fewer sections, four 90-degree sections having been found entirely adequate (see Figure 18). It is desirable to have the frequency for 360 degrees phase shift of the test line comparable with that for the switching lag line.

#### ROTOR SEGMENT TESTS

In cases where the electronic rotor is made up of a number of segments, each of which contains a lead line, a switching line, and switching components, it is desirable to have special test methods for a complete check on the individual segment. Arrangements should be provided to check the values of the components and also the correctness of the wiring. For checking rotor sectors of the type used in the submarine ER sonar, a *sonar switching test unit* was developed.<sup>6</sup> This test unit permits:

1. Tests for shorts between any terminal and ground.
2. A check on the frequency at which the circuits between certain pairs of terminals resonate. (This is a check on capacitive and inductive components.)
3. A measurement of the modulated signal amplitude obtained when the varistor is used as a modulator to apply 60-c modulation to a signal at operating frequency.

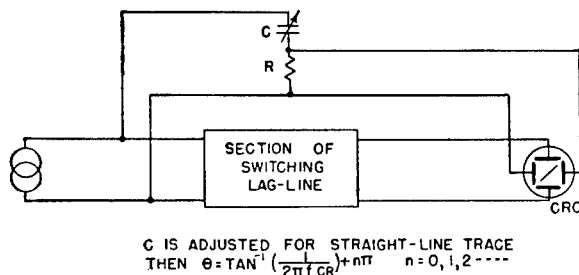


FIGURE 19. Arrangement for phase-shift measurement; RC reference.

4. A measurement of the phase shift of each section of the switching lag line at the switching frequency. The phase shift could have been measured with a standard lag line, but in this case it was more convenient to use an RC circuit as a reference, as shown in Figure 19.

#### TESTS ON COMPLETED ROTOR

Phase and amplitude measurements may be made upon the lead line in the completed rotor, with the switching signal turned off. A signal is applied by means of an artificial or an actual transducer. The signal amplitude is measured at each tap along the lead line by means of a vacuum-tube voltmeter. The phase is measured at each tap on the lead line, relative to any chosen tap, by means of a phasemeter or by the method utilizing a standard lag line. The cause of any obvious inconsistencies can then be investigated before patterns are taken.

The beam pattern is observed on an oscilloscope by means of the arrangement shown in Figure 14, omitting the sweep-synchronizing arrangement shown and substituting a synchronizing connection from the switching oscillator. Permanent record may be obtained by photographing the pattern, but direct chart recording of the patterns with the arrangement shown in Figure 15 is not possible. However, an electronic system was devised which allowed the use of a *portable polar chart recorder* [PPCR] to record the patterns obtained at the high scanning speed used in ER sonar. To do this, the circuit provides an electronic gate which accepts a signal from the rotor output only when its scanning operation passes through a certain limited bearing region. This bearing gate is then rotated slowly in synchronism with the rotation of the turntable of the polar chart recorder, and the pattern is traced out as the gate samples the continuously high-speed rotating pattern. Figure 20 is a block diagram of the circuits of the ER sonar pattern tracer. The device has been named the *polar inverse exponential pattern plotter for ER sonar* [PEPPER].<sup>7</sup>

The blocks in this diagram are labeled so that the various signals can be followed readily.

When varistors are used, it is desirable to take patterns at all azimuth bearings. This is because the amplitude is affected by the varistors. It is furthermore desirable that the varistor sectors be sorted and installed in such an order that those giving large amplitude and those giving small amplitude occur alter-

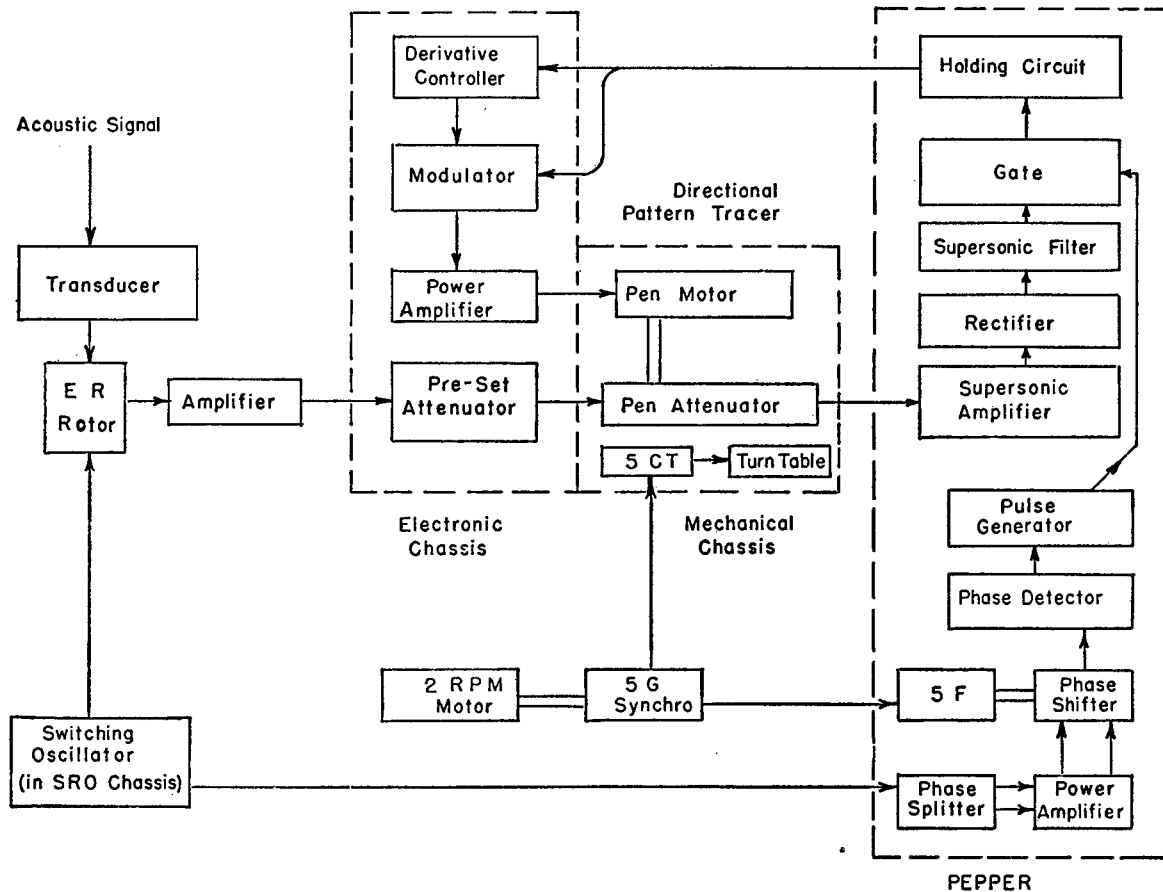


FIGURE 20. Block diagram of polar inverse exponential pattern plotter for ER sonar.

nately. This arrangement has been found to yield better patterns than when all the high-amplitude sectors are grouped together, and all the low-amplitude sectors are grouped together. In one specific instance the amplitude variations of the patterns were reduced from about  $\pm 3$  db to about  $\pm 1\frac{1}{2}$  db by the alternate arrangement.

A background of radial lines always appears on the indicator if the amplifier gain is raised sufficiently. This background of radial lines is due largely to deficiencies of the varistors as switching devices. An unsatisfactory varistor is evidenced by a strong radial line. Normally, the background is low enough to permit satisfactory operation. Reducing the amplitude of the switching pulse reduces the background noise but also reduces the amplitude of the desired signal. The use of the artificial transducer allows adjustment for optimum performance without interference from ambient water noise.

#### 8.2.5

### Artificial Transducer

An artificial transducer is a device that furnishes signals equivalent to those given by an actual transducer in water when it receives a sound wave from a distant source. Although the actual source of the electric signals could be built into the device, this is usually not done; rather a separate oscillator or signal generator is used. The artificial transducer is therefore a purely passive device that produces a group of signals having the proper relative phases and amplitudes to simulate those from the elements of an actual transducer when fed by an acoustic signal in the water.

Artificial transducers have been built to simulate searchlight sonar transducers<sup>8</sup> as well as scanning sonar transducers, but only the latter are discussed. Early models of such artificial transducers were designed to furnish the required signals at a negligibly

low impedance level; later models included networks which would also simulate the generator internal impedance of the actual transducer elements.<sup>9</sup> A further refinement was a multipole switch to permit control of the apparent direction of the sound source in integral steps equivalent to one transducer element. The complete artificial transducer then consists of three parts:

1. Artificial water.
2. Multipole switch.
3. Impedance network.

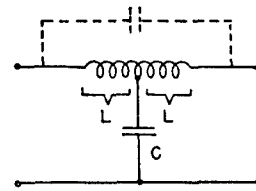
The order in which the last two parts are connected is a matter of wiring convenience, since the artificial water supplies signals to only part of the impedance network at any time, whereas each element of the latter is connected at all times to a corresponding input circuit on the commutator. In one case, for electronic rotor transmitting tests, the impedance networks were built up of components capable of withstanding high power, and this part was used without the artificial water and multipole switch.

Artificial transducers have proved of great value in permitting tests to be made in the laboratory of all parts of scanning sonar systems except the transducers, and it seems that they should be equally useful in production testing. A model constructed with this application in mind was the *trainable artificial HP-5 transducer*. Since it contains all the basic parts just mentioned it will serve as an appropriate example. In the following description, the basic parts are discussed in turn.

#### THE ARTIFICIAL WATER

The artificial water is that portion of the artificial transducer which introduces the required relative phase shifts and attenuations. While the phase-splitting process could be accomplished in other ways, it is done preferably with a multisection lag line tapped at appropriate points. This is because a lag line introduces essentially constant time lags which are independent of frequency, just as do the various paths over which the sound travels in the water. A lag line built for one frequency may therefore be used over a range of frequencies, and the phase shifts introduced will change just as do those in the outputs of an actual transducer. The only parameter of importance in the design of the lag line is therefore the size of the transducer to be simulated.

In constructing the time-delay network or lag line,



$$f_c = f \left[ \left( \frac{14.1}{31\pi B} \right)^2 - 198 \right]^{\frac{1}{2}}$$

$$L = \frac{0.00113 R_0}{(in\ mh) \ f_c (in\ mc)}$$

$$C (in\ \mu f) = \frac{4.49}{R_0 f_c (in\ mc)}$$

WHERE,

$f$  = DESIGN FREQUENCY

$B$  = PHASE SHIFT OF SECTION

$L$  = INDUCTANCE OF ONE HALF OF COIL

$R_0$  = ZERO FREQUENCY IMAGE IMPEDANCE OF LINE

FIGURE 21. Design data for linear phase-shift lag-line section.

it is desirable to use a network in which the phase shift is a linear function of the frequency. The type of section shown in Figure 21 approximates this condition. In order to avoid undesired coupling between sections, the coils for the lag line may be wound on high-permeability toroid cores. Since the zero-frequency image impedance of each section should be the same, and since in general the desired phase shift per section will vary from section to section, the same cutoff frequency cannot be used for all sections. This offers no difficulty so long as the cutoff frequency of any individual section is kept well above the operating frequency.

Each half of the toroidal winding must be trimmed separately. At the present time it is common practice to trim the coils and pick the capacitors within a tolerance of  $\pm 2$  per cent. If this tolerance is not maintained, trouble may arise because of the presence of standing waves on the line. The terminating resistors must also be carefully chosen to avoid standing waves.

Signals from taps are taken through isolating resistors to attenuating networks which are adjusted to introduce the required relative amplitudes. The required values may be measured on an actual transducer, or they may be computed on the basis of the theoretical work. Usual practice involves the computation of the pressure-transmission pattern of a transducer element in a pressure-release baffle,<sup>10</sup> although

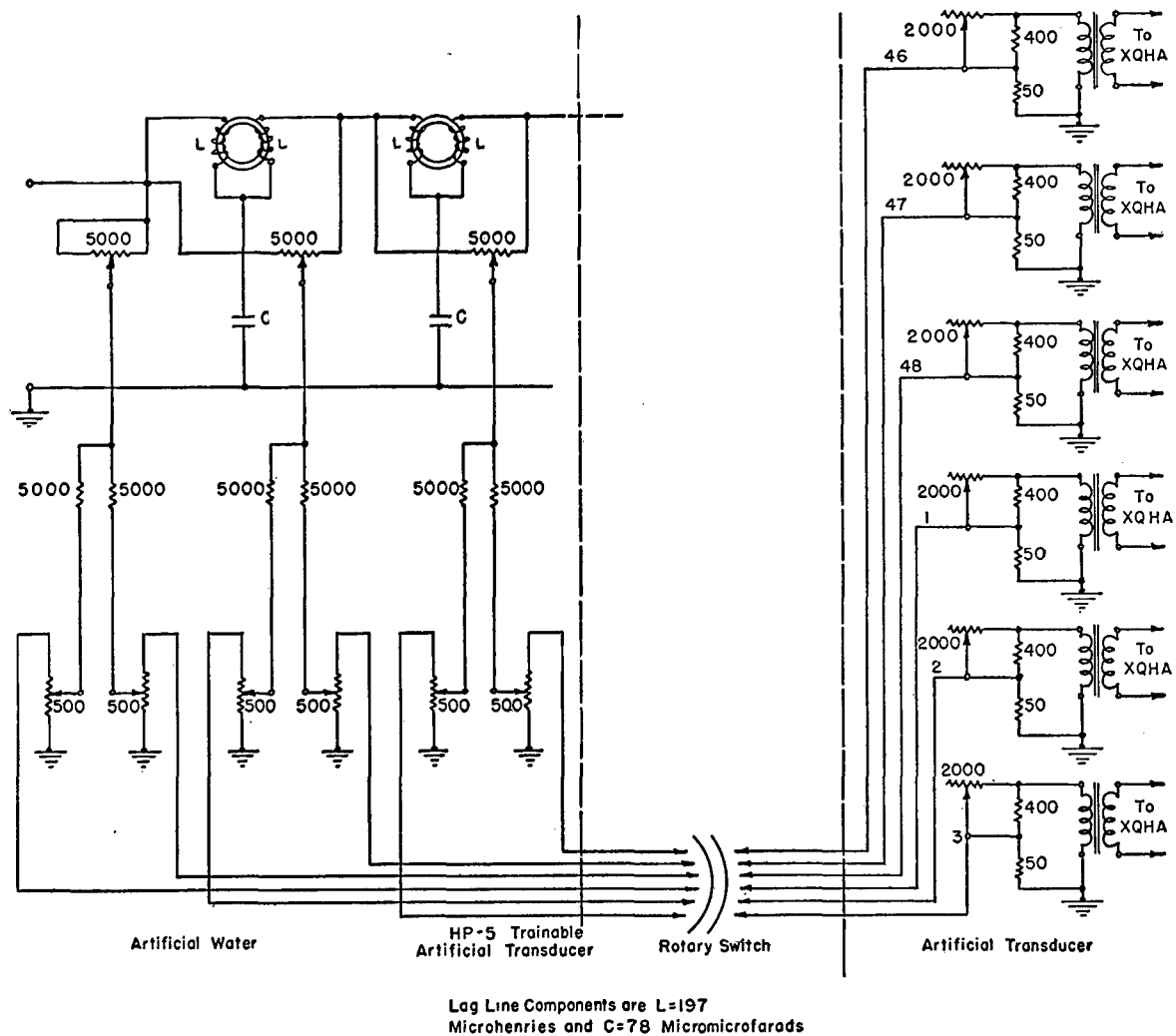


FIGURE 22. Wiring diagram of trainable artificial HP-5 transducer.

the amplitude ratios may be modified, if desired, to simulate more closely those from an actual transducer.

The isolating resistors are bridged onto the lag line at appropriate points as shown in Figure 22, the circuit diagram of the trainable artificial transducer. This particular unit was designed to simulate a 48-element cylindrical magnetostriction transducer having a diameter of  $18\frac{3}{4}$  inches and an operating frequency of 25.5 kc. The 5,000-ohm potentiometers permit exact adjustment of the relative phase, and the 500-ohm potentiometers permit exact adjustment of the amplitudes of the individual signals.

Two views of the unit under discussion appear in Figures 23 and 24.

#### MULTIPOLE SWITCH

The multipole switch is seen in the center section of Figure 24. This switch rotates the 24 output connections of the artificial water to coincide with any 24 consecutive output impedance networks. This corresponds to rotating the source of sound around the actual transducer in integral steps of one transducer element, or  $7\frac{1}{2}$  degrees. Appropriate dials are provided to indicate the apparent direction of the sound source, and stops furnished to limit the rotation in order to safeguard connecting wires. A phase-shifting transformer is coupled to the switch shaft to control the phase of synchronizing signals to a CRO on which the scanning pattern is displayed.

CONFIDENTIAL



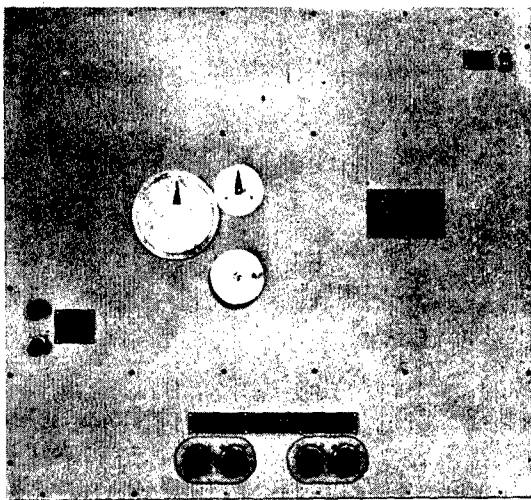


FIGURE 23. Front view of trainable artificial HP-5 transducer.

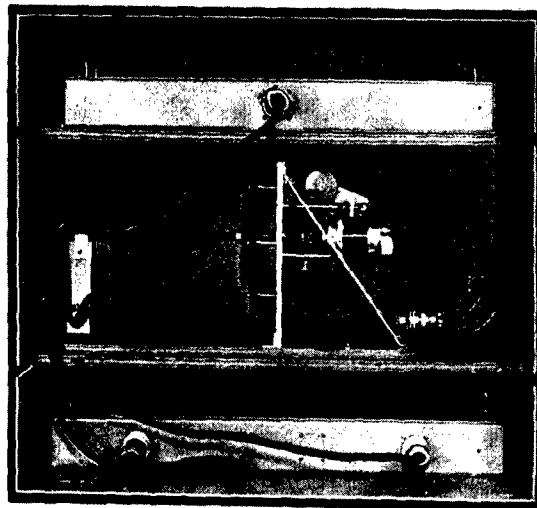


FIGURE 24. Rear view of trainable artificial HP-5 transducer.

#### IMPEDANCE NETWORKS

Impedance networks serve to simulate the generator source impedance of the individual transducer elements. This is desirable in order that pattern modifications at interregister positions be properly represented, particularly when two commutators are connected in parallel. Output transformers are used in the networks shown in Figure 22. The use of transformers avoids the necessity of a common ground lead from the artificial transducer to the commutator under test, and thus permits a complete simulation of the HP-5 transducer, which uses separate pairs of leads for each element. The design of suitable output transformers is discussed in the instruction book.<sup>3</sup>

Other networks may be used to simulate the impedance of a transducer element, depending upon the degree to which the actual transducer is to be simulated. (See Figure 25.) A first approximation may be made using only a resistor across the output terminals, as shown in Figure 25A. An actual magnetostrictive transducer element, however, has a reactive component of generator impedance. Its impedance may be simulated at a single frequency by a simple  $L$ - $R$  circuit as shown in Figure 25B or in Figure 25D. In some cases it is desirable to simulate exactly the transducer output impedance over a considerable range of frequencies. This can be accomplished by using the network shown in Figure 25C which includes all components of the transducer impedance, including the motional component, so that the actual

impedance circle will be obtained if the output of an element is measured.<sup>11</sup>

#### CONSTRUCTION PRACTICE

Care must be taken in the construction of the artificial transducer to minimize the effects of ground loops and of electrostatic and electromagnetic coupling.<sup>9</sup> Twisted pair wiring should be used wherever

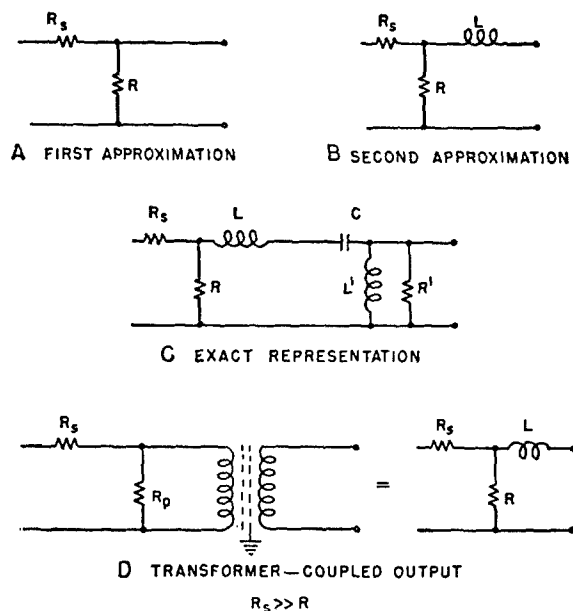


FIGURE 25. Networks that simulate generator impedance of actual magnetostrictive transducer elements.

CONFIDENTIAL

possible. An electrostatic shield should be used to separate the lag line from the attenuation and output circuit.

After the artificial transducer has been assembled and wired, the following check should be made to determine whether excessive coupling exists between elements. A signal should be applied to the input, and each attenuator adjusted for maximum output. The voltage should be read across a pair of output terminals. The corresponding potentiometer should then be set for maximum attenuation and the output voltage again read. These two readings should differ by at least 40 db. A difference of less than 40 db indicates undesired coupling in some part of the circuit. Each element should be checked in this manner. The adjustments for phase and amplitude differences may then be made.

### 8.3 TRANSFER NETWORK TESTS

#### 8.3.1 General Description

The term "transfer network" is used here to describe the send-receive switching arrangement which was used to switch the transducer connections from the transmitting to the receiving circuits in the scanning sonar system. Various types of transfer networks which were used at one time or another are described

in previous chapters. Two typical transfer networks are shown in Figures 26 and 27. In general the networks utilize the following components:

1. Tuning coil
2. Coupling capacitors and blocking capacitors
3. Polarizing chokes (used with d-c polarized transducers)
4. Receiving-matching transformers
5. Switching or change-over relays

#### 8.3.2 General Requirements of the Transfer Network Components

##### NETWORK TUNING COIL

This component was used in transfer networks in the following manner: in those ER systems which employed a crystal transducer, the transducer elements were connected in parallel during the transmitting periods and the group series-tuned by a coil. In the CR system, where the magnetostriction transducer was used mainly, a capacitor was series-connected to each element and these groups connected in parallel during the transmitting period. As the magnetostrictive elements had a low impedance, the tuning coil was placed in parallel with the group.

In addition to having the proper inductance, the coil was designed to meet two other fundamental requirements: first, to have a sufficiently high breakdown-voltage strength, and second, as high a  $Q$  as

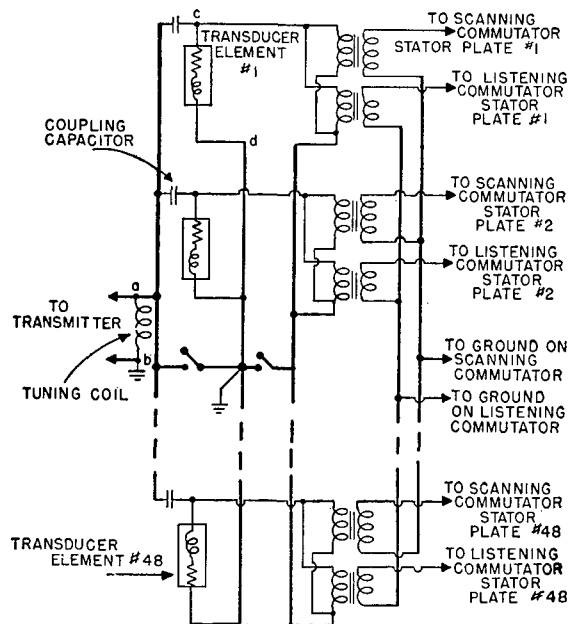


FIGURE 26. Circuit diagram of transfer network of Sangamo XQHA scanning sonar.

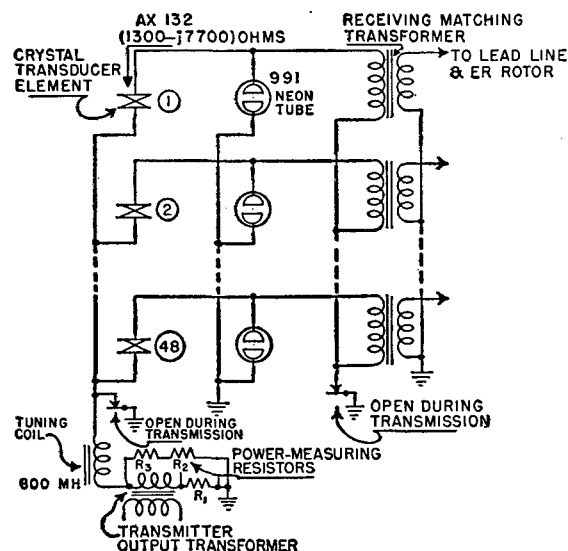


FIGURE 27. Circuit diagram of transfer network, ER submarine scanning sonar system.

CONFIDENTIAL

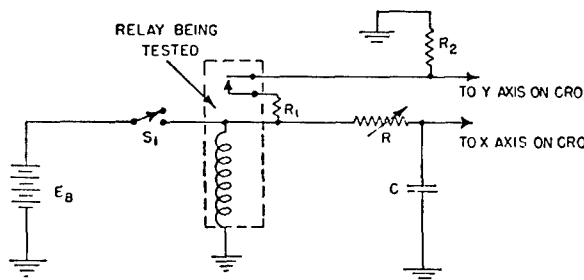


FIGURE 28. Circuit for testing Type A contact-relay operation.

possible. To insure an adequate breakdown-voltage strength, insulation was provided to avoid breakdown between turns, between coil layers, or from the coil to its supporting structure. In order that a minimum of power be lost in the coil, its ratio of reactance to resistance was made as high as possible. This was accomplished by the use of Litz wire, a judicious spacing of the coil turns, and the use of high-permeability, low-loss core materials. It was found that the toroidal type of winding best suited the application. Standard bridge methods of measuring the coil  $Q$  were used.

#### COUPLING OR TUNING CAPACITORS

Mica capacitors having a  $\pm 2$  per cent tolerance and a low drift were used for coupling capacitors to magnetostriction transducers. Their breakdown strength was at least twice the peak signal voltage to which they were subjected in use, plus 1,000 volts. Their losses were negligible at the signal frequency.

Blocking capacitors used in the early transfer networks to pass the signal current and to isolate the d-c polarizing current had low reactance values at the signal frequency in comparison with those of the other circuit elements.

#### POLARIZING CHOKE COILS

In those CR systems which used a d-c polarized transducer, a choke coil was necessary for each transducer element to pass the direct current and to isolate the signal from the polarizing current source. These chokes had an inductance of 4 to 7 mh at the current level used and as low a copper resistance as possible—in the neighborhood of 1 or 2 ohms. The insulation breakdown-voltage was at least twice the peak voltage of the transmission signal as measured on the high side of the choke, plus 1,000 volts.

$RC$  = CLOSING TIME IN SECONDS IF DEFLECTION OCCURS AT  $0.63x$

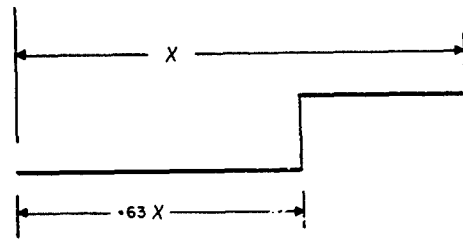


FIGURE 29. CRO trace. Type A contact-relay operation test.

#### RECEIVING-MATCHING TRANSFORMERS

In the CR system, transformers were used to match the low impedance of the individual transducer element with its parallel capacitor to the high impedance of the input circuit of the capacitive commutator. The transformers used were of the closely coupled type with the windings placed on a thin lamination core in such a way that the leakage inductance was at a minimum. Before installation, each was tested for proper impedance ratio, phase shift, and d-c resistance. When the transformers had a center tap on one winding, this was also checked. The tolerances were held to 1 per cent.

In the ER system with a crystal transducer, a transformer was used to match the high impedance of the crystal element to the low impedance of the ER lead line, so that in effect the transformer and transducer element became one of the mid-shunt elements on the line. These transformers were of the toroidal-wound type using high-permeability dust cores. Their coupling coefficient was somewhat lower than those used in the CR system. After fabrication, each was subjected to tests to check its primary and secondary inductance, coupling coefficient, and winding  $Q$  at the operating frequency. Test procedures followed those commonly used with an impedance bridge.

In addition to the above tests, the phase-shift and voltage-ratio characteristics of these transformers were checked in the following manner: the primaries of all the transformers to be used in one set were connected in parallel and to a common signal supply. One side of all the secondaries was connected to a common ground. The voltages appearing across the secondaries were then compared for phase and magnitude by means of a CRO. All secondary voltages should, of course, be equal in these two respects.

CONFIDENTIAL

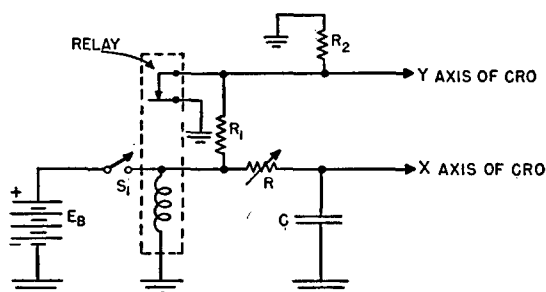


FIGURE 30. Circuit for testing Type B contact-relay operation.

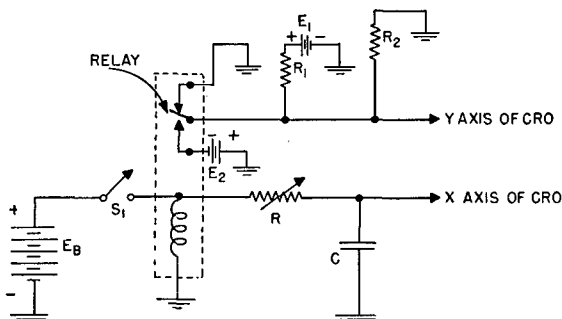


FIGURE 31. Circuit for testing Type C contact-relay operation.

### RELAYS

In both the ER and CR systems, relays were used to effect the change-over of the transducer connections from the transmitting to the receiving circuits. Relays may be classified as having Type A, Type B, or Type C contacts. Type A is the name given to a pair of contacts which are normally open when the relay coil is unenergized and closed when the relay coil is energized. Type B is a pair of contacts which are normally closed, and open when the relay coil is energized. Type C is a single-pole, double-throw type of switch, having three contacts. When the relay coil is energized, the first and second pair of contacts open, and the second and third contacts close.

Each relay unit used in a transfer network should be tested for contact resistance, time of opening and closing of contacts, and sequence of contact operation. Contact resistance may be tested by an ordinary ohmmeter. Figure 28 shows a circuit used to determine the closing time of a Type A contact relay. When the switch or hand-key  $S_1$  was closed, the battery voltage  $E_B$  was impressed across the relay coil and also across the RC circuit to charge the capacitor  $C$ . The horizontal deflection on a CRO was proportional to the voltage on this capacitor. The Y axis input of the CRO was connected through the relay contacts and the resistor ( $R_1$ ) to the relay-coil side of the key,  $S_1$ .

When the relay contacts closed, a positive deflection, whose magnitude depended upon the battery voltage and the values of  $R_1$  and  $R_2$ , was applied to the Y axis input of the oscilloscope (see Figure 29). By proper calibration of the deflection on the cathode-ray tube, the time of closing of the contacts could be determined.

The circuit shown in Figure 30 was used to test the

time of opening of the Type B contact relay. The same procedure was used as that described for testing the Type A contact relay. The trace on the CRO screen was similar to that shown in Figure 29.

The procedure for testing the Type C contact relay is somewhat more involved. The circuit used is shown in Figure 31. When the switch  $S_1$  was closed, the relay coil was energized, and the sweep started in the same manner as in the previous cases. After the coil was sufficiently energized, the upper contact opened, giving a positive pulse to the Y axis of the CRO. When the lower contact closed, the Y axis of the CRO received a negative pulse. If  $E_1 = E_2$  and  $R_1 = R_2$ , the trace on the CRO screen would be similar to that shown in Figure 32. The time required for contact No. 1 to open is shown as  $T_1$ , and the time after this until contact No. 2 closed is shown as  $T_2$ . These times were determined from the time constant of the RC circuit producing the horizontal deflection.

To test the sequence of operation of two Type A contacts, the circuit shown in Figure 33 was used. If  $A_1$  closed first, there would be deflection in the negative direction on the oscilloscope as shown in Figure 34. If  $A_2$  closed first, the pulse deflection would be positive, as illustrated.

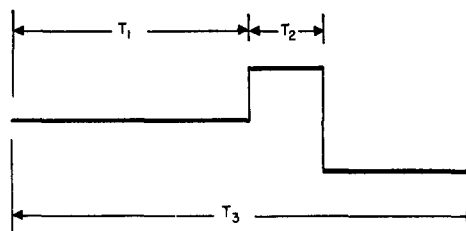


FIGURE 32. CRO trace, Type C contact-relay operation test.

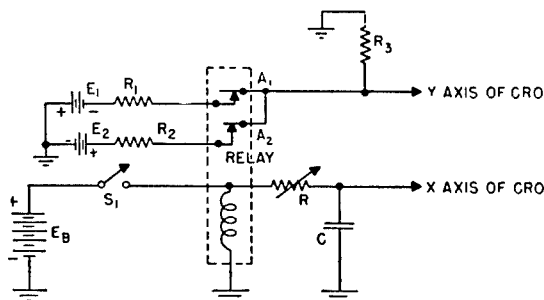


FIGURE 33. Circuit for testing sequence of operation of two Type A contact-relays.

To check the sequence of operation of two Type B contacts, the circuit of Figure 35 was used. After  $S_1$  was closed, if  $B_1$  opened before  $B_2$ , a positive pulse was applied to the Y axis. If  $B_2$  opened before  $B_1$ , a negative pulse was applied to the Y axis. The two possible CRO traces are shown in Figure 36.

The foregoing discussion on the testing of single and double A, B, and C types of relay contacts describes only one way to perform these tests. Another method of testing relay operation and time of opening or closing of contacts made use of a time interval meter. The General Electric time interval meter (Catalogue No. 8014478G1) proved quite satisfactory for this purpose.

### 8.3.3 Tests on Complete Transfer Network

In testing the operation of any scanning sonar the three following items pertaining to the operation of the transfer network were measured or checked:

1. The power factor and magnitude of the input impedance of the transfer network as seen by the transmitter.
2. The power input to, and power output of, the transfer network during the transmitting period, and its transfer efficiency.

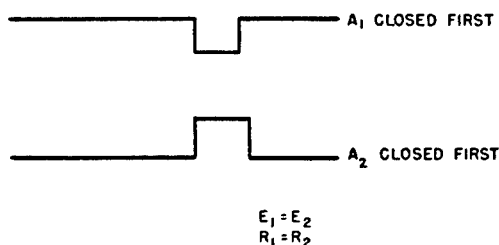


FIGURE 34. CRO trace, two Type A contact-relays sequence of operation test.

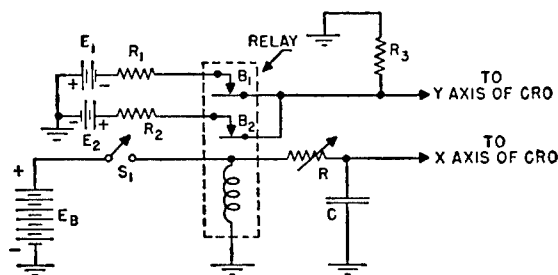


FIGURE 35. Circuit for testing sequence of operation of two Type B contact-relays.

3. The degree to which the network prevented the transmitted signal from entering the receiving circuits of the commutator or being picked up by them.

In the CR system the following procedures were used to check the above items:

1. A calibrated series resistor  $R_1$ , very small compared to the transmitter load impedance, was inserted in the line between the point  $b$  (see Figure 26) and the transmitter output, and a voltage divider in the form of two calibrated resistors,  $R_2$  and  $R_3$ , was bridged across between the points  $a$  and  $b$ . The series resistance  $R_2$  and  $R_3$  should be at least twenty times the transmitter load impedance, and the ratio  $R_2/(R_2 + R_3)$  about one-tenth. The voltages appearing across  $R_1$  and  $R_2$  were applied to the X and Y input deflection circuits of a CRO. From the resulting Lissajous figure (ellipse), the power factor was calculated. Proper tuning is indicated when the ellipse appears as a line or nearly so.

2. Proper calibration of the deflections of the CRO allowed determination of the voltage across the network input circuit and the current into the transfer network. The power input was then calculated from the expression  $P = EI \cos \theta$ . The transfer network input impedance was  $E/I$ .

The power input to any transducer element was found in the same way, that is, by bridging the voltage divider across any transducer element — for example, across the points  $c$  and  $d$  (Figure 26), and

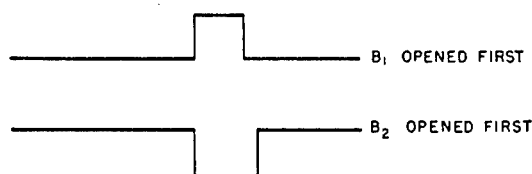


FIGURE 36. CRO trace, two Type B contact-relays sequence of operation test.

by inserting  $R_1$  in series with the element. Assuming uniform transducer elements, the total power output of the transfer network was that measured for one element times the number of transducer elements. The transfer network efficiency is a ratio of the power output to the power input. As described elsewhere,<sup>1</sup> the acoustic power delivered by the transducer may be found by means of a calibrated monitor hydrophone at a known distance; and the efficiency of the transducer found from the ratio of output acoustic power to electric input power. The efficiency of the transfer networks was usually 75 per cent or higher, but the overall efficiency of the combination was between 10 per cent and 40 per cent depending on the type of transducer, crystal transducers having the higher values.

3. To check the third item, a high-impedance voltmeter was connected across the secondary of any one of the commutator input transformers. The voltage appearing across the secondary during the transmitting period indicated how effectively the receiving channels were isolated during this period. No criteria have been established as to the allowable maximum value of this voltage. Certainly it should be sufficiently low to prevent any sparking between the capacitive commutator plates during the transmitting period.

In ER sonar the above items were measured similarly except for the transfer network output power. Since the crystal elements had a very high impedance, it was not feasible to attempt to measure their current input experimentally. The voltage across the element was determined by a high-resistance voltage divider and a calibrated CRO, and the current and power input calculated from the known electric impedance. Figure 27 shows where the resistors  $R_1$ ,  $R_2$ , and  $R_3$  were connected to measure the network input power.

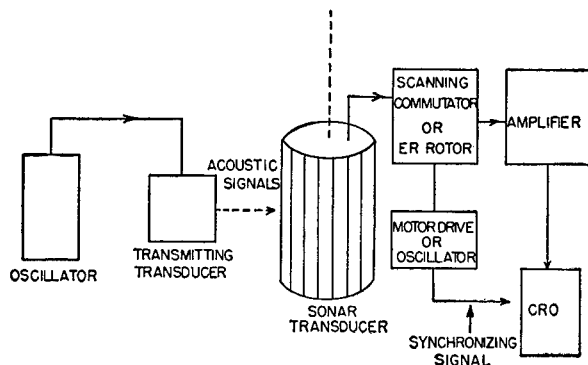


FIGURE 37. Block diagram of circuit arrangement for obtaining receiving patterns in high-speed scanning.

One other necessary check in regard to the ER sonar transfer network was to see that all protective neon tubes were conducting during the transmitting interval. An indication of the uniformity of their voltage-drops was given by measuring, by means of a calibrated CRO, the voltages appearing across the secondaries of the various matching transformers in the receiving circuit during the transmitting interval.

#### 8.4 ACOUSTIC RECEIVING PATTERNS AND NOISE TESTS—COMMUTATOR AND TRANSDUCER

Because the connections between the transfer network and commutator components were so complex, and because the resultant performance of these two components was so dependent upon their mutual interaction, it was found desirable in the development work to test these components together.

In testing the combination of transducer, transfer network, and commutator (or electronic rotor), it was desirable to determine the following:

1. Receiving beam patterns through the scanning commutator (or electronic rotor) with the sound source in various directions with respect to the transducer (commutator scanning). (Figures 37 and 38.)
2. Receiving beam patterns through the listening commutator as it is rotated, with the sound source in

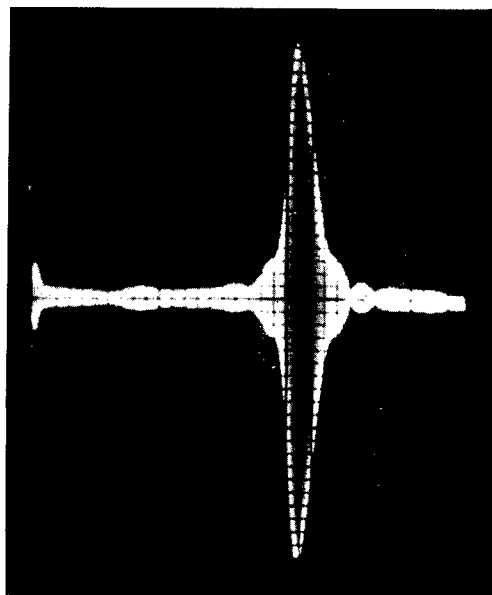


FIGURE 38. ER scanning sonar pattern.

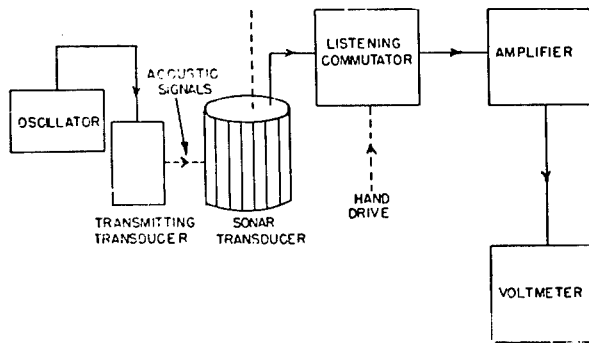


FIGURE 39. Block diagram for obtaining receiving pattern with commutator hand driven.

various fixed directions with respect to the transducer. (Figures 39 and 40.)

3. Receiving beam patterns through the listening commutator with the commutator in various fixed orientations and the sound source moving through a succession of directions with respect to the transducer (transducer rotated). (Figures 41, 42, and 43.)

4. Sensitivity as a function of frequency, in terms of commutator output vs intensity of sound in the water, through scanning and listening commutators. (Figure 44.)

5. Minimum detectable water signal for the scanning and listening commutators (or noise level).

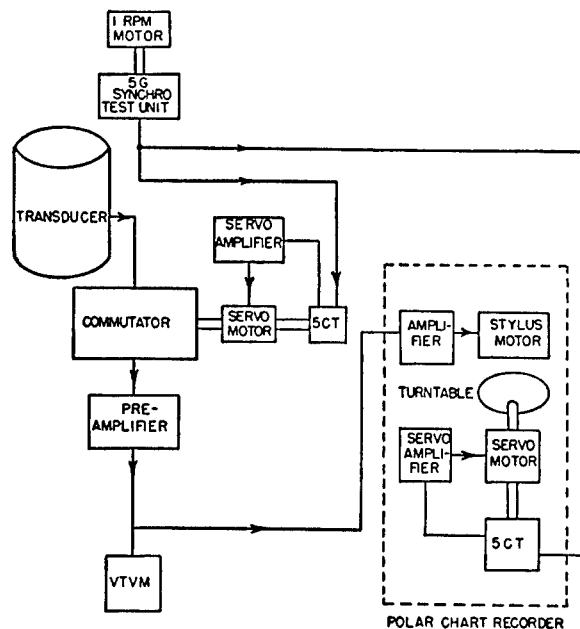


FIGURE 40. Block diagram of circuit connections to portable polar chart recorder with commutator servo driven.

Since these measurements were all based on the use of acoustic signals, a testing station with suitably calibrated equipment was required, just as it was for the acoustic tests of the transducer alone. Since pattern measurements are involved, the pattern measuring equipment needed for the tests of the transducers alone was also required. Figure numbers accompany each of the tabulated items, and the corresponding figures illustrate appropriate test arrangements that were found suitable.

#### 8.4.1 Receiving Beam Patterns with Commutator (or Rotor) Scanning

Following preliminary checks on the beam-forming and rotation equipment, beam patterns were taken on the transducer itself and its associated commutator or rotor by the transmission of an acoustic signal through the water to the transducer, where it was picked up and fed to the commutator or electronic rotor. The test signal was produced by a standard transmitting hydrophone. Equipment used in making these tests has been described elsewhere.<sup>1</sup>

As shown in Figure 37, the electric output from the scanning commutator (or ER rotor) was fed through a flat amplifier to a cathode-ray oscilloscope which had a linear sweep. A signal from the sweep generator on the scanning commutator was used to synchronize the linear sweep so that a stationary pattern could be observed on the scope. When the ER rotor was being tested, the synchronizing signal was obtained from

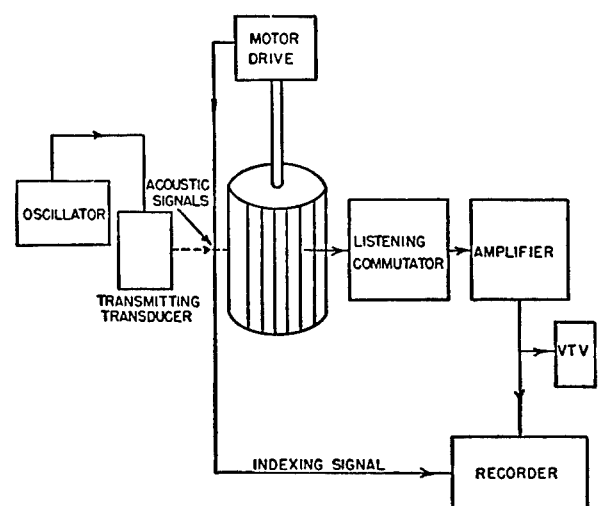


FIGURE 41. Block diagram of circuit connections for obtaining receiving patterns with transducer rotated.

was slowly rotated by means of a servo motor. A sound-level recorder with a rectangular coordinate plot was sometimes used in these measurements.

### 8.4.3 Receiving Beam Patterns through the Listening Commutator with the Transducer Rotating

Figure 41 shows a block diagram of this method of making pattern measurements. The transducer was rotated in steps of 2 degrees to 10 degrees for the point-by-point plotting method, or it was driven slowly by a motor as shown in Figure 42, when a recorder (PPCR or rectangular plot) was used. The commutator was fixed in position in either case. Sets of patterns were taken with the commutator set at different positions. Particular attention was paid to the inter-register positions of the commutator plates to be sure that the commutation process was smooth. Figure 43 shows a typical pattern.

#### 8.4.4 Sensitivity as a Function of Frequency

For comparative measurements of the sensitivity of the transducer – transfer-network – commutator combination, sound was put into the water by means of a calibrated hydrophone driven from a variable frequency oscillator. The output from the scanning commutator (or ER rotor) was fed through a flat amplifier to a cathode-ray oscilloscope by means of

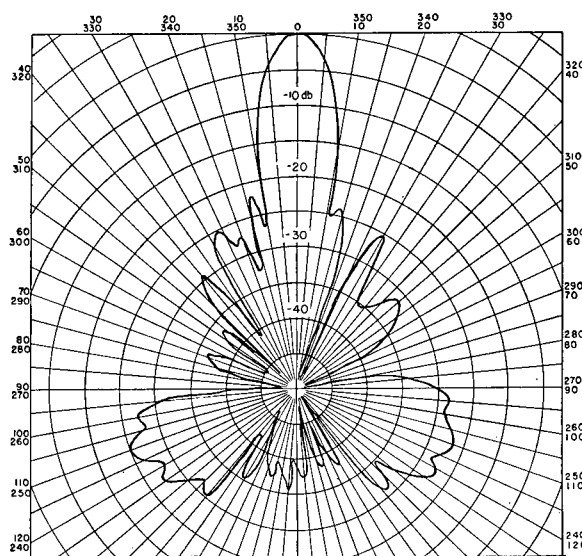


FIGURE 43. Receiving beam pattern taken with CR commutator fixed and transducer rotated.



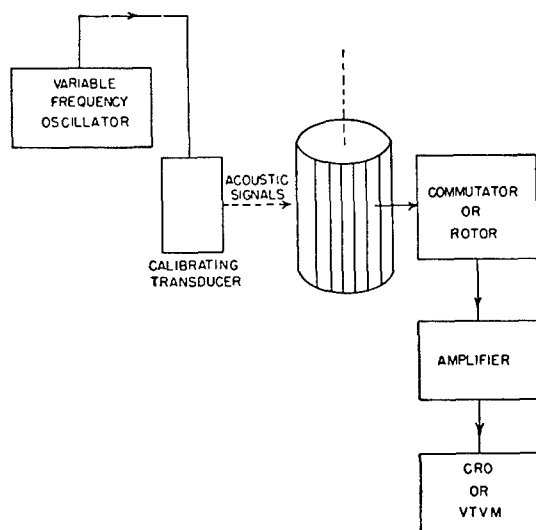


FIGURE 44. Block diagram of circuit connections for obtaining sensitivity measurement.

which the amplitude of the peak of the pattern could be observed. (See Figure 44.) A voltmeter was used in place of the CRO when the listening commutator was being tested. The frequency of the sound in the water was varied until the amplitude of the peak of the pattern was a maximum. This change in frequency affected the pattern shapes somewhat and the working frequency was chosen so as to get the best patterns and the greatest possible sensitivity. Relative sensitivities were usually measured although it was possible to calculate the sensitivity in absolute terms from the known calibration of the standard hydrophone and the distance between the hydrophone and the transducer.

## 8.5 TESTS OF RECEIVERS AND PREAMPLIFIERS

### 8.5.1 Introduction

Certain characteristics of the preamplifier and receiver must be tested to make sure that these units will function properly. Present discussion is confined to the tests to be made before installation of complete sonar equipment on a ship. A properly functioning preamplifier will accurately reproduce the signal at its input. Similarly, a satisfactory receiver will properly transmit the signal applied to its input circuit and modify this signal to forms suitable for both audible and visual indicators. Certain requirements

and prohibitions may be specified for both units: (1) excessive noise, distortion, blocking, cross-modulation, and instability should not accompany the reproduction of the signal; (2) characteristics of the units must not vary appreciably with changes in line voltage, tubes, and ambient conditions; (3) frequency response, gain, phase shift, linearity, input impedance, output impedance, and dynamic range should be within the designed values. In the receiver, the electronic circuits used for control purposes such as *reverberation-controlled gain* [RCG],<sup>12</sup> *time-varied gain* [TVG],<sup>13</sup> *own-doppler nullifier* [ODN],<sup>14</sup> or *automatic volume control* [AVC] should be properly adjusted for satisfactory performance.

Life tests on a representative preamplifier and receiver are highly desirable since they will show the change in operation with time. Sample units should also be subjected to standard acceptance test for humidity, temperature, and vibration.

In order to aid servicing and maintenance after the complete sonar gear is installed on a ship, operating data on the components should be obtained prior to installation. These data should consist of the measured d-c voltages at all tube pins, signal voltages at all significant points with a known value of input signal, output voltage of all local oscillators, and d-c power supply voltages.

### 8.5.2

### Preamplifier Tests

The overall frequency response of the preamplifier should be examined with both steady-state and pulse signals. With correct input and output impedance termination, the steady-state response is obtained by measuring gain as a function of the frequency of an input signal whose amplitude is below any overload point. The response to pulse signals is obtained by measuring gain and reproduction of pulse shape and wave form as a function of the duration of the pulse. This measurement should be made at the nominal operating frequency of the sonar gear with a calibrated CRO.

To measure linearity, the amplifier output voltage may be measured as a function of the input signal voltage at the nominal operating frequency, from zero to above the overload point. The linearity test also suffices as a measurement of dynamic range.

To determine noise level, a root-mean-square voltmeter is connected to the output through an auxiliary measuring amplifier of satisfactorily low noise level,

while a signal source of low internal impedance is applied in series with the first grid resistor. The input voltage is then increased until the output rises to  $\sqrt{2}$  times its value with zero input. This input voltage is the equivalent noise level. For this test a vacuum-tube voltmeter can be used as a root-mean-square voltmeter without appreciable error.

The four sources of noise within the preamplifier are thermal agitation, shot effect, microphonics, and hum from the power supply. An attempt should be made to classify and reduce these sources as much as possible. If the measured output voltage decreases when the first grid resistor is short-circuited, the decrease represents the percentage of noise created by thermal agitation in that resistor. The effect on noise level of mechanical vibration of the preamplifier should be noted. A cathode-ray oscillograph may be used to estimate roughly the amount of hum voltage in the noise. Stray magnetic and electric fields from an external source should not be present.

The phase shift through the preamplifier is important when a preamplifier is to be used in each of the two channels of a *bearing deviation indicator* [BDI] receiving system, since the phase shift through one BDI channel must be equal to that through the other over the operating frequency range. The phase-shift measurement in the preamplifier can be made by use of a standard lag line and a calibrated CRO, or by a calculation from the Lissajous figure on a calibrated CRO.

The differential phase shift between the two preamplifier units may be checked easily in the following manner: a calibrated CRO is used, the output of one preamplifier is connected to the CRO Y-axis input, and the output of the other is connected through a standard lag line to the X-axis input (see Figure 45). The preamplifier inputs are connected in parallel to an audio-oscillator output. The standard lag line is adjusted until the ellipse closes on the cathode-ray tube screen. Its phase reading then gives the difference between the phase shifts through the two preamplifiers. The entire procedure, including the calibration of the CRO, should be repeated in steps throughout the sonar frequency range.

For satisfactory BDI operation, the gains of both BDI preamplifiers for all sonar frequencies must be equal. The checking of this requirement is implied in the steady-state frequency-response measurement which has been discussed previously.

The stability of the preamplifier should be checked

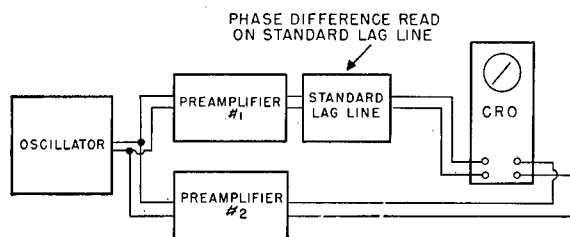


FIGURE 45. Circuit arrangement for testing differential phase shift through two amplifiers.

over the allowable range of a-c line-voltage variation. Gain, linearity, and output impedance are measured as functions of the line voltage to check stability. Any undesirable actions such as oscillations, periodic blocking of tubes, or cross-modulation should also be investigated, at the two limits of line voltage.

### 8.5.3

## Scanning Receiver

The overall frequency response of the receiver should be examined for a steady-state, or continuous, signal and for pulse signals. With correct input impedance termination, the correct setting of the unicontrol oscillator, and normal gain-control setting, the continuous signal response may be obtained by measuring gain as a function of the frequency of the input voltage, which is held constant and below the overload point. It is highly desirable that maximum response is obtained at the nominal sonar operating frequency. Another steady-state response, which gives mainly the characteristics of the r-f band-pass circuits, may be obtained by measuring gain as a function of the unicontrol setting, with the input signal held at the sonar operating frequency.

The frequency response to pulses may be obtained by measuring gain, and by reproduction of the pulse shape and wave form as provided by the signal-pulse generator through an artificial transducer and a test scanning commutator. This measurement should be made at the sonar operating frequency and with the use of a calibrated cathode-ray oscillograph. It is also adequate as a measurement of overall gain, if it is repeated for different settings of the gain control. The gains of the individual stages—r-f, 1st detector, i-f, 2nd detector, and cathode-follower stage—should be obtained also in order to check completely the operation of each receiver component. For the same reason, a point-to-point check of d-c voltages should be made. These component tests are highly desirable, for

the receiver may appear to be satisfactory in overall operation even though one or more components are not functioning as designed.

In measuring linearity the output voltage is recorded as a function of a steady-state input voltage of sonar operating frequency, from zero to above the overload point. If this procedure is repeated for gain settings throughout the control range, it serves as a measurement of dynamic range and noise.

In making noise measurements on the receiver, the output voltage may be measured with a d-c voltmeter. The input signal should have very low internal impedance and should be inserted in series with the proper input terminating impedance. The input voltage which produces a d-c voltmeter reading of  $\sqrt{2}$  times its reading with zero input is the equivalent noise level. As in the preamplifier tests, an attempt should be made to classify the noise and measure the contribution from each noise source.

The calibration of the unicontrol oscillator dial should also be checked. It is usually convenient to measure and calibrate the frequency of the local oscillator by comparison with some previously calibrated secondary standard, using the Lissajous method. If, in the frequency response tests, the peak response is obtained at the correct sonar operating frequency, the calibration of the unicontrol oscillator then checks by inference the frequency characteristics of the r-f and i-f stages. For a more complete check, however, the frequency response of the r-f stage alone may be measured. This response can be obtained by measuring the r-f output voltage as a function of the input frequency.

Improper termination of the output filter or of the r-f or i-f band-pass filters may result in the generation of damped transient oscillations when subject to pulse-type signals. It is highly important, therefore, to investigate the transient response of the receiver. This investigation requires an input signal in the form of a square pulse whose amplitude, duration, and signal frequency are variable. Under these different conditions of input pulse signal, the receiver output signal may be observed with a CRO to study its transient behavior.

Parasitic oscillations in the receiver sometimes occur, either continuously or only under certain input signal conditions. In many cases the parasitic frequency is so high that the oscillations cannot be detected with the use of a CRO or a vacuum-tube voltmeter. Frequently, however, the operation of the re-

ceiver is acceptable even when the oscillations exist. An effective test procedure is to measure the voltage at the output and individual stages of the receiver throughout the entire frequency spectrum to an upper limit of 300 to 500 megacycles. For completeness, the test should be made with different levels of continuous input signal, with different settings of gain control, and at the allowable limits of a-c line voltage.

One type of cross-modulation or cross talk exists only in dual-channel receivers. The scanning and listening receivers of the XQHA gear, for example, are located in the same chassis. It is therefore necessary to check the magnitude of the unwanted signal in the scanning-receiver output which is picked up from the listening receiver. This type of cross talk may be expressed as the ratio of scanning-receiver input voltage required to produce a certain scanning-receiver output voltage, to the listening-receiver input voltage that will produce the same output voltage in the scanning receiver. This measurement must be made at the correct sonar operating frequency.

Input voltage, current, and phase angle should each be measured as a function of frequency to determine the receiver's input impedance and its frequency characteristic. With correct input-impedance termination, the measurements can be made by a method similar to that used in measuring the output impedance of the preamplifier.

Reverberation-controlled gain<sup>12</sup> is a circuit arrangement whereby the gains of the receiver are decreased greatly at the instant of transmission. The receiver gain will be rapidly restored unless reverberation is present, in which case the gain restoration will be modified to correspond with the persistence of the reverberation. This circuit provides, in effect, a TVG circuit with time constant depending upon water conditions.

From the above general description of RCG, it will be seen that it is convenient to test only the two limiting conditions of operation during preinstallation tests. One limiting condition is obtained when there is no output from the receiver at the end of the keying impulse, thereby allowing the most rapid restoration of gain. The other limiting condition is obtained by applying to the control point of the RCG circuit, in place of reverberation, a steady signal of such magnitude that the slowest restoration of gain is obtained. A calibrated CRO is used to measure the control voltage from the RCG circuit, and to determine the rate of restoration of gain.

## 8.5.4

**Listening Receiver**

The same tests described in the foregoing section on scanning receivers should be made on the listening receiver, but with some modifications and additions. All these tests are made with the ODN switch in the off position. The overall frequency response to pulses of sonar frequency should be measured using a pulse generator whose output pulse is of the designed duration.

In addition, the operation of the beat-frequency oscillator, the audio band-pass filter, and ODN should be tested. The operation of the beat-frequency oscillator is checked by observing that a suitable audio frequency of proper amplitude is obtained throughout the range of operation of the receiver, with ODN off.

The audio band-pass filter should be tested as an individual component by measuring gain through the filter as a function of the frequency of signal inserted in series with the filter input impedance. This test may be performed with the receiver power supply turned off.

The ODN<sup>14</sup> circuit operation can be tested by measuring the audio output frequency as the receiver input frequency is varied. The test should be repeated for different levels of input signal throughout the expected range of reverberation level. It will be necessary to supply a recurrent keying pulse that is the same as the pulses which exist when the complete sonar equipment keys. For each input frequency the pulses must be applied at the proper terminals before the audio output frequency is measured a short time later. The time allowed to sample the introduced reverberation signal should also be measured by determining the length of time between the opening and closing of the relay or device which operates at the start and end of the sampling period.

## 8.5.5

**Sum-and-Difference BDI**

A BDI receiver consists essentially of two channels that are nearly identical. With the exception of the last two BDI stages and the audio output stage, each channel performs as a single-channel listening receiver. The next-to-the-last stage consists of a phase detector where signals from the two channels are combined, and the last stage is the deflection amplifier.

Both BDI channels, up to the input of the phase

detector and the audio output stage, should be given the tests discussed under Section 8.5.4 above. In addition to these tests, a check should be made on the balance in the two channels. For complete balance up to the input of the phase detector, linearity, phase shift, frequency response, and gain of both channels must be the same within specified tolerances.

In order to test the last two BDI stages, the measurement of a BDI deflection curve is necessary. A special device, such as the *artificial projector*, is required to make the test.<sup>8</sup> When used to simulate the receiving function of a split projector, the device furnishes to the connected circuit (BDI receiver) signals like those generated in an actual projector when receiving sound from a distant source, with proper dependence on projector rotation. With the artificial projector and auxiliary equipment providing input signals to the BDI receiver, a BDI deflection curve is obtained by recording d-c output voltage as a function of the angle of rotation of the artificial projector. Deflection curves should be obtained for values of input signal from zero amplitude to the overload point for a particular gain setting. This test should be repeated several times between the minimum and maximum setting of the gain control.

## 8.5.6

**Preinstallation Production Tests**

Preinstallation production tests necessarily include most of the tests already discussed. After the first few units of a production run have been tested completely, the total number of tests on succeeding units may be reduced. For instance, linearity may be tested at the minimum and maximum gain settings, thus being checked by inference throughout the gain control, rather than being tested at, for example, ten specific settings of the gain control. Moreover, it is possible to achieve several test objectives with one general test procedure. Testing for linearity may be combined with the measurement of noise level. By measuring overall gain as a function of frequency, with the use of a square pulse of sonar frequency at the input signal, three objectives are obtained: (1) measurement of overall frequency response, (2) measurement of gain, and (3) test of response to transients. It may be necessary only to determine the d-c power-supply voltage as a function of a-c voltage, rather than to check stability of gain, linearity, local oscillator frequency calibration, etc., as a function of



1. A cathode-ray oscilloscope having a moderately long-persistence screen (preferably a 5-inch tube). If the display on the screen is to be photographed, the screen should be an actinic-blue short-persistence type. The oscilloscope should be carefully calibrated over the sonar frequency range.

2. Calibrated voltage dividers are needed as the measurement of pulse voltages well beyond the range of the usual oscilloscope input circuits is frequently necessary. Noninductive carbonized resistors furnish the most convenient means of building up a voltage divider. Their wattage rating should be sufficiently great to preclude heating and subsequent change of resistance, and the overall resistance of the divider should be sufficiently high that it does not disturb materially the circuit being measured.

3. A simple heterodyne receiver of the type shown in Figure 46 for listening to the transmitter output. The local oscillator in the receiver should be well shielded and isolated from the input circuit by a buffer amplifier to prevent feeding a high-frequency signal back into the circuit being tested. Very little gain is required in the receiver since the signals to be studied are usually of comparatively high level.

4. Some type of pulse generator as an input keying-pulse simulator for keying the transmitter during various stages of the test program. If grid bias, plate, or other power supplies are needed which are external to the transmitter unit being tested, the input keying-pulse simulator should incorporate these so that an interconnection to the simulator will cause the transmitter to operate as if it were connected to the system of which it is a part.

5. The usual electrical measuring equipment such as oscillators, high-resistance d-c voltmeters, vacuum-tube voltmeters, etc.

Procedures in making many of the above-mentioned tests on the transmitter components follow known orthodox methods and do not require discussion here. However, certain tests peculiar to sonar pulse transmitters are described here.

### 8.6.2 Output Power Measurement

While noninductive resistors are useful as loading elements while the transmitter power output is being checked, it is often desirable to use a simulated transducer with its impedance-matching network. The simulated transducer impedance should have the same resistive and reactive components as the actual

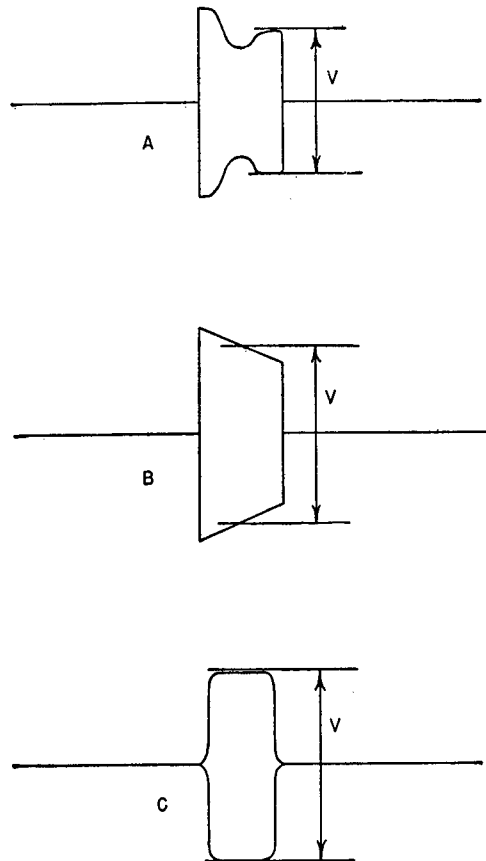


FIGURE 47. Representative pulse shapes.

transducer to be used with the transmitter unit under test, and should be capable of handling the power fed to it. In this manner the impedance-matching network, output transformer, protective devices, etc., can be tested along with the transmitter.

When determining the power output by using a calibrated CRO to measure the voltage amplitude of the output pulse into a known load resistor, it must be kept in mind that the pulse shape is not regular. Consequently, as power is proportional to the square of the voltage, the value of the power thus determined will vary widely, depending on the point on the pulse envelope at which the voltage is measured. To prevent any ambiguity regarding this measurement, it has been the custom to take an average value of the pulse voltage. In Figure 47, showing several common types of pulse envelopes, the points which are generally selected as average amplitudes are indicated; the choice of the point in any type is entirely arbitrary. The peak of the pulse should not be used

in determining power since such value will give an indicated power output considerably greater than the true value. For this reason, the use of a crest voltmeter to measure pulse voltage amplitudes is not feasible. In a series of power measurements, the same point should be selected throughout and indicated in the data report.

As previously mentioned, the output power should be measured for different tuning adjustments over the sonar frequency range and also as a function of the load impedance. The output impedance for the greatest power output should be determined, if the output transformer design has not been frozen, or if different power tubes are being studied. If definite specifications have been set up for power output versus ping rate, or if power-supply voltage-recovery rate is being changed, a measure of the output at various ping rates may be necessary. In systems intended to be used over a comparatively wide frequency range, the transducer characteristics may be such that only a small portion of that range is likely to be used; in this case a transmitter should be adjusted for optimum operation over that limited range.

### 8.6.3 Power and Current Input Measurement

Owing to the pulse-type operation of a sonar transmitter, usual methods of measuring plate power input to the final amplifier are inadequate. As its plate supply utilizes the energy storage principle, the plate voltage will vary over the ping period from a high initial value to a lower value at the end of the period. To measure the plate voltage over this short period, the calibrated CRO with its voltage divider is used. The initial and final values of the supply voltage are determined from the CRO screen pattern and the power input to the plate circuit of the final power amplifier is computed from the equation

$$P_{in} = \frac{1}{2}C [E_1^2 - E_2^2] \frac{1}{T}$$

where  $C$  represents the total capacitance of the storage capacitors,  $E_1$  and  $E_2$  are the initial and final values of the plate supply voltage during the ping period, and  $T$  is the length of the transmitted pulse.

Screen and plate currents of the driver and final power amplifier tubes may be measured by using a small calibrated resistor placed in the circuit whose current is to be determined, and a CRO to measure

the amplitude of the voltage pulse across the resistor. In the power amplifier stages employing certain tetrodes (Type 715B), it will be found that the screen current increases abruptly as the excitation voltage is raised above a critical value. The screen current measurement is therefore of value in determining the proper amplitude of the grid driving voltage.

The overall 60-cycle power consumption of the transmitter may be determined in the usual manner. The power factor should be checked and, if it is excessively low, power factor correction applied.

### STABILITY

Transients of any kind are to be avoided by correct circuit design and adjustments. Parasitics and regeneration can usually be detected in the output pulse by the use of a high enough sweep rate in the observation CRO. Experience will make it possible to distinguish between distortion of wave form caused by normal variations in envelope shape, and variations caused by parasitics and regeneration effects. In the latter case the wave form may be so poor that it is impossible to synchronize the sweep. Variations in envelope shape as indicated in Figure 47A and B show up as haziness of outline on the upper and lower peaks of the pulse, while parasitics or regeneration are indicated by a general "hash" not recognizable as any definite pattern.

In studying frequency stability of the transmitter oscillator, a suitable standard of frequency is needed for comparison. Usually a stable variable interpolation oscillator that has been previously calibrated may be used to check the transmitter frequency in conjunction with a CRO, following the Lissajous figure method.

In those sonar systems using unicontrol where the frequency of the whole system is controlled from the receiver unit, the oscillator in the transmitter must have a high degree of stability to insure proper operation of the receiver, and, moreover, the output of the converter stage must be high enough to give sufficient excitation on the succeeding amplifier stage, and must be free from harmonic distortion. This last qualification must be verified by thoroughly testing the band-pass characteristic of the filter associated with the converter. A standard calibrated oscillator and vacuum-tube voltmeter are the chief pieces of equipment needed to make these tests.

In a short-pulse system that uses frequency modulation, the frequency of the oscillator, which may also

be the sonar signal frequency, is usually modulated by means of a reactance tube (see Chapter 7). In general, frequency modulation is difficult to study in a short-pulse-length system. However, it will be frequently found that the voltage output of the frequency-modulated oscillator will vary as the frequency varies, affording thereby an approximate measure of the frequency change if the output voltage of the unit has first been calibrated against frequency with the oscillator operating continuously. A heterodyne receiver is useful in working with frequency-modulated signals if the pulse is sufficiently long (20 to 30 msec). Frequency modulation of short pulses can often be detected by noticing that the tone of the pulse does not vary as the heterodyne receiver is tuned past the center frequency of the pulse. The variation during the pulse of the d-c control voltage on the reactance-tube grid may be measured with an oscilloscope and compared with a plot of frequency-versus-control grid bias voltage, determined by varying the grid voltage with a potentiometer and measuring frequency at convenient points while operating the oscillator continuously. It is also possible to place the oscillator output on the Y axis of an oscilloscope and the reactance-tube grid bias voltage on the X axis amplifier for sweep control. The pattern thus obtained (see Figure 48) can be used to determine whether or not the frequency sweeps far enough during the ping interval. The intensity of the dot at the right end of the trace increases as the length of time the spot remains at the right increases. For this test, the X-axis amplifier must be calibrated in order to determine the total variation of bias voltage from the beginning to the end of the pulse. This variation is then compared with the frequency-versus-bias characteristic of the reactance tube, and the frequency variation is thereby determined.

Operation of the transmitter over a wide range of supply voltages must be checked to ascertain that cut-off bias and other possibly critical voltages remain within acceptable limits, and that the performance is satisfactory (if not optimum) under all expected conditions of operation.

If the transmitter design involves the building of special parts—transformers, coils, and so on—tests should be made on insulation breakdown, operation at high temperature and humidity, life expectancy, and suitability of general design.

Production tests, aside from the usual manufacturing procedures of complete parts inspection and cor-

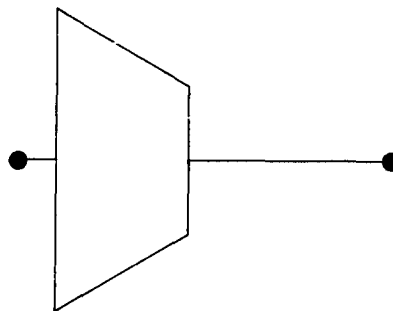


FIGURE 48. Oscillator output versus control grid bias on reactance tube.

rect connection checks, should involve the use of an input test set that will simulate the operation of the remainder of the sonar system as well as be an actual interconnection with the other units of the system. The power output, frequency, and pulse shape and length of the transmitted pulse should be measured and compared with the acceptable values determined by previous experiment on a prototype model.

## 8.7

## INDICATOR TESTS

### 8.7.1

### Spiral Sweep Tests

The indicator unit contains the *plan position indicator* [PPI] tubes, their associated power-supply circuits, various synchro units associated with the cursor controls, and other circuits, according to the type of sonar system. The details of testing and checking the PPI spiral-sweep and pulse circuits are discussed in the next section of this chapter. In the slower-speed CR scanning sonar, the linearity of the sweep may be checked by increasing beam intensity until the individual spirals are visible and then observing whether the turns are equally spaced from the beginning to the end of the spiral. In a high-speed scanning system, such as the ER sonar, an a-c brightening signal, whose frequency is a multiple of the rotation frequency, can be applied to the PPI control grid so that brightening will occur at even time intervals from the beginning to the end of the sweep. Uniformity of the spaces between the brightened turns can then be verified, and at the same time, the range start and range limit checked for all range settings, to make sure that the spiral begins and ends at the proper place. Methods of checking these two limits are outlined in the next section.

The circularity of the spiral should be checked



next. This can be done by applying a constant voltage to the spiral-sweep generator field or expander tube, so that a circle of constant radius is produced on the PPI. Excitation should be varied so that the circularity of the sweep at several diameters may be checked. Where range is to be determined from a measure of the spiral radius, the circle must be exact, but if a range recorder is used, circularity of the spiral is not so important.

Due to the higher tangential speed of the electron beam at the outer edge of the scope, the trace will be less intense there than at the center, if no compensating method is employed. Where compensation is used, it should be checked by observing the uniformity of the spiral intensity with the PPI screen. Observation of the intensity at the end of the spiral should be sufficient to check the beam intensity.

The deflection of the electron beam in the cathode-ray tube is affected by stray 60- and 120-cycle fields around the tube and deflection circuits. This is made evident by the periodically uneven spacing of the turns of the sweep, which, in the high-speed scanning system where the turns are very close together, may produce the apparent effect of uneven brightening.

The focus and intensity controls for the indicator tube should be checked to make sure that the operating position is near the center of the potentiometer and that there is sufficient range on both sides of the operating position to allow for variations which might arise from changes in line voltage, from surrounding light conditions, etc. The receiver should overload by the time the intensity of the scope trace reaches its greatest value.

If the indicator under test has an electronic cursor, this should also be observed to be sure that it follows properly and has the right intensity limits.

The blanking pulse usually applied to the cathode of the PPI tube should be checked with an oscilloscope to see that the pulse is of the proper duration and amplitude to produce blanking of the scope during the return of the spiral and pinging period, and for the reverberation immediately following the ping, if that is desired. Tests for checking the timing of this pulse in relation to the sweep are discussed in the next section.

#### 8.7.2 Checking Mechanical Parts

The various mechanical features incorporated in the indicator should be inspected. All the gear trains

should be checked to be sure that there is no roughness or stickiness and backlash. This can be done by operating all knobs and motor-driven parts and turning them several revolutions. Any stickiness should be readily noticed. The servo systems are most easily tested by applying a step function to their input. A step function for a position type of servo consists of a rapid displacement, that is, quick movement from one position to another without any movement immediately before or after. A properly adjusted servo system will follow this movement rapidly, coming to a stop with a very slight overshoot.

The servo system is out of adjustment, however, if it comes to the final position slowly, overshoots excessively, oscillates about the final position, or comes to an incorrect final position. If the final position reached by any mechanically driven part varies when the position is approached from different directions, there is backlash.

The indicator should be allowed to run for several hours to check any possible overheating of the equipment. Various circuit components should also be checked for excessive temperature rise to make certain all are properly designed.

The a-c supply line voltage should be varied over the range tolerated in the design to check the operation of the electronic circuits. Changes of intensity and focus of the beam, or variations in the radius of the spiral sweep, etc., with variation in the line voltage should be noted and corrected. With proper design and construction, slow variations in line voltage should have little effect on the intensity or focus of the beam or on the spiral-sweep rate.

### 8.8 SWEEP CIRCUIT AND KEYING CIRCUIT TESTS

Various factors which influence the performance of the sweep and keying circuits are noise (including hum and signal harmonics), changes in line voltage and frequency, temperature, humidity, change of components, stray fields, and switching operations in other parts of the equipment.

For many tests on these circuits, a d-c voltmeter and a Ballantine voltmeter covering the sonic range are adequate. The most useful instrument however is a CRO, since with it, wave form, length and amplitude of pulses, and synchronism between pulses are all measured. For certain measurements on time intervals, a time interval meter is useful.

## 8.8.1

**Sweep Circuit Tests**

The PPI sweep should be circular and accurately centered on the screen. Its radius should increase linearly with time and the flyback period must be synchronized with the transmitting interval. To determine the general performance of the spiral sweep, an inspection of the indicator display is necessary. If a low-frequency voltage is applied to the PPI brightening grid, certain individual spirals of the sweep, depending upon the brightening frequency, can be made to stand out so that both their circularity and linearity of spacing are checked. If the spiral is not circular, tests should be made for stray electrostatic and magnetic fields, and shielding provided when necessary. With a device such as the *dynamic monitor*, or another delayed pulser, an approximate check can be made of the performance of the range-determining circuits as well as of the effect of ping rate upon range and bearing indications. Stability of equipment for both slow and rapid changes of line frequency and voltage should be observed. Performance tests with vacuum tubes and other components that may be replaced during the life of the equipment should be made with components having values at both limits of the tolerance.

**SAWTOOTH SWEEP LINEARITY TESTS**

Relatively few tests have to be made to determine the linearity of the sawtooth sweep circuits, and since only approximate linearity is necessary, the tests consist largely of observations made with a CRO.<sup>15</sup>

Electronic sawtooth sweeps of the capacitor-charging type were designed to be linear over a voltage range from 10 per cent to 90 per cent of the B+ voltage supply, with an error in linearity of from 2 per cent to much less than 1 per cent.<sup>16, 17, 18</sup> In any of the capacitor-charging electronic sweeps, the deviation from linearity can be computed from the change in the charging current with sweep amplitude. The charging current can be determined by measuring the voltage across the charging resistor through which the current flows. If this voltage remains constant, the charging current will be constant and the sweep will be linear. If the charging current dies off exponentially, the extent of deviation from linearity of the sweep can be computed from the various voltage measurements by a method outlined in Puckle's *Time Bases*.<sup>19</sup>

Measurements of the sawtooth varying voltage itself, with the usual test instruments, are useful. A peak voltmeter is satisfactory in measuring the start and finish of the sawtooth voltage.

Static measurements are of some value in testing for linearity. If the supply, start, and finish voltages are measured, the deviation from linearity may be computed as indicated above. If the system utilizes a nonlinear sweep, with compensation in the modulator or in some other portion of the circuit to produce a linear sweep on the PPI, static measurements relating sawtooth sweep amplitude to the diameter of the circle upon the face of the cathode-ray tube may be helpful as an indication of the direction and extent to which the sawtooth sweep should deviate from linearity to give a linear display.

A laboratory CRO that has a *linear time base sweep* is useful in checking sweep linearity. If a direct-coupled amplifier is available, or if the sawtooth sweep amplitude is sufficiently great to be applied directly to the vertical deflection plates, the sweep may be viewed upon the screen of a CRO. The cathode-ray oscillograph can also be used to check the sawtooth sweep in the ER system after it has modulated the circular sweep, but before the sweep is split into polyphase voltages to be applied to the PPI.<sup>20, 21</sup>

In sonar systems, the slow speed of sound propagation makes it essential that as little time as possible be lost between the end of one sweep of the spiral and the beginning of the new one. This means that the sweep capacitor must be discharged at a rate which is considerably more rapid than its charging rate. This is often difficult to do, especially with the large capacitance needed to obtain the necessary magnitudes of the charging current, and because the capacitors are often oil-filled. Oil-filled capacitors are especially undesirable in the sense that the dielectric may be polarized to an uncertain extent, depending upon the capacitor's past history. When oil-filled capacitors are used they should be tested for this defect.

**CIRCULAR SWEEP TESTS**

The circuits or equipment generating the circular portion of the spiral sweep should be so designed that the phase of the spiral sweep is synchronized with the scanning operation to within  $\frac{1}{4}$  degree or better, since that is the desired accuracy of the system.<sup>22, 23, 24</sup> This degree of precision is necessary as the precision of the components of the scanning equipment and

the overall equipment is better than 1 degree.<sup>25, 26, 27</sup> To achieve a circular sweep with this degree of precision, it is necessary that any extraneous signal pick-up in the spiral sweep circuit be about -30 db. Such extraneous signals may be those due to a-c hum, harmonics of the circular sweep frequency, noise, or stray magnetic fields. Tests of the circular sweep should therefore include hum, harmonic, and noise measurements to insure that the level of these spurious components is sufficiently low. Stray magnetic fields can be eliminated by either shielding the magnetic circuits or removing the offending magnetic device from the vicinity of the equipment.<sup>20</sup>

With extraneous signal absent, the circularity of the sweep is assured if each of the polyphase signals is of the same amplitude and of a relative time phase equal to the space-phase relationship of the deflection coils. In the case of the 2-phase sweep generator, both the relative phase and amplitude of the 2-phase voltage may be checked simultaneously by applying one of the phase voltages to the vertical deflection plates of a CRO and the other to the horizontal deflection plates. The resulting Lissajous figure is a circle if the two voltages are 90 degrees in phase and of equal amplitude. If the figure is not a circle, then adjustment should be made. This test is performed with either a low-frequency sawtooth excitation or a d-c excitation on the 2-phase generator field. The phase-splitting network of a 2-phase electronic sweep may be tested by measuring the impedance of each of its components. If the impedance of each branch is equal to the impedance of the opposite branch, the 90-degree phase-relationships should be accurate.<sup>28, 29</sup>

With the ER system, the frequency of the switching-line oscillator is adjusted so that the time taken for a pulse to travel through the switching line is exactly equal to the period of one oscillation, and hence the scanning beam of sensitivity rotates uniformly without a jump between the elements attached to the beginning and end of the switching line. This frequency is maintained at a constant level by a closed-cycle control consisting of a discriminator attached to the beginning and end of the switching line, and a frequency-controlled oscillator (see Chapter 7). The performance of this frequency control is checked by opening the cycle at any point, inserting a signal into the sections following this point, and measuring the response at the other side of the opening. A high ratio of response to signal is desirable, as it provides a stiff control system that keeps the frequency accu-

rate. In the Models 1 and 2 of the submarine system the stiffness was approximately 50. The measurement is most easily made at some point between the output of the discriminator and the input to the reactance tube. A high-resistance voltmeter (sensitive to 1/100 volt) is used for this measurement. The proper operating potential for the line connecting the discriminator to the reactance tube is zero volts at the operating frequency.

The 3-phase circular sweep system used in CR sonar is more difficult to test since 3-phase deflection-coil cathode-ray oscilloscopes are not in common use. However, it might be possible to change to a 2-phase sweep system by means of Scott-connected transformers so that an ordinary cathode-ray oscilloscope could be used.

At HUSL the synchro generator, used for generating the 3-phase voltages for the spiral sweep, was tested statically for phase and amplitude accuracy in the following manner. Its rotor field was connected to a 60-cycle voltage source and its stator was connected to a CT synchro of known accuracy. The test for phase accuracy was to turn the CT synchro until the voltage at its rotor terminals was 0 degrees, and then to read its angular position, which should correspond within  $\frac{1}{2}$  degree to the angular position of the generator. After this point was found, the CT rotor was turned through 90 degrees and a notation was made of the amplitude of the voltage across its rotor terminals. After the above procedure is repeated, the amplitude of this voltage should be the same for all 90-degree test positions. A polyphase generator that responds properly to the above tests should generate a satisfactory circular sweep.

The complete spiral-sweep generating system, together with deflection coils around the cathode-ray tube, is tested as a unit. Two tests may be made. The purpose of the first is to insure that bearing indication is independent of the radius of the sweep. This can be done by attaching a pulse-forming device to the shaft of the scanning commutator and applying the resultant pulse to the brightening circuit of the PPI tube while the sweep is spiraling out. The pulse-forming apparatus may be a contactor that makes contact for only a degree or so during each revolution of the commutator. Correct operation of the sweep-generating system is indicated if the brightened spot on the screen appears always at the same angular region of the spiral sweep.

In the second test the linearity of the expansion of

the spiral in the overall system may be ascertained by applying a low-frequency brightening signal to the grid of the cathode-ray tube, so that approximately ten rings of the spiral sweep are brightened and appear on the screen. If these rings are evenly spaced the expansion of the spiral is linear.<sup>30, 31, 32</sup>

In the case of a circular sweep generated by mechanical means, a check was made to see that there was no whip or backlash in the mechanical coupling. Tests on the commutator driving motor were made to check its constancy of speed with normal changes of line voltage.<sup>33, 34, 35</sup>

### 8.8.2 Timing Circuit Tests

In the testing and adjusting of timing circuits, particularly during their operational intervals, care should be exercised in using time-interval measuring equipment and methods that are sufficiently accurate for the specific application. A clock offers a convenient means of measuring the time intervals between such current operations as keying pulses, provided these pulses do not occur at too rapid a rate to be counted over a fixed period. A special instrument, such as a *time-interval meter* may be used where the time interval is too short for the foregoing method to be employed. A timer of the contact type, driven by a synchronous motor that is fed from a power source of known constant frequency, may also be used.<sup>36</sup> This equipment should have contacts that open and close accurately at intervals corresponding to the desired operational interval of the device being tested.

A slight modification of this type of device exists already in the chemical recorder. Since its motor runs at constant speed when connected to a reasonably stable power supply, the recording pen also moves at constant speed and the distance it travels on the paper is directly proportional to time. This method is sufficiently accurate for measuring the ping interval. When it is not possible to synchronize the recorder with the device being tested, the recorder may be set to a time interval longer than the time interval being measured, so that a pair of marks will be made during each trace of the recorder. Then, for a known velocity of pen travel, the distance between this pair of marks is a measure of the time interval, and the consistency of this length with repeated trips across the paper is a measure of the precision of the time interval.<sup>18</sup>

There are several types of electronic circuits that

may be used for measuring time intervals; one of these is a calibrated trigger circuit, or relaxation oscillator, with a stabilized power supply. This may be used as a time divider for measuring a short interval.<sup>37</sup>

Another electronic method of securing known time intervals uses an integrator circuit equipped with an on-off switch. With constant input, the value of the integral is directly proportional to the time when the input is applied. This mechanism is usually a device for charging a capacitor with a meter attached for reading the final charge upon the capacitor. The device under test is used to switch the integrating circuit on and off.

A third electronic device for determining time intervals is the stabilized oscillator and counter. The oscillator may be operated at any convenient audio frequency; 800 cycles is most convenient, however, since each cycle corresponds to one yard of sound travel in water. The oscillator frequency is stabilized by some means such as a tuning fork. Circuit connections may be made so that the beginning and end of the pulse from the circuit being tested switch the oscillator into and out of an electronic counter. The indicated count then gives the time interval, in milliseconds, microseconds, or "range yards" of the pulse produced by the circuit under test.

The precision with which the keying circuit determines the ping interval may be affected by power-supply voltage, temperature, humidity, and change of components. The above tests should be made with these quantities varied so as to meet the extreme conditions under which operation is expected.<sup>38</sup>

The correctness of the sequence in a system's keying operations can be checked rather completely by turning the equipment on and observing its operation. Such things as bounce and double keying of relays can be observed by connecting a cathode-ray oscilloscope with a slow time-base sweep across the contact of the relay under test. The synchronization of the ping with the blanking pulse may be tested by applying both inputs simultaneously into the vertical deflection input of a CRO. Two 1-megohm resistors are attached to the input terminal of the scope; the blanking-pulse lead is connected to one of these, and a lead wire connected to the other is placed in such a position that it picks up stray energy from the transmitter.<sup>39</sup> Other functions that should occur simultaneously, or within a short time of each other, can be checked by the same method. The sweep rate of the

CRO may be calibrated against the 60-cycle power-supply frequency so as to give a rough indication of the time interval between events or of the duration of an event. In testing the range-change switch, the only test, other than simply trying it with the equipment on, is to check for continuity of the proper circuits for each switch position. Tests of local keying, recorder keying, hand keying, and interlocking of dual systems are best made by trying out the complete systems. If there are no extraneous marks upon the PPI scope, the various timing and interlocking functions are being performed correctly.<sup>40</sup>

The transmitted pulse length can be checked by allowing the screen to be brightened by the transmission of the ping, with the ordinary spiral sweep applied. Proper ping length is indicated by a circle of brightening with no gap and with only a slight amount of overlap.<sup>41</sup>

The brightening and blanking pulses may be checked by means of a scope and a peak-and-trough voltmeter. The CRO is used to measure the duration of the pulse while the peak-and-trough voltmeter is used to measure its amplitude. When only a peak voltmeter is available, it may be used to read the negative peak voltage from a reference level above that of the voltage to be measured.<sup>39</sup>

### 8.8.3

### Range Determination

Test requirements to determine the accuracy of range-determining devices have become more stringent as the need for greater accuracy has increased. The permissible error allowed for a scanning sonar system is at present  $\pm 15$  yards, a quantity which is determined by the depth-charge pattern.<sup>28</sup> For a sub-surface ship the permissible error is only  $\pm 5$  yards, and this is dependent upon the requisite accuracy of the information received by the torpedo data computer.<sup>22, 24</sup>

The accuracy of range determination obtainable with the early systems was inherently limited by the speed of rotation.<sup>42</sup> In the original MR sonar, range determination was probably accurate to within  $\pm 200$  yards. In the latest ER sonar, the rotation rate inherently limits the range determination to  $\pm 1$  yard, or even less, but the sound path in the water is so uncertain that the inherent error in sound transmission is more than the  $\pm 1$ -yard limit.

Early in the development of scanning sonar it became apparent that some method of testing the entire

system was needed.<sup>15</sup> This resulted in the development of the dynamic monitor,<sup>43</sup> which may be used as an approximate means of checking the accuracy of the less precise range-determining systems.

With present more accurate systems, the stable oscillator with electronic counter is preferable; an 800-cycle frequency is most convenient since each cycle corresponds to one yard of sound travel in water.

The types of range-determining devices which may have to be tested are:

1. Those in which there is no marking.
2. Those in which a separate recorder is used.
3. Those in which fixed range circles are used.
4. Those in which a range caliper is used.

There are certain tests which are specially adapted to each type of device. For the system in which there are no range marks on the face of the PPI, the best test for linearity and total range determination is to apply a signal of either 80 or 8 cycles (10- or 100-yard intervals) to the brightening grid of the cathode-ray display tube. Coordination of the display with the beam is tested best with the dynamic monitor, or some kind of calibrated delayed-pulsing device. The same low-frequency brightening method can be used to determine the scale accuracy of the chemical recorder if the oscillator frequency is known with a fair degree of accuracy. The latter quantity can be determined with some precision by using a chemical recorder as a time divider. This is done by determining the number of cycles of the oscillator for one complete cycle of the recorder. The former quantity is equal to the total number of marks upon the forward travel of the recorder, plus the number of cycles of the oscillator while the recorder is flying back and re-starting. The time for one cycle of the recorder is determined by counting the number of cycles that occur in some specific interval of time—ten minutes, for example—measured by an accurate timepiece.

In the case of fixed range circles, the interval between markings may be determined by the oscillator in the scanning sonar system, and it is necessary to determine only the frequency of that oscillator.

The caliper type of range-determining system is tested by using certain key points whose ranges are easily determined or which occupy strategic points on the range dial.<sup>18, 39, 44</sup>

A simple method of aligning the electronic timing and range-marking circuits has been worked out for the XQHA submarine sonar system. It requires only a high-resistance, low-range voltmeter, and an accu-

rate time standard such as a chronometer. This is described in the above references.

To insure adequate operation of the equipment under all possible operating conditions, tests of the accuracy of the range-determining devices should be made under the expected conditions of operation. These include high and low line voltage ( $\pm 20$  volts on 115-volt line), high and low power-supply frequency (from 50 to 70 cycles), high humidity, and/or high temperature.

#### 8.8.4 Sweep Tests for BDI

The sweep tests for the BDI used with the scanning sonar system are similar both to those given above for the other sweep circuits and to the tests given to the standard BDI. The linearity of the sweep is checked by 60-cycle modulation, and the interval is checked by a timer. In the past the timer has been built into a small box consisting of a control circuit and a thyatron, and calibrated by means of a stop watch. The first point to be tested is the range start, which should be the same for each range of the range-selector switch. Both the range start and the centering of the display should be reasonably stable with change of line voltage and with transients upon the line. A signal sufficient to give a deflection on the BDI should also give brightening; both should occur on all signals greater than 1-microvolt input. The sweep should be blanked for the return and the duration of any switching transients. The test in this case is visual examination.

### 8.9 STABILIZATION TESTS

When stabilization equipment is being installed, arrangements should be made with the ordnance section of the Navy Yard to have the platform of the stable element and the shaft of the projector measured with a surveyor's transit. The training shaft should always remain perpendicular to the plane of the base of the stable element. With proper care in installation, the errors can be held to within five minutes of angle. This work should be done while the ship is in dry dock, preferably one not of the floating type. Moreover, it is advisable to have a representative from the manufacturer's company present while the ship is still in dry dock to supervise installation and adjust the gyro balance in the stable element.

Before a test of the operation of the entire stabi-

lization system is attempted, a complete wiring check should be made from point to point. Particular care should be taken to check the synchro connections throughout the system; as, for example, to ascertain that the  $S_1$ ,  $S_2$ , and  $S_3$  wires from the generator are connected to  $S_1$ ,  $S_2$  and  $S_3$ , respectively, on each receiver. After all wiring checks have been made, all synchros should be adjusted to make the electrical zeros of the synchros correspond to the mechanical zeros of the system.<sup>45</sup>

After the wiring and synchros have been checked, normal tests for aligning the stable element should be made according to the instruction book published by the manufacturer. Directional tests should then be carried out to determine whether or not the system is stabilizing in the proper direction. The system should be followed through step by step, from the control handwheels through the stable element and trunnion-tilt corrector to the training shaft of the transducer and the commutators. The procedure can best be explained by describing the steps used in checking this part of the integrated Type B sonar (Chapter 6), which are as follows:

1. Set the ship's compass at zero. Set the true-target-bearing dials on the indicators at zero. The stable element train-indicator dial should now read 000 degrees. If it does not, check the alignment of the deck-tilt corrector synchros. The signal input to the trunnion-tilt corrector should be 0 degrees. If this is not true, check the zero of the 1- and 36-speed train-order synchros in the base of the stable element. The voltage across the  $S_1$  and  $S_3$  leads of each of these synchros should be 0 volts.

2. An increasing train angle should rotate the stable element yoke clockwise. If it does not rotate clockwise, reverse the leads  $S_1$  and  $S_3$  on both 1- and 36-speed deck-tilt corrector synchros. The director-train receivers in the trunnion-tilt corrector should now rotate clockwise. If the stable element yoke rotates correctly but the receivers in the trunnion-tilt corrector do not, reverse the  $S_1$  and  $S_3$  leads of the 1- and 36-speed train-order synchros in the base of the stable element.

3. Set the stable element on 0 degrees train. Facing the aft end of the stable element, exert a light downward pressure against the left side of the gyro. The level ring top will move toward the aft end of the stable element. The input to the trunnion-tilt corrector-sonar depression receiver should now decrease. This can be read on the small dial inside the

top cover. Exert a light downward pressure against the right side of the gyro. The sonar depression receiver on the trunnion-tilt corrector should now reverse and the reading on the dial should increase. If the above operations are reversed, interchange leads  $S_1$  and  $S_2$  of both the 2- and 36-speed level synchros in the stable element.

4. Exert a light downward pressure on the aft side of the gyro. The cross-level ring will rotate clockwise. The reading of the cross-level receiver dial in the trunnion-tilt corrector will increase in value. Exert a light downward pressure against the forward side of the gyro. The cross-level ring will rotate counter-clockwise. The cross-level receiver dial reading will decrease in value. If the cross-level dial in the trunnion-tilt corrector does not follow these changes, reverse leads  $S_1$  and  $S_2$  of both cross-level synchros in the stable element.

After the tests have been made on the stable element, the inputs to the trunnion-tilt corrector will have the proper polarity and the outputs of the trunnion-tilt corrector transmitters will be rotating in the proper manner. However, the direction of rotation of the transducer shaft may be reversed. This can be changed by reversing the  $S_1$  and  $S_2$  leads on the CT synchro attached to the transducer shaft. The commutators for depressing the beam may be corrected in a similar manner to reverse the direction of their servos.

#### 8.9.1

### Indicator Panel

The 26-kc depth-scanning sonar aboard the USS CYTHERA had an indicator panel associated with it containing synchros that were connected to repeat the various functions involved in the stabilization of the sonar equipment. It was planned that this panel would give information to determine the static displacement errors between given points. A movie camera was to be used to photograph the panel and any one frame of the film would indicate the dynamic displacement error. For example, the relative bearing inserted at the handwheel was to be repeated at the indicator panel as were the deck-tilt correction and the sonar train order from the stable element and the trunnion-tilt corrector respectively. Whenever the ship was tied alongside a dock, and was in a level position, any motion inserted at the handwheel would change all three quantities by the same amount. All three values were repeated at 1- and 36-speed; therefore the displacement error could be indicated to an

accuracy of 0.06 degree. This method of indicating different functions by recording on movie film was used to indicate the errors due to different speeds and accelerations. The movie camera was arranged to take five frames per second, and flash lamps were synchronized with the shutter operation so that the exposure time was  $1/30,000$  of a second. This was to make it possible to have the dials rotate at speeds in excess of 200 rpm and still have the pictures clear enough to read the dials down to 1 degree.

The indicator panel, as designed and built by HUSL, included special Sperry synchros for the indicating units. This type of voltage receiver had no damper; therefore, when a signal was applied, the rotors would overshoot, and if the signal changed direction, the voltage receiver would commence to rotate continuously as an induction motor. For this reason, the indicator panel built by HUSL was never actually used aboard the CYTHERA. The research section of ASDevLant adopted the principle of this indicator panel and designed a new unit using small dials mounted on standard size 1 receivers. It was expected that the inertia of the dials and rotors in this new panel would be so low as to cause no appreciable dynamic error, and therefore values could be read to 0.1 degree. Informal reports indicated that it was found to operate with reasonable satisfaction.

In addition to measuring the accuracies of the stable element and associated equipment, this method of measurement could be used to measure the roll and pitch of the ship and overall accuracy of the bearing determination. By having a moving-picture camera mounted on the bridge and having the lens arranged to point at the horizon with crossed hairlines in the field of the lens, any roll and pitch should show up on the film as a displacement of the horizon from the cross lines. Such arrangements were planned by ASDevLant and it was expected that they would be used in measuring the performance of both the Type A and Type B integrated sonars.

The accuracy of the bearing determination can be obtained by mounting a camera on a circular stand designed similar to a large pelorus. By graduation of the edge of this table and use of the viewfinder of the camera as a sighting device, the actual relative bearing of a submarine's periscope can be determined. If a synchro repeater that repeats the sonar relative bearing is brought into the field of the camera lens, then when a picture is made it will contain a record of the periscope bearing and also the dial of the sonar

bearing repeater. Much further study is required on this problem.

## 8.9.2

**Artificial Ship**

In order to test the 2-axis stabilization and to make accurate measurements of all functions of the stable element and the trunnion-tilt corrector under controlled conditions, a testing apparatus was designed and built, based on equipment developed for a similar purpose at the Radiation Laboratory (MIT). The central portion of this equipment was a Ransome welding positioner. This unit positioned a mounting plate about one axis and rotated this mounting plate about an axis perpendicular to the first axis. By positioning this mounting plate in a vertical plane, it was possible to attach a horizontal platform which could be tipped  $\pm 10$  degrees in a given direction and rotated  $\pm 30$  degrees in a plane 90 degrees from the original motion. Both motions were power-driven at variable speeds by means of a 3-phase induction motor and a Worthington all-speed hydraulic drive. With this arrangement, the pitch and roll of a ship could be duplicated as sinusoidal motions. Maximum pitch amplitude could be 10 degrees, with the period varying from 5 to 10 seconds. The rotary motion of the table was arranged to represent the roll of the ship with a maximum amplitude of  $\pm 30$  degrees, with periods varying from 5 to 10 seconds. Both motions were independent of each other and were not synchronized, in order that various amplitudes and phase relations between the two motions could be obtained.

In order to get instantaneous indications of roll and pitch, two synchros were attached to each axis of motion and were arranged to repeat roll and pitch at 1- and 36-speeds. If the repeater dials were photographed with a clock having a second hand, the evaluation of roll and pitch could then be plotted against time, and the speed and accelerations could be derived from these curves.

It was originally intended to use the synchro indicator panel described previously to repeat all the values of the stable element and trunnion-tilt corrector, in addition to the roll and pitch repeated directly from the positioner. By taking flash pictures of the dials for a period of one or two minutes, it was expected that all possible conditions of roll and pitch phasings for given amplitudes could be obtained. This would then be repeated for several different amplitudes and periods of roll and pitch corresponding

to particular types of ships such as a destroyer escort or destroyer. This test unit was designed in cooperation with the Ransome Machinery Corporation of Dunellen, New Jersey, and was built by them. However, the delivery was extended from the time originally planned, and as the stabilization equipment had already been installed aboard ship, the test equipment was never used.

## 8.9.3

**Attack Director Tests**

All attack director tests were carried on under the supervision of ASDevLant. In addition to two attack aids, three different attack directors were tested in a total of 2,993 runs on attack teachers and 696 runs at sea. These three directors were the Mark II, developed by the Armour Institute of Technology, the Mark III attack director, built at the Harvard Underwater Sound Laboratory,<sup>46</sup> and the Mark VI, built by the Librascope Corporation in cooperation with personnel from Naval Research Laboratories [NRL] and the Bureau of Ordnance.

In order to eliminate as many variables as possible, a set of 54 depth-charge runs was compiled by ASDevLant for use with the Sangamo attack teacher for testing attack directors. These runs included a large variety of submarine maneuvers ranging from straight courses to runs involving submarine maneuvers after loss of contact. The procedure for making these tests was to pick the runs at random until the entire set of 54 runs had been made. The cards describing these runs were then reshuffled and the set repeated. A fixed sinking time of 28 seconds was used for all runs. This time corresponds to a moderately deep target if Mark VI charges are assumed and a very deep submarine in the case of Mark IX, Model 2, charges.

The characteristics of the ship and submarine were kept constant for all trials on three different directors. The submarine was assumed to be a 517-ton German U-boat, and the ship to be a 1,500-ton destroyer. All tests were in charge of highly trained officers with considerable experience in conning antisubmarine attacks. In testing the different directors, complete attack teacher tests were made before commencing sea trials. During all the attack teacher runs, the courses of the submarine and the attacking ship were plotted on paper. These plots were preserved for later analysis to determine time and lead errors as well as total error.

CONFIDENTIAL



Sea tests of the three different directors were carried out aboard ships assigned to ASDevLant. The Mark II and Mark IV directors were tested aboard a destroyer escort, the USS JORDAN, while the Mark III was tested aboard the PCE-869. Sinking times of 25 or 15 seconds were employed. Results of the runs were scored by the OBC practice attack meter. The OBC readings were plotted, and time and lead errors determined from the plot.

Three different types of submarine runs were used: (1) straight course and constant speed; (2) restricted evasive; (3) fully evasive maneuvers. Restricted evasive maneuvers permitted a moderate change of speed and a maximum change of 60 degrees from the base course. Fully evasive maneuvers permitted all possible changes in submarine's course and speed. During all the sea trials the submarine was supposed to operate at a constant known depth.

Of the three directors tested, the Mark IV, built by the Librascope Corporation, seemed to possess the most promising qualifications for use with the integrated sonar systems.<sup>47</sup>

## 8.10 INSTALLATION TESTS

### 8.10.1 Introduction and Test Equipment

After the installation of a scanning sonar equipment, the nature of the equipment and its performance must be determined by a comprehensive test program. The objectives of the test program will naturally depend on the type of installation.

This section will describe first the different viewpoints for installation tests of scanning sonar equipment on experimental ships, as used in the field of experimental development by HUSL, and on ships in Navy service. A description will then be given of special test equipment, followed by a discussion of installation tests on experimental ships. These latter installation tests will then be abridged to a test program suitable for routine service installations of scanning sonar equipment on Navy ships.

On an experimental ship the objective of installation tests is to determine completely the physical characteristics of the scanning sonar equipment and its acoustic, electronic, electric, and mechanical performance, and thus obtain information which will lead to an efficient direction of development work. These tests include tests of equipment components. For example, the performance of the receiver com-

ponent will be known by measuring such quantities as gain, dynamic range, internal noise output, signal-to-noise factor, frequency response, sensitivity to line voltage changes, etc. These installation tests also include measurements on the equipment as a whole, such as the measurement of the sound pressure level of the minimum echo detectable by the equipment under various conditions of operation. Operational tests of one experimental installation will naturally differ to some extent from those of another installation. For example, tests on one installation may be made in order to obtain special detailed information about a component that has been newly redesigned. A discussion of such tests is omitted here. Two references are given which describe installation tests made on the Model XQHA installation on the USS GALAXY (IX-54).<sup>48, 49</sup> For routine service installations made at Navy yards, the main objective of installation tests should be to insure that the scanning sonar equipment is ready for operation and meets approved Navy specifications.

On an experimental ship, it is convenient to make installation tests with a calibrated monitor transducer and the following electronic equipment: (1) vacuum-tube voltmeter, (2) cathode-ray oscillograph, (3) audio oscillator, and (4) a calibrated frequency standard. Assuming that the sensitivity (in volts per dyne per cm<sup>2</sup>) of the monitor transducer, and the sound pressure level (in dynes per cm<sup>2</sup> per volt output) at one meter from the transducer, have been determined accurately for different frequencies, the use of the vacuum-tube voltmeter permits acoustic measurements in absolute units. The use of the cathode-ray oscillograph permits direct observation. The monitor transducer can be operated as a transmitter with a signal generator and vacuum-tube voltmeter to put sound of known intensity into the water, or as a receiver with the vacuum-tube voltmeter and cathode-ray oscillograph to pick up and measure the intensity of sound that has entered the water from the scanning sonar transducer, and to observe its wave form and pulse envelope. The setting of the frequency dial of the audio oscillator may be checked with the calibrated frequency standard.

A monitor transducer can be suspended from the ship's rail to make installation tests, provided the following conditions exist:

1. Ship is steady.
2. There are no strong currents running.
3. There is a fairly extensive stretch of water on at

least one side of the ship; there should be no large surface near the ship to reflect the sound beam of the sonar transducer.

It is necessary to suspend the monitor transducer vertically and in a relatively fixed position with respect to the sonar transducer and to have it remain so in order to obtain reliable measurements (conditions 1 and 2 above).

An installed monitor transducer differs from one suspended from the ship's rail in that the installed transducer is mounted on a streamlined strut that may be lowered through the hull of the ship. This mounting arrangement allows testing of the sonar equipment at any time, under any conditions of operation of the ship, and without regard to conditions of the sea or motion of the ship. It also provides a permanently fixed and known reference point for all measurements; that is, the bearing and distance of the monitor transducer from the sonar transducer are accurately known. The mounting arrangement may also be so designed that the installed monitor transducer can be lowered in depth in order to make tests on the sonar equipment at variable depth angles. In this case, the arrangement is known as a "deep monitor," and is of particular value in depth-scanning systems.

Installation tests can also be made by means of a *sound gear monitor* [SGM] of the OAX or OCP types.<sup>50, 51</sup> Each of these monitors consists of a hydrophone (suspended from a ship's rail) with an electronic unit and can be operated either as a transmitter to put sound of known intensity in the water or as a receiver to pick up and measure the intensity of sound that has entered the water from another source. Such sound gear monitor equipment is not so flexible in use as the installed- or deep-monitor type, and therefore may not be so useful on an experimental ship. However, they are standard items of Navy gear, available at installation yards and bases, and are therefore useful for routine installation tests on Service ships. The sound gear monitor's electronic unit can be used with either the streamlined strut-mounted transducer or with the deep-monitor hydrophone.

The dynamic monitor<sup>43</sup> is of use in making a specific installation test which provides a measure of the overall operating performance of the scanning sonar equipment. The performance of sonar equipment is influenced by its physical characteristics, the operator, the medium, and the target characteristic. The

dynamic monitor, by eliminating the effects of the last two variables on the target echo, allows measurements to be made from which the figure-of-merit can be determined. The dynamic monitor consists of a monitor hydrophone and an electronic unit. Its functions are: (1) to pick up from the water the transmitted sound pulse of the sonar gear by use of the monitor hydrophone; (2) to measure the sound pressure of this transmitted pulse; (3) to generate a small artificial echo, after an appropriate time delay, and put it into the water by use of the monitor hydrophone; and (4) to measure the sound pressure of this echo. The artificial echo is in the form of a pulse, rather than a continuous sound signal, and is adjustable in pulse duration, intensity, frequency, and range. Echo range corresponds to the appropriate time delay.

The portable polar chart recorder<sup>4</sup> may be used to plot automatically on polar graph paper the signal level as received through the transducer and commutator as a function of the bearing angle of the echo source from the sonar transducer.

The *split projector test unit* [SPTU]<sup>52</sup> is a special, portable test device for testing and evaluating the performance characteristics of sonar projectors that are split for use with the bearing deviation indicator. The SPTU comprises essentially the input circuits of a standard BDI auxiliary unit (HUSL Models X-3 and X-4) up to and including the lag line. Auxiliary equipment includes a suitable generator such as a sound gear monitor; a measuring amplifier and indicator, which may be the amplifier unit of a monitor or a sonar gear receiver; and, under certain conditions, a filter junction box. Tests that can be made on a split projector with the SPTU include measuring directivity patterns and determining the BDI deflection curve.

## 8.10.2 Installation Tests on Experimental Ship

### PRELIMINARY INSTALLATION TESTS

A desirable arrangement of preliminary tests follows:

1. Inspect units visually, looking for obvious defects in wiring, missing parts, loose parts, etc.
2. Check the continuity of interconnecting cables between units, and of the ground wiring system.
3. Measure the resistance to ground of each ele-

ment of the transducer after it has been in the water for at least several hours.

4. Measure the a-c power-supply voltages.

5. Close the main power switch, and then set to the on position the power switches of all units, except the transmitter unit.

6. Check the sequence of operation of all send-receive devices to avoid the following improper conditions:

a. The short-circuiting of the transmitter during the ping interval.

b. The applying of transmitter output power to receiving units during the pinging interval.

7. Check roughly the receiving response of the scanning sonar equipment to sound put into the water by the use of a monitor transducer and an oscillator.

8. Set the power switch of the transmitter to the on position.

9. Check the apparent normalcy of operation of all functional controls. If there is no obvious (visual or audible) evidence of improper operation of the scanning sonar equipment, then further installation tests may be made.

#### 8.10.3

### Transmission Tests

To make sure that the transmitter and transducer are operating at highest efficiency during transmission, it is desirable first to tune the transmitter. Transducer tests before installation are assumed to have already determined the correct center operating frequency, which is usually taken as that frequency for which the transducer is most sensitive in reception. The frequency control dial is adjusted so that the transmitter is working at the correct center operating frequency. This adjustment can be made conveniently by the Lissajous method, using a standard calibrated oscillator and CRO. The acoustic output of the transducer may be picked up from the water by a monitor hydrophone and its electric output applied to the deflection plate of the CRO.

The next step in checking the system operation is to make sure that the transmitter and transducer are operating at highest efficiency and that the transfer network is properly tuned so that the load on the transmitter unit is at unity power factor. Measurements for checking these factors are described earlier in the present chapter.

A third step in checking transmitting performance is to measure acoustic power output, first making sure that ping length is correct. At the same time, it is convenient to observe the shape of the sound pulse put into the water and the wave form of the individual cycles of sound pressure.

To determine the duration of the ping, the acoustic ping output of the scanning sonar transducer is picked up from the water by a monitor hydrophone, whose electric output is applied to a CRO. With the synchronizing signal amplitude control of the oscillograph set at zero, the rate at which the electron beam is swept across the screen of the cathode-ray tube is adjusted until the length of the ping signal is equal to the whole length of the horizontal time axis shown on the screen. Since the sweep of the electron beam is not synchronized with the ping signal, the start and end of the ping may appear at any point along the horizontal time axis. Adjustment of the electron beam sweep just described is fairly easy to make if the sweep frequency is gradually changed from a low frequency which makes the length of the ping signal equal to that of the horizontal time axis. Without changing the sweep rate of the electron beam set in the previous adjustment, the sweep rate can then be measured by applying a signal from the audio oscillator to the Y-axis input terminals of the oscillograph and adjusting the oscillator frequency until one stationary cycle is seen on the screen. The reciprocal of the frequency of the one stationary cycle, or its period, is therefore equal to the length of the ping.

Methods of measuring the acoustic power output are discussed in detail elsewhere.<sup>1</sup>

From the measurements of transmitter electric power output and transducer acoustic power output, the efficiency of the transducer and transfer network connected to the transmitter output terminals may be computed.

Other measurements which give valuable information on the transmitter and transducer are the following:

1. Measurement of sound pressure in the center of the transmitting beam at a known distance from the transducer as a function of transmitting frequency, for long-range automatic keying.

2. Measurement of the transmitted sound pressure as a function of transmitter keying rate, both for automatic and chemical recorder keying.

CONFIDENTIAL

#### 8.10.4 Transmitting Directivity Patterns

For an azimuth-scanning sonar equipment, two types of transmitting directivity patterns describe reasonably well the performance of the transducer. One type of pattern shows the variation with relative bearing of intensity of sound put into the water in the horizontal plane passing through the center of the transducer. For scanning sonar installations without domes, the sound intensity is usually approximately constant with bearing in the horizontal plane; however, certain streamlined domes are capable of distorting seriously the directivity pattern of an otherwise nondirectional sonar transducer. A reasonably complete picture of transducer performance in the horizontal plane can be obtained by measuring the ping intensity of sound at particular bearings relative to the sonar transducer and at intervals of 20 degrees on either the starboard or port side of the ship. The bearing range of the monitor transducer used to measure sound intensity, with respect to the sonar transducer, should be known accurately, and both transducers should be at exactly the same depth. If it is possible to rotate the transducer, it is easier to obtain the pattern in the horizontal plane by measuring the ping intensity of sound with the monitor transducer located at one particular point and the scanning sonar transducer rotated in 5-degree steps.

To investigate the effect of the dome on the transmitting directivity patterns, the intensity of the transmitted sound is measured at a particular bearing relative to the scanning transducer as the latter is rotated in azimuth. Such a pattern should not be confused with the horizontal distribution of sound intensity in the water present while the scanning transducer is pinging. This test cannot be made conveniently in installations where the transducer is fixed in bearing.

The other type of transmitting directivity pattern shows the variation of sound intensity with elevation angle measured in a vertical plane passing through the axis of the transducer. For azimuth-scanning installations without domes, this type of pattern should be approximately the same for vertical planes at all relative bearings. For installations with domes, it is necessary to obtain patterns, in the vertical plane, of several relative bearings in order to gain a reasonably complete picture of transducer performance. In measuring this type of pattern, it is advisable to suspend the monitor transducer in a horizontal rather than

the normal vertical position so that its sensitivity is independent of depth in the water. It is still better to use a very short transducer and to correct for its vertical pattern, since it is difficult to keep the direction of a horizontally suspended transducer correct.

#### 8.10.5 Receiving Directivity Patterns

Receiving directivity patterns were usually measured at the output terminals of the preamplifier. A monitor transducer, located at some particular relative bearing, produces a sound signal at the sonar operating frequency. The method for obtaining the receiving pattern under high-speed scanning conditions has been discussed earlier in this chapter. This method may be applied to the shipboard installation as well as at the laboratory test stations. The equivalent pattern of the hand-trained listening channel may be obtained by observing the output of the preamplifier on the listening commutator with a vacuum-tube voltmeter and rotating the cursor on the PPI through 360 degrees. Since training of the listening beam of sensitivity depends upon the setting of the PPI cursor, a plot of the observed voltages against angular position of the cursor will give the receiving beam pattern of the transducer and the listening commutator, and is termed the receiving pattern of the listening channel. Tests can be made to determine the effect of the capacitive commutator register and the uniformity of transducer elements on the receiving directivity pattern of the hand-trained listening channel. Because of the great number of patterns sometimes desired, it is convenient to use the PPCR.

If the scanning sonar equipment has a BDI receiving channel, a BDI deflection curve should be obtained. Before this is done, the acoustic power output of the monitor hydrophone and/or gain of BDI should be adjusted so that a maximum deflection of approximately 1.5 inches on the BDI scope is obtained when the bearing of the receiving beam of sensitivity is such as to produce this maximum deflection—roughly 8 degrees off bearing. The BDI deflection curve obtained by plotting readings of deflection versus bearing relative to the hydrophone should be similar to that shown in Figure 49. If the deflection curve thus obtained is not satisfactory, the split projector test unit can be used to test the performance characteristics of the transducer and commutators used in the BDI listening channel.

CONFIDENTIAL

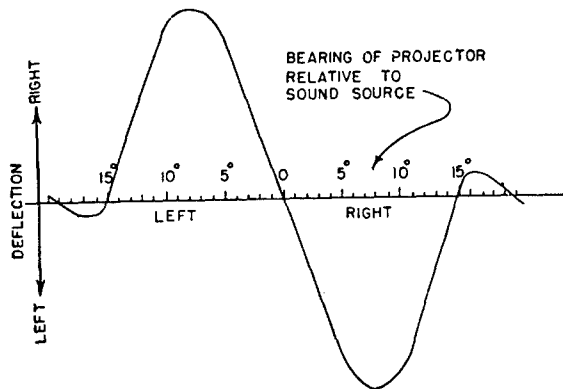


FIGURE 49. BDI deflection curve.

### 8.10.6 Receiver Frequency-Response Tests

To check the receiving frequency response of the transducer, commutators, and preamplifiers, a monitor transducer may be used to transmit sound through the water to the scanning sonar transducer. The voltage across the monitor-transducer input terminals should be recorded so that the intensity of the sound field may be known. The receiving response is obtained by measuring the output of each preamplifier for frequencies at suitable intervals over the receiver tuning range. The output of the scanning commutator preamplifier may be measured with the use of a cathode-ray oscillograph, which has been calibrated over the range of frequencies being measured.

Additional receiving frequency-response measurements similar to those just described should be obtained to check the components of the several receiving channels. The procedures are the same as those used in the above tests except that the output to the brightening grids of the PPI and/or the audio output of the listening receiver are measured. The receivers are tuned to the frequency of sound emitted by the monitor transducer, the TVG or RCG circuits being disabled.

To measure the overall frequency response of each receiving channel, a monitor transducer is again used as a sound source, and the output to the brightening channel is measured for frequencies at suitable intervals over the receiver tuning range. During these tests, the receivers should remain tuned to the center operating frequency of the scanning sonar equipment. The overall response thus obtained shows the effects of all band-pass filters.

### 8.10.7 Noise, Receiving Sensitivity, and Cross Talk

The noise level in the several receiving channels, expressed in terms of an equivalent sound field at the sonar transducer, should be measured in the quietest water obtainable. When the electric-circuit noise is higher than that of water-borne origin, the noise-level measurement becomes more significant in expressing performance of the equipment than when the reverse situation is true. If the reading of a root-mean-square voltmeter, connected to the output of the receiving channel, does not change when the sonar transducer is in the water or retracted into its sea chest, then the ambient water noise beneath the ship is well below the electric noise. For installations where it is not possible to retract the transducer into the ship's hull, the level of water noise must usually be calculated to determine its level relative to the electric noise level. For scanning sonar equipments, the electric noise level is usually greater than the ambient water noise level of sea state 2 or 3, mainly because of the narrow width of the equipment's receiving beams of sensitivity. It is usually possible then to measure the electric noise level, expressed in terms of an equivalent sound pressure at the sonar transducer, in quiet water.

To measure the noise level of the listening receiving channel, a root-mean-square voltmeter is connected to the audio output. Using a monitor transducer as a sound source, the sound pressure in the water is adjusted until the voltmeter reading has increased to  $\sqrt{2}$  times its original value. The sound pressure level at the sonar transducer is then the equivalent noise level. This quantity should be measured for several settings of the gain control. To obtain the same quantity for the scanning channel, a calibrated cathode-ray oscillograph may be used to measure the output to the brightening grid of the PPI cathode-ray tube. In this test, the sound pressure in the water is adjusted until the pattern corresponding to the sound is  $\sqrt{2}$  times the ambient background seen on the screen of the cathode-ray oscillograph.

To obtain the receiving sensitivity of the scanning receiver, its output to the brightening grid of a calibrated cathode-ray oscillograph is measured as a function of the sound pressure in the water at the sonar transducer for one setting of the gain control. The measurement should be repeated for settings of the gain control ranging from minimum to maximum

gain. The receiving sensitivity of the listening receiver is obtained by measuring the output to the loudspeaker, noting the distortion level at the same time.

#### 8.10.8 Figure-of-Merit Measurement

The figure of merit of the sonar system may be evaluated in the following manner: By a simple calculation, the sound pressure in the center of the transmitting beam at some known distance from the transducer, as previously determined in the acoustic-power-output measurement, may be converted to the equivalent pressure at one meter from the transducer. In the determination of the minimum echo detectable by the sound operator, a monitor transducer is used as a sound source to put sound of known pressure at the sonar transducer. The continuous sound signal is adjusted in level until the sound operator can just detect it. The ratio of these two pressures may then be calculated.

The ratio will vary for the different receiving channels of the scanning sonar equipment. It is a function of all factors that affect the intensity of the transmitted ping and the intensity of the minimum detectable signal. As far as the minimum signal is concerned, the deciding factors are usually ambient water noise level, the character of the reverberation, and the electric noise level of the gear. The figure of merit may also be measured directly by use of the dynamic monitor.<sup>43</sup>

#### 8.10.9 Mechanical Alignment

For proper mechanical alignment of a scanning sonar equipment, the synchro system must be adjusted with great precision, or systematic bearing errors will result. In order to make the angular indications at both ends of a synchro system correspond, it is necessary to orient the machines with respect to each other. Measurements of all angular displacements of the rotors of the synchro units are referred to a standard position which is designated as "electrical zero." This position may be checked accurately for synchro motors and generators by connecting the rotor winding across 115 volts a-c and a low-range voltmeter across the stator terminals  $S_1$  and  $S_3$ , with  $S_2$  open. The rotor is then turned until a minimum voltage indication is obtained. The adjustment procedure of "zeroing" synchros is not concerned with

the angular position of the transducer or the commutator, but it must be properly carried out before these elements can, in turn, be adjusted. The zeroing adjustments should be made in the equipment before installation. It will be necessary to check the adjustments if the installation tests about to be described indicate improper mechanical alignment of the scanning sonar equipment.

In checking mechanical alignment, it is customary first to determine whether the electron beams of the cathode-ray tubes which provide plan position indication occupy at each instant a position on the screen corresponding to the location from which echoes may be received at the corresponding instant. In the case of azimuth scanning, it is then necessary only to verify two different relative bearings. The use of an installed monitor transducer as a source of sound provides a known reference point to make the forward position on the cathode-ray face agree accurately with the zero bearing of the scanning beam of sensitivity. A monitor transducer can be suspended from the ship's rail at another relative bearing to verify that the scanning beam and the electron beam of the cathode-ray tube are rotating in the same direction.

Directly coupled to a capacitive scanning commutator is a 5 CT synchro used as the spiral-sweep generator. The output voltage of the synchro is applied to the 3-phase deflection coils surrounding the neck of the PPI tube. By adjusting the relative angular position of either the deflection coils, or the stator of the synchro, it is possible to make the forward position on the cathode-ray face agree with zero bearing of the scanning beam. In a CR sonar system, it is usually convenient to adjust the position of the stator of the synchro on the scanning commutator. In an ER sonar system, it is necessary to adjust the angular position of the deflection coils around the neck of the CRO. If the electron beam of the cathode-ray tube does not rotate in the same direction as the scanning beam of sensitivity, it can be made to do so by reversing two connections:  $S_1$  and  $S_3$  of the deflection coils. In a depth-scanning system, two different depression angles are verified to check plan position indications. An installed monitor transducer (deep monitor) which can be lowered in depth is used for this test.

The mechanical alignment of the listening commutator should be tested. Training of the listening channel depends upon the setting of the cursor on the PPI (*elevation position indicator* [EPI] in the depth-scanning system). The rotor of the listening commu-

tator is driven by a servo motor energized by the output of a servo amplifier, which in turn receives its signal from the rotor of a 5 CT synchro coupled with the listening commutator. The stator of the synchro is supplied from the stator windings of a 5 G synchro in the console, which is geared to turn one-to-one with the cursor. The original setting of the listening commutator rotor is made by using an installed monitor transducer as a source of sound and adjusting the position of the stator commutator synchro until the received signal is a maximum when the cursor is trained to the known azimuth (or depression angle) of the monitor transducer. A voltmeter at the listening receiver output can be used to supplement the ear in observing received signal level. A check should also be made to see if both the cursor and the listening commutator rotor rotate in the same direction by verifying the position of a sound source at another bearing (or depth angle).

In testing the alignment of the listening channel of a depth-scanning system, the depth-scanning transducer should be directed at the sound source. Also, it should be verified that the action of the stabilization components of the system is not interfering with the accuracy of the alignment. Since the listening channel commutator is used in conjunction with a difference-listening commutator to produce BDI operation in a horizontal plane, it should be determined that the two commutators are aligned so as to track together in a vertical plane.

Installation tests of the stabilization units of an integrated scanning sonar system are described previously in this chapter.

#### 8.10.10 Installation Tests on Service Ships at Navy Yard

A test program suitable for routine service installations of scanning sonar equipment on Navy ships should check the overall acoustic performance of the gear in all relative bearings with respect to the ship. A minimum, but reasonably complete, test program would include an overall acoustic test which would be made perhaps in steps of 20 degrees throughout 360 degrees of azimuth. It would also include detailed tests of equipment components, which would be made at one particular relative bearing. The overall test made in steps of 20 degrees could check by inference, throughout 360 degrees of azimuth, the detailed tests made at one bearing, and the combination of

these tests would constitute a satisfactory minimum test program.

The figure of merit provides a reliable numerical index of the overall acoustic performance. The measurement of this ratio (for the several receiving channels) and the ping intensity at one meter, in steps of 20 degrees throughout 360 degrees of azimuth, would be a desirable overall acoustic test.

The test would check:

1. Uniformity of transmitted intensity with direction in the horizontal plane through the center of the transducer.
2. Absolute level of acoustic power output.
3. By inference, the distribution of transmitted intensity with elevation angle in the vertical planes through the transducer axis. If the minor lobes of the vertical pattern were too high, the transmitted intensity in the center of the beam would be lower than normal.
4. Tuning of transmitter. Ping intensity would be lower if the transmitter were not tuned correctly.
5. Efficiency of transmitter and transducer.
6. Ping duration, frequency, shape, and wave form—if the dynamic monitor is used to measure figure of merit.
7. By inference, the receiving directivity pattern. If the receiving beam of sensitivity were wider than normal, the measurement of figure of merit would reflect a higher level of the minimum detectable echo.
8. Tuning of receiver.
9. Electric noise level, if the test were made in quiet water.
10. Receiving sensitivity to minimum signal.
11. Mechanical alignment. In making the test, it would be seen whether or not the electron beam of the cathode-ray tube, which provides plan position indication, occupies at each instant a position on the screen corresponding to the location from which echoes may be received at the same instant. The mechanical alignment of the listening channel would also be checked.

The detailed tests at one bearing for a routine service installation can be made by using a monitor transducer, located at a particular bearing, to put a steady sound signal into the water. It would be desirable to make the following detailed tests:

1. Measure the receiving directivity pattern of the scanning channel.
2. Measure the receiving directivity pattern for the listening channel.

CONFIDENTIAL

3. Obtain BDI deflection curves for a sound signal level just above electric noise and the maximum level which would be obtained in practice, if the gear has a BDI receiving channel.

4. Check receiving sensitivity by measuring the output of the scanning receiver and the listening receiver as a function of sound field in the water for maximum and minimum settings of the gain control.

To carry out the above test program, it would be necessary to design and construct a special test device, which would be similar to the dynamic monitor,<sup>43</sup> but with certain modifications and additional provisions. In order to measure receiving directivity patterns and receiving sensitivity, it would be necessary to modify the dynamic monitor so that it could be used (1) to put a steady sound signal of variable level and frequency into the water, and (2) to measure the electric output of the various receiving channels of a scanning sonar system.

To measure electric output, it would be desirable to use the cathode-ray oscillograph components of the dynamic monitor and to provide for its calibration as a measuring device.

If an installed monitor transducer were furnished with the modified dynamic monitor as just described—that is, if an installed monitor transducer were made a standard item on board the Navy ship—it would be possible also to check periodically the operating performance of the sonar gear while the ship is on sea duty. During extended sea duty, changes may occur in overall functioning, and routine tests would determine whether or not the sonar gear is ready for action and to what extent. The results of these routine checks at sea could be compared directly with the results of initial installation tests at the Navy yard. The direct comparison would emphasize and readily point out small changes in performance with time.

## 8.11 OPERATING TESTS PROCEDURE

### 8.11.1 Introduction

After the installation tests of an experimental scanning sonar system have been completed, it is desirable to conduct a series of field trials to determine the value of the system for the type of operations for which it was designed. In the discussion following these introductory remarks, the testing procedure is presented under three headings: "Horizontal-Scan-

ning Sonar," "Depth-Scanning Sonar," and "Submarine-Scanning Sonar." This arrangement is arbitrarily made for the purpose of clarification, and, as will be noted, some of the testing procedure is common to all three systems.

In a series of field trials, the principal aim is to obtain data from which to evaluate the tactical usefulness of the system in the conducting of antisubmarine attacks, torpedo detection, mine-field navigation, and surface-ship detection.

Data must be taken on the accuracy with which the system can be used, the effect on system performance of ship and target motion, the effect on its performance of the medium and geographic location, the operating efficiency of personnel, and security against giving useful information to the enemy. The field operations should also contribute to correction of faults, give information for future design improvement and changes, provide indications of the possibility of extending the field of application of the system, and give information on reliability of performance and maintenance problems.

### 8.11.2 Horizontal-Scanning Sonar Operating Test Procedure

The accuracy of position measurements can be conducted under three sets of conditions which are as follows:

1. Accuracy with a point source, an echo repeater as the target, and with both the echo-ranging ship and the target stationary.
2. Accuracy with a point source as the target and the echo-ranging ship under way as in attack, with the point source being stationary or moving.
3. Accuracy with a real target, such as a submarine, and with the echo-ranging ship and the submarine moving as in attack.

For all test conditions, the accuracy of range measurements can be determined by comparing ranges as measured with the values given by a range finder on the ship's bridge.

A second set of range tests are those to determine maximum discovery range for a submarine. In addition to the other factors that determine maximum discovery range, this range will depend to some extent on the sonar operator's knowledge of the positions of the target. It is desirable to conduct two types of measurements, one in which the sonar operator knows the relative bearing of the target as it is ap-



proached outside the maximum echo range, and the other in which the operator will be following a normal search procedure and have no knowledge of target location. In order that experimental results may be checked with theory, it is highly important that a record be kept of the following data:

1. Date, sea state, wind force, bathythermograph, a-c line voltage.
2. Area of operation, type and depth of bottom.
3. Target speed, aspect, name, length, and depth of keel.
4. Echo-ranging ship's speed and gear.

It is also true that the above list of data should be recorded for the other operating tests.

A field study related to maximum echo range consists of taking data showing the distribution of echo amplitudes and the percentages of visible and audible echoes as a function of the range, for a given set of test conditions.<sup>53, 54, 55, 56</sup> If sufficient data are obtained to plot the percentage of echoes versus range, it is possible to calculate the probability of detection at a given range and also to extrapolate the graph to give the maximum range of detection. An evaluation of the quantity known as "recognition differential" could be made from data showing the amplitude dis-

tribution of echoes and the percentages of visible and audible echoes.

A study of bearing accuracy can be conducted much like that for measurements of range accuracy. The accuracy of bearing indications can be determined by comparing sonar bearings with simultaneous values given by a pelorus on the ship's bridge. Correction should be made for the parallax between the positions of the pelorus and the transducer, and also between the positions of the center of the target and the identifying object sighted upon with the pelorus. The two sets of data should be plotted on the same graph as functions of time. Since in an operation of this type there would be comparatively long periods during which the bearings do not change, it would be possible to obtain from this portion of the data a determination of the absolute bearing accuracy of the system. In the case of determination of bearing accuracy for a submarine target, the data should also be recorded as a function of target aspect. In this connection it would be desirable to record data for a fixed aspect of the target, such as for beam position, quarter position, and bow position, so that a correlation could be made between target aspect and bearing accuracy. Course plans for bearing study, shown in Figures 50 and 51, were designed to avoid masking of the target echo by interference from the wake of the echo-ranging ship.

In addition to target-aspect studies, measurements of the effect of echo-ranging ship's speed on echo-ranging performance are necessary. One method of obtaining data on this point is to measure the system figure of merit by use of a streamlined installed monitor transducer and the electronic unit of the dynamic monitor. This method gives as a function of ship's speed,<sup>57</sup> the level of the minimum echo detectable by the sonar operator at a specific range and bearing.

Tests on the reliability of the system as a torpedo-

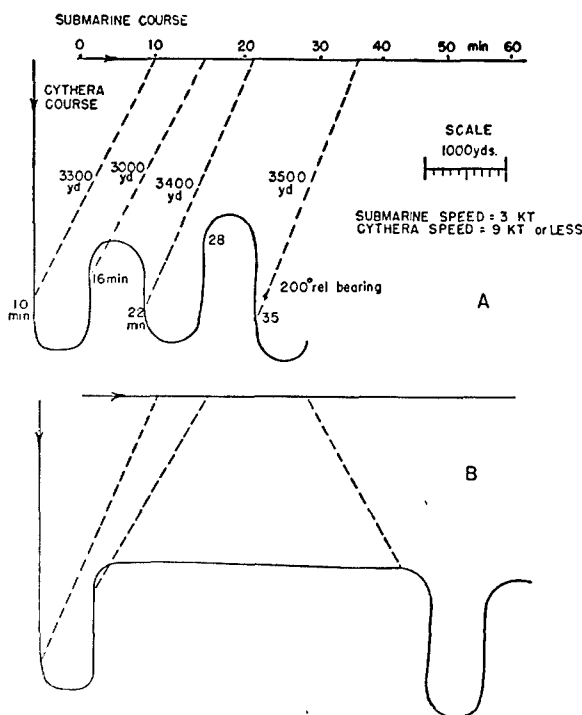


FIGURE 50. Course plan for bearing study - I.

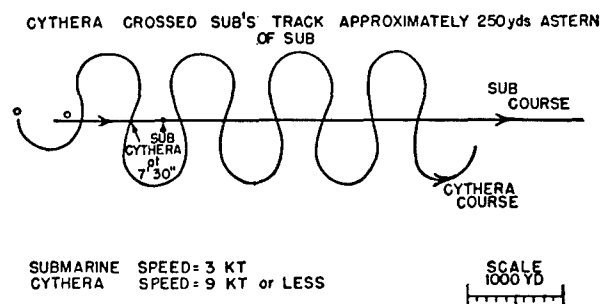


FIGURE 51. Course plan for bearing study - II.

CONFIDENTIAL

Remarks

FIGURE 52. QH sonar log data sheet.

In many of these measurements it would be highly desirable to record the PPI information photographically. An accurate operational log should be kept so that an indication of the reliability of the system is obtained. Figure 52 is an example of a typical log sheet.

### 8.11.3 Depth-Scanning Sonar Operating Test Procedure

The depth-scanning sonar operating tests included all of the measurements discussed under the horizontal-scanning system with the exception of torpedo detection, and included in addition depth determination.

Another test of interest was the determination of the target strength of a submarine as a function of target aspect. Current literature<sup>59</sup> has detailed information on this subject, but only on target aspects within depression angles of 0 degrees to 13 degrees. It was desirable, therefore, to obtain information on the target strength of a submarine at depression angles over the range of 13 degrees to 90 degrees. To secure reliable results, it was necessary to obtain a large number of samples for each measurement, preferably at constant target range.<sup>60</sup>

#### 8.11.4 Submarine-Scanning Sonar Operating Test Procedure

The submarine operating tests should include all measurements indicated under the horizontal-scanning sonar system. Mine-field navigation, torpedo detection, and surface-ship tracking are of special interest to the submarine system, since these are operations for which the system was designed. These three main classes of operation, therefore, will be discussed in the following paragraphs, and will naturally include many of the objectives of test procedure previously discussed.

## MINE-FIELD NAVIGATION

First in these tests should be the determination of the ability of the equipment to detect mines. A number of 3-foot mine cases or 1-foot triplanes should be

moored in an area of 1,000 yards radius in a depth of water of 10 to 40 fathoms. The targets should be located at different depths, from the surface down to a point several feet from the bottom and each target marked by a buoy. A steel shaft on the buoy should allow observation of buoy position by radar. The submarine should proceed around and through the target area and measurements should be made on accuracy of position determination, maximum discovery ranges, percentage of visible echoes as a function of range, and qualitative tests made on navigation of the submarine by its commanding officer through the target area.

These tests should be repeated for various depths of water, depths of submarine, speeds of submarine, types of target, and arrangements of targets.

#### TORPEDO-DETECTION TESTS

These tests are the same as the torpedo-detection tests mentioned previously, and include additional tests on torpedoes fired from the submarine in which the sonar gear is installed. It should be possible to compare directly some of the results for torpedoes proceeding away and results for approaching torpedoes. The direct comparison should give some information on the maximum range at which a torpedo could possibly be detected.

#### SURFACE-SHIP TESTS

The objectives of these tests,<sup>61</sup> which are of special interest to submarine-scanning systems, are to determine (1) detection range for noise of surface ship; (2) echo-ranging performance for surface-ship tracking; (3) reliability of single pings, at irregular intervals of time, in echo-ranging performance; and (4) security against giving useful information to the enemy while echo ranging. These tests should be divided into two groups: tests in shallow water of 20 to 50 fathoms and those in deeper water, preferably over 100 fathoms. The target should be a large surface ship (500 tons or more) capable of proceeding at 12 to 15 knots, so that considerable propeller noise will be present.

In measurements of the detection range for surface-ship noise, since the submarine sonar system gives information only on the bearing of the noise, it will be necessary to provide other means of measuring the range to the target when its noise is detected. One procedure for doing this is to have the target and the submarine proceed on fixed courses at fixed speeds so

that the geographic plot of the entire run will be predetermined and known as a function of time. In order to obtain complete information about the geographic plot, it will be necessary to measure the distance and true bearing between the vessels at the start of the run and provide means for synchronizing with time observations made on both vessels.

A desirable procedure for the conduct of tests is as follows: The target should proceed on a straight course at a speed of about 12 knots, starting the event about 8,000 yards from the intersection point of its course and the course of the submarine. The submarine should proceed on a course of 090 degrees from the target's course at a speed of three knots, starting the event about 2,000 yards from the intersection point. There is no need for the two vessels to approach nearer than about 500 yards. Observers on the target should record with time the radar range and bearing of the submarine, and signal by blinker the start of the run. The submarine should tow a radar target during submerged approaches, so that the surface ship can record its position. Periscope observation of the target is required, and an observer at the periscope should record at regular time intervals the relative bearing of the target. Observers stationed at the submarine sonar equipment should record the discovery time of target noise and its bearing at regular intervals.

The above procedure could also be used to determine echo-ranging performance for tracking of the surface ship. Observers at the submarine sonar equipment should also record, with time, the discovery range and bearing by echo ranging on the surface ship, as well as subsequent target positions. The percentage of visible echoes should also be recorded.

In echo-ranging performance, the reliability of single pings, spaced at irregular intervals of approximately one minute, should be determined in alternate runs. If one run is made with normal echo-ranging procedure and the next run with single pings, under the same test conditions for one day, a comparison of the two types of operation could be made readily.

During some of these operations, a sound operator on the target should attempt to locate and track the submarine by listening for the submarine's ping and by echo ranging. These tests should give qualitative information on security against the disclosure of useful information to the enemy.

## Chapter 9

# THEORY OF BEAM FORMATION

### 9.1 TRANSDUCERS

#### 9.1.1 Introduction

A STATIONARY radiator which is to produce a rotating radiation pattern of unchanging form preferably has a circular cross section in the plane of rotation of the pattern. The pattern in the plane perpendicular to that of rotation approximates that of a line source of a length equal to that of the cylinder. Dividing the surface of the cylinder into strips parallel to its axis, and providing these strips with separate excitation, gives a pattern which is controlled by the phase and amplitude of the separate elements. The receiving pattern of sensitivity may be rotated by a commutator or by purely electrical means as in the ER rotor.

#### 9.1.2 Reciprocity Theorem

The reciprocity theorem permits the patterns in transmission and in reception to be spoken of interchangeably. However, it is understood that ordinarily the elements of a cylindrical transducer are excited uniformly in transmission and that only in reception are the responses of the individual elements attenuated, phased, and combined to form a directive beam. When the pattern of a transducer is spoken of without further qualification, it means the directivity pattern in a plane normal to the axis of the cylinder; that is, in the plane of rotation.

#### 9.1.3 Continuous Cylindrical Radiators

A general statement can be made concerning the formation of radiation patterns by segmented cylindrical radiators; namely, that any desired pattern may be approximated as closely as desired provided that the width of the active strips of the radiator be chosen small enough. Actually, there is a lower limit to the width of the elements imposed by considerations of construction. Another consideration is based upon the fact that the formation of a very narrow pattern, in general, requires that the phase and amplitude of the signal change considerably from element to element. This makes it impossible to rotate the pattern smoothly, and also raises the objection that the

theory upon which the statement is based is inapplicable since it assumes that there is no interaction between the elements. Thus it is seen that analysis of pattern formation based on a continuous cylindrical radiator, whose elements are arbitrarily narrow, has very limited practical implications.

#### 9.1.4 Pattern of Sector of Cylinder<sup>1, 2, 3</sup>

The pattern of a segmented cylindrical transducer may be considered as being a superposition of the patterns of the single elements of the transducer. Therefore the pattern of a single element is first considered. It depends upon the angular width of the element, the diameter of the cylinder relative to the wavelength of the signal, and the baffle condition presented by the cylinder. Two separate baffle conditions are considered; namely (1) "stiff" or rigid, and (2) pressure release. When the cylinder is assumed to be stiff, the active element is presumed to move as a rigid piston with uniform velocity. When the cylinder is assumed to provide a pressure release (that is, to be incapable of supporting pressure) the active element itself is presumed to exert a uniform pressure. The justification for either baffle condition lies in the correlation between patterns of single elements obtained in practice and the computed theoretical patterns. It is found that the actual patterns lie between those given by theory for these two conditions, but closer to that based on the pressure release baffle conditions.

The pattern of a sector of a cylinder is given by:

$$P = P_0 \left[ D_0 + 2 \sum_{m=1}^{\infty} \frac{\sin m\alpha}{m\alpha} D_m \cos m\phi \right] \quad (1)$$

where

$$D_m = \begin{cases} \frac{j^{m-1}}{H'_m(ka)} & \text{Stiff Baffle} \\ \frac{j^m}{H_m(ka)} & \text{Release Baffle} \end{cases}$$

Here  $\phi$  is the angle between the direction of observation and a line bisecting the sector,  $2\alpha$  is the angular

width of the sector, and  $P_0$  is a normalizing factor.  $H_m(z)$  is the Hankel function of the second kind of order  $m$  (commonly denoted by  $H_m^{(2)}(z)$ ), and  $H'_m(z)$  is the derivative of  $H_m(z)$ . In terms of the Bessel function  $J_m(z)$  and the Neumann function  $N_m(z)$ ,

$$H_m(z) = J_m(z) - jN_m(z).$$

Table 1 gives the values of  $J_m(z)$  and  $N_m(z)$  for particular values of the argument and order of interest.

Values of the Neumann function were calculated by a recursion formula. The radius of the cylinder is  $a$  and  $k$  is the wave number of the signal; that is,

$$k = \frac{2\pi}{\lambda},$$

where  $\lambda$  is the wave length of the signal. Thus the dimensionless number  $ka$  is the number of wavelengths in the circumference of the cylinder.

TABLE 1

$m$	$J_m(12)$	$N_m(12)$	$J_m(16)$	$N_m(16)$	$J_m(20)$	$N_m(20)$	$m$	$J_m(24)$	$N_m(24)$	$J_m(28)$	$N_m(28)$
0	0.0477	-0.2252	-1.749	.0958	.1670	.0626	0	-0.0562	-0.1528	-0.0732	0.1318
1	-0.2234	-0.0571	.0904	.1780	.0668	-.1655	1	-0.1540	0.0531	0.1306	0.0755
2	0.0849	0.2157	.1862	.0736	.1603	.0792	2	0.0434	0.1573	0.0825	0.1264
3	0.1951	0.1290	.0438	.1964	.0989	.1497	3	0.1613	0.0269	0.1188	0.0936
4	0.1825	0.1512	.2026	.0001	.1307	.1211	4	0.0031	0.1640	0.1079	0.1061
5	0.0735	0.2298	.0575	.1963	.1512	.1000	5	0.1623	0.0278	0.0879	0.1240
6	0.2437	0.0403	.1667	.1228	.0551	.1741	6	0.0646	0.1524	0.1393	0.0621
7	0.1703	0.1895	.1825	.1042	.1842	.0044	7	0.1300	0.1040	0.0282	0.1506
8	0.0451	0.2614	.0070	.2140	.0739	.1710	8	0.1404	0.0917	0.1534	0.0132
9	0.2304	0.1590	.1895	.1098	.1251	.1412	9	0.0364	0.1651	0.0595	0.1431
10	0.3005	0.0229	.2062	.0905	.1865	.0439	10	0.1677	0.0321	0.1152	0.1052
11	0.2704	0.1972	.0682	.2229	.0614	.1851	11	0.1033	0.1384	0.1418	0.0679
12	0.1953	0.3386	.1124	.2160	.1190	.1598	12	0.0730	0.1590	0.0038	0.1585
13	0.1201	0.4800	.2368	.1011	.2041	.0066	13	0.1763	0.0206	0.1450	0.0679
14	0.0650	0.7014	.2724	.0518	.1464	.1512	14	0.1180	0.1366	0.1309	0.0955
15	0.0316	1.1566	.2399	.1916	.0008	.2183	15	0.0386	0.1800	0.0142	0.1634
16	0.0140	2.1901	.1775	.3076	.1452	.1762	16	0.1663	0.0884	0.1461	0.0796
17	0.00570	4.684	.1150	.4235	.2331	.0636	17	0.1831	0.0622	0.1527	0.0724
18	0.00215	11.080	.0668	.5923	.2511	.0680	18	0.0931	0.1765	0.0394	0.1675
19	0.000759	28.56	.0354	.9093	.2189	.1860	19	0.0435	0.2025	0.1021	0.1430
20	0.0002512	79.35	.0173	1.567	.1647	.2855	20	0.1619	0.1442	0.1779	0.0265
21	0.00007839	235.96	.0079	3.008	.1106	.3849	21	0.2264	0.0378	0.1521	0.1051
22	0.00002315	746.45	.0034	6.231	.0676	.5229	22	0.2343	0.0780	0.0502	0.1842
23			.0013	14.40	.0380	.7654	23	0.2031	0.1809	0.0732	0.1843
24			.0005	35.08	.0199	1.237	24	0.1550	0.2686	0.1704	0.1186
25					.0098	2.205	25	0.1070	0.3564	0.2190	0.0191
26					.0045	4.274	26	0.0678	0.4739	0.2207	0.0846
27					.0020	3.908	27	0.0399	0.6703	0.1908	0.1762
28					.0008	19.78	28	0.0220	1.034	0.1473	0.2552
29					.0003	46.47	29	0.0114	1.743	0.1038	0.3312
30					.0001	114.98	30	0.0056	3.178	0.0677	0.4370
31					0	298.48	31	0.0026	6.203	0.0413	0.6023
32					0	810.10	32	0.0012	12.85	0.0237	0.8967
33					0	2294.6	33	0.0005	28.05	0.0129	1.447
34					0	6761.7	34	0.0002	64.29	0.0066	2.515
35					0	20645.0	35	0.0001	154.1	0.0033	4.660
36					0	65672.0	36			0.0015	9.135
							37			0.0007	18.83
							38			0.0003	40.63
							39			0.0001	91.45
							40			0.00005	214.1
							41			0.00002	520.4

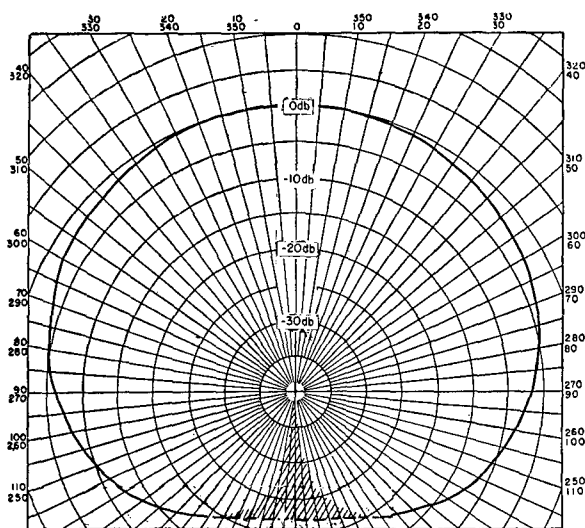


FIGURE 1. Amplitude pattern of single element 10 degrees wide in stiff baffle,  $ka = 16$ .

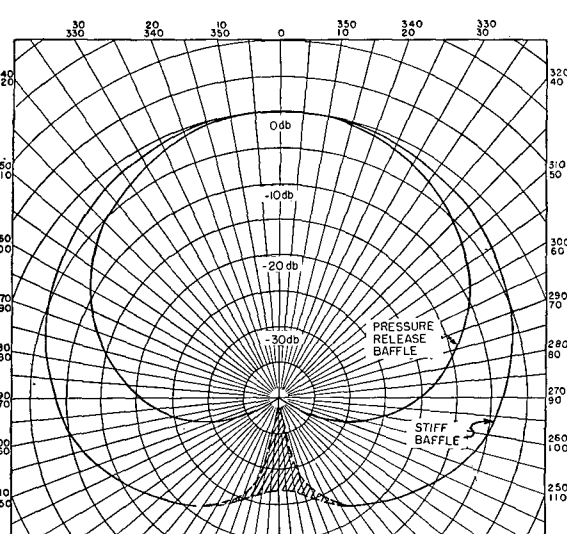


FIGURE 3. Amplitude pattern of single element 10 degrees wide,  $ka = 20$ .

### 9.1.5 Single-Element Patterns<sup>2,4</sup>

The amplitude and phase patterns of single elements in several cases have been computed from equation (1). Thus  $ka = 16$  and an element of 10 degrees in Figures 1 and 2,  $ka = 20$  and an element of 10 degrees in Figures 3 and 4, and  $ka = 24$  and an element of  $7\frac{1}{2}$  degrees in Figures 5 and 6. In the cases  $ka = 20$  and 24, the element patterns are shown under two baffle conditions. A diffraction pattern exists in the very back of the pattern in the stiff baffle cases with  $ka = 20$  and 24. The computations are not made at

small enough intervals to reveal the fine structure of this diffraction pattern, but it has a period of  $\frac{180}{ka}$  degrees. It is a low-level effect and relatively unimportant.

### 9.1.6 Simplified Single Element Theory

As may be seen from equation (1), the pressure pattern  $P$  of a sector of a cylinder is a complex function of  $\phi$ ; that is,  $P$  has a real and an imaginary part, which can be converted into amplitude and phase angle. When the radius of the cylinder is large and the

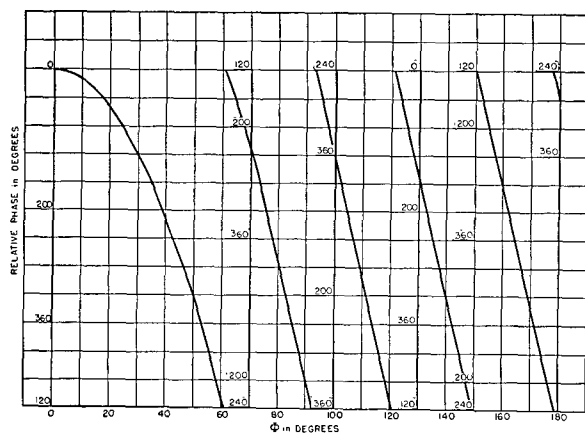


FIGURE 2. Phase pattern of single element 10 degrees wide in stiff baffle,  $ka = 16$ .

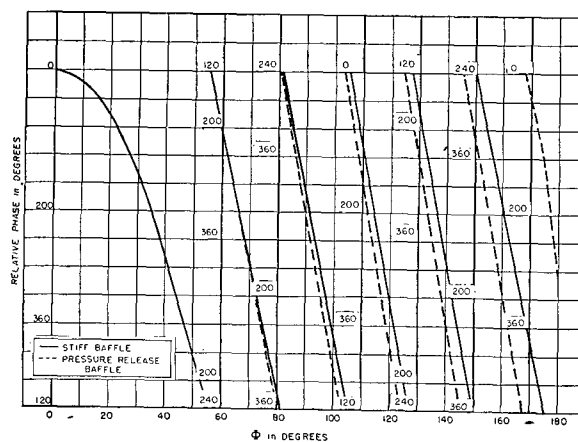


FIGURE 4. Phase pattern of single element 10 degrees wide,  $ka = 20$ .

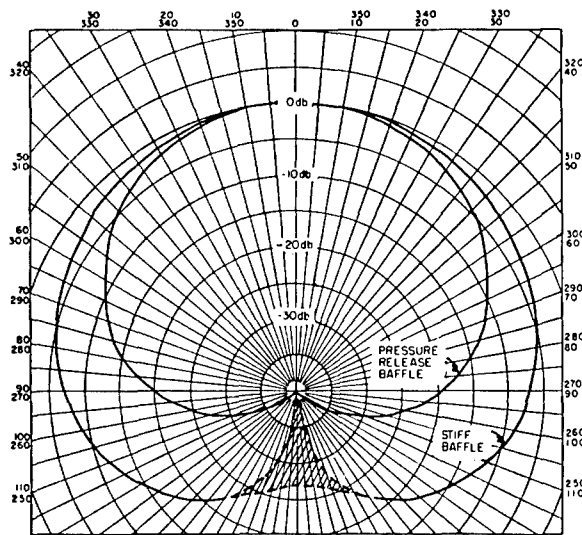


FIGURE 5. Amplitude pattern of element  $7\frac{1}{2}$  degrees wide,  $ka = 24$ .

width of the sector is small compared to the wavelength of the signal, simple geometric arguments may be used to obtain a good approximation to  $P$  over the front half of the transducer; that is,

$$-\pi/2 < \phi < \pi/2.$$

Now a cylindrical transducer is considered, having a narrow active sector receiving a signal from a distant source. It is assumed that the source is stationary and at an angle  $\phi = 0$ , so that the pattern of an element is obtained by measuring the response of the element as the transducer is rotated about its axis.

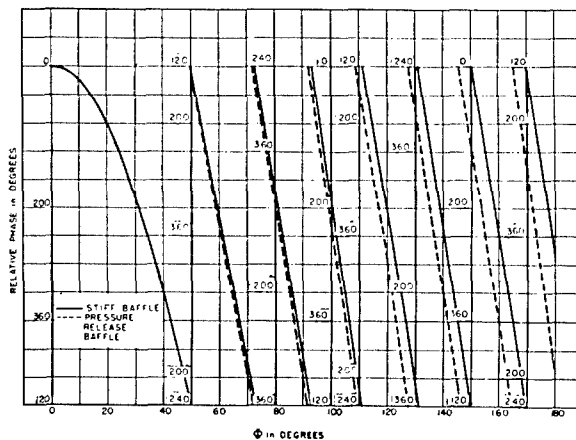


FIGURE 6. Phase pattern of element  $7\frac{1}{2}$  degrees wide,  $ka = 24$ .

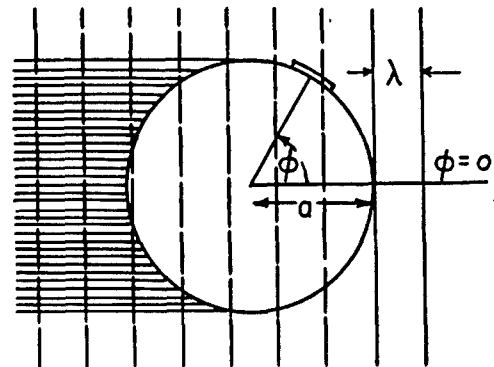


FIGURE 7. Section of cylindrical transducer showing path differences.

When the element is at a typical angle  $\phi$ , the situation is as shown in Figure 7; the extra distance which a signal must travel to reach the element in this position, as compared to when it is at  $\phi = 0$ , is  $a(1 - \cos \phi)$ . The lag in the phase of the signal is then

$$\angle P = ka(1 - \cos \phi) \text{ radians.} \quad (2)$$

The normalized amplitude of  $P$  is proportional to the projection of the element in the direction of the incoming signal, and is given by

$$|P| = \cos \phi. \quad (3)$$

Equations (2) and (3) hold only over the illuminated half of the cylinder. In the shadow region this simplified analysis gives  $P = 0$ . Actually, this is not the case, though the back sensitivity is well below the front sensitivity. To get an accurate picture of this diffraction effect, reference must be made once more to the exact formula for the pattern given in equation (1).

#### 9.1.7

### Time Delay Concept

Mention has been made of the phase pattern of  $P$  as determined from equation (1) or as approximately given by equation (2). It is perhaps more accurate to speak of time lags or delays, for the lag in phase is caused by the additional time delay of signals reaching elements removed from the acoustic axis of the transducer. If  $\tau'$  is the time it takes the signal to travel a distance equal to the radius of the cylinder, and if  $\tau$

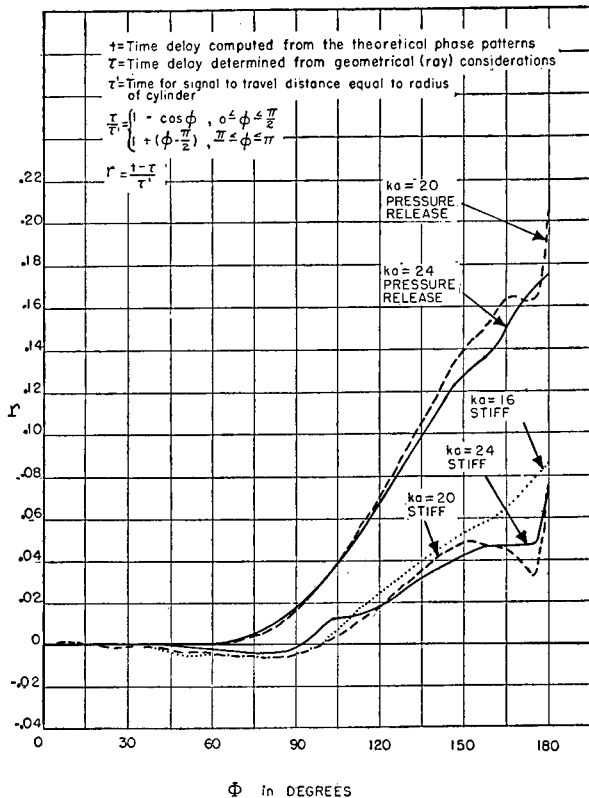


FIGURE 8. Single-element time delay patterns.

is the time lag of the signal in reaching the element at an angle  $\phi$  compared with the element at  $\phi = 0$ , then,

$$\frac{\tau}{\tau'} = 1 - \cos \phi. \quad (4)$$

This holds as long as  $-\pi/2 < \phi < \pi/2$ , and is based on the same simplified assumptions as those upon which

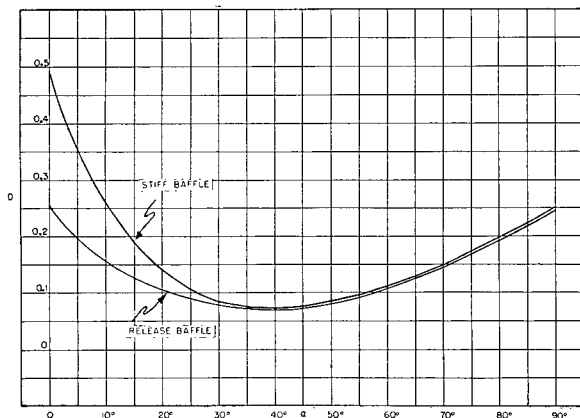


FIGURE 9. Directivity ratio of sector of cylinder of angle  $\alpha$ ,  $ka = 24$ .

(2) is based. An extension of this formula for elements in the shadow region may be obtained if it is assumed that the signal travels along the circumference in order to reach elements in the back of the transducer. Then

$$\frac{\tau}{\tau'} = 1 + \left( \phi - \frac{\pi}{2} \right). \quad (5)$$

This holds when  $\pi/2 \leq |\phi| \leq \pi$ . The curves in Figure 8 have been plotted to show how closely the actual time delays fit the relations above. Here the differences between the time delays computed from the exact equation (1), and the time delays given by equations (4) and (5), are plotted as functions of the angle  $\phi$ . The curves group themselves according to the baffle conditions assumed, but in both cases the approximations of equations (4) and (5) are good.

The concept of time delay was introduced for several reasons. One was that time delay has a simple and obvious geometrical explanation which is *independent of the frequency of the signal*. This fact is important, for example, in the construction of an electrical network to simulate in amplitude and phase the pattern of a single element of a transducer. An artificial transducer line, as a network of this type is sometimes called, is usually a tandem arrangement of phase-lagging sections and the desired voltages are tapped off at the proper points along the line. The phase-lagging sections are simple low-pass filters which have a fairly constant time delay per section over a range of frequencies. Hence the same artificial

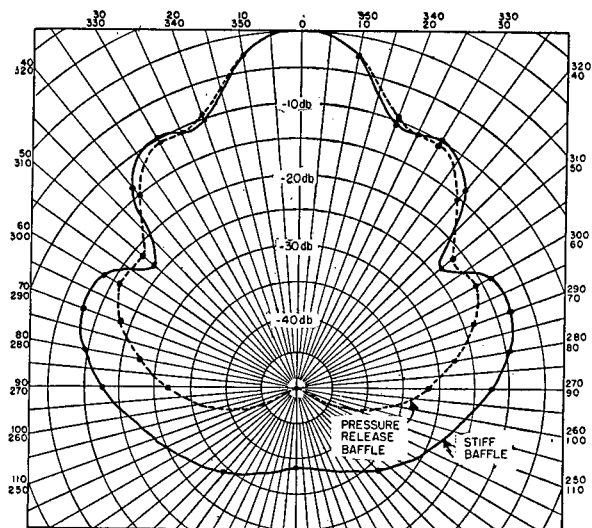
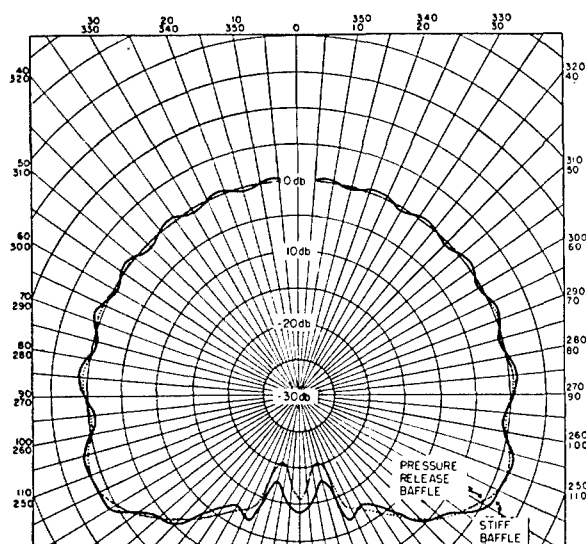
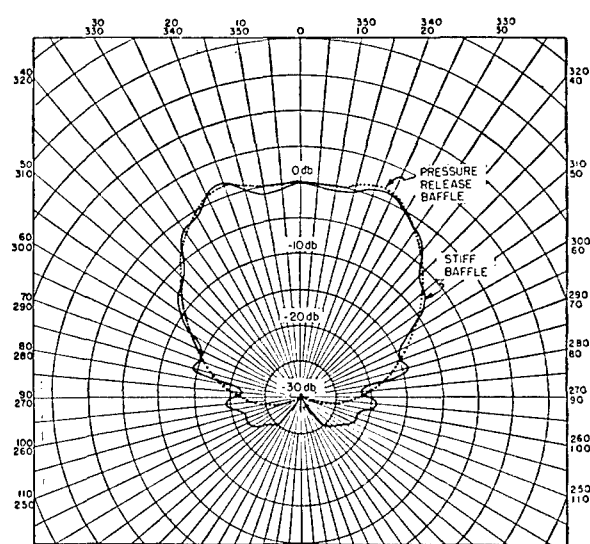


FIGURE 10. Amplitude pattern of 40-degree sector (minimum directivity index),  $ka = 24$ .



FIGURE 11. Pattern of 270-degree sector,  $ka = 24$ .FIGURE 12. Pattern of 90-degree sector,  $ka = 24$ .

transducer line can be used to simulate various real transducers as long as they are of equal size and have the same number of elements, even though they may operate at different frequencies.

#### 9.1.8 Sector Pattern of Minimum Directivity Ratio<sup>5</sup>

It is noticed that the amplitude pattern of a 10-degree sector is slightly narrower than that of a  $7\frac{1}{2}$ -degree sector. This narrowing of the pattern is expected as the width of the sector increases through small angles. On the other hand, the pattern of a sector of 360 degrees, a pulsating cylinder, is uniform in all directions. Hence a pattern of minimum width or minimum directivity ratio may be expected for some intermediate angular width of sector. In Figure 9, the directivity ratio of a sector of a cylinder of  $ka = 24$  is plotted against the angular width of the sector. The two-dimensional directivity ratio of a normalized pattern  $P(\phi)$  is defined as

$$D = \frac{1}{2\pi} \int_{-\pi}^{\pi} |P(\phi)|^2 d\phi.$$

The minimum is seen to exist for a sector of width 40 degrees under both baffle conditions; this minimum, however, is very broad. In Figure 10 the amplitude pattern of a sector of 40 degrees is shown.

#### 9.1.9 Patterns of 90-Degree and 270-Degree Sectors<sup>6</sup>

For depth-scanning purposes, it is of interest to know the patterns of a 270-degree and a 90-degree sector. These are shown in Figures 11 and 12 for  $ka = 24$ .

#### 9.2 COMMUTATED ROTATION [CR] SONAR

##### 9.2.1 Introduction<sup>1</sup>

In CR sonar the rotation of the pattern is accomplished by mechanically turning a circular array of plates. This array is capacitively coupled to a similar stationary array to which the signals of the individual elements of the transducer are applied. A detailed description of the CR sonar system is given in Chapter 5. In this section the theory of pattern formation for CR sonar is given. It is worth noting, however, that the theory developed here is to a considerable extent independent of the exact mechanism of the rotation. For example, it applies equally well to a system which uses inductive coupling between the rotor and the stator. The basic assumption in the theory is that the signals from the various elements are presented individually so that each can be phased and attenuated by a desired amount and then combined to form a resultant signal whose amplitude as a function of direction is the pattern.

### 9.2.2 Mathematical Theory of CR Sonar Pattern Formation<sup>1,7,8</sup>

If  $P(\phi)$  is the pattern of an element centered in the direction  $\phi = 0$ , then the pattern of an element whose midpoint is at  $\phi = \phi_k$  is  $P(\phi - \phi_k)$ . If the excitation of the  $k'$  element has a magnitude and an angle equal to that of the complex number  $U_k$ , then the resultant pattern formed by all the elements is

$$\begin{aligned} R(\phi) &= \sum_{k=0}^{N-1} U_k P(\phi - \phi_k) \\ &= P_0 \sum_{k=0}^{N-1} U_k \sum_{m=-\infty}^{\infty} \frac{\sin m\alpha}{m\alpha} D_m e^{jm(\phi - \phi_k)}, \end{aligned}$$

where  $N$  is the number of elements. If the transducer acts as a stiff baffle,  $U_k$  is spoken of as the velocity of the  $k'$  element and all  $U_k$  elements together form a velocity distribution. If the transducer presents a pressure release baffle,  $U_k$  is referred to as the pressure of the  $k'$  element and all  $U_k$  elements together form a pressure distribution. In either case, however, the attenuation and phasing of the patterns of single elements indicated by  $U_k$  are affected by electrical attenuation and phase-shifting networks which combine the excitations of the elements to form the final pattern. It may be assumed that the only interaction between the elements of the transducer is through the water; that is, each element may be considered as a baffle for all the others. Since the elements are contiguous and of equal angular width  $2\alpha$ ,

$$2\alpha = \frac{2\pi}{N}.$$

An effort may now be made by trial and error to find the  $U_k$  elements which yield the best pattern, assuming that  $ka$  (determined by the size of the transducer and the signal frequency) and  $N$  are given. This method of procedure was employed when the problem of pattern formation by a cylindrical transducer first arose, and some of the results are given in the *Report on Directivity Patterns*.<sup>1</sup> It is obvious that such a trial-and-error method has many limitations; for example, it is not known whether or not the pattern obtained is the best possible one, and the separate limitations imposed on the choice of  $ka$  and  $N$  cannot

be exhibited. It is much more desirable to set up a straightforward mathematical procedure by which the  $U_k$  elements may be determined to approximate a previously chosen desirable pattern. This is the method to be followed here.

A pattern which has a major lobe width of  $2\Delta$  radians 8.68 db (pressure  $1/e$ ) from the peak, and which has the desirable characteristics of low back radiation and no minor lobes is the Gaussian pattern,

$$R_0'(\phi) = e^{-(\phi/\Delta)^2}.$$

This is not a periodic function of  $\phi$  and is, therefore, not expandable in a Fourier series. However, when  $\pi/\Delta \gg 1$  the periodic function

$$R_0(\phi) = \sum_{n=-\infty}^{\infty} e^{-\left(\frac{\phi + 2n\pi}{\Delta}\right)^2}$$

closely approximates the Gaussian function. Its Fourier expansion is

$$\begin{aligned} R_0(\phi) &= \frac{\Delta}{2\sqrt{\pi}} \sum_{m=-\infty}^{\infty} e^{-\left(\frac{\Delta m}{2}\right)^2} e^{jm\phi} \\ &= \frac{\Delta}{2\sqrt{\pi}} \left[ 1 + 2 \sum_{m=1}^{\infty} e^{-\left(\frac{\Delta m}{2}\right)^2} \cos m\phi \right] \end{aligned}$$

Equating the corresponding terms of  $R_0(\phi)$  and  $R(\phi)$ , the following system of equations is obtained:

$$\sum_{k=0}^{N-1} U_k B_m e^{-jm\phi_k} = e^{-\left(\frac{\Delta m}{2}\right)^2}, \quad m = -\infty, \dots, 0, \dots, \infty \quad (6)$$

where

$$B_m = \frac{\sin m\alpha}{m\alpha} D_m = B_{-m},$$

with  $P_0$  chosen to equal  $\Delta/2$  for convenience. Equation (6) represents an infinite system of equations, since it holds for each integer value of  $m$ . Hence it cannot be solved exactly for the  $2N$  unknowns; namely, the real and imaginary parts of the  $U_k$  ele-

ments. However, the equations can be solved in a least square sense. If they are written in matrix form,

$$(b_{mk})(U_k) = (c_m),$$

where

$$b_{mk} = B_m e^{-jm\phi_k},$$

and

$$c_m = e^{-\left(\frac{\Delta m}{2}\right)^2},$$

then

$$(b_{mg}^*)^T (b_{mk})(U_k) = (b_{mg}^*)^T (c_m),$$

where  $(a)^T$  is the transform of  $(a)$ . This is a system of  $N$  equations in the  $N$  complex unknowns  $U_k$ . Applying this procedure to equation (6), the following is obtained:

$$\begin{aligned} \sum_{k=0}^{N-1} U_k \sum_{m=-\infty}^{\infty} B_m B_m^* e^{-jm(\phi_k - \phi_g)} \\ = \sum_{m=-\infty}^{\infty} B_m^* e^{jm\phi_g} e^{-\left(\frac{\Delta m}{2}\right)^2}, \quad g = 0, 1, \dots, N-1. \end{aligned} \quad (7)$$

Instead of adopting the above procedure, a solution may be attempted by minimizing the integral

$$\int_{-\pi}^{\pi} |R(\phi) - R_0(\phi)|^2 d\phi$$

with respect to the  $U_k$ 's where  $R(\phi)$  is the actual pattern and  $R_0(\phi)$  is the Gaussian pattern. However, it should lead to the same set of equations (7).

There are two cases to be considered; one in which the line of symmetry of the pattern passes through the midpoint of an element, and the other in which the line of symmetry passes between two contiguous elements. These are called Cases I and II respectively (see Figure 13).

$$\phi_k = \begin{cases} \frac{2\pi}{N} k & \text{Case I} \\ \frac{2\pi}{N} \left(k + \frac{1}{2}\right) & \text{Case II} \end{cases}$$

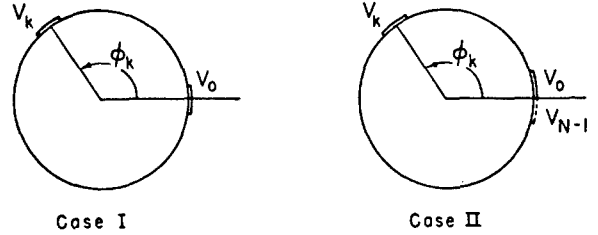


FIGURE 13. Two positions of acoustic axis relative to elements.

If these values are substituted in equation (7) and the periodicity of the coefficients is used, it leads to the system of equations

$$\begin{aligned} \sum_{k=0}^{N-1} U_k e^{-jm\phi_k} \sum_{n=-\infty}^{\infty} B_{m+nN} B_{m+nN}^* \\ = \sum_{n=-\infty}^{\infty} (\pm)^n B_{m+nN}^* e^{-\frac{\Delta^2 (m+nN)^2}{4}}. \end{aligned} \quad (8)$$

Thus

$$\sum_{k=0}^{N-1} U_k e^{-jm\phi_k} = A_m$$

where

$$A_m = \frac{\sum_{n=-\infty}^{\infty} (\pm)^n B_{m+nN}^* e^{-\frac{\Delta^2 (N-m)^2}{4}}}{\sum_{n=-\infty}^{\infty} B_{m+nN} B_{m+nN}^*}$$

The plus sign is used in Case I, the minus sign in Case II. Ordinarily, only the principal two terms in these series are important, so that

$$A_m = \frac{B_m^* e^{-\left(\frac{\Delta m}{2}\right)^2} \pm B_{N-m}^* e^{-\frac{\Delta^2 (N-m)^2}{4}}}{B_m B_m^* + B_{N-m} B_{N-m}^*}$$

The set of equations (8) can be solved for the  $U_k$ 's. The following is a summary of the relations between  $A_m$  and  $U_k$  in trigonometric form.  $N$  is assumed to be even.

Case I:

$$A_m = U_0 + 2 \sum_{k=1}^{\frac{N}{2}-1} U_k \cos \frac{2\pi}{N} mk + (-1)^m U_{(N/2)}$$

$$U_k = \frac{1}{N} \left[ A_0 + 2 \sum_{m=1}^{\frac{N}{2}-1} A_m \cos \frac{2\pi}{N} mk + (-)^k A_{(N/2)} \right]$$

Case II:

$$A_m = 2 \sum_{k=0}^{\frac{N}{2}-1} U_k \cos \frac{2\pi}{N} m \left( k + \frac{1}{2} \right)$$

$$U_k = \frac{1}{N} \left[ A_0 + 2 \sum_{m=1}^{\frac{N}{2}-1} A_m \cos \frac{2\pi}{N} m \left( k + \frac{1}{2} \right) \right]$$

### 9.2.3 Restrictions on Parameters

Substituting into the pattern  $R(\phi)$ , it is found that

$$R(\phi) = \frac{\Delta}{2\sqrt{\pi}} \sum_{m=-\infty}^{\infty} A_m B_m e^{jm\phi}$$

Comparing this with the Gaussian pattern  $R_0(\phi)$ , which is being approximated, it is found that the parameters  $ka$ ,  $N$ , and  $\Delta$  must satisfy certain inequalities if the approximation is to be good. First, in order that  $R(\phi)$  and  $R_0(\phi)$  coincide up to terms for which  $m \cong N/2$ , it must be that  $|B_m| \ll 1$  when  $m > N/2$ . Since  $|B_m|$  decreases rapidly only beyond  $m = ka$ ,

$$\begin{aligned} ka &\ll \frac{N}{2} \\ \frac{ka}{N} &\ll \frac{1}{2}. \end{aligned} \quad (9)$$

This states that the width of a single element of the transducer must be less than half a wavelength. On the other hand, in order that the terms beyond  $m = N/2$  (that is, the terms not being well approximated) may be small,

$$\left( \frac{\Delta N}{4} \right)^2 \gg 1$$

or,

$$\Delta \gg \frac{4}{N}. \quad (10)$$

The conditions (9) and (10) are actually interrelated, and are more stringent than they need to be. Transducers have been built in which (9) and (10) have both been violated and yet the patterns have been reasonably acceptable. Of course, everything depends upon what minor lobe structure and back sensitivity are acceptable. The order of magnitude of the principal minor lobe may be obtained by summing the terms of  $R_0(\phi)$  which are poorly approximated. The contribution of the terms exceeding  $m = N/2$  is

$$\frac{\Delta}{\sqrt{\pi}} \sum_{m=N/2}^{\infty} e^{-\left(\frac{\Delta m}{2}\right)^2} \cong \frac{2}{\sqrt{\pi}} \int_{\frac{\Delta N}{4}}^{\infty} e^{-x^2} dx$$

Thus the relation exists,

$$\frac{\text{Error in Pattern}}{\text{Maximum Ordinate}} = \text{Erfc} \left( \frac{\Delta N}{4} \right), \quad (11)$$

where  $\text{Erfc}$  is 1 minus the error integral

$$\text{Erf } x = \frac{2}{\sqrt{\pi}} \int_0^x e^{-u^2} du.$$

The error in the patterns sets an upper limit to the size of the minor lobes obtained with the given approximation. Thus if  $\Delta \geq 8/N$ , the minor lobes are more than 58 db below the principal maximum, while if  $\Delta = 4/N$ , the minor lobes are at least 16 db below the principal maximum provided that the other conditions are satisfied. These estimates are pessimistic as seen later from computed theoretical patterns. The agreement with actual patterns such as those shown in Figures 24 to 28 is much better. It is interesting that the criteria (9), (10), and (11) set no lower limit on the dimensions of the cylinder. This agrees with the statement at the outset that with a continuous cylindrical source of any radius there is always a velocity or pressure distribution which gives a Gaussian pattern of any width, and that the required distribution may be approximated by a sufficient subdivision of the cylinder into sections. Since the maximum power radiated decreases rapidly with

the dimensions of the radiator, it should be as large as possible, consistent with equation (9) and with mechanical limitations.

#### 9.2.4 Pattern of Minimum Directivity Ratio<sup>1</sup>

From equation (11) it can be seen that the less stringent the requirement put on the minor lobes, the narrower the main lobe can be made. It is of some interest to determine the narrowest pattern that can be obtained with a given size radiator and a given number of vibrating sections. This problem is solved in the *Report on Directivity Patterns*<sup>1</sup> by minimizing the two-dimensional directivity ratio; that is, the integral

$$\frac{1}{2\pi} \int_{-\pi}^{\pi} |\text{Actual Pattern}|^2 d\phi$$

subject to the auxiliary condition that the maximum ordinate is kept constant. It turns out that the velocity or pressure distribution required to obtain this pattern of minimum directivity ratio is the same as that required to approximate the Gaussian pattern of zero width, that is,  $2\Delta = 0$ . The actual pattern obtained then is the error in the approximation. Provided the width of the individual sections is less than half a wavelength as before, it is shown in the *Report on Directivity Patterns*<sup>1</sup> that the resulting directional pattern is approximately of the form

$$\frac{\sin(N+1)\phi/2}{(N+1)\sin\phi/2}.$$

This pattern is approximately that of a line source whose length is

$$l = (N+1) \frac{\lambda}{2\pi} = \frac{N+1}{k}.$$

It follows that  $l$  becomes larger with  $N$  and, hence, the width of the narrowest attainable pattern diminishes as  $N$  increases. If  $ka/N = 1/2$  and  $N \gg 1$ ,

$$l = \frac{Na}{ka} = 2a,$$

so that the length of the equivalent line source is then equal to the diameter of the transducer. The width of

the major lobe 6 db from the peak is approximately  $432/N$  degrees, which is 9 degrees when  $N = 48$ . From the above equations it can be seen that the total angular width of the major lobe is just twice the angular width of one of the elements. The principal objection to this pattern of minimum directivity ratio is the height of the minor lobes, which is only 13.5 db below the peak of the major lobes.

#### 9.2.5 Computation Program<sup>9</sup>

To what degree the conditions stated in (9) and (10) may be violated is one of the important unsolved problems of transducer design and pattern formation. It is interrelated with the problem of the optimum choice of the number of elements to use in forming the pattern, which in turn depends on the width of the pattern, minor lobe limitations, and back sensitivity. A scanning sonar pattern computer has been designed which should not only contribute appreciably to present knowledge of how best to choose the available parameters to form a desirable pattern for any given transducer, but should also reveal a good deal about the allowable tolerances on these parameters. The latter subject is one on which little is known at present.

The principle upon which the pattern computer is designed is a simulation of the transducer and beam-forming attenuation and phase-shift networks so that the parameters may be varied at will and the resulting patterns obtained. Let  ${}_iA_T$  and  ${}_i\theta_T$  be the amplitude and angle, respectively, of the voltage of the  $i$ th element of the transducer, and  ${}_iA_L$  and  ${}_i\theta_L$  be the amplitude and phase of the voltage transfer at the  $j$ th position of the electrical beam-forming line. Then the pattern voltage when the acoustic axis passes through the  $k'$  element is

$$P_k = \sum_i [{}_iA_T \angle {}_i\theta_T] [{}_{k-i}A_L \angle {}_{k-i}\theta_L].$$

Thus the pattern is obtained by varying  $k$ . A selected set of values of  $A_L$  and  $\theta_L$  is set on dials by the operator; then a cam which carries the transducer characteristics (that is, the  $A_T$  and  $\theta_T$  information) is pushed through the machine by a motor. By means of synchro transmission, a turntable on a directional pattern tracer is rotated and the result of the summation is plotted directly by the pattern tracer. The process of summation is carried out electrically through ad-

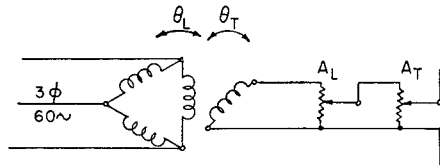


FIGURE 14. Schematic diagram of pattern computer.

dition of a number of 60-cycle voltages obtained from circuits of the form shown in Figure 14. A phase-shifting transformer is excited from a three-phase source; the voltage induced in the secondary is constant in amplitude but varies in phase according to the rotation of the secondary. This rotation is produced by rack and pinion connection to a cam follower, and the phase is further modified in accordance with  $\theta_L$  by hand-set of the stator angle.  $A_L$  is hand-set on one potentiometer, and the other is cam-controlled in accordance with the amplitude pattern of the transducer. One of these circuits is required for each active element. In the computer recently designed provision is made for a maximum of 24 such elements.

### 9.2.6 Determination of Pattern Width<sup>8</sup>

The results of the rather limited computations so far undertaken are given here. Investigation is first made of the effect of the choice of  $2\Delta$ , the width of the pattern on the required electrical phase shifts and attenuations as given by the angle and magnitude, respectively, of the  $U_k$ 's. The velocity distribution  $U_k$ 's have been calculated under stiff baffle conditions for  $ka = 20$ ,  $N = 36$ , and  $\Delta = 0.0, 0.100, 0.173$ . The

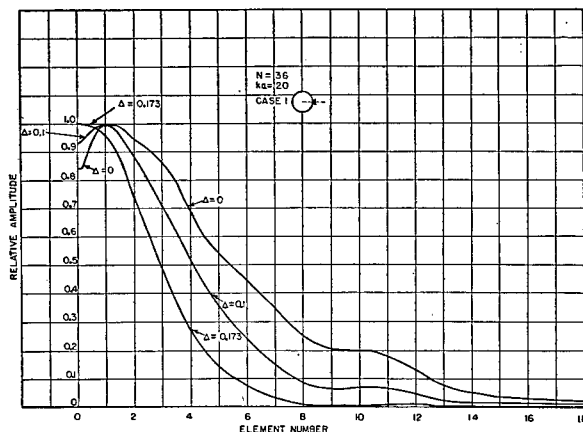


FIGURE 15. Comparison of amplitude distributions on circular transducer.

single-element patterns are shown in Figures 3 and 4. The required attenuations and phases are plotted in Figures 15 and 16, with smooth curves through the points. The curves are normalized with respect to the strongest element which is assumed to have unit amplitude, and the phases are referred to the front element. The line of symmetry of the pattern passes through the midpoint of the zero element, which is Case I shown in Figure 13. It is clear that the phase distribution is not critically dependent upon the choice of  $\Delta$ . The close grouping of all the phase distributions indicates the necessity of having them correct within narrow limits, a fact that has important implications on the uniformity of the resonances and  $Q$ 's of the elements of the transducer. The attenuation distributions for the various values of  $\Delta$  vary widely and hence can be considered the principal determinants of the width of the pattern.

### 9.2.7

### Rotatability<sup>8</sup>

First a general theory of rotation of cylindrical beam patterns is considered. This theory does not assume any special form for the pattern being rotated. Therefore, the results apply, in particular, to the case of a Gaussian pattern.

The essential idea for the production of rotating beam patterns is exceedingly simple. It is most easily demonstrated for the case of a continuous distribution of sources on a cylindrical radiator. As was stated in 9.1.3, by a proper adjustment of the amplitudes and phases of these sources any desired form of stationary radiation pattern may be produced. In order

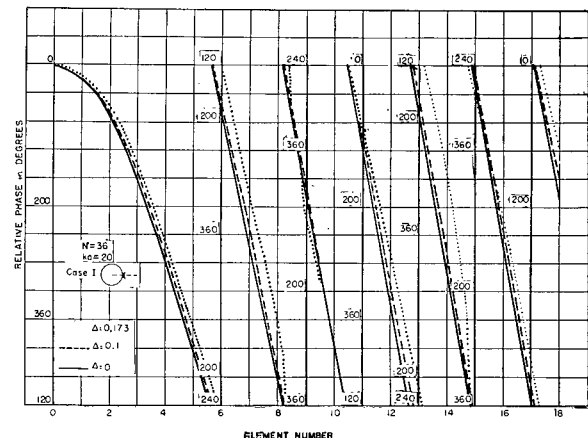


FIGURE 16. Comparison of phase distributions on circular transducer.

to generate the corresponding rotating pattern, it is only necessary to rotate the given phase and amplitude and distribution of the cylindrical radiator with the desired angular velocity. Let it be assumed that the phase and amplitude distribution necessary to produce the required stationary pattern is given by the function

$$A(\phi) e^{i\alpha(\phi)} e^{-i\omega_0 t}, \quad (12)$$

where  $\phi$  is the azimuth angle and  $\omega_0$  is the frequency of the signal. This function can be expanded in a complex Fourier series of the form

$$A(\phi) e^{i\alpha(\phi)} e^{-i\omega_0 t} = \sum_{R=-\infty}^{\infty} S_R e^{iR\phi} e^{-i\omega_0 t}.$$

The rotating distribution corresponding to equation (12) may be represented by the function

$$A(\phi - \omega_r t) e^{i\alpha(\phi - \omega_r t)} e^{-i\omega_0 t},$$

where  $\omega_r$  is the angular velocity of rotation. Written in the form of a Fourier series, this becomes

$$\begin{aligned} A(\phi - \omega_r t) e^{i\alpha(\phi - \omega_r t)} e^{-i\omega_0 t} \\ = \sum_{n=-\infty}^{\infty} S_n e^{in(\phi - \omega_r t)} e^{-i(\omega_0 + n\omega_r t)}. \end{aligned} \quad (13)$$

This represents the most general solution of the problem. The resulting equation (13) shows that *in order to produce a rotating pattern, it is necessary to use as many frequencies as there are Fourier components required to produce the desired stationary pattern.* In case equation (12) is a symmetrical function of  $\phi$ , as it is in most practical cases, it may be represented by a cosine series.

$$A(\phi) e^{i\alpha(\phi)} = \sum_{n=0}^{\infty} C_n \cos n\phi. \quad (14)$$

The result, equation (13) may then be written

$$\begin{aligned} A(\phi - \omega_r t) e^{i\alpha(\phi - \omega_r t)} e^{-i\omega_0 t} \\ = e^{-i\omega_0 t} \sum_{n=0}^{\infty} C_n \cos n(\phi - \omega_r t). \end{aligned} \quad (15)$$

This corresponds to the excitation of each source with a modulated signal, with the phase of the modulation distributed uniformly around the circle. In the general case, the modulating signal is non-sinusoidal and must contain several harmonics of the fundamental rotation frequency, the phase of each harmonic being controlled by the order of the harmonic. The relative amplitude of the harmonics and, hence, the wave form of the modulating signal is determined by the desired directional pattern.

In practice, it is not possible to achieve a continuous distribution of sources on the cylindrical radiator, and it is necessary to know what modifications must be introduced into the theory to deal with an array of discrete sources in the scanning sonar transducers considered in this report. The detailed mathematical analysis is set forth in Appendix V of the *Progress Report on Sonic Locator Developments*.<sup>10</sup>

A few of the main results obtained in the above report are presented here. In the first place, it is impossible to obtain a pure rotating pattern (that is, one which rotates without periodic distortion) with only a finite number of sources. In considering such a finite set of sources arranged at regular intervals on the circumference of a circle, the best which can be hoped for is a directional pattern which, as the rotation is followed, assumes only the same form after passing through an angle equal to an integral multiple of the angular distance between sources on the circle. Any pattern of such an array of sources can be represented as an undistorted rotating pattern plus a series of rotating patterns which oscillate rapidly as they rotate. In order that the oscillating part of the pattern may be small compared with the undistorted rotating part, it is necessary that the distance between adjacent sources on the circle be small compared with the wave length of the emitted radiation. This criterion is necessary, though the relationship attained in practice is not sufficient to ensure that the radiation pattern closely approximate an undistorted rotating pattern.

The sharpness of a pattern bears a direct relation to its Fourier coefficients. The sharper a pattern, the greater the number and the higher the order of the Fourier components necessary to produce it, according to equation (13). This implies, according to equation (14), the necessity of a correspondingly large number of modulation harmonics to produce the rotating directional pattern. Generally speaking,

$$\Delta \cong \frac{4\pi}{m},$$

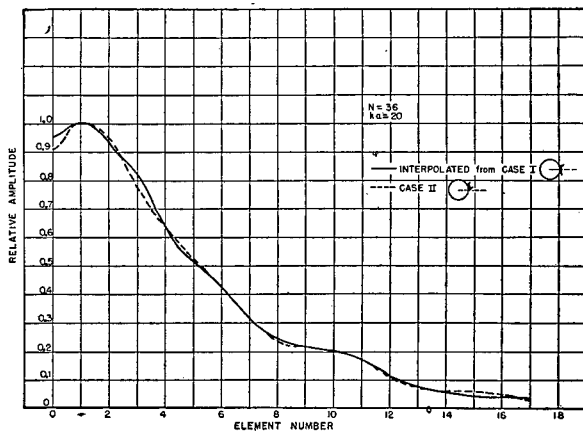


FIGURE 17. Amplitude distribution on circular transducer,  $\Delta = 0$ .

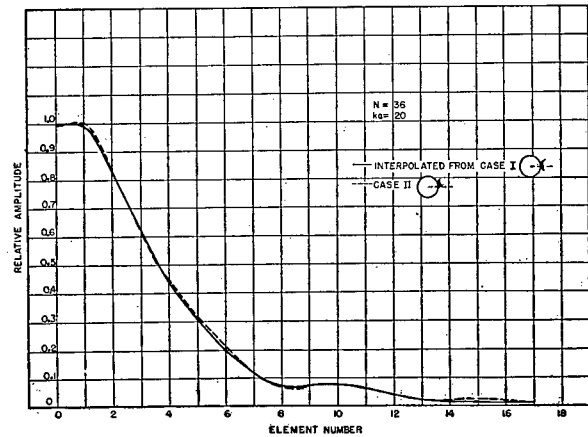


FIGURE 18. Amplitude distribution on circular transducer,  $\Delta = 0.1$ .

where  $\Delta$  is the angular width of the pattern and  $m$  is the order of highest harmonic changes used. It is shown in the above-mentioned report that it is necessary, in order that the pattern rotate without excessive distortion, for the number of sources to be at least twice the order of the highest harmonic used.

The foregoing discussion has assumed complete freedom of control over the phase and amplitude of the signal applied to each transducer element. One practical method of producing modulation of the phase and amplitude applied to such elements is to couple the signal source to (or from) the transducer elements by a condenser whose capacitance changes in a prescribed way with time. This may be recognized as one way to describe the function of the capacitive commutator, since its arrangement provides for a capacitive coupling which varies from zero to full registration.

It would theoretically be possible to consider analytically the time variation of excitation of a single transducer element as it is coupled capacitatively to successive points on the rotor lag line, to resolve this time variation into its 48 components, and to synthesize these components according to the prescription of equation (15). Such an approach has formidable difficulties, however, and it has not been undertaken.

Alternatively, the relative phase and amplitude distribution for the various elements of the transducer corresponding to a particular in-register position of the commutator might be considered, the directional pattern produced by this distribution of excitation might be computed and the results compared with a similar computation of the directional

pattern produced for the distribution of excitation provided by a mid-register position of the commutator. Unfortunately, this procedure also offers formidable computation difficulties. It has been found easier to compute the distribution required for an assigned directional pattern than to compute the directional pattern for an assigned distribution of excitation. Accordingly an indirect approach has been followed in examining analytically the special problems involved in the rotatability of the Gaussian patterns utilized in scanning applications.

In the preceding discussions of pattern formation, two cases have been distinguished: Case I in which the beam axis bisects a transducer element, and Case II in which the beam axis lies midway between two adjacent elements. If the beam pattern is rotatable, it might be expected that interpolation forms of  $U_{kr}$ , the complex excitation amplitude, at the midpoints of the curves drawn for Case I should approximate closely those obtained directly for Case II.

In fact, if the two velocity distributions obtained in this way differed greatly, it would seem likely that the pattern resulting from the velocity distributions is not rotatable; that is, there would be fluctuations in the shape of the pattern as the velocity distribution is rotated smoothly from position I to position II and then farther around to position I again. Therefore, the degree to which the velocity distribution of Case II coincides with the velocity distribution obtained from Case I by smooth curve interpolation may be taken as a measure of the "rotatability" of the pattern. It is not known how large a disparity between the two velocity distributions may be possible under



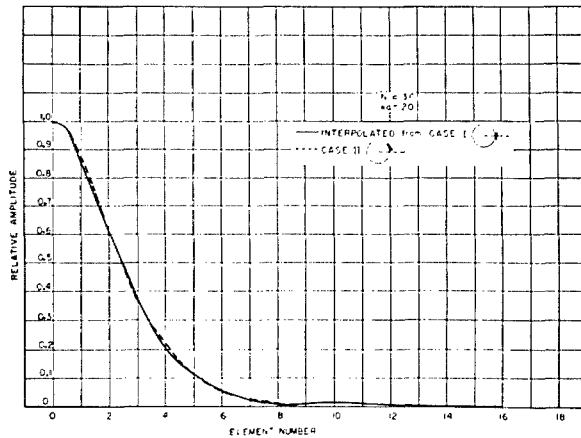


FIGURE 19. Amplitude distribution on circular transducer,  $\Delta = 0.173$ .

the requirement that the pattern, in actual practice, be rotatable. However, it has not been difficult to exercise judgment on the matter in those cases which have arisen thus far. In Figures 17 to 22 are shown the original and interpolated amplitude and phase distributions for  $\Delta = 0.0$ , 0.1, and 0.173. Fortunately, there is very little difference between the pairs of curves, even when  $\Delta = 0.0$  which is the pattern of minimum directivity ratio. It could, therefore, be expected that these patterns would be rotatable as has been verified in practice. A shifting in the major lobe has actually been observed when the acoustic axis is between the positions of Case I and Case II. This can be attributed to the chord rather than arc interpolation that occurs in practice. It is hoped that this source of error can be minimized by overlapping

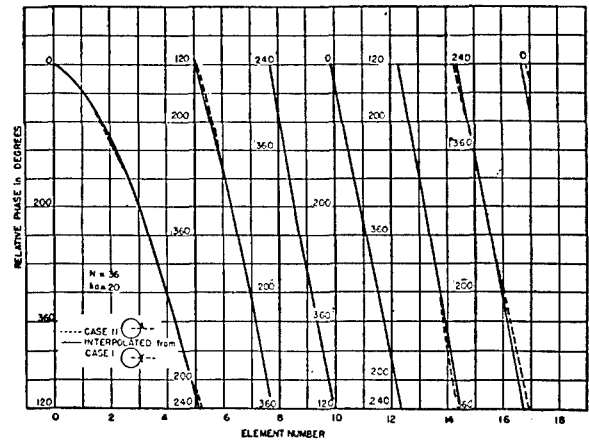


FIGURE 21. Phase distribution on circular transducer,  $\Delta = 0.1$ .

methods and by increasing the number of plates on the rotor.

### 9.2.8 Method for Improving Rotatability<sup>11</sup>

The latter suggestions are considered in more detail. It has been proposed that the rotor of the scanning commutator be subdivided into 96 (or more) sections, leaving the stator at 48. By this means twice as many voltages are obtained which can be applied to the beam-forming circuits to obtain improved rotation of the beam. It is to be understood that the transducer still has 48 elements and that the condition relating beam width and number of transducer sections still holds. Thus there is no improvement of

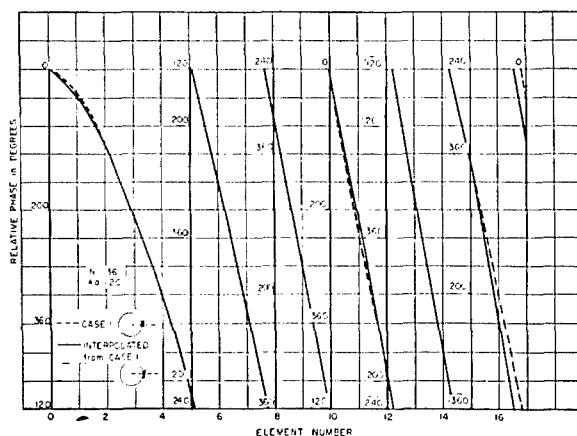


FIGURE 20. Phase distribution on circular transducer,  $\Delta = 0$ .

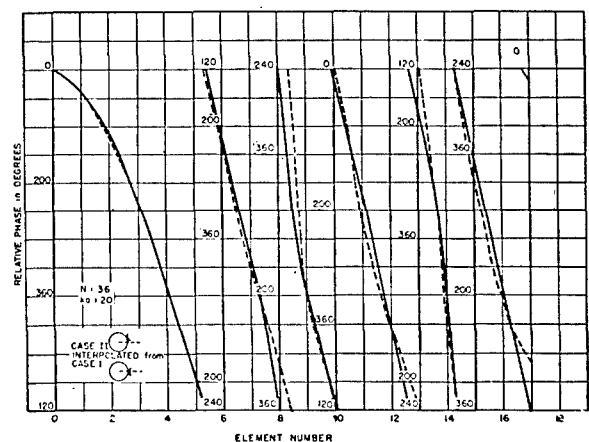


FIGURE 22. Phase distribution on circular transducer,  $\Delta = 0.173$ .

the theoretical pattern by this device, but only an increase in its smoothness of rotation.

In order to explain the proposal for improving the smoothness of rotation, the process of producing the rotation by a commutator can be explained with the help of Figure 23. The points on this diagram were computed to exhibit the values of the phase and amplitude which should be applied to successive elements of the transducer in order to produce a certain transmitting pattern. These points may also be interpreted to represent the attenuations and phase shifts which must be introduced by the lag line in order that the combined outputs of the transducer elements may produce the same pattern in reception. The points labeled 0, 1, 2, . . . give the amplitudes and phases to produce a pattern whose axis of symmetry bisects the "0" transducer element. It is noted that the transducer elements which correspond to the numerals 0, 1, 2, . . . occupy uniform angular intervals around the transducer, while the corresponding points on the diagram appear at angles and with amplitudes corresponding to the electrical response of corresponding transducer elements. The transducer elements are numbered symmetrically about "0" element . . . -2, -1, 0, 1, 2 . . . and the amplitude and phase of the response is the same for negatively numbered elements as for those positively numbered.

If it is now desired to produce a directional pattern whose axis lies midway between the elements 0 and +1, a position on the transducer which might be identified as  $+1/2$ , a similar set of points designating the phase and amplitude distribution for successive transducer elements may be added to the diagram. These points may be numbered  $1/2$ ,  $1 1/2$ , and  $2 1/2$ , and so forth. This distribution of phase and amplitude would correspond to the response of the successive elements of a transducer which had been rotated physically by half the angle of separation of the adjacent elements. This situation can be represented by renumbering the transducer elements  $-1 1/2$ ,  $-1/2$ ,  $+1/2$ ,  $+1 1/2$ , and again the points on the diagram may refer to elements of either sign.

When the commutator signals of the rotor and stator are "in register" there is a one-to-one correspondence between the elements of the transducer and the corresponding signals of the rotor. Beam-forming networks may be connected to the rotor elements to produce directional patterns centered either on the leading element "0" or on the  $1/2$ -position corresponding to the midpoint between the 0 and 1

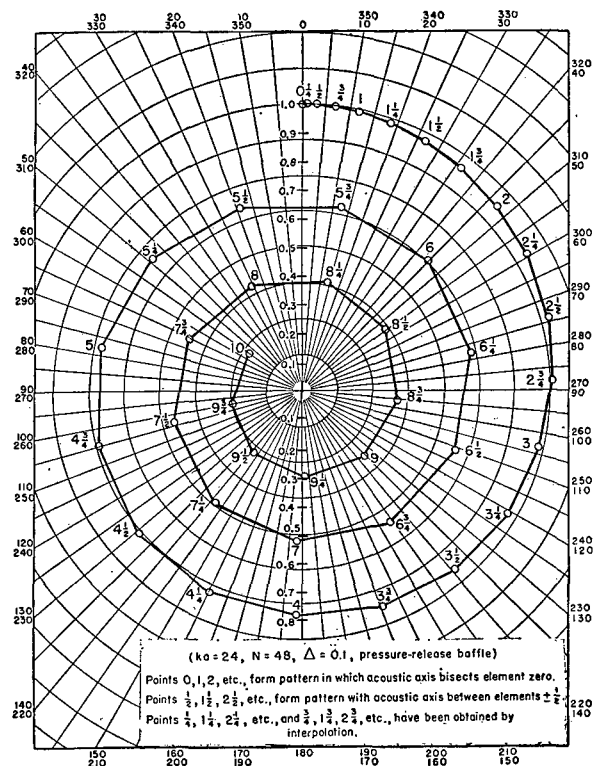


FIGURE 23. Amplitudes and phases to produce scanning pattern.

elements. Symmetry for BDI application predisposes for the latter choice which is now considered further. Principal attention focuses upon the situation arising when the rotor is not in register with the stator. For want of better information it is assumed that the phase and amplitude of the response observed for the successive rotor signals can be obtained by interpolating along a straight line joining the correspondingly numbered points in the figure. Thus when a rotor plate equally overlaps the two stator plates  $1/2$  and  $1 1/2$ , the interpolation would be along the straight line joining these two points in the figure. Inspection reveals that the midpoint of such a line does not fall far from the point 1 in the figure. This difference represents the error in the excitation of the corresponding element with regard to beam pattern formation for this intermediate rotor position. The error is small because the phase displacements for the first few transducer elements are small. The interpolation error increases rapidly, however, and is seen by inspection of the diagram to be quite large for elements more than 3 or 4 removed from the beam axis. It is also observed that the nature of the error at the mid-

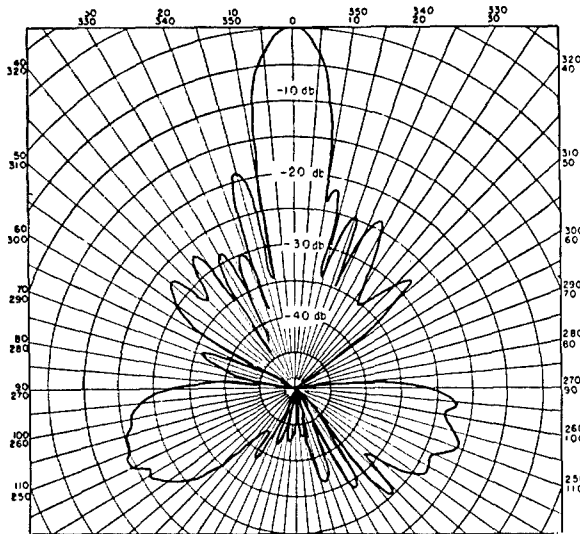


FIGURE 24. Actual pattern of Sangamo XQHA unit with rotor and stator in full register (Case II).

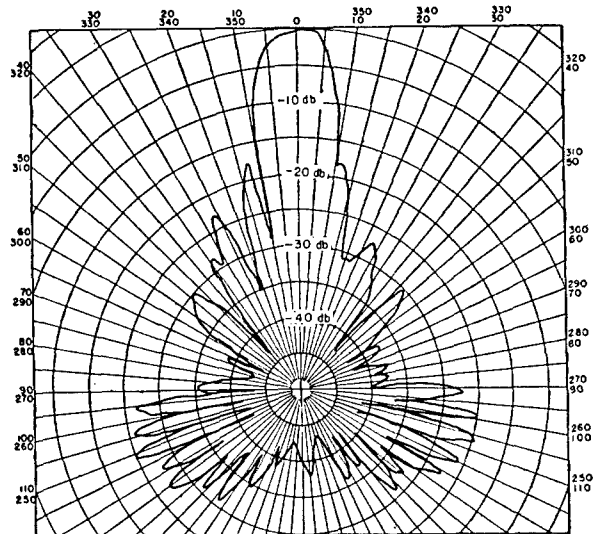


FIGURE 26. Actual pattern of Sangamo XQHA unit with acoustic axis in position of Case I.

position of the rotor (that is, midway between in-register positions) is a progressive reduction in amplitude of the elements removed from the center. This produces broadening of the major lobe and reduction of the minor lobes with respect to the patterns formed for in-register positions of the rotor. For positions other than the mid position, the errors in phase and amplitude produce distortion of the pattern and some bearing error. These effects are shown in Fig-

ures 24 to 28, which represent experimental patterns obtained with a unit of Sangamo XQHA.<sup>12</sup>

The proposal for subdivision of the rotor into 96 sectors can now be considered in detail. These sectors would be connected to a beam-forming network which, in order to produce a similar beam pattern, would be designed to provide attenuations and phasings as represented by the points  $\frac{1}{4}$ ,  $\frac{3}{4}$ ,  $1\frac{1}{4}$ , and so forth, which were obtained in preparing the diagram

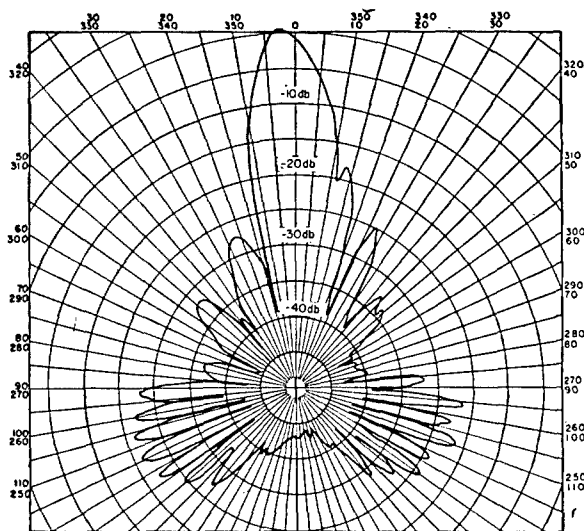


FIGURE 25. Actual pattern of Sangamo XQHA unit with acoustic axis midway between positions of Case I and Case II to the left.

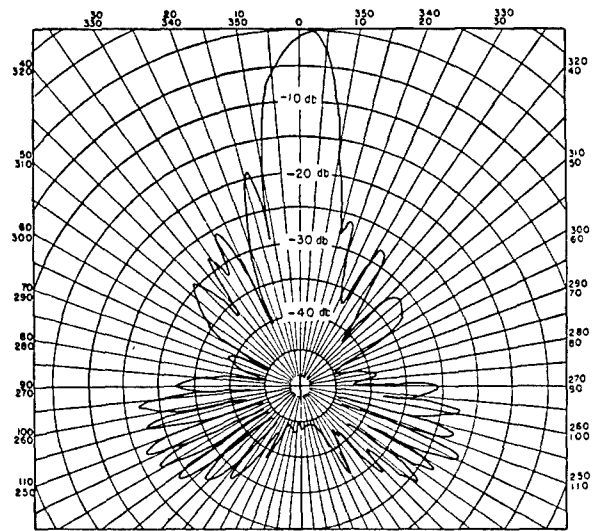


FIGURE 27. Actual pattern of Sangamo XQHA unit with acoustic axis midway between positions of Case I and Case II, Case II to the right.

CONFIDENTIAL

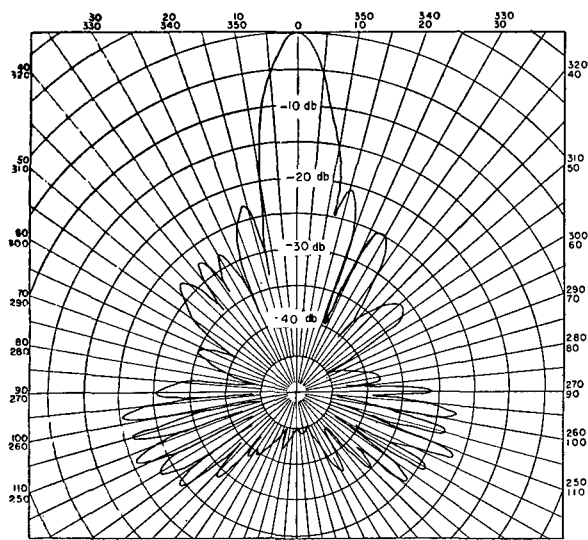


FIGURE 28. Actual pattern of Sangamo XQHA unit with acoustic axis in position of Case II, rotor is displaced 7.5 degrees with respect to Figure 24.

by interpolation. There are now two positions of registration corresponding to excitation of the transducer elements according to the mean of  $\frac{1}{4}$  and  $\frac{3}{4}$ , of  $1\frac{1}{4}$  and  $1\frac{3}{4}$ , and so forth. It is seen that these means always lie closest to the points  $\frac{1}{2}$ ,  $1\frac{1}{2}$ , and so forth. There is still some slight error arising from straight-line interpolation between the quarter points and the pattern, for this position of registration, would differ slightly from the reference pattern. In the second position of registration the excitation

would correspond to interpolation between the pairs of points numbered  $-\frac{1}{4}$  and  $+\frac{1}{4}$ ,  $\frac{3}{4}$  and  $1\frac{3}{4}$ , and so forth. Again these mean positions correspond closely to the points 0, 1, and so forth. Thus the pattern is nearly correct in both positions of registration, that is,  $3\frac{3}{4}$  degrees instead of every  $7\frac{1}{2}$  degrees as before. However, since the angular displacement between the points involved in the straight-line interpolation is smaller, the maximum errors occurring between the positions of registration are very much smaller than they were for the cases in which the number of rotor signals corresponded to the number of stator signals.

### 9.2.9

### Effect of Baffle Conditions

The patterns of single elements under the two conditions of stiff and release baffles have already been given. Because of the difference in these patterns, it is also expected that the required electrical attenuation and phase shifts differ. The extent of this difference is indicated in the curves in Figures 29 and 30. Here the required electrical attenuations and phase shifts are shown in Case II position under stiff and release baffle conditions with  $ka = 24$ ,  $N = 48$ ,  $\Delta = 0.1$ . The phase curves are very much the same to 45 degrees, and the difference is only slight from there to 60 degrees. However, the shading curves are seen to be quite distinct, just as were the amplitude patterns of the corresponding single elements.

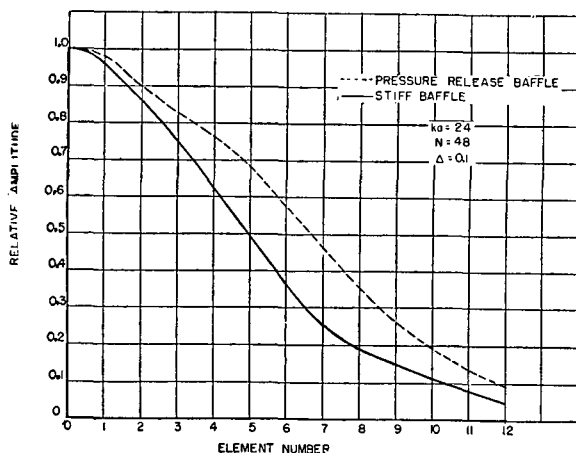


FIGURE 29. Attenuation required to produce pattern with transducer in position of Case II, and characteristics as given.

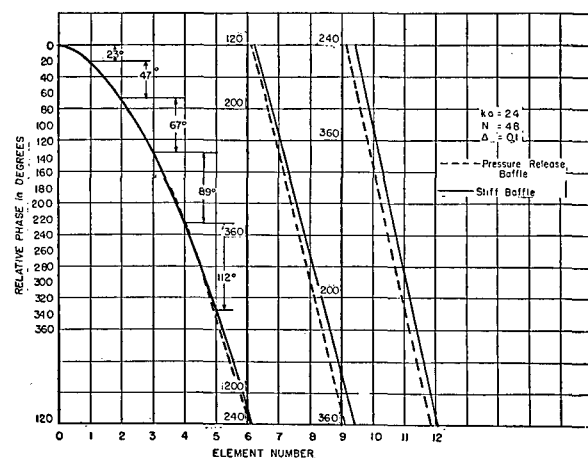


FIGURE 30. Phasing required to produce pattern with transducer in position of Case II, and characteristics as given.

CONFIDENTIAL

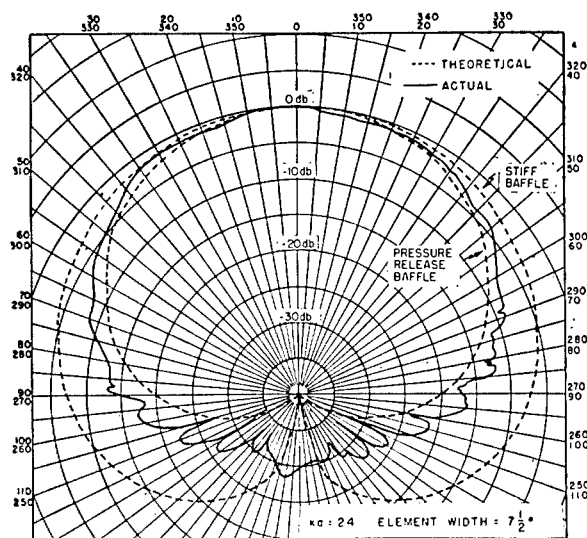


FIGURE 31. Comparison of actual single-element pattern with theoretical single-element patterns.

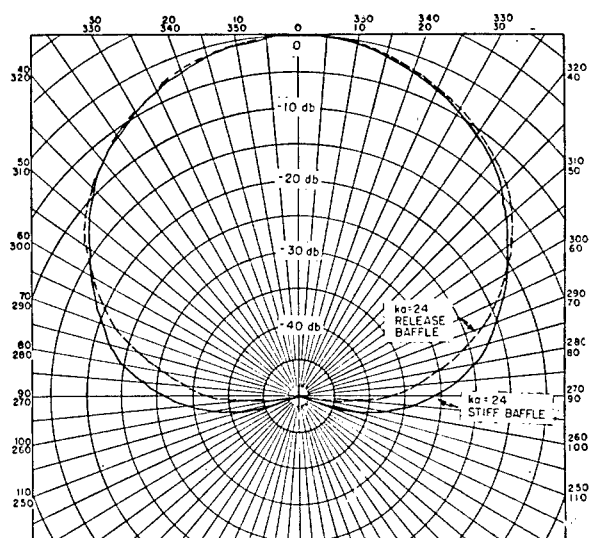


FIGURE 32. Comparison of total attenuation patterns for  $\Delta = 0.1$ .

### 9.2.10 Total Attenuation Pattern<sup>13,14,15</sup>

It has been found in practice that the amplitude patterns of single elements lie between those computed for stiff and release baffle conditions; on the whole they are closer to those for the release baffle conditions (see Figure 31). In the past, this difference between practice and theory was corrected by interpolating between the required electrical attenuations under the stiff and release baffle conditions. The extent of this interpolation was indicated by the position of the actual single-element pattern compared with those of the theoretical single-element patterns under corresponding baffle conditions. However, a recently adopted method of adjusting the electrical attenuations to the actual transducer is simple to apply and has theoretical justification.

To understand this method, the concept of total attenuation pattern must be introduced as the product of the single-element pattern and the electrical attenuation "pattern." In practice this product is the pattern obtained by measuring the amplitude of the signals from each of the elements at the input to the lag line (after they have been electrically attenuated) with a distant source on the acoustic axis of the transducer. This pattern includes the electrical attenuation as well as the attenuation in the water; that is, the attenuation caused by the fact that the element does not face the source. It may be expected that this total attenuation curve will yield a resultant pattern

of a given width independently of the single-element pattern. If this is true, it becomes a simple matter to take into account the actual single-element transducer patterns, since, once the single-element pattern is measured, it is necessary merely to introduce the appropriate electrical attenuations to give the correct total attenuation pattern.

To verify the validity of the assumption concerning the constancy of the total attenuation curve, this curve is shown in Figure 32 for stiff and release baffle conditions and  $ka = 24$ ,  $N = 48$ ,  $\Delta = 0.1$ . Already the difference in single-element patterns and required electrical attenuation patterns has been noted. Yet the curves in Figure 32 are surprisingly alike as far as 60 degrees and differ by only 4 db at 70 degrees. In practice it is only the elements in the front 120 degrees which are used in forming the pattern. There is justification, then, for adopting the method described above in using the total attenuation curve to adjust the electrical attenuation curve to a given transducer.

It would be desirable to have a family of curves giving the total attenuation patterns for various values of  $\Delta$  and  $ka$ , but this would require a rather extensive calculation program. Therefore, only the few results which are at hand are given. In Figure 33, the total attenuation curves are shown for  $\Delta = 0.0, 0.1, 0.173$  with  $ka = 20$ ,  $N = 36$ , computed from the stiff baffle case. A set of total attenuation curves for various values of  $ka$ , with  $\Delta$  fixed, can be obtained from one such curve by varying the angular scale inversely as

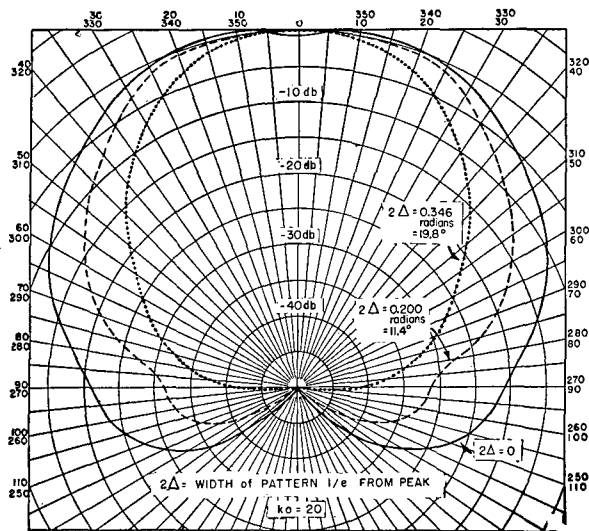


FIGURE 33. Total attenuation patterns for various pattern widths.

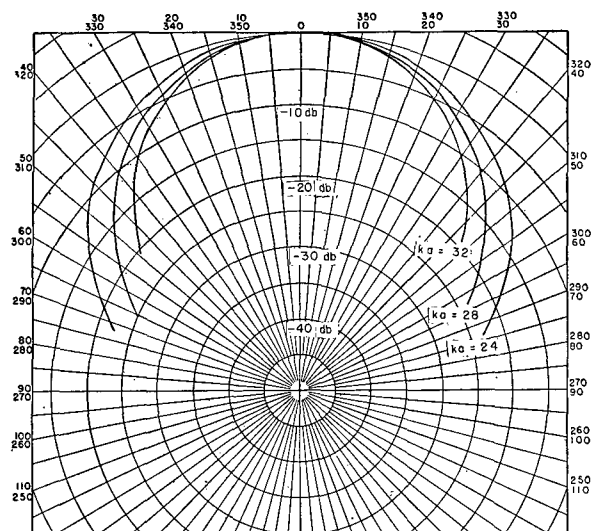


FIGURE 34. Total attenuation curves for various values of  $ka$  with  $\Delta = 0.1$ .

the  $ka$ . Thus the total attenuation curves for  $\Delta = 0.1$  can be obtained from the one in Figure 32 for  $ka > 24$ . Such a set of curves is shown in Figure 34. Care must be taken in extrapolating to smaller values of  $ka$ .

### 9.2.11 Phase-shift Requirements in Forming Pattern<sup>8, 16</sup>

It has been shown how to obtain the electrical attenuation which must be introduced to fit a given transducer and obtain a pattern of a given width. The corresponding electrical phase shifts or time delays which must be introduced are as easily obtainable, for it develops that time delays introduced electrically should be just enough to compensate the varying time delays in the water. This is admittedly not exact, but holds well around to  $\phi = 70$  degrees or 80 degrees when a pressure release baffle is assumed. This is shown in Figure 35, where the phase pattern of a single element is shown with the electrical phase pattern which must be introduced to obtain a pattern with  $\Delta = 0.1$ . Although this result does not hold so closely when a stiff baffle is assumed, there is no great difference between the two. As already stated, the transducer approximates a release baffle more closely than it does a stiff baffle (see Figure 31). It has already been seen that the electrical phase pattern is relatively insensitive to changes in  $\Delta$ . It is, therefore, recommended that the electrical phase pattern should coincide with the phase pattern of a single element.

If the pattern of a single element is not available but the dimensions of the transducer are known, time delays should be introduced into the signals of the various elements which just compensate for those suffered in the water. In this respect a phenomenon should be mentioned which is as yet unexplained.<sup>17</sup> It has been found that the phase pattern as based on actual measurements of a single-element pattern has corresponded to that of a transducer of larger  $ka$  than that which the actual frequency of the signal and physical

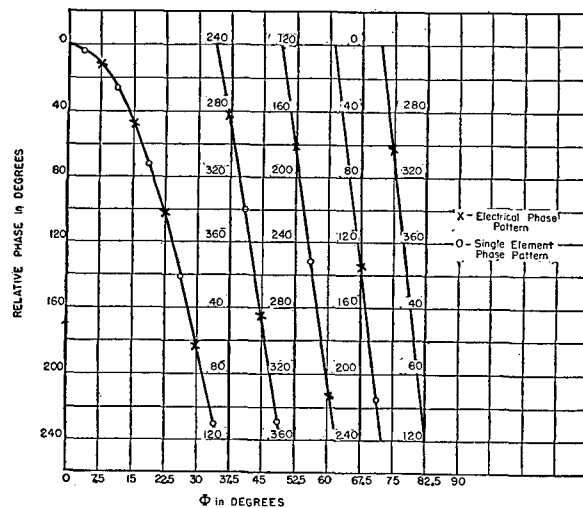


FIGURE 35. Comparison of single-element phase pattern with required electrical phase pattern to form acoustic pattern with release baffle;  $ka = 24$ ,  $\Delta = 0.1$ .

CONFIDENTIAL

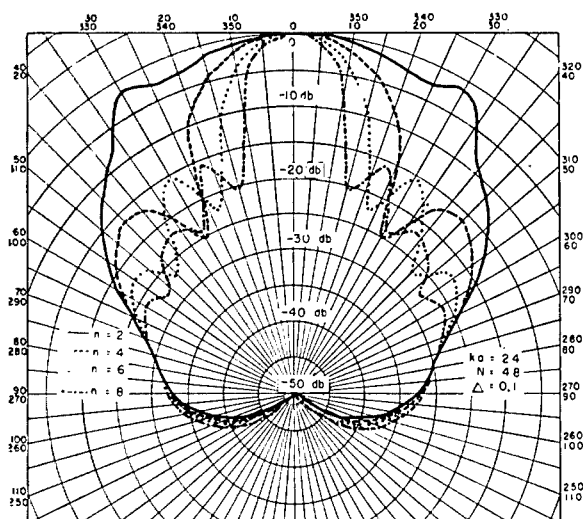


FIGURE 36. Theoretical pattern of segmented pressure release cylindrical transducer using  $N$  elements in beam formation: A.

dimensions of the transducer would indicate. This disparity has been found to be between 8 and 12 per cent. No satisfactory explanation of this effect is known at present. It would, therefore, seem highly desirable that the first recommendation above be followed whenever possible; that is, the phase pattern of a single element should be measured and the electrical phase pattern should be made to match it. If the second procedure of using the operating frequency and dimensions of the transducer to calculate

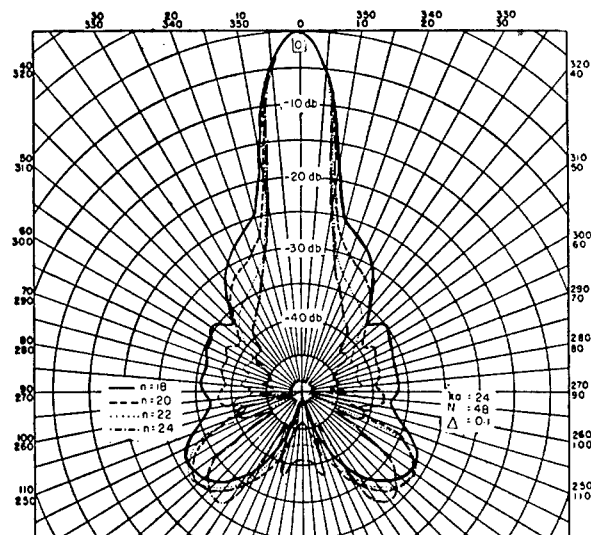


FIGURE 38. Theoretical pattern of segmented pressure release cylindrical transducer using  $N$  elements in beam formation: C.

$ka$  is adopted, the value thus obtained should be increased tentatively by 10 per cent until single-element patterns have been measured so that the first procedure may be used.

#### 9.2.12 Effect of Limiting Number of Active Elements<sup>18, 19</sup>

It has already been mentioned that in practice only a limited number, usually about one third, of the ele-

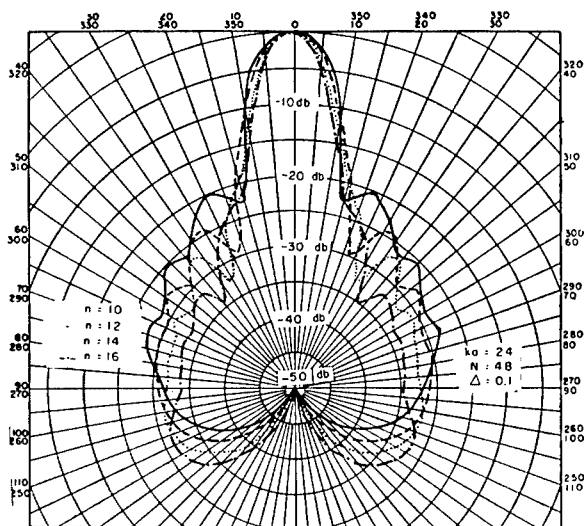


FIGURE 37. Theoretical pattern of segmented pressure release cylindrical transducer using  $N$  elements in beam formation: B.

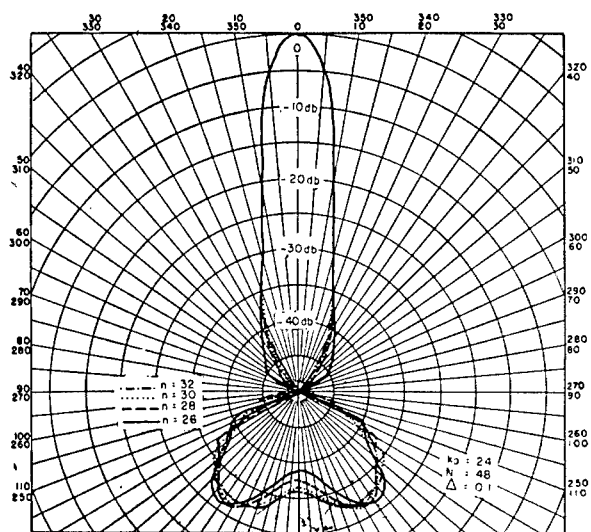


FIGURE 39. Theoretical pattern of segmented pressure release cylindrical transducer using  $N$  elements in beam formation: D.

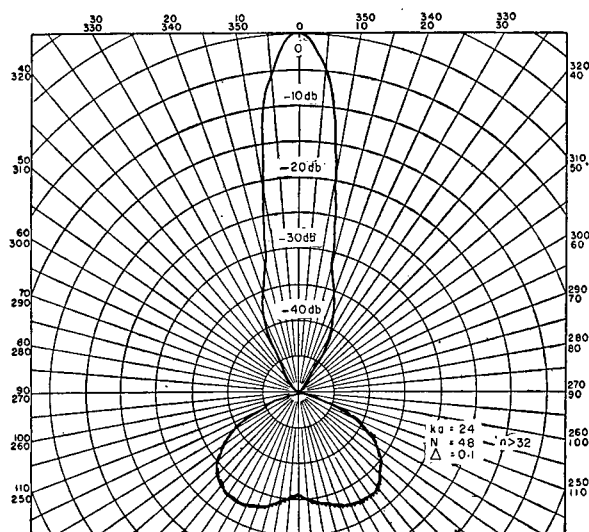


FIGURE 40. Theoretical pattern of segmented pressure-release cylindrical transducer using  $N$  elements in beam formation: E.

ments are used in forming the pattern. This is done to minimize the number of sections in the lag line and thereby to reduce the labor of building the high precision lag lines required, and also to reduce the space occupied by the lag line in the commutator. It, therefore, becomes of interest to know the effect on the width of major lobe and the minor side and back lobe structure of the resulting patterns when using a limited number of the elements in the pattern formation. Computations have been made with  $ka = 24$ ,  $N = 48$ ,  $\Delta = 0.1$ , and release baffle assumptions, to obtain the final pattern when 2, 4, 6, . . . elements are used in its formation, assuming in each case that the elements have the exact attenuations and phase shift required by theory. These patterns in groups of four are shown in Figures 36 to 39 and for  $N > 32$  in Figure 40. The pattern of special interest is that in which 16 elements are employed, since this is the number that has generally been used in practice. Here the width of the major lobe is practically at its required value, that is  $2\Delta$ , and the first minor lobe is about 31 db below the peak of the major lobe. A 32-db minor lobe appears at 120 degrees, while the sensitivity from 60 degrees to 120 degrees remains between 32 db and 34 db below the major lobe. In practice, the variations from theory can be expected to introduce minor lobes in this sector which are higher than 30 db below the major lobe. This has been found to be the case, with the 120-degree minor lobe being raised about 6 db above that predicted by theory.

This is shown in the pattern of Figure 24 of an XQHA Sangamo unit<sup>12</sup> in which 16 elements are used in forming the pattern. It is noticed that the 120-degree minor lobes are not improved by using more elements in the pattern formation. In Figure 41 a summary is shown of the characteristics of the pattern as a function of the number of elements used. It appears that the use of 16 elements gives close to optimum results. It has also been found in practice that these minor lobes deteriorate steadily as the condition  $\frac{ka}{N} < \frac{1}{2}$  is violated more and more.

### 9.2.13 Directivity Ratio in Transmission and Reception<sup>16, 18</sup>

In calculating the efficiency of a transducer, it is convenient to know the directivity ratio of the pattern. The patterns in transmission and reception for scanning sonar are quite distinct and hence must be treated separately. The pattern in transmission when all the elements are excited uniformly is closely that of a line source of length equal to the length of the transducer. If the length of the transducer is greater than several wavelengths, the directivity ratio is given by

$$D = \frac{\lambda}{2l}$$

If the pattern in transmission is available, it is advisable to use the curves in Figure 42 which gives the directivity ratio as a function of the major lobe width. These curves are based on the assumption of a line source whose first minor lobes are 13.5 db below

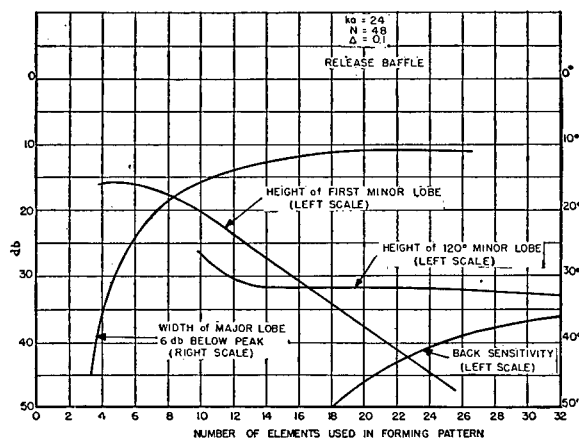


FIGURE 41. Characteristics of pattern as function of number of elements used in forming pattern.



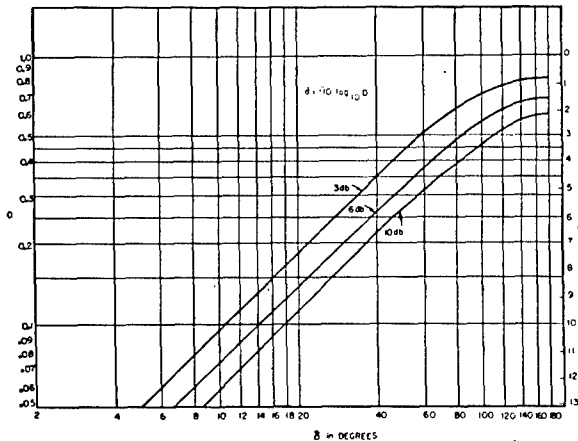


FIGURE 42. Directivity ratio  $D$  and directivity index  $d$  of line source as function of width  $\delta$  of pattern, 3, 6, and 10 db from peak.

the peak. If there is a difference between the minor lobe structure of the actual pattern and that of a line source, judgment may be exercised in making an incremental change in the directivity ratio which would account for the difference in patterns. In this way the directivity ratio should be obtained to within 10 per cent. Numerical integration must be resorted to if higher accuracy is desired.

The pattern in reception is quite directive in the horizontal as well as the vertical plane. If the vertical pattern is closely that of a line source, and if the pattern in the horizontal plane is narrow and with low minor lobes (better than 20 db), the directivity ratio is given to within 10 per cent by

$$D = \frac{3}{2} \delta_1 \delta_2 10^{-5},$$

where  $\delta_1$ ,  $\delta_2$  are the widths in degrees 6 db from the peak of the patterns in the vertical and horizontal planes. The middle chart of Figure 43 is based on this formula.

The single elements of a transducer have patterns which are quite directive in the plane through the axis of the transducer, but are quite broad in the plane normal to the transducer axis. The directivity ratio of such a pattern is difficult to obtain accurately without resorting to numerical integration. If 25 per cent accuracy in the directivity ratio is sufficient, however, corresponding to an accuracy of 1 db in directivity index, the charts on Figure 43 may be used. In general, the values of directivity index thus obtained are too large.

## 9.3 ELECTRONIC ROTATION [ER] SONAR

### 9.3.1 Introduction

The problem of pattern formation for ER Sonar is quite different from that for CR sonar, and more difficult. The difficulty is twofold because the number of available parameters is very limited, and further, the pattern is such a complicated function of these parameters that it is extremely difficult to decide on a choice of parameters which should yield the best obtainable pattern. There is an additional complicating factor due to the doppler effect introduced by the rotation. This effect is much more pronounced in ER sonar than in CR sonar because of the higher rotation speeds usually used.

### 9.3.2 Pattern Formation in Two Stages<sup>20</sup>

There are two stages in the ER sonar pattern formation. In the first stage, the signals from the various elements of the transducer are "mixed" on a lead line. Because of the required uniformity of the pattern in angle, the lead line sections must have the same attenuation and phase shift between elements of the transducer, so that there are two parameters, the phase shift and the attenuation per section of lead line. Thus, the voltage occurring at each section of the lead line is the vector sum of the voltage due to the transducer element, to which the point is directly connected, and the voltages of all the other transducer elements, attenuated and phased according to the lead line. This voltage, as a function of angle, is called the *lead line pattern*.

The second stage of pattern formation combines the voltages of a number of successive elements of the lead line. This combination is effected by switching devices to which the lead line voltages are applied. The amount of each signal to be combined is determined by the shape of the switching pulse, and combining involves no phase shifting. Both vacuum tube and varistor switching have been investigated experimentally. When triode switching is used, the Miller effect (that is, the increase in input capacitance due to gridplate capacitance) effectively shunts the lead line with a capacitance, thereby changing the attenuation and phase characteristics of the lead line. This effect introduces additional variables which may be used to alter the pattern. However, it also greatly

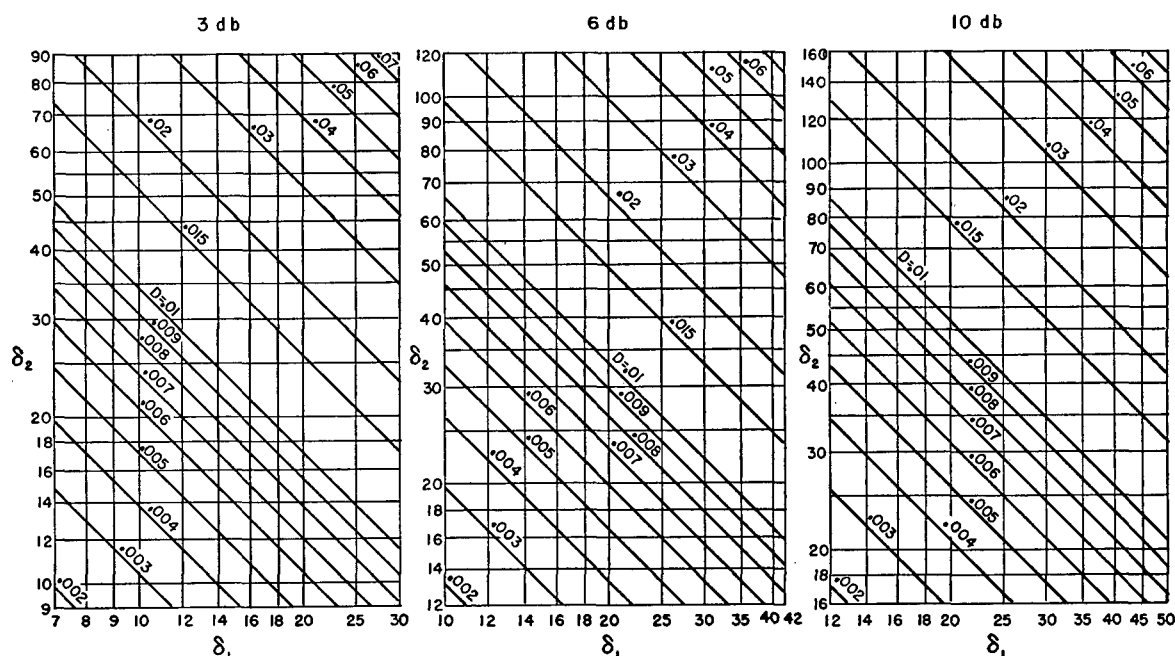


FIGURE 43. Directivity ratio  $D$  in terms of total pattern widths  $\delta_1$ ,  $\delta_2$  in degrees between points 3, 6, and 10 db below maximum.

complicates a mathematical analysis of the pattern formation. The Miller effect is not present in varistor switching unless artificially introduced, and in the remaining discussion it is assumed to be absent.

### 9.3.3 Mathematical Theory of ER Sonar Pattern Formation<sup>21,22,23</sup>

Equation (1) gives the pattern  $P(\phi)$  of a single element. To obtain the pattern of an element centered at an angle  $\phi_k$  with the principal direction,  $\phi - \phi_k$  is substituted for  $\phi$  in the equation. Let the attenuation and phase shift per section of the lead line be represented by the function

$$\Theta = e^{j\xi} = e^{j(\xi + j\eta)},$$

where  $\xi$  is the phase shift in radians and  $20\eta \log_{10} e$  is the attenuation in db per section. Then the voltage appearing at an angle  $\phi_l$ , assuming there are  $|k - l|$  elements between  $\phi_k$  and  $\phi_l$ , is

$$V(\phi_l) = \sum_{k=0}^{N-1} \Theta^{|k-l|} P(\phi_k),$$

where  $N$  is the number of elements in the transducer.

If now the pulse shape is given by

$$\Psi = \Psi(\phi),$$

the final pattern is

$$W(\phi_n) = \sum_{l=0}^{N-1} \Psi(\phi_n - \phi_l) V(\phi_l).$$

Various schemes have been suggested for introducing phase shifts by complex switching pulses.<sup>3,4</sup> None of these suggestions has been carried out, however, and discussion here is limited to the situation as it exists at present. This imposes a condition which is not easy to reckon with; namely,  $\Psi(\phi) \geq 0$  for all values of  $\phi$ .

The summations involved in the expressions for  $V$  and  $W$  may be replaced by integrations, provided that certain apparently justifiable assumptions are made. Let the lead line function be

$$\Theta(\psi) = e^{j\xi|\psi|} = e^{-(a-jb)|\psi|},$$

so that the attenuation and phase shift per radian are  $20a \log_{10} e$  db and  $b$  radians, respectively. Then the lead line pattern is given by

$$V(\theta) = \int_{-\infty}^{\infty} \Theta(\psi - \theta) P(\psi) d\psi = \int_{-\infty}^{\infty} \Theta(\psi) P(\theta + \psi) d\psi.$$

CONFIDENTIAL

Since

$$\Theta(\psi) = \Theta(-\psi),$$

$$V(\theta) = \int_0^\infty \Theta(\psi) [P(\theta + \psi) + P(\theta - \psi)] d\psi.$$

The final pattern can be written as

$$W(\phi) = \int_{\phi-\pi}^{\phi+\pi} V(\theta) \Psi(\theta - \phi) d\theta = \int_{-\pi}^{\pi} V(\theta + \phi) \Psi(\theta) d\theta.$$

Now

$$P(\theta + \psi) + P(\theta - \psi) = 2 \sum_{-\infty}^{\infty} D_m \cos m\psi e^{jm\theta},$$

and

$$\begin{aligned} \int_0^\infty \Theta(\psi) \cos m\psi d\psi &= \int_0^\infty e^{j\zeta\psi} \cos m\psi d\psi \\ &= \frac{j}{2} \left[ \frac{1}{\zeta + m} + \frac{1}{\zeta - m} \right]. \end{aligned}$$

Thus

$$V(\theta) = 2 \sum_{-\infty}^{\infty} \frac{j\zeta D_m e^{jm\theta}}{\zeta^2 - m^2} = 2 \sum_{-\infty}^{\infty} \frac{D_m \cos m\theta}{a - j(b + m)}.$$

Also

$$W(\phi) = 2\pi \sum_{-\infty}^{\infty} \frac{j\zeta D_m A_m e^{jm\phi}}{\zeta^2 - m^2}$$

where

$$A_m = \frac{1}{\pi} \int_{-\pi}^{\pi} e^{jm\theta} \Psi(\theta) d\theta,$$

or

$$A_m = \frac{2}{\pi} \int_0^\pi \Psi(\theta) \cos m\theta d\theta,$$

if  $\Psi(\phi) = \Psi(-\phi)$ . In the expression for  $W(\phi)$ ,  $D_m$  is a given complex number,  $\zeta$  is an arbitrary complex number with two parameters, and  $A_m$  is a real number and arbitrary except that it must be the Fourier coefficient of a one-signed function  $\Psi(\phi)$ . This last

condition is difficult to take into account mathematically. Since  $D_n = D_{-n}$  and  $A_m = A_{-m}$ ,

$$W(\phi) = 2\pi \left[ \frac{jD_0 A_0}{\zeta} + 2 \sum_{m=1}^{\infty} \frac{j\zeta D_m A_m}{\zeta^2 - m^2} \cos m\phi \right].$$

Now the amplitude pattern which it would be desirable to approximate is the Gaussian pattern  $e^{-(\phi/\Delta)^2}$  which has the Fourier expansion (provided  $\pi/\Delta \gg 1$ ),

$$R(\phi) = \frac{\Delta}{2\sqrt{\pi}} \left[ 1 + 2 \sum_{m=1}^{\infty} e^{-\frac{\Delta^2 m^2}{4}} \cos m\phi \right].$$

It is clear that the corresponding coefficients of  $W(\phi)$  and  $R(\phi)$  cannot be simply equated, since  $A_m$  must be real. An alternative procedure would be to obtain the expression for  $W(\phi) W^*(\phi)$  which has real coefficients, and then equate these coefficients with those of  $R^2(\phi)$ . This leads to quadratic equations in the  $A_m$ 's in which there are more equations than unknowns. At this point the method of least squares may be used to determine the  $A_m$ 's. However, it is extremely unlikely that the  $A_m$ 's obtained in this manner satisfy the required conditions that they be Fourier coefficients of a one-signed function. Also, the degree of approximation to a Gaussian pattern is known not a priori. This method of procedure has, therefore, been dropped.

The expression given at the outset for the pattern of a single element is an exact expression. It is approximated well over an angle of 90 degrees on either side of the element by

$$P(\phi) = \cos \phi e^{-jka(1 - \cos \phi)}.$$

If we make use of the expansion

$$e^{jka \cos \phi} = \sum_{p=-\infty}^{\infty} J_p(ka) e^{jp(\frac{\pi}{2} - \phi)},$$

the lead line pattern is then given by

$$V(\theta) = 2e^{-j(ka + \frac{\pi}{2})} \sum_{p=-\infty}^{\infty} \frac{J_p'(ka) e^{+jp\frac{\pi}{2}}}{a - j(b + p)} \cos p\theta.$$

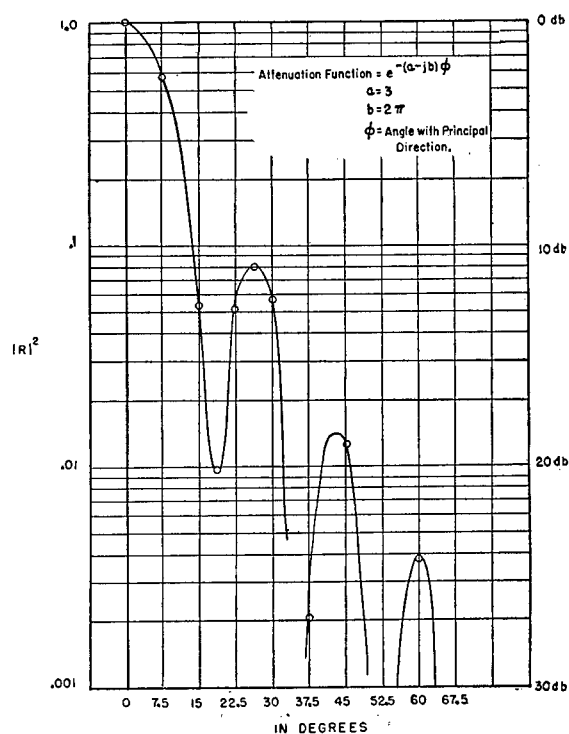


FIGURE 44. Amplitude pattern of first stage of ER sonar.

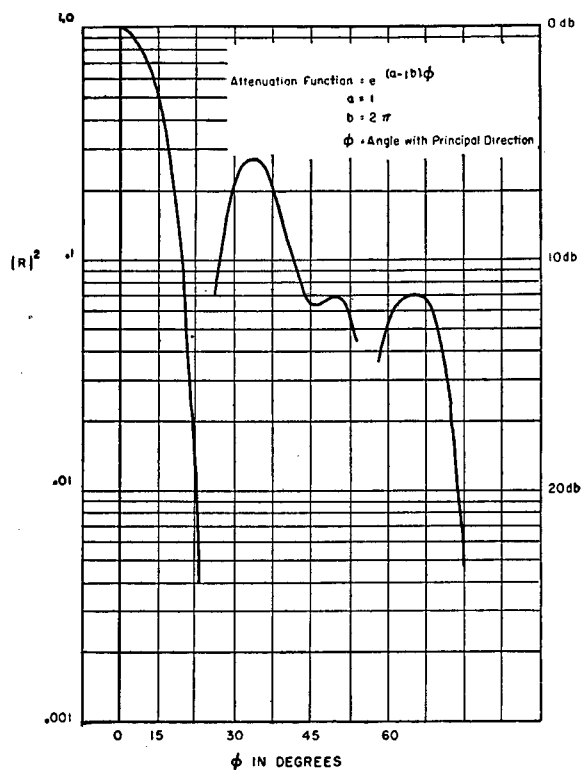


FIGURE 46. Amplitude pattern on ER sonar lead line.

This pattern has been computed when  $ka = 24$  in the two cases  $a = 3, b = 2\pi$ , and  $a = 1, b = 2\pi$ . The quantity  $b = 2\pi$  corresponds to a phase shift of about 1 radian per section of lead line for a 48-element transducer, while  $a = 3$  corresponds to a little over 3 db attenuation per similar section of lead line and  $a = 1$  to a proportionally smaller attenuation. The lead line amplitude patterns are shown in Figures 44 and

46, and the corresponding phase patterns are shown in Figures 45 and 47.

## 9.3.4

Rotation Doppler<sup>24</sup>

An examination of the patterns mentioned above reveals a correlation between the positions of the minor lobes on the amplitude patterns and the re-

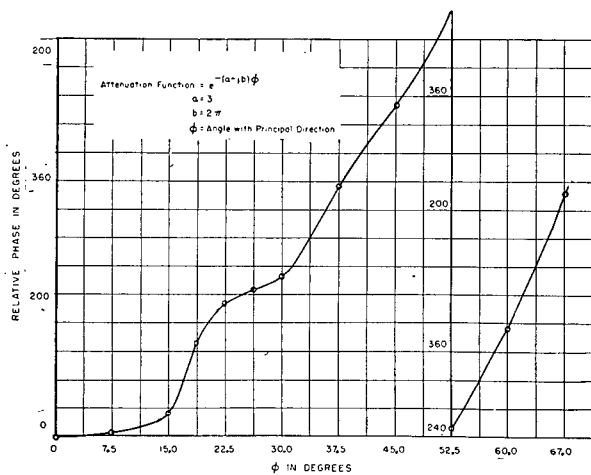


FIGURE 45. Phase pattern of first stage of ER sonar.

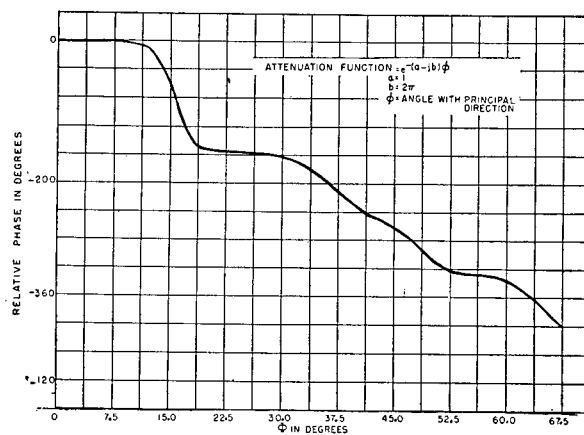


FIGURE 47. Phase pattern on ER sonar lead line.

CONFIDENTIAL

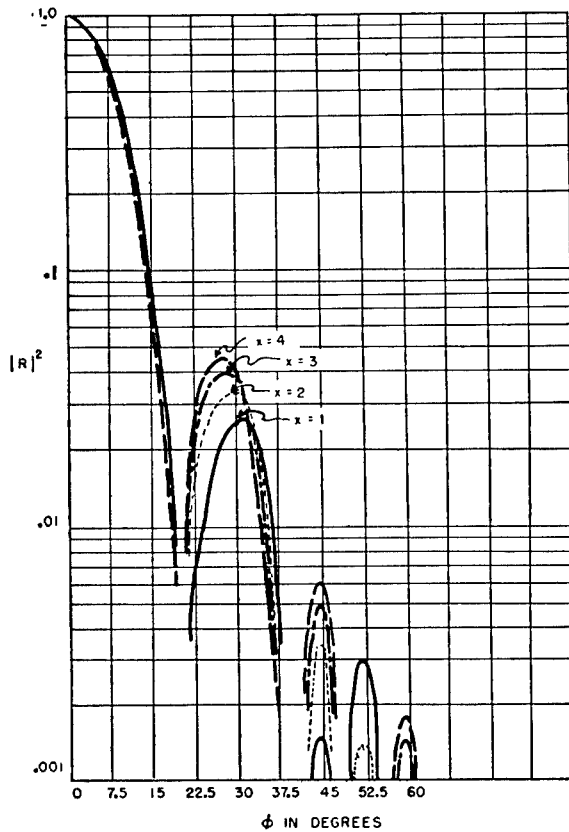


FIGURE 48. ER sonar amplitude patterns of three elements conducting in ratio 1:x:1; lead line constants,  $a = 3$ ,  $b = 2\pi$ .

gions of minimum slope on the corresponding phase patterns. This phenomenon has implications upon the doppler effect introduced by the rotation itself. Let  $\theta = \theta(t)$  be the phase in radians of a signal as a

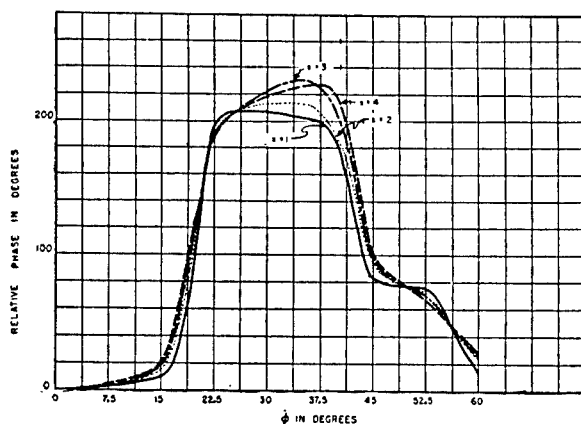


FIGURE 49. ER sonar phase patterns of three elements conducting in ratio 1:x:1, lead line constants,  $a = 3$ ,  $b = 2\pi$ .

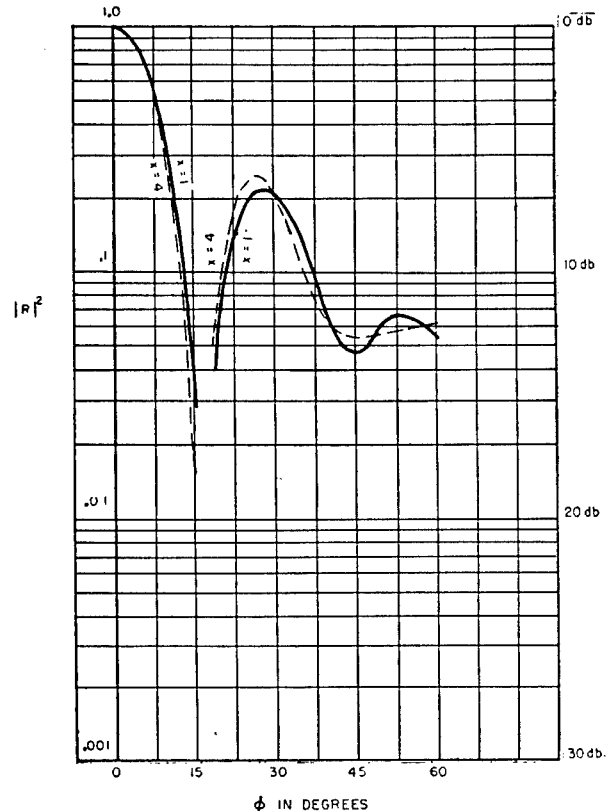


FIGURE 50. ER sonar amplitude patterns of three elements conducting in ratio 1:x:1, lead line constants,  $a = 1$ ,  $b = 2\pi$ .

function of time. Then the frequency shift in cycles per second caused by  $\theta$ 's being a function of time is

$$f = \frac{1}{2\pi} \frac{d\theta}{dt} = \frac{1}{2\pi} \frac{d\theta}{d\phi} \frac{d\phi}{dt},$$

where  $\phi$  is the angle with the principal direction. Thus, if  $n$  is the slope of the phase pattern, and  $r$  the speed of rotation in rps,

$$f = nr.$$

For example, in Figure 45, the slope from  $\phi = 15$  degrees to  $\phi = 22.5$  degrees is approximately  $154/7.5$ , while between  $\phi = 22.5$  degrees and  $\phi = 30$  degrees the slope is approximately  $38/7.5$ . If the rotational speed is 300 rps, these figures correspond to 6.16 and 1.52 kc of frequency shift. Thus, the rotation doppler may shift the frequency of the signal outside the band pass of the receiver. It should be remarked that, because of the high rotational speed of ER sonar, a rather wide pass band is required to permit the major

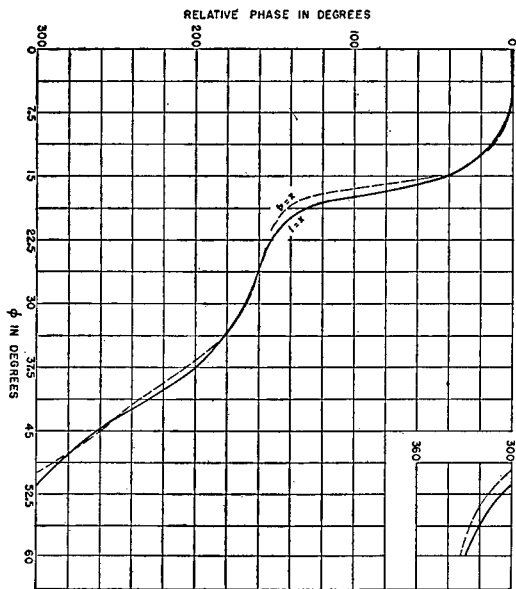


FIGURE 51. ER sonar phase patterns of three elements conducting in ratio 1:x:1, lead line constants  $a = 1$ ,  $b = 2\pi$ .

lobe signal to pass through without distortion. For example, a pattern 20 degrees wide requires a band

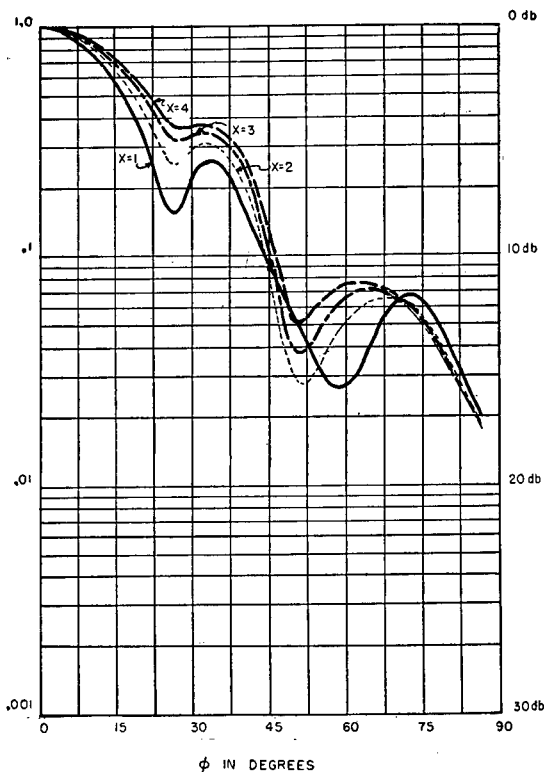


FIGURE 52. Amplitude patterns of three elements conducting in ratio 1:x:1, no lead line.

width of 5.4 kc. Considerations of own and target doppler are, therefore, unimportant. The smaller shift occurs where the most phase shift is needed; that is, at the minor lobe. The improvement in the minor lobe structure obtained by rotation doppler is difficult to evaluate since it depends upon the band-pass characteristics of the transformers, tuned circuits, and so forth. For example, it would not be known if a pattern with 15-db minor lobes and 5-kc doppler rotation at the minor lobe is better or worse than a pattern with 20-db minor lobes and 0.5-kc rotation doppler at the minor lobe, unless the frequency characteristic from the lead line to the point of rectification were known. It is worth noting that broad band noise is not discriminated against by the rotation doppler unless selectivity is introduced ahead of the rotor.

9.3.5

### Form of Switching Pulse<sup>19</sup>

Figures 48, 49, 50, 51 show families of patterns of amplitude and phase when three elements of the lead line contribute in the ratio 1:x:1 with  $x = 1, 2, 3, 4$ .

It appears that the lead line pattern is 23 degrees wide with minor lobes 11 db down when  $a = 3$ , which corresponds to the lead line in present operation, but when  $a = 1$ , the main lobe is 19 degrees wide and the minor lobe is only 5.5 db down. The minor lobe structure is greatly improved in the case  $a = 3$  when three elements contribute in the proportions indicated, as shown in Figure 48. The corresponding set of curves in Figure 50, for the case  $a = 1$ , shows only slight improvement. In both cases the major lobe width is only slightly increased.

It has been suggested that as good results may be

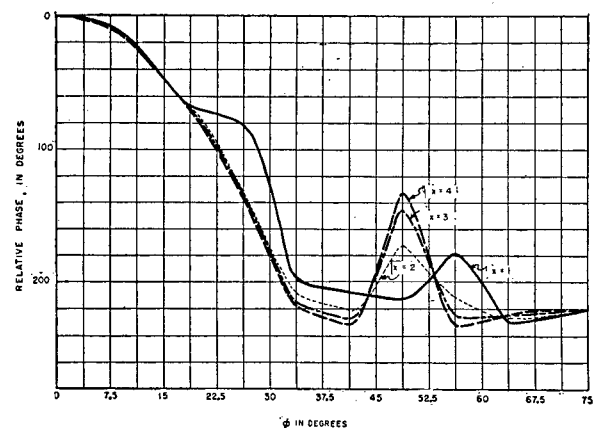


FIGURE 53. Phase patterns of three elements conducting in ratio 1:x:1, no lead line.

CONFIDENTIAL

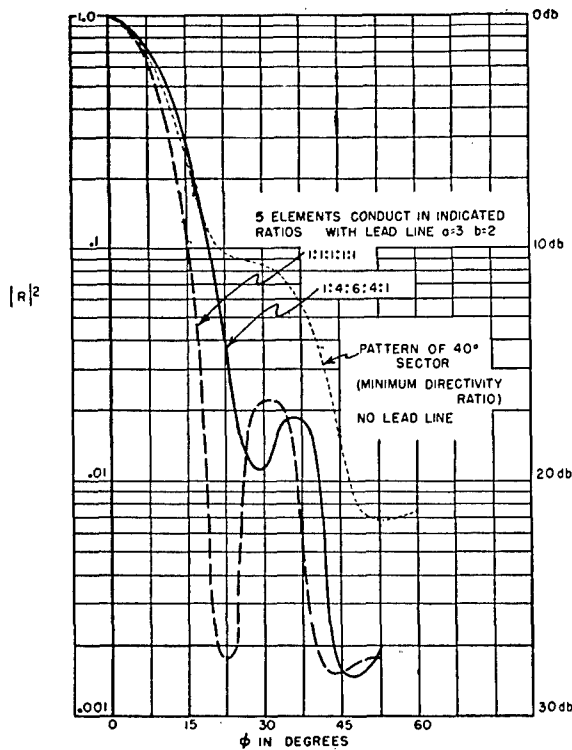


FIGURE 54. Comparison of amplitude patterns with and without lead lines.

obtained if the lead line is not used at all. In order to have a comparison with the results above, the patterns of three elements of the transducer in parallel and in varying proportions are shown in Figures 52 and 53. These patterns do not compare favorably

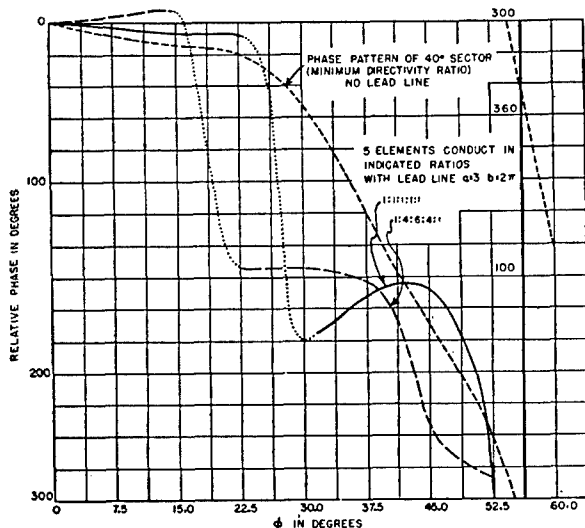


FIGURE 55. Comparison of phase patterns with and without lead lines.

with those for which a lead line is used. The curves in Figures 54 and 55 have a further bearing on the question. Here the patterns of minimum directivity index are shown. They are essentially the patterns of five transducer elements operated in parallel and with no lead line, as well as the patterns when five elements on the lead line ( $a = 3, b = 2\pi$ ) are conducting in the proportions 1:1:1:1:1 and 1:4:6:4:1.

#### 9.4

### CR LAG LINE DESIGN

#### 9.4.1

### Considerations on the Choice of the Line

It has been shown in Section 9.2 that signals received on the various elements of a scanning sonar transducer should be given time delays which are essentially independent of frequency in order to form a specified pattern. At any one frequency the desired time delays can be obtained with any nondissipating delay line. However, if the phase shift of this line is not a linear function of frequency, a change in the operating frequency necessitates a change in the beam-forming line.

Thus, although a simple filter section such as a constant- $k$  low-pass filter is satisfactory, it is necessary to use a section with a more linear phase shift if greater independence from changes in the operating frequency is desired.

#### 9.4.2

### Constant- $k$ Theory—Curves

The simplest type of delay line is the constant- $k$  low-pass filter of Figure 56A which is considered as a

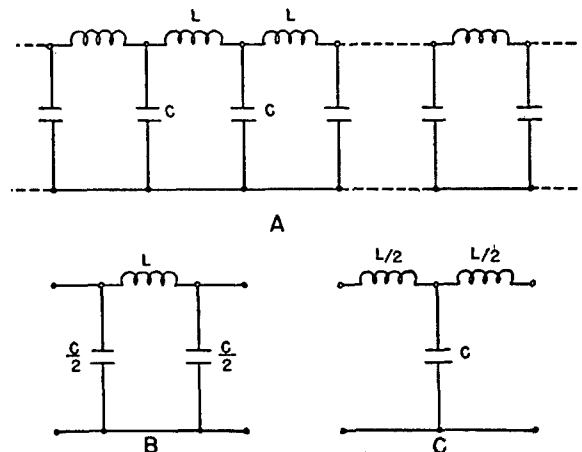


FIGURE 56. Constant- $k$  low-pass filter sections.

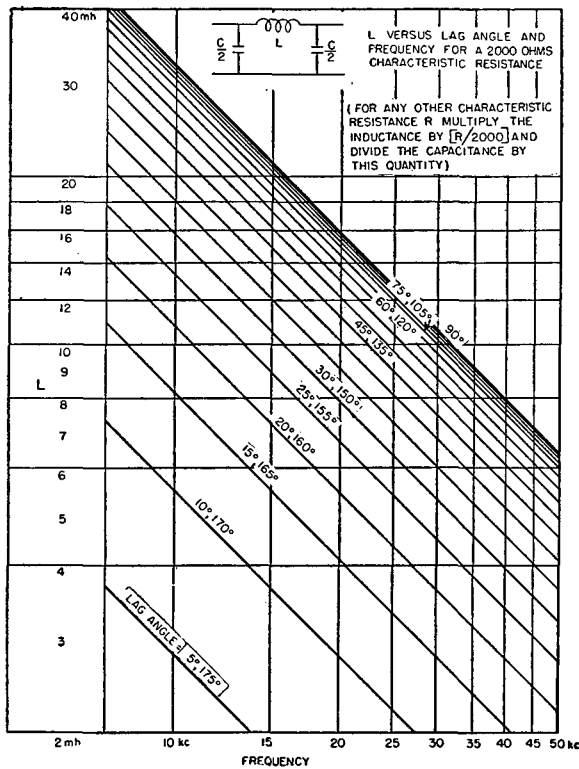


FIGURE 57. Curves for determination of inductance of constant- $k$  low-pass filter.

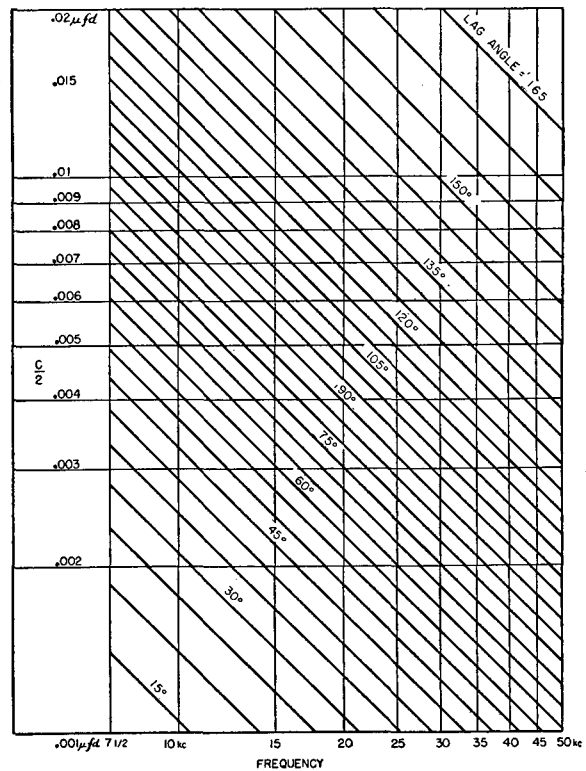


FIGURE 58. Curves for determination of capacitance of constant- $k$  low-pass filter.

tandem arrangement of symmetric  $\pi$ -sections or T-sections as in Figures 56B and 56C respectively.

If  $Z_{I0}$  is the desired image impedance at zero frequency, and if  $\beta$  is the desired phase shift at an angular frequency  $\omega$ , then it is easy to show that the design formulas for either the  $\pi$ - or the T-section are<sup>25</sup>

$$L = \frac{Z_{I0} \sin \beta}{\omega} \quad \text{henries,}$$

$$C = \frac{2 \tan \beta/2}{\omega Z_{I0}} \quad \text{farads.}$$

Figures 57 and 58 give design curves by means of which  $L$  and  $C$  may be chosen.

#### 9.4.3 Theory of $m$ -Derived Sections<sup>26</sup>

In the early work it was realized that a delay line with linear phase shift would have some advantages. This led to an investigation of the properties of the  $m$ -derived section of Figure 59.

If  $k$  is the coefficient of coupling, the section of Figure 59 is equivalent to an  $m$ -derived network with

$m = [(1+k)/(1-k)]^{1/2} > 1$ . Or conversely, a mid-series  $m$ -derived low-pass filter, whose prototype is the section of Figure 56, can be achieved by the use of the circuit of Figure 59 if  $k = (m^2 - 1)/(m^2 + 1)$ .

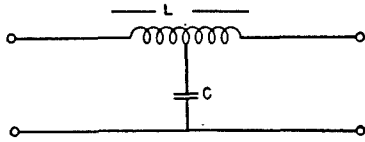
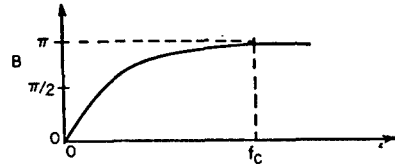
The use of iron-cored toroidal inductances in the section of Figure 59 gives a coupling coefficient of approximately 0.9 which corresponds to  $m \cong 4$ . Although the phase shift of an  $m$ -derived section with  $m = 4$  is linear over only a small portion of the pass band, it is still approximately linear up to large values of the phase shift. It is this latter consideration that has made the circuit of Figure 59 feasible, even though  $m$  may necessarily be as large as 4.

The circuit parameters are chosen on the basis of the assumption that the phase shift is linear from zero frequency up to the frequency of operation. This assumption is valid for phase shifts up to 120 degrees and leads to the following simple design formulas<sup>27</sup>

$$L = \frac{\beta Z_{I0}}{360^\circ f} \quad \text{henries,}$$

$$C = \frac{\beta}{360^\circ f Z_{I0}} \quad \text{farads.}$$



FIGURE 59. A mid-series  $m$ -derived low-pass filter section.FIGURE 60. Phase shift versus frequency for  $m$ -derived filter with  $m \cong 4$ .

Here  $\beta$  is the desired phase at the angular frequency  $\omega$ , and  $Z_{I0}$  is the image impedance at zero frequency.

#### 9.4.4 Aspects of $m$ -Derived Sections

If the prototype is a constant- $k$  low-pass filter, the phase shift of the  $m$ -derived filter with  $m \cong 4$  is of the form sketched in Figure 60. The phase shift is fairly linear up to  $\beta = \pi/2$ , although this represents only a small fraction of the pass region.

In some of the filter sections that were designed with a large impedance the measured phase shift was found to be linear over a much larger fraction of the pass region than could reasonably be expected on the basis of  $m$ -derived filter theory. This behavior was shown to be produced by distributed capacitance in the inductance  $L$ . The slope of the phase shift curve, evaluated at  $f = 0$ , is the same regardless of the amount of the distributed capacitance. This means that the section can usually be designed on the basis of  $m$ -derived sections without any corrections for the distributed capacitance.

If the distributed capacitance is of the same order of magnitude as the shunt capacitance  $C$ , the network is no longer an  $m$ -derived section but must be considered as a bridged-T section. A detailed analysis of the circuit of Figure 59, with explicit allowance for the distributed capacitance, is given in Section 9.6.2. It is briefly mentioned here that the main effect of a large distributed capacitance is to decrease the value of  $f_c$  without changing the initial slope. This effect obviously leads to an improvement in the linearity of the phase shift characteristics.

#### 9.4.5 Insertion of Signal

It has been assumed in the preceding discussion that the filter sections have no dissipation. This is not entirely true since at many points along the line the transducer elements are connected through bridging networks. If the series arm of the bridging network is

so large that it has little effect on the behavior of the line, an undue amount of voltage loss is produced. On the other hand, if the series arm is small, the assumption that the line has no dissipation is not justified. The practical solution is to compromise by using a bridging resistor that is several times the image impedance of the line. The details of the computation were discussed in the section on commutators in Chapter 6.

The effect of the bridging resistors is twofold. In the first place, they produce attenuation of a signal as it travels down the line, and if the outputs of the different transducer elements are properly attenuated before being inserted in the line, the fact that the different signals travel a different length of the line introduces errors, since the amount of attenuation is proportional to the length of the path. This difficulty must be corrected by individually altering the amplitude of the signals inserted at the different points until the total attenuation is the correct amount. The second effect is that the phase shift of a line is altered by the introduction of dissipation. This effect is less pronounced than the attenuation phenomena and is inappreciable in the lines so far constructed.

It should be emphasized that the method of using bridging resistors that are large and do not present much loading to the lag line is not the only solution to the problem of mixing the outputs of the transducer elements. Furthermore, it may not even be the best practical solution. There is a substantial margin for improvement since the bridging network now used introduces approximately 20 db of loss and the lag line itself introduces another 4 db of loss. Some, but not all, of these losses can be eliminated. The major advantage of the present system is that since all of the sections of the lag line are similar the possibility of errors in construction is reduced. On the other hand, most of the improvements that have been suggested require a change in the image impedance at each point where a voltage is inserted.

In the present method the signal voltages are intro-

duced through a parallel connection. It is also possible to insert each transducer element and its associated networks as part of a series arm of the lag line. This may be of advantage in an inductive commutator design; it is probable that the losses which must be accepted to obtain satisfactory combination are equal to those with parallel combination.

## 9.5 ER LEAD LINE DESIGN

Section 9.3 discussed the theoretical considerations involved in the formation of a pattern with a lead line. The practical details of incorporating the transducer element as part of the lead line were described in Chapter 7.

For the present needs it is sufficient to consider the lead line of Figure 61. The parallel shunt combination of  $R$  and  $L$  represents the transducer. Crystal transducer elements can be made to act as inductive sources by connecting them to transformers whose shunt inductance has larger susceptance than does the crystal transducer element.

To design a line, such as that in Figure 61, which gives an attenuation per section of  $\alpha$  nepers (8.68 db = 1 neper), and a phase shift per section  $\beta$  at the angular frequency  $\omega$ , the following expression<sup>28</sup> is used:

$$L = \frac{R \sinh \alpha \sin \beta}{\omega (1 - \cosh \alpha \cos \beta)} \text{ henries,}$$

$$C = \frac{1}{2\omega R \sinh \alpha \sin \beta} \text{ farads.}$$

Design curves for  $L$  and  $C$  versus the attenuation  $\alpha$  in decibels are given for  $\beta = 50, 55$ , and  $60$  degrees in Figure 62. The graph cannot readily be used backwards to get  $\alpha$  and  $\beta$  when  $R$ ,  $L$ , and  $C$  are given. In general this relation is complex; however,  $\alpha$  is usually sufficiently small that, without too great error,  $\sinh \alpha$  can be replaced by  $\alpha$  and  $\cosh \alpha$  by 1. Then  $\beta$  is approximately independent of  $R$  and

$$\sin(\beta/2) = 1/2\omega\sqrt{LC}$$

$$\alpha = \omega L/R\sqrt{4\omega^2 LC - 1}.$$

Contours of constant  $\alpha$  and  $\beta$  are plotted in Figure 63.  $R$  is assumed to be 1,000 ohms for the purpose of plot-

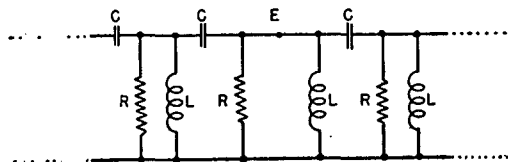


FIGURE 61. Constant- $k$  lead line modified by shunt dissipation.

ting  $\alpha$ . For any other value of  $R$ , the value of  $\alpha$  obtained from the graph should be multiplied by  $1,000/R$ . This graph can also be used to solve the problem of Figure 62: that of determining the appropriate  $L$  and  $C$ . If  $R$  has any other value than 1,000 ohms, the  $L$  and  $C$  thus obtained should be multiplied and divided, respectively, by  $R/1,000$ .

Since the output voltage is obtained by connecting at one or more of the points such as  $E$  in Figure 61,

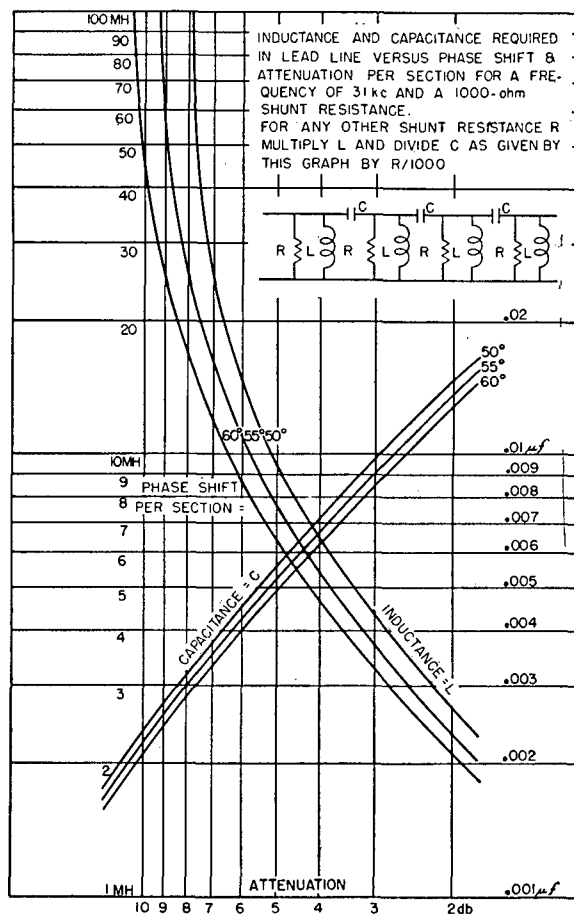


FIGURE 62. Curves for determination of inductances and capacitances for dissipative lead line.

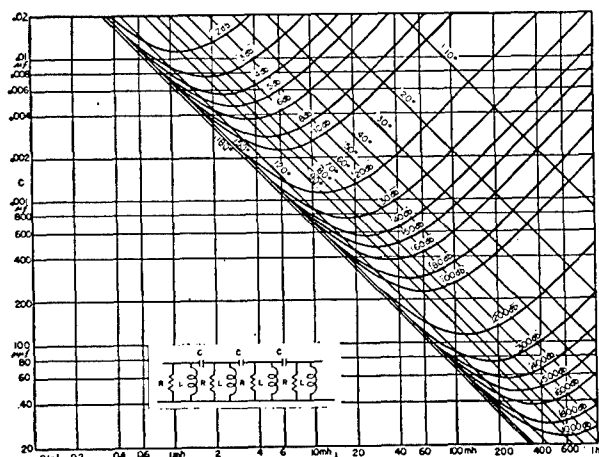


FIGURE 63. Approximate attenuation and phase shift per section versus capacitance and inductance for frequency of 31 kc and inductance shunted by 1,000-ohm resistance.

this leads to the question of the mid-shunt image admittance of one of the sections. This admittance is:

$$Y_{\pi} = \frac{G}{2 \tanh \alpha} + j \frac{G}{2 \tan \beta},$$

where  $G = 1/R$ . The admittance looking into any mid-shunt point of the properly terminated line is twice this value.

## 9.6 SWITCHING PULSE LINE DESIGN

### 9.6.1 Requirements and Uses

In the ER system all the transducer elements are connected into a lead line, and at each element a vacuum tube or other switching device, normally biased beyond cutoff, is connected. By means of a distortionless line, a pulse, commonly called the "switching" pulse, successively changes the bias on one or more tubes. Thus, at any given instant, the distribution of voltage along the lead line is such as to establish conduction in a group of adjacent tubes whose combined outputs produce the desired instantaneous directional pattern. Since the switching line is composed of lumped elements, it is referred to as an "artificial line" to distinguish it from a line with continuously distributed parameters.

It is obvious that if the system is to respond uniformly to signals received from any direction, the switching pulse must have very nearly the same shape and amplitude at the end of the switching line as it

had at the beginning. This requires that the phase shift be very closely proportional to frequency up to the frequency of the highest harmonic required for satisfactory transmission of the pulse form.

### 9.6.2 Basic Theory of Switching Lines

In the symmetric  $\pi$ - or T-section low-pass constant- $k$  filter there are two parameters, an inductance and a capacitance. Usually it is desired to specify the image impedance at zero frequency and the phase shift at the frequency of operation. These two specifications completely determine the circuit elements and there is no parameter left by means of which the attenuation or phase shift properties can be adjusted.

A new parameter may be introduced, however, by a process of  $m$ -derivation of the constant- $k$  prototype. The use of this parameter is equivalent to introducing a new circuit element, and with it changes can be made in the frequency behavior of the phase shift, the attenuation, or the image impedance.

In the construction of an artificial line it is important that the phase shift be a linear function of the frequency over a large fraction of the pass region. This is the criterion by which any new parameters are to be adjusted. If the phase shift curves of the  $m$ -derived sections are plotted with  $m$  as a parameter, it may be seen that when  $m$  is approximately equal to 1.4, a nearly linear phase shift curve is obtained.<sup>29</sup>

The simplest way to realize  $m$ -derived filter sections with  $m > 1$  is to use a center-tapped inductance with a coupling-coefficient  $k$  between the two halves. This is represented by the circuit of Figure 59 which is a mid-series  $m$ -derived low-pass filter. The parameter  $m$  is replaced by a new parameter  $k$ , the coupling coefficient. These parameters are related by  $m = \sqrt{(1+k)/(1-k)}$  or  $k = (m^2 - 1)/(m^2 + 1)$ . The value of  $m = 1.4$  corresponds to  $k = 0.33$ .

The first artificial transmission lines built at HUSL were designed to have a high image impedance. On that account inductances with iron cores were desirable, making it difficult to realize a coupling coefficient as small as 0.33. Furthermore, since a large number of these inductances were to be placed in a small space requiring that the effect of stray fields be minimized, toroidal coils were considered desirable.

It was found experimentally that for the sizes of inductance used in these lines the distributed capacitance was not negligible, the circuits did not behave as would be expected on the basis of a simple  $m$ -

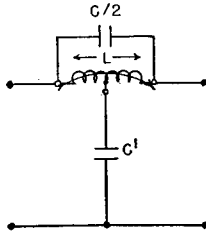
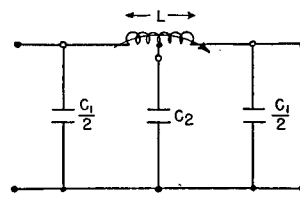


FIGURE 64. Bridged-T filter section.

FIGURE 65. Double- $\pi$  filter section.

derived section, and in some cases the effect of the distributed capacitance greatly improved the phase shift properties of the network.

These experimental observations led to an investigation of the general circuit of Figure 64. In this circuit the coupling coefficient  $k$  is not considered as an adjustable parameter since the use of toroidal coils imposes an essentially fixed value of  $k$ . The capacitance  $C/2$ , which includes the distributed capacitance, serves as a new parameter to adjust the phase shift versus frequency characteristics.

Later in the development of the technique of switching lines, the image impedance was reduced to the order of 50 ohms. This involved the use of small inductances so that the effects of distributed capacitance became negligible.

The phase shift of the network in Figure 59, with  $k \cong 0.9$ , could be made nearly linear by introducing additional capacitance in parallel with the inductance. Further study suggests the possibility of using, instead, the symmetric network of Figure 65. It may be objected that the circuit of Figure 65 requires three capacitors as compared to the two required by the circuit of Figure 64, but this objection is invalidated when a large number of sections are to be connected in tandem as is done in the artificial lines.

In the circuits of Figures 64 and 65 there are three parameters, the inductance and two capacitances. This statement is based on the assumption that the coupling coefficient  $k$  is not adjustable. The three parameters make it possible to specify three quantities regarding the behavior of the network. Two parameters are used, as before, in specifying the phase shift at the operating frequency and the image impedance at zero frequency. The third parameter is available for the purpose of linearizing the phase shift curve.

In order to have a quantitative process by means of which the third parameter can be selected, it was decided to make sure that the line which is tangent to

the phase shift curve at the origin would intersect the phase shift curve at  $\beta = 90$  degrees. To test the fairness of this criterion, it has been applied to the  $m$ -derived section of Figure 59. This criterion gives a value of  $m = 1.27$ . Independent computations<sup>29</sup> show that if  $m$  is varied in steps of 0.1, then 1.3 gives the best linear behavior from 0 to 90 degrees and gives good linear behavior from 0 to 145 degrees. It has been shown that the value  $m = 1.4$ , which was quoted before, gives the most nearly linear phase shift over the range from 0 to 145 degrees. This criterion is now applied to the circuits of Figures 64 and 65.

### 9.6.3 Switching Line for ER Sonar

The circuit of Figure 64 may be analyzed as follows: Let  $Z_I$  be the image impedance,  $\Theta$  the image transfer constant, and  $k$  the coefficient of coupling of the inductance. It can be shown that<sup>30</sup>

$$\tanh \Theta = j \frac{2\omega\omega_1 \sqrt{1+k} \sqrt{(\omega_1^2 - \omega^2)(\omega_2^2 - \omega^2)}}{(\Omega_1^2 - \omega^2)(\Omega_2^2 - \omega^2)},$$

or

$$\tanh \frac{\Theta}{2} = j \frac{\omega\omega_1 \sqrt{1+k}}{\sqrt{(\omega_1^2 - \omega^2)(\omega_2^2 - \omega^2)}},$$

$$Z_I = \sqrt{\frac{L}{2C}} \sqrt{\frac{1-k}{1+k}} \sqrt{\frac{\omega_2^2 - \omega^2}{\omega_1^2 - \omega^2}},$$

where

$$\omega_1^2 = 2/LC,$$

$$\omega_2^2 = 4 \left[ \frac{1+k}{1-k} \right] / LC,$$

$$\omega_3^2 = \left[ \frac{4}{1-k} \right] / LC,$$

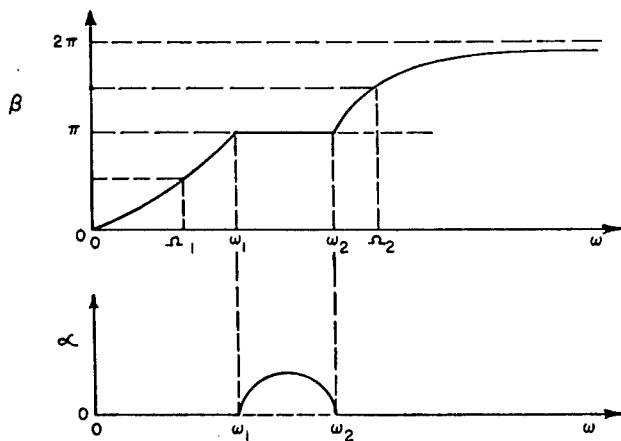


FIGURE 66. Phase shift and attenuation characteristics of circuit in Figure 64.

and  $\Omega_1^2$  and  $\Omega_2^2$  are the roots of

$$\omega^4 - \omega^2(\omega_2^2 + \omega_3^2) + \omega_1^2\omega_2^2 = 0.$$

It can be shown that<sup>30</sup>

$$0 < \Omega_1 < \omega_1 < \omega_2 < \Omega_2,$$

and so if  $\Theta = \alpha + j\beta$  the behavior of  $\alpha$  and  $\beta$  may be sketched as in Figure 66.

The design procedure is as follows: A lag line is to be constructed with a phase shift that has a specified slope when plotted against frequency and with a specified image impedance at zero frequency. The inductive elements of the line have a coupling coefficient of  $k$ .

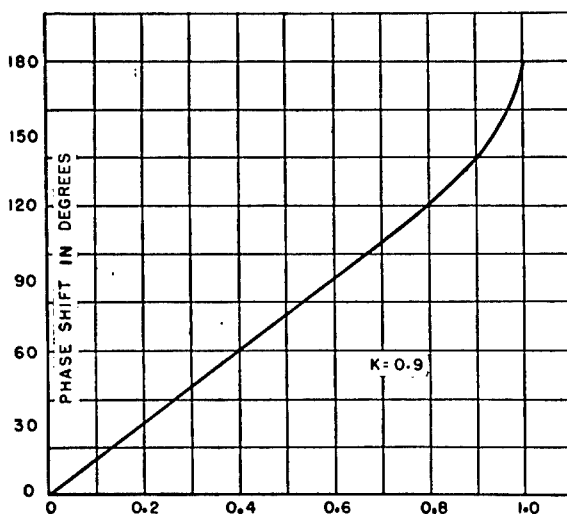


FIGURE 67. Phase shift versus frequency on linear scale for circuit in Figure 64.

The design parameters are fixed by specifying that the slope of the phase shift at zero frequency is the desired slope and that the frequency at which the phase shift is 90 degrees falls on the straight line. The slope  $\mu$  of the phase shift curve at a frequency of zero cycles per second is

$$\mu (\text{radians/cycle}) = \frac{4\pi\omega_1^2\omega_2^2}{\Omega_1^2\Omega_2^2} \sqrt{\frac{1+k}{1-k}} = \frac{4\pi}{\omega_2} \sqrt{\frac{1+k}{1-k}}.$$

This determines  $\omega_2$  (given  $k$ ) and finally

$$C' = \frac{m^2}{4\pi^2} \frac{1}{L}.$$

Now  $\Omega_1$ , the angular frequency at which the phase shift is 90 degrees, is specified in the problem and may be treated as known. The value of  $\omega_1^2$  can be determined by the equation

$$\omega_1^2 = \Omega_1^2 \frac{\Omega_1^2 - \omega_2^2}{\frac{2}{1-k} - \omega_2^2},$$

which in turn determines the cutoff frequency and the product  $LC$  in accordance with

$$LC = \frac{2}{\omega_1^2}.$$

If  $L$  is given,  $C$  is thus determined, or if the image impedance at zero cycles is specified, then  $L$  and  $C$  can be found with the aid of the equation

$$Z_l \Big|_{f=0} = \frac{\omega_2}{\omega_1} \sqrt{\frac{1-k}{1+k}} \sqrt{\frac{L}{2C}}.$$

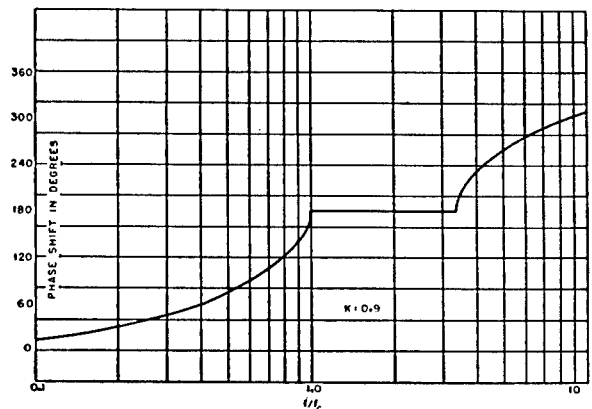


FIGURE 68. Phase shift versus frequency on logarithmic scale for circuit in Figure 64.

The phase shift of this network is shown in Figure 67 for the special case of  $k = 0.9$ . It can be seen that the phase shift is approximately linear for phase shift angles up to 120 degrees. In Figure 68 the phase shift is shown for a much wider range of frequencies in order that the attenuation band can be seen in its true aspect.

For the practical design of these filter sections it is desirable to solve the equation given above for the dependent variables expressed in terms of the independent variables.<sup>31</sup>

The basic independent variables are: (1) the frequency  $F_1$  at which the phase shift is 90 degrees (or  $\Omega_1 = 2\pi F_1$ ); (2) the inductance  $L$  of the coil; and (3) the coefficient of coupling  $k$  of the coil.

The dependent variables are: (1)  $f_1$ , the lower limit of the stop band, that is, the frequency at which the phase shift first becomes 180 degrees (or  $\omega_1 = 2\pi f_1$ ); (2) the frequency  $f_2$  of the upper limit of the stop band (or  $\omega_2 = 2\pi f_2$ ); (3) and (4) the capacitances  $C/2$  and  $C'$ ; and (5) the image impedance  $Z_{I0}$  at zero frequency.

If it is specified that the slope of the phase shift

curve at zero frequency is that of a straight line through the 90-degree point,

$$\frac{f_2}{f_1} = \frac{\omega_2}{\Omega_1} = \frac{4}{\pi} \sqrt{\frac{1+k}{1-k}}. \quad (16)$$

This curve is plotted in Figure 69.

By virtue of equation (16) it can be shown that

$$\frac{f_1}{F_1} = \frac{\omega_1}{\Omega_1} = \sqrt{\frac{25.87k + 6.13}{16k - 3.74}}. \quad (17)$$

This curve is plotted in Figure 70.

The shunt capacitance  $C'$ , is determined by

$$C' = \frac{1}{16F_1^2} \cdot \frac{1}{L}.$$

This equation is plotted in Figure 71 with  $L$  as a parameter.

After the lower frequency  $f_1$  of the stop band has been determined by equation (17), the bridging capacitance  $C/2$  can be determined by

$$\frac{C}{2} = \frac{1}{4\pi^2 f_1^2} \cdot \frac{1}{L}.$$

This equation has been plotted in Figure 72 with  $L$  as a parameter.

The image impedance at zero frequency  $Z_{I0}$  is given by

$$Z_{I0} = 4F_1 L.$$

This equation is plotted in Figure 73 with  $L$  as a parameter.

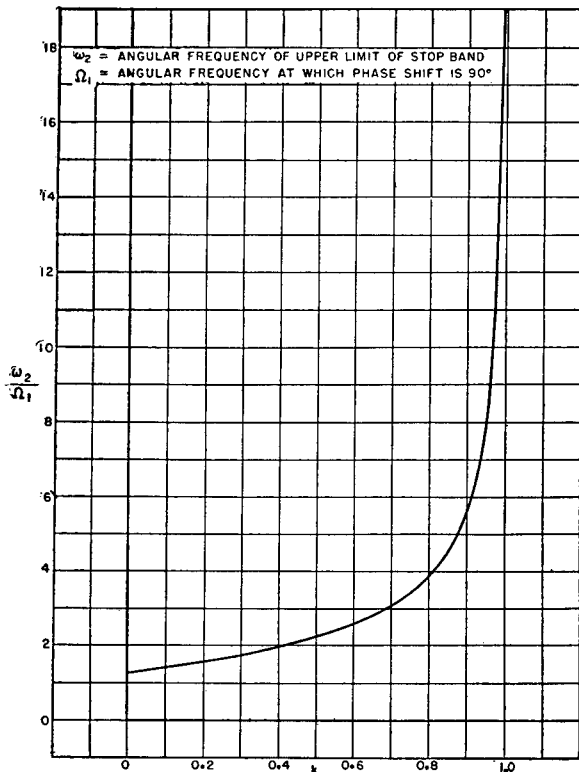


FIGURE 69. Dependence of upper limit of stop band on  $k$ , where  $k$  = coefficient of coupling of coil.

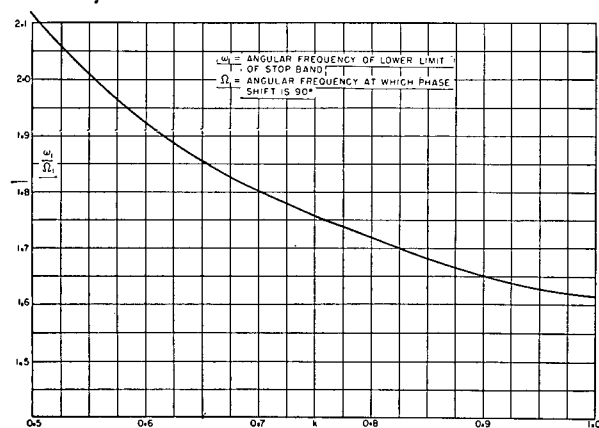


FIGURE 70. Dependence of lower limit of stop band on  $k$ , where  $k$  = coefficient of coupling of coil.

In the curves for which  $L$  is a parameter, the values of  $L$  were chosen to conform more or less with the inductances of standard toroidal coils supplied by the Western Electric Company and at the same time to give a uniform spacing of the curves. The values of  $L$

most commonly used in the construction of the artificial lines are 85, 130, and 210 millihenries. To save the trouble of interpolations, Figures 74 and 75 give curves for the determination of the capacitances  $C'$  and  $C/2$  respectively for these special values of  $L$ .

The design procedure may be summarized as follows:

1.  $F_1$  and  $L$  are chosen and  $k$  is measured.
2. From Figures 69 and 70 the auxiliary quantities  $f_1$  and  $f_2$  are determined. Actually  $f_2$  has no further importance except to show the upper limit of the stop band.
3. By means of Figure 71,  $C'$  may be determined.
4. From Figure 72 or 75,  $C/2$  may be determined.
5. From Figure 73 the image impedance at zero frequency is determined.

#### Example

Suppose that a section is to be designed which gives a phase lag of 10 degrees at 500 cycles and that the available inductance is 0.080 henry with a coupling coefficient of 0.885. If the phase shift were linear, the frequency  $F_1$  at which the phase shift is 90 degrees would be 4,500 cycles. From Figure 69 it is seen that

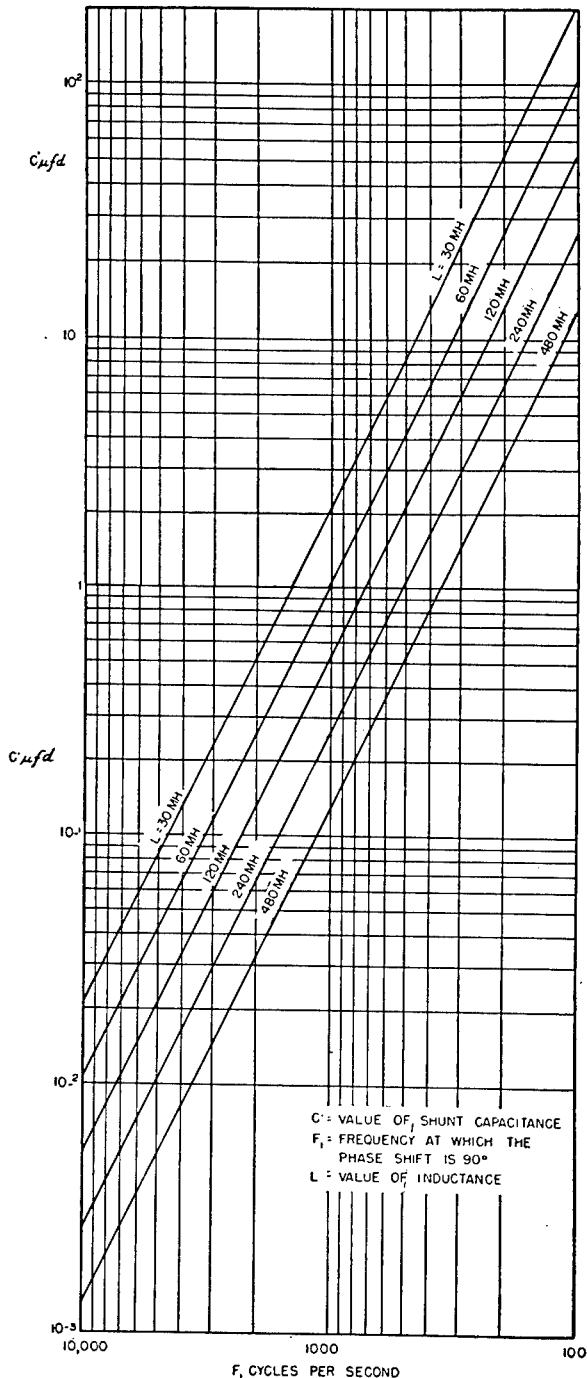


FIGURE 71. Curves for determination of  $C'$  of Figure 64.

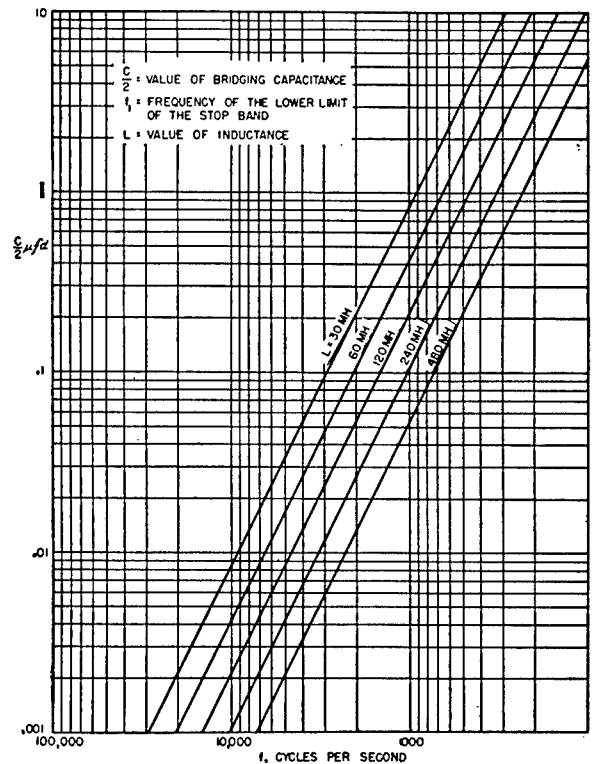


FIGURE 72. Curves for determination of  $C/2$  of Figure 64.

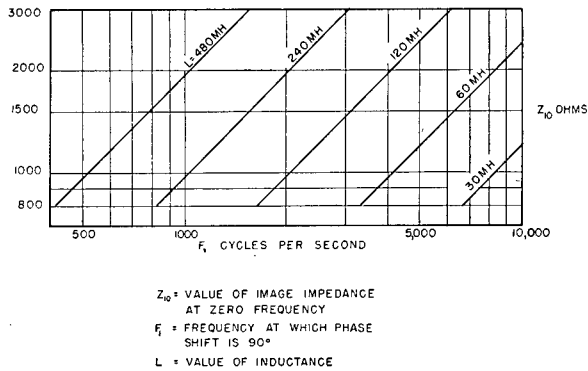


FIGURE 73. Curves for determination of image impedance of Figure 64.

for  $k = 0.885$ ,  $f_2/F_1 = 5.20$ . Thus the upper limit of the stop band is 23,400 cycles. From Figure 70,  $f_1/F_1 = 1.663$  and the lower limit of the stop band is 7,500 cycles.

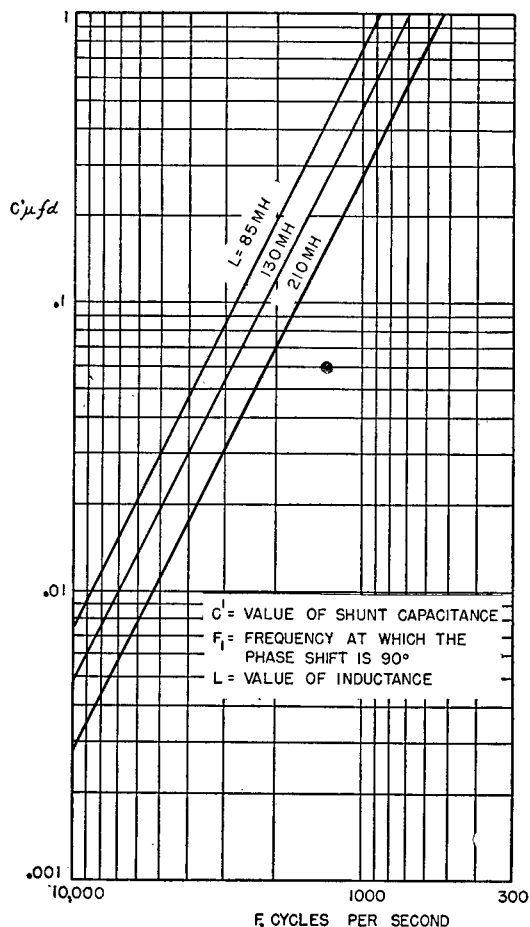


FIGURE 74. Curves for determination of  $C'$  of Figure 64 at common values of  $L$ .

In Figure 71, for  $F_1 = 4,500$  cycles, an interpolation is made at  $L = 80$  mH, and  $C' = 0.039 \mu\text{f}$  is found. On Figure 72, for  $f_1 = 7,500$  cycles,  $C/2 = 0.0056 \mu\text{f}$ . It should be noted that for inductances whose coupling coefficients are near 0.9, a check on the computations lies in the fact that the inductor and its bridging capacitor should have an antiresonance at a frequency very near  $1.65F_1$ . From Figure 73 the image impedance at zero cycles is seen to be 1,370 ohms.

#### 9.6.4 Switching Line Using Double-Pi Filter Sections

Consider the network of Figure 65 and let:

- $k$  = coefficient of coupling
- $L$  = total inductance
- $\Theta$  = image transfer constant of network
- and  $Z_I$  = image impedance.

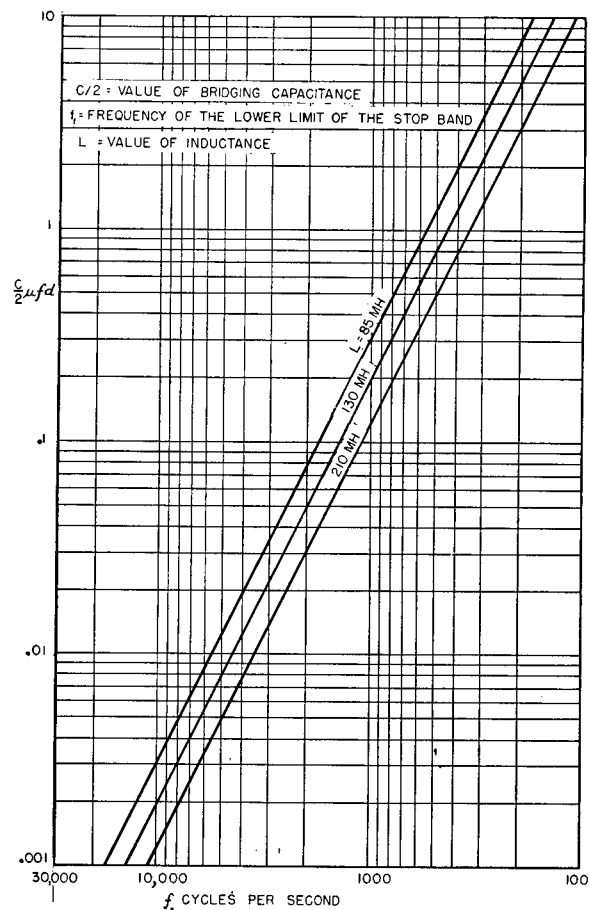


FIGURE 75. Curves for determination of  $C/2$  of Figure 64 for common values of  $L$ .



Then

$$\tanh \Theta = \frac{j\omega[(\omega_1^2 - \omega^2)(\omega_2^2 - \omega^2)(\omega_3^2 - \omega^2)]^{1/2}}{(\Omega_1^2 - \omega^2)(\Omega_2^2 - \omega^2)}$$

$$\tanh \frac{\Theta}{2} = j\omega \sqrt{\frac{(\omega_3^2 - \omega^2)}{(\omega_1^2 - \omega^2)(\omega_2^2 - \omega^2)}}$$

$$Z_I = \sqrt{\frac{L}{C_1 + C_2}} \sqrt{\frac{1 - \omega^2/\omega_2^2}{(1 - \omega^2/\omega_1^2)(1 - \omega^2/\omega_3^2)}}$$

or

$$Z_I = \frac{L\omega_2^2}{2} \sqrt{\frac{(\omega_2^2 - \omega^2)}{(\omega_1^2 - \omega^2)(\omega_3^2 - \omega^2)}}$$

where

$$\omega_1^2 = 4/LC_1$$

$$\omega_2^2 = 4 \left[ \frac{1+k}{1-k} \right] \frac{1}{LC_2}$$

$$\omega_3^2 = 4 \left[ \frac{1+k}{1-k} \right] \frac{1}{L} \left( \frac{1}{C_1} + \frac{1}{C_2} \right)$$

$$\omega_4^2 = \frac{4}{L(C_1 + C_2)}$$

and  $\Omega_1^2, \Omega_2^2$  ( $\Omega_1^2 < \Omega_2^2$ ) are the roots of

$$\omega^4 - \frac{1}{2} \omega^2 (\omega_1^2 + \omega_2^2 + \omega_3^2) + \frac{1}{2} \omega_1^2 \omega_2^2 = 0$$

treated as a quadratic in  $\omega^2$ .

As in the preceding case, it is desirable to specify the slope of the phase shift curve and the image impedance at zero frequency. The value of  $k$  is fixed by the kind of inductors that are used.

Let  $\beta'$  = slope of the phase shift curve in radians per cycle,

$Z_{I0}$  = image impedance at zero frequency.

Then

$$L = \beta' Z_{I0} / 2\pi,$$

also

$$C_1 + C_2 = \beta'^2 / 4\pi^2 L = \beta' / 2\pi Z_{I0}.$$

One more relationship is necessary in order to solve for  $C_1$  and  $C_2$  separately. This is obtained by specifying that the point on the phase shift curve at which  $\beta = \pi/2$  should fall on a line of slope  $\mu$  through the

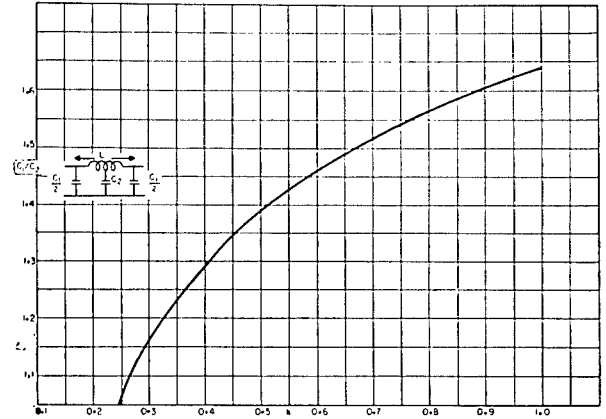


FIGURE 76. Dependence of  $C_1/C_2$  on  $k$  for circuit of Figure 65.

origin. This condition yields the following quadratic equation in  $C_1/C_2$ :

$$\left( \frac{C_1}{C_2} \right)^2 (1 - 2\lambda) + 2 \left( \frac{C_1}{C_2} \right) \cdot$$

$$\left[ 1 - \lambda + \frac{\lambda}{1+k} \left\{ (1-k)\lambda - 1 \right\} \right] + 1 - \frac{2\lambda}{1+k} = 0$$

where  $\lambda$  is used to denote  $(\pi/4)^2$ . Since the coefficients are functions of  $k$  only, and since only positive values of  $(C_1/C_2)$  are of interest,  $(C_1/C_2)$  can be plotted as a function of  $k$  as in Figure 76.

This network has two pass bands and two elimination bands. The dependence of phase shift, attenuation, and image impedance on frequency are shown in Figure 77.

For a given value of  $k$ , the phase shift curve may be plotted as a function of  $f/f_c$  where  $f_c$  is the first cutoff frequency or  $\omega_1/2\pi$ . It may be seen from Figure 78, in which the phase shift is plotted on a linear scale, that the phase shift is linear up to 90 degrees. The presence of dissipation tends to reduce the phase shift near the cutoff frequency, and the range of linear phase shift may consequently be even larger. In Figure 79 the phase shift for  $k = 0.9$  is plotted for a large range in order to show the relative positions of the pass bands.

If  $k = 0.9$ , then

$$\frac{f_1}{F_1} = 1.621, \frac{f_2}{F_1} = 8.95, \frac{f_3}{F_1} = 11.40,$$

where  $F_1$  is the frequency at which the phase shift is 90 degrees. In one application frequently used,

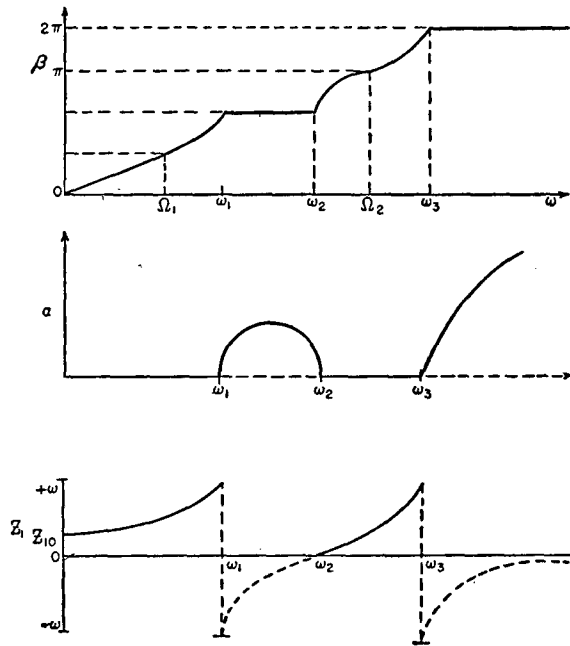


FIGURE 77. Dependence of phase shift, attenuation, and image impedance on frequency for circuit of Figure 65.

$F_1 = 4$  kc. In this case  $f_1 = 6.5$  kc,  $f_2 = 36$  kc, and  $f_3 = 45.6$  kc. If the echo-ranging frequency is under 36 kc, it falls in one of the elimination bands. If a frequency between 36 and 46 kc is used, trouble may result from cross-talk arising from free transmission at signal frequency along the switching line. The quantities  $f_2$  and  $f_3$  are each proportional to  $(1 - k)^{-1/2}$ , so that they may be increased by increasing  $k$ .

If the network of Figure 65 is to be treated as a filter, the cutoff frequency  $f_c$  is specified instead of the

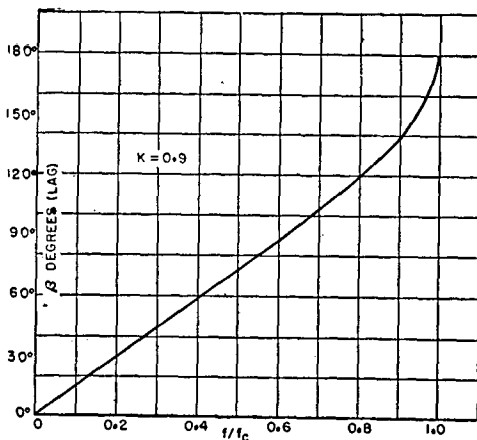


FIGURE 78. Phase shift versus frequency on linear scale of circuit of Figure 65.

slope of the phase shift curve. In this case, the cutoff frequency is determined by

$$LC_1 = \frac{1}{\pi^2 f_c^2}.$$

Since  $C_1/C_2$  is known,

$$LC_2 = \frac{C_2}{C_1} \frac{1}{\pi^2 f_c^2}.$$

Hence

$$\omega_4^2 = \frac{4}{L(C_1 + C_2)} = \frac{4\pi^2 f_c^2}{1 + C_2/C_1},$$

and finally

$$L = \frac{2Z_{I0}}{\omega_4} = \frac{Z_{I0}\sqrt{1 + C_2/C_1}}{\pi f_c}$$

and

$$C_1 = 1/\pi^2 f_c^2 L.$$

$C_2$  may be found since  $C_1/C_2$  is known.

### 9.6.5 Further Examples of Switching Lines

Several other networks have been studied but none of them has been used. These circuits are listed and a phase shift curve is presented for each.

Figure 80 is an all-pass constant-resistance network.<sup>30</sup>

Figure 81 is basically an  $m$ -derived section with  $m = 1.5$  in tandem with its constant- $k$  prototype.<sup>32</sup>

Figure 82 is basically two  $m$ -derived sections in tan-

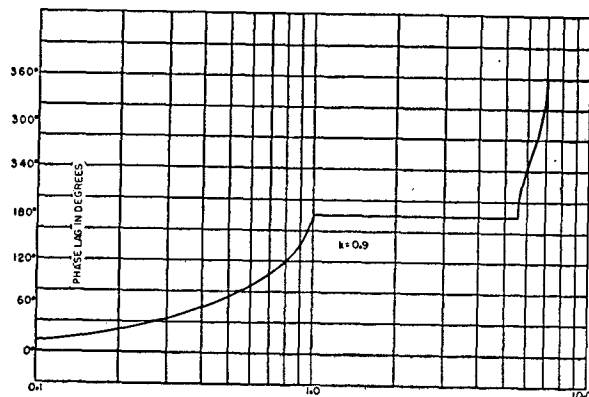


FIGURE 79. Phase shift versus frequency on logarithmic scale of circuit of Figure 65.

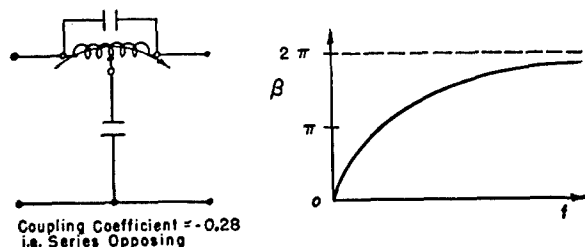


FIGURE 80. Constant-resistance filter section and its phase shift behavior with respect to frequency.

dem, with  $m = 1.6$  and  $m = 0.6$  respectively. The image impedance is fairly constant over most of the pass band.<sup>32</sup>

#### 9.6.6

### Power Storage Lines

Artificial lines, in addition to their use as delay networks and switching lines, can be employed for power storage in transmitter power supply circuits. Here the aim is to deliver a large amount of power to the transmitter for the short time in which the pulse is emitted. It is desirable that the power be constant during the length of the pulse, except for such pulse shaping as may be applied to reduce shock excitation of nearby (enemy) tuned circuits. For this purpose, the line may be composed of constant- $k$  low-pass filter sections (Figure 56), of  $m$ -derived sections (Figure 59) or of any of the more involved sections described above (Figures 64, 65, 80, 81, 82).

The theory is first developed in terms of an ideal<sup>33</sup> distortionless continuous lag line. If such a line is open-circuited at each end and is charged to a potential  $2V$ , the total energy ( $E$ ) stored is given by

$$E = 2V^2 C$$

where  $C$  is the total shunt capacitance.

The series of voltage distributions in Figure 83

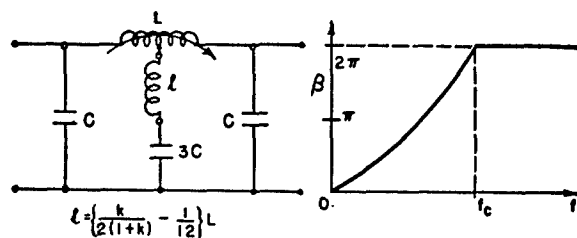


FIGURE 81. Complex filter section and its phase shift behavior with respect to frequency,  $m = 1.5$  (constant- $k$  prototype with  $m$ -derived section).

shows how the line behaves. If a load impedance  $Z_R$ , equal to the image impedance of the line, is suddenly connected to the right end, the voltage at this end falls to  $V$ . This is equivalent to applying a sudden d-c voltage of  $-V$  at the right end of the line (B). Since the line is ideal, this d-c pulse travels down the line to the open-circuited left end where it is reflected without change of sign (C, D). The pulse,  $-V$ , then returns to the right end (E). The voltage across the load impedances  $Z_R$  remains at  $V$  until the reflected pulse returns; the voltage across  $Z_R$  then drops to zero.

Thus if the line is initially charged to a potential  $2V$ , it delivers a voltage  $V$  for the length of time required for a pulse to travel twice the length of the line. The advantages of the system are twofold: (1) the delivered voltage is constant during the pulse; (2) all of the energy stored in the line is delivered during the pulse.

If the continuous line is replaced by one composed of a finite number of sections, the ideal behavior described above is approximated if the number of sections is sufficiently large. With a finite number of sections there is a cutoff frequency; as a result, only a finite frequency spectrum can be transmitted, and the ideal square pulse shown in Figure 83 is distorted. If sections are used which give zero attenuation and linear phase shift over the pass band, the theory of the response of an ideal low-pass filter is applicable.<sup>34</sup> Thus, if a constant voltage is suddenly applied to the input of an ideal low-pass filter, the delay time  $t_d$  in the arrival of the first portion of the pulse at the output is

$$t_d = \frac{\mu}{2\pi} \quad (18)$$

where  $\mu$  = slope of total phase shift curve in radians per cycle. The build-up time  $\tau_a$  is given by

$$\tau_a = \frac{1}{2f_c}$$

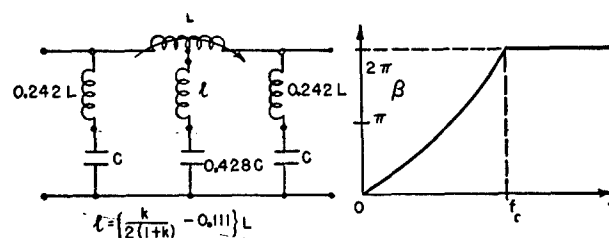


FIGURE 82. Second complex filter section and its phase shift behavior with respect to frequency (two  $m$ -derived sections with  $m = 1.6$  and  $m = 0.6$ ).

where  $f_c$  = cutoff frequency of the filter. These quantities are indicated in Figure 84, and the resultant output pulse shape for a storage line of ideal low-pass

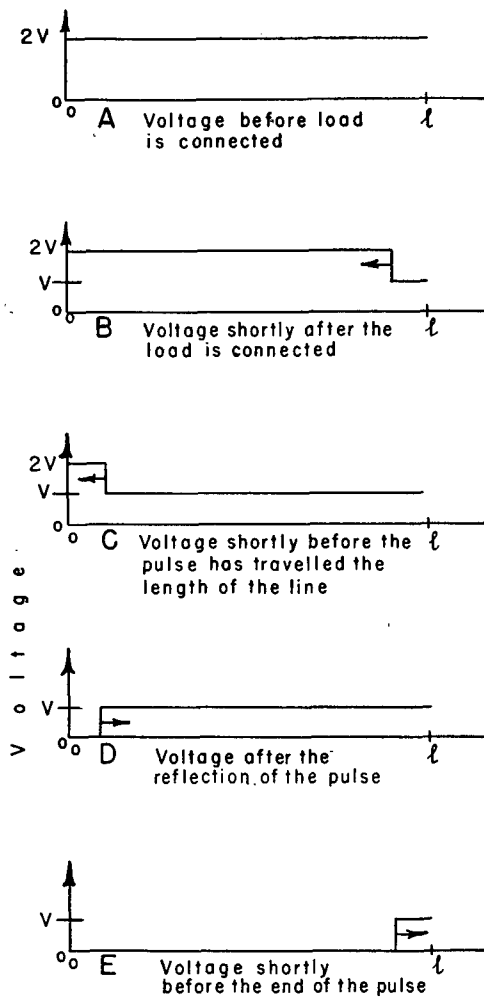


FIGURE 83. Distribution of voltage along charged lag line of length  $l$  at successive intervals after suitable load is connected at one end.

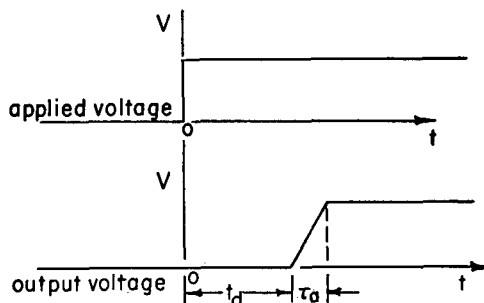


FIGURE 84. Shape of Heaviside unit step function before and after passing through ideal low-pass filter.

filter sections is shown in Figure 85. The higher the cutoff frequency, the less the build-up time  $\tau_a$  which is involved in considerations of pulse distortion. Since raising the cutoff frequency means increasing the number of sections for a given total time delay, a compromise has to be made between reduction of pulse distortion and reduction in numbers of components.

In designing a line consideration must be given to the power  $W$ , the voltage  $V$ , the load resistance  $R$ , and the pulse length  $\tau$ . These quantities are not entirely independent, since there exists the relationship

$$W = \frac{V^2}{R}.$$

If each of the  $n$  sections has a total shunt capacitance  $C_0$  and if the desired output voltage is  $V$ , the line must be charged to a potential  $2V$ , and the stored energy  $E$  is

$$E = 2V^2nC_0.$$

If all of this energy is to be delivered at the rate of  $W$  watts during  $\tau$  seconds,

$$E = W\tau = 2V^2nC_0$$

or

$$nC_0 = \frac{W\tau}{2V^2}.$$

This determines the total capacitance of the line if the voltage is fixed.

The pulse length  $\tau$  is equal to the time lag  $t_d$  for a pulse to travel twice the length of the line, and from equation (18)

$$t_d = \tau = \frac{nm_0}{\pi}$$

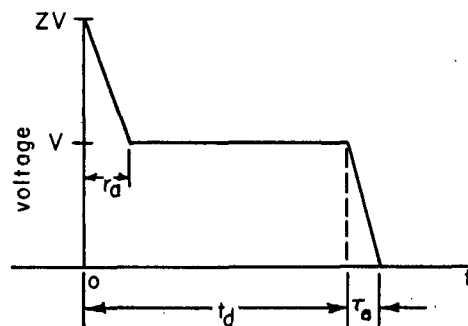


FIGURE 85. Shape of voltage developed across load resistance connected to ideal low-pass transmission line.

or

$$\mu_0 = \frac{\pi\tau}{n},$$

where  $\mu_0$  is the slope of the phase shift curve of one section in radians per cycle. It is recognized from this expression that the electrical length of the line is 180 degrees for a frequency of  $1/\tau$ , and that at this frequency the phase shift of a single section is 180 degrees/ $n$ . The number of sections  $n$ , as already implied, is preferably small in order to keep the number of components to a minimum. The lower limit can be determined by considering that the filter is ideal. If the phase shift at the cutoff frequency  $f_c$  for one section is  $\pi$  radians, as is usually the case, the build-up time  $\tau_a$  is given by

$$\tau_a = \frac{\tau}{2n}.$$

Thus two sections give a build-up time of one-quarter of the duration of the pulse. This may be acceptable

when some rounding of the corners is desired. Actually, since the line is composed of lumped elements, the terminating elements appreciably affect the shape of the pulse. If the network ends in a shunt capacitance, the initial discharge current is very large and a sharp voltage peak occurs at the beginning of the pulse. On the other hand, if the network ends in a series inductance, there is less tendency for the formation of this sharp voltage peak. It may be possible to adjust the amount of the terminating series inductance so that a minimum surge of voltage is produced at the beginning of the pulse, but this has not been investigated.

The theory derived above is limited in its application. If a line of only a few sections is suddenly discharged, the behavior is very complicated and may be determined only by a rigorous analysis of the Kirchhoff equations. The theory should, therefore, be considered only as a basic guide and final design adjustments should be made experimentally.

## SUMMARY DISCUSSION OF SCANNING SONAR PROBLEMS AND PROPOSALS FOR FUTURE WORK

### 10.1 SCANNING SYSTEM PROBLEMS: FUTURE WORK

#### 10.1.1 Transducer Improvements

EXPERIENCE in the development of transducers up to the time of the writing of this book has indicated a number of ways in which these particular components of scanning sonar gear may be improved. The present section deals with various aspects of this problem.

##### RELIABILITY

*Watertightness.* The complexity of scanning sonar transducers makes watertight construction difficult, but it is extremely important that the device should be able to operate in water without leaking for as long a period as several years at a time.

Steps toward improving the watertightness of transducers should consist chiefly in simplifying present designs, developing better materials, and making more convenient cable seals. For example, techniques should be developed whereby Navy M bronze and stainless steel castings can be cast in such a way as to be guaranteed absolutely nonporous. Some study should be devoted to forged and welded stainless steel construction which is inherently nonporous but needs to be made rustproof.

If, in the light of further experience, it should appear desirable to construct transducers with separately housed, removable elements, the problem of making the individual elements watertight and durable must be solved.

Although most of the important design factors of cable seals for use at low water pressures are known at the present time, they are not applied as well as they should be. Cable seals should be developed which are reliable up to water pressures as high as 1,000 psi, since at such pressures, cables (especially the larger ones) tend to slip or extrude through ordinary low-pressure cable seals.

The most satisfactory water seals are of the tongue-and-groove type in which the primary flange faces are drawn up tight. In this condition the volume of

gasket rubber in the groove should be 10 to 15 per cent greater than the space between the tongue and groove. The tongue is made to fit the groove loosely on the outside diameter so that the excess 10 to 15 per cent of gasket rubber can creep past the outer edge of the tongue.

Another type of seal which has been successful is one using a rather close-fitting tongue and groove with a corprene gasket. The corprene gasket is made with dimensions giving it a volume about 10 per cent greater than the closed volume of the tongue and groove. The compressibility and resilience of the cork particles in the corprene allow the gasket to compress, yet keep the seal tight regardless of temperature changes and aging.

*Corrosion and Deterioration of External Parts; New Materials.* Sea water corrodes most metals rapidly unless the surfaces are covered by protective coatings. Corrosion is increased by electrolytic action if the transducer and some dissimilar metal are electrically connected and both exposed to sea water. Consequently, further development of satisfactory metals, protective coatings, and methods of reducing electrolytic action is desirable.

Most transducers have rubber parts that are exposed to such agents as the sea water, mineral oil, and grease. This rubber is also subjected to the action of sunlight and air if the transducer is mounted on the topside of a submarine. The rubber used under such conditions should be highly resistant to deterioration by the agents mentioned, and in addition should be acoustically transparent and mechanically strong and tough. The  $\rho c$  rubber developed for the Navy by the Goodrich Tire and Rubber Company of Akron, Ohio, possesses most of the characteristics mentioned; it has low mechanical strength, however, and poor resistance to the action of sunlight. Further development work on rubber for use on transducers in sea water is therefore suggested.

There are many transducer arrangements in which troublesome reflections of sound are produced by surfaces in the vicinity of the transducer. An example of this is the combined arrangement in which the depth-scanning unit is mounted beneath the horizontal-

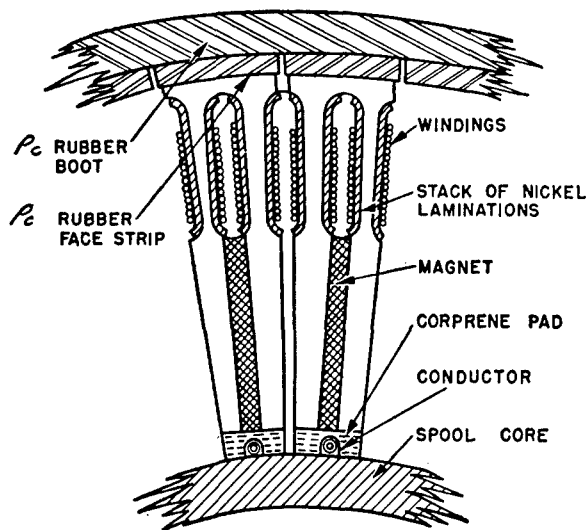


FIGURE 1. General design of element support and housing used in the Sangamo HP-5 scanning sonar transducer.

scanning unit. In this case the reflections of sound from the bottom plate of the upper transducer cause appreciable interference with the patterns and response of the lower transducer. If a rubber or rubber-like material can be developed which has a specific acoustic impedance very near that of water, and a very high coefficient of attenuation, it can be used to cover surfaces that give troublesome reflections. Such a material might also be used to cover the sides of submarines to render them incapable of reflecting sound pulses, in which case underwater sound echo-ranging systems would lose their usefulness. A material of this kind would be valuable in so many applications that its development would justify a great deal of time and expense. This problem could be attacked best by the combined efforts of a good rubber research laboratory and an underwater acoustics laboratory. Butyl rubber is the best material of this type now known.

There is also great need for a method of securing a strong, durable, and reliable bond between rubber of the acoustically transparent type and metals such as Navy M bronze and stainless steel. If such a bond were possible, the rubber face of the transducer could be bonded directly to the metal case and the use of clamping bands and bars of various kinds would be unnecessary when permanent water seals are needed.

*Strength Against Pressure and Impacts.* Several scanning sonar transducers have been constructed which withstand static pressures up to 200 to 300 psi,

and a few have been made which should operate successfully above 500 psi, although none has actually been tried at such a pressure. It is relatively easy to make the metal frames of the transducers strong enough to withstand any reasonable static or dynamic hydraulic pressures, but to construct the vibrating elements so that they are not deformed or rendered inoperative by such pressures is a much greater problem.

Consider, for example, the transducer elements and mounting shown in Figure 1. In this case the inward force due to external water pressure is transmitted through the rubber boot and rubber faces, through the laminated nickel stacks, and through the corprene pressure release backing pads to the core of the spool. The laminated stacks are capable of supporting a load of at least 3,000 psi and, consequently, do not limit the compressive strength of the transducer. The rubber faces withstand pressures of at least 1,000 psi if they are completely confined, but in this case there are small gaps between the stack faces into which the rubber can flow and this flow becomes serious at pressures above 350 psi. If the rubber is soft, very little improvement is made by increasing the thickness of the rubber boot so that it is necessary to use rubber having a greater Young's modulus and to reduce the gaps between neighboring stacks. The only supporting area at the bottom of the laminated stacks is the area of the two tail sections because the magnets are loose in the magnet slots. Since this area is only about 0.4 that of the face, the pressure on the corprene pads is about 2.5 times the external hydraulic pressure, causing the corprene to squeeze up into the magnet slots and into the small gaps between neighboring stacks. This effect could be minimized by placing thin strips of a strong material, such as impregnated laminated glass fiber board, between the bases of the stacks and the corprene pad. These strips could be about 1/16 inch thick and the thickness of the corprene could be reduced to about 1/8 inch without reducing perceptibly the pressure release effect. The thinner layer of corprene would have less tendency to flow under the pressure of the stack, and the fiber board strip would help to bridge the gaps over the magnet.

A typical method of constructing scanning sonar transducers in which the elements are made of piezoelectric crystals is illustrated in Figure 2. The crystals are arranged in stacks supported on pieces of molded corprene which have an L-shaped cross section. The

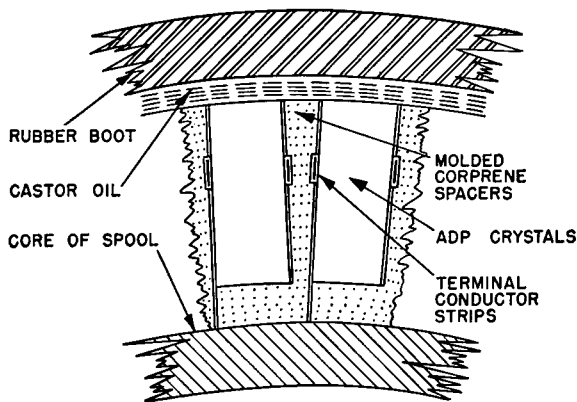


FIGURE 2. General design of element support and housing used in the Brush AX crystal scanning sonar transducer.

element space between the rubber boot and the core of the spool is vacuum-filled with castor oil. During the filling process, after the empty spaces are filled with castor oil, more oil is forced in under pressure so that the rubber boot bulges to some extent. When such a transducer is subjected to external hydraulic pressure, the oil in the element chamber must automatically come to the same static pressure. Owing to the fact that the cork particles in the corprene are compressible, the corprene changes its dimensions when the pressure is applied, while the crystals change very little. Consequently, there is some relative motion between the crystals and the corprene. If this relative motion is too great, the metal foil leads that connect to the terminal conductor strips are moved or torn. The motion may also tear loose the cemented joint between the crystals and the corprene and allow the crystals to become loose. These effects would be most pronounced at the top and bottom ends of the elements because of their relatively great lengths. There is also some possibility of damage to the assemblies of crystal elements due to pressure gradients set up in the oil of the element chamber by impulsive pressures caused by underwater explosions. In addition, the crystals could be damaged if the transducer were accidentally dropped on its side against some relatively sharp object or struck by such an object. Some thought should be given, therefore, to the problem of making crystal transducers capable of withstanding greater static pressures, greater impulsive pressure gradients, and greater impacts.

*Electrical Insulation.* In magnetostriction trans-

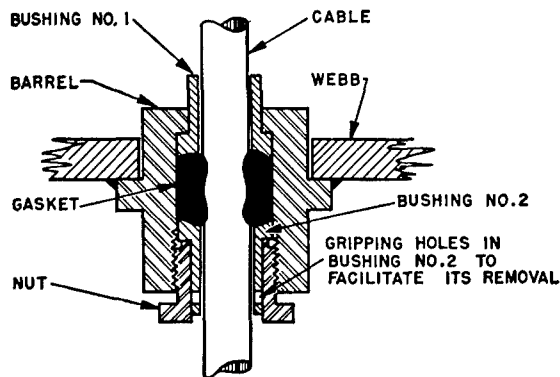
ducers the windings are usually designed to operate at relatively low impedance, so that the voltages used in high-power transmitting are generally not greater than 500 volts. However, because of the large number of elements and their intricacy, it is necessary to design the electric insulation of the windings, lead wires, terminal strips, etc., with considerable care. Places where improvement in this respect would be possible in the units already constructed include the insulation between the windings and the sharp corners of the laminated magnetostrictive stacks, the insulation and protection of the lead wires which run from the windings through the supporting flange to the terminal box, and the insulation in the terminal box itself.

In crystal transducers the impedances are high, and the terminal voltages consequently rise to thousands of volts during high-power driving. Since such voltages are too great for use in practical cables containing 50 or more twisted pairs of conductors, it has generally been the practice to install a transformer in the terminal box of the transducer for each element so that low impedance and voltage is retained in the cable. This means that the terminal box of a 48-element transducer must contain 48 transformers, each with a high-voltage winding connected to the proper crystal element terminals. Considerable improvement can be made in this connection with respect to present mechanical design and electrical insulation.

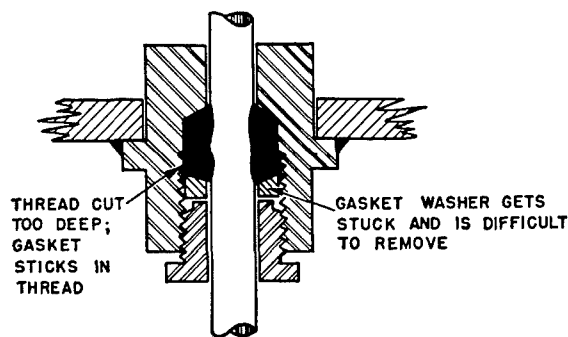
*Serviceability.* Scanning sonar transducers are so intricate and complicated that any internal repairs should be done by an expert in a place where the necessary tools and testing facilities are available. Two approaches are therefore suggested to improve the serviceability of such transducers. First, consideration should be given to increasing the ease of mounting or dismounting the transducer and its cable on a ship, with or without a sea chest. Second, a study should be made of the techniques of repairing and making changes in the interior parts of the transducer after it is brought to a servicing shop.

The cable gland should be so designed that it comes apart easily when the transducer is dismounted. One of the most common difficulties in this connection is binding the gasket or gasket washers to the side wall of the barrel. To illustrate this point, two seals are shown in Figure 3A and B which are equally good in sealing quality but differ considerably in ease of disassembly. In the A type, bushing No. 2 can be readily removed after the nut is removed





A. TYPE WHICH IS EASILY TAKEN APART



B. TYPE WHICH IS VERY DIFFICULT TO TAKE APART

FIGURE 3. Two cable seals for scanning sonar transducers which have equally good sealing qualities but widely different disassembly characteristics.

and the remainder of the seal comes out easily with a pull on the cable. In the B type, however, it is very difficult to remove the gasket washer and gasket because they tend to jam in the threads of the barrel.

It is also desirable to have the terminal box readily accessible while the transducer is attached to the mounting shaft. The favored design is to have the bottom cap of the transducer serve as the bottom wall of the terminal box.

It is desirable to make the elements so that they can be removed and replaced as mechanical units for repair in a servicing shop. The maximum to be desired in this respect would be to have separate interchangeable watertight elements with terminals that could be readily passed into the terminal box through convenient water seals. If the elements were to be housed in a single rubber boot, as they are in nearly all of the present transducers, then it would still be desirable to make them removable and replaceable as independent mechanical units. The interchangeability

of elements of a given type of transducer would be very convenient. Such interchangeability, however, would have to be based even more on uniformity of frequency and impedance than on uniformity of mechanical dimensions.

*Stability of Permanent Magnets.* It is assumed that no future models of magnetostriction scanning sonar transducers will be polarized by the use of direct current in the windings. While the present models employing permanent magnet polarization are satisfactory up to fairly high-power levels ( $5 \times 10^6$  dynes per sq cm sound pressure at the active faces) it is desired to operate underwater sound gear at still higher levels. There are three ways of increasing the power output of magnetostriction transducers for ultra-high-power use. First, with no auxiliary polarization at all, it is possible to drive the elements with a current whose frequency is half that of resonance of the stacks. While this solution is a very practical one for transmitting at very high-power levels, it complicates the process of receiving. Second, magnets might be found that are more difficult to depolarize than those now in use. Such magnets would have greater coercive force than those now employed, or would have greater dimensions in the direction of magnetization. This method would require redesign of the present laminations and would in general result in lower electromechanical coupling coefficients. Higher mechanical  $Q$ 's would have to be used to get the same efficiency, unless the core losses were reduced by using thinner laminations. Third, the laminations could be reshaped to give much higher  $Q$  and the use of thinner laminations would reduce core losses. Both of these modifications would increase the efficiency. Ultimately, however, the acoustic power that can be obtained from a magnetostriction transducer is limited by magnetic saturation and magnetic hysteresis losses in the magnetostrictive material.

*Stability of Impedance and Efficiency.* The efficient and satisfactory operation of a sonar system depends to a considerable extent upon proper impedance matching between the transducer and the associated electronic circuits. To maintain good impedance matching, it is usually necessary to maintain the impedances of circuits and of the transducer at stable values regardless of temperature, change in frequency, or aging.

In X-cut Rochelle salt crystals there is notably poor stability of impedance with temperature variation. Y-cut Rochelle salt, and more particularly ammo-

CONFIDENTIAL

nium dihydrogen phosphate [ADP] crystals, are considerably better in this respect and for this reason, in spite of the fact that their electromechanical coupling coefficient is only about half as great, are being used increasingly in place of X-cut Rochelle salt crystals. Of these two crystal materials, ADP is preferred because it does not dehydrate at temperatures below 300 F, whereas, Rochelle salt begins to dehydrate at about 110 F. The impedance of magnetostriction transducers changes very little with temperature.

Variation of impedance with frequency is most pronounced in transducers which have high efficiency and are sharply resonant. Thus, a change in the operating frequency of such a transducer introduces mismatch of impedances and consequent loss in overall efficiency. As a result, in practical systems it is often desirable to use a transducer with a relatively low mechanical  $Q$  even though its efficiency is not so great as the peak efficiency of a more sharply resonant one. One line of research to be continued in scanning sonar transducers should be the development of units which have lower mechanical  $Q$ 's than present units while maintaining the same efficiency.

Another method of solving the problem of variation of transducer impedance is to include in the circuit an automatic tuning or compensating network. Several such compensating networks are known but very little work has been done toward applying them to transducer circuits. For practical shipboard use, however, this solution is definitely less desirable than making the impedance variation in the transducer so small that further compensation is unnecessary.

*Simplicity of Design.* In developing a complete underwater sound system there is always the temptation to add such a multiplicity of accessories for the purpose of obtaining information that all the gear is seldom in good working order at any one time. The most troublesome complications arise when one component is used to serve two or more purposes; in such a case the failure of one part of the system may cripple the other unless further components are introduced to prevent such an occurrence. It is good practice, in designing a system that must be highly reliable, to separate the functions of the important parts so that each operates independently. This is particularly true of the mechanical components.

An example may be cited in the design of the transducer portion of the integrated Type B sonar in which the horizontal-scanning transducer and the depth-scanning transducer are mounted on the same

shaft. The depth-scanning transducer is attached to the bottom of the horizontal-scanning transducer and the cables from the first pass up through the core of the second through appropriate water seals. Ordinarily the horizontal-scanning transducer does not have to be rotated about the vertical axis, whereas the depth-scanning unit does. A simple arrangement is obtained by rotating both transducers and compensating for the rotation of the horizontal-scanning unit by appropriate phase shifting in the indicator and control circuits. Both transducers are housed in one large dome. The chief advantages of this complex combination are (1) that one transducer does not shade the other acoustically, (2) that only one supporting shaft is needed, and (3) that only one dome is needed. Some of the disadvantages are (1) that the rotation of the horizontal-scanning transducer is unnecessary and undesirable as far as its particular function is concerned; (2) that the passing of the cables from the lower transducer through the upper one and the support of the lower transducer by the upper one introduces undesirable complications in the mechanical assembly and the water seals; (3) that troublesome acoustical reflections are produced by the broad bottom cap of the upper transducer; and (4) that the unusually large dome requires extra-heavy internal structural reinforcement which not only causes acoustic interference but is vulnerable to damage because of the great distance it extends below the hull.

The reliability and the simplicity of the above system could be increased by separating the transducers so that the action of each one is independent of the other. They should preferably be housed in separate smaller domes far enough apart so that no appreciable acoustic interference is produced. Perhaps the preferred position of the depth-scanning transducer would be a considerable distance behind the horizontal-scanning transducer where it would interfere least with the routine horizontal searching. The two smaller domes would have less internal framework than the single large dome would have to interfere with the transmission of sound.

#### MANUFACTURABILITY

*Acoustical and Electrical Tolerances.* The perfection of the acoustical patterns formed by a scanning sonar system depends upon the uniformity of the elements of the electrical beam-forming network and the uniformity of the transducer elements. To give acceptable patterns, deviations from the proper

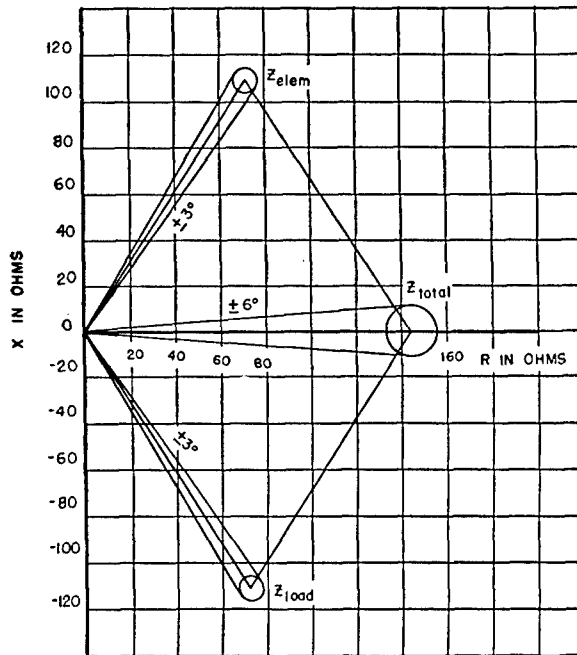


FIGURE 4. Impedance diagram for transducer elements, showing effects of variations.

phases and amplitudes of the signals from the various elements must fall within certain limits, dependent upon fundamental operational performance requirements. In the manufacture of transducers it is desired that the tolerance range of the sensitivities of the various elements be limited to  $\pm 1$  db of the average when they are terminated in their complex conjugate impedances. It is also desirable that the variation in the phases of the generated voltages across the conjugate impedance loads on the elements be not more than  $\pm 10$  degrees when the elements are excited by the same sound wave (in phase on all elements). This latter requirement means that the sum of the phase variations, which arise from variations of natural mechanical frequency and variations in electrical impedance of the elements, must be less than  $\pm 15$  degrees.

Figure 4 shows the effect on total impedance caused by variations in element and load impedance. In the circuit consisting of the element and load in series the voltage drop across the load is:

$$V = IZ_{(\text{load})} = E \cdot \frac{Z_{(\text{load})}}{Z_{(\text{total})}} \quad (1)$$

The phase of  $E$  (generated voltage) may vary  $\pm 6$  degrees because of variation in the frequencies of reso-

nance of the various elements. The phase angle of  $Z_{\text{load}}$  may vary as much as  $\pm 3$  degrees even when the components of the beam-forming network are carefully selected. The variation of the phase angle of  $Z_{\text{total}}$  is  $\pm 6$  degrees. (See Figure 4.) All of these variations when added together give a total possible phase variation of  $\pm 15$  degrees which means a total spread of 30 degrees. In optics or acoustics a change of phase of at least 45 degrees is usually considered necessary to bring about any appreciable change in diffraction pattern so that the 30 degrees mentioned above is a reasonably safe tolerance. The phase variation due to the dispersion of the frequencies of resonance of the elements is given in degrees by

$$\Delta \phi \approx 114 Q \frac{\Delta f}{f_{\text{avg}}} \quad (2)$$

where  $Q$  is the usual measure of the sharpness of resonance and  $\Delta f$  is the deviation of the actual frequency of resonance from the average frequency of resonance of all the elements. If  $\Delta \phi$  is to be kept within the limits of  $\pm 6$  degrees suggested, then  $(Q\Delta f)/f_{\text{avg}}$  should be kept less than  $6/114$ .

Necessary tolerances with regard to sensitivity, frequency of resonance, and impedance of the elements are fairly severe when compared with ordinary manufacturing tolerances. That suitable elements of the magnetostrictive laminated-stack type can be manufactured has been demonstrated by the Sangamo Electric Company. The same is true of the Brush Development Company with respect to elements of the piezoelectric crystal type. It is more difficult to meet the impedance tolerances than the frequency-variation tolerances in the crystal type. The  $Q$  of most crystal units is of the order of 3 and consequently the frequency tolerances are not so severe as those for magnetostriction units, which have  $Q$ 's ranging upward from 8.

The dimensional tolerances on the frames, water seals, etc., of scanning sonar transducers are fairly close but easily within the ranges held to in routine precision machining. No difficulty should be experienced if the manufacturer fully realizes the importance of properly fitting parts and makes the effort to meet specifications.

**Cost, Rate of Production, Critical Materials.** The magnetostriction scanning sonar transducers of the laminated-stack type, completed at the time of this writing, cost about \$8,000 each. Of this amount about

\$1,200 was paid for the nickel strip from which the laminations were punched. It is believed that in routine production the cost of transducers of this type could be brought down to \$5,000 or \$6,000. The cost of the nickel used in a tube-and-plate type of magnetostriction transducer would be almost insignificant, but the many small parts and the time required to maintain the close dimensional tolerances increase the total cost of this type to a similar figure.

The cost of scanning sonar transducers of the crystal type made up to the time of this writing ranges upward from \$6,000. In production this could probably be lowered to around \$5,000. Since the growing and cutting of ADP crystals require a considerable investment in equipment, time, and skilled workers, it is not likely that this figure can be lowered by any great amount.

The rate of production of magnetostriction transducers of the laminated-stack type is determined mainly by the rate at which the laminations can be punched and treated. If several dies are used simultaneously, the laminations from the various dies would have to be kept separate for use in separate transducers unless it could be demonstrated that the different groups of laminations all fall within the same frequency tolerances. One good die can be resharpened and used to punch at least 25,000 laminations during an eight-hour day. Since an ordinary horizontal-scanning transducer requires about 65,000 laminations, one die can punch enough laminations in one week for approximately two transducers.

The rate of production of crystal transducers depends on the rate at which the crystals can be grown and processed. A crystal-growing plant with a capacity great enough to grow crystals for 1,000 transducers per year would be very large but well within the bounds of possibility.

None of the materials that go into the construction of transducers is used in large enough quantities to be critical. About 400 tons of nickel (if the scrap is returned) would be required to manufacture 1,000 transducers of the magnetostrictive laminated-stack type. The amount of ADP needed for crystals in 1,000 transducers could be readily made and purified by the chemical industry, but growing the crystals might slow production.

*Testing Facilities.* Many routine tests should be made during the manufacture of the various parts of a transducer. These tests and the facilities necessary for their performance are discussed elsewhere.<sup>1</sup> Fu-

ture work in the field should be directed toward refining techniques for the purpose of securing more accurate and reliable data.

#### CABLES FOR SCANNING SONAR TRANSDUCERS

In most scanning sonar systems the scanning commutator is located inside the ship. This necessitates running wires from each element of the transducer to the commutator chassis, a distance usually measuring from 40 to 50 feet. In order to minimize electromagnetic and electric pickup, as well as cross talk in these long wires, it is good practice to use two conductors in the form of a twisted pair from each element. In cases where three or more leads are brought from each transducer element, the leads should be run in the cable as a twisted multiplet. When the lead wires are run in the cable either as twisted pairs or multiplets, there is no need of a common electric shield around the whole cable. The conductors forming the cable should be color-coded to facilitate identification.

The bundle of wires forming the cable should be surrounded by a watertight sheath. It is also desirable for the complete cable to be as flexible as possible to bending and twisting deformations, especially in installations where the transducer must be trained by the rotation of the transducer shaft. Stiff cables and cables with solid wire conductors fail quickly when mechanical rotation is required. The insulation on the individual conductors should be designed to avoid abrasion against adjacent conductors, possibly by use of certain waxy lubricants. If the cable is to be flexible the sheath should not bind the conductors together too compactly, and the core should be of such pliable material as hemp or jute. For installations in which the transducer must be rotated, a cable ten feet in length should be able to withstand, during continuous duty, torsional rotation of 360 degrees or more in both directions.

In addition to being as flexible as possible, the cable must have the nearly incompatible property of being impervious to the passage of water along its length. Cables of this type are known commercially as "blocked" cables. Blocking is usually accomplished by vulcanizing the conductors in a solid rubber-like matrix, although this makes a very stiff cable. It may also be accomplished by filling the spaces between conductors with certain waxy resins or with a granulated material which swells quickly to a large volume when water comes in contact with it.

Satisfactory cables should also have the following specific characteristics:

1. Resistance not greater than 10 ohms per 1,000 feet.
2. Insulation between any pair of wires, at least 10 megohms per 1,000 feet.
3. Capacitance between any two wires in a multiplet, not greater than 50  $\mu\text{mf}$  per foot; capacitance between any two wires in different multiplets, not greater than 30  $\mu\text{mf}$  per foot.
4. Cross talk between any two properly terminated twisted pairs less than -50 db.
5. Insulation strength, 1,000 volts; insulation of reasonably low dielectric hysteresis loss from 10 to 60 kc.
6. Sheath: watertight, tough, flexible, abrasion-resistant, fire-resistant, resistant to action of grease, oil, salt water, air, and sunlight; little tendency to cold flow when put under pressure by a gasket seal.
7. Stability of properties over temperature range from 20 to 170 F.
8. Ability to withstand external pressures up to 1,000 psi.

Among the commercial multiconductor cables which partially satisfy the above requirements is a Navy-approved armored telephone cable with the wires made up into twisted pairs [TTHFA]. It satisfies most of the specifications given above except that the individual conductors are made of solid wire and the assembly is too stiff. Such a cable is reasonably satisfactory for installations in which the transducer is not rotated in any way, but unsatisfactory if the transducer is to be rotated.

There are no other standard commercial cables that meet as many of the requirements for scanning sonar transducers as the TTHFA telephone cable mentioned above. It is recommended that prospective manufacturers of scanning sonar transducers enlist the aid of electrical cable companies to manufacture cable to meet the special requirements specified. For example, the Collyer Wire and Cable Company of Providence, Rhode Island, has made some special cable for HUSL which meets most of the specifications with reasonable satisfaction.

#### PATTERNS

*Vertical Patterns of Horizontal Scanning Transducers.* The type of vertical pattern most desirable for horizontal scanning depends upon a variety of factors including range and depth of the target, depth

of the water, roughness of the sea, roll and pitch of the ship, and thermal gradient in the water.

So far all but one of the horizontal scanning transducers of this project have been made with elements that are five to seven wavelengths long, with uniform amplitude from top to bottom. The single exception was the HP-3, which was equipped with three wires to each element to allow amplitude ratios of 0:1:1:0 or  $1/2:1:1:1/2$  on the four stacks of each element. This transducer has not yet been tried on shipboard so that no comparison can be made of the advantages and disadvantages of the different types of vertical patterns. However, it is expected that each transducer should be capable of giving a sharp vertical pattern for routine, long-range azimuthal search, and a very broad vertical pattern for use in maintaining contact with close deep targets. The HP-3 transducer is being modified to have a pair of lead wires from each of the four stacks of all 48 elements (192 pairs), and shipboard experiments will be conducted using all the reasonable combinations of amplitude and phasing. These tests should give fairly definite information about the most practical vertical patterns to use for different search conditions.

*Shading.* When the elements of a horizontal scanning transducer are operated at the same amplitude throughout their entire length, the first three pairs of minor lobes of the vertical pattern are only about 11 to 15 db below the major lobes. If the elements are divided into sections with inactive spaces between the active sections, the first three pairs of minor lobes are from 9 to 13 db below the major lobe if the sections are operated at the same amplitude. However, by shading, that is, by operating the sections at different amplitudes, the heights of the minor lobes relative to the major lobe, and the width of the major lobe, can be modified. The general theory of patterns<sup>1</sup> indicates that, if the centers of the active sections of the elements are spaced more than one wavelength apart, it is impossible to reduce the heights of minor lobes below the value they would have in the pattern of a single segment at the same angles. Moreover, inactive spaces between sections of an element make the minor lobes higher. Consequently, to get effective lobe reduction in the vertical pattern by amplitude shading and phasing, it is necessary to break the elements into sections which are less than one wavelength long and to have as little inactive space as possible between sections.

It should be recognized, however, that there is still

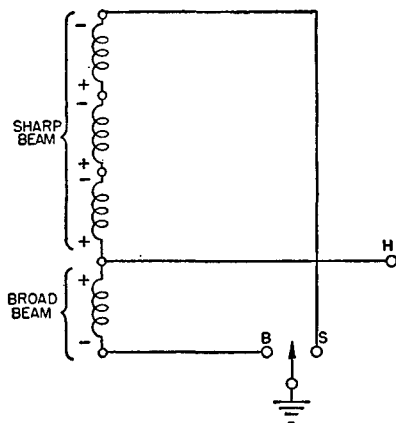


FIGURE 5. A proposed wiring diagram for a single element of a transducer to be used for sharp beam and broad beam operation.

some question as to whether or not minor lobe reduction in the vertical pattern is desirable in any case. It can be shown that the directivity index (that is, ratio of the average intensity over the whole sphere surrounding the transducer to the intensity on the main beam) is a minimum when the elements operate at full amplitude over their entire length. Now the satisfactory performance of an echo-ranging system depends largely on the signal-to-noise ratio, where the acoustical noise consists of reverberation and the noise generated in the water by the ship. This ratio should be as large as possible, which means the directivity index should be low. There are special cases, however, in which the bottom or water conditions make high side lobes undesirable even though the pattern has minimum directivity. The most satisfactory answer can only be obtained by shipboard tests made under actual echo-ranging conditions.

*Separate Layers of Elements for Regular Search and MCC.* One convenient way of getting a relatively sharp vertical beam for regular search purposes and a very broad beam for *maintenance of close contact* [MCC] is to divide each element into two sections; a long section for the sharp beam and a short section for the broad beam. The connections are as shown in Figure 5 where the common terminal *H* is used for either system. Sharp beam operation is obtained by throwing the grounding switch to the *S* contact and the broad beam operation by switching to the *B* contact. The approximate patterns that would be obtained with these two sets of connections are shown in Figure 6. These two patterns satisfy the requirements quite well, although it might be somewhat

better if the main lobe of the broad pattern were directed farther downward. This, however, would require either mechanically tilting the lower ring of stacks, or breaking the lower ring of stacks into sub-segments which could then be phased with respect to each other. It is doubtful whether the improvement in performance would justify this additional complication.

It has been suggested that by phase reversal a two-lobed difference pattern could be obtained that would provide a reasonably good MCC feature. The better of the other possible combinations should be tried on shipboard so that the best can be selected on an experimental basis.

#### HORIZONTAL PATTERNS

*Transmitting Patterns.* Most scanning sonar systems utilize a transmitting pattern which is uniform ( $\pm 1$  db) in all directions in the plane perpendicular to the axis of the transducer.

There are a few special cases in scanning sonar systems in which it may be desirable to transmit sound power into the water in preferred directions. For these, a limited amount of directionality can be obtained by energizing only a group of neighboring elements. It has been shown theoretically<sup>2</sup> and experimentally<sup>3</sup> that for conventional scanning sonar transducers the patterns produced by active sectors of less than 30 degrees are very similar to those set up by flat-faced transducers of equal extent. For sectors greater than 40 degrees the angular width of the patterns increases linearly with the angular extent of the sectors and is independent of any other factors. The minimum pattern width is then obtained with a 40-degree sector.

If it should be desired to transmit sound in a sharp beam with greatly reduced side lobes, phasing and amplitude shading would have to be introduced just as it is in the formation of a sharp receiving beam. At the present stage of development the insertion and removal of such a transmitting network before and after pinging would involve some complicated switching, but it might be that if more attention were given to the problem a reasonably simple and practical switching system could be devised.

*Receiving Patterns.* The ideal receiving pattern would consist of a sharp main lobe with no side or back lobes. To approximate such a pattern, it is necessary for all parts of the beam-forming system to be designed correctly and to operate accurately within

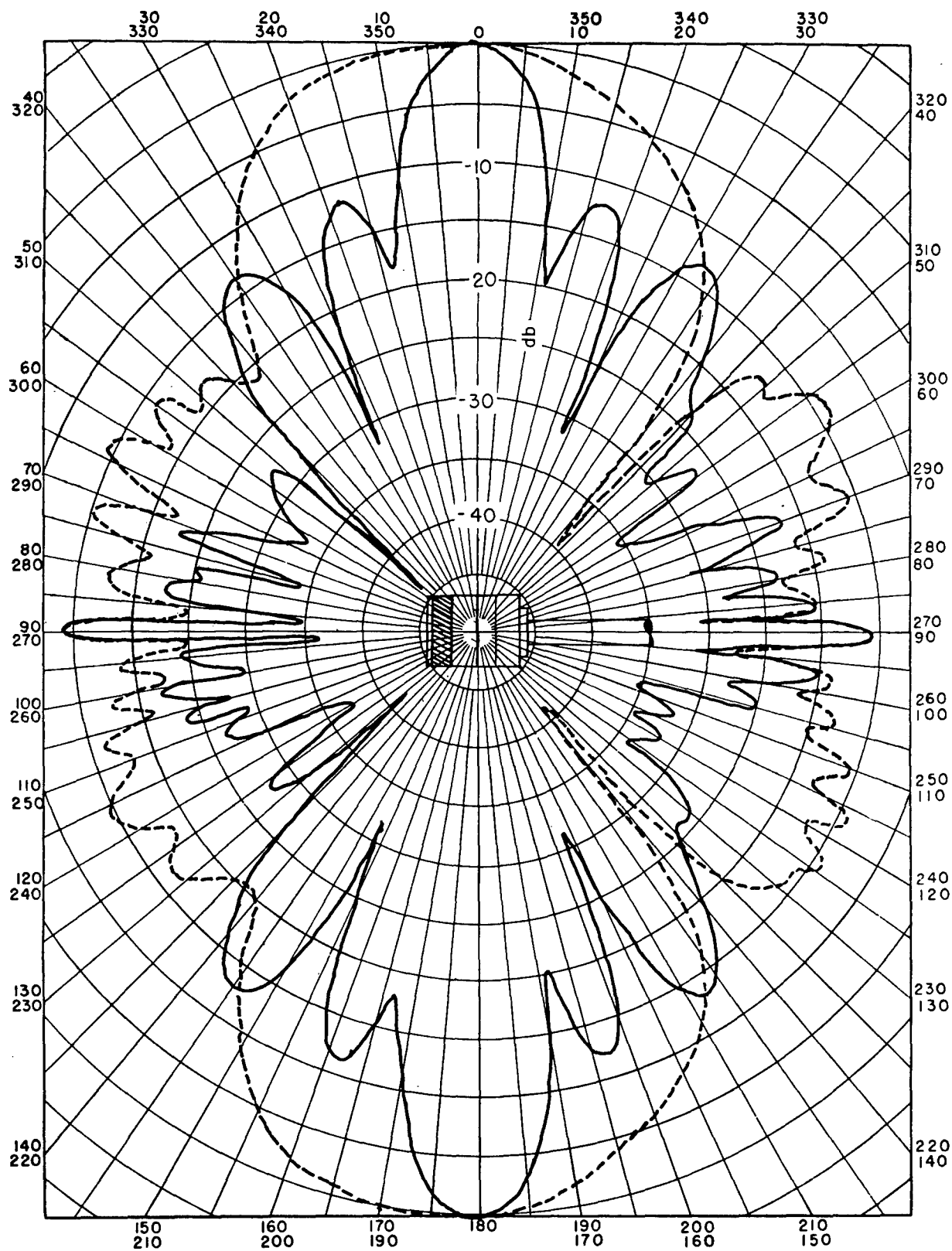


FIGURE 6. Approximate sharp and broad vertical patterns from a transducer connected as shown in Figure 5.

CONFIDENTIAL

very close tolerances. The tolerances on the transducer components have already been discussed in a previous section. The most promising place for improvement in pattern formation is in the beam-forming networks where many arrangements of different numbers of elements and of phasing and shading schemes remain to be tried. It would help the designer and builder of transducers if beam-forming networks could be devised that would give satisfactory patterns from transducer elements with a width of  $\frac{3}{4}$  wavelength or more, instead of the present narrow width of  $\frac{1}{2}$  wavelength.

#### FREQUENCY RESPONSE, IMPEDANCE, EFFICIENCY

*Mechanical Q.* Ideally, frequency response for a scanning sonar transducer would be uniform over the entire frequency range for which the system gave satisfactory patterns. This would make it possible to change the frequency of operation to the most favorable value when desirable. For example, when two or more ships operate as a search team within range of each other, to avoid interference, it would be of considerable help to be able to change frequency easily. If, however, the transducer has a sharp mechanical resonance it cannot be operated far from the frequency of resonance without the system becoming inefficient.

X-cut Rochelle salt crystals are capable of giving a uniform frequency response and efficiency over a relatively wide frequency range because of their high electromechanical coupling coefficient (0.6) and because their specific acoustic resistance is more nearly that of water than is the resistance of most of the metals, including nickel. It has already been pointed out, however, that these crystals are not entirely practical because of their vulnerability to high temperatures and their variation of impedance with temperature. ADP crystals have a lower electromechanical coupling coefficient (0.3) and, consequently, to give the same efficiency, must be operated at higher mechanical  $Q$ 's than X-cut Rochelle salt crystals. On the other hand, the ADP crystal units have a much lower rate of change of impedance with temperature and are much more stable at high temperatures. Transducers using ADP crystals may be made to operate with reasonable efficiency at  $Q$ 's as low as 3 or 4, while it is very difficult to make magnetostriction transducers with  $Q$ 's lower than 6 or 8 and still retain satisfactory efficiencies.

#### EFFICIENCY VERSUS $Q$

The designer of scanning sonar transducers must always strive toward the highest possible efficiency since present scanning systems require more than 1 kw of sound power in the water during pings and the trend is toward still higher powers. It was pointed out earlier in this report that it is not the best practice to go to higher  $Q$ 's simply to achieve high efficiency. It is obvious that a compromise must be made between high efficiency and low  $Q$  if the electromechanical coupling coefficient is low (that is, from 0.15 to 0.3). A detailed discussion of the design problem is given elsewhere.<sup>1</sup>

#### IMPEDANCE VERSUS FREQUENCY

The most common generators of the electronic type used to provide power for scanning sonar transducers are designed to operate into a load resistance that is constant with frequency. Consequently, if a transducer is to act as an ideal load, its impedance as seen by the generator should be resistive and constant. Unfortunately, both the resistance and reactance of transducers of the magnetostrictive or piezoelectric types vary with the frequency, and the higher the mechanical  $Q$  the greater is the rate of variation. This is one of the reasons that a transducer with a broad mechanical resonance is more desirable than one with a sharp resonance.

When the impedance of a transducer has a fairly large reactive component it may be rendered resistive at the frequency of resonance by electrical tuning. Several types of networks have been worked out for tuning, but much further development and improvement are indicated. One line of investigation is the use of automatic tuning networks or mechanisms which operate to keep the transducer network automatically tuned to the proper resistance to match the power source.

#### DOMES

An ideal dome should have the following characteristics:

1. The streamlined surface should be shaped so that no cavitation takes place at the highest ship speed at which the sonar gear is to operate.
2. The walls and supporting structure of the dome should produce no effect on the incoming or outgoing sound.
3. The dome structure should be strong enough to withstand any of the hydrodynamic forces it may en-

CONFIDENTIAL



counter in rough seas, and to withstand impacts with such underwater debris as is occasionally encountered around ports and harbors.

The domes, which consist of steel framework with a thin (0.050-inch) "skin" of stainless steel, have proved moderately satisfactory for sharp-beam echo-ranging gear of the QC type. The few experiments that have been made with scanning transducers mounted in domes of this type indicate that they may also be satisfactory for scanning sonar use. Some improvement could be made by decreasing the size and mass of the supporting framework through the use of stronger and more corrosion-resistant materials. It may also be possible to develop a skin of reinforced  $\rho$ c rubber with greater mechanical strength and greater sound transparency than the stainless steel skin mentioned above. The Naval Research Laboratory [NRL] in Washington, D. C., is working on this development.

Another type of dome, which seems to offer interesting possibilities, is a dome made of a thick, flat piece of molded  $\rho$ c rubber of oval shape and fastened securely at its boundary to the hull of the ship or the bottom of the sea chest. Before the transducer is lowered below the hull level, the rubber dome would be inflated by pumping water into it under pressure. An arrangement of this kind would provide a streamlined dome that is rigid and entirely free of objectionable metal framework or skin. In such a dome the transducer would, in effect, be in free water. It would also have the advantage of being highly resilient and able to withstand considerable impact without damage to itself or the transducer. Still another advantage is that the water (or liquid) between the transducer and the dome would be under a pressure of several atmospheres and there would be less danger of cavitation at the active face of the transducer at very high power levels of sound transmission. There would also be considerably less trouble than at present is caused by air coming out of solution with increase in temperature, and collecting on the transducer and dome walls.

There are many other dome designs and arrangements that should receive some consideration including combined forms of the stainless steel skin and reinforced rubber skin and combined forms of retractable domes of the British type with a rubber blister bottom. Domes molded from some of the plastic materials such as those used in airplane wings and bodies also should be investigated.

## 10.2

## CR PATTERN FORMATION

Although the capacitive commutator has been developed to the stage of practical use, there is still considerable room for improving beam-forming and beam-rotating devices. In general, future work should be directed toward:

1. Modifying the method of commutation to give greater simplification of assembly and more desirable electrical characteristics.
2. Improving the method of conducting the signal or signals out of the commutator so that the electric noise level is reduced.
3. Increasing the scanning speed.
4. Reducing the signal loss in the electric circuits associated with the commutator.
5. Securing better beam patterns.

The first three items present both mechanical and electrical design problems. The last two items mainly concern the electrical design of the beam-forming lag line and the method of introducing the echo signal into the line. The following proposals are offered for examination with the idea that they may accomplish the above objectives. They concern chiefly improvement of the capacitive type of commutator, although some are applicable also to the inductive type.

### 10.2.1 Smooth Rotation of Beam Pattern

In all commutators made so far, the commutator plates have been made identical, each having its capacitor segments uniformly patterned along radial lines in the case of the flat plate design, and along axial lines in the case of the cylindrical plate design. With this arrangement, there are objectionable pattern changes as the capacitor segments move from the in-register position to the inter-register position. The major lobe is somewhat distorted, widened, and decreased in amplitude. Moreover, the minor lobes in certain regions of the pattern are increased.

It is suggested that in order to eliminate such variations the capacitor segments on one of the plates be skewed in a manner similar to that shown in Figure 7. With such an arrangement there should be smoother phase changes in the signals fed to the beam-forming network and, hence, smoother rotation of the beam pattern.

An alternative proposal for securing smoother beam rotation is to subdivide the rotor plates into twice as many capacitor segments as there are on the

stator, thereby providing twice as many signal voltages which may be fed into the lag line<sup>4</sup> as described in Chapter 9.

The first proposal necessitates greater care in shaping the capacitor segments on the skewed plate, whereas the second involves more line feed-in points, which in turn means more resistors, etc. However, an experimental investigation of these suggestions is desirable in order to determine their respective merits.

### 10.2.2 Oil-Filled Listening Commutators

One disadvantage of the capacitive commutator is that a very small air gap (0.0035 inch) is necessary to provide a sufficiently high capacitance between segments. In the manually trained listening commutator this somewhat stringent requirement might be eased by immersing the commutator plate in a suitable oil whose dielectric constant is several times that of air. For example, the dielectric constant of castor oil is 5.6 and that of Transil oil is 2.1, so that with the same segment area the spacing might be increased several times without decreasing the commutator capacitance. This would permit relaxing the requirements for machining and assembly tolerance. The above proposal is not suitable for the high-speed scanning unit. In general, the loss of uniformity of the scanning and listening commutator parts, and the complications inherent in making the assembly liquid-tight, would probably outweigh the advantage of slightly more space between plates in the listening commutator unit.

### 10.2.3 Multi-Scan Commutator for High-Speed Scanning

The scanning speed in CR scanning systems is 30 rps, limiting the transmitted signal pulse length to a minimum value of about 35 milliseconds. Since the signal-to-reverberation ratio and the range resolution are increased as the ping length is decreased, it is very desirable that higher scanning speeds be obtained. Since doubling the rotational speed allows the ping length to be halved, a study of the possibilities of designing a commutator to rotate at 3,600 rpm should be made.

The following method of doubling the scanning speed without increasing the rotational speed is possible. Let the stator and rotor plates of the scanning

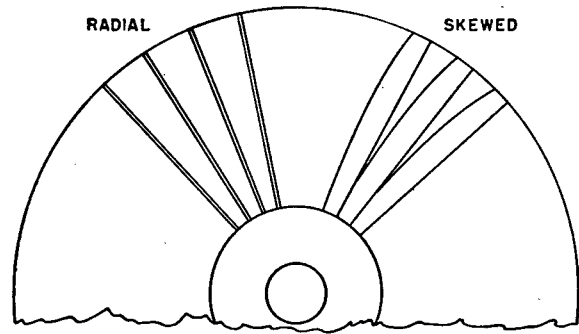


FIGURE 7. Skewed sector commutator plate.

commutator be built to have twice as many capacitor segments as there are staves around the transducer. With a 48-stave transducer, for example, the commutator plates would each have 96 segments. If one group of 48 stator segments, subtending an arc of 180 degrees, is then connected in parallel with the other group and to the transducer, the sound horizon is scanned twice during each revolution of the commutator rotor. To keep the high potential leads to the stator segments as short as possible, a transformer should probably be used for each stator segment, with the two groups paralleled in their low impedance primary sides. In the rotor, only one set of active segments would need to be used, although two sets would be required for maximum utilization of the received energy.

Doubling the rotational speed and at the same time using a multistator design would increase the scanning speed to 120 rps which would allow the use of a 9-millisecond ping length. Although both mechanical and electrical problems become more acute in a design of this kind, it is believed that such a commutator is practical and might materially improve the small-target detecting qualities of the CR scanning system. Inductive rather than capacitive coupling could also be adapted to such multiple scanning, in which case the possibility of operating all circuits at low impedance would be advantageous. Inductive commutators of this kind are discussed in a later section of this chapter.

### 10.2.4

### Tolerances

The principal factor determining the size of the air gap between the stators and the rotor is the total capacitance required in the circuit. The practical minimum capacitance between each stator and rotor

segment is about 100  $\mu\text{f}$ . However, it is desirable to have the value as high as possible since a high capacitance keeps the commutator reactance low and allows the impedance of the lag line input circuits to be kept at a minimum. Obviously if a fixed capacitance between each rotor and stator segment is to be maintained, any increase in the size of the air gap must be accompanied by a proportionate increase in the area of the capacitor segments. Although an air gap greater than that used at present would be desirable because the requirements on uniformity would then be less strict, as long as insulating plates are used, it is probable that rotors with diameters of 11 to 12 inches are about as large as are feasible. Even if metal plates were used it would be desirable to keep the size down.

A practical way of increasing the available area is to increase the number of plates and then connect them in parallel with the rotor between two stators, as was done in both the Model 1 and Model 1B commutators. This method has the additional advantage of compensating for any "wobble" of the rotating plate because, if the rotor plates are parallel, an increase of capacitance on one side is accompanied by a corresponding decrease on the other side. The commutators built to such a design are difficult to manufacture and assemble. It is doubtful if stators and rotors could be made identical, using three or more insulating plates. If metallic plates are used and fabricated as described in this chapter, the advantage in having them identical would no longer be so great, and a design utilizing three or more plates could be developed which would allow a simple assembly.

#### 10.2.5 Multiple Plate Commutator

The following brief discussion describes one possible way of simplifying the assembly of a multiple plate commutator. An outstanding defect in all the designs considered so far is that all electrical connections to the segments have to be made after assembly and alignment of the plates. The connections from the rotor segments to the lag line, where the latter is on the rotor, are particularly difficult to reach, since they have to be made through a large hole in the center of a stator. The Model 1B commutator utilized banana plugs that attached to each section of the lag line and were plugged into holes in the rotor. These connections should be more positively made for production models. The wiring problem would be considerably simplified if the lag line and rotor could be

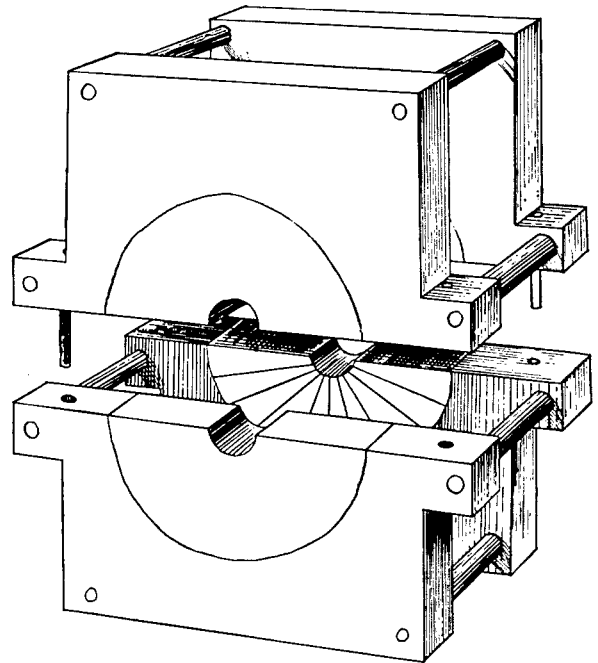


FIGURE 8. Split stator plate arrangements.

mounted on the shaft and the wiring done before the end plates and stators are assembled. The most obvious way of making this possible would be to split the stators in the center so that they could be added to the assembly last, a procedure which does not seem practical as long as insulating materials are used for the plates. It would be feasible, however, if metal-based plates were used. Such an arrangement is shown in Figure 8. During manufacture the stator base plates could be pinned together, the segments added, and the plates ground and finished as units. They could then be separated for assembly and as many plates as desired could be stacked up and fastened together to form the multiple stator. The stator plates would be separated by spacers equal to the thickness of the rotor plates plus twice the air gap desired. In previous models it has been difficult to connect the stator segments in parallel after assembly of the entire commutator, but with the stack described above these connections could be made before adding stators to the rotor assembly.

#### 10.2.6

#### Plate Materials

All commutators that have been built so far have been subject to the basic limitation that the insulating material is also the structural supporting mem-

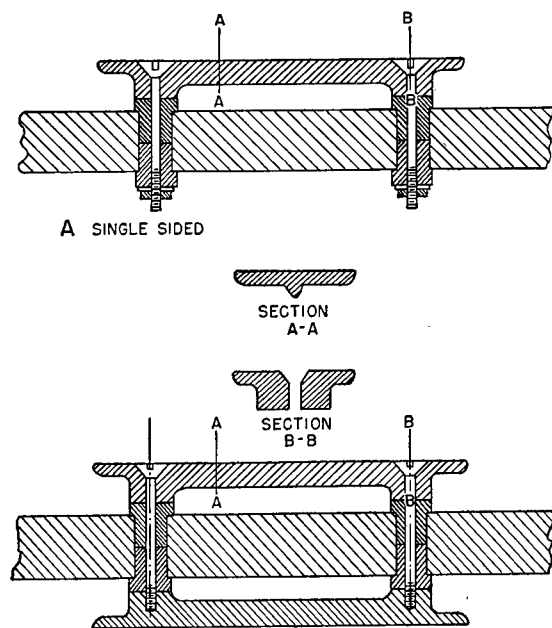


FIGURE 9. Composite capacitive commutator plate arrangements.

ber. The work that has already been done is described fully in Chapter 5, where it is suggested that, if the same method is to be used in future, the possibility of using a ceramic such as Alsimag instead of glass should be investigated further.

It is also suggested in Chapter 5 that any future study should include composite structures in which the separate functions of insulation and structural support are performed in each case by the most suitable material. The use of a heavy metal plate with metal segments attached to it through insulating bushings was considered for the first commutator design but was discarded because of its complexity. However, in production this method might prove quite practical. For example, the segments could be die-cast, molded, or possibly forged accurately enough so that only slight surface grinding would be necessary after assembly. Insulators could be molded and provisions could be included for locating them on the main plate and for locating the segments on them. In addition, provision for making electrical connection to each segment could be included in the die. The main plate to which these segments were to be attached could be of aluminum thick enough to remain flat. It would be considerably easier to mount such a plate and maintain alignment than it is with the insulating plates now being used. Sketches of possible composite arrangements are shown in Figure 9.

## 10.2.7

## Inductive Commutator

Early in the research program on electromechanical beam-rotating devices, an inductive type of commutator was proposed and partially designed. As originally planned, it was to have a number of transformers (as many as there were transducer staves) each having a stationary primary and movable secondary. Each secondary was to be mounted on a rotor located inside the primaries, with a small air gap between the magnetic cores. Each primary coil was to be connected to a transducer stave, with a certain number of secondary coils connected into the lag line. In the original design, the cores were to be built of laminated magnetic iron and clamped together in a brass supporting structure. However, owing to the difficulty of meeting the requirements of transformer design with the laminated materials then available, and to the rapid development of the capacitive commutator, an operating model of the inductive unit was never built.

It is strongly recommended that the possibilities of this type of commutator be re-examined. It seems probable that with the improved methods of molding and bonding dust core material now available, the requirements of transformer design can be readily met. Although the inductive commutator may be mechanically more complex in structure, nevertheless from the electrical point of view it has the following advantages:

1. No impedance-matching input transformers are needed since the stator coils themselves may be designed to match the transducer impedance.

2. The rotor coils may be wound to provide any desired transformation ratio to suit the lag line design, which may be of low impedance, and the signals may be introduced by series feed.

3. With series feed, the necessary attenuation of signal voltages can be secured by variation of the turns ratio between the rotor and stator coils, thus eliminating part of the resistor network now used in the capacitive commutator and requiring less space for the beam-forming lag line.

4. With low-impedance circuits, shielding, as well as avoidance of cross talk, becomes much less of a problem, and multiple-scan commutators become more practical. Mechanically, a much stronger structure can be built since the main stresses can be taken by metallic members. In this connection, Figure 10 illustrates a design which has rotating secondaries

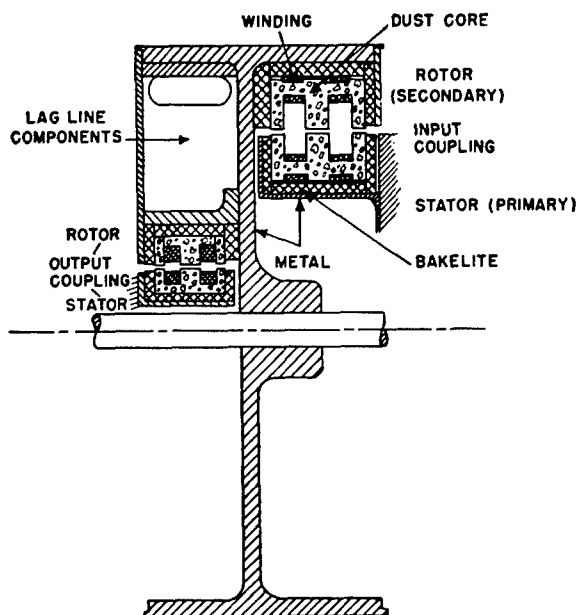


FIGURE 10. Suggested design for inductive commutator for CR scanning sonar.

outside of the stationary primaries so that they would be subject only to compressive stresses.<sup>5</sup> With greater structural strength higher rotation speeds could be realized, perhaps making feasible some of the schemes that have been proposed for short-ping CR sonar. Also larger air gaps might be satisfactory with consequent easing of machining tolerances.

#### 10.2.8 Capacitive and Inductive Output Rings

The contact type of slip ring has proved reasonably satisfactory for conducting lag line signals out of the commutator rotor. Electrical noise generated in the sliding contact has been kept fairly low by proper design and adjustment of brush pressure but is a limiting factor in determining the threshold sensitivity of the scanning sonar. Brush noise is likely to increase appreciably with time.

Two other types of pickup are possible, both of which have several advantages over the sliding contact. One of these, the capacitive ring output, was used with success in the earlier models of the scanning commutator. The second, which may be called the inductive output, has not been investigated to date. Both are free of the electric noise troubles that are inherent in the contact type of slip ring and have other advantages that justify further investigation.

For the capacitive output, a capacitance of around 500  $\mu\text{f}$  is desirable with a 10,000- to 15,000-ohm lag line. A significant difference between the commutating plates and the output rings is that the total capacitance is always used in the output, uniformity of the air gap not being important. Flat radial plates were found difficult to assemble and adjust and led to the adoption of slip ring output. It should be possible to design a capacitive output commutator whose assembly would not be unduly complicated. For example, the output rings could be made cylindrical and mounted to the rotor shaft in essentially the same way that the slip rings are now mounted. The stator could then be a complete cylinder slipped over the rotor, or two or more sections of a cylinder mounted independently and connected in parallel, as shown in Figure 11. An alternative arrangement would be to place the stators inside the rotor; such an arrangement would be well adapted to the Sangamo XQHA commutator design.

Where the capacitive ring is used, its capacitance may be utilized as a component of a band-pass filter between the rotor output and preamplifier, as shown in Figure 12. The chief disadvantage of this arrangement is that the filter characteristic is somewhat dependent on the ring air gap.

The capacitive ring output described above is not readily adaptable if a low-impedance lag line is used in the commutator. An inductive output arrangement on the other hand may be designed to match any desired lag line impedance. It also has the advantage over either the capacitive or sliding contact devices in that the two coils may be wound to provide any desired transformation ratio. A step-up ratio may be used to feed a closely adjacent preamplifier, or a low-impedance output may be provided so that the

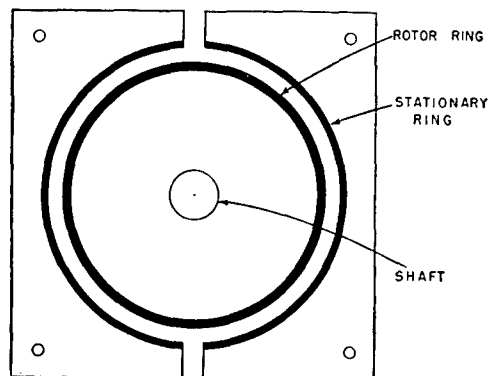


FIGURE 11. Split stator capacitive output ring.

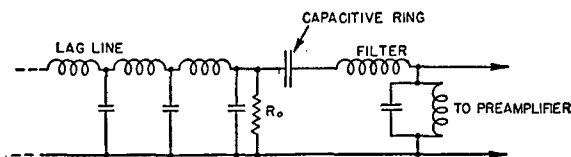


FIGURE 12. Output capacitive ring in filter arrangement.

signals are fed directly to a remotely placed receiver chassis. Furthermore, the secondary of the stationary coil can be ungrounded for a balanced output circuit. Only one ring, or its equivalent, would be needed for a single-channel output, and two where a two-channel output for BDI is needed. Several possible arrangements based on the use of molded dust cores are shown in Figure 13. At A is shown a radial gap design that has the feature of using identical cores for rotor and stator. At B is shown an axial gap design that is slightly more complicated, but which can be applied in dual-channel use, as shown at C. It also

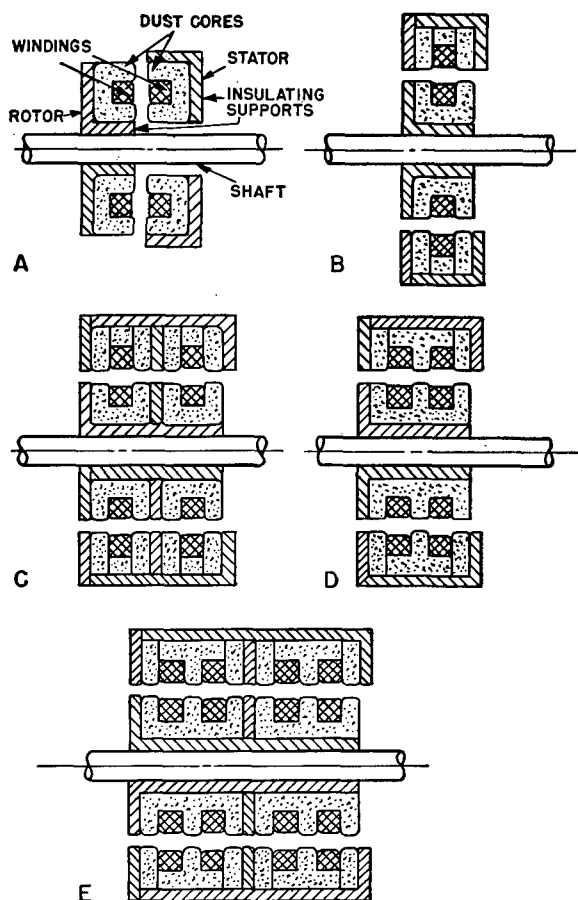


FIGURE 13. Inductive output arrangements.

lends itself to astatic winding, which may be necessary for reduction of hum pickup, as shown at D. Such an arrangement for dual-channel outputs is shown at E. The space between rotors and stators would be determined by the amount of leakage inductance that could be tolerated; a reasonable value is 0.005 inch. It should be pointed out that the leakage inductance could be employed as a component of a band-pass filter in the same manner as the capacitance of the capacitive ring output.

### 10.2.9 Double Lag Line Output Coupling Techniques

In past commutator designs where two singly fed lag lines were used, and one output channel was desired, the output leads were connected to the common junction of the lines as shown in Figure 14A. Where right and left output channels were desired, each line was resistance-terminated and the output signals were brought out directly to two separate preamplifiers.

It has been proposed that a transformer, or transformers, should be inserted at the output point, thereby obtaining a 5- to 10-db gain in the signal voltage

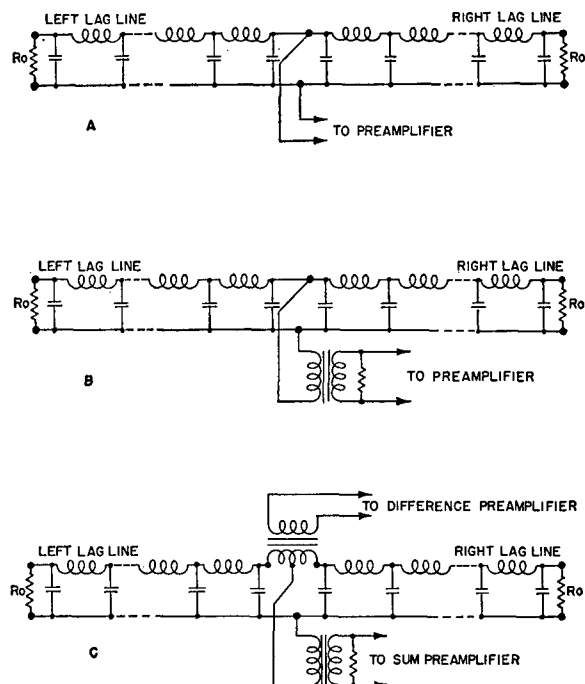


FIGURE 14. Methods of output coupling for one- and two-channel outputs.

on the grid of the preamplifier. Such an arrangement is shown at B in Figure 14 for a single-channel output. Where sum-and-difference outputs are desired from a double lag line commutator, transformer connections can be made as shown at C.

10.2.10

### Stationary Lag Line

One or two early models of the capacitive commutator were designed with stationary lag lines. To convey the signal from the active elements of the commutator rotor to the lag line, capacitive rings were used. This type of commutator design was quite satisfactory but was abandoned in favor of the mechanical simplicity achieved with a rotating lag line.

It now appears that commutator construction could be simplified considerably by having the lag line mounted outside the commutator, coupled to the commutating elements either inductively or capacitively. Certainly the manufacture of the lag line itself would be much easier if requirements of space and dynamic balancing were removed.

10.2.11

### Pattern Computer—Study of Phasing Tolerances

In developing the CR scanning technique, it has been apparent that a more exhaustive investigation of the beam formation was necessary than that which could be made during the emergency period. In lag line design the following problem is presented: Given a set of transducer signal voltages having certain amplitudes and mutual phase relationships, what are the amplitude and phase factors that must be incorporated into a beam-forming network to give the optimum pattern?

At present, the beam-forming lag line is designed to produce phase lags which approximate those that occur between signal voltages generated in the various staves of the cylindrical transducer. As far as phase relationships are concerned, the line merely compensates for the circularity of the transducer by making its directional sensitivity equivalent to that of a plane array of receiving elements. To aid in forming the desired beam, the signals from the staves on either side of the "head-on" point are further attenuated by a resistor network in the commutator. Actually, there is no assurance that the phase lags and attenuations now used in lag line design are necessarily those which gave *the best pattern* for a given number

of elements; nor is it known just how widely these factors may deviate from their theoretically correct values without materially affecting the beam pattern.

As far as is known there is no simple and direct theoretical approach to the above problem. However, a pattern computer has been proposed and designed as an experimental means of studying the problem of beam formation.

10.3

## ER PATTERN FORMATION

10.3.1

### Improvements in Present Methods of Electronic Switching

The greatest improvements in the *electronic rotation* [ER] sonar can be made in that portion of the system which forms and rotates the receiving pattern and by providing a listening channel. As described in Chapter 7, electronic rotation uses a beam-forming lead line with high-speed electronic switching elements to couple signals from desired positions to the receiving circuits. While the beam-forming abilities of such lead lines are now fairly well known (see Chapter 9), the switching elements have not thus far been entirely satisfactory in service. Copper oxide varistors have proved vulnerable to overload damage during transmission, and have been found to vary widely in transfer characteristics. Provision of protective devices (neon lamps) permitted mounting the commutator inside the transducer, thus eliminating the use of cables with large numbers of conductors, but recent developments in cable construction make this advantage of little importance. Once the pattern forming and rotating device is located inside the ship, instead of inside the transducer, the advantages of varistors over vacuum tubes as switching elements virtually disappear. Vacuum tubes are more uniform in transfer characteristics; they can be arranged to present less load to the lead line and to introduce less switching noise; and they are generally less vulnerable to damage from overload. The self-biasing circuit described in Chapter 7 seems desirable in order to ease amplitude tolerances on the switching line, and either diodes or multi-element tubes may be used.

Replacement of the separate switching elements with a single electronic unit seems very desirable, particularly if the unit is of a type in which physical motion of an electron beam accomplishes the switching and mixing functions. Such devices have been developed by the Western Electric Company<sup>6</sup> and the Fed-

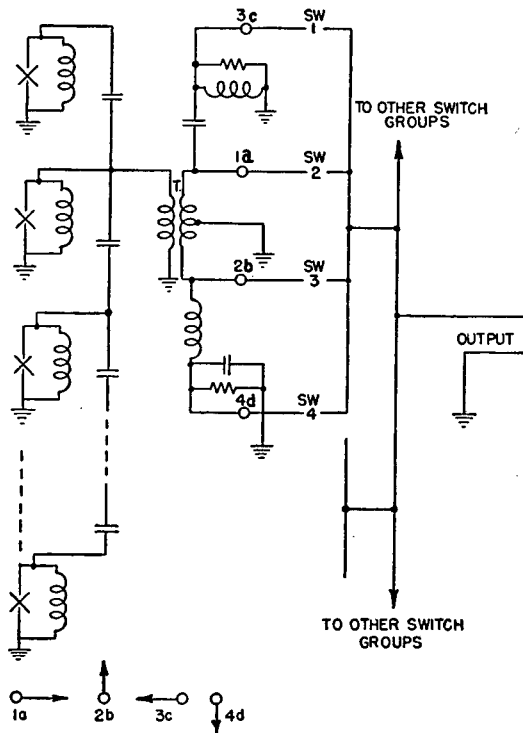


FIGURE 15. Complex vector switching arrangement.

eral Telephone and Radio Corporation<sup>7</sup> for multiplex communication purposes, and could probably be adapted for ER service. If the switching noise should prove too great at the signal levels obtained from the transducer, separate preamplifiers for each element or for each switching point might be necessary. They could conceivably be constructed as part of the switching device.

### 10.3.2 New Forms of ER Pattern Forming and Rotating Devices

With the present single lead-line arrangement, the pattern quality that can be obtained is distinctly limited by the design compromises necessary to obtain a uniform line, and the ER system is, therefore, at a distinct disadvantage when compared to the CR type. Improvement in ER pattern quality is much desired to afford better resolution and greater freedom from interference. The several directions of development which are possible include:

1. Phased switching.
2. Multiple-layer lead lines.
3. Preformed patterns.

In Chapter 9 it is pointed out that improved pat-

terns could be obtained if the signals from the points active at any instant were combined with appropriate phase changes, rather than directly combined as at present. Modifications of the present circuit to allow simply plus or minus control of phase seem reasonably easy,<sup>8</sup> and more exact control of phase (throughout 360 degrees) could be obtained with the arrangement shown in Figure 15. From each junction point of the lead line, the signal is taken to a phase-splitting and resolving circuit which delivers four-phase signals to four switching elements. Separate switching control potentials are applied to these elements from four switching lines, each of a form to give the desired overall transmission to the receiver.

Multiple-layer lead lines have been suggested as a means of avoiding, at least in part, the inherent limitations of the present single lead-line arrangement. The chief deterrent to their investigation has been the extreme difficulty of analyzing their behavior. At first glance, it seems possible that such lines could give much closer approximations to the required phase shifts and amplitudes than single-layer lead lines. For example, in the two-layer lead line shown in Figure 16, it would appear that signals from transducer elements near any particular point would, through the action of the transverse lag lines, be phase-advanced relatively less than those from more remote elements. The attenuation effects are not so easy to visualize, but it is believed that they too would be subject to control in the desired direction.

A scanning sonar using preformed patterns is already under development by the British Admiralty.<sup>9</sup> In such a system, as indicated in Figure 17, signals from each element are fed through separate bridging resistors into appropriate points on several lag lines. For a 48-element transducer, a maximum of perhaps

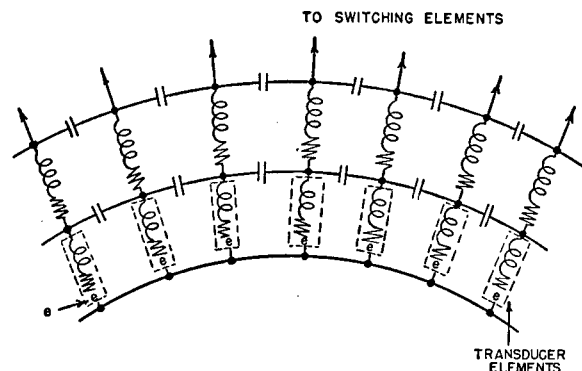


FIGURE 16. Two-layer lead line.



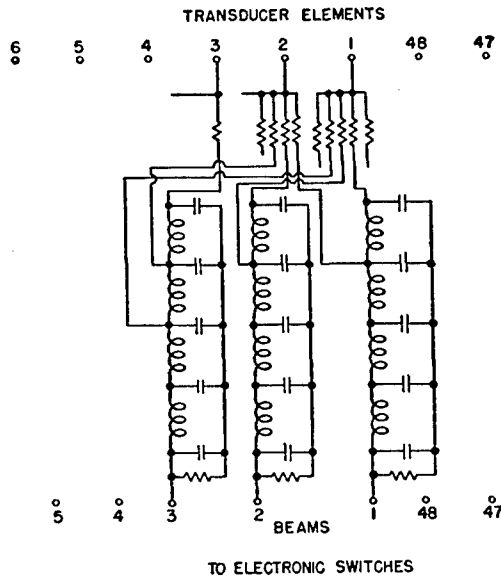


FIGURE 17. Preformed pattern scanning system.

16 elements would, therefore, feed each lag line. Each lag line is made to give the theoretically required phase shifts, and the required amplitude control is obtained by choice of the bridging resistors, as in the CR scanning sonar. In the British system, electronic switching is used to pass the output from each lag line in turn to the receiver, but smooth rotation of the receiving pattern could probably be achieved with proportional switches and a graduated switching pulse like that now used in the ER scanning system. It should be noted that the use of lag lines, rather than lead lines, makes the operation of this system relatively independent of frequency.

### 10.3.3 Storage of Received Energy

Present scanning sonar systems, employing either commutated or electronic rotation, make use of only a small fraction,  $1/10$  to  $1/13$ , of the incident echo energy. Unfortunately, the echo is not uniform in intensity like the transmitted pulse, but shows wide and rapid fluctuations.<sup>10</sup> Consequently, since the fraction used may happen to be taken at any part of the incident echo, it is much less consistent in intensity than is the average of the whole echo. In addition, rapid changes in intensity during the accepted fraction lead to errors in the indicated bearing of the echo. In CR scanning sonar the resulting inconsistencies in scanning indications are known to put the scanning channel at a basic disadvantage with respect to the listen-

ing channel which utilizes the whole echo. An obvious remedy for this undesirable situation is to make provision for energy storage, so that the average echo intensity can be indicated. Even if only partial integration must be accepted, some statistical improvement should result.

In the British system with preformed patterns described above, the signal energy output from each channel is stored, after rectification, on a capacitor which is scanned by the electronic switch. By proper choice of rectifier time constants a useful degree of integration can presumably be obtained.

Another approach is through storage of vibration energy in the transducer element itself, or of electric energy in an associated tuned electric circuit. Here the basic limitation is in the band width required to accommodate doppler and to allow for frequency drift, since band-width considerations based on the pulse length of the rapidly swept pattern are only valid after the pattern has been formed. A 30-kc transducer with a  $Q$  of 20 would, for example, give energy integration over about  $4/9$  of the returning pulse at 330-rps rotation speed, a considerable potential improvement over the  $1/12$  figure at present achieved with the ER scanning sonar. It must be pointed out, however, that this advantage is offset by the fact that the use of sharply resonant mechanical or electrical input circuits precludes change of system-operating frequency and increases the difficulty of adequate control of phase variations.

### 10.3.4 Sector Scanning Arrangements

Of the various scanning systems that have been built up to this time, only the depth-scanning sonar described in Chapter 6 has scanned less than 360 degrees. Other applications in which scanning of only a sector would be useful have been suggested, however, among them navigational aids and bottom surveys. The ER scanning system, with its possibility of giving high range resolution, should be worth investigating with regard to such sector scanning applications.

In order to make full use of the scanning time, it is desirable that a fully formed receiving pattern start at one edge of the sector and be swept to the other edge and then be cut off; at that instant a fully formed beam should start again at the beginning of the sector. If the present type of ER scanning system is used, a second switching pulse would have to start down

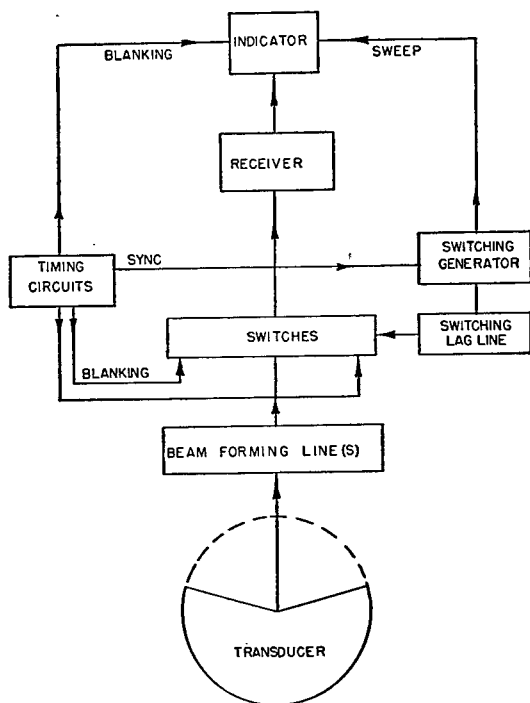


FIGURE 18. Sector scanning arrangement.

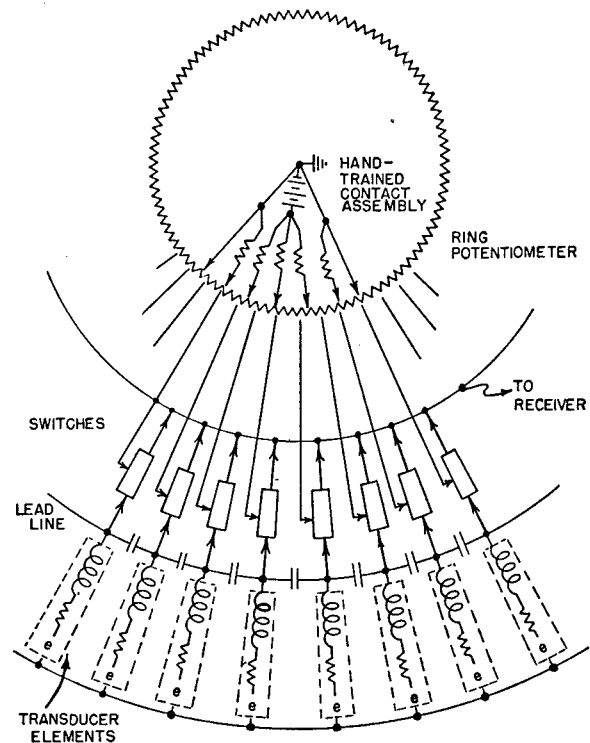


FIGURE 19. ER listening channel arrangement.

the switching line at just the right time to form a pattern at the beginning edge of the sector at the instant the preceding pulse is forming a pattern at the finishing edge. Suitable blanking pulses would have to be provided to block the switching devices at the beginning edge of the sector until the center of the pattern reaches the finishing edge, then to block those at the finishing edge as the new pattern starts at the beginning edge. Similar control of the indicator potentials would be required. A functional block diagram of such a system is shown in Figure 18.

A sector scanning system could be used in parallel with a full 360-degree system to permit more careful examination of a sector of interest, or it could be a separate special-purpose system. In the latter case, sector pinging, to put most of the transmitted energy into the sector of interest, would be desirable.

The greatest difficulty in applying the ER scanning method to sector scanning would be in realizing the narrow beam patterns that would probably be necessary in such applications. To this end the use of patterns preformed with multiple lag lines, as described in an earlier portion of this section, might be desirable.

## 10.3.5

## Listening Channel

At an early stage of its development, when ER scanning sonar operated at speeds of only 30 or 60 rps, the corresponding pulse length of 15 to 20 milliseconds was considered long enough to give useful audible information. The value of a separate listening channel in CR sonar was just beginning to be appreciated, and some preliminary proposals were made to provide a listening channel for the ER system. However, with the system operating at speeds of 200 rps and greater, the extreme shortness of the pulse seemed to preclude listening and no further work was done on this type of channel. This was unfortunate, since operating experience with the ER submarine sonar up to the time of this writing indicates that, despite the short pulse length, a trainable listening channel would be of sufficient value to justify its inclusion in the system. While the echo quality is admittedly poor with such a short pulse and doppler discrimination is low, the ability to get some measure of additional information by ear to help the eye interpret what is seen on the PPI seems valuable. In fact,

CONFIDENTIAL

on the basis of this experience even a nondirectional listening system would seem to have some merit.

A listening channel for an ER scanning sonar could use either CR or ER principles. If CR, it would be just like that described in Chapter 5, unless the cruder conductive commutation mentioned in Chapter 1 were thought desirable. If ER, it would be like the scanning channel, but operating statically rather than dynamically. Figure 19 shows a proposed arrangement using a single lead line. The electronic switches, instead of being controlled by connection to points on a switching line down which a pulse is traveling, are connected to points on a ring potentiometer. By means of the battery and the contacts on the hand-trained contact assembly, a static d-c potential distribution is developed which is equivalent to the active portion of the scanning switching pulse. A receiving beam pattern is thus formed in a direction determined by the setting of the contact assembly.

It is likely that training could be accomplished most conveniently through a servo system, so that this equipment could be located remote from the operator position (although preferably external to the transducer). If the switches were of a type that presented negligible load to the lead line, and if suitable isolation of switching control potentials were provided, both scanning and listening switching could be connected to the same lead line without mutual interference.

## 10.4 CIRCUIT IMPROVEMENTS

### 10.4.1 Introduction

Operating experience with the various scanning sonar systems, and the background of experience with searchlight sonar, indicate several lines of further circuit development that should be investigated further:

1. Increasing transmitted power.
2. Increasing receiving sensitivity, especially for desired echoes, and increasing the ratio of desired signal to reverberation and to noise.
3. Increasing the ease of operation.
4. Increasing reliability and ease of checking and maintenance.

The last is a general aim and is mentioned here to emphasize the great importance which considerations of reliability must always be given.

### 10.4.2 Increasing Transmitted Power

The problem of high-powered transmitter design is important because of the large transmitting power necessary to obtain a given intensity of sound at all distant targets around the horizon. Early solutions employed standard transmitter design, using larger tubes and components to obtain the power, leading to massive equipment. For the purpose of echo ranging, in which the pulse length is short compared to the interval between pulses, it is obviously unnecessary to provide a transmitter capable of continuously supplying the required peak powers. Pulse-type transmitters were developed that relied on a large capacitor to store energy during the interval between pulses and release it at the time of the pulse. This capacitor storage system has proved adequate for short pulse operation in spite of the fact that the actual amount of energy withdrawn from the capacitor on each pulse is only a small portion of the total available. For long pulses, the shape of the capacitor discharge curve produced a distorted pulse, so that the power at the end of the pulse was appreciably less than at its beginning. Hence for the longer pulse lengths, to avoid using excessively large capacitors to obtain a suitable pulse shape, a simple type of filter arrangement was incorporated in some of the transmitters.

As a result of developments in the radar field, the design of pulse-line-type power supplies has been investigated. (See Chapter 9 for discussion of design factors.) These supplies are of such nature as to yield, in the form of a single flat-topped pulse, all of the power stored in a set of capacitors.

If a pulse with sharp corners is required, the line must be designed to have linear phase-shift characteristics as a function of frequency and to have a high cutoff frequency. This required some departure from the simple type of low-pass filter. For many applications it is undesirable to have the corners of the pulse sharp, so that a simple low-pass filter design with the cutoff frequency at approximately three times the reciprocal of the pulse length is more desirable.

The energy available is in the form of a d-c pulse, and some method of converting it to the required ultrasonic frequency must be provided. If radar-type pulse modulators are used, the pulse may be applied directly to the output-tube plates and the output pulse initiated by suitable change in grid bias. If voltages other than those resulting from a readily available pulse line are desired, the pulse transformer

technique may be employed. The transformer size is quite reasonable for 3-millisecond pulses (see Chapter 7). It appears that the pulse transformer volume is dependent primarily upon the pulse length and nearly independent of the power rating, but further investigation of this method should be made. Recent suggestions have been made concerning the use of thyratrons, particularly of the hydrogen-filled variety, for converting d-c power into power at ultrasonic frequencies. Such a procedure may require the use of step-down pulse transformers, since in general these tubes have low impedance and are, therefore, low-voltage devices. An additional advantage resulting from the use of transformers is that all plate, screen, and grid voltages may be supplied simultaneously from a single pulse line by the use of taps on the transformer.<sup>11</sup>

One of the principal difficulties in designing transmitters is the absence of information on the behavior of available radar-type tubes under the longer pulse conditions required in sonar work.

Without doubt the present trend is toward higher and higher powers, and this introduces many problems that concern the associated equipment. Output transformers, send-receive networks, cables and transducers which are adequate for powers of less than 1 kw, are obviously inadequate in the 5- to 20-kw range now employed in scanning sonar and would have to be completely redesigned for use at the proposed 100-kw power levels. While the desirability of extremely high-power pulsing appears to be beyond question, it must be remembered also that the designer is attempting to compress a complete transmitter into spaces available on submarines and small surface ships. Full advantage must be taken, therefore, of the latest developments and improvements in components, while at the same time adequate safety factors must be zealously maintained to promote service reliability.

#### 10.4.3 Increasing Receiver Sensitivity to Desired Signals

Designing a receiver with enough gain to give an indication of a very weak signal poses no unusual problems. However, the design problems involved in getting the best possible ratio of desired to undesired signal are much more difficult to solve. The characteristics of the desired signals (echoes and target noise) and of the undesired signals (reverberation,

water noise, and electric noise) have been discussed in Chapter 3.

Reduction of electric noise originating within the system itself has long been a problem in electronic work and the techniques for its solution are well understood. It is quite possible to design a receiving system whose residual noise level is determined by thermal noise in the input circuit. Reduction of water noise is accomplished by improving dome design, by improving the receiving directivity (with limitations imposed by operating considerations) and by reducing the band width of the receiving system. In the latter case advantage is taken of the fact that water noise is fairly evenly distributed in frequency, and that the amount passing through the receiver is directly determined by the width of the pass band. (This assumes that any nonlinearity before the pass-band determination is sufficiently low so that appreciable cross-modulation does not occur.)

However, the pass band must be wide enough to pass the echo pulse without serious distortion, and it must also be wide enough to accommodate frequency changes caused by the doppler which results from the motion of own ship and target relative to the water. Which of these two limitations is the controlling one depends upon the characteristics of the system and its use. The pulse limitation usually controls in a high rotation speed ER sonar, while the doppler limitation is usually the controlling factor in the 30-rps CR scanning sonar.

Since the target may move at any speed within certain limits, there is no way to avoid making the pass band wide enough to accommodate target dopplers. Compensation may be made for own doppler by *own-doppler nullification* [ODN], permitting restriction of the pass band, with consequent improvement in signal-to-water-noise ratio.<sup>12</sup> Because of the pulse requirement, less improvement is possible in the scanning than in the listening channel by use of ODN. In the latter case, ODN is further advantageous in making operation easier.<sup>13</sup> It is also required in the operation of certain techniques whereby advantage is taken of target doppler to enhance the echo signal with respect to reverberation.<sup>13</sup> Considerable experience has been accumulated on ODN methods as applied to searchlight-type sonar<sup>13</sup> and some suggestions for its application to scanning sonar are given later in this chapter.

Since the level of the echo signal increases as the range decreases (see Chapter 3) the gain of the re-

ceiver must be appropriately adjusted with time after the ping is emitted. Reverberation is unpredictable, especially when bottom reflections are obtained, so that the maximum probability of distinguishing target echo signal from reverberation is obtained by adjusting the gain of the receiver in such a way that the reverberation signal is at every instant close to the threshold of indication. A target signal is then most likely to be detected. After reverberation falls below water noise, the gain must remain constant. Obviously, such complex gain variations must be handled automatically, and the *time-varied gain* [TVG] and *reverberation-controlled gain* [RCG] circuits were developed to perform this function in searchlight-type sonar systems.<sup>14, 15</sup> Similar circuits may be applied to the listening channel of a scanning sonar. In the case of the scanning channel, however, the problem is complicated by the rapidly varying conditions which the receiving beam encounters while in process of scanning. Reverberation may not be the same on all bearings; bottom echoes may be received in depth scanning; and considerable noise from own-ship's propellers may be picked up from the aft direction. What is really needed is a method of gain control that anticipates the level to be received and adjusts the gain of the scanning receiver continuously to keep background noise at threshold.

#### OWN-DOPPLER NULLIFIER IMPROVEMENTS

The doppler shift  $\Delta f$  caused by own-ship's motion is given by (see Chapter 3)

$$\Delta f \cong 2 \frac{f}{c} \cdot S_o \cdot \cos B_r, \quad (3)$$

where  $f$  = transmitted frequency,

$c$  = velocity of sound in water,

$S_o$  = speed of own ship,

$B_r$  = bearing (relative) of the center of the beam.

In a searchlight-type sonar, compensation at a particular bearing may be introduced either in transmission or in reception with equally satisfactory results. In a scanning sonar, introduction of such ODN compensation at the transmitter results in desensitiz-

ing the scanning receiver at bearings removed from that chosen for  $B_r$  in equation (3). It is, therefore, necessary to introduce ODN compensation in reception; for example, by changing the frequency of the heterodyne oscillator in the receivers. If this oscillator is also involved in a unicontrol circuit, the ODN compensation must be removed during the transmitting interval.

In a scanning channel,  $B_r$  in equation (3) is a time function, so that

$$\Delta f = \frac{2f}{c} \cdot S_o \cdot \cos (2\pi N t), \quad (4)$$

$N$  being the number of revolutions per second of the scanning beam, and time  $t$  being measured from the instant when the scanning beam is dead ahead. Obtaining ODN in the scanning channel, therefore, requires a sinusoidally varying compensation that is synchronous with the rotation of the scanning beam.

There are two general types of own-doppler nullification: *reverberation-controlled* and *computed-correction*.<sup>13</sup> The reverberation-controlled type functions by measuring the average reverberation frequency and automatically adjusting a heterodyne oscillator to bring this reverberation frequency to a standard value. It has been used in searchlight-type sonar systems and in the listening channel of scanning equipments, and has been reasonably satisfactory when rapid bearing changes are not required. In general, it is smaller and less expensive than a computed-correction type, but is more subject to errors due to roll velocity and water noise. This is particularly true when water noise has a higher level than early reverberation, as may be the case at high ship speeds in deep water.

The computed-correction type performs the operations indicated in equation (3) or (4). It obtains  $S_o$  from the pitometer log and  $B_r$  from the sonar gear, and applies the result of the computation in the form of a frequency correction. It is more complex than the reverberation-controlled type, and has the disadvantage that it must be connected to a pitometer log; this is not serious, however, since a pitometer log is always installed in ships having fire-control equipment. It has the advantages of being independent of the nature of reverberation, or water noise, and of using components similar to those used in fire-control computers.

Although the above discussion has been limited to

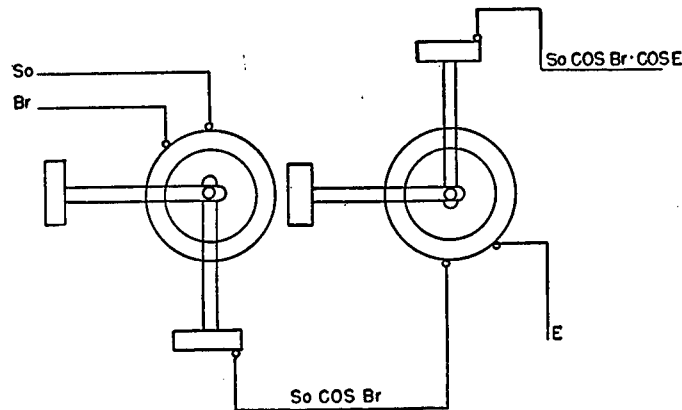


FIGURE 20. Connection of mechanical resolvers for computed-correction ODN.

azimuthal angles, it is obvious that the expression for any direction is:

$$\Delta f = \frac{2f}{c} \cdot S_o \cdot \cos B_r \cdot \cos E, \quad (5)$$

where  $E$  is the depth (negative elevation) angle. In depth-scanning sonar equation (4) becomes:

$$\Delta f = \frac{2f}{c} \cdot S_o \cdot \cos B_r \cdot \cos (2\pi N t). \quad (6)$$

The result of the computation to change the frequency of an oscillator may be applied by mechanically changing the inductance or capacitance in the frequency-determining circuit, or by electronic control with a reactance-tube circuit. Mechanical control is, in general, more stable and reliable, and for this reason is preferable for the listening channel, even though its use may require inclusion of a servo. Electronic control is, at the present writing, less stable, but has the great advantage of allowing rapid frequency changes and is accordingly desirable for the scanning channel.

The computation indicated in the above equations involves deriving a cosine from an angle and taking products, and includes the introduction of a suitable factor of proportionality. These are processes common in fire-control computers, and may be done mechanically or electrically. Figure 20 shows a mechanical method using standard fire-control resolvers, the schematic nomenclature being that used in fire-control drawings.<sup>16</sup> Figure 21 shows an electrical method adapted to the requirements of the inte-

grated Type B sonar (see Chapter 6). In this case the derivation of the cosine function is performed by electric resolvers, which may be standard synchros.

Figure 21 also illustrates a practical arrangement for applying ODN to both listening and scanning channels. A voltage proportional to ship's speed is obtained from the pitometer log. This voltage is properly combined with relative bearing and depth angle in resolvers, and the resultant output is used to position a condenser controlling the heterodyne oscillator frequency, through a null-balance servo. Since the percentage variation in frequency is small, particularly in the heterodyne oscillator, the variable capacitor may have a straight-line capacitance char-

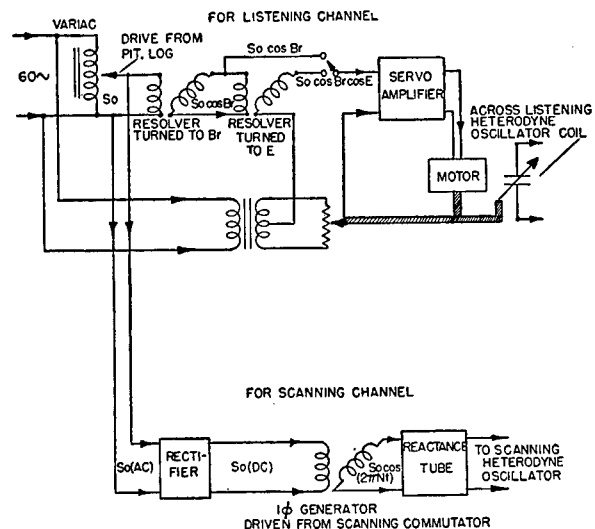


FIGURE 21. Computed-correction ODN with servoed capacitor, frequency control in listening channel.

CONFIDENTIAL

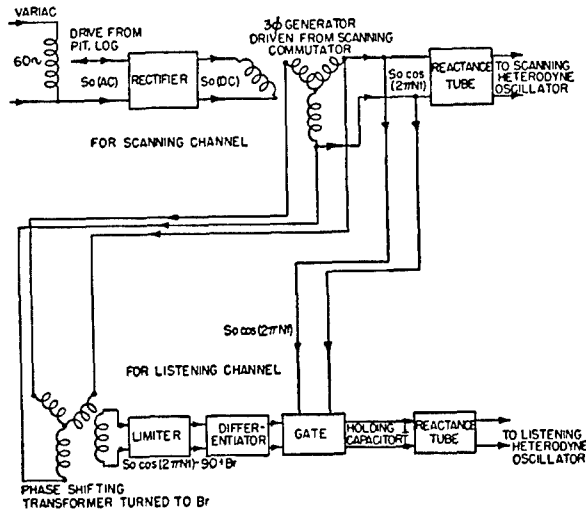


FIGURE 22. Computed-correction ODN with reactance-tube frequency control in both channels.

acteristic. Although the corrections are strictly accurate at one operating frequency only, the errors over the operating band can easily be kept acceptably small by proper choice of oscillator constants.

Operation of the scanning-channel ODN is similar to the above. Direct-current excitation for an a-c generator mounted on the scanning commutator is furnished by rectification of the  $S_0$  voltage derived from the pitometer log. The output voltage of this generator is, therefore, proportional to  $S_0 \cos(2\pi Nt)$  as required by equation (4), and is applied to a reactance-tube circuit which controls the frequency of the scanning-channel heterodyne oscillator in the proper manner. This is not a null method, and the magnitude of the correction, therefore, is dependent upon the line voltage and line frequency. As in the listening channel, tuning errors can be kept small by the proper choice of oscillator constants.

It is recognized that in the arrangement shown in Figure 21 the primary emphasis is on obtaining stability in the listening channel whose pass band is narrower than that of the scanning channel. If errors due to potential instability of reactance-tube circuits are not considered excessive, the capacitor servo of Figure 21 may be eliminated. A proposed arrangement for doing this is shown in Figure 22, using the same system for the scanning channel as described above. At the instant when the scanning beam has the same bearing as the listening beam, the ODN voltage for the scanning channel is that needed to control the reactance-tube circuit, which in turn con-

trols the frequency of the listening-channel heterodyne oscillator. A gating circuit opens just at this instant and charges a holding capacitor which accomplishes this control. Proper timing of the gating circuit is insured by controlling it from the output of a phase-shifting transformer mounted on the listening commutator. This receives 3-phase excitation from the generator on the scanning commutator. A similar arrangement could be worked out for a depth-scanning system.

#### 10.4.4 Increasing Ease of Operation

The primary function of the sonar operator is to recognize and identify target echoes or noise on the indicator and, once sonar contact has been made, to maintain contact and determine the bearing and range of the target. The problem of facilitating the performance of these duties is primarily one of indicator design, as explained in Chapter 2 and later in this chapter. It is clear that there should be a minimum of duties such as gain control and tuning required of the sonar operator. Gain control which is determined automatically by the background level has already been mentioned, but the operator must be permitted some additional degree of control to take care of variations in ambient conditions and personal abilities.

With sharply tuned projectors, tuning is of considerable concern to the operator, but with the broadly resonant transducers now in fairly common use and with improvements in circuit stability this is not now the case. No tuning should ever be necessary except to reduce interference from other-ships' gear by changing the operating frequency. To facilitate this operation, unicontrol arrangements are desirable; typical circuits for this are described in Chapters 5 and 6. Whether or not the price paid for the unicontrol feature, in terms of increased complexity, is justified depends upon how often the operating frequency has to be changed.

Bearing deviation indicators, of the types now in service, require frequent attention by the sonar operator to make certain that tuning and balance remain correct. Circuit improvements to increase stability are obviously necessary.<sup>17</sup> Steps already taken in this direction are described in Chapter 6.

With the present trend toward placing only the indicators and operating controls in the sonar hut, new requirements are placed on circuit design to per-

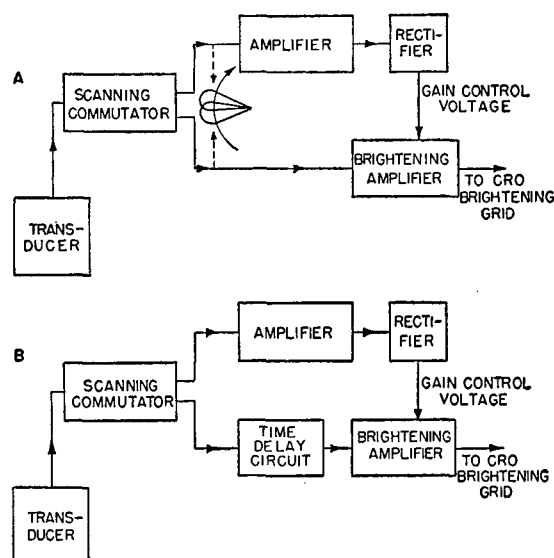


FIGURE 23. Anticipating gain control.

mit remote control of gain and tuning. Remote gain control, operating simultaneously on scanning, listening, and BDI receivers, is a problem of some magnitude. A possible but not entirely satisfactory solution is described in Chapter 6. Remote tuning control, if required, poses further problems. Servo motors might be used, or master oscillators could be located in the sonar hut; both introduce undesirable additional complexity which must be justified in terms of increased operating efficiency.

#### 10.4.5 Anticipating Gain Control

As pointed out previously, the fluctuating nature of the reverberation and noise background picked up by the scanning beam makes an anticipating gain control necessary if maximum target echo recognition is to be achieved. Two proposed arrangements for providing such control are shown in Figure 23. In A, two receiving beams are formed simultaneously, one leading the other in rotation by a small angle. Such simultaneous beam formation has been mentioned in Chapter 2 and is further described in Chapter 5. The leading beam is used to control the gain of the receiver connected to the lagging beam. The same result may be obtained by the arrangement marked B with the advantage that only a single beam need be formed by the commutator. In effect, the signal is delayed until the gain of the receiver can be adjusted to accommodate it properly. It is clear

that in both of these arrangements the envelope response of the rectifier and gain control circuits must be adjusted to give optimum averaging. Such arrangements may be of definite value in increasing weak echo recognition, and also in reducing the defocusing and broad indication phenomena observed with unusually strong echoes.

#### SYNCHRONOUS OR SECTOR-SELECTIVE GAIN CONTROL

In certain applications of scanning sonar it might be of advantage to control synchronously the gain of the receiver as a function of the instantaneous position of the scanning beam. For example, in depth-scanning sonar, it might be desirable to reduce the gain as the depression angle increases. Since the level of the target echo increases at the shorter ranges necessarily associated with the greater depression angles, the level of indication would tend to remain constant, and difficulties in handling bottom reflections might be reduced.

It might also prove desirable to vary the gain of the system in such a manner as to suppress signals in undesired sectors or to enhance signals in some desired sector. This could be done by an automatic control whose operation depended upon the position of the cursor. It might, for example, increase the sensitivity of the system throughout the sector of which the cursor line is the center. Such an arrangement might produce more favorable echo indications, but its greatest advantage would probably be in aiding the operator to concentrate his attention on the active sector. Techniques for synchronous gain control have not been developed, but would presumably be based on the principles and methods described under "Own-Doppler Nullifier Improvements."

#### 10.5

#### INDICATORS

The development of indicators, up to the time of this writing, seems to have been along two lines: first, toward methods and devices for providing a more complete picture of the tactical situation for the benefit of the conning officer, as well as for easing the duties of the sonar operator; and second, toward indicators whose primary function is to permit the transmission of data (after incorporating the judgment of the operator) to attack directors. The first category includes the PPI indicators on the simple QH-type scanning systems, the *mechanical geographical attack plotter* [MGAP],<sup>18</sup> and the modification of ASAP



for XQHA.<sup>19</sup> Into the second category fall the indicators on AD-3<sup>20</sup> and those on the integrated Type B sonar (see Chapter 6).

The trend of indicators at present (1945) is to provide the operator not only with a picture of the situation, but also with aided tracking through connection with the fire-control computer, so that his duty is limited to the insertion of small corrections. Future development of *automatic target training* [ATT]<sup>21</sup> may also contribute to this end.

On the listening portion of the scanning sonar an additional indicator of the BDI type does not in itself give any additional information. It simply provides an indication of the training accuracy of the listening channel. However, indicators of the *sector-scan indicator* [SSI] variety, which have proportional deflection characteristics, may provide some additional information, since the magnitude of the required correction, as well as its direction, is available from such an indicator. The use of SSI would thus be another step toward providing the sound operator with a picture of the target area, since this indicator shows a plot of a sector of the horizontal plane.

Even though at some future date the entire conning of the antisubmarine attack may be handled by a computer, there will probably still be a period during which it is desirable to plot relative motions of the attacking ship and target. It has been suggested that this plotting function may be facilitated by the use of the Skyatron.<sup>22</sup> The replacement of the standard cathode-ray tube by such a device permits large-scale, very long-persistence projection on standard plotting sheets or charts, rather than smaller and less permanent type of plotting on the face of a tube as is now done in the ASAP. If the plotting is performed by a separate plotting device, means of transmitting the information to this device are required at the indicator. In addition, the plot itself probably will not be sufficiently accurate for the attack, so that some means of obtaining numerical values for target range and bearing must be provided. Mechanical counters could be used in each of which the operator would read a single number as it appears in a small aperture.

As a general alternative to the present method of reading the position of a spot with respect to the center of a CRO tube or to the end of a scale, it has been suggested that the operator be provided with a control which would return the spot to an index so that the numerical value corresponding to the position of the target could be read from a dial operated

by the control. This proposal is in accord with the present practice of pointer-matching fire-control work.

If the display is to be plotted, it is not always advantageous to make a polar plot. For some purposes (depth scanning, for example) the range of values varies so much in different directions that the plot is better made with correspondingly different scales. This requires noncircular scanning. Likewise, since the accuracy required in the later stages of an attack is much greater than during the search or the approach, a logarithmic or otherwise nonlinear range scale on a polar plot, while greatly distorting the mapping, might make more efficient use of the available plotting space.

It has been suggested that additional information, particularly that concerned with doppler, might be presented on the PPI-type indicators by the utilization of color-television techniques in which the color of the indication is a function of doppler.

The ultimate in simplicity of operation, perhaps, would be a system in which a spot would appear on a scope screen and the only operator job would be to manipulate a single control so that the spot is kept between two lines. With improvements in sonar performance it may no longer be necessary for the operator to have in mind the tactical situation; in fact, it may even be preferable for him not to know the situation. During the brief and tense moments of an attack it is desirable that all necessary operations by the sonar operator be so simple that they are almost mechanical reflexes, with the machinery performing the complicated functions.

As an illustration, one proposal is described here which has several features of considerable merit. It follows radar practice rather closely, with the necessary allowances for the physical limitations of sonar. Figure 24 shows a sketch of the basic arrangement which has three cathode-ray tube indicators and functions as follows:

The PPI scope is of the usual form which presents a map of all targets in terms of azimuth angle with respect to the ship. This is used for general search procedure. Once a target is discovered, the operator stationed at this indicator sets a cursor upon the target and two listening channels (azimuth and depth) are thereby trained to the target bearing. The operator then makes a rough estimate of range, which he either calls to the operator of the A scope or sets on a range dial.

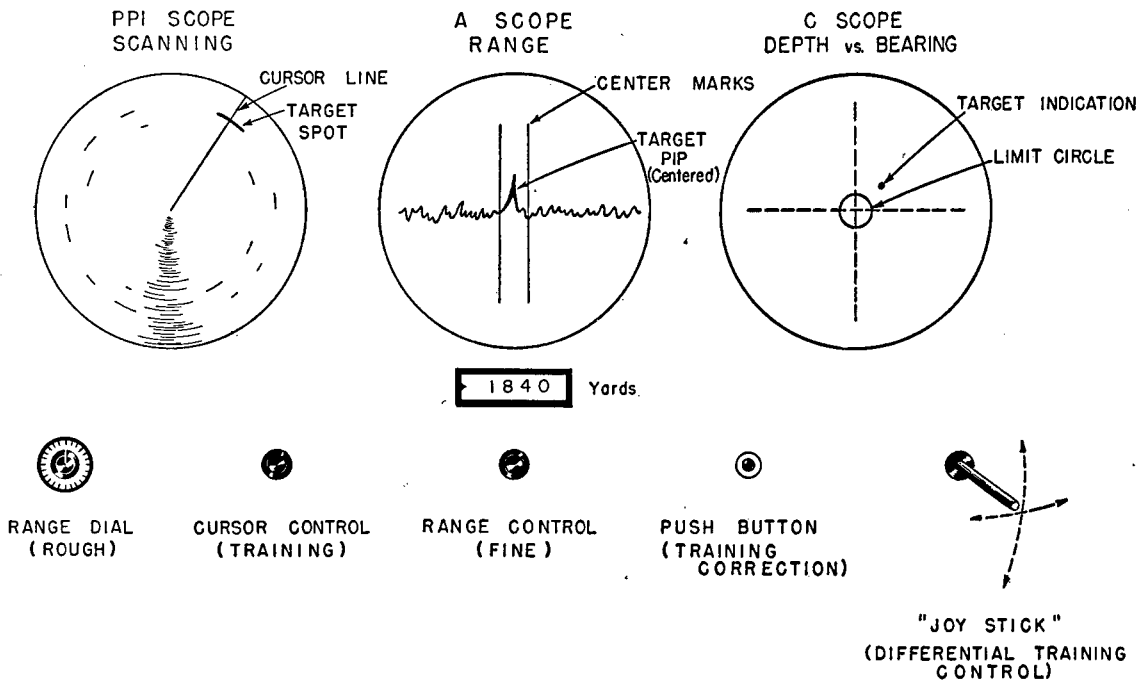


FIGURE 24. Suggested indicator system for advanced integrated sonar.

The A scope gives range only. A horizontal (or vertical) sweep is amplitude-deflected by the incoming signals. The sweep is so arranged that it shows only an expanded band of range values centered at the estimated target range. Thus, for an estimated target range of 2,000 yards the expanded sweep might cover the range band from 1,900 to 2,100 yards. The A scope operator, by means of a control knob, keeps the target indication centered between a pair of lines marked on the scope. This automatically feeds target range into the fire-control calculating gear. Range indications would be given on a counter.

After the above operations are performed by the operators of the PPI and A scopes, indications start to appear upon the C scope. The C scope is arranged to plot target depth against target bearings, and a spot appears continuously upon the scope, representing the deviation in azimuth and depth of the last received echo. This deviation of the spot is caused by the dual action of the azimuth and depth BDI, both of which are of the proportional type. A special narrow range gate, operating from the information derived from the A scope, allows only the target echo to act on the BDI circuits. The deflection voltages developed charge horizontal and vertical deflection circuits that hold the indication until receipt of the next echo (next gating period). This gives a continuous in-

dication on the C scope. During the time between echoes, the push button on the C scope can be depressed and the "joy stick" training control manipulated, causing slewing of the depth and azimuth training. The direction and speed of the training of the two systems is controlled by the direction and amount of deflection of the joy stick (as in turret control). As the training proceeds, bias voltages proportional to the amount of train are fed back and added to the deflection voltages already present, causing the spot to approach the center. After the spot has been centered, the push button is released, whereupon the spot returns to its original deflection. The next received echo should then return the spot to the centering circle ruled on the scope if the training was correct. The function of the push button described above can be performed automatically as a further development when proper circuits are available. The method of having a continuous spot and feeding-back voltages proportional to training allows the operator to judge immediately the amount of train necessary. The use of slow-speed slewing allows the operator to make up for any major errors in the training performed by the calculating gear, as well as to perform small differential training to correct for small deviations. This operation automatically feeds target depth and target bearing into the computer. After a

CONFIDENTIAL

few pings of the sonar system, the computer starts to return estimated target-position information back to the sonar gear and automatically train it to the target. Thus, the only function for the operators is to watch the appropriate scopes and put in small corrections representative of small errors in training and range prediction as performed by the calculating gear. These errors correspond to changes in target course and speed which had not yet had time to affect the computation. In addition, the computer acts as an attack director, giving information to the conning officer.

It may be seen that this system relieves the operators of the necessity of making any complicated judgments. In each case the operator turns a knob to match a cursor to a spot or to match a spot or pip to a prearranged line or limit circle. These manipulations are readily reduced to purely mechanical reflex reactions on the part of the operator.

The electronics and scanning devices required to operate in conjunction with such an indicator have not as yet been developed. It is felt, however, that the arrangement suggested here is one logical goal which might be pursued in the development of improved sonar equipment.

#### 10.6 STABILIZATION AND FIRE CONTROL

At present it is clear that sonar information has greater probable error and is obtained less frequently than other fire-control information. It is, therefore, to be expected that in future development each portion of the attack equipment (sonar, ordnance, and fire-control) will be designed with a fuller appreciation of the capabilities and limitations of the others. The discussion here deals with the antisubmarine problem, and it is recognized that similar considerations hold in the prosubmarine field.

##### 10.6.1 Sonar Considerations

Sonar information must always be limited in accuracy because of the nature and properties of the ocean as a medium for transmission of sound. In addition, the nature and extent of the target introduce uncertainties as to its position.<sup>23, 24, 25</sup> Sonar design should take into account these limitations.<sup>26, 27</sup> The methods described in Chapter 3 for determining performance

expectations on the basis of sonar characteristics should be useful in this connection.

As complete information as possible is required regarding the position of the target. Stabilization must be provided to remove the effect of own-ship's roll and pitch, by correcting the indications or by effectively leveling the sonar transducer. Where only the indications are corrected, great inconsistency of information may be experienced under conditions of considerable roll and pitch (see Chapter 3). This is a disadvantage because the amount of useful information received is decreased and the range of probable detection is reduced. Physical stabilization of a scanning sonar transducer presents formidable problems in mechanical design, but is presumed possible. Electrical beam shifting likewise seems very difficult, but it is possible in theory and should be investigated.

Choice of the type of stabilization, two-axis or three-axis, requires a careful study of operational requirements. The relative simplicity of the two-axis type makes it preferable if its limitations at large elevation angles are found operationally acceptable. Whether or not the stabilization units are used in common with other equipment is a matter involving considerations of space, reliability, and damage control, and must be studied in connection with the ship's whole fire-control system.

It has already been pointed out earlier in this chapter that the design of the sonar indicators is of great importance. It must be considered in relation both to the efficiency of the operators and the interconnection with the fire-control equipment.

##### 10.6.2 Ordnance Considerations

It has long been recognized that depth charges are inadequate for antisubmarine warfare. Slow sinking speed, stern-dropping attacks, a slow maneuvering of the attacking ship, and loss of sonar contact at short range give much opportunity for evasive action by the submarine.<sup>28</sup> Forward-thrown projectiles still are dependent to a considerable degree on proper maneuvering of the ship.

All of these ordnance types require that the ship make attack runs and allow only one firing per run. It seems clear that adaptation of gunnery methods to the antisubmarine attack would be highly advantageous, utilizing continuous firing and independence of ship's motion. If both range and bearing of the point at which the projectile entered the water

could be set in accordance with information from a fire-control computer, then maneuvering of the attacking ship would become much less critical. The conning officer would need only to keep the ship within reasonably wide range limits of the target and could adjust his aspect to present a minimum mark for torpedoes. Continuous sonar contact, including contact for short ranges and deep targets, would facilitate maneuvers.

Gunnery-type antisubmarine ordnance has long been under consideration, and development has recently been begun by the Bureau of Ordnance. This development should be prosecuted vigorously. The widest possible limits in both bearing and range should be striven for, to allow maximum latitude in maneuvering. Fuzing should be of the contact and proximity type rather than of the pressure type, so that only damaging explosions would interfere with sonar operation. On the other hand, the value of spotting techniques in gunnery has led to the suggestion<sup>29, 30</sup> that the antisubmarine projectiles be constructed to return identifiable sonar indications whose position may be compared with that of the target. Release of bubbles or the incorporation in each projectile of a very simple echo repeater<sup>31</sup> are possible means to this end.

### 10.6.3 Fire-Control Considerations

Fire control for surface and antiaircraft gunnery has reached a state of near perfection in so far as it is used with visual observation of the target. With the differences in the nature of sonar and visual information it is logical to expect great departures from normal fire-control methods to be desirable.<sup>32</sup> Present day fire-control methods should be more nearly applicable to the gunnery-type antisubmarine ordnance discussed above. However, it has been clearly shown that adequate provision must be made for the particular nature of sonar information, which is characterized by:

1. Time lag, due to the low velocity of sound in the medium, and operator lag (2 seconds).
2. Comparatively long time interval between observations, due to the nature of sonar equipment and the methods of operation.
3. Inaccuracy and dispersion of bearing data ( $\pm 1.5$  degrees), due to water dispersion, target extent, and operating errors.
4. Inaccuracy and dispersion of depth data ( $\pm 20$

feet), due to the causes listed in No. 3 above, plus thermal gradient refraction and surface reflections.

5. Dispersion of range data ( $\pm 20$  yards), due to the causes mentioned in No. 4 above.

In the present state of sonar art the values mentioned above are realistic averages for a submarine target at ranges of the order of 500 to 1,000 yards. Development of sonar fire control must, therefore, be based on making the best use of data which possess this degree of "roughness." Smoothing devices must be provided to keep the attack computation stable and based on the most probable position of the target, but the degree of smoothing (or acceptance lag) must be held to a minimum so that target maneuvers may be detected quickly. With erratic data more smoothing must be provided, but arrangement should be made for reducing the smoothing, and thereby increasing maneuver detectability, when the data are more consistent. Recorder methods allow intelligent judgment to be applied in smoothing the data, but these methods are subject to misjudgment. On the other hand, methods using automatic smoothing are not subject to operator misjudgment, but are unable to take full advantage of the consistency of data available at any given time. It is in this field that there is greatest need for study and development.

Given the smoothed data, the computation of the ordnance orders and predicted data is straightforward, and both mechanical and electrical methods are available. Complications of the computer for several types of attack should be evaluated in terms of tactical value.

A large proportion of initial contacts with surfaced submarines are made visually or by radar; moreover, submerged submarines frequently surface during the course of an attack. Therefore, to take full advantage of the ship's available ordnance, guns, torpedoes, and underwater projectiles, close coordination of all the ship's fire-control equipment is necessary. It should be possible, for example, to have guns and torpedoes ready and trained to attack the submarine if it surfaces, and to transfer contact smoothly from sonar to radar or visual at that time. On the other hand, target course and speed information gained from radar or visual contact should be available to the sonar fire control to give predicted sonar position for assistance in making initial sonar contact. Considerable study should be devoted to this problem, in order that the maximum cooperation may be achieved with the least chance for error and unsatisfactory operation.

Closely related to the problem of coordination is that of damage control. Considerable interconnection of various units is necessary to facilitate the coordination mentioned above, and suitable switching arrangements must be provided to isolate an inoperative portion so that the usefulness of other units is impaired as little as possible. For example, considering only the sonar and its associated fire-control equipment, it should be possible to operate the sonar without fire control, but with stabilization, or without either one. Even by itself, an operable sonar equipment might make possible a successful attack with ordinary depth charges, or might maintain contact until the submarine had to surface. The use of various units in common (as, for example, the stable element) must be carefully considered from this point of view; duplication of vital units in different portions of the ship may be desirable. Likewise, elements with similar functions in different portions, such as servo amplifiers, should be interchangeable.

The above discussion of isolation of units for damage control applies also to provision for testing, servicing, and maintenance. In such complicated systems it must be possible to test each portion separately. For example, testing sonar performance with an *installed sound gear monitor* [ISGM] as discussed in a later section of this chapter, requires temporary removal of sonar stabilization and aided tracking.

#### 10.7 MONITORING AND SERVICING DURING OPERATION

A suitable testing program has two functions: (1) to insure that the sonar equipment, having first been installed or maintained at a base, is operating as well as it should; and (2) to determine at frequent periods during its service that it continues to operate efficiently. An obvious accompanying need is provision for quickly finding and remedying trouble.

One section of Chapter 8 describes methods and techniques that have been used for the testing, after installation, of the experimental scanning sonar units developed by HUSL, and may provide a guide in considering this part of the problem.

In-service checking is usually carried out when a ship is at sea and in combat readiness, and should, therefore, be simple, easy, and rapid, as well as accurate. A method similar to that worked out for checking QC sonar with an ISGM<sup>33, 34</sup> seems indicated. In

this case, the checking procedure interrupts searching for only twelve seconds, and is, therefore, considered suitable for once-a-watch use.

Correction of faults indicated by the in-service check should be made easy and rapid by having components available for replacement. Circuits should be arranged and testing facilities provided, so that trouble may be quickly localized and defective components identified.

##### 10.7.1 What Needs to be Checked in Service

In order to be assured that the scanning sonar is performing properly the following questions represent the minimum to be answered:

1. Is normal power being transmitted into the water?
2. Is receiving sensitivity normal?
3. Is noise level normal for the operating speed?
4. Is the receiving pattern normal?

Positive answers to the first three questions determine, in effect, that the figure of merit of the sonar (see Chapter 2) is normal, and that detection ranges should be as expected except as limited by water conditions. A positive answer to the fourth furnishes a more sensitive check on the condition of the transducer-commutator combination. Noise level is obvious to the operator during normal search operation from the settings of the gain controls required for acceptable background at long ranges; therefore, it need not be specifically checked. Proper tuning of transmitter and receiver are checked implicitly in measurements of transmitted power and receiving sensitivity; also, changes are likely to be apparent audibly during normal operation. Frequency determination and retuning would accordingly be part of the procedures to locate the cause when either power or sensitivity was found below normal. (This is in contrast to requirements for checking QC-type sonar equipment, whose sharply resonant transducers make tuning critical.)

##### 10.7.2 Appropriate Procedures for In-Service Checking

A test transducer located outside the dome is necessary to meet the requirements for determination of power and sensitivity of a scanning sonar. It should be located on the horizontal center-line of the sonar

transducer, four to six diameters distant, and preferably forward from the transducer. It must be streamlined to allow use at any ship speed, and should be retractable and replaceable from within the ship. A mounting using a pitometer log-type strut, as developed for the installed sound gear monitor,<sup>34</sup> seems well suited for this service. The test transducer must have high stability and reasonably flat frequency response.

Since storage-type transmitters are used in scanning sonar equipment, steady-state measurements cannot be made. A peak voltmeter or calibrated cathode-ray tube indicator is accordingly indicated. The nondirectional nature of scanning sonar transmission permits the making of power measurements without interruption of sonar operation.

To measure receiving sensitivity, it is necessary to put a sound signal of known level into the water, and to note the setting of the receiver gain control which brings the resulting sonar indication to a reference level (or conversely, the gain control may be set and the required signal noted). The output reference level may often conveniently be the threshold of either visual or aural indications, depending on the specific sonar system.<sup>16</sup> Alternatively, an output meter may be incorporated.

In checking sensitivity, minimum interruption of search operation can be obtained by proper procedure. For example, in the case of the XQHA sonar, if the signal level in the water is set above the water noise level, it appears on the scanning indicator at long range (where the RCG has allowed the receiver gain to come to the value determined by the gain control setting). The sonar operator may then interrupt pinging by switching to the noise position, adjust the gain control to give threshold indication, note the setting, and return to search pinging.

In working out checking procedures that allow minimum interruption of search operation, the location of the test equipment and its indicators must be carefully considered. It may be desirable to locate the test indicators in the sonar hut to allow immediate checking by the operator. Standard indications, with which the results of the checking must agree, can be determined at the time the sonar is certified at the base as ready for action.

The importance of the figure of merit, which combines transmitting power and receiving sensitivity to give an overall performance figure for the sonar gear (see Chapter 3), makes it desirable to construct the

test equipment so that results obtained with it can be directly correlated with figure of merit measurements. However, since diminution of transmitted power and receiving sensitivity are independently possible, the procedures described above, in which they are observed separately, seem preferable for routine in-service checking.

A more speedy process can be developed for the checking of receiving beam patterns. Points of importance are the width of the major lobe, the heights of the first minor lobes, and the nature and magnitude of spurious side and back sensitivity. For example, for QH sonar, by putting a fairly strong signal into the water with the test transducer the sonar gain control can be adjusted until the scanning indication is just visible above threshold on the PPI screen. Increasing the gain by 6 db, for instance, gives an indication of the width of the major lobe; increasing it by 20 db, for example, if no further radials are indicated, shows that the minor lobes are below this value. For this purpose it is desirable that the gain control be calibrated in db, although check settings may be determined from a calibration of the control. The beam of the listening channel may be similarly checked, using the training control to train the beam first in the direction of the test transducer, then (observing the cursor on the PPI screen) in the direction of minor lobes and side or back lobes of interest.

As a corollary to the procedure just outlined, in which predetermined gain-control settings are made to show that the minor lobes and the spurious side and back sensitivity are below standard values, it is possible to get a good measurement of the receiving pattern by determining the gain control change needed to bring the various lobes to threshold. From such readings it is even possible to determine the pattern with reasonable accuracy.

Another specific method for delineating the receiving pattern is by changing the function of the PPI scope (by switching) to make it a polar pattern tracer, either linear or logarithmic.<sup>36</sup> This has not yet been proved satisfactory and the simplicity of the methods using the unaltered sonar equipment, as outlined above, makes them seem the more attractive.

#### 10.7.3 In-Service Operator Practice

Shore-based training facilities used at present are based on the requirements of searchlight-type sonar, and reach their culmination in the attack teacher.<sup>37</sup>

Modifications of shore-based training equipment, to allow training in the procedures required with scanning sonar, are already being studied,<sup>19</sup> and a suitable modification of the attack teacher, to permit practice in making attacks with scanning sonar information, has been under test.<sup>38</sup>

The further development of shore-based scanning sonar training aids, and of procedures for using them, must be pursued. Shipboard training aids and procedures should be developed for scanning sonar. In so doing it might be well to consider the possibility of combining, at least in part, the equipment used in checking sonar performance with that used in providing operator practice. Furthermore, since the practice equipment requires certain direct connections to the sonar gear, design of the two must be closely coordinated.

#### 10.8

### MODULATION

Various proposals have been made for increasing the visual contrast between the echo and reverberation traces as they appear on the screen of the cathode-ray tube indicator for scanning sonar. Present practice sets the visual threshold by means of the reverberation so that weak echoes are often lost.

In order to improve echo-signal recognition, it is necessary to investigate the fundamental questions of what factors may be present in the echo but absent in the reverberation, or what factors may be present in the reverberation but absent in the echo. Information on these questions should make possible the design of equipment which permits improved distinction between the desired echo and the undesired reverberation.

There are two possible solutions to this problem. The first is to earmark the transmitted ping in a manner that is preserved in the echo but lost in the reverberation, and to use receiving equipment sensitive only to such identification. The second is to make use of the fact that the echo returns from a particular direction, while the signals identified as reverberation appear to come from extended sources and, therefore, from a spread of directions. In the first case, the most profitable method seems to be through modulation of the ping signal to produce modulation in the echo, which does not appear in the reverberation. *Simultaneous lobe comparison* [SLC] techniques seem to offer some possibilities in the second line of approach.

Before much can be done in the way of circuit design, some fundamental research on the effect of modulation of acoustic pulses in water must be undertaken<sup>39</sup> to determine its effect on the returning echo. Some equipment was built and installed by HUSL for a program of experimentation<sup>40</sup> with various types of amplitude and frequency modulation, but time and facilities were insufficient to allow the program to be carried to completion. Work has been done elsewhere, however, with standard searchlight sonar on the same problem, and several equipment modifications have been developed that may be applicable to scanning sonar. For example, the reverberation equalizer<sup>41</sup> developed at the San Diego Laboratory has features that may be applied to the scanning problem. On a single-frequency ping the fundamental frequency of the returning reverberation variation is approximately the same as the returning echo pulse. With a frequency-modulated ping the fundamental frequency of the reverberation variation is much higher than the echo pulse, although the amplitude of the reverberation with and without modulation is the same.<sup>42</sup>

Since with a frequency-modulated pulse, the echo length is long compared to the reverberation-variation pulses, detection and filtering can be used to produce discrimination against reverberation in the receiving system.<sup>43</sup> This fundamental idea might be applied to the scanning sonar system if the modulation frequency were high enough so that several frequency changes occur while the receiving sensitivity beam is cutting the echo train. To be effective, however, a transducer and receiver with a wide frequency response would be required with correspondingly high noise sensitivity.

The case for amplitude modulation looks less promising. Experiments with searchlight-type systems, in which the transmitted pulse is amplitude-modulated, have not indicated that any improvement in performance is gained by the use of such modulation. Since reverberation appears to be modulated to the same degree as the desired echo, no additional information results by which the echo may be distinguished from the reverberation. Some experiments at New London using amplitude modulation have indicated that there might be some advantage gained by such use in improving the signal-to-noise ratio. In any sound gear the noise may be reduced by reducing the pass band. In normal design it is necessary to have the pass band sufficiently wide to pass the transmitted

pulse and any doppler shift in frequency. Own-doppler nullification reduces the band width required to that necessary to pass only target doppler. If the transmitted pulse is modulated and the selectivity is placed after a stage rectifying the carrier, the pass band required is that necessary to pass the doppler on a base frequency equal to the modulation. The signal-to-noise ratio is then increased by the ratio of the normal carrier frequency to the modulation frequency. In the scanning channel the pass band required is determined primarily by the pulse resulting from the scanning of the echo, and is only slightly increased by target-doppler or own-doppler considerations. Thus, it appears that very little gain can be obtained by the use of modulation on the outgoing pulse and selectivity after rectification. In the listening channel, however, ODN may be applied and the selectivity after rectification utilized as in the normal searchlight-type system.

On surface ships working against submerged targets in deep water, the use of modulation may result in a net disadvantage, since the target doppler is small and thus permits narrow pass bands if ODN is used, while use of amplitude modulation always destroys the ability of the operator to recognize echoes by their quality.

The use of amplitude modulation permits the transmission of constant peak power with a considerable reduction in average power, or conversely, if the transmitter and transducer permit, the transmission of higher peak powers for the same average power. Some experiments have been carried out utilizing the first alternative and overmodulating to a degree which resulted in the transmission of a burst of short pulses during each ping having a ratio of pulse to space of about 1:3. Experiments carried out under Navy auspices indicated that this form of transmission produced some improvement in the detectability of small targets, but quantitative data are not available.

### 10.9 THREE-DIMENSIONAL SCANNING

Standard searchlight sonar may be considered as a one-dimensional scanning device, since it examines successively regions lying at different ranges in a particular direction and portrays by some method of presentation the presence of targets lying in that particular direction. In a similar manner the QH-type sonar described in this report scans in two dimensions and

represents in polar coordinates all target points in a plane approximately parallel to the ocean surface. The integrated Type B sonar described in Chapter 6 adds, through a separate operation, scanning in a particular selected plane approximately perpendicular to the ocean surface. It remains to consider some of the fundamental problems involved in three-dimensional scanning of the entire subsurface hemisphere. Two basic problems must be considered: the physical problem of securing acoustical information from the medium, and the problem of portraying the information for interpretation by an observer.

Fundamental to scanning, by methods so far considered, is the movement of a beam of receiving sensitivity. As one example, the axis of the beam might trace out a cone of expanding angle around the downward vertical, as shown in Figure 25. The vertical inclination of the beam would thus change slowly from the vertical to the horizontal as the beam scanned rapidly in azimuth, and the whole process would need to be completed quickly enough to be repeated within a time interval corresponding to the range resolution. As an alternative, the axis of the receiving beam might scan rapidly through elevation angles from the horizontal to the downward vertical, while the plane containing this excursion rotates more slowly through all azimuth bearings. Again, the entire scanning process should be completed within the range resolution interval.

Apparatus for carrying out the scanning operations just described would undoubtedly be more complicated than those so far proposed. In order to accomplish these operations with techniques similar to those described in this report it would be necessary to arrange small transducer elements over a spherical surface and to arrange phasing networks and switching circuits to produce the desired formation and commutation of the beam. Since the added component of high-speed motion of the beam would increase considerably the difficulties arising from shortness of the signal pulse intercepted by the receiving beam, it would seem mandatory to utilize permanently connected phasing networks yielding preformed beams and an electronic system that would integrate the entire pulse length for the proposed high-speed scanning. Because high resolution is required for elevation angle, it seems probable that at least 600 transducer elements would be necessary, even if it were possible to sacrifice some coverage in the region of the downward vertical.





FIGURE 25. Example of three-dimensional scanning.

CONFIDENTIAL

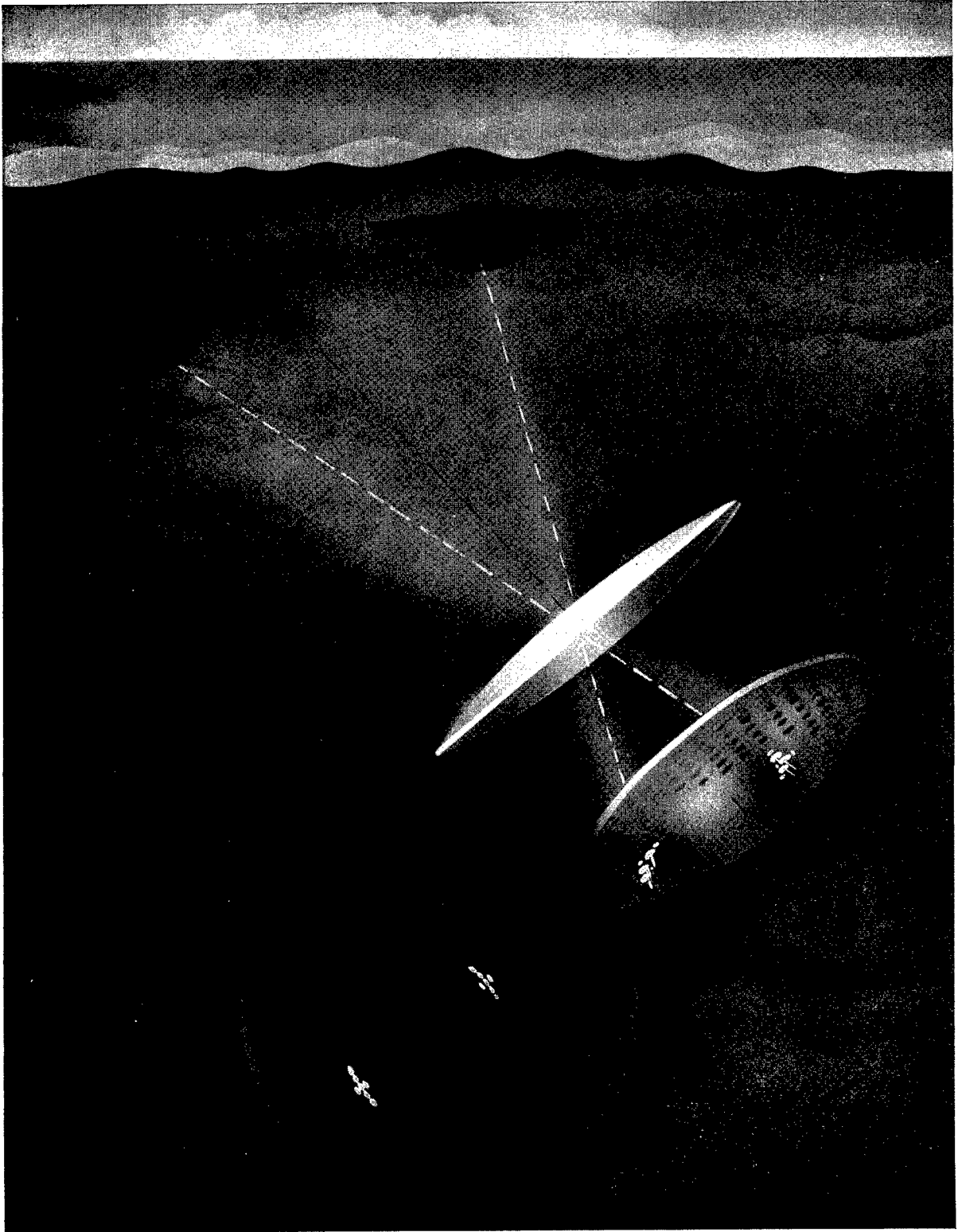


FIGURE 26. An acoustic analogue of television.

CONFIDENTIAL

Variations of the foregoing method have been proposed<sup>44, 45, 46</sup> which involve the use of an acoustic lens formed, as in the optical case, by an acoustically transparent volume bounded by appropriately curved surfaces and having a propagation velocity differing significantly from that of sea water. Such an acoustic lens would be expected to form an acoustical image of the region of interest (see Figure 26) on a mosaic of small transducers in the focal plane of the lens.<sup>47</sup> Beam formation would be accomplished by the lens, so that the only additional requirement would be to scan the output of the transducer array. This could be accomplished readily enough, but there is not yet available a method of integrating and storing the pulse signal at the individual points of the transducer mosaic without resorting to an undesirable multiplicity of amplifier and rectifier channels. If the suggested mosaic of transducers could be replaced by some substance or process which would utilize what might be called acoustic irradiation in a way that would permit the presence of the acoustical signal to be revealed by subsequent optical or electronic scanning, this system would present very attractive possibilities. It is recognized that this description proposes an electroacoustic analogue of the television iconoscope. Parabolic reflectors or other acoustical adaptations of optical devices could be invoked to surmount any difficulties arising in the acoustic lens, but this system will probably remain impractical until the electroacoustic transducing mosaic becomes available.

The most practical method of achieving a form of three-dimensional scanning at present appears to lie in an extension of the basic principles of the integrated Type B sonar. In this case two scanning systems are superimposed, one sweeping out a volume of the medium approximately parallel to the ocean surface, while the other examines another restricted volume of the medium covering all depression angles for a limited range of azimuth bearings. Application of sector-scan techniques to each of these scanning channels would provide for rapid location of any target within range. If it is necessary to guard against the possibility that a target might appear suddenly below the depression angle limits of the horizontal scanning system and off the bearing of the vertical scanning system, it might be feasible to utilize several vertical scanning channels, each covering, by a horizontal scan, overlapping fixed regions of azimuth bearing.

One of the most difficult problems associated with three-dimensional scanning is the adequate display of information to an operator. Present horizontal scanning systems exhibit position information on the plane surface of a cathode-ray indicator. The display is built up progressively in time and successive displays are superimposed, the limited persistence of the cathode-ray tube allowing the presentation to alter sluggishly. One proposal for representing an additional coordinate is to code the bright spot indication corresponding to the presence of a target. Thus a brightened line originating at the target location on a PPI display might indicate by its length or orientation the magnitude of another coordinate such as depth. This method produces interpretable indications only if targets do not overlap, and if the display is reasonably free from noise interference. It has the additional disadvantage of sacrificing any possibility of quality interpretation of the target indications appearing in the present QH PPI. It might be possible to arrange two PPI displays for stereoscopic viewing so that the target indication would appear to the operator at its appropriate depth. Other three-dimensional television techniques might be invoked similarly, but some new indicator principles must become available before a true picture of changing conditions in three-dimensional space can be formed and presented to an observer as they change with time.

The question may be raised as to whether it is desirable to present such complete three-dimensional position information to a single operator. The three-indicator type of presentation suggested in an earlier section of this chapter would present substantially all information gained from three-dimensional scanning, but would divide the problem of dealing with this information among three operators. Unless tactical advantages arise from the more compact, but more complicated unitary presentation, it appears now that some form of presentation similar to the three-indicator type of display represents the most practical approach to three-dimensional scanning.

In summary, systems for three-dimensional scanning appear to be very complicated. However, new conceptions and basic research on system elements may remove these handicaps. Even now, certain fundamental methods have been established which would make it feasible to undertake the design of a three-dimensional scanning system to provide any required degree of scrutiny of the subsurface hemisphere.

CONFIDENTIAL

## GLOSSARY

- ACOUSTIC AXIS.** A reference line adopted in calibration of any transducer, usually the direction of maximum response.
- ADP CRYSTAL.** Ammonium dihydrogen phosphate crystal having marked piezoelectric properties.
- AMBIENT NOISE.** Noise present in the medium apart from target and own-ship's noise.
- ARTIFICIAL TRANSDUCER.** A laboratory device used to furnish synthetic signals equivalent in phase relations and amplitude to those furnished by an actual transducer in water, receiving sound from a distant source.
- ASAP.** Antisubmarine attack plotter.
- A SCOPE.** A CRO indicator depicting echo intensities by vertical deflections, and ranges by the position of these deflections on the horizontal trace.
- BAFFLE.** A shield used to modify an acoustic path.
- BAFFLE, PRESSURE RELEASE.** A soft baffle incapable of supporting variational acoustic pressure.
- BAFFLE, STIFF.** An ideally rigid baffle.
- BDI.** Bearing deviation indicator.
- BEARING RATE.** Rate of change of bearing.
- B SCOPE.** A CRO indicator having a rectangular plot of range versus bearing. Spot brightness indicates echo intensity.
- CAVITATION.** Formation of gas or vapor cavities in water, caused by sharp reduction of local pressure.
- CHEMICAL RECORDER.** An indicator which records range on chemically treated paper.
- CR SYSTEM.** Commutated rotation scanning sonar.
- CRYSTAL TRANSDUCER.** A transducer which utilizes piezoelectric crystals, usually Rochelle salt, ADP, quartz, or tourmaline.
- CUT-ONS.** Method of bearing determination from initial and final echoes obtained as the echo-ranging beam is swept across the target.
- DEAD TIME.** Elapsed time between the will to fire and the instant when the charges strike the water.
- DEPTH ANGLE.** The angle between the horizontal and the bearing of the submerged target as seen from own ship.
- DG.** Differential generator (synchro).
- DIFFERENTIAL SYNCHRO.** A synchro unit which responds to the sum or difference of two rotation orders.
- DIRECTIVITY INDEX.** A measure of the directional properties of a transducer. It is the ratio, in decibels, of the average intensity, or response, over the whole sphere surrounding the projector, or hydrophone, to the intensity or response on the acoustic axis.
- DIRECTIVITY RATIO.** A measure of the directional properties of a transducer. It is the numerical ratio of the intensity, or response, on the acoustic axis to the average intensity, or response, over the whole sphere surrounding the projector, or hydrophone.
- DLC.** Delayed lobe comparison.
- DOMES.** A transducer enclosure, usually streamlined, used with echo-ranging or listening devices to minimize turbulence and cavitation noises arising from the transducer's passage through the water.
- DSS.** Depth scanning sonar.
- DYNAMIC MONITOR [DM].** A form of monitor giving an index known as the figure of merit of the dynamic performance of echo-ranging gear.
- ECHO REPEATER.** An artificial target, used in sonar calibration and training, which returns an echo by receiving, amplifying, and retransmitting an incident ping.
- EI.** Elevation indicator.
- E2I.** Expanded elevation indicator.
- ELECTRICAL ZERO.** An arbitrarily chosen electrical reference point for any specific system.
- EPI.** Elevation position indicator.
- ER SYSTEM.** Electronically rotated scanning sonar. A system utilizing an electronic circuit for beam rotation.
- FIGURE OF MERIT.** Ratio, in decibels, of pressure in transmitted ping at a distance of 1 yd to pressure of the minimum detectable echo under prevailing conditions.
- GEOGRAPHIC PLOT.** A plot which records motion of target relative to true north.
- HELIPOT.** A helical potentiometer whose slide wire is wound like a spring, so that the contact makes several complete revolutions in going from zero to maximum resistance.
- HP-TYPE TRANSDUCER.** Hebbphone, a longitudinally vibrating laminated stack transducer of type used in final QH design.
- HUSL.** Harvard Underwater Sound Laboratory.
- HYDROPHONE.** An underwater microphone.
- IN-REGISTER POSITION.** With capacitive commutator, in-register position occurs when stator and rotor electrodes are exactly opposite one another, producing maximum capacitive coupling.
- INTER-REGISTER POSITION.** With capacitive commutator, inter-register position occurs when rotor electrodes are in mid-positions giving equal capacitive coupling to two adjacent stator electrodes.
- ISGM.** Installed sound gear monitor.
- MAGNETOSTRICTION EFFECT.** A phenomenon exhibited by certain metals, particularly nickel and its alloys, which change in length when magnetized or (Villari effect) when magnetized and then mechanically distorted undergo a corresponding change in magnetization.
- MCC.** Maintenance of close contact.

- MR SYSTEM.** Mechanically rotated scanning system. An early scanning sonar system developed by HUSL.
- MTB.** Maintenance of true bearing.
- NOISE RADIALS.** The brightening of all range points on a specific PPI bearing, caused by the reception of noise from the direction indicated.
- NORMALIZED AMPLITUDE.** The response along the axis of the major lobe plotted with a value of unity (or 0 db).
- ODN.** Own-doppler nullifier.
- OTE.** Operator training equipment. Earlier a HUSL designation for operational test equipment.
- PEPPER.** Polar exponential pattern plotter for ER sonar.
- P2I.** Modified PPI.
- P3I.** Precision PPI.
- PHANTASTRON CIRCUIT.** A precision delay circuit.
- PIEZOELECTRIC EFFECT.** A phenomenon exhibited by certain crystals in which mechanical compression produces a potential difference between opposite crystal faces or an applied electric field produces corresponding changes in dimensions.
- PING.** An acoustic pulse signal projected from echo-ranging transducer.
- PIP.** An echo trace on indicator screen.
- PPCR.** Portable polar chart recorder.
- PPI.** Plan position indicator.
- PRESSURE RELEASE.** A material, such as air-cell rubber, which is incapable of supporting variational acoustic pressure.
- PROJECTOR.** An underwater acoustic transmitter.
- QH.** Navy designation for CR scanning sonar (originally applied to HUSL designs) employing magnetostrictive transducers.
- QL.** Navy designation for FM sonar of UCDWR design.
- RANGE RATE.** Rate of change of range between own ship and target.
- RCG.** Reverberation controlled gain.
- RECOGNITION DIFFERENTIAL.** The number of decibels by which a signal must exceed the background in order to be recognized 50 per cent of the time.
- REVERBERATION.** Sound scattered diffusely back towards the source, principally from the surface or bottom and from small scattering sources such as bubbles of air and suspended solid matter.
- REVERBERATION INDEX.** Measure of the ability of an echo-ranging transducer to distinguish the desired echo from the reverberation. Computed from the directivity patterns as the ratio in decibels of the bottom, surface, or volume reverberation response of a specific transducer to the corresponding response of a nondirectional transducer.
- $\rho c$  RUBBER.** A rubber compound with the same  $\rho c$  (density times velocity of sound) product as water.
- RING STACK.** A magnetostrictive transducer composed of ring laminations which vibrate radially.
- SEARCHLIGHT-TYPE SONAR.** Echo-ranging system in which the same narrow beam pattern is used for transmission and reception.
- SGM.** Sound gear monitor.
- SKYATRON.** A dark-trace, long-persistence, cathode-ray tube which can be used for projection of plan position indication.
- SLC.** Simultaneous lobe comparison.
- SONAR.** A generic term applied to apparatus or methods that use sound for navigation and ranging.
- SONIC.** Pertaining to the range of audible frequencies, sometimes taken as from 0.02 kc to 15 kc.
- SOUND CHANNEL.** A rare condition, occurring when a negative velocity gradient overlies a positive velocity gradient in the water, whereupon the sound energy is confined between horizontal planes and thus may be transmitted over very long ranges.
- SSI.** Sector scan indicator.
- STACK, LAMINATED.** A pile of consolidated laminations.
- STANDARD DEVIATION.** The square root of the average of the squares of the differences from the mean.
- STAVE.** Individual longitudinal element, a number of which make up a sonar transducer.
- STORAGE SYSTEM.** Scanning system in which the received signal from each direction is integrated in the capacitors associated with each of many directional channels for later sampling.
- SUPERSONIC.** Pertaining to the range of frequencies higher than sonic. Sometimes referred to as ultrasonic to avoid confusion with the use of supersonic to denote higher-than-sound velocities.
- TARGET ASPECT.** Orientation of the target as seen from own ship.
- TARGET STRENGTH.** Measure of reflecting power of the target. Ratio, in decibels, of the target echo to the echo from a 6-foot diameter perfectly reflecting sphere at the same range and depth.
- TRAIN.** To rotate the transducer in a given direction about its axis.
- TRANSDUCER.** Any device for converting energy from one form to another (electrical, mechanical, or acoustic). In sonar, usually combines the functions of a hydrophone and a projector.
- TRANSMISSION ANOMALY [A].** Dimensionless factor, depending on range and general ocean conditions, which accounts for transmission loss other than that caused by inverse square divergence.

**TRANSMITTED INTENSITY.** Sound intensity in decibels above 1 dyne per square centimeter usually measured at 1 m from the transmitter.

**TRIPLANE.** A device consisting of three sound-reflecting surfaces, mutually perpendicular, having the property of reflecting a sound pulse back along the axis of arrival, used to simulate a target.

**TRUE BEARING.** Bearing with respect to true north.

**TVG.** Time varied gain.

**VARIO-LOSSER CIRCUIT.** A varistor circuit using a d-c control voltage to vary the attenuation of the signal voltage in a circuit.

**VARISTOR.** Nonlinear resistance the value of which decreases with increasing applied voltage.

**WHITE NOISE.** A uniform continuous noise spectrum.

**XQHA.** Navy designation for development model of azimuth scanning system employing the capacity commutator rotation principle.

# BIBLIOGRAPHY

Numbers such as Div. 6-631.4-M1 indicate that the document listed has been microfilmed and that its title appears in the microfilm index printed in a separate volume. For access to the index volume and to the microfilm, consult the Army or Navy agency listed on the reverse of the half-title page.

## CHAPTER 1

1. *Bearing Deviation Indicator*, OSRD 6425, NDRC 6.1-sr287-2075, HUSL, Nov. 1, 1945. Div. 6-631.4-M1
2. *Sonic Location Developments*, NDRC C4-sr58-047, HUSL, Dec. 29, 1941. Div. 6-632.0-M3
3. "Preliminary Installation, Operation and Maintenance Instruction for the Torpedo Detection Modification of the WCA-2 Echo-Ranging Listening Sounding Equipment," *Brief Descriptions of Four New Submarine Sonar Developments*, P 49A/1313, CUDWR-NLL, Dec. 18, 1944.
4. *ER Sonar, A New Sharp Beam System*, Stanley R. Rich, M 02.453.27, HUSL, July 12, 1943. Div. 6-632.311-M4
5. *Preliminary Returns of the Field Trip of the Aide de Camp to New London*, Roderic M. Scott, M 02.45.4-35 (I), HUSL, Nov. 12, 1943. Div. 6-632.212-M6  
*New London Results II, Event B, November 3, 1943, ER Sonar*, Roderic M. Scott, M 02.45.5-35 (II), HUSL, Nov. 17, 1943. Div. 6-632.312-M3
6. *Artificial Line of Low Distortion*, Claude W. Horton, M 110.3-78, HUSL, May 12, 1944. Div. 6-632.62-M4
7. *A New Switching System for ER Sonar*, Stanley R. Rich, M 02.453.2-28, HUSL, Feb. 22, 1944. Div. 6-632.63-M3
8. *3-Foot Sphere Echo Ranging Data*, Thomas P. Merritt, David C. Whitmarsh, and Roderic M. Scott, M 02.453.4-60, HUSL, Nov. 10, 1944. Div. 6-632.312-M7
9. *The 53-kc ER Sonar System at Mountain Lakes Reference Laboratory*, Thomas P. Merritt and Arthur C. Clatfelter, M 02.453.7-22, HUSL, Aug. 21, 1944. Div. 6-632.312-M5
10. *The 53-kc ER Sonar System On Board the Aide de Camp at New London*, Thomas P. Merritt, Arthur C. Clatfelter, and David C. Whitmarsh, M 02.453.4-39, HUSL, Aug. 28, 1944. Div. 6-632.312-M6
11. *Varistors as Gain Controls*, Stanley R. Rich and William L. Detwiller, M 110.3-89, HUSL, June 6, 1944. Div. 6-632.63-M4
12. *ER Sonar Installation on USS Dolphin*, Robert B. Bowersox, Reuben H. Wallace, and Andrew Patterson, Jr., M 02.453.5-11, HUSL, Apr. 10, 1945. Div. 6-632.311-M14
13. *AX-89 No. 2 Varistor Rotor Tests*, Stanley R. Rich and M. S. McKittrick, M 02.453.7-49, HUSL, Feb. 14, 1945. Div. 6-632.63-M13
14. *Theory of ER Sonar*, Gerald I. Harrison, M 02.453-119, HUSL, Dec. 11, 1944. Div. 6-632.311-M11
15. *Varistors as Reactance Elements*, Stanley R. Rich, M 110.3-147, HUSL, Nov. 10, 1944. Div. 6-632.63-M8

## CHAPTER 2

1. *Reverberation Studies at 24 kc*, NDRC 6.1-sr30-401, UCDWR, Nov. 23, 1942. Div. 6-520.0-M2
2. *Conference on Sonar Display with J. W. Horton at New London, July 19, 1943*, William T. Bartholomew and Harold P. Knauss, M 02.45-59, HUSL, July 22, 1943. Div. 6-632.04-M3
3. *Status of Scanning Sonar Display and Fire Control Problems*, Harold P. Knauss and William T. Bartholomew, M 02.45-124, HUSL, Jan. 20, 1944. Div. 6-632.04-M7
4. *Changes Made in the General Electric Attack Plotter (known as the ASAP)*, Robert B. Bowersox, M 80-165, HUSL, Mar. 19, 1945. Div. 6-632.05-M1
5. *Cursor Design*, Frederick V. Hunt, M 02.45.2-136, HUSL, Nov. 3, 1944. Div. 6-632.04-M17  
*Cursor Design and Angle Subtended by Submarine*, Harold P. Knauss, M 02.45.2-132, HUSL, Nov. 1, 1944. Div. 6-632.04-M16
6. *Continuously Visible Electronic Cursor*, Harold P. Knauss, M 02.45.2-197, HUSL, Mar. 12, 1945. Div. 6-632.04-M19
7. *Range Marking Circuit for CR Sonar*, Kenneth N. Fromm, M 02.452-59, HUSL, July 6, 1943. Div. 6-632.211-M5
8. *The Range Marking Circuit for the Scanning Submarine System*, Norman B. Saunders, M 02.453.2-50, HUSL, Aug. 17, 1944. Div. 6-632.04-M13  
*J. L. Hathaway Notebook*, p. 125, June 27, 1944.
9. *Repetition of CRO Echo Indications*, Harold P. Knauss, M 110.60-45, HUSL, May 28, 1943. Div. 6-632.04-M1
10. *Depth Determination with QH Sonar*, Roderic M. Scott, M 02.50-32, HUSL, Apr. 12, 1944. Div. 6-632.421-M1  
*Depth Scanning Sonar Proposed System (as of 3 July 1944)*, O. Hugo Schuck, M 02.50-57, HUSL, July 3, 1944. Div. 6-632.421-M3  
*Fire Control Sonar. Critique on Depth-Scanning System*, O. Hugo Schuck, M 02.50-81, M 02.50-88, HUSL, Aug. 3, 1944, Aug. 7, 1944. Div. 6-632.421-M6  
*Depth Scanning Sonar; Proposed System*, Robert B. Watson, M 02.50-106, M 02.50-147, HUSL, Sept. 12, 1944, Mar. 3, 1945. Div. 6-632.421-M13
11. *Minutes of Twelfth Conference on Integrated Sonar Systems held 29 March 1945*, H 302 (12), HUSL, Apr. 19, 1945, p. 3. Div. 6-632.41-M9
12. *A Continuous Range and Bearing Mechanical Indicator*, John D. Lane, M 110.60-114, HUSL, Apr. 13, 1944. Div. 6-632.04-M8  
*Mechanical Oscilloscope for QH Sonar*, William T. Bartholomew, M 80-131, HUSL, May 24, 1944. Div. 6-632.04-M10

13. *Operational Accuracy of XQHA, With and Without BDI: With Stationary Echo-Repeater Target*, Robert E. Kirkland, M 02.45.4-165, HUSL, June 13, 1945.  
Div. 6-632.222-M13
14. *Sonar Doppler Applications*, OEMsr-287, OSRD 6558, NDRC 6.1-sr287-2069, HUSL, Nov. 15, 1945.  
Div. 6-631.3-M5
15. *Ultimate System Scanning Sonar. Own Doppler Nullifier Considerations*, O. Hugo Schuck, M 02.311.3-95, HUSL, Oct. 17, 1944.  
Div. 6-632.421-M9
16. *Slant Range Correction Recorder*, Hugh E. Harlow, Benjamin A. Wooten, and Dwight E. Gray, OEMsr-287, NDRC 6.1-sr287-1707, HUSL, July 15, 1944. Div. 6-644.21-M12  
*British A/S 393 Recorder Handbook*, Figure 9, B-364.
17. *Handbook for Type 147B ASDIC*, British Report, B-363.
18. *Automatic Target Training*, NDRC 6.1-sr287-2067, HUSL, Aug. 15, 1945.  
Div. 6-631.21-M14
19. *Bearing Deviation Indicator*, OSRD 6425, NDRC 6.1-sr287-2075, HUSL, Nov. 1, 1945. Div. 6-631.4-M1  
*Listening Systems for Patrol Craft*, NDRC 6.1-sr692-1698, BTL, Dec. 1, 1944. Div. 6-622.1-M5  
*Comparison of Bearing Deviation Indicator Systems*, Malcolm H. Hebb, Gerald I. Harrison, and Nelson M. Blachman, NDRC 6.1-sr287-1549, HUSL, May 20, 1944.  
Div. 6-631.41-M7
20. *Time-Variied Gain for Sonar Equipment*, OSRD 5340, NDRC 6.1-sr287-2076, HUSL, June 15, 1945.  
Div. 6-631.11-M3
21. *Reverberation-Controlled Gain for Sonar Equipment*, OSRD 5415, NDRC 6.1-sr287-2079, HUSL, July 15, 1945.  
Div. 6-631.12-M5
22. *Bearing Deviation Indicator*, OSRD 6425, NDRC 6.1-sr287-2075, HUSL, Nov. 1, 1945. Div. 6-631.4-M1
23. *Radio, Radar, and Sonar Equipments—General Requirements*, 916-925-240A/930D, RE 13A 554E, U. S. Navy Bu-Ships.
24. *Field Trip of the Aide de Camp, August 5, 1944*, David C. Whitmarsh, M 02.453.4-28, HUSL, Aug. 7, 1944.  
Div. 6-632.312-M4  
*Pulse Tailoring for Sonar Systems*, Frederick V. Hunt, M 02.45-202, HUSL, Aug. 12, 1944. Div. 6-632.01-M5
24. *Tailored Pulses in Sonar Transmitters*, Frederick V. Hunt, M 02.45.2-214, HUSL, July 10, 1945. Div. 6-632.01-M9  
*Detection of Scanning Sonar on Submarine by Surface Vessels*, Malcolm H. Hebb, M 02.453-92, HUSL, Aug. 11, 1944. Div. 6-632.0-M16  
*Scanning Sonar Doppler Due to Rotation of Pattern*, Gerald I. Harrison, M 02.45.1-16, HUSL, May 10, 1944.  
Div. 6-632.61-M1
25. *Miscellaneous Studies in Electrical Transmission Networks*, OSRD 6582, NDRC 6.1-sr287-2088, HUSL, Nov. 15, 1945.  
Div. 6-632.62-M16
26. *Temperature Compensation of QH Sonar Oscillator*, Robert L. Cumberow, M 02.45.7-108, HUSL, Sept. 21, 1944.  
Div. 6-632.01-M6
27. *Pro-Submarine Timer*, Reuben H. Wallace, M 02.453.2-90, HUSL, Nov. 8, 1944. Div. 6-632.02-M10
28. *Developments in Spiral Sweeps*, F. Burton Jones and Roderic M. Scott, M 02.45-31, HUSL, Mar. 13, 1943.  
Div. 6-632.02-M2
29. *Spiral Sweep Synchros at 30 rps*, F. Burton Jones, M 02.45-118, HUSL, Jan. 14, 1944. Div. 6-632.02-M5
30. *The Range Marking Circuits for the Scanning Submarine System*, Norman B. Saunders, M 02.453.2-50, HUSL, Aug. 17, 1944. Div. 6-632.04-M13
31. *Appearance of 90° Minor Lobes in Scanning Sonar Transducer Patterns*, Thomas P. Merritt and Francis P. Bundy, M 02.45.7-90, HUSL, May 13, 1944. Div. 6-632.61-M2
32. *Magnetostriction Transducers and High Power Supersonic Pulsing*, Frederick V. Hunt, Roger Hickman, Malcolm H. Hebb, and others, M 01.213-171, HUSL, Mar. 4, 1944.  
Div. 6-632.01-M4
33. *Magnetostriction Transducers*, NDRC. Summary Technical Report, Division 6, Volume 13.
34. *Capacitive Commutators*, F. Burton Jones and Reuben H. Wallace, M 02.452-86, HUSL, Oct. 5, 1944.  
Div. 6-632.211-M8

## CHAPTER 3

1. *Reverberation Studies at 24 kc*, NDRC 6.1-sr30-401, UCDWR, Nov. 23, 1942. Div. 6-520.0-M2
2. *Predicted Maximum Listening Ranges in Sonic and Supersonic Listening to Submarines and Surface Ships*, J. W. Emling and M. T. Dow, BTL, Aug. 30, 1943.  
Div. 6-580.1-M1
3. *Computed Maximum Echo and Detection Ranges for Submarine Echo-Ranging Gear*, William B. Snow and Edward Gerjuoy, NDRC 6.1-sr1131-1688, CUDWR, July 1944.  
Div. 6-580.0-M2
4. *Sound Ranges Under the Sea, 1944*, NDRC 6.1-sr1131-1880, CUDWR, November 1944. Div. 6-500.0-M2
5. *The Discrimination of Transducers Against Reverberation*, NDRC 6.1-sr30-968, UCDWR, May 31, 1943.  
Div. 6-520.1-M8
6. *Memos on Telegraph Theory, Submarine Detection, Reverberation in Sea Water, etc.*, Harry Nyquist and Kenneth W. Pfleger, III J (b) 18-10, BTL, Oct. 20, 1941 to Apr. 3, 1942.  
Div. 6-632.0-M1 Div. 6-540.2-M1  
Div. 6-632.0-M2 Div. 6-510.12-M2  
Div. 6-632.0-M4 Div. 6-570.4-M1  
Div. 6-632.0-M5 Div. 6-570.3-M1  
Div. 6-632.0-M6 Div. 6-570.1-M1  
Div. 6-632.0-M7 Div. 6-520.1-M4  
Div. 6-632.0-M8 Div. 6-520.1-M5  
Div. 6-632.0-M9 Div. 6-520.1-M6  
Div. 6-570.4-M2 Div. 6-570.31-M1  
Div. 6-520.1-M3 Div. 6-570.2-M2  
Div. 6-520.1-M2 Div. 6-520.11-M1
7. *Effect of Doppler on Echo Detection*, British Internal Report 81, OSRD WA-262-10, HMA/SEE, Fairlie Report, May 7, 1942.



8. *Speech and Hearing*, Harvey Fletcher, D. Van Nostrand Co., New York, N. Y., 1929.
9. *Telegraph Signaling. Aural Reception vs. Others*, R. S. Alford, 3410-RSA-MS, BTL, July 2, 1942. Div. 6-570.31-M2
10. *The Detection of an Echo in the Presence of Reverberation*, Carl F. Eckart, NDRC C4-sr30-175, UCDDR, May 12, 1942. Div. 6-570.32-M1
11. "Auditory Patterns," Harvey Fletcher, *Reviews of Modern Physics*, Vol. 12, Jan. 1940, pp. 47-65.
12. *Conference with Hector Willis of Fairlie*, O. Hugo Schuck, M 02.13-5, HUSL, June 20, 1944. Div. 6-632.0-M15
13. *Figure of Merit of QH Gear*, Charles A. Ewaskio, M 02.45.7-123, HUSL, Nov. 1, 1944. Div. 6-632.0-M20
14. *The Attenuation of Sound in the Sea*, Carl F. Eckart, NDRC 6.1-sr30-1532, UCDDR, July 6, 1944. Div. 6-510.22-M4
15. *Directivity Ratio of Long Sources*, Gerald I. Harrison, M 01.21-96, HUSL, Oct. 9, 1944. Div. 6-632.0-M19
16. *Maximum Echo Ranges in Shallow Water*, Technical Memorandum 5, CUDWR, Oct. 21, 1944. Div. 6-580.1-M5
17. *Bottom Reverberation in Very Shallow Water*, NDRC 6.1-sr30-1845, UCDDR, Aug. 18, 1944. Div. 6-520.21-M5
18. *Calibration of the 94111A, 94120, and 94211A Transducers and the 100-Inch Dome Used in the QGA Echo-Ranging System*, F. H. Graham, NDRC 6.1-sr1130-1626, CUDWR, June 7, 1944. Div. 6-556.1-M24
19. *Figure of Merit vs. Ship's Speed. Figure of Merit of QH Model II on November 19, 1944*, Charles A. Ewaskio, M 02.45.7-138, HUSL, Nov. 22, 1944. Div. 6-632.212-M19
20. *Power Output of QH Model II and Sensitivity of Installed Monitor on the Cythera*, Charles A. Ewaskio, M 02.45.7-131, HUSL, Nov. 10, 1944. Div. 6-632.212-M18
21. *Application of BDI to XQHA. Tests*, Robert E. Kirkland, M 02.45.4-153 HUSL, May 7, 1945. Div. 6-632.222-M10
22. *Report on Directivity Patterns of Sound Sources*, Walter O. Pennell, Malcolm H. Hebb, and others, NDRC 6.1-sr287-089, HUSL, Apr. 29, 1942. Div. 6-551.0-M2
23. *Principles of Naval Architecture*, Rossell and Chapman, Society of Naval Architects and Marine Engineers, 1942, Vol. II, R 5.9.
24. *Roll, Pitch, and Mast Deflection Characteristics*, G. J. Maslach, MIT Radiation Laboratory, Dec. 15, 1943. Div. 6-632.21-M1
27. *Volume Reverberation. Scattering and Attenuation vs. Frequency*, OSRD 1555, NDRC 6.1-sr30-670, UCDDR, Apr. 13, 1943. Div. 6-520.3-M1
28. *Prediction of Sound Ranges from Bathythermograph Observations*, NavShips 943-C2, March 1944.
2. *Sonic Locator Development II—MR Sonar. The Rotoscope*, NDRC 6.1-sr287-1346, HUSL, Feb. 5, 1944. Div. 6-632.11-M12
3. *An Anecdotal History of the Rotoscope to December 28, 1942*, Harold P. Knauss, M 02.451-27, HUSL, June 18, 1943. Div. 6-632.11-M11
4. *Field Test on Monday, July 27, 1942*, Harold P. Knauss, M 02.451(I).40-5, HUSL, July 27, 1942. Div. 6-632.12-M1
5. *MR Sonar as a Listening Device, Field Tests of August 21, 1942*, O. Hugo Schuck and James F. Bacon, M 02.451(I).40-11, HUSL, Aug. 27, 1942. Div. 6-632.12-M2
6. *Pleasure Bay, September 15, 1942*, Harold P. Knauss and Roland K. Blumberg, M 02.451(I).40-17, HUSL, Sept. 16, 1942. Div. 6-632.12-M3
7. *Rotoscope Field Trip off Spectacle Island, Friday, September 18, 1942*, Harold P. Knauss, M 02.451(I).40-19, HUSL, Sept. 21, 1942. Div. 6-632.12-M4
8. *Rotoscope Field Test, September 23, 1942*, Harold P. Knauss and Arthur L. Besse, M 02.451(I).40-21, HUSL, Sept. 24, 1942. Div. 6-632.12-M5
9. *Rotoscope Report on Tippy Model, October 6, 1942*, Harold P. Knauss, M 02.451(I)-18, HUSL, Oct. 6, 1942. Div. 6-632.11-M4
10. *Status Report: MR Sonar*, Harold P. Knauss and James F. Bacon, M 02.451-12, HUSL, Sept. 26, 1942. Div. 6-632.11-M3
11. *Rotoscope Conference, November 12 and 13, 1942*, Harold P. Knauss, M 02.451(II)-19, HUSL, Nov. 14, 1942. Div. 6-632.11-M5
12. *Installation of Rotoscope*, Harold P. Knauss, M 02.451(II).-50-9, HUSL, Dec. 15, 1942. Div. 6-632.11-M7
13. *Rotoscope Field Trip, December 19, 1942, Egg Rock*, Harold P. Knauss, M 02.451(II).40-16, HUSL, Dec. 22, 1942. Div. 6-632.12-M8
14. *Rotoscope Field Trip, November 6, 1942*, Harold P. Knauss, M 02.451(II).40-11, HUSL, Nov. 6, 1942. Div. 6-632.12-M7
15. *Rotoscope Field Tests, January 8, 1943, off Nahant*, Harold P. Knauss, M 02.451(II).40-21, HUSL, Jan. 8, 1943. Div. 6-632.12-M10
16. *Final Tests on the Rotoscope, June 16, 1943*, F. Burton Jones and David C. Whitmarsh, M 02.451(II).40-42, HUSL, June 16, 1943. Div. 6-632.12-M14
17. *The Trip of the Aide de Camp, May 12, 1943*, Roderic M. Scott, M 02.451(II).40-37, HUSL, May 12, 1943. Div. 6-632.12-M13
18. *Range Accuracy and Range Scale for Rotoscope*, Harold P. Knauss, M 02.451(II)-27, HUSL, Jan. 11, 1943. Div. 6-632.11-M8
19. *Rotoscope Trip to Gloucester and Return*, David C. Whitmarsh, M 02.451(II).40-35, HUSL, May 10, 1943. Div. 6-632.12-M12
20. *Rotoscope Field Trips, December 29 and 30 [1942], January 2, 4 and 5, 1943*, Harold P. Knauss, M 02.451(II).40-20, HUSL, Jan. 5, 1943. Div. 6-632.12-M9

## CHAPTER 4

1. *Some Notes on Echo-Ranging Receiving Amplifiers with Special Reference to the Sonar Receiving Amplifier*, Roland K. Blumberg, M 02.45-18, HUSL, Dec. 14, 1942.

CONFIDENTIAL

21. *Demonstrations of the Rotoscope, Friday, March 12 and Monday, March 15, 1943*, Harold P. Knauss, M 02.451(II).60-10, HUSL, Mar. 16, 1943. Div. 6-632.12-M11
22. *Magnetostrictive Transducers*, Malcolm Hebb and Harvey Brooks, NDRC 6.1-sr287-898, HUSL, June 22, 1943. Div. 6-612.1-M2
23. *Construction and Characteristics of the MR Sonar 12x12-Inch Hydrophone*, Francis P. Bundy, M 02.451(II)-14, HUSL, Oct. 19, Nov. 9, and Dec. 9, 1942. Div. 6-632.12-M6
24. *SLC Brightening for CR Sonar*, F. Burton Jones and Roderic M. Scott, M 02.452-48, HUSL, May 28, 1943. Div. 6-632.211-M2
25. *Some Remarks on the Fundamental Problem of Distinguishing an Echo from Reverberation in Sonar Type Devices*, Roderic M. Scott, M 02.45-41, HUSL, May 4, 1943. Div. 6-632.0-M11
26. *Bearing Deviation Indicator*, OSRD 6425, NDRC 6.1-sr287-2075, HUSL, Nov. 1, 1945. Div. 6-631.4-M1
27. *Tests on SLC Brightening*, Roderic M. Scott and F. Burton Jones, M 02.45-44, HUSL, May 8, 1943. Div. 6-632.212-M3
28. *Rotoscope Conference, September 16, 1942*, Harold P. Knauss, M 02.451(II)-10, HUSL. Div. 6-632.11-M13
29. *Data and Operating Instructions for 1.5-kw Power Amplifier*, Neil E. Handel, M 110.40-12, HUSL, Mar. 24, 1943. Div. 6-632.01-M1
30. *Electronic Problems of MR Sonar*, Harold P. Knauss, M 02.451(II).20-6, HUSL, Aug. 28, 1942. Div. 6-632.11-M1
31. *Report on Electronic Spiral Sweep*, David C. Whitmarsh and Roland K. Blumberg, M 02.451(II)-33, HUSL, Jan. 27, 1943. Div. 6-632.02-M1
32. *Proposed Rotoscope for Detection of Small Targets at Short Ranges*, Harold P. Knauss, M 02.451(III)-7, HUSL, Nov. 21, 1942. Div. 6-632.11-M6
8. *Miscellaneous Echo Repeaters*, NDRC 6.1-sr287-2070, HUSL, Sept. 1, 1945.
9. *Receiver for Semmes Installation, Field Trip of Aide de Camp, October 7, 1943*, Roderic M. Scott, M 02.45.40-20, HUSL, Oct. 8, 1943. Div. 6-632.03-M1
10. *Field Trip of July 12, 1943*, Roderic M. Scott, M 02.452.4-20(2), HUSL, July 13, 1943. Div. 6-632.212-M4
11. *Preliminary Returns of the Field Trip of the Aide de Camp, to New London*, Roderic M. Scott, M 02.45.4-35(I), HUSL, Nov. 12, 1943. Div. 6-632.212-M6
12. *New London Results III. Sensitivity of CR Sonar*, Roderic M. Scott and Charles A. Ewaskio, M 02.45.4-35(III), HUSL, Dec. 10, 1943. Div. 6-632.212-M7
13. *New London Results IV*, Roderic M. Scott and Charles A. Ewaskio, M 02.45.4-35, HUSL, Dec. 16, 1943. Div. 6-632.212-M8
14. *CR/ER Sonar Installation on USS Sardonyx*, H 245, HUSL, Feb. 21, 1944. Div. 6-632.212-M10
15. *CR Sonar (QH Sonar) Demonstration on the Sardonyx Installation*, Robert B. Bowersox, M 02.452.4-52, HUSL, Mar. 9, 1944. Div. 6-632.212-M11
16. *Performance of HP-2 No. 1 on USS Sardonyx*, Cedric E. Hesthal, Francis P. Bundy, and Thomas P. Merritt, M 02.45.4-50, HUSL, Mar. 4, 1944. Div. 6-612.712-M5
17. *Bearing Accuracy of QH Sonar, Model I*, Harold P. Knauss, M 02.45.7-93, HUSL, June 19, 1944. Div. 6-632.212-M12
18. *Figure of Merit of QH Gear*, Charles A. Ewaskio, M 02.45.7-123, HUSL, Nov. 1, 1944. Div. 6-632.0-M20
19. *Torpedo Observation Test on USS Cythera, July 20 to August 18, 1944*, Franklin E. Lowance, Charles A. Ewaskio, and Roger W. Boom, M 02.45.4-83, HUSL, Sept. 7, 1944. Div. 6-632.0-M17
20. *Field Tests on Cythera, October 4, 1944*, Charles A. Ewaskio, Franklin E. Lowance, Allen Chernosky, and others, M 02.45.4-105, HUSL, Oct. 5, 1944. Div. 6-632.212-M15

## CHAPTER 5

1. *Project Report and Instruction Book for Model XQHA Sonar Equipment*, NDRC 6.1-sr1288-2117, Sangamo Electric Co., April 1945. Div. 6-632.221-M3
2. *Field Tests on Medusa*, Roderic M. Scott and F. Burton Jones, M 02.452.7-10, HUSL, Oct. 2, 1942. Div. 6-632.212-M1
3. *Medusa*, Roderic M. Scott and F. Burton Jones, M 02.452.7-12, HUSL, Oct. 8, 1942. Div. 6-632.63-M1
4. *Sonar Conference of October 14, 1942*, Harold P. Knauss, M 02.452-20, HUSL, Oct. 15, 1942. Div. 6-632.311-M1
5. *ER Sonar Field Trip, October 20, 1942 off Spectacle Island*, Roderic M. Scott and Harold P. Knauss, M 02.452.4-6, HUSL, Oct. 20, 1942. Div. 6-632.312-M2
6. *Operator Training Equipment, Models 2 and 10*, NDRC 6.1-sr287-2055, HUSL, Jan. 1, 1945. Div. 6-321.21-M4
7. *Developments in Spiral Sweeps*, F. Burton Jones and Roderic M. Scott, M 02.45.31, HUSL, Mar. 13, 1943. Div. 6-632.02-M2
21. *Figure of Merit vs Ship's Speed, Figure of Merit of QH Model II on November 19, 1944*, Charles A. Ewaskio, M 02.45.7-138, HUSL, Nov. 22, 1944. Div. 6-632.212-M19
22. *Activities on USS Babbitt, March 12 to March 17, 1945, Inclusive*, C. E. Houston, M 02.45.4-138(3), HUSL, Mar. 20, 1945. Div. 6-632.222-M5
23. *Activities on USS Babbitt for the week of February 26 to March 3, 1945*, C. E. Houston, M 02.45.4-138(1), HUSL, Mar. 6, 1945. Div. 6-632.222-M2
24. *Interference Measurements on USS Galaxy and USS Babbitt April 3 to April 10, 1945*, C. E. Houston, M 02.45.4-158, HUSL, May 31, 1945. Div. 6-632.222-M12
25. *Report on Tests of the Partially Complete Sangamo XQHA System at the HUSL Barge*, Francis P. Bundy, M 02.45.7-158, HUSL, Mar. 1, 1945. Div. 6-632.222-M1
- 25a. *Recommendations on Attenuation and Lag Lines for the Sangamo XQHA System*, Gerald I. Harrison, HUSL, Apr. 2, 1945. Div. 6-632.221-M4

26. *Tests of Sangamo HP-5 No. 3 Transducer*, Cedric E. Hesthal and Francis P. Bundy, M 02.45.7-159, HUSL, Mar. 26, 1945. Addendum to above, M 02.45.7-160, Mar. 26, 1945.  
Div. 6-612.714-M11
27. *Calibration of XQHA Scanning Sonar*, Leslie L. Foldy, NDRC 6.1-sr1130-2370, USRL, Sept. 10, 1945.  
Div. 6-554.4-M13
28. *Operator Training Equipment, Model 5, Modification of Sangamo QFA-5 Attack Teacher and Associated Equipment for Scanning Sonar Training*, NDRC 6.1-sr287-2062, HUSL, Nov. 1, 1945.  
Div. 6-632.05-M3
29. *Tests of Sangamo HP-5 No. 4 Transducer*, Ray Rast and Francis P. Bundy, M 02.45.7-161, HUSL, Mar. 22, 1945.  
Div. 6-612.714-M10
30. *Tests to be Made on XQHA System No. 1 on USS Galaxy*, O. Hugo Schuck and Leon G. S. Wood, M 02.45.4-140, HUSL, Mar. 16, 1945.  
Div. 6-632.222-M4
31. *Evaluation of Measurements Made on XQHA System No. 1 on USS Galaxy, March 19 to March 28, 1945*, Robert E. Kirkland, M 02.45.4-149, HUSL, Apr. 24, 1945.  
Div. 6-632.222-M8
32. *Correction of Graph No. 7 of Memo: Evaluation of Measurements Made on XQHA on USS Galaxy March 19 to 29, 1945, and April 24, 1945*, Robert E. Kirkland, M 02.45.4-155, HUSL, May 14, 1945.  
Div. 6-632.222-M11
33. *Intensity of a Target Echo*, C. E. Houston, M 01.80-11, HUSL, Apr. 16, 1945.  
Div. 6-632.0-M24
34. *Two-Channel Preamplifier for XQHA BDI*, Leon G. S. Wood, M 02.302-46, HUSL, Mar. 22, 1945.  
Div. 6-632.221-M2
35. *Results of Measurements on Two-Channel Preamplifier for XQHA BDI*, Leon G. S. Wood, M 02.45.7-165, HUSL, Apr. 10, 1945.  
Div. 6-632.221-M5
36. *Tests to be Made on XQHA Aboard USS Galaxy After Installation of Dual Channel Preamplifier*, Leon G. S. Wood, M 02.45.4-144, HUSL, Apr. 4, 1945.  
Div. 6-632.222-M7
37. *Application of BDI to XQHA. Tests*, Robert E. Kirkland, M 02.45.4-153, HUSL, May 7, 1945.  
Div. 6-632.222-M10
38. *Scanning Sonar XQHA. BDI Operational Tests*, O. Hugo Schuck, M 02.45.4-151, HUSL, Apr. 29, 1945.  
Div. 6-632.222-M9
39. *Activities on USS Babbitt, March 6-10, 1945, Inclusive*, C. E. Houston, M 02.45.4-138(2), HUSL, Mar. 13, 1945.  
Div. 6-632.222-M3  
*Activities on the USS Babbitt from March 19 to March 31, 1945*, C. E. Houston, M 02.45.4-138(4), HUSL, Apr. 3, 1945.  
Div. 6-632.222-M6
40. *Tests of Sangamo HP-5 No. 5 Transducer*, Jack C. Cotton, M 02.45.7-172, HUSL, May 7, 1945.  
Div. 6-612.714-M12
41. *Report on Tests of Transducer No. 6*, J. S. Martin to F. C. Holtz of Sangamo Electric Co., Sangamo 30, HUSL, May 9, 1945.  
Div. 6-632.52-M14
42. *Magnetostriction Transducers*, NDRC Summary Technical Report, Division 6, Volume 13.
43. *Medusa*, Roderic M. Scott and F. Burton Jones, M 02.452.7-13, HUSL, Oct. 13, 1942.  
Div. 6-632.212-M2
44. *Tests on the Hebbphone*, Roderic M. Scott, M 01.213-33, HUSL, Mar. 18, 1943.  
Div. 6-612.71-M7
45. *Comparison of Three Scanning Sonar Input Systems*, J. Lewis Hathaway, M 02.45.2-50, HUSL, Jan. 7, 1944.  
Div. 6-632.03-M3
46. *Transmission Measurements on HP-1 and HP-2*, F. Burton Jones, Cedric E. Hesthal, Lou Fein, and Aaron B. Powers, M 02.45.7-102, HUSL, Sept. 8, 1944.  
Div. 6-632.51-M4
47. *Results of the Analysis of the Admittance Data on the Individual HP-2 Stacks, Including the Selection and Arrangement of the Elements in HP-2—No. 1B*, Robert E. Payne, M 02.45.7-78, HUSL, Apr. 13, 1944.  
Div. 6-612.55-M15
48. *Construction and First Tests of the HP-2 No. 1 Transducer*, Francis P. Bundy, Cedric E. Hesthal, Thomas P. Merritt, and Arthur C. Clatfelter, M 02.45-161, HUSL, Mar. 21, 1944.  
Div. 6-612.712-M6
49. *Comparison Tests on Hebbphone I and Hebbphone II*, Thomas P. Merritt, Francis P. Bundy, F. Burton Jones, Arthur C. Clatfelter, and Cedric E. Hesthal, M 02.45.7-85, HUSL, May 2, 1944.  
Div. 6-612.711-M7
50. *Acoustic Patterns of the HP-2B Scanning Sonar Transducer on the USS Cythera*, Harold P. Knauss, Aaron B. Powers, and Francis P. Bundy, M 02.45.7-114, HUSL, Oct. 10, 1944.  
Div. 6-632.51-M5
51. *Construction and Performance of HP-4 No. 5 Experimental Scanning Sonar Stack*, Francis P. Bundy and Milton Carlson, M 02.45-200, HUSL, July 26, 1944.  
Div. 6-632.51-M2
52. *Tests of HP-3, No. 1 Transducer*, Mervin J. Foral and Francis P. Bundy, M 02.45.7-174, HUSL, May 23, 1945.  
Div. 6-612.713-M16
53. *Impedance of HP-3 Stacks*, Francis P. Bundy, M 02.50-116, HUSL, Oct. 5, 1944.  
Div. 6-612.713-M6
54. *Final Tests on Sangamo HP-5 No. 1*, Francis P. Bundy, M 02.45.4-135, HUSL, Feb. 27, 1945.  
Div. 6-612.714-M8
55. *Millerphone*, John D. Lane, M 01.213-105, HUSL, Nov. 2, 1943.  
Div. 6-612.8-M10
56. *Millerphone, (Casketphone)*, John D. Lane and Julius O. Natwick, M 01.213-127, HUSL, Dec. 10, 1943.  
Div. 6-612.8-M12
57. *Millerphone II Report*, John D. Lane, M 01.213-166, HUSL, Feb. 29, 1944.  
Div. 6-612.8-M13
58. *Tests on the 36-Element X-Cut Crystal Sonar Transducer Built by the San Diego Laboratory*, Robert E. Payne, M 02.452.70-28, HUSL, Sept. 27, 1943.  
Div. 6-632.52-M1
59. *Pattern Tests on CPI-1, No. 770, San Diego 36-Element Crystal Transducer*, William T. Bartholomew, Julius O. Natwick, and Harold P. Knauss, M 02.45.70-43, HUSL, Oct. 21, 1943.  
Div. 6-632.52-M2
60. *Further Tests on CPI-1 No. 770, Crystal Transducer*, Harold P. Knauss, M 02.45.70-46, HUSL, Nov. 5, 1943.  
Div. 6-632.52-M3

61. *Tests on CPI-1, No. 770, Crystal Transducer—III*, Harold P. Knauss, M 02.45.70-51, HUSL, Nov. 22, 1943. Div. 6-632.52-M4
62. *Air Gap Tolerances on Commutators for CR Scanning Sonar*, Clifford M. Wallis, M 02.452.7-36, HUSL, June 29, 1944. Div. 6-632.211-M8
63. *ER Sonar Field Trip off Spectacle Island*, Roderic M. Scott and Harold P. Knauss, M 02.452.40-5, HUSL, Oct. 16, 1942. Div. 6-632.312-M1
64. *Report on Commutated Rotation Sonar*, Harold P. Knauss, H 132, HUSL, May 5, 1943. Div. 6-632.11-M10
65. *Sonar Production Plans*, John S. Coleman, M 02.452.30-6, HUSL, Nov. 23, 1943. Div. 6-632.0-M13
66. *Tests on the Magnetic Compass Follower*, Roderic M. Scott, M 101.20-70, HUSL, Oct. 22, 1943. Div. 6-632.04-M5
67. *Progress on the Aide de Camp up to Friday, September 24th [1943]*, Roderic M. Scott, M 02.452.40 40, HUSL, Sept. 24, 1943. Div. 6-632.212-M5
68. *PPI Bearing Accuracy on 5-inch, 7-inch, and 12-inch Scopes*, Roger W. Boom, M 02.45.50-55, HUSL, May 31, 1944. Div. 6-632.04-M12
69. *PPI Tube Size Demonstration*, Robert B. Bowersox and Harold P. Knauss, M 02.45.6-10, HUSL, May 12, 1944. Div. 6-632.04-M9
70. *QH Sonar, Model 2, Serial 1. Installation on USS Cythera*, H 328, Sept. 13, 1944. Div. 6-632.212-M13
71. *QH Depth Scanning Sonar. Experimental Model. Installation on USS Cythera*, H 382, Mar. 1, 1945. Div. 6-632.421-M12
72. *Attack Plotters Mark I, Models 1 and 2*, BuOrd Pamphlet 1101, January 1944.
73. *Changes Made in the General Electric Attack Plotter (known as the ASAP)*, Robert B. Bowersox, M 80-165, HUSL, Mar. 19, 1945. Div. 6-632.05-M1
74. *The ASAP Installation on USS Cythera*, Robert H. Hughes, M 80-167, HUSL, Apr. 17, 1945. Div. 6-632.05-M2
75. *Some Notes on Echo-Ranging Receiving Amplifiers with Special Reference to the Sonar Receiving Amplifier*, Roland K. Blumberg, M 02.45-18, HUSL, Dec. 14, 1942.
76. *Laboratory Tests of Simultaneous Independent Lobe Comparison for CR Sonar, at 23 kc*, F. Burton Jones and Reuben H. Wallace, M 02.452.40-31, HUSL, Aug. 20, 1943. Div. 6-632.211-M6
77. *Measurements on the Tuned Radio Frequency Amplitude Receiver*, Andrew Patterson, Jr., M 02.45.70-41, HUSL, Oct. 19, 1943. Div. 6-632.03-M2
78. *Results of Tests of the Second Sonar Console Listening Amplifier*, Frank S. Replogle, M 02.452.20-60, HUSL, Mar. 11, 1944. Div. 6-632.03-M4
79. *Sonar Preamplifier Band-Pass Filter*, John O. Hancock, M 02.45.2-183, HUSL, Jan. 10, 1945. Div. 6-632.03-M7
80. *Appendix to John Hancock's Memorandum: Sonar Preamplifier Band-Pass Filter*, Malcolm H. Hebb, M 02.45.2-187, HUSL, Jan. 18, 1945. Div. 6-632.03-M8
81. *Sonar Doppler Applications*, OSRD 6558, NDRC 6.1-sr287-2069, HUSL, Nov. 15, 1945. Div. 6-631.3-M5
82. *CR Sonar Electronics*, Roderic M. Scott and Harold P. Knauss, M 02.452-52, HUSL, June 15, 1943. Div. 6-632.211-M3
83. *Status of QH Sonar Model 2 Aboard USS Cythera. (PY 31)*, J. Lewis Hathaway, William C. Marlow, Franklin E. Lowance, and Julius O. Natwick, M 02.45.5-15, HUSL, Sept. 30, 1944. Div. 6-632.212-M14
84. *QH Sonar Revisions and Measurements—New London*, Arthur C. Clatfelter and Aaron B. Powers, M 02.45-223, HUSL, Oct. 19, 1944. Div. 6-632.212-M16
85. *Temperature Compensation of QH Sonar Oscillator*, Robert L. Cummerow, M 02.45.7-108, HUSL, Sept. 21, 1944. Div. 6-632.01-M6
86. *Anchored Vessel Screening (Completion Report)*, NDRC 6.1-sr287-2057, HUSL, May 5, 1945. Div. 6-633.11-M7
87. *Pulse Shaping for High Duty Cycle Circuits*, Frederick V. Hunt, M 110.3-19, HUSL, July 4, 1943. Div. 6-632.01-M2
88. *DC Pulse Generator*, F. Burton Jones and Reuben H. Wallace, M 110.3-20, HUSL, July 16, 1943. Div. 6-632.63-M2
89. *Line Type Modulators (Radiation Laboratory Seminar, August 10 [1943])*, O. Hugo Schuck and Harold P. Knauss, M 02.45-76, HUSL, Aug. 11, 1943. Div. 6-632.62-M1
90. *Sharp Pulse High Power Transmitters*, Nelson Butz and F. Burton Jones, M 110-214, HUSL, Dec. 4, 1943. Div. 6-632.01-M3
91. *Miscellaneous Studies in Electrical Transmission Networks*, OSRD 6582, NDRC 6.1-sr287-2088, HUSL, Nov. 15, 1945. Div. 6-632.62-M16
92. *On the So-Called Bump-Back Filter Advocated by Professor Jones*, Claude W. Horton, M 110.3-203, HUSL, June 11, 1945. Div. 6-632.01-M8
93. *Pulse Tailoring for Sonar Systems*, Frederick V. Hunt, M 02.45-202, HUSL, Aug. 12, 1944. Div. 6-632.01-M5
94. *Tailored Pulses in Sonar Transmitters*, Frederick V. Hunt, M 02.45.2-214, HUSL, July 10, 1945. Div. 6-632.01-M9
95. *Report on Electronic Spiral Sweep*, David C. Whitmarsh and Roland K. Blumberg, M 02.451(II)-33, HUSL, Jan. 27, 1943. Div. 6-632.02-M1
96. *Knauss's Memorandum on Sonar Program, Dated January 25th, 1943*, Frederick V. Hunt, M 02.451(II)-35, HUSL, Jan. 31, 1943. Div. 6-632.211-M1
97. *Sonic Locator Development II, MR Sonar. The Rotoscope*, NDRC 6.1-sr287-1346, HUSL, Feb. 5, 1944. Div. 6-632.11-M12  
*Report on the Rotoscope and the Status of MR and ER Sonar Research*, Harold P. Knauss, H110, HUSL, Jan. 18, 1943. Div. 6-632.11-M9
98. *Rotoscope Conference, November 12 and 13*, Harold P. Knauss, M 02.451(II)-19, HUSL, Nov. 14, 1942. Div. 6-632.11-M5
99. *Sonar Conference, October 28, 1942*, Harold P. Knauss, M 02.45-14, HUSL, Oct. 29, 1942. Div. 6-632.311-M2

100. *Present Status of the ER Sonar Department*, Roderic M. Scott and F. Burton Jones, M 02.452-34, HUSL, Jan. 8, 1943. Div. 6-632.311-M3
101. *Spiral Sweep Synchros at 30 rps*, F. Burton Jones, M 02.45-118, HUSL, Jan. 14, 1944. Div. 6-632.02-M5
102. *Mechanical Recorder for Sonar*, John D. Lane, M 02.45-50, HUSL, June 12, 1943. Div. 6-632.04-M2
103. *CR Sonar Electronics Conference, June 16, 1943*, Harold P. Knauss, M 02.452-54, HUSL, June 19, 1943. Div. 6-632.211-M4
104. *Range Marking Circuit for CR Sonar*, Kenneth N. Fromm, M 02.452-59, HUSL, July 6, 1943. Div. 6-632.211-M5
105. *Sweep Requirements for Integrated B Sonar*, Norman B. Saunders, M 02.302-44, HUSL, Mar. 14, 1945. Div. 6-632.41-M8
106. *Chemical Recorder, Bearing Repeater, Automatic Training Applied to Sonar*, J. Lewis Hathaway, M 02.45-94, HUSL, Nov. 11, 1943. Div. 6-632.04-M6
107. *Aide de Camp Field Trip, December 29, 1943*, David C. Whitmarsh, M 02.452.40-20(27), HUSL, Dec. 29, 1943. Div. 6-632.212-M9
108. *San Diego Range Marking System*, Harold P. Knauss, M 110.3-27, HUSL, Sept. 22, 1943. Div. 6-632.04-M4
109. *Sonar Signal Injector*, Frederick V. Hunt, M 02.45.70-49, HUSL, Nov. 18, 1943. Div. 6-632.06-M1
110. *Stable Extended Range Linear Sweeps*, F. Burton Jones and Reuben H. Wallace, M 110-202, HUSL, Nov. 11, 1943. Div. 6-632.02-M4
111. *Linear Sweeps*, F. Burton Jones and Reuben H. Wallace, M 110-183, HUSL, Oct. 5, 1943. Div. 6-632.02-M3
112. *Use of Chemical Range Recorder with QH Sonar*, Harold P. Knauss, M 02.45-192, HUSL, May 26, 1944. Div. 6-632.04-M11
113. *Mechanical Sweep Circuit*, Kenneth N. Fromm, M 02.45.2-70, HUSL, Mar. 20, 1944. Div. 6-632.02-M6
114. *Sangamo Timer*, J. Lewis Hathaway, M 02.45.2-74, HUSL, Apr. 4, 1944. Div. 6-632.02-M7
115. *QH Sonar Devices Being Processed*, Hayward Henderson, M 02.45-177, HUSL, Apr. 28, 1944. Div. 6-632.0-M14
116. *Conference with Sangamo Electric Company Representatives, February 29*, Harold P. Knauss, M 02.452.3-18, HUSL, Mar. 2, 1944. Div. 6-632.221-M1
117. *Sangamo's Cursors and Range Recorders*, Frederick V. Hunt, M 02.45-225, HUSL, Oct. 20, 1944. Div. 6-632.04-M15
118. *Continuously Visible Electronic Cursor*, Harold P. Knauss, M 02.45.2-197, HUSL, Mar. 12, 1945. Div. 6-632.04-M19
1. *Relationships between Ship and True Coordinates*, W. A. Mersman, R L Report 8, MIT, Apr. 8, 1944. Div. 6-632.41-M1
2. *Train Rates in a Two-Axis Director*, H. W. James, RL Report 8, MIT, Sept. 18, 1943.
3. *Fire Control Sonar Critique on Depth-Scanning System*, O. Hugo Schuck, M 02.50-88, HUSL, Aug. 7, 1944. Div. 6-632.421-M6
4. *Depth-Scanning Sonar; Proposed System (as of 3 July 1944)*, O. Hugo Schuck, M 02.50-57, HUSL, July 3, 1944. Div. 6-632.421-M3
5. *Combined Minutes of Series of Conferences Held in Washington, July 13-15, 1944*, H 298, HUSL, July 17, 1944. Div. 6-632.41-M2
6. *QH Depth Scanning Sonar (Experimental Model) Installation on USS Cythera*, H 382, HUSL, Mar. 1, 1945. Div. 6-632.421-M12
7. *The 26-kc Projectors for Aide de Camp*, Gerard W. Renner, M 02.45-228, HUSL, Nov. 2, 1944. Div. 6-632.51-M7
8. *Comments on the Monitor Hoist to be Installed on the Cythera*, Roderic M. Scott, M 02.331.5-27, HUSL, Feb. 26, 1944. Div. 6-632.06-M2
9. *Additional Comments on the Monitor Hoist Which Has Been Installed on the Cythera*, Roderic M. Scott, M 02.331.5-33, HUSL, Mar. 13, 1944. Div. 6-632.06-M3
10. *Measurements on the 26-kc Depth-Scanning System on USS Cythera*, Robert B. Watson, M 02.507-12, HUSL, Feb. 17, 1945. Div. 6-632.422-M2
11. *Measurements on HP-3DS as Installed on USS Cythera*, Robert B. Watson, M 02.507-21, HUSL, Mar. 3, 1945. Div. 6-612.713-M11
12. *Portable Polar Chart Recorder*, NDRC 6.1-sr287-2060, HUSL, Sept. 15, 1945. Div. 6-553.5-M2
13. *Construction and First Tests of the Magnetostrictive Scanning Sonar Transducer, HP-3DS*, Robert B. Watson and Francis P. Bundy, M 02.502-6, HUSL, Dec. 13, 1944. Div. 6-632.51-M8
14. *Transmitting Patterns for Installed Depth-Scanning Transducer on USS Cythera*, Robert B. Watson, M 02.507-25, HUSL, Mar. 14, 1945. Div. 6-632.422-M8
15. *Vertical Patterns and Ping Pressures of Transmitting Beams, 26-kc DSS, on USS Cythera*, Charles R. Rutherford, Cassius M. Clay, and Robert A. Westervelt, M 02.507-34, HUSL, May 28, 1945. Div. 6-632.422-M12
16. *Measurements of the Depth-Scanning System on USS Cythera*, Robert B. Watson, M 02.507-22, HUSL, Mar. 8, 1945. Div. 6-632.422-M5
17. *Strength of Ocean Bottom Echoes off Florida East Coast Using 26-kc DSS*, Cassius M. Clay and Robert A. Westervelt, M 02.80-14, HUSL, May 24, 1945. Div. 6-632.422-M11
18. *Progress Report on USS Cythera*, Charles R. Rutherford, M 02.504-18, HUSL, Apr. 11, 1945. Div. 6-632.422-M10
19. *Submarine Runs with Directional and Nondirectional Transmitting Beams, 26-kc DSS, on USS Cythera*, Cassius M. Clay, M 02.507-40, HUSL, June 18, 1945. Div. 6-632.422-M13

## CHAPTER 6

CONFIDENTIAL

20. *Measurements Made with 26-kc DSS on USS Cythera*, Charles A. Ewaskio, M 02.507-14, HUSL, Feb. 21, 1945.  
Div. 6-632.422-M3
21. *Acoustical Power and Figure of Merit of 26 kc DSS System and Bottom Echo Strength*, Charles A. Ewaskio, M 02.507-8, HUSL, Feb. 12, 1945.  
Div. 6-632.422-M1
22. *Figure of Merit vs Ship's Speed. Figure of Merit of QH Model II on November 19, 1944*, Charles A. Ewaskio, M 02.45.7-138, HUSL, Nov. 22, 1944.  
Div. 6-632.212-M19
23. *Log of HUSL Observations, USS Cythera, February 8 to 12, 1945*, Cassius M. Clay, M 02.504-12(1), HUSL, Mar. 3, 1945.  
Div. 6-632.422-M4
24. *Log of HUSL Operations on USS Cythera, February 27-March 3, 1945*, Neil E. Handel, M 02.504-12(4), HUSL, Mar. 10, 1945.  
Div. 6-632.422-M7
25. *Log of HUSL Operations on USS Cythera, February 13 through February 17, [1945]*, Robert C. Morton, M 02.504-12(2), HUSL, Mar. 8, 1945.  
Div. 6-632.422-M6
26. *Directional Transmission for Depth Scanning*, Robert B. Watson, M 02.502-40, HUSL, Apr. 5, 1945.  
Div. 6-632.421-M15
27. *Transmission Pattern for Constant Echo Strength*, Gerald I. Harrison, M 01.75-15, HUSL, Mar. 26, 1945.  
Div. 6-632.61-M5
28. *Directional Transmission for Depth Scanning*, Frederick V. Hunt, M 02.502-20, HUSL, Feb. 15, 1945.  
Div. 6-632.421-M10
29. *Directional Transmitting Beam for Scanning Sonar*, O. Hugo Schuck, M 02.502-25, HUSL, Feb. 19, 1945.  
Div. 6-632.421-M11
30. *Arrangement for Beam-Forming Transmission for Depth Scanning*, Robert B. Watson, M 02.502-45, HUSL, Apr. 13, 1945.  
Div. 6-632.421-M18
31. *Magnetostriction Transducers*, NDRC Summary Technical Report, Division 6, Volume 13.
32. *Sonar-Lamination Dimensions as Functions of the Number of Sections*, Nelson M. Blachman, M 01.213-203, HUSL, June 26, 1944.  
Div. 6-632.51-M1
33. *Minutes of Second Conference on Ultimate Sonar System, Held July 27, 1944*, H 302(2), HUSL, July 27, 1944.  
Div. 6-632.41-M3
34. *The Scanning-Sonar Depth-Angle Transducer Lamination*, Nelson M. Blachman, M 02.50-97, HUSL, Aug. 18, 1944.  
Div. 6-632.51-M3
35. *Construction and First Tests of Magnetostrictive Scanning Sonar Transducer, HP-8D No. 2*, Leon W. Camp and Robert B. Watson, M 02.502-50, HUSL, July 3, 1945.  
Div. 6-632.51-M9
36. *The HP-8 Laminated Stacks*, Leon W. Camp, M 01.213-302, HUSL, Feb. 5, 1945.  
Div. 6-612.715-M3
37. *Cable for Ultimate Type B and Submarine Systems*, Robert B. Watson, M 02.502-43, HUSL, Apr. 12, 1945.  
Div. 6-632.421-M17
38. *Cable for Depth Scanning Transducer Supplied by Collyer Wire and Cable Co.*, Robert B. Watson, M 02.502-31, HUSL, Mar. 1, 1945.  
Div. 6-632.53-M4
39. *Scanning Sonar Transducer Cable*, Hugh E. Harlow, M 02.45.2-204, HUSL, May 11, 1945.  
Div. 6-632.53-M6
40. *Trip to Bell Telephone Laboratories on the Question of HP-8 Cable*, Hugh E. Harlow, M 02.502-10, HUSL, Jan. 15, 1945.  
Div. 6-632.53-M3
41. *Water Seal for 100-Conductor Cable*, Alan H. Selker, M 110.1-163, HUSL, Dec. 6, 1944.  
Div. 6-632.53-M1
42. *Cable Seals for HP-8 Cable*, Hugh E. Harlow, M 02.502-8, HUSL, Jan. 3, 1945.  
Div. 6-632.53-M2
43. *Method for Sealing Collyer 50-Pair Flexible, Blocked Cable*, Alan H. Selker, M 02.502-36, HUSL, Mar. 9, 1945.  
Div. 6-632.53-M5
44. *Tests of Sangamo HP-5 No. 5 Transducer*, Jack C. Cotton, M 02.45.7-172, HUSL, May 7, 1945.  
Div. 6-612.714-M12
45. *Depth Scanning Sonar Indicator, Orthogonalization of*, O. Hugo Schuck, M 02.50-107, HUSL, Sept. 12, 1944.  
Div. 6-632.421-M7
46. *Experimental Work on Orthogonalization*, Robert H. Hughes, M 02.50-149, HUSL, Apr. 11, 1945.  
Div. 6-632.421-M16
47. *Study of Differences Between Commutators No. 1 and No. 2 of the Depth Scanning System*, Robert H. Hughes, M 02.507-28, HUSL, Mar. 23, 1945.  
Div. 6-632.422-M9
48. *Results of Measurements of Two Channel Preamplifier for XQH-4 BDI*, Leon G. S. Wood, M 02.45.7-165, HUSL, Apr. 10, 1945.  
Div. 6-632.221-M5
49. *Loud Speakers for Sonar Equipment*, Neil E. Handel and John D. Watt, M 02.45.7-135, HUSL, Nov. 18, 1944.  
Div. 6-632.03-M6
50. *Stabilization System for Depth Scanning Sonar*, Robert B. Watson, M 02.50-85, HUSL, Aug. 4, 1944.  
Div. 6-632.421-M5
51. *Minutes of Tenth Conference on Integrated Sonar Systems Held February 1, 1945*, H 302(10), HUSL, Feb. 8, 1945.  
Div. 6-632.41-M5
52. *Minutes of Eleventh Conference on Integrated Sonar Systems Held March 1, 1945*, H 302(11), HUSL, Mar. 8, 1945.  
Div. 6-632.41-M6
53. *Integrated Sonar System*, Hayward W. Henderson, M 02.30-203, HUSL, Mar. 12, 1945.  
Div. 6-632.41-M7
54. *Notes on Details of Depth Scanning Console*, Hayward W. Henderson, M 02.302-28, HUSL, Sept. 28, 1944.  
Div. 6-632.421-M8
55. *Trip to Washington and Conference There on Fire-Control Equipment for Ultimate Sonar, November 21, 1944*, Robert B. Watson, M 80-161, HUSL, Nov. 24, 1944.  
Div. 6-632.41-M4
56. *Attack Directors and Attack Aids, Review Report on Depth Charge Trials of Projects Nos. 108, 109, 110, 111, and 144*, ASDD/S68, ASDevLant, Jan. 3, 1945.
57. *Sonar Preamplifier Band-Pass Filter*, John O. Hancock, M 02.45.2-183, HUSL, Jan. 10, 1945.  
Div. 6-632.03-M7

58. *Bearing Deviation Indicator*, OSRD 6425, NDRC 6.1-sr287-2075, HUSL, Nov. 1, 1945. Div. 6-631.4-M1
59. *Integrated B Sonar, Sweep Requirements for*, O. Hugo Schuck, M 02.302-42, HUSL, Mar. 8, 1945. Div. 6-632.421-M14

## CHAPTER 7

1. *Instruction Manual for Submarine Scanning Sonar System XQKA*, File 369, HUSL, Feb. 1945. Div. 6-632.311-M12
2. *Preliminary Returns of the Field Trip of the Aide de Camp to New London*, Roderic M. Scott, M 02.45.4-35(1), HUSL, Nov. 12, 1943. Div. 6-632.212-M6
3. *New London Results II, Event B, November 3, 1943. ER Sonar*, Roderick M. Scott, M 02.45.4-35(II), HUSL, Nov. 17, 1943. Div. 6-632.312-M3
4. *The 3-Foot Sphere Echo Ranging Data*, Thomas P. Merritt, Roderic M. Scott, and David C. Whitmarsh, M 02.453.4-60, HUSL, Nov. 10, 1944. Div. 6-632.312-M7
5. *Field Trip of the Aide de Camp*, David C. Whitmarsh, M 02.453.4-28, HUSL, Aug. 7, 1944. Div. 6-632.312-M4
6. *Pulse Tailoring for Sonar Systems*, Frederick V. Hunt, M 02.45-202, HUSL, Aug. 12, 1944. Div. 6-632.01-M5
7. *The 53-kc ER Sonar System at Mountain Lakes Reference Laboratory*, Thomas P. Merritt and Arthur C. Clatfelter, M 02.453.7-22, HUSL, Aug. 21, 1944. Div. 6-632.312-M5
8. *ER Installation on USS Dolphin*, Reuben H. Wallace, Robert B. Bowersox, and Andrew Patterson, Jr., M 02.453.5-11, HUSL, Apr. 10, 1945. Div. 6-632.311-M14
9. *Answer to "Thyrte Protection for Input Circuits" by F. V. Hunt, March 5, 1945*, Robert B. Bowersox, M 110.3-181, HUSL, Mar. 6, 1945. Div. 6-632.03-M9
10. *Submarine Transducers and Lighting Systems*, Harold E. Nash, M 02.453.2-140, HUSL, Mar. 15, 1945. Div. 6-632.52-M8
11. *Installation and Tests of the XQKA Scanning Sonar System on the USS Dolphin*, Andrew Patterson, Jr., M 02.453.4-80, HUSL, May 30, 1945. Div. 6-632.312-M8
12. *Report on Data Obtained from Brush AX-104 Crystal Transducer*, Thomas P. Merritt, M 02.45.7-91, HUSL, June 14, 1944. Div. 6-632.52-M5
13. *Spy Pond Measurements on AX-132, No. 1*, Thomas P. Merritt and Roderic M. Scott, M 01.211-69, HUSL, Dec. 26, 1944. Div. 6-632.52-M6
14. *Preliminary Measurements Made at Spy Pond on AX-132, No. 2*, Stanley R. Rich, M 02.453.7-55, HUSL, Mar. 26, 1945. Div. 6-632.52-M9
15. *Tests on Brush AX-132, No. 3*, James J. Faran, Jr., M 02.453.7-65, HUSL, Apr. 27, 1945. Div. 6-632.52-M10
16. *Tests on Brush AX-132, No. 4*, James J. Faran, Jr., M 02.453.7-74, HUSL, May 23, 1945. Div. 6-632.52-M16
17. *Tests on Brush AX-132, No. 5*, James J. Faran, Jr., M 02.453.7-66, HUSL, Apr. 28, 1945. Div. 6-632.52-M11
18. *Tests on Brush AX-132, No. 6*, James J. Faran, Jr., M 02.453.7-70, HUSL, May 9, 1945. Div. 6-632.52-M13
19. *Preliminary Measurements on AX-136, No. 1*, Robert B. Bowersox, M 02.453.7-53, HUSL, Mar. 6, 1945. Div. 6-632.52-M7
20. *Efficiency of AX-136 Transducers*, Harold E. Nash, M 02.453.3-49, HUSL, June 21, 1945. Div. 6-632.52-M20
21. *Reason for Return of AX-136, No. 3 Transducer to Brush*, James J. Faran, Jr., M 02.453.7-68, HUSL, May 4, 1945. Div. 6-632.52-M12
22. *Tests on Brush AX-136, No. 2*, James J. Faran, Jr., M 02.453.7-72, HUSL, May 16, 1945. Div. 6-632.52-M15
23. *Tests on Brush AX-136, No. 4*, James J. Faran, Jr., M 02.453.7-78, HUSL, June 4, 1945. Div. 6-632.52-M17
24. *Further Tests on Brush AX-136, No. 2*, James J. Faran, Jr., M 02.453.70, HUSL, June 6, 1945. Div. 6-632.52-M18
25. *Tests on Brush AX-136, No. 5*, James J. Farran, Jr., M 02.453.7-82, HUSL, June 11, 1945. Div. 6-632.52-M19
26. *Magnetostriction Transducers*, NDRC Summary Technical Report, Division 6, Volume 13.
27. *Varistors as Reactance Elements*, Stanley R. Rich, M 110.3-147, HUSL, Nov. 10, 1944. Div. 6-632.63-M8
28. *AX-89 No. 2 Varistor Rotor Tests*, Stanley R. Rich and M. S. McKittrick, M 02.453.7-49, HUSL, Feb. 14, 1945. Div. 6-632.63-M13
29. *Effect of Band-Pass Filters on a Pulse*, Gerald I. Harrison, M 110.3-183, HUSL, Mar. 20, 1945. Div. 6-632.03-M10
30. *A New Design for the Vacuum Tube Electronic Rotor*, Roderic M. Scott, M 02.453.2-66, HUSL, Oct. 2, 1944. Div. 6-632.63-M6
31. *New Electronic Rotors*, Stanley R. Rich, M 02.453.2-69, HUSL, Oct. 14, 1944. Div. 6-632.63-M7
32. *A New Switching System for ER Sonar*, Stanley R. Rich, M 02.453.2-28, HUSL, Feb. 22, 1944. Div. 6-632.63-M3
33. *Varistor Rotor Troubles*, Stanley R. Rich, M 02.45.2-126, HUSL, Feb. 12, 1945. Div. 6-632.63-M12
34. *ER Sonar. A New Sharp Beam System*, Stanley R. Rich, M 02.453.27, HUSL, July 12, 1943. Div. 6-632.311-M4
35. *Artificial Line of Low Distortion*, Claude W. Horton, M 110.3-78, HUSL, May 12, 1944. Div. 6-632.62-M4
36. *Design of Artificial Line of Low Distortion*, Claude W. Horton, M 110.3-83, HUSL, May 23, 1944. Div. 6-632.62-M5
37. *A New Artificial Line of Low Distortion*, Claude W. Horton, M 110.3-113, HUSL, Aug. 21, 1944. Div. 6-632.62-M7
38. *Maximum Echo Ranges and Listening Ranges for Submarine Scanning Sonar Gear*, Roderic M. Scott and Thomas P. Merritt, M 02.453-102, HUSL, Sept. 18, 1944. Div. 6-632.0-M18
39. *SLC without the S. A New Pattern Comparison Scheme for E R Sonar*, Stanley R. Rich, M 02.453-34, HUSL, Aug. 20, 1943. Div. 6-632.011-M5

40. *Interference Measurements USS Galaxy and USS Babbitt, April 3-April 10, 1945*, C. E. Houston, M 02.45.4-158, HUSL, May 31, 1945. Div. 6-632.222-M12
41. *Pro-Submarine Receivers*, Arthur C. Clatfelter, M 02.453.2-154, HUSL, Apr. 13, 1945. Div. 6-632.03-M11
42. *Tentative Specifications [of] Pro-Submarine Electronic Equipment*, J. Lewis Hathaway, M 02.453-79, HUSL, July 12, 1944. Div. 6-632.311-M8
43. *More Artificial Lines with Linear Phase Shifts*, Claude W. Horton, M 110.3-138, HUSL, Oct. 18, 1944. Div. 6-632.62-M10
44. *Magnetostriction Transducers and High Power Supersonic Pulsing*, Frederick V. Hunt, Roger W. Hickman, Malcolm H. Hebb, and Francis P. Bundy, M 01.213-171, HUSL, Mar. 4, 1944. Div. 6-632.01-M4
45. *Five Millisecond Pulse High Power Transmitter for ER Sonar Equipment Aboard the Aide de Camp*, David C. Whitmarsh and Andrew Patterson, Jr., M 02.453.2-120, HUSL, Jan. 17, 1945. Div. 6-632.01-M7
46. *Miscellaneous Studies in Electrical Transmission Network*, OSRD 6582, NDRC 6.1-sr287-2088, HUSL, Nov. 15, 1945. Div. 6-632.62-M16
47. *Use of Artificial Lines as a Power Supply*, Claude W. Horton, M 110.3-142, HUSL, Nov. 1, 1944. Div. 6-632.62-M11
48. *High Voltage Pulse Line*, Robert E. Payne, M 02.453.2-132, HUSL, Feb. 22, 1945. Div. 6-632.62-M13
49. *A Defense of Constant-K Pulse Lines and Their Designer*, Robert E. Payne, M 02.453.2-136, HUSL, Feb. 27, 1945. Div. 6-632.62-M14
50. *Low Impedance Pulsing Storage Lines for Submarine Sonar*, Francis R. Nitchie, M 110.3-204, HUSL, June 11, 1945. Div. 6-632.62-M15
51. *Stable Extended Range Linear Sweeps*, F. Burton Jones and Reuben H. Wallace, M 110-202, HUSL, Nov. 11, 1943. Div. 6-632.02-M4
52. *The Range Marking Circuit for the Scanning Submarine System*, Norman B. Saunders, M 02.453.2-50, HUSL, Aug. 17, 1944. Div. 6-632.04-M13
53. *ER Spiral Sweep Experiences and Comments*, Stanley R. Rich, M 02.453.2-38, HUSL, May 8, 1944. Div. 6-632.02-M8
54. *Modifications to ER Spiral Sweep*, Stanley R. Rich, M 02.453.2-41, HUSL, May 29, 1944. Div. 6-632.02-M9
55. *A Low Frequency Modulator*, John I. Evers and Stanley R. Rich, M 110-282, HUSL, May 10, 1944. Div. 6-632.62-M3
56. "Frequency Modulation of Resistance-Capacitance Oscillators," Maurice Artzt, *Proceedings of the Institute of Radio Engineers*, July 1944.
57. *The Range Marking Circuit for the Scanning Submarine System (Revised)*, Norman B. Saunders, M 02.453.2-60, HUSL, Sept. 6, 1944. Div. 6-632.04-M14
58. *Submarine Sonar System Range Marking Circuit. Tentative Instructions for Calibration and a More Detailed Explanation of the Operation of the Sweep Circuit*, Norman B. Saunders, M 02.453.2-77, HUSL, Nov. 3, 1944. Div. 6-632.04-M18
59. *Meeting in New York Office on Submarine Sonar Program, September 7, 1944*, Charles P. Boner, M 02.453-95, HUSL, Sept. 8, 1944. Div. 6-632.311-M9
60. *Pro-Submarine Requirements*, F. Burton Jones, M 02.45-119, HUSL, Jan. 15, 1944. Div. 6-632.311-M6
61. *Pulse Generator for the Electronic Rotor for the Scanning Submarine System*, Norman B. Saunders, M 02.453.2-55, HUSL, Aug. 29, 1944. Div. 6-632.63-M5
62. *Recommended Change in Pro-Submarine Rotor Design*, Stanley R. Rich, M 02.453.2-101, HUSL, Nov. 29, 1944. Div. 6-632.63-M9
63. *Pro-Submarine Timer*, Reuben H. Wallace, M 02.453.2-90, HUSL, Nov. 8, 1944. Div. 6-632.02-M10
64. *Sweep Requirements for Integrated B Sonar*, Norman B. Saunders, M 02.302-44, HUSL, Mar. 14, 1945. Div. 6-632.41-M8
65. *Range Marking Circuit for CR Sonar*, Kenneth N. Fromm, M 02.452-59, HUSL, July 6, 1943. Div. 6-632.211-M5
66. *Alignment of the Electronic Timer and Range Marking Circuit of the Submarine Scanning Sonar, Model II*, Norman B. Saunders, M 02.453.2-152, HUSL, Apr. 9, 1945. Div. 6-632.311-M13
67. *Mechanical Sweep Circuit*, Kenneth N. Fromm, M 02.45.2-70, HUSL, Mar. 20, 1944. Div. 6-632.02-M6
68. *Temperature Compensation of QH Sonar Oscillator*, Robert L. Cummerow, M 02.45.7-108, HUSL, Sept. 21, 1944. Div. 6-632.01-M6

## CHAPTER 8

1. *Magnetostriction Transducers*, NDRC Summary Technical Report, Division 6, Volume 13.
2. *Miscellaneous Studies in Electrical Transmission Networks*, OSRD 6582, NDRC 6.1-sr287-2088, HUSL, Nov. 15, 1945. Div. 6-632.62-M16
3. *Instruction Manual for HP-5 Trainable Artificial Transducer, Model 1*, File 465, HUSL, July 15, 1945. Div. 6-632.51-M10
4. *Portable Polar Chart Recorder*, NDRC 6.1-sr287-2060, HUSL, Sept. 15, 1945. Div. 6-553.5-M2
5. *Design of Potentiometer Phase Shifter for Phase Measurements over a Broad Frequency Band*, Robert L. Cummerow, M 110-373, HUSL, Mar. 5, 1945. Div. 6-632.06-M7
6. *Operating Instructions for ER Sonar Switching Test Unit*, M 02.453.4-83, HUSL, June 14, 1945. Div. 6-632.311-M15
7. *Polar Inverse Exponential Pattern Plotter for ER Sonar (Pepper)*, Norman B. Saunders, M 02.333-55, HUSL, Mar. 6, 1945. Div. 6-632.06-M8
8. *Artificial Projector*, NDRC 6.1-sr287-2054, HUSL, Sept. 1, 1945.
9. *Artificial Transducers for Scanning Sonar*, Robert E. Payne, M 91.20-242, HUSL, Oct. 30, 1944. Div. 6-632.51-M6
10. *Single Element Scanning Sonar Patterns*, Gerald I. Harrison, M 02.45.7-143, HUSL, Nov. 24, 1944. Div. 6-632.61-M3



11. *Equivalent Circuit for Magnetostrictive Transducers*, Robert E. Payne, M 01.213-213, HUSL, Aug. 3, 1944.  
Div. 6-612.31-M9
12. *Reverberation-Controlled Gain for Sonar Equipment*, NDRC 6.1-sr287-2079, HUSL, July 15, 1945.  
Div. 6-631.12-M5
13. *Time-Variied Gain for Sonar Equipment*, OSRD 5340, NDRC 6.1-sr287-2076, HUSL, June 15, 1945.  
Div. 6-631.11-M3
14. *Sonar Doppler Applications*, OSRD 6558, NDRC 6.1-sr287-2069, HUSL, Nov. 15, 1945.  
Div. 6-631.3-M5
15. *Sonar Signal Injector*, Frederick V. Hunt, M 02.45.70-49, HUSL, Nov. 18, 1943.  
Div. 6-632.06-M1
16. *Linear Sweeps*, F. Burton Jones and Reuben H. Wallace, M 110-183, HUSL, Oct. 5, 1943.  
Div. 6-632.02-M3
17. *Stable Extended Range Linear Sweeps*, F. Burton Jones and Reuben H. Wallace, M 110-202, HUSL, Oct. 11, 1943.  
Div. 6-632.02-M4
18. *Alignment of the Electronic Timer and Range Marking Circuit of the Submarine Scanning Sonar System, Model II*, Norman B. Saunders, M 02.453.2-152, HUSL, Apr. 9, 1945.  
Div. 6-632.311-M13
19. *Time Bases (Scanning Generators), Their Design and Development, with Notes on the Cathode-Ray Tubes*, O. S. Puckle, John Wiley and Sons, New York, N. Y., 1943.
20. *Tentative Specifications [of] Pro-Submarine Electronic Equipment*, J. Lewis Hathaway, M 02.453-79, HUSL, July 12, 1944.  
Div. 6-632.311-M8
21. *Program and Work Schedule for Submarine Scanning Sonar*, Roderic M. Scott, M 02.453-109, HUSL, Nov. 2, 1944.  
Div. 6-632.311-M10
22. *Pro-Submarine Requirements*, F. Burton Jones, M 02.45-119, HUSL, Jan. 15, 1944.  
Div. 6-632.311-M6
23. *Conference on Sangamo Specifications for CR Sonar*, Harold P. Knauss, M 02.452-78, HUSL, Feb. 1, 1944.  
Div. 6-632.211-M7
24. *Meeting in New York Office on Submarine Sonar Program, September 7, 1944*, Charles P. Boner, M 02.453-95, HUSL, Sept. 8, 1944.  
Div. 6-632.311-M9
25. *PPI Bearing Accuracy on 5-inch, 7-inch, and 12-inch Scopes*, Roger W. Boom, M 02.45.4-55, HUSL, May 31, 1944.  
Div. 6-632.04-M12
26. *Bearing Accuracy of QH Model I*, Harold P. Knauss, M 02.45.7-93, HUSL, June 19, 1944.  
Div. 6-632.212-M12
27. *Pattern Amplitude Uniformity in ER Sonar Rotor No. 1*, Robert L. Cumberow and David C. Whitmarsh, M 02.453.7-57, HUSL, Mar. 30, 1945.  
Div. 6-632.63-M14
28. *Sonar Conference, October 28, 1942*, Harold P. Knauss, M 02.45-14, HUSL, Oct. 29, 1942.  
Div. 6-632.311-M2
29. *Developments in Spiral Sweeps*, F. Burton Jones and Roderic M. Scott, M 02.45-31, HUSL, Mar. 13, 1943.  
Div. 6-632.02-M2
30. *Rotoscope Field Trips, December 29 and 30 [1942], January 2, 4, and 5, 1943*, Harold P. Knauss, M 02.451(II).40-20, HUSL, Jan. 5, 1943.  
Div. 6-632.12-M9
31. *Aide de Camp Field Trip, December 29, 1943*, David C. Whitmarsh, M 02.452.40-20(27), HUSL, Dec. 29, 1943.  
Div. 6-632.212-M9
32. *Spiral Sweep Synchros at 30 rps*, F. Burton Jones, M 02.45-118, HUSL, Jan. 14, 1945.  
Div. 6-632.02-M5
33. *MR Sonar Status*, Harold P. Knauss, M 02.451-6, HUSL, Sept. 4, 1942.  
Div. 6-632.11-M2
34. *Rotoscope. Report on "Tippy" Model*, Harold P. Knauss, M 02.451(1)-18, HUSL, June 12, 1943.  
Div. 6-632.11-M4
35. *Mechanical Recorder for Sonar*, John D. Lane, M 02.45-50, HUSL, June 12, 1943.  
Div. 6-632.04-M2
36. *Sangamo Timer*, J. Lewis Hathaway, M 02.45.2-74, HUSL, Apr. 4, 1944.  
Div. 6-632.02-M7
37. *The Range Marking Circuit for the Scanning Submarine System*, Norman B. Saunders, M 02.453.2-50, HUSL, Aug. 17, 1944; Revised, M 02.453.2-60, Sept. 6, 1944.  
Div. 6-632.04-M14
38. *Temperature Compensation of QH Sonar Oscillator*, Robert L. Cumberow, M 02.45.7-108, HUSL, Sept. 21, 1944.  
Div. 6-632.01-M6
39. *Instruction Manual for Submarine Scanning Sonar System, XQKA*, File 369, HUSL, Feb. 1945.  
Div. 6-632.311-M12
40. *Sweep Requirements for Integrated B Sonar*, O. Hugo Schuck, M 02.302-42, HUSL, Mar. 8, 1945.  
Div. 6-632.421-M14
41. *Project Report and Instruction Book for Model XQHA Sonar Equipment*, NDRC 6.1-sr1288-2117, Sangamo Electric Co., Springfield, Ill.  
Div. 6-632.221-M3
42. *Range Accuracy and Range Scale for Rotoscope*, Harold P. Knauss, M 02.451(II)-27, HUSL, Jan. 11, 1943.  
Div. 6-632.11-M8
43. *The Dynamic Monitor*, NDRC 6.1-sr287-2058, HUSL, Apr. 10, 1945.  
Div. 6-641.2-M6
44. *Submarine Sonar System Range Marking Circuit. Tentative Instructions for Calibration and a More Detailed Explanation of the Operation of the Sweep Circuit*, Norman B. Saunders, M 02.453.2-77 (5P), HUSL, Nov. 3, 1944.  
Div. 6-632.04-M18
45. *United States Navy Synchros, Ordnance Pamphlet 1303*.
46. *Attack Director III and Related Developments*, NDRC 6.1-sr287-2082, HUSL, Sept. 1, 1945.  
Div. 6-644.21-M13
47. *Review Report on Depth Charge Trials of Attack Directors and Attack Aids*, Projects 108, 109, 110, 111, 144, ASDD/S68, ASDevLant, Jan. 3, 1945.
48. *Tests to be Made on XQHA System No. 1 on USS Galaxy*, Leon G. S. Wood and O. Hugo Schuck, M 02.45.4-140, HUSL, Mar. 16, 1945.  
Div. 6-632.222-M4
49. *Tests to be Made on XQHA Aboard USS Galaxy After Installation of Dual Channel Preamplifier*, Leon G. S. Wood, M 02.45.4-144, HUSL, Apr. 4, 1945.  
Div. 6-632.222-M7

50. *Sound Gear Monitor. Underwater Sound Portable Test Equipment*, NDRC 6.1-sr287-2086, HUSL, Nov. 1, 1945. Div. 6-611.1-M9
51. *Operator's Manual for Underwater Sound Portable Testing Equipment, (Sound Gear Monitor), Model OAX*, File 177, HUSL, Oct. 1, 1943.
52. *Split Projector Test Unit*, NDRC 6.1-sr287-2051, HUSL, Dec. 1, 1944. Div. 6-611.14-M1
53. *New London Results II, Event B, November 3, 1943, ER Sonar*, Roderic M. Scott, M 02.45.40-35(II), HUSL, Nov. 17, 1943. Div. 6-632.312-M3
54. *Variation in Visual and Audio Echoes with QH Model II in Shallow Water*, Franklin E. Lowance, Robert M. Hughes, and Charles A. Ewaskio, M 02.45.4-118, HUSL, Nov. 8, 1944. Div. 6-632.212-M17
55. *Variation in Visual and Audio Echoes with QH Model II in Deep Water*, Charles A. Ewaskio and Franklin E. Lowance, M 02.45.4-126, HUSL, Dec. 9, 1944. Div. 6-632.212-M20
56. *The 3-Foot Sphere Echo Ranging Data*, Thomas P. Merritt, David C. Whitmarsh, and Roderic M. Scott, M 02.453.4-60, HUSL, Nov. 10, 1944. Div. 6-632.312-M7
57. *Figure of Merit vs Ship's Speed. Figure of Merit of QH Model II on November 19, 1944*, Charles A. Ewaskio, M 02.45.7-138, HUSL, Nov. 22, 1944. Div. 6-632.212-M19
58. *Torpedo Detection with QH Sonar*, NDRC 6.1-sr287-1954, HUSL, Jan. 15, 1945. Div. 6-632.0-M23
59. *An Analysis of Reflections from Submarines*, NDRC 6.1-sr1131-1846, CUDWR, Sept. 9, 1944. Div. 6-530.22-M9
60. *Measurements made with 26 kc DSS on USS Cythera*, Charles A. Ewaskio, M 02.507-14, HUSL, Feb. 21, 1945. Div. 6-632.422-M3
61. *Dentada Tests of Scanning Sonar XQKA*, Roderic M. Scott, M 02.453.4-70, HUSL. Div. 6-632.312-M9
8. *Circular Transducer Patterns*, Gerald I. Harrison, M 01.21-62, HUSL, Apr. 7, 1944. Div. 6-612.21-M14
9. *Scanning Sonar Pattern Computer*, O. Hugo Schuck, M 110-341, HUSL, Oct. 23, 1944. Div. 6-632.06-M5
10. *Sonic Locator Developments*, NDRC C4-sr58-047, HUSL, Dec. 29, 1941. Div. 6-632.0-M3
11. *Further Subdivision of Scanning Rotor to Achieve More Uniform Rotation of Beam*, Malcolm H. Hebb, M 02.45.1-31, HUSL, Apr. 19, 1945. Div. 6-632.61-M8
12. *Report on Tests of the Partially Complete Sangamo XQHA System at the HUSL Barge*, Francis P. Bundy, M 02.45.7-158, HUSL, Mar. 1, 1945. Div. 6-632.222-M1
13. *Total Attenuation Patterns*, Gerald I. Harrison, M 01.21-119, HUSL, Mar. 24, 1945. Div. 6-612.21-M32
14. *Design B for Scanning Sonar XQHA*, Gerald I. Harrison, M 02.45.1-26, HUSL, Apr. 14, 1945. Div. 6-632.221-M6
15. *Scanning Sonar Pattern Formation*, Gerald I. Harrison, M 02.45.1-27, HUSL, Apr. 14, 1945. Div. 6-632.61-M5
16. *Directivity Ratio of Long Sources*, Gerald I. Harrison, M 01.21-96, HUSL, Oct. 9, 1944. Div. 6-632.0-M19
17. *Construction and First Tests of Magnetostrictive Scanning Sonar Transducer HP-8D No. 2*, Leon W. Camp and Robert B. Watson, M 02.502-50, HUSL, July 3, 1945. Div. 6-632.51-M9
18. *Theoretical Scanning Sonar Patterns*, Gerald I. Harrison, M 02.45.1-22, HUSL, Jan. 19, 1945. Div. 6-632.61-M4
19. *Theoretical Scanning Sonar Patterns*, Gerald I. Harrison, M 02.45.1-29, HUSL, Apr. 16, 1945. Div. 6-632.61-M7
20. *Theory of ER Sonar*, Gerald I. Harrison, M 02.453-119, HUSL, Dec. 11, 1944. Div. 6-632.311-M11
21. *Plus or Minus Switching in ER Sonar*, Gerald I. Harrison, M 02.453-123, HUSL, Dec. 23, 1944. Div. 6-632.63-M11
22. *Ideal Switching Wave Form*, Stanley R. Rich, M 02.453.2-105, HUSL, Dec. 8, 1944. Div. 6-632.63-M10
23. *Harrison's 180° Reversals*, Stanley R. Rich, M 02.453.2-104, HUSL, Dec. 8, 1944. Div. 6-632.62-M12
24. *Scanning Sonar Doppler Due to Rotation of Pattern*, Gerald I. Harrison, M 02.45.1-16, HUSL, May 10, 1944. Div. 6-632.61-M1
25. *The  $\pi$  Lag Section Charts*, Nelson M. Blachman, M 110.70-13, HUSL, Jan. 28, 1944. Div. 6-632.62-M2
26. *Miscellaneous Studies in Electrical Transmission Networks*, OSRD 6582, NDRC 6.1-sr287-2088, HUSL, Nov. 15, 1945. Div. 6-632.62-M16
27. *Capacitive Commutators*, F. Burton Jones and Reuben H. Wallace, M 02.452-86, Technical Memorandum 37, HUSL, Oct. 24, 1944. Div. 6-632.211-M9
28. *A Lead Line With Attenuation*, Nelson M. Blachman, M 110.3-135, HUSL, Oct. 12, 1944. Div. 6-632.62-M9
29. *Notes on M-Derived Filters*, Claude W. Horton, M 110.3-119, HUSL, Sept. 8, 1944. Div. 6-632.62-M8

## CHAPTER 9

1. *Report on Directivity Patterns of Sound Sources*, Walter O. Pennell, Malcolm H. Hebb, and others, NDRC C4-sr287-089, HUSL, Apr. 29, 1942. Div. 6-551.0-M2
2. *Patterns of Radiators in Pressure-Release Baffles*, Gerald I. Harrison, M 01.21-65, HUSL, Apr. 12, 1944. Div. 6-612.21-M15
3. *Single Element Pattern of Cylindrical Transducer*, Gerald I. Harrison, M 01.21-68, HUSL, Apr. 28, 1944. Div. 6-612.21-M16
4. *Single Element Scanning Sonar Patterns*, Gerald I. Harrison, M 02.45.7-143, HUSL, Nov. 24, 1944. Div. 6-632.61-M3
5. *Pattern of a Sector of a Cylinder*, Gerald I. Harrison, M 01.21-107, HUSL, Nov. 14, 1944. Div. 6-612.21-M22
6. *Pattern of 270° and 90° Sectors (Really Correct)*, Gerald I. Harrison, M 01.21-115, HUSL, Feb. 26, 1945. Div. 6-612.21-M30
7. *Vibration and Sound*, Philip M. Morse, McGraw-Hill Book Co., New York, N. Y., 1936.

30. *Artificial Line of Low Distortion*, Claude W. Horton, M 110.3-78, HUSL, May 12, 1944. Div. 6-632.62-M4
31. *Design of Artificial Line of Low Distortion*, Claude W. Horton, M 110.3-83, HUSL, May 23, 1944. Div. 6-632.62-M5
32. *More Artificial Lines with Linear Phase Shifts*, Claude W. Horton, M 110.3-138, HUSL, Oct. 18, 1944. Div. 6-632.62-M10
33. *Use of Artificial Lines as a Power Supply*, Claude W. Horton, M 110.3-142, HUSL, Nov. 1, 1944. Div. 6-632.62-M11
34. *Communication Networks*, Volume II, Ernst A. Guillemin, John Wiley and Sons, New York, N. Y., 1943, pp. 477-480.
16. *Description of Standard Mechanical and Electrical Units Used in Ford Fire Control Instruments*, W. I. Tamlyn and J. M. Scutt, File V185, HUSL, June 17, 1940.
17. *Bearing Deviation Indicator*, OSRD 6425, NDRC 6.1-sr287-2075, HUSL, Nov. 1, 1945. Div. 6-631.4-M1
18. *Mechanical Geographic Attack Plotters*, NDRC 6.1-sr287-2061, HUSL, Jan. 15, 1945. Div. 6-644.13-M6
19. *Operational Training Equipment-5*, NDRC 6.1-sr287-2062, HUSL, Nov. 1, 1945.
20. *Attack Director, Mark III, and Related Developments*, NDRC 6.1-sr287-2082, HUSL, Sept. 1, 1945. Div. 6-644.21-M13

## CHAPTER 10

1. *Magnetostriction Transducers*, NDRC Summary Technical Report, Division 6, Volume 13.
2. *Pattern of a Sector of a Cylinder*, Gerald I. Harrison, M 01.21-107, HUSL, Nov. 14, 1944. Div. 6-612.21-M22
3. *Tests of HP-3, No. 1 Transducer*, Marvin J. Foral and Francis P. Bundy, M 02.45.7-174, HUSL, May 23, 1945. Div. 6-612.713-M16
4. *Further Subdivision of Scanning Rotor to Achieve More Uniform Rotation of Beam*, Malcolm H. Hebb, M 02.45.1-31, HUSL, Apr. 19, 1945. Div. 6-632.61-M8
5. *Scanning Sonar. Inductive Commutators*, O. Hugo Schuck, M 02.45.2-207, HUSL, June 15, 1945. Div. 6-632.63-M16
6. "The Magnetically Focused Radial Beam Vacuum Tube," A. M. Skellet, *Bell System Technical Journal*, April 1944.
7. *Report on Meeting at Federal Telephone and Radio Corporation on Special-Purpose Multi-Element Tubes*, Robert L. Cummerow, M 02.453.2-162, HUSL, May 17, 1945. Div. 6-632.63-M15
8. *Plus or Minus Switching in ER Sonar*, Gerald I. Harrison, M 02.453-123, HUSL, Dec. 23, 1944. Div. 6-632.63-M11
9. *ASW Technical Memorandum No. 33; PPI ASDIC*, R. F. Simons, NDRC 6.1-100 (33), OSRD, London (WA-1540-8"), Jan. 31, 1944.
10. *Status Report on Task No. 5. Effect of Short Pulse Lengths and Receiver Bandwidth on Echo Ranging*, Robert W. Kirkland, HUSL File BT 200, BTL, July 15, 1944. Div. 6-632.03-M5
11. *Low Impedance Pulsing Storage Lines for Submarine Sonar*, Francis R. Nitchie, M 110.3-204, HUSL, June 11, 1945. Div. 6-632.62-M15
12. *Ultimate System Scanning Sonar. Own Doppler Nullifier Considerations*, O. Hugo Schuck, M 02.311.3-95, HUSL, Oct. 17, 1944. Div. 6-632.421-M9
13. *Sonar Doppler Applications*, OSRD 6558, NDRC 6.1-sr287-2069, HUSL, Nov. 15, 1945. Div. 6-631.3-M5
14. *Time-Variied Gain for Sonar Equipment*, OSRD 5340, NDRC 6.1-sr287-2076, HUSL, June 15, 1945. Div. 6-631.11-M3
15. *Reverberation-Controlled Gain for Sonar Equipment*, OSRD 5415, NDRC 6.1-sr287-2079, HUSL, July 15, 1945. Div. 6-631.12-M5
21. *Automatic Target Training*, NDRC 6.1-sr287-2067, HUSL, Aug. 15, 1945. Div. 6-631.21-M14
22. *Skyatron Display Systems*, John S. Coleman, OSRD Liaison Office Reference Wa-2730-12, Aug. 24, 1944.
23. *Progress Report on Activities at Sylph, June 1943*, Carl M. Herget, M 02.314.30-39, HUSL, July 6, 1943. Div. 6-632.0-M12
24. *Fire Control Sonar. Critique on Depth-Scanning System*, O. Hugo Schuck, M 02.50-88, HUSL, Aug. 7, 1944. Div. 6-632.421-M6
25. *Studies of Optical Reflections from Submarine Models*, Part I, NDRC 6.1-sr1046-1053, MIT, Apr. 12, 1944; Part II, NDRC 6.1-sr1046-1668, MIT, Aug. 15, 1944. Div. 6-530.23-M4
26. *Operational Accuracy of XQHA; with and without BDI; with Stationary Echo-Repeater Target*, Robert E. Kirkland, M 02.45.4-165, HUSL, June 13, 1945. Div. 6-632.222-M13
27. *The Dependence of the Operational Efficacy of Echo-Ranging Gear on Its Physical Characteristics*, Henry Primakoff and M. J. Klein, NDRC 6.1-sr1130-2141, Mar. 15, 1945. Div. 6-551.0-M14
28. *Probable Effectiveness of Antisubmarine Attacks and Choice of Size and Type of Antisubmarine Barrages*, Louis B. Slichter, NDRC C4-sr20-054, CUDWR, Jan. 19, 1942.
29. *Bi-Weekly Report Covering Period December 24, 1944 to January 6, 1945*, NDRC 6.1-sr287-1964, HUSL, Jan. 8, 1945. Div. 6-632.0-M22
30. *Spotting with QH Sonar*, Harold P. Knauss, M 02.45.4-129, HUSL, Dec. 21, 1944. Div. 6-632.0-M21
31. *Miscellaneous Echo Repeaters*, NDRC 6.1-sr287-2070, HUSL, Sept. 1, 1945.
32. *Attack Directors and Attack Aids, Review Report on Depth Charge Trials of Projects 108, 109, 110, 111, 144, ASDD/S68; ASDevLant*, Jan. 3, 1945.
33. *ISGM Procedure for Tuning Driver and Receiver Quickly Under Way*, O. Hugo Schuck, M 02.331.4-38, HUSL, Mar. 21, 1944. Div. 6-632.06-M4
34. *Sound Gear Monitor. Underwater Sound Portable Test Equipment*, NDRC 6.1-sr287-2086, HUSL, Nov. 1, 1945, pp. 106-107. Div. 6-641.1-M9
35. *The Dynamic Monitor*, NDRC 6.1-sr287-2058, HUSL, Apr. 10, 1945. Div. 6-641.2-M6

CONFIDENTIAL

36. *Plotting of Scanning Sonar Transducer Pattern on Equipment Scope*, Charles R. Rutherford, M 02.45.7-129, HUSL, Nov. 9, 1944. Div. 6-632.06-M6
37. *Installation, Operation and Maintenance Instruction Book for Underwater Sound Attack Teachers, Model QFA and Model QFA-1*, NOs-94981, Sangamo Electric Co., Dec. 6, 1941. Div. 6-323.1-M1
38. *Operator Training Equipment, Model 5 (Modification of Sangamo QFA-5 Attack Teacher and Associated Equipment for Scanning Sonar Training)*, NDRC 6.1-sr287-2062, HUSL, Nov. 1, 1945. Div. 6-632.05-M3
39. *Some Remarks on the Fundamental Problem of Distinguishing an Echo from Reverberation in Sonar Type Devices*, Roderic M. Scott, M 02.45-41, HUSL, May 4, 1943. Div. 6-632.0-M11
40. *Tentative Research Program for Sonar. Points to be Discussed at the First Meeting of the Program Committee*, Roderic M. Scott, M 02.45-122, HUSL, Jan. 19, 1944. Div. 6-632.311-M7
41. *The Reverberation Equalizer*, George W. Downs, NDRC 6.1-sr30-692, UCDWR, Sept. 18, 1943. Div. 6-520.2-M2
42. *Observations of Echo Signals Obtained Using Variable Frequency Transmission*, Edwin M. McMillan, NDRC 6.1-sr30-208, UCDWR, July 4, 1942. Div. 6-510.3-M1
43. *Echo Detection of Small Targets*, H. F. Willis, D. W. Boston, and others, OSRD WA-1154-16, British Internal Report 145, HMA/SEE, Fairlie Report, Sept. 23, 1943.
44. *Depth Scanning Sonar. Phasing Network for a Two-Dimensional Array of Transducers*, Norman B. Saunders, M 02.50-50, HUSL, June 23, 1944. Div. 6-632.62-M6
45. *Acoustic Lens Scanning Sonar System*, O. Hugo Schuck, M 02.45-198, HUSL, July 17, 1944. Div. 6-632.421-M4
46. *Depth Scanning Sonar. Material for Acoustic Lens*, Norman B. Saunders, M 113.5-141, HUSL, June 30, 1944. Div. 6-632.421-M2
47. *Sonavision*, Roland K. Blumberg and David C. Whitmarsh, M24-5, HUSL, Feb. 22, 1943. Div. 6-632.0-M10

# CONTRACT NUMBERS, CONTRACTORS, AND SUBJECT OF CONTRACTS

<i>Contract Number</i>	<i>Name and Address of Contractor</i>	<i>Subject</i>
OEMsr-287	President and Fellows of Harvard College Cambridge, Massachusetts	Studies and experimental investigations in submarine and subsurface warfare.
OEMsr-1288	Sangamo Electric Company Springfield, Illinois	Engineering development of a sonar scanning system for shipboard installation and construction of three preliminary models of same.

#### SERVICE PROJECT NUMBER

The project listed below was transmitted to the Executive Secretary, NDRC, from the War or Navy Department through either the War Department Liaison Officer for NDRC or the Office of Research and Inventions (formerly the Coordinator of Research and Development), Navy Department.

<i>Service Project Number</i>	<i>Subject</i>
NS-142	Basic improvement of echo-ranging gear.

## INDEX

The subject indexes of all STR volumes are combined in a master index printed in a separate volume.  
For access to the index volume consult the Army or Navy Agency listed on the reverse of the half-title page.

- A scope, 26, 503
- Acoustic lens for three-dimensional scanning, 512
- Acoustic patterns
  - see* Directivity patterns
- Acoustic power radiated, relation to directivity ratio, 71
- Acoustic pulse modulation, 508
- Adcock antenna system, 5
- ADP crystal transducers
  - see* AX-132 transducer; AX-136 transducer
- ADP crystals, 478-479, 485
- Aided-tracking mechanisms, 275
- Air-gap tolerances on commutators for CR sonar, 148
- "All-around" search
  - see* Scanning sonar
- Alsimag used in sonar commutators, 154
- Ambient noise of the sea, 59-60, 68
- Ambient noise pressure, 73
- Ammonium dihydrogen phosphate, 478-479, 485
- Amplitude-brightening receiver, 174
- "Anchor" project, 200
- Annular search device, 4
- Anticipating gain control, 501
- Antisubmarine attack plotter (ASAP), 23, 43-44, 166, 216-218
- Antisubmarine ordnance, gunnery-type, 505
- Armour Institute of Technology, 421
- Artificial projector, 409
- Artificial ship, 421
- Artificial transducer, 395-399
- Artificial transducer line, 437
- Artificial water, 9, 392, 396
- A-scope, 26, 503
- Attack directors, 275, 421
  - see also* Fire control with sonar
- Attack plotters
  - ASAP, 43-44, 166
  - MGAP, 501
- Attack teacher, 126, 166, 421, 507
- Attack-search switch, 291
- Attenuation, total, 51
- Attenuation coefficient, 69
- Attenuation curve, 450
- Auditorium system, CR sonar, 119-120, 210
- Auditory indicators, 22, 27
- Automatic gain control for ER receivers, 355
- Automatic keying unit (AKU), 216
- Automatic target training (ATT), 502
- Automatic volume control (AVC), 8-9, 32, 92
  - see also* RCG circuit; TVG circuit
- AX-89 transducer, 49, 124, 142, 318, 334
- AX-104 transducer, 49, 311, 318
- AX-127 transducer, 49
- AX-132 transducer, 49, 313, 316, 319, 347
- AX-136 transducer, 49, 314-316, 323, 347
- AX-142 transducer, 49
- Azimuth scanning
  - see also* PPI
  - 26-kc sonar, 264-266
  - 38-kc sonar, 250-252
  - commutators, 264
  - directivity patterns, 425
  - transducer (H-5 modified), 250
- B scope, 27
- B19-J hydrophone, 316
- Bandwidth for ER receivers, 353
- Bathothermograph, 276
- BDI (bearing deviation indicator)
  - construction, 279-280
  - deflection curves, 286
  - distortion effect, 286
  - doppler shift compensation, 291
  - functions, 279, 502
  - gain control, 285
  - general principles, 227
  - heterodyne BDI systems, 28
  - improvement, 286
  - lag line lobe comparison, types X3 and X4; 29, 34-35, 97
  - phase shifting circuits, 279-280
  - phase-actuated locator (PAL), 28-29, 34-35
  - power supply, 283-284
  - RCG circuit, 284, 288-289
  - right-left indicator (RLI), 28-29, 34-35
  - search-attack switch, 291
  - sector scan indicator (SSI), 27, 34-35, 221, 502
  - sum-and-difference principle, 34, 227, 279
  - tests, 284-288, 409
  - types, 29
  - use as a monitor, 95-97
  - use with integrated type B sonar, 222, 289
  - use with searchlight sonar, 1
- use with 26 kc depth-scanning sonar, 226, 279-288
- varistor circuit, 280
- BDI brightening, 97
- Beam formation
  - see* Directivity patterns
- Beam patterns
  - see* Directivity patterns
- Beam rotation
  - see* Commutators
- Bearing accuracy, 430
- Bearing cursors, 24
- Bearing deviation indicator
  - see* BDI
- Bearing information
  - see* BDI; PPI
- Bearing repeaters, 29
- Binary counter-switching, 339
- Blanking PPI screen, CR systems, 206
- "Blockbusters" (transmitters), 191
- "Blocked" cables, 481
- Blocking, ER receivers, 358
- Bottom reverberation, 63, 66-68, 73
- Bottom scattering coefficients, 66
- B'r director train, 43
- Bridged T switching lag lines, 340
- Brightening pulse measurements, 418
- Brightening receiver, 278-279
- British Admiralty, preformed directivity patterns, 493
- British Navy sonar system, 4
- B'r'q-train order, 269
- Brush crystal transducers
  - AX-89; 49, 124, 142, 318, 334
  - AX-104; 49, 311, 318
- B-scope, 27
- Bump-back filters, 199
- C scope, 503
- Cable seals for transducers, 475
- Cables for scanning transducers, 481
- Caliper type of range-determining system, 418
- Capacitive commutators, 143-153
  - see also* Commutators
  - capacitive rings, 54-55
  - capacitor material, 54-55
  - Die-Block model, 144
  - Models 1-5; 146-153
  - Whirling Dervish, 144
- Capacitive rotation sonar
  - see* CR sonar
- Capacitive transmit-receive network, 345

- Cardboard commutator, 143
- Cathode-ray switching generator, 339
- Cathode-ray tubes
- choice of size, 25
  - dynamic range, 32
  - varying background intensity, 350
- Cavitation, 46
- Chemical range recorder
- functions, 28
  - use with Aide de Camp ER/CR system, 214
  - use with ER systems, 385
  - use with integrated type B sonar, 224
  - use with Model XQHA system, 166
  - use with QH sonar, Model I and Model 2; 214-215, 218
  - use with searchlight sonar, 1
- Circuit improvements recommended, 496-501
- anticipating gain control, 501
  - increasing ease of operation, 500
  - increasing receiver sensitivity, 497
  - increasing transmitted power, 497
- Circuits, electronic
- discriminator circuit, 385, 393
  - electronic timing circuits, 40
  - expander circuit for electronic sweep, 111-113
  - for relay elimination, 130
  - gain-control circuits, 116, 284-289, 355
  - Hartley oscillator circuit, 366
  - integrator circuit, 417
  - keying circuit, 203-204
  - Miller-effect circuit, 330
  - ODN circuit, 187, 409
  - PAL circuits, 35
  - ping-delay circuit, 106-110
  - pulse-sharpening circuit, 121
  - range marking circuit, 377, 379
  - RCG circuit, 116, 284-289
  - sweep circuit, 111
  - timing circuits, 40
  - trigger circuit, 78, 362, 417
  - TVG circuit, 355
  - varistor bridge circuits, 279, 290
  - X-3 and X-4 circuits for BDI, 34
- Circuit-testing meter and switch, 308
- Circular sweep tests, 416
- Circulatory control (definition), 379
- Code transmission for underwater communication, 40
- Coefficient of backward volume scattering, 64
- Commutated rotation scanning sonar
- see* CR sonar
- Commutators
- capacitive rings, 54-55
  - capacitor material, 54-55
  - cylindrical forms, 54
  - design, 50-55
  - for integrated type B sonar, 259-266
  - for 26-kc azimuth-scanning sonar, 264
  - for 26-kc depth-scanning sonar, 252-259
  - for 38-kc depth-scanning sonar, 259-263
  - for XQHA system, 54
  - multiple plate, 488
  - multi-scan, 487
  - oil filled, 487
  - plate forms, 54
  - plate material, 153-156, 488
  - preamplifier, 53
  - slip rings, 55
- Commutators, CR
- air-gap tolerances, 54
  - brushes, 54-55
  - connections to segments, 54-55
  - Dic-Block model, 144
  - double lag line coupling, 491
  - first cardboard model, 143
  - for early HUSL system, 7-8
  - general description, 3
  - input transformers, 51
  - interregister error, 53
  - lag line, 52
  - lag line designs, 252-259
  - metallizing plates, 154
  - Model I, 146
  - Model IB, 149
  - Model II, 147
  - Model III, 148
  - Model IV (cylindrical rotor), 149
  - Model V, 153
  - Model 5 (48 element, cylindrical), 252-259
  - pattern measurements, 393
  - recommendations for future research, 486
  - rotor, 50
  - smooth rotation of beam pattern, 486
  - stationary lag line, 492
  - stator, 50
  - tolerances, 487
  - "Whirling Dervish," 144
- Commutators, ER
- beam patterns, 394
  - discriminator adjustment, 393
  - general specifications, 55
  - mechanical requirements, 57
- Commutators, tests, 387-393
- assembly tests, 391
  - component tests, 387
  - input transformer measurements, 388
  - input impedance measurements, 387
  - lag line and lead line measurements, 389
  - phase shift measurements, 388
  - subassembly tests, 389
  - termination resistor tests, 389
  - transducer and commutator tested together, 403-406
- Commutators, types
- capacitive, 9, 50, 143-153
  - CR vs ER, 50
  - electronic rotation, 55
  - inductive, 50, 143, 489
- Console indicators
- for integrated type B sonar, 271
  - for QH sonar, Models 1 and 2; 157-162
- Control rack for integrated type B sonar, 271
- Copper oxide varistors, 17
- Corning Glass Works, 155
- Corrosion prevention in transducers, 475
- Counter
- use in timing, 417
  - use in Aide de Camp sweep circuits, 212
- CPI-1 transducer, 49, 141
- CR repeater scope, 349
- CR sonar, 116-221
- commutators, 143-155, 391
  - directivity patterns, 438, 486
  - elements, 116-118
  - evaluation, 220-221
  - experimental work, 118-128
  - figure of merit, 122-125
  - functions that require time control, 205
  - general description, 116-118
  - indicators, 116-118, 155-168
  - laboratory tests and equipment, 119-120
  - lag line design, 460
  - length of times between pings, 118
  - limitations, 303
  - mathematics of pattern formation, 439
  - Medusa, 118
  - operation, 116
  - own-doppler nullification, 117, 187, 497
  - PPI display, 117, 205
  - RCG circuit, 116
  - receivers, 116, 168-189
  - recommendations for future research, 221, 486
  - spiral sweep, 41, 205
  - storage of received energy, 494
  - sweep and timing circuits, 205-219
  - tests, 402, 404, 410, 416
  - tolerances, 487
  - torpedo detection with, 121, 124
  - transducers, 118, 128-143
  - transmitters, 116, 189-204
- CR sonar, recommendations, 486-492
- commutator plates, 486-487
  - commutators, 487
  - high-speed scanning, 487
  - inductive commutator, 489



- lag line, 491  
 multiple plate commutator, 488  
 pattern computer, 492  
 plate material for commutators, 488  
 slip rings, 490  
 smooth rotation of beam pattern, 486  
 tolerances, 487
- CR sonar, systems  
*see also* QH sonar  
 Aide de Camp system, 120-122  
 auditorium system, 119-120, 210  
 Model 1 CR/ER sonar, 122-125  
 Model 2 CR system, 125-126  
 XQHA system, 116, 126-128
- CR/ER console, Model 1; 122
- Crossed-dipole system, 5
- Cross-modulation, 408
- Crystal transducers  
*see* Transducers, crystal
- Cursors for depth-scanning display, 26
- Cylindrical radiators, 433
- Cylindrical transducer, 47
- Delayed lobe comparator (DLC), 121, 306, 356
- Depth charge detection with submarine ER sonar, 316
- Depth charge thrower, gun type, 277
- Depth-scanning display (DDS), 26
- Depth-scanning sonar, 26 kc, 226-241  
 BDI receiver, 227, 239, 279-288  
 bottom echo, 235-237  
 commutator, 252-259  
 components, 227  
 deep monitor, 229  
 design considerations, 226  
 directivity patterns, 230, 259  
 dome, 229  
 EPI scope, 229, 237  
 figure of merit, 238  
 historical summary, 14  
 indicator panel, 420  
 indicators, 162, 266-268  
 installation book, 229  
 installed sound gear monitor, 230  
 interference patterns, 234-235  
 lag lines, 254  
 maximum range, 238  
 ocean bottom echoes, 235  
 preamplifiers, 277  
 propeller noise, 238  
 QBF projector, 237  
 range recorder, 229  
 receiver, 185, 227, 239  
 recommendations, 241  
 scanning receivers, 277-279  
 signal circuits, 228  
 stabilization, 268-270  
 submarine runs, 237-238
- sweep circuits, 296-298
- synchro control and display circuits, 228
- tests on USS Cythera, 222, 230
- transducers, 222, 226-229, 241-250
- transmitter, 202, 292-295
- transmitting patterns, 234
- trunnion tilt corrector, 229
- Depth-scanning sonar, 38-kc, 259-263
- Depth-scanning sonar, operating tests, 431
- Depth-scanning transducers  
 HP-3DS, 226, 229, 241-245  
 HP-8D, 222, 245-250
- Detection of torpedo echoes, 124
- Die-Block model commutator, 144
- Directivity index, 60, 66
- Directivity patterns, 433-474  
 90° and 270° sectors, 438  
 commutator and transducer tests, 403-406  
 computer, 442, 492  
 CR sonar, 47, 438-455  
 cylindrical transducers, 47  
 depth-scanning sonar, 26 kc, 230  
 effect of baffle conditions, 449  
 effect of dome, 425  
 ER sonar, 49, 455-462, 492-496  
 Gaussian pattern, 439  
 horizontal patterns, 483  
 HP-1 transducer, 129-133  
 HP-3 transducer, 137  
 measurements used for testing transducers and commutators, 405-406  
 Medusa (transducer), 129  
 number of active elements, 452  
 pattern width, 443  
 phase shift requirements, 451  
 preformed patterns, 493  
 principles of formation, 47  
 receiving patterns, 47, 403-406, 425  
 reciprocity theorem, 433  
 rotatability, 443, 446  
 rotation doppler, 457  
 sector of a transducer cylinder, 433  
 sector pattern of minimum directivity ratio, 438  
 shading, 482  
 sharpness, 444  
 single-element patterns, 435  
 testing by adjusting sonar gain control, 507  
 time delay concept, 436  
 total attenuation pattern, 450  
 transducers, 433-438  
 transmitting patterns, 7, 425  
 vertical patterns, 44, 482
- Directivity ratio  
 HP-1 transducer, 129-133  
 HP-5 transducer, 138
- in transmission and reception, 453  
 minimum directivity ratio, 438, 442
- Director train (stabilized sight), 43
- Discriminator circuit, 385, 393
- Display for three-dimensional scanning, 512
- Dome, effect on receiving hydrophone pattern, 80
- Domes, lubricating solutions, 90
- Domes for scanning transducers, 485
- Doppler, rotational, 457
- Doppler shift corrections, 498
- Dynamic monitor, 214, 415, 418, 423
- Dynamic range of scanning receivers, 53, 358
- Echo detectability  
*see* Echo recognition
- "Echo injector," 9-10
- Echo ranging  
 acoustic power radiated, 71  
 basis of comparison, 76  
 calculations, 73  
 figure of merit, 76  
 optimum frequency, 20  
 roll and pitch of ship, 71
- Echo recognition, 59-76  
 effect of large targets, 76  
 effect of thermal gradients, 70  
 maximum detection ranges, 75  
 noise, 59-63, 68-69  
 probability formula with visual detector, 62-63  
 refraction, 70  
 reverberation, 63-68  
 target strength, 70  
 transmission loss, 69
- Echo storage, 494
- Echo-ranging paths, 67-68
- Echo-ranging systems  
*see* Scanning sonar systems
- Electric noise, 60, 68, 73, 426, 490
- Electrically rotated sonar  
*see* ER sonar
- Electroacoustic analogue of the television iconoscope, 512
- Electromechanical commutators  
*see* Commutators
- Electronic rotation scanning sonar  
*see* ER sonar
- Electronic spiral sweep for CR sonar, 207
- Electronic switches, 16, 55  
 multielement switch (pentagrid), 337  
 plate switching, 337  
 triode type, 337  
 varistor switch, 336
- Electronic switching improvements, 492
- Elevation angle, 269
- Elevation indicator (EI), 27
- Elevation order, 269

CONFIDENTIAL

- Elevation position indicator (EPI), 14, 27, 224, 229, 278
- Energy-storage systems for scanning-sonar transmitter, 36
- Eq-elevation angle, 269
- Eq-elevation order, 269
- ER rotors, 326-348
- 60 cycle rotor, 331, 343
  - 200 cycle rotor, 343
  - 500 cycle rotor, 343, 347
  - design details, 343
  - directivity patterns, 326
  - lead lines, 326, 331
  - mechanical construction, 346
  - parts, 326
  - rotation speed, 330
  - submarine systems rotor, 343
  - switches, 335
  - tests, 393-394
  - transmission lines, 339
  - transmit-receive networks, 344
- ER sonar, 303-385
- applications, 18
  - chart system for Aide de Camp, 73
  - commutators, 55-58
  - directivity pattern, 47, 455, 492
  - discriminator circuit, 385, 393
  - echo storage, 494
  - general description, 303-304
  - historical survey, 15-19
  - improvements in directivity patterns, 492-496
  - improvements in electronic switching, 492
  - indicators and controls, 348-353
  - lead lines, 331, 463
  - listening beam, 495
  - maximum detection ranges, 75
  - own-doppler nullification (ODN), 497
  - pulse lines, 370
  - range determination, 372, 418
  - receivers, 353-362
  - rotation doppler, 457
  - rotors, 326-348
  - scanning speed, 303
  - sector scanning, 494
  - spiral sweep, 41, 371
  - sweep and timing circuits, 371-385
  - sweep linearization and stabilization, 383
  - switching line, 465
  - transducers, 317-326
  - transmitters, 362-371
- ER sonar, 200 cycle system
- circuit testing meter and switch, 309
  - directivity patterns, 309
  - HP-1 transducer, 317
  - indicators, 349
  - lag line, 309
  - new equipment, 309
  - receiver, 359
  - rotor, 343
  - scanning ranges, 349
  - sweep and timing circuits, 372
  - tests on Aide de Camp, 308, 311
  - transmitter, 362
  - use in submarine, 312
- ER sonar, 500 cycle system
- AX-104 transducer, 49, 311, 318
  - detectability tests, 312
  - directivity patterns, 311
  - indicators, 350
  - receiver, 359
  - rotor, 343, 347
  - scanning ranges, 351
  - sweep and timing circuits, 373
  - tests, 312
  - transmitter, 367
- ER sonar, recommendations
- electronic switching, 492
  - listening channel, 495
  - multiple-layer lead lines, 493
  - phased switching, 493
  - preformed patterns, 493
  - sector scanning, 494
  - storage of received energy, 494
- ER sonar, systems
- 60 cycle systems, 304
  - 200 cycle system, 16
  - 300 cycle submarine sonar, 313
  - 500 cycle system, 311
  - 53 kilocycle system, 16, 359, 373
  - Aide de Camp installations, 15, 304
  - early systems, 9
  - model I CR/ER sonar, 122
  - submarine sonar, XQKA, 304
- ER sonar, tests
- circular sweep tests, 416
  - complete transfer network, 402
  - on Aide de Camp, 15
  - on Tippecanoe, 18
  - transmitter tests, 411
- Error integral, 71
- Expanded elevation indicator (EI), 27
- Expander circuit for electronic sweep, 111-113
- Federal Telephone and Radio Corporation, 492-493
- 53 kc ER sonar, 16, 359, 373
- Figure of merit, 507
- Aide de Camp CR system, 122
  - definition, 76
  - depth-scanning sonar, 26 kc, 238
  - measurement upon installation, 427
  - Model I CR/ER system, 124
  - Model II CR sonar system, 125
- Filters
- band-pass for capacitive commutators, 491
  - band-pass for preamplifier, 277
  - band-pass for 26 kc depth-scanning BDI receiver, 279
  - band-pass for XQKA, 361
  - bump-back, 199-204, 363
  - for QH sonar, 183
  - preamplifier, 183
  - tests on band-pass filters, 409
- Fire control with sonar
- accuracy limitations, 504-505
  - coordination, 506
  - damage control, 505
  - equipment, 275
  - for antisubmarine warfare, 504-505
  - for type B integrated sonar, 275
  - General Electric attack plotter, 44
  - general requirements, 43-44
  - gun type thrower for large charges, 277
  - Mark 4 attack director, 43-44, 275
  - ordnance, 504
- 500 cycle ER sonar
- see ER sonar, 500 cycle system
- Fixed-tuned signal frequency type receivers, 360
- FM sonar, 4
- Fogging of the PPI screen, 15
- Formulas
- CR sonar directivity pattern, 439
  - echo recognition probability, 62
  - ER sonar directivity pattern, 455
  - pattern of a sector of a cylinder, 433
- Frequency discriminator circuit, 56-57
- Frequency modulation, 508
- Frequency modulation (FM) sonar, 4
- Gain-control circuits
- RCG, 116, 284-289
  - sector-selective gain control, 501
  - TVG, 355
- Gaskets, corprene, 475
- Gaussian directivity pattern, 439
- Gencaseal insulation for transducer windings, 129
- General Electric attack plotter, 43-44, 166
- Geographic plotting, 23, 166
- German scanning systems, 5
- Gunnery-type antisubmarine ordnance, 505
- Gyro-compass converter unit, 228
- Hanovia Chemical Company, 154
- Hartley oscillator circuit, 366
- Harvard Underwater Sound Laboratory
- see HUSL
- Hebbphone 1 (HP-1), 10, 48, 120, 129, 306, 317
- Hebbphone 2 (HP-2), 48, 124, 133
- Hebbphone 2B (HP-2B), 48, 125, 133

- Hebbphone 3 (HP-3), 48, 136, 482  
 Hebbphone 3DS (HP-3DS), 48, 226, 241-245  
 Hebbphone 3S (HP-3S), 48, 317  
 Hebbphone 4 (HP-4), 48  
 Hebbphone 5 (HP-5), 48, 138, 250, 396  
 Hebbphone 6 (HP-6), 48  
 Hebbphone 7 (HP-7), 48  
 Hebbphone 8 (HP-8), 48  
 Hebbphone 8D (HP-8D), 222, 245-250  
 Hebbphone 9 (HP-9), 48  
 Heterodyne oscillator, 33  
 Hewlett-Packard oscillator, 92, 99-100  
 High power transmission, circuit improvements, 497  
 High speed scanning with CR sonar, 487  
 Horizontal scanning sonar  
   *see also* QH sonar  
   operating test procedure, 429  
 HP transducers  
   *see* Hebbphone  
 Human ear as noise detector, 61  
 HUSL, 1  
   indicator panel, 421  
   Mark III attack director, 421  
   modulation of acoustic pulses in water, 508  
 HUSL scanning system  
   *see* QH sonar  
 HUSL Spy Pond Calibration Station, 18  
 Hydrophones, crystal, 6 x 6 inch, 85
- Ideal detector (echo ranging), 61  
 Impedance, transducers, 47  
 Impedance networks, 398  
 Impedance ratio, 388  
 Indicators  
   A scope, 26, 503  
   arrangement, 29  
   auditory indicators, 27-28  
   B scope, 27  
   bearing deviation indicator; *see* BDI  
   bearing repeaters, 29  
   C scope, 503  
   captain's, 224  
   depth-scanning display, 25  
   design, 22, 30  
   EPI scope, 235  
   helmsman's, 224  
   mechanical oscilloscopes and recorders, 27  
   plan position indicator; *see* PPI  
   proposed improvements, 501-504  
   range recorders, 28  
   remote plan position indicator, 29  
   scope display, 26-27  
   skyatron, 502  
   tests, 413-419  
   tube size, 25  
   types, 22, 501
- Indicators for CR sonar, 155-168  
   commercial cathode-ray oscilloscope, 155  
   console, Model 1, 157  
   console, Model 2, 159  
   geographic plot, 166  
   MR indicator, 155  
   PPI - 7 in., 156  
   PPI - 12 in., 156  
   XQHA, 162  
 Indicators for ER sonar, 348-353  
   60 cycle ER sonar, 349  
   200 cycle ER sonar, 349  
   500 cycle ER sonar, 352  
   submarine ER sonar, 352  
 Indicators for integrated type B sonar, 13, 270  
 Indicators for MR scanning sonar, 90  
 Indicators for 26-kc depth-scanning sonar, 266  
 Inductive commutator, 50, 143, 489  
 Input transformer measurements on commutators, 387  
 Installation tests, 422-429  
   cross talk, 425  
   directivity patterns, 425  
   equipment needed, 422  
   figure-of-merit, 427  
   mechanical alignment, 427  
   noise level, 426  
   on experimental ships, 422-423  
   on service ships at Navy Yard, 428  
   receiver frequency response tests, 426  
   receiving sensitivity, 426  
 Installed sound gear monitor (ISGM), 136, 230, 506  
 Integrated type B sonar, 14, 43, 222-302  
   *see also* Depth-scanning sonar, 26 kc  
   accuracy, 300  
   azimuth equipment and operator, 224  
   BDI and listening equipment, 222, 224, 289  
   bearing accuracy, 222  
   chemical range recorder, 224  
   commutators, 252-266  
   console design, 271  
   control circuits for receiver, 290  
   control circuits for transmitters, 295  
   control rack, 271  
   depth operator, 224  
   depth scanning, 222, 300  
   disadvantages, 301  
   echo-ranging system, 299  
   EPI, 224  
   errors in operation of control circuits, 300  
   evaluation of system, 300-302  
   fire control, 226, 275-277  
   gain control, 291  
   general description, 222-226
- horizontal-scanning system, 222  
 indicators, 270-272  
 operation of system during attack, 224  
 own-doppler nullification (ODN), 500  
 PPI, 224  
 preamplifier, 288  
 range recorder, 271  
 receivers, 277-292  
 recommendations, 300  
 requirements, 222  
 speaker, 271  
 stabilization, 272-275, 419  
 sweep and timing circuits, 296-300  
 three-dimensional scanning, 512  
 training control, 275  
 transducers, 241-252, 479  
 transmitter, 292-296  
 uses, 300  
 work at HUSL, 300
- Integrator circuit, 417  
 International Projector Company, 84
- "Joy stick" training control, 503
- Ka/N (definition), 44  
 Keying circuit, 203-204  
 Kollsman two-phase synchro spiral sweep generator, 211
- L level angle, 43  
 Lag line  
   26-kc azimuth scanning, 264  
   38-kc depth-scanning sonar, 259  
   artificial transducer, 395  
   bridged T, switching, 340  
   CR sonar, 460, 492  
   ER sonar, 340  
   impedance, 52  
   in commutators, 50, 254
- Lead lines  
   ER sonar, 331, 463, 493  
   multiple-layer, 493
- Lead-line measurements for electronic rotors, 393  
 Librascope Corp., Mark VI attack director, 421  
 Line impedance, 52  
 Linear amplitude receiver, 121  
 Lissajous ellipse, 388  
 Lissajous method, 424  
 Listening receiver tests, 409  
 Listening receivers, 33  
 Listening rotor, Model 1B, 149  
 Lubricating solutions for domes, 90
- Magnetostrictive transducers  
   *see* Transducers, magnetostrictive  
 Maintenance of close contact (MCC), 483  
 Maintenance of scanning sonar equipment, 506

- Maintenance of true bearing (MTB), 13, 23, 117-118, 352
- Massachusetts Institute of Technology, artificial ship, 421
- Master-oscillator-power-amplifier (MOPA), 192
- Maximum echo range, 430
- Mechanical geographical attack plotter (MGAP), 501
- Mechanical rotation scanning sonar  
see MR sonar
- Mechanical sweep for Model 1 Rotoscope, 110
- Mechanical timer for QH scanning sonar, Model 2; 216
- Medusa, magnetostrictive transducer, 9, 48, 118, 128
- Metallizing methods for securing conducting surfaces on insulating plates, 154
- Microphonics, 60
- Miller-effect circuit, 330
- Millerphone, 48
- Mine detection with submarine ER sonar, 315
- Mine-field navigation with submarine scanning sonar, 431
- Model 1 CR/ER sonar, 122
- Modified plan position indicator (P<sup>2</sup>I), 27
- Modulation of acoustic pulses in water, 508
- Modulator for 53-kc ER sonar sweep circuit, 373
- Monitor transducer, 422
- Mountain Lakes test station, 127, 312
- Movie camera used to check displacement error of indicator panels, 420
- MR sonar, 77-115  
Aide de Camp installations, 8, 79, 170  
brightening, 97  
disadvantages, 114  
electronic sweep, 111  
elements, 77-78  
evaluation, 84  
experimental results, 79-84  
functions, 77  
historical summary, 8  
improvements, 82  
indicators, 90-92, 155  
mechanical sweep, 110  
noise tests, 80  
pattern of receiving hydrophone, 80  
ping control, 106  
power consumption, 81  
PPI display, 90  
range determination, 418  
receivers, 92-99  
recommendations for future research, 114-115  
reverberation studies, 83  
rotating rigs, 89-90
- Rotoscope; see Rotoscope, Model 1; Rotoscope, Model 2  
spiral sweep, 110-114  
Tippecanoe installations, 78  
transducers, 84-89, 190, 386  
transmitters, 99-110
- Multipole switch, 397
- "Musa" system, 5
- Mycalex as commutator plate material, 146, 153
- Mykroy as commutator plate material, 153
- Networks, transfer, 122, 399-403
- New London Laboratory, 34
- Noise  
ambient noise of the sea, 59, 68  
discrimination against, 60  
distinguishing characteristics, 59  
electric noise, 60, 68  
human ear as detector, 61  
"ideal" detector, 60-61  
measurements, 408, 425  
narrow bandwidth, 61  
receiver discrimination against, 497  
reverberation, 59  
self noise, 68  
ship noise, 59  
shrimp noise, 59-60  
sources, 32  
target noise, 59-60, 68  
tests for MR sonar, 78-80  
tests on the preamplifier, 406  
visual detector, 61
- Noise radial, 3
- Noise reduction in receivers, 497
- ODN circuit, 187, 409
- Omnidirectional search systems  
see Scanning sonar systems
- Operator training equipment (OTE), 120
- Ordnance considerations for scanning sonar, 504
- Orthogonalization, 258
- Output filters for ER receivers, 355
- Own-doppler nullification (ODN), 28, 117, 353, 497-499
- PAI circuit, 35
- Pattern computer for CR sonar, 492
- Pattern formation, scanning sonar  
see Directivity patterns
- Pattern of minimum directivity ratio, 47
- Pentagrid, 337
- Pentagrid convertor switch, 342
- Permanent magnet polarization of magnetostrictive transducers, 478
- Phase lags, 53
- Phase splitter, bridge type, 208
- Piezoelectric transducers  
see Transducers, crystal
- Ping control  
for CR sonar, 205  
for Rotoscope, 106-110
- Ping delay circuit, 106-110
- Pinging rate, 12
- Plan position indicator  
see PPI
- Plate switching, 336
- Plotting device, 502
- Pointer-matching fire control, 502
- Polar inverse exponential pattern plotter for ER sonar (PEPPER), 394
- Polyphase generators, 338
- Portable polar chart recorder (PPCR), 230, 394, 423
- Power storage lines, 472
- PPI (plan position indicator)  
advantages, 1  
bearing information, 23  
CR sonar, 117, 155  
design limitations, 20  
development at HUSL, 5  
geographic plot, 23  
integrated type B sonar, 222  
modified plan position indicator (P<sup>2</sup>I), 27  
MR scanning sonar, 89  
power supplies location, 30  
precision plan position indicator (P<sup>3</sup>I), 27  
range information, 24  
ship-centered, 23  
spiral sweep generation, 40-41  
tube size, 25  
use, 502
- Preamplifiers  
design requirements, 53  
filter for QH sonar, 183  
for 26 kc depth-scanning sonar, 277-292  
tests for scanning sonar, 406
- Precision plan position indicator (P<sup>3</sup>I), 27
- Pre-scanning sonar, 1
- Propeller noise, 60
- Pulse generators, 342
- Pulse lines for ER sonar, 370
- Pulse-sharpening circuit, 121
- Pyrex for commutator plates, 154
- Q of scanning transducers, 51, 485
- QBF projector, 237
- QC sonar, 1

- QFA-5 attack teacher, 166
- QH sonar  
   general description, 2  
   historical development, 5, 11  
   scanning rate, 2  
   tests, 11-14
- QH sonar, Model 1  
   indicator console, 157  
   listening receiver, 174  
   range determination, 214-215  
   scanning receiver, 174  
   sweep and timing circuits, 214  
   tests on USS Cythera, 124  
   transmitter, 193
- QH sonar, Model 2  
   attack plotter, 218  
   automatic keying unit, 216  
   BDI, 125  
   figure of merit, 76, 125  
   filter design, 183  
   HP-2B transducer, 133  
   maximum discovery range, 125  
   mechanical timer, 216  
   receiver, 181  
   tests on USS Cythera, 136  
   tests with submarine target, 255  
   timing and sweep circuits, 216  
   transmitters, 194, 203
- QL sonar, 4
- Radar methods of energy storage compared to sonar, 200
- Radiation patterns  
   *see* Directivity patterns
- Radio direction finding, 5
- Range determination  
   tests, 418, 429  
   with CR sonar, 206  
   with ER sonar, 372
- Range information from PPI, 24
- Range marker circuit, 121, 377, 379
- Range recorders, 28, 228, 271
- Range selector switch, 299, 377
- Ranging on a deep target, 276
- Ransome welding positioner, 421
- RC phase-shift type vacillator, 341-342
- RCG circuit, 116, 284-289
- Receivers  
   bandwidth, 31, 497  
   BDI receivers, 34, 279-291  
   design, 30-35  
   doppler effect, 31  
   frequency, 30  
   gain, 355, 497-498  
   gear control, 32  
   listening receivers, 33, 409  
   noise, 31-32  
   scanning receivers, 30, 407  
   sensitivity, 497  
   sum and difference BDI, 409  
   tests, 406-410, 426  
   tuning range, 31
- Receivers for CR sonar, 168-189  
   amplitude brightening receiver, 174  
   depth scanning sonar receiver, 185  
   QH sonar, Model 1; 174  
   QH sonar, Model 2; 181  
   receiver used with Aide de Camp  
     ER/CR sonar, 170  
   SIC brightening, 169  
   TRF type, 168  
   XQHA receivers, 185
- Receivers for ER sonar, 353-361  
   53-kc ER sonar, 359  
   60 cycle ER sonar, 358  
   200 cycle ER sonar, 359  
   automatic gain control, 355  
   bandwidth, 353  
   blocking, 358  
   delayed lobe comparison, 356  
   doppler shift, 355  
   dynamic range, 358  
   fixed-tuned signal frequency type, 360  
   output filters, 355  
   receiver gain, 355  
   submarine ER sonar, 360  
   Submarine Signal Co. receiver 755-J, 359  
   tuning frequency of range, 357
- Receivers for integrated type B sonar, 288-292  
   BDI listening receivers, 289  
   control circuits, 290  
   preamplifier, 288  
   scanning receivers, 288
- Receivers for MR sonar, 92-99  
   Rotoscope, Model 1; 92-93  
   Rotoscope, Model 2; 93-99
- Receivers for 26-kc depth-scanning sonar, 185, 277
- Receiving directivity index, 60
- Receiving patterns  
   *see* Directivity patterns
- Reciprocity theorem, 433
- Recognition differential (echo recognition), 62
- Recommendations for future research, 475-512  
   circuit improvements, 496-501  
   CR sonar, 221, 486-492  
   ER sonar pattern formation, 492-496  
   fire control, 277, 504-506  
   indicators, 501-504  
   integrated type B sonar, 301  
   maintenance, 506-508  
   modulation, 508  
   scanning sonar, 475-512  
   stabilization and fire control, 504-507  
   three-dimensional scanning, 509-512  
   transducer improvements, 475-486
- Remote plan position indicators, 29
- Reverberation  
   bottom reverberation, 66-68  
   characteristics of, 59  
   power transmitted, 71  
   sound intensity, 71  
   surface reverberation, 66-68  
   volume reverberation, 63-66
- Reverberation controlled gain (RCG)  
   circuit, 32, 116, 239, 278, 408
- Reverberation equalizer, 508
- Ring ladderphone, 48
- Ring stack transducers, 84, 325
- RLL receiver, 35
- Rochelle salt crystal transducers  
   AX-89 No. 2; 141, 318  
   AX-104; 49, 142, 318  
   CPI-1 No. 770; 141-142  
   impedance, 47
- Rotating hydrophone, 8
- Rotating rigs for MR sonar, 89
- Rotation doppler, 457
- Rotor segment tests for electronic rotors, 394
- Rotors, electronic  
   *see* ER rotors
- Rotoscope, Model 1; 78  
   indicators, 90, 92  
   mechanical sweep, 110  
   noise reduction, 82  
   ping control, 106  
   receiver, 92-94  
   rotating rigs, 89  
   test results, 82
- Rotoscope, Model 2; 79  
   evaluation, 84  
   electronic sweep, 111-114  
   indicators, 91-92  
   ping control, 106-110  
   proposed improvements, 83  
   receiver, 93-99  
   rotating rigs, 89  
   tests on components, 83
- Rubber for transducers, 475
- San Diego Laboratory, reverberation equalizer, 508
- Sangamo attack teacher, 126, 421
- Sangamo Electric Company  
   automatic keying unit, 216  
   chemical range recorder, 28  
   Model XQHA scanning sonar, 11, 116, 126, 138  
   scanning commutator, 264  
   timer for 53-kc ER sonar, 373
- Sawtooth sweep linearity tests, 415
- Scanning, three-dimensional, 509
- Scanning frequency, 20
- Scanning indicator (EPI), 241

CONFIDENTIAL

Unclassified

- Scanning receivers  
*see* Receivers
- Scanning sonar  
 advantages, 1  
 commutator design, 50-58  
 echo recognition, 59-76  
 electronic timing circuits, 40  
 fire-control information, 43  
 indicators and controls, 22-30  
 maintenance, 506  
 mechanical motions, 42-44  
 ordnance considerations, 504  
 pattern formation, 47-50  
 performance expectations, 59-76  
 preliminary work, 5  
 receivers, 30-35  
 sequence of functions, 40-42  
 stabilization, 43  
 switching pulse lines, 464  
 synchro and servo requirements, 44  
 theory of directivity pattern formation, 433  
 transducers, 44-50  
 transmitters, 35-40
- Scanning sonar pattern computer, 442
- Scanning sonar recommendations, 19, 475-512  
 circuit improvements, 496-501  
 CR pattern formation, 486-492  
 ER pattern formation, 492-496  
 fire control, 504-506  
 improving echo-signal recognition, 508  
 indicators, 501-504  
 in-service checking, 506  
 maintenance, 506-508  
 pulse modulation, 508-509  
 stabilization, 504-506  
 three dimensional scanning, 509-512  
 transducer improvements, 475-486
- Scanning sonar systems  
 British Navy system, 4  
 CR sonar, 11, 116-221  
 depth-scanning system, 26 kc, 13, 226, 259  
 ER sonar, 9, 15, 303-385  
 integrated type B, 13, 222-302  
 MR sonar, 8-9, 77-115  
 QH sonar, 3, 157, 174-183, 193, 214  
 QL sonar, 4  
 SSC sonar, 4  
 vertical scanning system, 13
- Scanning sonar tests, 386-432  
 commutator tests, 387-399  
 indicator tests, 413  
 installation tests, 422  
 performance tests, 429  
 preamplifier tests, 406  
 range determination, 418  
 receiver tests, 406-407  
 stabilization tests, 419  
 sweep circuit tests, 415  
 testing commutator and transducer together, 403-406  
 timing circuit tests, 417  
 transducer tests, 386  
 transfer network tests, 399-401  
 transmitter tests, 410
- Scanning sonar transducers  
*see* Transducers
- Scopes  
*see* Indicators
- Search-attack switch, 299
- Searchlight sonar, 122-125, 395, 498
- Sector scan indicator (SSI), 27, 34-35, 221, 502
- Sector-selective gain control, 501
- Self noise, 68, 73
- Send-receive switching arrangements, 122, 399-403
- Sequence control with ER sonar, 371
- Shading, 482
- Ship motion, effect on echo ranging, 71
- Ship-centered PPI display, 23
- Shock mounting for hydrophone, 83
- Shrimp noise, 59-60, 73
- Simultaneous lobe comparison (SLC), 8-9, 358, 508
- Sintered oxide magnets for HP-3 transducer, 136-137
- 60 cycle ER sonar  
 general description, 304  
 HP-1 transducer, 317  
 indicators, 347  
 lead lines, 331  
 receivers, 358  
 sweep and timing circuits, 372  
 transmit-receive networks, 344  
 transmitter, 362
- Skyatron, 502
- SLC brightening receiver, 83, 121, 169
- Slip rings, 490
- Sonar depression order, 228
- Sonar fire control  
*see* Fire control with sonar
- Sonar methods of energy storage compared to radar, 200
- Sonar operator, 500, 508
- Sonar switching test unit, 394
- Sonar train order, 228
- Sonar training aids, 508
- Sound attenuation, effect on frequency, 20
- Sound channel, 70
- Sound gear monitor (SGM), 423
- Sound gear monitor (SGM) transducer (Type S 3), 128
- Sound paths, 67-68
- Speaker for the integrated type B sonar, 271
- Specifications for transducer cables, 481
- Spiral sweep  
 electronic, 111  
 for CR sonar, 205, 207  
 for ER sonar, 371  
 for MR sonar, 110  
 generation, 40-41, 207, 214  
 Kollsman two phase generator, 211  
 mechanical, 110  
 tests, 413
- Split projector test unit (SPTU), 423
- Spy Pond testing station, 231
- SRO circuit, 377
- SSC sonar, 4
- Stabilization for the sonar equipment, 43
- Stabilization tests, 419-422  
 artificial ship, 421  
 attack director tests, 421  
 indicator panel tests, 420
- Stabilized oscillator and counter, 417
- Submarine ER sonar  
 bearing, 316, 352  
 chemical recorder, 385  
 depth charge detection, 316  
 doppler effect, 328-330  
 HP-3S transducer, 317  
 indicators, 352  
 interval timer, 382  
 laglines, 313-314, 339-340  
 linear sweeps, 383  
 maximum range, 313, 315  
 mine detection, 315  
 operating test procedure, 431  
 oscillator, 381  
 pulse length determination, 381  
 pulse-generating circuit, 380  
 range determination, 379  
 range-marking circuit, 377, 379  
 receiver bandwidth, 353  
 receivers, 360  
 rotor, 347  
 sonar switching test unit, 394  
 SRO circuit, 377  
 sweep and timing circuits, 376  
 sweep calibration, 384  
 test line, 313  
 tests on Spy Pond, 314  
 torpedo detection, 316  
 transducers, 313  
 transmitters, 367  
 triplane detection, 315
- Submarine Signal Company (SSC), 4, 356, 368
- Sum-and-difference BDI principle, 34, 279
- Surface reverberation, 63, 66, 73
- Surface "reverberation index," 60
- Surface ship noise detection, 432
- Surface-ship tests of submarine scanning sonar, 432

- Sweep and timing circuits for CR sonar, 205-219
  - Aide de Camp ER/CR system, 211
  - auditorium demonstration system, 119, 210
  - electronic spiral sweep, 207
  - Kollsman two-phase synchro spiral sweep generator, 211
  - QH scanning sonar, Model 1; 214
  - QH scanning sonar, Model 2; 216
  - rotating capacitive sweep generator, 209
  - XQHA scanning sonar, 219
- Sweep and timing circuits for ER sonar
  - 53-kc ER sonar, 373
  - 60-cycle ER sonar, 372
  - 200-cycle ER sonar, 372
  - linearization and stabilization, 383
  - submarine ER sonar, 376
- Sweep and timing circuits for integrated type B sonar, 296-300
- Sweep and timing circuits for 26-kc depth-scanning sonar, 296
- Sweep circuit tests
  - circular sweep tests, 416
  - linearity tests, 415
  - sweep tests for BDI, 419
- Sweep generator, 147, 207
- Switches, nonrectifying, 342
- Switches for electronic rotors, 335-343
  - binary counter-switching, 339
  - cathode-ray switching generator, 339
  - lag lines, 340
  - pentagrid convertor switch, 342
  - synchronization, 340
  - transmission lines, 339
  - vacuum tube switches, 342
  - varistor switches, 335-336, 342
- Switching lag-line measurements for electronic rotors, 393
- Switching pulse lines, 464-474
  - ER sonar, 465
  - mathematical analysis, 464
  - power storage lines, 472
  - requirements, 464
  - theory, 464
  - uses, 464
  - with double filter section, 469
- Switching voltage generators, 16, 337
- Synchro and servo requirements for scanning sonar, 44
- Synchro systems, 427
- Target doppler effect, 59
- Target echoes, 59-60
- Target noise, 68, 73
- Target strength, 70
- Temperature-gradient corrector, 276
- Thermal noise, 60
- Three-dimensional scanning, 509
- Thyrite, use in transducers, 131
- Time lags, 50
- Time-interval meter, 417
- Time-varied gain (TVG), 9, 32
- Timing circuit tests, 417
- Timing circuits
  - see Sweep and timing circuits
- Torpedo detection
  - submarine scanning sonar tests, 432
  - with CR sonar, 121, 124
  - with MR sonar, 8-9
  - with submarine ER sonar, 316
- Train order, 269
- Trainable artificial HP-5 transducer, 396
- Transducers
  - cables, 46, 481
  - CR sonar, 118-119, 128-143, 438-454
  - depth scanning, 26 kc, 222, 226, 241
  - design factors, 44
  - directivity patterns, 60, 433-438
  - effective diameter, 262
  - ER sonar, 317-326, 454-464
  - evaluation for scanning, 386
  - frequency, 44-45
  - impedance, 47
  - magnetostrictive, 45
  - manufacturability, 479
  - materials, 44-45, 475, 478
  - mechanical Q, 478
  - MR sonar, 84, 190, 386
  - phase angle, 44-45
  - serviceability, 477
  - shock, 45
  - switching pulse lines, 464-474
  - table of all types, 48-49
  - tests, 386-389, 403
  - training speed, 44
  - types, 386
- Transducers, artificial, 395
- Transducers, crystal
  - 6 x 6 inches, 85
  - AX-89; 49, 124, 142, 318, 334
  - AX-104; 49, 311, 318
  - AX-127; 49
  - AX-132; 49, 314, 319, 347
  - AX-136; 49, 314, 323, 347
  - AX-142; 49
  - CP1-1 #770; 49, 141
  - electrical insulation, 477
  - strength against impact and pressure, 476
- Transducers, magnetostrictive
  - 54-kc ring stack, 325
  - design considerations, 44
  - electrical insulation, 477
  - Hebbphone-1; 10, 48, 120, 128-129, 317
  - Hebbphone-2; 48, 124, 133
  - Hebbphone-2B; 48, 125, 133
  - Hebbphone-3; 48, 127, 136
  - Hebbphone-3DS; 48, 241
  - Hebbphone-3S; 48, 317
  - Hebbphone-4; 48
  - Hebbphone-5; 48, 127, 138, 250, 396
  - Hebbphone-6; 48
  - Hebbphone-7; 48
  - Hebbphone-8; 48
  - Hebbphone-8D; 222, 245-250
  - Hebbphone-9; 48
  - Medusa, 48, 118, 128
  - Millerphone, 48
  - Ring Ladderphone, 48
  - ring-stack emitter, 15 inch, 84, 325
  - stability of permanent magnets, 478
  - strength against impact and pressure, 476
  - tube hydrophone, 12 x 12 inch, 86
- Transducers, recommendations, 475-486
  - acoustical and electrical tolerances in manufacture, 479
  - cable seals, 475
  - cables, 481
  - corrosion prevention, 475
  - cost, 480-481
  - critical materials, 480-481
  - directivity patterns, 482
  - domes, 485
  - efficiency, 485
  - electrical insulation, 477
  - impedance, 485
  - mechanical Q, 485
  - production rate, 480-481
  - serviceability, 477
  - simplicity of design, 479
  - stability of impedance, 478
  - strength against impact and pressure, 476
  - testing facilities, 481
  - uniformity of elements, 479
  - watertightness, 475
- Transfer networks, 122, 399-403
  - coupling or tuning capacitors, 400
  - general description, 399
  - network tuning coil, 399
  - polarizing choke coils, 400
  - receiving-matching transformers, 400
  - relays, 401
  - requirements, 399-402
  - tests on complete network, 402-403
- Transmission anomaly, 69
- Transmission loss, 69
- Transmit-receive networks for ER rotors, 344
- Transmitter tests, 410-413
  - equipment needed, 410
  - frequency stability, 412
  - general tests, 410
  - output power measurements, 411
  - power and current input measurement, 412

- Transmitters  
 1.5 kw, 102, 362  
 36 tube driver, 190  
 400-watt, 99  
 circuits, 36  
 design requirements, 35  
 power supply, 36  
 power tubes, 39  
 pulse shape, 35  
 "unicontrol" system, 38
- Transmitters for CR sonar, 189-204  
 "Blockbusters," 191  
 model XQHA, 204  
 MR transmitter, 190  
 problems, 189  
 QH scanning sonar, Model 1; 193  
 QH scanning sonar, Model 2; 194  
 transmitter with 36 tube driver, 190
- Transmitters for ER sonar, 362-371  
 53-kc ER sonar, 367  
 60 cycle ER sonar, 362  
 200 cycle ER sonar, 362  
 submarine ER sonar, 367
- Transmitters for integrated type B sonar, 292
- Transmitters for MR scanning sonar, 99
- Transmitting directivity patterns, 7, 425
- Trigger circuit, 78, 366, 417
- Triplane detection with submarine ER sonar, 315
- True-bearing PPI, 121
- Trunnion-tilt corrector, 225, 228, 269
- Tubes for transmitters, 39
- Tuning range for ER receivers, 357
- Turn ratio, 387
- TVG circuit, 355
- TVG-AVC amplifier-receiver, 93-95
- 26 kc Depth-scanning sonar  
*see* Depth-scanning sonar, 26 kc
- 200 cycle ER sonar system  
*see* ER sonar, 200 cycle system
- Type B integrated sonar  
*see* Integrated type B sonar
- Ultimate type A scanning sonar, 222
- Ultimate type B scanning sonar  
*see* Integrated type B sonar
- Underwater direction finding, work of Germans, 5
- Underwater sound detection systems  
*see* Scanning sonar systems
- Unicontrol system, 38, 293
- University of California Division of War Research (UCDWR), 4, 141
- Vacuum tube rotors, 342
- Vacuum-tube switches, 337
- Varistor bridge circuits, 280, 290
- Varistor electronic switches, 335-336
- Varistors, 17, 313, 342
- Vertical scanning system, 13
- Visual detector, 63
- Volume reverberation, 63
- Volume reverberation curve, 73
- Volume reverberation index, 60
- Wakes shown on PPI, 2
- Watertightness of transducers, 475
- Western Electric Company, 492
- "Whirling Dervish," 118, 144
- Wide-range monitor, 317
- X-cut Rochelle salt crystals, 85, 478-479, 485
- XQHA sonar  
 accuracy of bearing information, 221  
 BDI improvement, 127  
 blanking of PPI screen, 206-207  
 commutators, 54  
 evaluation, 220  
 general description, 116  
 indicators, 162  
 in-service checking, 507  
 modifications, 127  
 noise tests, 128  
 receivers, 185  
 sweep and timing circuits, 219  
 tests, 127, 392  
 transducers, 127, 139  
 transmitter, 204  
 tuning range, 357
- XQKA  
*see* Submarine ER sonar
- Y-cut Rochelle salt crystals, 334, 478-479
- Z'd cross level angle, 43



~~CONFIDENTIAL~~

**TITLE:** Underwater Sound Equipment III - Scanning Sonar Systems

AVL- 53930

CYCODE

(None)

ORIG. AGENCY ED.  
Vol. 18

PRECEDING AGENCY ED.  
(Same)

**AUTHOR(S)** : Schuck, O. H.; Scott, R. M.; Watson, R. B.  
**ORIG. AGENCY** : OSRD, NDRC, Division 6, Washington, D. C.  
**PUBLISHED BY** : (Same)

**DATE**  
1946

**DOC. CLASS.**  
~~Secret~~

**COUNTRY**  
U.S.

**LANGUAGE**  
English

**PAGES**  
542

**ILLUSTRATIONS**  
photos, tables, diagrs, graphs

**ABSTRACT:**

An account is given of the development of scanning sonar, a method of underwater sound signaling which provides a continuous display of the position of all underwater objects within the acoustical detection range. The basic principles of omnidirectional scanning sonar systems are discussed along with equipment design considerations, the construction of prototype equipment, an analysis of operating tests, and recommendations for future work. The preparation of this information represents a group effort of members of the scanning sonar division and the editorial division of the Underwater Sound Laboratory, Harvard University.

**DISTRIBUTION:** Copies of this report obtainable from CADO.

(1)

**DIVISION:** Electronics (3)  
**SECTION:** Communications (1)

**SUBJECT HEADINGS:** Sonar, Sonar (89810.1)

**ATI SHEET NO.:** C-9-1-32

Control Air Documents Office  
Wright-Patterson Air Force Base, Dayton, Ohio

**AD TECHNICAL DATA**

~~CONFIDENTIAL~~